

LTR-LCPT-20-06-NP Attachment

Application for Certificate of Compliance for the Traveller PWR Fuel Shipping Package

NRC Certificate of Compliance
USA/9297/AF-96
Docket 71-9297

Safety Analysis Report, Revision 15

Application for Certificate of Compliance for the Traveller PWR Fuel Shipping Package

**NRC Certificate of Compliance
USA/9297/AF-96
Docket 71-9297**

Safety Analysis Report, Revision 15



RECORD OF REVISIONS

Rev. No.	Date	Description of Revision
0	March 2004	Original application. (Ref: NMS-NRC-04-004)
1	November 2004	Response to NRC request for additional information. (Ref: NMS-NRC-04-009, NMS-NRC-04-011)
2	February 2005	Response to NRC request for additional information. (Ref: NMS-NRC-05-002)
3	March 2005	Response to NRC request for additional information. Correct one error, revise certain tables to make the SAR parameter tables consistent with those that will be published in the CoC, clarify the results of the rod container analysis, and clarify the maintenance requirements for the shock mounts. (Ref: NMS-NRC-05-003)
4	March 2005	Response to NRC request for additional information. Correct entries in various tables that list the Traveller design weights. Clarify in Sections 2 and 3 that the shock mounts were intact following the drop and fire tests. Provide justification in Section 2 for establishing payload weights that are higher than fuel assembly weights used in actual testing. (Ref: NMS-NRC-05-004)
5	March 2006	Information about loose rod pipe packaging in license drawings and revision to Safety Analysis Report to describe this new loose rod pipe packaging. (Ref: UAM-NRC-06-005)
6	September 2006	A packaging component used to secure these non-Westinghouse fuel assembly types in the Traveller was designed after approval of the Traveller. Information about packaging components used to secure the contents. (Ref: UAM-NRC-06-011)
7	October 2007	Response to NRC request for additional information. Added sketch of package in Chapter 1 and revised Section 1.1 Revised Sections 2.6.3 and 2.6.4 to delete reference to calculations because the package is not sealed against pressure. Revised Section 2.7.1.2 regarding test sequence justification. Revised Section 8.2.3.3 to clarify shock mount inspection frequency. Revised Section 8.2.5 to clarify BORAL plate inspection frequency. Administrative change to Table 6-21, showing the correct number of fuel and non-fuel rods in a 15x15 STD/OFA fuel assembly. (Ref: LCPT-10-6)
8	May 2010	Add CE16NGF and CE16VA fuel assemblies to criticality safety evaluation. (Ref: LCPT-10-14)

RECORD OF REVISIONS (cont.)

<u>Rev. No.</u>	<u>Date</u>	<u>Description of Revision</u>
9	November 2010	<p><u>Style and Composition</u> An appendix is added to each section of the application as recommended in Regulatory Guide 7.9 to provide a list of documents that are referenced in the text of that section. The addition of this first appendix may result in renumbering of headings and pages where other appendices already existed for that section. Typographical changes have also been made. <u>Section 1 – General Information</u></p> <p>1.2.1.2 Outerpack Added description of vibration and shock dampening system.</p> <p>1.2.1.3 Clamshell Revised to provide more detailed description of clamshell features, including a design change for an alternate top end plate. Figures were revised to show typical configurations for the axial restraint and axial spacer.</p> <p>1.2.1.4 Rod Container Removed rod box as an option.</p> <p>1.2.3 Contents Revised description to add more detailed description of fuel assembly and components that may be transported in the fuel assembly. Added a Figure 1-8 showing a typical PWR fuel assembly. Added wording to describe the number of rods per pipe and how the rods are loaded.</p> <p>1.4 Appendices Added Appendix 1.4.1, References. Renamed Appendix 1.4.2, Engineering Drawings for Packaging The engineering drawings for packaging Drawing No. 10004E58 Safety Related Items, Traveller XL and STD was revised to show modifications to the clamshell top end plate and changes to the outer pack such as silicone rubber weather gasket, tie down chain tray gussets, new swing bolts, and clamshell cam lock wave washer.</p> <p><u>Section 2 – Structural Evaluation</u></p> <p>2.12.3.2.4.1 Internal/External Pressure Added silicone foam rubber seal and removed description of seal function as providing thermal protection.</p> <p>2.12 Appendices Added Appendix 2.12.1, References Added Appendix 2.12.6, Supplement to Drop Analysis for the Traveller XL Shipping Package – Clamshell Axial Spacer Structural Evaluation. Added Appendix 2.12.7, Supplement to Drop Analysis for the Traveller XL Shipping Package – Clamshell Removable Top Plate Structural Evaluation.</p>

RECORD OF REVISIONS (cont.)

<u>Rev. No.</u>	<u>Date</u>	<u>Description of Revision</u>
9 (cont.)		<p><u>Section 3 – Thermal Evaluation</u> Revised introduction to clarify that there is no heat generating material. Tables 3-2 and 3-3 and bullets in the text were revised to be consistent with ASME Code</p> <p>3.1.3 Description of maximum temperatures Added silicone rubber gasket to Table 3-1, Summary Table of Temperatures for Traveller Materials</p> <p>3.1.4 Description of maximum pressures Added silicone rubber gasket.</p> <p>3.4 Thermal Evaluation Under Normal Conditions of Transport Revised to clarify that there is no heat generating material.</p> <p>3.5.3 Maximum Temperatures and Pressures Revised description of the purpose for seals used around the Outerpack door. Added silicone foam rubber as an acceptable seal material. Added Figure 3-8A to show location of weather seal gaskets.</p> <p><u>Section 4 – Containment</u> Added Section 4.3, Appendices, and 4.3.1 References. No references are cited.</p> <p><u>Section 5 – Shielding Evaluation</u> Added Section 5.1, Appendices, and 5.1.1 References. No references are cited.</p> <p><u>Section 6 – Criticality Evaluation</u> Section 6.2, Fissile Material Contents Added statement that reactor control cluster (RCC) assemblies, secondary source assemblies, and solid stainless steel rods that may be placed in the PWR fuel assembly are non-fissile material.</p> <p>6.2.1 PWR Fuel Assemblies Added justification for allowing RCC, secondary source rods, or stainless steel rods in fuel assembly contents.</p> <p>6.2.2 PWR and BWR Rods Revise limit for wrapping or sleeving in Table 6-5 Fuel Rod Parameters</p> <p>6.3.1.1 Contents Models Removed rod box as an option.</p> <p>6.10.2 PWR Fuel Assembly Parameters Revised dimensions for guide tube and pellet in Table 6-22 Parameters for 16X16 Fuel Assemblies</p> <p>6.10 Appendices Added Appendix 6.10.1, References</p> <p><u>Section 7 – Package Operations</u> Revised all sections to incorporate operating experience and more accurately represent the current package operations. Added Section 7.4, Appendices, and 7.4.1 References. No references are cited.</p>

RECORD OF REVISIONS (cont.)

<u>Rev. No.</u>	<u>Date</u>	<u>Description of Revision</u>
9 (cont.)		<p><u>Section 8 – Acceptance tests and Maintenance Program</u> Replace “poison plate” with term “neutron absorber plate”, and replace “neutronics testing” with term “neutron absorber testing” to standardize reference to BORAL neutron absorber material. Add criteria for visual inspection of neutron absorber plates to Section 8.2.5. 8.1.5.1.4 Thermal Properties Thermal properties is revised to show the thermal conductivity for FR-3706, FR-3610, and FR-3620.</p>
10	September 2013	<p><u>Style and Composition</u> A number of typographical errors throughout the entire document have been corrected in this revision. A side result of the typographical corrections has been the addition of several pages, in order to accommodate paragraphs or figures which no longer had room to fit on the pages they previously occupied. <u>Section 1 – General Information</u> 1.2.1.1 Package Types Revised weights of packages where required. 1.2.1.4 Rod Pipe Further corrections added to clarify that the Rod Pipe will be the only rod container moving forward. 1.4.2 Engineering Drawings for Packaging Included the most recent revisions to the licensing drawings <u>Section 2 – Structural Evaluation</u> Updated equations and weights throughout the Section. 2.11.1 Rod Pipe Further corrections added to clarify that the Rod Pipe will be the only rod container moving forward. 2.12 Appendices Revised the appendices to provide an updated structural analysis which accounts for the revised weight of the Traveller package. 2.12.3.2.2 Lifting Provided additional information on Traveller STD four-point lift. Tables 2-7, 2-8, and 2-9 Removed, as the information was either already present or was consolidated elsewhere. <u>Section 6 – Criticality</u> 6.1.2, and 6.1.3 Corrections added to clarify that the Rod Pipe will be the only rod container moving forward. Figure 6-17 Replaced with the correct figure. <u>Section 7 – Package Operations</u> 7.1.1.3 Clarification and consolidation of information. 7.1.2, 7.12.1, and 7.2.2 Added tolerances for Torque figures.</p>

RECORD OF REVISIONS (cont.)

<u>Rev. No.</u>	<u>Date</u>	<u>Description of Revision</u>
10 (cont.)		<u>Section 8 – Acceptance Tests and Maintenance Program</u> Clarification and consolidation of information.
11	December 2013	<u>Section 1 – General Information</u> 1.2.1.3 Maximum Quantity of Material per Package Revised allowable weight for packing materials which are equivalent to polyethylene.
12	March 2015	Addition of the Traveller-VVER packaging with VVER fuel assembly contents in each chapter as required for design approval. Chapters 1, 2, 3 and 6 contain majority of the content addition (including Sections 1.2.1.1.3 and 1.2.1.3, Section 2.12.8, Section 3.3.1.1, and Section 6.10.11). Addition of tie-down detail calculations (Section 2.12.3.2.3). Revision of text to clarify acceptable seal materials, however no changes to materials made (Chapter 2 and Chapter 8). Minor style and composition, non-technical edits made throughout SAR to clarify text.
13	January 2017	Complete revision of Section 6, including development of bounding fuel parameters defined for each fuel bin as categorized fuel assemblies (CFAs), which represent a combination of fuels, as discussed in Sections 6.9.2 and 6.2. Revision of method for establishing subcriticality, by evaluation of uncertainties as independent sensitivities and accumulation of penalties, as discussed in Section 6.3.4. Updated code version to SCALE 6.1.2, and SCALE model of Traveller packaging, as discussed in Section 6.3. Clarifications added to Sections 1, 4, 5, 7, and 8, major details have not changed. Sections 1, 4, 5, 7, and 8 are fully updated to Revision 13 pages and change bars are not used. Sections 7 and 8 include additional details to represent current usage of the packages, and activities that are applicable to all sites that use the packages. Section 2 and 3 include an update to reference sections to address the update of IAEA regulations, as incorporated by 49 CFR 171.7. Section 2.12.8.3 (pages 2-240 – 2-240C) includes additional details of the VVER fuel assembly performance expectations resultant of the previously defined Traveller VVER FEA. New Section 2.12.9 has been added to discuss performance comparison of zirconium alloys. Section 3.2.1 and tables have been revised to incorporate additional material property references. Section 3.6.5.1 (pages 3-46, 3-46A) includes additional details of the condition of the moderator block after fire testing, as justification to support the evaluations defined in Section 6.3.4.3.3.

RECORD OF REVISIONS (cont.)

<u>Rev. No.</u>	<u>Date</u>	<u>Description of Revision</u>
14	February 2019	<p>Non-technical changes in Chapters 1, 6, 7, and 8 to add clarification of existing analyses. Additional grammatical changes made in Chapter 1.</p> <p>No changes are made to Chapters 2, 3, 4, and 5.</p> <p>Chapter 1 changes</p> <ul style="list-style-type: none"> • Section 1.1 - Added paragraph for approved WEC QA program • Section 1.2.1.5.3 – clarified that axial restraints are for all Traveller variants; removed text specific to Traveller XL • Throughout – clarified, where needed, component name such as Clamshell main door versus access door and Clamshell base; clarified containment boundary and burnable absorbers; additional minor changes made to clarify text and correct grammar <p>Chapter 6 changes</p> <ul style="list-style-type: none"> • Sections 6.1.2 and 6.3.4.3 – clarified when penalties are and are not applied to the total penalty summary • Sections 6.1.2.1, 6.4.2.1, 6.4.2.2.1, 6.4.2.2.3 – for HAC single package revised polyethylene packing material penalty to assess 2 kg penalty, as 2 kg is defined as the license limit (impacted Tables 6-36, 6-27, 6-26, 6-2) • Section 6.4.2.2.3 (pg 6-50, 6-51), 6.4.2.2.4.1 (pg 6-58), 6.4.2.2.4.2 (pg 6-62), 6.6.2.2.2 (pg 6-92) – clarified the polyethylene packing material limit • Throughout – clarified model and evaluation where needed; reference corrections also <p>Chapter 7 changes</p> <ul style="list-style-type: none"> • Section 7.1 and 7.2 – clarified the package loading and unloading operations cover a range of activities; Added reference to applicable information in Section 1 • Added detail for further inspection of Clamshell and BORAL neutron absorber plates • Section 7.1.3.1 – added restrictions for lifting stacked packages • Throughout – minor clarifications of activities <p>Chapter 8 changes</p> <ul style="list-style-type: none"> • Section 8.1 – added statement regarding approved WEC QA program • Throughout – minor clarifications of testing and acceptance criteria

RECORD OF REVISIONS (cont.)

<u>Rev. No.</u>	<u>Date</u>	<u>Description of Revision</u>
15	February 2020	<p>No changes are made to Chapters 4, 5, and 7.</p> <p>Chapter 1 changes</p> <ul style="list-style-type: none"> • Section 1.1, 1.2.2.1, and 1.2.2.2 – revised text to clarify that the allowable enrichments of 5 wt.% for fuel assemblies and U₃Si₂ loose rods, or 7 wt.% for UO₂ loose rods. • Section 1.2.2.1.1 – added text to state the allowance of clad chromium coating and Optimized ZIRLO Liner • Section 1.3.2 – updated Rod Pipe licensing drawing 10006E58 Rev. 6 <p>Chapter 2 changes</p> <ul style="list-style-type: none"> • Section 2.12.9 – revised to include cladding comparison with advanced variations of chromium coating or an Optimized ZIRLO Liner <p>Chapter 3 changes</p> <ul style="list-style-type: none"> • Section 3.2.1.1 added to address thermal comparison of advanced cladding variations including cladding treated with a chromium coating or an Optimized ZIRLO Liner • Uranium silicide (U₃Si₂) fuel to Table 3-3A, <p>Chapter 6 changes</p> <ul style="list-style-type: none"> • No changes to SCALE inputs or results for baseline cases and previous sensitivity studies for fuel assemblies. • ADOPT UO₂ rod sensitivity study evaluated for all transport conditions: single package NCT and HAC, package array NCT and HAC • UO₂ fuel rods evaluated for 7wt.% ²³⁵U for all transport conditions and added ADOPT fuel rod sensitivity study: single package NCT and HAC, package array NCT and HAC • Sections 6.1.2 and 6.3.4.3 – defined criteria for statistical significance for when a penalty is applied, which impacted the penalty summary tables and <i>Maximum k_{eff}</i> values (Section 6.1.2.1) • Section 6.1.2 and 6.8 – two new benchmark series (7.4 w.t% and 6.9 wt.% enrichments) added to supplement the addition of 7 wt.% UO₂ loose rod contents. New USL equation generated and USL values in Table 6-1 updated. • Section 6.2 – Text revised to include 7 wt.% loose rods and ADOPT rods • Sections 6.2.1 and 6.9.2.1 – Typographical errors corrected in Tables 6-5 and 6-97 (no effect on analysis) • Sections 6.2.1 and 6.2.2 – added allowance for ADOPT rods and advanced cladding variations of chromium coating or an Optimized ZIRLO Liner • Section 6.2.3 – added allowance for clad coatings • Section 6.2.4 – added allowance for ADOPT rods and advanced cladding variations, as well as 7 wt.% UO₂ loose rods. • Section 6.3.4.3 – Table 6-18 as well as Sections 6.3.4.3.2 and 6.3.4.3.14 updated to include single package HAC fuel assembly shift study and ADOPT rod study. • Sections 6.4.1, 6.5.1 and 6.6.1 – Updated results based on total penalty with the statistical significance criteria applied

<u>Rev. No.</u>	<u>Date</u>	<u>Description of Revision</u>
		<ul style="list-style-type: none"> • Sections 6.4.2, 6.5.2, 6.6.2, and 6.9.3 – Updated results with the statistical significance criteria applied. All UO₂ loose rod baseline and sensitivity study results updated for 7 wt.% ²³⁵U enrichment. Single package HAC fuel assembly shift study and ADOPT rod studies added. • Section 6.3.4 and 6.9.4 – supplemental combined case study added to appendix 6.9.4 and referenced in section 6.3.4. • Throughout – highlighting in sensitivity study tables corrected to most reactive case to reflect revised statistical significance criteria (not marked with rev bars) <p>Chapter 8 changes</p> <ul style="list-style-type: none"> • Section 8.1.2 reference to ASME Code revised to allow later edition at time of manufacturing as approved by Engineering • Section 8.2.3.2 heading changed from “Weather Seal” to “Weather Gasket” • Added Section 8.2.6 to address “Periodic Weld Examinations” • Added Section 8.2.7 to address “Periodic Acetate Plug Examinations”

TABLE OF CONTENTS

1.0	GENERAL INFORMATION	1-1
2.0	STRUCTURAL EVALUATION.....	2-1
3.0	THERMAL EVALUATION.....	3-1
4.0	CONTAINMENT.....	4-1
5.0	SHIELDING EVALUATION.....	5-1
6.0	CRITICALITY EVALUATION.....	6-1
7.0	PACKAGE OPERATIONS	7-1
8.0	ACCEPTANCE TESTS AND MAINTENANCE PROGRAM	8-1

TRAVELLER SAFETY ANALYSIS REPORT ACRONYM LIST

Acronym	Definition	Acronym	Definition
ADOPT	Advanced Doped Pellet Technology	LWR	Light-water reactor
ASME	American Society of Mechanical Engineers	NCT	Normal Conditions of Transport
ANSI	American National Standards Institute	NFD	Nuclear Fuel Division of Westinghouse
ASTM	American Society for Testing and Materials	OD	Outer diameter
AWS	American Welding Society	OR	Outer radius
BORAL	Borated aluminum	PWR	Pressurized water reactor
BWR	Boiling water reactor	QC	Quality control
CFA	Categorized fuel assembly	QTC	Qualified test unit
CFR	Code of Federal Regulation	SAR	Safety Analysis Report
CG	Center of gravity	SS	Stainless steel
CS	Clamshell	SSR	Specific Safety Requirements
CSI	Criticality safety index	TE	Total energy
CTE	Coefficient of thermal expansion	UHMW	Ultra-high molecular weight
CTU	Certified test unit	UNC	Unified thread coarse
DFT	Directional flame thermometers	USL	Upper subcritical limit
DTE	Differential thermal expansion	WtF	Water-to-Fuel
EALF	Energy of average lethargy causing fission		
FA	Fuel assembly		
FAA	Federal Aviation Administration		
FEA	Finite Element Analysis		
FEM	Finite Element Model		
GT/IT	Guide tubes/instrument tubes		
HAC	Hypothetical Accident Conditions		
IAEA	International Atomic Energy Agency		
ICRP	International Commission on Radiological Protection		
ID	Inner diameter		
IE	Internal energy		
IR	Inner radius		
KE	Kinetic energy		
k _{eff}	Effective neutron multiplication factor		
LEU	Low-enriched uranium		

TRAVELLER SAFETY ANALYSIS REPORT
LIST OF EFFECTIVE PAGES

Page	Rev.	Date	Page	Rev.	Date	Page	Rev.	Date
i	8	5/2010	2-1	12	3/2015	2-37	0	3/2004
ii - iii	9	11/2010	2-1A	1	11/2004	2-38	10	9/2013
iv	10	9/2013	2-2	0	3/2004	2-39	10	9/2013
v	13	1/2017	2-3	9	11/2010	2-40	10	9/2013
vi	14	2/2019	2-4	12	3/2015	2-41	10	9/2013
vii - viii	15	3/2020	2-5	10	9/2013	2-42	10	9/2013
ix	0	3/2004	2-6	9	11/2010	2-43	10	9/2013
x - xiv	15	3/2020	2-7	12	3/2015	2-44	10	9/2013
			2-8	9	11/2010	2-45	10	9/2013
1-i - 1-iii	14	2/2019	2-9	10	9/2013	2-46	10	9/2013
1-1	15	3/2020	2-10	9	11/2010	2-47	10	9/2013
1-2	14	2/2019	2-11	10	9/2013	2-48	10	9/2013
1-3	14	2/2019	2-11A	12	3/2015	2-49	10	9/2013
1-4	13	1/2017	2-12	9	11/2010	2-49A	10	9/2013
1-5	14	2/2019	2-13	10	9/2013	2-50	10	9/2013
1-6	14	2/2019	2-14	10	9/2013	2-50A	10	9/2013
1-7	13	1/2017	2-14A	13	1/2017	2-50B	10	9/2013
1-8	13	1/2017	2-14B	1	11/2004	2-50C	10	9/2013
1-9	13	1/2017	2-15	9	11/2010	2-51	10	9/2013
1-10	13	1/2017	2-16	10	9/2013	2-51A	12	3/2015
1-11	13	1/2017	2-17	2	2/2005	2-51B	12	3/2015
1-12	13	1/2017	2-18	2	2/2005	2-51C	12	3/2015
1-13	13	1/2017	2-19	0	3/2004	2-51D	12	3/2015
1-14	13	1/2017	2-20	0	3/2004	2-51E	12	3/2015
1-15	14	2/2019	2-21	0	3/2004	2-51F	12	3/2015
1-16	13	1/2017	2-22	1	11/2004	2-51G	12	3/2015
1-17	15	3/2020	2-22A	1	11/2004	2-51H	12	3/2015
1-18	15	3/2020	2-22B	1	11/2004	2-51I	12	3/2015
1-19	14	2/2019	2-22C	1	11/2004	2-52	0	3/2004
1-20	14	2/2019	2-22D	1	11/2004	2-53	0	3/2004
1-21	15	3/2020	2-23	10	9/2013	2-54	0	3/2004
10004E58	9		2-24	10	9/2013	2-55	0	3/2004
10037E43	3		2-24A	10	9/2013	2-56	1	11/2004
10006E58	6		2-24B	9	11/2010	2-57	12	3/2015
			2-25	10	9/2013	2-58	10	9/2013
2-i	4	3/2005	2-26	9	11/2010	2-59	10	9/2013
2-ii	10	9/2013	2-27	9	11/2010	2-60	10	9/2013
2-iii	15	3/2020	2-28	0	3/2004	2-61	0	3/2004
2-iv	12	3/2015	2-29	0	3/2004	2-62	0	3/2004
2-v	13	1/2017	2-30	0	3/2004	2-63	10	9/2013
2-vi	12	3/2015	2-31	0	3/2004	2-64	10	9/2013
2-vii	1	11/2004	2-32	10	9/2013	2-65	10	9/2013
2-viii	2	2/2005	2-32A	10	9/2013	2-66	12	3/2015
2-ix	1	11/2004	2-32B	1	11/2004	2-67	9	11/2010
2-x	1	11/2004	2-33	13	1/2017	2-67A	9	11/2010
2-xi	2	2/2005	2-34	12	3/2015	2-67B	2	2/2005
2-xii	9	11/2010	2-35	12	3/2015	2-68	9	11/2010
2-xiii	15	3/2020	2-36	12	3/2015	2-69	0	3/2004

TRAVELLER SAFETY ANALYSIS REPORT
LIST OF EFFECTIVE PAGES (cont.)

Page	Rev.	Date	Page	Rev.	Date	Page	Rev.	Date
2-70	0	3/2004	2-116	9	11/2010	2-154	0	3/2004
2-71	0	3/2004	2-117	0	3/2004	2-155	1	11/2004
2-72	9	11/2010	2-118	9	11/2010	2-155A	1	11/2004
2-73	0	3/2004	2-119	0	3/2004	2-155B	1	11/2004
2-74	0	3/2004	2-120	0	3/2004	2-156	2	2/2005
2-75	0	3/2004	2-121	0	3/2004	2-157	2	2/2005
2-76	0	3/2004	2-122	0	3/2004	2-158	1	11/2004
2-77	0	3/2004	2-123	0	3/2004	2-159	0	3/2004
2-78	0	3/2004	2-124	0	3/2004	2-160	0	3/2004
2-79	0	3/2004	2-125	9	11/2010	2-161	0	3/2004
2-80	0	3/2004	2-126	2	2/2005	2-162	0	3/2004
2-81	0	3/2004	2-127	1	11/2004	2-163	0	3/2004
2-82	0	3/2004	2-128	9	11/2010	2-164	0	3/2004
2-83	0	3/2004	2-129	9	11/2010	2-165	0	3/2004
2-84	0	3/2004	2-130	1	11/2004	2-166	0	3/2004
2-85	0	3/2004	2-131	1	11/2004	2-167	9	11/2010
2-86	9	11/2010	2-132	0	3/2004	2-168	1	11/2004
2-87	0	3/2004	2-133	9	11/2010	2-169	0	3/2004
2-88	0	3/2004	2-134	9	11/2010	2-170	0	3/2004
2-89	1	11/2004	2-134A	1	11/2004	2-171	0	3/2004
2-90	0	3/2004	2-134B	1	11/2004	2-172	2	2/2005
2-91	0	3/2004	2-134C	1	11/2004	2-173	0	3/2004
2-92	0	3/2004	2-134D	1	11/2004	2-174	0	3/2004
2-93	0	3/2004	2-135	1	11/2004	2-175	9	11/2010
2-94	0	3/2004	2-135A	9	11/2010	2-176	0	3/2004
2-95	0	3/2004	2-135B	1	11/2004	2-177	1	11/2004
2-96	0	3/2004	2-135C	9	11/2010	2-178	0	3/2004
2-97	10	9/2013	2-135D	1	11/2004	2-179	0	3/2004
2-98	9	11/2010	2-136	9	11/2010	2-180	0	3/2004
2-99	10	9/2013	2-137	0	3/2004	2-181	0	3/2004
2-100	0	3/2004	2-138	9	11/2010	2-182	0	3/2004
2-101	1	11/2004	2-139	1	11/2004	2-183	9	11/2010
2-102	0	3/2004	2-139A	1	11/2004	2-184	0	3/2004
2-103	1	11/2004	2-139B	1	11/2004	2-185	0	3/2004
2-104	9	11/2010	2-140	0	3/2004	2-186	0	3/2004
2-105	2	2/2005	2-141	1	11/2004	2-187	0	3/2004
2-106	1	11/2004	2-142	9	11/2010	2-188	0	3/2004
2-106A	9	11/2010	2-143	9	11/2010	2-189	0	3/2004
2-106B	1	11/2004	2-144	9	11/2010	2-190	4	3/2005
2-107	0	3/2004	2-145	1	11/2004	2-191	0	3/2004
2-108	0	3/2004	2-146	0	3/2004	2-192	9	11/2010
2-109	0	3/2004	2-147	0	3/2004	2-192A	4	3/2005
2-110	0	3/2004	2-148	12	3/2015	2-192B	4	3/2005
2-111	0	3/2004	2-149	0	3/2004	2-192C	9	11/2010
2-112	0	3/2004	2-150	0	3/2004	2-192D	4	3/2005
2-113	0	3/2004	2-151	0	3/2004	2-193	0	3/2004
2-114	0	3/2004	2-152	0	3/2004	2-194	0	3/2004
2-115	0	3/2004	2-153	0	3/2004	2-195	0	3/2004

TRAVELLER SAFETY ANALYSIS REPORT
LIST OF EFFECTIVE PAGES (cont.)

Page	Rev.	Date	Page	Rev.	Date	Page	Rev.	Date
2-196	0	3/2004	2-241	12	3/2015	3-21	10	9/2013
2-197	0	3/2004	2-242	12	3/2015	3-22	0	3/2004
2-198	0	3/2004	2-243	12	3/2015	3-23	0	3/2004
2-199	0	3/2004	2-244	12	3/2015	3-24	0	3/2004
2-200	0	3/2004	2-245	15	3/2020	3-25	9	11/2010
2-201	10	9/2013	2-246	15	3/2020	3-26	10	9/2013
2-202	10	9/2013	2-247	15	3/2020	3-27	0	3/2004
2-203	10	9/2013	2-248	15	3/2020	3-28	9	11/2010
2-204	9	11/2010	2-249	15	3/2020	3-29	0	3/2004
2-205	9	11/2010	2-250	15	3/2020	3-30	0	3/2004
2-206	9	11/2010	2-251	15	3/2020	3-31	9	11/2010
2-207	9	11/2010	2-252	15	3/2020	3-32	0	3/2004
2-208	10	9/2013	2-253	15	3/2020	3-33	9	11/2010
2-209	9	11/2010	2-254	15	3/2020	3-34	0	3/2004
2-210	10	9/2013				3-35	10	9/2013
2-211	9	11/2010	3-i	15	3/2020	3-35A	1	11/2004
2-212	10	9/2013	3-ii	13	1/2017	3-35B	10	9/2013
2-213	9	11/2010	3-iii	15	3/2020	3-36	0	3/2004
2-214	10	9/2013	3-iv	9	11/2010	3-37	0	3/2004
2-215	9	11/2010	3-1	10	9/2013	3-38	1	11/2004
2-216	9	11/2010	3-2	9	11/2010	3-39	0	3/2004
2-217	9	11/2010	3-3	13	1/2017	3-40	10	9/2013
2-218	9	11/2010	3-4	15	3/2020	3-41	0	3/2004
2-219	12	3/2015	3-4A	15	3/2020	3-42	1	11/2004
2-220	12	3/2015	3-4B	15	3/2020	3-42A	1	11/2004
2-221	12	3/2015	3-4C	15	3/2020	3-42B	1	11/2004
2-222	12	3/2015	3-5	13	1/2017	3-43	0	3/2004
2-223	12	3/2015	3-5A	12	3/2015	3-44	0	3/2004
2-224	12	3/2015	3-5B	12	3/2015	3-45	0	3/2004
2-225	12	3/2015	3-6	0	3/2004	3-46	13	1/2017
2-226	12	3/2015	3-7	0	3/2004	3-46A	13	1/2017
2-227	12	3/2015	3-8	0	3/2004	3-46B	1	11/2004
2-228	12	3/2015	3-9	0	3/2004	3-47	0	3/2004
2-229	12	3/2015	3-10	10	9/2013	3-48	0	3/2004
2-230	12	3/2015	3-11	0	3/2004	3-49	10	9/2013
2-231	12	3/2015	3-12	0	3/2004	3-50	1	11/2004
2-232	12	3/2015	3-13	10	9/2013			
2-233	12	3/2015	3-14	10	9/2013	4-i	13	1/2017
2-234	12	3/2015	3-14A	9	11/2010	4-1	13	1/2017
2-235	12	3/2015	3-14B	9	11/2010			
2-236	12	3/2015	3-15	9	11/2010	5-i	13	1/2017
2-237	12	3/2015	3-15A	13	1/2017	5-1	13	1/2017
2-238	12	3/2015	3-15B	9	11/2010			
2-239	12	3/2015	3-16	10	9/2013			
2-240	13	1/2017	3-17	12	3/2015			
2-240A	13	1/2017	3-18	1	11/2004			
2-240B	13	1/2017	3-19	9	11/2010			
2-240C	13	1/2017	3-20	0	3/2004			

TRAVELLER SAFETY ANALYSIS REPORT
LIST OF EFFECTIVE PAGES (cont.)

Page	Rev.	Date	Page	Rev.	Date
6-i - 6-vii	15	3/2020	6-117 - 6-134	13	2/2017
6-1	14	2/2019	6-135 - 6-136	14	2/2019
6-2 - 6-7	15	3/2020	6-137	13	2/2017
6-8	13	2/2017	6-138 - 6-141	15	3/2020
6-9 - 6-11	15	3/2020	6-142 - 6-143	13	2/2017
6-12	13	1/2017	6-144	15	3/2020
6-13	14	2/2019	6-145 - 6-150	13	2/2017
6-14 - 6-16	13	2/2017	6-151 - 6-155	15	3/2020
6-17	15	3/2020			
6-18 - 6-19	13	2/2017	7-i	14	2/2019
6-20 - 6-22	15	3/2020	7-1 - 7-5	14	2/2019
6-23	13	2/2017	7-6	13	2/2017
6-24	15	3/2020			
6-25	13	2/2017	8-i	15	3/2020
6-26	14	2/2019	8-ii	14	2/2019
6-27 - 6-29	13	2/2017	8-1	15	3/2020
6-30 - 6-32	15	3/2020	8-2	14	2/2019
6-33 - 6-37	13	2/2017	8-3	13	2/2017
6-38	15	3/2020	8-4 - 8-8	14	2/2019
6-39 - 6-41	13	2/2017	8-9	15	3/2020
6-42	15	3/2020	8-10	15	3/2020
6-43 - 6-44	13	2/2017	8-11	13	2/2017
6-45 - 6-47	15	3/2020			
6-48 - 6-50	13	2/2017			
6-51	15	3/2020			
6-52	13	2/2017			
6-53	15	3/2020			
6-54 - 6-55	14	2/2019			
6-56	13	2/2017			
6-57	15	3/2020			
6-58	13	2/2017			
6-59 - 6-69	15	3/2020			
6-70 - 6-71	13	2/2017			
6-72 - 6-75	15	3/2020			
6-76 - 6-80	13	2/2017			
6-81 - 6-85	15	3/2020			
6-86 - 6-87	13	2/2017			
6-88	15	3/2020			
6-89	13	2/2017			
6-90 - 6-92	15	3/2020			
6-93 - 6-94	13	2/2017			
6-95	14	2/2019			
6-96 - 6-101	13	2/2017			
6-102 - 6-109	15	3/2020			
6-110	13	2/2017			
6-111 - 6-114	15	3/2020			
6-115	13	2/2017			
6-116	15	3/2020			

TABLE OF CONTENTS

1.0	GENERAL INFORMATION.....	1-1
1.1	INTRODUCTION.....	1-1
1.2	PACKAGE DESCRIPTION.....	1-1
1.2.1	Packaging	1-1
1.2.1.1	Overall Dimensions and Weights of the Traveller Variants.....	1-2
1.2.1.2	Containment Features.....	1-2
1.2.1.3	Neutron and Gamma Shielding Features.....	1-2
1.2.1.4	Criticality Control Features	1-3
1.2.1.5	Structural Features.....	1-3
1.2.2	Contents.....	1-17
1.2.2.1	Type and Form	1-17
1.2.2.2	Maximum Quantity of Material per Package	1-18
1.2.3	Special Requirements for Plutonium	1-20
1.2.4	Operational Features	1-20
1.3	APPENDICES.....	1-21
1.3.1	References	1-21
1.3.2	Licensing Drawings for Packaging.....	1-21

LIST OF TABLES

Table 1-1 Traveller CSIs 1-1
Table 1-2 Isotopic Content Specification 1-19

LIST OF FIGURES

Figure 1-1 Outerpack Closed Position (left) and Opened Position (right) 1-4
Figure 1-2 Outerpack and Clamshell Cross-Section View (typical) 1-4
Figure 1-3 Clamshell with Fixed Top Plate (FTP) 1-7
Figure 1-4 Clamshell with Removable Top Plate (RTP) 1-7
Figure 1-5 Clamshell Latch Locked Position (left) and Open Position (right) 1-8
Figure 1-6 Corner Post Axial Restraint – Removable Top Plate (left), Fixed Top Plate (right) 1-9
Figure 1-7 Center Plate Axial Restraint – Removable Top Plate (left), Fixed Top Plate (right) 1-10
Figure 1-8 Corner Post Axial Restraint 1-10
Figure 1-9 Axial Spacer Assembly (length depends on fuel assembly type) 1-11
Figure 1-10 XL Clamshell Fuel Spacer Assembly 1-11
Figure 1-11 Comparison of Standard Clamshell to VVER Clamshell 1-12
Figure 1-12 VVER Clamshell with VVER Top Plate (VTP) 1-12
Figure 1-13 VTP Locking Mechanism 1-13
Figure 1-14 Comparison of Clamshell Door Hinges and Latches 1-13
Figure 1-15 Axial Clamp as Installed on VTP 1-14
Figure 1-16 Rod Pipe 1-15
Figure 1-17 Generic Sketch of the Traveller Representing the Package as Prepared for Transport 1-16

1.0 GENERAL INFORMATION

1.1 INTRODUCTION

The Traveller is a shipping package designed to transport enriched commercial grade uranium fuel assemblies or rods. It will carry several types of pressurized water reactor (PWR) fuel assemblies with uranium dioxide (UO₂) enrichments up to 5.0 weight percent (wt.%) ²³⁵U, as well as either PWR or boiling water reactor (BWR) fuel rods with UO₂ enrichments up to 7.0 wt.% ²³⁵U and uranium silicide (U₃Si₂) enrichments up to 5.0 wt.% ²³⁵U. The Traveller package is designed to carry one (1) fuel assembly or one (1) Rod Pipe for loose fuel rods. There are three packaging variants in the Traveller family: Traveller Standard (STD), Traveller XL (XL), and Traveller VVER (VVER).

In the criticality analysis, PWR fuel assemblies are organized with similar fuel assemblies into defined bins. Three PWR groups define the allowable fuel assembly contents, with each group containing like bins. The bounding parameters of the fuel assembly contents in a bin are represented by categorized fuel assemblies (CFA), for the criticality analyses. All CFAs among the three PWR groups are evaluated and organized by Criticality Safety Indices (CSI) and Traveller packaging variants. This is described further in Section 6, with contents parameter details in Section 6.2, Fissile Material Contents.

The CSI of each content for the Traveller are provided in Table 1-1. The following sections describe the package design and testing program in detail. Licensing drawings are presented in Section 1.3.2. A generic sketch of the Traveller representing the package as prepared for transport is provided in Figure 1-17.

Content	Traveller Packaging Variant	CSI
PWR Group 1	Traveller STD/XL	1.0
PWR Group 2	Traveller XL	4.2
PWR Group 3	Traveller VVER	1.0
Rod Pipe	Traveller STD/XL	0.7

The analyses and testing are performed under an NRC-approved quality assurance program, which specifically complies with Title 10 of the Code of Federal Regulations, Part 50 (10 CFR 50), Appendix B requirements and is adopted to meet the requirements of 10 CFR 71, Subpart H, for the transportation of radioactive material.

1.2 PACKAGE DESCRIPTION

1.2.1 Packaging

The packaging is made up of two basic components: 1) an Outerpack and 2) a Clamshell. The package is made up of the packaging and the contents, which consist of either a fuel assembly or Rod Pipe with loose fuel rods. The Outerpack and Clamshell are connected together with a suspension system that reduces the forces applied to the contents during transport. The contents, either a fuel assembly or Rod Pipe, are secured

inside the Clamshell during transport.

1.2.1.1 Overall Dimensions and Weights of the Traveller Variants

There are three packaging variants in the Traveller family: Traveller STD (STD), Traveller XL (XL), and Traveller VVER (VVER). General parameters for each packaging variant are as defined in the following subsections. Dimensions represent an as manufactured outer-most measurement. Weights represent a bounding maximum weight.

1.2.1.1.1 Traveller STD

- Gross Weight = 4,500 pounds (2,041 kg)
- Tare Weight = 2,850 pounds (1,293 kg)
- Outer Dimensions = LxWxH- 197.0 in. x 27.1 in. x 39.3 in. (5004 mm x 686 mm x 998 mm)
- Accommodates standard length fuel assemblies or Rod Pipe

1.2.1.1.2 Traveller XL

- Gross Weight = 5,230 pounds (2,372 kg)
- Tare Weight = 3,255 pounds (1,476 kg)
- Outer Dimensions = LxWxH- 226.0 in. x 27.1 in. x 39.3 in. (5740 mm x 688 mm x 998 mm)
- Accommodates standard or long length fuel assemblies or Rod Pipe

1.2.1.1.3 Traveller VVER

- Gross Weight = 5,105 pounds (2,316 kg)
- Tare Weight = 3,255 pounds (1,476 kg)
- Outer Dimensions = LxWxH- 226.0 in. x 27.1 in. x 39.3 in. (5740 mm x 688 mm x 998 mm)
- Accommodates VVER type fuel assemblies

1.2.1.2 Containment Features

The Containment System is described in both IAEA Regulations for the Safe Transport of Radioactive Material, Specific Safety Requirements No. SSR-6 para. 213 [1] and 10 CFR 71.4 [2] as, “the assembly of components of the packaging intended to retain the radioactive material during transport.” The Containment System for the Traveller is the zirconium alloy clad and end plugs of the fuel rods. Containment is described further in Section 4.

The fuel rod is assembled by loading the UO₂ or U₃Si₂ pellets into a cladding tube. The tubes are pressurized with helium and end plugs are welded to the tube which effectively seals and contains the radioactive material. Welds of the fuel rods are verified for integrity by non-destructive methods such as radiographic or ultrasonic testing. As the containment boundary is welded closed, it cannot be opened unintentionally. Thus, the requirements of 10 CFR 71.43(c) are satisfied.

1.2.1.3 Neutron and Gamma Shielding Features

The Traveller packaging does not contain neutron or gamma shielding features because neutron and gamma radiation emitted from the allowable contents is negligible in quantity, as discussed in Section 5. Due to the

insignificant decay heat of the allowable contents, payload personnel barriers are not necessary. The Traveller packaging meets the requirements of 10 CFR 71.47.

1.2.1.4 Criticality Control Features

The confinement system for the Traveller consists of the fuel rods, the fuel assembly (or Rod Pipe), the Clamshell assembly including the neutron absorber plates, and the Outerpack. The Traveller features a flux trap system that reduces neutron communication between packages in an array. This system features BORAL® neutron absorber plates located at each lateral side of the Clamshell that act in conjunction with ultra-high molecular weight (UHMW) polyethylene moderator blocks, which are affixed to the walls of the Outerpack inner cavity. Neutrons leaving one package must pass through two regions of moderator blocks and then BORAL neutron absorber plates before reaching the contents of another package. In addition, the structural materials of the Traveller for which credit is taken in the criticality safety analysis provide additional neutron absorption.

1.2.1.5 Structural Features

1.2.1.5.1 Outerpack

The Outerpack is a structural component that serves as the primary impact and thermal protection for the contents. It also includes components that provide for lifting, stacking, and tie down during transportation. The Outerpack is a long tubular design consisting of a top and bottom half, as shown in Figure 1-1. Each half consists of a stainless steel outer shell, a layer of rigid 10-pcf polyurethane foam, and an inner stainless steel shell. The stainless steel provides structural strength and acts as a protective covering to the foam. A typical cross-section showing key elements of the package is depicted in Figure 1-2.

The Outerpack also has independent impact limiters at the top and lower ends. Each Endcap Impact Limiter system contains an Inner Pillow Impact Limiter adjacent to 20-pcf polyurethane foam. The 20-pcf foam is encased by the package Outerpack stainless steel skins. The top Inner Pillow Impact Limiter consists of 6-pcf foam encased between two stainless steel plates to allow mating with the upper Outerpack. The lower Inner Pillow Impact Limiter consists of 6-pcf foam encased in a stainless steel circular housing, which allows mating with the lower Outerpack. Details of the top and lower Inner Pillow Impact Limiters are also shown on Sheet 6 of 10004E58 and 10037E43 for the Traveller STD and XL and Traveller VVER, respectively.

The foam is a rigid, closed-cell polyurethane that is an excellent impact absorber and thermal insulator, and has well-defined characteristics that make it ideal for this application. The steel-foam-steel “sandwich” is the primary fire protection, and is described in more detail in Section 3.

The inside of the Outerpack is lined with UHMW polyethylene moderator blocks. The polyethylene provides a conformal cavity for the Clamshell and fuel assembly to fall into during low-angle drops. The Clamshell is fastened to the lower Outerpack using shock absorbing rubber mounts. Polyethylene foam sheeting may be positioned between the Clamshell and lower Outerpack to augment the shock absorbing characteristics for transport. A weather gasket between the mating surfaces of the upper and lower Outerpack is used to mitigate water and debris from entering the package .

The Traveller VVER Outerpack is identical to the Traveller XL Outerpack except that the shock mounts on the Traveller VVER are slightly smaller and stiffer. The Traveller VVER Outerpack utilizes a bolted bracket for attachment to the Clamshell versus just a bolt for the Traveller XL. This change was needed because the sway space inside the Traveller VVER package is smaller than the Traveller XL package. The shock mount spacing positions are identical for the Traveller VVER and the Traveller XL Outerpacks.

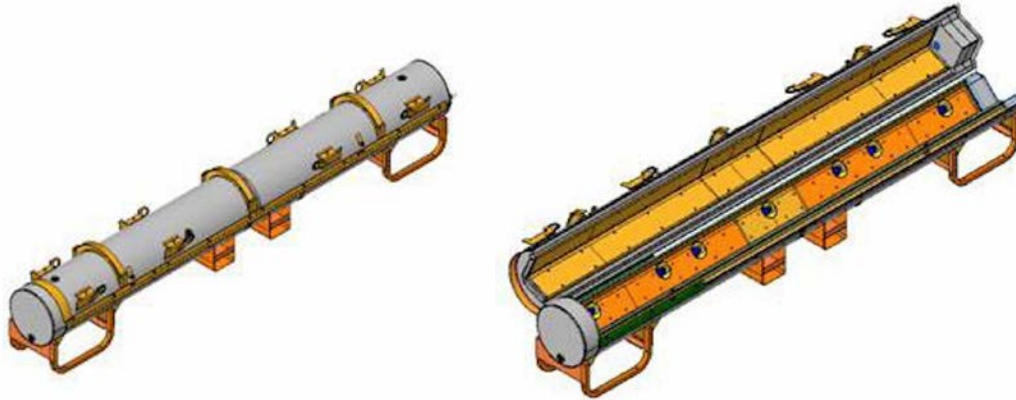


Figure 1-1 Outerpack Closed Position (left) and Opened Position (right)

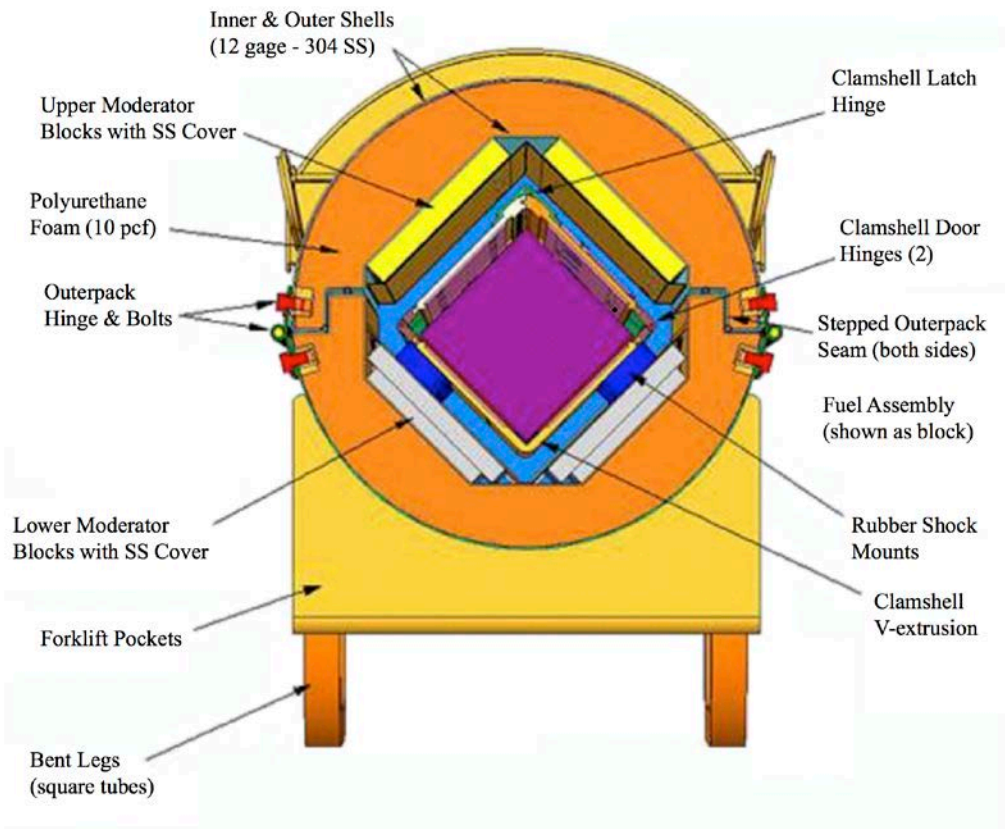


Figure 1-2 Outerpack and Clamshell Cross-Section View (typical)

1.2.1.5.2 Clamshell

The purpose of the Clamshell is to protect the contents during routine handling and to limit rearrangement of the contents in the event of a transport accident. During routine handling, the Clamshell main doors open to load the contents and are secured with multi-point cammed latches and hinge pins. The Clamshell protects and restrains the fuel assembly or Rod Pipe contents during all transport conditions. During accident transport conditions, the Clamshell remains closed and its structure limits rearrangement of the fuel assembly. Neutron absorber plates are installed on the inside surface of the Clamshell along the full length of each side.

There are two general types of Clamshells used: a typical, rectangular Clamshell and a hexagonal VVER Clamshell. The rectangular Clamshell is used in both the Traveller STD and XL packages as two slightly different Clamshell variants, with these differences between the STD and XL Clamshells described below. The hexagonal VVER Clamshell is used in the Traveller VVER package. Within this document, "Clamshell" will reference the commonly used rectangular Clamshell, while any use of the VVER Clamshell will be specifically referenced as such.

1.2.1.5.3 STD and XL Clamshell

The Clamshell structural components consist of an aluminum "V" base, two aluminum main doors, a small top "V" access door, bottom and top end plates, and multi-point cammed latch closure mechanisms. Piano type hinges (continuous hinges) connect each main door and the small top "V" access door to the "V" base. The BORAL neutron absorber plates are secured to the Clamshell with threaded fasteners and do not provide any structural strength to the Clamshell. The "V" base and bottom plate are lined with a cork rubber pad to cushion the contents and prevent damage during normal handling and routine transport conditions.

The top plate of the Clamshell has two configurations in order to accommodate different fuel types. Each uses a combination of flat head cap screws and tongue and groove joints in order to be fastened securely to the Clamshell. The Fixed Top Plate (FTP), shown in Figure 1-3, is secured directly to the top access door with cap screws. It has a tongue edge that fits into grooved shear bars that are attached directly to both faces of the Clamshell base with cap screws. The Removable Top Plate (RTP), shown in Figure 1-4, has grooved edges all around, and mates with shear bars that are fastened to all four faces of the Clamshell base. The bottom plate is secured to the Clamshell base with cap screws. Closure is provided by tongue and groove joining with the Clamshell doors.

Multi-point cammed latches that are spaced along the length of the Clamshell secure the main doors. These mechanical fasteners consist of a cam latch on the right main door that engages a keeper on the left main door. The cam latch is rotated a quarter-turn to engage the keeper as shown in Figure 1-5. A wave spring washer prevents inadvertent movement of the cam latch. There are nine (9) cam latches on the Traveller STD Clamshell and 11 cam latches on the Traveller XL Clamshell. The top access door is secured with a short hinge pin inserted into the hinge knuckles when the small top access door is closed.

Clamping mechanisms that interface with the contents provide axial and lateral restraint during all transport conditions. An adjustable, threaded rod-clamping device provides axial restraint at the top of the fuel assembly or Rod Pipe. The design of the top axial restraint components, as shown in Figure 1-6, Figure 1-7,

and Figure 1-8, depends on the Clamshell top plate configuration (FTP or RTP) and the fuel assembly type. An additional restraint may be added to secure non-fissile, non-radioactive reactor core components when shipped within the fuel assembly. Rubber pads are positioned at axial locations along the inside of the Clamshell doors to restrain lateral movement. These restraints, referred to as grid pads, are positioned to match the structural grid locations for each fuel assembly type.

Some fuel assemblies require an axial spacer to ensure proper axial fit into the Clamshell. The Clamshell is adapted axially for shorter fuel assemblies by adding an aluminum spacer component, as shown in Figure 1-9. The spacer is placed on the bottom end plate to elevate the fuel assembly in the longer Clamshell so it can be secured with the axial restraints at the top of the Clamshell. The larger cross-section dimension may be adapted for fuel assemblies with smaller cross sections by adding fuel spacer assemblies in the aluminum "V" base, as shown in Figure 1-10.

1.2.1.5.4 VVER Clamshell

The VVER Clamshell is similar in build to the standard Clamshell, however it has been designed for the transport of hexagonal fuel assemblies. A comparison of the two can be seen in Figure 1-11. The VVER Clamshell consists of an aluminum base and two aluminum main doors, bottom and top end plates, and similar multi-point cammed latch closure mechanisms as are used in the standard Clamshell. The VVER Clamshell also uses piano type hinges to connect each main door to the base, and neutron absorber plates are likewise installed on each lateral side of the VVER Clamshell using threaded fasteners. The base and bottom plate are also lined with a cork rubber pad to prevent damage during normal transport conditions.

The VVER Top Plate (VTP) also utilizes a combination of locking mechanisms and tongue and groove joints to fasten itself to the VVER Clamshell. As is shown in Figure 1-12, the VTP has a grooved tongue edge which slides into a shear lip that is directly fastened to the base of the VVER Clamshell. The top plate is then secured to the shear lip by a pair of quarter-turn locking knobs, see Figure 1-13. A wave spring under each knob prevents them from inadvertently rotating. The bottom plate is secured to the Clamshell with cap screws, and closure is provided by a tongue and groove joining with the VVER Clamshell doors.

The main doors of the VVER Clamshell operate in the same manner as the standard Clamshell, and are secured with identical locking mechanisms, see Figure 1-14. There are nine (9) cam latches on the VVER Clamshell.

Lateral and axial clamping mechanisms exist to provide restraint for the contents during all transport conditions. A circular clamping plate secured by a friction roll pin or a welded nut provides axial restraint at the top of the fuel assembly, shown in Figure 1-15. This clamping plate is adjustable by using the center clamp plate stud installed on the VTP, which lowers the clamp until it contacts the fuel assembly. This is similar in operation to the axial restraint, shown in Figure 1-7. A jam nut is used to keep the stud from turning during shipment. Rubber grid pads are positioned at axial locations along the inside of the VVER Clamshell doors to restrain lateral movement. Similar to the standard Clamshell, these grid pads are positioned to match the structural grid locations for each assembly type.

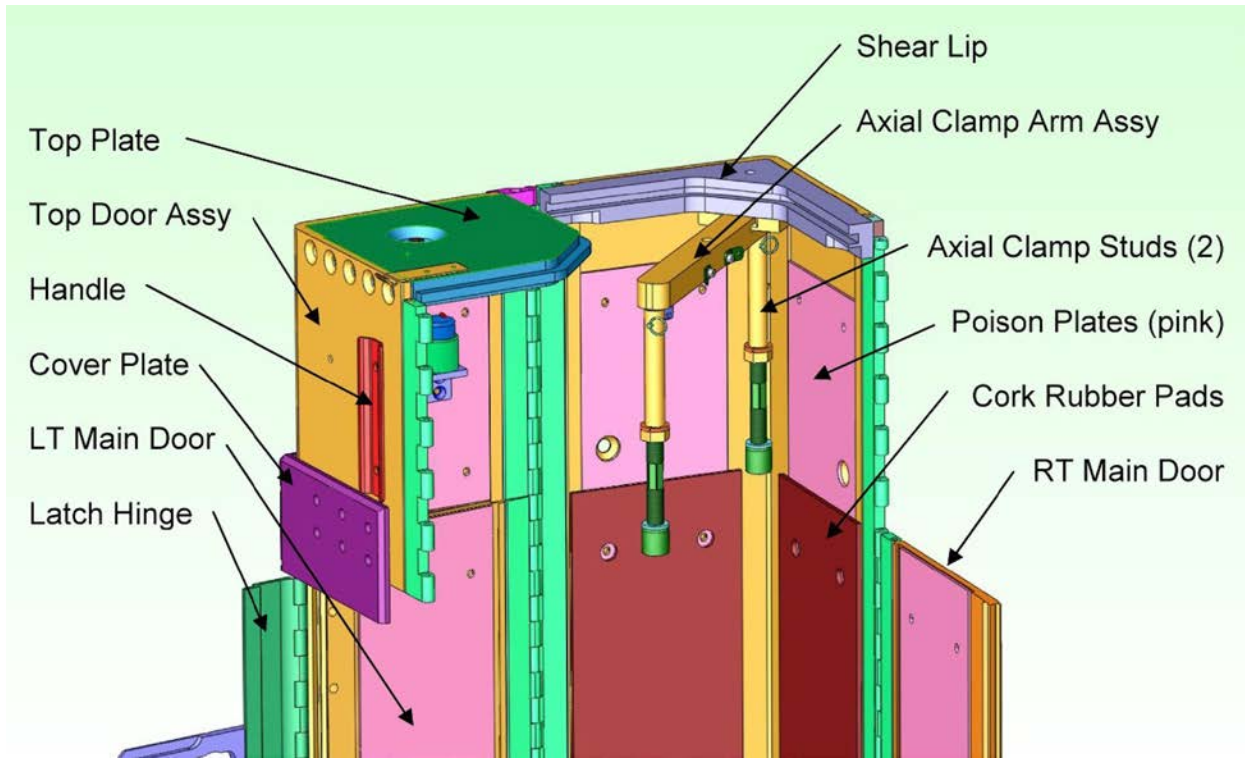


Figure 1-3 Clamshell with Fixed Top Plate (FTP)

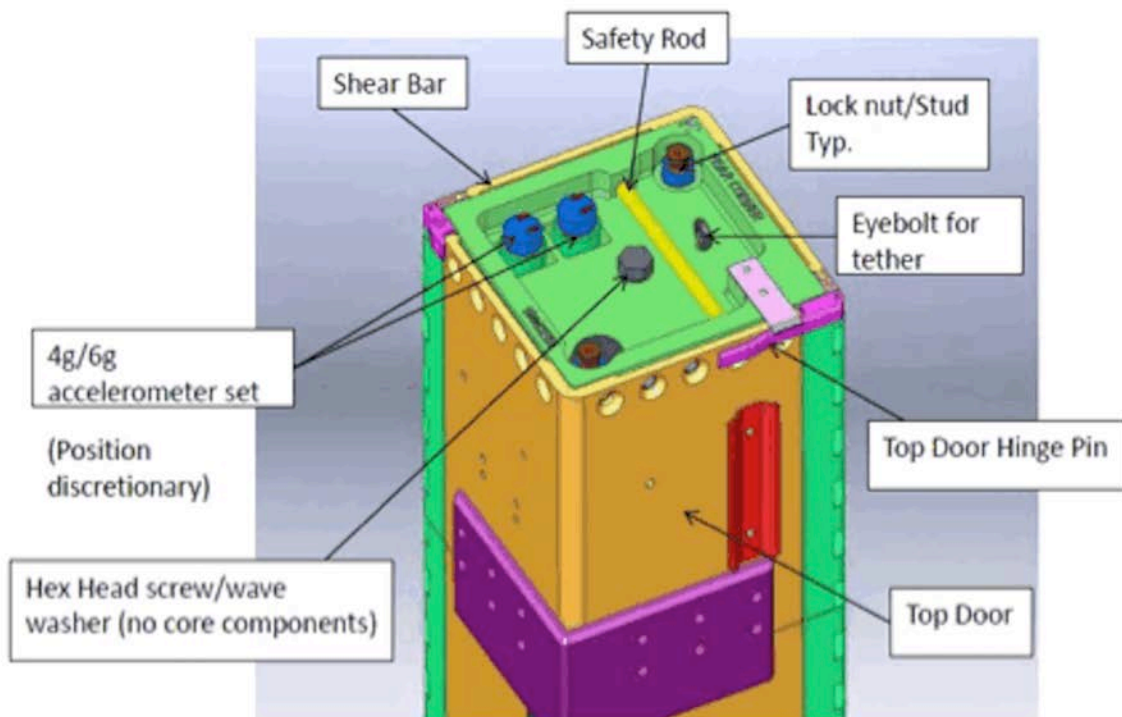


Figure 1-4 Clamshell with Removable Top Plate (RTP)

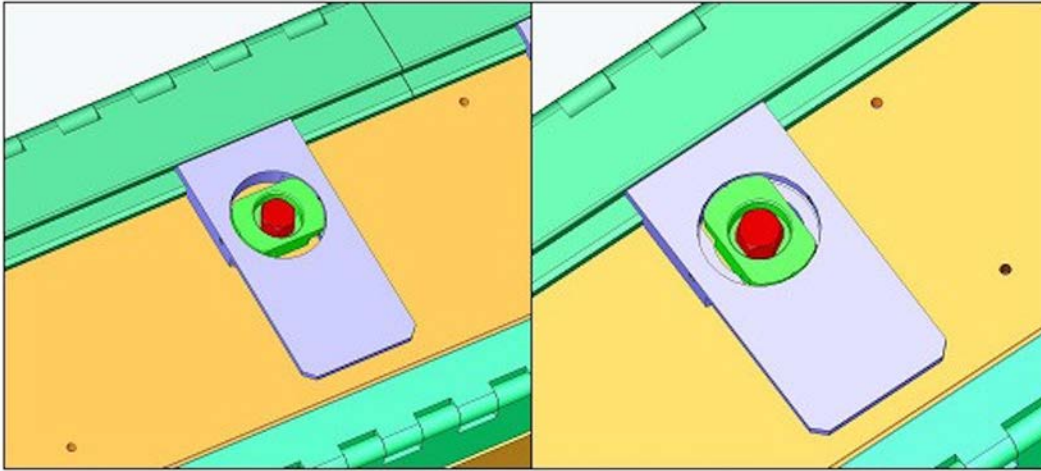
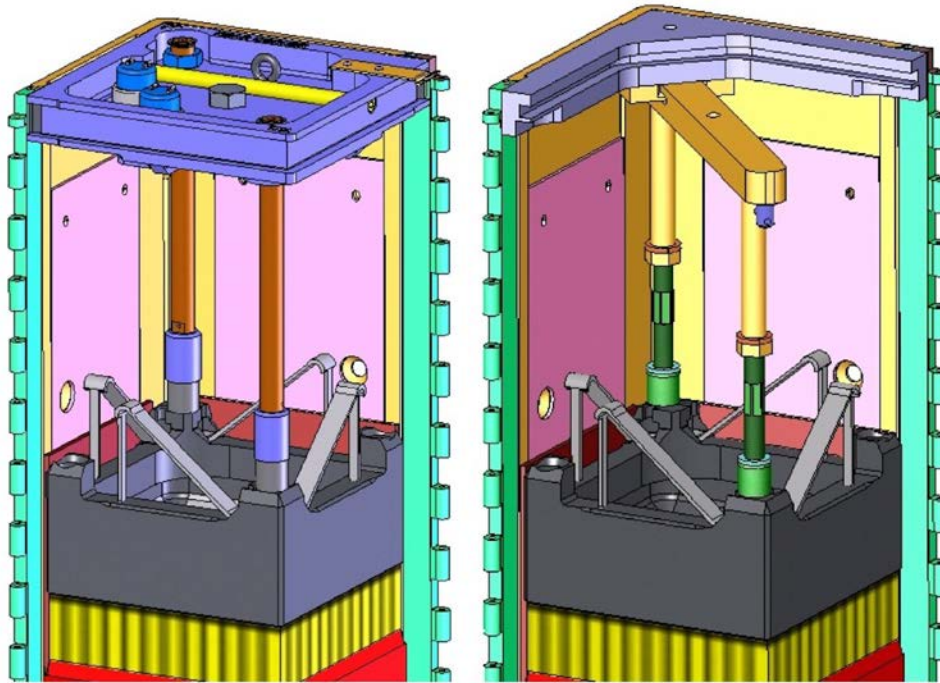
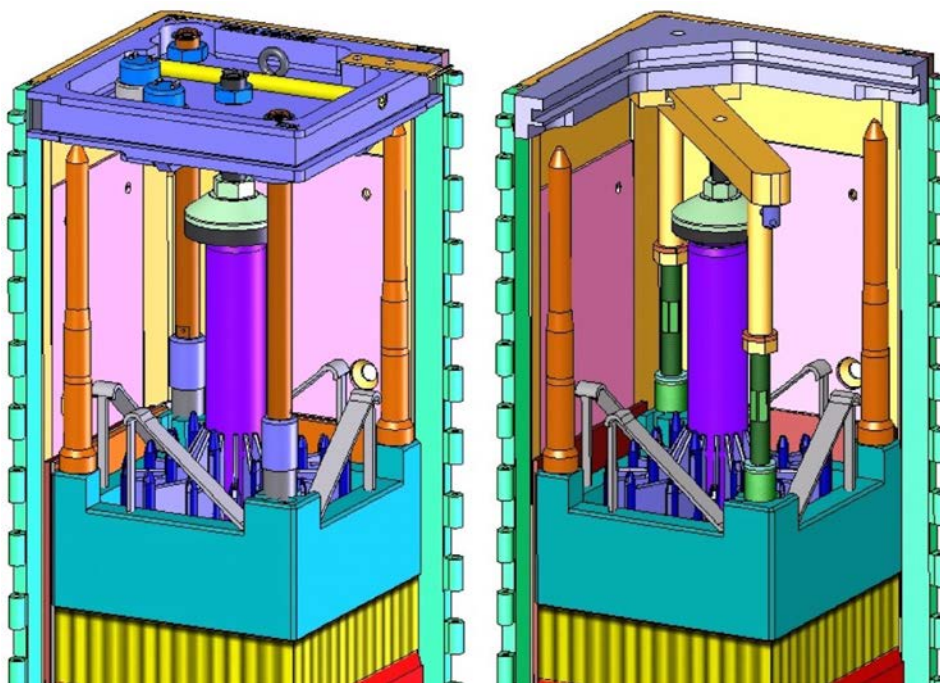


Figure 1-5 Clamshell Latch Locked Position (left) and Open Position (right)



Fuel Assembly



Fuel Assembly with Reactor Core Component

Figure 1-6 Corner Post Axial Restraint – Removable Top Plate (left), Fixed Top Plate (right)

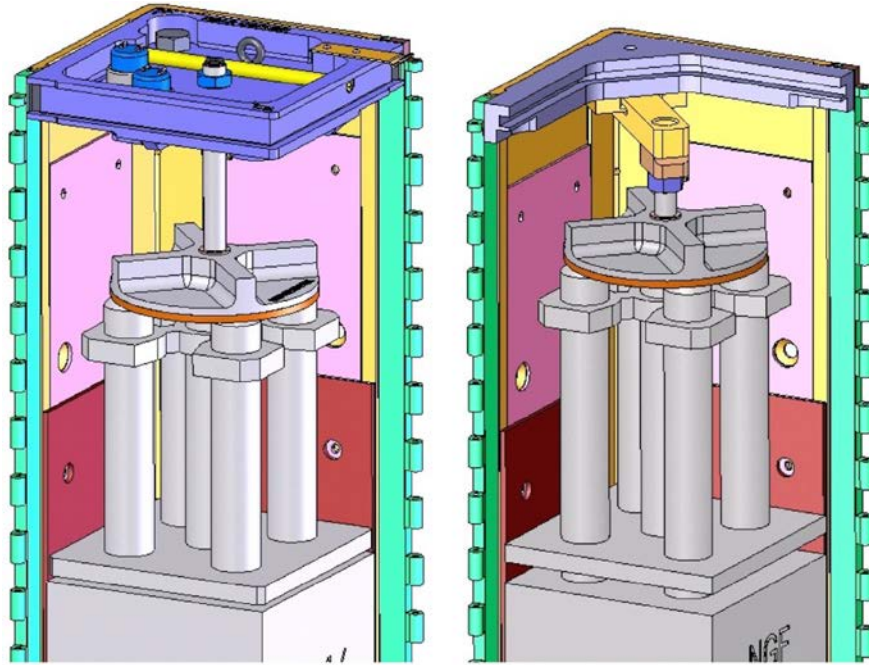


Figure 1-7 Center Plate Axial Restraint – Removable Top Plate (left), Fixed Top Plate (right)

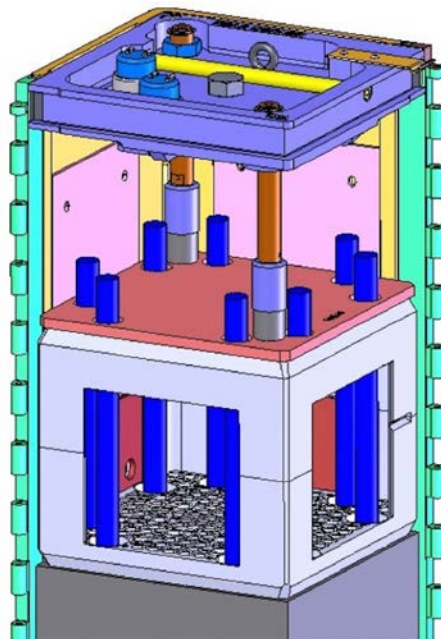


Figure 1-8 Corner Post Axial Restraint

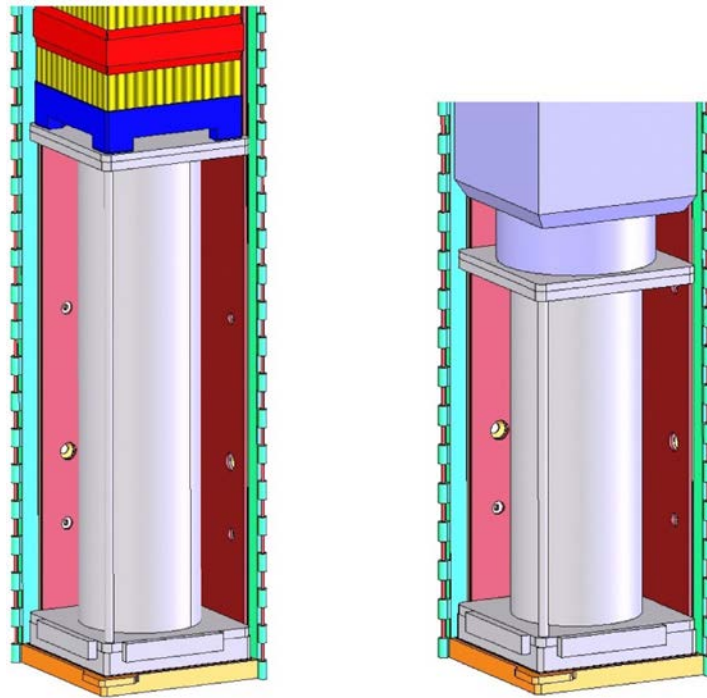


Figure 1-9 Axial Spacer Assembly (length depends on fuel assembly type)

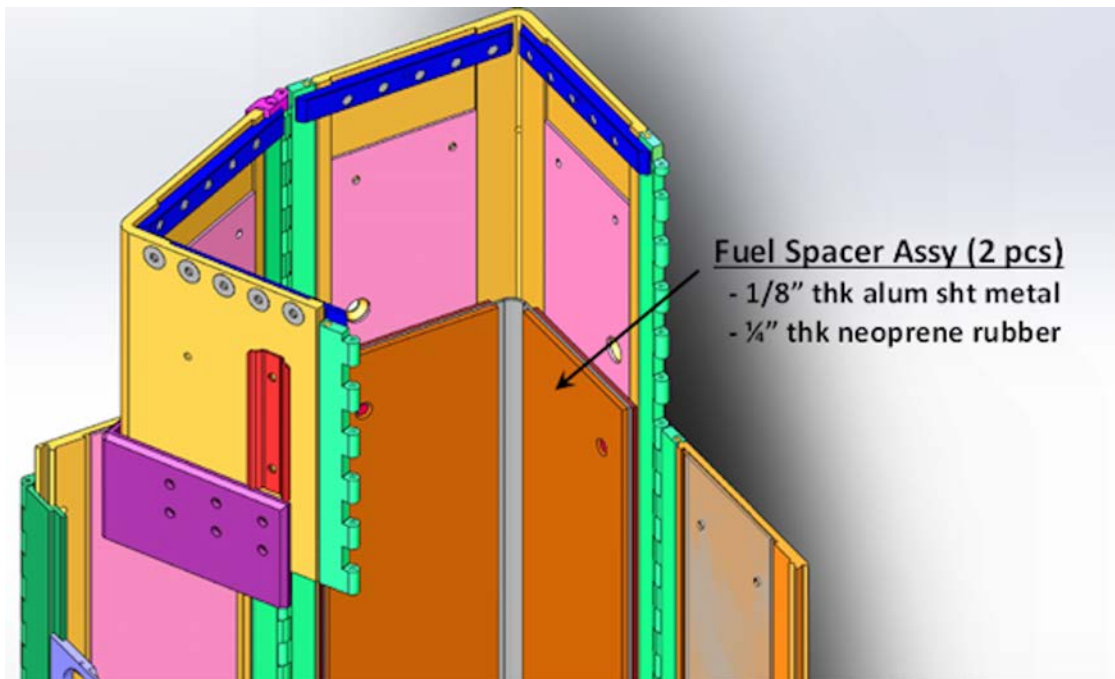


Figure 1-10 XL Clamshell Fuel Spacer Assembly

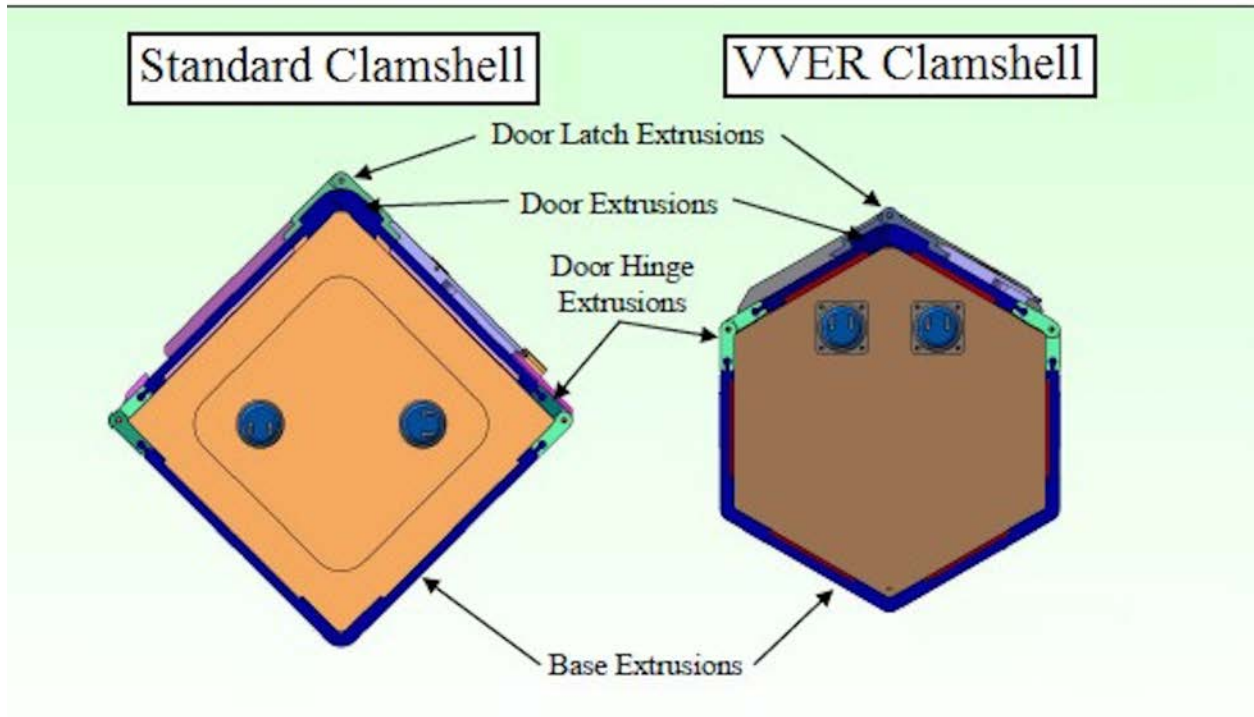


Figure 1-11 Comparison of Standard Clamshell to VVER Clamshell

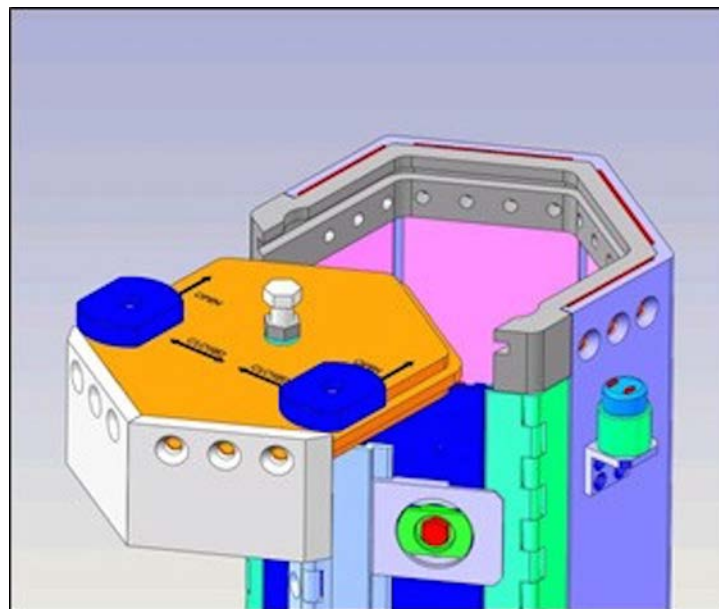


Figure 1-12 VVER Clamshell with VVER Top Plate (VTP)

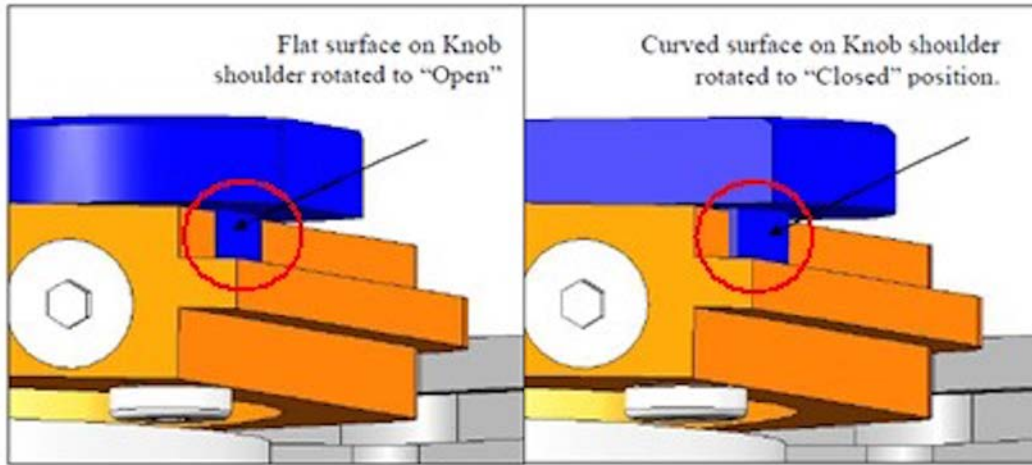


Figure 1-13 VTP Locking Mechanism

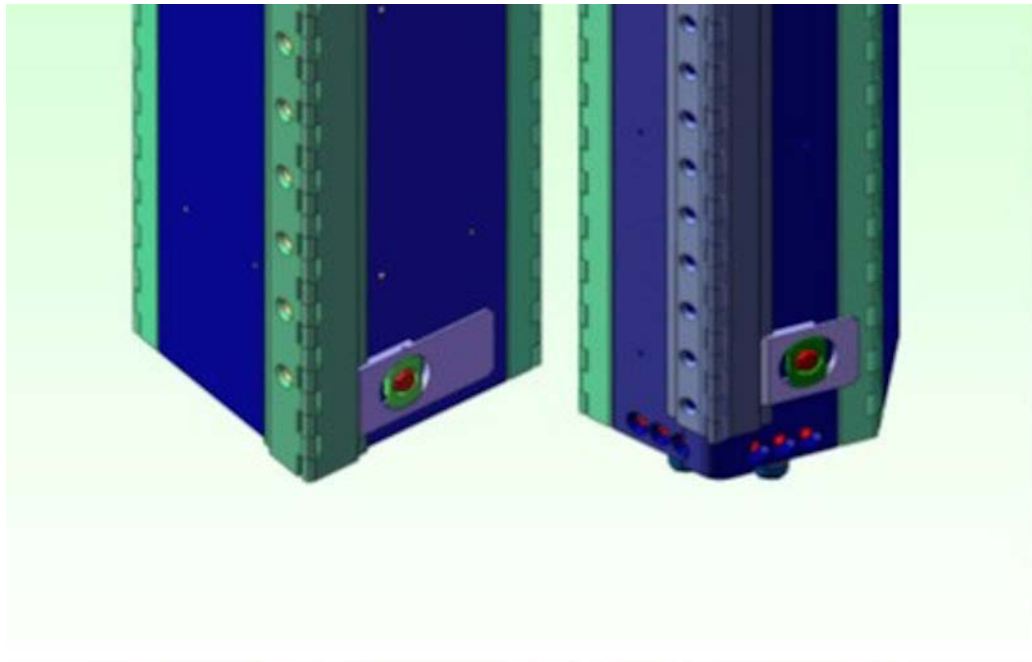


Figure 1-14 Comparison of Clamshell Door Hinges and Latches

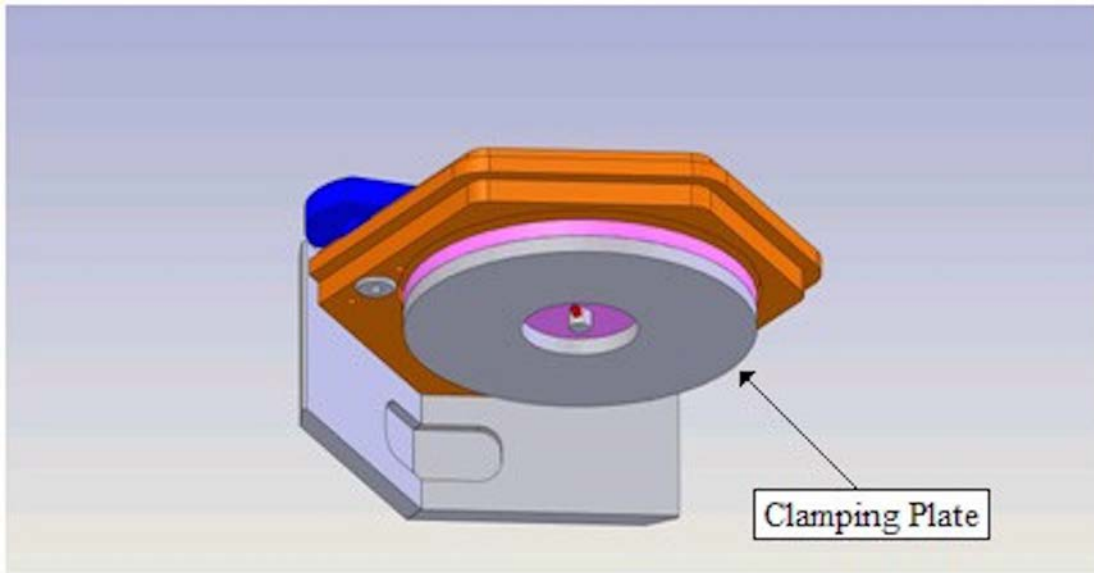


Figure 1-15 Axial Clamp as Installed on VTP

1.2.1.5.5 Rod Pipe

The Traveller is designed to carry loose fuel rods using the Rod Ripe shown in Figure 1-16. The Rod Pipe consists of a 6 in. (15.2 cm) 304 stainless steel, Schedule 40 pipe with 304 stainless steel closures at each end. The end closures are a 0.25 in. (6.35 mm) thick cover secured to a flange fabricated from 0.25 in. (6.35 mm) thick plate.

The Rod Ripe is held in place inside the Clamshell with positive restraining devices. The axial clamp assembly provides axial restraint for the Traveller XL. The axial clamp arm is bolted into the top shear lip and contacts the Rod Pipe by means of an adjustable jackscrew. For Traveller STD, the Clamshell top plate provides the axial restraint, and contact between the Clamshell top plate and the Rod Pipe is achieved by means of a conformal shipping spacer. Lateral and vertical restraint is accomplished through the use of removable rubber pads located inside the Clamshell door lip in conjunction with the latch assemblies on the Clamshell doors. The rubber pads are of varying thickness to accommodate the Rod Pipe in the Traveller variants. The Rod Pipe design has a maximum loaded weight of 1650 lb. (748 kg).

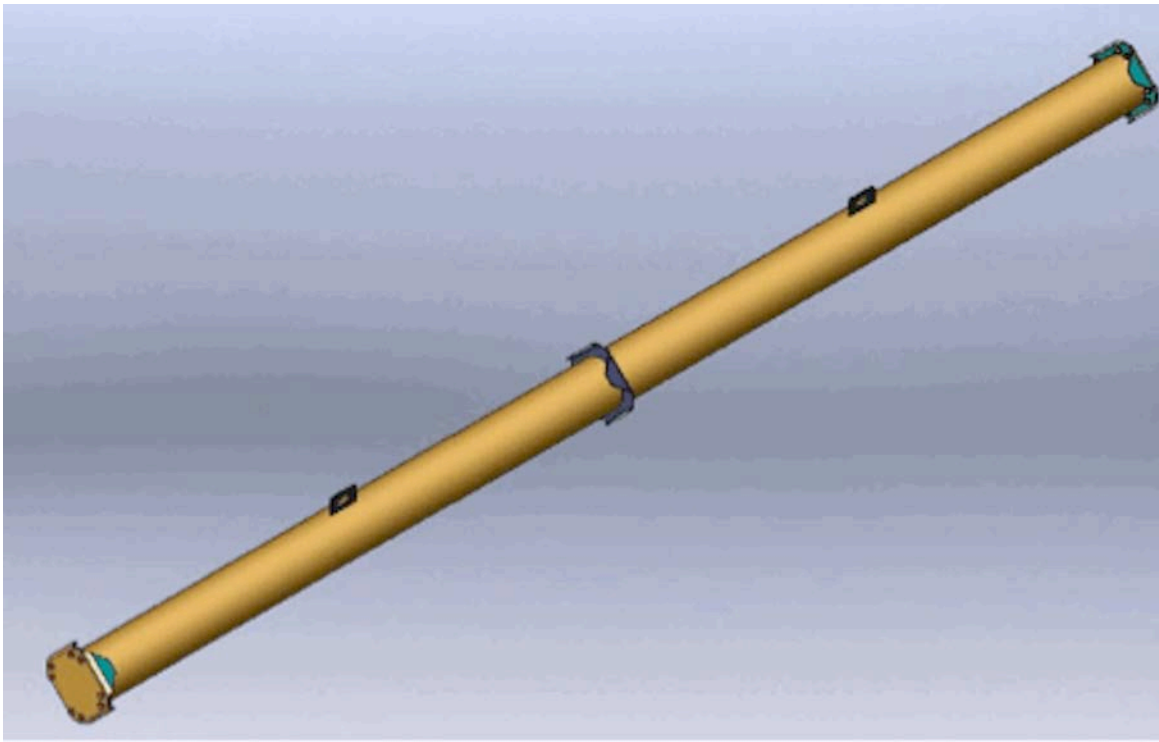


Figure 1-16 Rod Pipe

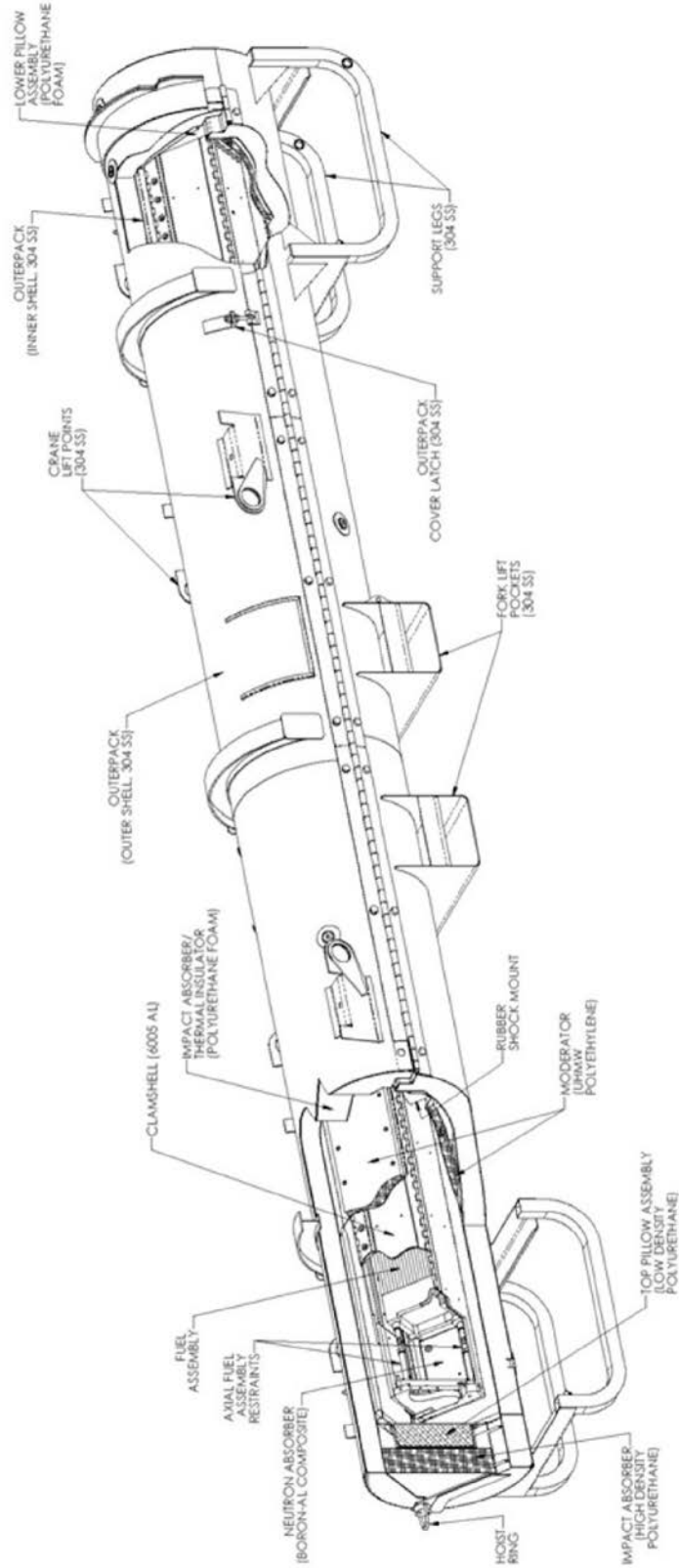


Figure 1-17 Generic Sketch of the Traveller Representing the Package as Prepared for Transport

1.2.2 Contents

1.2.2.1 Type and Form

The contents consist of either a single PWR fuel assembly or loose fuel rods. Fissile material is in the form of ^{235}U . For Uranium dioxide (UO_2) contents, fuel assemblies are limited to an enrichment of 5 wt.% ^{235}U and loose fuel rods are limited to an enrichment of 7 wt.% ^{235}U . For uranium silicide (U_3Si_2) contents, loose fuel rods are limited to an enrichment of 7 wt.% ^{235}U . Additionally, UO_2 contents in the form of loose fuel rods or fuel assemblies under PWR Group 1 or Group 2 may be Advanced Doped Pellet Technology (ADOPT™) rods, doped with up to 700 ppm Cr_2O_3 and up to 200 ppm Al_2O_3 . A single fuel assembly or a single Rod Pipe is transported in a package.

Any number of loose UO_2 fuel rods or 60 loose U_3Si_2 fuel rods may be transported in a Rod Pipe at a time. Fuel rods in the Rod Pipe include designs for both PWR and BWR. For the range of fuel rod diameters (≥ 0.308 in. (0.7823 cm)), the theoretical maximum number of fuel rods that can fit inside the Rod Pipe is ~250 fuel rods. The physical number of fuel rods placed in the Rod Pipe is less than the theoretical maximum value as some space is required to accommodate the packing materials and allow for the handling of fuel rods.

The PWR fuel assembly may be transported with non-fissile, non-radioactive reactor core components, as discussed in Section 1.2.2.1.3. In addition, a solid stainless steel rod may replace any of the fuel rods in a fuel assembly. The maximum contents weight for the three Traveller variants is:

- Traveller STD: 1,650 lb (748 kg)
- Traveller XL: 1,971 lb (894 kg)
- Traveller VVER: 1,850 lb (839 kg)

1.2.2.1.1 Fuel Rods

Uranium dioxide (UO_2) or uranium silicide (U_3Si_2) pellets are inserted into a zirconium alloy tube and welded-on end plugs seal each end of the tube, which together forms a fuel rod. The pellets are prevented from shifting during handling and shipment by a compression spring located between the top of the fuel pellet stack and the top end plug. See Section 6.2.4 for the limitations and requirements for fuel rod shipments in the Rod Pipe.

The fuel rod is designed as a pressure vessel, which significantly reduces the number and extent of cyclic stresses experienced by the cladding. The result is a marked extension of the fatigue life margin of cladding with enhanced cladding reliability. The rods are pressurized with helium and end plugs are welded to the rod, which effectively seals and contains the radioactive material. A representative nominal internal pressure of fuel rods at room temperature conditions is 380 psig (2.62 MPa gauge). There is no pressure relief device that would allow radioactive contents to escape. Cladding may include a chromium coating of 25 μm thick, nominally or include an Optimized ZIRLO Liner (OZL), per Section 2.12.9.

The ASME Boiler and Pressure Vessel Code, Section III, is used as a guide in the mechanical design and stress analysis of the fuel rod. The rod is designed to withstand the applied loads, both external and internal. Welds of the fuel rods are verified for integrity by non-destructive methods, such as radiographic or

ultrasonic testing, and process controls. As the containment boundary is welded closed, it cannot be opened unintentionally.

1.2.2.1.2 Fuel Assembly

A fuel assembly is a square or hexagonal array of fuel rods of UO₂ pellets in zirconium alloy tubes that are structurally bound together in a skeleton, which consists of thimble tubes, grids, a top nozzle, a bottom nozzle, and other hardware (i.e., springs, nuts, etc.). A reactor core component may be inserted into the fuel assembly and is fastened to the top and bottom nozzles of the assembly. Grid assemblies are mechanically fastened to the guide thimbles along the height of the fuel assembly to provide support for the fuel rods. The fuel rods are contained and supported, and the rod-to-rod centerline spacing is maintained, within the skeletal framework. See Section 6.2 for the limitations and requirements for fuel assembly contents in the Traveller variants.

1.2.2.1.3 Non-Fissile, Non-Radioactive Reactor Core Components

Reactor core components that may be shipped with the radioactive/fissile contents of the Traveller are non-fissile, non-radioactive components that have specific functions within a reactor core but have no primary function in a transport scenario. As a result, these components are not represented in transport analyses and no credit is taken for their presence in transport evaluations. Reactor core components include various types of rod control assemblies, base plate-mounted core components, spider-body core components, burnable absorbers, and secondary neutron sources.

A reactor core component is fitted into the guide/instrument tube locations of a fuel assembly. The core component may function as a flux suppressant, flow by-pass, or as a neutron absorber during reactor operation and does not alter the design of the fuel assembly. As such, it is not evaluated in the package criticality safety analysis because its function as a neutron absorber decreases the reactivity of the system.

Various components may include integral absorbers/poisons including, but not limited to, gadolinium, boron, erbium, and hafnium. For example, aluminum oxide-boron carbide burnable absorber or gadolinium oxides material may be integrated in the fuel assembly in order to provide additional reactivity control during reactor operation. This material depletes during the reactor cycle in the same manner as ²³⁵U. Fuel assembly integral burnable absorbers are not credited in the criticality safety analysis of Section 6 because its function as a neutron absorber decreases the reactivity of the system.

Startup neutron sources are typically of two types: 1) primary sources and 2) secondary sources. Primary sources are not an acceptable content for the Traveller package. Secondary sources are an acceptable content for the Traveller package. Secondary sources typically contain a mixture of antimony and beryllium (Sb-Be), and are used for restart of the reactor, which require in-core neutron activation to become a source.

1.2.2.2 Maximum Quantity of Material per Package

The maximum quantity of radioisotopes in the contents of the package is limited to the quantity contained in a single fuel assembly or in the maximum number of fuel rods that can be transported in the Rod Pipe. The only fissile material is low-enriched uranium that is less than or equal to 5 wt.% ²³⁵U for fuel assemblies and U₃Si₂ loose fuel rods or a maximum enrichment of 7.0 wt.% for UO₂ loose fuel rods. The maximum quantity

of fissile material is approximately 32 kg of ²³⁵U for the largest fuel assembly. The fuel pellets adhere to the isotopic content specified by ASTM C 753 [3], which is equivalent to enriched commercial grade uranium, as defined in ASTM C 996 [4] and summarized in Table 1-2. Table 1-2 is applicable to both UO₂ and U₃Si₂ fuel rods.

In the Rod Pipe configuration, individual fuel rods are wrapped in a protective polyethylene sleeve. When the Rod Pipe is filled with a desired number of rods, a plastic disc is inserted to protect the ends of the fuel rods. The space between the plastic disc and the Rod Pipe is filled with packing materials, such as “bubble wrap”, so that the rods are secured axially. Fuel assemblies are also wrapped in a protective polyethylene sleeve.

Content	Enriched Commercial Grade ¹
²³² U	0.0001 µg/gU
²³⁴ U	11.0 × 10 ³ µg/g ²³⁵ U
²³⁶ U	250 µg/gU
⁹⁹ Tc	0.01 µg/gU
Alpha Activity from Np and Pu ²	Expected to be below the detection limits of commonly used measurement methodology
Total Gamma Activity from Fission Products ²	Expected to be below the detection limits of the measurement methodology

NOTE: ¹ as defined in ASTM C 996 [4]. ² Plutonium and fission products are not allowed in the Traveller packages.

For contents to be acceptable for shipment in the Traveller package, the requirements of (a) or (b) shall be met:

- a. The uranium content meets the “unirradiated uranium” definition of SSR-6 para. 527 [1] and 10 CFR 71.4 [2]:

Unirradiated uranium means uranium containing not more than 2 x 10³ Bq of plutonium per gram of uranium-235, not more than 9 x 10⁶ Bq of fission products per gram of uranium-235, and not more than 5 x 10⁻³ g of uranium-236 per gram of uranium-235.
- b. If the ²³⁶U requirement of the unirradiated definition is not met, the content may still be shipped if the following criteria are met:
 - 1) The contents meet the requirements of the Enriched Commercial Grade specification of ASTM C 996 [4], specifically the ²³⁶U limit (250 µg²³⁶U/gU), as outlined in Table 1-2.
 - 2) There is less than a Type A quantity of material in the content.
 - For an A₂ calculation, the *U (enriched to 20% or less) - Unlimited* value may not be used.
 - The A₂ calculation must be completed using the A₂ values in 10 CFR 71 Appendix A Table A-1 for the individual isotopes in the fuel content, using the “slow lung absorption” values for uranium isotopes (i.e. for a UO₂ or U₃Si₂ compound).

Packing materials that have a moderating effectiveness greater than water, such as polyethylene sleeves and dunnage used to protect the fuel assembly or fuel rod contents during transport, are limited as follows:

- Such hydrogen-dense packing materials must have a moderating effectiveness which is less than or equal to a hydrogen density of 0.1325 g/cm³;

- For PWR fuel assemblies, packing material is limited to a maximum of 2.0 kg per package in the Clamshell;
- For loose fuel rods, packing material is unlimited inside the Rod Pipe.

1.2.3 Special Requirements for Plutonium

Plutonium will not be shipped in the Traveller Type A packages; therefore, this section is not applicable to the Traveller Type A.

1.2.4 Operational Features

Forklift pockets and tubular legs are attached to the bottom half of the Outerpack. Stacking brackets, which double as lift points, are attached to the top half of the Outerpack and are located in eight (8) locations. The package must be up-righted on one end for loading and unloading of contents. Two lifting points are attached to the top half of the Outerpack. Section 7 further describes the operation of the Traveller packages. A generic sketch of the Traveller representing the package as prepared for transport is provided in Figure 1-17.

1.3 APPENDICES

1.3.1 References

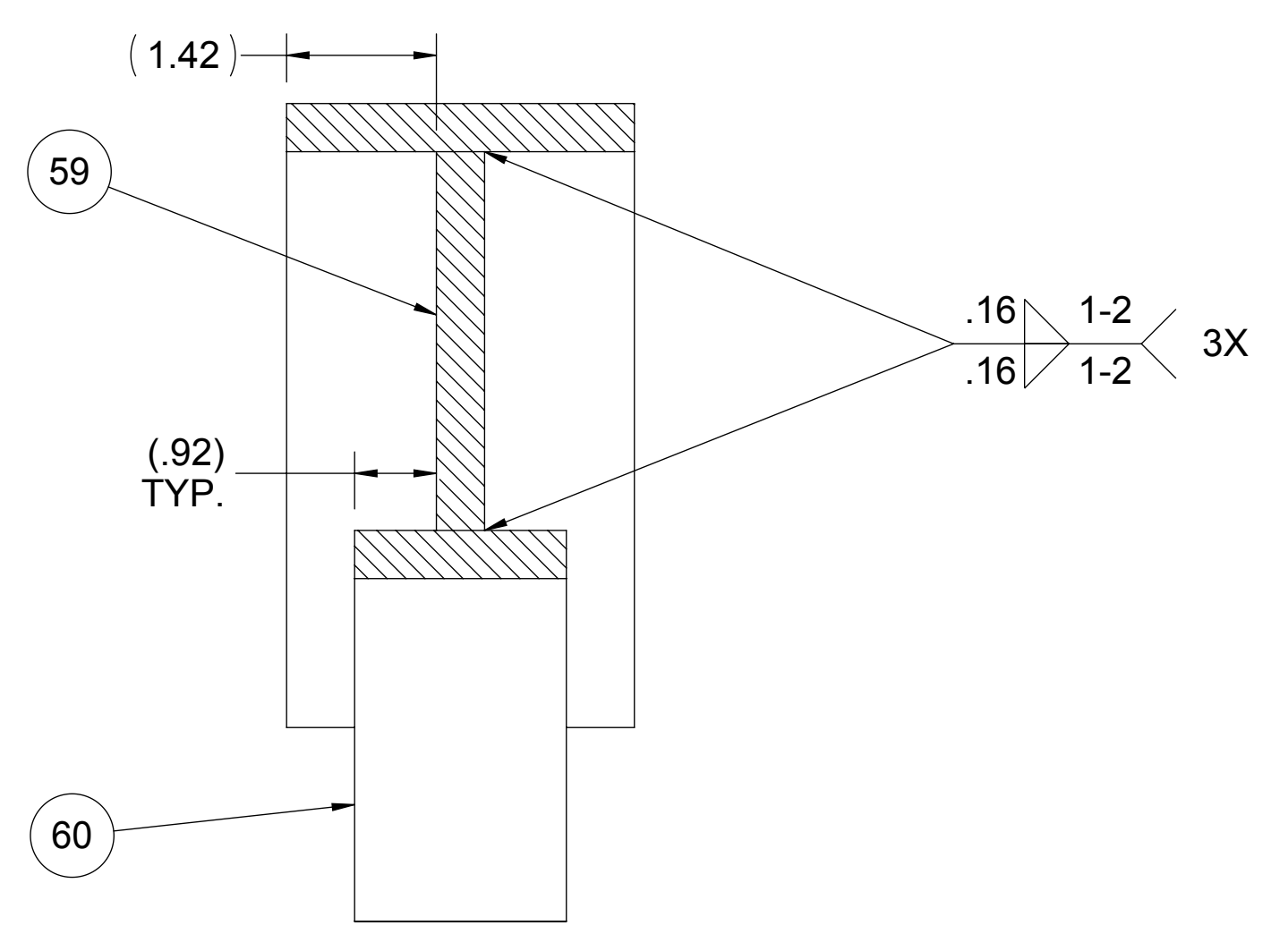
- [1] International Atomic Energy Agency, "Regulations for the Safe Transport of Radioactive Material," 2012.
- [2] U.S. Nuclear Regulatory Commission Code of Federal Regulations, Title 10 Part 71, "Packaging and Transport of Radioactive Material," 2016.
- [3] American Society for Testing and Materials, "Standard Specification for Nuclear-Grade, Sinterable Uranium Dioxide Powder," 2009.
- [4] American Society for Testing and Materials, "Standard Specification for Uranium Hexafluoride Enriched to Less Than 5% 235U," 2015.

1.3.2 Licensing Drawings for Packaging

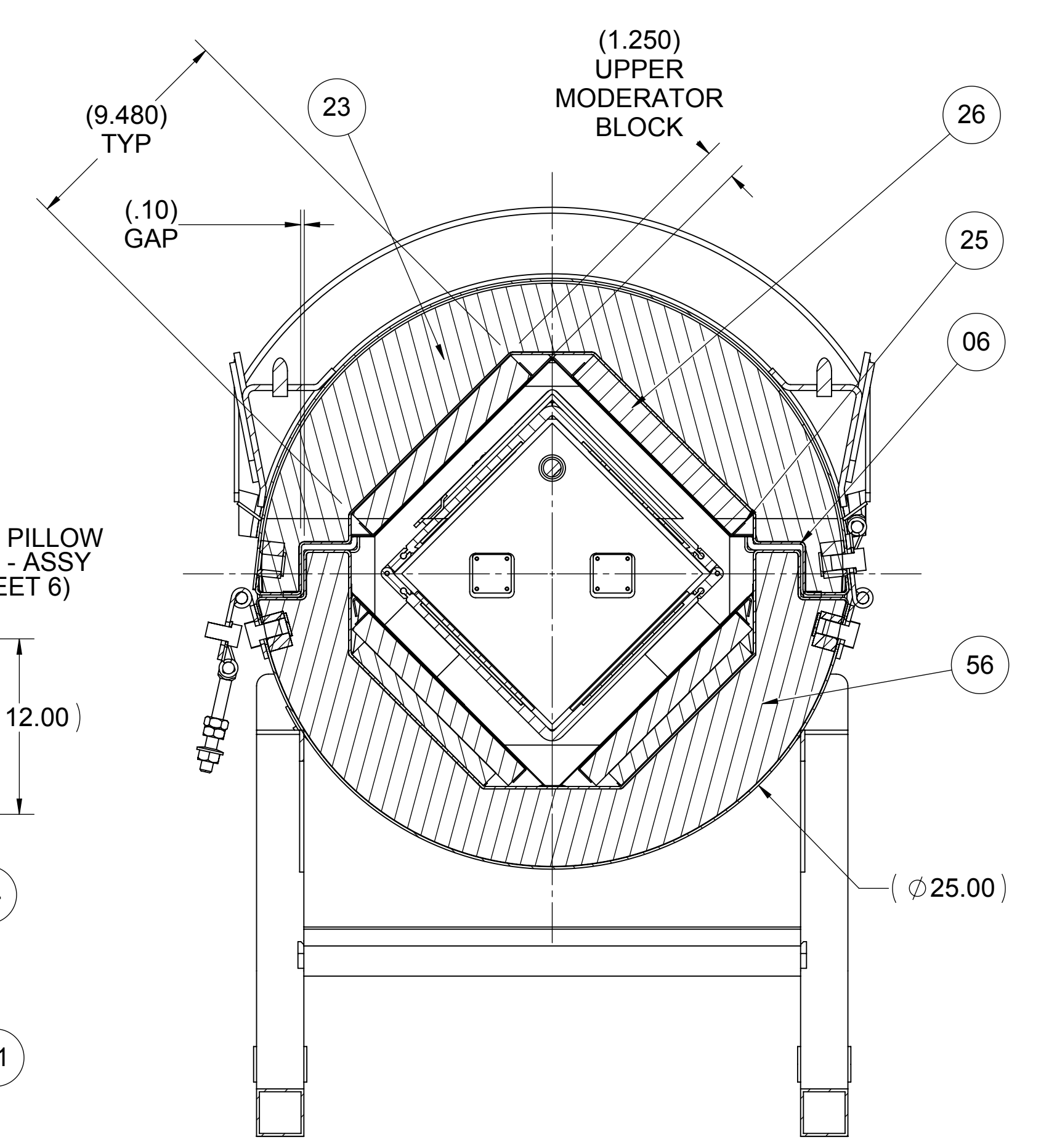
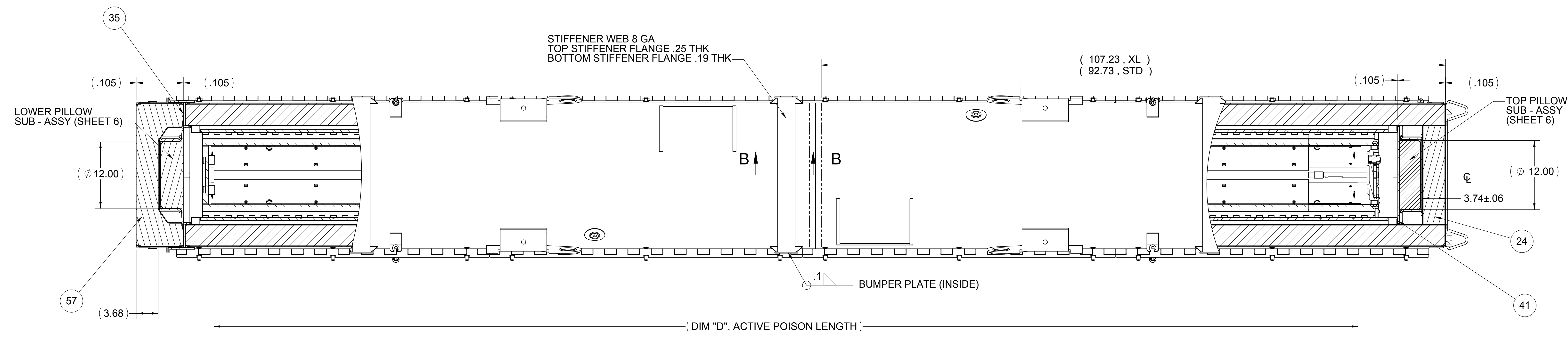
Traveller Type A Design (RTP and FTP) – Licensing Drawings
10004E58, Rev. 9 (Sheets 1-9)

Traveller Type A VVER Design (RTP and FTP) – Licensing Drawings
10037E43, Rev. 3 (Sheets 1-8)

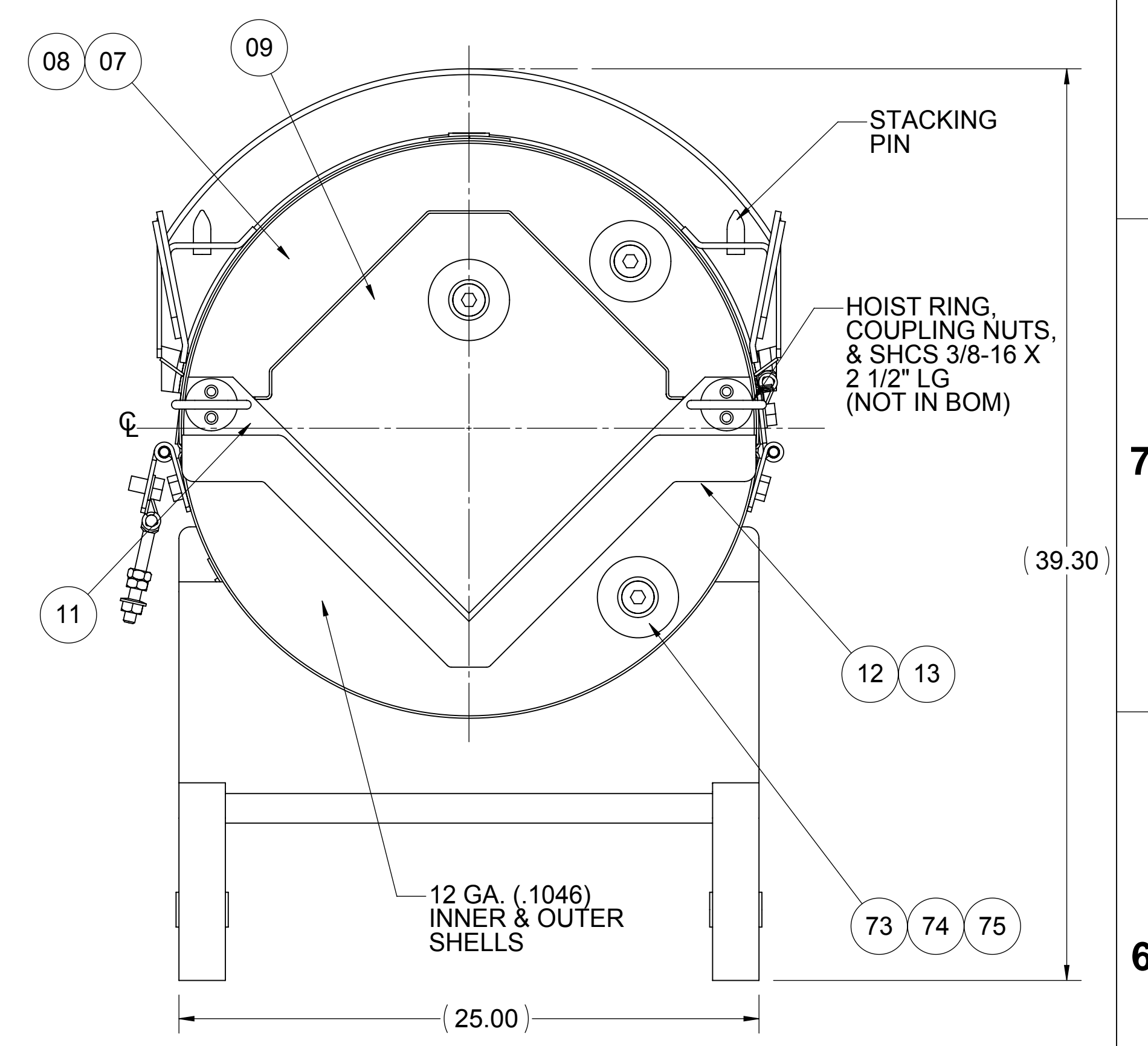
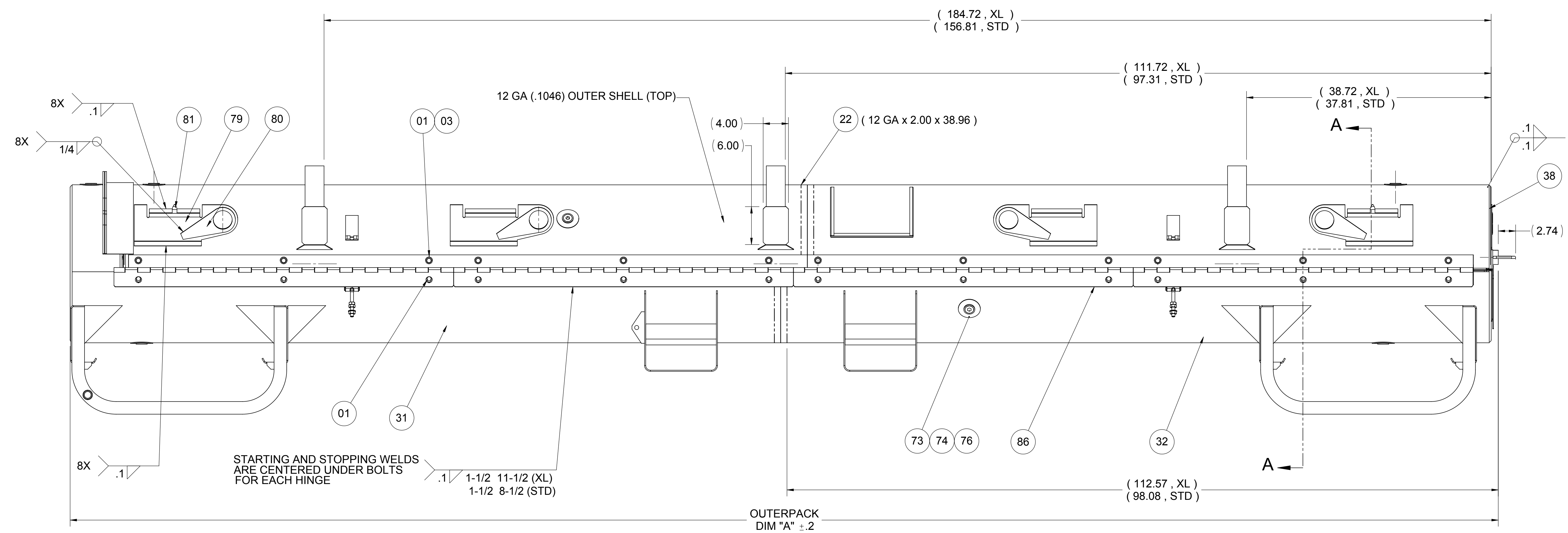
Rod Pipe – Licensing Drawing
10006E58, Rev. 6



SECTION B-B



SECTION A-A
SCALE 1:5



SCALE 1:5

SO 752255	ECN 61148-0	DESCRIPTION
ZONE DC	DESCRIPTION	PKGSUPPORT
ECN 0002409-0	DESCRIPTION	ZONE DC
CD	DIM (2.74) WAS 2.739	
DWN BY: C. GIBBS	2015/07/06	USPKGSUPPORT
ECN 0002789-0	DESCRIPTION	ZONE DC
CD	SEE SHEET 1 FOR CHANGES	
DWN BY: C. GIBBS	2013/08/19	BUD12879
ECN 0003155-0	DESCRIPTION	ZONE DC
CD	SEE SHEET 1 FOR CHANGES	
DWN BY: C. GIBBS	2015/09/22	

SEE PRODUCT SPECIFICATION PDINF000 FOR SUPPLEMENTAL PRODUCT INFORMATION
DIMENSIONS ARE IN INCHES

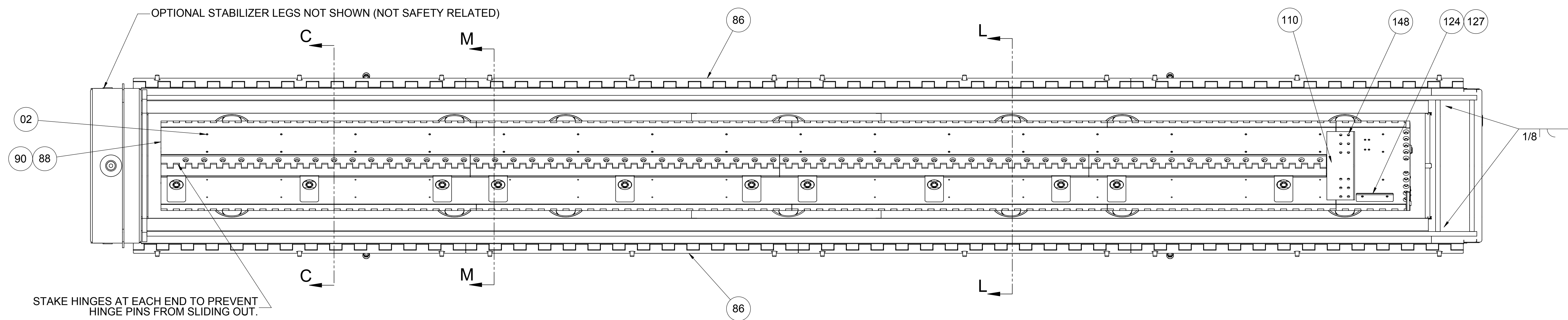
DATE	DESCRIPTION	BY	CHKD
DESIGN			
MFG ENG			
PA ENG			
DESIGN MGR			
APPROV			
SCALE	1:8	WEIGHT	

Westinghouse ELECTRIC COMPANY LLC - NUCLEAR FUEL COLUMBIA, SC USA

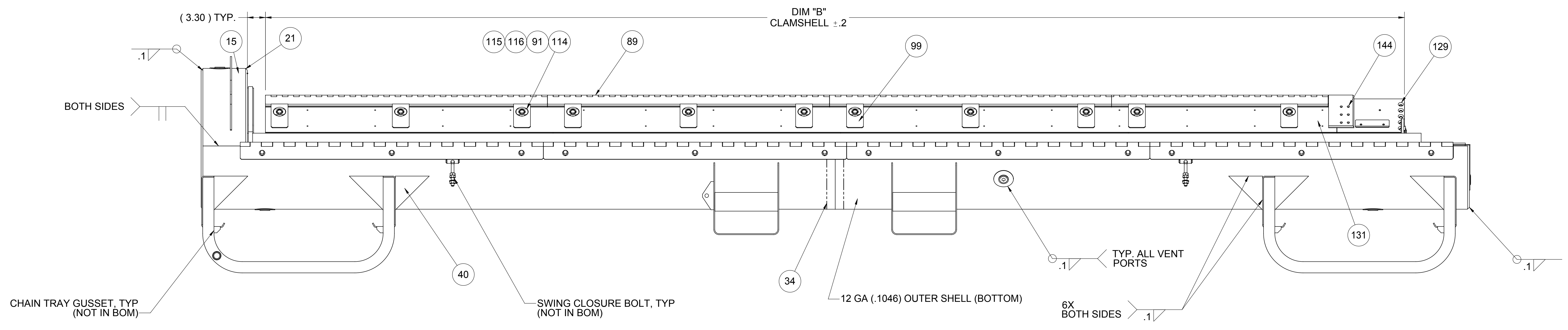
SAFETY RELATED ITEMS TRAVELLER XL & STD

TRCH NO: 9 DWG NO: 10004E58

SCALE: 1:8 SHEET 2 OF 9



© K 9F C I H P F D 5 7 ? 5 G G 9 A 6 @ M
 17 @ 5 A G < 9 @ @ B G F 5 @ 9 8 L
 SEE SHEET 4 FOR SECTION VIEWS



SO	752255		
ECN	61148-0		
ZNE	OC	DESCRIPTION	
PKGSUPPORT	ECN	0002409-0	
ZNE	OC	DESCRIPTION	
C3		EDITED WELD SYMBOL	
DWN BY	C. GIBBS	2015/09/22	
USPKGSUPPORT	ECN	0002789-0	
ZNE	OC	DESCRIPTION	
		SEE SHEET 1 FOR CHANGES	
DWN BY	C. GIBBS	2013/08/19	
BUD	128779		
ECN	0003155-0		
ZNE	OC	DESCRIPTION	
		SEE SHEET 1 FOR CHANGES	
DWN BY	C. GIBBS	2015/09/22	

SEE PRODUCT SPECIFICATION PDINFD00 FOR SUPPLEMENTAL PRODUCT INFORMATION

DIMENSIONS ARE IN INCHES

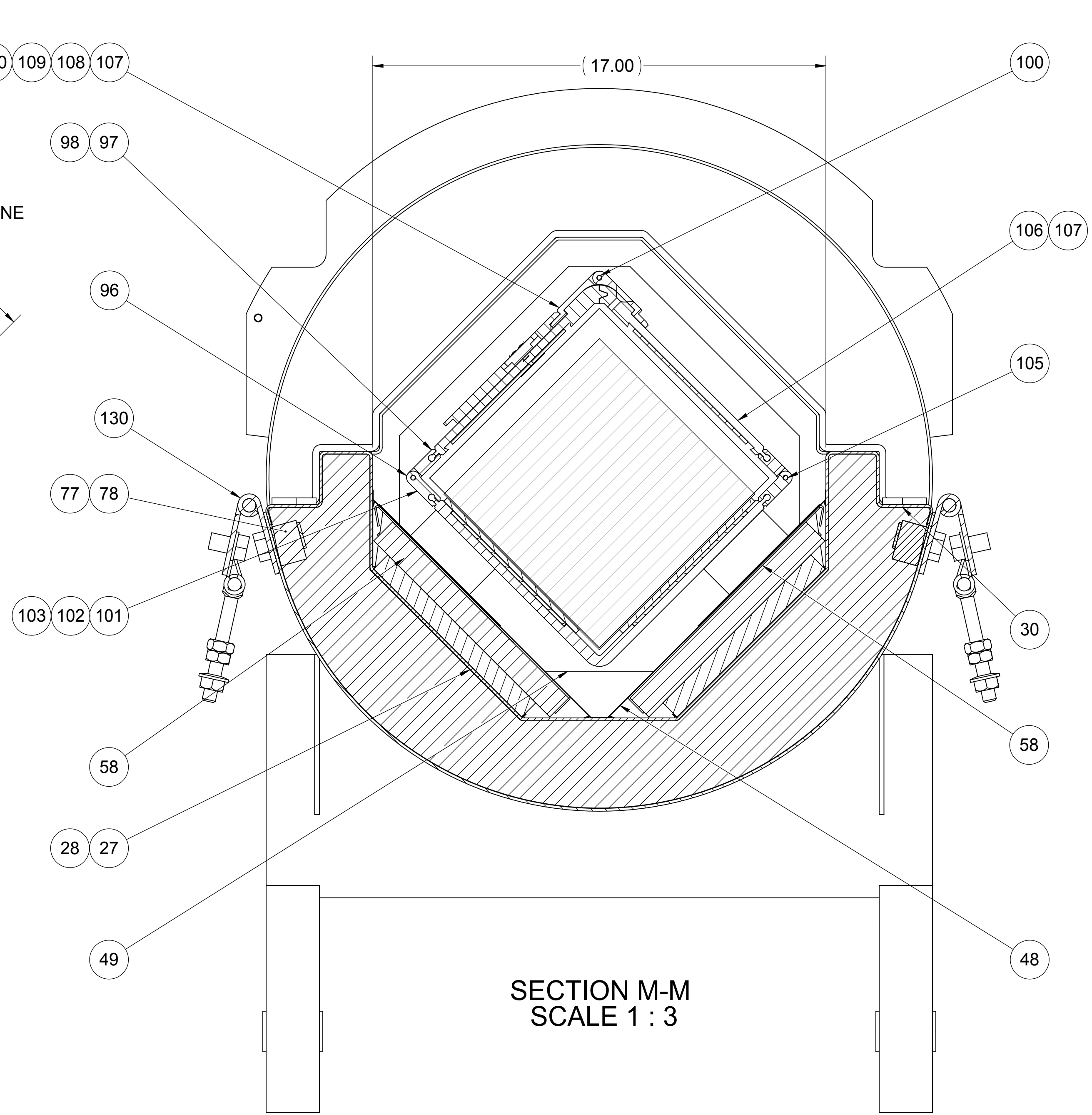
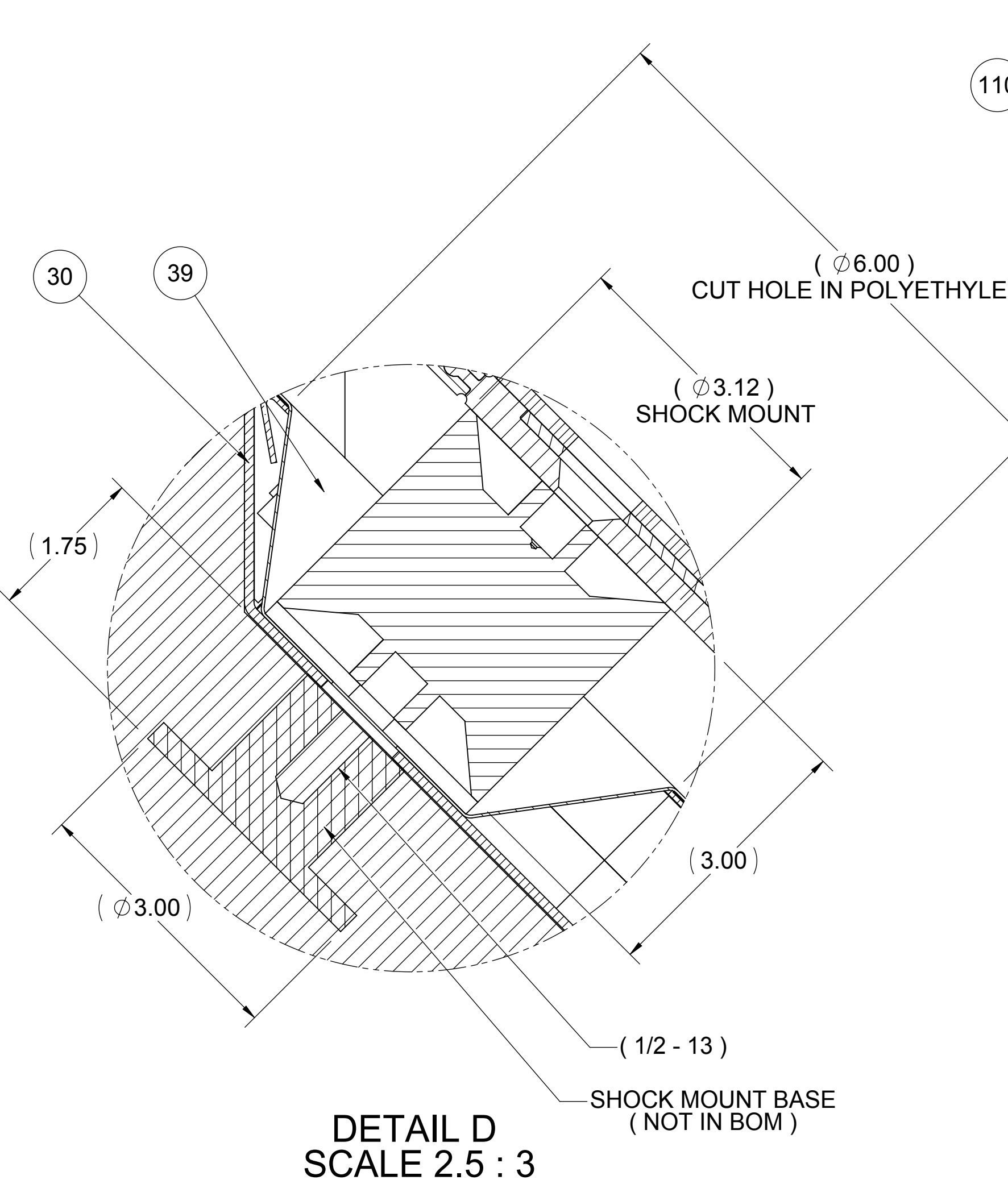
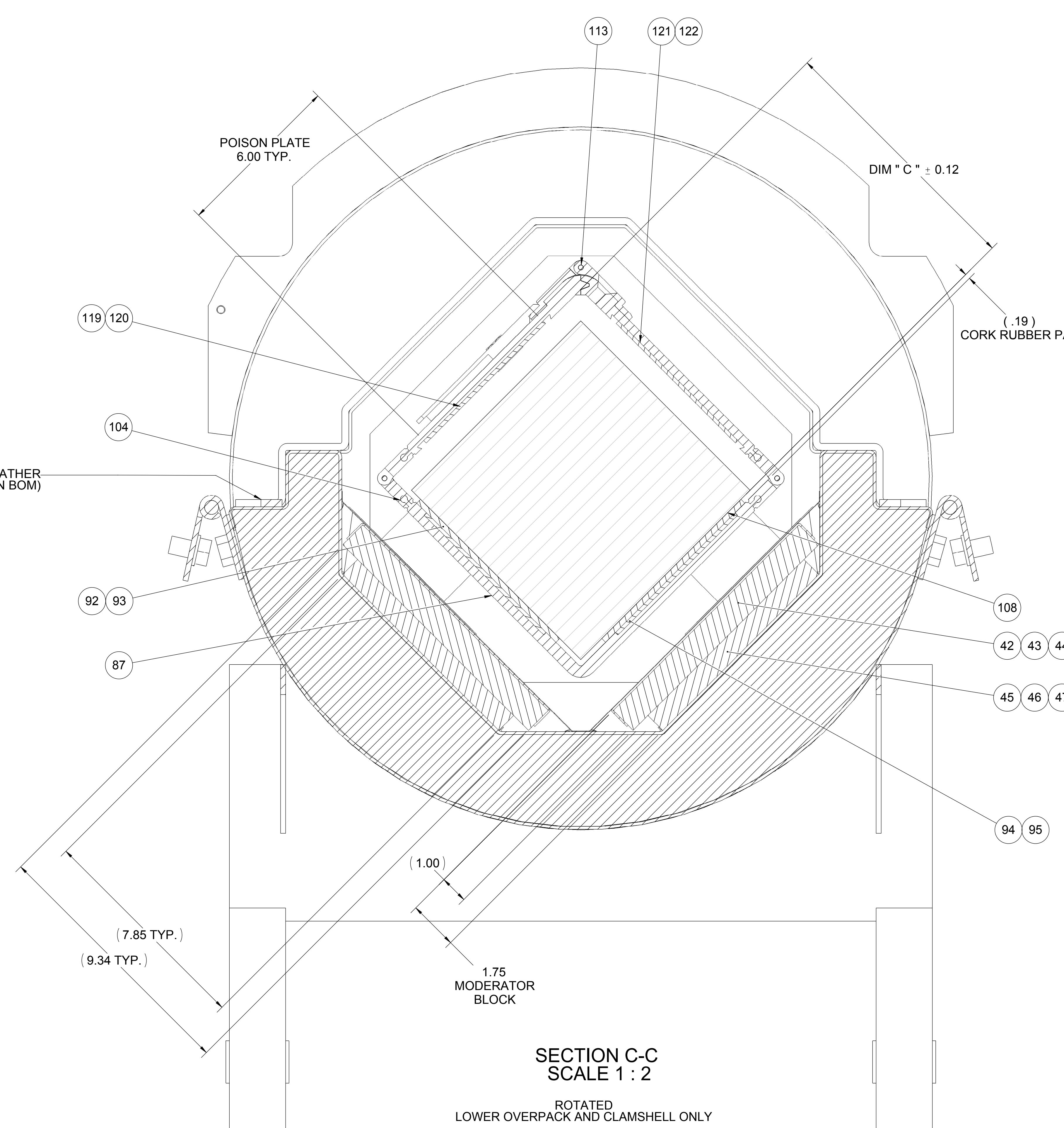
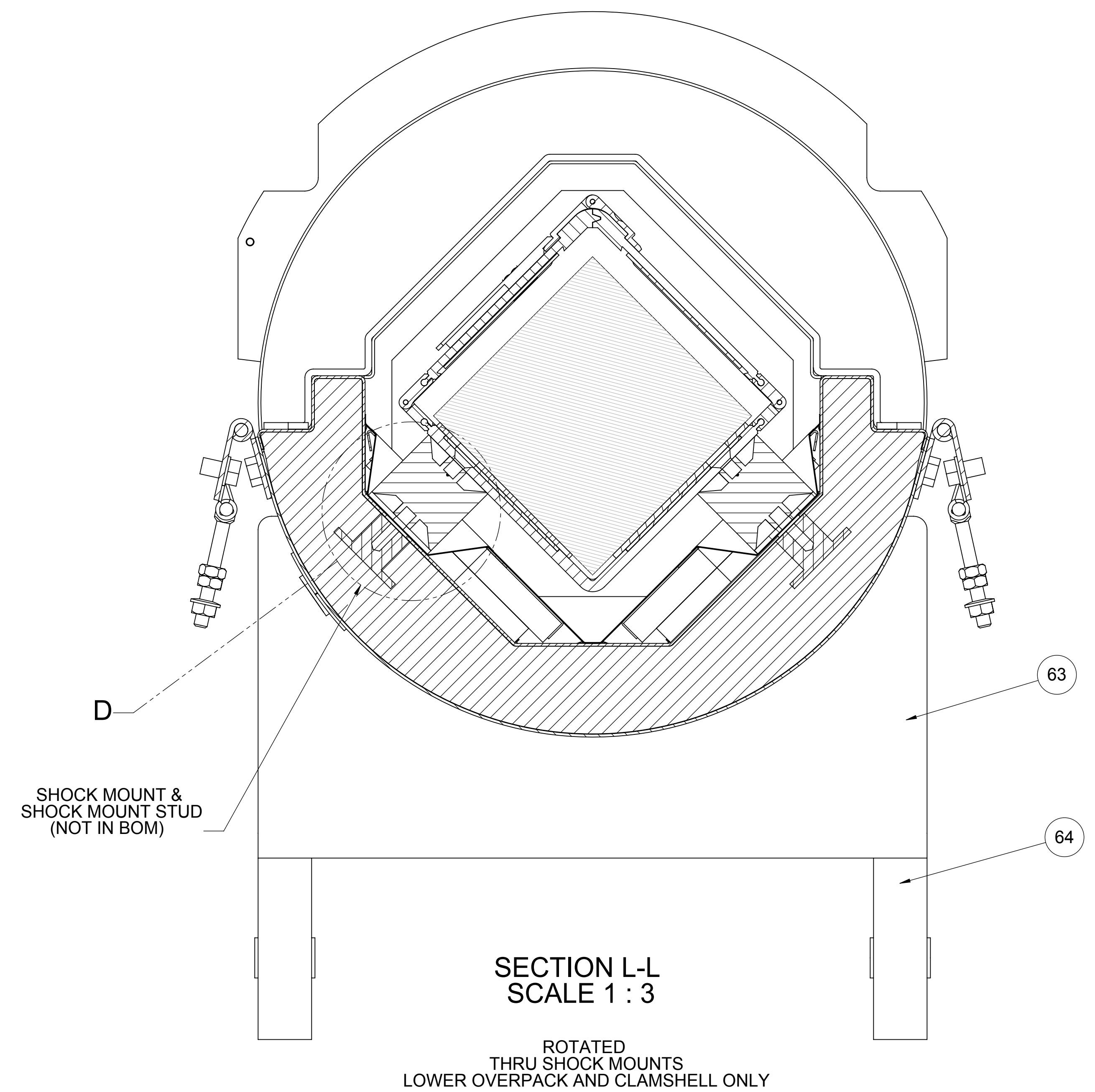
DWG REF -

NEXT ASSY -

THIRD ANGLE PROJECTION

DESIGN			
CHKD			
DESIGN			
MFG ENG			
PA ENG			
DESIGN			
MR			
APPROV			
APPROV			
APPROV			
SCALE	1:8	WEIGHTS	

ELECTRIC COMPANY LLC - NUCLEAR FUEL COLUMBIA, SC USA
SAFETY RELATED ITEMS TRAVELLER XL & STD
 DWG NO: 10004E58
 SHEET 3 OF 9



SO	75255		
ECN	61148-0		
ZNE	DC	DESCRIPTION	
PKGSUPPORT	ECN	0002409-0	
ZNE	DC	DESCRIPTION	
HT		REMOVED WELD CALL OUTS.	
DWN BY	C. GIBBS	20150922	
USPKGSUPPORT	ECN	0002784-0	
ZNE	DC	DESCRIPTION	
HT		SEE SHEET 1 FOR CHANGES.	
DWN BY	C. GIBBS	201310819	
BUD	28279		
ECN	0003155-0		
ZNE	DC	DESCRIPTION	
HT		SEE SHEET 1 FOR CHANGES.	
DWN BY	C. GIBBS	20150922	

SEE PRODUCT SPECIFICATION PDIN000 FOR SUPPLEMENTAL PRODUCT INFORMATION

DIMENSIONS ARE IN INCHES

DWG REF -
NEXT ASSY -

THIRD ANGLE PROJECTION

DESIGN			
CHKD			
DESIGN			
MISC ENG			
FIN ENG			
DESIGN			
APPROV			
SCALE	1:1	WEIGHTS	
TITLE	TRCH NO	DWG NO	REV
9		10004E58	-
SCALE 1:1		WEIGHTS	SHEET 4 OF 9

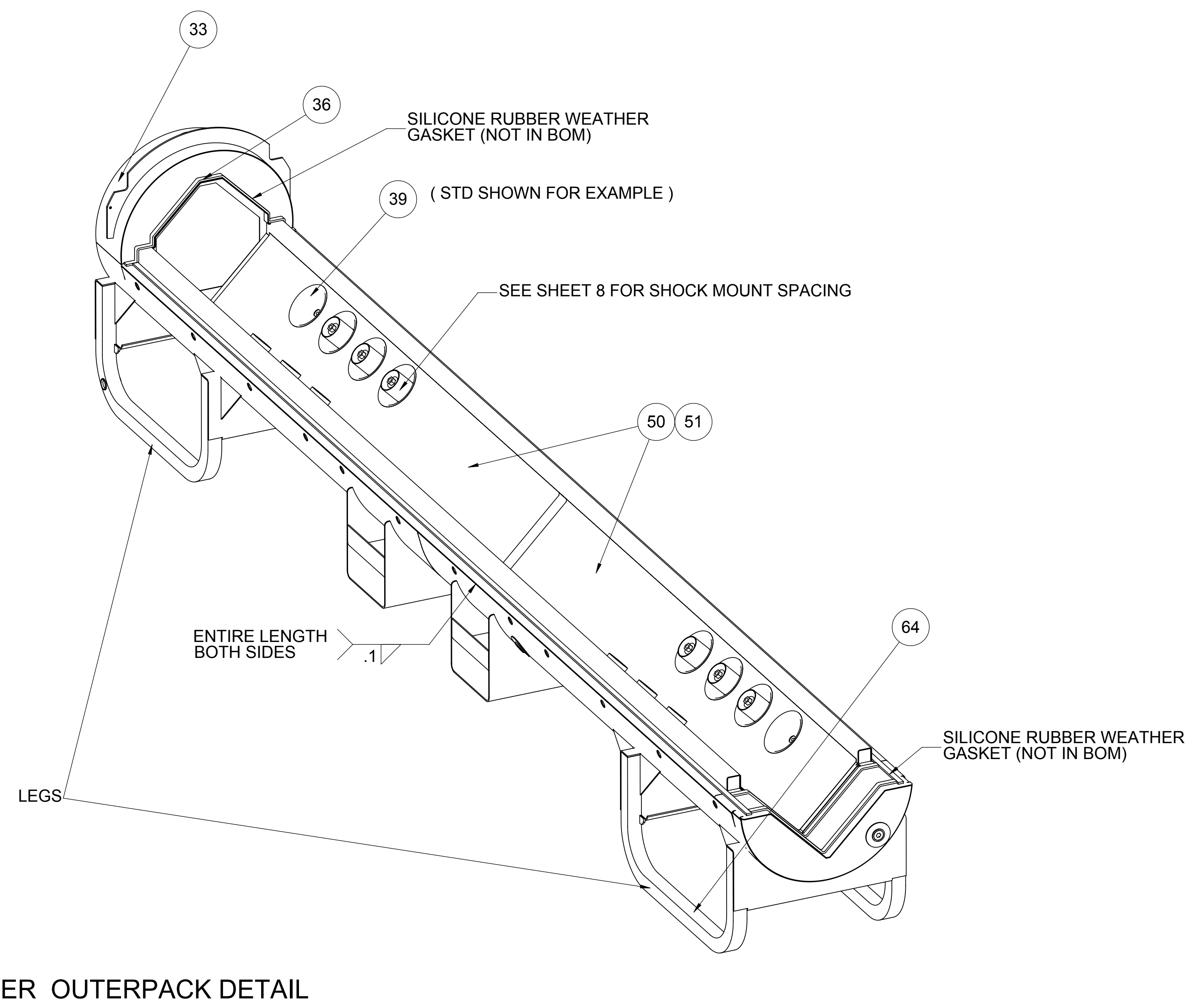
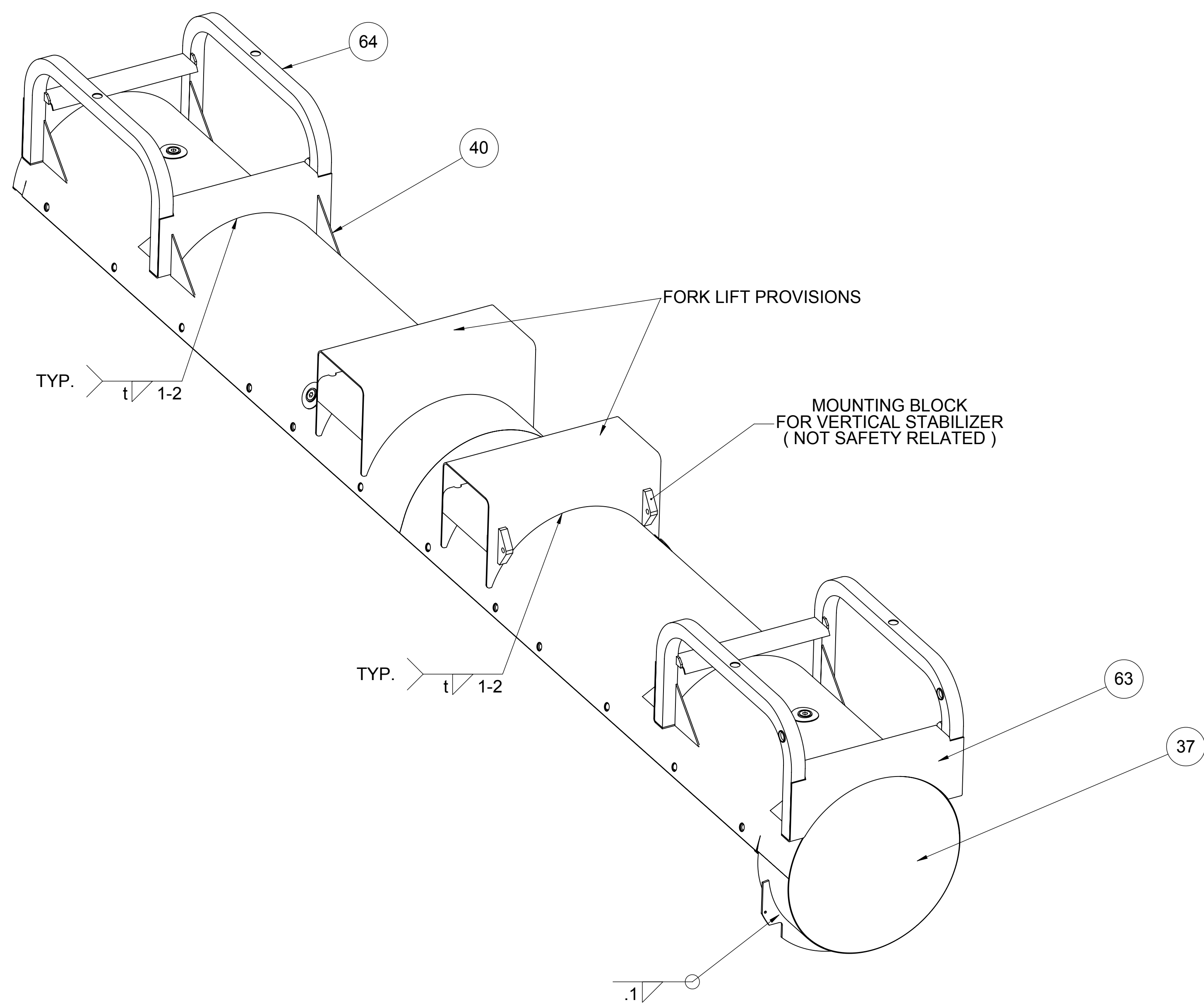
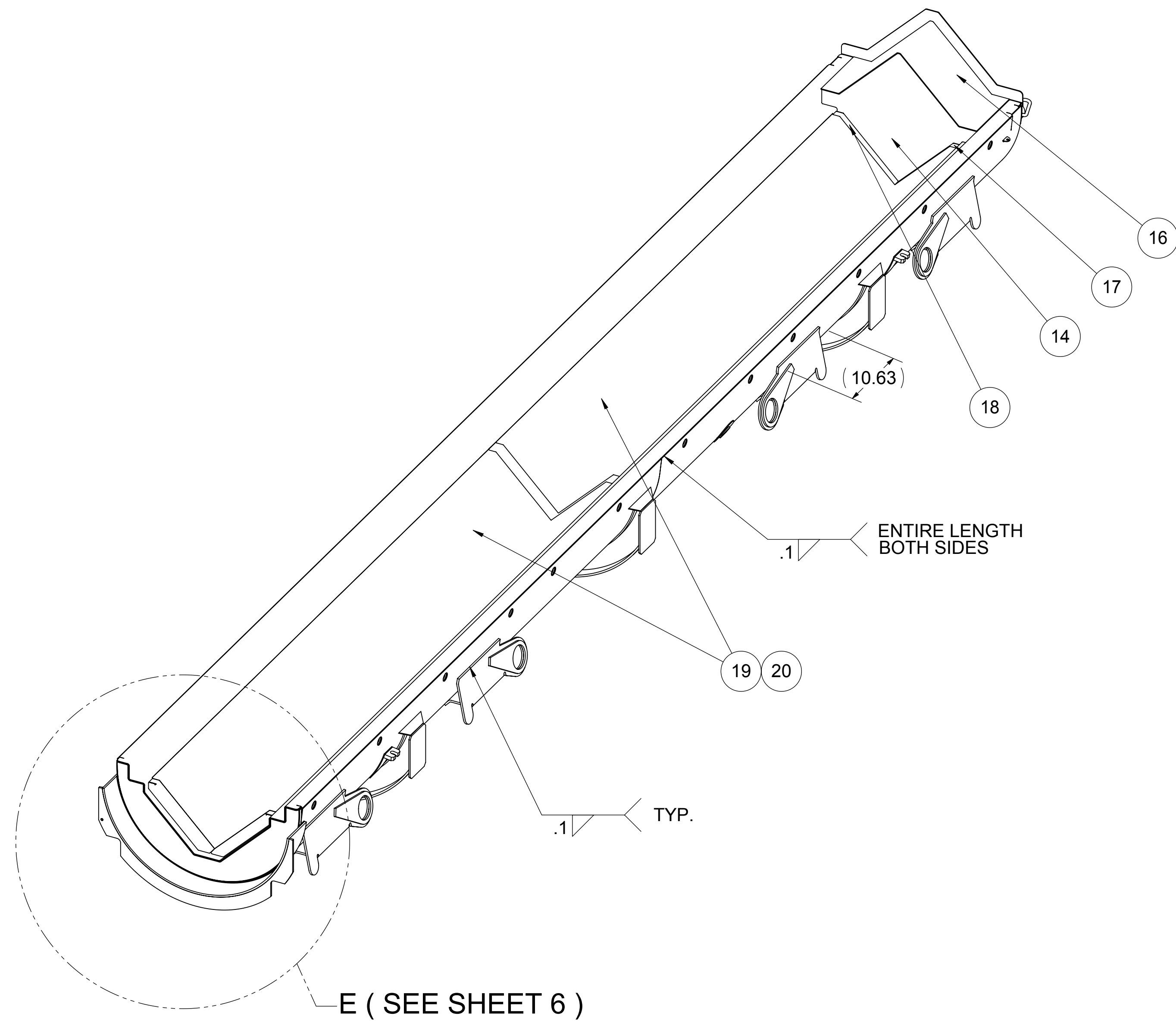
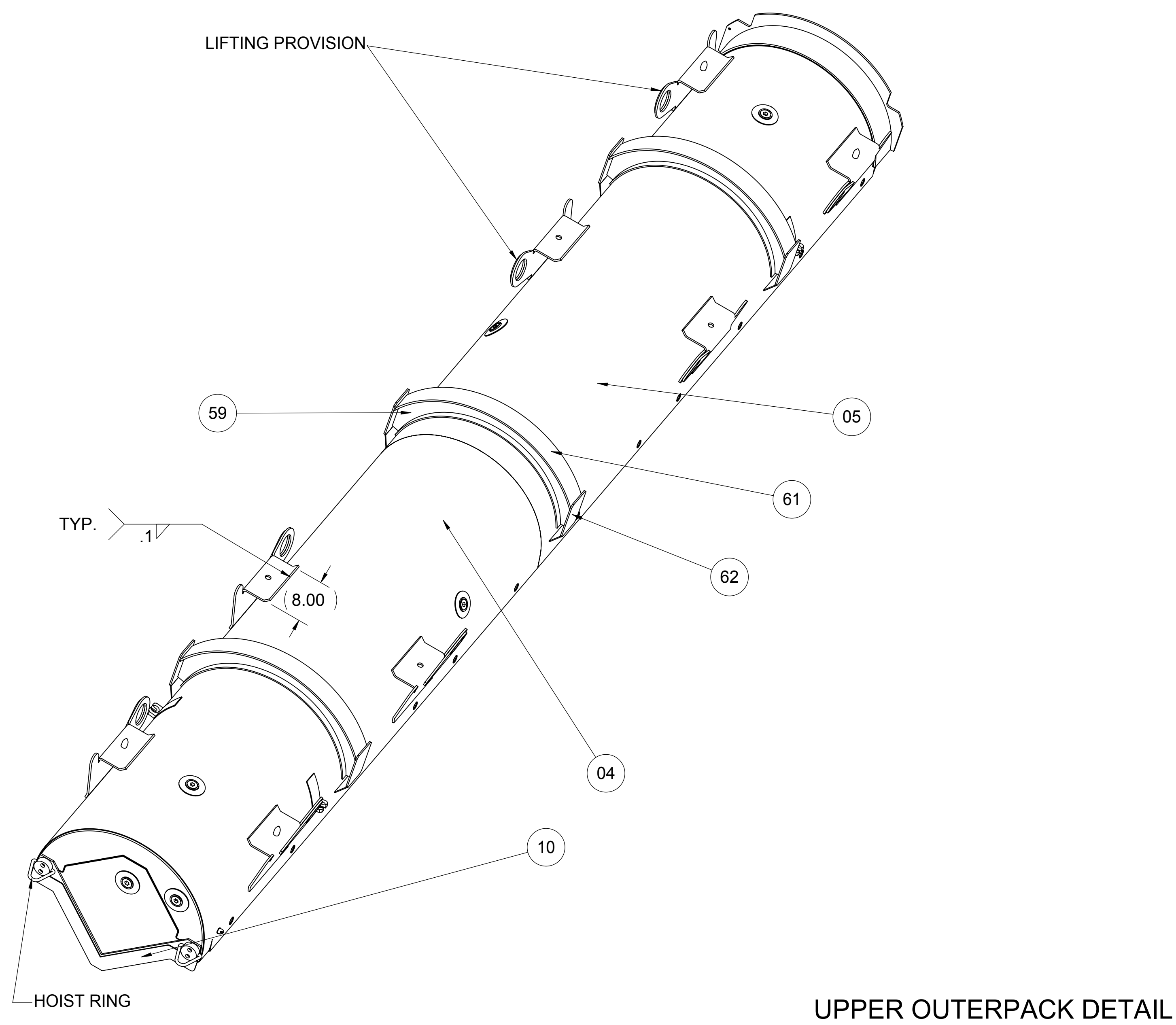
Westinghouse ELECTRIC COMPANY LLC - NUCLEAR FUEL COLUMBIA, SC USA

SAFETY RELATED ITEMS TRAVELLER XL & STD

10004E58

SHEET 4 OF 9

© 2015 Westinghouse Electric Company LLC All Rights Reserved



SO	752255		
ECN	61148-0		
ZNE	OC	DESCRIPTION	
PKGSUPPORT			
ECN	0002409-0		
ZNE	OC	DESCRIPTION	
BR		ADDED WELD SYMBOL CALLOUT	
DWN BY	C. GIBBS	2015/07/06	
USPKGSUPPORT			
ECN	0002789-0		
ZNE	OC	DESCRIPTION	
		SEE SHEET 1 FOR CHANGES	
DWN BY	C. GIBBS	2013/08/19	
BUD	128779		
ECN	0003155-0		
ZNE	OC	DESCRIPTION	
		SEE SHEET 1 FOR CHANGES	
DWN BY	C. GIBBS	2015/09/22	

SEE PRODUCT SPECIFICATION PDIN000 FOR SUPPLEMENTAL PRODUCT INFORMATION

DIMENSIONS ARE IN INCHES

DWG REF -

NEXT ASSY -

THIRD ANGLE PROJECTION

DESIGN	-	-
CHKD	-	-
DESIGN	-	-
MFG ENG	-	-
FIN ENG	-	-
DESIGN	-	-
MSR	-	-
APVD	-	-
APVD	-	-
APVD	-	-
SCALE	1:1	

Westinghouse ELECTRIC COMPANY LLC - NUCLEAR FUEL COLUMBIA, SC USA

SAFETY RELATED ITEMS TRAVELLER XL & STD

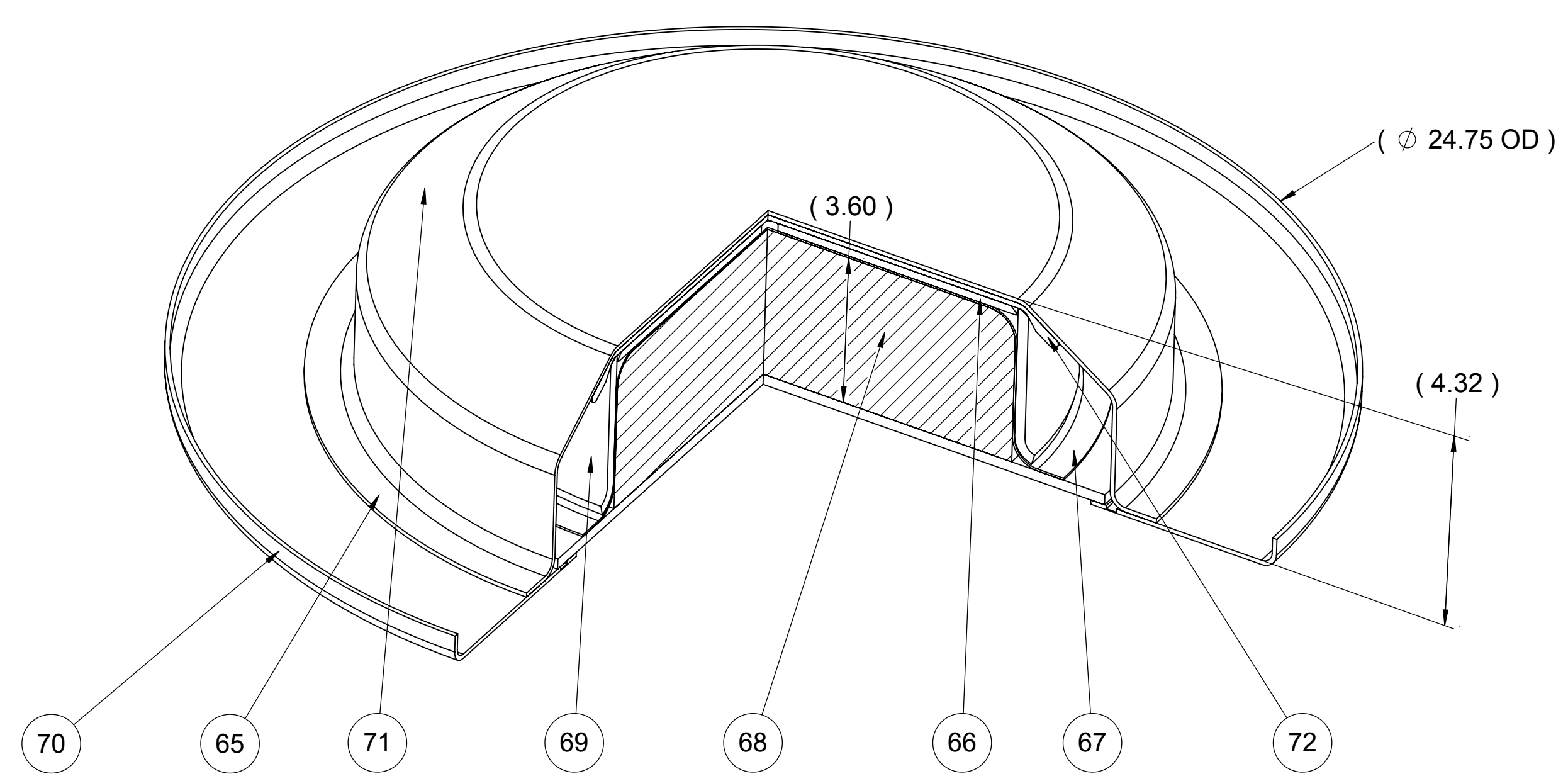
9

10004E58

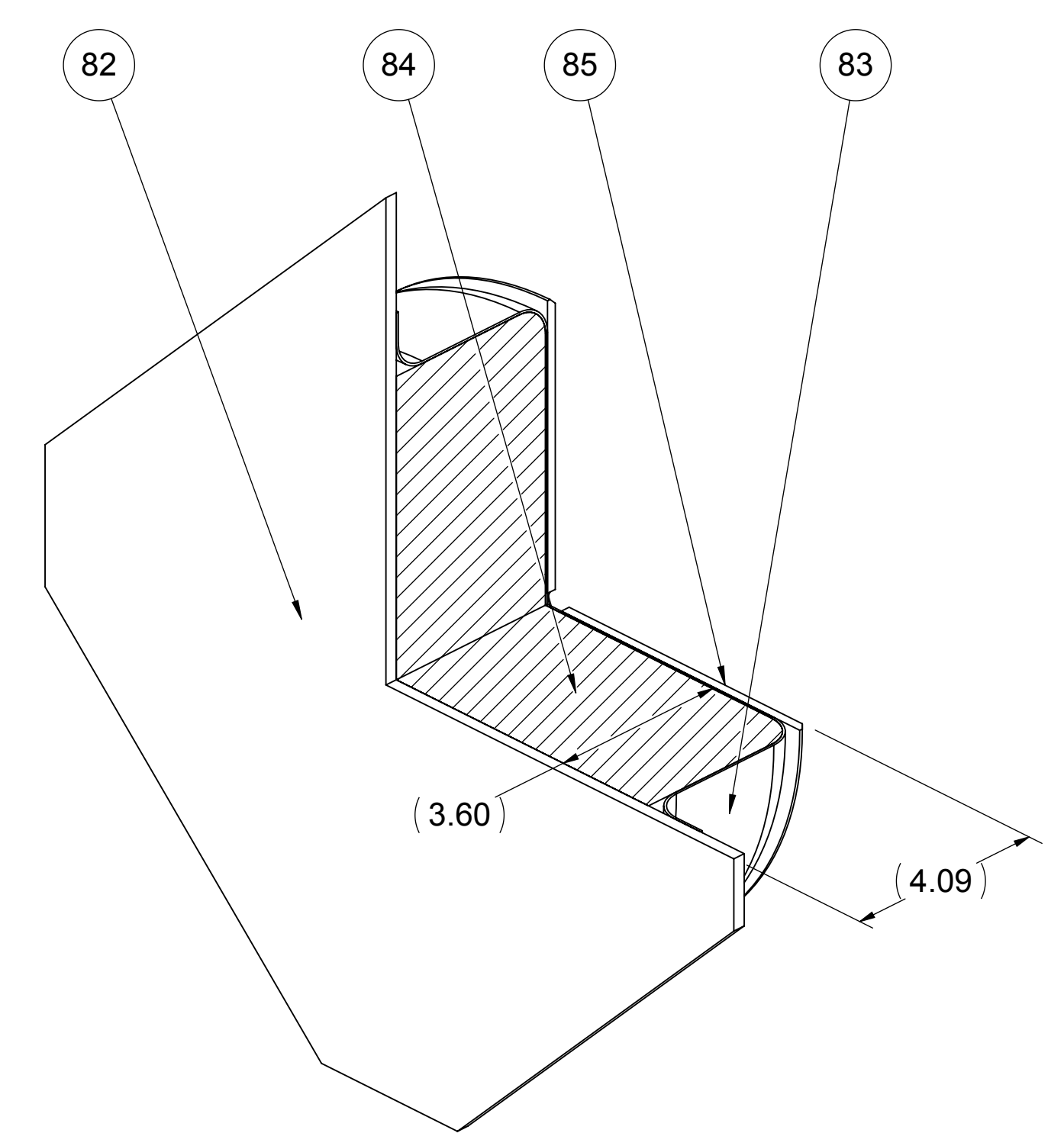
SCALE 1:1

WEIGHT (LBS)

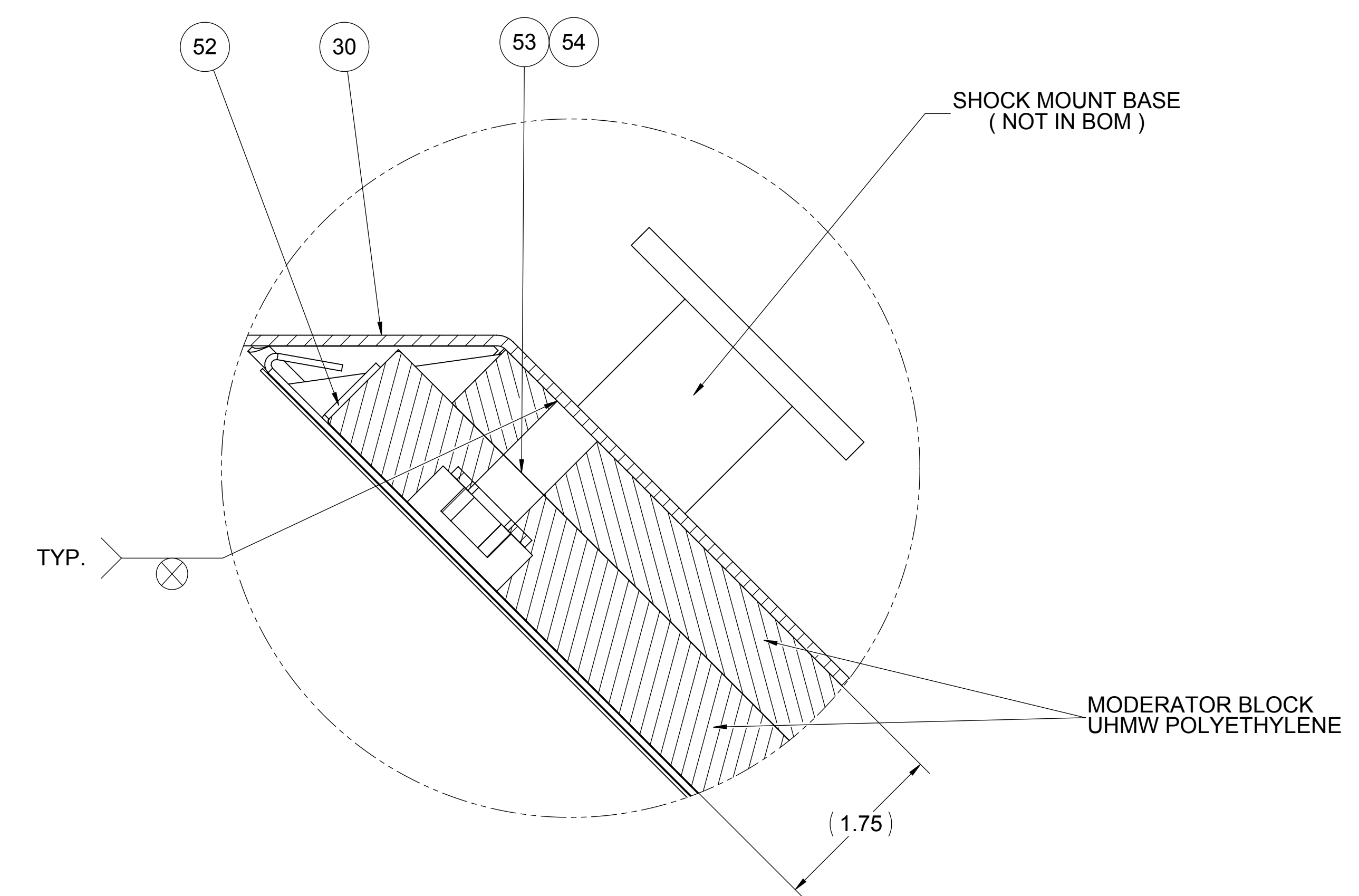
SHEET 5 OF 9



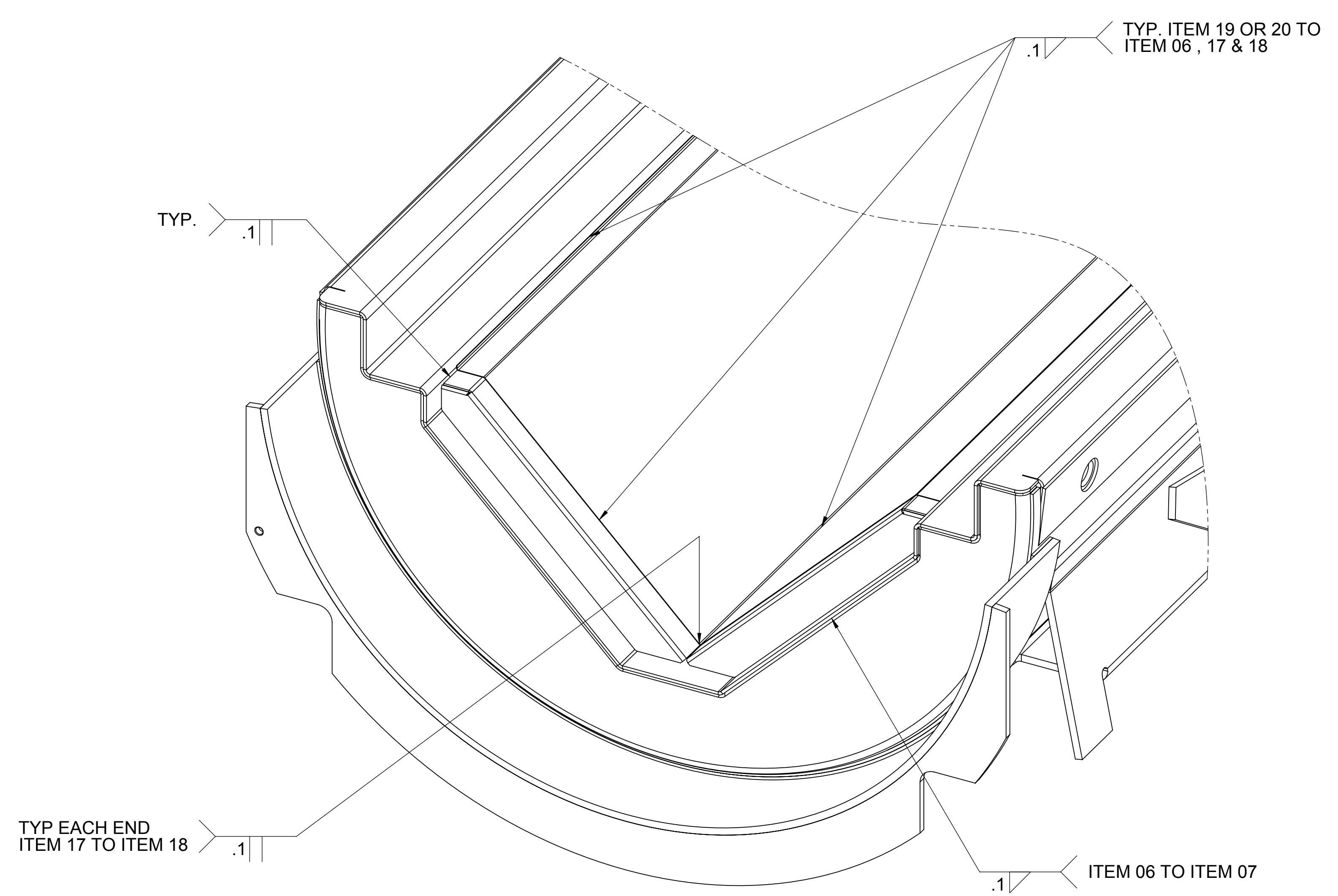
LOWER PILLOW SUB - ASSY



TOP PILLOW SUB - ASSY



MODERATOR BLOCK INSTALLATION



DETAIL E

SO	75255	%
ECN	61148-0	
ZNE	OC	DESCRIPTION
PKGSUPPORT		
ECN	0002409-0	+
ZNE	OC	DESCRIPTION
		SEE SHEETS 2 - 5 FOR CHANGES.
DWN BY	C. GIBBS	2015/07/06
USPKGSUPPORT		
ECN	0002789-0	1
ZNE	OC	DESCRIPTION
		SEE SHEET 1 FOR CHANGES.
DWN BY	C. GIBBS	2013/08/19
BUD	12879	
ECN	0003155-0	-
ZNE	OC	DESCRIPTION
		SEE SHEET 1 FOR CHANGES.
DWN BY	C. GIBBS	2015/09/22

SEE PRODUCT SPECIFICATION PDIN000 FOR SUPPLEMENTAL PRODUCT INFORMATION
DIMENSIONS ARE IN INCHES

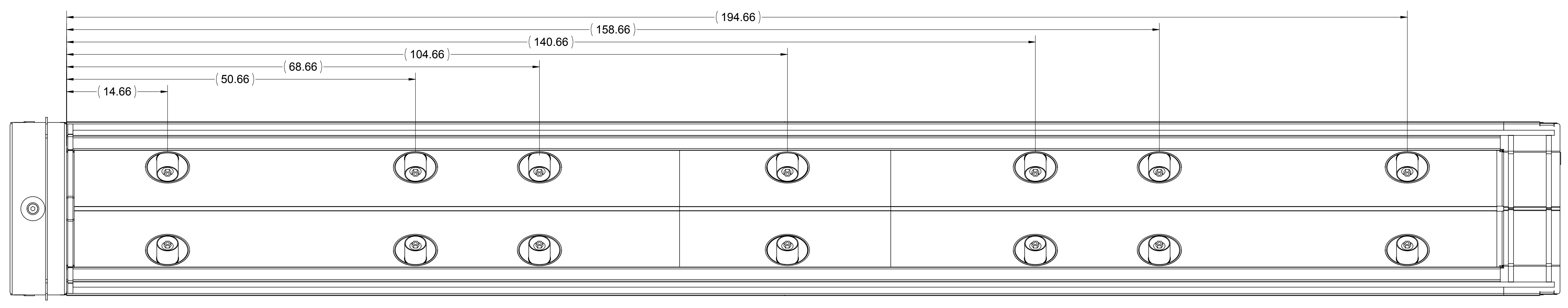
DWG REF -
NEXT ASSY -

THIRD ANGLE PROJECTION

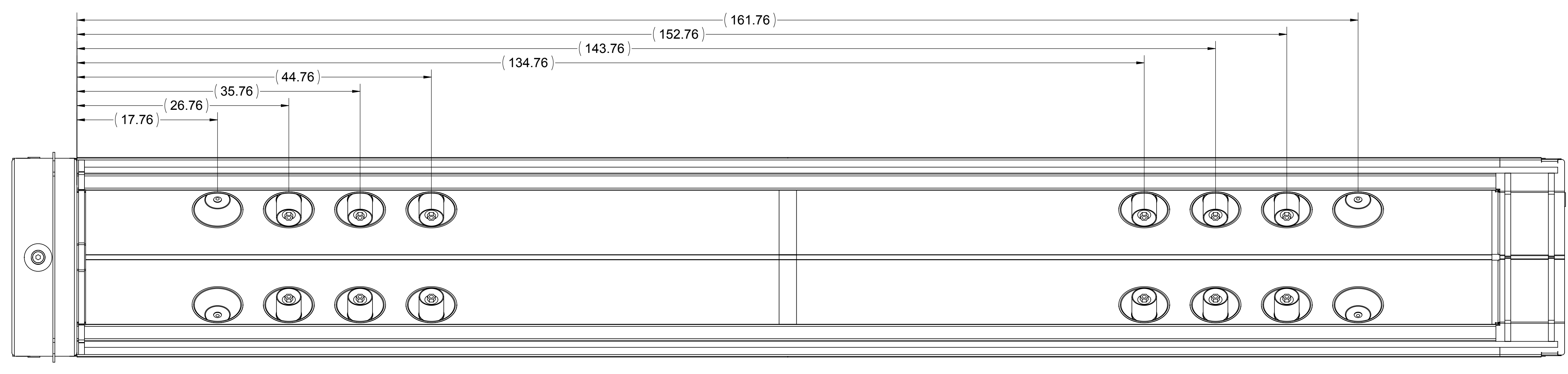
DESIGN	-		
CHNG	-		
DESIGN	-		
MFG ENG	-		
FIN ENG	-		
DESIGN	-		
MSR	-		
APPRO	-		
APPRO	-		
APPRO	-		
SCALE	1:1	WEIGHT(LBS)	
TITLE	TRCH NO	DWG NO	REV
9		10004E58	-
SCALE		SHEET 6 OF 9	



SAFETY RELATED ITEMS TRAVELLER XL & STD



SHOCK MOUNT SPACING - XL



SHOCK MOUNT SPACING - STD

SO	75255	%
ECN	61148-0	
ZNE	OC	DESCRIPTION
PKGSUPPORT		
ECN	0002409-0	
ZNE	OC	DESCRIPTION
		SEE SHEETS 2 - 5 FOR CHANGES.
DWN BY	C. GIBBS	2015/07/06
USPKGSUPPORT		
ECN	0002789-0	
ZNE	OC	DESCRIPTION
		SEE SHEET 1 FOR CHANGES.
DWN BY	C. GIBBS	2013/08/19
BUD	128779	
ECN	0003155-0	
ZNE	OC	DESCRIPTION
		SEE SHEET 1 FOR CHANGES.
DWN BY	C. GIBBS	2015/09/22

SEE PRODUCT SPECIFICATION PDIN000 FOR SUPPLEMENTAL PRODUCT INFORMATION
DIMENSIONS ARE IN INCHES

DWG REF -
NEXT ASSY -

THIRD ANGLE PROJECTION

DESIGN	-	-
CHKD	-	-
DESIGN	-	-
MFG ENG	-	-
PRG ENG	-	-
DESIGN	-	-
MSR	-	-
APPRO	-	-
APPRO	-	-
APPRO	-	-

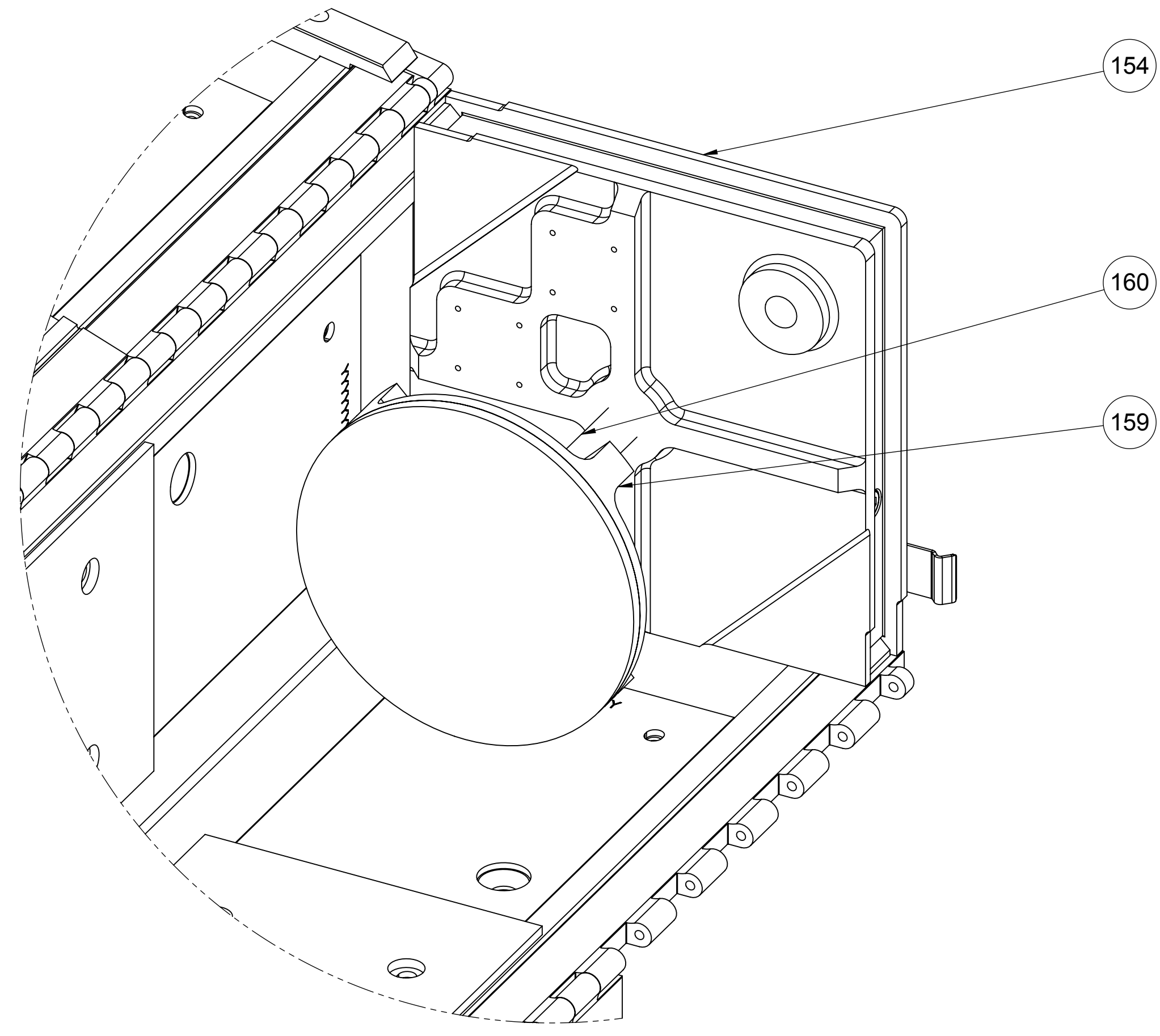
Westinghouse ELECTRIC COMPANY LLC - NUCLEAR FUEL COLUMBIA, SC USA

SAFETY RELATED ITEMS TRAVELLER XL & STD

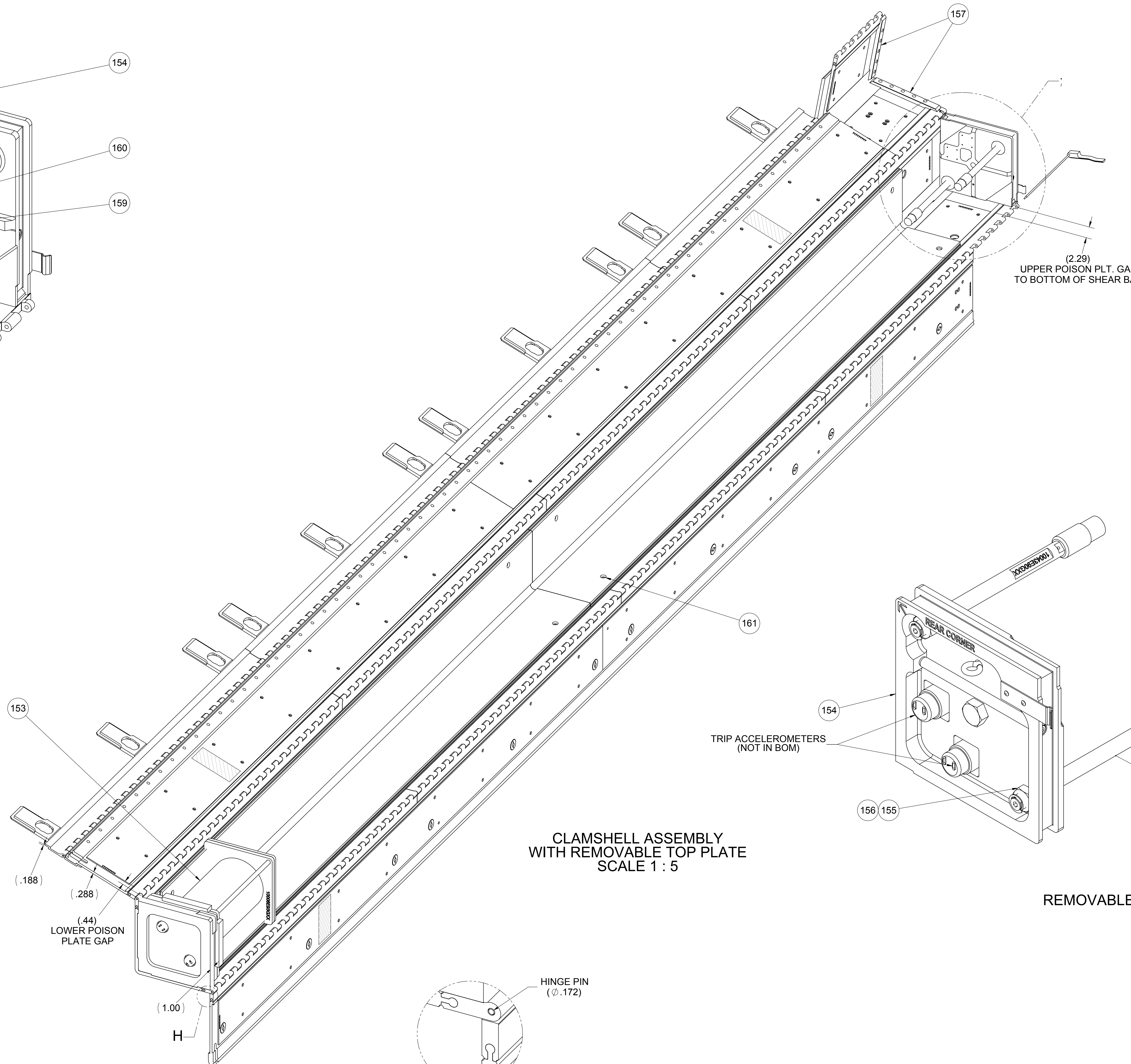
TITLE: **9** TFSM NO: **10004E58** REV: **-**

SCALE: 1:7.5 WEIGHT(LBS): SHEET 8 OF 9

ALTERNATE TOP AXIAL
RESTRAINT CONFIGURATION
(SQUARE OR CIRCULAR
CROSS-SECTION)

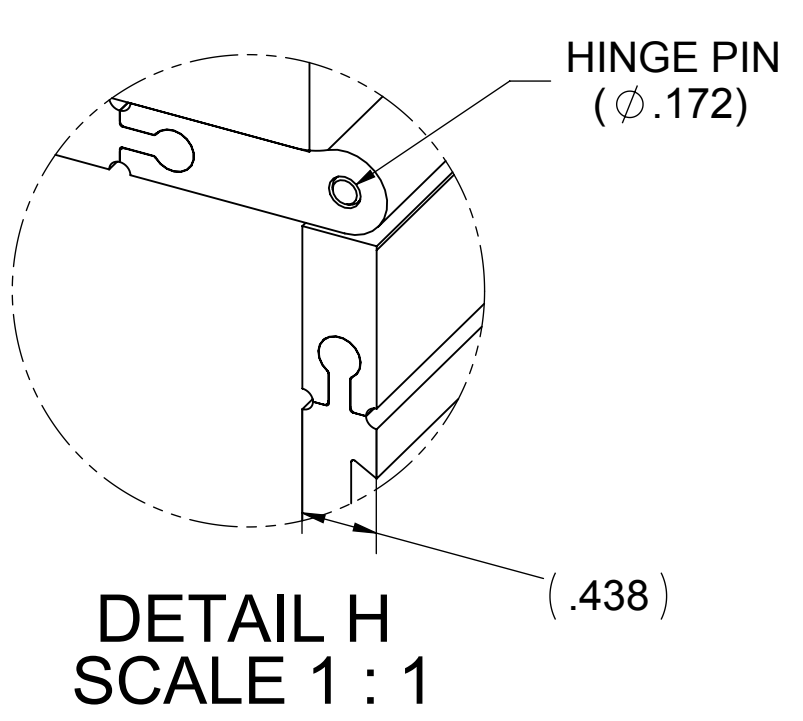


DETAIL G



CLAMSHELL ASSEMBLY
WITH REMOVABLE TOP PLATE
SCALE 1 : 5

REMOVABLE TOP PLATE DETAIL



DETAIL H
SCALE 1 : 1

SO	752255		
ECN	61148-0		
ZONE	DC	DESCRIPTION	
PKGSUPPORT	ECN	0002409-0	
ZONE	DC	DESCRIPTION	
SEE SHEETS 2 - 5 FOR CHANGES.			
DWN BY	C. GIBBS	2015/07/06	
USPKGSUPPORT	ECN	0002789-0	
ZONE	DC	DESCRIPTION	
SEE SHEET 1 FOR CHANGES.			
DWN BY	C. GIBBS	2013/08/19	
BUD	128779		
ECN	0003155-0		
ZONE	DC	DESCRIPTION	
SEE SHEET 1 FOR CHANGES.			
DWN BY	C. GIBBS	2015/09/22	

SEE PRODUCT SPECIFICATION PDIN000 FOR SUPPLEMENTAL PRODUCT INFORMATION
DIMENSIONS ARE IN INCHES

DWG REF -
NEXT ASSY -

THIRD ANGLE PROJECTION

DESIGN			
CHKD			
DESIGN			
MFG ENG			
FIN ENG			
DESIGN			
MRGR			
APPROV			
DATE			

Westinghouse ELECTRIC COMPANY LLC - NUCLEAR FUEL COLUMBIA, SC USA

SAFETY RELATED ITEMS TRAVELLER XL & STD

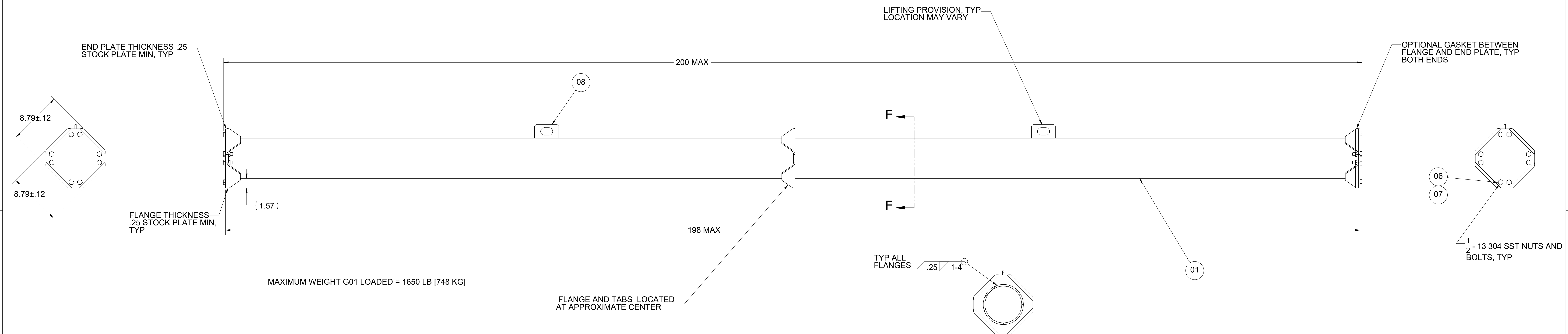
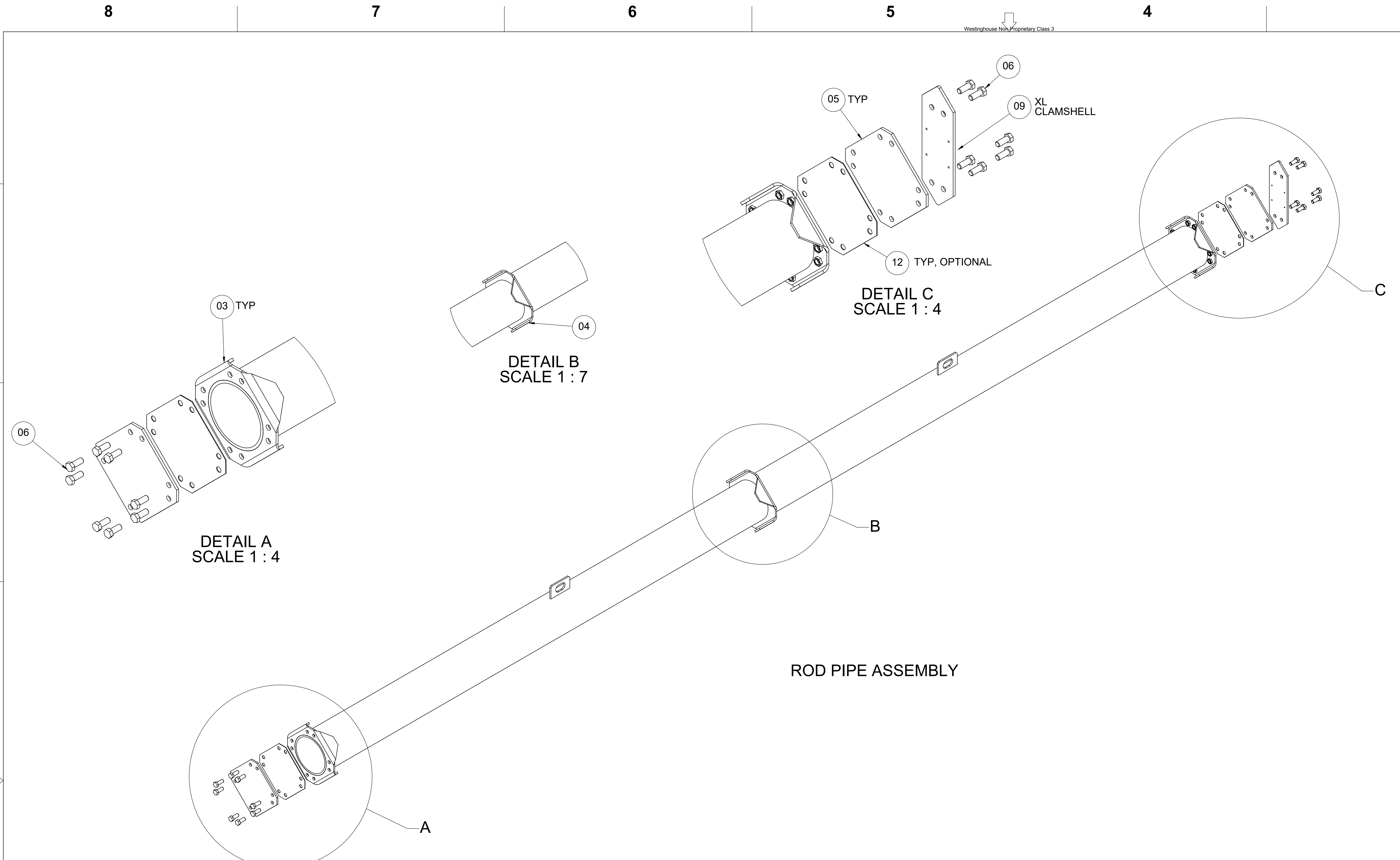
TRCH NO: 9 DWG NO: 10004E58

SCALE: 1:2 WEIGHT(LBS): SHEET 9 OF 9

© 2015 Westinghouse Electric Company LLC All Rights Reserved

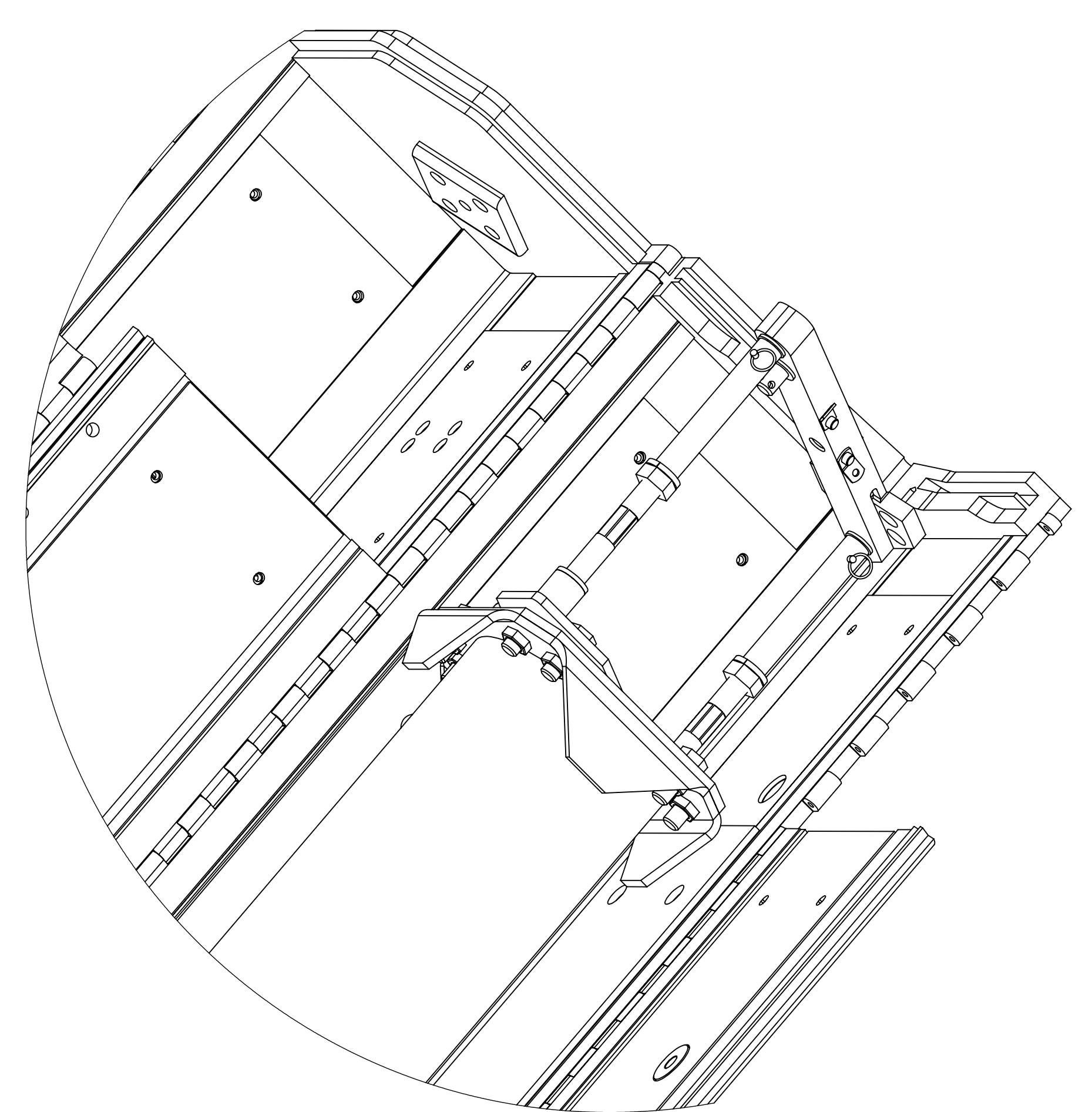
REQD		ITEM	QTY	UNIT	PART NAME	REFERENCE INFORMATION (SIZE)	MATL SIZE CODE PART NUMBER OR REF DWG
04	03	02	01	1	01	6" PIPE	SCHED 40
				2	03	END FLANGE	.25 THK STK
				1	04	SOLID FLANGE	.25 THK STK
				2	05	END PLATE	.25 THK STK
				16	06	BOLT	$\frac{1}{2}$ " - 13 X 1.25" LG
				16	07	NUT	$\frac{1}{2}$ " - 13
				2	08	LIFTING LUG	.25 THK STK
				1	09	TOP SHIM PLATE	.25" X 3.75" X 12.33"
				1	10	SHIPPING PAD	2.50" REF
				6	11	PACKING FOAM	$\frac{5}{8}$ " MAX. REF
				AR	12	GASKET	$\frac{1}{16}$ " REF
				1	13	BOTTOM PLATE SPACER	1.25" X 9.0"

- NOTES:
- PARTS TOLERANCES:
 DECIMAL: 2 PLACES UNDER 6 IN ±.03 6-12 IN ±.03 12-24 IN ±.04 OVER 24 IN ±.04
 DECIMAL: 3 PLACES UNDER 6 IN ±.020 6-12 IN ±.020 12-24 IN ±.030 OVER 24 IN ±.030
 ANGULAR: ±1
 - ASSEMBLY TOLERANCES:
 DECIMAL: 2 PLACES UNDER 6 IN ±.06 6-12 IN ±.06 12-24 IN ±.12 OVER 24 IN ±.2
 DECIMAL: 3 PLACES UNDER 6 IN ±.050 6-12 IN ±.050 12-24 IN ±.115 OVER 24 IN ±.188
 ANGULAR: ±2
 - 302, 303, 304L, 316 AND 316L SST ARE ACCEPTABLE FOR ALL 304 SST ASSEMBLY FASTENERS AND 304 SST SUB-ASSEMBLY FASTENERS.
 - WELD ALL ASSEMBLIES AND SUB-ASSEMBLIES PER ASME SECTION IX OR APPROVED EQUIVALENT STANDARD. INSPECT SST WELDS PER AWS D1.6 OR EQUIVALENT STANDARD.
 - PRIOR TO SHIPPING, TIGHTEN ITEM 06 (16 PLACES) TO A TORQUE OF 20 ±1 FT-LB OR 27 ±1 N-m.

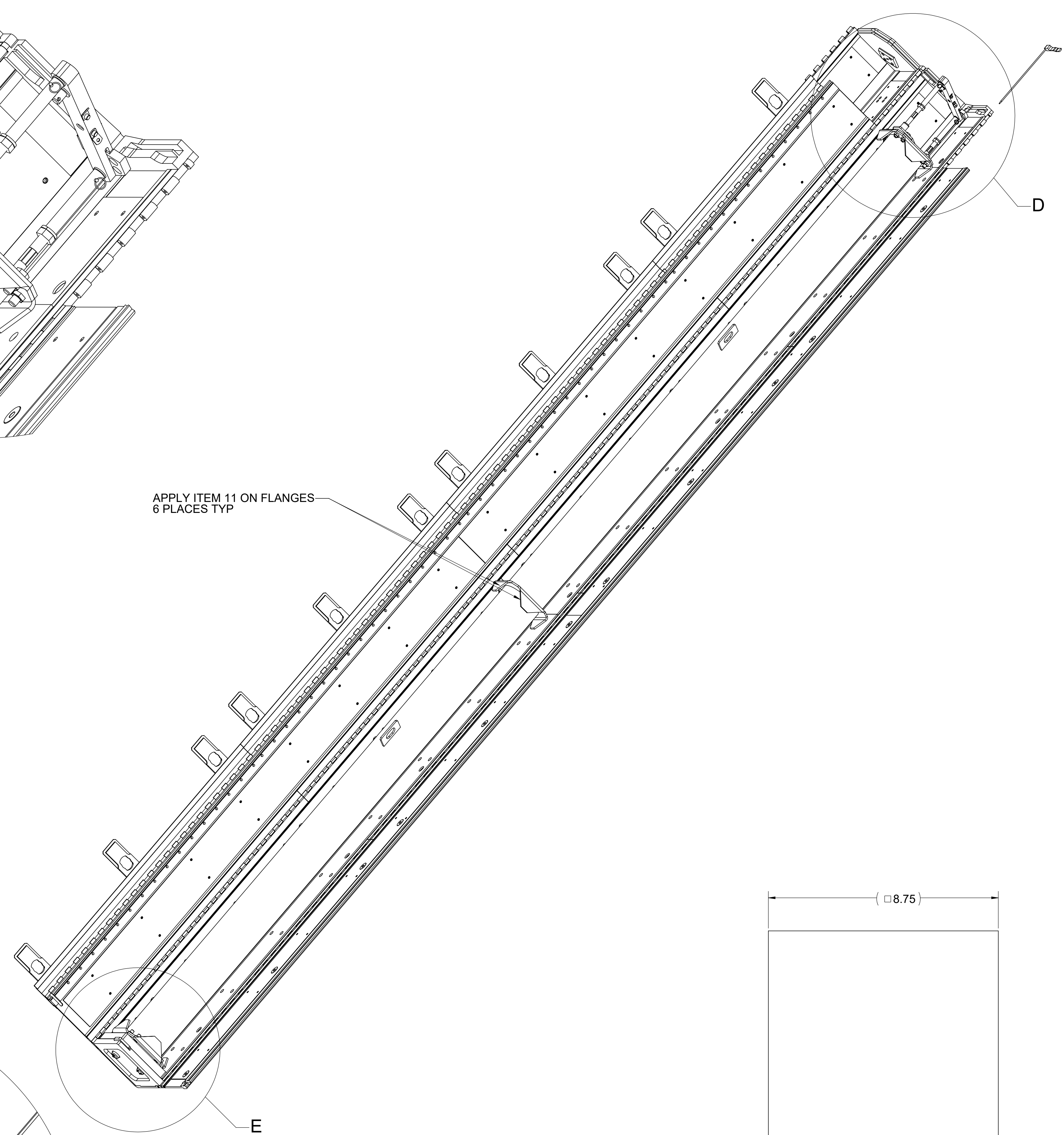


SO 752255	ECN 61146-0	DESCRIPTION NOSEUP	ECN 0003725-0	DESCRIPTION SEE ECN FOR CHANGES	DRAWN BY C. GIBBS	20190802
<p>SEE PRODUCT SPECIFICATION PDIN000 FOR SUPPLEMENTAL PRODUCT INFORMATION</p> <p>DIMENSIONS ARE IN INCHES</p> <p>ALL TOLERANCES ±.1/8" UNLESS OTHERWISE NOTED</p> <p>THIRD ANGLE PROJECTION</p>						
<p>WESTINGHOUSE</p> <p>ELECTRIC COMPANY LLC - NUCLEAR FUEL COLUMBIA, SC USA</p>			<p>SHIPPING PACKAGE LOOSE ROD PIPE</p> <p>SCALE 1:6</p> <p>WEIGHTS SEE DWG</p>			
<p>10006E58</p>			<p>SHEET 1 OF 2</p>			

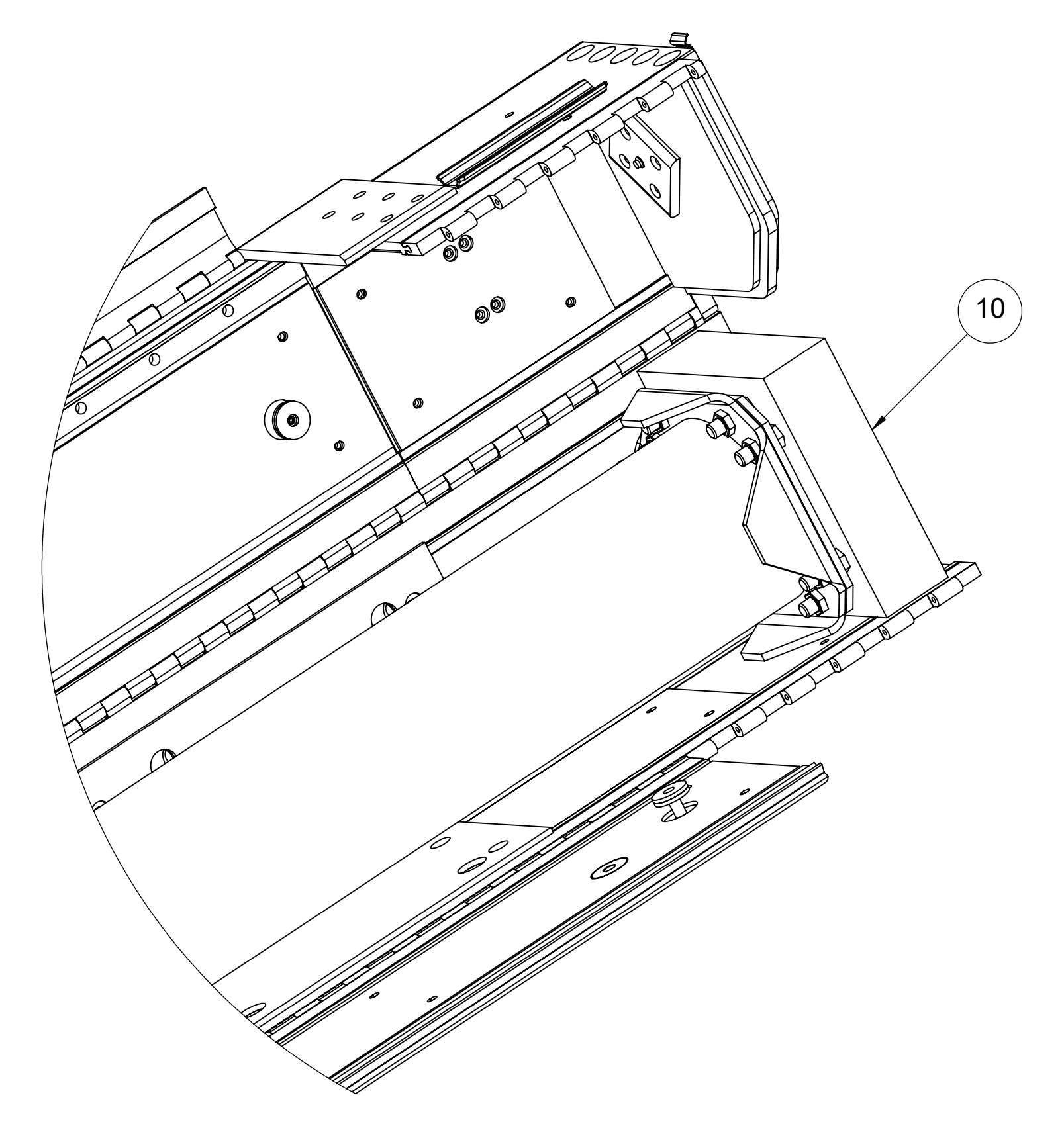
Westinghouse Non-Proprietary Class 3



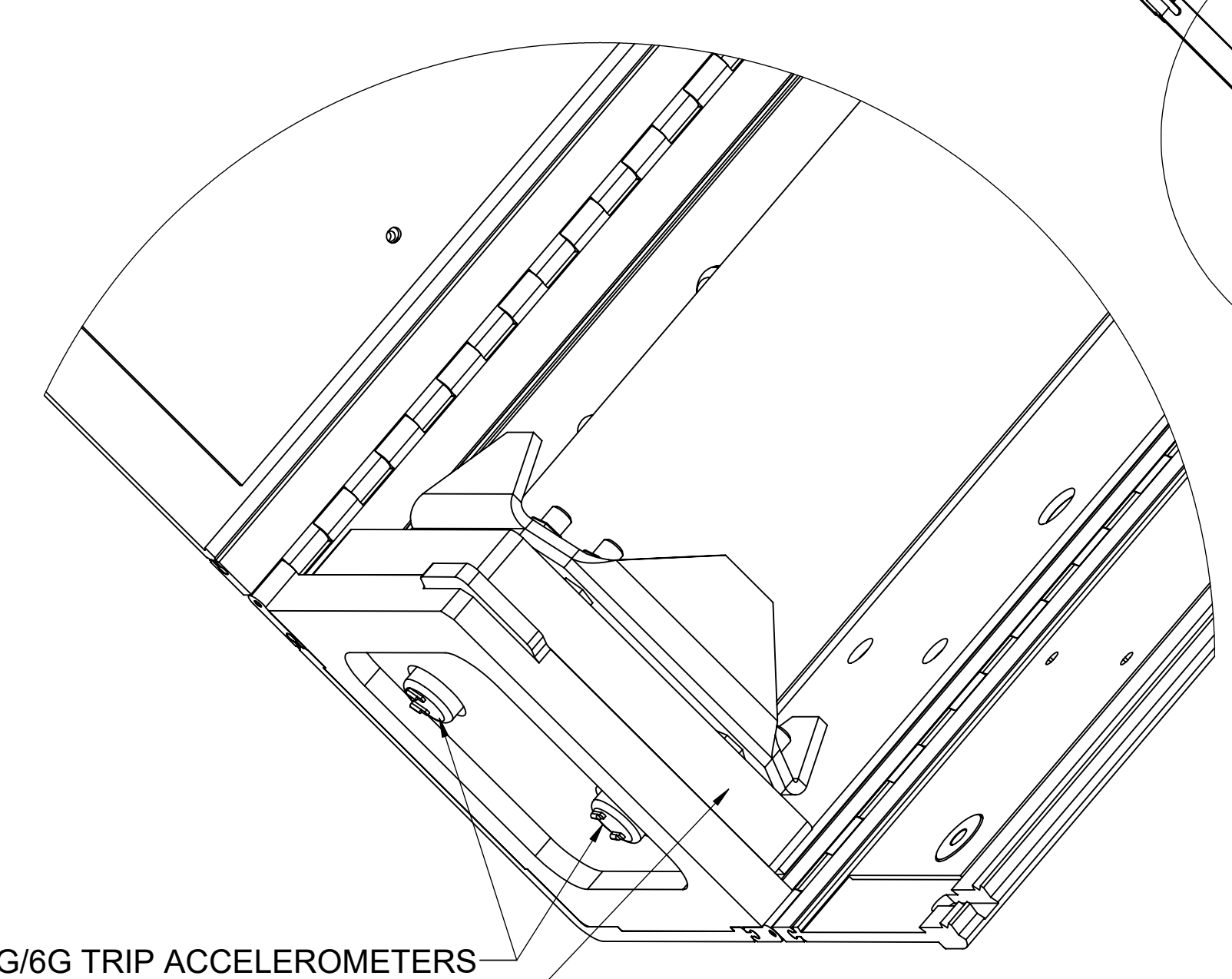
DETAIL D
SCALE 1 : 3
XL CLAMSHELL



APPLY ITEM 11 ON FLANGES
6 PLACES TYP

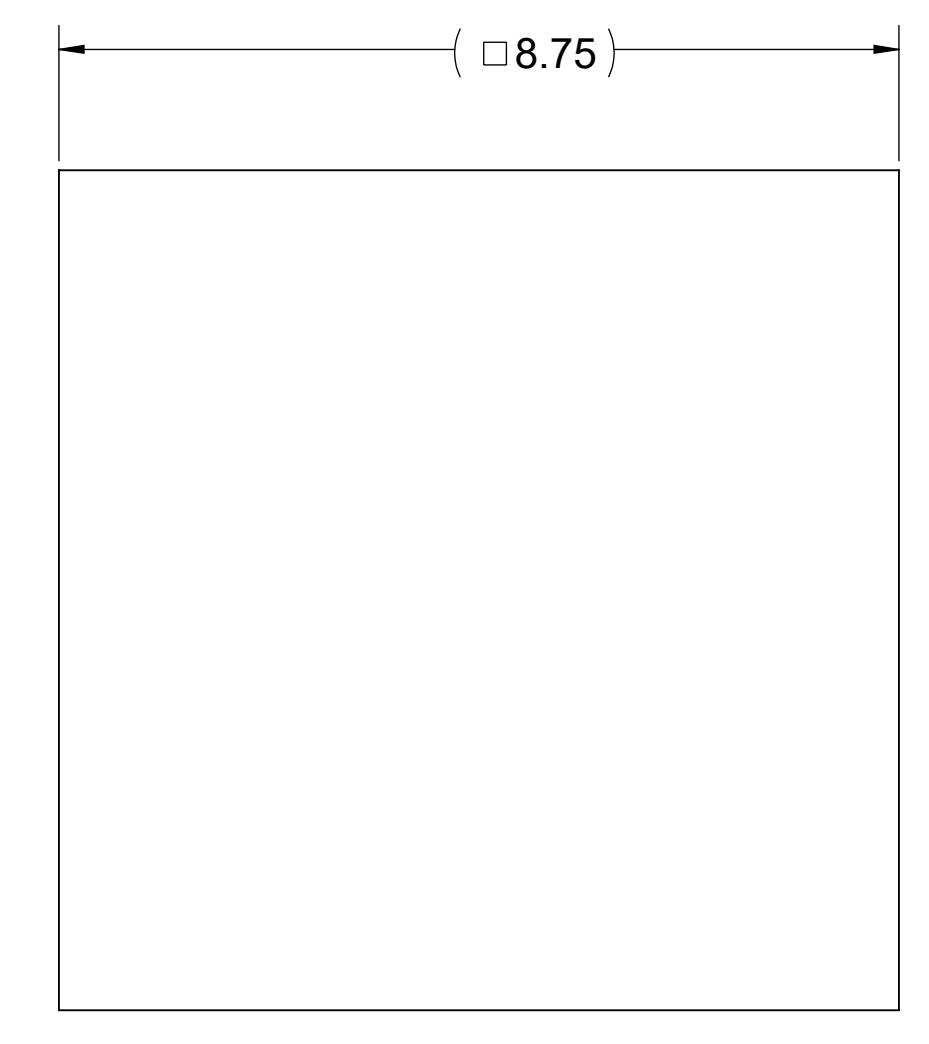


DETAIL D
SCALE 1 : 4
STD CLAMSHELL

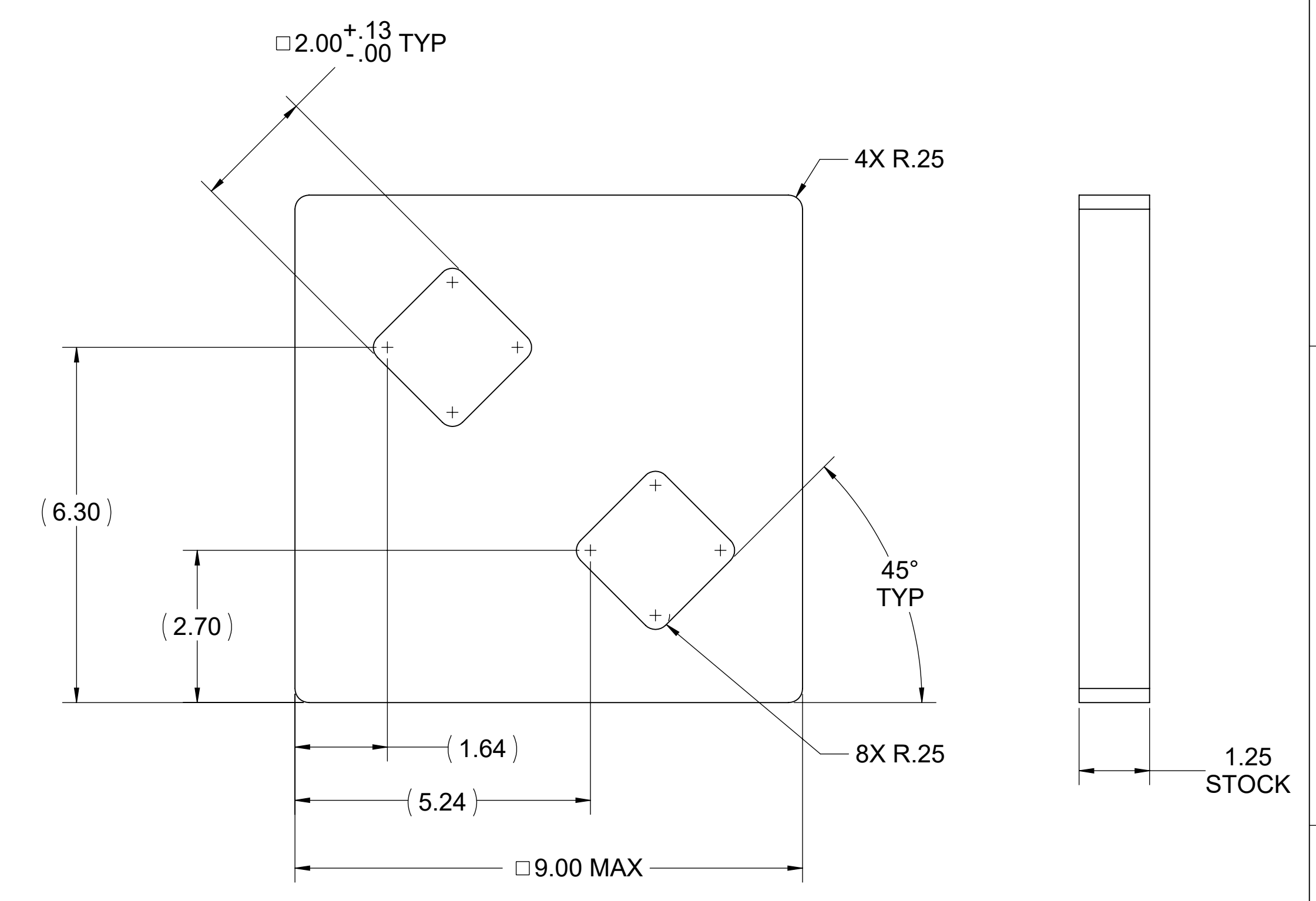


DETAIL E
SCALE 1 : 3

4G/6G TRIP ACCELEROMETERS
(NOT IN BOM)



SHIPPING PAD
SCALE 1:2
ITEM 10



BOTTOM PLATE SPACER
SCALE 1:2
ITEM 13

SO	75255		
ECN	61146-0		
ZNE	DC	DESCRIPTION	
		NOSEUP	
ECN	000375-0		
ZNE	DC	DESCRIPTION	
		SEE ECN FOR CHANGES	
DRAWN BY	C. GIBBS	DATE	20190822

SEE PRODUCT SPECIFICATION PDINFO00 FOR SUPPLEMENTAL PRODUCT INFORMATION
DIMENSIONS ARE IN INCHES

ALL TOLERANCES $\pm .1/8"$ UNLESS OTHERWISE NOTED

REV			
DATE			
DESIGN			
MFG			
FIN			
ASSEMBLY			
APPROVED			
DATE			

Westinghouse ELECTRIC COMPANY LLC - NUCLEAR FUEL COLUMBIA, SC USA

SHIPPING PACKAGE LOOSE ROD PIPE

SCALE: 1:8 WEIGHTS: SEE DWG SHEET 2 OF 2

DWG NO: 10006E58

REV: E

BILL OF MATERIAL table with columns: REQ'D, ITEM, NOTE, IDENT, PART NAME, REFERENCE INFORMATION (SIZE). Rows include: 48 01 A HEX HEAD SCREW (3/4-10 X 1" LONG), 182 02 - BORAL PLATE SHOULDER BOLT (1/4-28), 24 03 - LOCK WASHER (3/4), 1 04 - UPPER OUTER SHELL (SXXN. 1), 1 05 - UPPER OUTER SHELL (SXXN. 2, BACK), 1 06 - UPPER INNER SHELL, 1 07 - UPPER OUTER HEAD (SXXN. 1), 1 08 - UPPER OUTER HEAD (SXXN. 2), 1 09 - LIMITER END CAP, 1 10 - END SEAM COVER, 1 11 - END SEAM COVER SPACER, 1 12 - BOTTOM SEAM COVER, 1 13 - BOTTOM SEAM COVER SPACER, 1 14 - LIMITER END CAP (SXXN. 1), 1 15 - LIMITER END CAP (SXXN. 2), 1 16 - BOTTOM INNER COVER, 2 17 - MODERATOR END COVER (RH), 2 18 - MODERATOR END COVER (LH), AR 19 - UPPER MODERATOR COVER - LG., AR 20 - UPPER MODERATOR COVER - SHORT, AR 21 - CERAMIC FIBER BLANKET, 1 22 - OUTER SHELL BACKING BAR - LG., AR 23 - 10 PCF FOAM (UPPER), 1 24 - 20 PCF FOAM (UPPER), AR 25 - CERAMIC PAPER, AR 26 - MODERATOR - UPPER UNIT, AR 27 - WELD STUD, AR 28 - WELD STUD HEX NUT, 6 29 - FHCS (1/2-13 X 1 1/2" LONG), 1 30 - LOWER INNER SHELL, 1 31 - LOWER OUTER SHELL - BACK, 1 32 - LOWER OUTER SHELL - FRONT, 1 33 - LOWER IMPACT LIMITER COVER, 1 34 - BACKER BAR - SHORT, 1 35 - LOWER IMPACT LIMITER COVER, 1 36 - FRONT CLOSURE LIP, 1 37 - FRONT HEAD, 1 38 - BACK HEAD, AR 39 - SHOCK MOUNT COVER, 12 40 - GUSSET PLATE, 1 41 - BACK FOAM COVER, AR 42 - MODERATOR - LOWER SXXN. 1, AR 43 - MODERATOR - LOWER SXXN. 2

BILL OF MATERIAL table with columns: REQ'D, ITEM, NOTE, IDENT, PART NAME, REFERENCE INFORMATION (SIZE). Rows include: AR 44 - MODERATOR - LOWER SXXN. 3, AR 45 - MODERATOR - LOWER SXXN. 4, AR 46 - MODERATOR - LOWER SXXN. 5, AR 47 - MODERATOR - LOWER SXXN. 6, 4 48 - END RIB MODERATOR COVER (RH), AR 49 - MODERATOR CENTER COVER, AR 50 - MODERATOR END COVER - UPPER, AR 51 - MODERATOR END COVER - LOWER, AR 52 - CERAMIC PAPER (LOWER), AR 53 - WELD STUD, AR 54 - WELD STUD HEX NUT, 14 55 - FHCS (1/2-13 X 3/4" LONG), AR 56 - 10 PCF FOAM (LOWER), AR 57 - 20 PCF FOAM (LOWER), AR 58 - CERAMIC FIBER BLANKET, 3 59 - STIFFENER WEB, 3 60 - BOTTOM STIFFENER FLANGE, 3 61 - TOP STIFFENER FLANGE, 6 62 - BUMPER PLATE, 4 63 - CROSS MEMBER, 4 64 - LEG, 1 65 - LOWER PILLOW BASE PLATE, 1 66 - LOWER PILLOW LIP, 1 67 - LOWER PILLOW SPUN HEAD - MIDDLE, 1 68 - LOWER PILLOW SOFT FOAM, 1 69 - LOWER PILLOW INSULATION, 1 70 - LOWER PILLOW SPUN HEAD - BASE, 1 71 - LOWER PILLOW SPUN HEAD - TOP, 1 72 - INSULATION - TOP, 12 73 - VENT PORT COUPLING, 12 74 - VENT PORT NPT PLUG, 3 75 - FLAT VENT PORT PLATE, 9 76 - BENT VENT PORT PLATE, AR 77 - BOLTING BLOCK BASE, AR 78 - BOLTING BLOCK CAP, 8 79 - SHELF SUPPORT PLATE, 8 80 - SHELF DOUBLER, 4 81 - LOCATOR PIN, 1 82 - TOP PILLOW COVER PLATE

BILL OF MATERIAL table with columns: REQ'D, ITEM, NOTE, IDENT, PART NAME, REFERENCE INFORMATION (SIZE). Rows include: 1 83 - TOP PILLOW SPUN HEAD - INNER, 1 84 - TOP PILLOW FOAM, 1 85 - TOP PILLOW BACK PLATE, AR 86 - HINGE, 1 87 - BASE EXTRUSION / MACHINING, 1 88 - BOTTOM PLATE, AR 89 - DOOR HINGE EXTRUSION, 14 90 - FHCS (1/2-13 X 1.25" LONG), AR 91 - WAVE WASHER, 2 92 B POISON PLATE - SIDE TOP END, 2 93 B COMPOSITE BORON PLATE, 2 94 B POISON PLATE - LOWER TOP END, 2 95 B POISON PLATE - LOWER BOTTOM END, 1 96 - VVER BASE ASSEMBLY, AR 97 - LATCH EXTRUSION SHORT / MACHINED, AR 98 - LATCH EXTRUSION SHORT W/HOLES / MACHINED, AR 99 - VVER LATCH HANDLE, 1 100 - AXIAL HOLDDOWN JAM NUT (5/8-11), AR 101 - LATCH EXTRUSION LONG / MACHINED, AR 102 - LATCH EXTRUSION LONG W/HOLES / MACHINED, 1 103 - LEFT DOOR EXTRUSION / MACHINED, 1 104 - VVER LEFT DOOR ASSEMBLY, 28 105 - FHCS (3/8-16 X 7/8" LONG), 1 106 - RIGHT DOOR EXTRUSION / MACHINED, 1 107 - VVER RIGHT DOOR ASSEMBLY, AR 108 - DOOR HINGE MACHINED SHORT, AR 109 - DOOR HINGE MACHINED LONG, AR 110 - LEFT DOOR BOTTOM SHEAR LIP, AR 111 - HINGE PIN A, AR 112 - HINGE PIN B, AR 113 - HINGE PIN C, AR 114 - VVER LATCH NUT, AR 115 - VVER LATCH RETAINER, AR 116 - VVER LATCH HEX BOLT (1/2-20 X 1/2" LG.), 1 117 - TOP PLATE, 1 118 - TOP SHEAR LIP, 1 119 - AXIAL HOLD DOWN PLATE, 2 120 B POISON PLATE - LEFT DOOR, 1 121 B POISON PLATE - RIGHT DOOR TOP END, 1 122 B POISON PLATE - RIGHT DOOR BOTTOM END, 1 123 - RIGHT DOOR BOTTOM SHEAR LIP, 2 124 - TOP PLATE LOCKING KNOB, 6 125 - FHCS (1/2-13 X 3/4" LONG), 83 126 - FHCS (3/8-16 X 5/8" LONG), 2 127 - LOCKING KNOB SHOULDER BOLT, 1 128 - VVER TOP PLATE ASSEMBLY, 14 129 - FHCS (1/2-13 X 7/8" LONG), AR 130 - HINGE PIN, 1 131 - TOP PLATE COVER A, 1 132 - TOP PLATE COVER B, 10 133 - VVER CLAMHELL MOUNTING BRACKET - MIDDLE, 2 134 - VVER CLAMHELL MOUNTING BRACKET - RIGHT, 2 135 - VVER CLAMHELL MOUNTING BRACKET - LEFT, 1 136 - AXIAL HOLDDOWN BOLT (5/8-11)

- NOTES:
A. UPPER OUTERPACK HINGE BOLTS TORQUED TO 60 FT-LB (- 5 FT-LB) PRIOR TO SHIPPING. LOWER OUTERPACK HINGE BOLTS TORQUED TO 20 FT-LB (± 1 FT-LB) PRIOR TO TACK WELDING.
B. THE LAMINATE/COMPOSITE POISON PLATE (BORAL) SHALL POSSESS A MINIMUM AREAL DENSITY OF [] OF B-10. THE POISON PLATE THICKNESS SHALL BE []
C. WELDING SHALL BE PER ASME SECTION IX .
D. 302, 303, 304L, 316 AND 316L STAINLESS STEELS ARE ACCEPTABLE FOR ALL ASSEMBLY 304 SST FASTENERS AND SUB - ASSEMBLY 304 SST FASTENERS.
E. ASTM B221 6005A-T61 ALUMINUM IS AN ACCEPTABLE SUBSTITUTE FOR ASTM B209/B221 6005-T5 ALUMINUM.

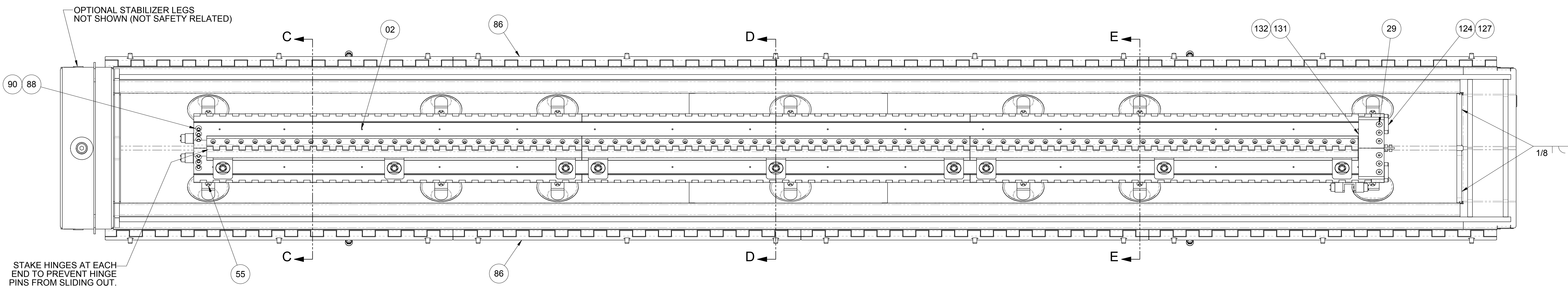
TOLERANCES (UNLESS OTHERWISE NOTED) table with columns: DECIMAL: 2 PLACES, DECIMAL: 3 PLACES, ANGULAR: ± 2, UNDER 6 IN., 6-12 IN., 12-24 IN., OVER 24 IN.

MAXIMUM PACKAGE ESTIMATED WEIGHTS
TRAVELLER VVER:
LOADED - 5105 LBS
EMPTY - 3255 LBS

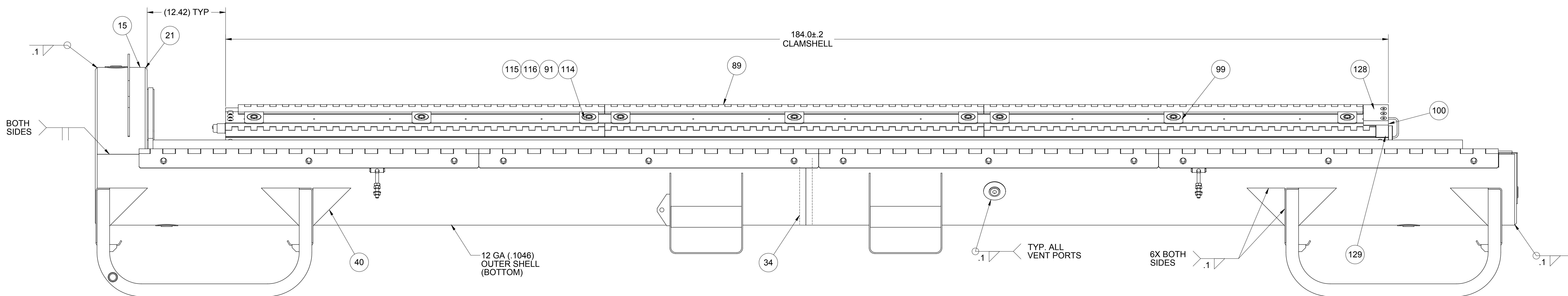
Revision table with columns: SO, WERDEY, ECN, 0002396-0, ZNE, DC, DESCRIPTION, BUD, 128779, ECN, 0003024-0, AT, BT, EDITED NOTES, DWG BY, C. GIBBS, 20150925, BUD, 128779, ECN, 0003184-0, ZNE, DC, DESCRIPTION, ADDED NOTE E, EDITED BILL OF MATERIAL, DWG BY, C. GIBBS, 20150922

SEE PRODUCT SPECIFICATION PDINP000 FOR SUPPLEMENTAL PRODUCT INFORMATION
DIMENSIONS ARE IN INCHES
THIRD ANGLE PROJECTION

WESTINGHOUSE logo, SAFETY RELATED ITEMS TRAVELLER VVER, PART NO. 10037E43, SHEET 1 OF 8, DATE, C. GIBBS, 2012/06/28, G. HILL, 2012/07/04, B. HEMPY, 2012/04/19, S. PALMER, 2012/04/23, B. JOYNER, 2012/05/22, D. ROWLAND, 2012/05/22, R. MAURER, 2012/04/24, J. HALLIGAN, 2012/04/24, J. RANDOLPH, 2012/04/20, SCALE 1:1, WEIGHT(LBS) -



LOWER OUTERPACK ASSEMBLY
VVER CLAMSHELL INSTALLED
(SEE SHEET 4 FOR SECTION VIEWS)



1	SO WVERDEV	ECN 0002396-0	DESCRIPTION
2	BUD12879	ECN 0003024-0	DESCRIPTION
3	DRAWN BY C. GIBBS	2015/02/25	DESCRIPTION
	BUD12879	ECN 0003156-0	DESCRIPTION
	DRAWN BY C. GIBBS	2015/02/22	DESCRIPTION

SEE PRODUCT SPECIFICATION
PDIN000 FOR SUPPLEMENTAL
PRODUCT INFORMATION
DIMENSIONS ARE IN INCHES

DATE	C. GIBBS	2012/06/28		ELECTRIC COMPANY LLC, NUCLEAR FUEL COLUMBIA, SC USA
DATE	G. HILL	2012/07/04		
DATE	B. HEMPY	2012/04/19	SAFETY RELATED ITEMS TRAVELLER VVER	
DATE	S. PALMER	2012/04/23		
DATE	B. JOYNER	2012/05/22		
DATE	D. ROWLAND	2012/05/22		
DATE	R. MAURER	2012/04/24	TITL TRCH NO E	DWG NO 10037E43
DATE	J. HALLIGAN	2012/04/24	SCALE 1:6	SHEET 3 OF 8
DATE	J. RANDOLPH	2012/04/20		

8

7

6

5

4

3

2

1

H

G

F

E

D

C

B

A

H

G

F

E

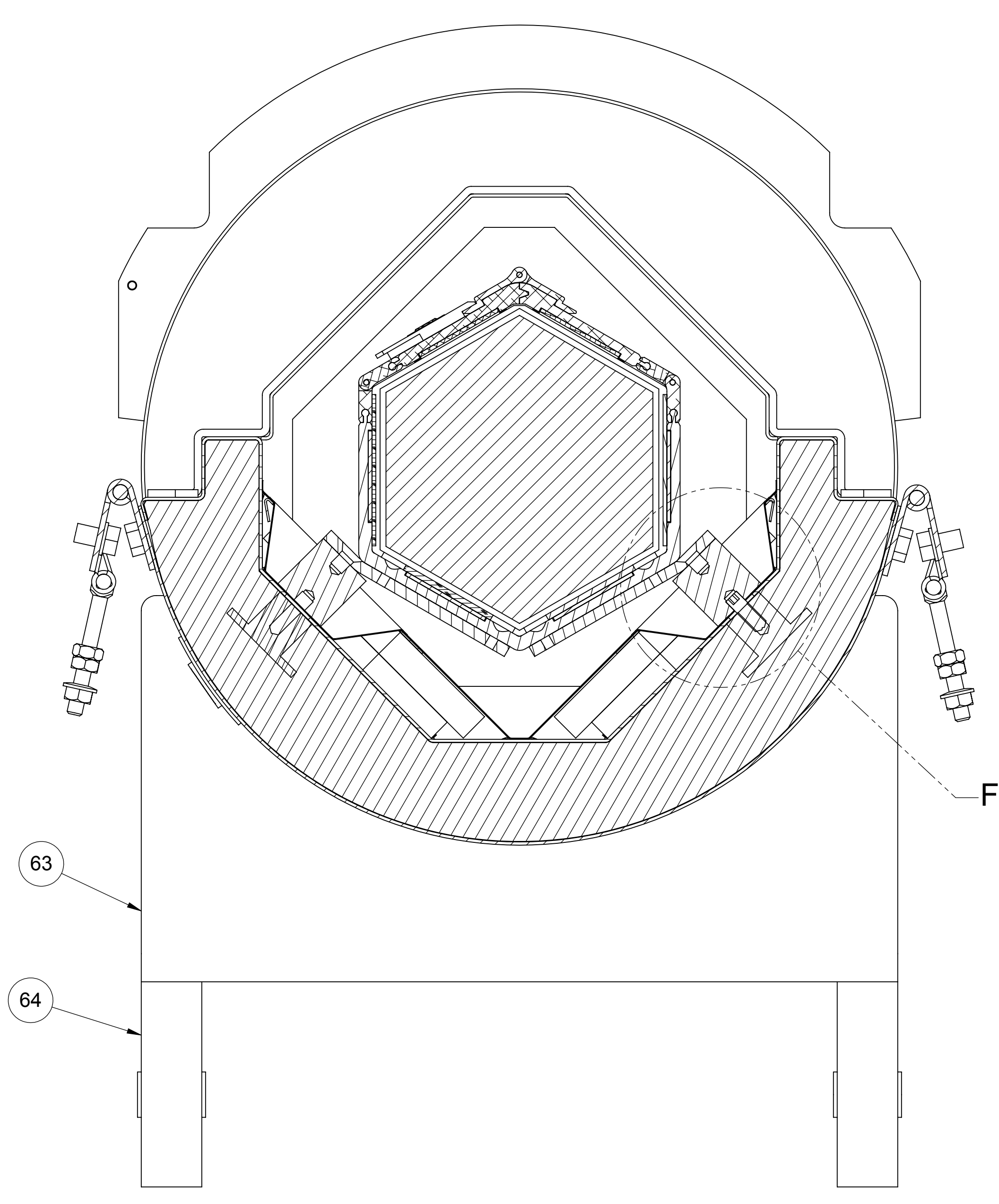
D

C

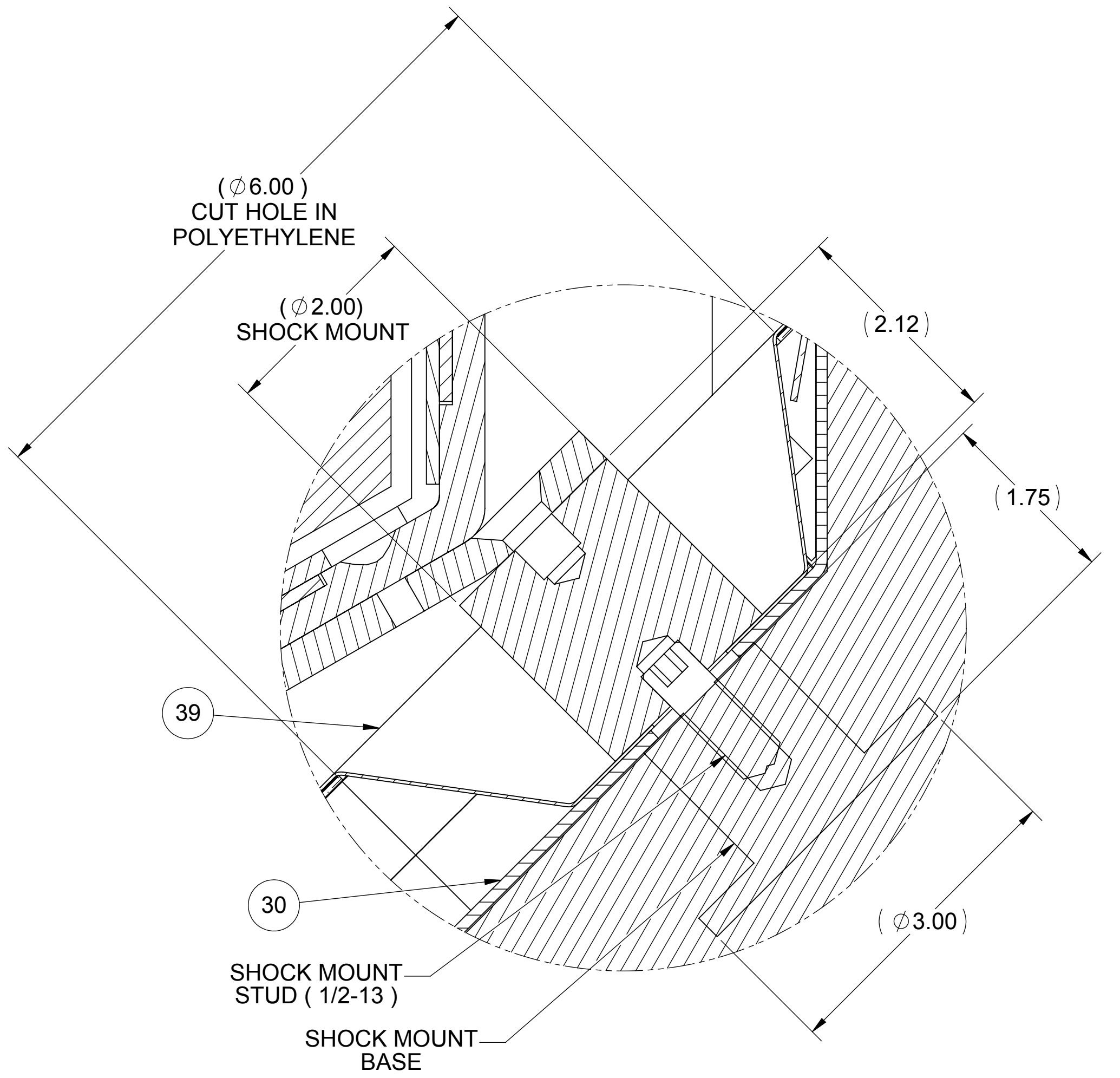
B

A

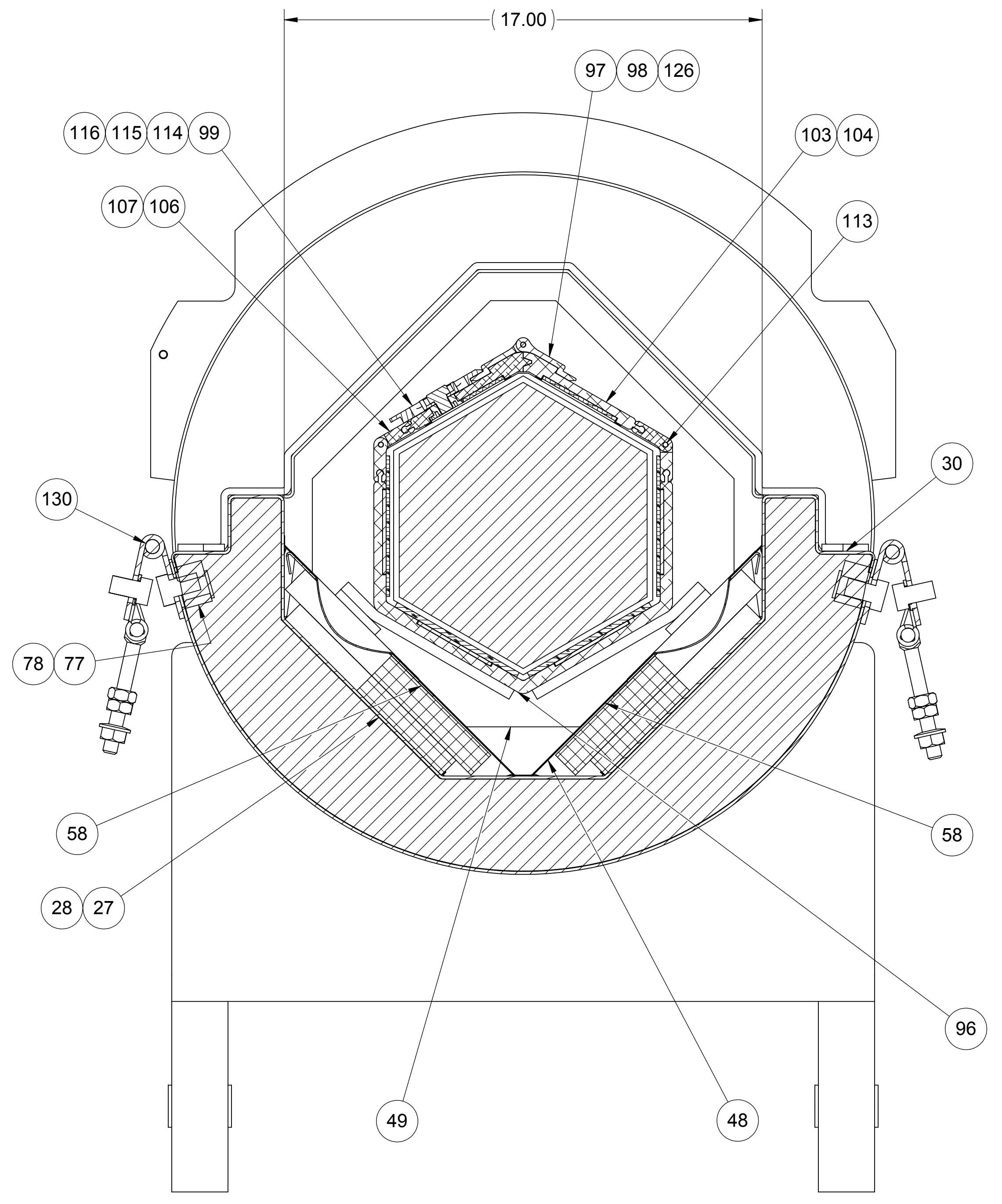
Westinghouse Non-Proprietary Class 3



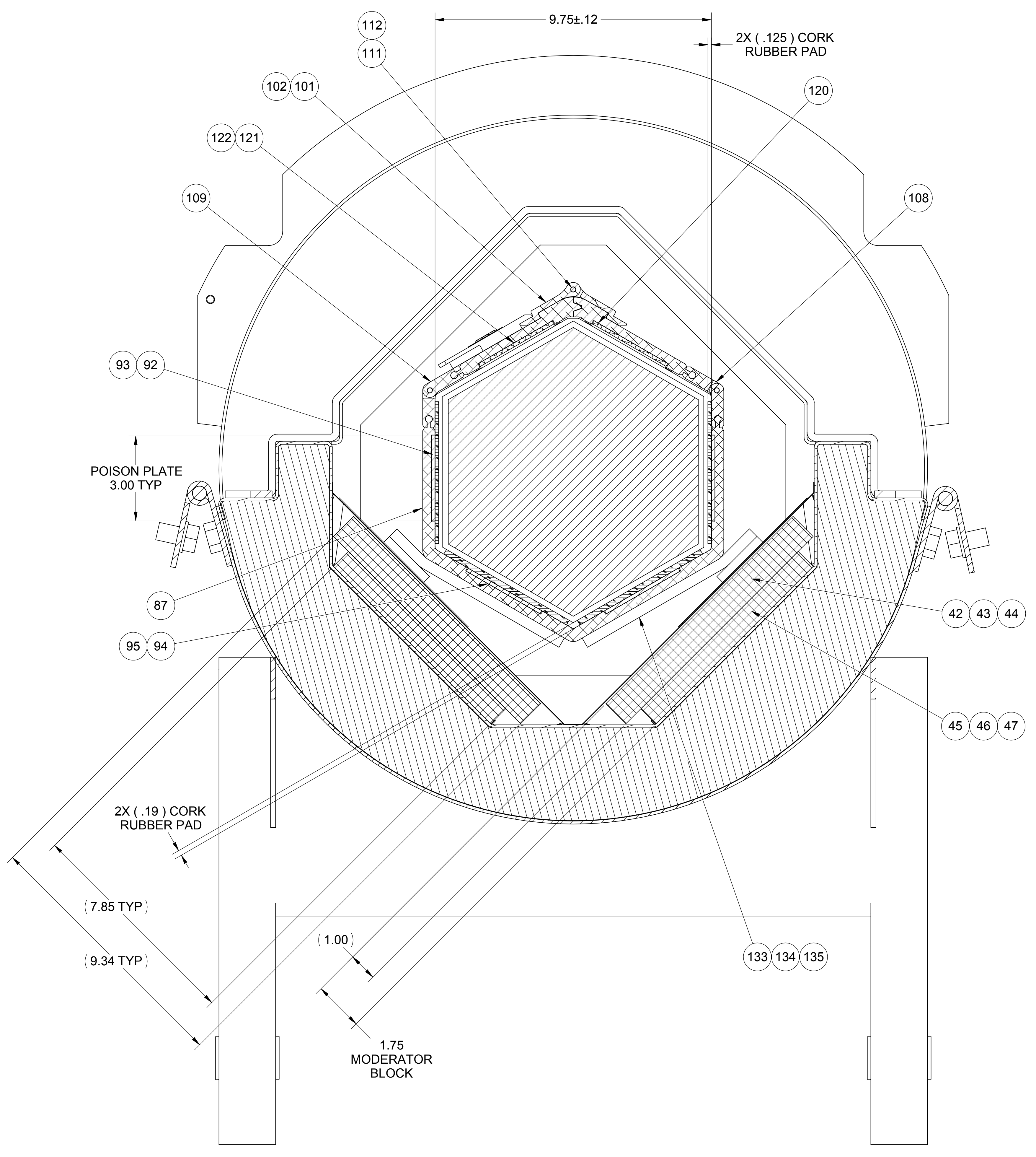
SECTION E-E



DETAIL F
SCALE 1 : 1
SHOCK MOUNT, SHOCK MOUNT STUD
& SHOCK MOUNT BASE ARE NOT IN BOM



SECTION D-D



SECTION C-C
SCALE 1 : 2

1	SO WVERDEV	ECN 0002396-0	DESCRIPTION
2	ZNE DC	BUD128779	DESCRIPTION
3	ECN 0003024-0	DESCRIPTION	SEE SHEET 1 FOR CHANGES.
	DRAWN BY	C. GIBBS	2015/09/25
	BUD128779	DESCRIPTION	EDITED BALLOONS.
	ECN 0003156-0	DESCRIPTION	
	DRAWN BY	C. GIBBS	2015/09/22

SEE PRODUCT SPECIFICATION PDIN000 FOR SUPPLEMENTAL PRODUCT INFORMATION
DIMENSIONS ARE IN INCHES

DWG REF -
NEXT ASSY -

THIRD ANGLE PROJECTION

DATE	C. GIBBS	2012/06/28		ELECTRIC COMPANY LLC - NUCLEAR FUEL COLUMBIA, SC USA							
DATE	G. HILL	2012/07/04									
DESIGN	B. HEMPY	2012/04/19	SAFETY RELATED ITEMS TRAVELLER VVER								
DESIGN	S. PALMER	2012/04/23									
DESIGN	B. JOYNER	2012/05/22									
DESIGN	D. ROWLAND	2012/05/22									
DESIGN	R. MAURER	2012/04/24									
APPROV	J. HALLIGAN	2012/04/24	<table border="1"> <tr> <td>SCALE</td> <td>1:3</td> </tr> </table>	SCALE	1:3	<table border="1"> <tr> <td>DWG NO</td> <td>10037E43</td> </tr> </table>	DWG NO	10037E43	<table border="1"> <tr> <td>SHEET</td> <td>4 OF 8</td> </tr> </table>	SHEET	4 OF 8
SCALE	1:3										
DWG NO	10037E43										
SHEET	4 OF 8										
APPROV	J. RANDOLPH	2012/04/20	SOLIDWORKS DRAWING DO NOT REVISE MANUALLY © 2015 Westinghouse Electric Company LLC All Rights Reserved								

8

7

6

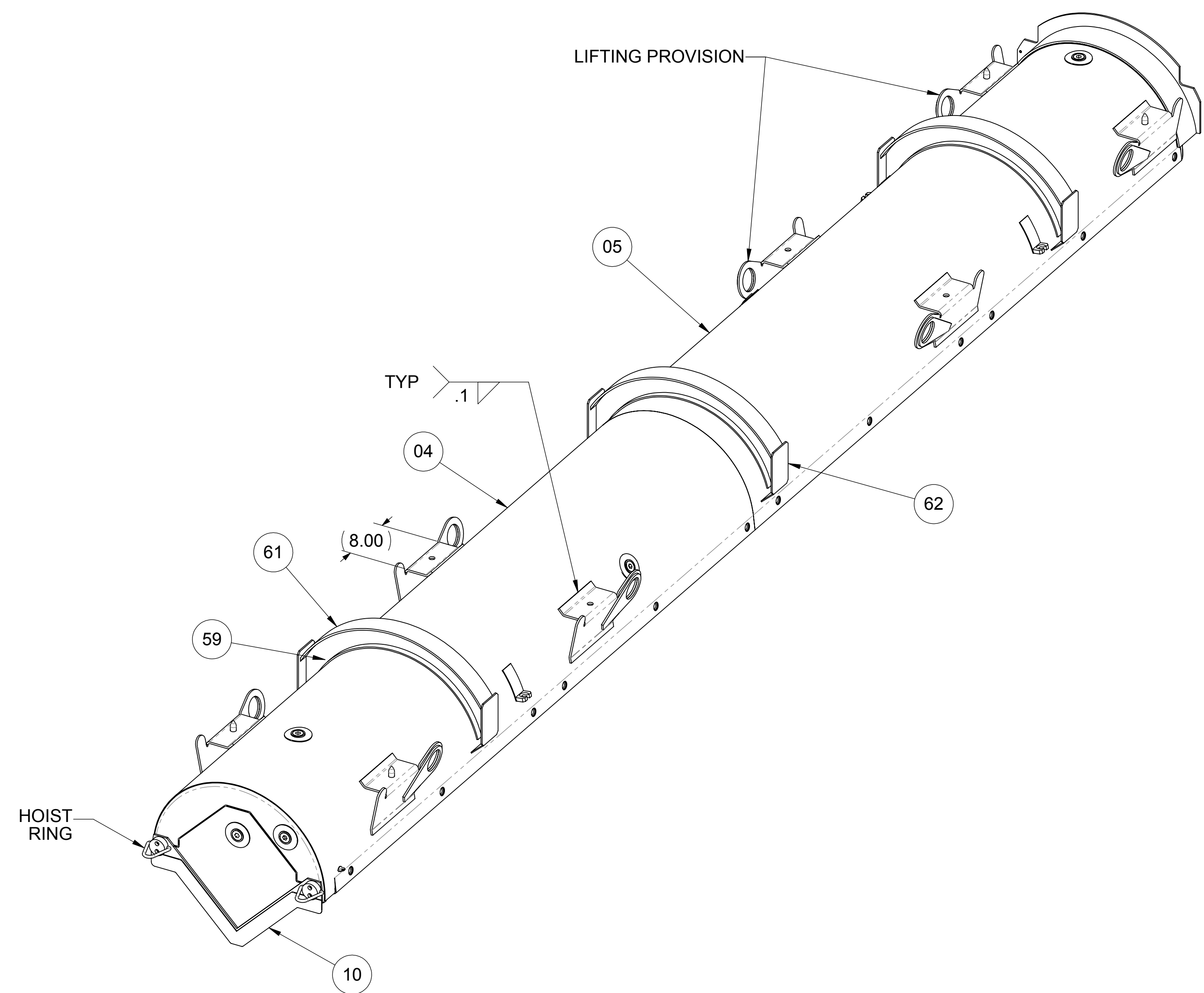
5

4

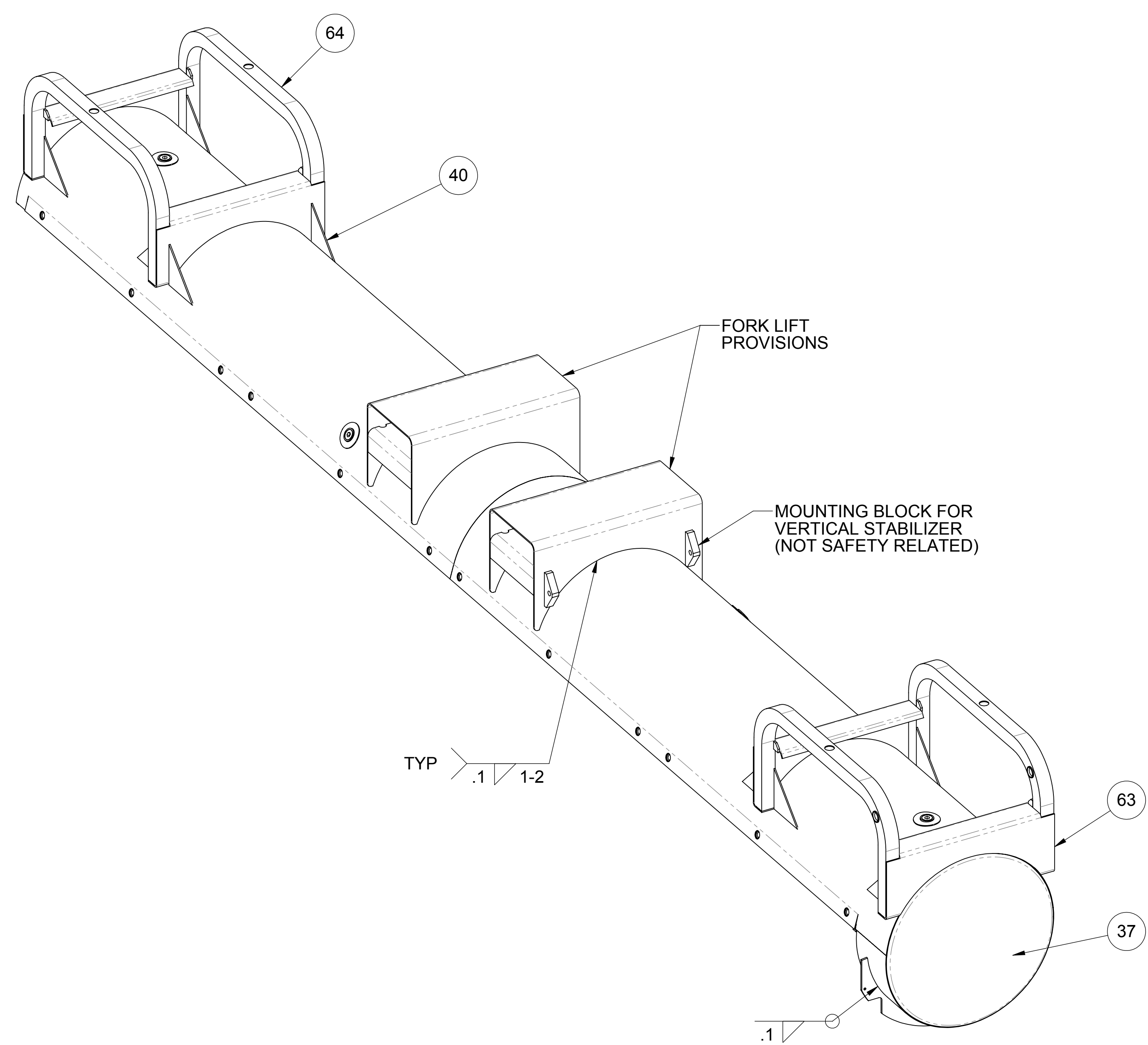
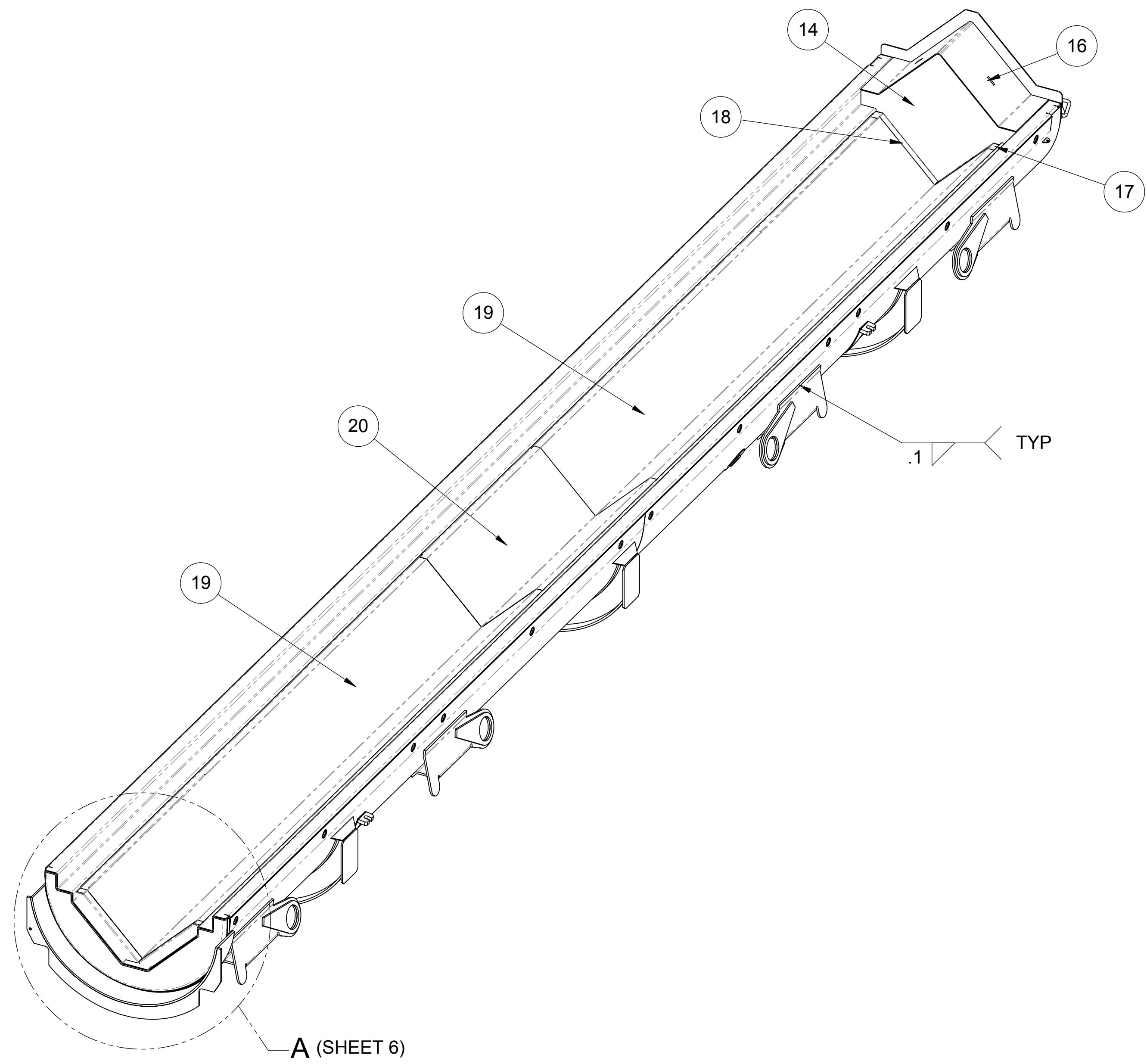
3

2

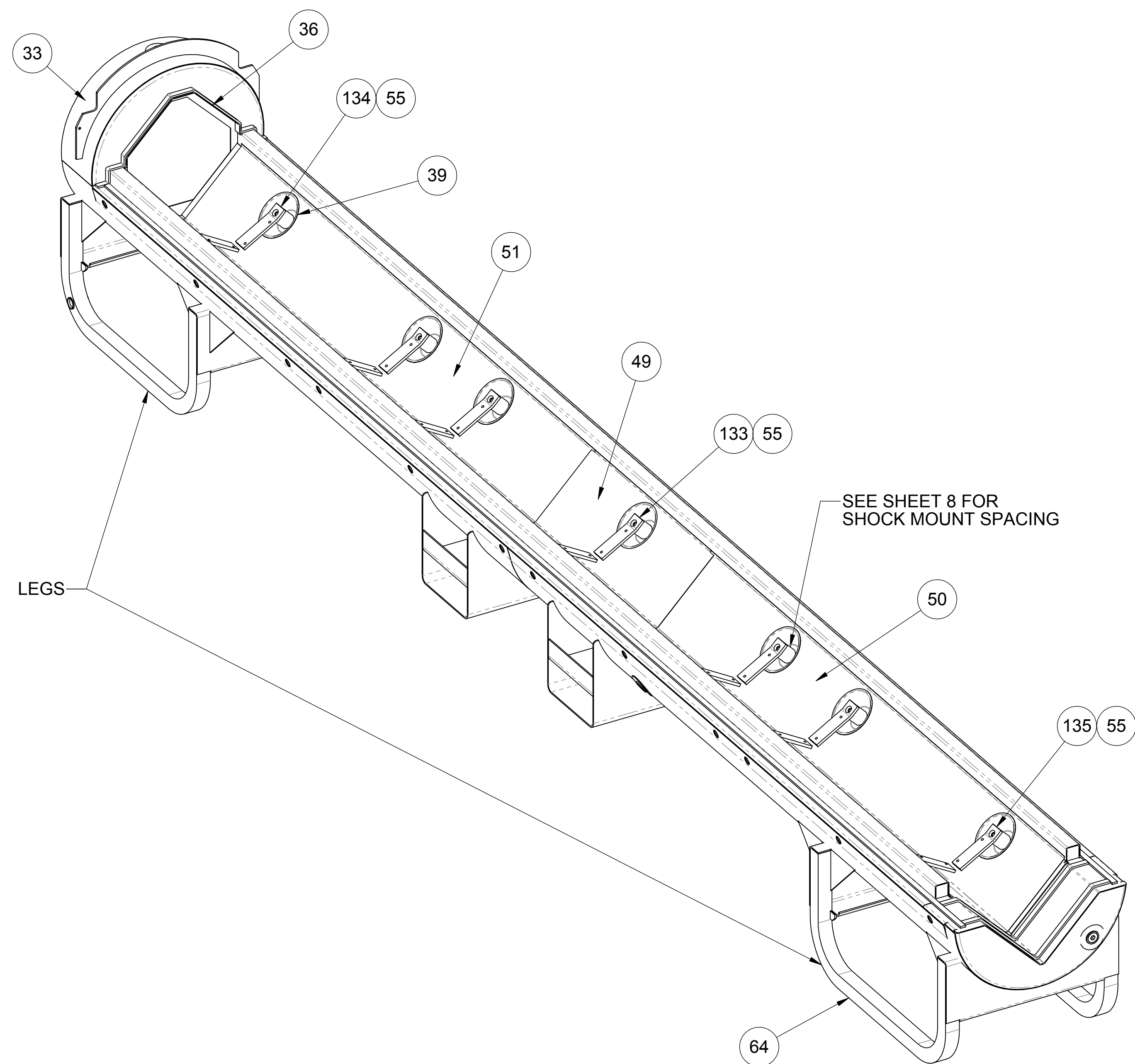
1



UPPER OUTERPACK DETAIL



LOWER OUTERPACK DETAIL



1	SO WVERDEV	ECN 0002396-0	DESCRIPTION
2	ZNE DC	BUD128779	DESCRIPTION
	ECN 0003024-0		DESCRIPTION
			SEE SHEET 1 FOR CHANGES.
3	DRAWN BY C. GIBBS	2015/02/25	
	BUD128779		DESCRIPTION
	ECN 0003156-0		DESCRIPTION
			SEE SHEET 6 AND 7 FOR CHANGES.
	DRAWN BY C. GIBBS	2015/02/22	

SEE PRODUCT SPECIFICATION PDINF000 FOR SUPPLEMENTAL PRODUCT INFORMATION
DIMENSIONS ARE IN INCHES

DWG REF	THIRD ANGLE PROJECTION
NEXT ASSY	

DATE	2012/06/28	Westinghouse	ELECTRIC COMPANY LLC - NUCLEAR FUEL COLUMBIA, SC USA
DRWD	2012/07/04		
DESIGN	2012/04/19	SAFETY RELATED ITEMS TRAVELLER VVER	
MISNG	2012/04/23		
PRDNG	2012/05/22		
DESIGN	2012/05/22		
APVD	2012/04/24	SCALE	1:10
APVD	2012/04/24	WEIGHTS	
APVD	2012/04/20		

10037E43	3
SHEET 5 OF 8	

8

7

6

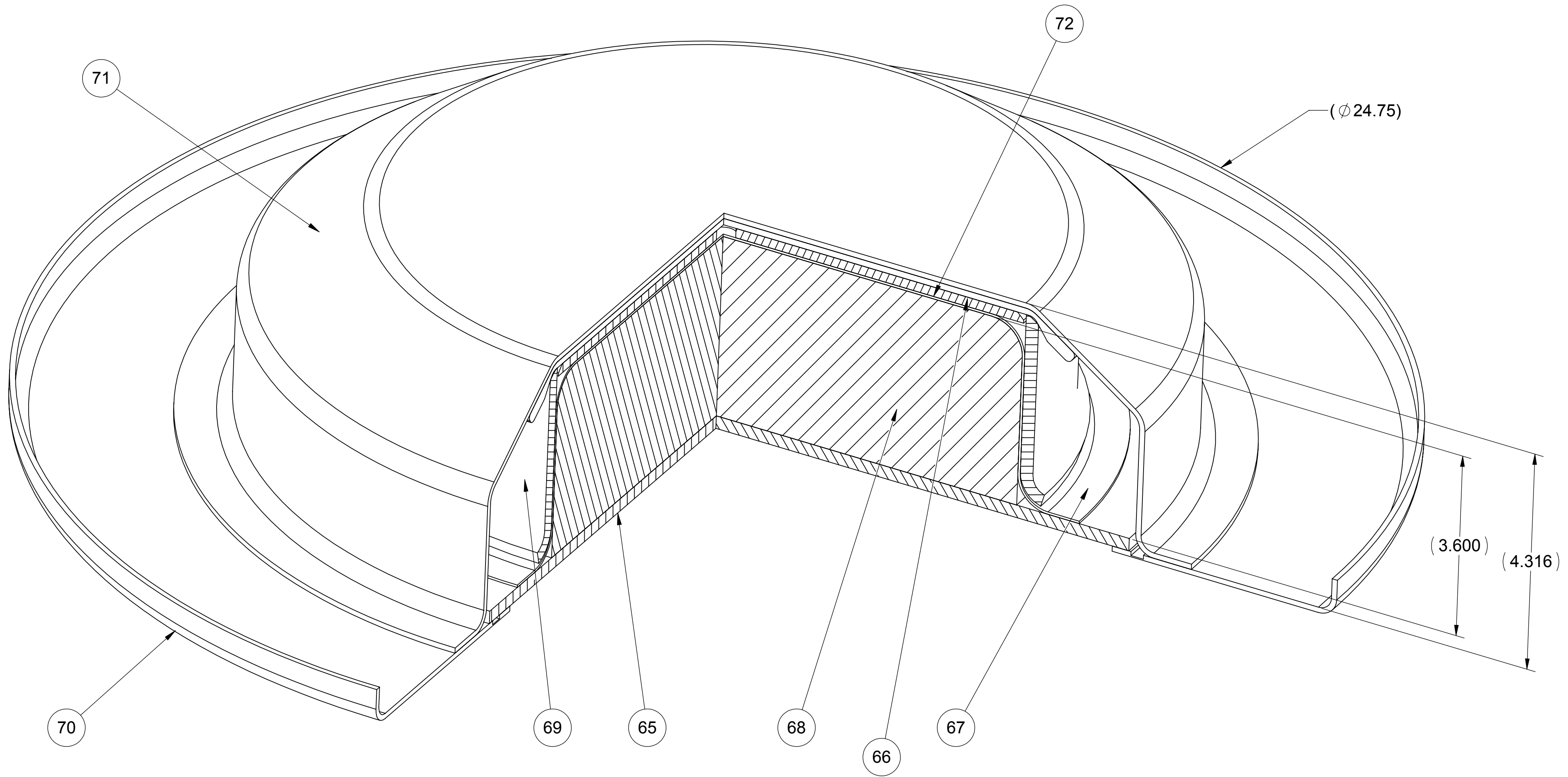
5

4

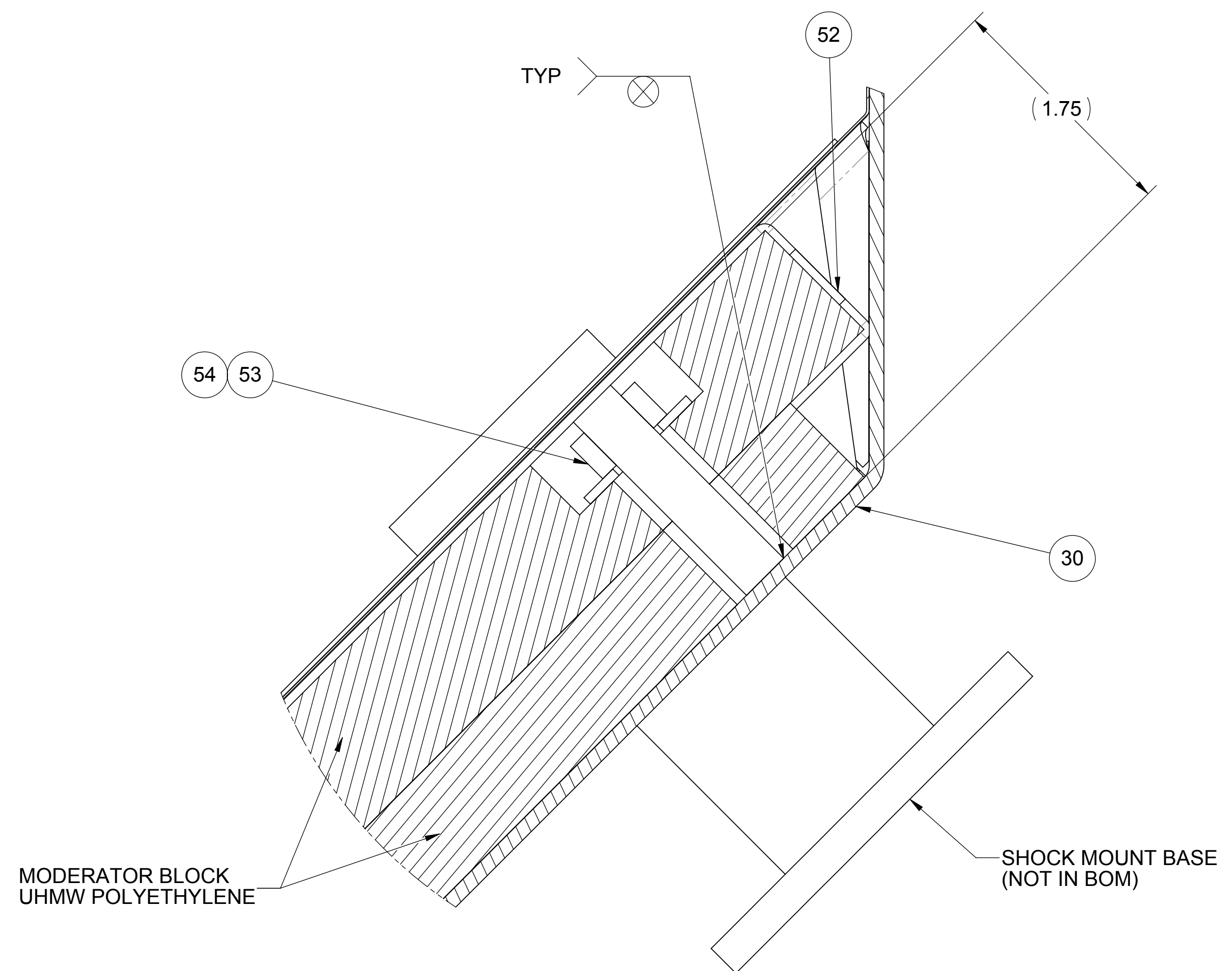
3

2

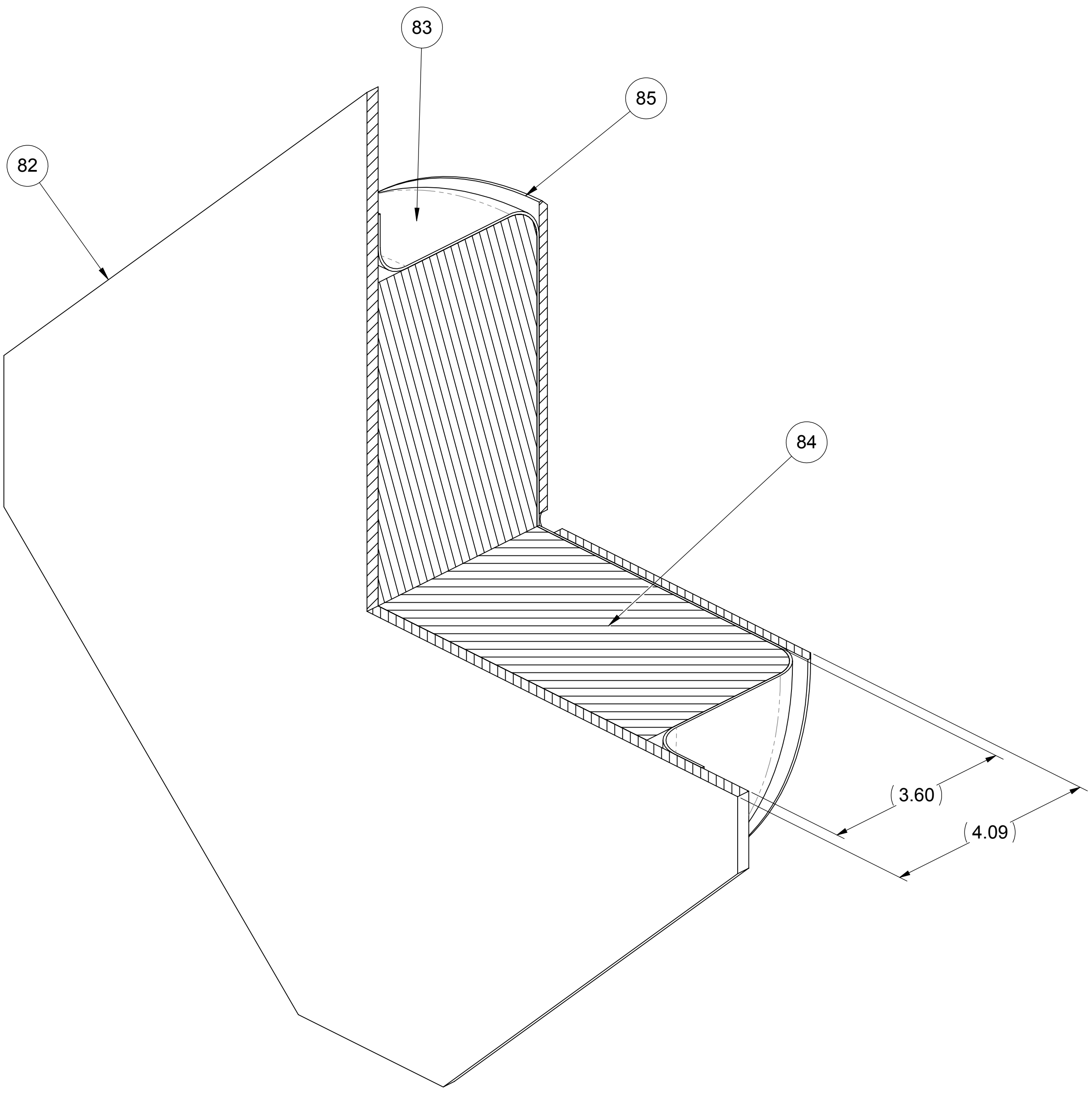
1



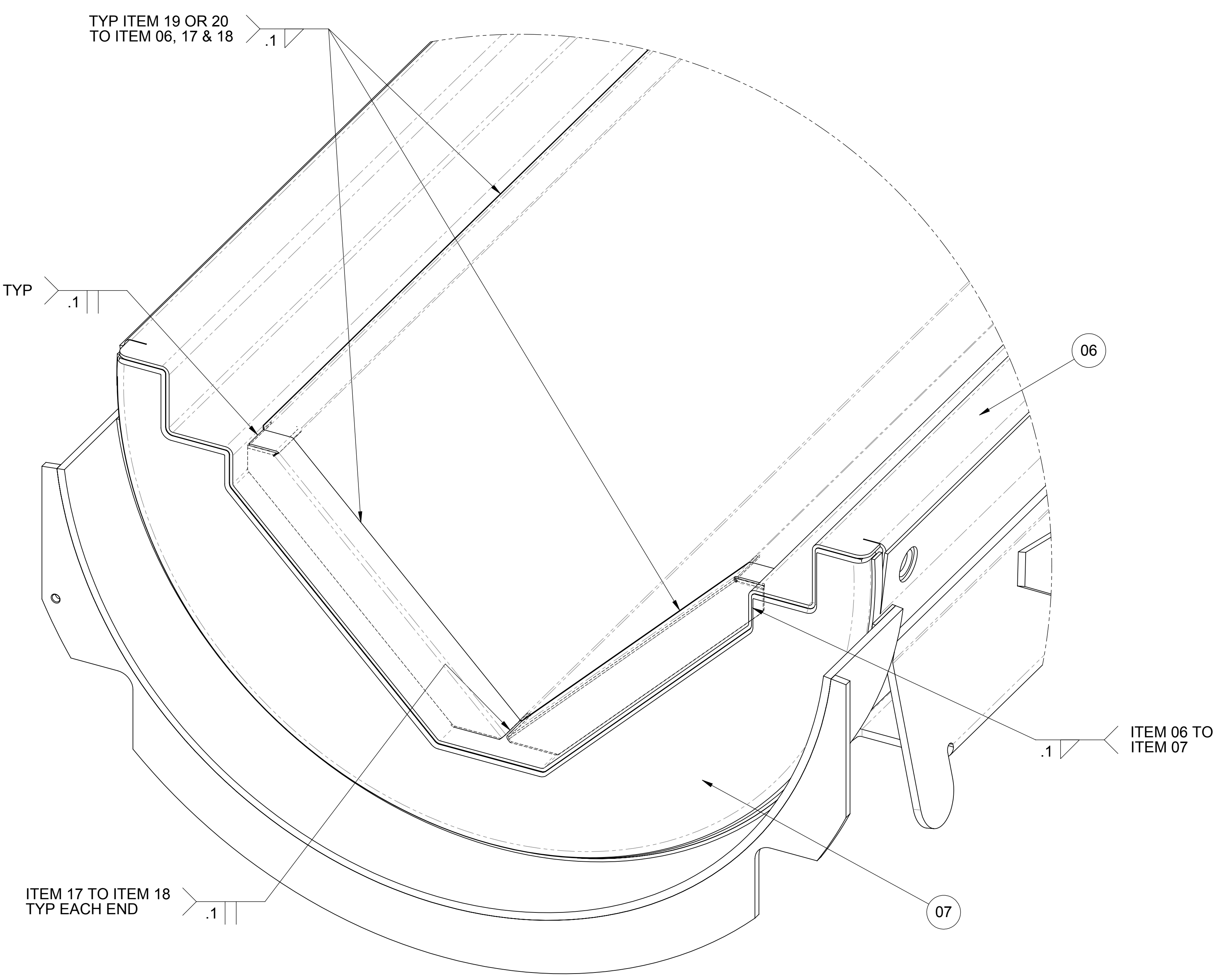
LOWER PILLOW
SUB-ASSEMBLY
SCALE 3 : 4



MODERATOR BLOCK
INSTALLATION
SCALE 3 : 2

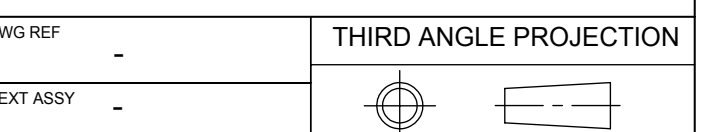


TOP PILLOW
SUB-ASSEMBLY
SCALE 3 : 4



DETAIL A

SEE PRODUCT SPECIFICATION
PDIN000 FOR SUPPLEMENTAL
PRODUCT INFORMATION
DIMENSIONS ARE IN INCHES



DATE	C. GIBBS	2012/06/28		ELECTRIC COMPANY LLC, NUCLEAR FUEL COLUMBIA, SC USA
DRAWN	G. HILL	2012/07/04		
DESIGNED	B. HEMPY	2012/04/19	SAFETY RELATED ITEMS TRAVELLER VVER	
REVISION	S. PALMER	2012/04/23		
APPROVED	B. JOYNER	2012/05/22		
DESIGNED	D. ROWLAND	2012/05/22		
APPROVED	R. MAURER	2012/04/24	SCALE	1:2
APPROVED	J. HALLIGAN	2012/04/24	WEIGHT	
APPROVED	J. RANDOLPH	2012/04/20	ITEM NO	10037E43
			SHEET	6 OF 8

SO	WVERDEV	0002396-0
ZONE	DC	DESCRIPTION
BUD	128779	
ECN	0003024-0	
ZONE	DC	DESCRIPTION
		SEE SHEET 1 FOR CHANGES.
DRAWN BY	C. GIBBS	2015/02/25
BUD	128779	
ECN	0003156-0	
ZONE	DC	DESCRIPTION
		FAST BALLOON FOR ITEM 06
DRAWN BY	C. GIBBS	2015/02/22

8

7

6

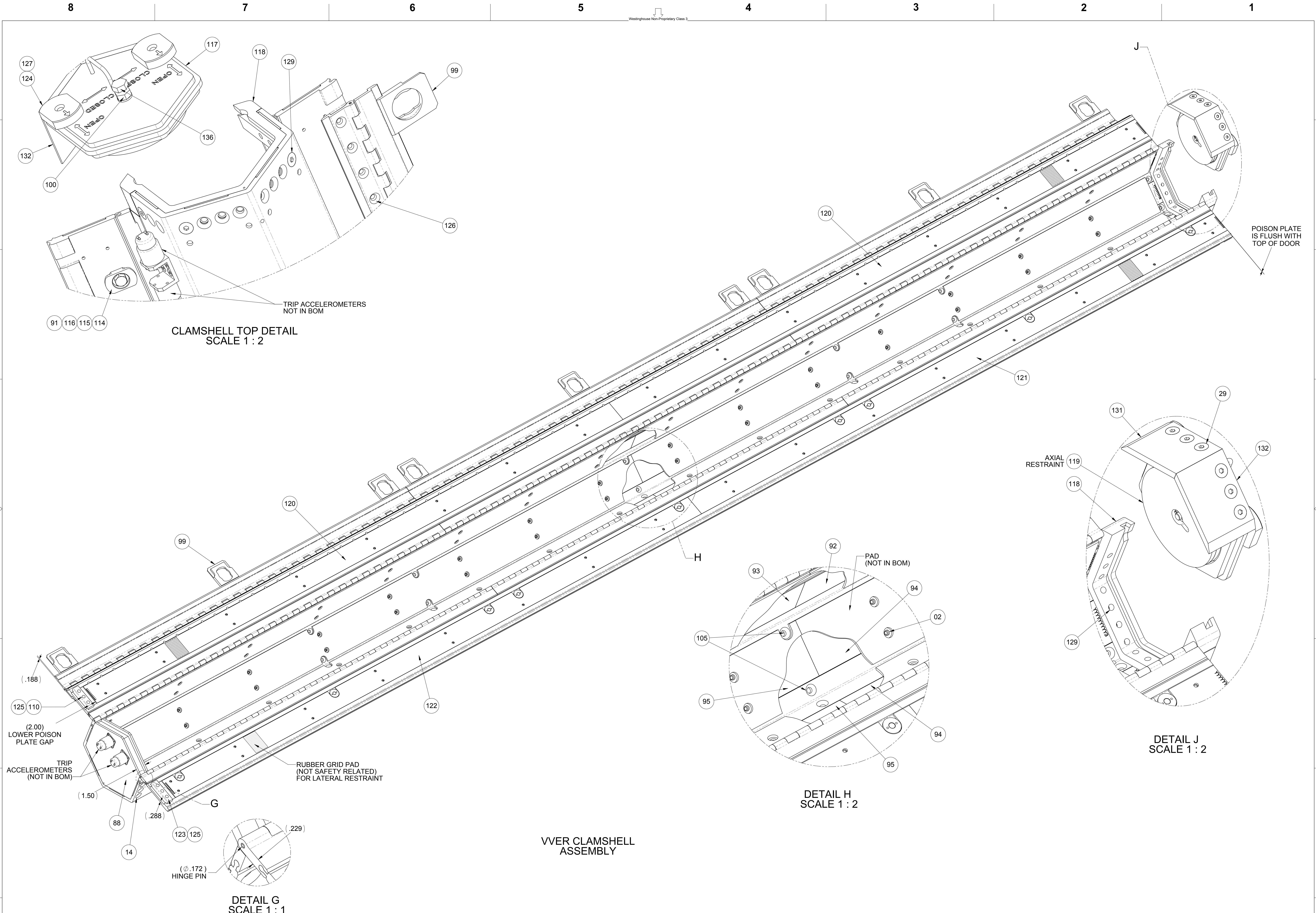
5

4

3

2

1



CLAMSHELL TOP DETAIL
SCALE 1 : 2

DETAIL J
SCALE 1 : 2

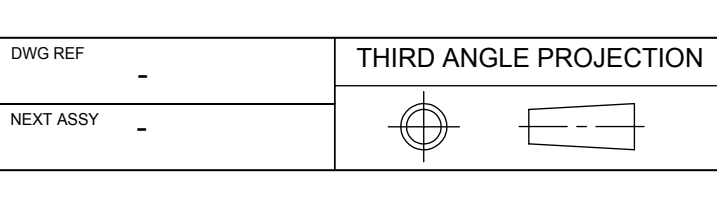
DETAIL H
SCALE 1 : 2

DETAIL G
SCALE 1 : 1

VVER CLAMSHELL
ASSEMBLY

1	SO	WVERDEV	0002396-0	DESCRIPTION
2	ZNE	DC	BUD128779	DESCRIPTION
3	ECN	0003024-0	DESCRIPTION	SEE SHEET 1 FOR CHANGES.
4	ZNE	DC	ADDED BALLOON.	DESCRIPTION
5	ECN	0003184-0	DESCRIPTION	ADDED BALLOON.
6	ZNE	DC	ADDED BALLOON.	DESCRIPTION
7	ECN	0003184-0	DESCRIPTION	ADDED BALLOON.
8	ZNE	DC	ADDED BALLOON.	DESCRIPTION

SEE PRODUCT SPECIFICATION PDIN000 FOR SUPPLEMENTAL PRODUCT INFORMATION
DIMENSIONS ARE IN INCHES

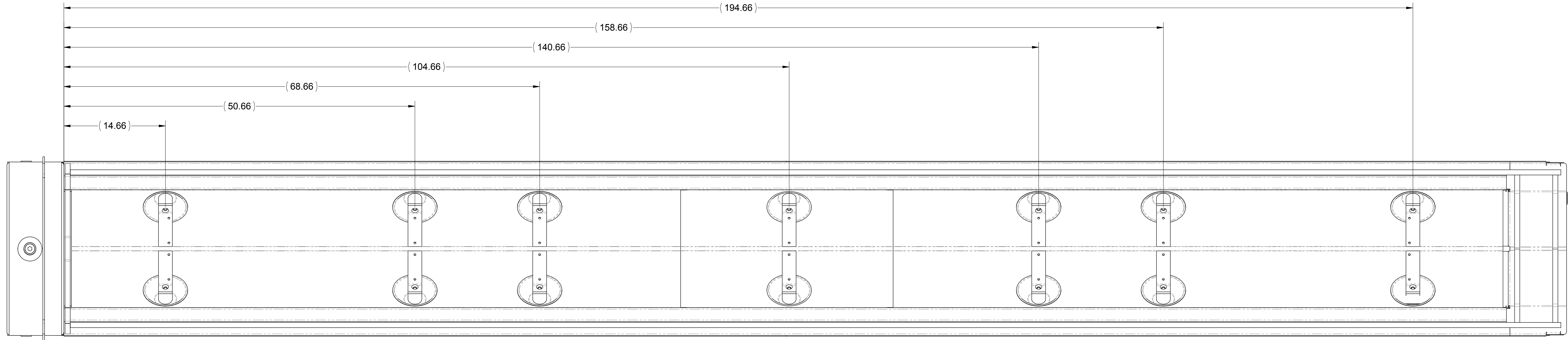


DATE	2012/06/28	DESIGNED BY	C. GIBBS
DATE	2012/07/04	DESIGNED BY	G. HILL
DATE	2012/04/19	DESIGNED BY	B. HEMPY
DATE	2012/04/23	DESIGNED BY	S. PALMER
DATE	2012/05/22	DESIGNED BY	B. JOYNER
DATE	2012/05/22	DESIGNED BY	D. ROWLAND
DATE	2012/04/24	DESIGNED BY	R. MAURER
DATE	2012/04/24	DESIGNED BY	J. HALLIGAN
DATE	2012/04/20	DESIGNED BY	J. RANDOLPH

Westinghouse ELECTRIC COMPANY LLC - NUCLEAR FUEL COLUMBIA, SC USA

SAFETY RELATED ITEMS TRAVELLER VVER

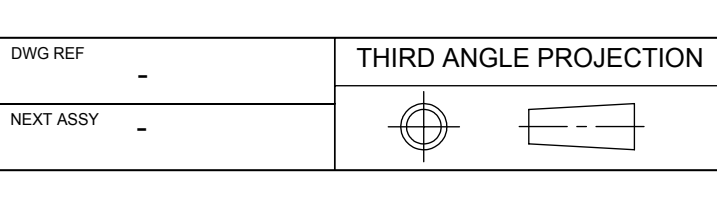
SCALE: 1:4
WEIGHTS: -
SHEET 7 OF 8



SHOCK MOUNT SPACING

1	SO WVERDEV	ECN 0002396-0	DESCRIPTION
2	BUD12879	ECN 0003024-0	DESCRIPTION
3	DWN BY C. GIBBS	20150225	DESCRIPTION
	BUD12879	ECN 0003156-0	DESCRIPTION
	DWN BY C. GIBBS	20150922	DESCRIPTION

SEE PRODUCT SPECIFICATION PDINFO00 FOR SUPPLEMENTAL PRODUCT INFORMATION
DIMENSIONS ARE IN INCHES



DATE	C. GIBBS	2012/06/28		ELECTRIC COMPANY LLC, NUCLEAR FUEL COLUMBIA, SC USA
DATE	G. HILL	2012/07/04		
DESIGN	B. HEMPHY	2012/04/19	SAFETY RELATED ITEMS TRAVELLER VVER	
DESIGN	S. PALMER	2012/04/23		
DATE	B. JOYNER	2012/05/22		
DATE	D. ROWLAND	2012/05/22		
DATE	R. MAURER	2012/04/24	SCALE	1:6
DATE	J. HALLIGAN	2012/04/24	WEIGHT(LBS)	
DATE	J. RANDOLPH	2012/04/20	SCALE	1:6

10037E43
SHEET 8 OF 8

TABLE OF CONTENTS

2.0	STRUCTURAL EVALUATION.....	2-1
2.1	Description of Structural Design.....	2-1
2.1.1	Discussion.....	2-1
2.1.2	Design Criteria.....	2-3
2.1.2.1	Basic Design Criteria.....	2-3
2.1.2.2	Miscellaneous Structural Failure Modes.....	2-3
2.1.3	Weights and Centers of Gravity.....	2-4
2.1.4	Identification of Codes and Standards for Package Design.....	2-4
2.2	Materials.....	2-5
2.2.1	Material Properties and Specifications.....	2-5
2.2.2	Chemical, Galvanic, or Other Reactions.....	2-5
2.2.3	Effects of Radiation on Materials.....	2-5
2.3	Fabrication and Examination.....	2-7
2.3.1	Fabrication.....	2-7
2.3.2	Examination.....	2-7
2.4	Lifting and Tie-down Standards for All Packages.....	2-8
2.4.1	Lifting Devices.....	2-8
2.5	General Considerations.....	2-9
2.5.1	Evaluation by Test.....	2-9
2.5.2	Evaluation by Analysis.....	2-11
2.6	Normal Conditions of Transport.....	2-12
2.6.1	Heat.....	2-12
2.6.1.1	Summary of Pressures and Temperatures.....	2-12
2.6.1.2	Differential Thermal Expansion.....	2-12
2.6.1.3	Stress Calculations.....	2-12
2.6.1.4	Comparison with Allowable Stresses.....	2-13
2.6.2	Cold.....	2-13
2.6.3	Reduced External Pressure.....	2-13
2.6.4	Increased External Pressure.....	2-13
2.6.5	Vibration.....	2-13
2.6.6	Water Spray.....	2-14A
2.6.7	Free Drop.....	2-14A
2.6.8	Corner Drop.....	2-15
2.6.9	Compression – Stacking Test.....	2-15
2.6.10	Penetration.....	2-15
2.7	Hypothetical Accident Conditions.....	2-16
2.7.1	Free Drop.....	2-23
2.7.1.1	Technical Basis for the Free Drop Tests.....	2-23
2.7.1.2	Test Sequence for the Selected Tests.....	2-24
2.7.1.3	Summary of Results from the Free Drop Tests.....	2-24
2.7.2	Crush.....	2-24
2.7.3	Puncture.....	2-25

TABLE OF CONTENTS (cont)

2.7.3.1	Technical Basis for the Puncture Drop Tests	2-25
2.7.3.2	Summary of Results from the Puncture Drop Test	2-26
2.7.4	Thermal.....	2-26
2.7.4.1	Summary of Pressures and Temperatures	2-27
2.7.4.2	Differential Thermal Expansion.....	2-27
2.7.4.3	Stress Calculations	2-27
2.7.4.4	Comparison with Allowable Stresses.....	2-27
2.7.5	Immersion – Fissile Material	2-27
2.7.6	Immersion – All Packages	2-28
2.7.7	Summary of Damage	2-28
2.8	Accident Conditions for Air Transport of Plutonium.....	2-29
2.9	Accident Conditions for Fissile Material for Air Transport.....	2-30
2.10	Special Form.....	2-31
2.11	Fuel Rods.....	2-32
2.11.1	Rod Pipe.....	2-32
2.12	Appendices	2-33
2.12.1	References	2-33
2.12.2	Container Weights and Centers of Gravity	2-34
2.12.2.1	Container Weights	2-34
2.12.2.2	Centers of Gravity	2-34
2.12.3	Mechanical Design Calculations for the Traveller XL Shipping Package	2-36
2.12.3.1	Analysis Results and Conclusions	2-38
2.12.3.2	Calculations.....	2-40
2.12.4	Drop Analysis for the Traveller XL Shipping Package	2-67
2.12.4.1	Conclusion and Summary of Results	2-67
2.12.4.2	Predicted Performance of the Traveller Qualification Test Unit.....	2-68
2.12.4.3	Comparison of Test Results and Predictions.....	2-116
2.12.4.4	Discussion of Major Assumptions	2-128
2.12.4.5	Calculations.....	2-129
2.12.4.6	Model Input.....	2-135C
2.12.4.7	Evaluations, Analysis and Detailed Calculations	2-142
2.12.4.8	Accelerometer Test Setup	2-143
2.12.4.9	Bolt Factor of Safety Calculation.....	2-144
2.12.5	Traveller Drop Tests Results.....	2-148
2.12.5.1	Prototype Test Unit Drop Tests	2-148
2.12.5.2	Qualification Test Unit Drop Tests	2-167
2.12.5.3	Certification Test Unit Drop Tests	2-183
2.12.5.4	Application to Higher Contents Weights	2-192
2.12.5.5	Conclusions.....	2-192C

TABLE OF CONTENTS (cont)

2.12.6 Supplement to Drop Analysis for the Traveller XL Shipping Package –	
Clamshell Axial Spacer Structural Evaluation.....	2-201
2.12.6.1 Background	2-202
2.12.6.2 Conclusions	2-202
2.12.6.3 Detailed Calculations and Evaluations	2-202
2.12.7 Supplement to Drop Analysis for the Traveller XL Shipping Package –	
Clamshell Removable Top Plate Structural Evaluation	2-212
2.12.7.1 Background	2-212
2.12.7.2 Conclusions	2-214
2.12.7.3 Detailed Calculations and Evaluations	2-214
2.12.8 Supplement to Drop Analysis for the Traveller XL Shipping Package –	
Structural Analysis of the Traveller VVER Shipping Package.....	2-219
2.12.9 Zirconium Alloy Performance During Testing.....	2-245
2.12.9.1 Strain Energy Absorption Capability Calculation Method.....	2-246
2.12.9.2 Chromium Coated and OZL Cladding Evaluation	2-249
2.12.9.3 Advanced Fuel Cladding Feature Additional Details	2-251

LIST OF TABLES

Table 2-1	Summary of Traveller STD, Traveller XL and Traveller VVER Design Weights	2-4
Table 2-2	Safety-Related Materials Used in the Traveller Packages	2-6
Table 2-3	Summary of Regulatory Requirements	2-9
Table 2-4	Summary of Traveller Mechanical Analysis	2-11
Table 2-5	Summary of the Development of the Traveller	2-17
Table 2-6	Traveller STD, Traveller XL, and Traveller VVER Design Weights	2-34
Table 2-7	Deleted	
Table 2-8	Deleted	
Table 2-9	Deleted	
Table 2-10	Top Outpack Latch Bolt Minimum Factors of Safety (FS) for 9m Side Dropped	2-77
Table 2-11	Top Outpack Hinge Bolt Minimum Factors of Safety (FS) for 9m Side Drop	2-78
Table 2-12	Clamshell Keeper Bolt Minimum Factors of Safety for 9m Side Drop	2-80
Table 2-13	Clamshell Bottom Plate Bolt Minimum Factor of Safety for 9m Side Drops	2-81
Table 2-14	Clamshell Grooved Top Plate Bolt Minimum Factors of Safety for 9m Side Drops	2-82
Table 2-15	Clamshell Lipped Top Plate Bolt Minimum Factors of Safety for 9m Side Drops	2-83
Table 2-16	Top Outpack Latch Bolt Minimum Factors of Safety for 9m CB-Forward of Corner Drops	2-93
Table 2-17	Top Outpack Hinge Bolt Minimum Factors of Safety for 9m CB Forward of Corner Drops	2-93
Table 2-18	Clamshell Keeper Bolt Minimum Factors of Safety for 9m CG-Forward-of- Corner Drops	2-94
Table 2-19	Clamshell Bottom Plate bolt Minimum Factors of Safety for 9m CG-Forward- of-Corner Drops	2-95
Table 2-20	Clamshell Grooved Top Plate Bolt Minimum Factors of Safety for 9m CG-Forward-of-Corner Drops	2-95
Table 2-21	Clamshell Lipped Top Plate Bolt Minimum Factors of Safety for 9m CG-Forward-of-Corner Drops	2-96
Table 2-22	Prototype Tests Used to Compare with Analysis	2-117
Table 2-23	Comparison of Predicted and Actual Deformations for Test 1-1	2-121
Table 2-24	Initial Velocities 9 Meter Drop and 1 Meter Pin Puncture Analyses	2-136
Table 2-25	Summary of Elastic Properties	2-142
Table 2-26	Bolt Strength Summary	2-145

LIST OF TABLES (cont.)

Table 2-27	Strengths of Various Classifications of Bolts [14]	2-146
Table 2-28	Bolt Strength Ratio	2-147
Table 2-29	Series 1 As-Tested Drop Conditions	2-150
Table 2-30	Measured Decelerations in Prototype Test 1.1	2-156
Table 2-31	Measured Accelerations in Test 1.2	2-158
Table 2-32	Prototype Test Series 2	2-159
Table 2-33	Traveller Prototype Drop Tests Performed in Test Series 3.....	2-165
Table 2-34	QTU-1 Measured Weight	2-167
Table 2-35	QTU-1 Drop Test Orientations.....	2-168
Table 2-36	Key Dimensions of QTU-1 Fuel Assembly Before Testing	2-173
Table 2-37	QTU-1 Fuel Assembly Grid Envelope After Testing.....	2-174
Table 2-38	QTU-1 Fuel Rod Pitch Data After Testing.....	2-175
Table 2-39	QTU Series 2 As-Tested Drop Conditions.....	2-175
Table 2-40	QTU-2 Weights	2-176
Table 2-41	Key Dimensions of QTU-2 Fuel Assembly Before Testing	2-181
Table 2-42	QTU-2 Fuel Assembly Grid Envelope After Testing.....	2-182
Table 2-43	QTU-2 Fuel Rod Pitch Data After Testing.....	2-183
Table 2-44	Test Weights.....	2-185
Table 2-45	CTU Drop Test Orientations	2-186
Table 2-46	Fuel Assembly Key Dimension Before Drop Test.....	2-196
Table 2-47	CTU Fuel Assembly Grid Envelop Dimensions After Testing.....	2-197
Table 2-48	CTU Fuel Assembly Rod Envelope Data After Testing	2-198
Table 2-49	CTU Fuel Assembly Rod Envelope After Testing.....	2-199
Table 2-50	CTU Fuel Rod Gap and Pitch Inspection After Testing.....	2-200
Table 2-51	Dimension and Material Properties of Axial Spacer.....	2-205
Table 2-52	Aluminum Properties.....	2-206
Table 2-53	Annealed 304 Stainless Steel Properties	2-206
Table 2-54	Crushable Foam Properties.....	2-206
Table 2-55	Neoprene (60 durometer) Properties	2-206
Table 2-56	Aluminum Properties for Traveller VVER Analysis	2-232
Table 2-57	Annealed 304 Stainless Steel Properties for Traveller VVER Analysis	2-232
Table 2-58	Crushable Foam Properties for Traveller VVER Analysis	2-233
Table 2-59	Traveller VVER and Traveller XL Comparative Energy Absorption Capabilities.....	2-240A
Table 2-60	Traveller VVER and Traveller XL Resultant FEA Comparisons.....	2-240A
Table 2-61	Fuel Rod Strain Energy Absorption Using Minimum Tensile Mechanical Properties.....	2-245
Table 2-62	Fuel Cladding Yield Stress Values vs Temperature.....	2-245
Table 2-63	Fuel Cladding Ultimate Stress Values vs Temperature.....	2-246

LIST OF FIGURES

Figure 2-1	Traveller STD Exploded View	2-2
Figure 2-1A	Sample of Clamshell Accelerations Measured During Road Test (May 11, 2004)	2-14
Figure 2-1B	Impact Limiter “Pillow” Assembly	2-22A
Figure 2-1C	Container Bottom End	2-22A
Figure 2-1D	Impact Limiter “Pillow” Assembly	2-22B
Figure 2-1E	Bottom Plate – Viewed from Inside	2-22B
Figure 2-1F	CTU Package Bottom End	2-22C
Figure 2-2	Traveller XL and Traveller STD Dimensions and Center of Gravity (Note: End View is Common to both Models)	2-35
Figure 2-3	Westinghouse Fresh Fuel Shipping Package, the Traveller XL	2-36
Figure 2-4	Internal View of the Traveller Shipping Package	2-37
Figure 2-5	Traveller Lifting Configurations	2-43
Figure 2-6	Lifting Hole Force Detail	2-44
Figure 2-7	Lifting Bracket Fabrication Detail	2-45
Figure 2-8	Hole Tear-out Model and Mohr’s Circle Stress State	2-46
Figure 2-9	Traveller STD Stacked Lifting Configuration	2-48
Figure 2-10a	Forklift Handling XL Model and Assumed Cross Section	2-49
Figure 2-10b	Forklift Pocket Weld Detail	2-50A
Figure 2-10c	Leg Assembly Loading Condition During Inadvertent Tie-Down	2-51
Figure 2-10d	Welding Depiction at Representative Gusset Plate	2-51A
Figure 2-10e	Welding Depiction at Cross Member	2-51B
Figure 2-10f	Lift Eye Loading Assumed Conditions During Inadvertent Tie-Down	2-51C
Figure 2-10g	Vertical Lift Eye Welding Configuration	2-51D
Figure 2-10h	Combined Shear Lift Eye Welding Configuration	2-51F
Figure 2-11	Typical Temperature Dependent Tensile Properties for Tempered 6000 Series Al	2-52
Figure 2-12	Temperature Dependent Tensile Properties for 304 SS	2-53
Figure 2-13	Temperature Dependent Crush Strength for 10 PCF Polyurethane Foam	2-54
Figure 2-14	Temperature Dependent Crush Strength for 20 PCF Polyurethane Foam	2-54
Figure 2-15	Temperature Dependent Crush Strength for 6 PCF Polyurethane Foam	2-55
Figure 2-16	Temperature Dependent Crush Strength for Traveller Foam at 10% Strain	2-55

Figure 2-17	Compression/Stacking Requirement Analysis Model.....	2-58
Figure 2-18	Stacking Force Model on Stacking Bracket.....	2-59
Figure 2-19	Outerpack Section Compression Model.....	2-60
Figure 2-20	Leg Support Section Compression Model.....	2-63
Figure 2-21	Traveller Stiffeners, Legs, and Forklift Pockets.....	2-69
Figure 2-22	Results of Prototype Drop Test.....	2-70
Figure 2-23	Side Drop Orientation.....	2-70
Figure 2-24	Low Angle Drop Orientation.....	2-71
Figure 2-25	Damage from Prototype Low Angle Drop (Test 1.1).....	2-71
Figure 2-26	Horizontal Drop Orientation.....	2-72
Figure 2-27	Predicted Energy and Work for 9m Horizontal Drop Onto Outerpack Hinges.....	2-73
Figure 2-28	Predicted Energy and Work Histories for a 9m Horizontal Drop Onto the Outerpack Hinges.....	2-73
Figure 2-29	Predicted Rigid Wall Force Histories for 9m Horizontal Drops Onto the Outerpack Latches and Hinges.....	2-74
Figure 2-30	De-coupled Impacts for 9 m Horizontal Side Drop.....	2-75
Figure 2-31	Bolts on Prototype Outerpack.....	2-76
Figure 2-32	Bolt Labels for Right Outerpack.....	2-77
Figure 2-33	Bolt Labels for Left Outerpack.....	2-79
Figure 2-34	Clamshell Closure Latches and Keeper Bolts.....	2-79
Figure 2-35	Clamshell Keeper Bolt Labels.....	2-80
Figure 2-36	Clamshell Top and Bottom End Plates.....	2-81
Figure 2-37	Clamshell Bottom Plate Bolt Labels.....	2-82
Figure 2-38	Clamshell Bottom Plate Bolt Labels.....	2-83
Figure 2-39	Clamshell Doors.....	2-84
Figure 2-40	Clamshell Response during Side Drop.....	2-85
Figure 2-41	Clamshell Doors at Bottom Plate.....	2-85
Figure 2-42	Predicted Response of Clamshell Bottom Plate and Doors During 9m Horizontal Drop onto Outerpack Latches.....	2-86
Figure 2-43	Top Nozzle Analysis Drop Orientation.....	2-87
Figure 2-44	Location of Impact.....	2-87

LIST OF FIGURES (cont.)

Figure 2-45 Damage to Outerpack During Angled Drop onto Top Nozzle End of Package..... 2-88

Figure 2-46 Predicted Deformation of Outerpack Top Nozzle Impact Limiter..... 2-88

Figure 2-47 Predicted Pin Puncture Orientation after a CG-Forward-of-Corner Test..... 2-89

Figure 2-48 Outerpack Top Separation vs. Drop Angle 2-90

Figure 2-49 Predicted Energy and Work Histories for 9 m CG-over-Corner Drop onto the Top Nozzle End at Various Angles..... 2-91

Figure 2-50 Predicted Rigid Wall Forces 2-92

Figure 2-51 Clamshell Top Plate Geometry 2-96

Figure 2-52 Traveller Drop Orientations Analyzed For Maximum Fuel Assembly Damage 2-97

Figure 2-53 Predicted Energy and Work Histories for a 9m Vertical Drop Onto the Top Nozzle End of the Package 2-99

Figure 2-54 Predicted Energy and Work Histories for a 9m Vertical Drop Onto the Bottom Nozzle End of the Package 2-99

Figure 2-55 Predicted Rigid Wall Histories for 9m Vertical Drops onto the Bottom (QU-1) and Top (QU-8B) Ends of the Package 2-100

Figure 2-56 Predicted Force Between Clamshell and Impact Limiter for 9m Vertical Drops 2-101

Figure 2-57 Predicted Fuel Assembly Accelerations for 9m Vertical Drops 2-102

Figure 2-58 Impact Between Clamshell and Bottom Impact Limiter for Vertical Drop onto Bottom End of Package..... 2-102

Figure 2-59 First Impact Between Clamshell and Top Impact Limiter for Vertical Drop onto Top End of Package..... 2-103

Figure 2-60 Second Impact Between Clamshell and Top Impact Limiter for Vertical Drop onto Top End of Package..... 2-103

Figure 2-61 Third Impact Between Clamshell and Top Impact Limiter for Vertical Drop onto Top End of Package..... 2-104

Figure 2-62 Predicted Temperature and Foam Density Effect on Outerpack/Drop Pad Interface Forces (9m CG-Forward-of-Corner with 18° Rotation Drop onto the Top End of the Package)..... 2-105

Figure 2-63 Predicted Temperature and Foam Density Effect on Outerpack/Drop Pad Accelerations (9m CG-Forward-of-Corner with 18° Rotation Drop onto the Top End of the Package)..... 2-105

Figure 2-63A Predicted Temperature and Foam Density Effect on Outerpack/Drop Pad Interface Forces (9m Vertical Drop onto the Bottom End of the Package) 2-106

Figure 2-63BPredicted Temperature and Foam Density Effect on Fuel Assembly Acceleration (9m Vertical Drop onto the Bottom End of the Package) 2-106

LIST OF FIGURES (cont.)

Figure 2-64 Predicted Energy and Work Histories at Various Temperatures 2-107

Figure 2-65 Pin Drop Orientation 2-108

Figure 2-66 Predicted Outerpack/Pin Interference Forces (1m Drop onto 15mm Diameter Steel Pin) 2-108

Figure 2-67 Predicted Fuel Assembly Accelerations (1m Drop onto 15mm Diameter Steel Pin) 2-109

Figure 2-68 Pin Drop onto Outerpack Hinges 2-109

Figure 2-69 Predicted Outerpack/Pin Interface Forces (1m Drop onto 15mm Diameter Steel Pin) 2-110

Figure 2-70 Predicted Fuel Assembly Accelerations (1m Drop onto 15mm Diameter Steel Pin) 2-110

Figure 2-71 Predicted Energy and Work Histories for a 1 m Horizontal Pin Drop (Pin Underneath the Package CG)..... 2-111

Figure 2-72 Predicted Energy and Work Histories for a 1 m Tilted Pin Drop (20° Tilt With TN End Down..... 2-112

Figure 2-73 Predicted Energy and Work Histories for a 1 m Horizontal Pin Drop (Pin Hitting Hinge at Package CG) 2-112

Figure 2-74 Comparison of Predicted Maximum Pin Indentations 2-113

Figure 2-75 Predicted Outerpack/Pin Interface Forces (1 m Drop onto 15 mm Diameter Steel Pin After 9m Drop)..... 2-114

Figure 2-76 Predicted Fuel Assembly Accelerations (1 m Drop onto 15mm Diameter Steel Pin after 9 m Drop)..... 2-115

Figure 2-77 Predicted Energy and Work Histories (1 m Drop onto 15 mm Diameter Steel Pin after 9 m Drop)..... 2-116

Figure 2-78 Prototype Drop Tests Used To Benchmark Analysis..... 2-117

Figure 2-79 Prototype Unit 1 Drop Test 2-118

Figure 2-80 Comparison of Test 1.1 with Analytical Results..... 2-119

Figure 2-81 Comparison of Test 1.1 with Analytical Results..... 2-120

Figure 2-82 Deformations at End of Package 2-122

Figure 2-83 Internal Deformations at Inside Outerpack 2-123

Figure 2-84 Outerpack Deformations at Bottom Nozzle End of Package 2-124

Figure 2-85 Pin Puncture Deformations..... 2-124

Figure 2-86 Dimensions of Pin Puncture Deformations 2-124

LIST OF FIGURES (cont.)

Figure 2-87 Outerpack Predicted Deformations of Pin Drop 2-125

Figure 2-88 Predicted and Measured Y Accelerations..... 2-126

Figure 2-89 Three Axis Measured Accelerations..... 2-126

Figure 2-90 Predicted and Measured Y Accelerations..... 2-127

Figure 2-91 Predicted and Measured Y Accelerations..... 2-127

Figure 2-92 Measured Primary and Secondary Accelerations 2-128

Figure 2-93 FEA Model Input Files 2-130

Figure 2-94 Outerpack Mesh in Prototype Model..... 2-131

Figure 2-95 Impact Limiter in Prototype Unit Model 2-131

Figure 2-96 Clamshell Mesh in Qualification Unit Model 2-132

Figure 2-97 Fuel Assembly in Both Prototype and Qualification Unit Models..... 2-132

Figure 2-98 Outerpack Hinge Model 2-133

Figure 2-99 FEA Input Files 2-134

Figure 2-100 Outerpack Mesh in Qualification Unit Model 2-134A

Figure 2-100A FE Meshes of Outerpack Legs and Forklift Pockets 2-134A

Figure 2-100B Lower Outerpack Mesh for Qualification Unit Model..... 2-134B

Figure 2-100C Qualification Unit Model Mesh Detail..... 2-134C

Figure 2-100D Upper Outerpack Mesh for Qualification Unit Model 2-134D

Figure 2-101 Impact Limiter Meshes in Qualification Unit Model 2-135

Figure 2-101A Hinge/Latch Feature in Qualification Unit Model..... 2-135A

Figure 2-102 Clamshell Mesh in Qualification Unit Model 2-135B

Figure 2-102A Clamshell Top Head in Qualification Unit Model 2-135B

Figure 2-102B Clamshell Top Nozzle Hold-down Bars in Qualification Unit Model..... 2-135C

Figure 2-102C Clamshell Hinges and Latches in Qualification Unit Model..... 2-135C

Figure 2-103 Package Drop Angle 2-137

Figure 2-104 Gravity Load Profile 2-138

Figure 2-105 Stress Strain Data for LAST-A_FOAM 2-139

Figure 2-105A Foam Response at Strains from 0-10% 2-139A

Figure 2-106 Stress-Strain Curves for 304 Stainless Steel..... 2-140

Figure 2-107 Temperature Effects on Tensile Properties of Annealed Stainless Steel..... 2-140

LIST OF FIGURES (cont.)

Figure 2-108	Stress-Strain Characteristics of Aluminum in Clamshell	2-141
Figure 2-109	Temperature Effects on Tensile Properties of Aluminum in Clamshell.....	2-141
Figure 2-110	Accelerometer Locations on Prototype Unit 1	2-144
Figure 2-111	Traveller Prototype Internal View	2-149
Figure 2-112	Traveller Prototype External View	2-150
Figure 2-113	Drop Orientations for Prototype Test Series 1	2-151
Figure 2-114	Traveller Prototype Exterior After Test 1.1.....	2-152
Figure 2-115	Traveller Prototype Interior After Test 1.1.....	2-153
Figure 2-116	Traveller Prototype Exterior After Test 1.2.....	2-154
Figure 2-117	Traveller Prototype Interior After Test 1.2.....	2-155
Figure 2-117A	Accelerometer Locations on Prototype Drop Test	2-155A
Figure 2-118	Clamshell Accelerometer Trace for Prototype Test 1.1	2-156
Figure 2-119	Outerpack Accelerometer Trace for Prototype Test 1.1	2-157
Figure 2-120	Clamshell Accelerometer Trace for Prototype Test 1.2	2-157
Figure 2-121	Traveller Prototype After Test 1.3.....	2-159
Figure 2-122	Drop Orientations for Traveller Prototype Test Series 2.....	2-160
Figure 2-123	Traveller Prototype After Test 2.1	2-161
Figure 2-124	Traveller Prototype After Test 2.2.....	2-162
Figure 2-125	Traveller Prototype After Test 2.3.....	2-163
Figure 2-126	Traveller Prototype Interior After Test Series 2	2-164
Figure 2-127	Traveller Prototype Clamshell and Bottom Impact Limiter After Test Series 3.....	2-166
Figure 2-128	Traveller Prototype Clamshell and Bottom Impact Limiter After Test Series 3.....	2-166
Figure 2-129	Drop Orientation for QTU Test Series 1	2-168
Figure 2-130	QTU-1 Outerpack After Test 1.1	2-169
Figure 2-131	QTU-1 Outerpack After Test 1.2.....	2-170
Figure 2-132	QTU-1 Outerpack After Test 1.3.....	2-170
Figure 2-133	QTU-1 Fuel Assembly After Drop and Burn Tests.....	2-171
Figure 2-134	Measurements Made on QTU-1 Fuel Assemblies Before and After Drop Tests	2-172

LIST OF FIGURES (cont.)

Figure 2-135	QTU Test Series 2 Drop Orientations.....	2-177
Figure 2-136	QTU Outerpack After Test 2.1	2-178
Figure 2-137	QTU Outerpack After Test 2.2	2-178
Figure 2-138	QTU Outerpack After Test 2.3	2-179
Figure 2-139	QTU-2 Clamshell and Fuel Assembly After Drop Tests.....	2-180
Figure 2-140	Traveller CTU Test Article Internal View	2-184
Figure 2-141	Traveller CTU External View.....	2-185
Figure 2-142	CTU Drop Test Orientations.....	2-186
Figure 2-143	Top Nozzle End Outerpack Impact Damage	2-187
Figure 2-144	CTU Outerpack Stiffener After Test 1.....	2-188
Figure 2-145	CTU Outerpack After Test 2.....	2-188
Figure 2-146	CTU Outerpack After Test 2.....	2-189
Figure 2-147	Hinge Separation at Bottom Nozzle End From Test 2.....	2-189
Figure 2-148	CTU Outerpack After Test 3.....	2-190
Figure 2-149	CTU Clamshell After Drop and Fire Tests	2-191
Figure 2-150	Outerpack Lid Moderator After Testing	2-191
Figure 2-151	Fuel Assembly Damage Sketch and Pre-test Assembly	2-193
Figure 2-152	CTU Fuel Assembly After Testing	2-194
Figure 2-153	CTU Fuel Assembly Top End After Testing	2-194
Figure 2-154	Cracked Rod From CTU Fuel Assembly	2-195
Figure 2-155	Cracked Rod Locations on CTU Fuel Assembly.....	2-195
Figure 2-156	Axial Spacer below Fuel Assembly in Traveller XL Clamshell.....	2-201
Figure 2-157	FEA Model – Axial Spacer.....	2-204
Figure 2-158	Dynamic Crush Strengths for Foam Materials Utilized in the Traveller.....	2-207
Figure 2-159	Annealed 304 Stainless Steel Stress-Strain Characteristics	2-207
Figure 2-160	Deformed Model with Axial Spacer at 23 ms (the end of the impact)	2-208
Figure 2-161	Predicted Total End Crushing (mm) with Axial Spacer	2-209
Figure 2-162	Kinetic Energy History (mJ) of the Axial Spacer Model.....	2-209
Figure 2-163	Fuel Handling Tool Grappled to a 17x17 Top Nozzle (in blue) within the Opened Outerpack and Clamshell	2-213
Figure 2-164	Fuel Handling Tool Shown Attached to a 17x17 XL Fuel Assembly and Behind the Overhanging Shear Lip.....	2-213
Figure 2-165	Traveller Top End Plate FEA Model	2-215
Figure 2-166	RTP Model at Beginning of Impact (0 ms) and End of Impact (33 ms).....	2-216
Figure 2-167	Rigid Wall Impact Force History of RTP Model.....	2-217
Figure 2-168	Kinetic Energy History of RTP Model (mJ vs s).....	2-217
Figure 2-169	Comparison of Simulated Top Nozzle Damage (left) to Drop Test (right).....	2-218

LIST OF FIGURES (cont.)

Figure 2-170	Traveller VVER Exploded View	2-220
Figure 2-171	Traveller VVER Clamshell Top Detail.....	2-220
Figure 2-172	Cross-Section views of Traveller XL and Traveller VVER Shipping Packages.....	2-221
Figure 2-173	XL and VVER Clamshell Lengths Shown with the Outerpack Lid Removed.....	2-222
Figure 2-174	Similarity of XL and VVER Clamshell Extrusions	2-223
Figure 2-175	Identical Hardware for XL and VVER Clamshell Quarter-turn Latches.....	2-223
Figure 2-176	Traveller VVER Clamshell Top Plate Assembly	2-224
Figure 2-177	VVER Fuel Assembly Installed - Top Nozzle Region	2-225
Figure 2-178	VVER Fuel Assembly Installed - Bottom Nozzle Region.....	2-225
Figure 2-179	Puncture Plate Distance from Ground During Impact	2-227
Figure 2-180	Traveller VVER Clamshell Model Showing Key Components	2-228
Figure 2-181	Traveller VVER Finite Element Model	2-229
Figure 2-182	Traveller VVER Model with Clamshell Walls and End Limiter Cover Plate Hidden	2-230
Figure 2-183	Traveller VVER Top Plate Assembly Showing Integral Axial Clamp and Rubber Pad.....	2-230
Figure 2-184	Comparison of Dynamic Crush Strengths of the Foams Components	2-233
Figure 2-185	Annealed 304 Stainless Steel Stress-strain Characteristics.....	2-234
Figure 2-186	Traveller XL Shown in a Top-down Impact Orientation.....	2-235
Figure 2-187	Top Down 9m Impact of Traveller VVER Package in 5 ms Increments	2-236
Figure 2-188	Kinetic Energy Plot for VVER Model.....	2-237
Figure 2-189	Deformed Shape of Model at 25ms	2-238
Figure 2-190	Max. Plastic Strain in the Clamshell Main Walls	2-238
Figure 2-191	Slap-down Model.....	2-241
Figure 2-192	Model with Upper Outerpack Hidden to Show VVER Clamshell	2-241
Figure 2-193	Outerpack Max. Longitudinal Bending Load History	2-242
Figure 2-194	Slight Plastic Strain in Clamshell Extrusion	2-243
Figure 2-195	Traveller VVER Top Plate "Shear lip"	2-244
Figure 2-196	Resilience and Toughness (Strain Area)	2-247
Figure 2-197	ZIRLO Cladding Stress-Strain Plot	2-248
Figure 2-198	Chromium Coated Optimized ZIRLO Cladding Stress-Strain Curve	2-249
Figure 2-199	OZL Lined Optimized ZIRLO Cladding Stress-Strain Curve	2-250
Figure 2-200	17x17 STD OFA Fuel Assembly, Tube Dimensions and Grid Elevations	2-253
Figure 2-201	Design Endurance Limits for Zircalloy Claddings.....	2-254

2.0 STRUCTURAL EVALUATION

This section presents the structural design criteria, weights, mechanical properties of material, and structural evaluations which demonstrate that the Traveller series of packages meet all applicable structural criteria for transportation as defined in 10 CFR 71¹ and TS-R-1².

2.1 DESCRIPTION OF STRUCTURAL DESIGN

The structural evaluation of the standard length Traveller (Traveller STD) and the longer length Traveller (Traveller XL) packages was performed with various tests and computer simulation using finite element analysis. Since the Traveller VVER utilizes the same Outerpack as the Traveller XL and recent design changes (e.g., the removable top plate) were evaluated using a benchmarked finite element model, the VVER package was also analyzed using finite element computer simulation. The results of the computer simulations and testing are provided in the following sections. Supporting analyses and analyses of not-tested structural aspects are also provided. See Figure 2-170 for an exploded view of the Traveller VVER package.

The Traveller shipping package consists of two major fabricated components: 1) an Outerpack assembly, and 2) a Clamshell assembly. The Outerpack consists of a stainless steel outer shell for structural strength, a layer of rigid polyurethane foam for thermal and impact protection, and a stainless steel inner shell for structural strength. Polyethylene blocks are affixed to the inner shell of the Outerpack for criticality safety. See Section 6, Criticality Evaluation, for full criticality safety description. The Clamshell consists of an aluminum container to structurally enclose the contents. Neutron absorber panels are affixed to the inner faces of the Clamshell. Rubber shock mounts separate and isolate the Clamshell from the Outerpack assembly. See Figure 2-1 for an exploded view of the Traveller STD package.

2.1.1 Discussion

The designs of the Traveller STD and Traveller XL unirradiated fuel shipping packages are the same except for length (and therefore weight). The Traveller VVER design is a hexagonal Clamshell mounted inside a Traveller XL Outerpack. Any reference to the Traveller XL Outerpack is applicable to Traveller VVER Outerpack for structural considerations. Details of the packages, including dimensions, and materials can be found in Section 1, General Information. Both packages consist of an Outerpack, and a Clamshell. Positive closure of the Outerpack is accomplished by means of high strength stainless steel bolts. The number of bolts is the same for the XL and STD designs, thus the loading per bolt is lower for the STD design. There are 48 bolts $\frac{3}{4}$ -inch bolts in the Outerpack, 24 attaching the hinge sections to the lower Outerpack and 24 attaching the upper Outerpack to the hinge sections. To remove the upper Outerpack, the 24 bolts must be removed. In the preferred approach, the Outerpack is opened when it is in a vertical orientation by removing the 12 bolts attaching the upper Outerpack to the hinges on one side. This allows the upper Outerpack to be opened on the other hinge sections, like a door. The design loadings for both

1. Title 10, Code of Federal Regulations, Part 71 (10 CFR 71), Packaging and Transportation of Radioactive Material, January 1, 2004 Edition
2. TS-R-1 1996 Edition (Revised), Regulations for the Safe Transport of Radioactive Material.

packages are below the ultimate design loads for the Outerpack bolts. The worst case forces for the package are presented in Section 2.12.3.2.2, Horizontal Side Drops, and a discussion regarding the design allowable is presented in Section 2.12.3.7, Evaluation, Analysis and Detailed Calculations, and Section 2.12.3.9, Bolt Factor of Safety Calculation. Further evidence of the adequacy of the Outerpack bolts is demonstrated through 9m drop testing whereby only one (1) Outerpack bolt failed in a total of nine (9) 9m drop tests. The single bolt that failed did so as a result of direct impact with the drop pad. The Clamshell is closed using ¼-turn nuts which lock latches on the doors of the assembly.

The Outerpack bolts and the Clamshell closure mechanisms have been subjected to the drop conditions of 10 CFR 71 and TS-R-1 without failure. Therefore, these designs are more than adequate to withstand the loads experienced during normal conditions of transport.

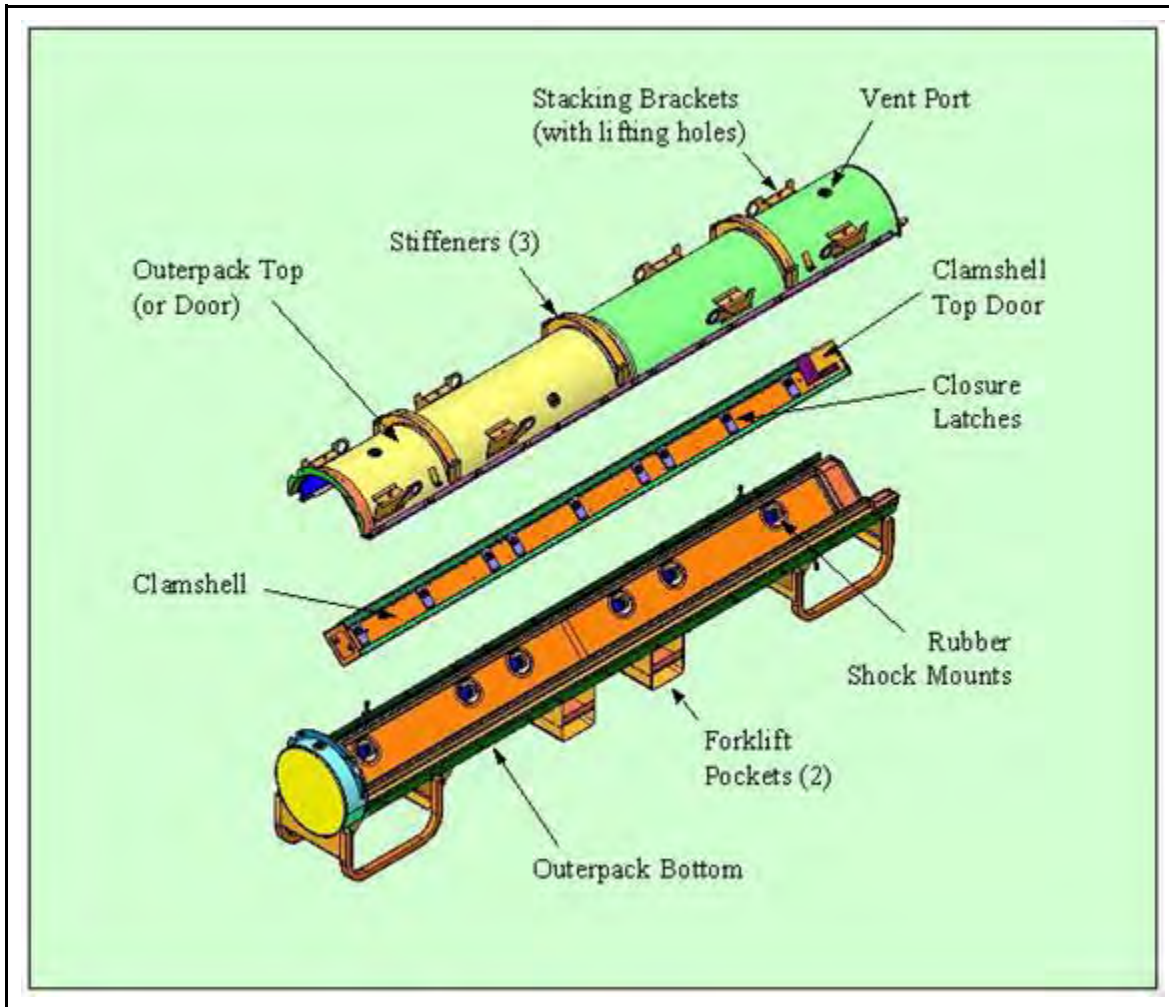


Figure 2-1 Traveller STD Exploded View

Closure of the Outerpack is provided by (12) $\frac{3}{4}$ -10UNC hex head bolts, which allows the top half of the Outerpack assembly to swing open on a series of hinges. The Outerpack top half or “door” may be opened in either direction, depending on which bolts are removed. Optionally, the top Outerpack assembly may also be completely removed by removal of (24) $\frac{3}{4}$ -10UNC hex head bolts. Closure of the Traveller STD and Traveller XL Clamshells are provided by latch assemblies that are secured with nine (9) $\frac{1}{4}$ -turn nuts, and eleven (11) $\frac{1}{4}$ -turn nuts, respectively.

The Traveller packages are not pressure sealed from the ambient environment, therefore, no differential pressures can occur within the package.

Handling of the packages is performed using the forklift pockets on the lower Outerpack. Handling may also utilize the lifting holes in the stacking brackets on the upper Outerpack.

Standard fabrication methods are utilized to fabricate the Traveller series of packages. Visual weld examinations are performed on all welds of the Traveller packages in accordance with AWS D1.6. and ASME Section III, Subsection NF-5360, for stainless steel and aluminum respectively.

2.1.2 Design Criteria

2.1.2.1 Basic Design Criteria

Evidence of performance for the Traveller XL package is achieved by (1) empirical evaluations using full-scale packages and (2) large-strain capable Finite Element Analysis (FEA). The Traveller XL is bounding due to its increased weight and length when compared to Traveller STD. The criteria that was used for impact evaluation is a demonstration that the containment and confinement systems maintain integrity throughout Normal Conditions of Transport (NCT) and Hypothetical Accident Condition (HAC) certification testing. That is, it is necessary to demonstrate that there is no release of material, no loss of moderator or neutron absorber, no decrease in Outerpack geometry, and no increase in Clamshell geometry. The as-found condition of the package (packaging and contents) is the baseline configuration for the criticality safety evaluation that can be found in Chapter 6, Criticality Evaluation.

A detailed discussion related to Traveller XL design criteria, can be found in Appendix 2.12.3, Mechanical Design Calculations for the Traveller XL Shipping Package.

2.1.2.2 Miscellaneous Structural Failure Modes

2.1.2.2.1 Brittle Fracture

The primary structural materials of the Traveller packages are austenitic stainless steel (ASTM A240 Type 304 SS) and 6000 Series aluminum (extruded components 6005-T5, all else 6061-T6). These materials do not undergo a ductile-to-brittle transition in the temperature range of interest [i.e., down to -40°F (-40°C)], and thus do not require evaluation for brittle fracture.

2.1.2.2.2 Fatigue

Because the shells of the Outerpack are constructed of ductile stainless steel and they are formed into a very stiff body with low resulting stresses, no structural failures of the Outerpack due to fatigue will occur. Because the Clamshell is structurally isolated from the Outerpack through the rubber shock mounts, no Clamshell fatigue will occur. The Clamshell is, for practical purposes, decoupled from the Outerpack through the rubber shock mounts. These rubber shock mounts also provide excellent damping to the Clamshell.

2.1.2.2.3 Buckling

For normal condition and hypothetical accident conditions, the Clamshell which structurally encloses the fuel, will not buckle due to free or puncture drops. This behavior has been demonstrated via full-scale testing of the bounding Traveller XL package.

2.1.3 Weights and Centers of Gravity

The Traveller XL weight bounds the Traveller STD and Traveller VVER weight as shown in Table 2-1. The calculated weight breakdown for the major individual subassemblies, including the shipping components for both packages, is listed below. For licensing purposes, the maximum bounding Traveller XL design weight is assumed to be 5,230 lb (2,372 kg). The general, Traveller structural analysis applicable to STD, XL and VVER is located in Section 2.12.2. The Traveller VVER specific structural analysis is located in Section 2.12.8.

Table 2-1 Summary of Traveller STD, Traveller XL, Traveller VVER Design Weights			
	Traveller STD	Traveller XL	Traveller VVER
Max. Fuel Assembly Weight, lb (kg)	1650 (748)	1971 (894)	1850 (839)
Max. Tare Weight, lb (kg)	2850 (1293)	3255 (1476)	3255 (1476)
Design and Licensing Basis Gross Weight, lb (kg)	4500 (2041)	5230 (2372)	5105 (2316)

The center of gravity of both Traveller packages is approximately at the geometric center of the Outerpack, i.e., approximately 23 inches above ground level, at the axial mid-station for both packages. Appendix 2.12.2, Container Weights and Centers of Gravity, shows the overall dimensions, locations of the centers of gravity for both packages, and detailed major component weights.

2.1.4 Identification of Codes and Standards for Package Design

The Traveller packages are evaluated with respect to the general standards for all packaging specified in 10 CFR §71.43, and TS-R-1 (paragraphs 606 – 649, as applicable). The fabrication, assembly, testing, maintenance, and operation will be accomplished with the use of generally accepted codes and standards such as ASME, ASTM, AWS. Special processes will be documented with procedures that will be evaluated and approved.

2.2 MATERIALS

2.2.1 Material Properties and Specifications

Mechanical properties for the materials used for the structural components of the Traveller packages are provided in this section. Temperature-dependent material properties for structural components are primarily obtained from Section II, Part D, of the ASME Boiler and Pressure Vessel (B&PV) Code. The analytic evaluation of the Traveller packages is via computer simulation (ANSYS/LS-DYNA[®]), only the material properties specific to the analysis portion and computer simulation portion of the evaluation are given. Table 2-2 lists the materials used in the Traveller packages and summarized key properties and specifications. More detailed material properties can be found in Appendix 2.12.3, Mechanical Design Calculations for the Traveller XL Shipping Package, and Appendix 2.12.4, Drop Analysis for the Traveller XL Shipping Package.

All materials used in the fabrication of the Certification Test Unit (CTU) meet 10 CFR 71 and TS-R-1 requirements. However, simulated neutron absorber plates were affixed to the inner faces of the Clamshell. These were fabricated from 1100-T0 aluminum (“dead soft” aluminum). These component plates did not contain boron, and were used to simulate the mechanical and thermal properties of the neutron absorber plates. The 1100-T0 aluminum was used due to its low mechanical properties. In production units, the actual neutron absorber plates will have insignificant differences in the material properties compared to the material used in the prototypes and CTU package.

2.2.2 Chemical, Galvanic, or Other Reactions

The Traveller series of packages are fabricated from ASTM A240 Type 304 stainless steel, 6000-series aluminum, borated 1100-series aluminum, polyurethane foam, and polyethylene sheeting. The stainless steel Outerpack does not have significant chemical or galvanic reactions with the interfacing components, air, or water.

The aluminum Clamshell is physically isolated, and environmentally protected, by the Outerpack and therefore will have negligible chemical or galvanic reactions with the interfacing components, air, or water. In addition, the Type 304 stainless steel fasteners which attach various Clamshell components represent a very small area ratio (cathode-to-anode ratio), which will render the reaction insignificant. Therefore, the requirements of 10 CFR §71.43(d), TS-R-1 (613) are met.

The Outerpack hinge bolts are zinc plated for the purpose of improving galling resistance which can be a significant problem when stainless steel fasteners are inserted in stainless steel threaded holes. The plating is not required for chemical or galvanic protection.

2.2.3 Effects of Radiation on Materials

There are no materials used in the Traveller packages which will be adversely affected by radiation under normal handling and transport conditions.

Material	Critical Properties	Reference Specifications/Codes	Comments
304 Stainless Steel	UTS: 75 ksi (517 MPa) YLD: 30 ksi (206 MPa) τ_{allow} : 18 ksi (124 MPa) E: 29.4 E6 psi (203 GPa)	ASTM A240 ASTM A276	Fully annealed material and not subject to brittle fracture.
6005-T5 Aluminum	UTS: 38 ksi (262 MPa) YLD: 35 ksi (241 MPa) τ_{allow} : 21 ksi (145 MPa) E: 10 E6 psi (69 GPa)	ASTM B221 ASTM B209	Reference standard UNS A96005
6061-T6 Aluminum	UTS: 38 ksi (262 MPa) YLD: 35 ksi (241 MPa) τ_{allow} : 21 ksi (145 MPa) E: 10 E6 psi (69 GPa)	ASTM B221 ASTM B209	Reference standard UNS A96061
Polyurethane Closed Cell Foam	Densities: 6 ± 1 pcf (0.096 ± 0.016 gm/cm ³), 10 ± 1 pcf (0.16 ± 0.016 gm/cm ³), 20 ± 2 pcf (0.32 ± 0.016 gm/cm ³) Crush Strengths: See Appendix 2.12.3	Westinghouse Specification PDSHIP02 ASTM D1621-94 ASTM D1622-93 ASTM D2842	Burn Characteristics verified by ASTM F-501, with exceptions noted in PDSHIP02.
UHMW Polyethylene	Specific Gravity: > 0.93 Molecular Wt: >3 million	ASTM D4020	N/A
Borated Aluminum Laminate Composite	Minimum areal densities: Borated Al Composite: [] ^{a,c}	Westinghouse Specification PDSHIP04 ASTM E748	The minimum areal densities are defined for the finished plate or laminate final thickness of [] ^{a,c} . No structural credit is taken for the neutron poison plates.
Ceramic Insulation (Paper and Felt)	Max. use temp: >1800°F (982°C) Conductivity: ≤ 1.2 Btu-in/hr-ft ² @ 500°F, (0.173 W/m-K @ 260°C)	N/A	The paper thickness is 0.0625" (1.59 mm), and the blanket thickness is 0.25" (6.35 mm)

2.3 FABRICATION AND EXAMINATION

2.3.1 Fabrication

The Traveller packages (XL, VVER and STD) are manufactured using standard fabrication techniques. No exotic materials or processes are required. Safety related items which are needed for criticality safety purposes have specific manufacturing specifications which clearly delineate all necessary codes, standards, and specifications required to meet design intent. All fabrication specifications are listed on the engineering drawings.

The fabrication processes of the Traveller include basic processes such as cutting, rolling, bending, machining, welding, and bolting. All welding is performed in accordance with ASME Section IX.

The manufacturing flow of the Traveller units includes fixturing of the inner and outer shells of the upper and lower Outerpack assemblies. Individual closure components are then aligned and welded in place. Sub-assemblies such as the forklift pockets, leg structures and stacking brackets are assembled in a parallel manner and appended to the main assemblies at appropriate times. Upon welding closure of the assemblies, the upper and lower Outerpack assemblies are secured together and poured with polyurethane foam material. Pouring of this material is tightly controlled through the foam manufacturing specification.

When the Traveller is filled with foam, it is ready for final assembly and installation of the Clamshell which has followed a parallel fabrication process. One difference for the Clamshell is that the faces are manufactured extrusions as opposed to “off-the-shelf” material. The extrusions are fabricated to industry standard specifications. Upon integration of the Clamshell to the Outerpack, final assembly and light grit blasting conclude the manufacturing process.

2.3.2 Examination

Manufacture of all Traveller packages shall be performed in accordance with strict Quality Assurance (QA) requirements. Included in the manufacture of the packages are examinations to verify that each package is being built to the required specifications. These examinations include the following:

1. Receipt inspections whereby the received components are visually inspected for workmanship, overall part quality, dimensional compliance, and material certification compliance.
2. All welds (which shall be performed by qualified welders/processes) shall be visually examined by a qualified inspector in accordance with AWS D1.6 and ASME Section III, Subsection NF-5360, for stainless steel and aluminum respectively.
3. Examinations which evaluate form, fit, and function shall be performed on each package to verify its operability and assess its overall quality.

2.4 LIFTING AND TIE-DOWN STANDARDS FOR ALL PACKAGES

2.4.1 Lifting Devices

The lifting criteria is governed by 10 CFR §71.45(a) and TS-R-1 (607). 10 CFR §71.45(a) states that any lifting attachment that is a structural part of the package must be designed with a minimum safety factor of three against yielding when used to lift the package in its intended manner. In addition, it must be designed so that failure of any lifting device under excessive load would not impair the ability of the package to meet other requirements of 10 CFR 71. The following calculations are based on the features of the Traveller XL package which bounds the Traveller STD for these requirements. Lifting and tie-down are described in detail in Appendix 2.12.3, Mechanical Design Calculations for the Traveller XL Shipping Package. |

2.5 GENERAL CONSIDERATIONS

The Traveller package structural evaluation consists of a combination of mechanical design calculations, finite element analysis, and testing. Table 2-3 shows the regulatory requirements and the means by which satisfactory compliance was demonstrated.

Requirement Description	US NRC	TS-R-1	Applicable Condition	Means Demonstrated
Lifting attachments	10 CFR 71.45(a)	TS-R-1, § 607	General Package Standard	Mech. Design Calc.
Tie-Down devices	10 CFR 71.45(b)(1,2)	TS-R-1, § 636	General Package Standard	Mech. Design Calc.
Design temperatures between -40°F (-40°C) and 158°F (70°C)	10 CFR 71.71(c)(1,2)	TS-R-1, § 637 and 676	General Package Standard	Mech. Design Calc.
Internal/External Pressure	10 CFR 71.71(c)(3,4)	TS-R-1, § 615	Normal transport condition	Mech. Design Calc.
Vibration	10 CFR 71.71(c)(5)	TS-R-1, § 612	Normal transport condition	Mech. Design Calc.
Water spray	10 CFR 71.71(c)(6)	TS-R-1, § 721	Normal transport condition	Mech. Design Calc.
Compression/Stacking test	10 CFR 71.71(c)(9)	TS-R-1, § 723	Normal transport condition	Mech. Design Calc.
Penetration	10 CFR 71.71(c)(10)	TS-R-1, § 724	Normal transport condition	Mech. Design Calc.
Immersion	10 CFR 71.73(c)(6)	TS-R-1, § 729	Accident transport condition	Mech. Design Calc.

2.5.1 Evaluation by Test

The development of the Traveller packages included mechanical scoping tests to quantify the critical characteristics of the components or subsystems of the design. These scoping tests included:

1. Outerpack Hinge Strength-to-Failure Testing
2. Hinge Alignments Tests
3. Foam Pouring Tests
4. Foam Burn Tests (pail type)
5. Clamshell Hinge Strength-to-Failure Testing
6. Clamshell Weld Tests

7. Clamshell impact tests
8. Impact limiter testing including “pillow” impact testing

The scoping tests provided designers with performance data. However, proof of performance in the Traveller package was obtained through full-scale testing. As such, these tests were not required to be performed in accordance with full QA standard. However, all full-scale Traveller XL packages were fabricated and tested under all QA requirements.

The development of the Traveller consisted of essentially three (3) full-scale test campaigns. These campaigns consisted of what are called the Prototype units (2), the Qualification Test Units (QTU) (2), and finally the Certification Test Units (CTU) (1). In general, these packages are very similar. The overall configuration of the Outerpack and Clamshell remain essentially identical throughout the design evolution. With each test campaign, the design was modified to increase structural or thermal margin, or to reduce excess design margin when appropriate. The significant design changes from Prototype to CTU were:

1. The reduction in Outerpack shell thicknesses from 11 gage (0.120", 0.30 cm) to 12 gage (0.105", 0.27 cm),
2. The adjusting of polyurethane foam densities (first a lowering of density for structural reasons, then an increase for improve thermal performance),
3. The addition of a thin stainless steel covering of the moderator blocks,
4. The replacement of short individual Outerpack hinges with a continuous Outerpack hinge,
5. A redesign of the Clamshell head attachment configuration, and finally,
6. A reduction in the number and size of the Outerpack hinge bolts.

The purpose of the computer simulation was to assist in evaluating these minor changes and predict performance of the modified packages. The computer simulation was also used to show the impact of initial test conditions (temperature of package) and manufacturing variability (foam density tolerances, skin thickness variations, etc.). These factors showed negligible effects on the overall performance of the packages. Details can be found in Appendix 2.12.4, Drop Analysis for the Traveller XL Shipping Package. |

A summary of the development and testing of the Traveller XL full-scale test packages is described in Table 2-5, and the detailed results of each test are described in Appendix 2.12.5, Traveller Drop Test Results. |

2.5.2 Evaluation by Analysis

Analysis consisted of mechanical design calculations and finite element analysis. Mechanical design calculations are described in detail in Appendix 2.12.3. Finite element analysis, utilizing LS-DYNA software, is described in detail in Appendix 2.12.4.

Table 2-4 gives a summary of the regulatory requirements that are demonstrated through mechanical design calculations

Table 2-4 Summary of Traveller Mechanical Analysis		
Requirement Description	Allowable Design Value(s) or Acceptance Criteria	Component Calculated Value vs. Allowable
Lifting attachments	Tensile Yield Stress, $\sigma_y < 30$ ksi Shear Yield Stress, $\tau_y < 18$ ksi Weld shear Yield Stress, $\tau_y < 12$ ksi Hoist Screw Shear Stress, $\tau < 72$ ksi Coupling Nut Shear Stress, $\tau < 18$ ksi Hoist Ring Tensile Stress, $\tau < 130$ ksi	Hole tear-out (4-pt. lifting) XL: $\tau = 5,230$ psi < 18 ksi STD: $\tau = 6,364$ psi < 18 ksi Weld shear (4-pt. lifting) XL: $\tau = 7,565$ psi < 12 ksi STD: $\tau = 9,205$ psi < 12 ksi Forklift XL Bending: $\sigma = 17,528$ psi < 30 ksi STD Bending: $\sigma = 26,260$ psi < 30 ksi XL Weld shear: $\tau = 3,533$ psi < 12 ksi STD Weld shear: $\tau = 6,080$ psi < 12 ksi Hoist Ring Assembly Bolt shear: $\tau = 50,619$ psi < 72 ksi Coupling Nut Shear Stress: $\tau = 17,671$ psi < 18 ksi Hoist ring tensile: $\sigma = 35,659$ psi < 130 ksi
Tie-Down	Weld shear Yield Stress, $\sigma_y < 12$ ksi	Leg Assembly Weld shear: $\tau = 11,648$ psi < 12 ksi Lift Eyes Weld shear (vertical): $\tau = 7,158$ psi < 12 ksi Weld shear (combined): $\tau = 7,173$ psi < 12 ksi
Temperatures Effects	No brittle fracture No impact from Differential Thermal Expansion (DTE)	No brittle fracture No DTE Impact
Internal/External Pressure	Compressive Yield Stress, $\sigma_y < 30$ ksi	No stress developed
Vibration	No impact on structural performance $f_{natOP} > f_{nat TRANS}$	No impact, 23 Hz $> 3.7-8$ Hz
Water spray	No impact on structural performance	No impact
Compression/Stacking	Weld shear Yield Stress, $\tau_y < 12$ ksi Compressive Yield Stress, $\sigma_y < 30$ ksi Elastic Stability (Critical Buckling), $F < P_{cr}$	Stacking Bracket: Weld shear: $\tau = 4,729$ psi < 12 ksi Bending: $\sigma = 1,827$ psi < 30 ksi Outerpack Buckling: Buckling: 26,150 lb $< 78,583$ lb Leg Support Buckling: Buckling: 3,269 lb $< 71,978$ lb
Penetration	No perforation of outer skin	Bounded by 1.0m HAC pin-puncture; No perforation of outer skin.
Immersion	Compressive Yield Stress, $\sigma_y < 30$ ksi	No stress developed

2.6 NORMAL CONDITIONS OF TRANSPORT

2.6.1 Heat

The thermal evaluation for the heat test is described and reported in Section 3, Thermal Evaluation.

2.6.1.1 Summary of Pressures and Temperatures

There is no pressure seal in the Traveller series of packages. Therefore, there is no pressure build up within the package. Maximum temperature for the following sections were evaluated to 158°F (70°C) and minimum temperatures to -40°F (-40°C).

2.6.1.2 Differential Thermal Expansion

The effects differential thermal expansion for the Traveller series of packages is negligible due to the design of the package. The most significant differential is between the aluminum Clamshell and the fuel assembly, and is less than 0.25 inches. The differential thermal expansion is accommodated by rubber-cork spacers between the Clamshell and fuel assembly.

Ultra-high Molecular Weight (UHMW) polyethylene does have a significantly higher coefficient of thermal expansion (CTE) when compared to Type 304 stainless steel. For this reason, the moderator panels are segmented along their lengths to accommodate the differential thermal expansion between the polyethylene and the inner stainless steel shells of the Outerpack. Additionally, oversized holes in the polyethylene panel are used to accommodate the effects of both temperature extremes.

See Appendix 2.12.3, Mechanical Design Calculations for the Traveller XL Shipping Package, for detailed differential thermal expansion calculations.

2.6.1.3 Stress Calculations

The Traveller packages are fabricated from relatively thin sheet metal parts which are not subject to thermal gradients generated from the interior of the package. The packages are also not sealed to the environment, therefore pressure stress is negated. The most significant stress potential occurs from the differential expansion rates of the bolted polyethylene moderator panels to the inner steel shells of the Outerpack. This potential stress is also negated by design, whereby the panels are made in sections and the bolt clearances and gaps between panels are adequately sized to allow unrestrained growth and contraction.

Successful testing of full scale Traveller XL packages indicates that the stresses associated with differential thermal expansion of the various packaging components are negligible.

2.6.1.4 Comparison with Allowable Stresses

As discussed in Section 2.6.1.3, Stress Calculations, further evaluation of stresses associated with differential thermal expansion for the various Traveller package components is not required.

2.6.2 Cold

The materials used in construction of the Traveller packages are not degraded by cold at -40°C (-40°F). Stainless steel and aluminum exhibit no brittle fracture at these temperatures. Therefore, the requirements of 10 CFR §71.71(c)(2) and TS-R-1 (618) are satisfied.

2.6.3 Reduced External Pressure

Since the Traveller series of packages are not sealed against pressure, there can not be any significant differential pressure. *See Appendix 2.12.3.2.4.1 for additional explanation.*

2.6.4 Increased External Pressure

Since the Traveller series of packages are not sealed against pressure, there can not be any significant differential pressure. *See Appendix 2.12.3.2.4.1 for additional explanation.*

2.6.5 Vibration

The package must be evaluated to consider the effects of normal vibration on the design performance. The isolation system is designed to dampen normally induced vibrations from transport, and is not fundamental to the safe operation of the package. However, the Outerpack must maintain its structural integrity during transport to maintain a safe transport condition as specified in 10 CFR §71.71(5), TS-R-1 (612). Typical attachment to a transport conveyance for the Traveller packages includes nylon straps or chain mounted both over the package and on the gusset tray connected to the support legs pointed inboard. The loading configuration can be modeled as a simply supported beam. Furthermore, the Outerpack is conservatively modeled considering only the outer shell at the first mode of vibration. The typical natural frequency range for transportation vehicles, $f_{nat\ TRANS}$, is 3.7-8 Hz. The natural frequency of the Outerpack can be determined from: l

$$f_{natOP} = a\sqrt{(EIg/l^3)/m}$$

where $a=1.57$ (primary mode coefficient assuming hinge-hinge end conditions for additional conservatism), $E = 29.4E6$ psi, $I = 634$ in⁴, $m = 2834$ pounds, $g = 386.4$ in/s² and $l = 226.2$ in. Substituting values:

$$f_{natOP} = 1.57 \sqrt{[(29.4E6)(634)(386.4)/(226.2)^3] / 2834} \text{ 1/s (Hz)}$$

$$f_{natOP} = 1.57 \sqrt{220} \text{ Hz}$$

$$f_{natOP} = 23 \text{ Hz}$$

Since the natural frequency of the Outerpack is greater than the natural frequency typical of a transportation vehicle, resonance of the Outerpack is not expected and normally induced vibrations will not preclude the package from performing its design function.

The rubber shock mounts effectively isolate and dampen loads and vibrations to the Clamshell and its contents. No resonant vibration conditions which could fatigue the Clamshell shall occur during normal conditions of transport.

There are several natural frequencies of the shock mount system depending on direction of movement. The dominant frequency is for vertical movement. This frequency is between 5.9 and 6.7 Hz (for Traveller XL) depending on the weight of the fuel assembly being transported. The fore and aft pitch frequency is slightly higher (6.9-7.9 Hz) but has a lower amplitude. Road tests have been performed with the suspension system to measure amplitudes during shipping. Figure 2-1A is characteristic of the results seen. When the truck travels over a bump, the clamshell initially sees relatively large accelerations (2-3 g's) but this oscillation quickly damps out to accelerations less than 1 g. This 300 mi trip involved approximately five and a half hours on the road with 1.4×10^5 total cycles.

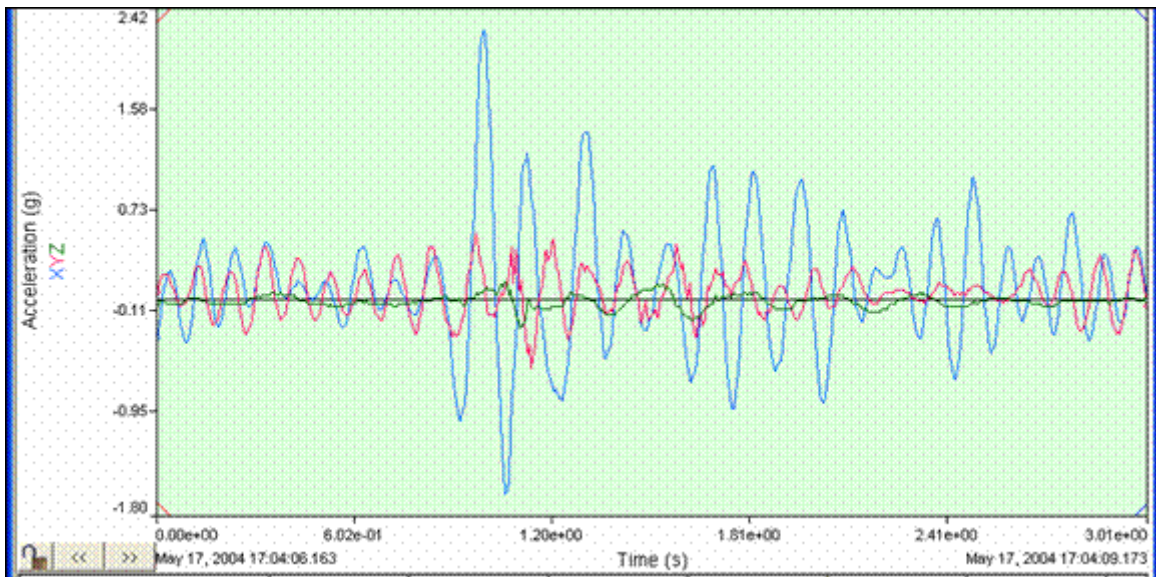


Figure 2-1A Sample of Clamshell Accelerations Measured During Road Test (May 11, 2004)

2.6.6 Water Spray

The materials of construction utilized for the Traveller packages are such that the water spray test identified in 10 CFR §71.71(c)(6), TS-R-1 (721), will have negligible effect on the package. Further, the Traveller Outerpack is cylindrical, and is specifically shaped to negate water collection. Since the Outerpack shell is fabricated from ASTM A240 Type 304 SS, the water spray will not impact the structural integrity of the package.

2.6.7 Free Drop

Since the gross weight of the bounding Traveller XL package is less than 5,000 kg (11,000 lb), a 1.2 m (4 feet) free drop is conservatively required per 10 CFR §71.71(c)(7), TS-R-1 (722). As discussed in Appendix 2.12.5, Traveller Drop Test Results, 1.2 m drops were performed on the Traveller CTU as an initial condition for subsequent Hypothetical Accident Condition (HAC) tests.

The Traveller packages are well protected during drop testing. In particular, the leg structure including fork lift structure, stacking structure, and upper Outerpack stiffener I-beam structure, all protect the Traveller during impact. Traveller CTU free drop testing and engineering evaluations indicated that this testing have negligible impact on the integrity of the package. However, the orientation selected for the free drop testing was a low angle slap-down, approximately 10 degrees, with the package inverted. The basis for selection of this orientation was that this orientation offered the greatest opportunity to stress the welded joints at the ends of the package. Detailed descriptions of the test results are given in Appendix 2.12.5, Traveller Drop Test Results. Applicability to VVER type fuel designs is provided in Appendix 2.12.8. Examinations following the prototypic and CTU testing proved the ability of the Traveller packaging to maintain its structural and criticality control integrity. Therefore, the requirements of 10 CFR §71.71(c)(7) are satisfied.

This page intentionally left blank.

2.6.8 Corner Drop

The corner drop test does not apply, since the gross weight of the package exceeds 100 pounds (50 kg), as specified in 10 CFR §71.71(c)(8) or 100 kg (221 lb) as specified in TS-R-1 (722).

2.6.9 Compression – Stacking Test

The compressive load requirement of 10 CFR §71.71(c)(9), TS-R-1 (723) is satisfied by the Traveller packages. Details of the analysis can be found in Appendix 2.12.3, Mechanical Design Calculations for the Traveller XL Shipping Package.

2.6.10 Penetration

The 1 m (40 inch) drop of a 1 ¼-inch (3.2 cm) diameter, 6 kg (13 pound), hemispherical end steel rod, as specified in 10 CFR §71.71(c)(10), TS-R-1 (724), is of negligible consequence to the Traveller series of packages. This conclusion is due to the fact that the Traveller packages are designed to minimize the consequences associated with the much more limiting case of a 1 m (40 inch) drop of the entire package onto a puncture rod, as discussed in Section 2.7.3, Puncture. The 12-gauge (2.7 mm) minimum thickness of the outer shell of the Outerpack is not damaged by the penetration event. Therefore, the requirements of 10 CFR §71.71(c)(10), TS-R-1 (724), are satisfied.

2.7 HYPOTHETICAL ACCIDENT CONDITIONS

When subjected to the hypothetical accident conditions as specified in 10 CFR §71.73, the Traveller package meets the performance requirements specified in Subpart E of 10 CFR 71, and TS-R-1 (726-737 as applicable). This conclusion is demonstrated in the following subsections, where the most severe accident condition is addressed and the package is shown to meet the applicable design criteria. The method of demonstration is through both computer analysis and by testing. The loads specified in 10 CFR §71.73 are applied sequentially, per Regulatory Guides 7.8 and 7.9 (draft).

The Traveller XL Certification Test Unit (CTU) test results are summarized in Section 2.7.7, Summary of Damage, with details provided in Appendix 2.12.5, Traveller Drop Test Results. Additional full-scale test results conducted prior to the certification tests are also included in Appendix 2.12.5. These tests describe the improvements to the Traveller XL design, substantiate the basis for the most severe hypothetical accident condition, and were used to validate the computer simulations.

The following table summarizes the development of the Traveller XL shipping package from the first prototype through the Certification Test Unit, or CTU. As can be seen, satisfying the thermal test requirements proved more difficult than expected. However, the culmination of the development effort has yielded a shipping package that has been thoroughly tested and meets the requirements of both 10 CFR 71 and TS-R-1.

Table 2-5 Summary of the Development of the Traveller			
Traveller XL	Test Sequence(s)	Structural Performance	Fire/Thermal Performance
Prototype-1 Drop testing: Jan 27-28, 2003 Burn Testing: Feb 28, 2003	Objective: FEA validation - 9 m low angle slap down (14.5 degrees) - 9 m high angle (71 degrees) - 1 m pin puncture (through CG, low angle) - 35 minute pool fire burn test.	- Outerpack – <u>Satisfied</u> requirements. Minor, local damage only. - Clamshell – <u>Satisfied</u> requirements for 9 m low angle test. <u>Failed</u> requirements for 9 m high angle test. <u>Satisfied</u> 1 m pin puncture test.	Outerpack <u>failed</u> to prevent ignition of polyethylene sheets in one location. Clamshell temperature away from interior combustion <u>satisfied</u> fire requirements.
<p>Comments:</p> <p>The Traveller XL Prototype-1 demonstrated robust structural performance, except for the Clamshell head(s) attachment which was not adequate. The most probable root cause of ignition of polyethylene sheeting was polyurethane foam combustion products entering the inside of the Outerpack as a result of holes drilled into inner Outerpack shell for thermocouples. No seals were used in the Outerpack for conservatism.</p> <p>Fire testing failed to prevent ignition of the combustible materials in the Outerpack. However, the components not adjacent to the internal fire remained well within thermal limitations, thus, demonstrating that the Outerpack had sufficient thermal resistance to external heat flow into package.</p> <p>Design Changes as a Result of Testing:</p> <p>Additional bolts were added to secure the top Clamshell head for Prototype-2 testing (see below).</p> <p>The package was subjected to the applicable tests for Normal and Hypothetical Accident conditions as described below. Following this series, the package was modified again to assess the robustness of the design. The center Outerpack hinge bolts were removed (1 of 3 bolts) from each hinge section. The number of locking pins on the Clamshell latches was also reduced, from 18 to 12.</p>			
Prototype-2 Drop Testing: Jan 30, 2003 Burn Testing: N/A	- 1.2 m low angle slapdown (20 degrees) - 1 m pin puncture (through CG, low angle) - 9 m high angle (72 degrees) Bolts and locking pins removed (described above) - 9 m end drop (bottom end down) - 9 m horizontal (feet down) - 9 m horizontal (side down)	- Outerpack – <u>Satisfied</u> requirements for all 9 m drops and pin puncture tests. Minor, local damage only. - Clamshell – <u>Satisfied</u> requirements for first 9 m drop. Bottom head separated in second 9 m drop (bottom end drop) because the fuel assembly was not properly seated against bottom Clamshell head as a result of prior drop. No other significant damage.	- Prototype 2 was not subjected to HAC fire testing.

Table 2-5 Summary of the Development of the Traveller (cont.)			
Traveller XL	Test Sequence(s)	Structural Performance	Fire/Thermal Performance
<p>Comments:</p> <p>The performance of the Prototypes (1 & 2) associated with the first testing campaign clearly demonstrated the robustness of the Overpack and Clamshell (except for the Clamshell head attachments). In all, six (6) drops were performed on 2 full-scale prototypes from 9 m. The Outerpack retained its overall integrity and functionality. Most importantly, all design features important to criticality safety performed as intended. Moderator blocks and simulated neutron absorber plates remained intact and attached to their respective structural components.</p> <p>Design Changes as a Result of Testing:</p> <p>Based on the robust structural performance of the Prototype units, several design changes were made to the Traveller XL for subsequent testing in the second test campaign. The Traveller units fabricated for the second campaign were called the Qualification Test Units, or QTUs. A total of two units were fabricated and tested. The significant changes to the QTUs were as follows:</p> <ol style="list-style-type: none"> 1. The Outerpack stainless steel shells were reduced from 11 gauge (0.1196 in., 3.04 mm) to 12 gauge (0.1046 in., 2.66 mm). This change was made primarily to lower weight and reduce excessive structural margin. 2. The hinge bolts were reduced in both number and size, from ten 7/8" (2.22 cm) diameter bolts to ten 3/4" (1.91 cm) bolts. This change was made to reduce excessive design margin. 3. A total of 2 seal materials were added to the design to act as: 1) an environmental seal, and 2) to minimize hot gases from entering the Outerpack seams. 4. The Outerpack leg structure, circumferential stiffeners, stacking brackets, and forklift pocket structures were changed. These changes were made for simplified manufacturing purposes and to reduce excessive design margin. 5. The polyurethane foam density of the center section of the package was reduced from 11 pcf to 10 pcf. The axial limiter foam sections of the package were also reduced from 16 pcf to 14 pcf. This change was made to lower the impact deceleration, and therefore loads experienced by the Clamshell. 6. The Clamshell extrusions were made thicker, from a nominal 0.375" (0.95 cm) to 0.438" (1.11 cm). This change was made primarily to eliminate welding of the heads to the extrusions. Bolted connections were utilized to attach the heads. 7. The welded simulated poison plates were redesigned for a bolted connection. This change was made to reduce the distortion of the aluminum Clamshell extrusions due to welding. 8. The Clamshell door locking latches were redesigned for quarter-turn nuts. This change was made for manufacturing and aesthetic purposes. 9. The Clamshell axial restraint system for restraint of the fuel assembly was redesigned. This change was made to simplify the fuel handling. 			

Table 2-5 Summary of the Development of the Traveller (cont.)			
Traveller XL	Test Sequence(s)	Structural Performance	Fire/Thermal Performance
QTU-1 Drop Testing: Sep 11, 2003 Burn Testing: Sep 15, 2003	<ul style="list-style-type: none"> - 1.2 m low angle slapdown (10 degree) - 9 m high angle (72 degrees) - 1 m pin-puncture (83 degrees at bottom end) - 37 minute pool-fire burn test. 	<ul style="list-style-type: none"> - Outerpack – <u>Satisfied</u> requirements for both drops and pin puncture tests. Minor, local damage only. - Clamshell – <u>Satisfied</u> requirements for both drops and pin puncture tests. 	<p><u>Failed</u> to prevent ignition of the polyethylene sheeting inside the Outerpack. Temperatures inside the Outerpack exceeded design limits. The package was extinguished approximately 1 hour after the conclusion of the pool fire testing.</p>
<p>Comments:</p> <p>The Traveller XL QTU-1 demonstrated robust structural performance. No Outerpack bolts failed. The Outerpack did not separate, and the pin puncture did not perforate the inner or outer shells nor did it effect the Clamshell in any detrimental way.</p> <p>One hour after the pool fire, the package burning was extinguished. Upon inspection of the QTU-1 unit, it was determined that excessive distortion of the Outerpack shells between the hinges, allowed sufficient hot gases to ignite the polyethylene sheeting on the top half of the Outerpack. The burnt polyethylene sheeting was directly in line with the gaps in between the hinges. The burnt zones (4) were located only on the upper half of the Outerpack. This is most likely due to the flanges on the mating Outerpack halves which preferentially directs incoming gases to the upper portion of the Outerpack.</p> <p>Design Changes as a Result of Testing:</p> <p>Based on unsuccessful fire testing of the QTU-1 unit, the QTU-2 unit was modified for improved thermal performance. Since the QTU-2 had already been drop tested in accordance with 10 CFR 71, and TS-R-1 requirements, only minor modifications were deemed acceptable. Only changes considered for the QTU-2 were ones that would not have affected the drop characteristics and performance. The changes made to the QTU-2 unit subsequent to drop testing are listed as follows:</p> <ol style="list-style-type: none"> 1. The 10 short Outerpack hinge sections were removed and replaced with 8 (four per side) long hinge sections that butted together forming a continuous hinge covering essentially all of the Outerpack mating seams. 2. The polyethylene moderator sheeting (both top and bottom sections) was covered with 26 gage stainless steel sheet metal. This sheet material was welded to the inner shells of the Outerpack along the sides of the covers, the ends (both top and bottom) were sealed with adhesive. The coverings therefore, were not completely welded closed. 			
QTU-2 Drop Testing: Sep 11, 2003 Burn Testing: Oct 20, 2003	<ul style="list-style-type: none"> - 1.2 m low angle slapdown (10 degrees) - 9 m end drop (bottom end down) - 1 m pin puncture (22 degrees through CG) - 32 minute pool-fire burn test. 	<ul style="list-style-type: none"> - Outerpack – <u>Satisfied</u> requirements for both drops and pin puncture tests. Minor, local damage only. - Clamshell – <u>Satisfied</u> requirements for both drop tests and thermal tests. No failures were noted in any structure, or fasteners. The maximum temperature of the Clamshell and its contents never exceeded design limits 	<p>- <u>Failed</u> to prevent ignition of the polyethylene sheeting inside the Outerpack. However, the maximum temperature of the Clamshell and contents remained below 200°C. The package was extinguished approximately 7 hours after the conclusion of the pool fire testing.</p>

Table 2-5 Summary of the Development of the Traveller (cont.)			
Traveller XL	Test Sequence(s)	Structural Performance	Fire/Thermal Performance
<p>Comments:</p> <p>The Traveller XL QTU-2 demonstrated robust structural performance. No Outerpack bolts failed. The Outerpack did not separate, and the pin puncture did not perforate the inner or outer shells nor did it effect the Clamshell in any detrimental way.</p> <p>Seven hours after the pool fire, the package burning was extinguished. During this seven hour period there was continuous low level smoldering. Upon inspection of the QTU-2 unit, it was determined that ignition occurred at the bottom end of the package. This was most likely caused by distortion of the Outerpack halves in the area of the bottom end where the impact limiter warped away from the top Outerpack half during the fire. The continuous hinge sections also did not cover the last 3 inches of the Outerpack seams on both sides of the package, which may have allowed additional hot gases to enter the package. The hot gas ingress occurred at a location where there was exposed polyurethane foam (the inner axial limiter foam) due to the thin stainless steel limiter cover being punched out by the Clamshell. This was an expected consequence of the bottom end drop.</p> <p>The long sheet metal covers which were welded along their sides but applied adhesive at the ends did not perform as anticipated. The covers distorted during the testing and opened the adhesive joint. This allowed the polyethylene moderator to ignite. The areas around the shock mounts also were not covered with sheet metal thus exposing the moderator to the conditions inside the Outerpack. These exposed areas showed signs of burning in post-test examinations.</p> <p>The QTU-2 test demonstrated that the polyethylene sheeting must be completely welded, or “canned”, by sheet metal to prevent ignition. However, this test was further evidence that the “bulk” heating of the inside of the Outerpack was acceptable, even with burning occurring within the Outerpack. This is a result of the fact that there is insufficient oxygen to support large amounts of burning. It was estimated that over the 7.5 hours of total burning, only about 10-15% of the moderator material was consumed.</p> <p>Design Changes as a Result of Testing:</p> <p>Based on the structural success of the QTU units and the thermal failures of the units, several changes were made to the design. These changes are listed below:</p> <ol style="list-style-type: none"> 1. The 26 gage moderator sheet metal covers were redesigned so that the polyethylene was completely encapsulated by sheet metal. This mandated the use of sheet metal “cones” around each shock mount. Additionally, thin ceramic insulating material was incorporated between the moderator sheet and the metal covers, around the cones, and over a length of 30 inches at both the top and bottom ends. The ceramic “paper” is nominally 0.06 inches (0.15 cm) in thickness. Ceramic felt was also incorporated to fill the voids under the shock mount cones and at the ends of the moderator sheets. 2. The thin sheet metal impact limiter cover which were design to be punched out by high angle Clamshell impacts were redesigned to have thicker (0.25", 0.64 cm) puncture-resistant plates. These “pillows” were separate structures that were tested in a separate series of mechanical and thermal tests prior to CTU testing. The purpose of the pillows was to prevent polyurethane foam from becoming exposed to the inside of the outerpack, even in end drops. The pillow also incorporated a thick (0.25", 0.64 cm) plate at its base to act as a heat capacitor for incoming heat during the fire testing. Finally, the void space between the pillow and the outer sections of the impact limiters was filled with ceramic felt and paper to further reduce the heat load to the pillows and the internal contents of the Outerpack. 3. The foam density within the inner section of the impact limiters, or pillows, was reduced from 7 pcf to 6 pcf to allow more crushing of the foam. This change was made to lower the impact forces on the Clamshell and its contents. 			

Table 2-5 Summary of the Development of the Traveller (cont.)			
Traveller XL	Test Sequence(s)	Structural Performance	Fire/Thermal Performance
<p>4. The four (4) long Outerpack hinge sections were lengthened to cover all of the Outerpack seams. There existed a nominal 3 inch (7.6 cm) uncovered section at the bottom end.</p> <p>5. The bottom limiter cover which curves around the bottom impact limiter was extended an additional 1.5 inches axially. Ribs (or lips) were added to this cover, and to the bottom limiter, to further reduce the ingress of hot gases.</p> <p>6. The foam density in the outer sections of impact limiters was increased from 14 pcf to 20 pcf to reduce the heat flow through these sections.</p> <p>7. The polyethylene moderator sheets were redesigned for manufacturing purposes.</p> <p>8. The silicone rubber Omega seal, was replaced with acrylic impregnated fiberglass braided tubing. This change was made to eliminate a potential source of combustion inside the Outerpack.</p> <p>The design changes listed above were retrofitted onto the QTU-1 unit (which had already been burned). The QTU-1 unit was then instrumented and taken through a series of fire tests in an effort to quantify the thermal design margins associated with these design changes. This testing was considered necessary to quantify the thermal design margins before the final Certification Test Unit (CTU) test article was tested. The modified unit was tested twice. It was first burned for 40 minutes, then it was re-burned for another 30 minutes the following day. The results of the tests were excellent. The impact limiter pillow temperature never exceeded 120°C, and the data confirms the primary heating to the inside of the Outerpack is by conduction.</p> <p>Based on the successful testing of the modified QTU-1 article, the design changes were incorporated in the manufacturing of the Traveller XL CTU package.</p>			
<p>CTU Drop Testing: Feb 5, 2004 Burn Testing: Feb 10, 2004</p>	<ul style="list-style-type: none"> - 1.2 m low angle slapdown (9 degrees) - 9 m end drop (bottom end down) - 1 m pin puncture (21 degrees through CG, directly onto Outerpack hinge) - 32 minute pool-fire burn test. 	<ul style="list-style-type: none"> - Outerpack – <u>Satisfied</u> requirements for both drops and pin puncture tests. Minor, local damage only. - Clamshell – <u>Satisfied</u> requirements for both drop tests and thermal tests. The Clamshell retained its shape and remained closed and latched after drop testing. 	<p>Clamshell – <u>Satisfied</u> requirements for fuel containment and criticality safety. The Clamshell and its contents remained below a maximum of 150°C.</p>
<p>The Traveller XL CTU demonstrated robust structural performance. No Outerpack bolts failed and the Outerpack retained its circular pre-test shape. The Outerpack did not separate, and the pin puncture did not perforate the inner or outer shells nor did it affect the Clamshell in any detrimental way. Minor weld failures on the Outerpack, in the region near the impact, were observed in post-test examinations. These failures had negligible effect on the performance of the CTU. The two (2) quick release pins on the cover lips detached during the drop test, therefore, they could not be used where they were intended, in the burn test (as such, they were not re-installed for the burn testing).</p>			

Table 2-5 Summary of the Development of the Traveller (cont.)			
Traveller XL	Test Sequence(s)	Structural Performance	Fire/Thermal Performance
<p>The impact limiter pillows performed as intended, however, they did not crush as much as intended due to the inherent axial flexibility of the 17x17 XL fuel assembly. The moderator sheeting remained completely contained within the sheet metal covering. A small brown spot was observed on the back side of one moderator sheet attached to the Outerpack top half. A very small amount of flow occurred away from the hot spot. This melt spot was small, affecting only a few cubic centimeters of material.</p> <p>The Clamshell was found intact and closed, and the simulated poison plates maintained their attached position with very little distortion. Minor damage was observed at the location of the impact with the pillow, however, the damage had negligible effect on the performance of the Clamshell. All closure nuts remained intact with no signs of distortion or stress.</p> <p>The most significant observation from the post-test examinations were 20 cracked fuel rod bottom end plug welds. These cracks occurred in the regions corresponding to the corners of the bottom nozzle. At these corners, the buckled bottom nozzle has steep faces (in excess of 45 degrees), which was exacerbated by the characteristically long legs of the 17XL assembly. The angled faces apply a side force to the local fuel rods as they are decelerated in the impact. The largest crack occurred in a fuel rod located in the outermost row within the assembly. The crack in the rod had a maximum width of approximately 0.075" (1.91 mm). This width is not sufficiently large enough for loss of fuel from the rod. Further, in all cases of cracked rods, the bottom end plugs did not separate. Therefore, fuel pellets are prevented from exiting any of the cracked rods.</p> <p>Design Changes as a Result of Testing:</p> <p>The CTU satisfied the HAC drop-test and burn-test requirements in all aspects. However, as with any development program, improvements can be envisioned after every series of tests. Based on the results of the CTU tests, several minor changes shall be incorporated into production units to enhance the performance of the package. These changes do not change the performance or characteristics of the package, but merely improve the safety margin of the package by incorporating rather obvious improvements as listed below. The basis for the change is also listed below:</p> <ol style="list-style-type: none"> 1. The studs which hold the moderator blocks to the upper Outerpack half failed during the drop testing. The moderator remained contained within the sheet metal covering. However, the number of 3/8" (0.95 cm) diameter studs shall be increased by 50% on the top Outerpack assembly only. 2. The bottom impact limiter pillow is welded at the top plate to the Outerpack inner plate. This weld is design to break in a high angle impact. It performed well in the drop test, however, it did not completely break. This joint shall be redesigned with a small groove cut into the inner plate to form a weakened break point. The break shall therefore not necessarily occur at the weld location. 3. The quick release pins used to secure the bottom end seam flange cover failed during drop testing but had negligible effect on the performance (intended for thermal performance only). Therefore, they were not used in the thermal test and will not be used in production units. <p>The figure below (Figure 2-1B) shows the impact limiter, or Pillow, assembly (shown without insulation). This assembly is shown installed in the Traveller package bottom (the configurations are the same for STD and XL packages) in Figure 2-1C. The weld between the bottom plate (yellow) and the puncture plate (red) is also shown. During testing this weld failed as expected, however, it did not completely allow the components to separate. This design change weakens the bottom plate by reducing its thickness to a nominal 0.025" thickness, as shown in Figures 2-1D and 2-1E. A .25 inch wide channel was added to weaken the part.</p>			

Table 2-5 Summary of the Development of the Traveller (cont.)

Traveller XL	Test Sequence(s)	Structural Performance	Fire/Thermal Performance
--------------	------------------	------------------------	--------------------------

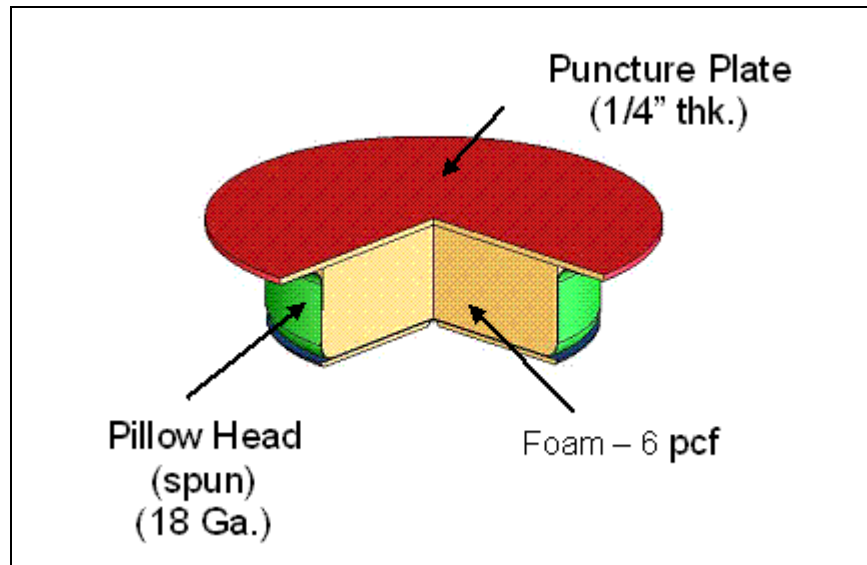


Figure 2-1B Impact Limiter "Pillow" Assembly

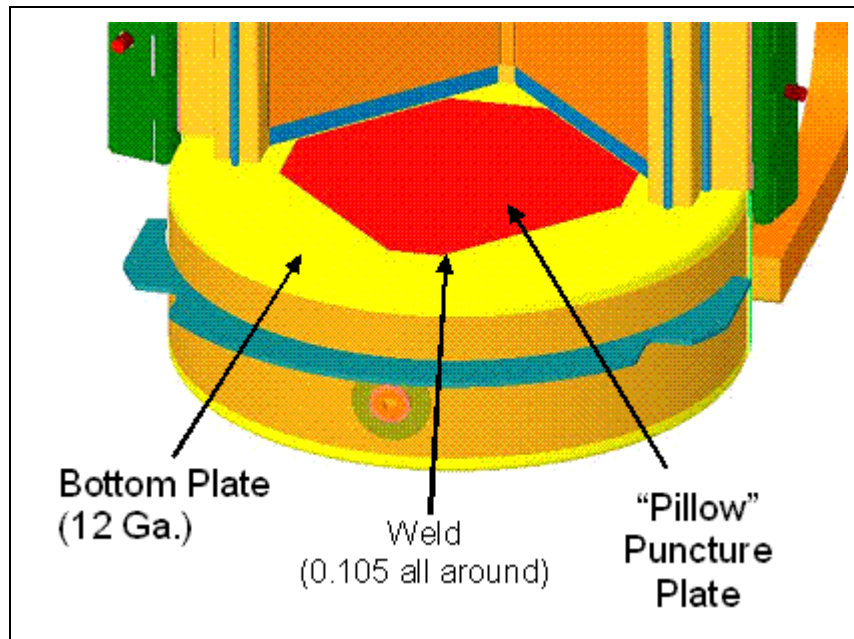


Figure 2-1C Container Bottom End

**Table 2-5 Summary of the Development of the Traveller
(cont.)**

Traveller XL	Test Sequence(s)	Structural Performance	Fire/Thermal Performance
--------------	------------------	------------------------	--------------------------

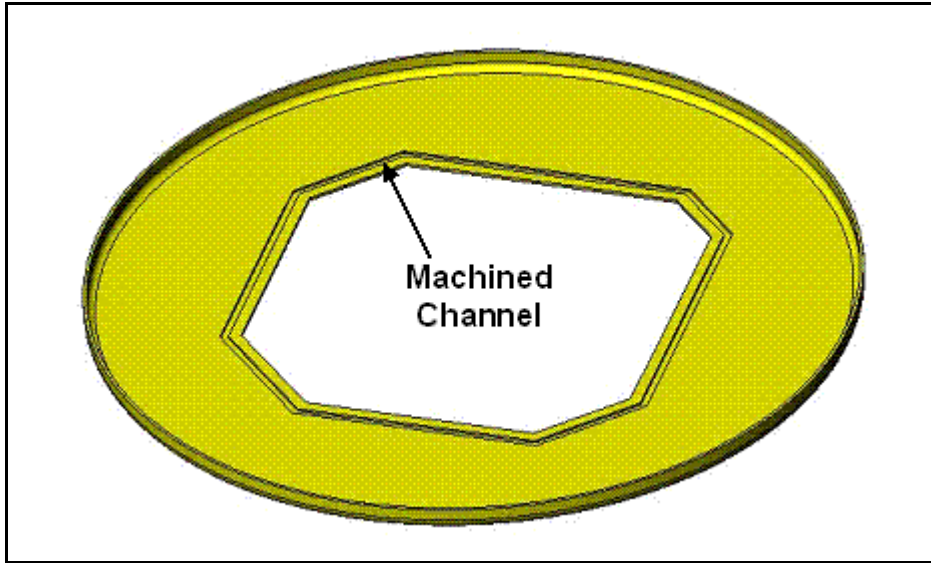


Figure 2-1D Impact Limiter "Pillow" Assembly

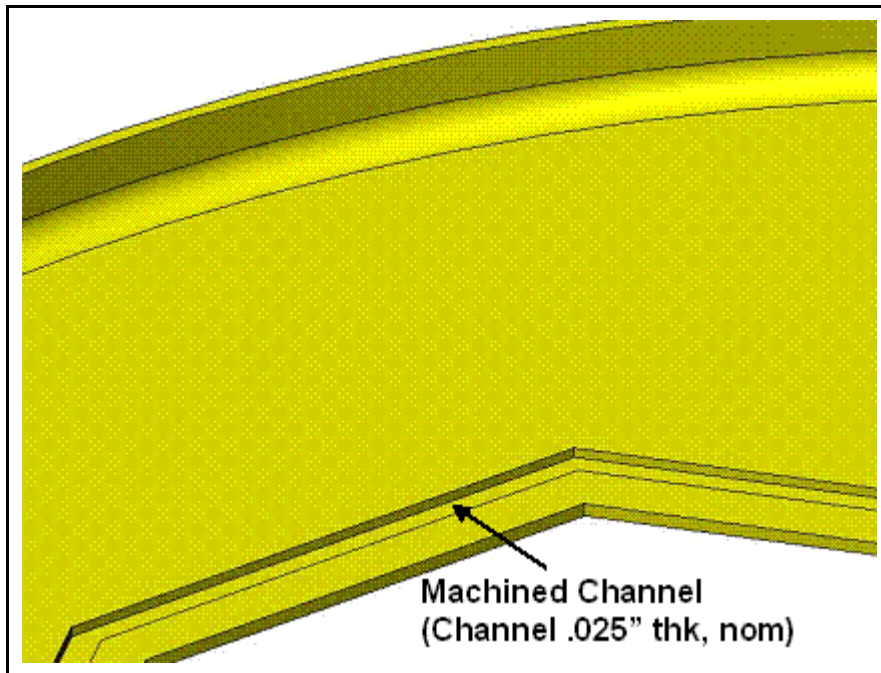
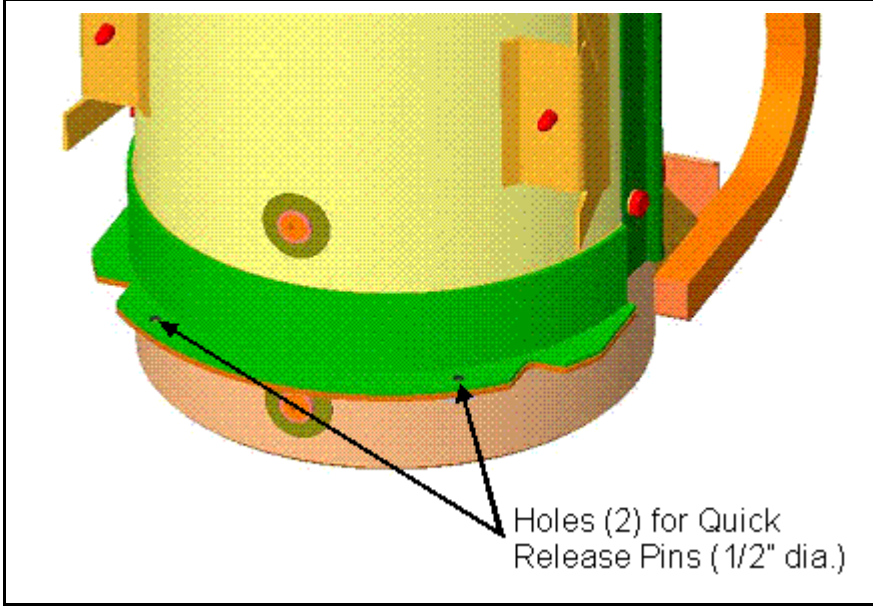


Figure 2-1E Bottom Plate – Viewed from Inside

Table 2-5 Summary of the Development of the Traveller (cont.)			
Traveller XL	Test Sequence(s)	Structural Performance	Fire/Thermal Performance
<p>The CTU design included a pinned connection (2 quick release pins – 0.5" diameter) between Outerpack halves at the bottom end of the package. Quick release pins were designed to help prevent the halves from warping and opening a gap locally during fire testing. Figure 2-1F shows the location of the quick release pins. During drop testing, the pins failed, therefore, they could not be used in the fire testing</p>			
 <p>The image is a 3D CAD model of the bottom end of a cylindrical package. It shows a green outer shell and a tan inner shell. Two circular holes are visible on the bottom surface of the green shell, indicated by two black arrows. A text label 'Holes (2) for Quick Release Pins (1/2" dia.)' is positioned to the right of the arrows. The model also shows some orange and yellow structural components on the sides.</p>			
<p>Figure 2-1F CTU Package Bottom End</p>			

This page intentionally left blank.

2.7.1 Free Drop

Subpart F of 10 CFR 71, TS-R-1 (727) requires that a 9-meter (30 foot) free drop be considered for the Traveller series of packages. The free drop is to occur onto a flat, essentially unyielding, horizontal surface, and the package is to strike the surface in an orientation for which the maximum damage is expected. The free drop is addressed by test, in which the most severe orientation is used. The free drop precedes both the puncture and fire tests. The ability of the Traveller packages to adequately withstand this specified drop condition is demonstrated via drop testing of the full-scale Traveller XL Certification Test Unit (CTU). The Traveller XL variant bounds the shorter and lighter Traveller STD design. Simulations using finite element analysis are performed to demonstrate the response of the package to free drop tests with the Clamshell axial spacer and removable top end plate.

2.7.1.1 Technical Basis for the Free Drop Tests

To properly select a worst case package orientation for the 9 m (30 feet) free drop event, the foremost item that could potentially compromise the criticality control integrity of the Traveller series of packages must be clearly identified.

The criticality control integrity may be compromised by four methods: 1) excessive movement of the fuel rods such that they form a critical geometry, 2) damage/destruction of the neutron absorber and polyethylene sheeting, 3) degradation of the neutron absorber/polyethylene sheeting and/or 4) other structural damage that could affect the nuclear reactivity of an array of packages.

For the above considerations, testing and FEA predictive methodology must include orientations that affect the Clamshell geometry and integrity. Throughout the development of the Traveller XL, minor design changes were made to optimize the structural and thermal performance of the package.

A total of nine (9) 30 foot (9 m) free drops were performed using full-scale prototypes at a variety of orientations to determine the most severe orientation and to assist in benchmarking the computer simulation model. Based on these tests, and the predictions of the analytic analyses, it was determined that the most severe 9 m free drop orientation was a bottom-end down drop due to; 1) the relatively high deceleration, 2) the greatest opportunity for lattice expansion of the fuel, and 3) the greatest opportunity for fire damage as a result of the subsequent pool-fire thermal testing.

The bottom-down end drop causes the greatest damage to the axial impact limiters, or “pillows.” These pillows were incorporated as a re-design from QTU-2 testing whereby the Clamshell punched through the plate covering the inner section of the axial impact limiter. This exposed foam later burned within the interior of the Outerpack and ignited the moderator panels. The concept of a puncture plate was redesigned to incorporate a “puncture resistant” plate. The inner foam limiter was therefore protected by the puncture resistant plate (1/4" thk, 0.64 cm), and was enclosed by a spun metal “can” welded to the plate to completely seal the pillow assembly. CTU test results confirmed that no polyurethane foam was exposed as a result of the bottom-down end impact.

The long bottom nozzle “legs” associated with the Westinghouse 17x17 XL fuel assembly are considered the most severe because they allow considerable strain of the bottom nozzle (particularly the flow plate, or

adapter plate) during a bottom-down end drop. The bowed adapter plate offers the greatest opportunity to damage fuel rods during the impact.

The top-down end drop produces significantly lower deceleration due to buckling of the axial clamp bolts. As these buckle, considerable energy is absorbed, thus lower the buckling of the top nozzle. By comparison, the bottom-down end drop is more severe.

2.7.1.2 Test Sequence for the Selected Tests

Analyses indicated and testing demonstrated that the puncture tests did not cause any damage to the package that would lead to further damage in the fire test, and neither did they compromise package containment or confinement. Therefore either order in which the 9m drop test and the puncture test are performed is equally valid.

TS-R-1, para 727, states that the drop test sequence shall be such that, upon completion, the specimen will have suffered such damage as to lead to maximum damage in the thermal test that follows. The TS-R-1 advisory document, TS-G-1.1, expands on this, saying that the assessment of maximum damage should consider what affect the drops have on package containment, shielding, and confinement. TS-G-1.1 further cautions that the most damaging package orientation may not be a flat impact onto the bar top surface, but an angle in the range 20° –30° range, because such an angle causes tearing of the outer skin as well as puncturing.

Section 2.7.3.1 discusses the technical basis for the puncture test, indicating that the greatest possibility of cumulative damage to this package occurs when the pin puncture is located within the area of impact of the 9m drop. Thus, maximum damage would occur when the puncture test follows the 9m drop test. During the Traveller development period, several test specimens were subjected to puncture drops onto different parts of the package in an effort to determine which location was most damaging. In one instance the drop test sequence was altered to assess whether or not a different order would cause more damage. As mentioned above, it was found that the puncture tests did not cause any damage to the package that would jeopardize either package containment or confinement. Therefore either order in which the 9m drop test and the puncture test are performed is equally valid.

Section 2.7.3.2 summarizes the results from the puncture drop tests. The several puncture tests are described in detail in the SAR and are summarized below.

Test Specimen	SAR	Test Sequence	Inspection Results
FEA Analysis	2.12.3.2.7	Two cases modeled: – Horizontal drop onto belly – Horizontal drop onto hinge	<ul style="list-style-type: none"> • Predicted unlikely that the outer shell would be penetrated in either case • (Good agreement between FEA results and prototype test results)
Prototype I	2.12.4.1	<p>(1) 9m Drop</p> – Bottom nozzle drop – 71° angle CG over corner on hinge	<ul style="list-style-type: none"> • Outerpack outer skin was locally indented 1.63" • Impact punch zone width was 10.5" • Pin did not perforate the outer skin • Internal inspection findings – small dent about 7/16" to 1/2" and 15" wide resulted from the pin puncture test • Moderator blocks were not impacted by the pin test.
		<p>(2) Puncture</p> – Package at 20° angle upside down over center of gravity	

Test Specimen	SAR	Test Sequence	Inspection Results
Prototype II	2.12.4.1	(1) Puncture – Drop onto package side – Package at 20° angle, CG (2) 9m Drop – Top nozzle drop – 72° angle CG over corner	<ul style="list-style-type: none"> • Outerpack outer skin was locally indented about 2" • Impact punch zone was 10" tall and 14" wide • Pin did not perforate the inner and outer shell • Moderator blocks and neutron poison plates maintained position
Qualification Test Unit I	2.12.4.2.1	(1) 9m Drop – Top nozzle drop – 72° angle CG over corner (2) Puncture – Drop onto top nozzle end – Package at 83° angle – Dropped on hinge to add to damage from 9m drop	<ul style="list-style-type: none"> • Indentation was approximately 1-1/2" deep • Additional tearing of the joint was noted which resulted in measured tear of approximately 1-1/8" • Moderator blocks and neutron poison plates maintained position
Qualification Test Unit II	2.12.4.2.2	(1) 9m Drop – Bottom nozzle drop – 90° angle (2) Puncture – Drop onto underbelly of package – Package at 22° angle	<ul style="list-style-type: none"> • Damage zone was 9" long x 6" wide x 2-7/8" deep • Moderator blocks and neutron poison plates maintained position
Certification Test Unit	2.12.4.3	(1) 9m Drop – Bottom nozzle drop – 90° angle (2) Puncture – Drop onto side of package, onto hinge – Package at 21° angle	<ul style="list-style-type: none"> • 6" length of hinge dented length to a maximum depth of 1.375" • Hinge separation of 1/2" from package about 7-1/2" from the impact point towards the top nozzle end • Hinge knuckles were not compromised • Moderator blocks and neutron poison plates maintained position

2.7.1.3 Summary of Results from the Free Drop Tests

Successful HAC free drop testing of the Traveller XL CTU certification unit indicates that the various structural features are adequately designed to withstand the 9 m (30 foot) free drop event. The most important result of the testing program was the demonstrated ability of the bounding Traveller XL package to maintain its criticality safety integrity.

Significant results of the free drop tests, including the thermal test, are as follows:

1. There was no breach or distortion of the Clamshell aluminum container.
2. There was no evidence of melting or material degradation on the polyethylene sheeting.
3. The Outerpack remained closed and structurally intact.
4. A small number of rods (20) were cracked during drop testing (only seen in bottom-end drops).
5. Rod damage has been at the end of the rods only. No damage anywhere else.
6. None of the end plugs have separated from the rods.
7. No pellet material is lost from the cracked rods.

Further details of the free drop test results are provided in Appendix 2.12.5, Traveller Drop Test Results. |

2.7.2 Crush

The crush test specified in 10 CFR §71.73(c)(2), TS-R-1 (727) is required only when the specimen has mass not greater than 500 kg (1,100 pounds), an overall density not greater than 1,000 kg/m³ (62.4 lb/ft³), and radioactive contents greater than 1,000 A2, not as special form. The gross weights of the Traveller packages are greater than 500 kg (1,100 pounds). Therefore, the dynamic crush test of 10 CFR §71.73(c)(2), TS-R-1 (727) is not applicable to the Traveller series of packages.

2.7.3 Puncture

Subpart F of 10 CFR 71 requires performing a puncture test in accordance with the requirements of 10 CFR §71.71(c)(3), TS-R-1 (727). The puncture test involves a 1 m (40 inch) drop onto the upper end of a solid, vertical, cylindrical, mild steel bar mounting on an essentially unyielding, horizontal surface. The bar must be 15 cm (6 inches) in diameter, with the top surface horizontal and its edge rounded to a radius of not more than 6 mm (1/4 inch). The minimum length of the bar is to be 20 cm (8 inches). The ability of the bounding Traveller XL packages to adequately withstand this specified drop condition is demonstrated via testing of numerous full-scale Traveller XL prototypes and the Certification Test Unit (CTU).

2.7.3.1 Technical Basis for the Puncture Drop Tests

To properly select a worst case package orientation for the puncture drop test, items that could potentially compromise criticality integrity of the Traveller package must be clearly identified. For the Traveller XL package design, the foremost item to be addressed is the integrity of the Clamshell and the neutron moderation and absorption materials (i.e., neutron absorber plate and polyethylene sheeting).

The integrity of the Clamshell and the criticality control features may be compromised by two methods: 1) breach of the Clamshell boundary, and 2) degradation of the neutron moderation/control materials due to fire.

For the above reasons, testing must consider orientations that attack the Outerpack closure assembly, which may result in an excessive opening into the interior for subsequent fire event, and/or the Clamshell which contains the fuel assembly. Based on prototype testing and computer simulations of the pin puncture event, the pin puncture has insufficient energy to cause significant damage to the Outerpack hinge closure system nor to the Clamshell (including components within the Clamshell).

The greatest possibility of cumulative damage to the package occurs when the pin puncture is located within the area of impact of the 9m drop. These locations further attack the welded joints adjacent to the crushed area between the Outerpack outer shell and the end cap. Many pin puncture locations were tested in prototype testing, and all had insignificant impact on the structural and thermal performance of the package. See Table 2-2 above, and Appendix 2.12.5, Traveller Drop Test Results, for more information regarding pin puncture testing.

Based on the above discussion, the Traveller XL CTU was specifically evaluated at a “new” location. The pin puncture was located such that the pin impacted directly on an Outerpack hinge at a low impact angle. This test had not previously been performed, and it was desired to test the hinge’s ability to take a pin impact and still perform its important function of thermally protecting the seam between Outerpack bottom and top assemblies. The thermal protection offered by the hinge is described in more detail in Section 3.

2.7.3.2 Summary of Results from the Puncture Drop Test

Successful HAC puncture drop testing of the CTU indicates that the various Traveller XL packaging features are adequately designed to withstand the HAC puncture drop event. The most important result of the testing program was the demonstrated ability of the bounding Traveller XL to maintain its structural integrity. Significant results of the puncture drop testing are as follows:

1. Minor damage to the Outerpack and Outerpack hinge
2. No affect on the structural or thermal performance of the package.
3. There was no evidence of separation of the Outerpack seam which would allow hot gases to enter the Outerpack.
4. No evidence of movement occurred that would have significantly affected the geometry or structural integrity of the Clamshell.
5. There was no evidence of loss of contents from the Clamshell due to the puncture events.
6. There was no evidence of deterioration of the polyethylene sheeting in the subsequent fire event.
7. There was no evidence of deterioration of the borated-aluminum sheeting (simulated) in the subsequent fire event.

Further details of the puncture drop test results are provided in Appendix 2.12.5, Traveller Drop Test Results. |

2.7.4 Thermal

Subpart F of 10 CFR 71, TS-R-1 requires performing a thermal test in accordance with the requirements of 10 CFR §71.71(c)(4), TS-R-1 (728). To demonstrate the performance capabilities of the Traveller packaging when subjected to the HAC thermal test specified in 10 CFR §71.71(c)(4), TS-R-1 (727), a full-scale CTU was burned in a fully engulfing pool fire. The test unit was subjected to a 9 m (30 foot) free drop, and a 1.2 m (4 foot) puncture drop, prior to being burned, as discussed above. Further details of the thermal performance of the Traveller XL CTU are provided in Section 3, Thermal Evaluation.

Type K thermocouples were installed on the exterior surface of the packaging (each side, top, and bottom) to monitor the package's temperature during the test. In addition, passive, non-reversible temperature indicating labels were installed on the Clamshell, fuel assembly, and inner surfaces of the Outerpack.

The CTU was exposed to a minimum 800°C (1,475°F), 30-minute pool fire. As discussed in Appendix 2.12.5, Traveller Drop Test Results, the package was orientated such that the Outerpack was on its side. This orientation offered the greatest opportunity for formation of a chimney and thus result in maximum combustion of the Outerpack foam and degradation of the polyethylene sheeting. |

Following the minimum 30-minute fire, the CTU was allowed to cool naturally in air, without any active cooling systems.

2.7.4.1 Summary of Pressures and Temperatures

The accident case pressure is assumed to be 0 psig since the Outerpack and Clamshell are not sealed.

The peak temperatures for the Clamshell, as recorded by five (5) temperature indicating strips, was 104°C (217°F). No loss of material was observed in the polyethylene material.

2.7.4.2 Differential Thermal Expansion

Fire testing of a full-scale Traveller XL package indicates that the stresses associated with differential thermal expansion of the various components are negligible.

2.7.4.3 Stress Calculations

Successful fire testing of a full-scale Traveller XL CTU package, as well as prior tested prototypes, indicates that the stresses associated with differential thermal expansion of the various packaging components are negligible.

2.7.4.4 Comparison with Allowable Stresses

As discussed in Section 2.7.4.3, Stress Calculations, further evaluation of stresses associated with differential thermal expansion for the various Traveller package components is not required.

Successful HAC thermal testing of the CTU indicates that the various Traveller packaging design features are adequately designed to withstand the HAC thermal test event. The most significant result of the testing program was the demonstrated ability of the Traveller XL CTU to maintain its criticality control integrity, as demonstrated by post-test inspection of; the moderator and poison materials, the remaining polyurethane foam, and the integrity of the Clamshell.

Further details of the thermal test results are provided in Appendix 2.12.5, Traveller Drop Tests Results and Section 3, Thermal Evaluation.

2.7.5 Immersion – Fissile Material

Subpart F of 10 CFR 71 requires performing an immersion test for fissile material packages in accordance with the requirements of 10 CFR §71.73(c)(6), TS-R-1 (733). Because of the seal configuration (see Section 1, General Information), the Traveller STD and Traveller XL packages are not leak-tight under external overpressure. Under the immersion test, water will fill all internal void space. Because of the pressure equalization, the packaging structure is therefore not subjected to loading during these tests.

2.7.6 Immersion – All Packages

Subpart F of 10 CFR 71 requires performing an immersion test for fissile material packages in accordance with the requirements of 10 CFR §71.73(c)(6), TS-R-1 (729). Because of the seal configuration (see Section 1, General Information), the Traveller STD and Traveller XL series of packages are not leak-tight under external overpressure. Under the immersion test, water will fill all voids. Because of the pressure equalization, the packaging structure is therefore not subjected to loading during these tests.

As the package model criticality study assumes the worst-case flooding scenario, the Traveller XL CTU is exempted from this water immersion test.

2.7.7 Summary of Damage

As discussed in the previous sections, the cumulative damaging effects of the free drops, puncture drop, and thermal tests were satisfactorily withstood by the Traveller XL CTU. Subsequent examinations of the CTU confirmed that integrity of the criticality control components was maintained throughout the test series. The geometry of the Clamshell remained essentially unchanged from the pretest condition. In addition, the Fuel Assembly was well protected and experienced damage that was within acceptance criteria. Therefore, the requirements of 10 CFR §71.73, TS-R-1 (726-729) have been adequately satisfied.

2.8 ACCIDENT CONDITIONS FOR AIR TRANSPORT OF PLUTONIUM

Not applicable.

2.9 ACCIDENT CONDITIONS FOR FISSILE MATERIAL FOR AIR TRANSPORT

Application to be made at a later date.

2.10 SPECIAL FORM

The contents of the Traveller series of packages do not classify as special form material.

2.11 FUEL RODS

In the Traveller XL and STD packages, the fuel rods within the package provide containment for the nuclear fuel. This containment was successfully demonstrated in 3 full-scale test campaigns comprising a total of nine (9) 30 foot free drops, and the corresponding 1.3 meter free-drops and pin puncture tests. These tests resulted in 100% containment of the fuel pellets within rod of every fuel assembly.

For all 9-meter drop test orientations except for the bottom-down end drop (long axis of package aligned with the gravity vector), every fuel rod survived with no damage except slight to moderate buckling of the cladding. Rod pressure test sampling was routinely performed on these fuel assemblies. Except for the bottom-down end drop, all of the rods sampled remained intact and pressurized. All rods visually appeared in excellent condition.

A total of two (2) full-scale Traveller XL packages (QTU-2 and CTU) were tested in a bottom-down end drop orientation. Both of these fuel assemblies (dummy Westinghouse 17x17 XLs) experienced a small percentage of rods with cracked welds in the location of the bottom end plug. In the worst case assembly (CTU), post-test inspection of the fuel assembly indicated that approximately 7.5% of the fuel rods were visibly cracked at the end plug weld zone. The average magnitude of the crack widths measured approximately 0.030 inches (0.76 mm) encompassing about one-half of a rod diameter. This minor cracking is considered insignificant since fuel pellets of diameter 0.374 inches (9.50 mm) are approximately 12.5 times larger than the average visible crack widths. A crack width of 0.075 inches (1.91 mm) was the largest observed. This width is not sufficient for fuel pellets to escape. Therefore, the containment system satisfies its requirement of containing loss of fuel.

Due to the nature of the bottom-down end impact, the fuel rod array is tightly packed and forced into the bottom nozzle. As the bottom nozzle buckles, the rods located nearest the corners of the adapter plate experience a side loading due to the deformed shape of the plate. This moment is sufficient to crack the weld, however, it is clearly not sufficient to completely break off the bottom end plug since the array of rods is so tightly packed. No complete separation of the bottom end plug was observed in any fuel rods for both fuel assemblies. Therefore, the fuel pellets are safely contained within each fuel rod. Further details can be found in Appendix 2.12.5, Traveller Drop Tests Results.

2.11.1 Rod Pipe

The Traveller Clamshell is primarily designed to transport PWR fuel assemblies. To accommodate loose fuel rods, a rod pipe has been designed. It is a 304 stainless steel rod pipe with a maximum diameter of 6.625 inches (6" Schedule 40 pipe), maximum length 200 inches, and a maximum loaded weight of 1650 lbs.

The loose rod pipe is a relatively rigid structure as compared to a fuel assembly. The rod pipe is a single structural member closed by rigid mechanisms. Because the fuel assembly is less stiff than the rod pipe, the fuel assembly is more likely to deform plastically from localized buckling.

The rod pipe is fit to conform into the clamshell axially with a rubber spacer, and is restrained laterally by the bent flanges with foam rubber "clamps" similar to retraining a fuel assembly at the spacer grid locations.

The TRAVELLER response to the 9-meter HAC drop test resulted in the kinetic energy due to the combined mass of the fuel assembly and clamshell being absorbed by the outerpack impact limiter and minor fuel assembly buckling. As a result, the strain damage to the fuel assembly was minimal, and the clamshell retained its pre-test geometry and its structural integrity even though the full stroke of the impact limiter was not utilized. When subject to the 9-meter impact test described in 10CRF71.73, the rod pipe is expected to utilize the full stroke of the impact limiter due to their rigidity. The resulting applied impact force to the rod pipe is expected to be less than that imparted to the fuel assembly. Furthermore, the rod pipe is expected to act in a coupled manner similar to the fuel assembly and result in similar load paths. With the maximum mass of 1650 pounds, the rod pipe will have less impact energy imparted on their rigid structure as well. The maximum rod pipe mass is less than the maximum fuel assembly mass used in the 9-meter impact test. Therefore, the performance of the TRAVELLER packaging with rod pipe contents would be similar to and bounded by the performance of the TRAVELLER packaging that was demonstrated by the 9-meter HAC drop with the fuel assembly contents.

This page intentionally left blank.

2.12 APPENDICES

2.12.1 References

SSR-6, 2012 Ed. [1] has been incorporated by reference into 49 CFR 171.7 [2], replacing TS-R-1, 1996 Ed. (Revised) [3]. The intention of the regulation has not been changed by the new IAEA regulation reference, therefore, the package design maintains compliance to the intension of the updated regulatory reference. Note the section in-text reference has not been revised.

- [1] International Atomic Energy Agency, "Regulations for the Safe Transport of Radioactive Material," SSR-6, 2012.
- [2] U.S. Department of Transportation, Commission Code of Federal Regulations, Title 49 Subchapter C—Hazardous Materials Regulations, October 2016.
- [3] International Atomic Energy Agency, "Regulations for the Safe Transport of Radioactive Material," TS-R-1, 1996 Ed. (Revised).

2.12.2 Container Weights and Centers of Gravity

2.12.3 Mechanical Design Calculations for the Traveller XL Shipping Package

2.12.4 Drop Analysis for the Traveller XL Shipping Package

2.12.5 Traveller Drop Test Results

2.12.6 Supplement to Drop Analysis for the Traveller XL Shipping Package – Clamshell Axial Spacer Structural Evaluation

2.12.7 Supplement to Drop Analysis for the Traveller XL Shipping Package – Clamshell Removable Top Plate Structural Evaluation

2.12.8 Supplement to Drop Analysis for the Traveller XL Shipping Package - Structural Analysis of the Traveller VVER Shipping Package

2.12.2 Container Weights and Centers of Gravity

2.12.2.1 Container Weights

This section provides the Traveller XL, VVER and STD weight breakdown to establish design and licensing weights, and centers of gravity for each package. The Design and Licensing Basis Gross Weight is calculated from the Nominal Total Weight plus the 2.3% manufacturing uncertainty. The maximum tare weight is the Design and Licensing Basis Gross Weight less the maximum fuel assembly weight. Maximum tare and Design and Licensing weights are rounded up to the nearest tenth after the maximum tare weight is determined.

	Traveller STD	Traveller XL	Traveller VVER
Nominal Outerpack Weight, lb (kg)	2368 (1074)	2670 (1211)	2670 (1211)
Max. Fuel Assembly Weight, lb (kg)	1650 (748)	1971 (894)	1850 (839)
Nominal Clamshell Weight, lb (kg)	378 (171)	467 (212)	463 (210)
NOMINAL TOTAL WEIGHT, lb (kg)	4396 (1994)	5108 (2317)	4983 (2260)
DESIGN and LICENSING BASIS GROSS WEIGHT, lb (kg)	4500 (2041)	5230 (2372)	5105 (2316)
DESIGN TARE WEIGHT, lb (kg)	2850 (1293)	3255 (1476)	3255 (1476)

2.12.2.2 Centers of Gravity

This section provides the location of the center of gravity for empty Traveller XL/VVER and Traveller STD packages.

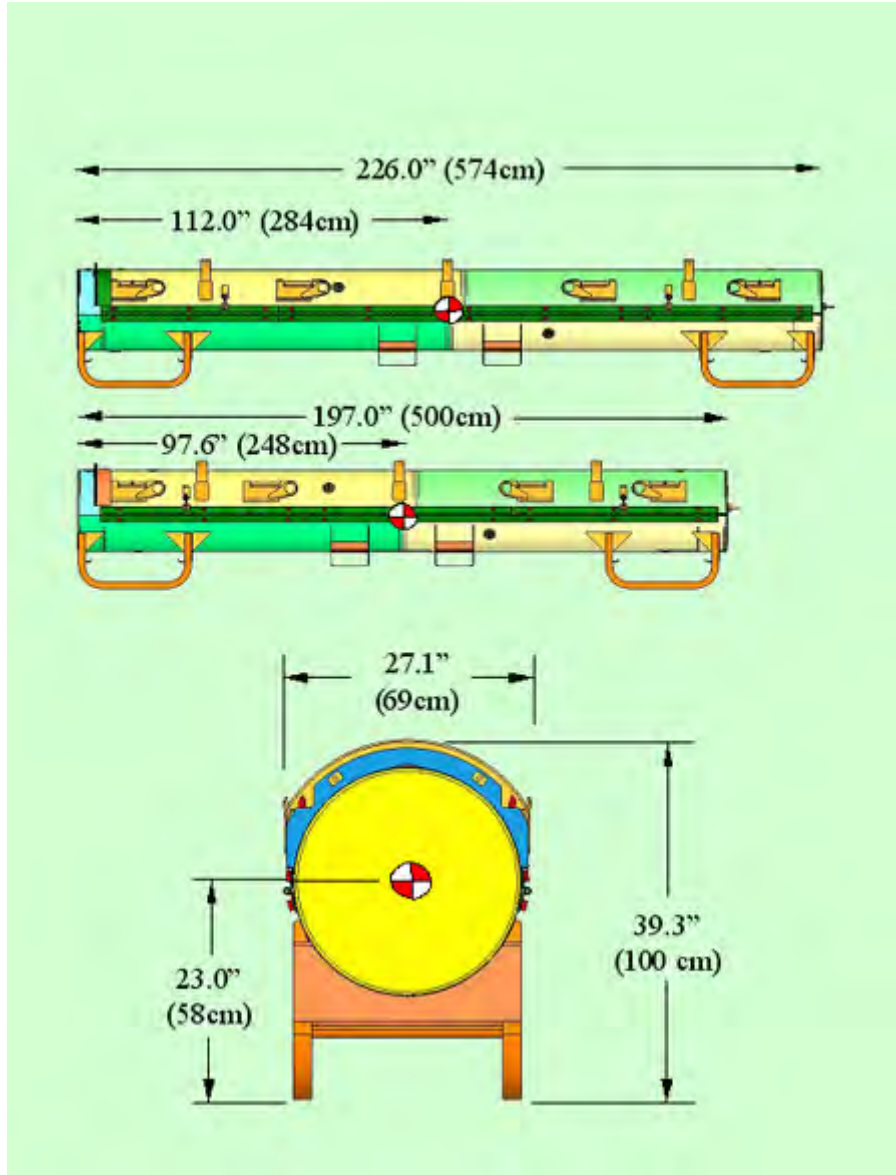


Figure 2-2 Traveller XL/VVER and Traveller STD Dimensions and Center of Gravity
(Note: End View is Common to both Models)

2.12.3 Mechanical Design Calculations for the Traveller XL Shipping Package

During Traveller package development, normal transport and hypothetical accident condition testing were performed to demonstrate package compliance to test conditions described in 10 CFR 71 and TS-R-1. For those requirements not demonstrated by testing, a mechanical analysis was performed to demonstrate package compliance. This section outlines the non-tested requirements to be satisfied and provides an analysis for each requirement.

The Traveller XL package is depicted in Figure 2-3. The exterior view of the Outerpack is shown. The internal packaging including the Clamshell is shown in Figure 2-4. The Traveller XL package structurally and mechanically bounds the Traveller VVER and Traveller STD packages because the XL is more massive than either the VVER or STD (except in the case of stacking where a double stacked Traveller STD bounds the Traveller XL and Traveller VVER). Additionally, the computer simulations and full-scale testing of the Traveller XL units demonstrate a robust design with considerable safety margins with respect to all structural and mechanical requirements.

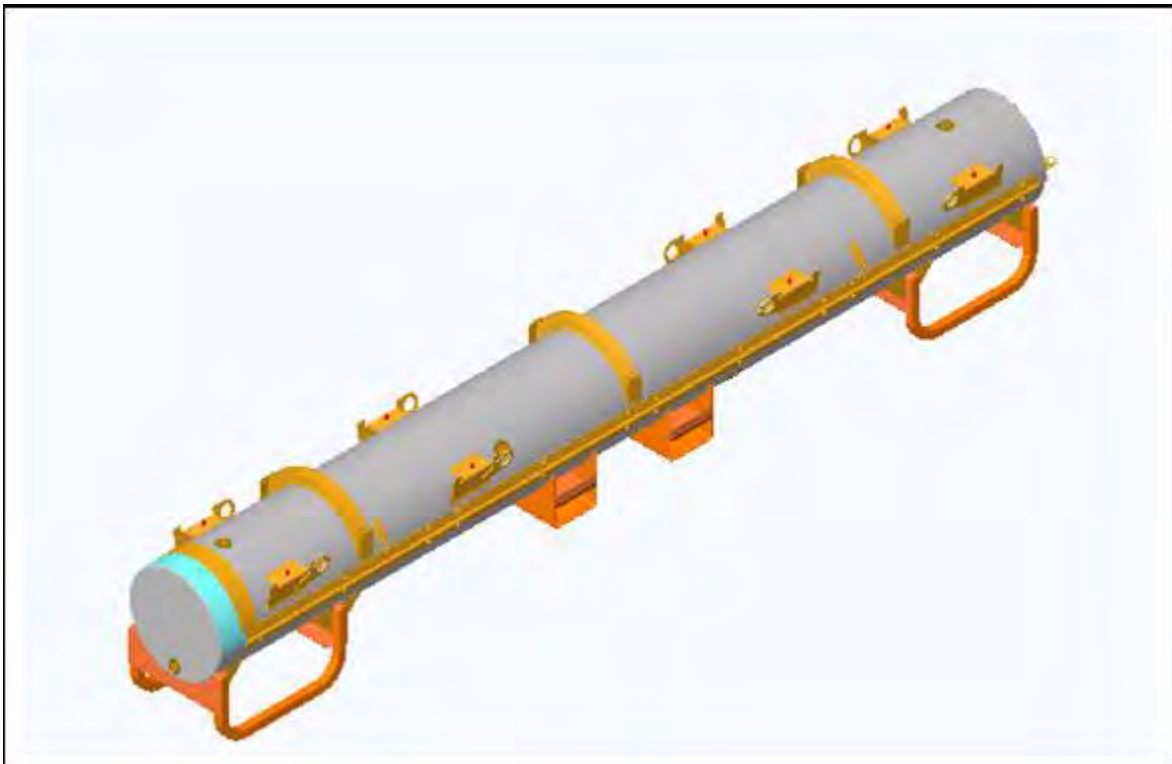


Figure 2-3 Westinghouse Fresh Fuel Shipping Package, the Traveller XL

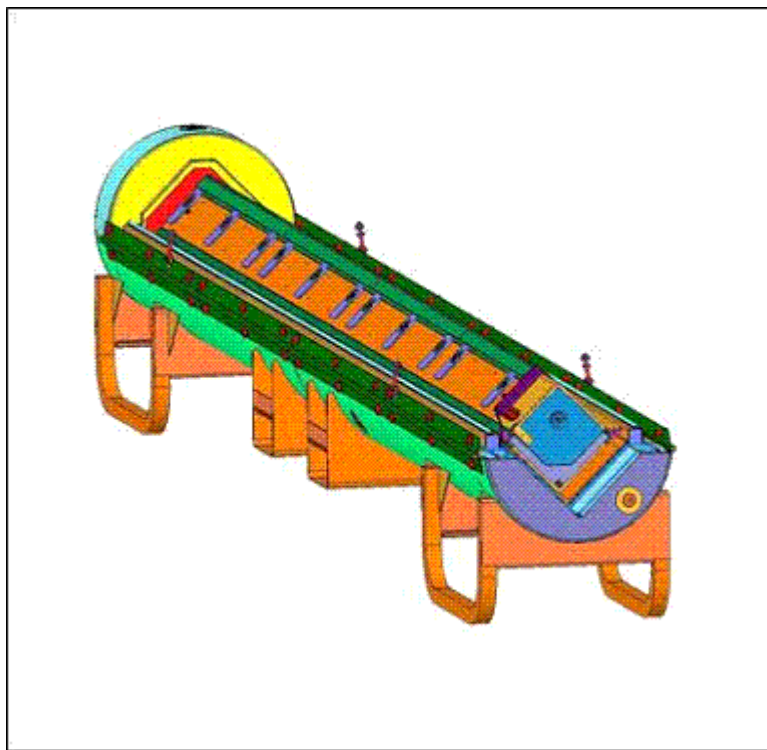


Figure 2-4 Internal View of the Traveller Shipping Package

2.12.3.1 Analysis Results and Conclusions

These analyses were performed to demonstrate Traveller XL package compliance to the mechanical requirements described in 10 CFR 71 and TS-R-1 for which no formal testing was conducted. These calculations bound the lighter, shorter Traveller STD unit. The applicable requirements were summarized in Table 2-3. The results of the design calculations (where applicable), acceptance criteria, and conditional acceptance shown in Table 2-4. Based on the results in Table 2-4, the Traveller package is shown to be compliant to mechanical requirements described in 10 CFR 71 and TS-R-1

Table 2-7 has been deleted.

Table 2-8 has been deleted.

Assumptions

The calculations to determine the maximum Outerpack allowable stresses for yield, shear, and weld shear are based on the properties of ASTM A240 Type 304 Stainless Steel. It is further assumed that the weld consumable possess greater mechanical properties than that of the base metal. Hence, the mechanical properties of the base metal will be employed for weld stress analysis. The reference drawings included in this analysis represent the Certification Test Unit (CTU) Traveller XL, which was fabricated for the drop and fire tests.

Acceptance Criteria

The Traveller package was structurally evaluated to demonstrate compliance to the conditions described in Table 2-3. The package's Outerpack structure is composed of ASTM A240 Type 304 Stainless steel. The mechanical properties are of listed below:

- Tensile strength, Minimum: 75 ksi
- Yield strength, Minimum: 30 ksi

For mechanical analysis where tensile, shear, or weld shear stresses were determined, the acceptance criteria was as follows:

- Maximum allowable tensile yield stress, $\sigma_y = 30$ ksi
- Maximum allowable shear stress, $\tau_{\max} = .6\sigma_y = 18$ ksi
- Maximum allowable weld shear stress, $\tau_{\text{weld}} = .4\sigma_y = 12$ ksi

The material constant Young's Modulus for 304 Stainless steel is:

$$E = 29.4E6 \text{ psi}$$

2.12.3.2 Calculations

Nine mechanical conditions were evaluated for Traveller package. These conditions are outlined in Table 2-3. Standard engineering methods were used for these calculations.

2.12.3.2.1 Input

The design loads were determined according to the criteria described in 10 CFR 71 and TS-R-1, 1996 where appropriate. The Traveller XL package weight bounds the Traveller STD design as shown in Table 2-6. The total weights for each Traveller design include shipping components where applicable.

Table 2-9 has been deleted.

Lifting – The lifting criteria is governed by 10 CFR 71.45(a) and TS-R-1, Paragraph 607. 10 CFR 71.45(a) states that any lifting attachment that is a structural part of the package must be designed with a minimum safety factor of three against yielding when used to lift the package in its intended manner. In addition, it must be designed so that failure of any lifting device under excessive load would not impair the ability of the package to meet other requirements of 10 CFR 71. The applied loads to the package lifting attachments are then:

For the case of Traveller XL:

$$F_l = 3W_{XL}$$

$$F_l = 3(5,230) \text{ lb}$$

$$F_l = 15,690 \text{ lb for the Traveller XL}$$

For the case of stacked Traveller STD:

$$F_l = 3W_{2STD}$$

$$F_l = 3(2*4,500) \text{ lb}$$

$$F_l = 27,000 \text{ lb}$$

Tie-Downs – The tie-down requirements are described in 10 CFR 71.45(b)(1,2) and TS-R-1, Paragraph 636. 10 CFR 71.45 states that a system of tie-downs that is a structural part of the package must be capable of withstanding, without generating stress in excess of its yield strength, a static force applied to the center of gravity having the following components:

- Vertical: 2 g
- Axial: 10 g
- Transverse: 5 g

Thus, the applied tie-down loads for the Traveller are:

- Vertical: 10,460 lb
- Axial: 52,300 lb
- Transverse: 26,150 lb

Design Temperatures between -40°F (-40°C) and 158°F (70°C) – The package must account for temperatures ranging from -40°F (-40°C) to 158°F (70°C) per TS-R-1 (637), and from -40°F (-40°C) to 100°F (38°C) per 10 CFR 71.71(c)(1,2). Thus, the bounding temperature range to consider for package design is -40°F (-40°C) to 158°F (70°C). The analysis of the Traveller package will consider the effects of temperature on thermally induced stress.

Internal/External Pressure – The package must account for the effects of external pressure conditions. The effects of reduced and increased external pressure are described in 10 CFR 71.71(c)(3,4) and TS-R-1 (615). The reduced external pressure is 25 kPa (3.5 psi) absolute, and the increased external pressure is 140 kPa (20 psi) as stated in 10 CFR 71.71.

Water Spray – A water spray test is required for the Traveller package to consider the effects of excessive rainfall on the structural integrity of the package. The water spray test is described by 10 CFR 71.71(c)(6) and TS-R-1 (721). The water spray test is to simulate a rainfall rate of approximately 5 cm/hr (2 in/hr) for at least one hour.

Compression/Stacking Test – The Traveller package must be subjected to a static compression test per by 10 CFR 71.71(c)(9) and TS-R-1 (723). Both regulations require that the applied load be the greater of the following:

An equivalent load of five times the mass of the package or the equivalent of 13 kPa (2 psi) multiplied by the vertically projected area of the package. Evaluating each case:

Case 1

The applied stacking force for case 1 is:

$$F_s = 5W_{XL}$$

$$F_s = 5(5230) \text{ lb}$$

$$F_s = 26,150 \text{ lb}$$

Case 2

The applied stacking force for case 2 is:

$$F_s = (Length)(OD)(P)$$

$$F_s = (226.2)(27.1)in^2(2)psi$$

$$F_s = 12,260 \text{ lb}$$

Thus, the applied stacking load is $F_s = 26,150 \text{ lb}$.

Penetration – The penetration test is an impact test described by 10 CFR 71.71(c)(10) and TS-R-1 (724). The package must be subject to the impact of the hemispherical end of a vertical steel cylinder of 3.2 cm (1.25 in) diameter and a mass of 6 kg (13 lb) dropped from 1 m (40 in) onto the surface of the package that is expected to be the most vulnerable to puncture.

Immersion – The immersion test is a hypothetical accident condition test that evaluates the effects of static water pressure head on the structural integrity of the package. The test condition is described by 10 CFR 71.73(c)(6) and TS-R-1 (729). The regulations state that the package must be immersed under a head of water of at least 15 m (50 ft) for at least 8 hours in the most damaging orientation. For demonstration purposes, an external gauge pressure of 150 kPa (21.7 psi) is considered to meet the test conditions.

2.12.3.2.2 Lifting

Traveller XL Four Point Lift – The Traveller package is crane lifted using a 4-point lift with attachment points located on the stacking bracket. Figure 2-5 shows a sample package with the lifting configurations. The assumed sling angle is 30°. The applied load, $F_l = 15,690$ lb.

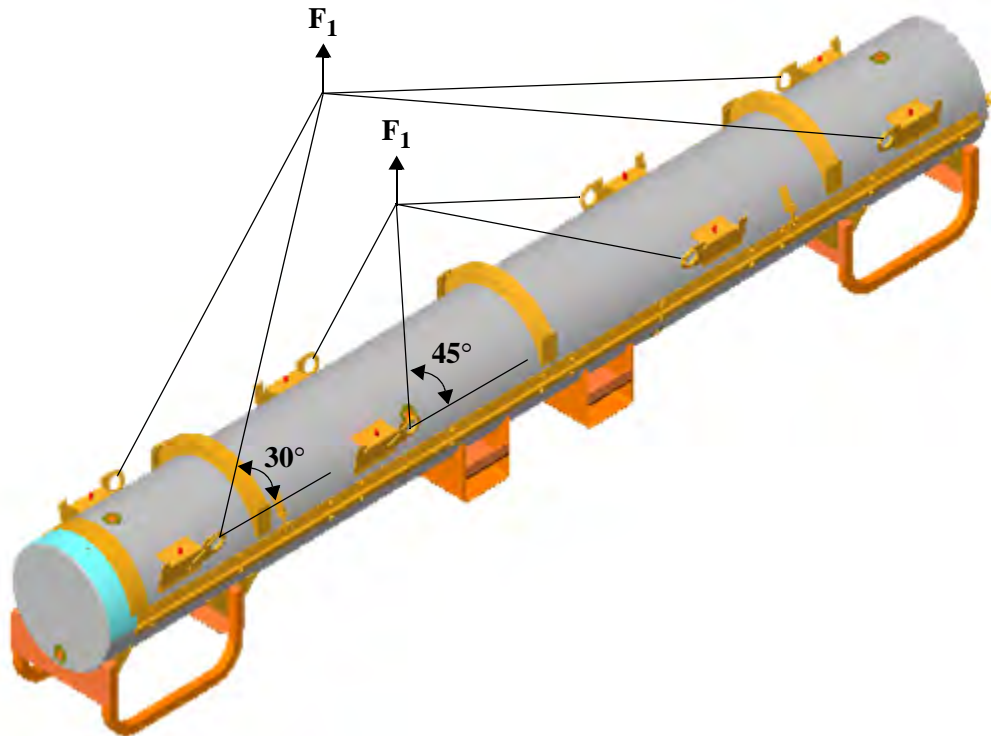


Figure 2-5 Traveller XL Lifting Configurations

Based on the lifting configuration, the applied load transferred to each lifting hole, F , is:

$$F = \frac{F_l}{4 \sin 30}$$

$$F = \frac{15,690}{4} / .5 \text{ lb}$$

$$F = 7,845 \text{ lb/hole}$$

The applied forces and resultant components for a single lifting hole are shown in Figure 2-6.

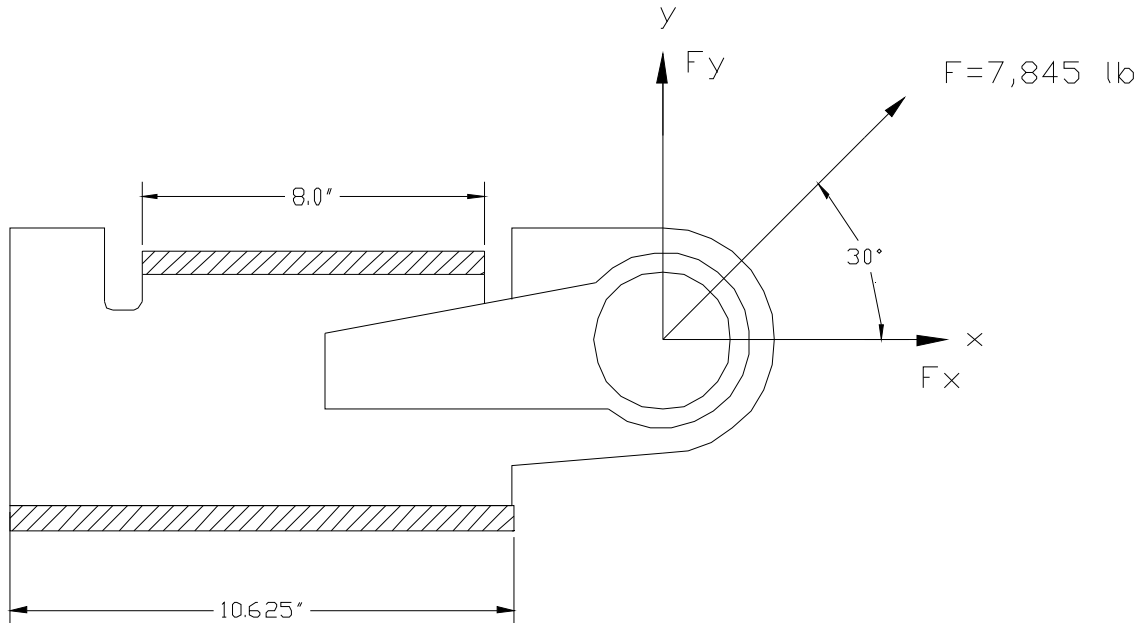


Figure 2-6 Lifting Hole Force Detail

The resulting force components are then:

$$F_x = F(\cos 30)$$

$$F_x = 7,845(0.866) \text{ lb}$$

$$F_x = 6,794 \text{ lb, and}$$

$$F_y = F(\sin 30)$$

$$F_y = 7,845(0.50) \text{ lb}$$

$$F_y = 3,923 \text{ lb}$$

The lifting bracket consists of ASTM A276 SS plate with an attached lifting eye. The lifting eye is 0.25" thick ASTM A276 SS plate and is reinforced with a 0.25" plate doubler. A lifting bracket detail is shown in Figure 2-7.

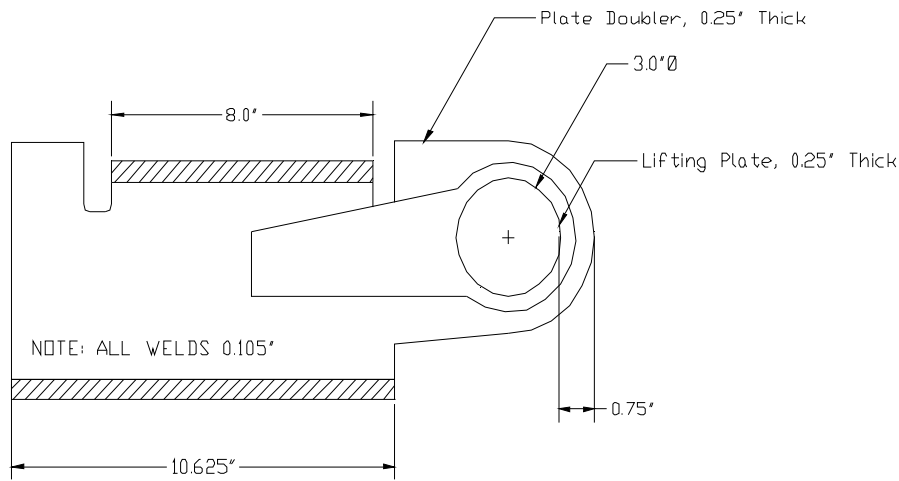


Figure 2-7 Lifting Bracket Fabrication Detail

The lifting analysis consists of two calculations: 1) hole tear-out and, 2) weld strength.

The hole tear-out is assumed to occur at the minimum 0.75" section of material in the lifting eye plate. From Table 2-4, the maximum allowable Shear Yield Stress, τ_y is 18 ksi. The stressed area is the minimum thickness of 0.5" times the section width of the tear out, 0.75" and double shear is assumed. Thus,

$$A = 2(.75)(.5) \text{ in}$$

$$A = 0.75 \text{ in}$$

The elemental volume stress state is described by the Mohr's Circle as shown in Figure 2-8. The resulting stress on the element due to applied load of 7,500 lbs is:

$$\sigma_x = F / A$$

$$\sigma_x = 7,845 / .75 \text{ psi}$$

$$\sigma_x = 10,460 \text{ psi}$$

The maximum shear stress on the element is then:

$$\tau_{\max} = \sqrt{\left[\frac{(\sigma_{x'} - \sigma_{y'})}{2}\right]^2 + \tau_{x'y'}^2}$$

$$\tau_{\max} = \sqrt{\left[\frac{(10,460 - 0)}{2}\right]^2 + 0^2}$$

$$\tau_{\max} = 5,230 \text{ psi}$$

Shear tear-out of the hole is not expected since $\tau_{\max} = 5,230 \text{ psi} < \tau_{\text{allowx}} = 18,000 \text{ psi}$.

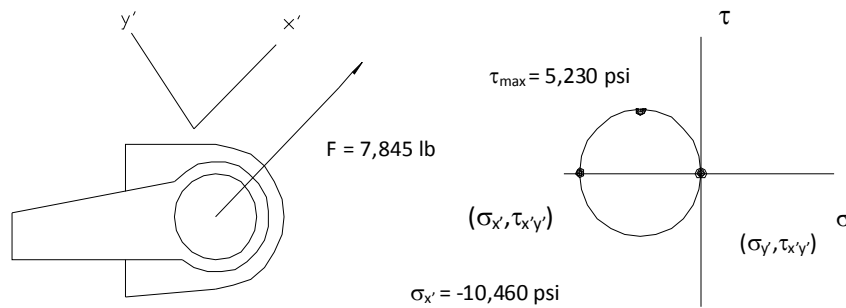


Figure 2-8 Hole Tear-out Model and Mohr's Circle Stress State

- The weld attaching the lift plates to the Outerpack shell are required to demonstrate that they are adequate to preclude local weld yielding. The analysis assumes that one of the wire ropes is non-functional and three of the four welds bear the lifting load. The weld shear stress is found by $\tau_{\text{weld}} = F/A$, where F is the applied vertical or horizontal load and A is the weld area. The assumed weld area is:

$$A = hl \sin 45, \text{ where } l \text{ is } (.75)(10.625+8") = 13.97" \text{ from Figure 2-6, and } h \text{ is the weld thickness, } 0.105".$$

The applied loads are $F_x = 6,794 \text{ lbs}$ in the vertical direction and $F_y = 3,923$ in the horizontal direction. The weld stresses are then:

$$\tau_x = F_x/A \text{ and } \tau_y = F_y/A$$

Substituting values,

$$\tau_x = 6,794 / (.105)(13.97)(.707) \text{ psi}$$

$$\tau_x = 6,551 \text{ psi, and}$$

$$\tau_y = \frac{F_y}{A}$$

$$\tau_y = 3,923 / (.105)(13.97)(.707) \text{ psi}$$

$$\tau_y = 3,783 \text{ psi}$$

The stresses τ_x and τ_y are perpendicular to each other, and the resulting weld shear stress is:

$$\tau = \sqrt{(\tau_x^2 + \tau_y^2)}$$

$$\tau = \sqrt{(6,551^2 + 3,783^2)}$$

$$\tau = 7,565 \text{ psi}$$

The welds are sufficient to prevent local yielding since $\tau_{\max} = 7,565 \text{ psi} < \tau_{\text{allow}} = 12,000 \text{ psi}$.

Traveller STD Four Point Lift – The Traveller STD package may be crane lifted using a 4-point lift with attachment points located on the inner stacking bracket. Figure 2-9 shows sample STD packages with the lifting configuration. The assumed sling angle is 45° since the inner lifting brackets are utilized. The applied load is $F_l = 27,000 \text{ lb}$ from Section 2.12.3.2.1. The methodology is the same as for the Traveller XL since the load path and structure is assumed nearly identical. However, the force components are greater:

$$F = \frac{F_l}{4 \sin 45}$$

$$F = \frac{27,000}{4 \cdot .707} \text{ lb/hole}$$

$$F = 9,546 \text{ lb/hole}$$

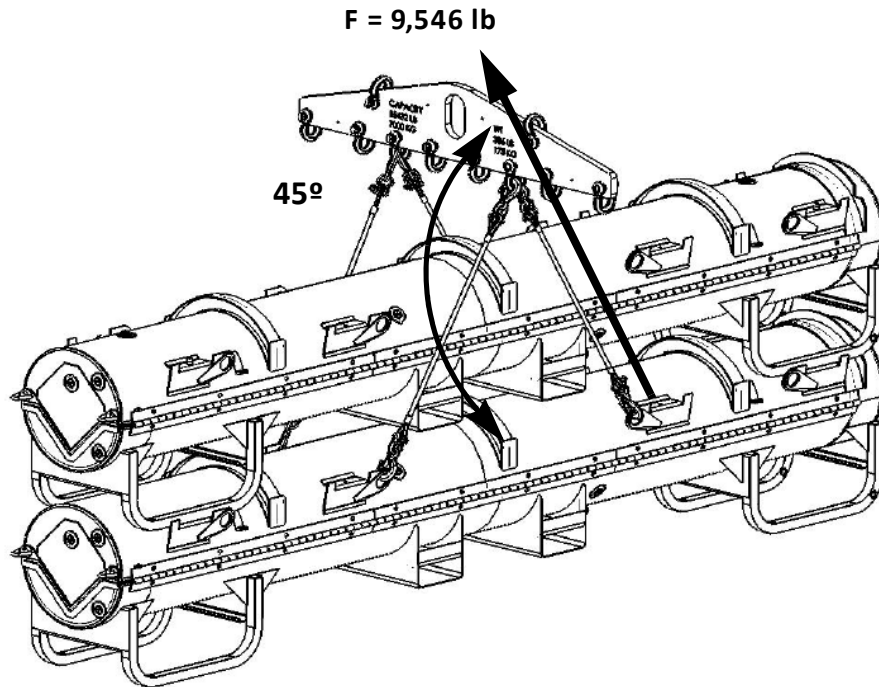


Figure 2-9 Traveller STD Stacked Lifting Configuration

Substituting into the force component geometric relationships:

$$F_x = F_y = 6,750 \text{ lb}$$

These resultant forces result in the following hole tear-out and weld shear loads using the same equations shown for the Traveller XL and substituting Traveller STD values:

Hole tear-out

$$\tau_{\max} = 6,364 \text{ psi}$$

Shear tear-out of the hole is not expected since $\tau_{\max} = 6,364 \text{ psi} < \tau_{\text{allowx}} = 18,000 \text{ psi}$.

Weld Shear

$$\tau = 9,205 \text{ psi}$$

The welds are sufficient to prevent local yielding since $\tau_{\max} = 9,205 \text{ psi} < \tau_{\text{allowx}} = 12,000 \text{ psi}$.

Forklift Analysis – During package lift by a forklift, only the center portion of the package is supported by the forklift extension arms. Consequently, the package is subject to a bending load due to the unsupported weight of the package. The loading conditions include a single Traveller XL and two stacked Traveller STDs.

For the bending evaluation, the Traveller package is conservatively modeled as a cantilever beam with the length equal to half of the overall Traveller length. For XL, $L_f = 113.1$ inches and the design lifting load is distributed over the length of the package as shown in Figure 2-10a. The outer shell is the only assumed structure of the package carrying the bending load. This calculation is repeated for Traveller STD with $L_f = 98.6$ inches. The design weights are calculated in Section 2.12.3.2.1. as 15,690 and 27,000 pounds for Traveller XL and two Traveller STD stacked, respectively.

The forklift pockets weldments are also subjected to a shear load during lifting as the forks will apply a normal force along the top plate as shown in Figure 2-10b. Both the Traveller XL and Traveller STD doubled stacked conditions are evaluated.

Bending

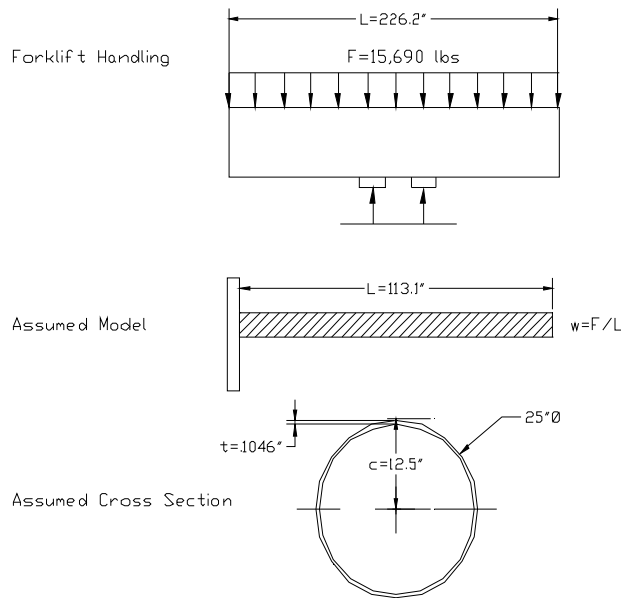


Figure 2-10a Forklift Handling XL Model and Assumed Cross Section

The bending stress can be determined from the classic flexure equation:

$$\sigma = \frac{Mc}{I}, \text{ where}$$

c is the distance from the neutral axis to the outer fibers, M is the applied bending moment, and I is the moment of inertia of the section.

The applied moment is given by:

$$M = \frac{wL^2}{2}$$

where w equals F/L from Figure 2-10a. The value for w is:

$$w = \frac{F}{L}$$

$$w = \frac{15,690}{113.1} \text{ lb/in} = 139 \text{ lb/in}$$

Thus,

$$M = \frac{(139)(113.1)^2}{2} \text{ in-lb}$$

$$M = 889,017 \text{ in-lb}$$

The moment of inertia for the shell, I, is calculated as follows:

$$I = \frac{\pi}{4}(R_o^4 - R_i^4)$$

where $R_o = 12.5"$ and $R_i = (12.5 - .1046)"$, $R_i = 12.395"$.

Thus,

$$I = \frac{\pi}{4}(12.5^4 - 12.395^4) \text{ in}^4$$

$$I = 634 \text{ in}^4$$

The bending stress is then:

$$\sigma = \frac{(889,017)(12.5)}{634} \text{ psi}$$

$$\sigma = 17,528 \text{ psi}$$

Forklift loading is not expected to impact the XL package by bending since $\sigma = 17,528 \text{ psi} < \sigma_{yield} = 30,000 \text{ psi}$.

In the case of the Traveller STD stacked:

$$w = \frac{27,000}{98.6} \text{ lb/in} = 274 \text{ lb/in}$$

$$M = \frac{(274)(98.6)^2}{2} \text{ in-lb}$$

$$M = 1,331,909 \text{ in-lb}$$

The bending stress is then:

$$\sigma = \frac{(1,331,909)(12.5)}{634} \text{ psi}$$

$$\sigma = 26,260 \text{ psi}$$

Forklift loading is not expected to impact the STD package by bending since $\sigma = 26,260 \text{ psi} < \sigma_{yield} = 30,000 \text{ psi}$.

As previously noted, the model conservatively assumes the outer shell is loaded, and the actual Outerpack structure with foam would provide even greater margin against bending.

Weld Shear

The forklift pocket (Item 01 in Figure 2-10b) weldments are also subjected to a shear load during lifting as the forks will apply a normal force along the top plate (Item 02) bottom surface as shown in Figure 2-10b. There are two cases to be evaluated: Traveller XL and Traveller STD doubled stacked. The applied forces are:

$$F_1 = 15,690 \text{ lb for the Traveller XL}$$

$$F_1 = 27,000 \text{ lb for two Traveller STDs stacked}$$

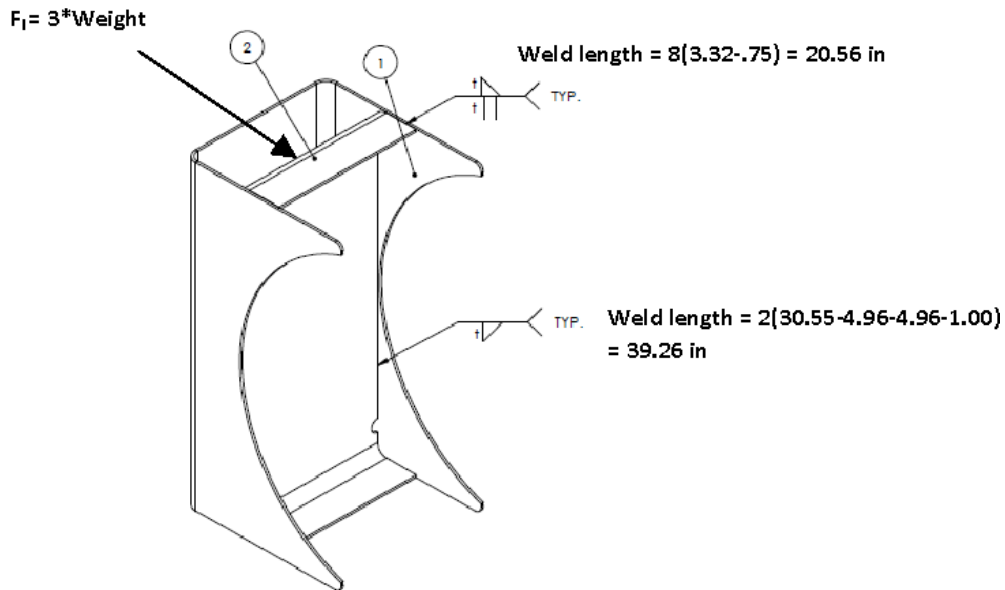


Figure 2-10b Forklift Pocket Weld Detail

The assumed weld area is:

$$A = hl \sin 45, \text{ where } l \text{ is } (20.56''+39.26'') = 59.82'' \text{ and } h \text{ is the weld thickness, } 0.105''.$$

The weld stresses are then:

$$\tau_{XL} = F_{XL}/A \text{ and } \tau_{STD} = F_{STD}/A$$

Substituting values for Traveller XL,

$$\tau_{XL} = 15,690 / (.105)(59.82)(.707) \text{ psi}$$

$$\tau_{XL} = 3,533 \text{ psi}$$

The welds are sufficient to prevent local yielding since $\tau_{XL} = 3,533 \text{ psi} < \tau_{allowx} = 12,000 \text{ psi}$.

Substituting values for Traveller STD,

$$\tau_{STD} = 27,000 / (.105)(59.82)(.707)$$

$$\tau_{STD} = 6,080 \text{ psi}$$

The welds are sufficient to prevent local yielding since $\tau_{STD} = 6,080 \text{ psi} < \tau_{allowx} = 12,000 \text{ psi}$.

Bolts

During package lift for fuel loading and unloading, the package is hoisted using the two rings attached to the top nozzle end of the Outerpack top. The hoist rings attach to the Outerpack using two 3/8-16 UNC Grade 8 Medium-Carbon socket head cap screws per hoist ring into a welded nut. The four screws are subject to shear loading in the most limiting case. The screws are fabricated to a minimum proof load of 120,000 psi. The load per bolt is the design lifting load of 15,690 pounds distributed by the four bolts. Thus, the load per bolt is 3,923 pounds. The allowable axial stress is the yield stress of 120,000 psi and the allowable shear stress is .6Sy, 72,000 psi. The stressed area is 0.0775 in². The applied stress is then:

$$\tau = F/A$$

$$\tau = 3,923 / .0775 \text{ psi}$$

$\tau = 50,619$ psi, which is less than the allowable shear stress of 72,000 psi as well as the axial allowable stress of 120,000 psi and is acceptable.

Coupling Nut

When the package is vertical, the coupling nut will be subject to a shear load. The nut is 3/8-16 and the material is 304 stainless steel. The allowable shear stress is 18,000 psi.

The stressed area of the internal thread is found by:

$$A = .7845(D - \frac{.9743}{n})^2 \text{ where } D \text{ is the nominal diameter } 0.375 \text{ inches, and } n \text{ is the number of threads per inch; } 16.$$

$$A = .0775 \text{ in}^2$$

The shear area A_n is found by:

$$A_n = (3.1416)(n)(L_e)(D_s \text{ min}) \left[\frac{1}{2n} + .57735(D_s \text{ min} - E_n \text{ max}) \right] \text{ in}^2$$

where:

n =	16
L _e =	0.269
D _{s_min} =	0.364
E _{n_max} =	0.340

Thus, $A_n = 0.222 \text{ in}^2$. The shear stress is then:

$$\tau = F / A$$

$$\tau = 3,923 / .222 \text{ psi}$$

$\tau = 17,671$ psi, which is less than the allowable material shear stress of 18,000 and is acceptable.

Hoist Ring

After the package is in the vertical position, the hoists will be loaded in tension. The applied tensile stress for normal up-ending is found from $\sigma = P/A$. The load per 3/8 inch diameter hoist ring is:

$$P = 15,690/2 \text{ lbs}$$

$$P = 7,845 \text{ lbs}$$

The tensile stress per hoist ring is:

$$\sigma = 7,845/[2][(\pi)(0.375^2)/4]$$

$$\sigma = 7,845/0.22 \text{ psi}$$

$$\sigma = 35,659 \text{ ksi.}$$

Since the allowable tensile yield strength is 130 ksi minimum, the hoist ring satisfies the lifting requirements.

2.12.3.2.3 Tie-Down Analysis

The Traveller packages are secured to the transport conveyance by means nylon straps (or chains) across the top of the Outerpack, and by chains that are passed through the leg assembly tray and connected inboard to the conveyance tie-down point. Thus, there are no structural devices designed for tie-down. However, it is possible that the leg assembly or the eight lift eyes could be inadvertently used for tie-downs. According to 10CFR71.45 these component require analysis to demonstrate that the inadvertent tie-down locations have the strength capability to that required for a tie-down device (or be rendered inoperable).

Leg Assembly

In the event that the leg assemblies are used as tie-downs and not rendered inoperable for tie-down, the two leg assemblies on the Outerpack base will be loaded. A depiction of this loading configuration is shown in Figure 2-10c.

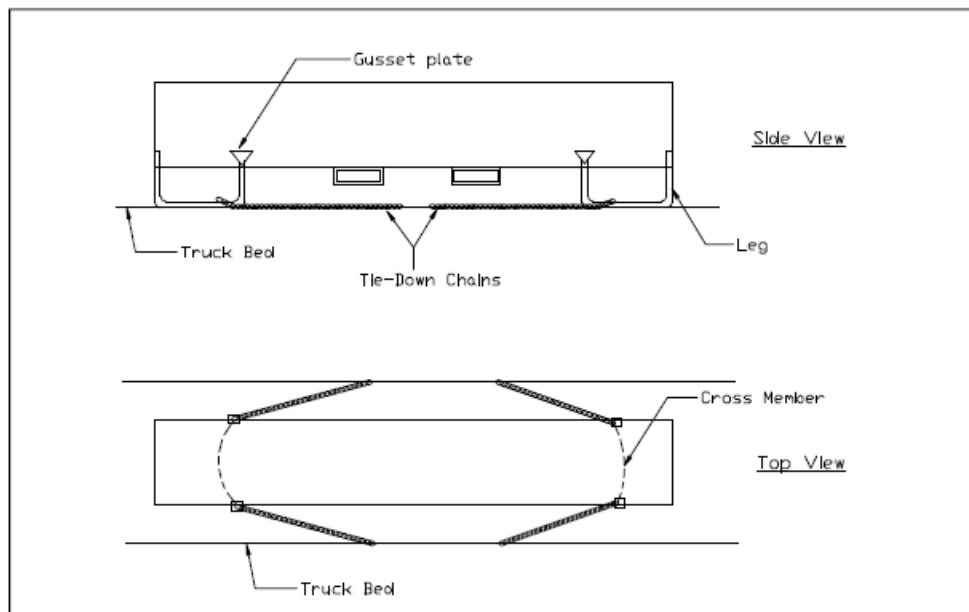


Figure 2-10c Leg Assembly Loading Condition During Inadvertent Tie-Down

The chains are assumed to be attached to each leg pair near the truck bed base so that the resulting chain angle (from the side perspective) is small enough to constitute an axially applied resultant load. For this loading condition, both leg pairs are loaded in the axial direction. The resultant applied force is the vector summation of the vertical, axial, and transverse components:

$$F = \sqrt{F_x^2 + F_y^2 + F_z^2}$$

$$F = \sqrt{52,300^2 + 26,150^2 + 10,460^2} \text{ lbs}$$

$$F = 59,401 \text{ lbs for both pairs.}$$

Therefore, the applied load for a single leg pair is .5F, or 29,701 lbs.

The leg assembly is attached to the Outerpack using a gusset plate, and also by an arced cross. Two gusset plates (6 inches wide each) are welded to the Outerpack base by a continuous 0.10 inch fillet weld on the outside of the skin. Thus, for single leg pair loading, the total weld length of the cross member section is 12+12, or 24 inches (Figure 2-10d).

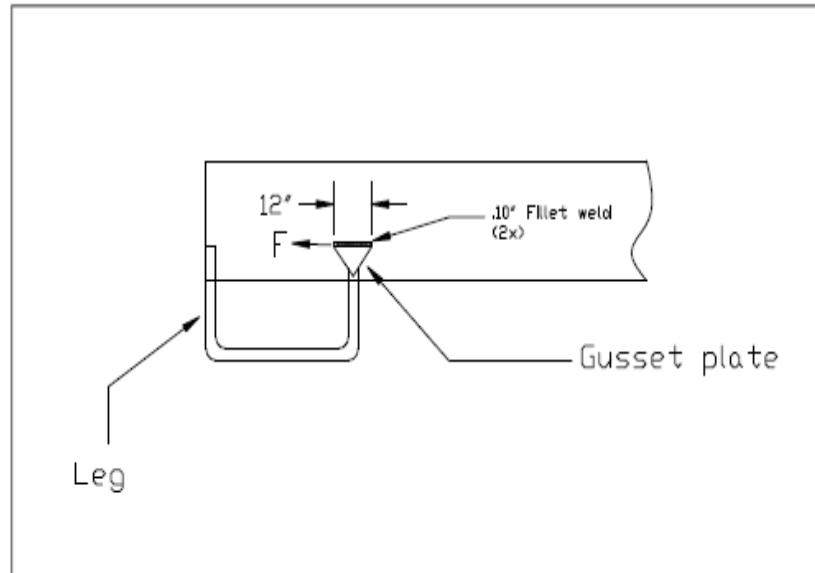


Figure 2-10d Welding Depiction at Representative Gusset Plate

The cross members are curved 7 gage plates welded to the Outerpack base using minimum 0.10 fillet welds, 1 inch long at 12 places per side as shown in Figure 2-10e. Thus, the total weld length each cross members is 12 inches.

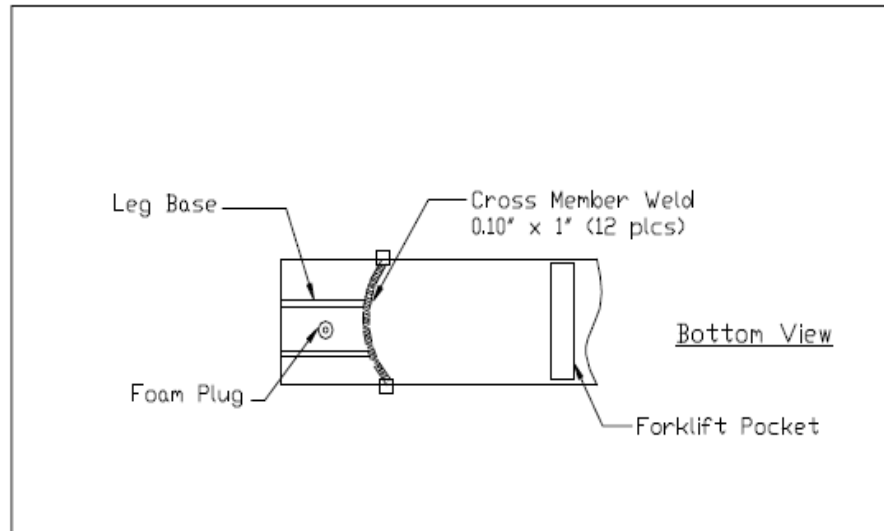


Figure 2-10e Welding Depiction at Cross Member

Weld Shear Analysis

The leg assembly is attached to the Outerpack shell by both the gusset and cross member welds. These welds are required to demonstrate that they are adequate to preclude local yielding. Axial loading of the resultant force results in a shear load on the welds.

The weld shear stress is found by:

$$\tau_{weld} = F/A,$$

where F is the applied vector shear load of 29,701 lbs and A is the weld area.

The weld area is:

$$A = hl \sin 45, \text{ where } l \text{ is } 24+12 = 36", \text{ and } h \text{ is the weld thickness, } 0.10".$$

$$A = (0.10)(36)(.707) \text{ in}^2$$

$$A = 2.55 \text{ in}^2$$

The weld shear stress is then:

$$\tau_{weld} = \frac{29,701}{2.55} \text{ psi}$$

$$\tau = 11,648 \text{ psi}$$

Thus, the welds are sufficient to prevent local yielding since $\tau_{weld} = 11,648 \text{ psi} < \tau_{allowx} = 12,000 \text{ psi}$.

Lift Eyes

In the event that the lift eyes are used as tie-down, the normal system of tie down would include eight (8) point loads (Figure 2-10f). The analysis will assume that one of the chains fails per side, so the applied load is for six (6) lift eyes. The chains may be angled at an assumed 30 degrees or vertical as shown in Figure 2-10f.

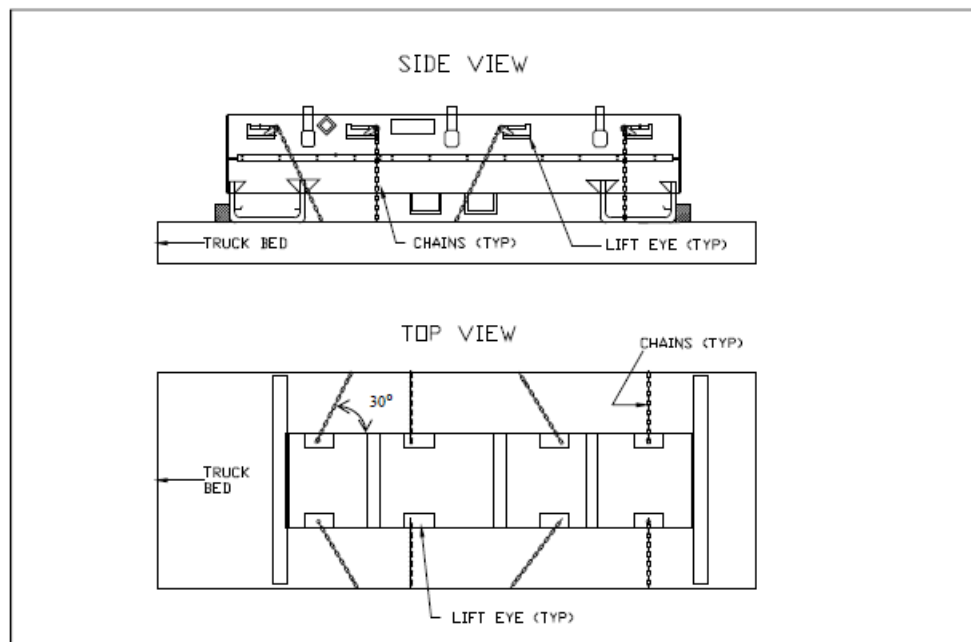


Figure 2-10f Lift Eye Loading Assumed Conditions During Inadvertent Tie-Down

The applied load is a combined vector load to the center of gravity of a single package. For this loading condition, each attached lift eye is loaded with 1/6th of the total load. The resultant applied force is the vector summation of the vertical, axial, and transverse components:

$$F = \sqrt{F_x^2 + F_y^2 + F_z^2}$$

$$F = \sqrt{52,300^2 + 26,150^2 + 10,460^2} \text{ lbs}$$

$$F = 59,401 \text{ lbs.}$$

Therefore, the applied load for a single lift eye is .167F, or 9,900 lbs.

Weld Shear Analysis - Vertical Direction

The lift eye is fillet welded to the Outerpack shell. The top and bottom part of the lift eyes are welded at 8 inches and 10.63 inches, respectively. Thus, the total weld length for the top and bottom weld subject to shear is 18.63 inches. A depiction of the loading configuration and lift eye sketch is shown in Figure 2-10g for the vertical chain orientation.

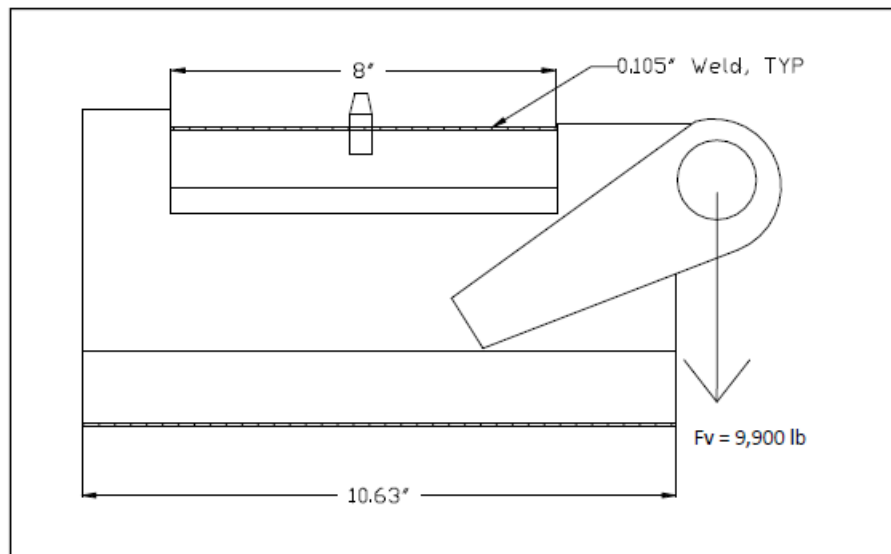


Figure 2-10g Vertical Lift Eye Welding Configuration

These welds are required to demonstrate that they are adequate to preclude local yielding for the vertical direction.

The weld shear stress is found by:

$$\tau_{weld} = F/A,$$

where F is the applied vector shear load of 9,900 lbs and A is the weld area. The weld area is:

$$A = hl \sin 45, \text{ where } l \text{ is } 18.63", \text{ and } h \text{ is the weld thickness, } 0.105".$$

$$A = (0.105)(18.63)(.707) \text{ in}^2$$

$$A = 1.38 \text{ in}^2$$

The weld stress is then:

$$\tau_{weld} = 9,900 / 1.38 \text{ psi}$$

$$\tau = 7,158 \text{ psi}$$

Thus, the welds are sufficient to prevent local yielding since $\tau_{weld} = 7,158 \text{ psi} < \tau_{allow} = 12,000 \text{ psi}$.

Weld Shear Analysis - Combined Shear

A depiction of the combined shear loading configuration and lift eye sketch is shown in Figure 2-10h for the angled chain orientation. Since there are horizontal and axial components, the principal shear force will be calculated. The vector stress components are shown pictorially below:

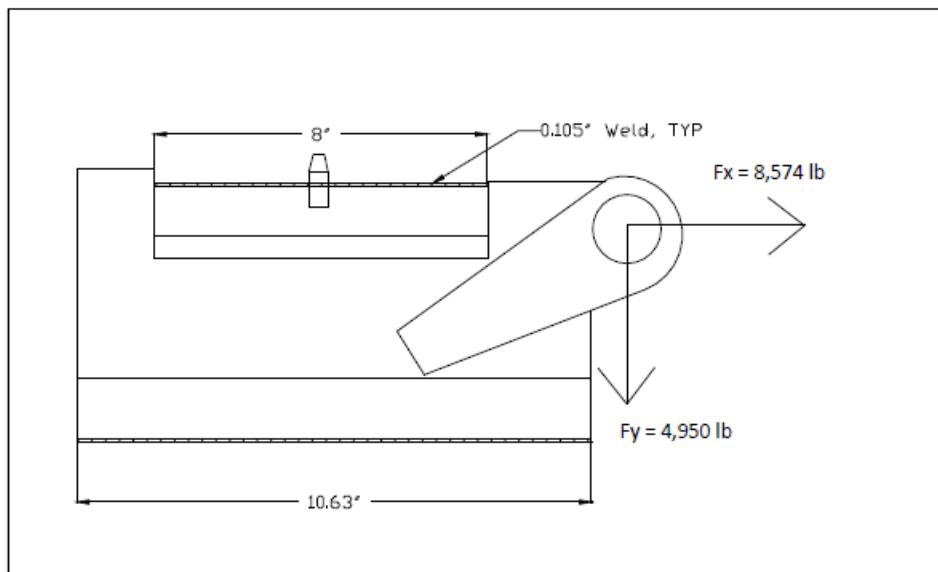
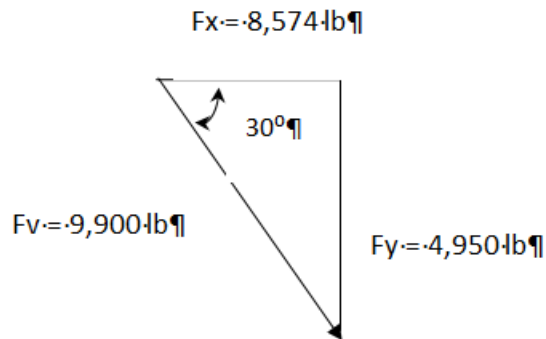


Figure 2-10h Combined Shear Lift Eye Welding Configuration

The x-direction weld shear stress is found by:

$$\tau_{weld\ x} = \frac{Fx}{A},$$

where F is the applied vector shear load of 9,900 lbs and A is the weld area.

The weld area is:

$$A = hl \sin 45, \text{ where } l \text{ is } 18.63", \text{ and } h \text{ is the weld thickness, } 0.105".$$

$$A = (0.105)(18.63)(.707) \text{ in}^2$$

$$A = 1.38 \text{ in}^2$$

The weld stress is then:

$$\tau_{weld x} = 8,574 / 1.38 \text{ psi}$$

$$\tau_{weld x} = 6,213 \text{ psi}$$

The y-direction weld shear stress is found by:

$$\tau_{weld y} = Fx / A,$$

where F is the applied vector shear load of 9,900 lbs and A is the weld area.

The weld area is:

$$A = hl \sin 45, \text{ where } l \text{ is } 18.63", \text{ and } h \text{ is the weld thickness, } 0.105".$$

$$A = (0.105)(18.63)(.707) \text{ in}^2$$

$$A = 1.38 \text{ in}^2$$

The weld stress is then:

$$\tau_{weld y} = 4,950 / 1.38 \text{ psi}$$

$$\tau_{weld y} = 3,586 \text{ psi}$$

Therefore, the principle shear stress is:

$$\tau = \sqrt{(\tau_x^2 + \tau_y^2)}$$

$$\tau = \sqrt{(6,213^2 + 3,586^2)}$$

$$\tau = 7,173 \text{ psi}$$

The welds are sufficient to prevent local yielding since $\tau_{\max} = 7,173 \text{ psi} < \tau_{\text{allow}} = 12,000 \text{ psi}$.

2.12.3.2.4 Design Temperature Analysis –40°F (-40°C) and 158°F (70°C)

The materials of construction of the Traveller Outerpack include ASTM A240 Type 304 Stainless Steel for the shells and low density, closed cell polyurethane impact limiter/thermal insulator (10 pcf along the axis, 6 pcf inside the top and lower pillows, and 20 pcf between the top and lower pillows). The Clamshell is comprised of ASTM B209/B221 Type 6005-T5 Aluminum. As demonstrated in the below sections, the package is suitable for transport operations over the required design temperature range.

Brittle Fracture – Aluminum alloys, including 6005-T5 Aluminum, do not exhibit a ductile-to-brittle temperature transition; consequently, neither ASTM nor ASME specifications require low temperature Charpy or Izod tests of aluminum alloys. Thus, brittle fracture of the aluminum components is not expected. Austenitic steels such as 304 Stainless Steel have a Face Centered Cubic (FCC) structure and consequently exhibit a ductile-to-brittle transition at cryogenic temperatures near -297°F (-183°C). Thus, brittle fracture of the stainless steel components is not expected.

Mechanical Properties For Design Temperature Range – The range of tensile and yield strength of 6005 series Aluminum over the design temperature range will not preclude the package from performing its intended design function. Figure 2-11 provides the temperature dependent yield and tensile strengths typical for a 6000-series aluminum up to approximately 212°F (100°C). Furthermore, the recommended operating temperature of aluminum alloys for structural applications is up to a temperature of 400°F (204°C), which is well below the maximum design temperature of 158°F (70°C).

The range of tensile and yield strength of 304 stainless steel over the design temperature range will not preclude the package from performing its intended design function. Figure 2-12 provides the temperature dependent yield and tensile strengths for 304 SS up to approximately 194°F (90°C).

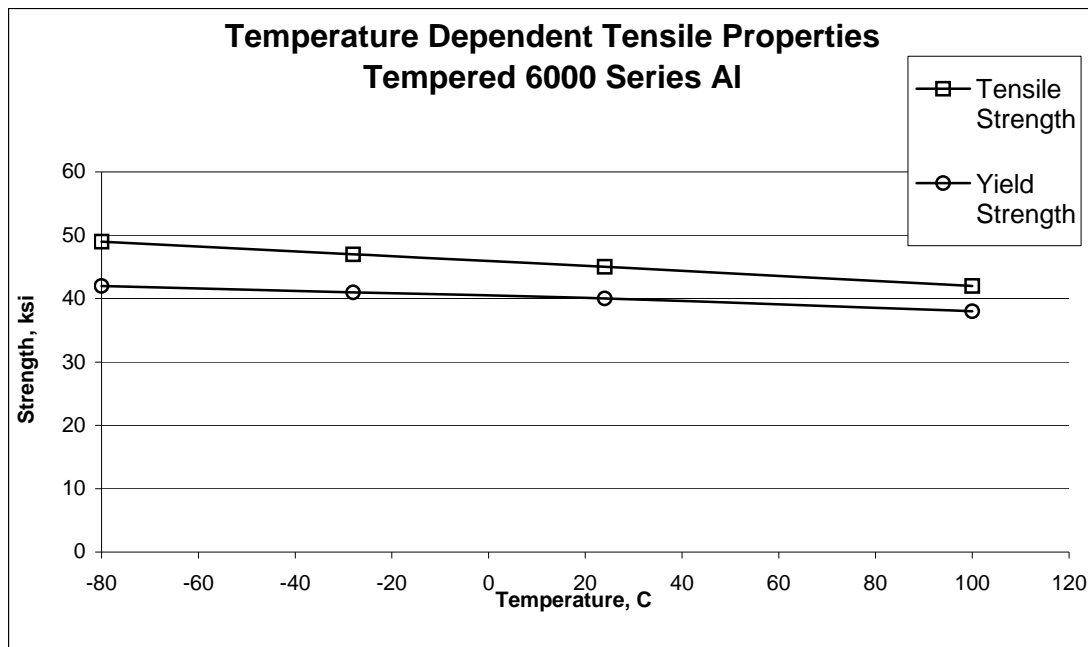


Figure 2-11 Typical Temperature Dependent Tensile Properties for Tempered 6000 Series Al

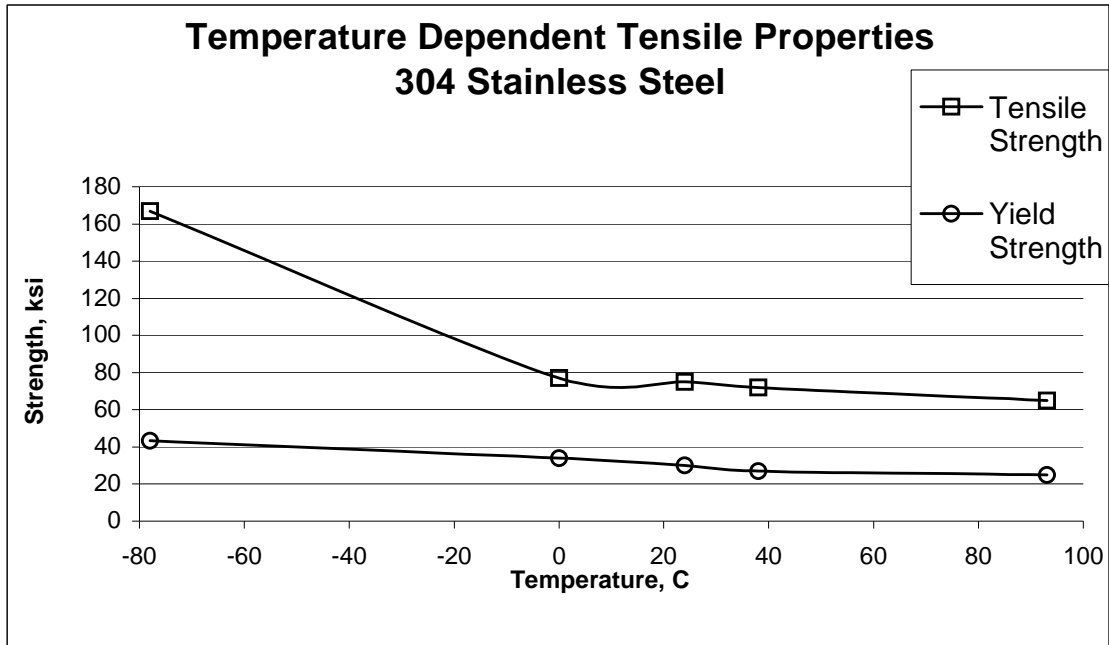


Figure 2-12 Temperature Dependent Tensile Properties for 304 SS

Temperature Evaluation of Foam – The foam is used as a crushable impact limiter and a special thermal insulator. This section only considers the mechanical properties since the thermal functions are evaluated in Section 3, Thermal Evaluation. The foam exhibits a general increase in compressive strength as temperature decreases. Figures 2-13, 14 and 15 show the compressive strength for the 10 pcf (pound per cubic foot), 20 pcf, and 6 pcf foam as a function of temperature, respectively. Of interest is the area under each temperature curve from 0-60% strain (the recommended energy absorption operation range of the foam). For each foam density, the temperature range considered does not significantly impact the energy absorption characteristics. Also, Figures 2-15 show that the compressive strength difference between -29°C and 24°C are relatively similar indicating at -40°C the behavior of the foam will not significantly change. Figure 2-16 provides the temperature dependent strength of each foam density at 10% strain from -54°C to 82°C. The curves show essentially a linear increase in crush strength as temperature decreases. Therefore, the impact properties of the foam are acceptable for use in the temperature range from -40°F (-40°C) to 158°F (70°C).

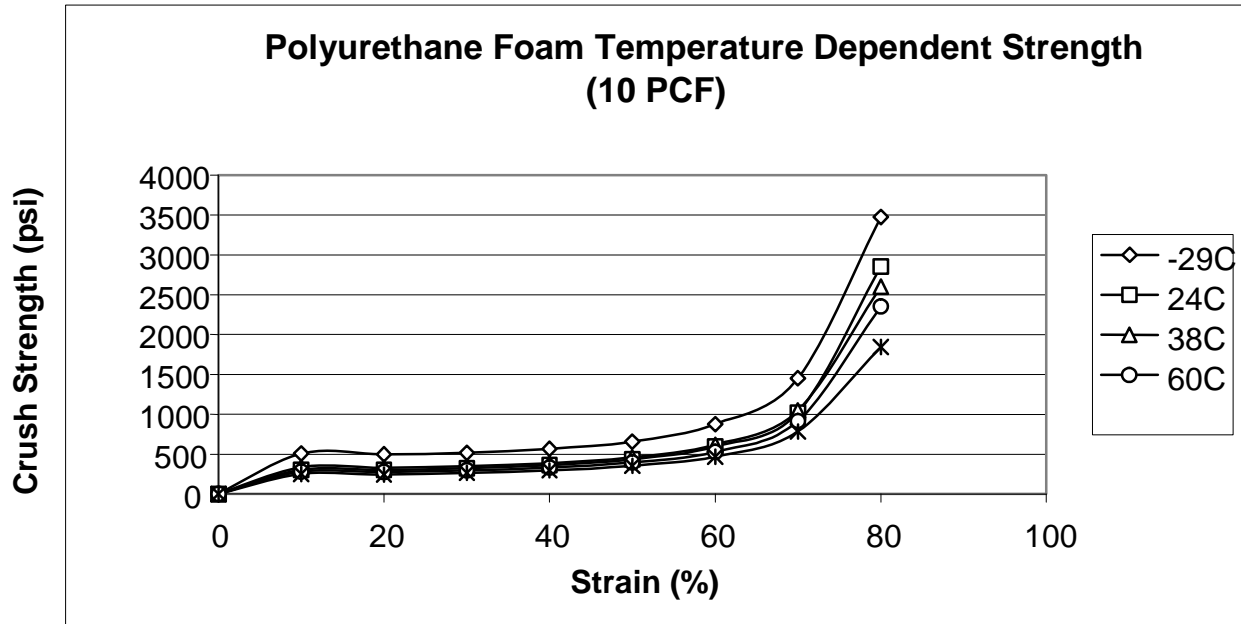


Figure 2-13 Temperature Dependent Crush Strength for 10 PCF Polyurethane Foam

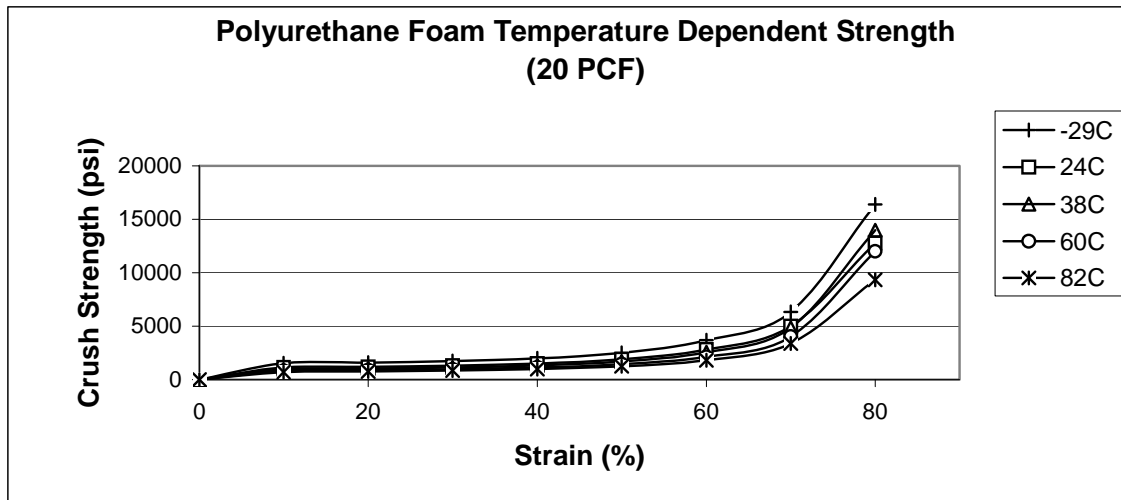


Figure 2-14 Temperature Dependent Crush Strength for 20 PCF Polyurethane Foam

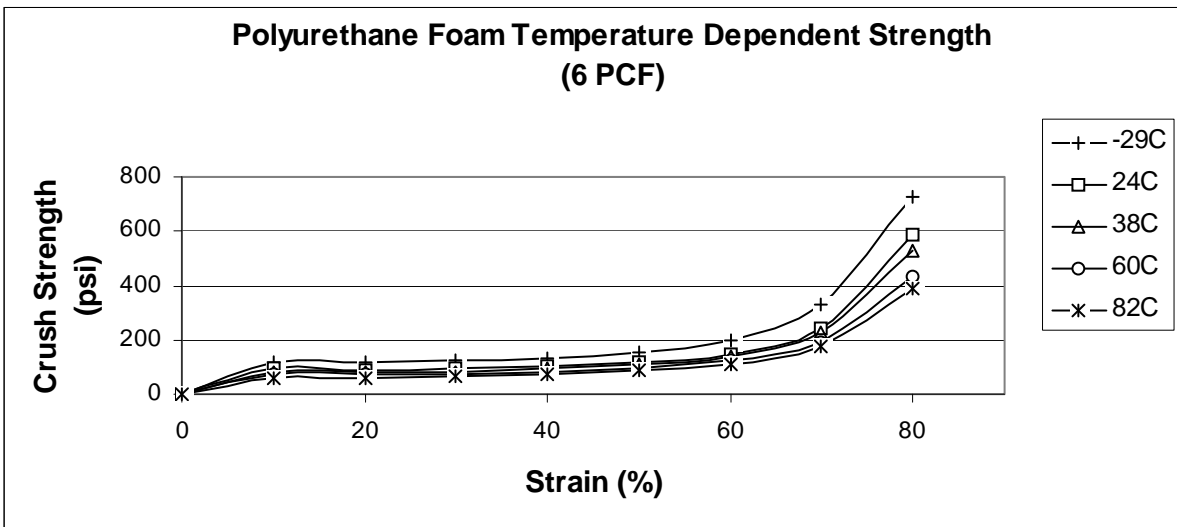


Figure 2-15 Temperature Dependent Crush Strength for 6 PCF Polyurethane Foam

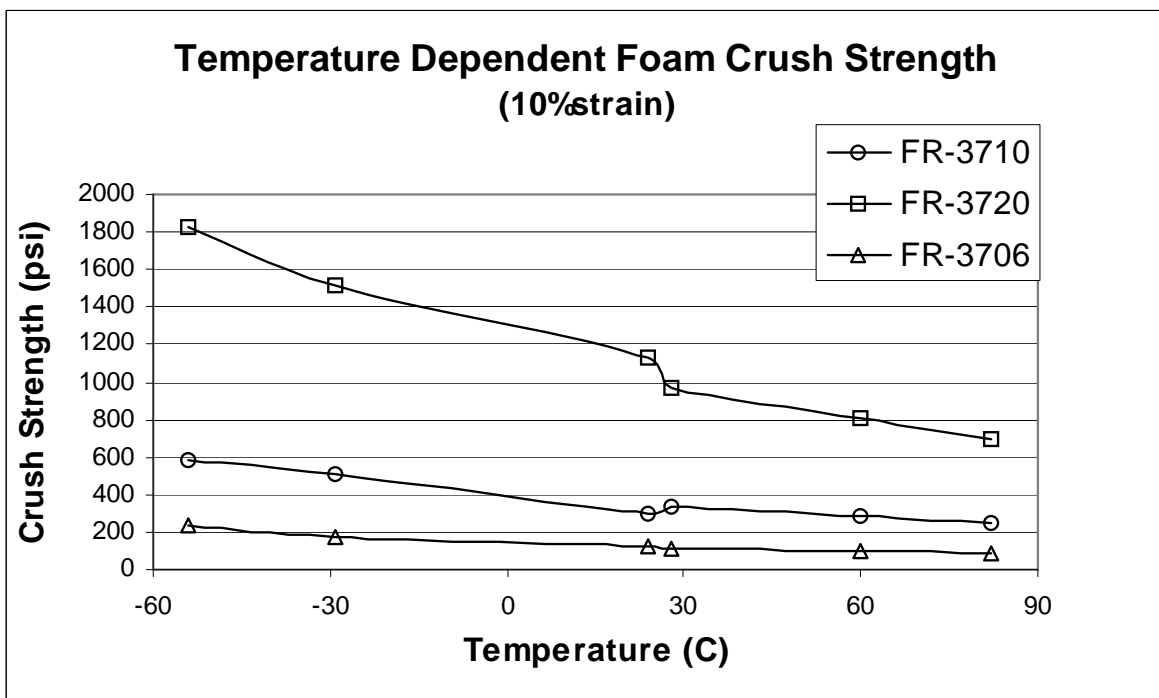


Figure 2-16 Temperature Dependent Crush Strength for Traveller Foam at 10% Strain

Differential Thermal Expansion – Differential thermal expansion (DTE) is expected to only impact the fuel assembly and Clamshell interface. The Outerpack is not under physical constraints and can accommodate thermal growth. Differential thermal expansion between the foam and the stainless steel shells of the Outerpack is easily accommodated by the elastic properties (low modulus value) of the foam.

However, the Ultra-high Molecular Weight (UHMW) polyethylene does have a significantly higher coefficient of thermal expansion (CTE) when compared to 304 stainless steel. For this reason, the moderator panels are segmented along their lengths to accommodate the differential thermal expansion between the polyethylene and the inner stainless steel shells of the Outerpack. Holes in the polyethylene segments are used to attach the panels to the inner Outerpack shells using threaded studs. These studs must not be loaded by the individual panel differential thermal expansion, or contraction. For this reason, each hole drilled into the polyethylene panel is significantly large to preclude thermally induced stresses in the bolt studs. The following calculation addresses this case.

The polyethylene moderator blocks are attached by 0.375 inch diameter weld studs on the inner skin of the on the Outerpack. The weld studs penetrate the moderator blocks through 0.563 inch diameter holes. The blocks are mounted with a nominal gap, block to block, of 0.260 inches. The coefficients of thermal expansions are:

- 304 stainless steel 9.6 μ in/in-F
- UHMW polyethylene 72 – 111 μ in/in-F

Using the worst difference in expansion coefficients, 100 μ in/in-F, the gaps between the blocks will accommodate heat up from 70° to 167°F. In addition, there is an additional 0.094 inch of clearance between the weld studs and each side of the holes in the polyethylene that will allow blocks with less than nominal clearance to slide in a direction to provide uniform clearance along the length of the Traveller.

Because the polyethylene's coefficient of expansion is much greater than stainless steel, interference between moderator blocks is not an issue when temperature drops. Instead, it is the interference between the blocks and the weld studs. Based on nominal clearances and a maximum distance of 17.0 inches from outboard hole-to-outboard hole, the package temperature can drop from 70°F to -41°F before the polyethylene is stressed. Most of the moderator blocks have significantly smaller distances between the outboard holes (6.5 to 12.5 inches) allowing them to accommodate larger temperature changes.

See Licensing drawings for additional details.

Analyzing the DTE between the fuel assembly and the Clamshell is evaluated assuming fuel loading is performed at 70°F (21°C) and shipped to a cold environment of -40°F (-40°C) since the aluminum will tend to contract more than the fuel assembly. The thermal growth is found by the familiar equation:

$\Delta L = \alpha(\Delta T)L_o$, where ΔL is the total growth, L_o CS is the original length of the Clamshell (202 inches), L_o FA is the original length of the fuel assembly (188.86 inches, per drawing 1453E86), ΔT is the temperature change (110°F), and α is the coefficient of thermal expansion.

For Aluminum, $\alpha = 13 \mu\text{in/in-}^\circ\text{F}$. For Zircalloy, $\alpha = 2.79 \mu\text{in/in-}^\circ\text{F}$.

The differential thermal growth between the Clamshell and the fuel assembly is then:

$$\begin{aligned} \text{DTE} &= \{\Delta L = \alpha(\Delta T)L_{oCS} \text{ Al}\} - \{\Delta L = \alpha(\Delta T)L_{oFA} \text{ Zirlo}\} \\ &= \{13\text{e-}6 \times 110 \times 202\} \text{ inches} - \{2.79\text{e-}6 \times 110 \times 188.86\} \text{ inches} \\ &= 0.29 - 0.058 \text{ inches} \end{aligned}$$

Thus,

$$\text{DTE} = 0.23 \text{ inches (the fuel assembly grows 0.23 inches relative to the Clamshell).}$$

The combined thickness of the base cork rubber and axial clamp cork rubber is 0.50 inches and can accommodate the growth due to differential thermal expansion. Thus, DTE is not a concern. Since the total differential growth associated with the XL Clamshell is greater than the STD Clamshell, it is the bounding calculation.

2.12.3.2.4.1 Internal/External Pressure

The Traveller package utilizes silicone rubber or fiberglass seals to preclude dust and other contaminants from entering the package. These seals are not continuous, and do not form an airtight pressure boundary. The package does not maintain a boundary between pressure gradients and is not designed to be pressurized during transport. Thus, internal/external reduced pressure will not impact the structural integrity of the package.

2.12.3.2.4.2 Vibration

The package must be evaluated to consider the effects of normal vibration on the design performance. The isolation system is designed to dampen normally induced vibrations from transport, and is not fundamental to the safe operation of the package. However, the Outerpack must maintain its structural integrity during transport to maintain a safe transport condition. Typical package attachment to a transport conveyance for the Traveller includes nylon straps or chain mounted both over the package and on the gusset tray connected to the support legs pointed inboard. The loading configuration can be modeled as a simply supported beam. Furthermore, the Outerpack is conservatively modeled considering only the outer shell at the first mode of vibration. The typical natural frequency range for transportation vehicles, $f_{\text{nat TRANS}}$, is 3.7-8 Hz. The natural frequency of the Outerpack can be determined from.

$$f_{\text{natOP}} = a \sqrt{(EIg/l^3)/m}$$

where $a=1.57$ (primary mode coefficient assuming hinge-hinge end conditions for additional conservatism), $E=29.4\text{E}6$ psi, $I=634$ in⁴, $m = 2,834$ pounds, $g = 386.4$ in/s² and $l = 226.2$ in (distance from gusset tray to gusset tray). Substituting values:

$$f_{\text{natOP}} = 1.57 \sqrt{[(29.4\text{E}6)(634)(386.4)/(226.2)^3]/(2,834)} \text{ 1/s (Hz)}$$

$$f_{natOP} = 1.57\sqrt{220} \text{ Hz}$$

$$f_{natOP} = 23 \text{ Hz}$$

Since the natural frequency of the Outerpack is greater than the natural frequency typical of a transportation vehicle, resonance of the Outerpack is not expected and normally induced vibrations will not preclude the package from performing its design function.

2.12.3.2.5 Water Spray

The Traveller Outerpack is cylindrical, and shaped so that water will not be collected. Since the shell is fabricated of 304 SS, the water spray will not impact the structural integrity of the package.

2.12.3.2.6 Compression/Stacking test

The Traveller package must demonstrate elastic stability for a 5 g static load. No credit is taken for the circumferential stiffeners or the forklift support tubes. The analysis assumes the stacking load is uniformly distributed over the four outermost stacking brackets on the Outerpack. Figure 2-17 depicts the shell compression/stacking model.

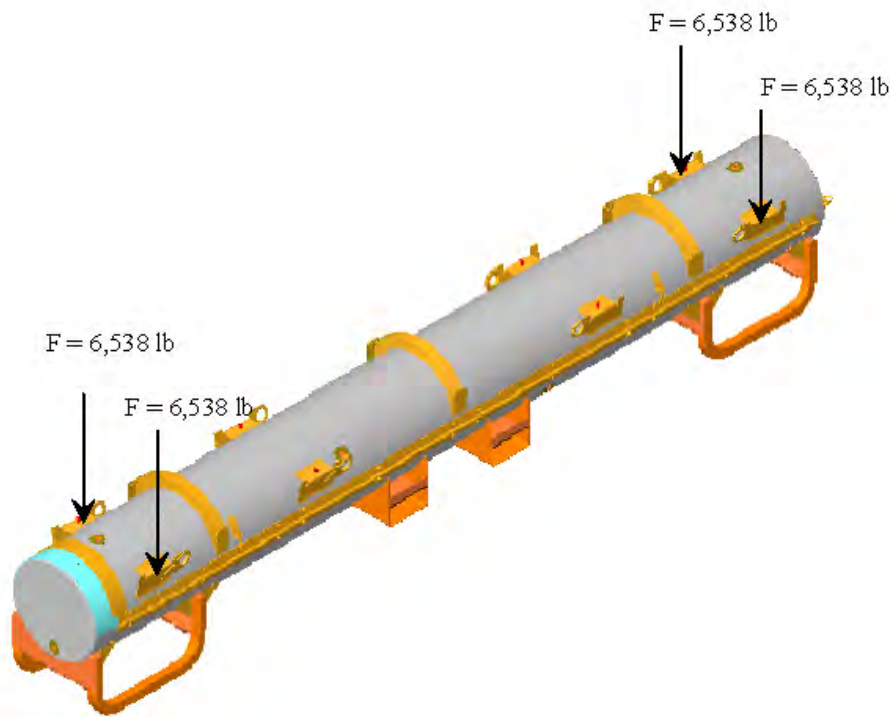


Figure 2-17 Compression/Stacking Requirement Analysis Model

The applied stacking force for the stacking test was determined to be:

$$F_s = 26,150 \text{ lb from Section 2.12.3.2.1.}$$

The load path is assumed to follow through the welds of the stacking brackets, through the Outerpack side, and then to the leg supports. This assumption is based on the package stacking configuration or the placement of weight on the package top. Each loaded section will be analyzed for its structural integrity.

Stacking Bracket – The stacking bracket is expected to experience a shear load on the weld during stacking. The loading configuration for a single bracket is shown in Figure 2-18.

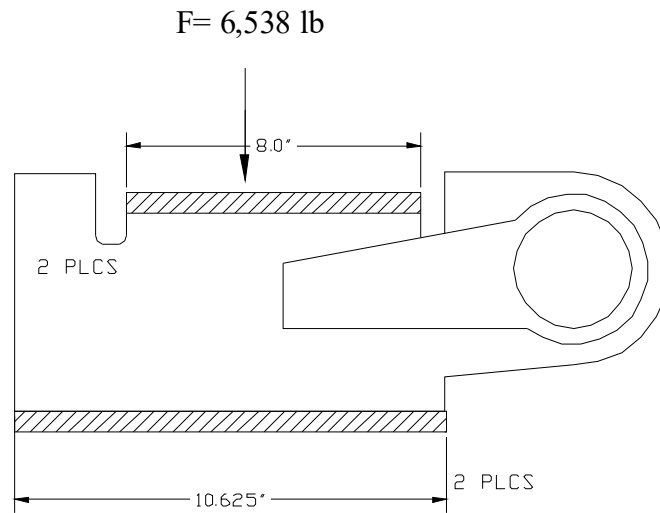


Figure 2-18 Stacking Force Model on Stacking Bracket

The load on each stacking bracket is found by dividing the applied load of 26,150 pounds by the four brackets that support the load:

$$F = 26,150 \text{ lb}$$

$$F = 6,538 \text{ lb}$$

The weld shear stress is found by $\tau_{weld} = F/A$, where F is the applied vertical or horizontal load and A is the weld area. The assumed weld area is the total weld area of each bracket and is found by:

$$A = hl \sin 45, \text{ where } l \text{ is } (10.625" + 8") = 18.625" \text{ from Figure 2-18 and } h \text{ is the weld thickness, } 0.105".$$

The weld stress is then:

$$\tau = F/A$$

Substituting values,

$$\tau = 6,538 / (.105)(18.625)(.707) \text{ psi}$$

$$\tau = 4,729 \text{ psi, which is less the allowable weld shear stress of 12 ksi.}$$

2.12.3.2.6.1 Outerpack Section

The stacking bracket is expected to experience a compressive load through the package side cross section during stacking as the force follows the projected load path. The loading configuration and model for the Outerpack section is shown in Figure 2-19.

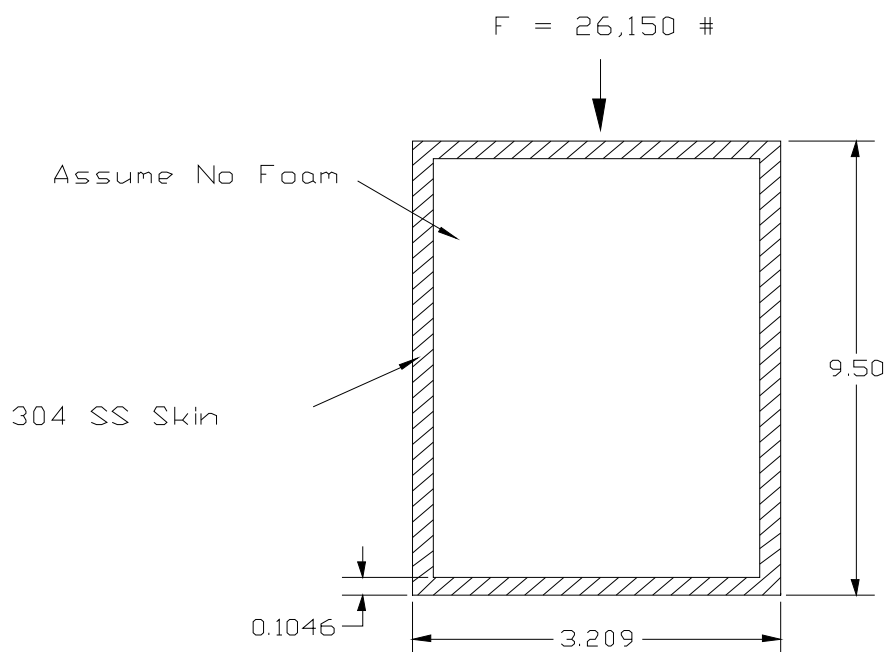


Figure 2-19 Outerpack Section Compression Model

The evaluation first examined the slenderness ratio of this section to determine if buckling is applicable. The model conservatively assumed no structural credit for the foam. In addition, the model assumed the force path section is from the base of the stacking bracket to the top of the support leg. The cross section consisted of a rectangular section of dimensions 9.50" x 3.209" with a wall thickness of 0.1046". The critical buckling load will be calculated and compared to the actual load to determine elastic stability of the Outerpack section.

The slenderness ratio, SR, can be expressed as:

$$SR = l/k$$

where l is the effective length, 9.50 inches, and the radius of gyration, k, is:

$$k = \sqrt{I/A}$$

For the Outerpack section, the moment of inertia, I, and the cross section area, A are:

$$I = (wl^3 - w_i l_i^3)/12 \text{ in}^4$$

$$I = (3.209\{9.50\}^3 - 3.0\{9.29\}^3)/12 \text{ in}^4$$

$$I = 28.8 \text{ in}^4$$

$$A = wl - w_i l_i \text{ in}^2$$

$$A = (3.209\{9.50\} - 3.0\{9.29\}) \text{ in}^2$$

$$A = 2.62 \text{ in}^2$$

Thus, the value for k is:

$$k = \sqrt{28.8/2.62} \text{ in}$$

$$k = 3.32 \text{ in}$$

The corresponding slenderness ratio is then:

$$SR = 9.50/3.32 \text{ in/in}$$

$$SR = 2.86$$

The limiting slenderness ratios for columns are as follows:

Long Columns

$\left(\frac{l}{k}\right)_1 = \sqrt{\frac{2\pi^2 CE}{\sigma_y}}$ where the end condition C is conservatively assumed to be unity, E is Young's Modulus, and σ_y is the tensile yield stress.

Substituting values:

$$\left(\frac{l}{k}\right)_1 = \sqrt{\frac{2\pi^2(29.4E6)}{30000}}$$

$$\left(\frac{l}{k}\right)_1 = 139$$

Short Columns

$$\left(\frac{l}{k}\right)_2 = .282\sqrt{\frac{AI^2}{\pi^2 I}}$$

Substituting values:

$$\left(\frac{l}{k}\right)_2 = .282\sqrt{\frac{2.62(9.50)^2}{\pi^2 28.8}}$$

$$\left(\frac{l}{k}\right)_2 = .257$$

Thus, $.257 < 2.86 \text{ (SR)} < 139$ and the Outerpack section is considered an intermediate column. The critical load for this column is given by:

$$P_{cr} = A\left(\sigma_y - \left\{\frac{\sigma_y l}{2\pi k}\right\}^2 \frac{1}{CE}\right)$$

$$P_{cr} = 2.62\left(30000 - \left\{\frac{30000 \cdot 9.50}{2\pi \cdot 3.32}\right\}^2 \frac{1}{29.4E6}\right)$$

$$P_{cr} = 78,583 \text{ lb}$$

Since the actual load of 26,150 pounds is less than the critical buckling load of 78,583 pounds, the Outerpack section is considered stable during compression from stacking.

2.12.3.2.6.2 Leg Support

The leg support is expected to experience a compressive load through the straight top cross section during stacking as the force follows the projected load path. The loading configuration and model for the leg support section is shown in Figure 2-20. There are eight (8) leg sections of 2"x2"x.120" 304 SS tubing of approximately 10" length. The expected load for each leg section is 26,150/8 pounds, or 3,269 pounds.

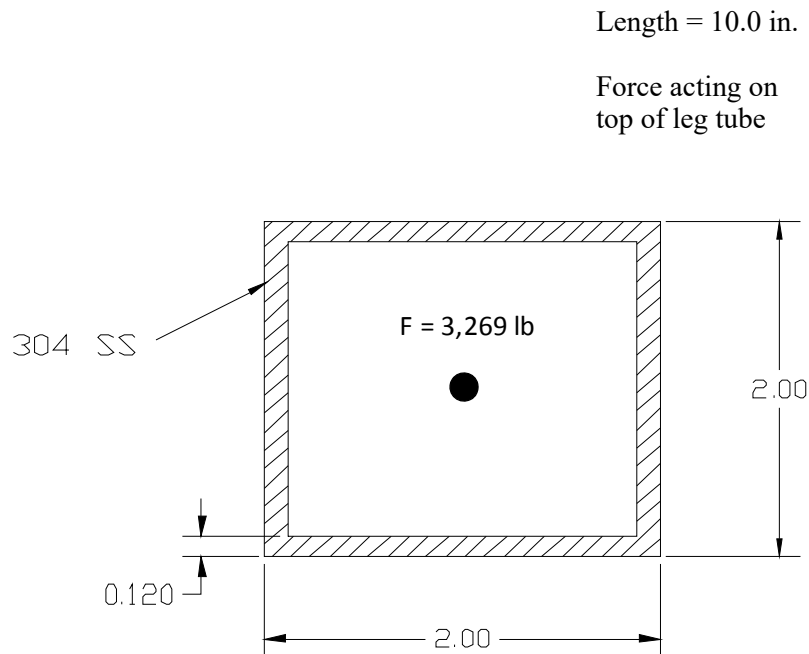


Figure 2-20 Leg Support Section Compression Model

The evaluation will first consider the slenderness ratio of this section to determine if buckling is applicable. The critical buckling load will be calculated and compared to the actual load to determine elastic stability of the leg support section.

The slenderness ratio, SR, is:

$$SR = l / k$$

where l is the effective length, 10.0 inches, and the radius of gyration, k , is:

$$k = \sqrt{I/A}$$

For the Outerpack section, the moment of inertia, I, and the cross section area, A are:

$$I = (wl^3 - w_i l_i^3) / 12 \text{ in}^4$$

$$I = (2.0\{10.0\}^3 - 1.76\{10.0\}^3) / 12 \text{ in}^4$$

$$I = 20 \text{ in}^4$$

$$A = wl - w_i l_i \text{ in}^2$$

$$A = (2.0\{10.0\} - 1.76\{10.0\}) \text{ in}^2$$

$$A = 2.4 \text{ in}^2$$

Thus, the value for k is:

$$k = \sqrt{20/2.4} \text{ in}$$

$$k = 2.9 \text{ in}$$

The corresponding slenderness ratio is then:

$$SR = 10.0/2.9 \text{ in/in}$$

$$SR = 3.4$$

The limiting slenderness ratios for columns is:

Long Columns

$\left(\frac{l}{k}\right)_1 = \sqrt{\frac{2\pi^2 CE}{\sigma_y}}$ where the end condition C is conservatively assumed to be unity, E is Young's Modulus, and σ_y is the tensile yield stress.

Substituting values:

$$\left(\frac{l}{k}\right)_1 = \sqrt{\frac{2\pi^2(29.4E6)}{30000}}$$

$$\left(\frac{l}{k}\right)_1 = 139$$

Short Columns

$$\left(\frac{l}{k}\right)_2 = .282 \sqrt{\frac{AI^2}{\pi^2 I}}$$

Substituting values:

$$\left(\frac{l}{k}\right)_2 = 0.282 \sqrt{\frac{2.4(10.0)^2}{\pi^2 20}}$$

$$\left(\frac{l}{k}\right)_2 = .31$$

Thus, .31 < 3.4 (SR) < 139 and the leg support section is considered an intermediate column. The critical load for this column is:

$$P_{cr} = A \left(\sigma_y - \left\{ \frac{\sigma_y}{2\pi} \frac{1}{k} \right\}^2 \frac{1}{CE} \right)$$

$$P_{cr} = 2.4 \left(30,000 - \left\{ \frac{30,000}{2\pi} \frac{10.0}{2.9} \right\}^2 \frac{1}{29.4E6} \right)$$

$$P_{cr} = 71,978 \text{ lb}$$

Since the actual load of 3,269 pounds is less than the critical buckling load of 71,978 pounds, the leg support section is considered stable during compression from stacking.

2.12.3.2.7 Penetration

The penetration test can be characterized as a localized impact event on the outer skin of the Outerpack. The energy imparted onto the outer skin is equal to the potential energy of the falling pin:

$PE = mgh$, where the mass of the pin is 13 lb and the drop height is 40 inches. To obtain correct units of energy, the gravitational constant g_c must be used in the energy equation. Thus,

$$PE_{penetration} = \frac{(13)(40)(32.2)}{32.2} \text{ in-lb (ft*s}^2\text{)/ft*s}^2$$

$$PE_{penetration} = 520 \text{ in-lb.}$$

By comparison, the energy locally imparted to the outer skin from the pin-puncture drop test is determined from the dropped package mass and the drop height. The mass of the package is 5,230 lb, and the drop height is 40 inches. Thus,

$$PE_{pin} = \frac{mgh}{g_c} = mh$$

$$PE_{pin} = (5,230)(40) \text{ in-lb.}$$

$$PE_{pin} = 209,200 \text{ in-lb.}$$

Pin puncture drop tests have demonstrated that the outer skin was not perforated as a result of impact onto the pin. Since the impact energy of the pin puncture drop test is approximately 400 times greater than that of the pin penetration, the pin puncture drop test bounds the pin penetration. Thus, the pin penetration impact is not expected to result in any significant structural damage to the Outerpack.

2.12.3.2.8 Immersion Analysis

The Traveller package uses silicone rubber or fiberglass seals for thermal protection and to preclude dust and other contaminants from entering the package. The seals are not continuous around the perimeter of the package and do not form a pressure boundary. In the event of water submersion, the inner portion of the package will fill with water creating equal hydrostatic pressure on the Outerpack and Clamshell surfaces. This condition would not result in a stress gradient through the Outerpack or Clamshell. Thus, immersion will not impact the structural integrity of the package.

2.12.4 DROP ANALYSIS FOR THE TRAVELLER XL SHIPPING PACKAGE

The primary method for evaluating the performance of the Traveller under hypothetical accident condition scenarios was actual testing of full-scale prototype packages. During the development program eighteen drop tests were conducted using a variety of orientations. Most of the drops were from greater than 9m. The drop tests are summarized in Table 2-5 and reported in detail in Section 2.12.4.

To supplement the actual test data, a finite element analysis (FEA) study was conducted using two models that were developed for the Traveller XL package. The first FEA model was based on the design of the two prototypes that were tested in January 2003. The second FEA model was based on the design of the two Qualification Test Units that were tested in September 2003. The QTU (actual package and FEA model) incorporated the modifications that were made to the design as a result of the prototype test results.

The objectives of the drop analysis effort were:

- Demonstrate that the first model acceptably predicted actual test results. This was accomplished by comparing the permanent mechanical deformations that resulted from the actual prototype drops with those predicted by the FEA model.
- Assist in the evaluation of test results. Because the FEA prototype model acceptably predicted actual test results, it could be used with confidence as a tool to evaluate possible changes to the packaging design in order to finalize a design that would pass the hypothetical drop tests.
- Assist in planning final tests. The FEA results, combined with the data obtained by prototype drop testing, were used to establish drop orientations for the qualification test unit (QTU) and certification test unit (CTU) tests.

Limitations were observed in the FEA process. For example, mesh density limitations meant that actual stress and strain predicted values could not be considered highly accurate. The models could identify regions of high stress and strain but could not accurately predict component failure unless predicted values were significantly above or below failure points. Instead, the models were developed to evaluate relative deformations, decelerations and energy absorption between drop orientations. The analyses provided a qualitative means for comparing predicted stresses and strains for different drop orientations to allow intelligent selection of drop orientations for testing. The Traveller program utilized extensive full-scale tests to prove the acceptability of the Traveller design. These tests results are described in sections 2.12.4 below and the results are compared with the FEA in this section.

2.12.4.1 Conclusion and Summary of Results

2.12.4.1.1 Conclusion

Analysis indicates that the Traveller XL shipping package complies with 10 CFR 71 and TS-R-1 requirements, respectively for all drop orientations. Test orientations which are most challenging are a 9 meter vertical drop with the bottom end of the package hitting first as shown in Figure 2-52A and a 9 meter

CG-forward-of-corner drop onto the TN end of package with an 18° forward rotation, Figures 2-44 and Figure 2-45. The former has the greatest potential to damage the fuel assembly and the latter is most damaging to the shipping package itself. Based on this analysis, successful drop tests in these two orientations are adequate to demonstrate that the Traveller XL design meets/exceeds the HAC drop test requirements.

2.12.4.1.2 Summary of Results

Analyses were conducted for horizontal side drops, center-of-gravity-over-corner onto the top nozzle drops, and vertical drops onto the top nozzle and bottom nozzle. A significant amount of analytical data is presented in the following sections. Below is an summary of the major points in the order presented:

Determination of Most Damaging Orientations

- The most damaging orientation for the outerpack may not be most damaging for the fuel assembly. Because of the robust design of the packaging, drop orientations that were most damaging to the fuel assembly took precedence.
- Analysis of drop orientations most damaging to the outerpack focused on three orientations: horizontal drop onto the side, vertical end drop (top and bottom nozzle end), and near-vertical drop (center-of-gravity over corner).
- Analysis of drop orientations most damaging to the fuel assembly focused on the vertical end drop (top and bottom nozzle end).

Most Damaging Orientations to Outerpack

- Horizontal drop onto the side gave highest predicted outerpack loads.
- CG forward of corner onto top predicted to be most damaging to outerpack because of potential damage that might compromise package ability to survive the thermal test.
- Damage to the Traveller XL shipping package from the HAC drop tests is predicted to be minor and primarily involves localized deformations in the region of impact. Both the Outerpack and Clamshell structures remain intact and closed.

Most Damaging Orientations to Fuel Assembly

- Bottom nozzle end drop predicted to be more damaging than top nozzle end drop.
- Fuel assembly damage is predicted to be confined to the top or bottom region depending on drop orientation. This damage primarily involves localized buckling and deformation of the nozzles.

Temperature and Foam Density Effects

- Temperature and foam density have a minor effect on drop performance of the Traveller XL package.
- For the orientation predicted most damaging to the Outerpack, a package with nominal foam density and dropped at “normal temperature” (75°F) experiences 8.5 and 13.7% higher loads than, respectively, one containing low density foam and dropped at 160°F or one containing high density foam and dropped at -40°F, Figure 2-62.
- Fuel assemblies in packages containing the highest allowable density foam and dropped at the lowest temperature extreme will experience accelerations that are very similar to those in packages with lowest allowable density foam and dropped at the highest temperature extreme, Figure 2-63. However, the accelerations at these extremes are only 5% greater than for a package dropped at 75°F containing nominal density foam.
- Bottom nozzle end drop predicted to be more damaging than top nozzle end drop.

Pin Puncture

- Analysis indicates that the Traveller XL is capable of withstanding the 1 m pin puncture test. The steel outer skin should not be ruptured.
- A maximum indentation of 67 mm is predicted for the 1 m pin puncture test when the package is impacted from underneath and dropped horizontally with its CG directly above the pin. during this test.

Comparison of Prototype Test Results to Analysis Predicted Results.

- There was good overall agreement between predicted and actual drop performance. This is evident by comparisons of predicted and actual permanent deformations, failed parts, and measured and predicted accelerations at specific positions on the Outerpack and Clamshell.

Bolt Factor-of-Safety Calculations.

- The Traveller XL shipping package will survive the HAC drop tests in any orientation with few or no closure bolt failures. Horizontal side drops onto the hinges or latches, Figures 26A and B, result in the highest hinge/latch bolt loads. The analyses indicate ten ¾-10 stainless steel bolts/side are sufficient to ensure the Outerpack remains closed during such drops. The minimum predicted factor of safety for the Outerpack latch and hinge bolts is 1.12.

[Rev 2 redistributed this information in Section 2.12.3.1 above.]

2.12.4.2 Predicted Performance of the Traveller Qualification Test Unit

2.12.4.2.1 Most Damaging Drop Orientations

A primary objective of this study was to determine the worst case drop orientation(s) for the HAC drop tests. This requirement is to drop test the shipping package in orientations that most damage: a) the shipping package, and b) the fuel assembly. It was quickly realized that the most damaging orientation for the shipping package, would not necessarily be the same for the fuel assembly. Based on the robust performance of the Traveller XL drop units during testing, orientations that were most severe to the fuel assembly became more significant.

Determination of the worst case orientation for the shipping package was facilitated by the Traveller XL computer analysis and results of the prototype tests. Many orientations can be eliminated from consideration due to inherent design features of the Traveller. For example, the circumferential stiffeners on the upper Outerpak, and the legs/forklift pocket structure, Figure 2-21, greatly reduce the crushing of the Outerpak since they crush prior to impact of the main body of the Outerpak. Drop orientations where one or the other

of these structures directly contacts the drop pad, Outerpack damage is reduced in comparison to orientations where these features are not impacted. This is because the energy absorbed in crushing these features cannot be absorbed by the Outerpack.

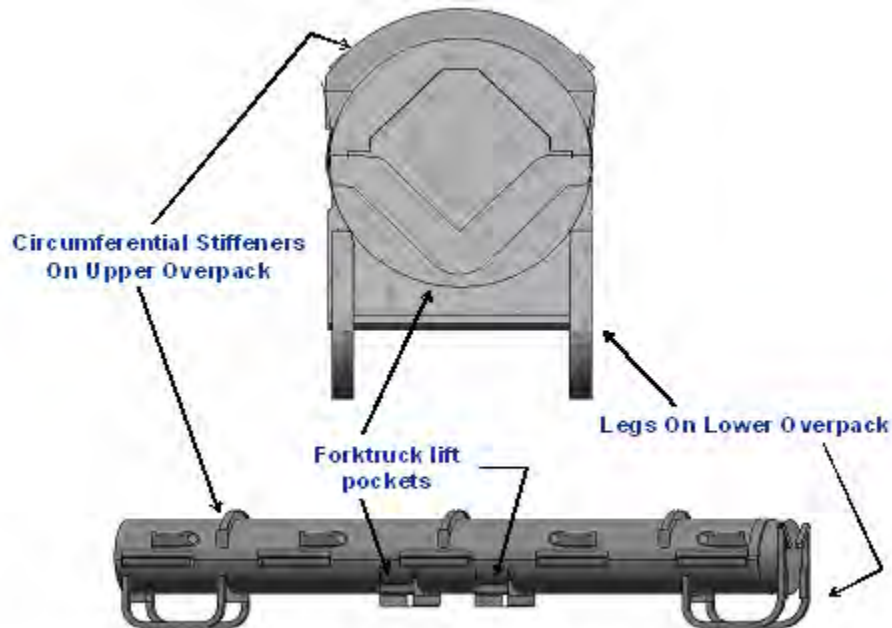


Figure 2-21 Traveller Stiffeners, Legs, and Forklift Pockets

Test results supported this hypothesis. Indeed, in the two available tests of relevance, these features absorbed almost all the energy and very little damage was incurred by the Outerpack. For example, Prototype-1, Test 1.1 was a low angle slap down test resulting in extensive crushing of the upper Outerpack stiffeners, Figure 2-22. Aside from this crushing, very little Outerpack damage was incurred. Prototype-2, Test 3.2 was the second example. In this test, the Outerpack was dropped horizontally onto its legs from 9 m. This resulted in significant crushing of the Outerpack legs and feet, Figure 2-22B, and the forklift supports, not shown. However, the Outerpack was otherwise not significantly damaged.

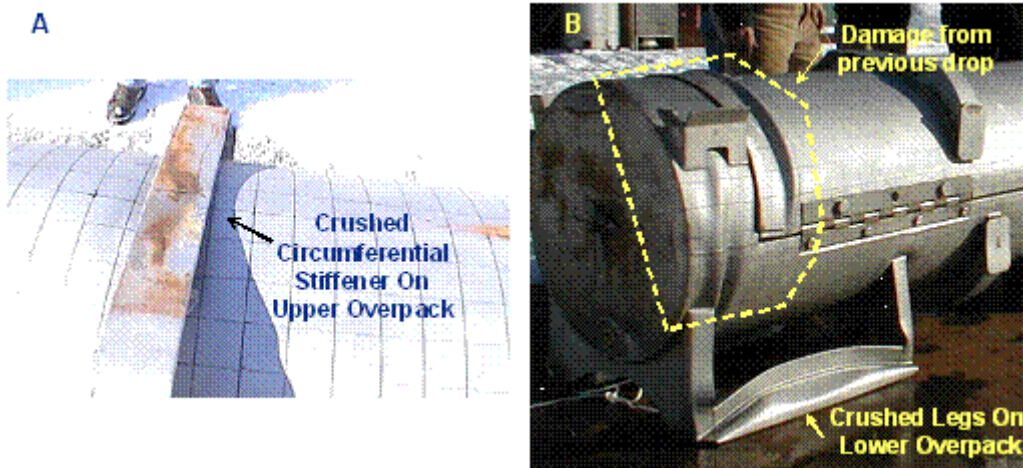


Figure 2-22 Results of Prototype Drop Test

Alternately, neither the stiffeners, nor legs hit first for orientations in which the Outerpack ZX plane defined in is perpendicular to the impact surface, Figure 2-23. Such orientations include side drops or slap downs onto the hinged sides of the Outerpack and vertical drops onto the either end of the package. Thus, our analysis of the most damaging Outerpack orientations focused on these orientations.

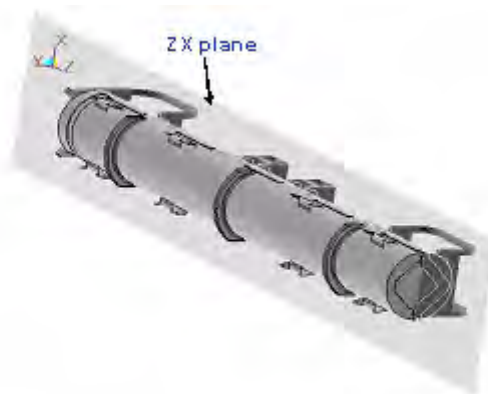


Figure 2-23 Side Drop Orientation

Determining which drop orientations in the ZX plane most damage the shipping package was also facilitated by the Traveller XL design itself. In particular, “slap down” drops, low- to medium-angle impacts where one end of the package hits before the other, as shown in Figure 2-24, divide the impact energy primarily between the top and bottom impact limiters. Generally, this energy is absorbed in a manner that induces relatively little damage for this design. An example of the damage associated with a 15° slap down is shown in Figure 2-25. This figure reflects the damage obtained in Test 1.1 of the Prototype test campaign.

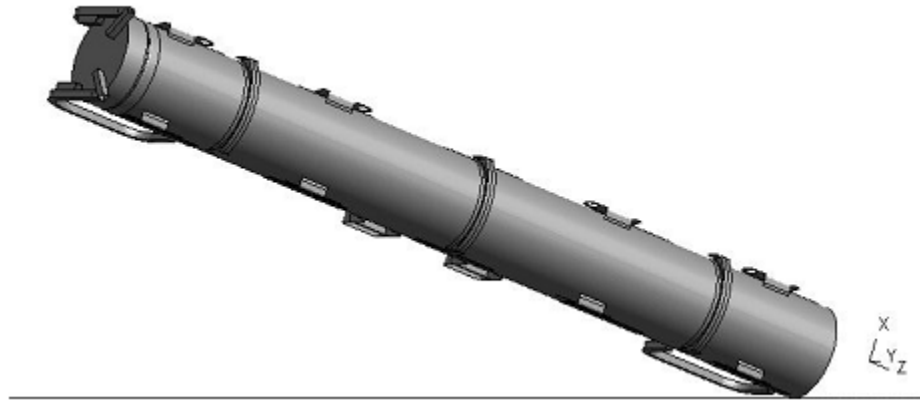


Figure 2-24 Low Angle Drop Orientation

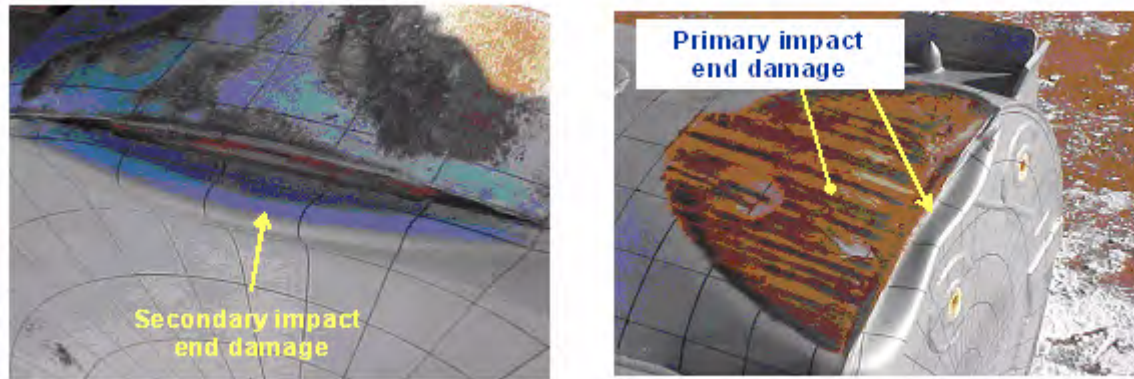


Figure 2-25 Damage from Prototype Low Angle Drop (Test 1.1)

The shipping package may be dropped in some orientations outside the ZX plane and still not be protected by its stiffeners and legs/forklift pocket structure, Figure 2-21. In vertical and nearly vertical orientations, the impact limiter will hit the drop pad first. In these cases, the primary impact energy may be entirely absorbed by the impact limiters and Outerpack walls with little, if any, being channeled into the stiffeners or legs. Indeed, the stiffeners and legs provide no benefit unless the shipping package actually falls over for a secondary impact.

Thus, analysis of orientations most damaging to the Outerpack was focused on horizontal drops onto the Outerpack side (i.e., onto the hinges/latches), vertical drops (onto either end of the package) and nearly vertical drops.

2.12.4.2.2 Horizontal Side Drops

The two possible orientations for a horizontal side drop test involve either a drop onto the opening or latched side of the Outerpack, Figure 2-26A, or a drop onto the permanently (or semi-permanently) hinged side, Figure 2-26B.

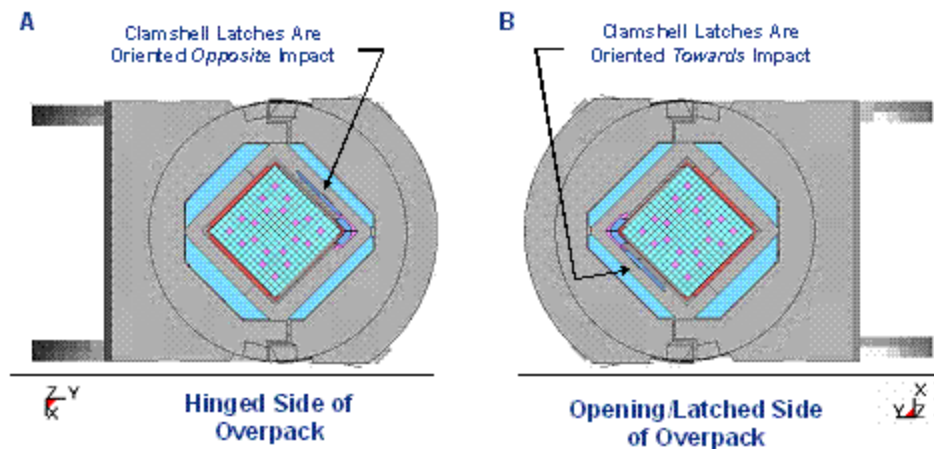


Figure 2-26 Horizontal Drop Orientation

Energy and Work Histories – Global energy and work for the Outerpack horizontal side drops are shown in Figures 2-27 and 2-28. The similarity of these two drops is reflected in these plots. Both plots (as do all the 9.14m (30ft) drops reported herein for the qualification unit) have an initial total energy (TE) of 204 kJ. This value correctly reflects the initial velocity (v) of 13.4 m/s applied to the 2,270 kg (5,005 lb) package mass (m) since our simulation is initiated at the end of Outerpack free fall from 9.14 m (30 ft.); the total energy is comprised only of kinetic energy (KE), and $KE = \frac{1}{2}mv^2$. Total energy remains nearly constant throughout both drop simulations. This reflects the relatively small overall deformations predicted for this drop, i.e., the almost negligible external work done by the package under gravity loading. In both simulations, the event was essentially completed within 10 milliseconds as seen by the flattening of the kinetic energy and internal energies after that time. Moreover, acceptable levels of hourglass, sliding, and stonewall energies were obtained although the sliding energy ultimately reached 10% of the internal energy. This latter issue is not critical since it occurs after the maximum Outerpack/drop pad force has been reached.

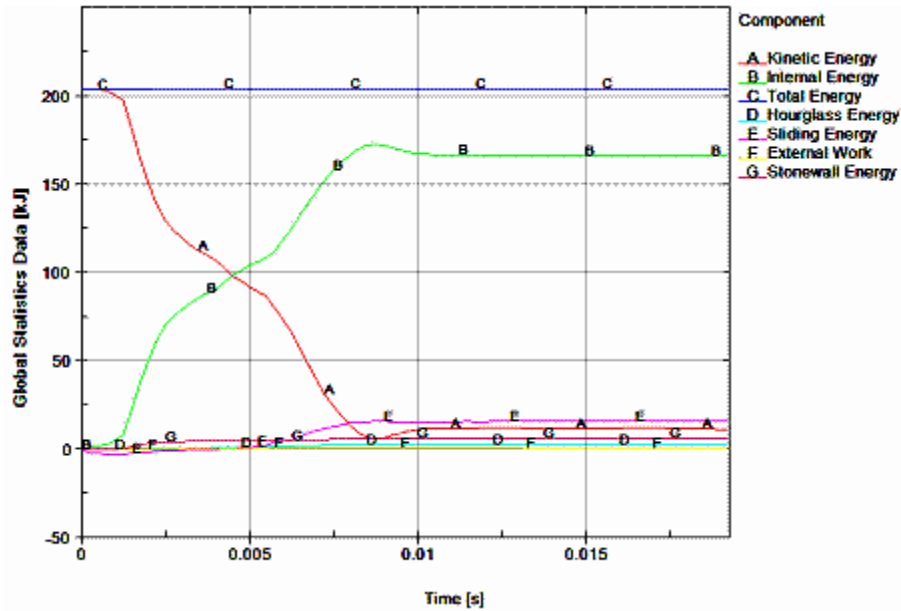


Figure 2-27 Predicted Energy and Work for 9m Horizontal Drop Onto Outerpack Hinges

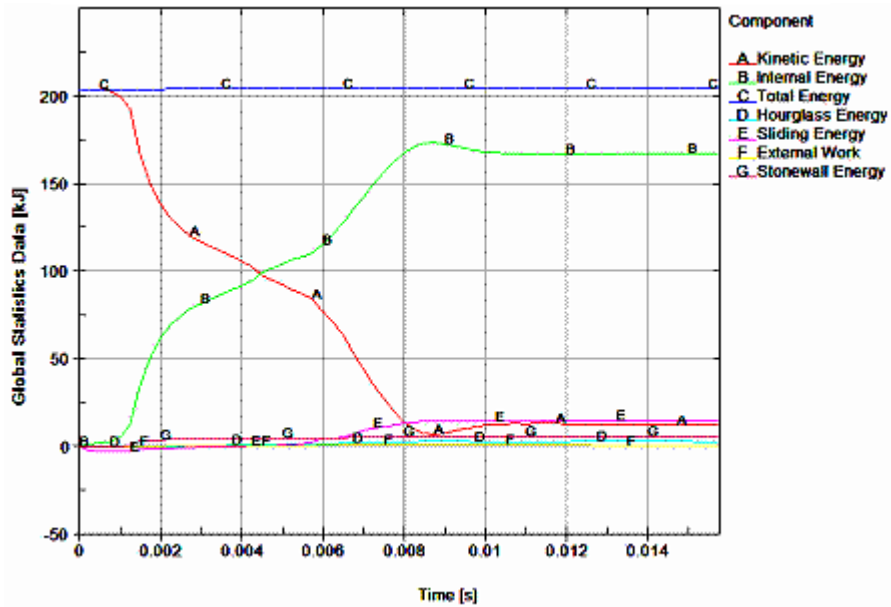


Figure 2-28 Predicted Energy and Work Histories for a 9m Horizontal Drop Onto the Outerpack Hinges

Rigid Wall Forces – Neglecting the very soft shock mounts that tie them together, the Traveller XL shipping package consists of an essentially de-coupled Outerpack and Clamshell/fuel pair. Indeed, the predicted drop scenario consists of the Outerpack crushing onto the pad while the Clamshell/fuel assembly continues falling until it hits the inner surfaces of the Outerpack. Then the Outerpack, Clamshell, and fuel assembly crush further onto the pad. This scenario is reflected in the rigid wall force history shown in Figure 2-29.

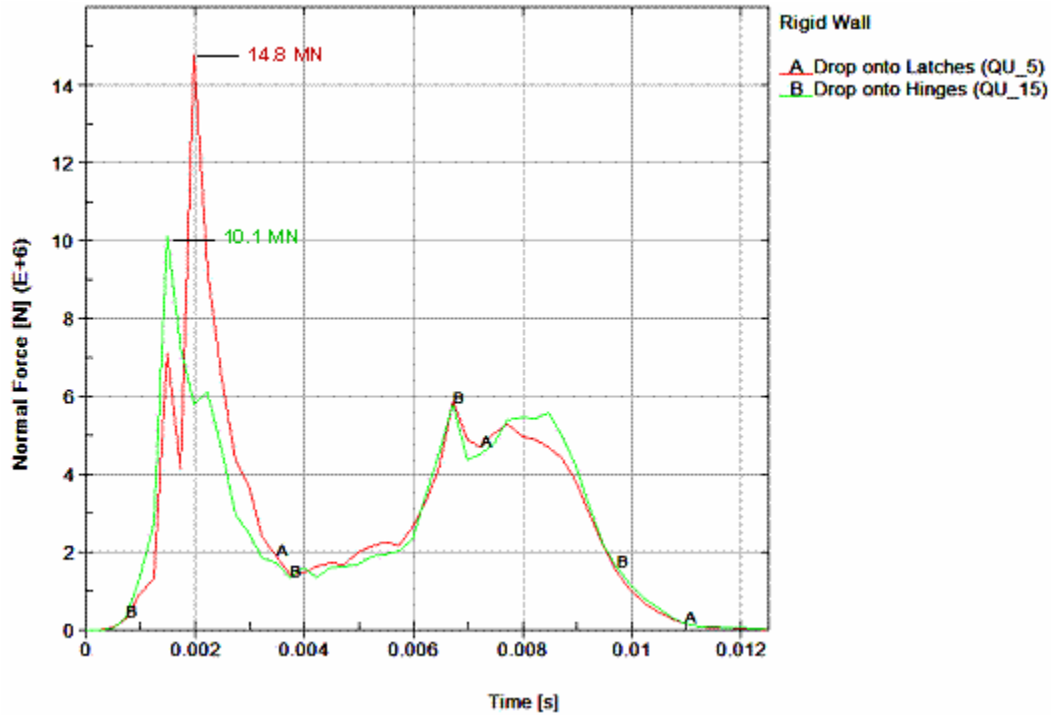


Figure 2-29 Predicted Rigid Wall Force Histories for 9m Horizontal Drops Onto the Outerpack Latches and Hinges

In Figure 2-30A, the initial impact between the Outerpack and pad is seen in the first 4 milliseconds, peaking at approximately 1.5 milliseconds for the drop onto hinge (run QU_15) and 2.0 milliseconds for the drop onto latches (run QU_5). This disparity is attributed to slight errors in the model geometrical definition (rather than to any actual non-symmetry within the design itself). Further, we postulate resolution of this disparity would lower the predicted forces for the drop onto Outerpack latch simulation (run QU_5) and increase those for the simulated drop onto the Outerpack hinges (run QU_15). However, we choose not to resolve this difference but simply used the QU_5 predictions as a bounding and conservative case. At approximately 4.0 milliseconds, the force between the Outerpack and drop pad has decreased and it appears the Outerpack might soon rebound. However, the Clamshell/fuel assembly then contacts the inner surface of the Outerpack and drives it into back into the drop pad, Figure 2-30B.

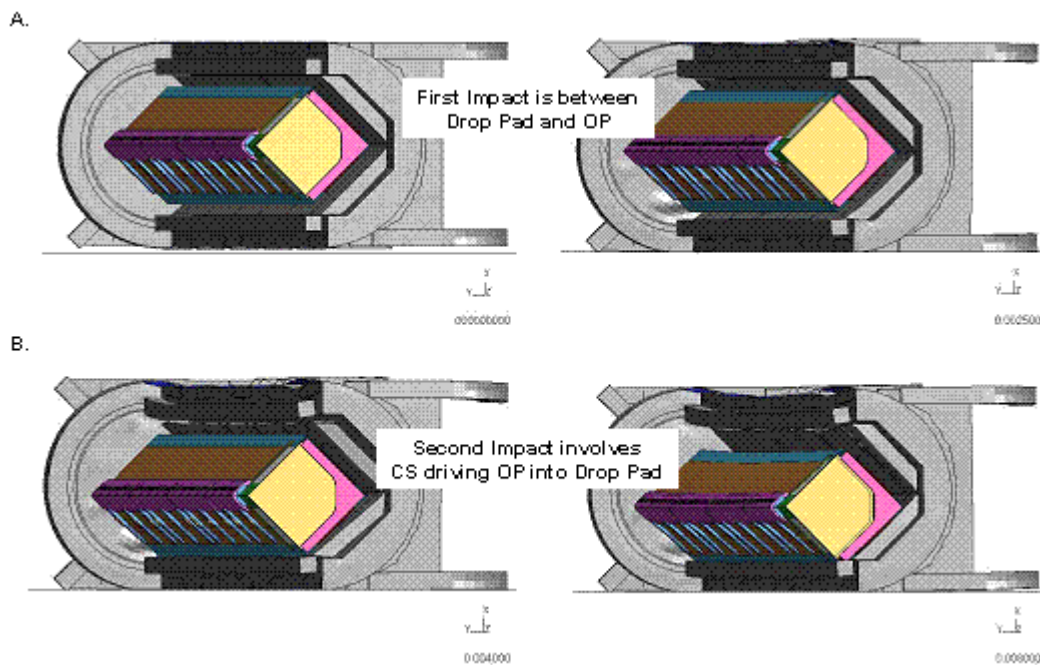


Figure 2-30 De-coupled Impacts for 9 m Horizontal Side Drop

The forces between the Outerpack and drop pad during the first portion of a horizontal side drop are the highest predicted forces for any orientations analyzed. However, these forces are so high because the deformations (i.e., cushioning) are small. Thus, despite the high forces, the package (Outerpack and Clamshell) should be relatively undamaged provided its components remain closed. For the Outerpack, this requires that the majority of the Outerpack latch/hinge bolts do not fail. In the case of the Clamshell, the latch bolts, the top and bottom end plate bolts, and, as will be described, the lipped/groove interfaces between the Clamshell end plates themselves (top end) and between the Clamshell doors and plate (bottom end) must not be comprised. During Prototype testing the robustness of these features was confirmed, as no Outerpack bolts failed, and the Clamshell latches remained closed.

Note that the Clamshell cross-sectional shape is predicted to stay essentially unchanged during the horizontal side drops, Figure 2-30. This is due in large part to the moderator blocks which form a “cradle” for the Clamshell. These moderator blocks prevent the Clamshell from radically changing shape as might otherwise happen since three of the Clamshell edges are either hinged or latched. This is an important structural benefit of the conformal shape of the interior of the Outerpack.

Outerpack Hinge Bolts – The Outerpack hinges are secured to the Outerpack with Type 304 stainless steel bolts, Figure 2-31. The bolts securing the bottom flange of the hinge (or latch) to the lower Outerpack are not removed during normal operation. Thus, the number of bolts used in this area is not critical from a user/operation standpoint. However, the bolts securing the top half of the latch to the upper Outerpack must be removed whenever the package is opened. Thus, the desire is to minimize the number of these bolts while

still insuring the package is not compromised during HAC drop tests. As such, the development of the Traveller XL design started with three 7/8" diameter (2.2 cm) for each hinge segment. A total of five (5) hinge segments per Outerpack side were utilized. The second Prototype unit therefore was tested with only 2 of 3 bolts in each hinge section (10 per side) to verify that design margins were present in the design.

Based on the successful testing of 10 bolts per side, evaluations were initiated to determine if smaller 3/4" diameter (1.91 cm) bolts had sufficient strength to sustain impact loads. These were shown to be acceptable. The QTU-1 and QTU-2 units were dropped with ten 3/4" (1.91 cm) bolts on each side.

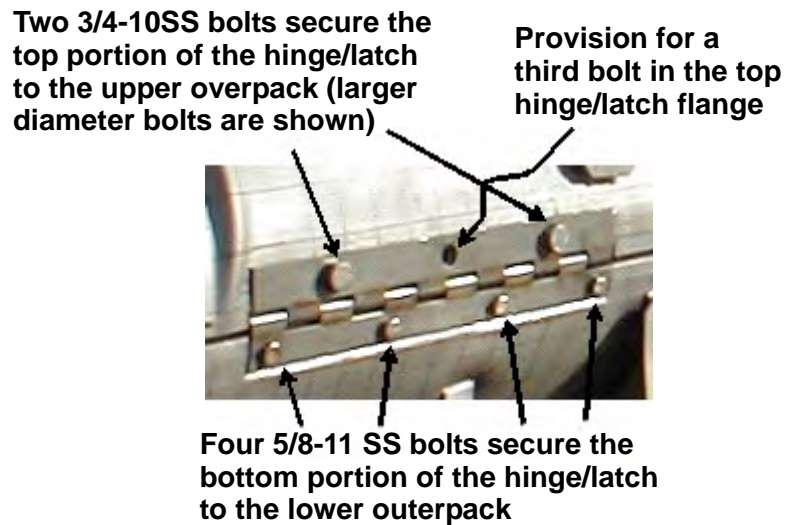


Figure 2-31 Bolts on Prototype Outerpack

Prototype-2, Test 3.3 was a side drop in which two 7/8-9 stainless steel bolts were used to secure the top portion of the hinge to the upper Outerpack and four 5/8-11 stainless steel bolts were used to secure the bottom hinge flange to the lower Outerpack. In this test, no bolts were broken. Our analyses indicate two 3/4-10 stainless steel bolts/latch and hinge are sufficient to insure the Outerpack remains closed during the 9m side drop. This is seen by reviewing the predicted safety factors of the top latch bolts when the package is dropped on its latching side, Figure 2-26B. As shown in Table 2-10, the minimum factor-of-safety (FS) for the top Outerpack latch bolts was 2.15 based on the bolt minimum tensile (125 ksi). This minimum was calculated for a latch bolt when the Outerpack was dropped onto its latched side, Figure 2-26B.

Table 2-10 Top Outerpack Latch Bolt Minimum Factors of Safety (FS) for 9m Side Dropped		
ID (Figure 2-32)	FS/Time	
	Dropped On OP Latches (Figure 2-30B)	Dropped On OP Hinges (Figure 2-30A)
B917	2.22/0.0082 s	2.20/0.0077 s
B921	2.15/0.0065 s	2.21/0.0065 s
B923	2.16/0.0065 s	2.17/0.0065 s
B927	2.20/0.0062 s	2.18/0.0065 s
B929	2.19/0.0057 s	2.19/0.0062 s
B933	2.19/0.0067 s	2.20/0.0077 s
B935	2.20/0.0067 s	2.16/0.0065 s
B939	2.18/0.0065 s	2.18/0.0065 s
B941	2.21/0.0085 s	2.23/0.008 s
B945	2.32/0.0045 s	2.43/0.0045 s



Figure 2-32 Bolt Labels for Right Outerpack

Hinge bolt FS for horizontal 9m side drops on the latched and hinged side of the Outerpack are shown in Table 2-10. If the shipping package were exactly symmetrical, FS for the hinge bolts calculated for a drop on the Outerpack hinges would correspond with those for the latch bolts when the package was dropped onto the latches, etc. However, this was not the case as can be seen by comparing the results shown in Table 2-10 with those in Table 2-11. This small irregularity is primarily attributed to slight errors in the model geometrical definition and to a lesser extent on actual non-symmetry within the design itself. The analysis indicates little likelihood of compromising the Outerpack closure during a 9m side drop.

Table 2-11 Top Outerpack Hinge Bolt Minimum Factors of Safety (FS) for 9m Side Drop		
ID (Figure 2-33)	FS/Time	
	Dropped On OP Latches (Figure 2-30B)	Dropped On OP Hinges (Figure 2-30A)
B947	2.34/0.0025 s	2.20/0.0077 s
B951	3.05/0.0027 s	2.21/0.0065 s
B953	2.58/0.0022 s	2.17/0.0065 s
B957	2.93/0.0022 s	2.18/0.0065 s
B959	2.82/0.0017 s	2.19/0.0062 s
B963	3.19/0.0017 s	2.20/0.0077 s
B965	2.52/0.0022 s	2.16/0.0065 s
B969	2.22/0.0117 s	2.18/0.0065 s
B971	2.52/0.0055 s	2.23/0.008 s
B975	2.54/0.0032 s	2.43/0.0045 s

For the CTU and production designs, minor changes to the design were made to improve burn test performance, as well as simplify manufacturing. To ensure a conservative design, two additional bolts were added on each side of the Outerpack full-length hinge sections. Therefore, the CTU and production packages utilize 12 bolts per side per hinge leaf. This change allowed the reduction of the planned high strength (125 ksi ultimate strength) bolt to be replaced with a lower strength bolt, since there are more bolts, and since the 70 ksi bolts were marginal in performance. It should also be noted that the Prototype-2 package was dropped on its side from 9 m and showed no visible signs of strain on any of the bolts. One explanation for this may be that friction is ignored in the calculation of bolt factors of safety.

The increase in number of bolts, 20%, (= 12/10) and the increase in strength of the allowable bolt material, ASTM A193 Class 1 B8, of 7% (= 75 ksi/70ksi – 1) causes the factors of safety of the worst bolt in a side drop to be reduced from 2.15 to 1.12. Since this is the greatest loading for any orientation, all bolts have an adequate safety margin.

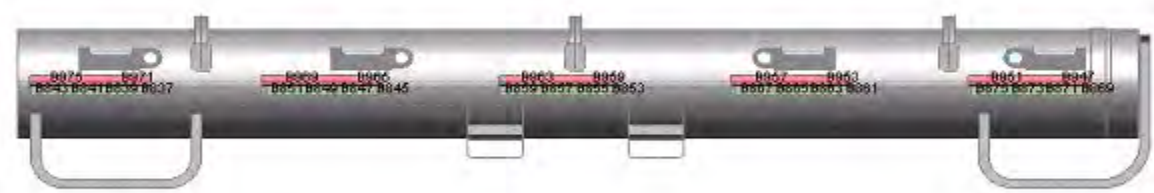


Figure 2-33 Bolt Labels for Left Outerpack

Clamshell Keeper Bolts – The inner Clamshell is restrained during shipment by eleven (11) quarter-turn latches as shown in Figure 2-34. This design was incorporated after Prototype testing, primarily for improved handling characteristics. One half of the latch, the latch handle, is welded to the one Clamshell door hinge. The portion of the latches which is physically turned to allow opening and closing is attached to the opposite door is called the “keeper.” Each keeper is attached to the Clamshell door with ½-13 stainless steel bolts.

Factors-of-safety for the Clamshell keeper bolts are shown in Table 2-12. The analyses indicate that these bolts are unlikely to fail during side drops onto either the Outerpack latches or Outerpack hinges. Further, the modeling of the fuel assembly as a rigid structure likely makes little difference to these predictions since the fuel rods would not be expected to buckle in this drop orientation.

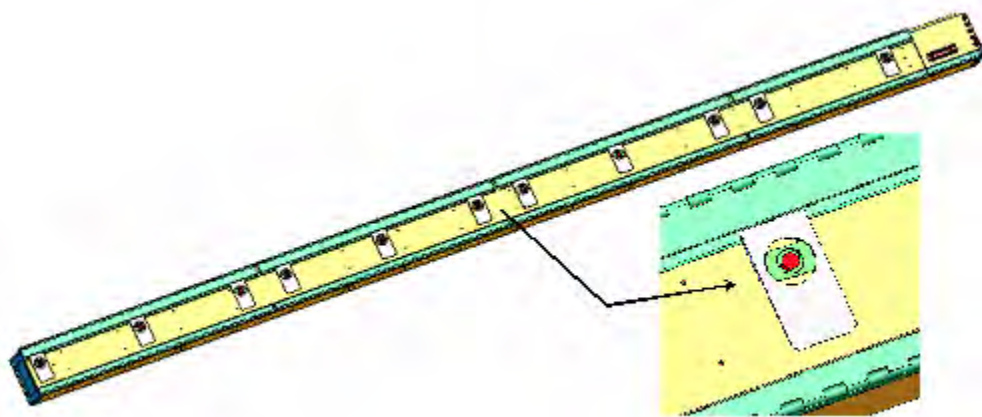


Figure 2-34 Clamshell Closure Latches and Keeper Bolts

Table 2-12 Clamshell Keeper Bolt Minimum Factors of Safety for 9m Side Drop		
ID (Figure 2-35)	FS/Time	
	Dropped On OP Latches (Figure 2-30B)	Dropped On OP Hinges (Figure 2-30A)
B6271277	2.10/0.0067 s	1.72/0.006 s
B6271278	2.15/0.007 s	1.72/0.0085 s
B6271279	3.17/0.0062 s	3.36/0.0075 s
B6271280	2.12/0.0072 s	4.40/0.01 s
B6271281	2.90/0.008 s	4.03/0.0092 s
B6271282	2.50/0.0082 s	2.48/0.0067 s
B6271283	3.70/0.0055 s	2.16/0.0067 s
B6271284	2.56/0.007 s	1.84/0.0062 s
B6271285	1.93/0.0072 s	2.64/0.008 s
B6271286	2.62/0.0072 s	3.00/0.0082 s
B6271287	1.94/0.0075 s	2.29/0.0082 s

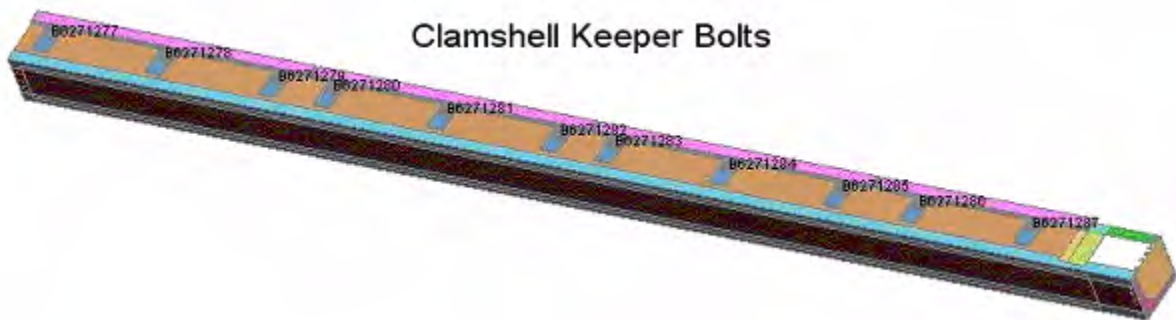


Figure 2-35 Clamshell Keeper Bolt Labels

Clamshell Top and Bottom Plate Bolts – In addition to the Clamshell latch bolts, there are thirty ½-13 stainless steel bolts securing the Clamshell top and bottom end plates. The twenty bolts securing the top end plate are distributed five per side as shown in Figure 2-36A. These bolts are not removed during normal operation and are permanently adhered to the plates. The ten bolts securing the bottom end plate are distributed equally to the two walls of the Clamshell V-shaped bottom extrusion as shown in Figure 2-36B. These bolts are also permanently adhered.

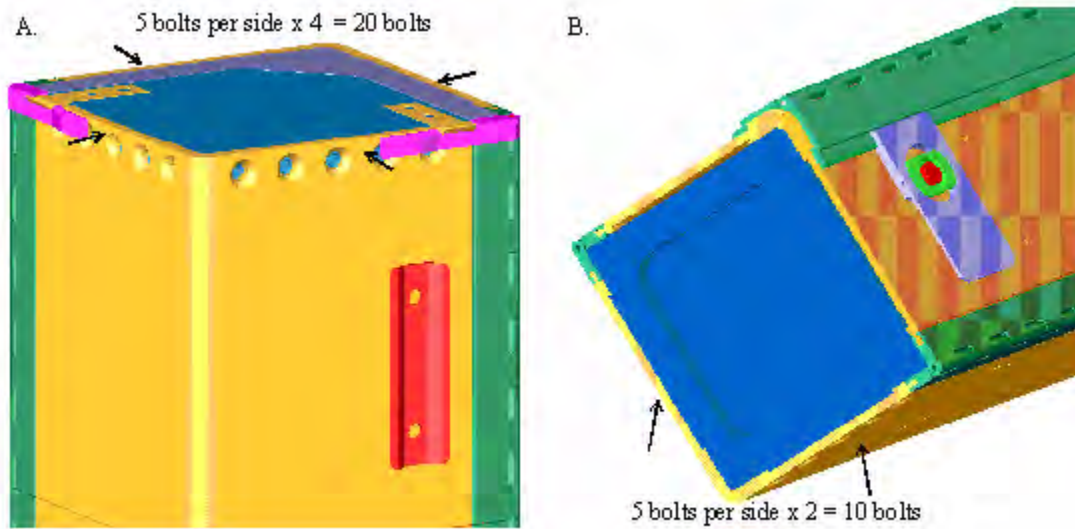


Figure 2-36 Clamshell Top and Bottom End Plates

The analyses indicates that none of the Clamshell bolts at the top and bottom ends will fail during a side drop on either the Outerpack latches or Outerpack hinges. This is evident from the minimum factors of safety shown in Tables 2-14, 2-15 and 2-16. (Our modeling of the fuel assembly as a rigid structure likely makes little difference to these predictions since the fuel rods would not be expected to buckle in this drop orientation.)

Table 2-13 Clamshell Bottom Plate Bolt Minimum Factor of Safety for 9m Side Drops		
ID (Figure 2-37)	FS/Time	
	Dropped on OP Latches (Figure 2-30B)	Dropped on OP Hinges (Figure 2-30A)
B6168785	2.39/0.0047 s	2.33/0.0107 s
B6168786	2.84/0.0070 s	4.29/0.0065 s
B6168787	6.40/0.0092 s	6.96/0.0062 s
B6168788	9.56/0.0092 s	6.26/0.0062 s
B6168789	6.62/0.0190 s	3.96/0.0060 s
B6168794	3.84/0.0062 s	5.43/0.0102 s
B6168793	19.4/0.0050 s	7.61/0.0102 s
B6168792	13.5/0.0087 s	7.88/0.0102 s
B6168791	4.37/0.0065 s	3.57/0.0055 s
B6168790	2.41/0.0060 s	2.48/0.0050 s

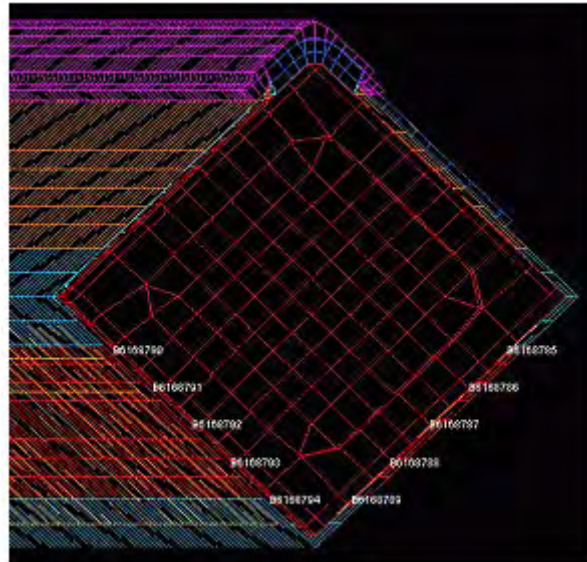


Figure 2-37 Clamshell Bottom Plate Bolt Labels

ID (Figure 2-38)	FS/Time	
	Dropped on OP Latches (Figure 2-30B)	Dropped on OP Hinges (Figure 2-30A)
B6168781	4.19/0.006 s	5.21/0.0052 s
B6168780	21.1/0.0065 s	12.67/0.0057 s
B6168779	32.1/0.0077 s	21.22/0.0057 s
B6168778	17.5/0.0095 s	33.37/0.007 s
B6168773	2.29/0.0065 s	2.73/0.005 s
B6168774	2.25/0.0062 s	4.97/0.0087 s
B6168775	3.88/0.0075 s	33.54/0.0092 s
B6168776	24.5/0.0057 s	52.4/0.0077 s
B6168777	13.2/0.0057 s	54.49/0.009 s
B6168769	2.99/0.0052 s	4.77/0.006 s

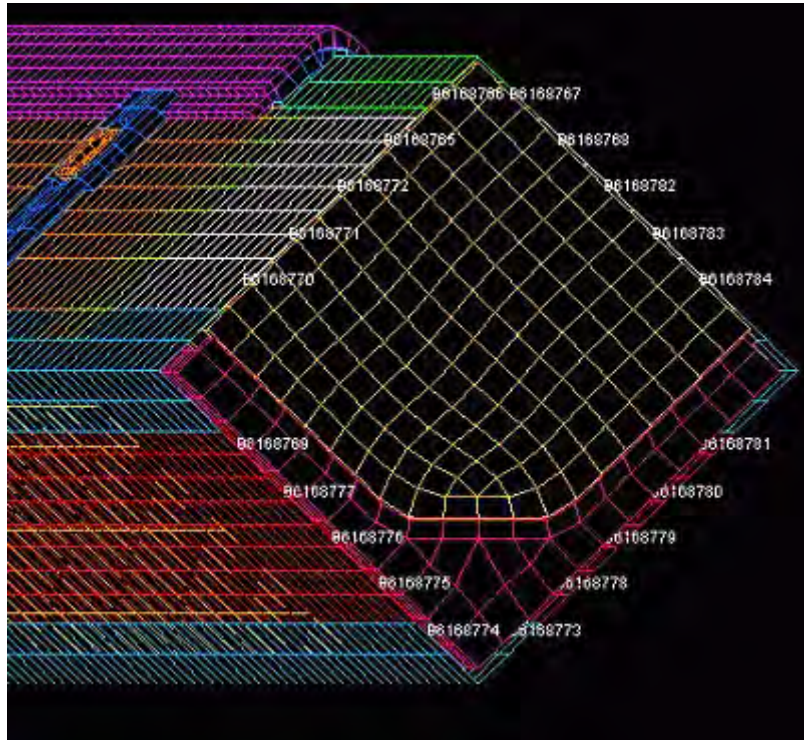


Figure 2-38 Clamshell Bottom Plate Bolt Labels

ID (Figure 2-38)	FS/Time	
	Dropped on OP Latches (Figure 2-30B)	Dropped on OP Hinges (Figure 2-30A)
B6168770	2.32/0.005 s	3.38/0.0077 s
B6168771	5.65/0.005 s	10.4/0.006 s
B6168772	5.95/0.005 s	11.6/0.007 s
B6168765	9.29/0.0085 s	18.8/0.0065 s
B6168766	7.27/0.0057 s	7.99/0.007 s
B6168767	6.54/0.007 s	6.58/0.006 s
B6168768	9.68/0.007 s	11.7/0.006 s
B6168762	9.14/0.007 s	9.16/0.006 s
B6168783	6.18/0.0085 s	5.65/0.0122 s
B6168784	4.22/0.008 s	2.25/0.0047 s

Clamshell Top End Plate Joint – One goal of the Traveller package design was to minimize the time and effort associated with loading and unloading the fuel. This necessitated the number of bolts that had to be removed during these operations be as kept as low as possible. To accomplish this, the top end of the Clamshell consists of two interlocking plates as shown in Figure 2-39. One of these plates is grooved and is permanently attached to the V-shaped lower portion of the Clamshell, Figure 2-36A. The other has a lip and is permanently attached to an upper housing above the Clamshell doors, Figure 2-39. This groove-and-lip design should indeed facilitate rapid loading and unloading, however, the joint must not separate to any significant extent during the HAC drop tests that the fuel rods might slip out of the Clamshell.

Fortunately, our analysis indicates that the separation during impact is small, Figure 2-40. Furthermore, the separation is transient/temporary as can be seen by the reduction in the separation distance in the later stages of the analysis, Figure 2-40B compared with Figure 2-40A. These predicted results were obtained from the analysis of the Outerpack drop onto its latches. In this case, the Clamshell latches are positioned underneath the fuel, towards the ground, Figure 2-26B. Analysis of the Outerpack drop onto its hinges yielded similar results although the predicted separation of this joint was slightly less.

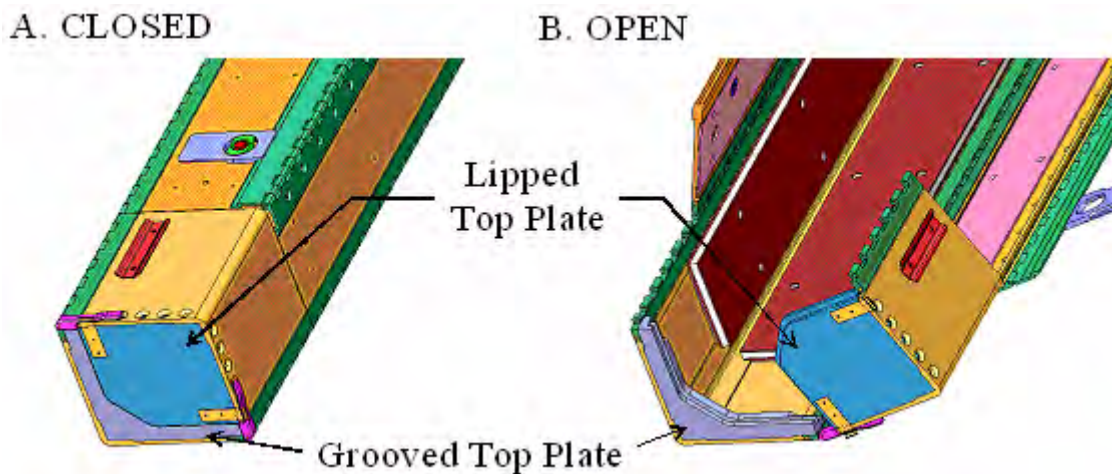


Figure 2-39 Clamshell Doors

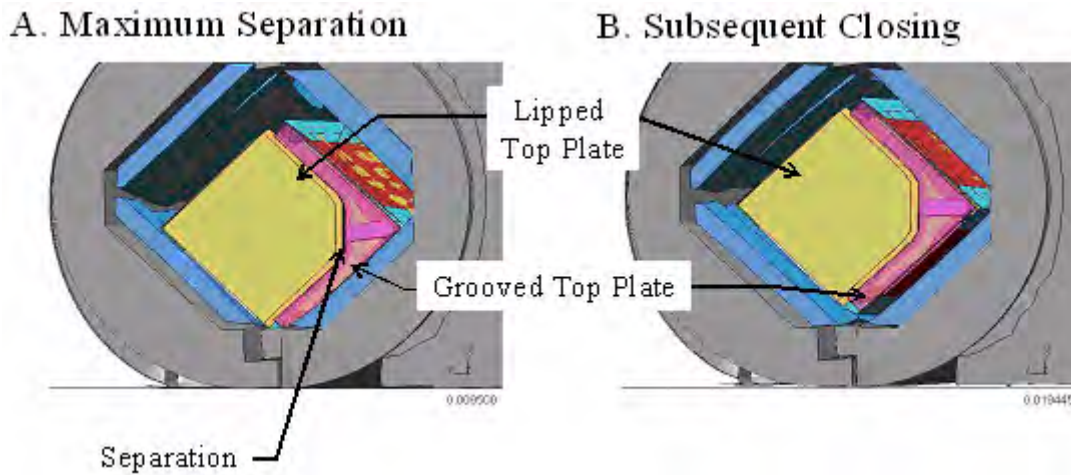


Figure 2-40 Clamshell Response during Side Drop

Clamshell Bottom End Plate/Door Joints – In keeping with the goal of minimizing the time and of loading and unloading the fuel, no bolts must be removed at the bottom end of the Clamshell during these operations. To accomplish this, the bottom Clamshell plate and doors have an interlocking feature consisting of a lip on the bottom end plate and corresponding grooves in both Clamshell doors, Figure 2-41. As described previously for the top end, these joints also do not separate to the extent that a fuel rod could slip through the opening

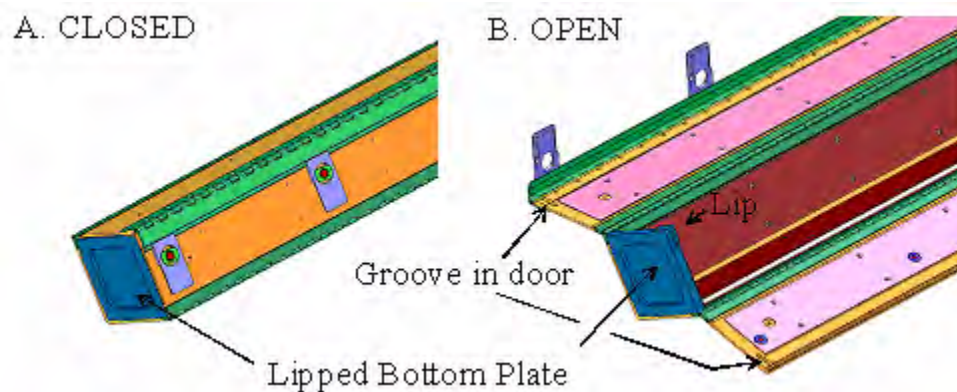


Figure 2-41 Clamshell Doors at Bottom Plate

A small separation of one of these joint during impact is predicted, Figure 2-42. Because the separation is at the upper joint is small, it is not possible that a fuel rod could slip through this joint. Furthermore, the other joint is predicted to remain closed and the bottom end plate should remain intact. These predicted results were obtained from the analysis of the Outerpack drop onto its latches. In this case, the Clamshell latches are positioned underneath the fuel, towards the ground, Figure 2-26B. As with the joint at the top Clamshell plate, the predicted separation of this joint was slightly less for a drop onto the Outerpack hinges.

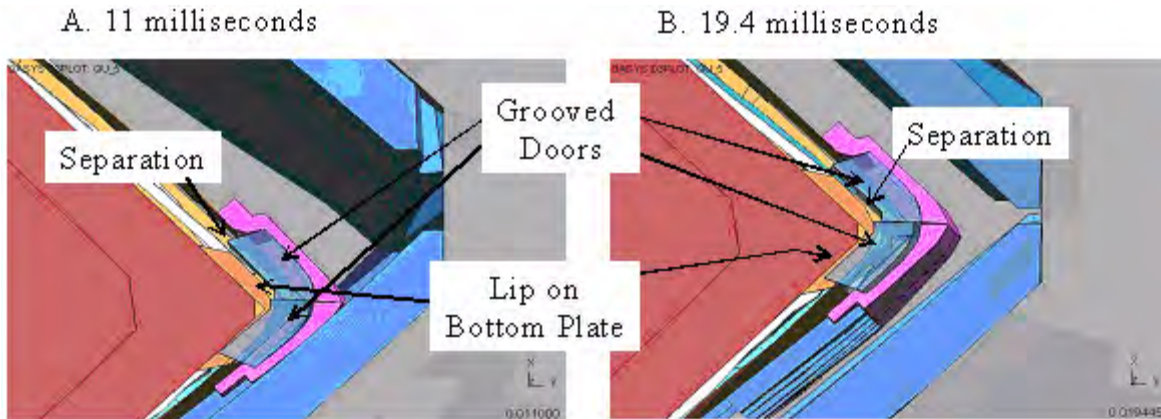


Figure 2-42 Predicted Response of Clamshell Bottom Plate and Doors During 9m Horizontal Drop onto Outerpack Latches

2.12.4.2.3 “CG-over-Corner” and “CG-forward-of-Corner” Drops onto Top Nozzle End of Package

As indicated in Figure 2-43, almost vertical orientations may result in the package center of gravity (CG) being positioned directly above the impacting corner of the package. When this occurs, the drop is designated as a “CG-over-corner” impact. In a CG-over-corner impact, the shipping package will initially continue translating in the direction of impact without rotating. However, deformation of the impacted corner may eventually result in the package tilting and falling over.



Figure 2-43 Top Nozzle Analysis Drop Orientation

CG-over-corner impacts direct all the drop energy to only a portion of the impact limiter. Thus, except for a specific feature of the Traveller XL package, a CG-over-corner impact (either onto the top or bottom end of the package) would probably be the most damaging “nearly vertical” drop. However, as subsequently shown, some drops onto the top nozzle at angles that put the CG forward of the impact corner, i.e., in the “fall” direction of Figure 2-44, are predicted to be more damaging. This is because the resulting deformation involves the Outerpack top corner bending about an (imaginary) axis between the knuckles of the first hinge and latch Figure 2-45.

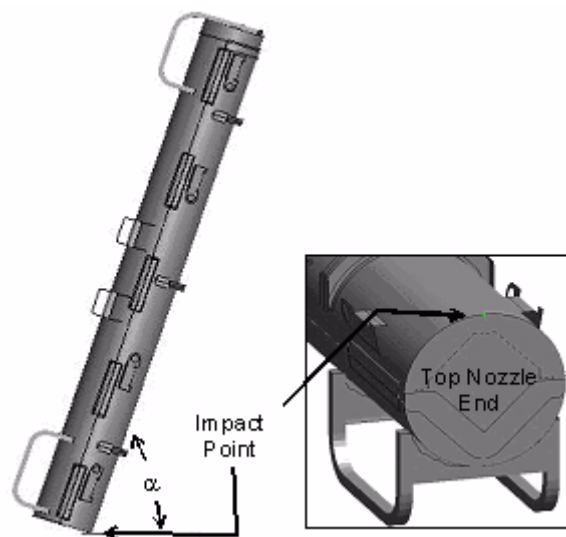


Figure 2-44 Location of Impact

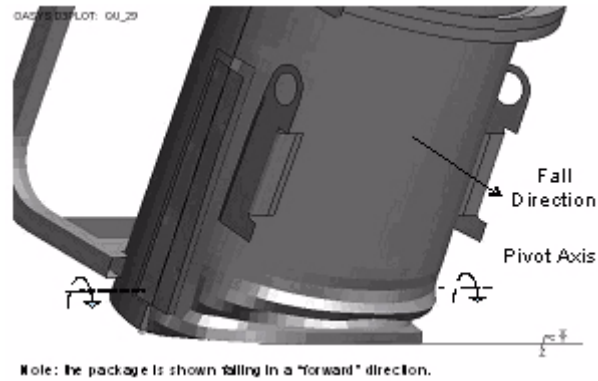


Figure 2-45 Damage to Outerpack During Angled Drop onto Top Nozzle End of Package

The most damaging drop orientation for the Outerpack is a top nozzle down, CG-forward-of-corner configuration having an 18° rotation ($\alpha=72^\circ$), see Figure 2-44. With smaller rotations, the detrimental opening of the Outerpack seam is predicted to be less despite a greater amount of energy being absorbed by the impact limiter. This is because portions of both the upper and lower Outerpack assemblies contact the drop pad and this significantly reduces their relative motion. With larger rotations, Outerpack seam opening is also predicted to be less. This is because the pivot axis moves well in front of the hinge knuckles in Figures 2-45 and 2-46.

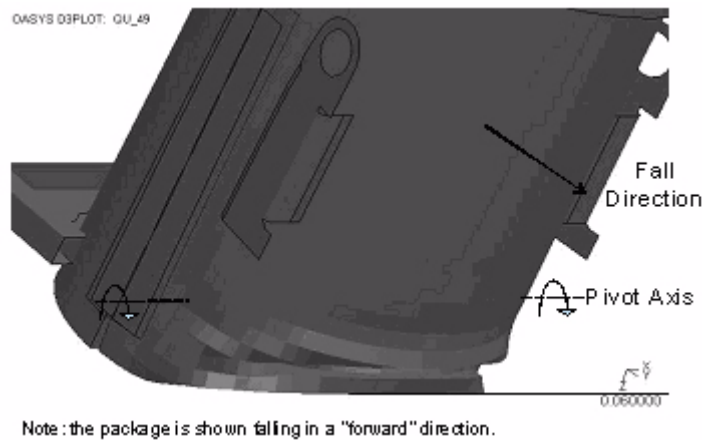


Figure 2-46 Predicted Deformation of Outerpack Top Nozzle Impact Limiter

For the subsequent 1 meter pin puncture drop, the premise is that this is the worst possible additional damage for the Outerpack seam to be further opened. Thus, the most damaging pin puncture orientation following a CG-forward-of-corner test is clearly one where the damaged face of the Outerpack is perpendicular to the pin as depicted in Figure 2-47. The combination of these scenarios; a high angle drop followed by a pin puncture in the location of the initial impact was the basis for the QTU-1 unit testing.

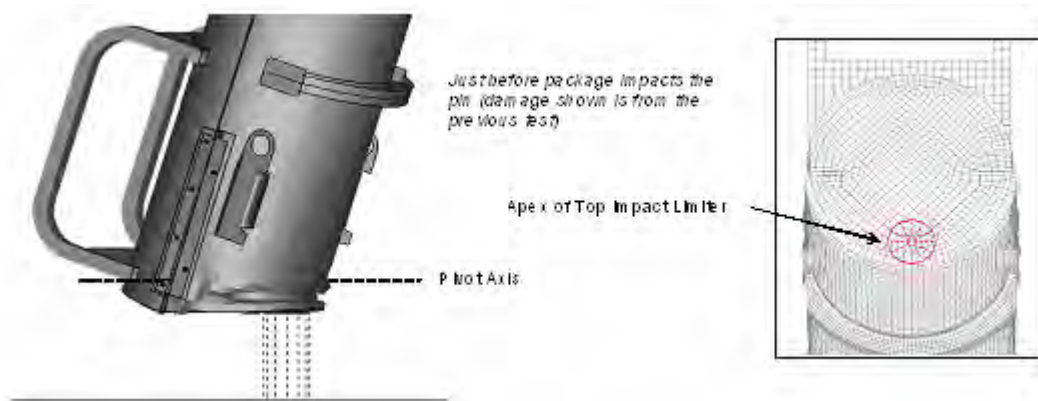


Figure 2-47 Predicted Pin Puncture Orientation after a CG-Forward-of-Corner Test

The FEA of the pin drop incorporated package deformations and stresses calculated to result from the 9m drop. The methodology for including the deformation and stresses involved defining the nodal coordinates in the pin puncture model as the deformed nodal positions of the previous analysis plus a rigid-body-rotation to locate the “model with previous damage” to the proper position/orientation for the pin puncture test. The element stresses were extracted from the first analysis and included as initial stresses in the second analysis.

Finally, from a computation standpoint, it was not practical to compute the secondary impact. This is because the secondary impact is preceded by a lengthy free-fall. Long (multi-day) computations would have been required to run an analysis through the free-fall and secondary impact. Fortunately, secondary impacts for such nearly vertical drops as this are known not to cause much additional damage. This is especially so for the Traveller XL design which will be protected by the circumferential stiffeners on the upper Outerpack. Thus, not having predictions of the secondary impact should be no limitation.

“Worst Case Drop Angle” Determination – As previously discussed, our damage criterion for the CG-forward-of-corner drops onto the top nozzle end of the package was the degree of separation between the upper and lower Outerpack assemblies. Three orientations: 11, 18, and 25° were investigated and it was determined that an angle of 18° resulted in the most separation, Figure 2-48.

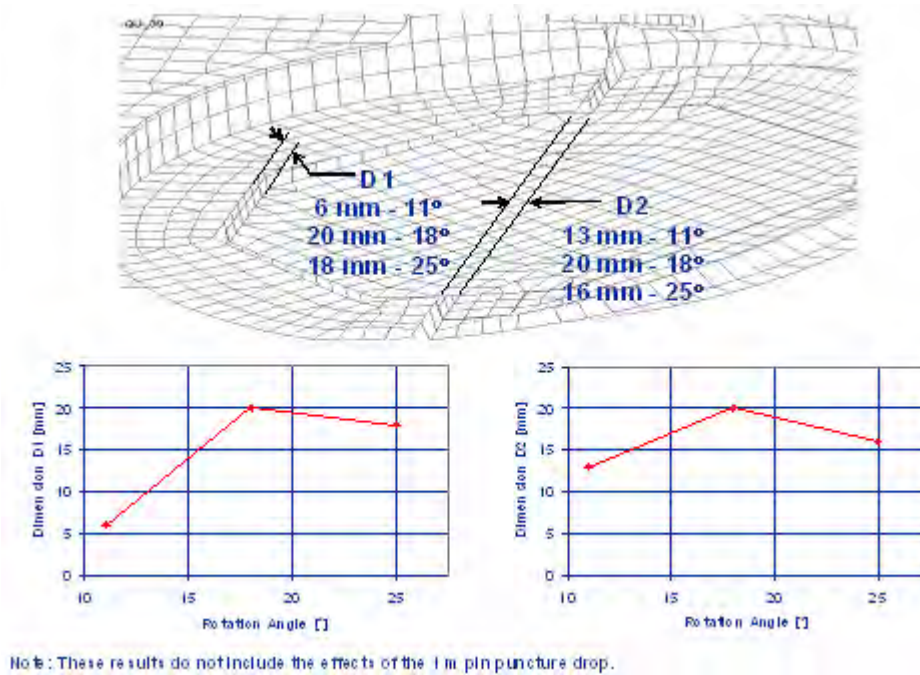


Figure 2-48 Outerpack Top Separation vs. Drop Angle

Energy and Work Histories – Predicted global energy and work histories for the primary impact of three CG-forward-of-corner drops onto the top nozzle end of the package are shown in Figure 2-49. These plots were obtained for forward rotations of 11, 18, and 25°, respectively. As before, the initial total energy (TE) of 204 kJ and increases slightly during the run in concert with the external work due to gravity. In each of these plots, the internal energy (IE) and kinetic energy (KE) traces become flat between 50-60 milliseconds into the impact event. This indicates completion of the primary impact and initiation of rollover. (Rollover and secondary impact were not numerically investigated as previously justified.) Note as drop rotation angle decreases, the internal energy absorbed by the Outerpack is predicted to increase. However, as explained earlier, this should not result in the largest Outerpack seam opening. Finally, hourglass, sliding and stonewall energies are low in each plot. This indicates overall numerically sound analyses. However, late in the analysis, hourglass energy does reach 4.1% of the total energy. While this is a low percentage, the hourglass error is concentrated in the XL pins (PID 10764) and the Clamshell cushioning pads (PIDS 2003 and 2013) in the vicinity of impact. An investigation of this error which involved using fully integrated elements found the energy previously dissipated as hourglass deformation was now (correctly) forced into the bottom impact limiter. This had only a marginal effect on the predicted force in the primary impact of Figure 2-50 and Figure 2-62. However, it did reduce predicted FA accelerations by about 17% (from the 47.3 g's shown in Figure 2-63 to 39.3 g's.). This latter effect was not significant enough to change any conclusions within the report.

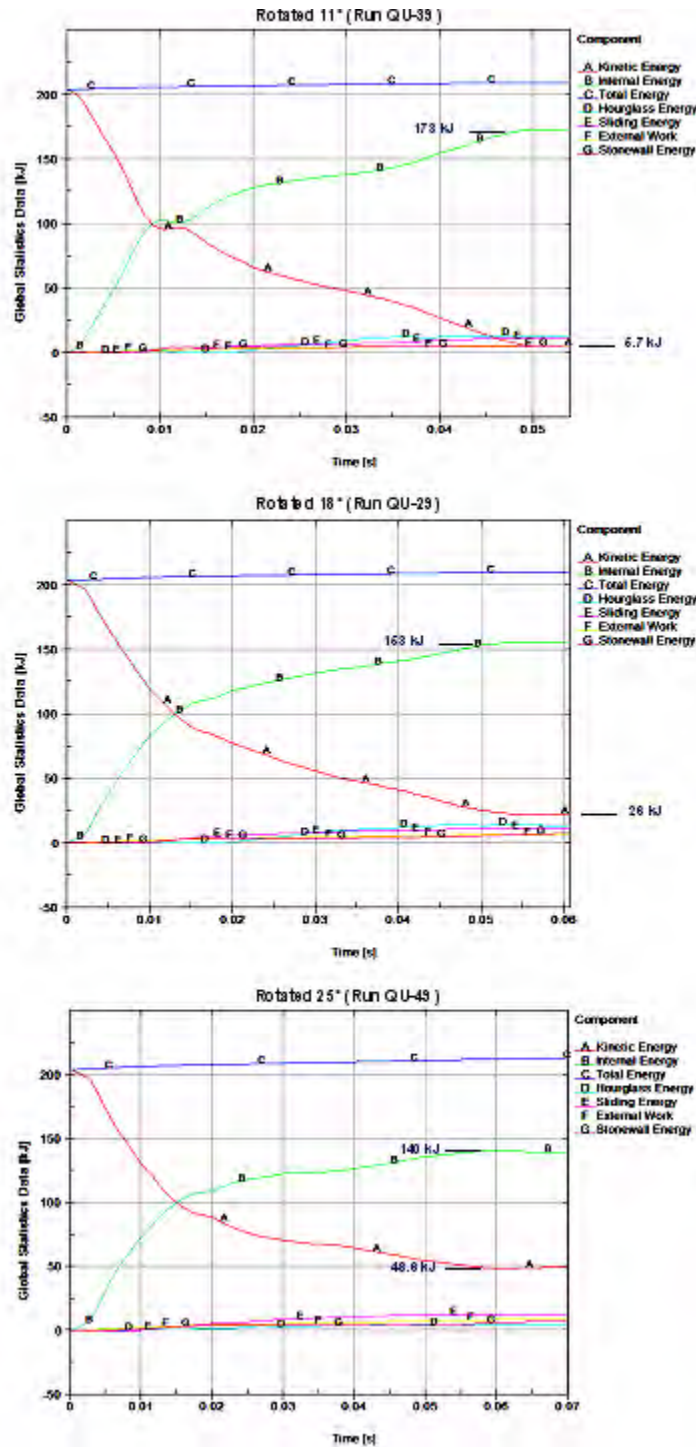


Figure 2-49 Predicted Energy and Work Histories for 9 m CG-over-Corner Drop onto the Top Nozzle End at Various Angles

Rigid Wall Forces – The predicted rigid wall force histories are shown in Figure 2-50 for CG-forward-of-corner drops on to the top end of the package rotated 11, 18, and 25°. These plots show only the primary impact (since the secondary impact due to fall-over was not calculated). The primary impact is divided into two separate events. From impact onset to approximately 25 milliseconds, the Outerpack impacts the drop pad while the Clamshell is still in free-fall. (This is due to the de-coupling between Outerpack and Clamshell previously discussed in section 2.1.1.1.1.) Secondly, the Clamshell hits the inner surfaces of the Outerpack and drives it back into the drop pad from approximately 25 milliseconds into the impact until about 70 milliseconds. Figure 2-50 shows the highest predicted loads for the Outerpack in these three orientations will be encountered at an 11° rotation. This agrees with the previous prediction that as drop rotation angle decreases, the internal energy absorbed by the Outerpack increases.

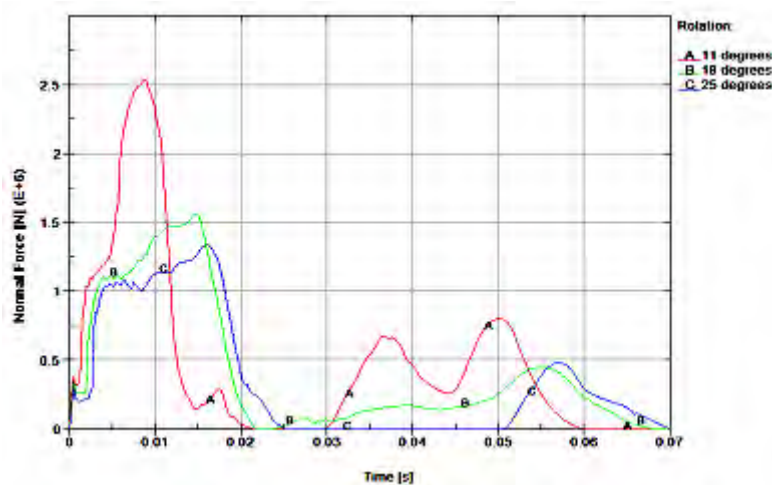


Figure 2-50 Predicted Rigid Wall Forces

As previously stated, the primary concern with CG-forward-of-corner drops onto the top nozzle end of the package is whether or not the thermal integrity needed to protect against the 30 min burn test will be compromised. It was shown that the deformation most likely to induce such damage is greatest when the Traveller XL package is rotated approx. 18° forward from a vertical orientation Figure 2-48. The main concern with the higher loads sustained and additional energy absorbed by the Outerpack at smaller rotation angles is if this jeopardized the Outerpack bolts. This issue is addressed in the following section.

Outerpack Hinge/Latch Bolts – The analysis indicates there is little likelihood of the Outerpack latch and hinge top bolts failing during a 9m CG-forward-of-corner drop onto the top end of the package. This is evident from the relatively high predicted factors of safety for these bolts, Tables 2-16 and 2-17.

ID (Figure 32)	FS/Time		
	11° Forward Rotation	18° Forward Rotation	25° Forward Rotation
B917	3.80/0.0143 s	7.57/0.0102 s	5.08/0.0105 s
B921	3.94/0.014 s	6.89/0.0247 s	6.19/0.0102 s
B923	3.10/0.0225 s	2.63/0.0245 s	3.87/0.0245 s
B927	3.28/0.0227 s	2.70/0.0247 s	4.04/0.0262 s
B929	2.61/0.012 s	2.29/0.0112 s	2.36/0.0147 s
B933	2.45/0.0065 s	2.25/0.0112 s	2.38/0.0147 s
B935	2.22/0.0117 s	2.22/0.0072 s	2.22/0.008 s
B939	2.22/0.0117 s	2.22/0.0072 s	2.22/0.0075 s
B941	2.23/0.0032 s	2.23/0.0052 s	2.23/0.0057 s
B945	2.22/0.0057 s	2.23/0.0077 s	2.23/0.0097 s

ID (Figure 33)	FS/Time		
	11° Forward Rotation	18° Forward Rotation	25° Forward Rotation
B947	3.59/0.014 s	6.37/0.0337 s	5.13/0.0105 s
B951	3.73/0.014 s	7.49/0.0232 s	6.17/0.0135 s
B953	2.95/0.0225 s	3.04/0.0245 s	4.19/0.0322 s
B957	3.19/0.0225 s	3.26/0.0245 s	4.30/0.0322 s
B959	2.65/0.0065 s	2.32/0.0115 s	2.34/0.0147 s
B963	2.51/0.0065 s	2.27/0.011 s	2.40/0.0122 s
B965	2.21/0.0062 s	2.21/0.0243 s	2.21/0.0077 s
B969	2.22/0.006 s	2.21/0.0235 s	2.23/0.0072 s
B971	2.20/0.006 s	2.20/0.0095 s	2.20/0.0110 s
B975	2.22/0.0055 s	2.23/0.0072 s	2.23/0.0077 s

It should also be noted that the latch and hinge bolts nearest impact were predicted to have the smallest (although still very adequate) safety factors. This is logical.

Clamshell Keeper Bolts – Our analysis indicates there is little likelihood of the Clamshell keeper bolts failing during a 9m CG-forward-of-corner drop onto the top nozzle end of the package. This is evident from the relatively high predicted factors of safety for these bolts, Table 2-18.

ID (Figure 35)	FS/Time		
	11° Forward Rotation	18° Forward Rotation	25° Forward Rotation
B6271277	5.86/0.0255 s	8.71/0.038 s	10.86/0.0237 s
B6271278	5.75/0.027 s	4.79/0.0285 s	4.43/0.0277 s
B6271279	22.6/0.029 s	8.46/0.0287 s	6.63/0.0237 s
B6271280	17.4/0.0258 s	10.89/0.026 s	3.29/0.0225 s
B6271281	13.38/0.023 s	12.31/0.0522 s	7.96/0.024 s
B6271282	19.48/0.0455 s	8.13/0.0375 s	8.85/0.0282 s
B6271283	16.85/0.0207 s	5.41/0.0332 s	5.78/0.0258 s
B6271284	33.54/0.0285 s	8.89/0.0392 s	7.3/0.0252 s
B6271285	17.56/0.0405 s	11.32/0.0132 s	11.69/0.0197 s
B6271286	14.73/0.016 s	9.67/0.0415 s	8.09/0.024 s

It should be noted that the keeper bolt nearest impact was predicted to have the smallest (although still very adequate) safety factor.

Clamshell Top and Bottom Plate Bolts – The analyses indicate that none of the Clamshell bolts at the top and bottom ends will fail during a 9m CG-forward-of-corner drop onto the top nozzle end of the package. This is evident from the minimum factors of safety shown in Tables 2-19, 2-20 and 2-21. (The modeling of the fuel assembly as a rigid structure likely makes little difference to these predictions since the fuel rods would not be expected to buckle in this drop orientation.)

Table 2-19 Clamshell Bottom Plate bolt Minimum Factors of Safety for 9m CG-Forward-of-Corner Drops			
ID (Figure 37)	FS/Time		
	11° Forward Rotation	18° Forward Rotation	25° Forward Rotation
B6168785	2.36/0.0495 s	2.38/0.0245 s	2.50/0.0197 s
B6168786	8.27/0.0497 s	5.85/0.0243 s	4.48/0.0235 s
B6168787	100.3/0.0262 s	94.5/0.0225 s	60.8/0.0235 s
B6168788	97.8/0.0262 s	112/0.0515 s	89.5/0.0235 s
B6168789	51.1/0.0227 s	27.0/0.0230 s	43.3/0.0437 s
B6168794	40.2/0.0222 s	31.0/0.0317 s	27.7/0.0317 s
B6168793	99.9/0.0262 s	83.3/0.0305 s	59.3/0.0385 s
B6168792	100.7/0.0618 s	86.7/0.0202 s	44.2/0.0402 s
B6168791	11.2/0.0412 s	6.55/0.0202 s	7.69/0.0200 s
B6168790	2.84/0.0412 s	2.43/0.0205 s	2.33/0.0280 s

Table 2-20 Clamshell Grooved Top Plate Bolt Minimum Factors of Safety for 9m CG-Forward-of-Corner Drops			
ID (Figure 38)	FS/Time		
	11° Forward Rotation	18° Forward Rotation	25° Forward Rotation
B6168781	2.33/0.0182 s	2.29/0.0187 s	2.31/0.0197 s
B6168780	3.86/0.0397 s	5.32/0.0200 s	4.32/0.0200 s
B6168779	2.84/0.049 s	6.08/0.0510 s	12.06/0.0217 s
B6168778	2.31/0.039 s	2.34/0.0447 s	2.37/0.0470 s
B6168773	2.25/0.0367 s	2.26/0.0430 s	2.26/0.0410 s
B6168774	2.23/0.0367 s	2.22/0.0427 s	2.22/0.0410 s
B6168775	2.31/0.0387 s	2.30/0.0435 s	2.32/0.0467 s
B6168776	2.91/0.0485 s	5.39/0.0555 s	9.58/0.0465 s
B6168777	7.04/0.0495 s	6.20/0.0467 s	4.84/0.0205 s

ID (Figure 38)	FS/Time		
	11° Forward Rotation	18° Forward Rotation	25° Forward Rotation
B6168770	1.76/0.0165 s	1.81/0.0180 s	1.77/0.0195 s
B6168771	1.79/0.0207 s	1.77/0.0177 s	1.75/0.0197 s
B6168772	1.78/0.0360 s	1.76/0.0477 s	1.80/0.0117 s
B6168765	1.76/0.0350 s	1.76/0.0170 s	1.73/0.0135 s
B6168766	1.77/0.0125 s	1.77/0.0150 s	1.72/0.0125 s
B6168767	1.78/0.0200 s	1.75/0.0150 s	1.72/0.0127 s
B6168768	1.77/0.0362 s	1.76/0.0152 s	1.76/0.0277 s
B6168762	1.76/0.0362 s	1.77/0.0510 s	1.76/0.0187 s
B6168783	1.77/0.0192 s	1.77/0.0155 s	1.77/0.0202 s

Clamshell Top End Plate Joint – The analyses indicate the Clamshell top end plate joint (Figure 2-39) will separate slightly, but not come completely apart during CG-forward-of-corner impacts. In particular, the lip on the top plate is predicted to remain within the groove in the V-shaped top plate along both edges but slip completely out in the middle. This is shown in Figure 2-51 for the CG-forward-of-corner drop rotated 11°. It should be noted that this separation is predicted to be permanent, not transient. It should also be noted that predicted deformations were similar but lesser for CG-forward-of-corner drops rotated 18° and 25°. However, in these latter two orientations, the lip on the top plate is predicted to remain within the groove in the V-shaped top plate along its entire length. **This extent of deformation was not observed in full-scale testing of Traveller XL prototypes and is therefore conservative.**

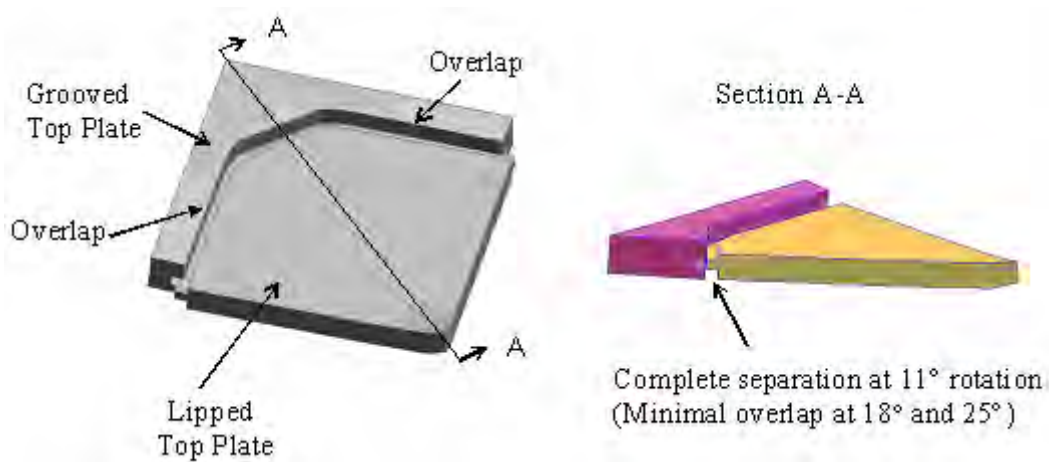


Figure 2-51 Clamshell Top Plate Geometry

Clamshell Bottom End Plate/Door Joints – The analyses indicated the Clamshell bottom end plate is minimally loaded during CG-forward-of-corner drops onto the top end of the shipping package. These trivial loads are not reported herein.

In summary, horizontal side drops onto the Outerpack hinges/latches result in the highest predicted Outerpack loads. Even so, a CG-forward-of-corner drop onto the top nozzle end of the package with 18° forward rotation, Figure 2-48 is predicted most damaging to the Outerpack. This is because the predicted opening of the seam between the upper and lower Outerpack assemblies may compromise the ability of the Traveller XL shipping package to withstand the 30 minute HAC burn test. Drop tests are described in Appendix 2.12.5 and the fire tests are described in Section 3, all of which demonstrate that this is not a serious concern.

2.12.4.2.4 Orientation Predicted Most Damaging to the Fuel Assembly

Determining the drop orientation most damaging to a fuel assembly is greatly facilitated by the geometry of the assembly itself. In particular, the fuel rods within a fuel assembly are very long (4.4 m or more), slender (approx. 9 mm), and relatively flexible. Thus, they are quite susceptible to buckling. For this reason, our hypothesis is that drop orientations which impart the highest axial loads to the assembly are most damaging. Buckling of the fuel rods is also of paramount importance with respect to criticality safety. For criticality safety, fuel rods must not be allowed to buckle in a configuration which results in an unsafe nuclear condition. See Section 6 for a complete description of the criticality safety of the Traveller packages.

Obviously, highest axial loads are generated by vertical or nearly vertical loadings. Near-vertical orientations may impart higher loads to a portion of the fuel rods than the average load applied to a fuel rod in truly vertical drops. However, in these orientations, the adjacent rods or Clamshell structure will provide lateral support. Thus, our focus was entirely on (truly) vertical drops for fuel assembly damage, Figure 2-52. Vertical orientations result in higher impact loads because the larger footprint impacts the ground and therefore the system is stiffer than a high angle orientation where the initial contact is a point which “grows” a footprint.

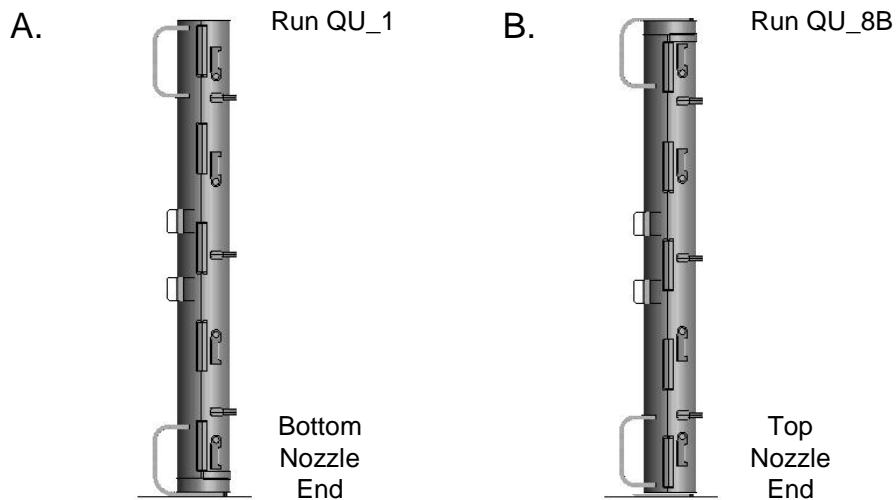


Figure 2-52 Traveller Drop Orientations Analyzed For Maximum Fuel Assembly Damage

The tendency of the fuel rods to buckle proved a severe modeling limitation because post-buckling behavior was simply beyond our current modeling capability. Post-buckling involves one or more buckled fuel rods impacting a nearby rod or Clamshell wall. These collisions involved a large momentum transfer because the fuel rods are so heavy. In our model, the mesh of the walls and nearby rods and was simply not capable of properly absorbing this energy. The result was the analysis aborted almost immediately once any fuel rods buckled. This was due to “negative volumes” (highly distorted solid elements) which resulted from the inability of the Clamshell walls, as meshed, to properly absorb the momentum transferred from the fuel rods. This occurred in all analyses we attempted and often with as much as 30 percent of the drop energy not yet absorbed. The mesh of the surrounding structure was simply not capable of properly absorbing this energy. Successful resolution of this problem would have required significantly finer meshes of both the fuel rods and surrounding structure and perhaps many other changes. From a practical standpoint, this level of analysis is beyond the capabilities of current computer systems. Rather, the fuel rods and associated fuel assembly structure (i.e., the grids), except for the top and bottom nozzles, were converted into a rigid part using the LS-DYNA[®] deformable-to-rigid option. This prevented the fuel rods from buckling and eliminated the associated problems with negative volumes allowing an analysis that absorbed all the available energy.

This approach prevented any associated loading of the structure surrounding the sides of the fuel assembly (the Clamshell walls), forfeiting the ability to predict the maximum loads and stresses on the Clamshell walls and latches in regions adjacent to the fuel rods. Since the fuel nozzles and other structures near the Clamshell top and bottom ends were kept deformable, Clamshell loads and stresses at the ends of the Clamshell were still fairly accurate. Further, the energy not transferred to the Clamshell walls was now forced into other structures – primarily the fuel assembly nozzles (which were kept deformable) and the end impact limiters in the case of axial drops. Thus, our analyses should be non-conservative for Clamshell regions adjacent to the fuel rods, accurate for the Clamshell top and bottom ends, and probably overly conservative for the displacements in the Outerpack impact limiters.

2.12.4.2.5 Vertical Drops

Our analysis determined that a vertical drop onto the bottom end of the package would be more damaging to the fuel assembly than a drop onto the top end. This is because the Clamshell is subjected to larger impact forces and the fuel assembly must withstand larger accelerations.

Energy and Work Histories – Global energy and work for vertical drops onto the top and bottom end of the package are shown in Figures 2-53 and 2-54, respectively. As before, both plots have an initial total energy (TE) of 204 kJ. The total energy rises slightly, reflecting the external work done by the package under gravity loading. Hourglass, sliding, and stonewall energies were small relative to the total energy. This indicates a good overall numerical analysis was obtained in both simulations.

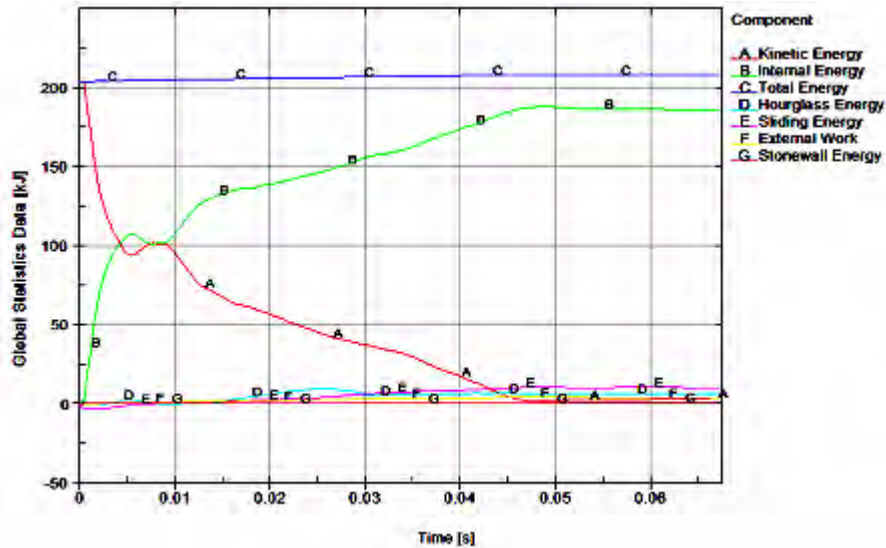


Figure 2-53 Predicted Energy and Work Histories for a 9m Vertical Drop Onto the Top Nozzle End of the Package

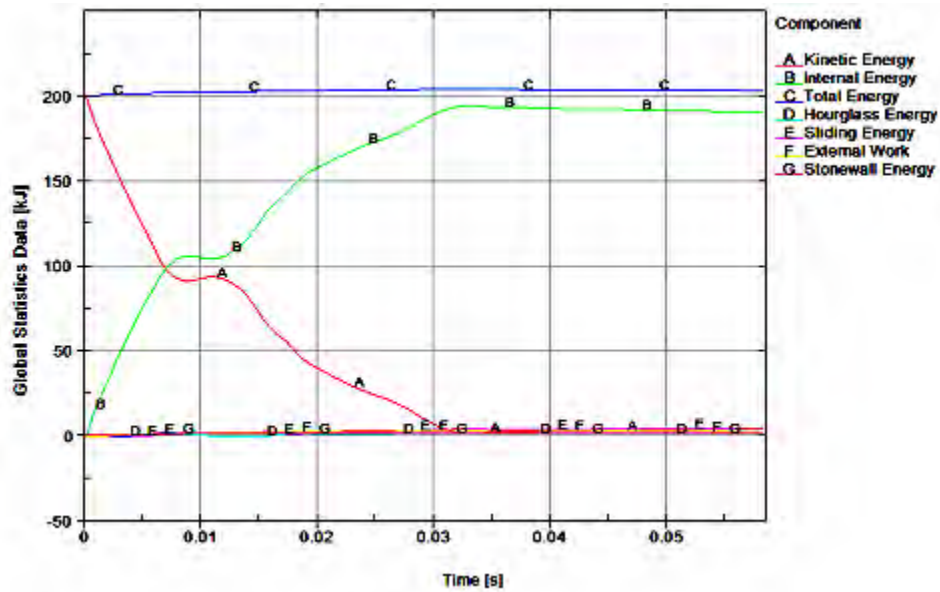


Figure 2-54 Predicted Energy and Work Histories for a 9m Vertical Drop Onto the Bottom Nozzle End of the Package

Rigid Wall Forces – Predicted force histories between the Outerpack and drop pad are shown in Figure 2–49 for top and bottom end vertical drops. The near de-coupling of the Clamshell and Outerpack is clearly evident in both simulations. In the drop onto the bottom end of the package, the initial impact between

Outerpack and drop pad has a 12 milliseconds (approx.) duration. The Clamshell is not involved in this impact as it is still in free-fall (neglecting the small forces of the shock mounts.) At approximately 15 milliseconds into the simulation, the Clamshell contacts the inner surface of the bottom impact limiter and pushes it back into the drop pad. The Clamshell and Outerpack impact further into the drop pad while the fuel assembly is now essentially decoupled from the Clamshell and still in free-fall. As the Outerpack and Clamshell begin to re-bound (at ~25 milliseconds into the simulation) the fuel assembly impacts the Clamshell and all three components (Outerpack, Clamshell and fuel assembly) crash back into the drop pad. The shipping package begins to rebound at approximately 31 milliseconds into the simulation and has left the drop pad after 45 milliseconds. A similar scenario is evident for the vertical drop onto the top nozzle end of the package.

Referring to Figure 2-55, it is noted that the predicted maximum Outerpack load for the top end drop is more than 2X that for the bottom end drop (5.1 versus 2.5 MN, respectively). This shows the higher cushioning capability of the bottom impact limiter design. Further, this indicates that bolts in the Outerpack hinges and latches in the vicinity of impact will be loaded more significantly in a vertical drop onto the top end of the package. Finally, the predicted 5.1 MN load on the Outerpack for a vertical top end drop is still 2-3X less than that predicted for horizontal side drops, Figure 2-29.

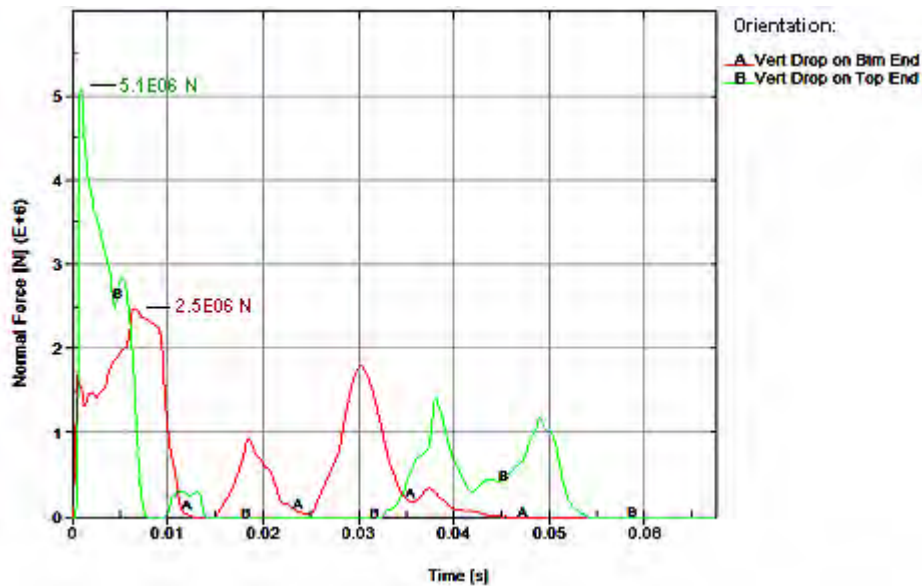


Figure 2-55 Predicted Rigid Wall Histories for 9m Vertical Drops onto the Bottom (QU-1) and Top (QU-8B) Ends of the Package

Clamshell Loads and Accelerations – The force between Clamshell and impact limiter was determined for vertical drops by specifying contacts between the CS top and bottom plates and the innermost impact limiter covers. For drops onto the top end of the package, this required defining contacts between the two CS top plates (the grooved and the lipped plate) and the innermost plate of the top impact limiter and summing

the predicted forces. This technique was only used for vertical drops because these are the only drop orientations in which the Clamshell impacts into only one surface.

Results are shown in Figure 2-56 (for the primary impact only as previously explained.) Note that the force is zero until almost 9 milliseconds into the drop simulation (which starts right before the Outerpack hits the drop pad. This is the time it takes the Clamshell to fall through the approximate 120 mm sway space separating the Clamshell and inner and the top and bottom impact limiters.

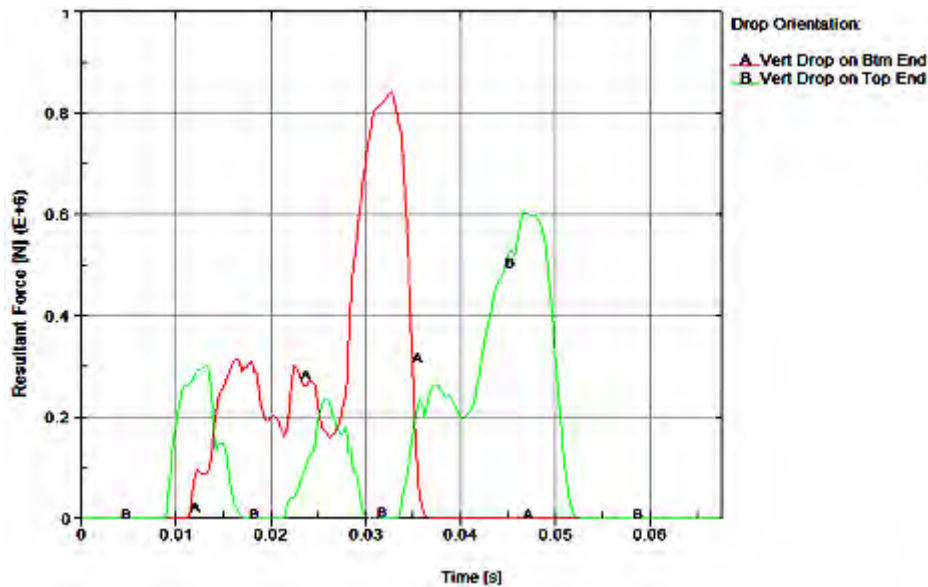


Figure 2-56 Predicted Force Between Clamshell and Impact Limiter for 9m Vertical Drops

Note also in Figure 2-56 that drops onto the bottom end of the package are more severe for the Clamshell than those onto the top end. Indeed, predicted CS loads for vertical drops onto the top and bottom end of the package are, respectively, 605 and 843 kN. These loads resulted in higher accelerations for the fuel assembly (FA) as well. As shown in Figure 2-57, predicted FA accelerations are 102 and 126 g's, respectively, for drops onto the bottom and top ends of the package.

The predicted sequence for a drop onto the bottom nozzle end of the package is shown in Figure 2-58. Impact between the Clamshell and inside covering of the bottom impact limiter occurs at approximately 13 milliseconds into the simulation; the maximum load between CS and bottom impact limiter is predicted to occur at approx. 33 milliseconds; and, the Clamshell is in full rebound by 40 milliseconds. Note the predicted crushing of the bottom nozzle legs shown in Figure 2-58.

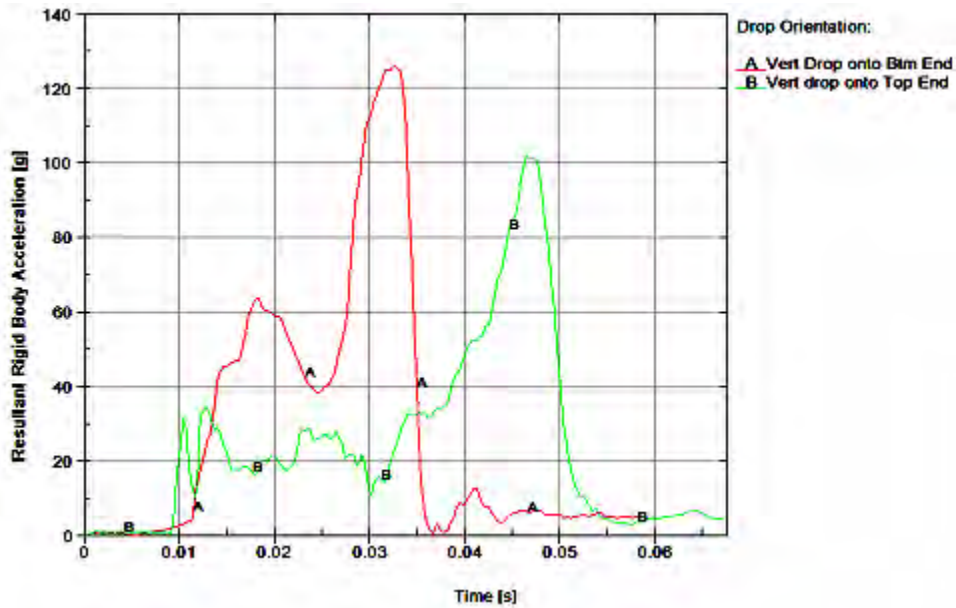


Figure 2-57 Predicted Fuel Assembly Accelerations for 9m Vertical Drops

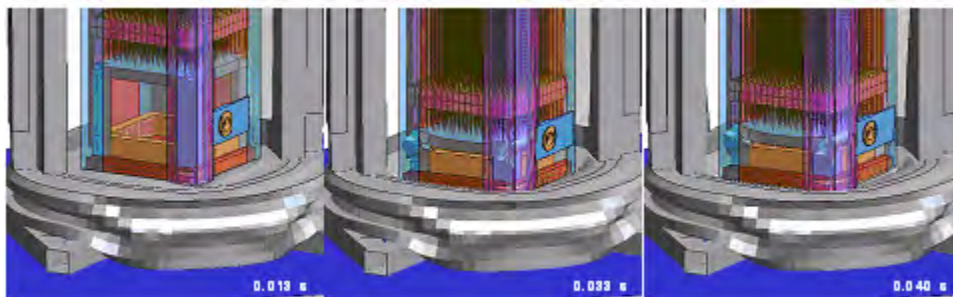


Figure 2-58 Impact Between Clamshell and Bottom Impact Limiter for Vertical Drop onto Bottom End of Package

It is interesting to note the Clamshell and top impact limiter are predicted to collide three times during the primary impact of top end drops. These impacts are depicted in Figures 2-59, 2-60 and 2-61. As shown in Figure 2-59, the first impact involves the Clamshell hitting the top impact limiter from free-fall (at ~9 milliseconds) and the XL pins and top nozzle hold-down posts buckling under the load of the fuel assembly until the top nozzle slides off the hold-down posts (at ~17 milliseconds.) The Clamshell now begins to rebound and leaves the top impact limiter. However, as shown in Figure 2-60, the fuel assembly

continues its downward motion and the top nozzle contacts the midsection of the hold-down posts at about 21.5 milliseconds. At approximately 30.5 milliseconds, Figure 2-60, the hold-down posts are predicted to break near their connection to the cross member connecting them. Then, the fuel assembly pushes the Clamshell back into the top impact limiter. This momentarily removes the fuel assembly loading from the Clamshell and it no longer is pushed into the Outerpack. However, the FA continues falling and the top nozzle begins pushing into the cross member at approximately 33.5 milliseconds. The FA continues its downward fall until motion is arrested at approximately 53 milliseconds, Figure 2-61.

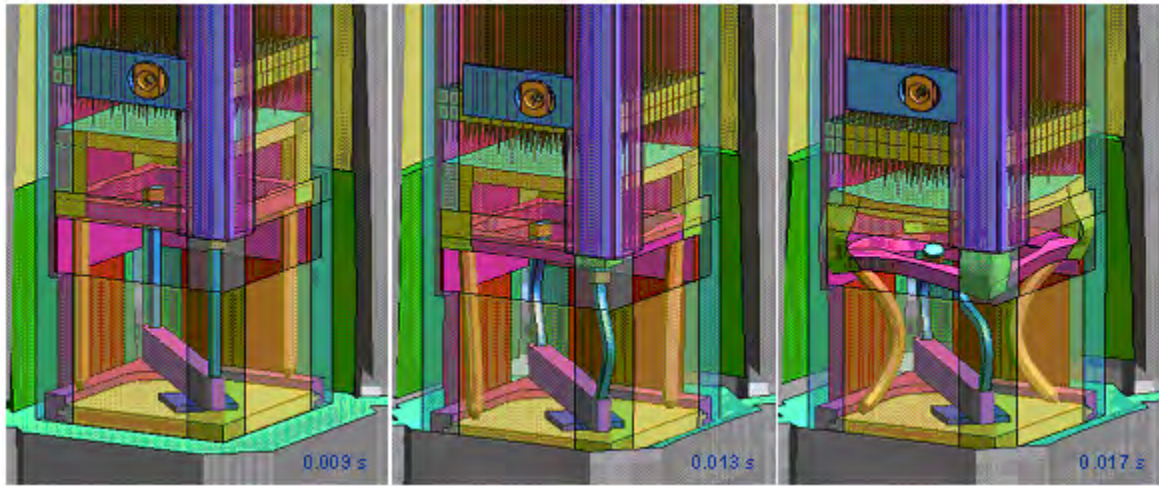


Figure 2-59 First Impact Between Clamshell and Top Impact Limiter for Vertical Drop onto Top End of Package

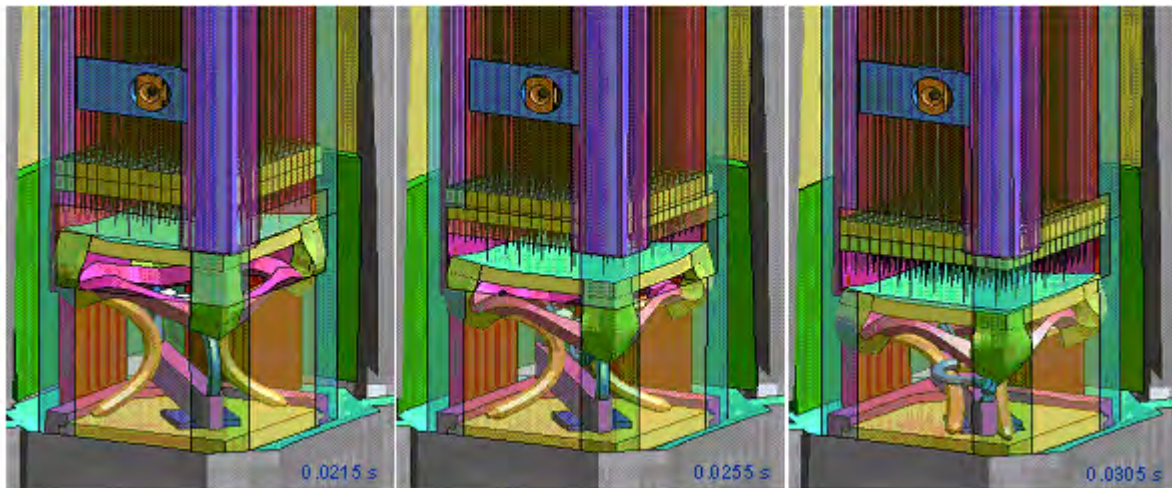


Figure 2-60 Second Impact Between Clamshell and Top Impact Limiter for Vertical Drop onto Top End of Package

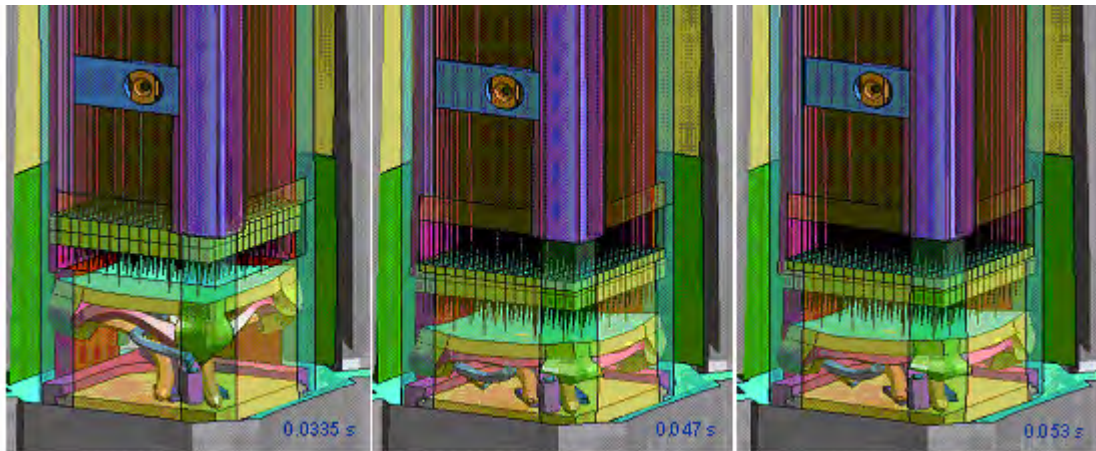


Figure 2-61 Third Impact Between Clamshell and Top Impact Limiter for Vertical Drop onto Top End of Package

From the results shown in this section, we conclude that a CG-forward-of-corner drop onto the top nozzle end of the package with an 18° forward rotation, Figures 2-44 and 2-45 is most damaging to the Outerpack. Further, as also shown, we conclude that the drop most damaging to a fuel assembly is a vertical one onto the bottom nozzle end of the package, Figure 2-52A. Thus, successful drop tests in these two orientations are an adequate demonstration that the Traveller XL design meets/exceeds the HAC drop test requirements.

2.12.4.2.6 Temperature and Foam Density Effects

The Traveller XL package must be capable of passing the HAC drop tests at any temperature within the range -40 to 160°F. Furthermore, foam crush strength is also directly related to foam density. The drop orientation previously determined most damaging to the Outerpack was selected to study the effect of temperature and density (the 9 meter CG-forward-of-corner drops onto the TN end of package with an 18° forward rotation, Figure 2-44). Our finding is that a Traveller XL package with nominal foam density and at “normal temperature” (75°F) experiences slightly higher Outerpack loads when dropped in this orientation compared with packages containing low density foam and dropped at 160°F or containing high density foam and dropped at -40°F, see Figure 2-62. In particular, the predicted maximum Outerpack load for the 75°F temperature/nominal density scenario is 1.69 MN. This is 8.5% more than the maximum load predicted for the -40°F/high density scenario and 13.7% more than that for the 160°F/low density scenario. Our analyses also indicates fuel assemblies in packages containing the highest allowable density foam and dropped at the lowest temperature extreme will experience accelerations that are very similar to those in packages with lowest allowable density foam and dropped at the highest temperature extreme, see Figure 2-63. However, the accelerations at these extremes are only 5% greater than for a package dropped at 75°F containing nominal density foam. Thus, temperature and foam density have a minor effect on drop performance of the Traveller XL package.

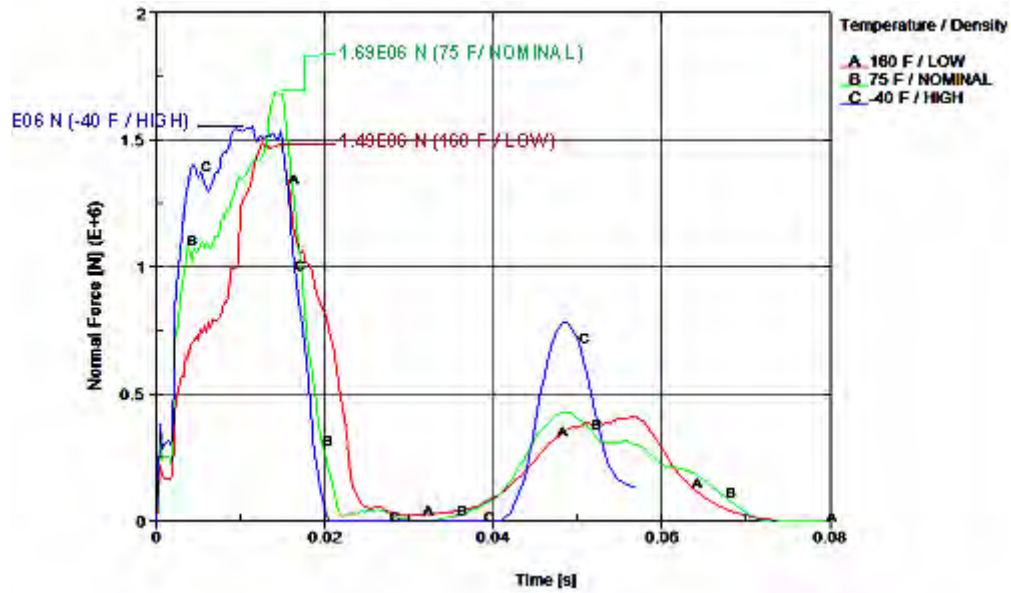


Figure 2-62 Predicted Temperature and Foam Density Effect on Outerpack/Drop Pad Interface Forces (9m CG-Forward-of-Corner with 18° Rotation Drop onto the Top End of the Package)

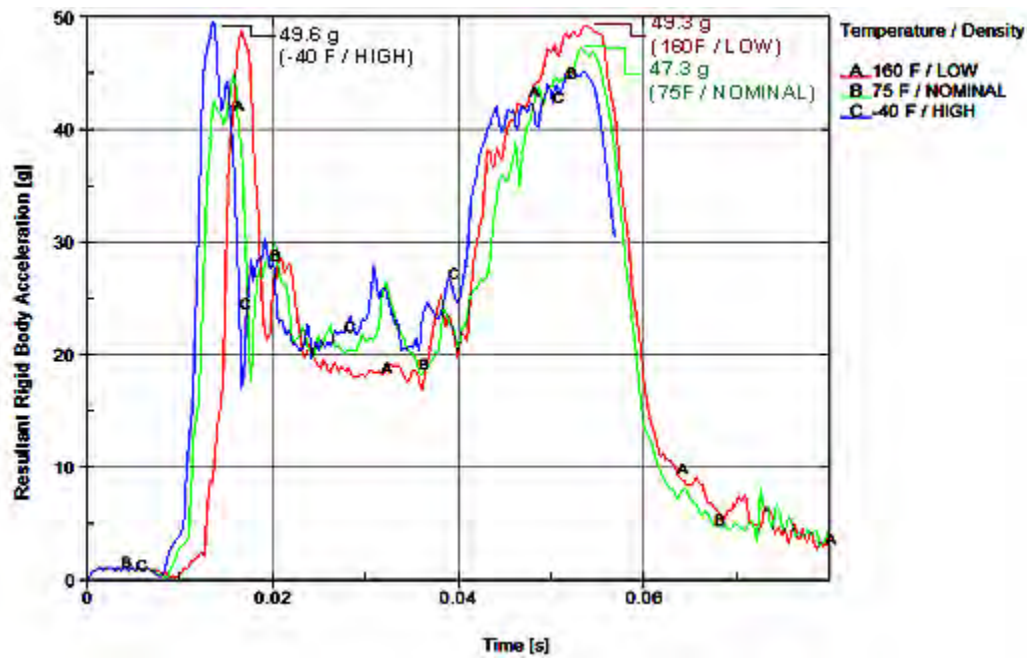


Figure 2-63 Predicted Temperature and Foam Density Effect on Outerpack/Drop Pad Accelerations (9m CG-Forward-of-Corner with 18° Rotation Drop onto the Top End of the Package)

In addition, the 9 meter vertical bottom-end down drop was analyzed using material properties for -40°C (-40°F) with foam density at the upper end of the tolerance band and 71°C (160°F) with foam density at the lower end of the tolerance band. The predicted results were compared with each other and with those at 24°C (75°F) and nominal foam density previously reported in Section 2.12.3.2.5. The results support the conclusions obtained from analysis of the 9 meter CG-forward-of-corner drops: temperature and variation in foam density due to manufacturing tolerances have only a minor effect on the drop performance of the Traveller package.

Temperature/foam tolerance effects for the 9 meter vertical drop onto the bottom nozzle end of the package were evaluated for the three previously noted conditions. Both predicted outerpack/drop pad force histories and fuel assembly accelerations were compared as shown in Figures 2-63A and 2-63B.

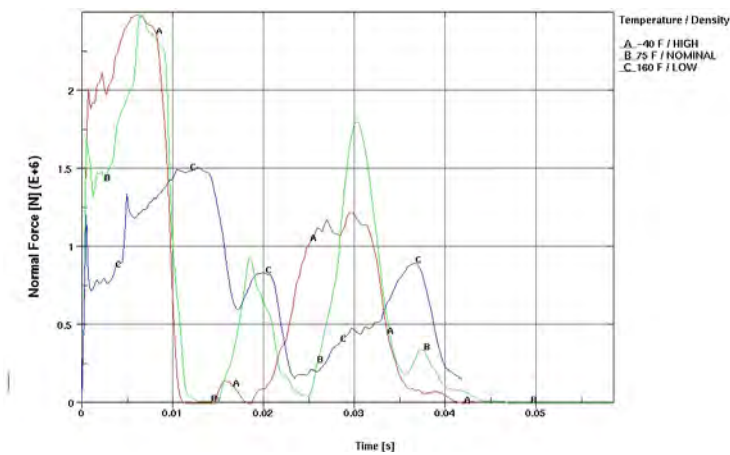


Figure 2-63A Predicted Temperature and Foam Density Effect on Outerpack/Drop Pad Interface Forces (9m Vertical Drop onto the Bottom End of the Package)

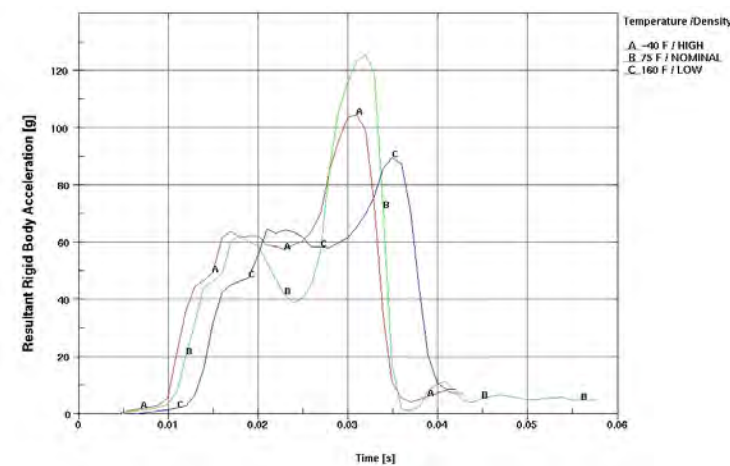


Figure 2-63B Predicted Temperature and Foam Density Effect on Fuel Assembly Acceleration (9m Vertical Drop onto the Bottom End of the Package)

Both of these figures predict that the highest forces occur when the package is 24°C (75°F) with the package having nominal foam density. (This does not necessarily mean that a package dropped at 24°C/75°F having foam densities at either the high or low end of the tolerance band would have had lower outerpack/drop pad forces and lower FA accelerations since that was not investigated.) In particular, the predicted maximum outerpack load for the 75°F (24°C)/nominal foam density scenario was 2.5E6 N. This was equal to that predicted for -40°C (-40°F) with foam density at the upper end of the tolerance band and about 67% greater than the 1.5E6 N load predicted for 71°C (160°F) with foam density at the lower end of the tolerance band. Moreover, a maximum FA acceleration of 126 g's was predicted for drops at 24°C (75°F) with the package having nominal foam density. This was approximately 20% higher than the 105 g's predicted for the -40°C (-40°F) with foam density at the upper end of the tolerance band scenario and approximately 40% higher than the 90.1 g's predicted for 71°C (160°F) with foam density at the lower end of the tolerance band case.

Energy and Work Histories – The predicted global energy and work histories for the package at 75°F containing nominal density foam was previously shown in Figure 2-29 (18° rotation.) This information is repeated in Figure 2-64 along with the corresponding results for a package dropped at 160°F with low density foam and at -40°F and high density foam. Although not discernable from these graphs, the initial total energies were slightly different for the three runs. In particular, the initial energy for the 160°F/low foam density run was 202 kJ, 204 kJ for the 75°F/nominal foam density run, and 205 kJ for the -40°F/high foam density run. These slight differences were obviously a result of the slight differences in predicted weight. Hourglass, sliding, and stonewall energies were small relative to the total energy. This indicates good overall numerical analyses.

2.12.4.2.7 Pin Puncture

In addition to the 9m drops, the package must survive a “pin puncture” test. The pin puncture test involves dropping the shipping package onto a flat-headed (15 cm diameter with 6 mm chamfer all around) steel pin from a 1 m height. The orientation of the package and location of pin impact must be chosen to achieve the greatest damage to the package.

The pin damage investigation consisted of two approaches. First, the pin drop was analyzed, based on maximum impact forces imparted to the Outerpack. Then, the cumulative damage that a pin drop could cause following a 9 m drop was studied. The latter study was naturally based on the 9 m drop predicted to cause the most Outerpack damage.

Maximum Loads – Our analysis indicates the shipping package will be subjected to the higher loads when dropped in a horizontal orientation, Figure 2-65A, compared to an inclined one Figure 2-65B. For example, when the package is tilted 20° (with the top nozzle end of the package towards the ground), our analysis predicts the maximum impact load is 561 kN. This is 10% less than the 624 kN load predicted for a fully horizontal drop Figure 2-66.

This page intentionally left blank.

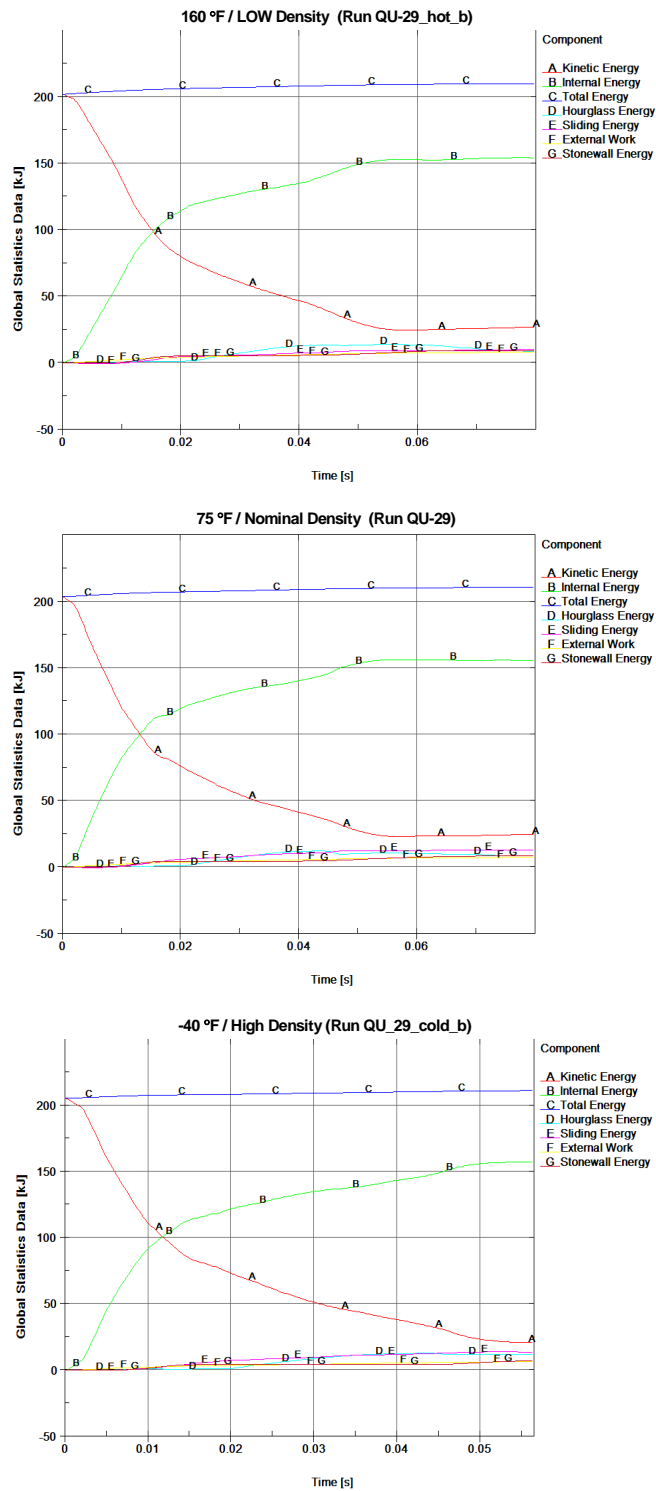


Figure 2-64 Predicted Energy and Work Histories at Various Temperatures



Figure 2-65 Pin Drop Orientation

A comparison of predicted fuel assembly accelerations is shown in Figure 2-67. Note the fuel assembly is predicted to experience approximately 9% higher accelerations in a fully horizontal pin drop than one inclined at 20 degrees.

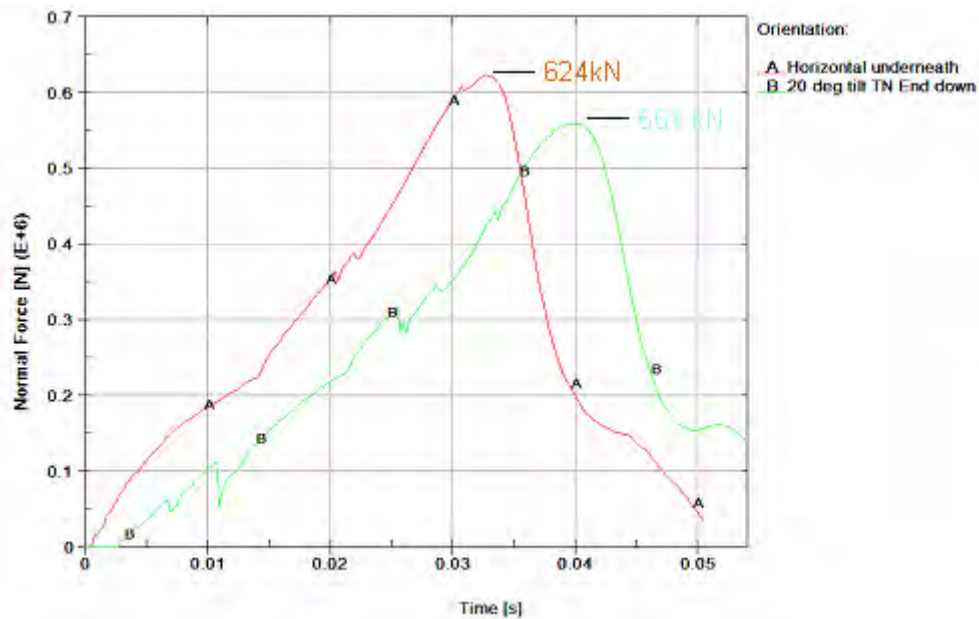


Figure 2-66 Predicted Outerpack/Pin Interference Forces (1m Drop onto 15mm Diameter Steel Pin)

Thus, a fully horizontal pin puncture drop produces higher Outerpack loads and fuel assembly accelerations than inclined pin puncture drops.

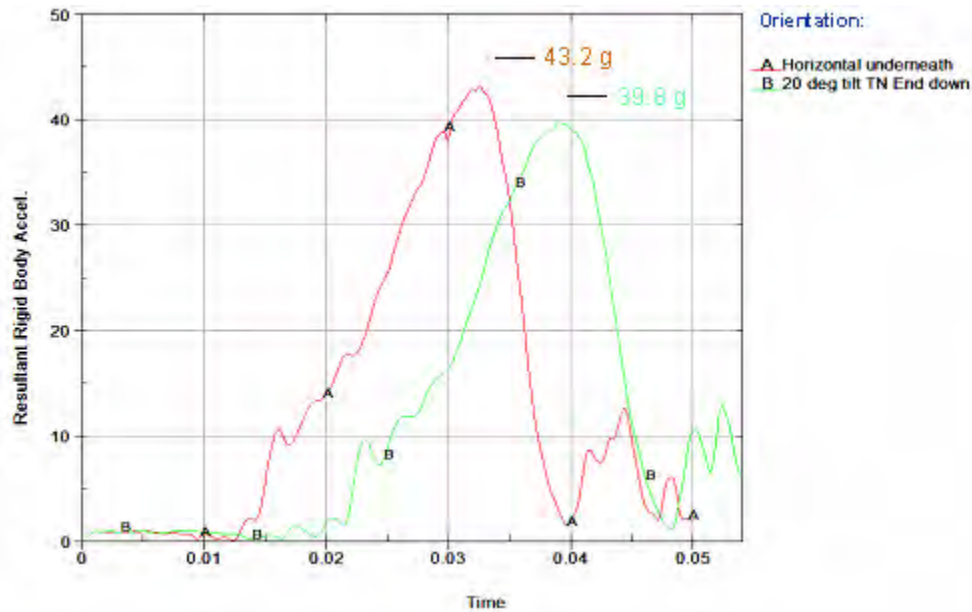


Figure 2-67 Predicted Fuel Assembly Accelerations (1m Drop onto 15mm Diameter Steel Pin)

Worst Horizontal Pin Drop – Two axial rotations were compared when studying the horizontal pin puncture drops. These were the previously described orientation in which the pin impacts the shipping package from underneath, Figure 2-65A, and one where the pin impacts the Outerpack hinges, Figure 2-68. In both cases, the pin was positioned directly under the package CG.

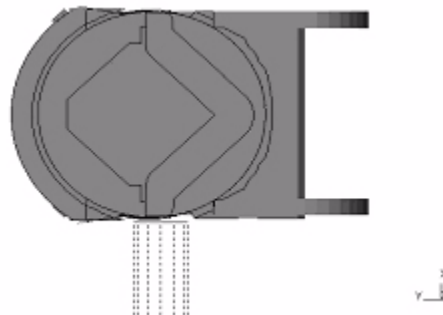


Figure 2-68 Pin Drop onto Outerpack Hinges

Interestingly, predicted Outerpack loads were practically the same for a horizontal pin puncture to the underneath side of the Outerpack and a pin impact directly to a hinge, Figure 2-69. However, there was less cushioning for the fuel assembly in the latter drop. This is evident from the predicted fuel assembly accelerations of 43.2 g’s for the impact to the underneath region of the Outerpack and 82.1 g’s for the hinge impact, Figure 2-70.

In fact, all of these pin puncture orientations were tested using full-scale Traveller XL units. In all cases, the pin puncture tests were passed without any puncturing of the outer skins of the units, nor any detrimental effects to the Clamshell/fuel assembly, or criticality safety aspects of the package.

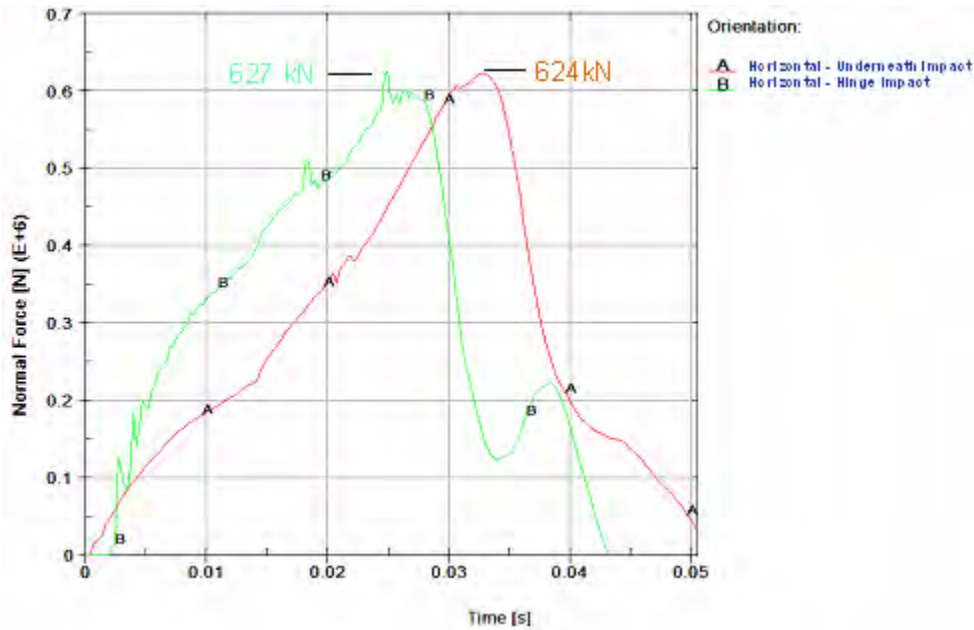


Figure 2-69 Predicted Outerpack/Pin Interface Forces (1m Drop onto 15mm Diameter Steel Pin)

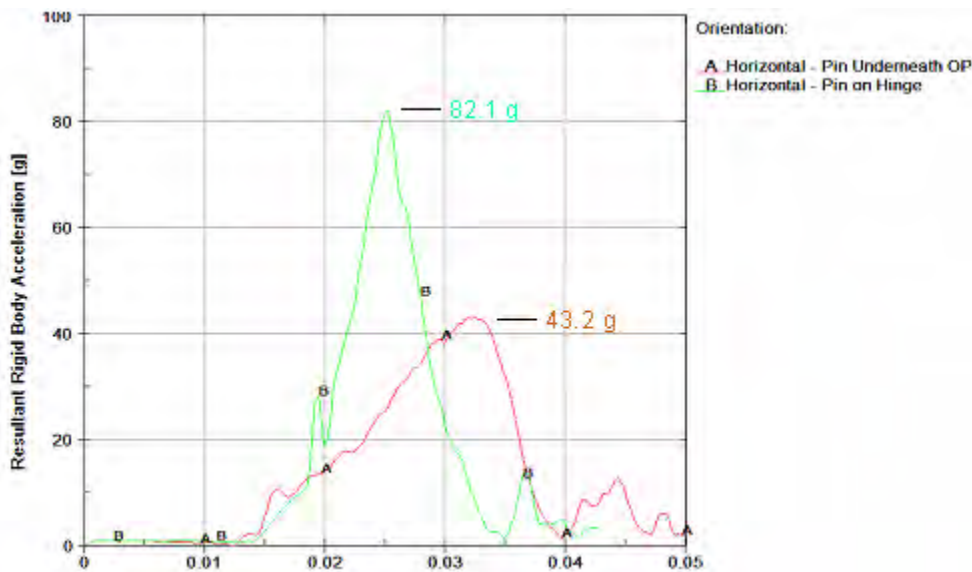


Figure 2-70 Predicted Fuel Assembly Accelerations (1m Drop onto 15mm Diameter Steel Pin)

Energy and Work Histories – Global energy and work for the 1 m pin puncture drops discussed above are shown in Figures 2-71, 2-72 and 2-73. These plots have an initial total energy (TE) of 22.3 kJ. This value correctly reflects the initial velocity (v) of 4.43 m/s applied to the 2,270 kg package mass (m) since our pin puncture simulations are initiated at the end of Outerpack free fall from 1 m; the total energy is comprised only of kinetic energy (KE), and $KE = \frac{1}{2}mv^2$. Total energy rises about 8% in these drop simulations. This reflects the work done by the package under gravity loading, i.e., the bending of the shipping package around the pin. Depending on drop orientation, the event was completed within 4 to 5 milliseconds as seen by the flattening of the kinetic energy and internal energies after that time. Moreover, acceptable levels of hourglass, sliding, and stonewall energies were obtained. This indicates a good overall numerical analysis was obtained in each simulation.

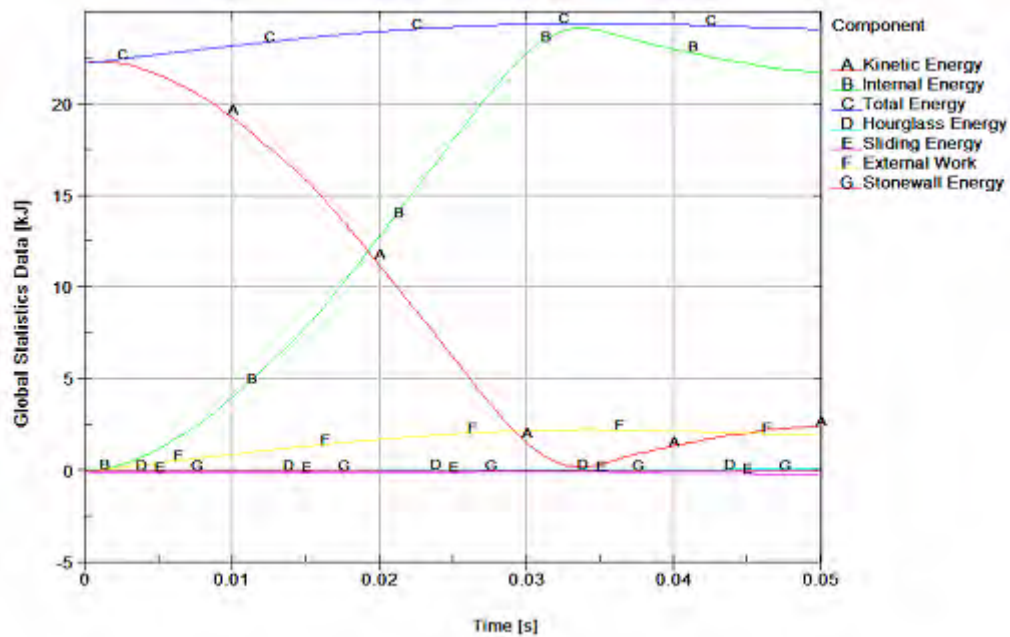


Figure 2-71 Predicted Energy and Work Histories for a 1 m Horizontal Pin Drop (Pin Underneath the Package CG)

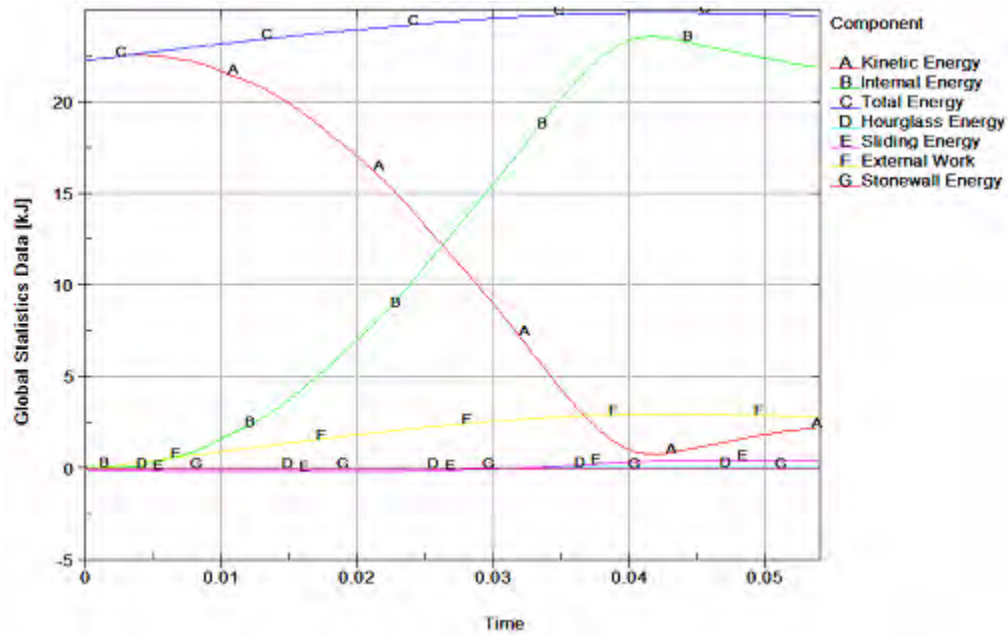


Figure 2-72 Predicted Energy and Work Histories for a 1 m Tilted Pin Drop (20° Tilt With TN End Down)

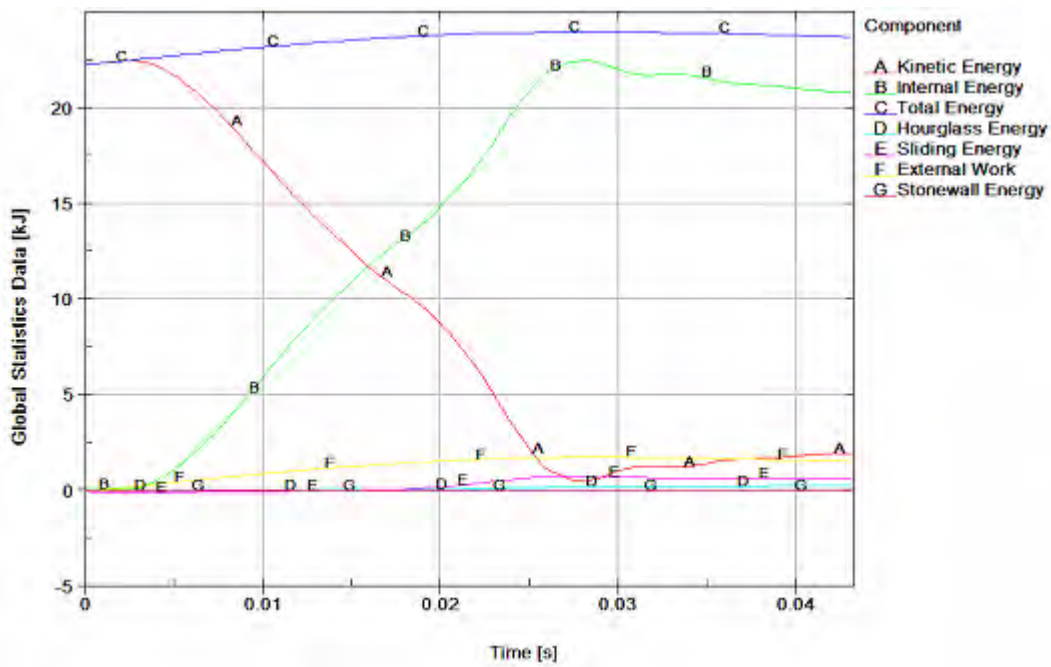


Figure 2-73 Predicted Energy and Work Histories for a 1 m Horizontal Pin Drop (Pin Hitting Hinge at Package CG)

Maximum Pin Indentation – Predicted maximum pin indentation for the horizontal underneath, inclined, Figure 2-65 and hinge pin puncture drops Figures 2-68 were, 67, 54 and 50 mm, respectively. This is shown in Figure 2-74.

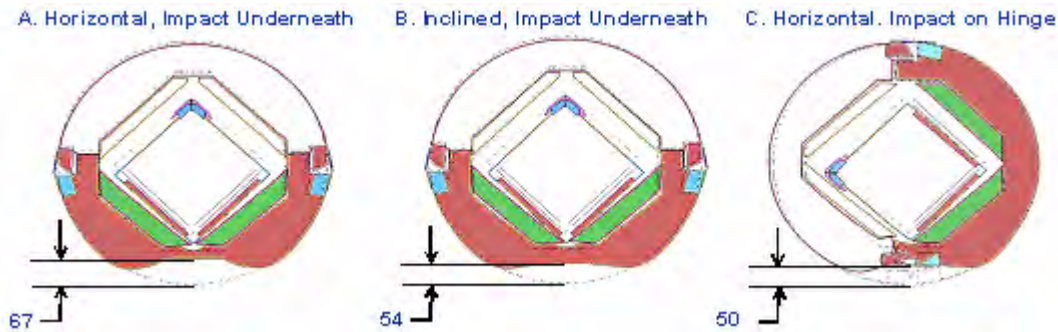


Figure 2-74 Comparison of Predicted Maximum Pin Indentations

Outer Steel Skin Damage – Predicted maximum plastic strains in the steel skin were only 12.6 and 15.7% for the horizontal and 20° tilted pin puncture simulations Figures 2-65A and 2-65B, respectively. These values are much less than the allowable 46.7% failure strain. Thus, it is unlikely the steel skin will be ruptured by the pin puncture test. Initial testing of the Traveller XL Prototype units were demonstrated that 11 gage (0.120" nominal thickness, 3.0 mm) 304 stainless steel had little difficulty passing the pin puncture tests. Those full-scale tests, in addition to the analytic work discussed previously, allowed designers the confidence to reduce the thickness of the Outerpack shells to 12 gage material (0.105" nominal thickness, 2.7 mm). Therefore, the QTU and CTU packages were all fabricated using 12 gage sheet material of the outer shells. Pin drop tests of QTU-1, QTU-2 and CTU packages confirmed that 12 gage material survived the pin puncture tests without failure.

Cumulative Damage – As previously stated, analysis of cumulative pin damage was based on the 9 m drop predicted to cause the most Outerpack damage. Indeed, this analysis placed the pin 1 m under, and normal to, the region of the top impact limiter which was (previously) predicted to flatten during the 9 meter CG-forward-of-corner drop onto the TN end of package with an 18° forward rotation Figures 2-64 and 2-25. The position of the pin was at the apex of the top impact limiter Figure 2-67. This location was chosen since it would most exacerbate the opening of the Outerpack seam predicted from the 9 m drop analysis.

Deformations, strains, and stresses from the previous 9 m analysis were used as the initial starting point for the cumulative pin puncture drop analysis. Inclusion of deformations was accomplished by use of the LSTC/LSPOST¹ capability to output deformations at the appropriate time (state) in LS-DYNA keyword format. The corresponding strains and stresses from the 9m analysis were written to a file (in LS-DYNA keyword format) via the LS-DYNA *INTERFACE_SPRINGBACK_DYNA3D command. A new master 1 m pin puncture analysis keyword file was created that defined all parts, materials, nodes (with deformed

1. LSPOST is the pre- and postprocessor by LSTC provided with LS-DYNA.

positions), element connectivity, loading, etc. Stresses and strains were then brought into the analysis by use of the LS-DYNA *INCLUDE and *STRESS_INITIALIZATION commands.

Maximum Loads – The Westinghouse analysis indicates the shipping package is subjected to higher loads when dropped on a previously damaged end than in any other orientation analyzed, including a drop onto a hinge. Indeed the maximum predicted Outerpack load was 734 kN for the 2nd hit Figure 2-75. This is 17% higher than the 627 kN predicted for a drop onto the Outerpack hinge Figure 2-69. The greater load is attributed to the lower cushioning available due to the foam in being highly compressed during the 9m drop. Even so, the maximum predicted fuel assembly acceleration was just 38.2 g's Figure 2-76.

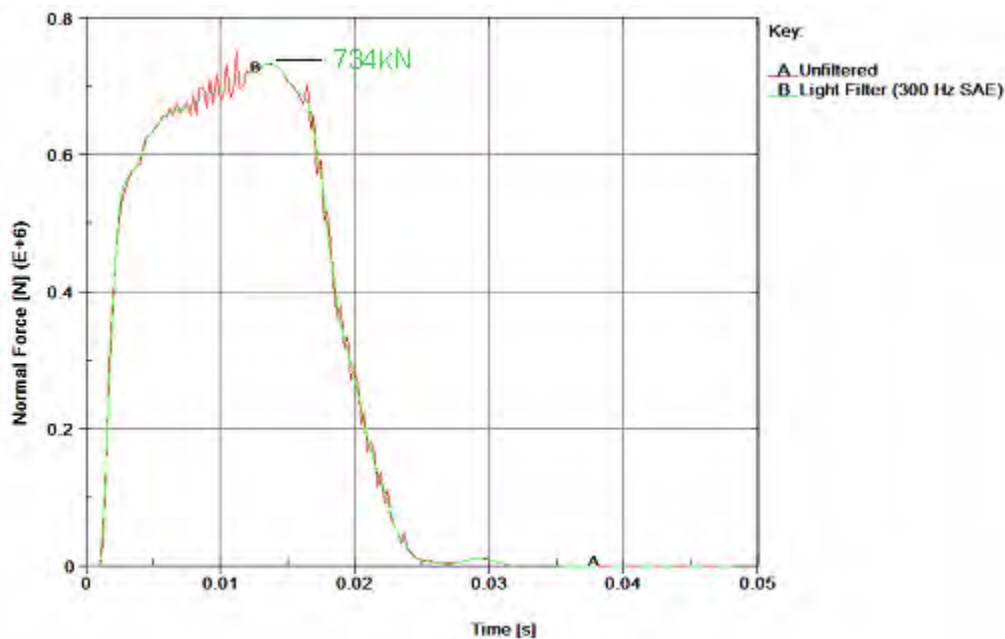


Figure 2-75 Predicted Outerpack/Pin Interface Forces (1 m Drop onto 15 mm Diameter Steel Pin After 9m Drop)

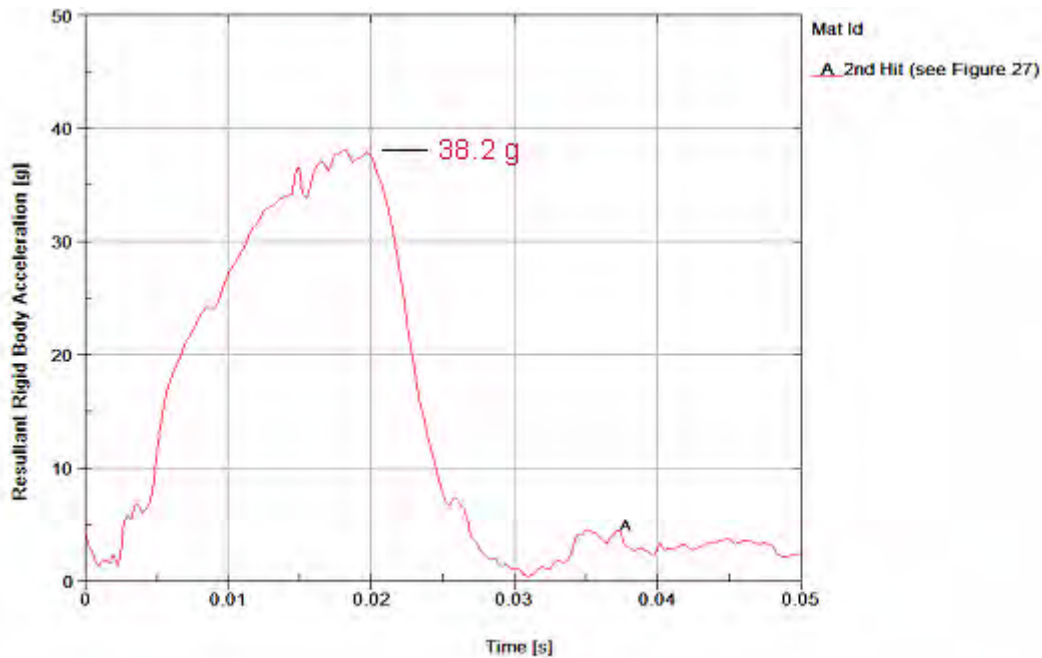


Figure 2-76 Predicted Fuel Assembly Accelerations (1 m Drop onto 15mm Diameter Steel Pin after 9 m Drop)

Additional Damage – As previously discussed, our primary concern for this sequence of drops (a 9 m CG-forward-of-corner drop onto the top nozzle end of the package followed by the 1 m pin puncture) was the extent of Outerpack seam opening Figure 2-28. Our measures of Outerpack seam opening, D1 and D2 (see Figure 2-48), would increase from 20 to 22.9 mm and from 20 to 22.2 mm, respectively.

Energy and Work Histories – Predicted global energy and work for the 1 m pin puncture drop following a 9 m CG-forward-of-corner drop onto the top nozzle end of the package is shown in Figure 2-77. The sliding energy in this plot is related to the initial penetration between the crushed impact limiter foam and outer steel skins. It is not necessarily an error. Moreover, the predicted increase in damage due to the pin puncture test simply does not warrant further investigation of this issue.

Pin Puncture Summary – Our analyses indicate the Traveller XL package is very capable of withstanding the 1 m pin puncture test. Indeed, it was determined that the likelihood of rupturing the outer steel skin is very low. Thus, the 1 m pin puncture test is a relatively benign test for the Traveller XL package. These conclusions were confirmed by the prototype test results as subsequently discussed.

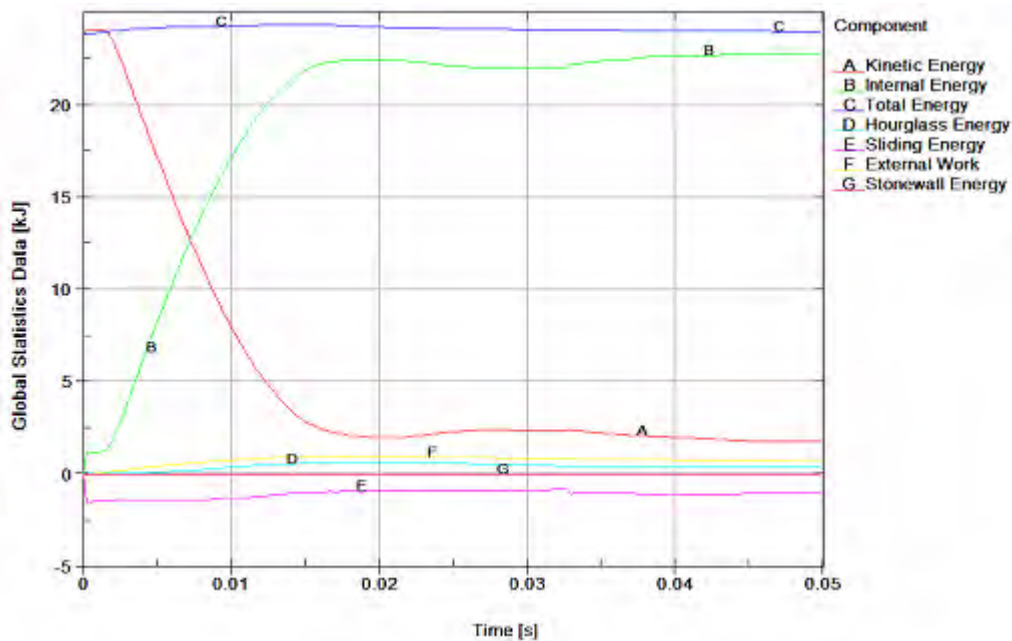


Figure 2-77 Predicted Energy and Work Histories (1 m Drop onto 15 mm Diameter Steel Pin after 9 m Drop)

2.12.4.3 Comparison of Test Results and Predictions

Two prototype Traveller XL packages were drop tested on January 28 and 29, 2003. Details of these tests are provided in Appendix 2.12.5, Traveller Drop Test Results.

Results from the extensive prototype tests in January, 2003 were reviewed to find the best ones for comparison with FEA predictions. Comparison cases were chosen to include tests with prototype units which did not have extensive previous test damage, those which represented a unique test configuration (i.e., the pin puncture) and those in which accelerometer data was obtained. The four selected cases are identified in Table 2-22 and Figure 2-78.

There was good overall agreement between predicted and actual drop performance of the prototype Traveller XL package. This is evident by comparisons of predicted and actual permanent deformations, failed parts and measured and predicted accelerations at specific positions on the Outerpack and Clamshell.

Test ID (corresponds to [6])	Analysis ID	Drop Height [m]	\dot{E}_x	\dot{E}_z	Comment
1.1, 9 m Low Angle	C1-25	9.1	14.5°	180°	T/N primary impact on OP top
1.2, 9 m CG-over-corner	C1-31	9.1	-71°	90°	B/N primary impact on OP hinge
2.2, 1 m Pin-puncture	Punc2-2nh	1.04	20°	135°	CG (Axial) on OP topside, T/N end down
2.3, 9 m CG-over-corner	C1-29	9.1	108°	0°	T/N primary impact on OP top

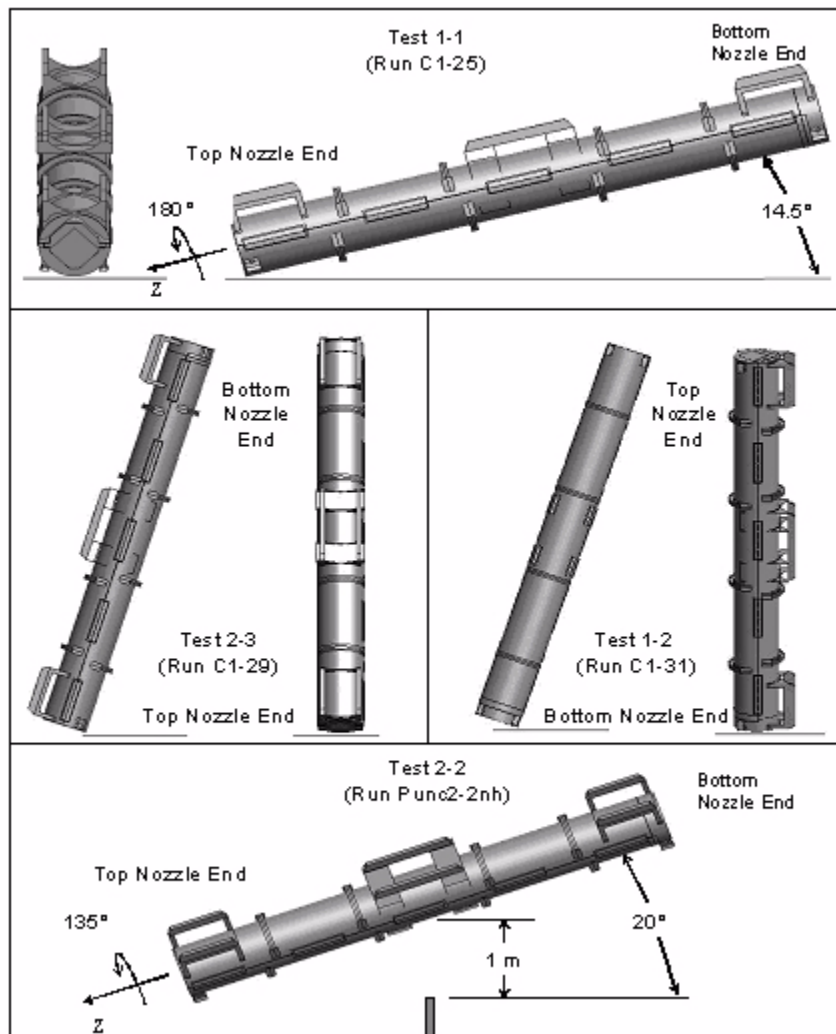


Figure 2-78 Prototype Drop Tests Used To Benchmark Analysis

2.12.4.3.1 Prototype Unit-1 Test 1.1

Prototype Unit-1, Test 1.1 was chosen for the first comparison. As indicated in Table 2-22 and Figure 2-78, this was an inclined drop from 9.1 meters onto the upper Outerpack (the unit was rotated 175° about its long axis and inclined 14.5° with the end of the package nearest the top of the fuel assembly hitting first.¹ Four frames taken from a video recording of test 1.1 are shown in Figure 2-79. These frames show the test sequence was comprised of the initial impact on the top nozzle end of the package (frame 1), rollover (frames 2 and 3), and a secondary impact to the bottom nozzle end of the package (frame 4).



Figure 2-79 Prototype Unit 1 Drop Test

Deformations – As reported in, test 1.1 produced noticeable permanent deformations in several locations of the Outerpack and no significant permanent deformations in the Clamshell. Outerpack permanent deformations were primarily at the ends of the package.

1. This will be referred to as the “top nozzle end” of the package. Likewise, the end of the package nearest the bottom of the fuel assembly will be called the “bottom nozzle end.”

An overall sense of the correspondence between predicted and actual Outerpack permanent deformations may be obtained by reviewing Figures 2-80 through 2-87. Quantitative comparison between predicted and documented measurements is given in Table 2-23.

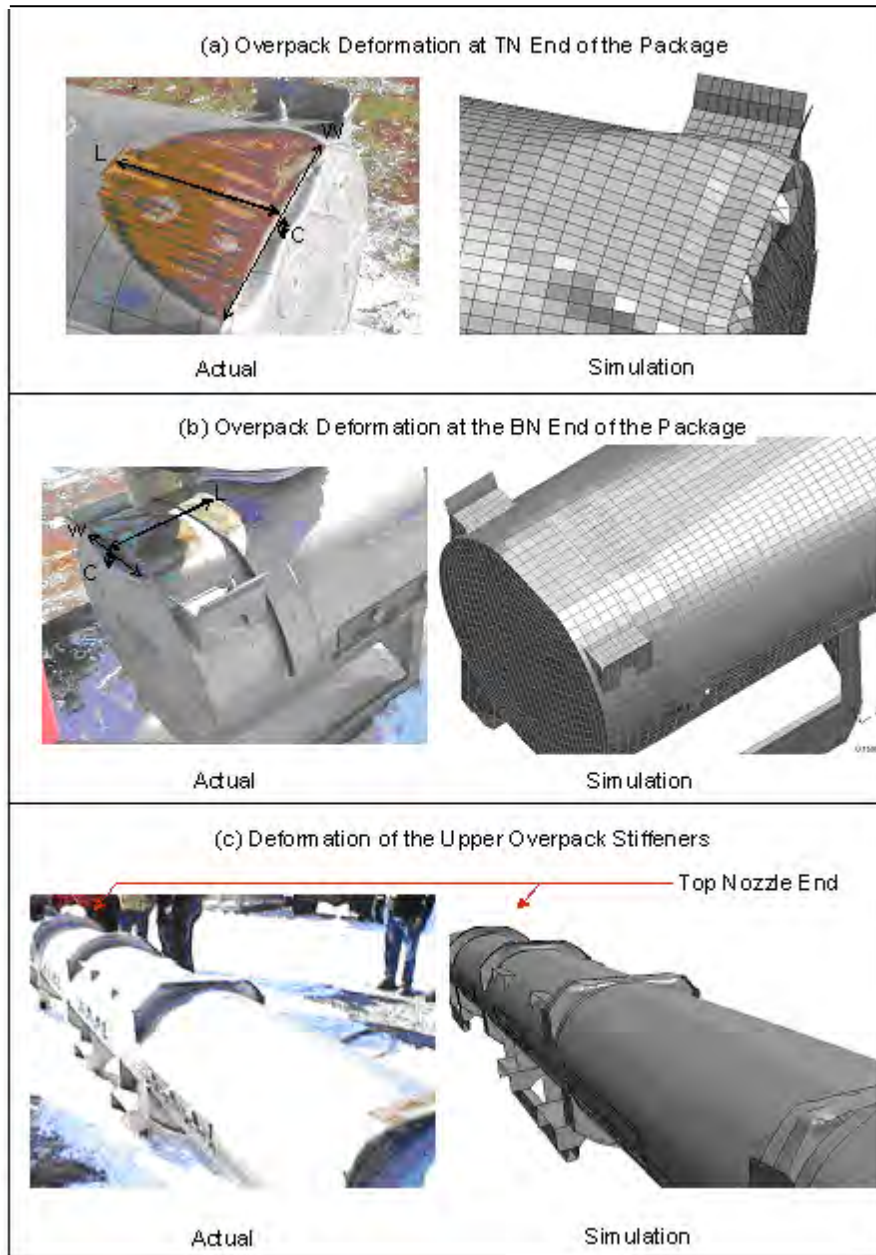


Figure 2-80 Comparison of Test 1.1 with Analytical Results

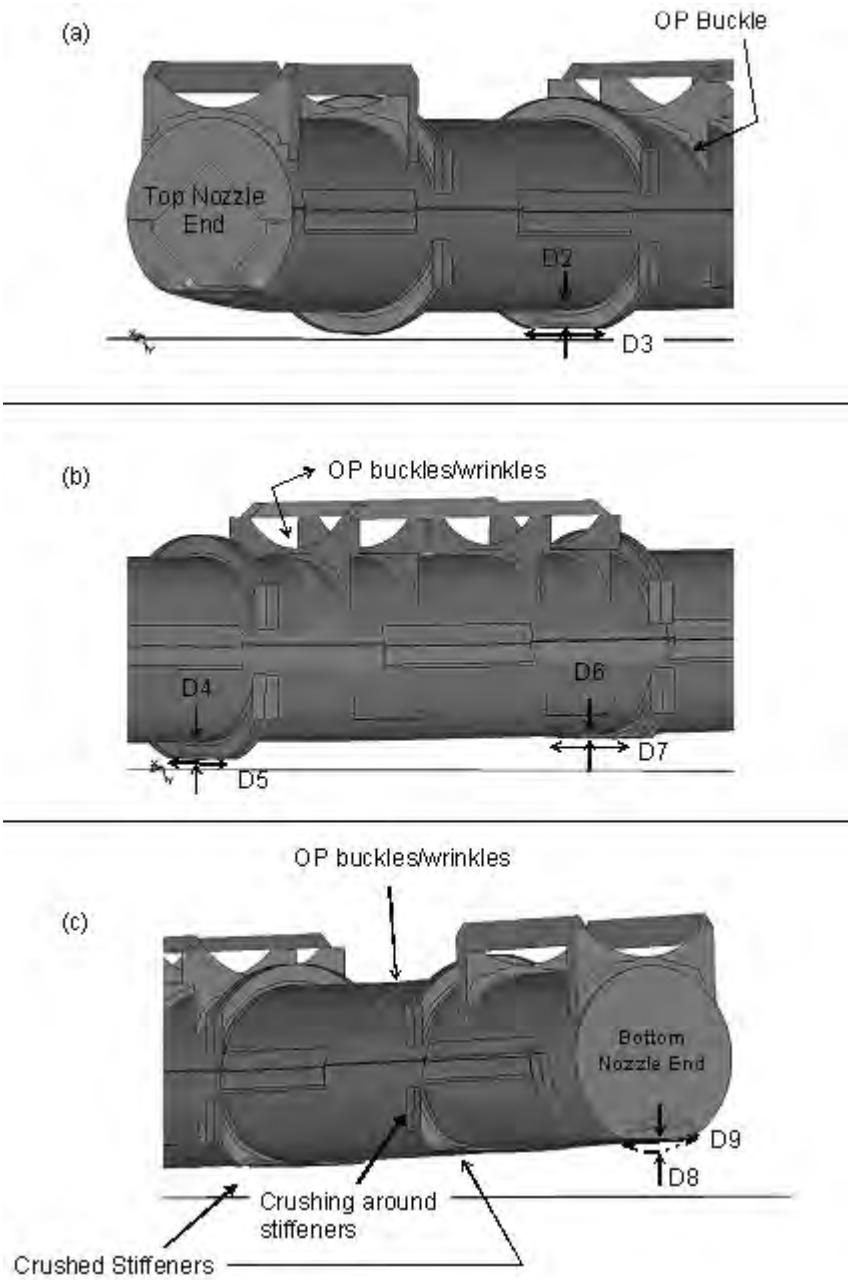


Figure 2-81 Comparison of Test 1.1 with Analytical Results

Item	Location	Measured (Reference 6)		Predicted		Nodes used to make Prediction		Difference	Conservative
		(in)	(mm)	(in)	(mm)				
1	Top nozzle end								
	Dim L in Figure 2-80	9.0	229	11.9	302	192658	134223	32.2%	Yes
	Dim W in Figure 2-80	12.0	305	14.6	371	134052	134170	21.7%	Yes
	Dim C in Figure 2-80	1.5	38	1.65	42	134062	223918	10.0%	Yes
2	Bottom nozzle end								
	Dim W in Figure 2-80	11.5	292	11.9	302	214342	190946	3.5%	Yes
	Dim L in Figure 2-80	10.57	268	13.0	330	94120	213639	23.0%	Yes
	Dim C in Figure 2-80	0.75	19	1.5	38	93833	214433	100.0%	No
3	Upper Overpack Stiffeners								
	Dim D2 in Figure 2-81	0.8	19	0.7	17	115715	115853	-10.7%	Yes
	Dim D3 in Figure 2-81	N/A		11.9	303	115702	116484	-	
	Dim D4 in Figure 2-81	2.4	60	2.2	56	112621	112759	-6.4%	No
	Dim D5 in Figure 2-81	N/A			-			-	
	Dim D6 in Figure 2-81	N/A		1.0	26	109526	110131	-	
	Dim D7 in Figure 2-81	16.0	406	18.4	468			15.1%	Yes
	Dim D8 in Figure 2-81	N/A			-			-	
	Dim D9 in Figure 2-81	23	584	22.6	574			-1.7%	No
Average Difference:								22.4%	

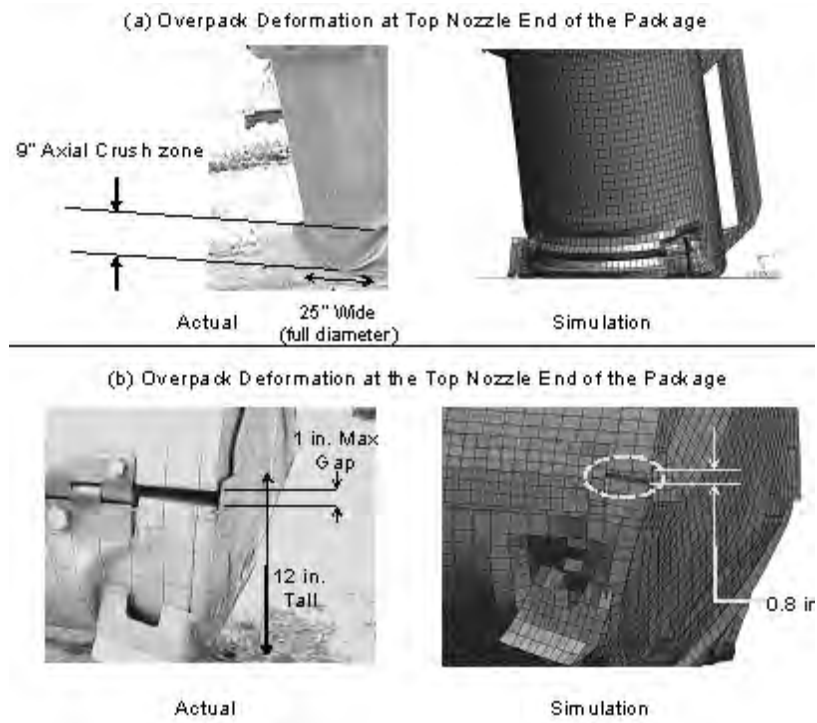
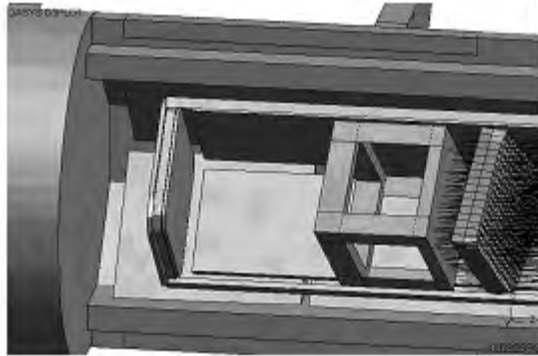


Figure 2-82 Deformations at End of Package

(a) FA Displacement at Bottom Nozzle End of the Package



Actual

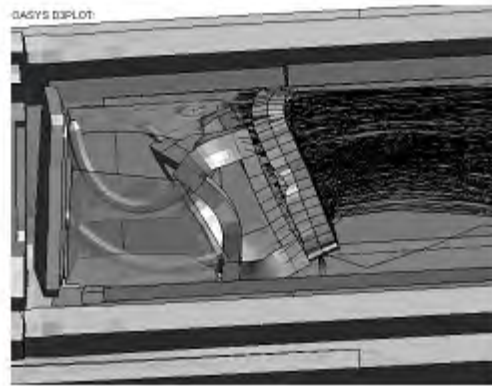


Simulation

(b) Deformation at the Top Nozzle End of the Package



Actual



Simulation

Figure 2-83 Internal Deformations at Inside Outerpack



Figure 2-84 Outerpack Deformations at Bottom Nozzle End of Package

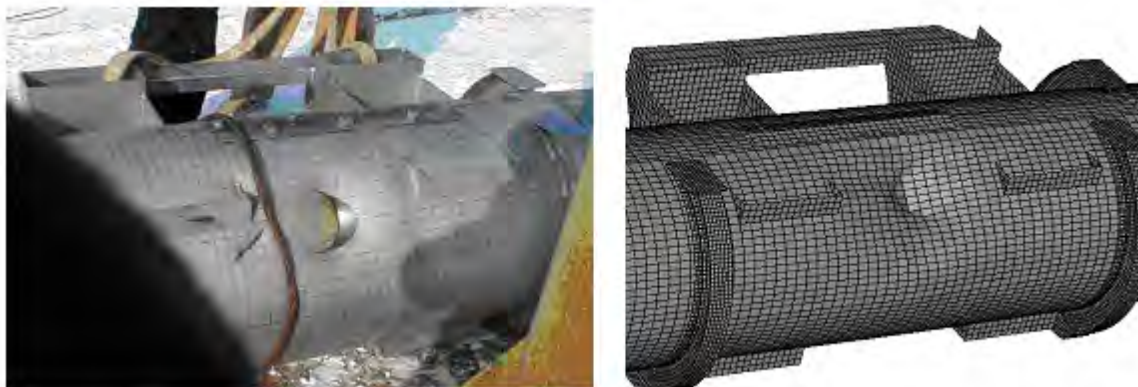


Figure 2-85 Pin Puncture Deformations

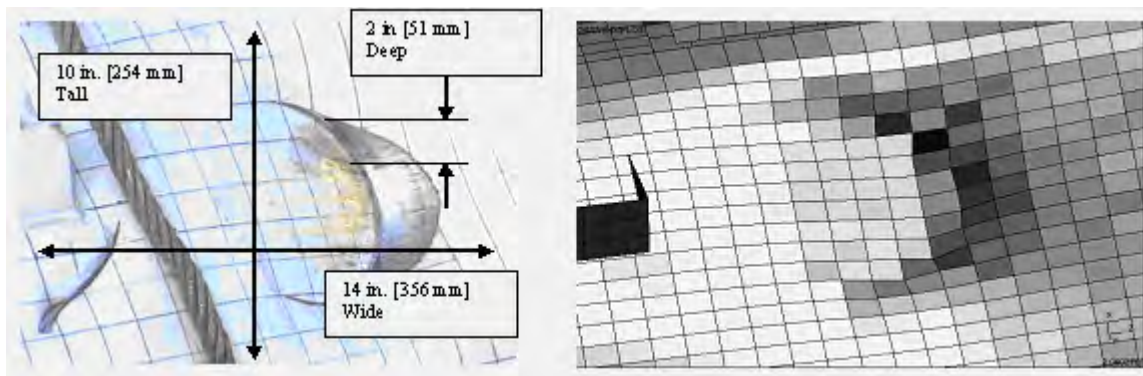


Figure 2-86 Dimensions of Pin Puncture Deformations

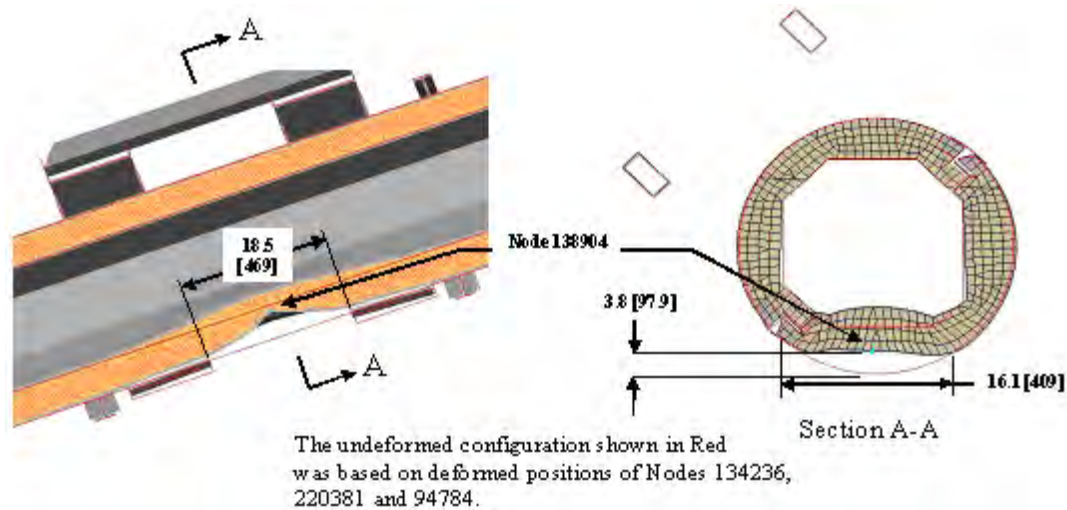


Figure 2-87 Outerpak Predicted Deformations of Pin Drop

2.12.4.3.2 Accelerations

Vertical accelerations (Y-direction) measured during test 1.1 are compared with the FE-based predictions in Figures 2-88 through 2-92. Agreement was good. Indeed, discrepancies between the two could easily be attributed to the inherent error associated with obtaining such data.

For the Outerpak, both measured and predicted traces contained two peaks, Figure 2-88. These corresponded to the two impacts associated with this test as illustrated in Figure 2-78. (Note: the larger acceleration with the secondary impact should not be interpreted as meaning larger forces were associated with the second impact. Rather, the larger magnitude simply reflects that the accelerometer was much nearer the secondary impact end.) While there were two visible peaks, the measured response was very small for the primary impact. For the secondary impact, the predicted acceleration was 1270 g's. This was in accordance with the measured peak acceleration which indicated accelerations were greater than 950 g's.

For unknown reasons, the accelerometers on both the Clamshell top and bottom plates gave erroneous readings late into the drop. This is clearly evident from accelerometer data in Appendix 2.12.5 that the accelerometers “saturate” for over 0.025 seconds and provide no meaningful response afterwards. Thus, only the first 0.05 seconds of the Clamshell data was compared in this report. For the accelerometer on the Clamshell top plate, measured and predicted accelerations corresponding to the first impact (at time 0.01 seconds in Figure 2-90) were 555 g's. This was also in accordance with measurements which indicated a peak acceleration greater than 525 g's was experienced. As shown in Figure 2-91, peak accelerations of 205 g's were measured on the Clamshell bottom plate. The corresponding predicted acceleration is also shown. Note the peak predicted acceleration was 155 g's.

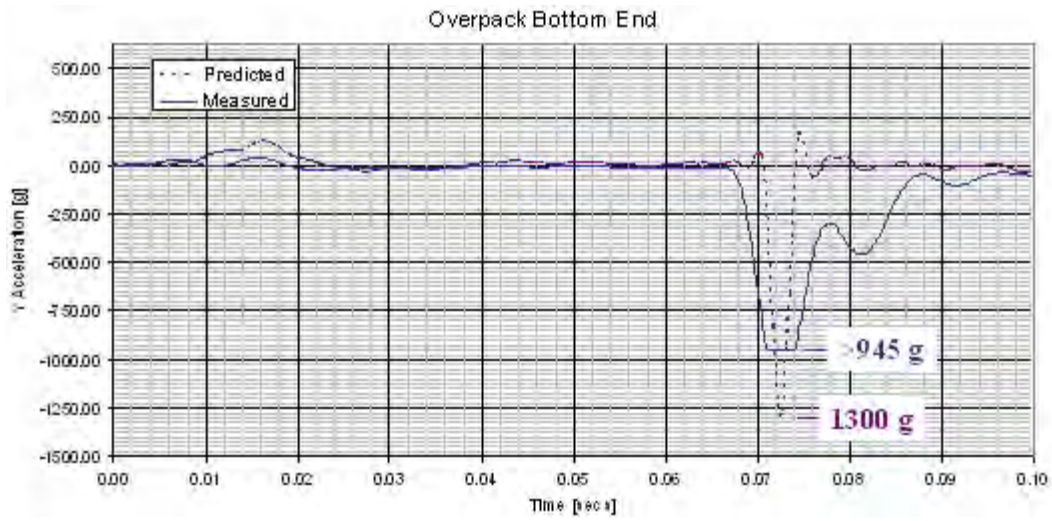


Figure 2-88 Predicted and Measured Y Accelerations

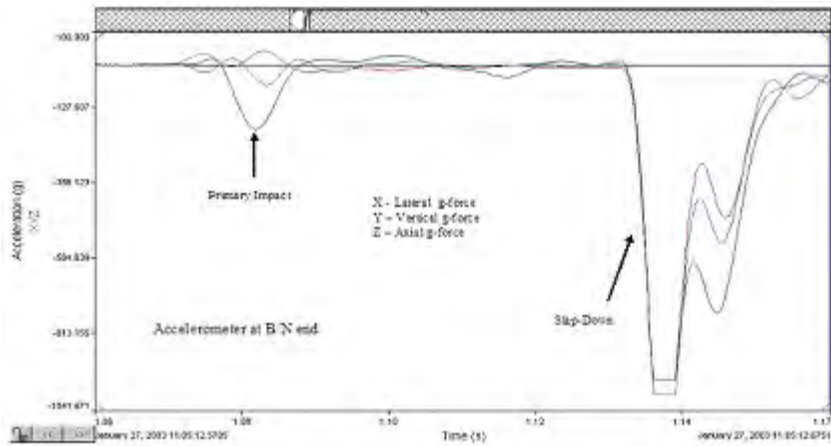


Figure 2-89 Three Axis Measured Accelerations

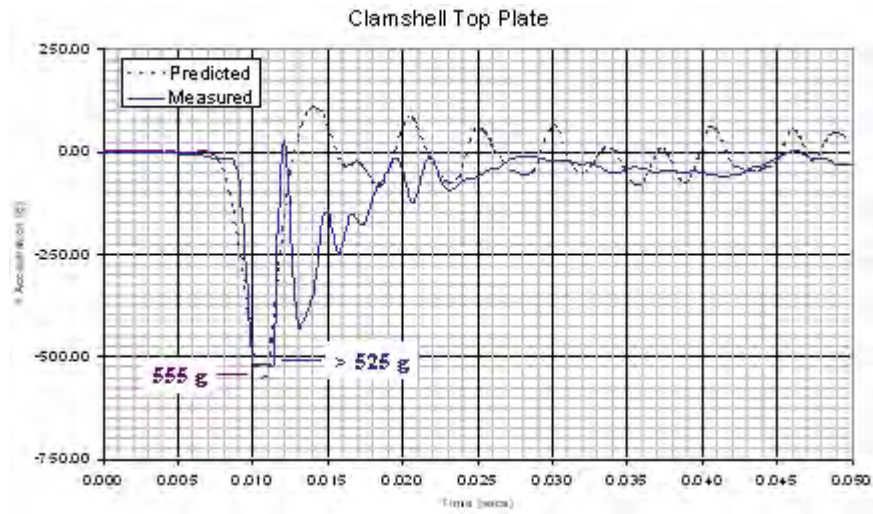


Figure 2-90 Predicted and Measured Y Accelerations

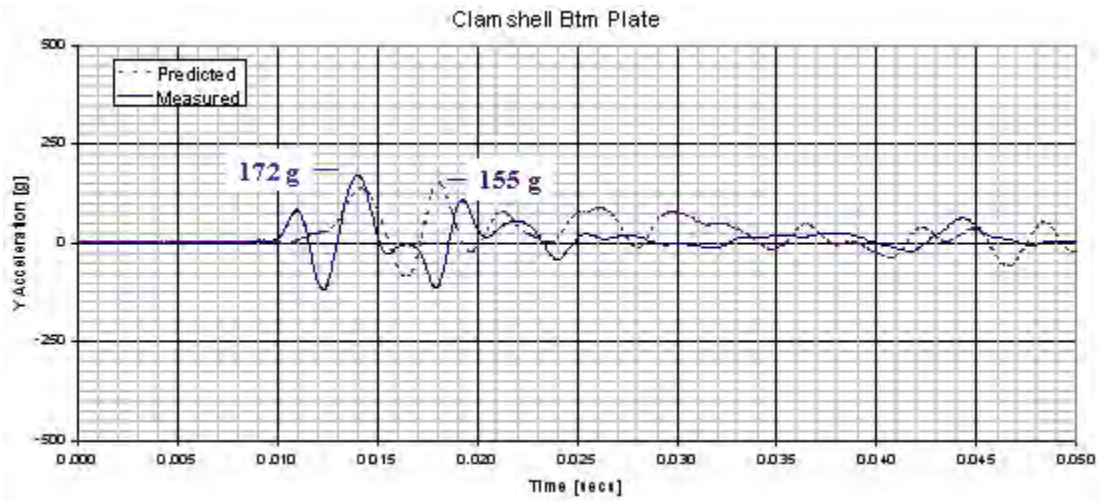


Figure 2-91 Predicted and Measured Y Accelerations

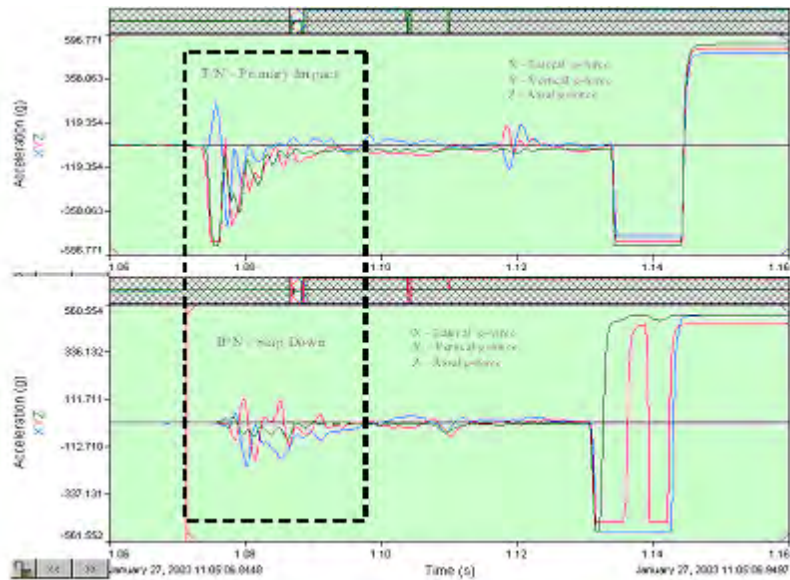


Figure 2-92 Measured Primary and Secondary Accelerations

2.12.4.4 Discussion of Major Assumptions

The many assumptions used to develop the LS-DYNA non-linear finite element stress code, including those needed to model the materials and impact, were found valid for simulating drop tests of the Traveller XL package. It is clearly evident from comparisons between prototype test results and predictions that the key physical phenomena governing shipping container impacts is captured within the LS-DYNA code.

The only major additional assumption was that bowing of the fuel assembly did not result in excessive additional loading of the Clamshell side walls, hinges and latches. Test results showed this was a valid assumption.

LS-DYNA 960 build no. 1647 (single precision, MPP) was used in these calculations because it has the very needed “no put-back” contact capability. However, the official quality tested and assured version is currently DYNA 960 build no. 1106 (single precision, MPP) which does not have the no put-back contact capability. ARUP is expecting to officially release LS-DYNA 970 (probably build no. 3858) in late October, 2004. This version, which does have the no put-back capability, must be installed and tested on the claxgen computers. Then a Traveller XL drop test case must be run to verify results in this calculation note correspond with results from the quality-assured version of LS-DYNA.

2.12.4.5 Calculations

2.12.4.5.1 Method Discussion

The finite element method was used to determine the loads, displacements, accelerations, strains, etc. of a Traveller XL shipping package containing an XL fuel assembly when dropped on a flat surface from 9 m and onto a 15 mm diameter pin from 1 m. The LS-DYNA explicit finite element code was used. This software was selected because it allowed the analysis to include the effects of large deformation, large strain, material non-linearity, contact, and failure of connections between parts and assemblies.

The goal of the analysis was to predict the deformation and damage that the Traveller XL shipping package and contained fuel will experience when subjected to the HAC impact tests. Although it would have been more conservative, it was not feasible to build a model which allowed failure of all joints and any deformation pattern. Such a model would have been unduly complex and calculation intensive and have required extraordinary development time. Rather, the Traveller XL prototype and qualification unit finite element models were constructed with consideration of all probable relative displacements, contact and failures. The premise in choosing this deliberately restrictive approach was that it would not affect accuracy because it would include provisions for the actual deformation and damage. Test results substantiated the accuracy of the prototype unit model, see Appendix 2.12.5.

The models described herein were primarily developed to aid in determining the drop orientations and number of drops needed to meet the HAC requirements. Thus, any point on the Outerpack outer periphery was a potential impact point and there was no one point in which a finer mesh could be afforded. Thus, the actual strains and stresses determined in the model can not be considered refined. Rather, the relative deformations, decelerations and energy absorption between drop orientations should be considered. This limitation applies to both models of the prototype unit and the qualification unit.

Model Descriptions – A basic description of the Traveller XL prototype and qualification units is discussed in section 1 above. All design details are available in and. Details of the finite element models are described in the following two sections.

In both models, units were tonnes (mass), millimeters (length), seconds (times) and Newtons (force).

2.12.4.5.2 Prototype Models

The Prototype models, Units 1 and 2, were constructed from many input files, Figure 2-94. These files defined various details of the model and were included with, or without, transformations of coordinates and renumbering of identities as the model was assembled.

The main file, Apr6.key, contains the control cards, specifies outputs, contact definitions, and many attributes common to more than one subassembly. The major subassemblies were the Outerpack, Clamshell, and fuel assembly. These were defined in the OP.key, CS.key, and XL_FAR.key files, respectively. These subassemblies are detailed in Figures 2-95 through 2-97. A total of 363,646 elements were used in the model (199128 shells, 150717 solids and 13801 beams).

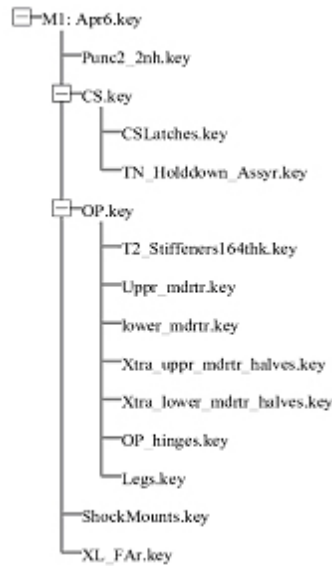


Figure 2-93 FEA Model Input Files

The orientation for each run was defined in individual load case files. Obviously, only one load case file and one material file was invoked per run.

The Clamshell Figure 2-96 is mounted to the Outerpack, Figure 2-94 with 22 rubber shock mounts. These shock mounts were modeled as discrete elements (springs). The stiffness of these elements was 92.7 N/mm in the global X direction, 135.4 N/mm in the global Y direction and 42.3 N/mm in the global Z direction. These values were obtained through tests. These details are included in the 'ShockMounts.key' file.

Predicted model weight for the Prototype units was 2.39 tonnes (5258 lbs). This matched the Prototype unit's 5065 lb. average weight within 3.8%.

Predicted model weight for the Qualification units was 2.27 tonnes (4994 lbs). This matched the Qualification unit's 4786 lb. average weight within 4.4%.

The Traveller program performed drop tests as input into the design process. As a result, there were changes in the design of the Traveller between the prototypes discussed on page 2-130 and the qualification test units described on page 2-133. The changes resulted in slightly different weights as noted in the descriptions.

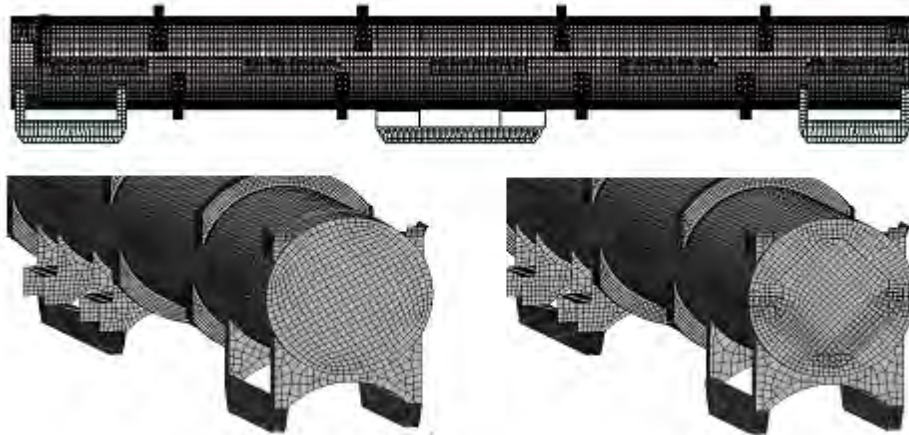


Figure 2-94 Outerpack Mesh in Prototype Model

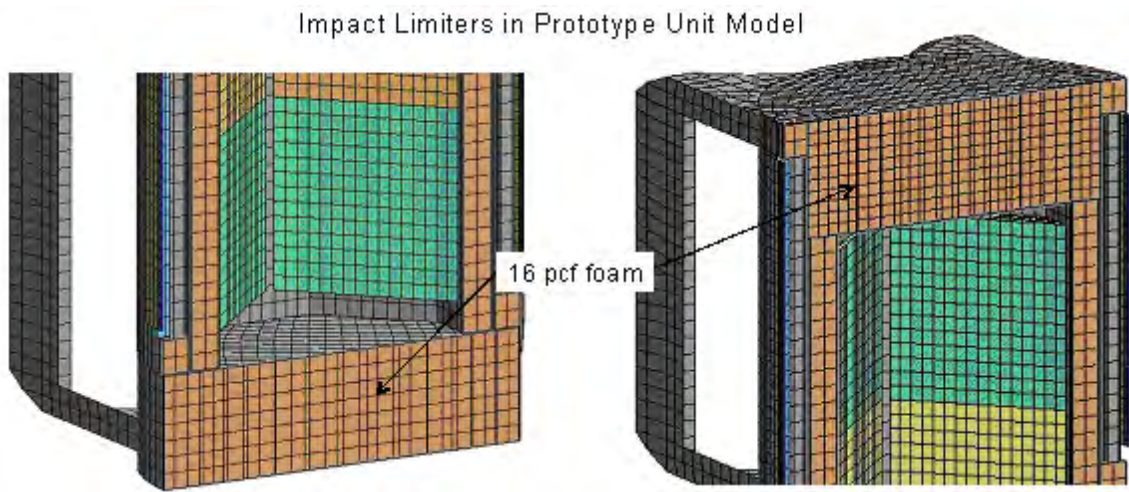


Figure 2-95 Impact Limiter in Prototype Unit Model

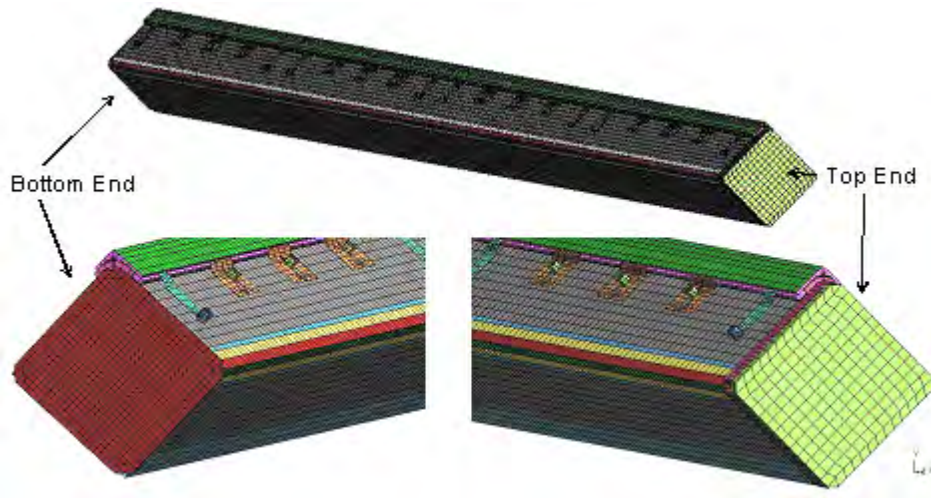


Figure 2-96 Clamshell Mesh in Qualification Unit Model



Figure 2-97 Fuel Assembly in Both Prototype and Qualification Unit Models

The Outerpack hinge details are shown in Figure 2-98. There were three bolts in the upper hinge plate in the Prototype models and only two for the Qualification unit models (shown). The bolts were modeled as spotweld beams. The spotweld beams and hinge plate shared nodes. The spotweld beam node at the hinge block was tied with LS-DYNA's NODAL_RIGID_BODIES. It should be noted that the manner of modeling the bolts allows for compression loading of the bolt, whereas in reality compression loads are not typically carried in bolted joints. However, in the horizontal side impact drops, the bolt heads themselves may impact the drop pad and compressive bolt loads are expected. Thus, our bolt model should be accurate in instances where compressive loads are developed and conservative elsewhere. The hinge pin was simulated using the LS-DYNA REVOLUTE_JOINT feature.

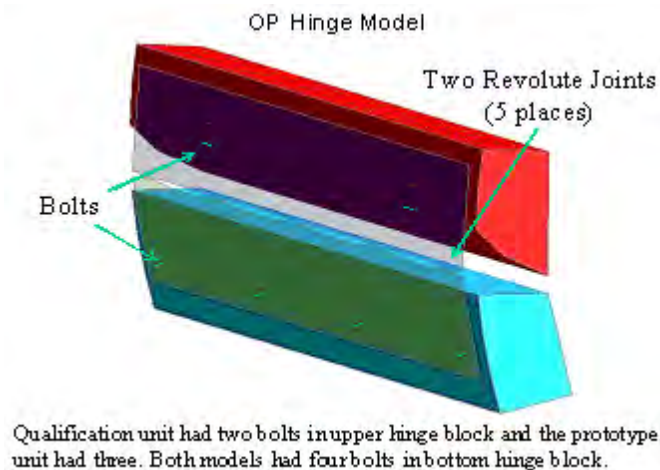


Figure 2-98 Outerpack Hinge Model

2.12.4.5.3 Qualification Unit Models (QTUs)

As with the Prototype units, the QTUs were constructed from many input files, see Figure 2-99. These files defined various details of the model and were included with, or without, transformations of coordinates and renumbering of identities as the model was assembled.

The main file, Aug19.key, contains the control cards, specifies outputs, contact definitions, and many attributes common to more than one subassembly. The major subassemblies were the Outerpack, Clamshell, and fuel assembly. These were defined in the OPs.key, CS_06_26sl6.key, and FA_remesh_FRslip.key files, respectively. The Outerpack and Clamshell subassemblies are detailed in Figures 2-101, 2-102 and 2-103 (The fuel assembly model was very similar to the one depicted previously in Figure 2-97. A total of 361,333 elements were used in the model (185985 shells, 157031 solids and 18317 beams).

The orientation for each run was defined in individual load case files. Likewise, the material property data was defined in three files which represented three different temperatures and foam densities. Obviously, only one load case file and one material file was invoked per run.

The Clamshell, Figure 2-102 is mounted to the Outerpack, Figure 2-100, with 14 rubber shock mounts. These shock mounts were modeled as discrete elements (springs). Outerpack hinge details were described in the previous section, see Figure 2-98.

Predicted model weight was 2.27 tonnes (4994 lbs). This matched the qualification unit's 4786 lb. average weight within 4.4%.

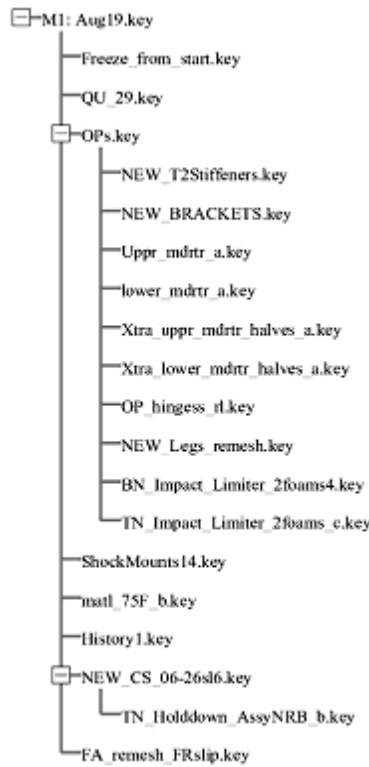


Figure 2-99 FEA Input Files

2.12.4.5.4 Qualification Unit – Outerpack Model Details

The FE model of the outerpack is shown in Figures 2-100 through 2-101A. Key features of the outerpack include the combination circumferential stiffeners/legs, the forklift pockets, the upper and lower outerpack halves, the hinges/latches on the sides, the stacking brackets, and the circumferential stiffeners on the upper outerpack. These features were included in the FE model as described below.

The circumferential stiffeners/legs and forklift pockets (Figure 2-100A) were modeled using 4-node Belytschko-Tsay shell elements (LS-DYNA elform = 2). These elements were integrated at three locations through the thickness using Gaussian quadrature. 1,008 of these elements were used to model the forklift pockets and 4,436 were used modeling the legs.

Both the circumferential stiffeners/legs and forklift pockets are welded to the lower outerpack outer casing. In the model, these parts were attached to one another using a penalty based tied contact algorithm (LS-DYNA's TIED_NODES_TO_SURFACE_OFFSET contact algorithm).

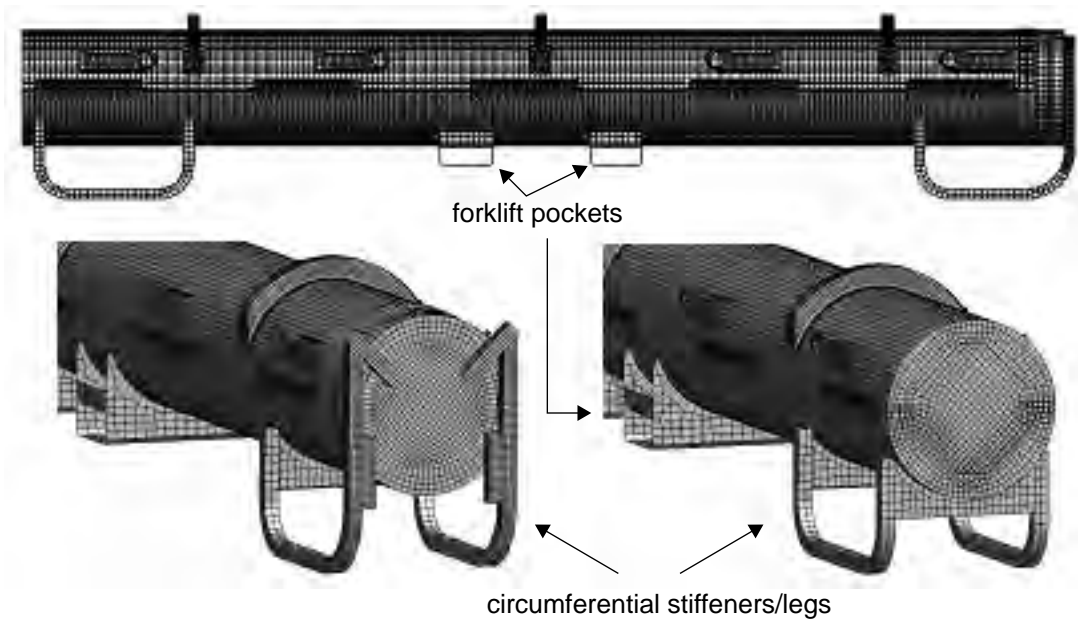


Figure 2-100 Outerpack Mesh in Qualification Unit Model

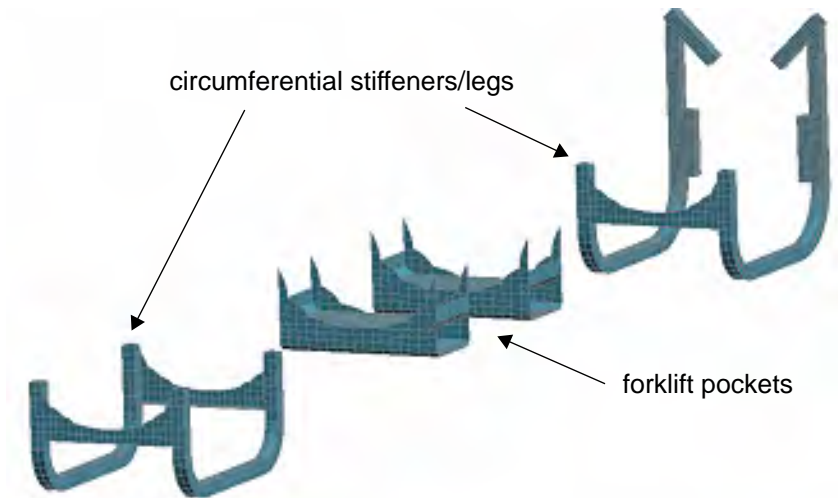


Figure 2-100A FE Meshes of Outerpack Legs and Forklift Pockets

The FE model of the QTU lower outerpack is depicted in Figures 2-100B and 2-100C. In addition to the previously mentioned circumferential stiffeners/legs, the lower outerpack is comprised of a long thick-walled “half-barrel” body and an impact limiter attached to one end (Figure 2-100A). The “half barrel” body is a sandwich construct of 10 pcf foam encased in 0.105 inch thick 304 stainless steel (Figure 2-100C). The outer steel casing was modeled using the same element formulation and integration scheme used for the

circumferential stiffeners/legs. 19,516 elements were required. The 10 pcf foam was modeled using 8 node selectively reduced fully integrated solid elements (LS-DYNA elform = 2) in conjunction with a material formulation developed especially for crushable foam (LS-DYNA material type = 63). Modeling the 10 pcf foam in the lower outerpack required 36,617 elements. Since this foam was poured-in-place, it is adhered to the stainless steel casing. This was modeled by enforcing tied contact between the outer nodes of the foam and the casing. The moderator blocks in the lower outerpack were modeled using 26,368 constant stress solid elements (LS-DYNA elform =1). Linear elastic material properties were used. The moderator blocks were attached to the lower outerpack using four bolts each for the full length moderator sections and two bolts each for the half-length moderator sections at the ends. These bolts were modeled using beam elements (LS-DYNA elform = 9) with a “spot weld” material formulation (LS-DYNA material type = 100.) Contacts between the moderator blocks, the lower outerpack, and the clamshell were defined using a penalty-based contact algorithm that accounts for shell thicknesses and for self contact as well as contact between different parts (LS-DYNA’s AUTOMATIC_SINGLE_SURFACE contact algorithm). Contact stiffness was found by dividing the nodal mass by the square of the time step size with a scale factor to ensure stability (LS-DYNA’s SOFT=1 contact option.) This approach was used because the foam has stiffness that is one or more orders of magnitude less than the metal parts. (Contact would possibly have broken down with other approaches that basically use the minimum stiffness of the two contact surfaces.)

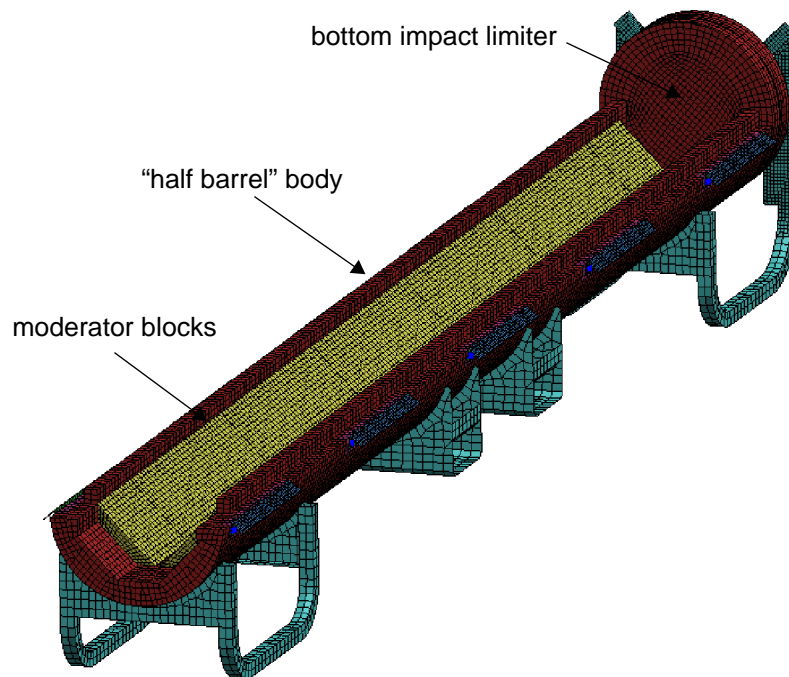


Figure 2-100B Lower Outerpack Mesh for Qualification Unit Model

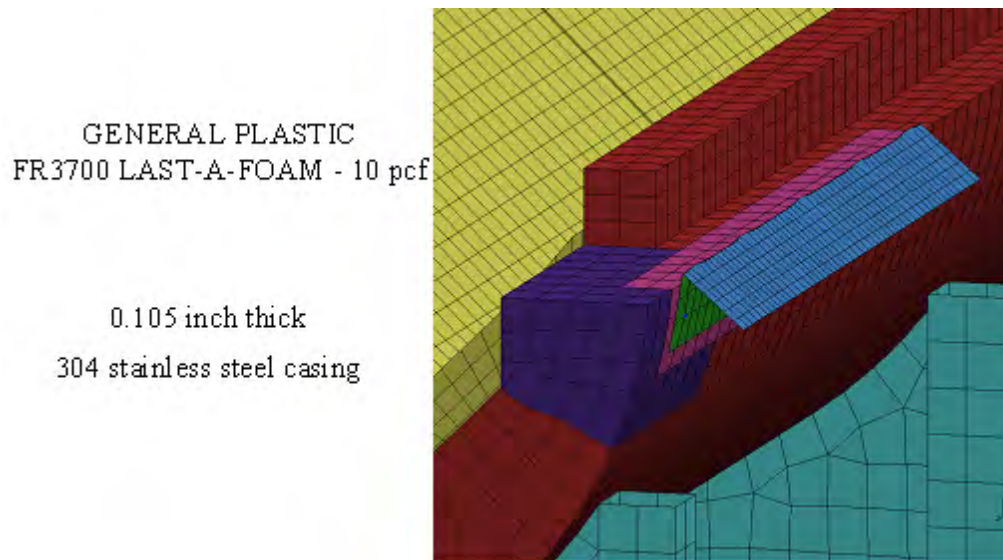


Figure 2-100C Qualification Unit Model Mesh Detail

The FE model of the QTU upper outerpack is depicted in Figure 2-100D. It primarily consists of a long thick-walled “half-barrel” body and an impact limiter attached to one end (Figure 2-100D). The “half barrel” body is a sandwich construct of 10 pcf foam encased in 0.105 inch thick 304 stainless steel. The outer steel casing was modeled using the same element formulation and integration scheme used for the circumferential stiffeners/legs and lower outerpack casing. 18,634 elements were required. The 10 pcf foam was modeled using 8 node selectively reduced fully integrated solid elements (LS-DYNA elform = 2) in conjunction with a material formulation developed especially for crushable foam (LS-DYNA material type = 63). Modeling the 10 pcf foam in the lower outerpack required 36,094 elements. Since this foam was poured-in-place, it is adhered to the stainless steel casing. This was modeled by enforcing tied contact between the outer nodes of the foam and the casing. The moderator blocks in the upper outerpack were modeled using 26,368 constant stress solid elements (LS-DYNA elform = 1). Linear elastic material properties were used. The moderator blocks were attached to the upper outerpack using four bolts each for the full length moderator sections and two bolts each for the half-length moderator sections at the ends. These bolts were modeled using beam elements (LS-DYNA elform = 9) with a “spot weld” material formulation (LS-DYNA material type = 100). Contacts between the moderator blocks, the upper outerpack, and the clamshell were defined using a penalty-based contact algorithm as described for the lower outerpack.

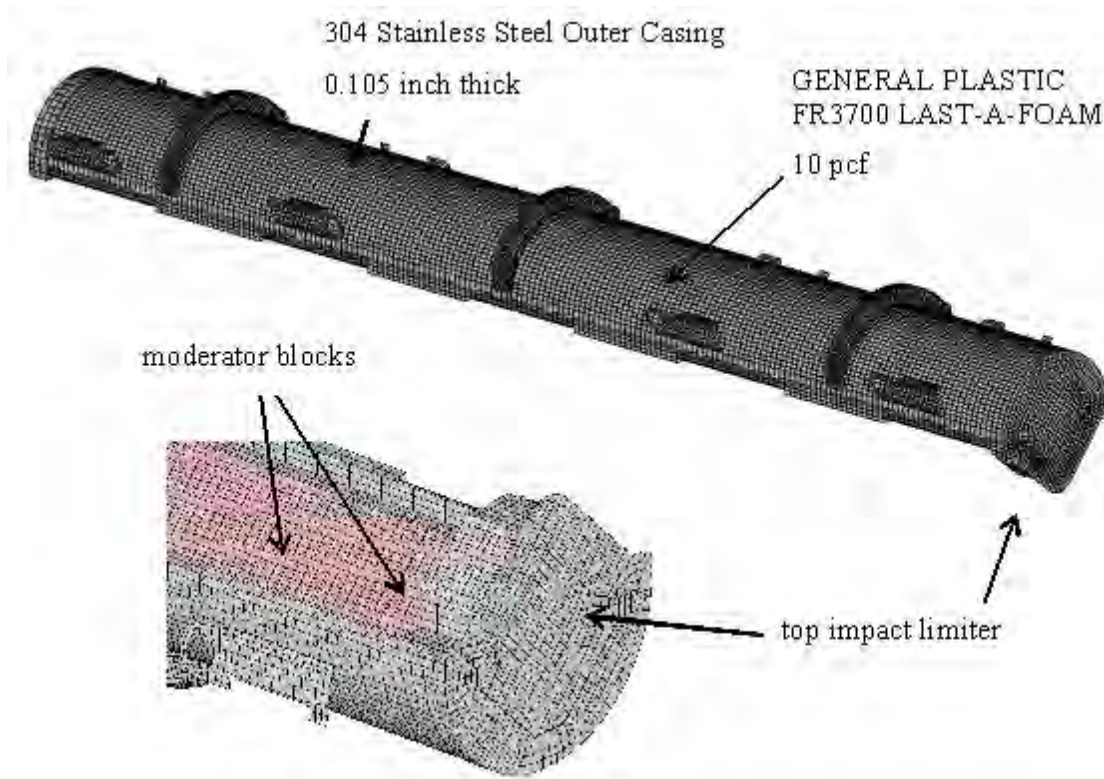


Figure 2-100D Upper Outerpack Mesh for Qualification Unit Model

Model details of the impact limiters are shown in Figure 2-101. Both consisted of two separate foam pieces: a 7 pcf foam block was placed inboard nearest the clamshell and 14 pcf foam covered both ends of the overpacks. These foam pieces were separated and covered by stainless steel. The foams were modeled using the same element formulation and material model as described for the 10 pcf foam in the overpack “barrels” except that each foam density had its own stress-strain curve. The 7 pcf foam in the bottom impact limiter was modeled with 2112 solid elements; the 14 pcf foam was modeled with 4480. The 7 pcf foam in the top impact limiter was modeled with 5248 elements; the 14 pcf foam was modeled with 1755 elements. Because these foams were “cut-to-fit,” they were not bonded to the steel cases. Thus, contact between the steel casings and the foam was defined using LS-DYNA’s AUTOMATIC_SINGLE_SURFACE contact algorithm as previously described (for contact between the lower outerpack, moderator blocks and clamshell).

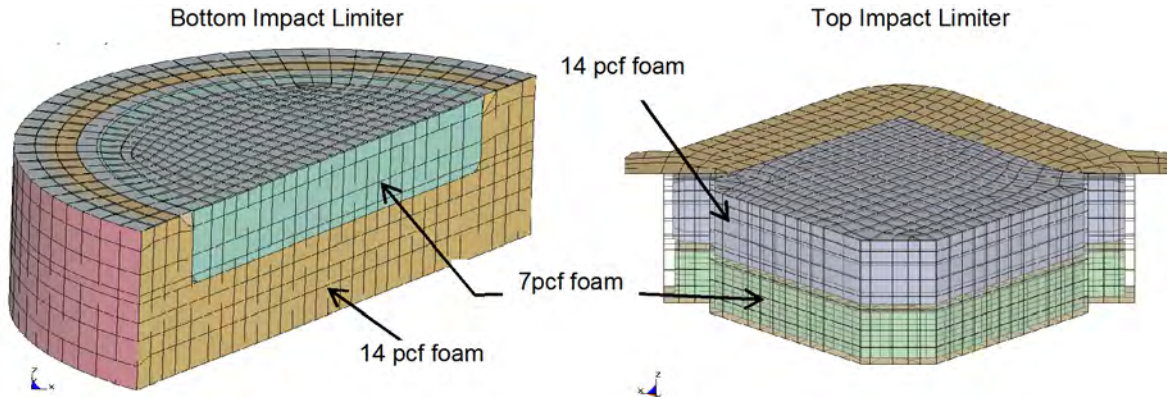


Figure 2-101 Impact Limiter Meshes in Qualification Unit Model

The stacking brackets and circumferential stiffeners on the upper overpack (Figure 2-100D) were modeled using the same element formulation and integration scheme used for the circumferential stiffeners/legs and overpack casings. 4,404 of these elements were used to model the stiffeners and 1,376 were used modeling the stacking brackets. Both the stiffeners and brackets were secured to the upper overpack casing using a tied contact algorithm as described for the circumferential stiffeners/forklift pockets and lower overpack casing.

The bolts which secure the overpack hinges/latches are all that prevent the upper and lower overpacks from separating upon impact. This was simulated in the model by replication of each physical part of the hinge/latch assemblies. In particular, hinge/latch assemblies including mounting blocks, hinge leaves, and the bolts were modeled (see Figure 2-98 and associated description in Section 2.12.3.5). These assemblies were attached to the upper and lower overpacks via tied (penalty-based) constraints. This methodology permitted relative rotations between the upper and lower overpacks along the axes of the hinges/latches while resisting any relative translations. Thus, the model forced the overpack latch bolts to prevent the displacement shown in Figure 2-101A. This allowed predicted deformations at the overpack seam to be realistic (e.g., Figures 2-30B and 2-74.)

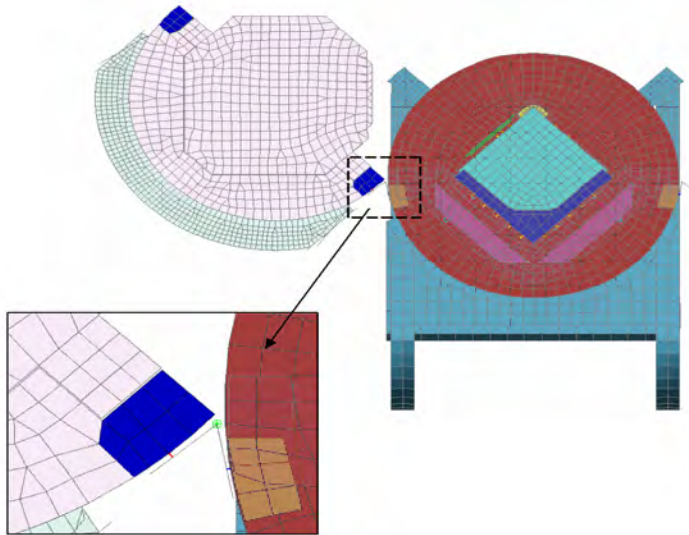


Figure 2-101A Hinge/Latch Feature in Qualification Unit Model

2.12.4.5.5 Qualification Unit – Clamshell Model Details

The FE model of the clamshell is shown in Figures 2-102 through 2-102C. Key features of the clamshell include: the clamshell top assembly, the V-shaped extrusion, the two doors including the hinges, middle latch and locks, and the bottom plate. These features were included in the FE model as described below.

The clamshell top assembly has two major features. First it can swivel from either side to allow access to the top portion of the fuel assembly. This is shown in Figure 2-102A where the CS head is swiveling about its right side. This feature was built into the FE model using the LS-DYNA revolute joint elements. (This is very similar to what was done for the overpack hinges/latches.)

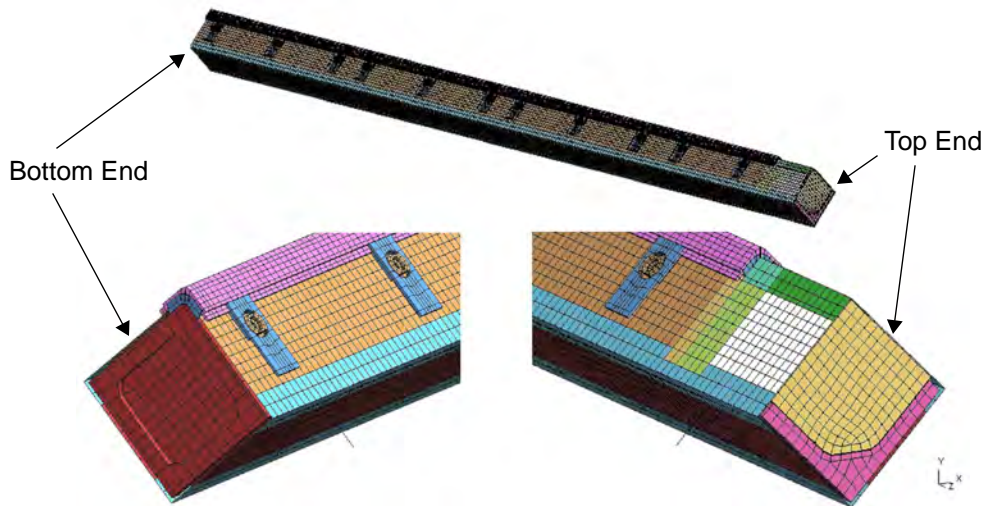


Figure 2-102 Clamshell Mesh in Qualification Unit Model

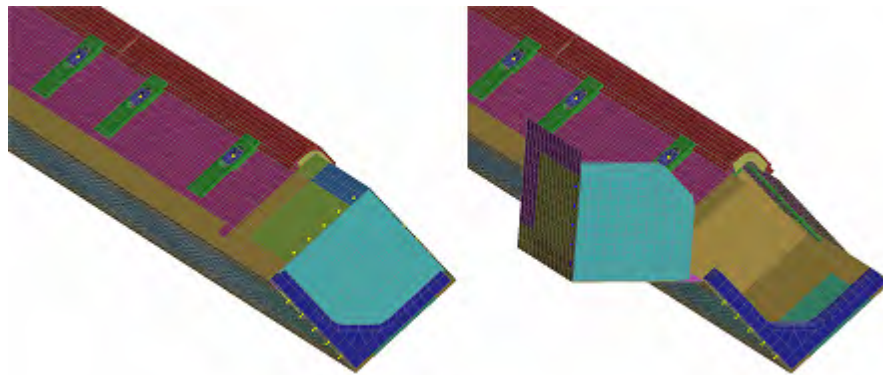


Figure 2-102A Clamshell Top Head in Qualification Unit Model

The second major feature was the top nozzle hold-down bars as shown in Figure 2-102B. Although this hardware has length adjustments to accommodate different fuel assembly heights, the hold-down bar was modeled for the height of an XL fuel assembly. If other fuels were to be modeled, the hold-down bars would need to be scaled in the z-direction. The hold-down bars were modeled with 8 node solid elements and contact between the top nozzle and other fuel and clamshell parts in the near vicinity was defined using LS-DYNA's AUTOMATIC_SINGLE_SURFACE contact algorithm.

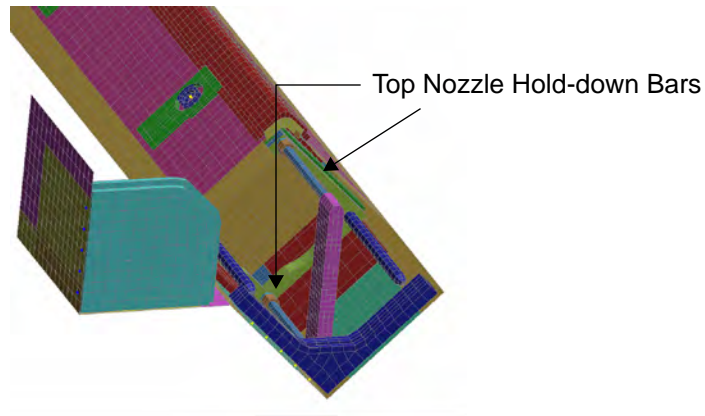


Figure 2-102B Clamshell Top Nozzle Hold-down Bars in Qualification Unit Model

The model of the clamshell latch and hinges allow the doors to rotate about the hinge centerlines as depicted in Figure 2-102C. These features were added using the LS-DYNA revolute joint element as already described.

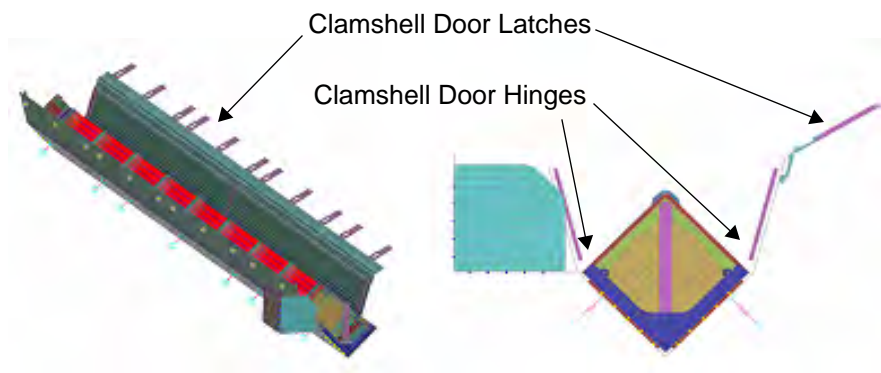


Figure 2-102C Clamshell Hinges and Latches in Qualification Unit Model

2.12.4.6 Model Input

Information needed to construct finite element models of the prototype and qualification units included load and boundary condition details, the stiffness and density of the comprising materials, the shipping package geometry, and the interconnections between the various shipping container subassemblies.

Drop Orientation and Initial Conditions – For modeling convenience, different drop orientations were modeled by changing the velocity and gravitational fields instead of rotating the model relative to the

This page intentionally left blank.

|

model global axes. Loadings were therefore specific to each drop orientation. Further, each analysis was initiated just prior to impact with the shipping package positioned just above the impact surface, having an initial velocity based on drop height (9.14 m for the free drops and 1 m for the pin puncture), and undergoing earth's gravitational pull. This analysis approach minimized computation effort since only minimal calculations of the shipping package during free-fall were needed. The required calculations were as follows.

2.12.4.6.1 Initial Velocity Magnitude (Speed)

The velocity, V , of any object having fallen for a drop height, h , in a constant gravitational field, g , is:

$$V = \sqrt{2gh}$$

Thus, using 9810 mm/s as the value of g , the calculated magnitude of the initial velocities (speed) for the 9 meter free drop and 1 meter pin puncture tests were as shown in Table 2-24.

Table 2-24 Initial Velocities 9 Meter Drop and 1 Meter Pin Puncture Analyses		
Test	Drop Height [m]	Initial Velocity (Speed) [mm/s]
9 m drop		
Prototype model	9.0	13288
Qualification model	9.14 (30 ft)	13389
Pin Puncture		
Prototype & Qualification models	1.0	4429

Velocity and Gravitational Fields – In general, a complete description of the position and orientation of an object in 3-dimensional space requires three coordinates and three direction cosines. However, for these drop tests, specification of only two direction cosines is sufficient. This is because both the drop pad and impact pin may be modeled as two-dimensional rigid walls or surfaces. In other words, these items have no distinct feature with respect to the shipping package that requires specification of the angle θ_y in Figure 2-103. Thus, only the angles θ_x and θ_z are needed to define the velocity and gravitational fields.

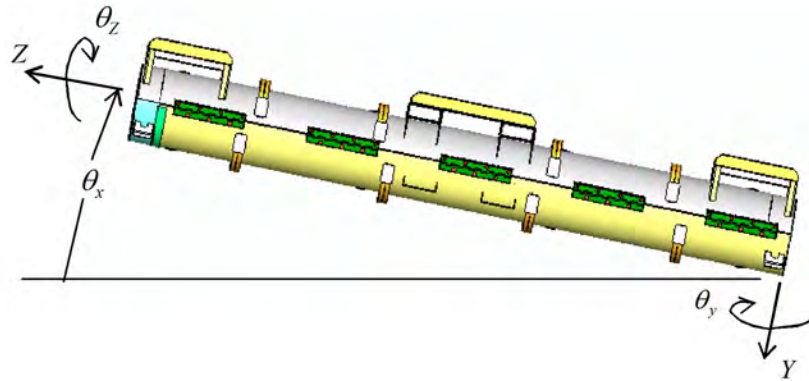


Figure 2-103 Package Drop Angle

Using the angles θ_x and θ_z shown in Figure 2-69, the velocity and gravitational fields are, respectively,

$$v = A^T \begin{Bmatrix} 0 \\ -V \\ 0 \end{Bmatrix}$$

and

$$a = A^T \begin{Bmatrix} 0 \\ g \\ 0 \end{Bmatrix}$$

where

$$A = \begin{bmatrix} \cos \theta_z & \sin \theta_z & 0 \\ \cos \theta_x \cdot \sin \theta_z & \cos \theta_z \cdot \cos \theta_x & -\sin \theta_x \\ \sin \theta_x \cdot \sin \theta_z & \sin \theta_x \cdot \cos \theta_z & \cos \theta_x \end{bmatrix}$$

The normal to the plane of impact (drop pad surface or pin face) is given by

$$n = A^T \begin{Bmatrix} 0 \\ -1 \\ 0 \end{Bmatrix}$$

The initial velocity field was implemented into the finite element model with the *INITIAL_VELOCITY command in LS-DYNA. The gravity field was applied using the *LOAD_BODY_GENERALIZED command. Finally, the impact plane was defined using the *RIGIDWALL_PLANAR or *RIGIDWALL_GEOMETRIC_CYLINDER commands. This approach allowed the drop orientation to be changed without altering the model coordinates. It should be noted that the gravity load was applied as a ramped load as shown in Figure 2-70. This was done as a precaution to minimize any numerical oscillations. However, this was probably unnecessary – applying the full gravity load at time zero would most likely produced equivalent results.

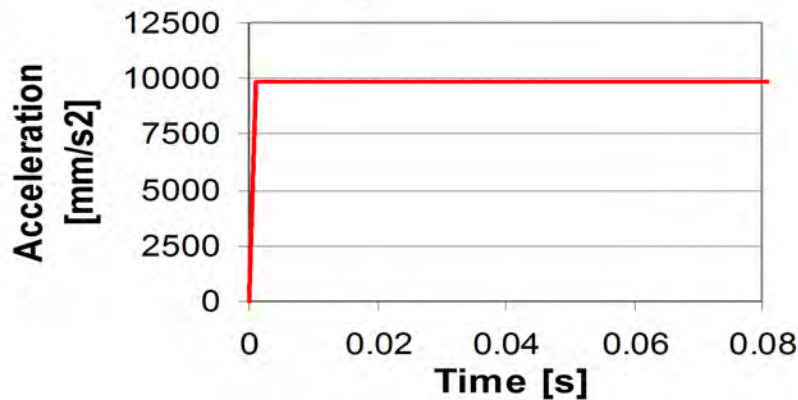


Figure 2-104 Gravity Load Profile

2.12.4.6.2 Material Properties

The crush strength of the polyurethane foam used in the Traveller XL package (LAST-A-FOAM[®] from General Plastics Manufacturing Company) is strongly influenced by temperature. For example, the perpendicular-to-rise dynamic crush strength of 10 pcf foam at 40% strain is approximately 940 psi at -40°F, 550 psi at 75°F, and just 338 psi at 160°F. Furthermore, foam crush strength is also directly related to foam density. Per the foam procurement specification, density is held within ± 1 pcf for the 7 and 10 pcf foam and $\pm 10\%$ for the 14 pcf foam. Both effects were included in our analyses. This was accomplished by specifying the foam crush strength at highest temperature (160°F) and lowest density (nominal density minus 1 pcf or 10%) and at lowest temperature (-40°F) and highest density (nominal density plus 1 pcf or 10%). Foam stress-strain curves used in the qualification unit analysis are shown in Figure 2-105. These were obtained from General Plastics data except that; 1) the curves were extended past General Plastics' recommend maximum strain limit to fully compressed (100% strain) using linear regressions of the last three known points, and 2) the two most crushable foams (6 pcf @160°F and 7 pcf @75°F) were made to follow the 8 pcf @ -40°F curves at strains above 50%, Figure 2-105). The latter adjustment was needed to prevent the foam elements from inverting under the high strains (i.e., this prevented “negative volumes”).

Stress-Strain Characteristics of General Plastics FR-3700 LAST-A-FOAM

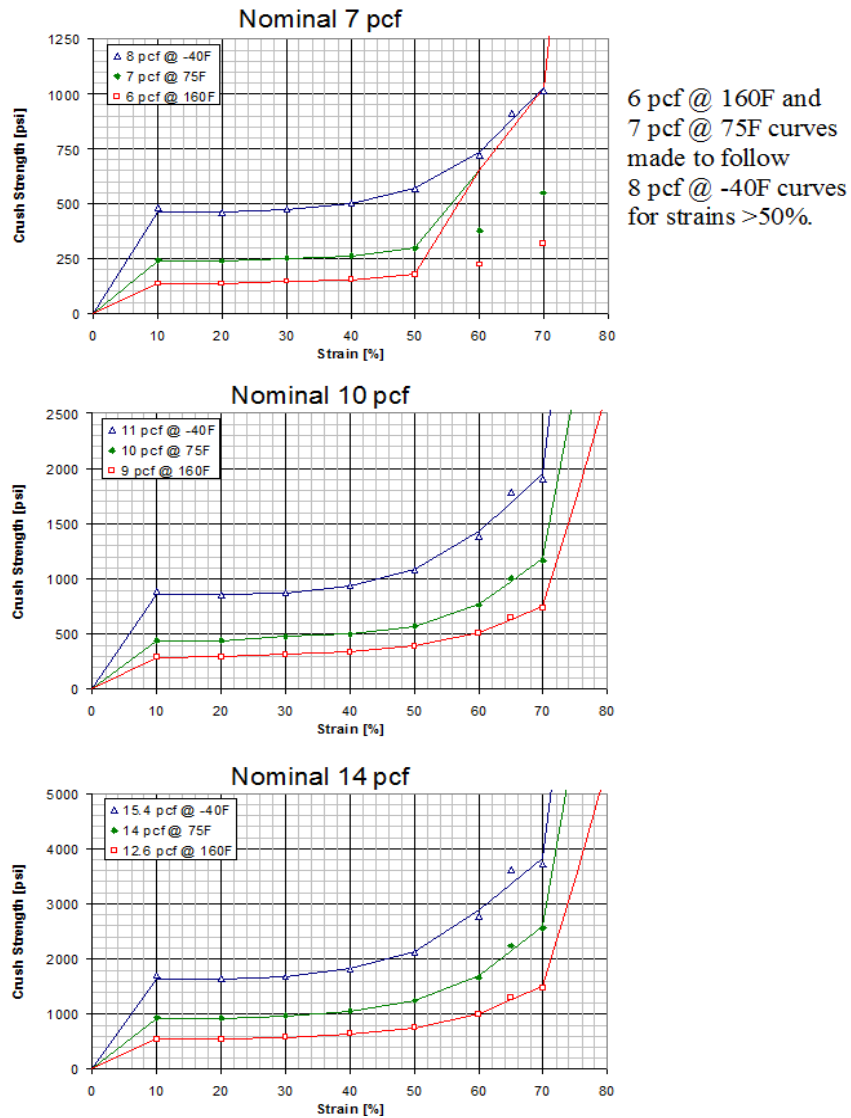


Figure 2-105 Stress Strain Data for LAST-A_FOAM

The use of a linear elastic material model from 0-10% strain was selected to evaluate the effects of temperature and foam density on drop test reaction forces. From Section 2.12.3.2.6, foam linear data demonstrated that temperature and foam density have a minor effect on the drop test response of the Traveller. The use of true stress-strain data ranging from 0-10% would not impact the conclusions of the comparative analysis.

A typical comparison of foam stress-strain behavior demonstrates that the available strain energy of a linear model is less than that observed with true stress-strain data. The use of true stress-strain data is expected to result in greater foam deflection when compared to linear modeling. Since greater crushing would absorb more kinetic energy, the predicted reaction force of the outerpack using true stress-strain data is expected to be less compared to linear data. It is concluded that the use of linear stress-strain data in the 0-10% range adds additional conservatism to the model.

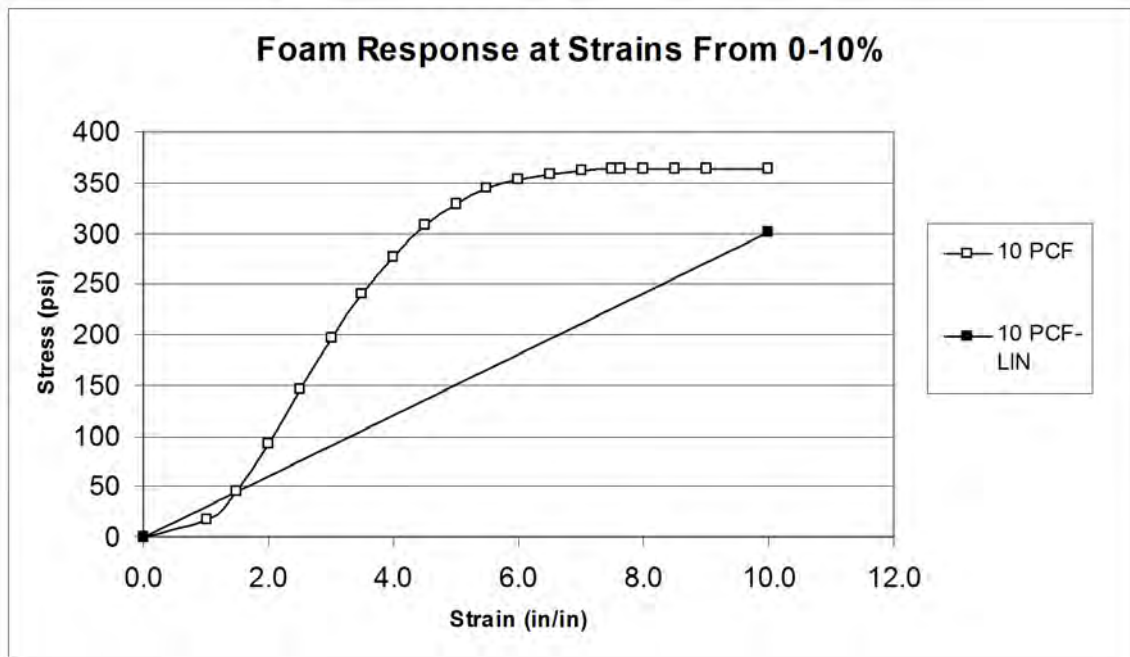


Figure 2-105A Foam Response at Strains from 0-10%

Stress strain characteristics for the 304 stainless steel used in these analyses are shown in Figure 2-106. The 75°F characteristics were obtained from pull tests of samples used in the prototype unit. Based on MIL_HDBK-5H “Metallic Materials and Elements for Aerospace Vehicle Structures,” see Figure 2-107, performance at 160°F was estimated by lowering both yield and ultimate strengths to 90% of their values at 75°F. Similarly, the performance at minus 40°F was estimated by raising yield and ultimate strengths to, respectively, 112 and 132% of their values at 75°F, Figure 2-107.

This page intentionally left blank.

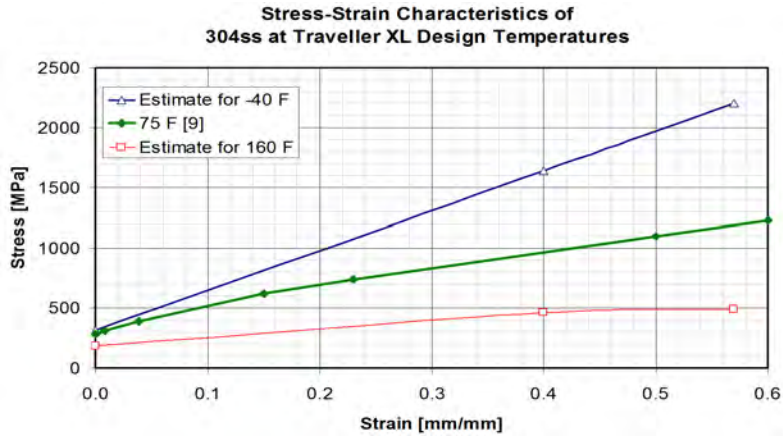


Figure 2-106 Stress-Strain Curves for 304 Stainless Steel

Temperature Effects on Tensile Properties of Annealed Stainless Steel

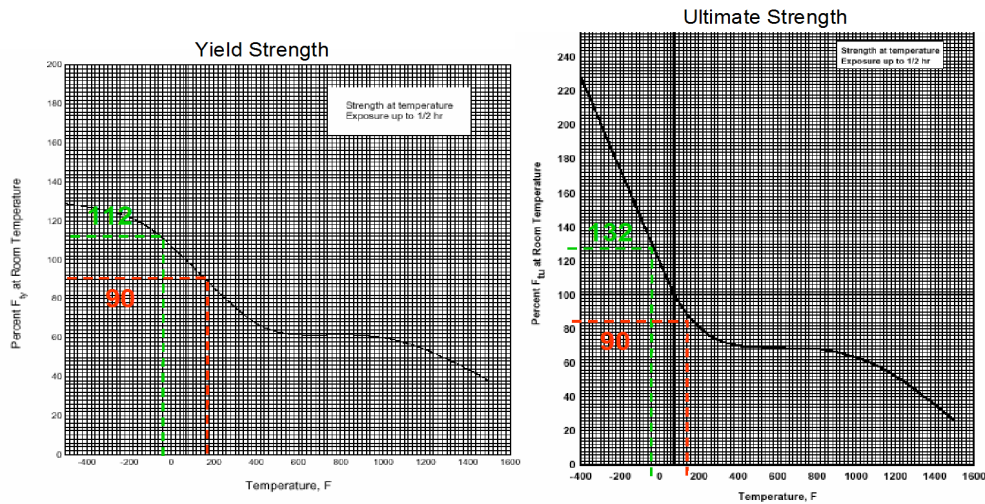


FIGURE 2.7.1.1.1(a) Effect of temperature on the tensile yield strength (F_y) of AISI 301, 302, 304, 304L, 321, and 347 annealed stainless steel. [16]

FIGURE 2.7.1.1.1(b) Effect of temperature on the tensile ultimate strength (F_u) of AISI 301, 302, 304, 304L, 321, and 347 annealed stainless steel. [16]

Figure 2-107 Temperature Effects on Tensile Properties of Annealed Stainless Steel

Estimated stress strain characteristics for the 6005-T5 aluminum used in these analyses are shown in Figure 2-108. The 75°F characteristics are typical of those for 6061-T6 used in the aerospace and automotive industries.¹ The 6005-T5 properties are similar based on their similar yield and ultimate strength and elongation. Because there was no available temperature dependent data, the curves for -40°F and 160°F were estimated based on the temperature dependence of aluminum alloy 6061T6. This was judged acceptable because alloy 6061-T6 is very similar to 6005-T5. However, for conservatism, we doubled

1. This data is not published. However, a similar curve is available from ALCAN

the impact that temperature had on 6061-T6 when estimating the temperature dependence of 6005-T5. For example, yield and ultimate strengths of 6061-T6 at 160°F is expected to be 6 and 4% less than at 75°F, Figure 2-109. However, we estimated these quantities for 6005-T5 by lowering the 75°F values by 12 and 8%. Likewise, when estimating the performance of 6006-T5 at -40°F, we increased the yield and ultimate strengths at 75°F by 8 and 12%, respectively. This is twice the reported impact this temperature reduction has on 6061-T6, Figures 2-109.

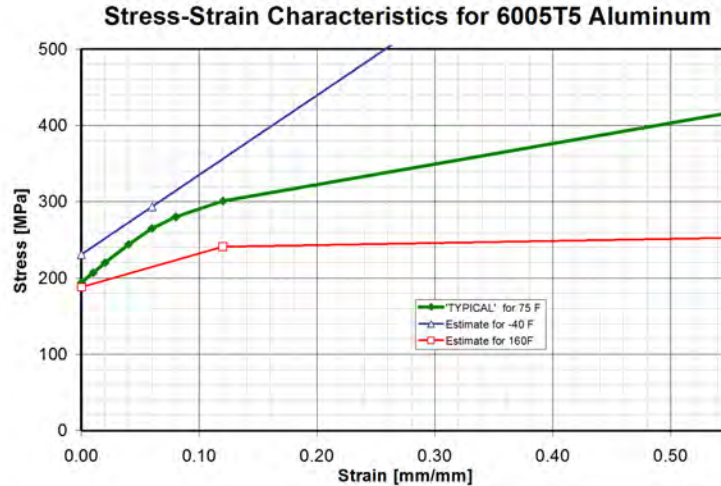


Figure 2-108 Stress-Strain Characteristics of Aluminum in Clamshell

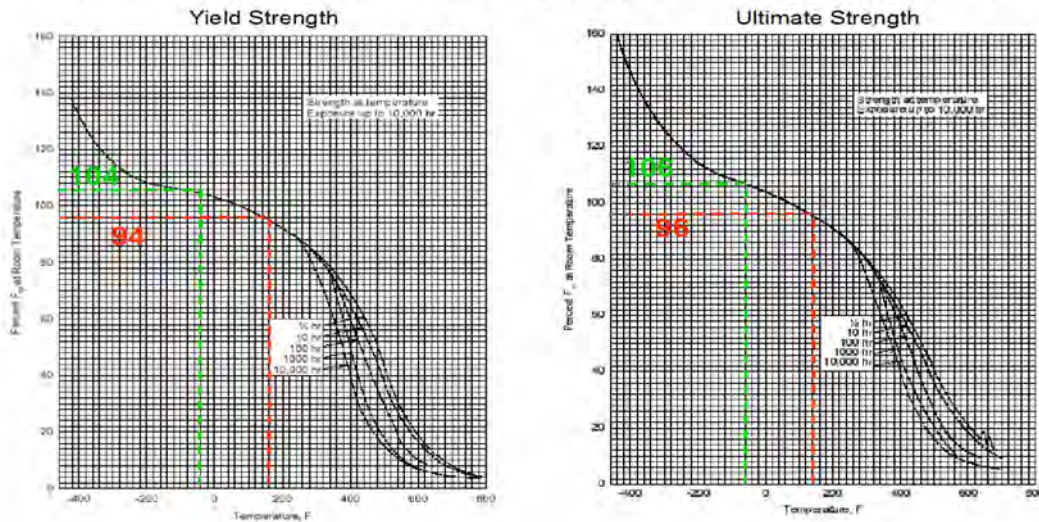


Figure 3-6-2.2 1(b). Effect of temperature on the tensile yield strength (F_y) of 6061-T6 aluminum alloy (all products). [16]

Figure 3-6-2.2 1(a). Effect of temperature on the tensile ultimate strength (F_u) of 6061-T6 aluminum alloy (all products). [16]

Figure 2-109 Temperature Effects on Tensile Properties of Aluminum in Clamshell

Finally, modulus of elasticity and Poisson’s ratio are also influenced by temperature. However, this effect is minimal and was neglected in this highly inelastic analysis. Thus, elastic properties determined at 75°F were used in the model. These are shown in Table 2-25.

Material	Modulus of Elasticity [GPa]	Poisson’s Ratio
304 stainless steel	206.7 ^a	0.32 ^a
6005T5 aluminum	70 [10]	0.3 [10]
Foam	0.37 ^b	N/A

Notes:
 a. This value of modulus is approximately 8% higher than the 192.0 GPa recommended at Westinghouse. This Poisson’s ratio is approximately 23% higher than the 0.26 recommendation. However, these elastic values were consistently used and these differences likely had little effect in this highly non-elastic analysis.
 b. Determined by using stress value at 10% strain instead of offset yield point.

2.12.4.7 Evaluations, Analysis and Detailed Calculations

Many billions of calculations required in these analyses were performed on the HPJ6000 workstation cluster (claxgen1, 2, 3 and 4). However, three additional sets of calculations were required. These were; 1) the calculations of the gravity and velocity fields and the orientation for the rigid wall surface or pin, 2) calculations of bolt factors of safety, and 3) calculations of accelerations from differentiated velocities. Example Calculations of Impact Plane Normal, Gravity Field, and Velocity Field

Horizontal Drop onto Outerpack Latches – A horizontal drop onto the Outerpack latches is shown in Figure 2-26. Using the coordinate system shown in Figure 2-103, this orientation is obtained when $\theta_x = 0$ and $\theta_z = 90^\circ$. Further, $V=13,389$ mm/s for a 9.14 m drop, Table 2-24, and $g=9810$ mm/s². Thus,

$$A = \begin{bmatrix} 0.0 & 1.0 & 0.0 \\ 1.0 & 0.0 & 0.0 \\ 0.0 & 0.0 & 1.0 \end{bmatrix},$$

$$n = \begin{bmatrix} 0.0 & 1.0 & 0.0 \\ 1.0 & 0.0 & 0.0 \\ 0.0 & 0.0 & 1.0 \end{bmatrix}^T \cdot \begin{bmatrix} 0 \\ -1 \\ 0 \end{bmatrix} = \begin{bmatrix} 1 \\ 0 \\ 0 \end{bmatrix},$$

$$v = \begin{bmatrix} 0.0 & 1.0 & 0.0 \\ 1.0 & 0.0 & 0.0 \\ 0.0 & 0.0 & 1.0 \end{bmatrix}^T \cdot \begin{bmatrix} 0 \\ -13,389 \\ 0 \end{bmatrix} = \begin{bmatrix} -13,389 \\ 0 \\ 0 \end{bmatrix},$$

and

$$g = \begin{bmatrix} 0.0 & 1.0 & 0.0 \\ 1.0 & 0.0 & 0.0 \\ 0.0 & 0.0 & 1.0 \end{bmatrix}^T \cdot \begin{Bmatrix} 0 \\ 9,810 \\ 0 \end{Bmatrix} = \begin{Bmatrix} 9,810 \\ 0 \\ 0 \end{Bmatrix}$$

Example Calculation of Bolt Factor of Safety – The equation below is utilized to calculate bolt factor of safety. For example, suppose a Clamshell bolt is subjected to an axial force of 5,134 lb_f and shear forces of 925 and 3380 lb_f. A factor of safety is calculated by first calculating the “Actual” (load) using these values of load, Table 2-26.

$$\begin{aligned} Actual &= \left(\frac{F_{axial}}{FN_{ult}} \right)^2 + \left(\frac{F_{yshear}}{FS_{ult}} \right)^2 + \left(\frac{F_{zshear}}{FS_{ult}} \right)^2 \\ &= \left(\frac{5,134}{12,070} \right)^2 + \left(\frac{925}{6,040} \right)^2 + \left(\frac{3,380}{6,040} \right)^2 \\ &= 0.5175 \end{aligned}$$

This value must be divided into the “Allowable” which is 1.0. Thus, the factor of safety for the bolt in this example is 1.93. (These loads correspond to those predicted for the Clamshell keeper bolt which is third down from the top end of the Clamshell during a horizontal side drop onto the latches at time 0.0072s. The calculated value for factor of safety corresponds to that shown in Table 2-11.

Description of Acceleration Calculations – Predicted accelerations, as shown in Figures 2-88 through 2-92, were obtained by differentiating predicted nodal velocities sampled at a frequency of 4 KHz and applying a “light” (SAE 180 Hz) filter. This technique was used because the finite-difference technique used in LS-DYNA yields very noisy accelerations. These nodal accelerations are indeed accurate in an average sense, but not in an absolute value. The differentiated velocity technique allowed the true trend in accelerations to be discerned. The calculations were accomplished with the LS-POST program.

2.12.4.8 Accelerometer Test Setup

Prior to testing, piezoelectric accelerometers were mounted on the Outerpack and Clamshells of both test prototypes. The intent was to measure the accelerations at a few critical points so that the forces involved in the drops would be better known and so that the FEA results could be validated.

Three accelerometers were positioned on the Prototype Unit-1 Test series 1, Figure 2-110. One accelerometer was on the Clamshell top plate and thus was near the initial impact end. The other two were positioned on the secondary impact end at the Clamshell bottom plate and bottom impact limiter. Further details of this instrumentation are available in Appendix 2.12.5.

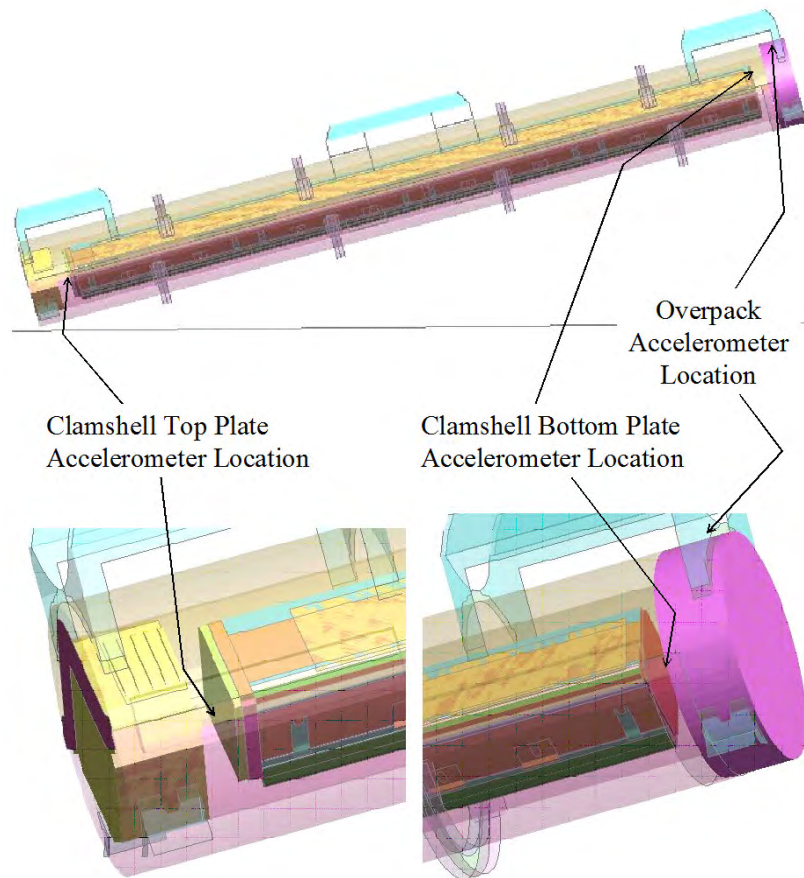


Figure 2-110 Accelerometer Locations on Prototype Unit 1

2.12.4.9 Bolt Factor of Safety Calculation

Bolt factors of safety (FS)

$$F.S. = \frac{\text{Allowable}}{\text{Actual}} \tag{H-1}$$

were based on the failure criteria

$$\left(\frac{F_{\text{axial}}}{F_{N_ult}} \right)^2 + \left(\frac{F_{\text{yshear}}}{F_{S_ult}} \right)^2 + \left(\frac{F_{\text{zshear}}}{F_{S_ult}} \right)^2 \geq 1. \tag{H-2}$$

This commonly-used criterion was chosen because it accounts for the effects of both axial and shear forces. (Note: the left side of equation H-2 is the “Actual” in equation H-1 and the “Allowable” is unity.)

The loads in equation H-2 were determined from the finite element analysis; the tensile and shear strengths are shown in Table 2-26. Initially, the tensile strengths were estimated from the tensile to proof strength ratios for Grade 2 bolts, Tables 2-27 and 2-28, obtained from. Use of the ratios obtained for Grade 2 bolts was justified because the proof strengths of these bolts should be just above Grade 2 levels based on their minimum strength of 70 ksi. However, bolt strengths estimated in this manner did not result in adequate factors of safety for each Outerpack bolt when the Traveller XL package was dropped horizontally, Figure 2-26. However, the specification for the Outerpack bolts was changed in the design of the CTU unit. The new bolt specification for CTU and production packages is ASTM A193 Class 1 B8 which has an ultimate tensile strength minimum of 75 ksi. Additionally, the number of Outerpack hinge bolts has increased to 12 bolts per side on the top leaf and bottom hinge leaf for both the XL and STD packages. This increase in the number of bolts, and the increase in strength results in a factor of safety of 1.12 for the bounding Traveller XL's worst bolt, in the worst case bolt failure orientation (the side drop).

Location	Size	Thread Area [in²] [13]	Minimum Yield Strength [ksi]	Estimated Minimum Proof Strength [lbf]⁽¹⁾	Ratio of Tensile to Proof Strength⁽²⁾	FN_ult [lbf]	NS_ult [lbs]⁽⁵⁾
CS bolts	1/2"-13	0.142	70 [14]	8,940	1.35	12,070 ⁽³⁾	6,040
Bottom OP hinge bolts	5/8"-11	0.226	70 [14]	14,240	1.35	19,200 ⁽³⁾	9,600
Top OP hinge bolts	3/4"-10	0.334	70 [14]	21,040	1.34	28,200 ⁽³⁾	14,100
			100 [18]	30,060	N/A	41,750 ⁽⁴⁾	20,900

Notes:

- (1) 0.9 * thread area * min yield strength
- (2) Based on estimated proof strength and Table 2-28
- (3) Estimated min proof strength * ratio of Tensile to proof strength
- (4) Minimum Ultimate Tensile Strength of 125 ksi * thread area
- (5) 0.5 * FN_ult

Nominal Dia of Product and Threads per in	Stress Area, in ²	Grade 1		Grade 2		Grade 4		Grades 5 and 5.2		Grade 5.1		Grade 7		Grades 8, 8.1, and 8.2	
		Proof Load, lb	Tensile Strength min, lb	Proof Load, lb	Tensile Strength min, lb	Proof Load, lb	Tensile Strength min, lb	Proof Load, lb	Tensile Strength min, lb	Proof Load, lb	Tensile Strength min, lb	Proof Load, lb	Tensile Strength min, lb	Proof Load, lb	Tensile Strength min, lb
Coarse-Thread Series – UNC															
No. 6-32	0.00909	–	–	–	–	–	–	–	–	750	1,100	–	–	–	–
8-32	0.0140	–	–	–	–	–	–	–	–	1,200	1,700	–	–	–	–
10-24	0.0175	–	–	–	–	–	–	–	–	1,500	2,100	–	–	–	–
12-24	0.0242	–	–	–	–	–	–	–	–	2,050	2,900	–	–	–	–
1/4-20	0.0318	1,050	1,900	1,750	2,350	2,050	3,650	2,700	3,800	2,700	3,800	3,350	4,250	3,800	4,750
5/16-18	0.0524	1,750	3,150	2,900	3,900	3,400	6,000	4,450	6,300	4,450	6,300	5,500	6,950	6,300	7,850
3/8-16	0.0775	2,550	4,650	4,250	5,750	5,050	8,400	6,600	9,300	6,600	9,300	8,150	10,300	9,300	11,600
7/16-14	0.1063	3,500	6,400	5,850	7,850	6,900	12,200	9,050	12,800	9,050	12,800	11,200	14,100	12,800	15,900
1/2-13	0.1419	4,700	8,500	7,800	10,500	9,200	16,300	12,100	17,000	12,100	17,000	14,900	18,900	17,000	21,300
9/16-12	0.182	6,000	10,900	10,000	13,500	11,800	20,900	15,500	21,800	15,500	21,800	19,100	24,200	21,800	27,300
5/8-11	0.226	7,450	13,600	12,400	16,700	14,700	25,400	19,200	27,100	19,200	27,100	23,700	30,100	27,100	33,900
3/4-10	0.334	11,000	20,000	18,400	24,700	21,700	38,400	28,400	40,100	–	–	35,100	44,400	40,100	50,100
7/8-9	0.462	15,200	27,700	15,200	27,700	30,000	53,100	39,300	55,400	–	–	48,500	61,400	55,400	69,300
1-8	0.606	20,000	36,400	20,000	36,400	39,400	69,700	51,500	72,700	–	–	63,600	80,600	72,700	90,900
1-1/8 - 7	0.763	25,200	45,800	25,200	45,800	49,600	87,700	56,500	80,100	–	–	80,100	101,500	91,600	114,400
1-1/4 - 7	0.969	32,000	58,100	32,000	58,100	63,000	111,400	71,700	101,700	–	–	101,700	127,700	116,300	145,400
1-3/8 - 6	1.155	38,100	69,300	38,100	69,300	75,100	132,800	85,500	121,300	–	–	121,300	153,600	138,600	173,200
1-1/2 - 6	1.405	46,400	84,300	46,400	84,300	91,300	161,600	104,000	147,500	–	–	147,500	186,900	168,600	210,800

Table 2-28 Bolt Strength Ratio						
Size	Tensile to Proof Strength Ratio					
	Grade 1	Grade 2	Grade 4	Grades 5, 5.1 and 5.2	Grade 7	Grades 8, 8.1 and 8.2
½-13	1.81	1.35	1.77	1.40	1.27	1.25
5/8-11	1.83	1.35	1.73	1.41	1.27	1.25
¾-10	1.82	1.34	1.77	1.41	1.26	1.25

2.12.5 TRAVELLER DROP TESTS RESULTS

Three series of full scale drop tests have been performed on the Traveller package to evaluate the performance of the design. This appendix will summarize structural performance of the Traveller during these tests. The objectives, test articles, results and lessons learned will be described. The three series were:

- Prototype Tests
- Qualification Tests
- Certification Tests

2.12.5.1 Prototype Test Unit Drop Tests

Testing was conducted at Columbiana High Tech Company (CHT) in Columbiana, Ohio during the week of January 27-30, 2003 (Ref. 3).

An as-built Traveller package prototype is shown in Figures 2-111 and 2-112. Figure 2-111 shows the internal packaging including the 17x17 XL fuel assembly, Clamshell, and moderator blocks. Figure 2-112 shows the closed Outerpack. The prototype packages employed 11 pcf foam along the axial section of the package and 16 pcf foam in the endcaps. Furthermore, the Outerpack consisted of 11 gage inner and outer skin. Each package also contained 22 shock mounts to connect the Clamshell to the Outerpack.

Test Series 1 – Test series 1 was conducted on January 27th through 28th and included two 9 meter drop tests plus a pin-puncture test. The package’s test weight was 5072 pounds. Drop orientations are shown in Figure 2-113 and Table 2-29.

The Outerpack retained its basic circular pre-test shape except for localized plastic deformation from the 9 meter drop tests and the pin-puncture test. One bolt on the lower Outerpack hinge failed after completion of the last 9 meter drop test. The Outerpack did not separate after any impacts, and the pin did not perforate the inner or outer shell. The internal damage was minimal. The fuel assembly’s envelope decreased from 8.418" nominal to 8.25" maximum after the first 9 meter drop test, and reduced further to 8.13" maximum after second 9 meter drop test. Fuel rod gaps globally decreased (the fuel envelope decreased), but local expansion was noted between a few rods with a maximum measured gap of .188" for the first 9 meter drop test and .625" maximum measured gap for second 9 meter drop test (compared to the nominal gap of .122"). The polyethylene moderator blocks and aluminum neutron “poison plates” maintained position. The Clamshell doors remained closed, but the top and bottom heads were separated from the Clamshell. The separation was caused by the fuel assembly deceleration forces reacting against the clamshell end plate. The bearing force of the bolts (a shear effect on the top head plate) from impact was sufficient to fail the material in the bolt slots for both head pieces. The fuel inspection indicated that no fuel rods had ruptured, and that the axial position of fuel rods maintained location between bottom and top nozzle. The failure the clamshell endplates was due to the bolt slots being modified as a result of warping of the clamshell during fabrication.

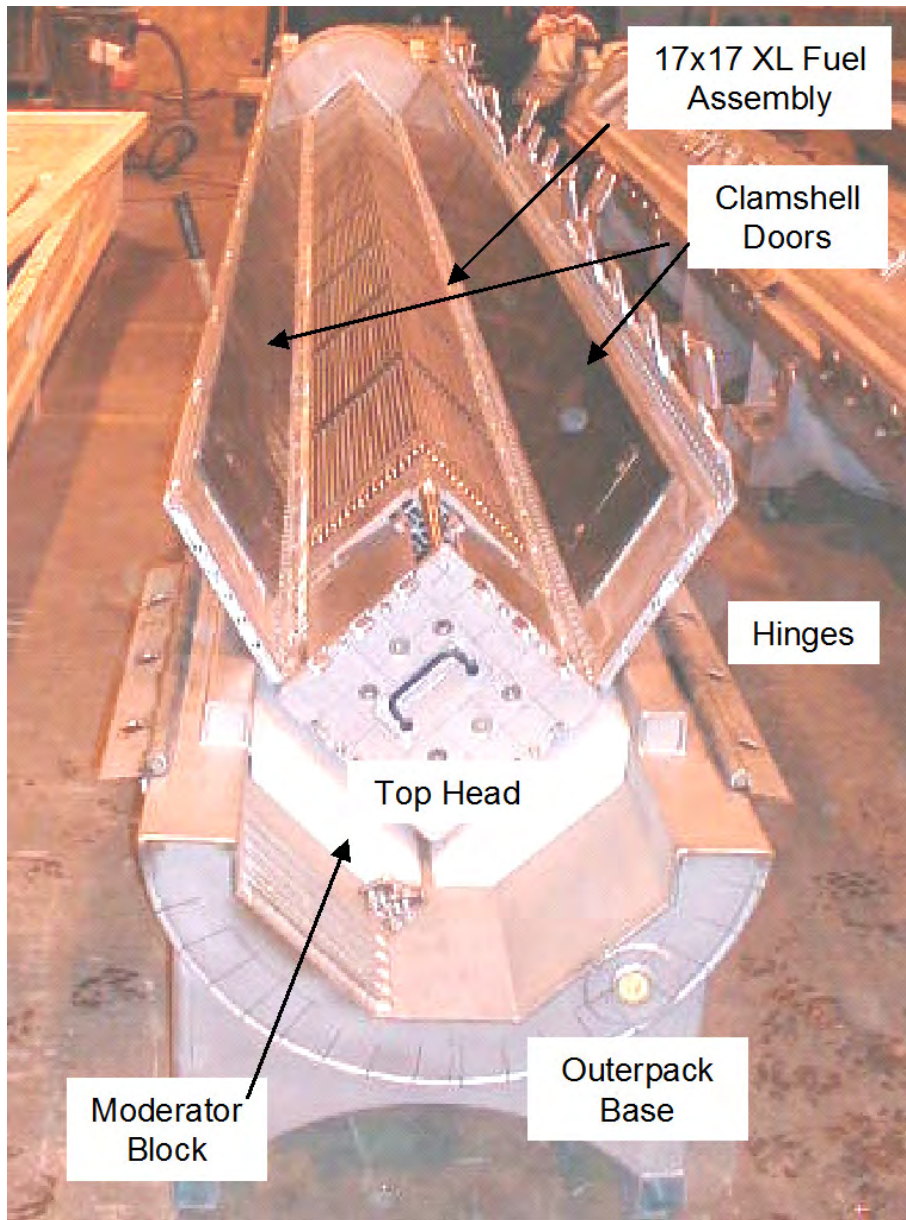


Figure 2-111 Traveller Prototype Internal View

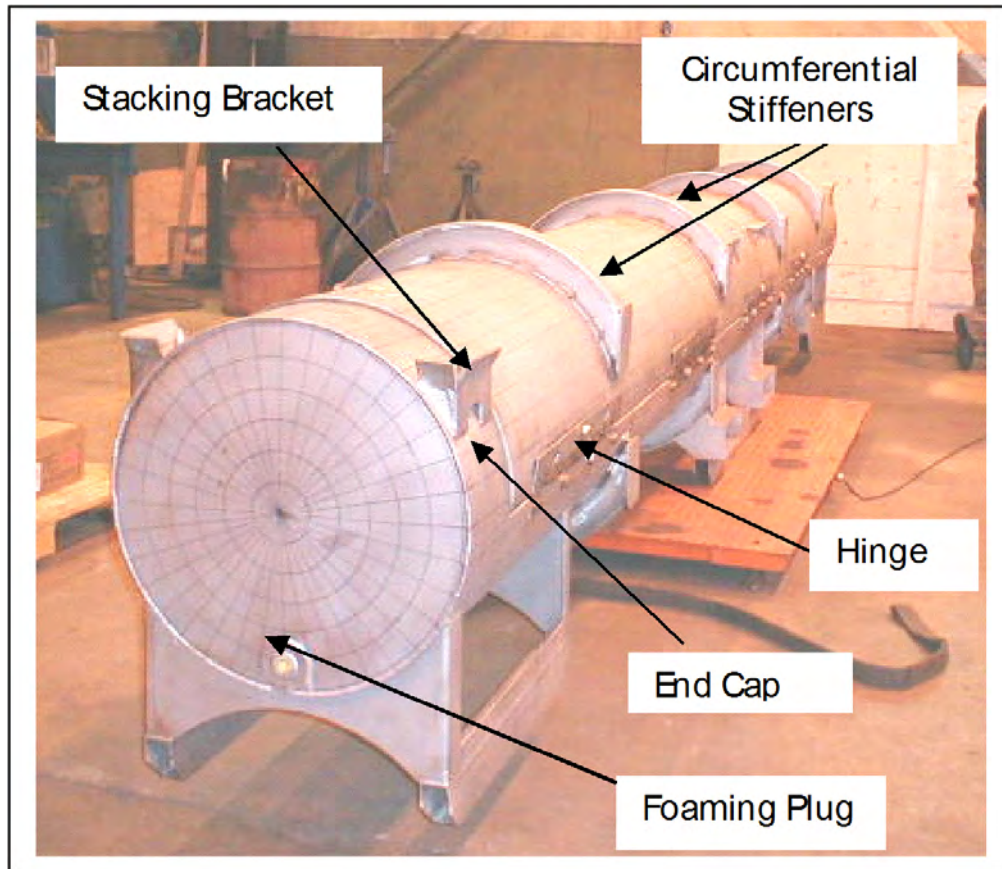


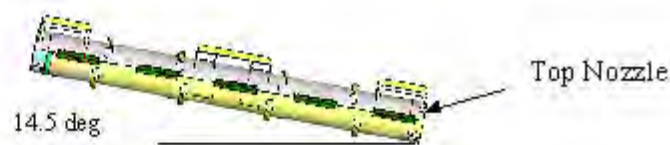
Figure 2-112 Traveller Prototype External View

Test Sequence	Test Pitch Attitude	Test Roll Attitude	Impact Location
1.1) 9 m Low Angle	14.5°	180°	T/N primary impact on OP top
1.2) 9 m CG-over-corner	71°	90°	B/N primary impact on OP hinge
1.3) 1 m Pin-puncture	20°	180°	Center of Gravity (Axial) on OP top, T/N end down

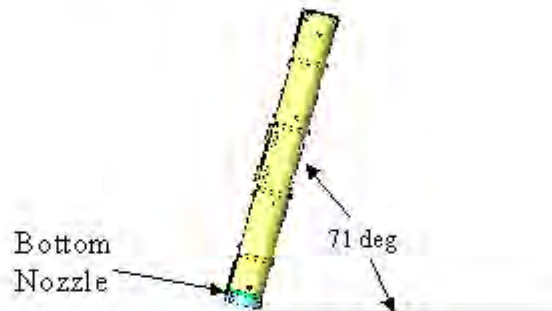
Test 1.1 – The Outerpack retained its basic circular pre-test shape except for localized plastic deformation from the 9 meter drop test. Impact zones from the drop test were localized at the nozzle impact locations on the package ends. The Outerpack did not separate after the impact, and no bolt failures on the Outerpack hinge were noted. The top nozzle damage zone consisted of local crush approximately 12" wide, 9" axially and a maximum crush of approximately 1.5". The circumferential stiffeners were crushed (Figure 2-114) and inhibited global crushing on the Outerpack. The bottom nozzle damage zone consisted of local crush approximately 11.5" wide, a maximum crush of approximately 3/4", and axially from the package end to

the edge of the stiffening ring. The internal damage was minimal as shown in Figures 2-113 and 2-114. The polyethylene moderator blocks and aluminum neutron “poison plates” maintained position. The Clamshell doors remained closed, but the Clamshell bulged outwardly approximately 0.25" locally at the grid locations in a section 54" long at the bottom nozzle end. The fuel inspection indicated that no fuel rods had ruptured, and that the axial position of fuel rods maintained location between bottom and top nozzle. The average measured fuel envelope decreased from 8.418" nominally to 8.25" maximum, and the maximum measured fuel rod gap was found to be 0.188" locally (observed at one or two rods along the envelope) compared to the nominal gap of 0.122". Figures 2-114 and 2-115 summarize the results of this drop test.

Test 1.1
9 m Low Angle
Slap Down



Test 1.2
9 m CG over corner
on Hinge



Test 1.3
1m Pin Puncture

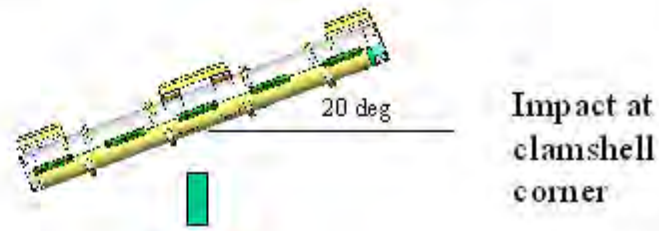
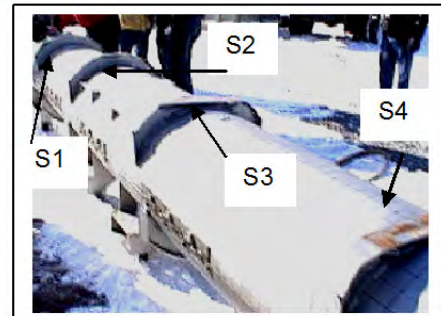
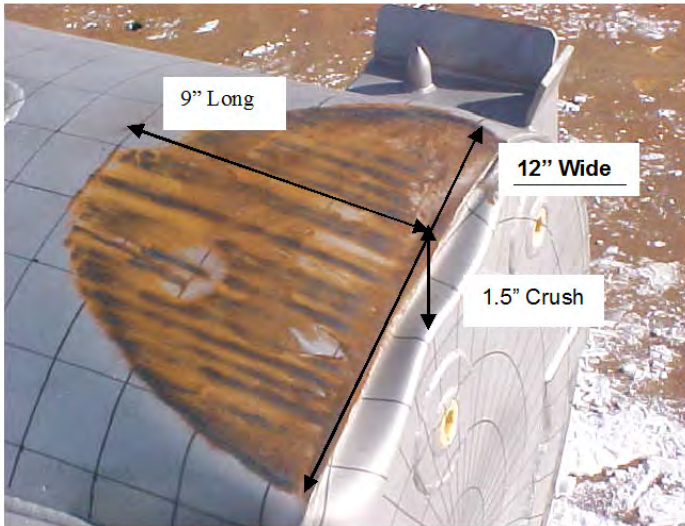
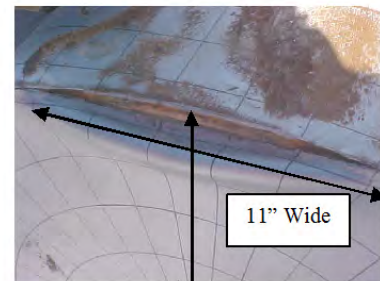
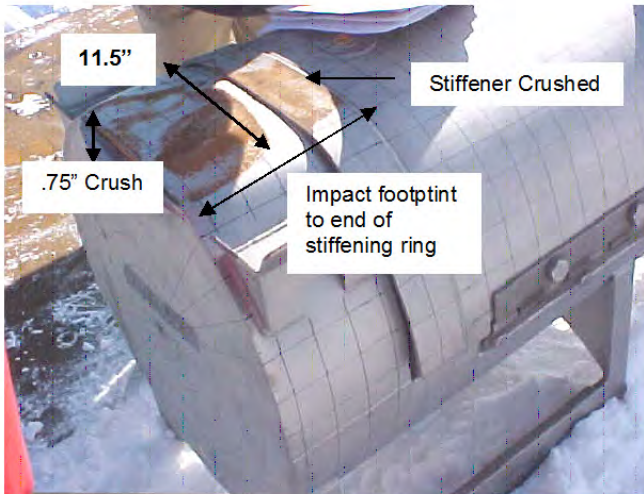


Figure 2-113 Drop Orientations for Prototype Test Series 1



Stiffening rings show progressive damage from T/N



Small tear at Bottom End cap/Plate Seam

Figure 2-114 Traveller Prototype Exterior After Test 1.1

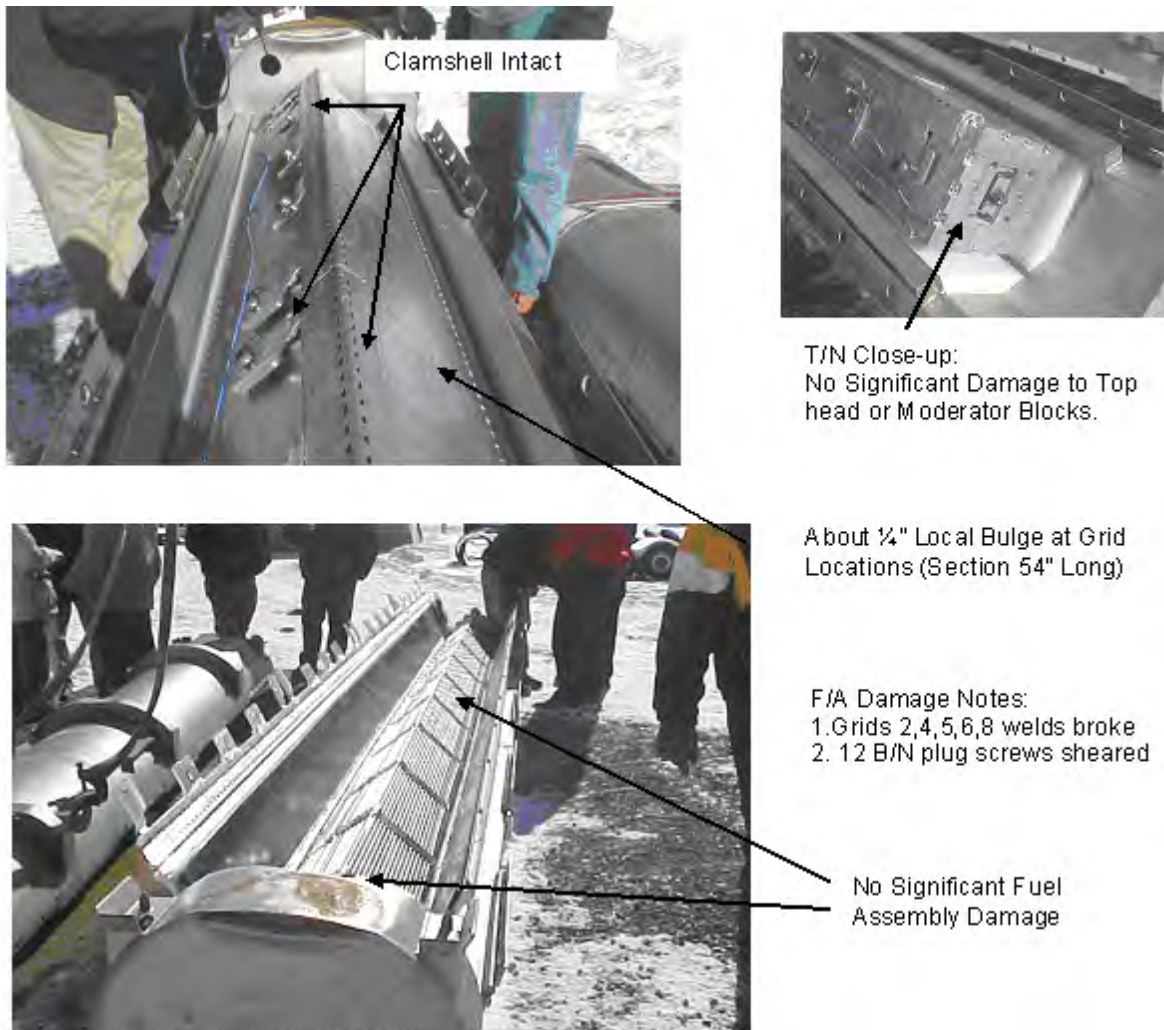


Figure 2-115 Traveller Prototype Interior After Test 1.1

Test 1.2 – The Outerpack retained its basic circular pre-test shape except for localized plastic deformation from the 9 meter drop test. Impact zones from the drop test were localized at the nozzle impact locations on the package ends. The Outerpack did not separate after the impact. One bolt failure on the Outerpack lower hinge, top nozzle end was noted. The bottom nozzle damage zone consisted of local crush approximately 10" wide, 22" tall and a maximum crush of approximately 3". The impact encompassed the stacking bracket which caused local buckling at the top/bottom Outerpack joint. A small ripple occurred in the Outerpack at this location. In addition, a tear in the Outerpack end cap measuring 8" wide resulted from the impact. The top nozzle damage zone consisted of local crush approximately 6" wide, 13" long and a maximum crush of approximately 1/4". The relatively small amount of crushing is attributed the stacking bracket impacting the Outerpack in a normal direction and spreading the load more uniformly along the Outerpack length. The internal damage was more substantial than the previous drop test. The polyethylene moderator blocks and aluminum neutron "poison plates" maintained position. The Clamshell doors remained closed, but the top

and bottom head pieces separated from the Clamshell. The separation was caused by material shear-out as the top head connector bolts beared against the bolt slots. The bearing force of the bolts (a shear effect on the top head plate) from impact was of sufficient load to fail the material in the bolt slots for both head pieces. The fuel inspection indicated that no fuel rods had ruptured, and that the position of fuel rods maintained axial location between bottom and top nozzle. The maximum measured fuel envelope compressed from 8.25" after test 1.1 to 8.13", and the maximum measured fuel rod gap increased from 0.188" to 0.625" locally (observed at one or two rods along the envelope). The fuel rod gap expansion was also localized to Grids P, 1, 2, 3, and 4. In addition, Grid 2 failed by means of the weld joint tearing on the grid corner. External and internal results are summarized in Figures 2-116 and 2-117.

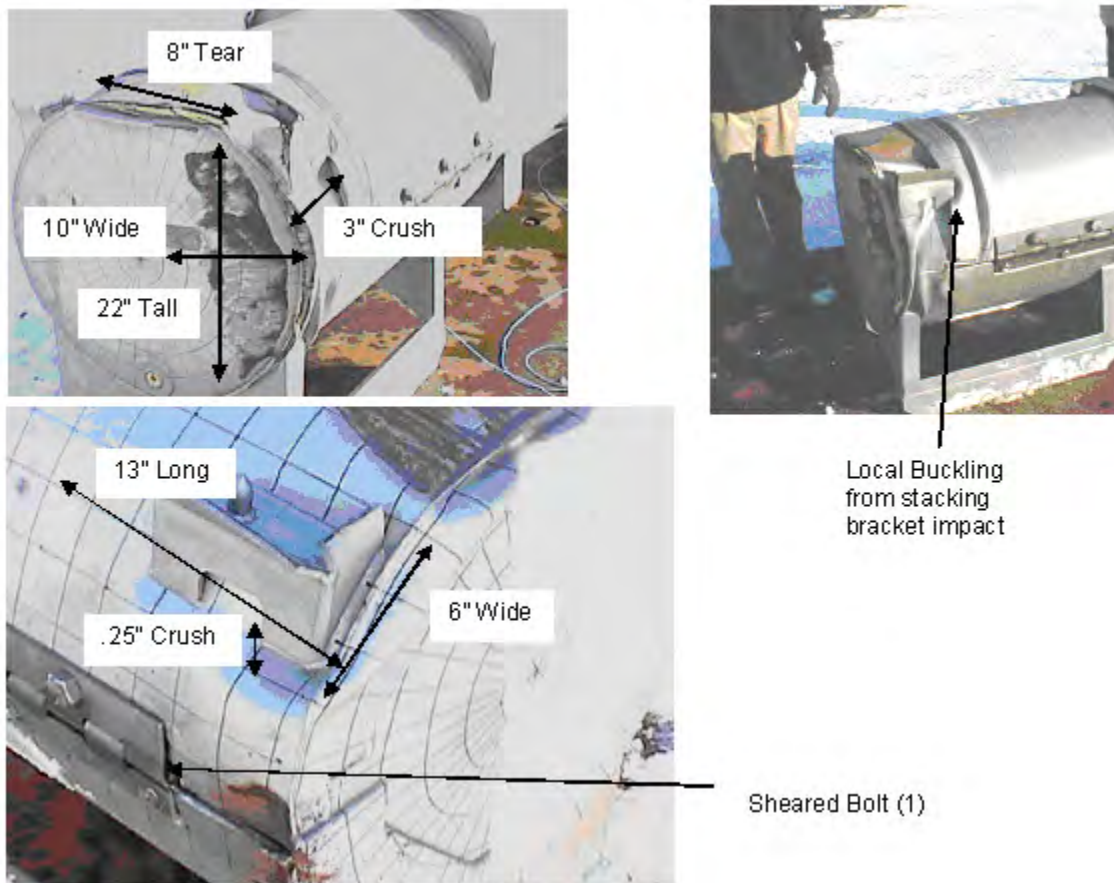


Figure 2-116 Traveller Prototype Exterior After Test 1.2

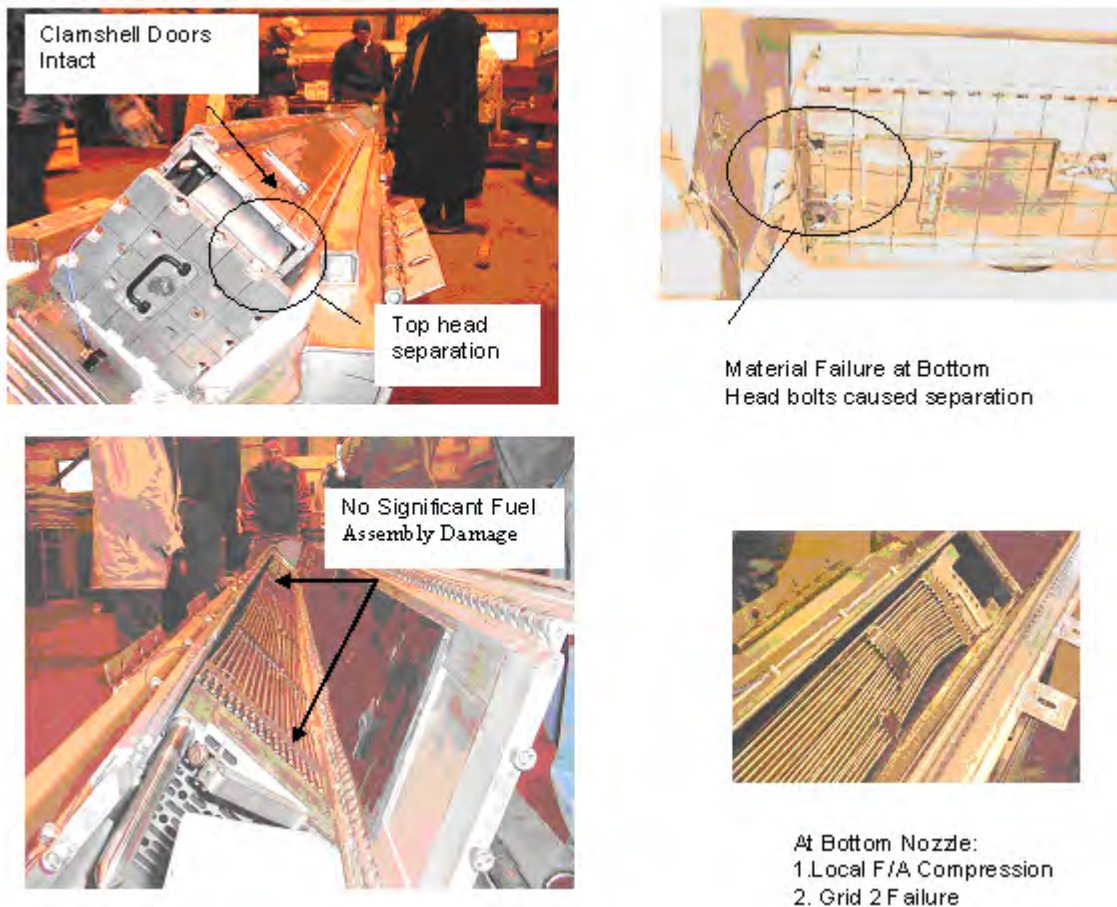


Figure 2-117 Traveller Prototype Interior After Test 1.2

Piezoelectric accelerometers were mounted on the Clamshell and Outerpack for drop tests 1.1 and 1.2. On the Clamshell, one 0-500 g accelerometer was mounted on the top head, and the other 0-500 g accelerometer on the bottom head. On the Outerpack, one 0-1000 g accelerometer was mounted on the underside of the bottom nozzle end (secondary impact location for test 1.1). After test 1.1, the accelerometer on the top head was replaced. The locations of these accelerometers are shown in Figure 2-117A. Figure 2-118 shows the accelerometer traces for the Clamshell from test 1.1. On the primary impact end (top nozzle), the accelerometer saturated in the vertical and axial directions, and the peak lateral deceleration was 453 g. The peak deceleration was 203 g and the resultant vector deceleration sum was 247 g at the secondary impact end (bottom nozzle).

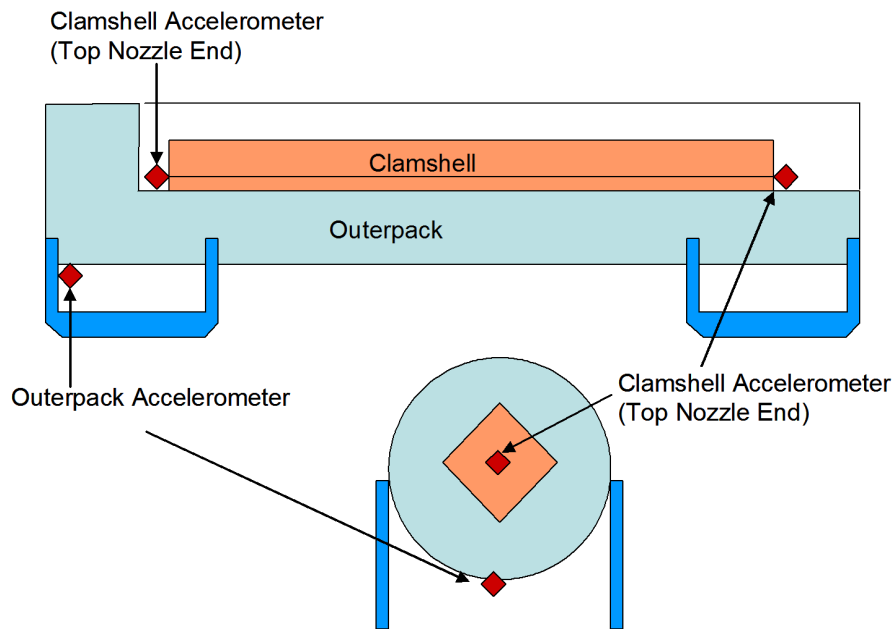


Figure 2-117A Accelerometer Locations on Prototype Drop Test

The 0-1000 g accelerometer trace for the Outerpak is shown in Figure 2-119. The Outerpak vector deceleration sum for the primary impact measured 204 g, and the peak deceleration force measured 191 g in the vertical direction. The slap-down (secondary impact) resulted in decelerations which saturated each directional accelerometer.

The deceleration data for test 1.1 is summarized in Table 2-30.

This page intentionally left blank.

|

Table 2-30 Measured Decelerations in Prototype Test 1.1				
Accelerometer Position	Measured Deceleration Force, g			
	Vertical	Lateral	Axial	Vector Sum
Clamshell T/N end	>500	435	>500	N/A
Clamshell B/N end	205	118	78	247
Outerpack – Primary Impact	191	59	42	204
Outerpack – Slap Down	>1000	>1000	>1000	N/A

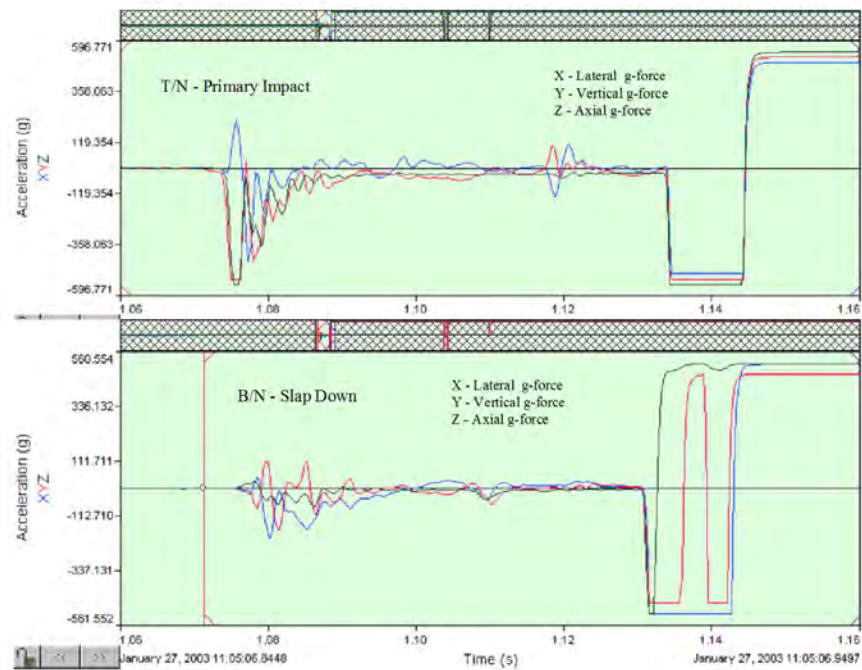


Figure 2-118 Clamshell Accelerometer Trace for Prototype Test 1.1

The top head accelerometer was replaced prior to test 1.2. Due to damaged instrumentation, no data was recorded for the bottom head or the Outerpack. The primary impact occurred on the bottom nozzle end. The top head accelerometer measured the deceleration trace of the primary impact as shown in Figure 2-119. The vector deceleration sum of the primary impact measured 417 g, and the peak deceleration force measured 260 g in the axial direction. The deceleration data for test 1.2 is summarized in Table 2-31.

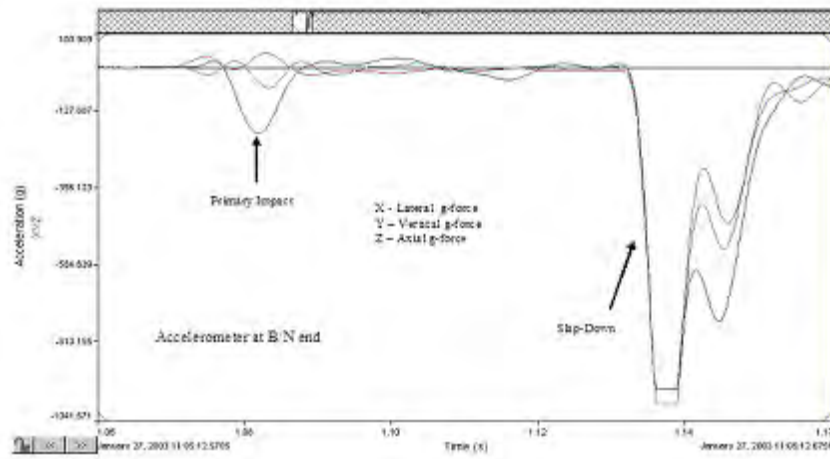


Figure 2-119 Outerpack Accelerometer Trace for Prototype Test 1.1

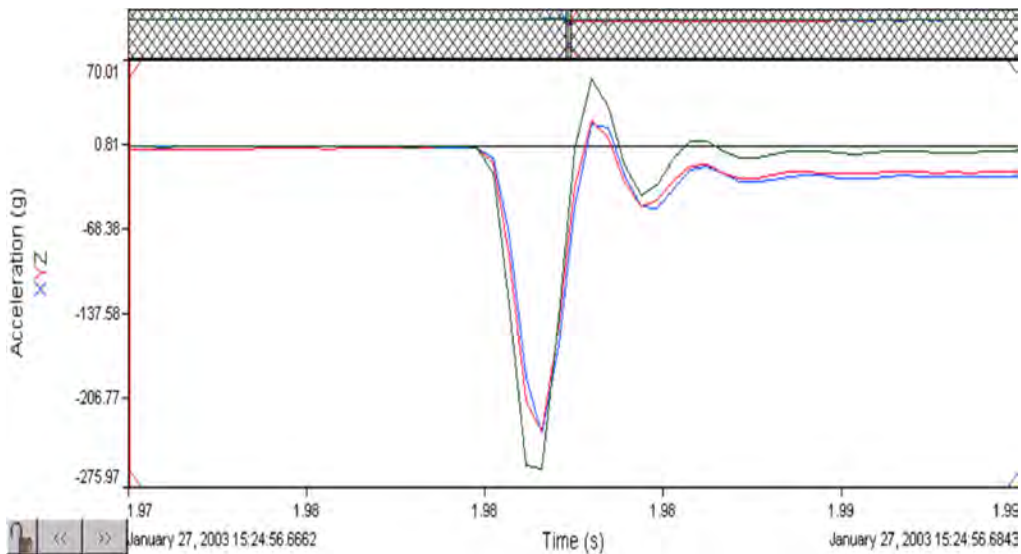


Figure 2-120 Clamshell Accelerometer Trace for Prototype Test 1.2

Table 2-31 Measured Accelerations in Test 1.2				
Accelerometer Position	Measured Deceleration Force, g			
	Vertical	Lateral	Axial	Vector Sum
Clamshell T/N end	230	232	260	417
Clamshell B/N end	No data	No data	No data	N/A
Outerpack – Primary Impact	No data	No data	No data	N/A
Outerpack – Slap Down	No data	No data	No data	N/A

Test 1.3 – The 1-meter pin puncture test resulted in little damage to the package. The outer skin of the Outerpack was locally punched approximately 1.63" and the width of the impact was approximately 10.5" as shown in Figure 2-121. The impact did not perforate the outer skin. The subsequent inspection of the inner side of the Outerpack top indicated that a small dent approximately 7/16" to 1/2" and 15" wide resulted from the pin puncture test. The moderator blocks were not impacted by the pin test.

Test Series 2 – Test series 2 was conducted on January 30th (Table 2-32) and included a 1.2-meter Normal accident condition free drop, a 1-meter pin-puncture test, and a 9-meter free drop test. The package’s test weight was 5057 pounds.

The cumulative external damage from the regulatory drop test sequence was localized to plastic deformation at the impact zones. There was no significant changes in the Outerpack geometry, and no bolt failures were noted. Upon an internal inspection, the pin did not perforate the inner or outer shell. The internal damage was minimal. The fuel assembly’s envelope decreased from 8.418" nominal to 8.25" maximum. Fuel rod gaps globally decreased (the fuel envelope decreased), but local expansion was noted between a few rods with a maximum measured gap of .188" compared to the nominal gap of .122". The polyethylene moderator blocks and aluminum neutron “poison plates” maintained position. The Clamshell doors remained closed, and the modified top head and bottom heads maintained position. A subsequent fuel inspection indicated that no fuel rods had ruptured, and that the axial position of fuel rods maintained location between bottom and top nozzle.

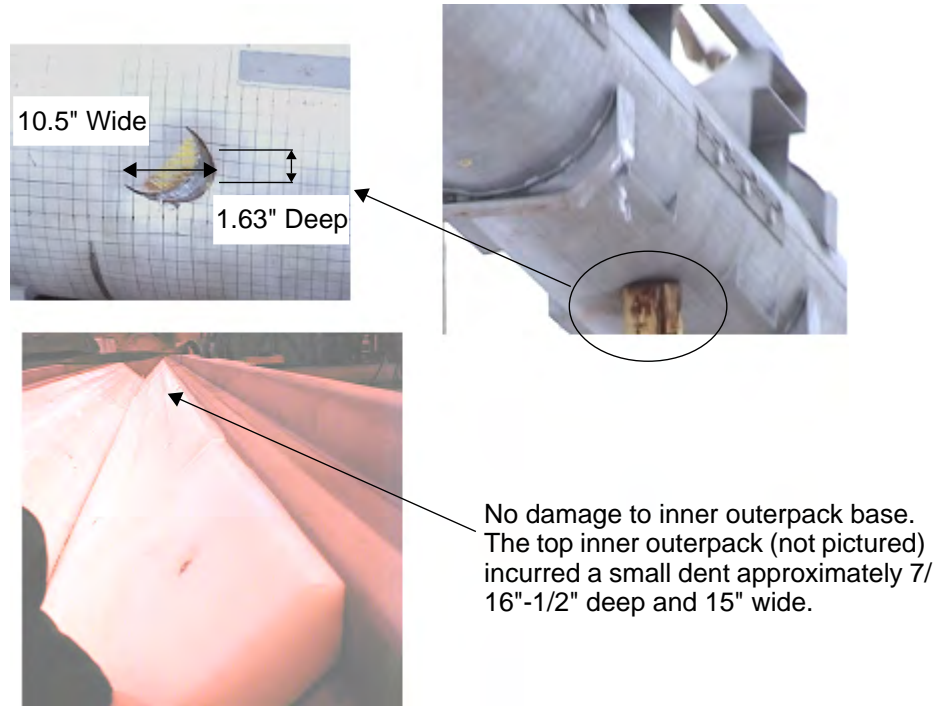
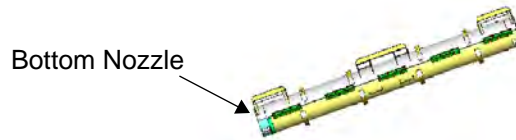


Figure 2-121 Traveller Prototype After Test 1.3

Table 2-32 Prototype Test Series 2			
Test Sequence	Test Pitch Attitude	Test Roll Attitude	Impact Location
2.1) 1.2-m NAC drop	20°	180°	B/N primary impact on OP top
2.2) 1-m Pin-puncture	20°	135°	CG (Axial) on OP topside, T/N end down
2.3) 9-m CG-over-corner	72°	180°	T/N primary impact on OP top

Test 2.1
1.2 m Low Angle
Step Down



Test 2.2
1 m Pin Puncture



Test 2.3
9 m CG over Corner
on Top

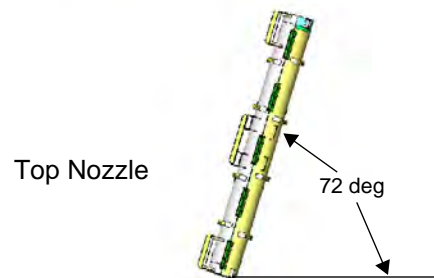


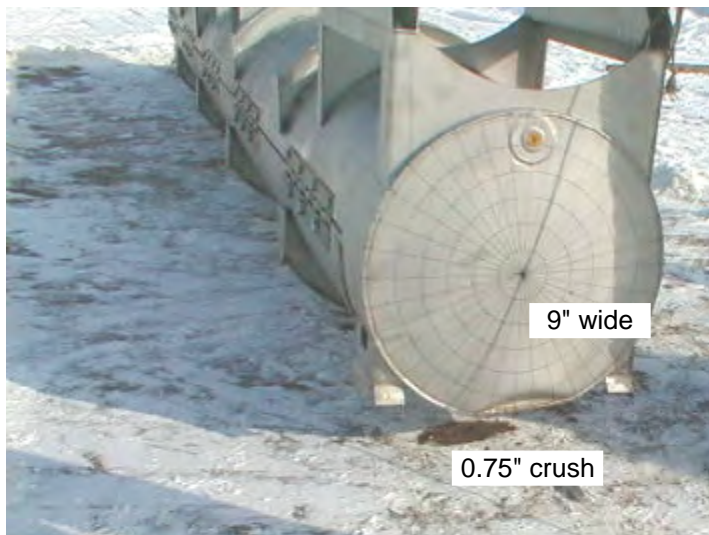
Figure 2-122 Drop Orientations for Traveller Prototype Test Series 2

Test 2.1 – The 1.2 meter normal condition drop test resulted in minimal damage to the Outerpack. The impact created an impact zone at the bottom end 9" wide, 2.5" in axial length, and crushed the Outerpack .75" as shown in Figure 2-123. Two stiffeners near the Outerpack center crushed approximately .75" over a width of 6". The energy absorption of the circumferential stiffeners precluded damage to the secondary impact end (top nozzle).

Test 2.2 – The second test of this drop sequence was a 1-meter pin drop on the package side, Figure 2-122. The 1-meter pin puncture test resulted in little damage to the package. The outer skin of the Outerpack was locally punched in approximately 2" as shown in Figure 2-124. The impact punch zone was 10" tall and the width of the impact was approximately 14". The impact did not perforate the outer skin.

Test 2.3 – The 9-meter drop test resulted in local damage to the primary impact region (top nozzle end). The secondary impact region was in the vicinity of the impact region of the 1.2-meter free drop and did not result in additional damage. From Figure 2-125, the damage zone was approximately 25" wide, 12" tall, and produced a crush zone approximately 9" axially. Due to the impact attitude, the Outerpack top tended to shear relative to the Outerpack bottom. A gap approximately 1" resulted from the impact, but did not comprise the Outerpack closure. No bolt failures were noted.

In general, the test sequence resulted in minimal Clamshell and fuel damage. The top nozzle end of the Clamshell was slightly bowed in a localized region at the top nozzle end (Figure 2-126), but did not result in fuel expansion. The modified top and bottom head pieces remained intact, and no shock mount failures were noted. The fuel inspection indicated that the assembly had moved axially toward the top nozzle 3-3/8" as a result of the spacer movement. There was no significant fuel damage at the bottom nozzle. Also the top nozzle region of the fuel assembly incurred some local damage. The guide pins buckled. Four (4) fuel rods moved axially (maximum of 1"), but did not extend beyond the neutron poison plates. The fuel inspection also indicated that no fuel rods had ruptured. The fuel rod gap measurements indicated the maximum measured fuel rod gap increased from 0.122" nominally to 0.188" locally (observed at one or two rods along the envelope). The measured fuel envelope compressed from 8.418" nominally to 8.25" maximum. The moderator blocks did not move from their original position even though two studs were sheared off. The pin-puncture test produced a 24" long by 5/8" deep dent on the inner Outerpack surface.



The axial damage zone is approximately 2.5".

No damage at T/N end.



Stiffeners crushed about .75" and also dented OP about .75". Crush width 6".

Figure 2-123 Traveller Prototype After Test 2.1

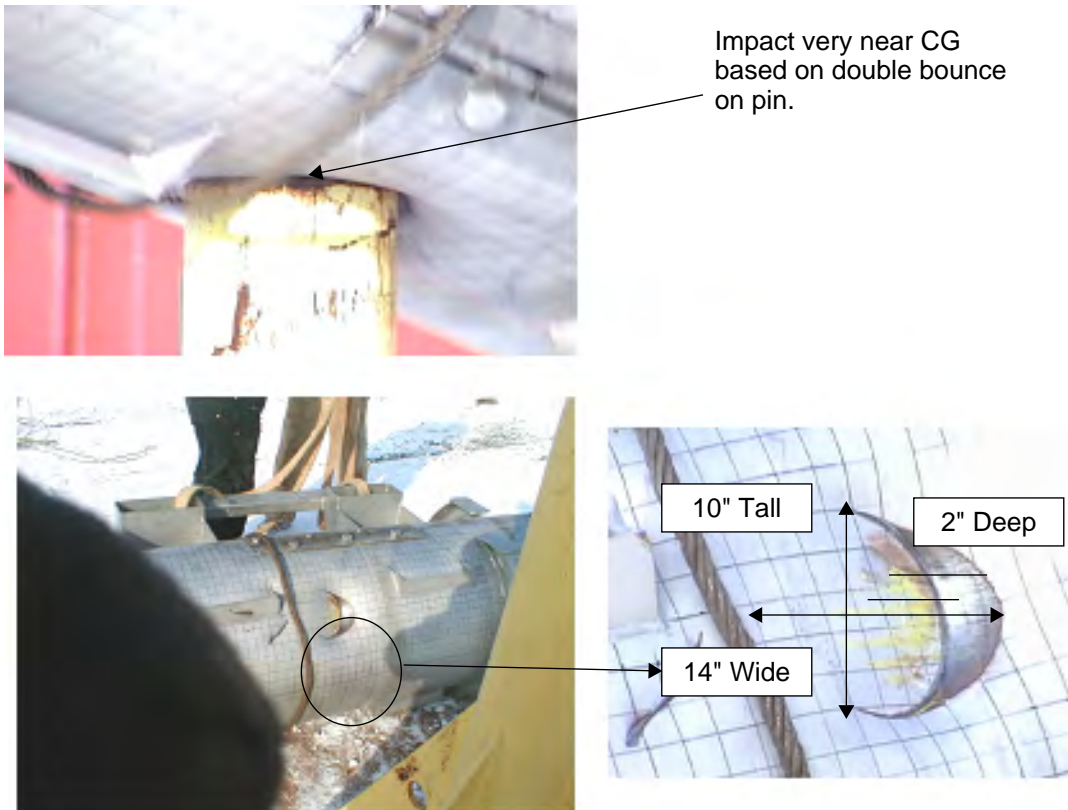


Figure 2-124 Traveller Prototype After Test 2.2

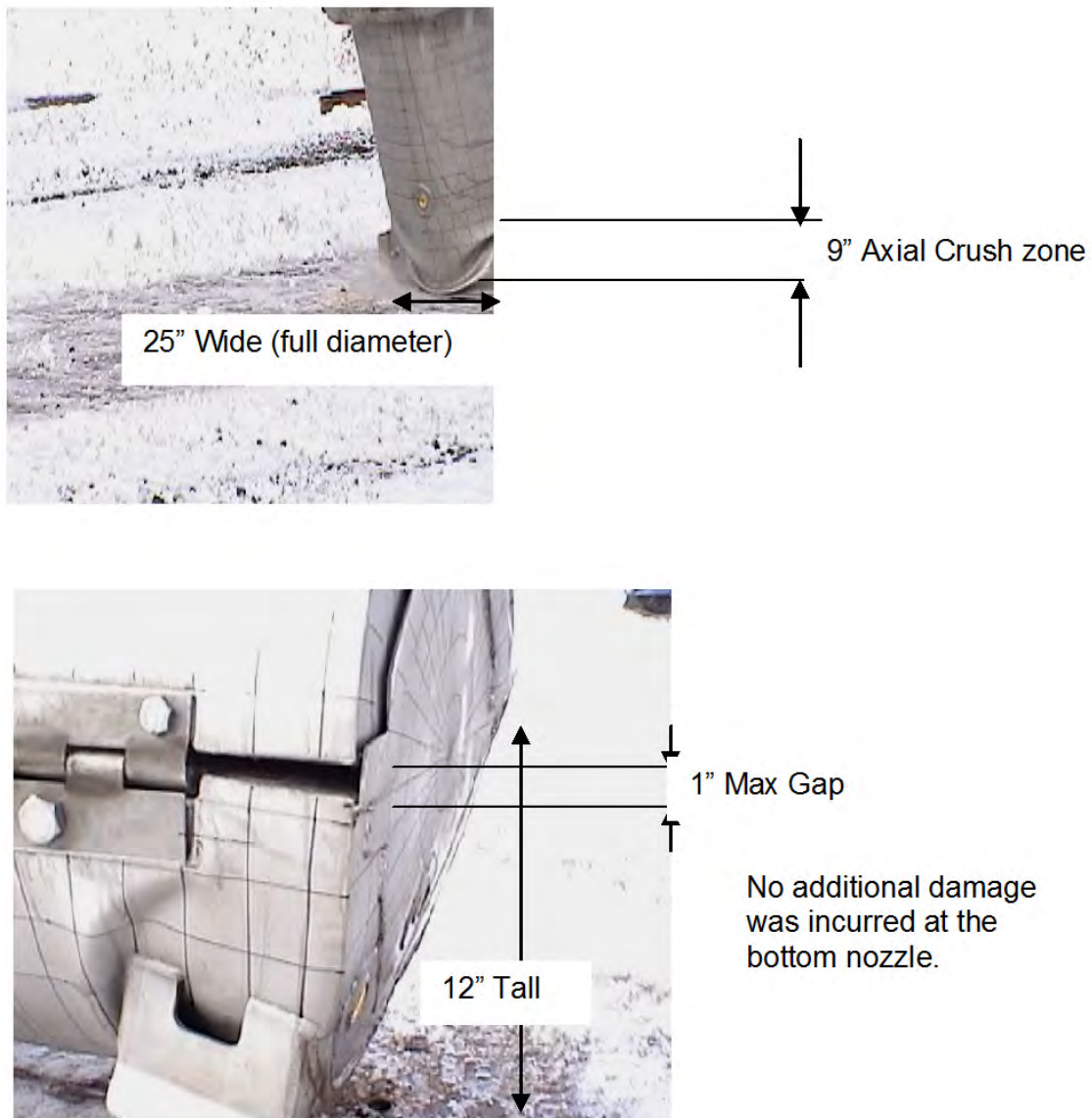


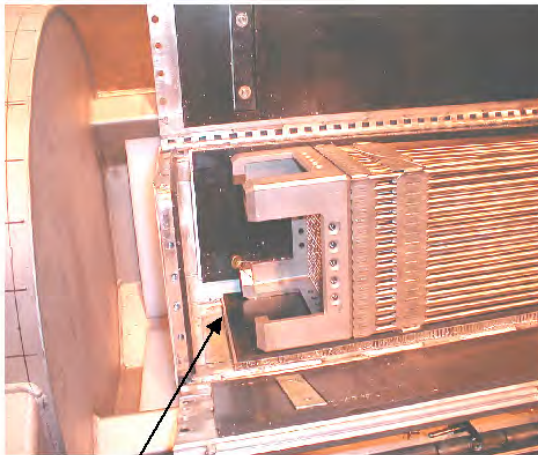
Figure 2-125 Traveller Prototype After Test 2.3



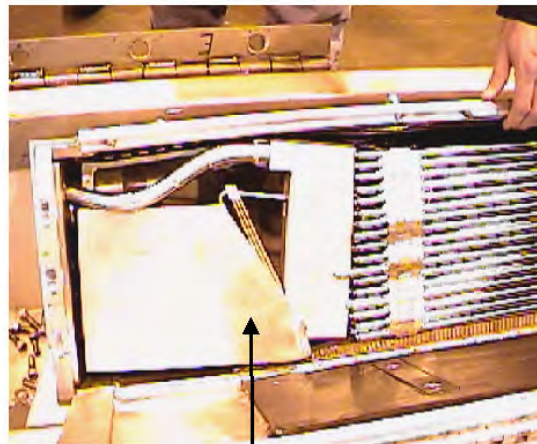
The modified top and bottom head maintained position.

The clamshell remained closed and 3 pins failed.

The T/N end bowed out about 3/16" over a 12" length.



Spacer and fuel moved 3-3/8".
No fuel damage at Bottom Nozzle.



Rod moved axially 1" maximum,
but within absorber plate region.

Figure 2-126 Traveller Prototype Interior After Test Series 2

Test Series 3 – Test Series 3 consisted of three 9-meter drop tests conducted to evaluate design features of the Outerpack after modifications to the Clamshell and Outerpack. The test sequence and measured drop attitudes are summarized in Table 2-33. The test series employed was Prototype 2 that had been used for test Series 2. The purpose of this test series was to evaluate design features and evaluate design margin. External damage assessments were performed following each supplementary drop test, and a general internal assessment was conducted after the completion of test 3.3. However, the inspections for this test series were

not intended for use in nuclear criticality safety analysis. Prior to test 3.1, the following modifications were made to the package:

- Removed 1 bolt from each of the 5 top Outerpack hinges (reduced bolt count by 33%).
- Removed sheet metal from endcap inner surface
- Removed 2 of the 5 pins that secure each Clamshell clip

Test Sequence	Test Pitch Attitude	Test Roll Attitude	Impact Location
3.1) 9-m Axial End drop	90°	0°	B/N impact
3.2) 9-m Flat drop	0.5°	0°	Impact on OP feet
3.3) 9-m Side drop	0°	270°(90°CCW)	Impact on OP hinges

Figure 2-127 shows that the Outerpack sustained minimal damage. The Outerpack remained closed and no bolts failed after the completion of drop test series 3. The first drop test of this series resulted in slight crushing (approximately 1-5/8" deep) at the bottom nozzle end. The crushed circumferential stiffeners precluded excessive Outerpack damage as the package slapped down after the axial drop. Drop test 3.2 crushed the feet and forklift supports completely, but otherwise did not compromise the Outerpack structural integrity. The direct hinge impact (test 3.3) did not fail any hinges or result in any substantial damage to the Outerpack.

The cumulative overall damage to the Clamshell was also minimal as shown in Figure 2-127. The Clamshell retained its geometry, no Clamshell clip pins failed, and no shock mount failures were noted. The notable Clamshell damage was located at the bottom head, which was separated from the Clamshell by the impacting fuel, Figure 2-128. It is presumed that the 3-3/8" gap from the Clamshell bottom plate to the base of the fuel assembly bottom nozzle provided sufficient distance for the fuel assembly to attain enough kinetic energy to separate the Clamshell bottom head upon impact.

The fuel was in good condition. No measurements were taken since this test series was qualitative in nature.



Figure 2-127 Traveller Prototype Clamshell and Bottom Impact Limiter After Test Series 3



Figure 2-128 Traveller Prototype Clamshell and Bottom Impact Limiter After Test Series 3

Minor design modifications were recommended for the Traveller package based on this testing. The top and bottom heads required additional bolting to preclude Clamshell separation. The number of Clamshell clip retaining pins (and clips) could be reduced. It was found that sufficient design margin against material failure existed allowing the Outerpack gage metal can be reduced slightly in thickness. In addition, the number of Outerpack bolts can be reduced on the top hinge by at least 1/3.

2.12.5.2 Qualification Test Unit Drop Tests

The following section delineates the second of three (3) full-scale testing campaigns of the Traveller development program. This campaign utilized two units called Quality Test Units, or QTU-1 and 2. A total of two (2) QTUs were built and tested, with minor changes to improve burn performance incorporated into the second QTU article.

2.12.5.2.1 QTU Test Series 1

Test series 1 was conducted on the afternoon of September 11 and included a 50 inch (1.27 m) slap down, a 33.3 feet (10.15 m) center of gravity-over-corner free drop test, and a 42 inch (1.07 m) pin-puncture test. The package’s test weight was 4793 pounds (Table 2-34). The internal inspection of the fuel assembly was conducted after completion of the fire test on September 16, 2003.

Test Weights	Nominal	Actual
Weight of Outerpack (Empty):	3033 lb	3032 lb
Weight of Clamshell (Empty):	425 lb	400 lb
Weight of package (Empty):	3477 lb	3432 lb
Total package test weight:	5422 lb	4793 lb

Test series 1 was conducted on the afternoon of September 11 and included a 50.75 inch (1.29 m) slap down, a 33.3 feet (10.15 m) free drop test, and a 42 inch (1.07 m) pin-puncture test. QTU1 pre-test data and observations are shown in Form 1A. The test sequence and measured drop attitudes are summarized in Table 2-35 and shown in Figure 2-129. A pitch angle of 72 degrees was measured along the outerpack surface for Test 1.2. The angle of 108 degrees should be located as shown in Figure 2-129. The reference to “hinge side” in Test 1.3 indicates the package side that pivots, rather than the actual hinge. The impact point of Test 1.3 (Figure 2-132) was on the top nozzle end and on the pivot (left) side of the package. A fuel damage assessment was conducted after the completion of the hypothetical fire condition test conducted on September 16, 2003 at the South Carolina Fire Academy near Columbia, SC.

The Outerpack retained its basic circular pre-test shape except for localized plastic deformation at the top nozzle end accumulated from the drop test series. No bolts failed on the Outerpack after completion of the drop test series. The Outerpack did not separate after any impacts, and the pin did not perforate the inner or outer shell. The most notable Outerpack damage was the resulting joint tear of approximately 1-1/8" at the Outerpack corner located at the top, left hinge side. The fuel assembly damage was minimal. At the top nozzle portion, the fuel assembly locally expanded from 8.375" nominal to 8.625" maximum over a length of approximately 2-3". The fuel rod gaps were globally unchanged but local expansion was noted between one rod near Grid 10 with a maximum measured gap of 0.250". The resulting measured maximum local pitch was 0.625 inches. Three rods were found to be in contact with each other while the remaining rods

were nominally positioned. Intermediate grids 2-7 were buckled locally, but the fuel rod envelope was unchanged. The bottom nozzle portion of the fuel assembly was slightly compressed from 8.375" nominally to 8.250" measured. Based on the condition of the fuel assembly, the Clamshell was concluded to have performed successfully. The fuel inspection also indicated that no fuel rods had visibly ruptured, and that the axial position of fuel rods maintained location between bottom and top nozzle.

Test Article ID	F/A Type	Test Sequence	Test Pitch Attitude	Test Roll Attitude	Design Feature Tested
QTU1	17x17 XL	P1.1)1.2 m, NAC, Low angle ¹	10°	180°	Operations of hinges/doors
		P1.2)9 m CG-over-Corner ¹	108°	90°	OP hinge shear, CS latches
		P1.3)1 m Pin-puncture ¹	83°	90°	Joint Integrity – Fire test

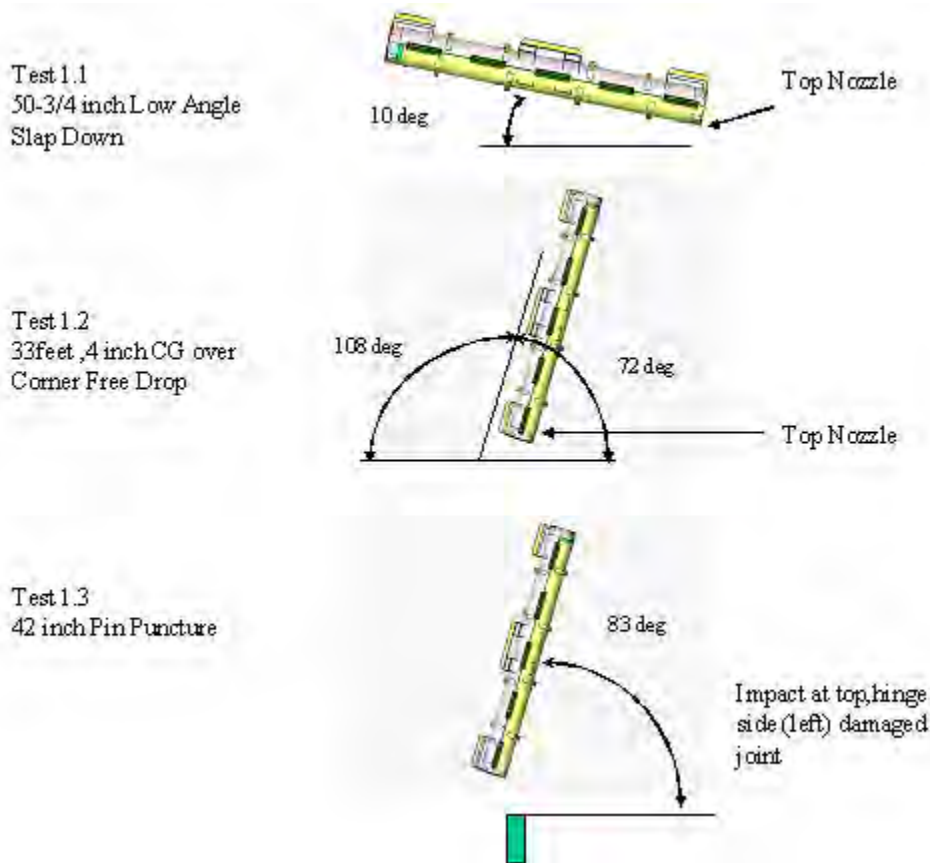


Figure 2-129 Drop Orientation for QTU Test Series 1

Test 1.1 – The 50.75 inches (1.29 m) drop onto the Outerpack lid was performed first. As shown in Figure 2-130, this drop resulted in a small indentation in the outer skin of the Outerpack.

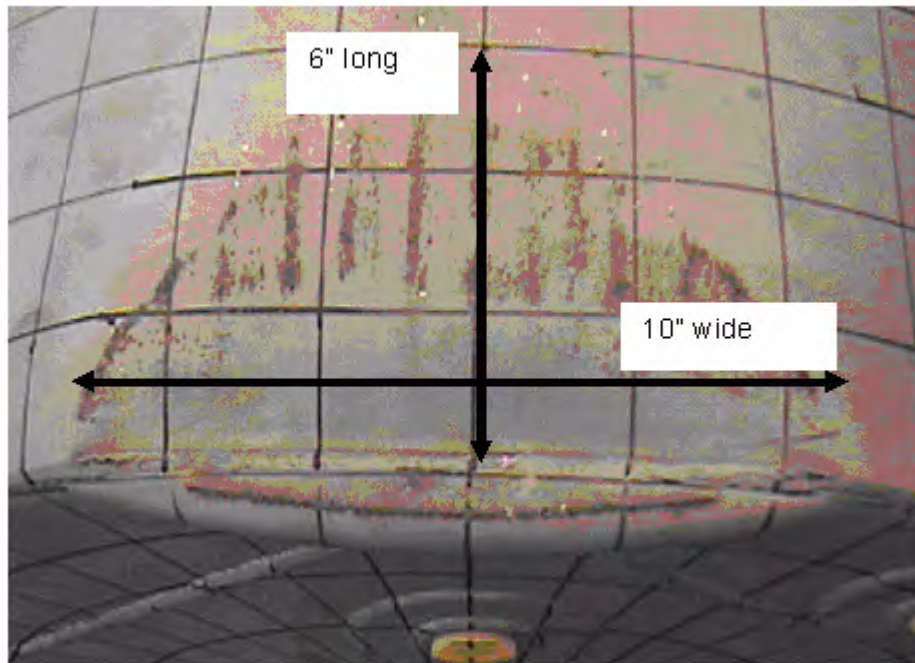


Figure 2-130 QUTU-1 Outerpack After Test 1.1

Test 1.2 – The 33.3-foot free drop resulted in localized damage to the top nozzle end region. One of the hoist rings was sheared off as a result of the impact, Figure 2-131. The impact opened a small tear at the top and bottom Outerpack seam (also in circled region). The entire 25" diameter face of the top nozzle end was dented approximately 3-1/2". The stiffeners were also dented across their tops, but were intact. Two welds located at the bottom nozzle end stiffener were broken, but this did not compromise the stiffener position.

Test 1.3 – The pin puncture test was located in the top left (hinge) side of the Outerpack top nozzle end. The objective of the test was attempt to increase the Outerpack separation incurred by the previous 33.3-ft drop. Additional tearing of the joint was noted which resulted in measured tear of approximately 1-1/8". The indentation resulting from the pin puncture was approximately 1-1/2" deep (Figure 2-132).

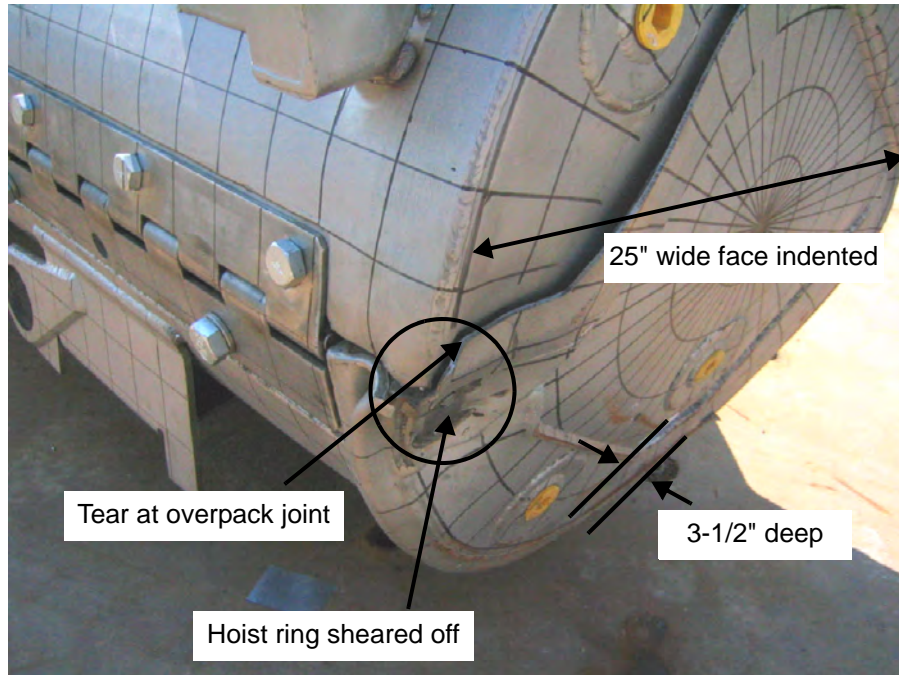


Figure 2-131 QTU-1 Outerpack After Test 1.2

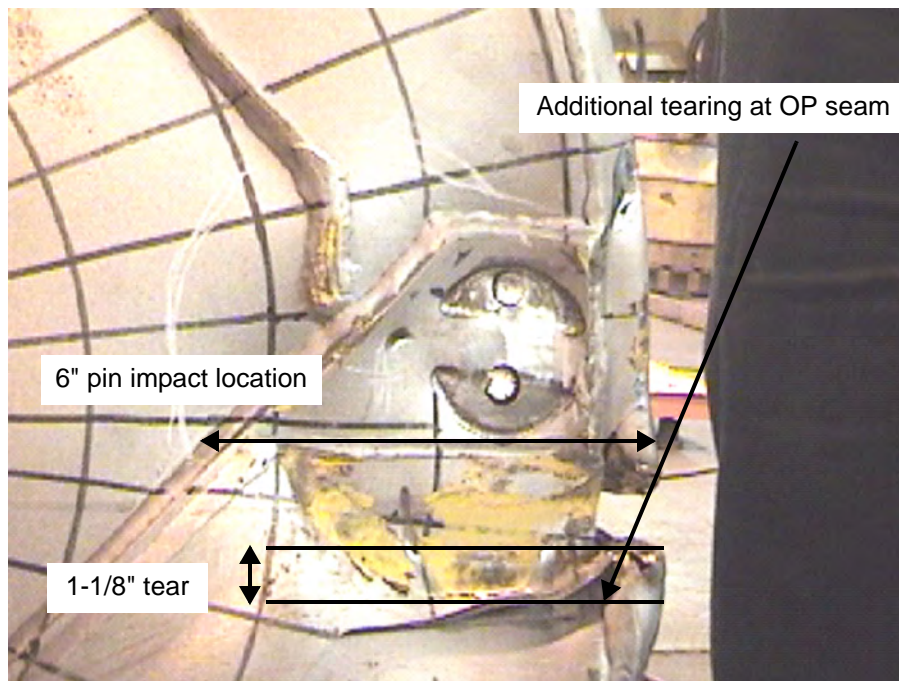


Figure 2-132 QTU-1 Outerpack After Test 1.3

QTU-1 was not opened until after the fire test. The Clamshell and fuel assembly were examined for damage at that time. The fuel assembly of QTU-1 was essentially undamaged, Figure 2-133. The most damage occurred at the top nozzle section where an area of approximately 2-3" in length increased from 8.375" nominal to 8.625". Grid 10 was torn, and all other grids were buckled but intact. The nozzles were essentially undamaged. The impact resulted in buckling of the core line-up pins attached to the top nozzle. The fuel rods appeared visibly undamaged.

The fuel assembly in QTU-1 was measured before the test and after the burn test at locations shown in Figure 2-134. Table 2-36 provides the pretest dimensions. Tables 2-37 and 2-38 provide the post test dimensions.

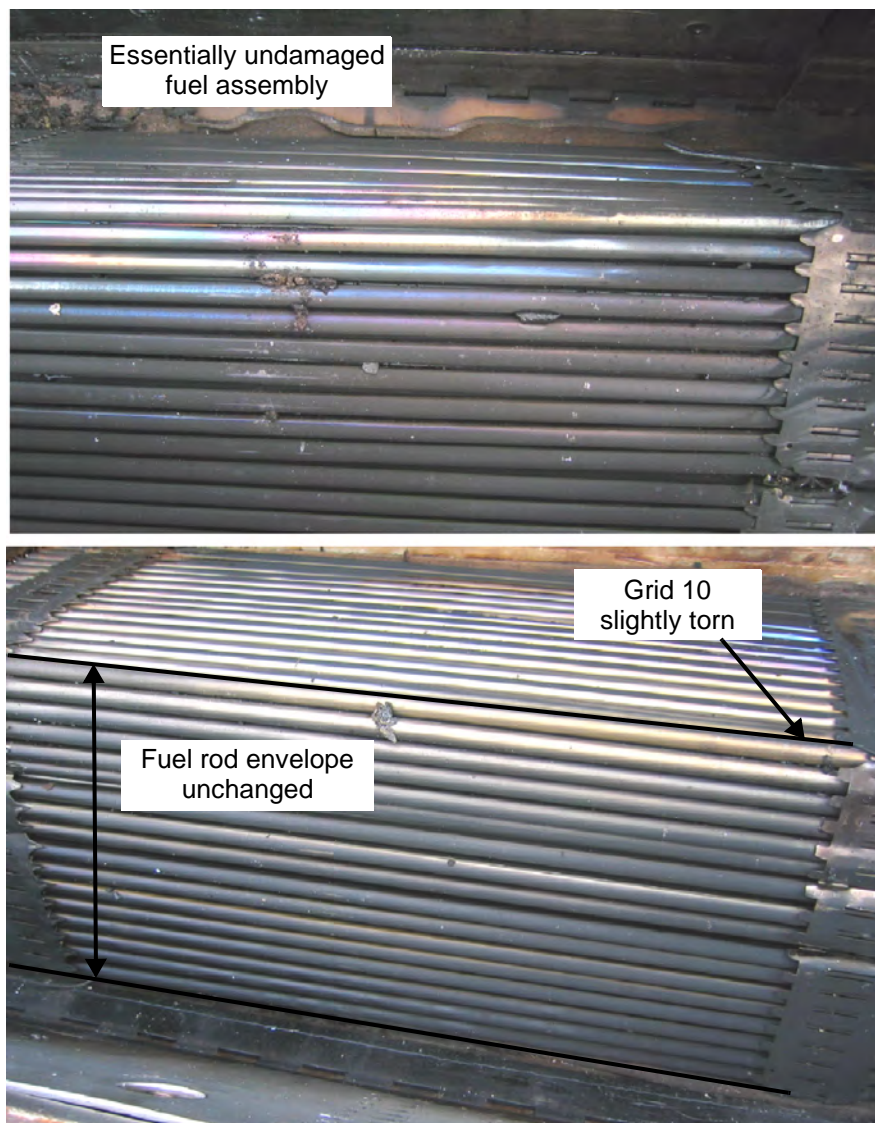


Figure 2-133 QTU-1 Fuel Assembly After Drop and Burn Tests

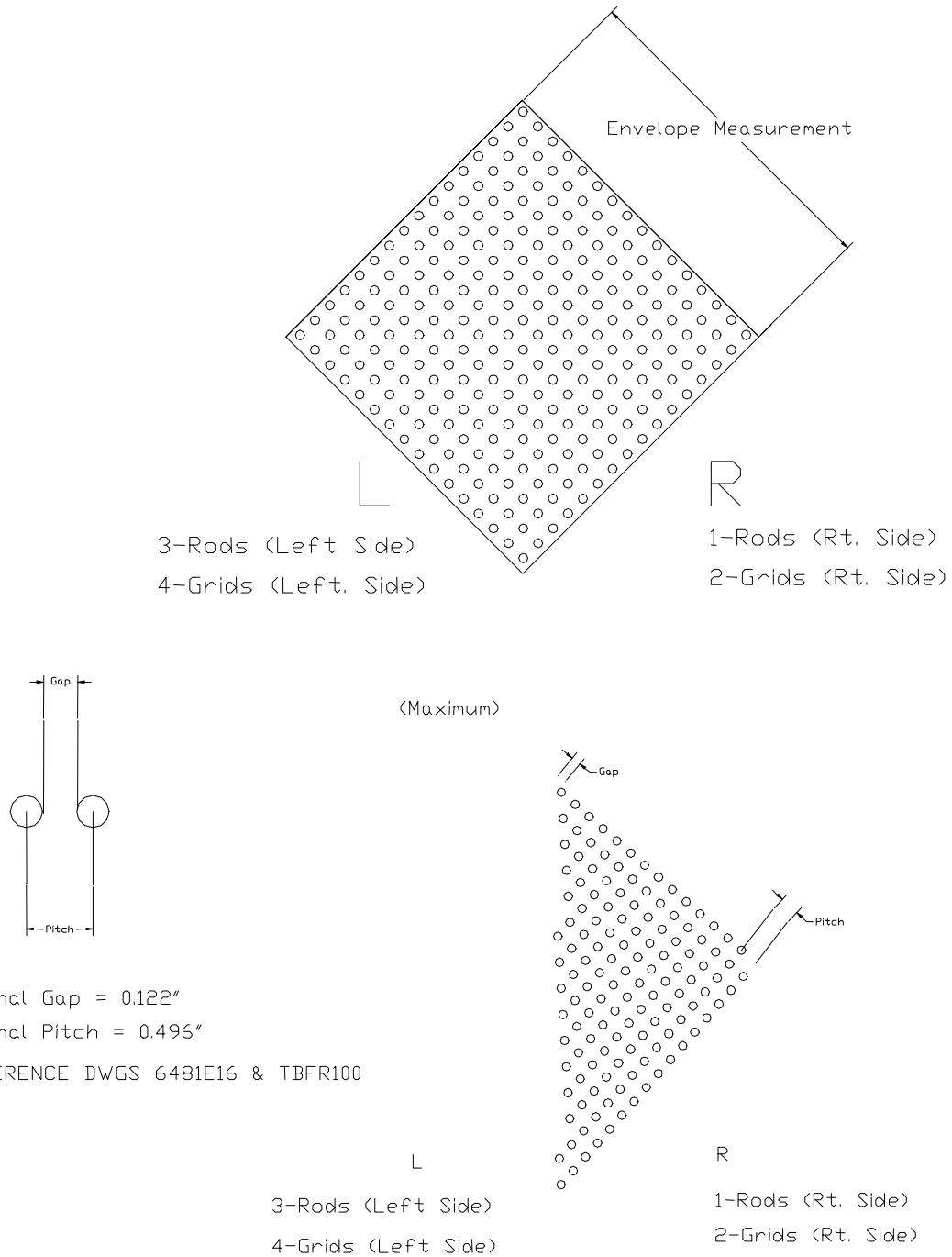


Figure 2-134 Measurements Made on QTU-1 Fuel Assemblies Before and After Drop Tests

Table 2-36 Key Dimensions of QTU-1 Fuel Assembly Before Testing			
Fuel Assembly ID: 503007, B/N # 02-6703			
F/A Location	Fuel Envelope (inches)	Gap (inches)	Pitch (inches)
B/N – Grid 1	1 – 8.330 2 – 8.455 3 – 8.250 4 – 8.446 8.375 Meas. Nominal*	L – 0.122 R – 0.123 0.125 Meas. Nominal*	L – 0.497 R – 0.498 0.500 Meas. Nominal*
Grid 1 – Grid 2	1 – 8.338 2 – 8.418 3 – 8.326 4 – 8.415 8.375 Meas. Nominal*	L – 0.124 R – 0.124 0.125 Meas. Nominal*	L – 0.499 R – 0.499 0.500 Meas. Nominal*
Grid 2 – Grid 3	8.375 Meas. Nominal*	L – 0.123 R – 0.120 0.125 Meas. Nominal*	L – 0.498 R – 0.495 0.500 Meas. Nominal*
Grid 3 – Grid 4	8.375 Meas. Nominal*	0.125 Meas. Nominal*	0.500 Meas. Nominal*
Grid 4 – Grid 5	8.375 Meas. Nominal*	0.125 Meas. Nominal*	0.500 Meas. Nominal*
Grid 5 – Grid 6	8.375 Meas. Nominal*	0.125 Meas. Nominal*	0.500 Meas. Nominal*
Grid 6 – Grid 7	8.375 Meas. Nominal*	0.125 Meas. Nominal*	0.500 Meas. Nominal*
Grid 8 – Grid 9	8.375 Meas. Nominal*	0.125 Meas. Nominal*	0.500 Meas. Nominal*
Grid 9 – Grid 10	8.375 Meas. Nominal*	0.125 Meas. Nominal*	0.500 Meas. Nominal*
Grid 10 – T/N	8.375 Meas. Nominal*	0.125 Meas. Nominal*	0.500 Meas. Nominal*
Note: * Measured nominal values were measured to nearest 1/8".			

Table 2-37 QTU-1 Fuel Assembly Grid Envelope After Testing			
Fuel Assembly Envelope Inspection Table			
Location	Envelope Dimension, Inches		Maximum Fuel Rod Gap from Form 1F (Nominal Gap = 0.122")
	Left Side, LS	Right Side, RS	
Between B/N and Grid 1	8.125	8.250	0.250
Between Grids 1 and 2	8.125	8.000	0.250
Between Grids 2 and 3	8.000	8.250	0.188
Between Grids 3 and 4	8.375	8.375	0.125
Between Grids 4 and 5	8.375	8.375	0.125
Between Grids 5 and 6	8.375	8.375	0.188
Between Grids 6 and 7	8.375	8.375	0.188
Between Grids 7 and 8	8.375	8.375	0.188
Between Grids 8 and 9	8.375	8.375	0.188
Between Grids 9 and 10	8.375	8.500	0.250
Between Grid 10 and T/N	8.500	8.625	0.250
MAXIMUM VALUE	8.500	8.625	0.250

Fuel Rod Pitch Inspection Table			
Location	Maximum Gap, inches		Maximum Pitch
	Left Side, LS	Right Side, RS	
Between B/N Grid 1	0.250	0.188	0.625
Between Grids 1 and 2	0.250	0.250	0.625
Between Grids 2 and 3	0.188	0.188	0.563
Between Grids 3 and 4	0.125	0.125	0.500
Between Grids 4 and 5	0.125	0.125	0.500
Between Grids 5 and 6	0.125	0.188	0.563
Between Grids 6 and 7	0.125	0.188	0.563
Between Grids 7 and 8	0.188	0.188	0.563
Between Grids 8 and 9	0.188	0.188	0.563
Between Grids 9 and 10	0.125	0.250	0.625
Between Grid 10 and T/N	0.125	0.250	0.625
MAXIMUM VALUE	0.250	0.250	0.625

2.12.5.2.2 QTU Test Series 2

Test series 2 was conducted on the afternoon of September 11 and included a 50 inch (1.27 m) slap down, a 33.4 feet (10.18 m) free drop test, and a 42 inch (1.07 m) pin-puncture test. The test sequence and measured drop attitudes are summarized in Table 2-39 and shown in Figure 2-135. Weights for QTU-2 are recorded on Table 2-40.

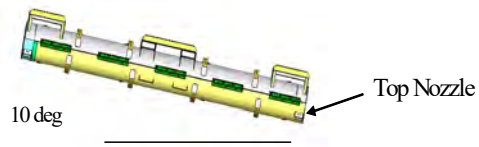
Test Article ID	F/A Type	Test Sequence	Test Pitch Attitude	Test Roll Attitude	Design Feature Tested
QTU2	17x17 XL	P2.1) 1.2-m, NAC, Low angle ⁽¹⁾	10°	180°	Operations of hinges/doors
		P2.2) 9-m End (B/N) ⁽¹⁾	90°	0°	Lattice exp., FR axial position
		P2.3) 1-m Pin-puncture ⁽¹⁾	22°	0°	OP stiffness
Note: (1) Actual test heights are reported in Figure 163 and post-test forms.					

Table 2-40 QTU-2 Weights		
Test Weights	Nominal	Actual
Weight of Outerpack (Empty):	3033 lb	2611 lb
Weight of Clamshell (Empty):	425 lb	400 lb
Weight of package (Empty) :	3477 lb	3011 lb
Total package test weight:	5422 lb	4778 lb

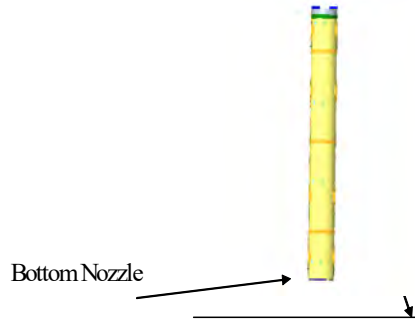
The Outerpack retained its basic circular pre-test shape except for localized plastic deformation accumulated from the 1.2 meter and 33.4 foot (10.18m) drop test. Damage zones from the drop test were localized to impact locations on the package end. The Outerpack did not separate after the impact, and no bolt failures on the Outerpack hinges were noted. From Figure 2-136, the 1.2 meter free drop resulted in a local crush zone at the top nozzle end measuring approximately 9-1/2" wide, 6" long axially and 7/8" deep. The Outerpack damage from the 33.4 foot drop, Figure 2-136 consisted of local crumple zone approximately 7" long maximum as demonstrated by the buckled Outerpack at the bottom nozzle end. A small weld tear was noted on each side of the Outerpack where the leg stand is connected to the end cap. The pin puncture damage was isolated to the impact point located at the package center-of-gravity. From As shown in Figure 2-138, pin puncture damage zone was an indented oval of measured dimensions 9" long by 6" wide and 2-7/8" deep.

The Clamshell was essentially undamaged from the drop test series, Figure 2-138. No change in the Clamshell grid markings were noted indicating that the Clamshell had not bulged outward (nor compressed). The polyethylene moderator blocks and aluminum neutron "poison plates" maintained position. The fuel assembly was found to be within the confines of the Clamshell and intact. The impact resulted in a slight ovalizing of the fuel assembly at the bottom nozzle region. Figure 2-139 shows the approximate angle of ovality is 118° at Grid 1 location. Localized expansion from 8.375" nominal to 8.625" was measured over a length of approximately 12" (30.48cm). The maximum fuel rod gap measured was 0.722 inches resulting in a maximum measured fuel rod pitch of 1.097 inches. The top nozzle portion of the tested fuel assembly was essentially undamaged. The axial position of fuel rods maintained location between bottom and top nozzles.

Test 2.1
50 inch Low Angle
Slap Down



Test 2.2
33 feet, 5 inch End
on Bottom Nozzle



Test 2.3
42-1/2 inch Pin Puncture



Figure 2-135 QTU Test Series 2 Drop Orientations

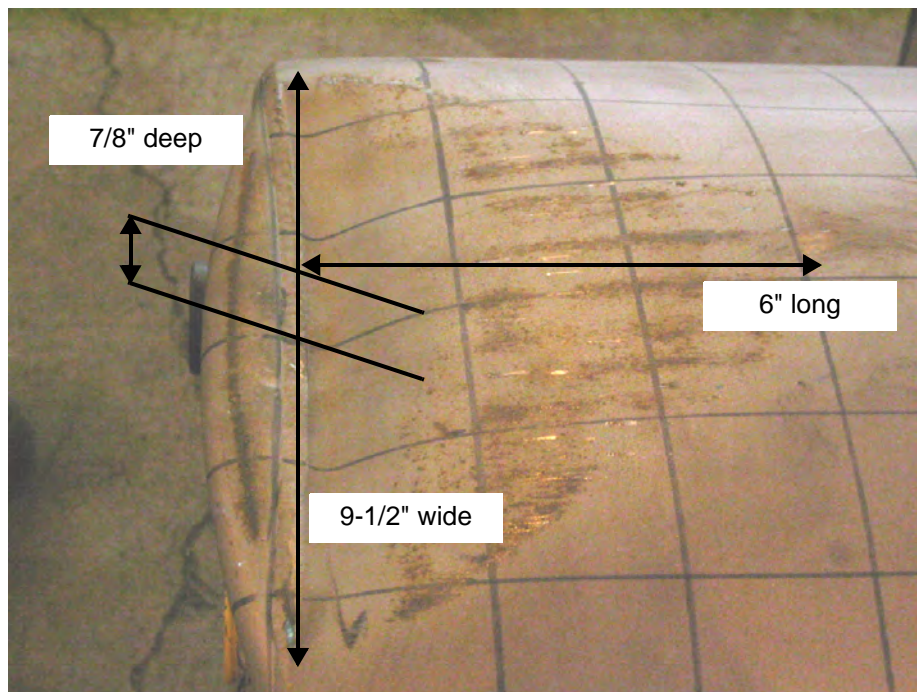


Figure 2-136 QTU Outerpack After Test 2.1

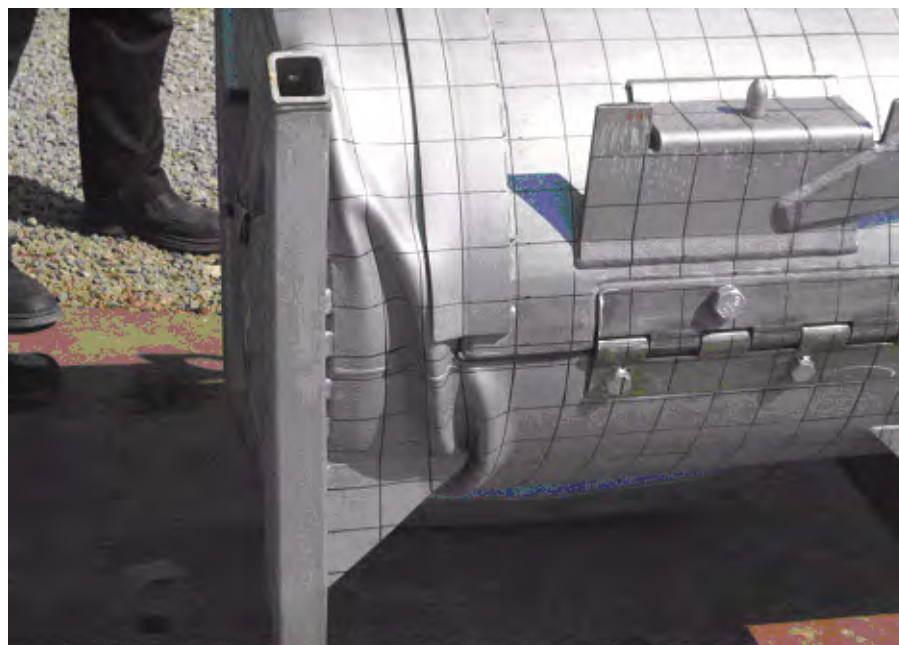


Figure 2-137 QTU Outerpack After Test 2.2

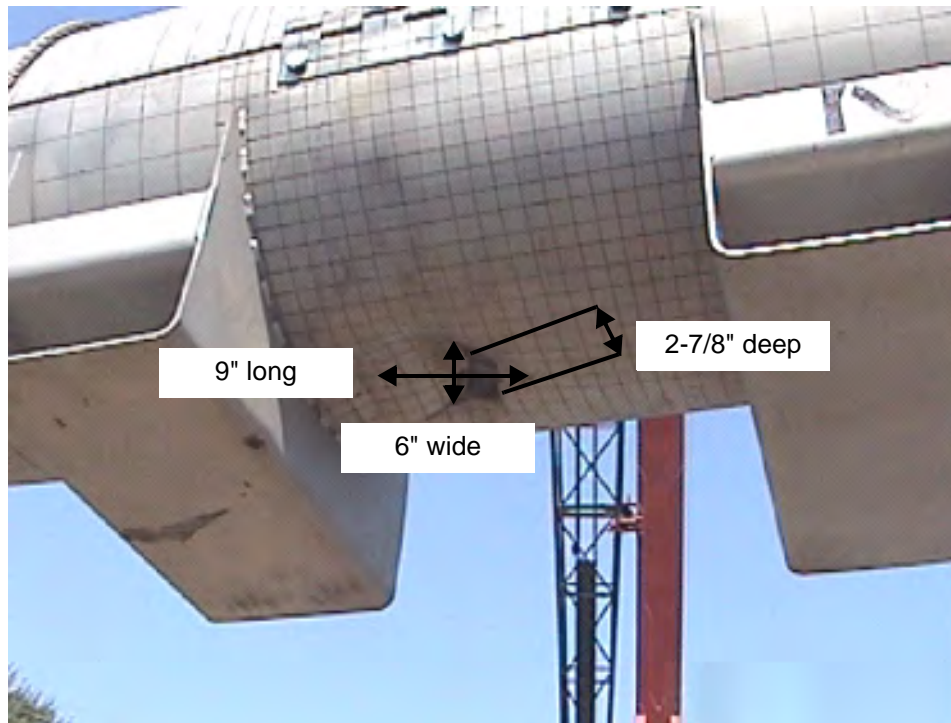


Figure 2-138 QTU Outerpack After Test 2.3

The fuel assembly in QTU-1 was measured before the test and after the burn test at locations shown in Figure 2-134 above. Table 2-41 provides the pretest dimensions. Tables 2-42 and 2-43 provide the post test dimensions.

The post-test inspections concluded that the tested configuration of the Traveller Outerpacks and Clamshells were acceptable. Furthermore, the tests concluded that Test Series 1 imparted the most damage to the Outerpack, and Test Series 2 imparted the most damage to the fuel assembly. Also, testing demonstrated that the Traveller Outerpack is suitable for transport with two top Outerpack bolts per hinge. The post-test geometry of the fuel assemblies for both test series was also acceptable.

In summary, testing demonstrated the Traveller package is suitable for compliance to normal and hypothetical mechanical drop test conditions described in 10 CFR 71 and TS-R-1.

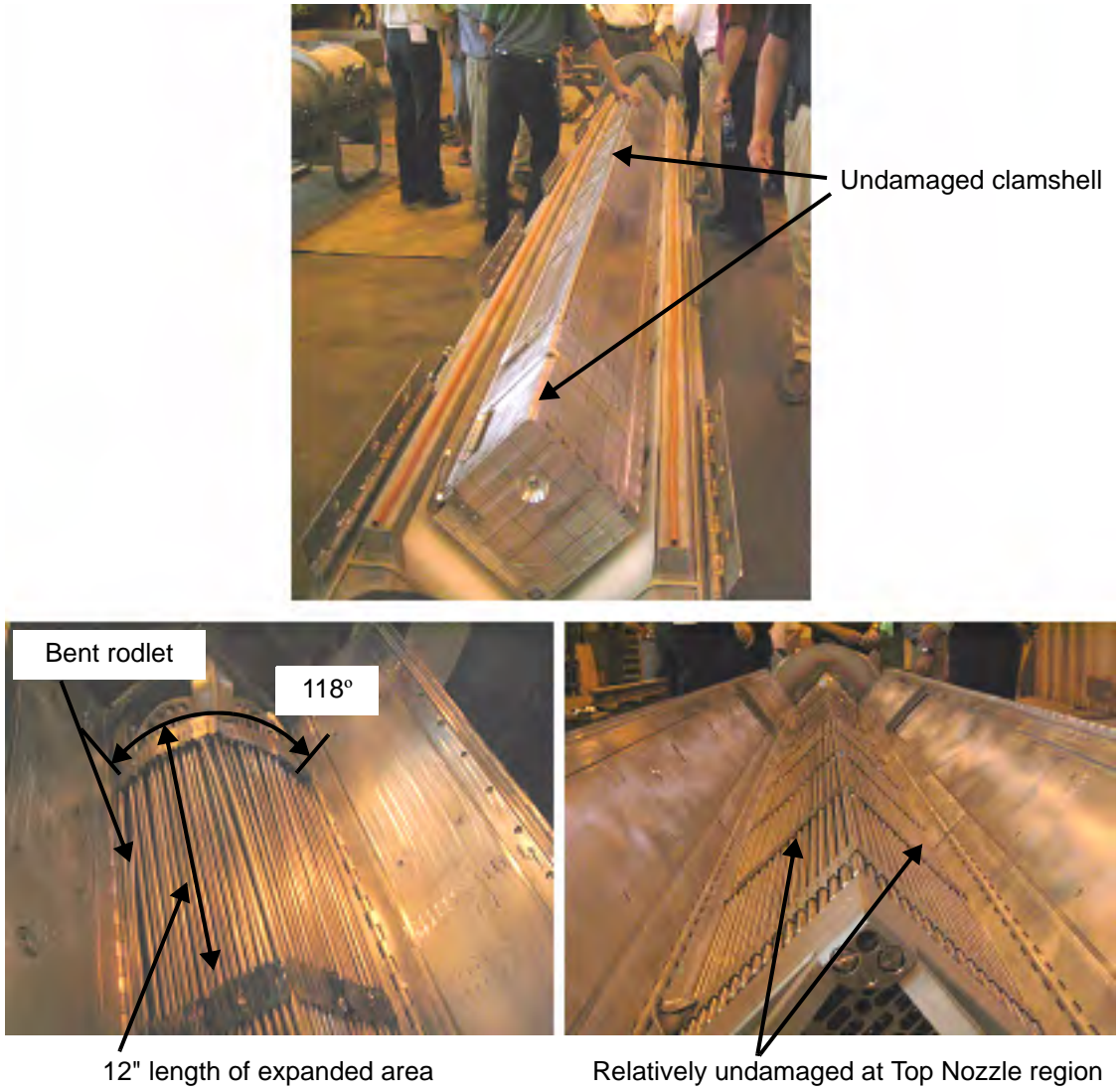


Figure 2-139 QTU-2 Clamshell and Fuel Assembly After Drop Tests

Table 2-41 Key Dimensions of QTU-2 Fuel Assembly Before Testing			
Fuel Assembly ID: 503005, B/N # 97-2480Y			
F/A Location	Fuel Envelope (inches)	Gap (inches)	Pitch (inches)
B/N – Grid 1	1 – 8.356 2 – 8.463 3 – 8.329 4 – 8.430 8.375 Meas. Nominal*	L – 0.124 R – 0.123 0.125 Meas. Nominal*	L – 0.499 R – 0.498 0.500 Meas. Nominal*
Grid 1 – Grid 2	1 – 8.325 2 – 8.415 3 – 8.319 4 – 8.420 8.375 Meas. Nominal*	L – 0.121 R – 0.123 0.125 Meas. Nominal*	L – 0.496 R – 0.498 0.500 Meas. Nominal*
Grid 2 – Grid 3	1 – 8.333 2 – 8.410 3 – 8.329 4 – 8.411 8.375 Meas. Nominal*	L – 0.121 R – 0.123 0.125 Meas. Nominal*	L – 0.496 R – 0.498 0.500 Meas. Nominal*
Grid 3 – Grid 4	1 – 8.311 2 – 8.435 3 – 8.310 4 – 8.24 8.375 Meas. Nominal*	L – 0.124 R – 0.123 0.125 Meas. Nominal*	L – 0.499 R – 0.498 0.500 Meas. Nominal*
Grid 4 – Grid 5	8.375 Meas. Nominal*	0.125 Meas. Nominal*	0.500 Meas. Nominal*
Grid 5 – Grid 6	8.375 Meas. Nominal*	0.125 Meas. Nominal*	0.500 Meas. Nominal*
Grid 6 – Grid 7	8.375 Meas. Nominal*	0.125 Meas. Nominal*	0.500 Meas. Nominal*
Grid 8 – Grid 9	8.375 Meas. Nominal*	0.125 Meas. Nominal*	0.500 Meas. Nominal*
Grid 9 – Grid 10	8.375 Meas. Nominal*	0.125 Meas. Nominal*	0.500 Meas. Nominal*
Grid 10 – T/N	8.375 Meas. Nominal*	0.125 Meas. Nominal*	0.500 Meas. Nominal*
Note: * Measured nominal values were measured to nearest 1/8".			

Table 2-42 QTU-2 Fuel Assembly Grid Envelope After Testing			
Fuel Assembly Envelope Inspection Table			
Location	Envelope Dimension, Inches		Maximum Fuel Rod Gap from Form 2F (Nominal Gap = 0.122")
	Left Side, LS	Right Side, RS	
Between B/N and Grid 1	8.625	8.500	0.722
Between Grids 1 and 2	8.000	7.938	0.539
Between Grids 2 and 3	7.938	7.688	0.316
Between Grids 3 and 4	7.813	7.625	0.137
Between Grids 4 and 5	8.063	7.875	0.153
Between Grids 5 and 6	8.250	8.250	0.143
Between Grids 6 and 7	8.375	8.375	0.146
Between Grids 7 and 8	8.375	8.375	0.141
Between Grids 8 and 9	8.375	8.375	0.162
Between Grids 9 and 10	8.375	8.375	0.141
Between Grid 10 and T/N	8.438	8.438	0.127
MAXIMUM VALUE	8.625	8.500	0.722

Table 2-43 QTU-2 Fuel Rod Pitch Data After Testing			
Fuel Rod Pitch Inspection Table			
Location	Maximum Gap, inches		Maximum Pitch, inches
	Left Side, LS	Right Side, RS	
Between B/N and Grid 1	0.722	0.501	1.097
Between Grids 1 and 2	0.539	0.501	0.914
Between Grids 2 and 3	0.250	0.316	0.691
Between Grids 3 and 4	0.137	0.125	0.512
Between Grids 4 and 5	0.153	0.132	0.528
Between Grids 5 and 6	0.142	0.143	0.518
Between Grids 6 and 7	0.145	0.146	0.521
Between Grids 7 and 8	0.141	0.138	0.516
Between Grids 8 and 9	0.162	0.122	0.537
Between Grids 9 and 10	0.139	0.141	0.516
Between Grid 10 and T/N	0.127	0.123	0.502
MAXIMUM VALUE	0.722	0.501	1.097

2.12.5.3 Certification Test Unit Drop Tests

A Traveller XL package was fabricated by Columbiana High Tech to serve as the certification test unit (CTU), Figures 2-140 and 2-141 and Table 2-44. This unit was subjected to a regulatory drop test performed February 5, 2004 in Columbiana, Ohio. The test included a 50 inch (1.27 m) slap down, a 32.8 feet (10.0 m) free drop test impacting the bottom nozzle, and a 42 inch (1.07 m) pin-puncture test, Figure 2-142 and Table 2-45. The CTU package was thermally saturated for approximately 15 hours prior to testing at a temperature of about 17°F (-8.3°C). At the time of testing the temperature was approximately 24°F (-4.4°C). The package’s test weight was 4863 pounds.

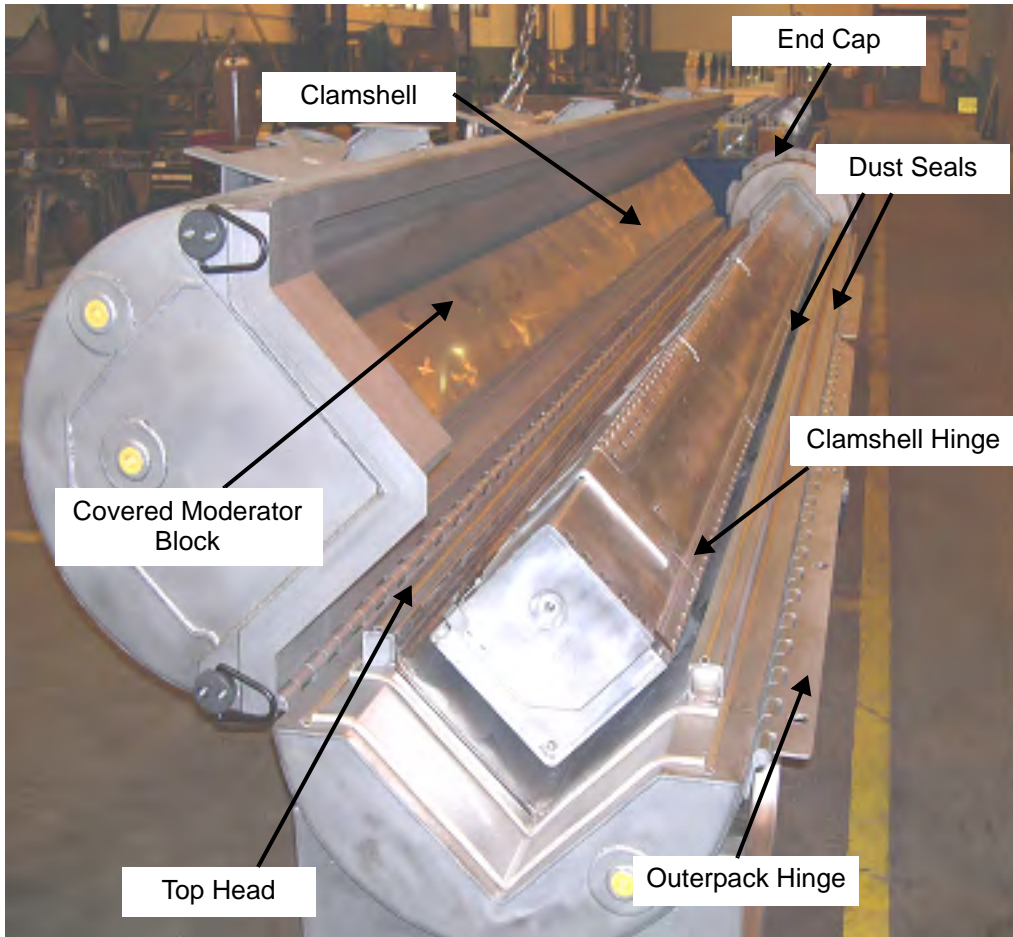


Figure 2-140 Traveller CTU Test Article Internal View

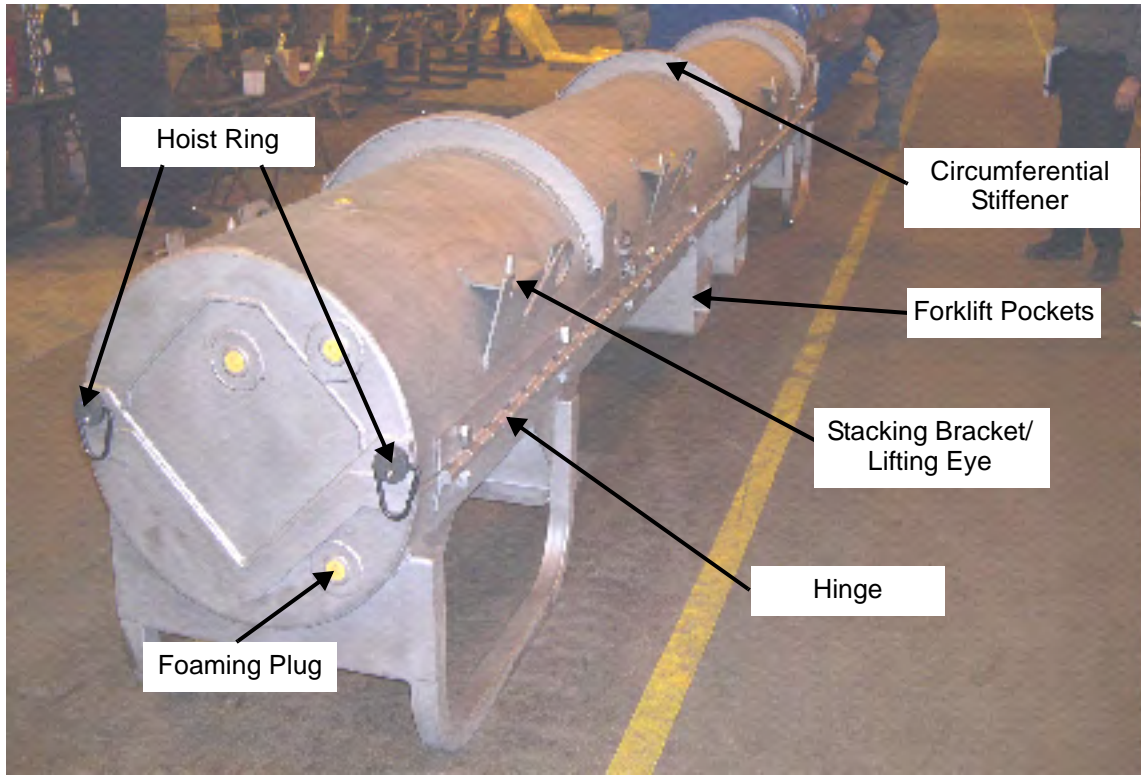


Figure 2-141 Traveller CTU External View

Table 2-44 Test Weights		
	Nominal* Wt	Actual Wt
Weight of Outerpack (Empty):	2633 lb	2671 lb
Weight of Clamshell (Empty):	425 lb	440 lb
Weight of package (Empty) :	3058 lb	3111 lb
Total package test weight:	4810 lb	4863 lb
Note: * Nominal total weight includes only Fuel Assembly since drop test was conducted without RCCA. Maximum expected design weight is estimated to be 5071 pounds (Ref. 3). The top Outerpack section weight is 1063 pounds empty and the bottom Outerpack section weight is 1608 pounds empty.		

Exterior Inspections After Drop Tests – The exterior of the package was examined after each drop. The inspections found that the Outerpack retained its circular pre-test shape except for localized plastic deformation at the ends. No hinge bolts failed on the Outerpack, the Outerpack did not separate, and neither the inner nor outer shell were perforated in the pin drop test.

Test 1.1
 50 inch Low Angle
 Slap Down



Test 1.2
 32 feet, 10 inch End
 Drop on B/N



Test 1.3
 42 inch Pin Puncture

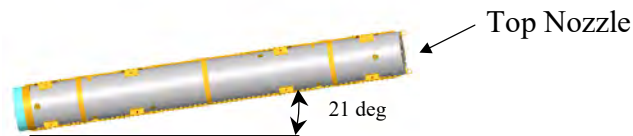


Figure 2-142 CTU Drop Test Orientations

Table 2-45 CTU Drop Test Orientations					
Test Article ID	F/A Type	Test Sequence	Test Pitch Attitude	Test Roll Attitude	Design Feature Tested
CTU	17x17 XL	P1.1) 1.2-m, NCT, Low angle ¹	9°	180°	Operations of hinges/doors
		P1.2) 9-m End Drop ¹	90°	0°	Lattice exp., FR axial position
		P1.3) 1-m Pin-puncture ¹	21°	90°	Hinge structural integrity

Test 1 – The 1.2 meter drop test resulted in a localized dent at the top nozzle end, and near the bottom nozzle end, the stiffener was dented over a length of about 8". Figures 2-143 and 2-144 shows the damage observed. The normal condition drop produced only local damage to the impact area. The depth of the crush was minimal.

Test 2 – The 9m (32.8-foot) free drop resulted in localized damage to the bottom nozzle end region. The two bottom nozzle stiffener keeper pins were detached as a result of the impact. The impact created a circumferential ripple located at 9" (bottom Outerpack) and 12" (top Outerpack) from the package bottom

end. The ripple resulted in a 1/2" crumple impact, which effectively shortened that section of the package slightly. Two stitch welds located inside the bottom nozzle end stiffener were broken, but this did not compromise the stiffener position. The bottom nozzle end cap stiffener separated to form a 1-3/16" gap, and the gap between the hinge and the cover lip was measured to be approximately 7/16". The hinge at the bottom nozzle end was separated about 1/16" from the Outerpack skin surface after the drop test. Figures 2-145 – 2-147 shows the damage observed.

Test 3 – The pin puncture test was located on the hinge of the Outerpack at approximately the axial center of gravity. The impact zone locally dented 6" of hinge length to a maximum measured depth of approximately 1-3/8", Figure 2-148. The hinge knuckles were not compromised as a result of the test. Hinge separation of 1/2" was noted about 7-1/2" from the impact point towards the top nozzle end.

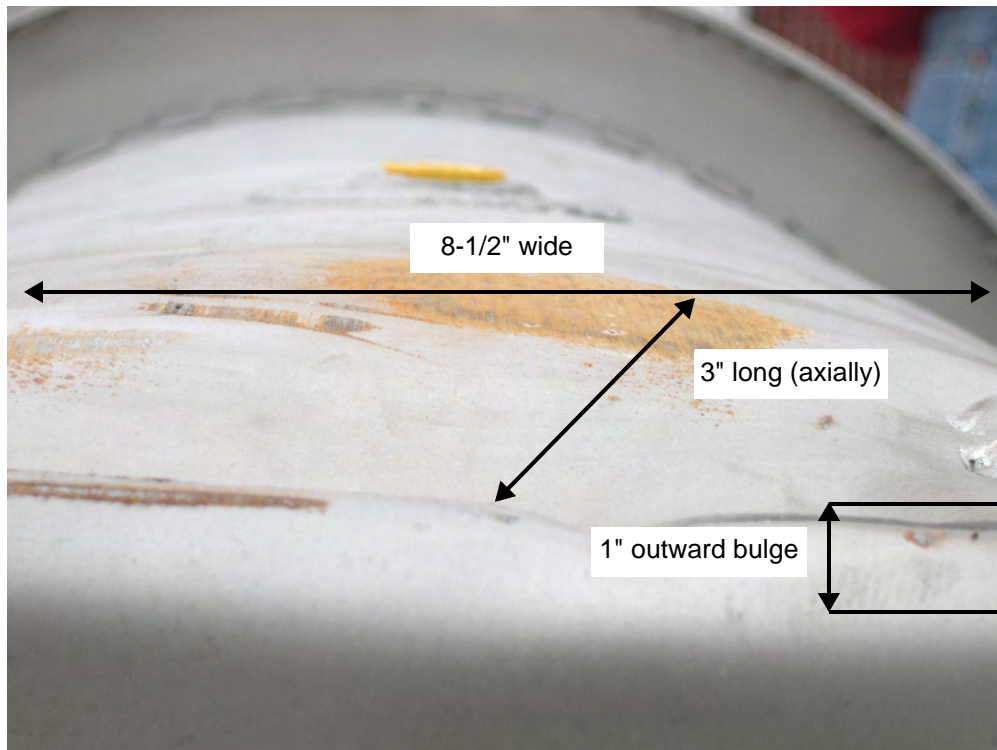


Figure 2-143 Top Nozzle End Outerpack Impact Damage

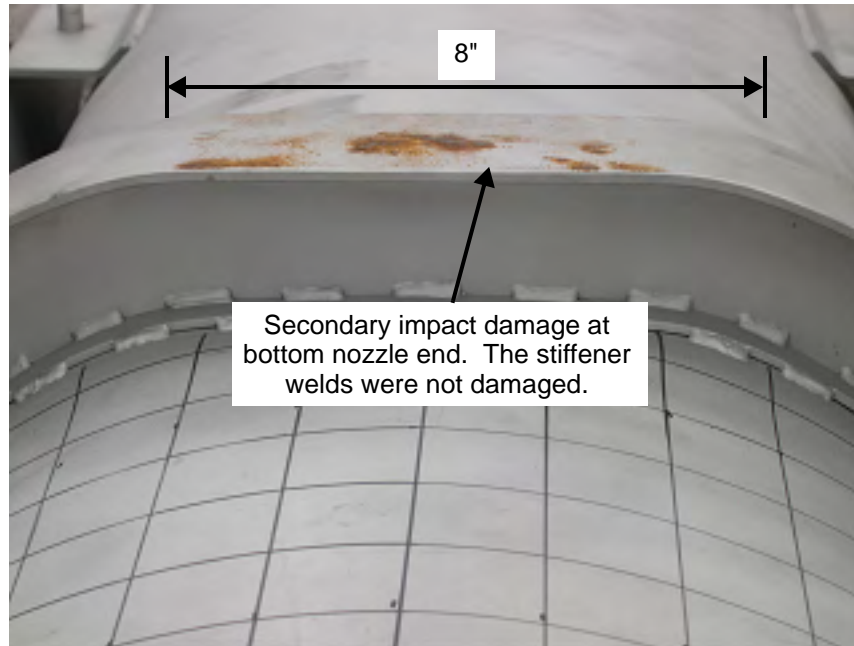


Figure 2-144 CTU Outerpack Stiffener After Test 1

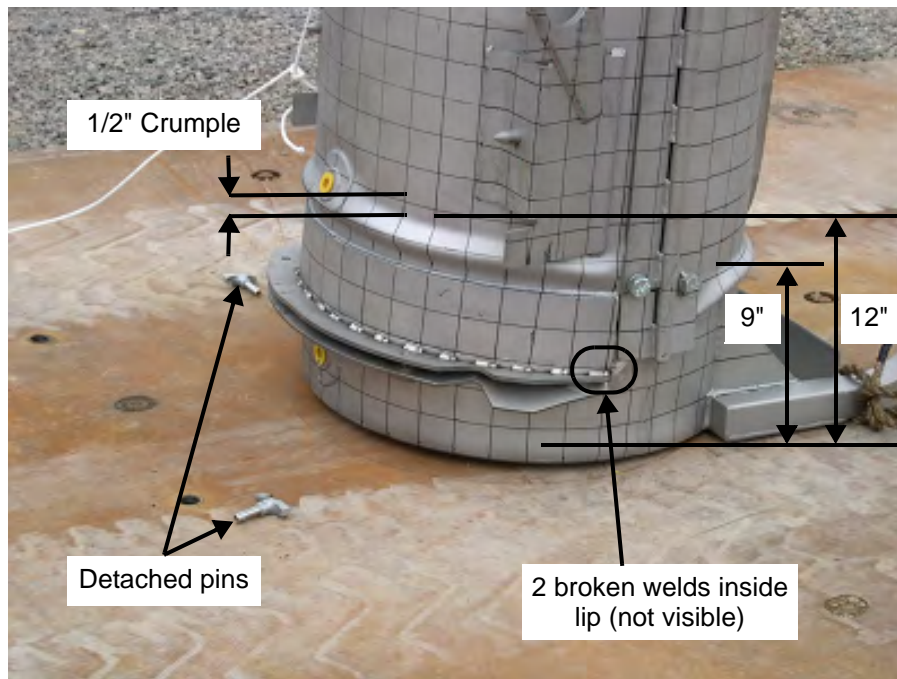


Figure 2-145 CTU Outerpack After Test 2

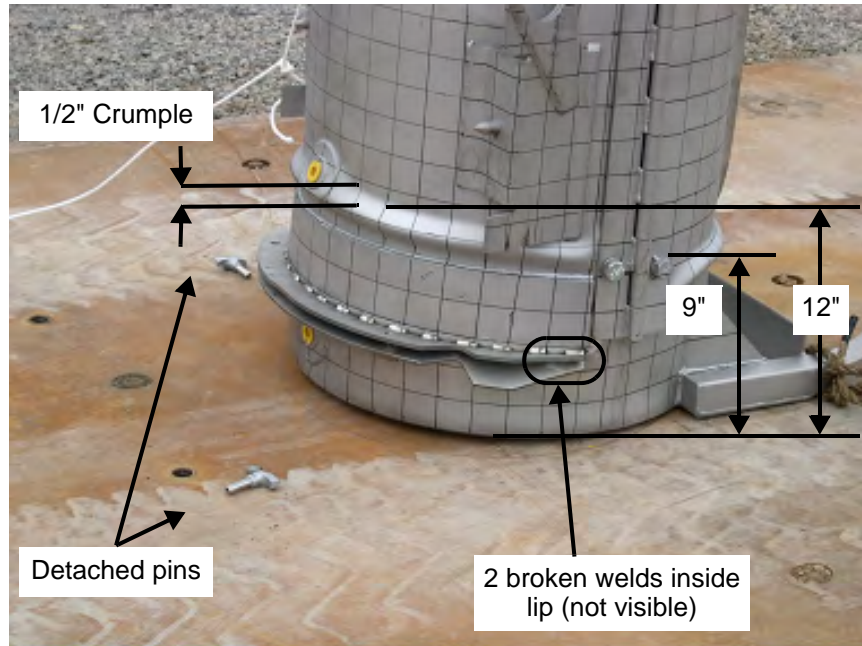


Figure 2-146 CTU Outerpack After Test 2

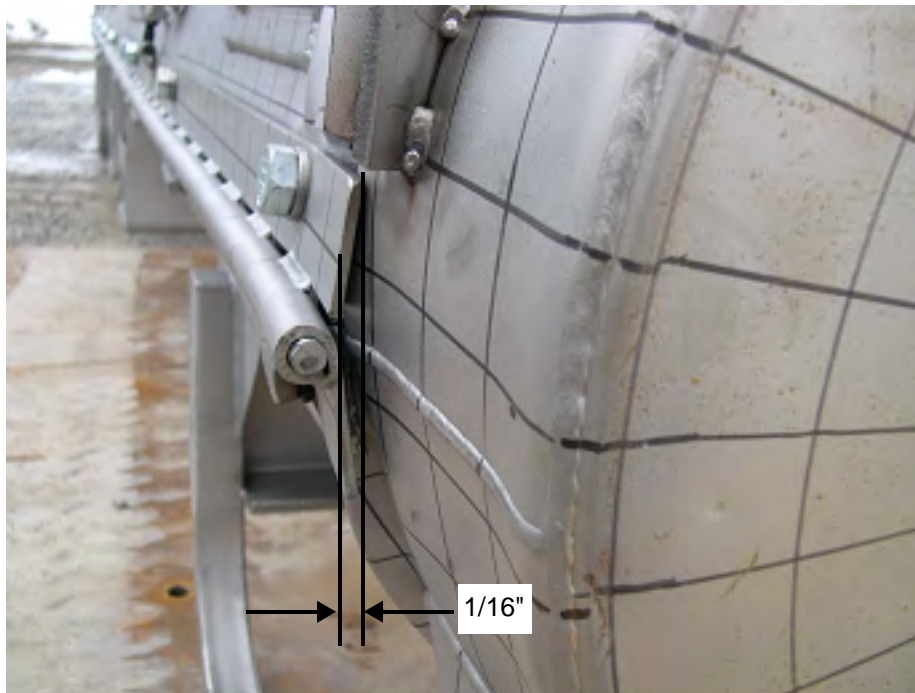


Figure 2-147 Hinge Separation at Bottom Nozzle End From Test 2

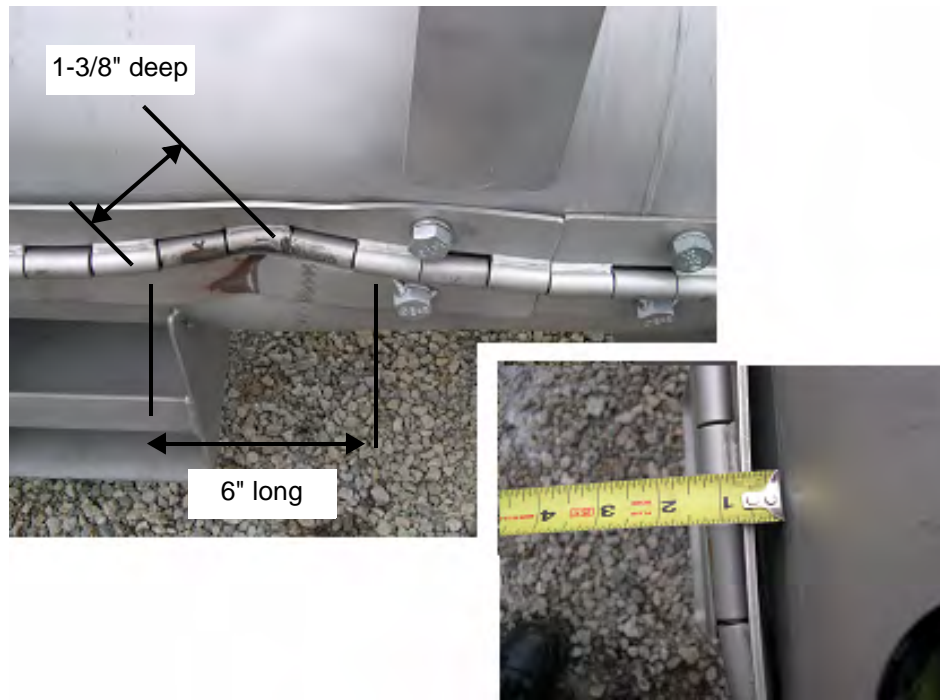


Figure 2-148 CTU Outerpack After Test 3

Interior Inspection Results – The CTU was sent to the South Carolina Fire Academy for the burn test immediately after the drop tests were completed. The package was not opened until the following week, approximately five hours after the fire test was completed. In general, the drop test and fire test resulted in minor damage to the Traveller internal structural components. The Clamshell was found intact and closed, Figure 2-149, and the simulated poison plates maintained position. All shock mounts were found to be visibly intact. At the bottom Clamshell plate, a 2-1/2" and a 2-3/4" piece of end lip sheared off. The measured gap was less than 1/16" and in the axial direction. The axial location of the fuel rods maintained position between the bottom and top nozzle. Finally, the moderator blocks were found to be intact and essentially undamaged after the completion of the drop and fire test. The moderator stud bolts on the top Outerpack were found sheared off, but the moderator cover maintained the moderator position. The stainless steel moderator cover was removed and the polyethylene moderator was examined. As shown in Figure 2-150, the moderator was intact and essentially undamaged.

Figure 2-151 provides the damage sketch overlaying the pre-tested fuel assembly for comparative purposes. For the 20" span from the bottom nozzle to Grid 2 of the fuel assembly, the fuel rod envelope expanded from 8-3/8" average nominal to 9-3/16". The grid envelope expanded from 8-7/16" nominal to 8-5/8" over the same 20" axial distance. The maximum measured fuel rod pitch in this region increased from 0.496" nominal to 0.990". This was caused by a single bent rod which was bent outward approximately 1/2". Otherwise, the typical pitch pattern consisted of 2 rod rows touching and the remaining 14 rows at nominal pitch, Figure 2-152.



Figure 2-149 CTU Clamshell After Drop and Fire Tests

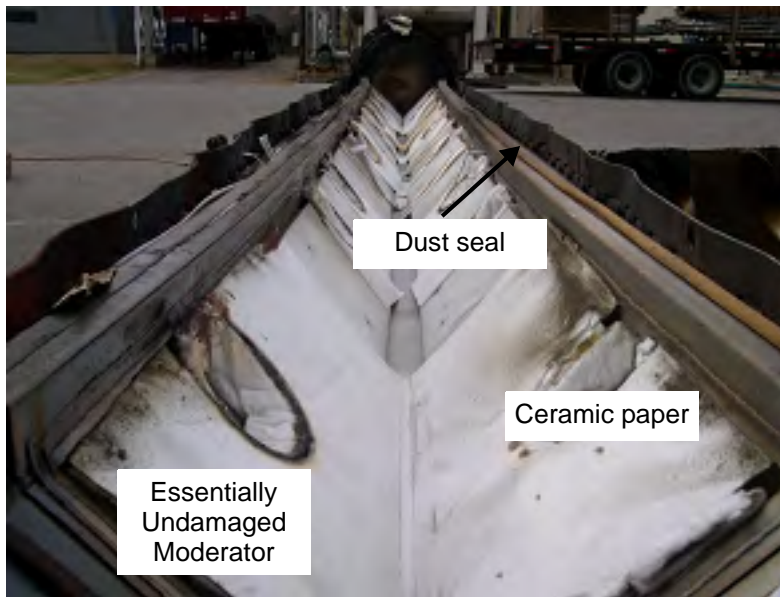


Figure 2-150 Outerpack Lid Moderator After Testing

For a length of 10" above Grid 2, the fuel rod envelope compressed from 8-3/8" nominal to 8-1/4". This slight compression is due to the single top rod slightly compressed inward. Above this 10" region, the single rod bent outward about 1/2" for a length of approximately 25".

For the 25" length from between Grids 2 and 3 and up to Grid 4, the single rod resulted in a measured envelope of 8-7/8", but the remaining envelope of 16 rows was slightly compressed (about 1/16"). The maximum pitch caused by the single rod was 0.740" compared to 0.496" nominal. Otherwise, the average pitch was nominal.

For the remainder of the fuel assembly from Grid 4 to the top nozzle, the fuel rod envelope compressed about 0.15" and the grid envelope compressed about 1/4". The average pitch decreased from 0.496" to 0.459" in this region.

Grid 1 was severely buckled, and the ovality was measured to be 120° for a length of about 20", Figure 2-153. Grids 2 and 3 were broken at the top corner, but otherwise intact. Grids 4-10 were relatively undamaged. The fuel inspection also indicated that 7.5% (20 of 265 rods) were cracked at the end plug locations (Figure 2-154). The average crack width measured was approximately 0.030" (30 mils) and the average length was 50% of the rod diameter. The cracked rods were located at the four corners, indicating the vertical impact created symmetrical impact forces to be transmitted through the bottom nozzle and fuel rods (Figure 2-155).

The fuel assembly in QTU-1 was measured before the test and after the burn test at locations shown in Figure 2-134 above. Table 2-46 provides the pretest dimensions. Tables 2-47 through 2-50 provide the post test dimensions.

2.12.5.4 Application to Higher Contents Weights

As discussed in section 2.12.3.2, the vertical drops on the bottom nozzle end of the package were determined to be the most damaging to the fuel assembly. Therefore, vertical drops were performed in the last two drop tests series, QTU-2 and CTU. This provided the maximum challenge to the fuel assembly and the clamshell heads. The tests were performed with lead filled fuel assemblies that did not incorporate rod cluster control assemblies (RCCA) or other internals. This was done because the RCCA, although adding weight, would increase the rigidity of the fuel assembly. This increased rigidity would decrease the forces on the clamshell walls. Additionally, when the fuel assembly is shipped with an RCCA, an additional axial restraint is provided to secure the total payload.

The two vertical drop tests are summarized below:

QTU-2 – 9 m drop test

Outerpack wt.	2611 lbs
Clamshell wt.	400 lbs
FA wt.	1767 lbs

Total wt. 4778 lbs
Drop ht 33.4 ft (10.2 m)

CTU – 9 m drop test

Outerpack wt. 2671 lbs
Clamshell wt. 440 lbs
FA wt. 1752 lbs
Total wt. 4863 lb
Drop ht 32.8 ft (10.0 m)

Drop heights greater than 9 m were used to bound maximum possible weights and other uncertainties. Because potential energy is directly proportional to drop height the bounding weights for each test result as:

QTU-2 at 9 meters

FA wt. 2000 lb
FA & Clamshell wt. 2453 lb
Total package wt. 5409 lb

CTU at 9 m

FA wt. 1947 lb
FA & Clamshell wt. 2433 lb
Total package wt. 5398 lb

During the vertical drop, the fuel assembly remains stationary with respect to the clamshell until the clamshell hits the outerpack impact limiter and begins to decelerate. When the outerpack hits the ground, it quickly decelerates as the foam and outerpack metal skin absorb the outerpack kinetic energy. As shown Figures 2-136 and 2-137, the amount of deformation to the outerpack was very small with a total crush of the outside of the bottom impact limiter < 0.5 inches (averaged).

The dynamic characteristics of the actual test performed with QTU-2 from 10.2 m are slightly different than a 9.0 m drop of a heavier package (and heavier fuel assembly), as described below. The terminal velocity of the test was approximately 14.2 m/s instead of the 13.3 m/s from a 9.0 meter drop. This will result in slightly different impact times between the clamshell and outerpack. The magnitude of this difference can be estimated with the following assumptions:

- Although the outerpack impact limiter has a total crush of approximately 0.5 inches (0.013 m) before the clamshell impact, the interior dimensions of the outerpack remain essentially the same as before impact.
- Initial separation distance between the clamshell and outerpack interior of 4.0 inches (0.102 m)
- There are no interaction between the clamshell/fuel assembly and the outerpack occurs until the clamshell hits the inside of the outerpack.

The actual QTU-2 drop was performed with a gross weight of 4778 lbs (2167 kg) from a 10.2 meter height. This is compared with a second theoretical Traveller drop test with a gross weight of 5409 lbs (2452 kg) from a 9.0 meter height. The outerpack cavity on QTU-2 was approximately eight inches longer than clamshell inside that cavity.

In the actual QTU-2 drop, the Traveller was falling at 14.2 m/s when the outerpack hits the ground. Assuming the clamshell was in its nominal position, it would continue to fall over a distance of four inches (0.102 m) before it hits the inside of the outerpack impact limiter. It takes the clamshell approximately 7.2 milliseconds for the clamshell to hit the inside of the outerpack after the outerpack comes to rest. This is calculated by:

$$0.102 = 14.15 t + 0.5 \cdot 9.81 t^2$$

In the theoretical Traveller drop, the clamshell package velocity at the time of outerpack impact is 13.2 m/s. If the clamshell is in the nominal position within the outerpack cavity, it will take approximately 7.7 milliseconds for the clamshell to hit the inside of the outerpack after the outerpack comes to rest. This is calculated by:

$$0.102 = 13.29 t + 0.5 \times 9.81 t^2$$

This results in a time difference between the two scenarios of 0.5 milliseconds. If the clamshell is located the maximum distance from the bottom impact limiter (8 inches or 0.204 m) the time to hit the impact limiter increases to 14.5 milliseconds and 15.3 milliseconds for the actual and theoretical drops respectively. In this case, there is a time difference of 0.8 milliseconds.

This simplified analysis does not include the deformation of the outerpack and the resulting deceleration profile which is not instantaneous. The FEA model provides a reasonable estimation of these deformations and predicts that the clamshell will hit the interior of the outerpack 15 milliseconds after the outerpack touches the ground (section 2.12.3.2.5). Because a small portion of the outerpack deformation is elastic, the outerpack probably rebounds slightly. The rebound was not observed in the tests but the FEA model does predict it to occur approximately 25 milliseconds after the outerpack impact.

The analysis above does show, however, the relative magnitude of the two different situations. The time difference between the actual drop and theoretical drop described above is only 0.5 to 0.8 milliseconds. This difference will not cause the clamshell to hit during the outerpack rebound (approximately 10 milliseconds

after clamshell contact) and the actual positions and velocities of the Traveller components will not be significantly different between the two drop scenarios.

The comparison above was made for the QTU-2 test. The general observations are applicable to the CTU tests however. As a result, the QTU-2 and CTU test drops justify payload weights significantly higher than the 1767 and 1752 lb fuel assemblies actually used in the testing.

2.12.5.5 Conclusions

Three series of drop tests were performed during the development and certification of the Traveller shipping package. This included two prototype units, two qualification test units and one certification test unit. Design improvements were made at each step based on the results of the drop tests and subsequent fire tests. The drop test series included a regulatory normal free drop of 1.2 meters, a 9-meter end drop onto the bottom nozzle, and a 1-meter pin-puncture test on the hinge. Minor structural Outerpack damage indicated that the Traveller Outerpack design satisfied the hypothetical accident condition defined in 10 CFR 71 and TS-R-1. Furthermore, the Clamshell was found to meet the acceptance criteria of the test by maintaining closure and its pre-test shape. The post-test geometry of the fuel assembly was determined to meet the acceptance criteria since only local expansion was noted in the lower 20" of the bottom nozzle region and the cracked rod gaps were all measured less than a pellet diameter.

In summary, testing demonstrated the Traveller package is suitable for compliance to normal and hypothetical mechanical drop test conditions described in 10 CFR 71 and TS-R-1.

This page intentionally blank.

|

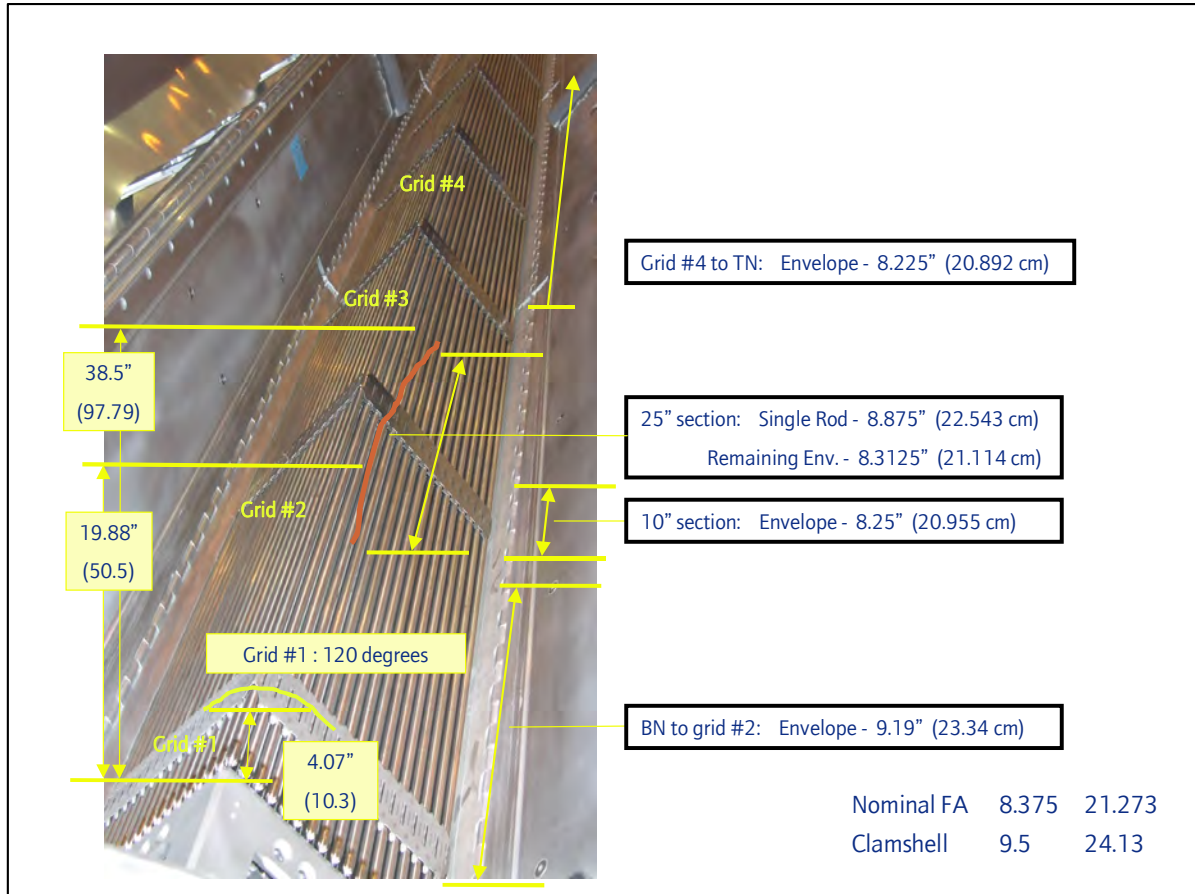


Figure 2-151 Fuel Assembly Damage Sketch and Pre-test Assembly

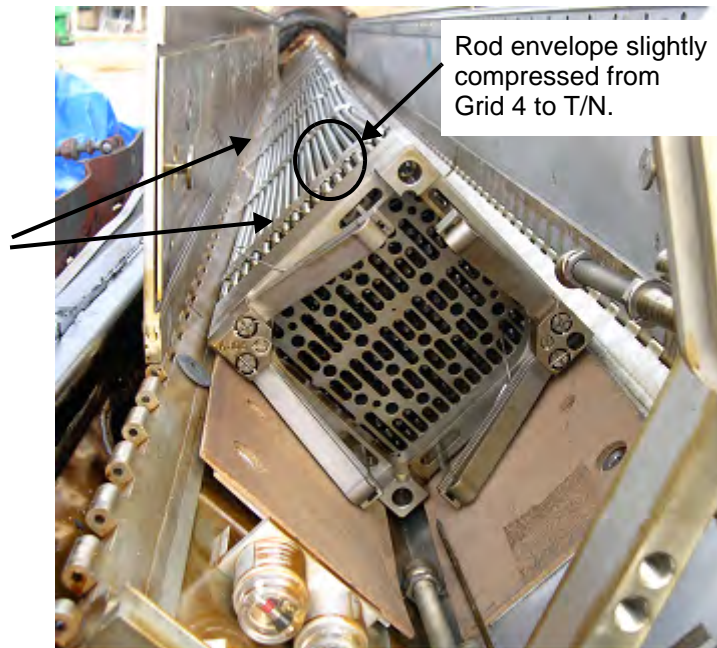


Figure 2-152 CTU Fuel Assembly After Testing

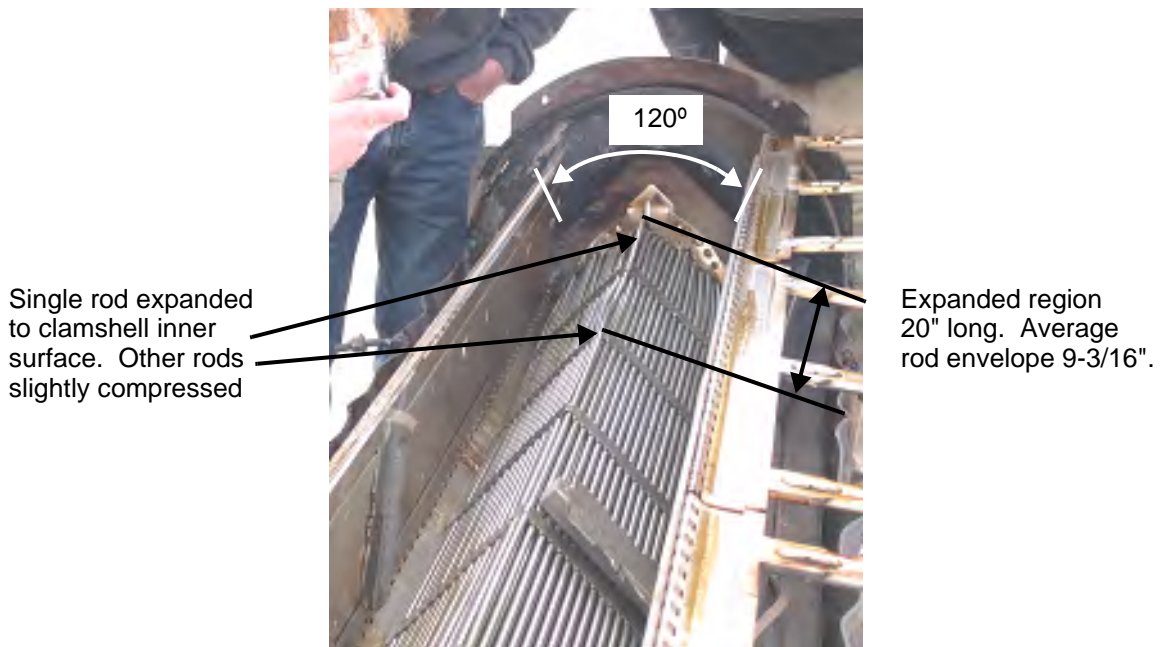


Figure 2-153 CTU Fuel Assembly Top End After Testing

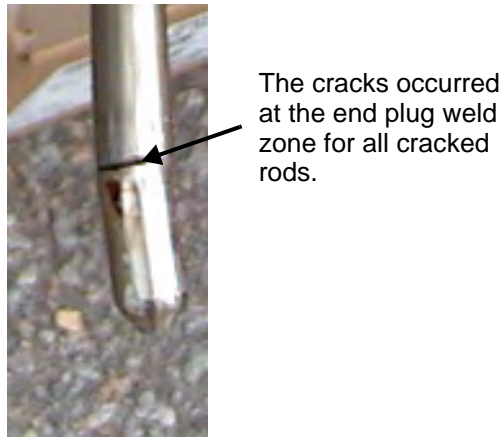


Figure 2-154 Cracked Rod From CTU Fuel Assembly

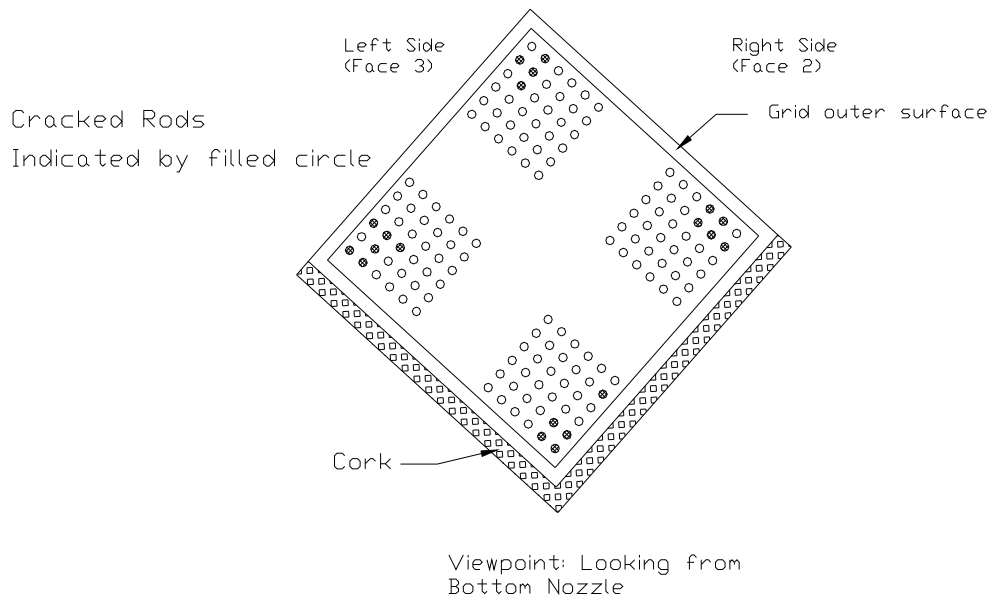


Figure 2-155 Cracked Rod Locations on CTU Fuel Assembly

Table 2-46 Fuel Assembly Key Dimension Before Drop Test			
Fuel Assembly ID: T/N # LM1F2N			
F/A Location	Fuel Envelope (inches)	Gap (inches)	Pitch (inches)
B/N – Grid 1	1: 8-3/8 2: 8-7/16 3: 8-3/8 4: 8-7/16	L – 0.123 R – 0.121	L – 0.498 R – 0.495
Grid 1- Grid 2	1: 8-3/8 2: 8-7/16 3: 8-3/8 4: 8-7/16	L – 0.123 R – 0.124	L – 0.497 R – 0.499
Grid 2- Grid 3	1: 8-3/8 2: 8-7/16 3: 8-3/8 4: 8-7/16	L – 0.121 R – 0.121	L – 0.495 R – 0.495
Grid 3- Grid 4	1: 8-3/8 2: 8-7/16 3: 8-3/8 4: 8-7/16	L – 0.123 R – 0.123	L – 0.497 R – 0.498
Grid 4- Grid 5	Rods: 8-3/8 Grids: 8-7/16	0.121	0.495
Grid 5- Grid 6	Rods: 8-3/8 Grids: 8-7/16	0.123	0.498
Grid 6- Grid 7	Rods: 8-3/8 Grids: 8-7/16	0.122	0.497
Grid 7- Grid 8	Rods: 8-3/8 Grids: 8-7/16	0.123	0.497
Grid 8- Grid 9	Rods: 8-3/8 Grids: 8-7/16	0.123	0.498
Grid 9- Grid 10	Rods: 8-3/8 Grids: 8-7/16	0.121	0.495
Grid 10 – T/N	Rods: 8-3/8 Grids: 8-7/16	0.122	0.497
AVERAGE	Rods: 8-3/8 Grids: 8-7/16:	0.122	0.497
Note: * Measured fractional values were measured to nearest 1/16". Measured decimal values were measured to the nearest 0.001".			

Table 2-47 CTU Fuel Assembly Grid Envelop Dimensions After Testing		
Location	Measured Grid Envelope Dimension, Inches	
	Left Side, LS	Right Side, RS
Grid 1	9-0	8-3/4
Grid 2	8-7/16	8-3/8
Grid 3	9-1/2	9-1/2
Grid 4	8-1/8	8-1/4
Grid 5	8-1/8	8-1/4
Grid 6	8-1/4	8-1/4
Grid 7	8-1/8	8-3/16
Grid 8	8-5/16	8-3/16
Grid 9	8-5/16	7-7/8
Grid 10	8-3/8	8-1/2
MAXIMUM VALUE	9-1/2	9-1/2

Table 2-48 CTU Fuel Assembly Rod Envelope Data After Testing			
Fuel Assembly Rod Envelope Inspection Table			
Location	Measured Envelope Dimension, In.		Calculated Maximum Fuel Rod Pitch from Form 1G (Nominal Pitch = 0.496")
	Left Side, LS	Right Side, RS	
Between B/N and Grid 1	9-0	8-3/4	0.566
Between Grids 1 and 2	8-5/16 ⁽¹⁾	8-5/16 ⁽¹⁾	0.990
Between Grids 2 and 3	8-1/2	8-0	0.740
Between Grids 3 and 4	8-7/16	8-1/2	0.715
Between Grids 4 and 5	8-3/16	8-3/16	0.472
Between Grids 5 and 6	8-3/16	8-3/8	0.578
Between Grids 6 and 7	8-1/16	8-1/16	0.550
Between Grids 7 and 8	8-3/8	8-3/16	0.541
Between Grids 8 and 9	8-0	7-13/16	0.483
Between Grids 9 and 10	8-3/8	8-1/2	0.498
Between Grid 10 and T/N	8-3/8	8-0	0.497
MAXIMUM VALUE	9-0	8-3/4	0.990
Note: (1) A single rod was measured to the inner Clamshell surface (9-1/2"). See Figure 2-153.			

Table 2-49 CTU Fuel Assembly Rod Envelope After Testing			
Fuel Assembly Rod Envelope Inspection Table			
Location	Measured Envelope Dimension, In.		Calculated Maximum Fuel Rod Pitch from Form 1G (Nominal Pitch = 0.496")
	Left Side, LS	Right Side, RS	
Between B/N and Grid 1	9-0	8-3/4	0.566
Between Grids 1 and 2	8-5/16 ⁽¹⁾	8-5/16 ⁽¹⁾	0.990
Between Grids 2 and 3	8-1/2	8-0	0.740
Between Grids 3 and 4	8-7/16	8-1/2	0.715
Between Grids 4 and 5	8-3/16	8-3/16	0.472
Between Grids 5 and 6	8-3/16	8-3/8	0.578
Between Grids 6 and 7	8-1/16	8-1/16	0.550
Between Grids 7 and 8	8-3/8	8-3/16	0.541
Between Grids 8 and 9	8-0	7-13/16	0.483
Between Grids 9 and 10	8-3/8	8-1/2	0.498
Between Grid 10 and T/N	8-3/8	8-0	0.497
MAXIMUM VALUE	9-0	8-3/4	0.990
Note: (1) A single rod was measured to the inner Clamshell surface (9-1/2"). See Figure 2-153.			

Table 2-50 CTU Fuel Rod Gap and Pitch Inspection After Testing			
Fuel Rod Gap and Pitch Inspection Table			
Location	Measured Maximum Gap, Inches		Calculated Maximum Pitch, Inches
	Left Side, LS	Right Side, RS	
Between B/N Grid 1	0.093 (between rows 9 & 10)	0.193 (between rows 6 & 7)	0.566
Between Grids 1 and 2	0.616 (out-lying rod only)	0.563 (out-lying rod only)	0.990
Between Grids 2 and 3	0.207 (one rod) Others touching	0.366 (one rod) Others touching	0.740
Between Grids 3 and 4	0.336	0.340	0.715
Between Grids 4 and 5	0.099	0.050	0.472
Between Grids 5 and 6	0.204	0.084	0.578
Between Grids 6 and 7	0.173 (between rows 2 & 3) Others Nominal	0.176 (between rows 6 & 7) Others Nominal	0.550
Between Grids 7 and 8	0.166	0.064	0.541
Between Grids 8 and 9	0.109	0.060	0.483
Between Grids 9 and 10	0.124	0.090	0.498
Between Grid 10 and T/N	0.123	0.074	0.497
MAXIMUM VALUE	0.616	0.563	0.990
Note: The pitch is calculated by adding the measured gap to the fuel rod diameter.			

2.12.6 SUPPLEMENT TO DROP ANALYSIS FOR THE TRAVELLER XL SHIPPING PACKAGE –CLAMSHELL AXIAL SPACER STRUCTURAL EVALUATION

2.12.6.1 Background

The XL Clamshell may be configured to include an aluminum spacer assembly to ship fuel types that normally would ship inside a Traveller STD package as shown in Figure 2-158. The structural performance of the spacer assembly in a bottom-down 9m hypothetical drop is evaluated to determine if there is any buckling of the spacer, a 6-inch Schedule 40 aluminum pipe, that could then damage or deform the Clamshell.

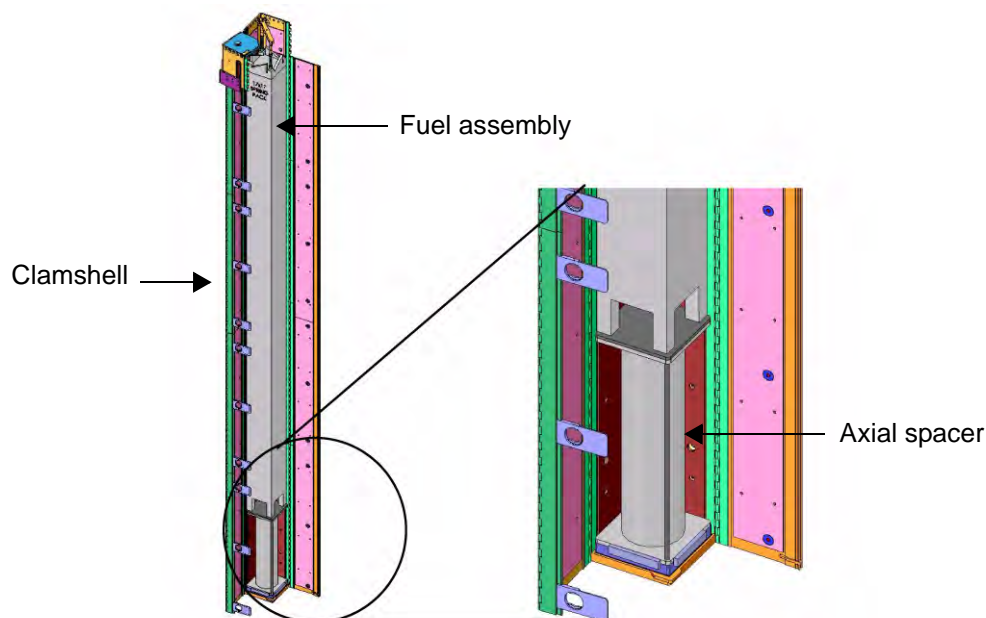


Figure 2-156 Axial Spacer below Fuel Assembly in Traveller XL Clamshell

The fuel assembly is assumed to be restrained in the clamshell to prevent any secondary impact within the clamshell. The spacer below the fuel assembly, when needed, and a top axial restraint restrain the contents to the clamshell, and as such the clamshell and contents decelerate as a coupled mass. The top axial restraint, fuel assembly structure, or spacer may absorb kinetic energy during the deceleration that results from an end drop impact.

Any structural deformation of the spacer assembly shall not change the shape of the clamshell or compromise the ability of the clamshell to confine the fuel assembly. The clamshell panel doors shall remain securely closed, end plates shall remain securely in place, hinges attaching the panel doors and multi-point cammed latch shall remain intact, and dimensions of the clamshell shall not be altered.

The primary impact with the unyielding surface occurs on the Outerpack end impact limiter. The Outerpack decelerates quickly within a few milliseconds of the primary impact because the contact area of the end surface is large and stiff, and there is no significant rebound. The Outerpack is completely decelerated by the time a secondary impact occurs inside the package as the Clamshell, suspended in the lower Outerpack on rubber mounts, continues to fall and contact the inside surface of the end impact limiter.

A crushable foam “pillow” is integrated into the end impact limiter to absorb kinetic energy from the secondary impact between the Clamshell and inside surface of the lower Outerpack end impact limiter. This pillow is a solid disk made from 6 pcf polyurethane foam. It has a nominal diameter of 12.00 inches (305 mm) and a nominal height of 3.60 inches (91 mm). The stiffer foam in the Outerpack end impact limiter, 20 lb/cu. ft. (0.32 g/cc) density, is located below and around the soft pillow. This stiffer component end impact limiter functions to decelerate the Outerpack at all high drop angle orientations.

2.12.6.2 Conclusions

Results of the simulated bottom-down 10m impact predict that there is no significant risk of damage to the Clamshell due to buckling of the spacer assembly. The 28.94 inch (735.1mm) long spacer assembly is too short to fail in a classic Euler buckling manner. Instead, the spacer pipe locally may crumple near its bottom and top ends during the impact. This local crumpling does not result in large column bowing displacements that could impart forces on the Clamshell panel doors or base.

2.12.6.3 Detailed Calculations and Evaluations

A Traveller TX finite element (FE) model of the entire package was originally used to simulate the impact testing. A new LS-DYNA Traveller model was created to simulate features of the TX package affected by the end impact orientation. The new model is more efficient and was used to evaluate the structural performance of the axial spacer in the vertical end impact.

Assumptions

Specific assumptions used in the FEA simulation are as follows:

1. The assumed mass of the 17STD FA (1,496 lbs, 678 kg) includes the heaviest core component, a Rod Control Cluster Assembly (RCCA) (180 lbs, 82 kg), Reference 5. The total FA mass was therefore, 1,676 lbs (760 kg) (RCCA dwg: 1554E27).
2. The FA is modeled with distributed point-element masses and is therefore not elastic. This is very conservative since actual drop testing revealed the weak axial stiffness of a FA (it vibrates and bows during end impacts).
3. The drop height was conservatively increased from 9m to 10m.
4. The FA bottom nozzle and spacer assembly were modeled without any restraints and they are therefore free to rotate/tilt. In actuality, the FA itself would keep the bottom nozzle relatively horizontal and the Clamshell walls will further restrain both items.

5. The majority of the mass of the Outerpak has not been included in this analysis because it does not significantly affect the Clamshell impact. More specifically, the Outerpak impact event is finished within only a few milliseconds, therefore the bottom limiter is simply waiting for the Clamshell impact into it. This assumption has been validated in a separate run which did include the remaining Outerpak mass.
6. The foam crush characteristics include extrapolation from 80% crush to 100% crush for model stability purposes. As mentioned earlier, actual pillow crushing was measured to be only about 50%. This is because the FA is not a rigid “hammer” that has no axial elasticity. This effect has been proven to be quite significant. However, in these simulations, the severe impact of the rigid-mass modeling of the fuel assembly was used. In some cases, this forces the crush curves to be extrapolated to 100%.
7. The longest spacer assembly is considered the bounding FA/Spacer combination.
8. LS-DYNA incorporates strain capability into the plastic regions of metallic material properties, therefore the “strain hardening” effects for aluminum were included in the model. These values are difficult to obtain, and therefore engineering judgement was used to assume the modulus after the yield. This was assumed to be a very low, linear value, of 268 MPa. This is almost no strain hardening from yield to failure.

Method

The Lawrence Livermore, LS-DYNA[®] finite element code was used to determine the loads, displacements, accelerations, strains, etc. of a Traveller XL shipping package containing a 17x17STD fuel assembly with RCCA when dropped onto a flat unyielding surface from a height of 10m. LS-DYNA 970, Revision 5434a, is a general purpose finite element code for analyzing the large deformation dynamic response of structures. This software was selected because it allows the analysis to include the effects of large deformation, large strain, material non-linearity, contact, and failure of materials.

Only the bottom end of the FA is modeled, the remainder of the assembly mass is simulated through point-mass elements. The weight of the remainder of the Clamshell is also modeled with point-mass elements. The Clamshell is an aluminum box with a solid 1 inch thick bottom plate. The spacer assembly is modeled with the 1.25 inch (31.8 mm) thick bottom rubber pad included, however, the 3/8 inch (9.5 mm) thick rubber pad on the top surface was not modeled.

Figure 2-157 shows components, materials, and meshing for the FEA simulation. The material properties assumed for the aluminum, stainless steel, and the crushable foams, and rubber pad are summarized in Tables 1 through 5. The compressive strength difference between the crushable foams is shown in Figure 2-158. Figure 2-159 shows the stress-strain curve of the 304 Stainless Steel properties used in the LS-Dyna simulation.

The appropriate properties of neoprene rubber for this simulation are difficult to determine exactly. Further, neoprene rubber does not obey Hook's law because it exhibits non-linear behavior. For this simulation, a value of 6.21 MPa was used for the shear modulus (G) of the 30 mm thick lower rubber pad.

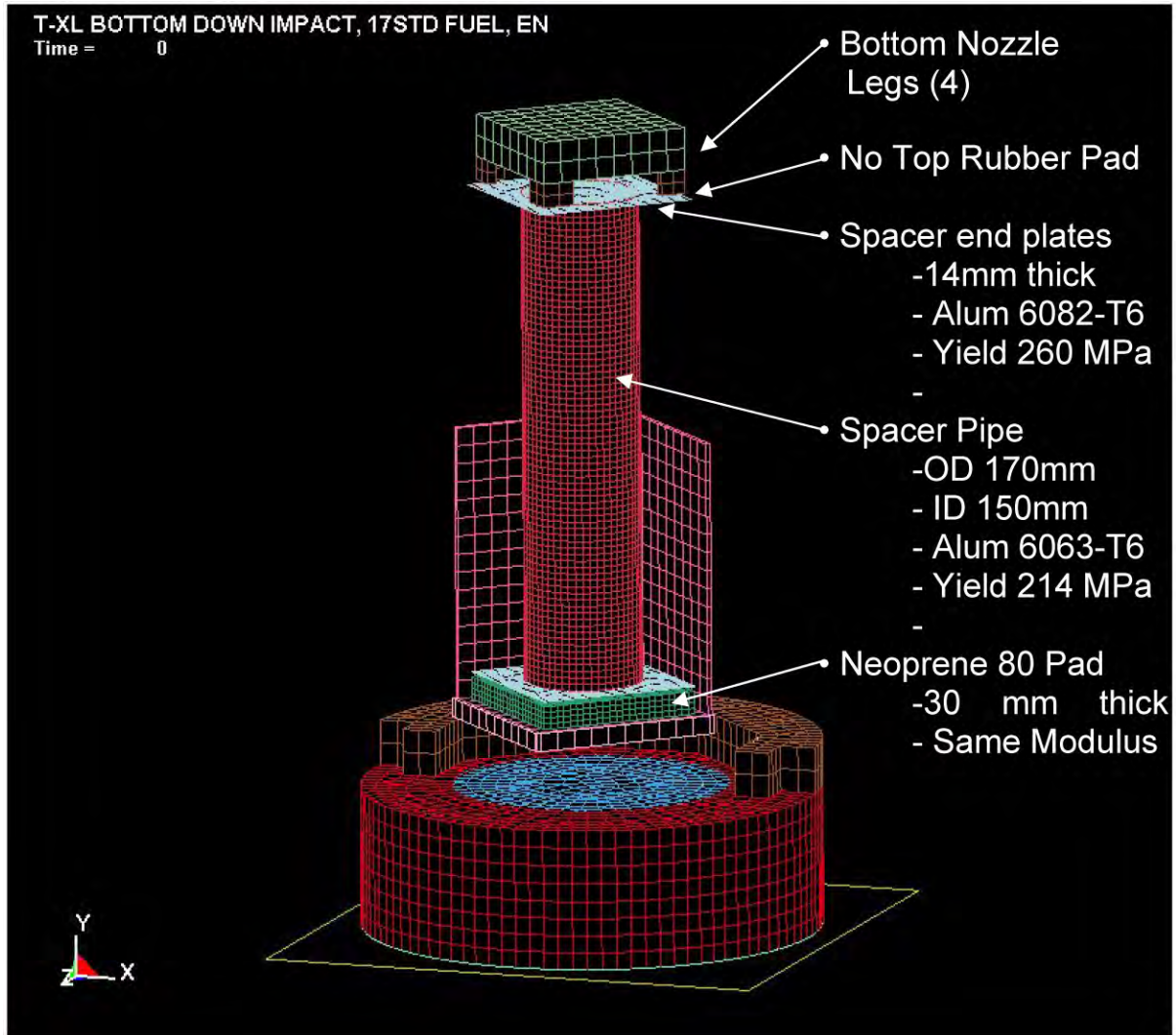


Figure 2-157 FEA Model – Axial Spacer

Table 2-51 Dimension and Material Properties of Axial Spacer	
Support Pipe:	
Exterior Diameter - mm (in):	170 (6.69)
Interior Diameter - mm (in):	150 (5.91)
Length - mm (in):	671.1 (26.42)
Wall Thickness - mm (in):	10 (0.39)
Material	6063-T6
Yield Strength - MPa (Ksi)	214 (31.0)*
Base Plates:	
Thickness - mm (in)	14 (.55)
Length - mm (in):	228.6 (9.00)
Material	6082-T6
Yield Strength - MPa (Ksi)	262 (38.0)*
Top Rubber Pad:	
Length - mm (in):	228.6 (9.00)
Thickness - mm (in)	10 (0.39)
Material	Neoprene 80
Bottom Rubber Pad:	
Length - mm (in):	228.6 (9.00)
Thickness - mm (in)	30 (1.18)
Material	Neoprene 80
Rod Handle:	No
Side Rubber Pad:	No
Total Assembly Length - mm (in):	735.1 (28.94)

Table 2-52 Aluminum Properties			
Aluminum Properties			
6005-T5 and 6061-T6 Aluminum at 75 degrees F			
Property	Symbol	Value	Units
Density	RO	2.71E-09	Mg/mm ³
Modulus	E	70	kN/mm ² (GPa)
Poisson's Ratio	PR	0.30	dimensionless
Yield Strength	SIGY	0.241	kN/mm ² (GPa)
Hardening Modulus	ETAN	0.25	kN/mm ²
Failure Strain	FAIL	0.35	In compression

Table 2-53 Annealed 304 Stainless Steel Properties			
Annealed 304 SS Properties			
Property	Symbol	Value	Units
Density	RO	8.00E-09	Mg/mm ³
Modulus	E	203	kN/mm ² (GPa)
Poisson's Ratio	PR	0.30	dimensionless

Table 2-54 Crushable Foam Properties			
Crushable Foam Properties			
	Density	Modulus	Poisson's Ratio
	Mg/mm ³	(MPa)	(dimensionless)
6 pcf Last-A-Foam	9.61E-11	30.14	0
10 pcf Last-A-Foam	1.60E-10	66.23	0
20 pcf Last-A-Foam	2.24E-10	192.76	0

Table 2-55 Neoprene (60 durometer) Properties			
Neoprene (Rubber) at 75 degrees F			
Property	Symbol	Value	Units
Density	RO	9.13E-10	Mg/mm ³
Shear Modulus	G	6.21E+00	MPa

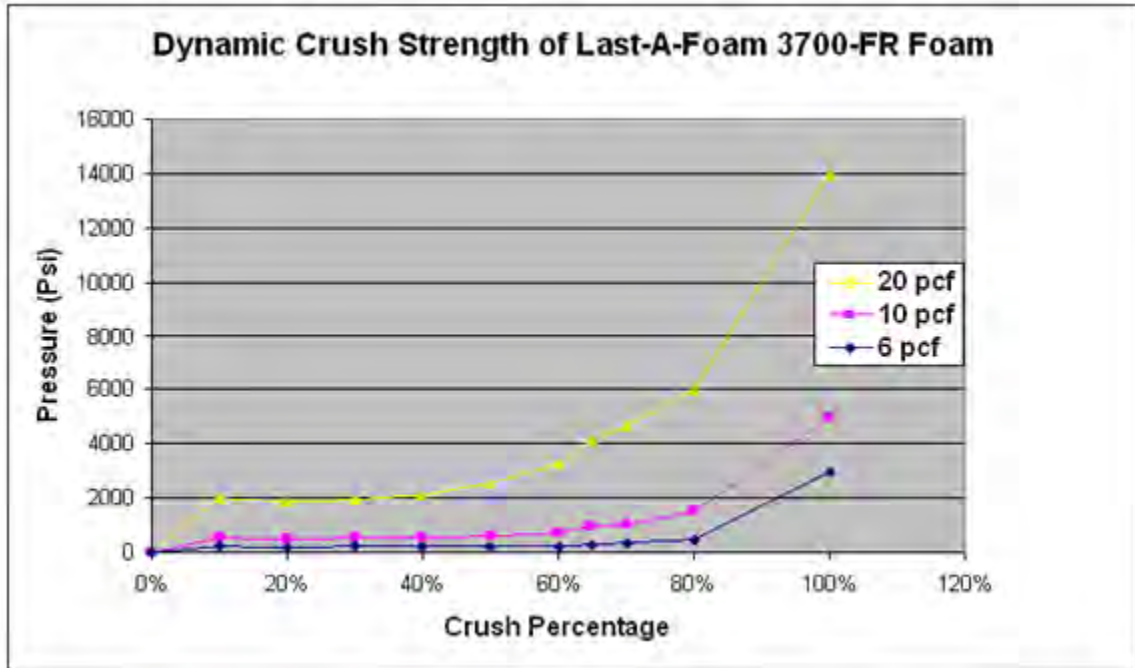


Figure 2-158 Dynamic Crush Strengths for Foam Materials Utilized in the Traveller

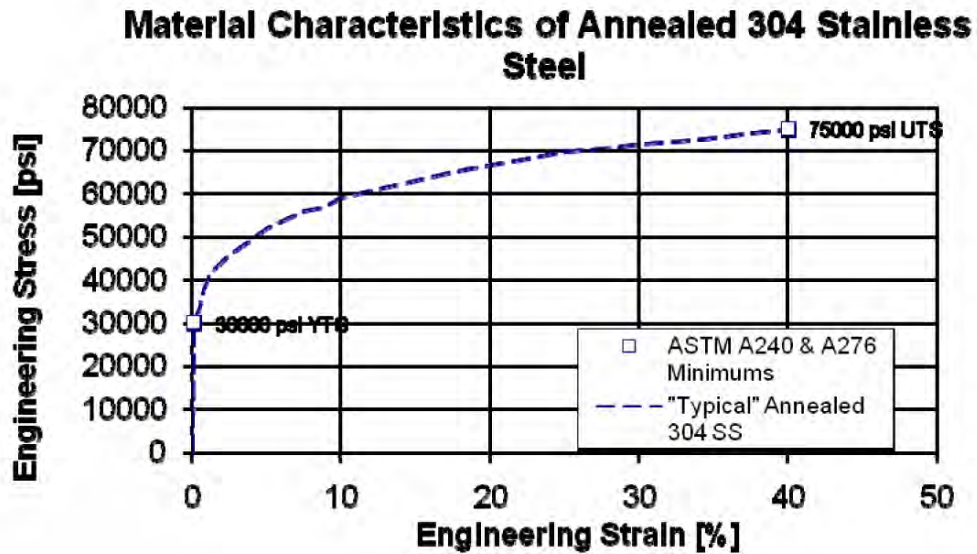


Figure 2-159 Annealed 304 Stainless Steel Stress-Strain Characteristics

Calculation Results

The 10m initial drop height of the Traveller simulation yields an impact velocity of 45.93 ft/sec (14.00 m/s). The FEA simulation shown in Figure 2-160 predicts deformation of the top spacer end plate, but no buckling or plastic deformation of the spacer pipe. From the displacement history of the top surface of the pillow shown in Figure 2-161, the total crush distance into the end impact limiter is approximately 94 mm (3.70 in). Figure 2-162 shows the kinetic energy history (mJ) of the axial spacer model.

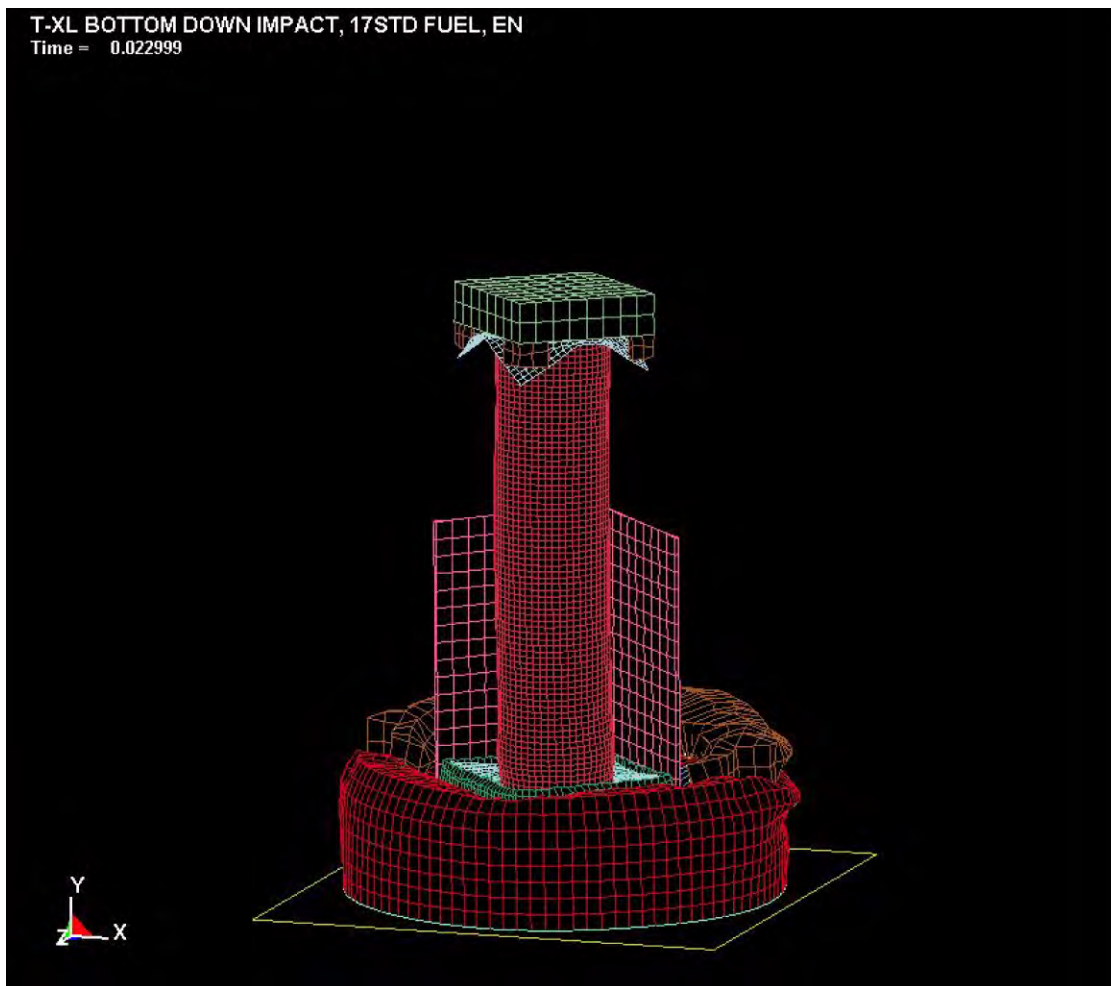


Figure 2-160 Deformed Model with Axial Spacer at 23 ms (the end of the impact)

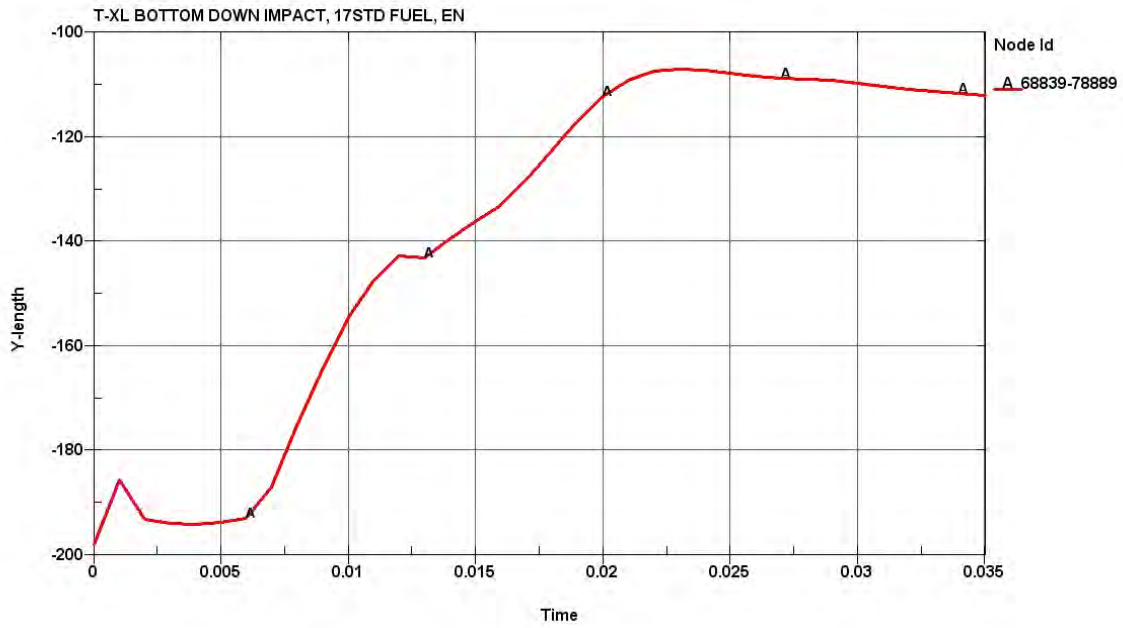


Figure 2-161 Predicted Total End Crushing (mm) with Axial Spacer

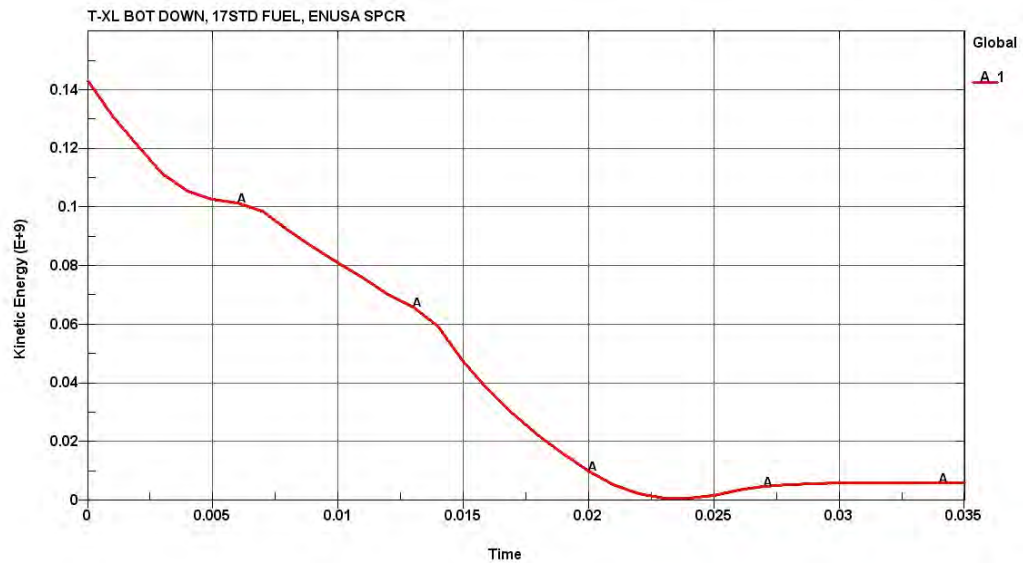


Figure 2-162 Kinetic Energy History (mJ) of the Axial Spacer Model

Validation

The many assumptions used to develop the LS-DYNA non-linear finite element stress code, including those needed to model the materials and impact, are validated by comparing the simulation results to the actual drop tests for the Traveller XL. Comparisons between certification test unit results and FEA simulation demonstrates that physical phenomenon governing shipping package impacts are simulated with adequate fidelity using the LS-DYNA model.

The pillow from a 10.0 m free drop impacting the bottom end of the package, CTU Test 1.2, was observed to crush approximately 1.8 inches. The simulation with axial spacer predicted the end limiter assembly (Pillow and high density end limiter) is crushed 92 mm (3.62 inches). The simulation predicts more absorption of the kinetic energy in the end impact limiter than observed in the actual drop test. This is due primarily to the assumption in the simulation that the fuel assembly is a rigid mass while for the actual drop test there was a significant energy absorbed in the deformation of the fuel assembly bottom nozzle and fuel rods during the deceleration.

In addition to the comparison energy absorbed by the end impact limiter, the axial force required to cause buckling of the spacer pipe, P_{cr} , can be estimated using the Euler buckling equation assuming that neither end is fixed (Reference: Shigley, "Mechanical Engineering Design", 3rd Edition, page 115):

$$P_{cr} = \pi^2 \times E \times I / L^2, \text{ where}$$

E = Modulus of elasticity, 1.00E+07 psi

I = Moment of inertia, $\pi/64 \times (D^4 - d^4)$, D =Outer diameter, d =Inner diameter

L = Length of the column

Using the dimensions from Table 1 the critical axial force is calculated as follows:

$$I = \pi/64 \times (6.69^4 - 5.91^4) = 38.44$$

$$P_{cr} = \pi^2 \times 1.00E+07 \text{ psi} \times 38.44 / 26.42^2 = 5.44E+06 = \text{lb f}$$

Assuming a conservative fuel assembly gross weight of 2,000 lbs and a deceleration of 200 g, the maximum load on the spacer would be approximately 400,000 lbs. This is significantly lower critical Euler values calculated for the axial spacer pipe. This result is consistent FEA simulation that predicted no buckling of the axial spacer.

Computer Code Input Files

CTUWSPCR.K Bottom-down end drop from 10m, with 17STD fuel and ENUSA Spacer Assy (dwg: CECT100, rev 1). This is Traveller XL pkg, production type, with 6pcf pillow. Temp = 75 F, Nominal foam densities

References

1. SFAD-10-72, Revision 2 (July 6, 2010), "Analysis of a Traveller XL Package in a Hypothetical Bottom-Down Impact With 17x17 STD Fuel and Spacer Assembly."

2.12.7 SUPPLEMENT TO DROP ANALYSIS FOR THE TRAVELLER XL SHIPPING PACKAGE – CLAMSHELL REMOVABLE TOP PLATE STRUCTURAL EVALUATION

2.12.7.1 Background

The fuel assembly is assumed to be restrained in the clamshell to prevent any secondary impact within the clamshell. The spacer below the fuel assembly, when needed, and an axial restraint restrain the contents to the clamshell, and as such the clamshell and contents decelerate as a coupled mass. The top end axial restraint, fuel assembly structure, or spacer may absorb kinetic energy during the deceleration that results from an end drop impact.

Operational experience with Traveller package revealed that some fuel types could not be loaded or unloaded vertically with existing customer handling tools. In particular, the 17x17 XL fuel with guide pins could not be vertically loaded/unloaded into the Traveller due to an interference between the handling tool and the Clamshell Shear Lip. Figure 2-163 shows the 17x17 XL top nozzle with the handling tool attached and fully seated. Figure 2-165 shows the potential interference. The tool cannot be installed or removed without tilting the fuel handling tool and potentially damaging the fuel assembly.

Additional evaluation revealed similar interference issues when handling fuel assemblies which include Core Component Assemblies (CCA). A new Clamshell top head configuration was designed to eliminate the interference from the Shear Lip. Both the original Fixed Top Plate (FTP) configuration and an alternate configuration called the Removable Top Plate (RTP) are described in Section 1 of the Safety Analysis Report (SAR).

The primary impact with the unyielding surface occurs on the Outerpack end impact limiter. The Outerpack decelerates quickly within a few milliseconds of the primary impact because contact area of the end surface is large and stiff, and there is no significant rebound. The Outerpack is completely decelerated by the time a secondary impact occurs inside the package as the Clamshell, suspended on rubber mounts, continues to fall and contact the inside surface of the end impact limiter.

A crushable foam “pillow” is integrated into the end impact limiter to absorb kinetic energy from the secondary impact between the Clamshell and inside surface of the Outerpack end impact limiter. This pillow is a solid disk made from 6 pcf polyurethane foam. It has a diameter of 12.00 inches (305 mm) and a height of 3.60 inches (91 mm). The stiffer foam in the Overpack end impact limiter, 20 lb/cu. ft. (0.32 g/cc) density, is located below and around the soft pillow. This stiffer component end impact limiter functions to decelerate the Outerpack at all high drop angle orientations.

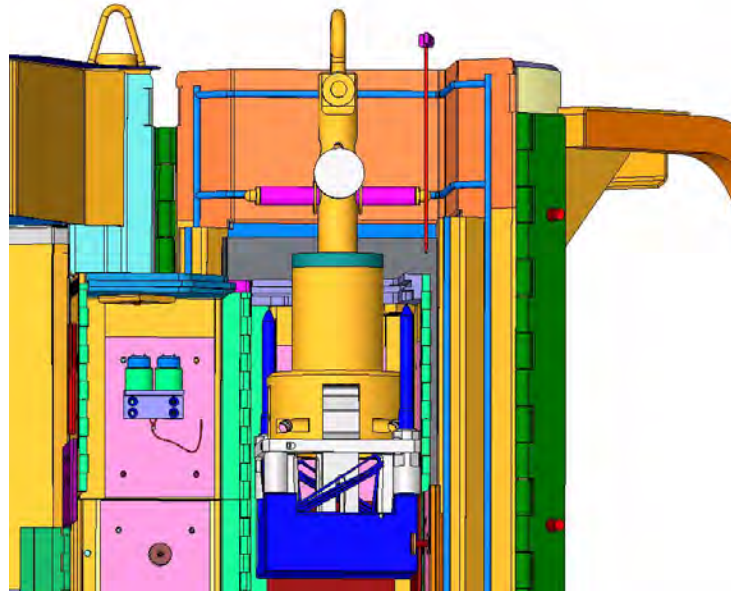


Figure 2-163 Fuel Handling Tool Grappled to a 17x17 Top Nozzle (in blue) within the Opened Outerpack and Clamshell

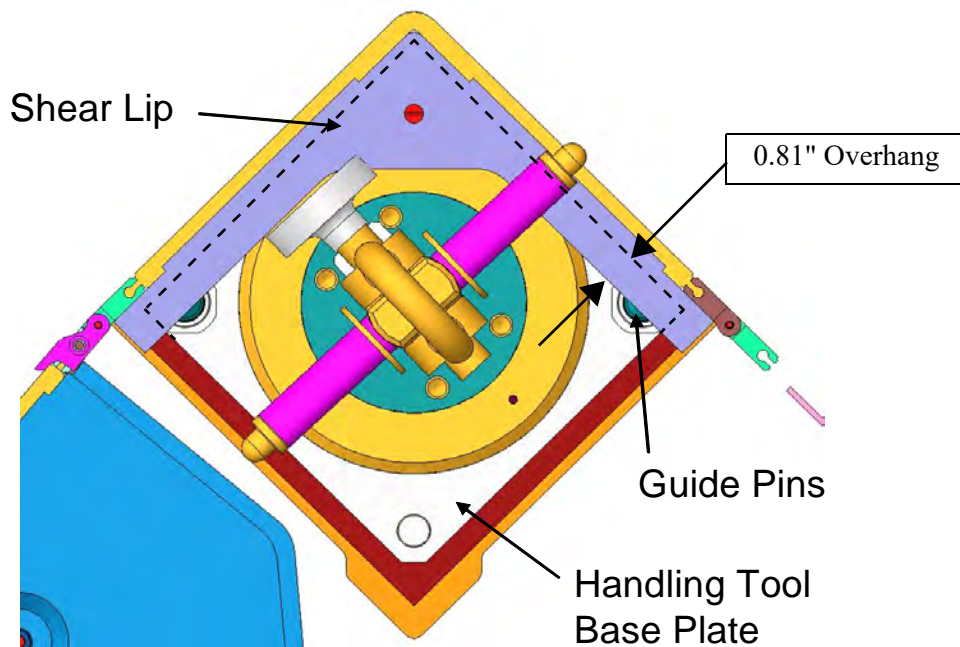


Figure 2-164 Fuel Handling Tool Shown Attached to a 17x17 XL Fuel Assembly and Behind the Overhanging Shear Lip

2.12.7.2 Conclusions

One of the most damaging orientations for the Clamshell and contents during impact is the end over center of gravity. The top-down impact challenges the integrity of the Clamshell's top end plate. End over center of gravity drop testing was performed using a certification test unit (CTU) and simulated using a finite element (FE) model. Both the actual drop tests and the FE model showed that the FTP design was acceptable. Simulation of the drop test with the RTP shows that this alternate end top plate design is also acceptable.

The screw fasteners that secure the top end plate components to the top access door and clamshell base are the weakest structure in either the FTP or RTP. These screws resist shear forces resulting from the secondary impact of the fuel assembly or fuel rod box on the top end plate during an end drop. Each screw is a stainless steel flat head cap screw, ½ inch diameter -13 threads per inch (1/2-13). These screw fasteners are not subject to large shear forces because the fuel assembly or fuel rod box is restrained in the Clamshell to prevent secondary impact on the end plate.

2.12.7.3 Detailed Calculations and Evaluations

A Traveller XL finite element (FE) model of the entire package was originally used to simulate the impact testing. A new LS-DYNA Traveller model was created to simulate features of the XL package affected by the end impact orientation. The new model is more efficient and was used to evaluate the structural performance of the axial space in the vertical end impact.

Method

The Lawrence Livermore, LS-DYNA[®] finite element code was used to determine the loads, displacements, accelerations, strains, etc. of a Traveller XL shipping package containing a 17x17 XL fuel assembly with RCCA when dropped onto a flat unyielding surface from a height of 10m. LS-DYNA 970, Revision 5434a, is a general purpose finite element code for analyzing the large deformation dynamic response of structures. This software was selected because it allows the analysis to include the effects of large deformation, large strain, material non-linearity, contact, and failure of materials.

Only the top end of the FA is modeled, the remainder of the assembly mass is simulated through point-mass elements. The weight of the remainder of the Clamshell is also modeled with point-mass elements. The Clamshell is an aluminum box with a solid 1 inch thick top plate. Figure 2-165 shows components and meshing for the FEA simulation.

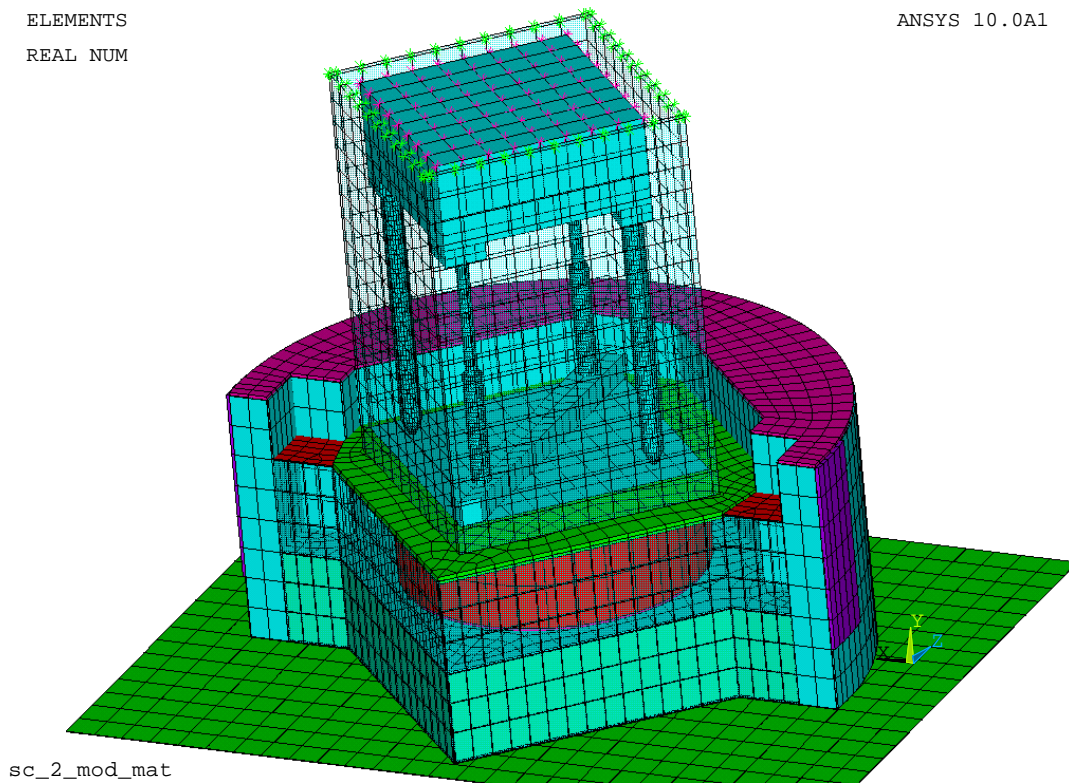


Figure 2-165 Traveller Top End Plate FEA Model

Calculation Results

The LS-Dyna model was also used to evaluate the maximum shear forces in the shear bar screws (simulated as the shear forces at the interfaces between the top plate and the extrusion walls). The peak shear force of the worst wall (i.e. across 5 screws) still showed a factor of safety of approximately 2.02 using conservative assumptions (i.e. ignoring friction between the wall and the plate for example).

The complete impact event for the RTP design without guide pins is shown in Figure 2-166 at various times. Figure 2-167 shows the rigid wall impact force history of RTP model and Figure 2-168 shows the kinetic energy history (mJ) of the axial spacer model.

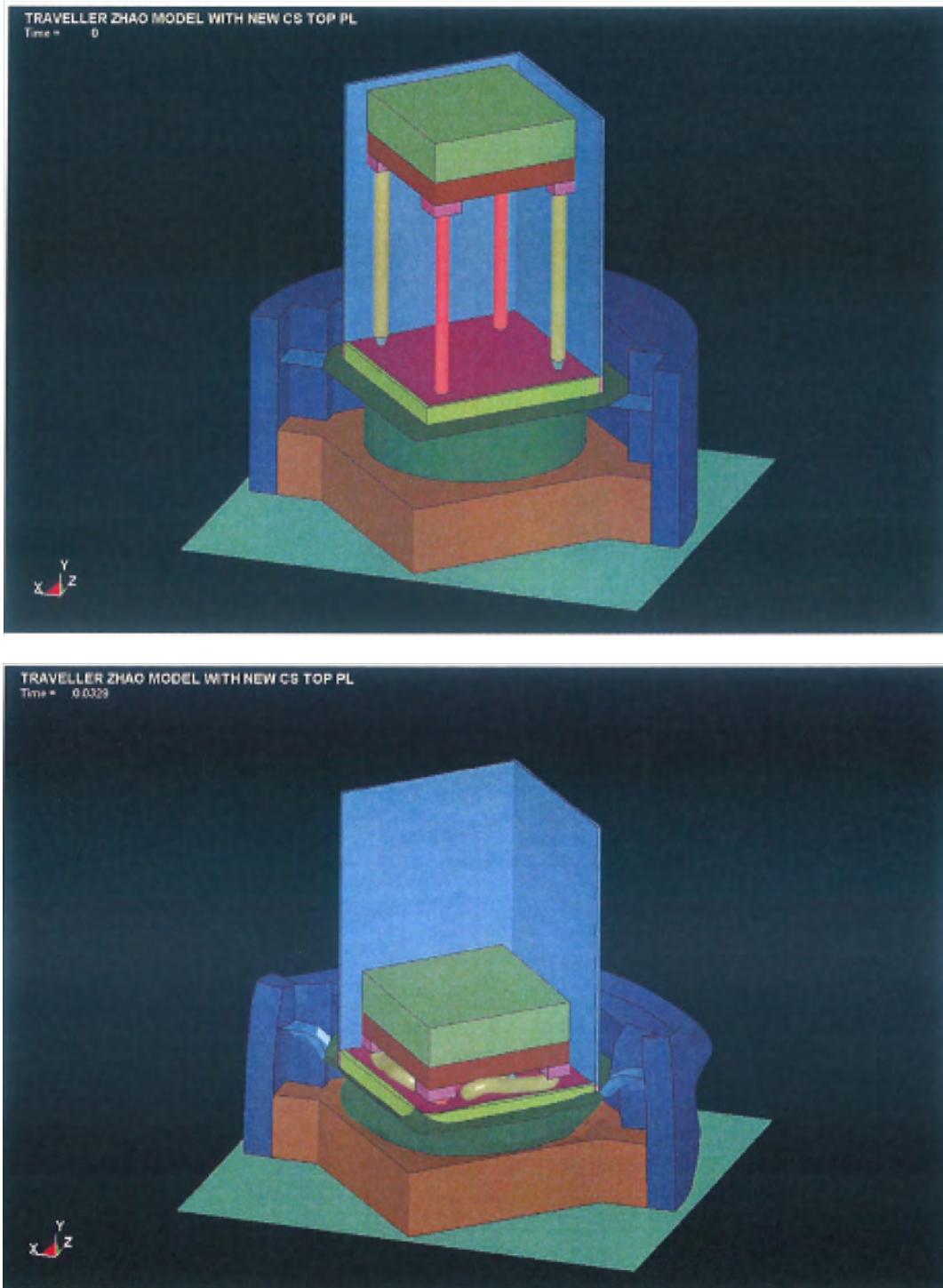


Figure 2-166 RTP Model at Beginning of Impact (0 ms) and End of Impact (33 ms)

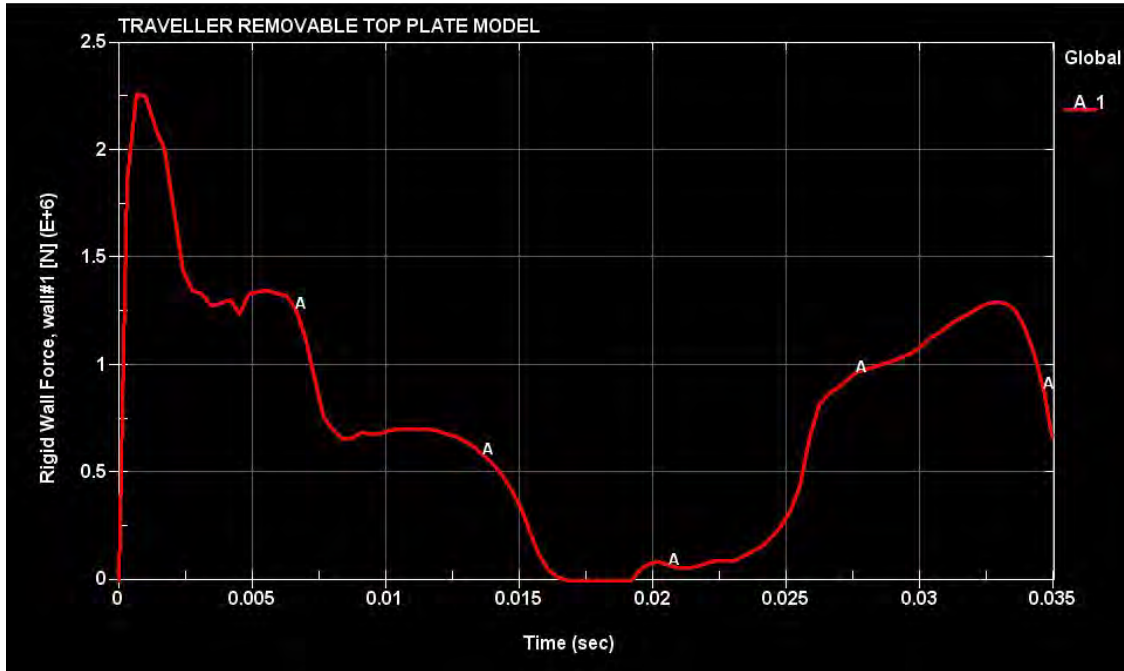


Figure 2-167 Rigid Wall Impact Force History of RTP Model

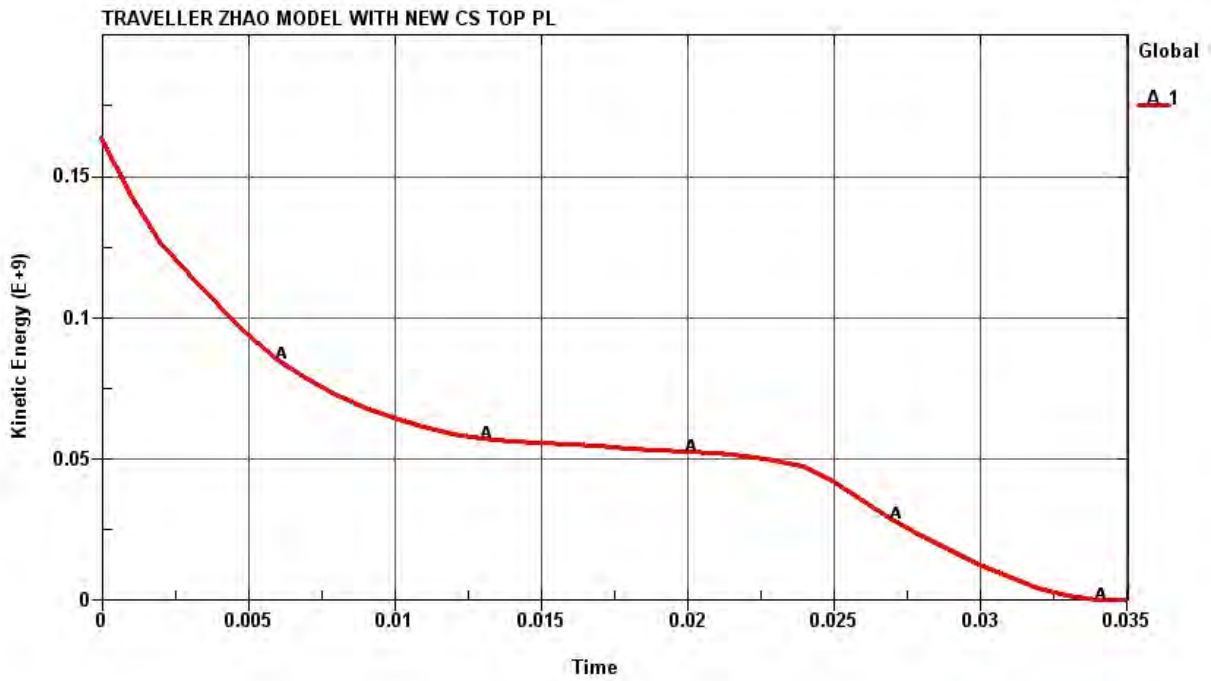


Figure 2-168 Kinetic Energy History of RTP Model (mJ vs s)

Validation

The many assumptions used to develop the LS-DYNA non-linear finite element stress code, including those needed to model the materials and impact, are validate by comparing the simulation results to the actual drop tests for the Traveller XL. Comparisons between certification test unit results and FEA simulation demonstrates that physical phenomenon governing shipping package impacts is simulated with adequate fidelity using the LS-DYNA model.

The buckling of the axial clamp studs and the Pillow are very similar to the previous the drop tests done with the qualification test unit (QTU). Figure 2-169 shows prediction of the post drop deformed shape of the top nozzle compared to the actual dropped onzzle.

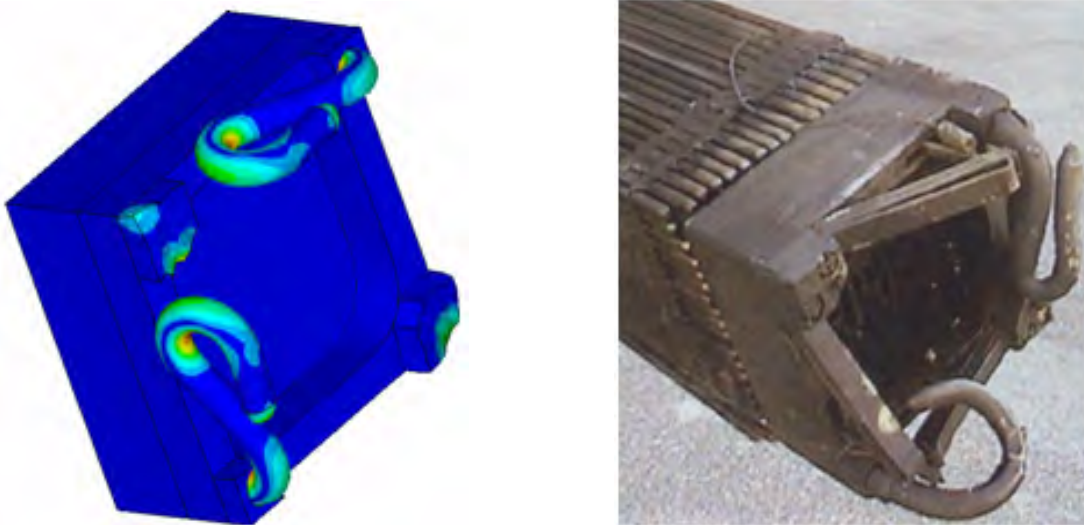


Figure 2-169 Comparison of Simulated Top Nozzle Damage (left) to Drop Test (right)

Computer Code Input Files

QTU1_9 w big axial studs 3.k

Traveller Top Nozzle Impact Study, New Top Plate Model

References

1. SFAD-09-184, Revision 1 (May 24, 2010) “ER 09-6 – Engineering Review Data Package for Revised Traveller Shear Lip”

2.12.8 Supplement to Drop Analysis for the Traveller XL Shipping Package - Structural Analysis of the Traveller VVER Shipping Package

2.12.8.1 Purpose and Background

Purpose

The purpose of this analysis is to evaluate the Traveller VVER shipping package for structural adequacy. Since the top-down impact represented one of the worst-case orientations for the Traveller XL Clamshell, it is therefore being used as a worst case study. Another “worst case” orientation is the low angle drop, or “slap-down.” A second finite element model was created to evaluate the VVER Clamshell in a 10 degree slap-down.

The Traveller VVER Clamshell will be shown to be as robust as the existing, and bounding, Traveller XL Clamshell. Evaluation of the Traveller VVER package’s Clamshell structural adequacy is presented by both by finite element modeling and standard engineering hand calculations.

Background

The Traveller VVER package is designed to carry one (1) hexagonal fuel assembly. The packaging is comprised of two basic components: 1) an Outerpack, and 2) a Clamshell. These are connected together with a suspension system that reduces the forces and shock loads to the fuel assembly during transport. Figure 2-170 shows an exploded view of the VVER shipping package. The fuel assembly is secured inside the Clamshell during transport using laterally with foam pads, and axially with a screw-activated top plate. Figure 2-171 shows the VVER Clamshell top detail view with the top plate and a closure latch identified.

The Traveller VVER package will be the third Traveller version; currently manufactured Traveller versions include the shorter Traveller STD and the slightly heavier Traveller XL package. The Traveller VVER Outerpack is identical to the Traveller XL Outerpack except that the shock mounts on the VVER are slightly smaller and stiffer and are attached to the lower Outerpack with a bracket. This change was needed because the sway space inside the VVER package is less than the XL package.

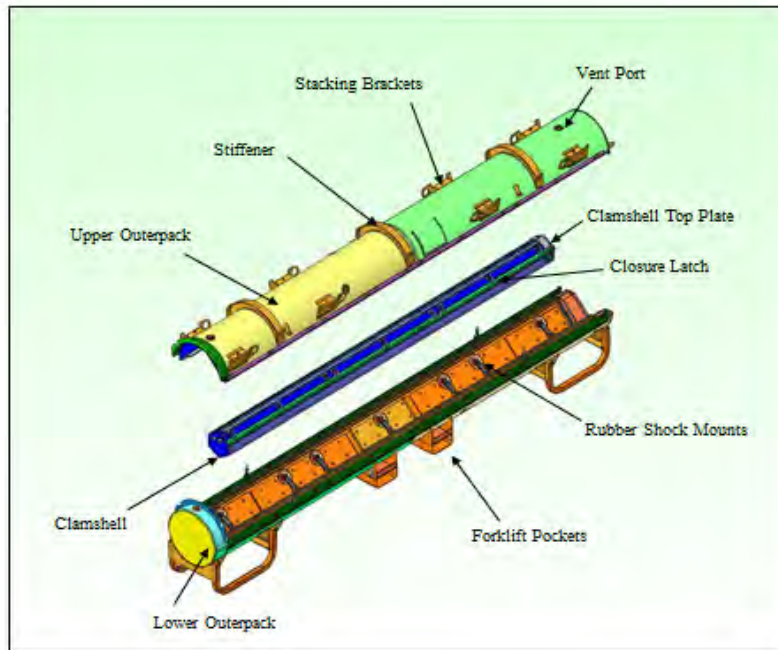


Figure 2-170 Traveller VVER Exploded View

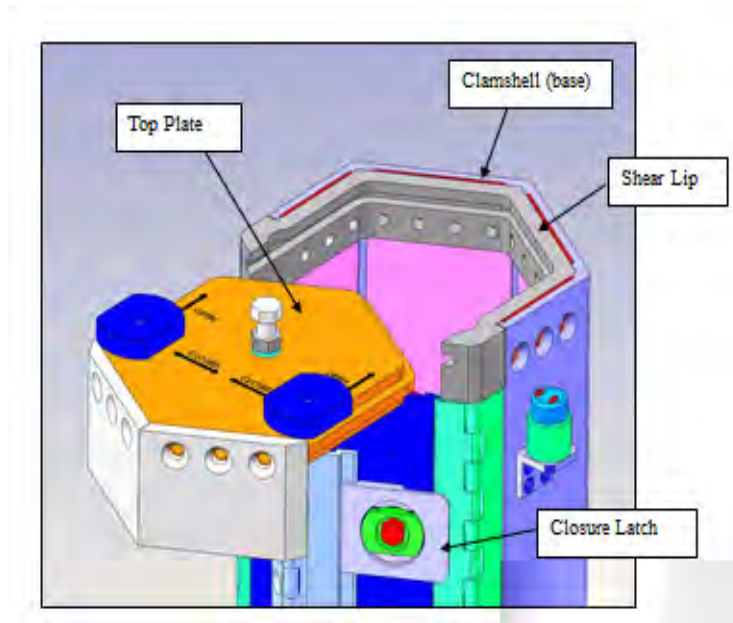


Figure 2-171 Traveller VVER Clamshell Top Detail

While the identical Traveller XL Outerpack will be used for VVER packages (albeit with different shock mounts), the Clamshell will be replaced with a hexagonal cross-section Clamshell. A cross-section comparison between the existing Traveller XL package and the VVER package is shown in Figure 2-172. As can be seen in Figure 2-172, the hexagonally-shaped Clamshell does fit within the Traveller XL Outerpack envelope. However, the Traveller VVER sway space is slightly less when compared to a Traveller XL package. The Traveller XL sway space is approximately 0.86 inches (21.8 mm) with no gravity effects to compress the shock mounts. This occurs at the upper faces of the Clamshell. The minimum sway space for the VVER Clamshell is 0.64 inches (16.3 mm) with no gravity effects. Actual sway space on the upper half of the VVER Clamshell will be higher due to the weight of the fuel which compresses the rubber shock mounts slightly. The shock mounts themselves behave as non-linear springs so impact with the bottom halves is not likely since they stiffen considerably as they are compressed.

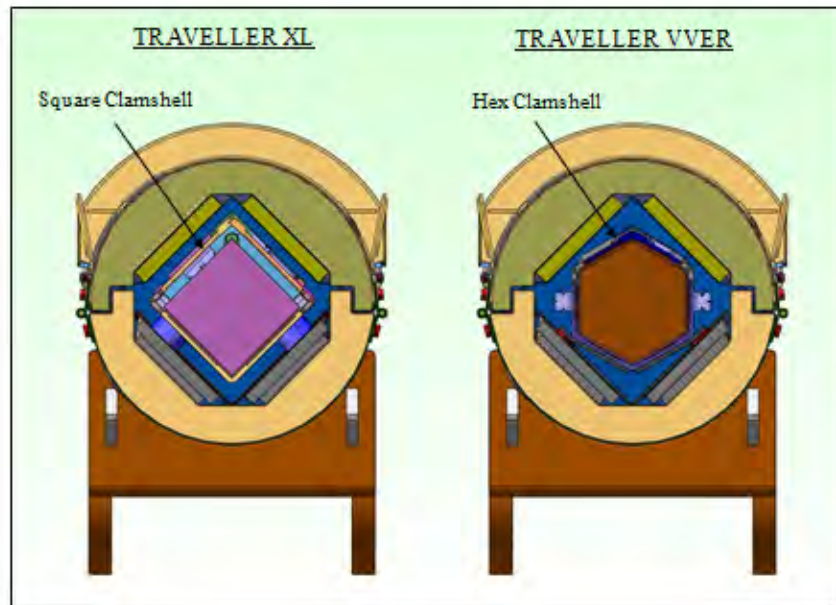


Figure 2-172 Cross-Section Views of Traveller XL and Traveller VVER Shipping Packages

The VVER type fuel is shorter than the bounding 17x17XL fuel carried by the XL package; 180.4 inches [4582.2 mm] vs. 199.2 inches [5059.7 mm], respectively. This allows a much shorter, therefore lighter, VVER Clamshell to be designed. Figure 2-173 provides a comparison of the Traveller VVER and Traveller XL Clamshells within the Outerpack.

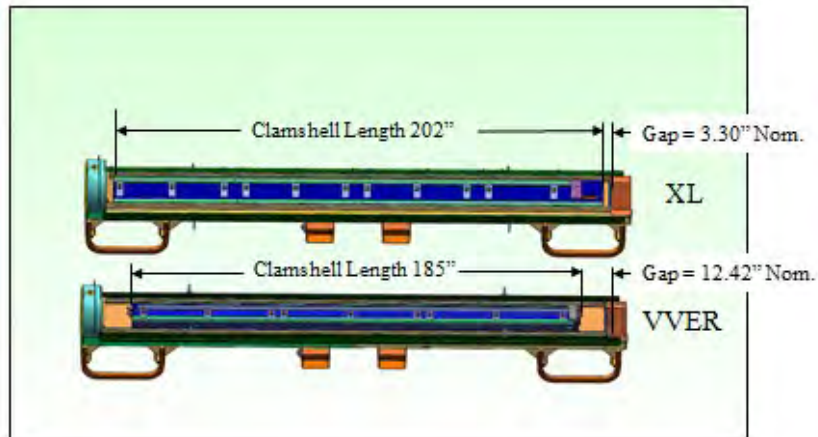


Figure 2-173 XL and VVER Clamshell Lengths Shown with the Outerpack Lid Removed

The structural design development and licensing strategy for the Traveller VVER package incorporates the existing Traveller XL Outerpack, so only the Traveller VVER Clamshell and suspension system needed to be developed and integrated with the Outerpack. As such, every effort was made to design the VVER Clamshell with the same, or greater, strength, as the Traveller XL Clamshell. The bounding fuel assembly for the Traveller XL package (17x17XL) is heavier than the fuel carried by the Traveller VVER package. A 17x17XL fuel assembly weighs 1971 lbs, including RCCA. The VVER type fuel weighs 1850 lbs maximum, including RCCA. Design basis weights of all Traveller models, including major components and maximum fuel assembly masses are shown in Table 2-6.

The Traveller VVER Clamshell design process began with the aluminum extrusion design. These were designed with the same wall thicknesses as the Traveller XL Clamshell, as shown in Figure 2-174. The wall thicknesses of all extrusions are the same, the door hinges are identical, the door "tongue and groove" joint is the same, and the latch extrusions are nearly identical. The nominal wall thicknesses are 0.438 inches near the corners and 0.313" at the thinner "pockets." The thinner sections along the faces are to accommodate []^{a,c} thick poison plates (for neutron absorption).

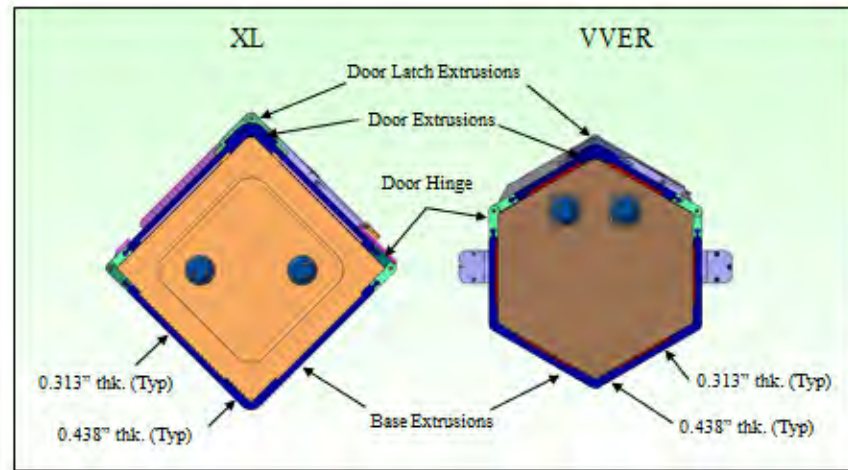
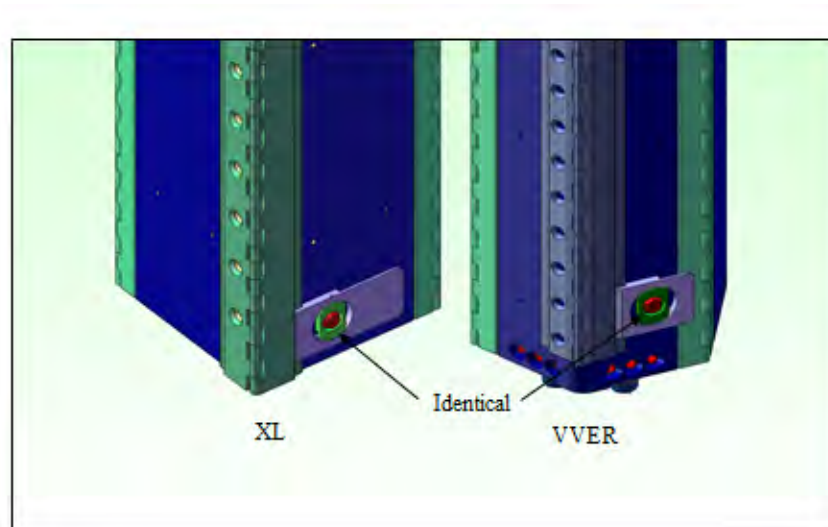


Figure 2-174 Similarity of XL and VVER Clamshell Extrusions

The Traveller VVER Clamshell main doors operate in the same manner as the Traveller XL package and are secured with identical hinge extrusions and door locking mechanisms as shown in Figure 2-175. The door latch for the Traveller VVER is shorter than the Traveller XL, but its function is the same. As with the Traveller XL, the Traveller VVER hinge extrusions are welded to the doors and the base extrusions.



**Figure 2-175 Identical hardware for XL and VVER Clamshell Quarter-turn Latches
(Shown in Locked Orientation)**

The fuel assembly top plate axial restraint was shown in Figure 2-171 as it fits into the Clamshell shear lip. Figure 2-176 provides the Traveller VVER top plate detail (underside isometric view); specifically the retractable top clamp plate is shown. Once the fuel is loaded into the Clamshell and the main doors are closed, the top plate assembly is slid into position with the clamp plate retracted. After locking the top plate to the shear lip, using the quarter-turn locking knobs, the center clamp plate actuating stud (Figure 2-176) is turned. This lowers the round clamp plate until the rubber pad contacts the fuel. A jam nut is used to keep the stud from turning during shipment.

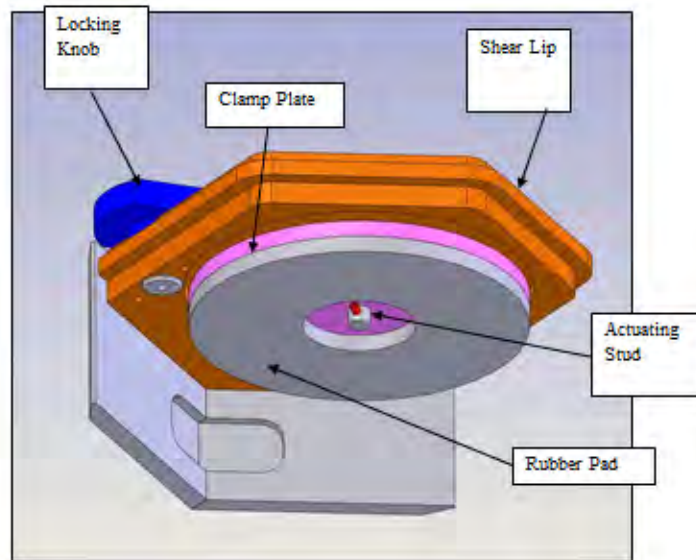


Figure 2-176 Traveller VVER Clamshell Top Plate Assembly

The VVER type fuel assembly is positioned into the Traveller VVER in the same manner as fuel of square cross-section design (for Traveller STD and XL). Figure 2-177 shows an open upper Outerpack; the top plate assembly installed and the round axial clamp extended into the clamped position contacting the VVER fuel assembly (model). Note that the main Clamshell doors are open in the figure for visual purposes only. They would be closed and locked during transport. One side of the top plate assembly covers (gray in color) is also hidden in the figure for visualization purposes. Figure 2-178 shows a VVER type fuel assembly (model) inside the Clamshell and seated against the bottom plate.

The Traveller VVER top and bottom end plates were designed thicker than their respective Traveller XL counterparts. The Traveller VVER top plate thickness is 1.25" (31.8 mm) and the bottom plate thickness is 1.50" (38.1 mm) thick as compared to 1.00" (25.4 mm) thick plates for both the Traveller XL (and STD) Clamshell end plates.

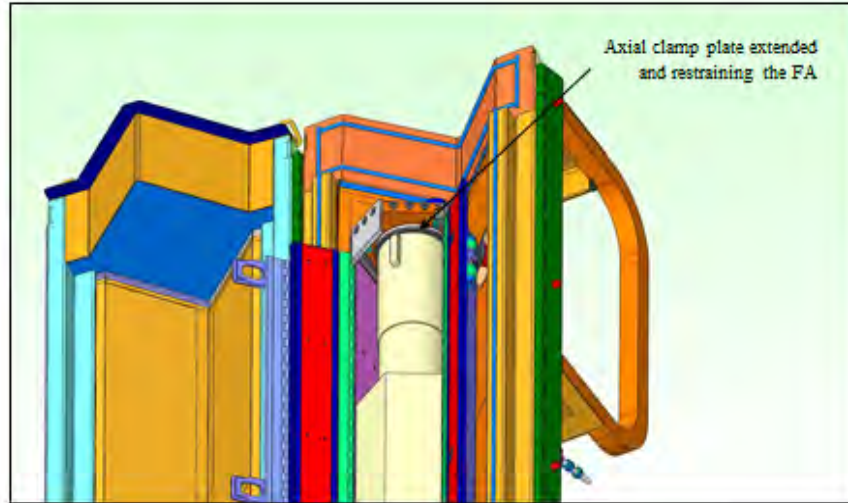


Figure 2-177 VVER Fuel Assembly Installed - Top Nozzle Region

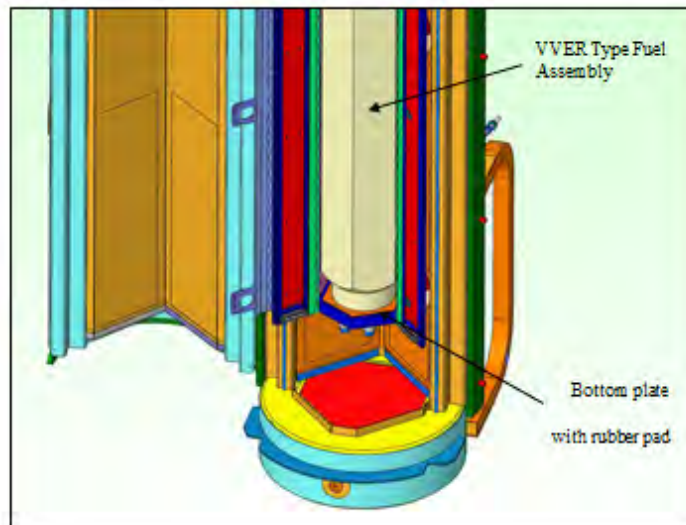


Figure 2-178 VVER Fuel Assembly Installed - Bottom Nozzle Region

Since the Hypothetical Accident Condition (HAC) top-down impact represented one of the most structurally challenging orientations for the Traveller XL Clamshell, it was also used for the Traveller VVER evaluation. During the top-down impact, most of the fuel assembly impact load path force is directed through the top plate. Hence, calculations were performed to demonstrate the robust structural design of the top plate shear lip by accommodating the entire shear load from the fuel assembly deceleration. Another structurally challenging orientation is the low angle drop, or "slap-down." A second finite element model was created to evaluate the VVER Clamshell in a 10 degree slap-down. The model simulated the fuel assembly as a solid rubber mass so as to minimize the bending stiffness of the fuel assembly itself. This assumption forced the Clamshell to resist all fuel assembly forces and accelerations.

2.12.8.2 Results and Conclusions

Results of the VVER top-down impact analysis indicate robust performance. The calculated deceleration of the VVER Clamshell was 72.5 g's, and, as expected, is less than the calculated Traveller XL top-down impact of 102 g's. This relatively low deceleration ensures that the retaining top plate bolts are stressed to a lesser degree than the XL Clamshell in the same orientation. Additionally, the strength and stability of the Clamshell walls, top plate assembly and other components are structurally adequate. Subsequent shear lip joint hand calculations demonstrate the structure has adequate strength to absorb the maximum impact load without significant damage.

The results of the low angle impact also indicated robust performance. No significant Clamshell damage at the first or second impact end was noted by virtue of the calculated 0.12% plastic strain at peak bending, in the bottom edge, near the mid-span. The Clamshell provided excellent structural performance in the slap-down event.

It is concluded that the VVER Clamshell survives the most damaging 9m drop orientations, a top-down end drop and a low angle slap-down. The walls of the Clamshell do not significantly deform and thus they keep the fuel envelope confined. The top plate assembly also exhibits a low degree of plastic deformation, which only occurs locally.

2.12.8.3 Detailed Calculations and Evaluations

Finite Element Modeling

Computer analysis of the Traveller VVER shipping package was performed using a large-strain capable, nonlinear, finite element code to verify Traveller VVER package performance. No actual drop testing was performed due to the similarity of the design with the Traveller XL. The finite element code used for this work was LS-Dyna, which is commercially available through Livermore Software Technology Corporation.

The bounding Traveller XL was also analyzed with this software. At that time, the analysis was only used for worst case drop orientation parametric studies. For example, how the package would behave for different drop angles. These were compared against each other and not for actual performance verification. Other factors such as skin thickness changes, foam density effects, and temperature effects were compared. The "sensitivity study" nature of the finite element modeling was to compare relative hypothetical drop

orientations. As a result, the primary basis for package compliance was through execution of actual drop testing. Agreement between computer modeling and actual drop testing was remarkably good. The original finite element model was extremely detailed and could accommodate all drop orientations. Subsequent to the Traveller licensing, a new, simplified LS-Dyna model was created to explore other changes and parametric studies. This new model was benchmarked against the original model and used to demonstrate structural adequacy of the Removable Top Plate (Section 2.12.7). In this analysis, the simple model was modified for the VVER design.

The computer model was created to simulate a 30 ft free-drop onto an unyielding surface. The entire model except the unyielding "ground" was initially set with a velocity of 13,380 mm/s (43.91 ft/s). This corresponds to free drop height of 9.13 m (30.0 ft). In the model coordinate system the velocity vector is pointed in the Y direction (see coordinate triad in Figure 2-182, in the lower left corner).

Using the results of the large-strain dynamic finite element analysis, the average deceleration of the Clamshell can be calculated and compared to the bench-marked Traveller XL analysis. The deceleration is based upon the total crushing Y-distance of the components below the Clamshell top plate. This includes the Pillow and the end limiter foam. At the top of the Pillow is a relatively thick stainless steel "puncture plate." It is the green plate shown in Figures 2-181 and 2-182. The displacement of this plate represents the total displacement of the Clamshell. LS-Dyna was queried for the time dependent displacement (Y-direction in model axis) for a node (node #120) in the center of the puncture plate. A plot is shown in Figure 2-179 below.

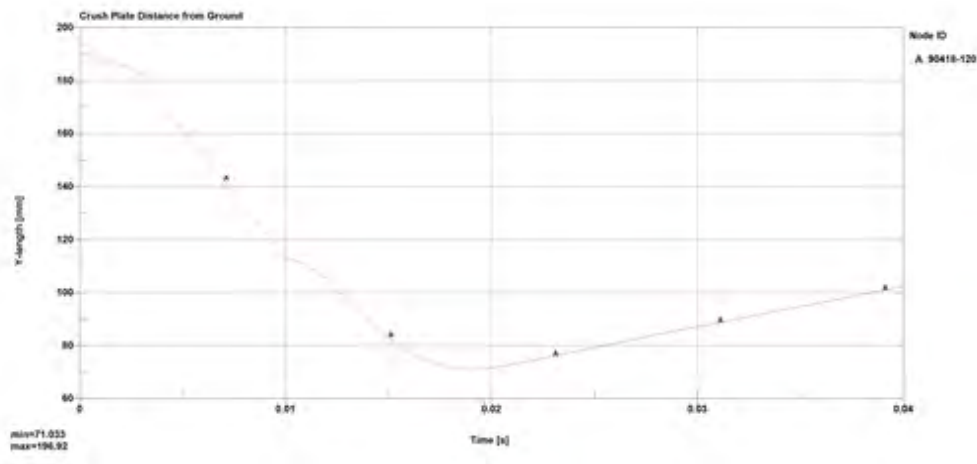


Figure 2-179 Puncture Plate Distance from Ground During Impact

The Traveller Clamshell is a long aluminum structure (hexagonal cross-section box) which is attached to the Outerpack with rubber shock mounts. While these shock mounts were not explicitly modeled in this analysis, their contribution to Clamshell stability and restraint was incorporated by applying a non-rotation boundary condition on the Clamshell "cut" face (at the upper face in Figure 2-181). With this boundary condition, the Clamshell cut face was not allowed to move or rotate about the X and Z axes. Similarly, the fuel assembly mass (see Figure 2-182) is also restrained from rotation because an actual fuel assembly is a long and fully supported mass. The fuel assembly mass was not allowed to rotate around the X and Z axes.

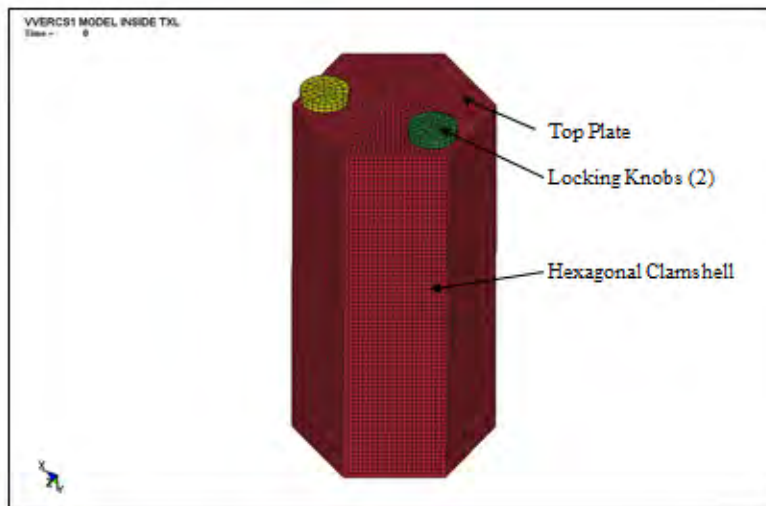


Figure 2-180 Traveller VVER Clamshell Model Showing Key Components

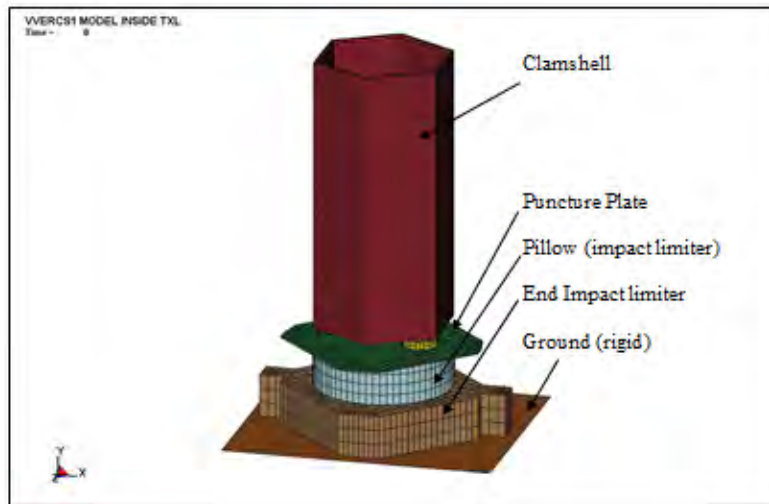


Figure 2-181 Traveller VVER Finite Element Model

Previous Traveller XL drop test analyses were revised based upon increased measured Outerpack weights. The remainder of the upper Outerpack was not discretely modeled because it does not affect performance of the Clamshell. The impact of the upper and lower Outerpack halves does not affect the performance of the Clamshell in a significant way. To bound the as-measured condition, 122 pounds was added to the SAR weights, and subsequent analysis used this weight increase for the Clamshell. This condition was applied to the Traveller VVER finite element analysis. Although the nominal Clamshell weight is 463 pounds (210 kg), the analyzed weight is 585 pounds (265 kg). The VVER fuel assembly weight used for the analysis is 1850 pounds (839 kg). This mass is simulated with very high density material within the hexagonal FA component as shown in Figure 2-181.

Figure 2-183 shows the underside of the top plate assembly and the axial clamp plate and stud. The plate is 0.5" thick 6061-T6 aluminum and the rubber is neoprene, 60 durometer. The center stud is 5/8"-11 bolt with a jam nut on the outside of the top plate to keep it from rotating during shipment.

For this analysis, the structural integrity of Clamshell is of key interest. To obtain this information, the initial material parameters were set, which included the initial impact velocity of 13,380 mm/s (43.91 ft/s). This corresponds to free drop height of 9.13 m (30.0 ft), see Section 2.12.8.2. All part configurations were obtained from the SolidWorks® CAD models and transferred into LS-Dyna using IGES files. Material properties for the various materials can be found in the Assumptions section below.

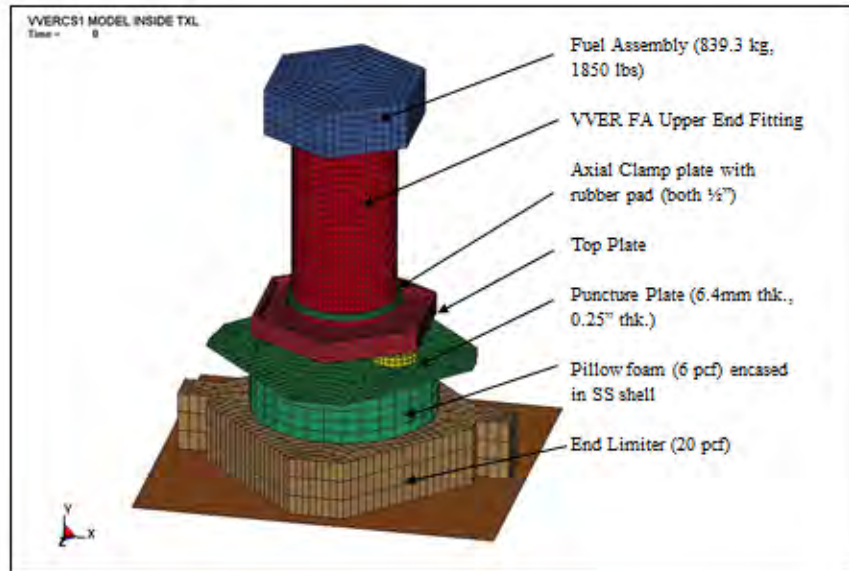


Figure 2-182 Traveller VVER Model with Clamshell Walls and End Limiter Cover Plate Hidden

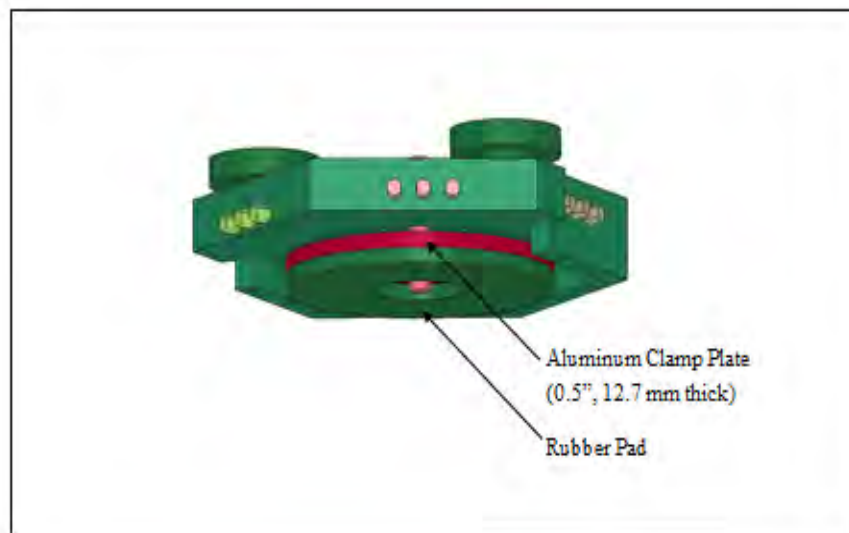


Figure 2-183 Traveller VVER Top Plate Assembly Showing Integral Axial Clamp and Rubber Pad

Assumptions

Many assumptions are used to develop a model for the LS-DYNA non-linear finite element stress code, including those needed for material properties and boundary conditions. These assumptions were found valid for simulating drop tests of the Traveller XL package through comparison with actual drop tests. It is clearly evident from comparisons between prototype test results and predictions that the key physical phenomena governing shipping package impacts is captured within the LS-DYNA code.

This simulation was performed using conservative assumptions which include the following:

- 1) The assumed mass of the VVER FA in the model was 1,850 lbs (839 kg).
- 2) The FA is modeled as an upper end fitting (pipe) and a hexagonal lump of steel with a higher than normal density. It is therefore essentially rigid. This is very conservative since actual drop testing revealed the weak axial stiffness of a fuel assembly (it vibrates and bows during end impacts). Fuel rod "slip" also tends to reduce the stiffness of the fuel.
- 3) The drop height corresponds to 9.13m (30 ft), slightly greater than the 10CFR71.73, 9 m drop height requirement.
- 4) The majority of the mass of the Outerpack has not been included in this analysis (i.e. the lower Outerpack) because it does not significantly affect the Clamshell impact. More specifically, the Outerpack impact event is finished within only a few milliseconds, therefore the bottom limiter (the Pillow) is simply waiting for the Clamshell impact into it.
- 5) The foam crush characteristics shown in Figure 2-184 include extrapolation from 80% crush to 100% crush for model stability purposes. As mentioned earlier, actual pillow crushing during actual testing was measured to be only about 50%. This is because the fuel assembly is not a rigid "hammer" that have no axial elasticity. This effect has been proven to be quite significant. However, in these simulations, the severe impact of inelastic modeling of the fuel assembly was used. In some cases, this forces the crush curves to be extrapolated to 100%.
- 6) In the slap-down model, the FA was modeled as rubber so that the Clamshell had to stabilize it. A stiff fuel assembly would have prevented the Clamshell from large scale deformations and plastic strain.

Axial Free Space Between the Clamshell and the Impact Limiter

The Traveller VVER design has an additional 9.12 inches of free space between the end of its Clamshell and the contact surface of the Outerpack impact limiter compared to the Traveller XL (12.42 inches versus 3.30 inches; Figure 2-173). The Traveller XL finite element models simulate a 30 foot free-drop onto an unyielding surface and the start of the simulation places the Outerpack just above the ground plane. The Outerpack impacts the unyielding surface and comes to rest before the Clamshell impacts it.

The gap for the Traveller XL finite element analysis was set at 0.048 inches. The Clamshell is positioned near the Outerpack so as to minimize the "free fall" of the Clamshell to optimize the model. However, a sufficient gap exists to allow the Outerpack to essentially come to rest first, before the Clamshell impacts it. This occurs over an approximate 2 millisecond duration. Because the Outerpack does not have time to bounce in these few milliseconds, it is essentially at rest awaiting the Clamshell impact. The Clamshell then impacts the Outerpack with the same initial velocity as it had at the start of the simulation. Even though the Traveller XL actual 3.30 inch gap was not explicitly modeled, the finite element analysis results were in a good agreement with the physical drop testing. The same finite element analysis techniques were employed for the Traveller VVER. In both cases, the Outerpack and the Clamshell have an initial velocity of approximately 43.9 feet/second to simulate the 30 foot free-fall impact forces.

Material Properties

The material properties assumed for the aluminum, stainless steel, and the crushable foams can be seen in Tables 2-56, 2-57, and 2-58, respectively.

Table 2-56 Aluminum Properties for Traveller VVER Analysis				
6005-T5 and 6061-T6 Aluminum at 75 Degrees F				
Property	Symbol	Value	Units	
Density	RO	2.71E-09	Mg/mm ³	
Modulus	E	69	kN/mm ² (GPa)	
Poisson's Ratio	PR	0.33	Dimensionless	
Yield Strength	SIGY	0.241	kN/mm ² (GPa)	

Table 2-57 Annealed 304 Stainless Steel Properties for Traveller VVER Analysis				
Property	Symbol	Value	Units	
Density	RO	7.85E-09	Mg/mm ³	
Modulus	E	207	kN/mm ² (GPa)	
Poisson's Ratio	PR	0.30	Dimensionless	

Property	Density Mg/mm³	Modulus kN/mm² (GPa)	Poisson's Ratio Dimensionless
6 pcf Last-A-Foam	9.61E-11	30.14	0
10 pcf Last-A-Foam	1.60E-10	66.23	0
20 pcf Last-A-Foam	3.20E-10	192.76	0

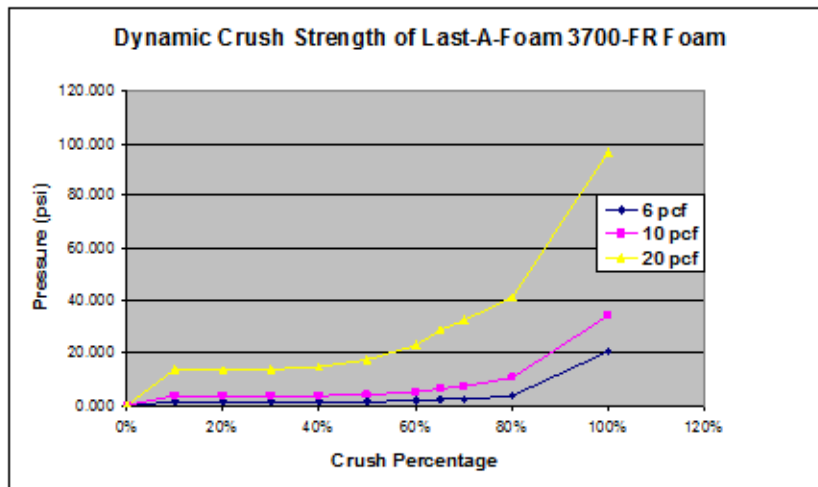


Figure 2-184 Comparison of Dynamic Crush Strengths of the Foams Components

Figure 2-185 shows the stress-strain curve of the stainless steel properties used in the LS-Dyna simulations.

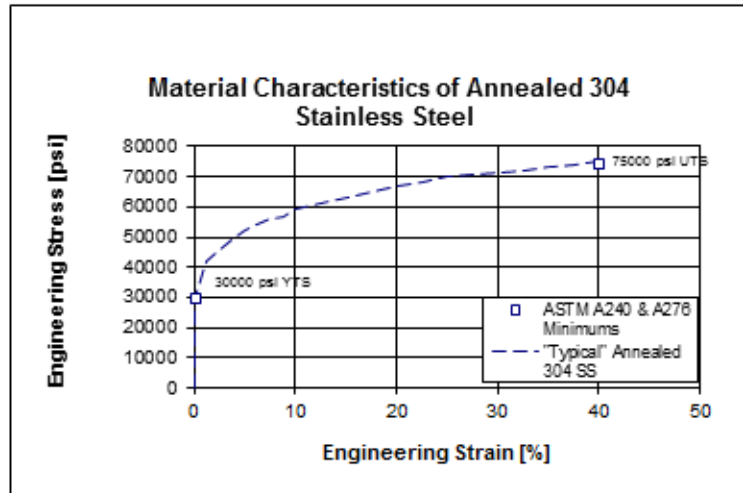


Figure 2-185 Annealed 304 Stainless Steel Stress-strain Characteristics

Top-down Evaluation and Results

Results of the VVER top-down impact analysis (see Figure 2-186, below) with VVER fuel indicate robust performance. The calculated deceleration of the Clamshell was 72.5 g's compared to the calculated XL top-down impact of 102 g's. The Traveller XL Clamshell demonstrated robust structural integrity for the applied 102g deceleration load. The strength and stability of the Clamshell walls, top plate assembly and other components are adequate. As with all Traveller variants, in high-angle drops, the soft "Pillow" foam provides a crushable cushion for the Clamshell (and fuel) to impact.

The analysis conservatively models the fuel as a solid mass with a simulated top end fitting. This is very conservative because the fuel is not a rigid mass; it is very susceptible to fuel rod bowing, buckling, and vibrations, as well as fuel rod slippage within the skeleton. All of these factors lessen the impact energy and subsequent forces through the Clamshell.

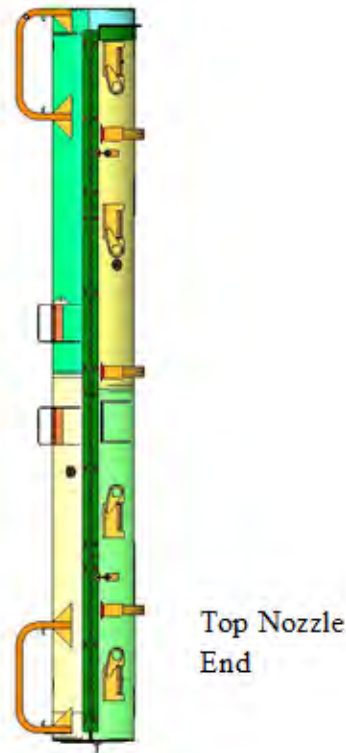


Figure 2-186 Traveller XL Shown in a Top-down Impact Orientation

The axial load path in the top-down end drop is primarily from the fuel through the top plate and into the Pillow foam, however, any axial differential shearing loads (Clamshell walls and top plate) are reacted by the ½ inch diameter screws which fix the top plate and shear lip to the Clamshell walls. In the case of the Traveller XL, 20 screws are used to make this attachment. Despite the reduced weight of the VVER fuel, the VVER Clamshell also utilizes 20 screws to affix the top plate and shear lip to the walls and doors.

The model results are shown in Figure 2-187, in 5 ms increments. The VVER Clamshell walls and bottom limiter cover plate have been hidden for viewing of the fuel assembly and Pillow. The end foam components crushed a total of 125.9 mm (4.96 inches) during the 20ms impact. A plot of the kinetic energy of the model is also shown in Figure 2-188. Note that the impact event is over by 20 milliseconds (i.e., kinetic energy is near zero). Note that a small amount of energy is retained due to rotation of the Clamshell within the Outerpack. This moment will be balanced by the Outerpack walls.

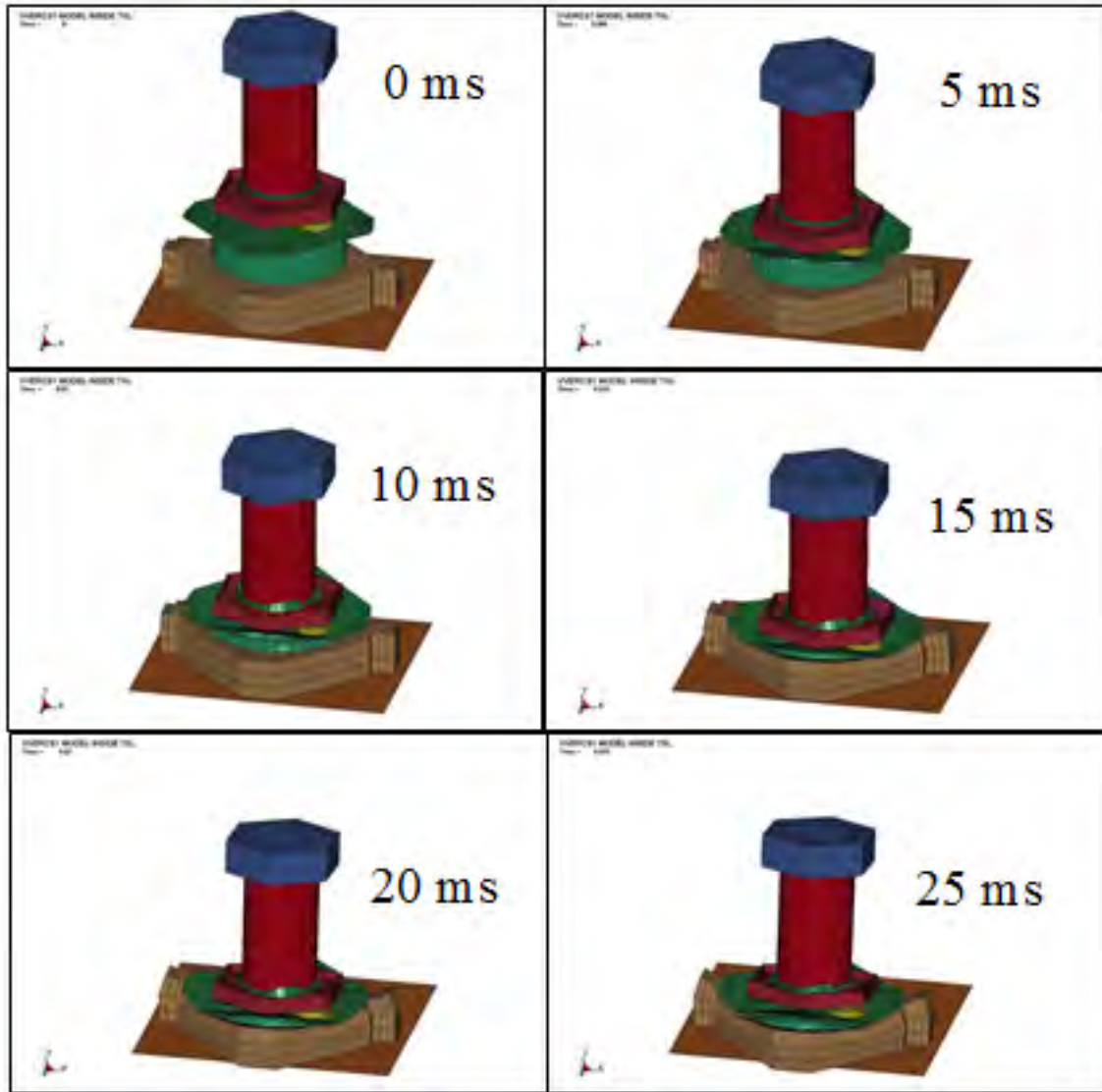


Figure 2-187 Top Down 9m Impact of Traveller VVER Package in 5 ms Increments

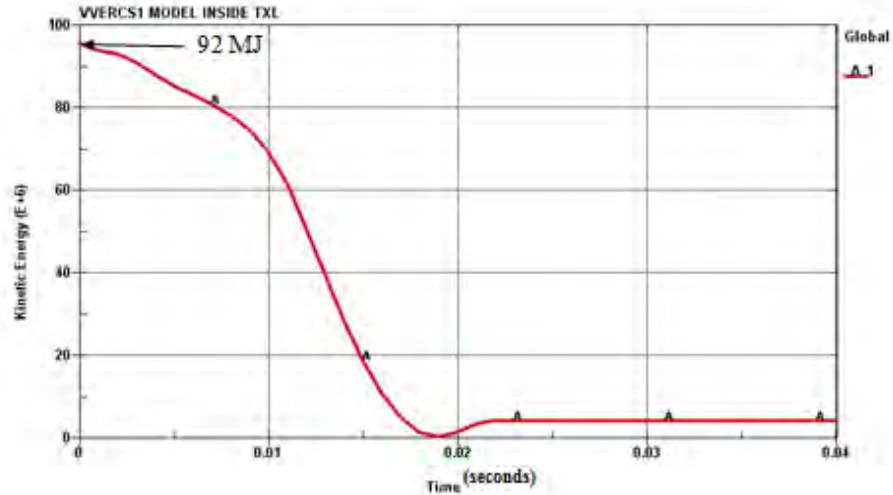


Figure 2-188 Kinetic Energy Plot for VVER Model (Time in Seconds, Energy in J)

The model predicts no crumpling of either the Clamshell walls or the VVER fuel assembly top nozzle (upper end fitting). Both components remain geometrically stable throughout the impact event.

Figure 2-189 shows the final shape of the VVER Clamshell and Outerpack at the end of the impact, 20 ms. As expected the aluminum axial clamp plate and the rubber pad are considerably deformed during a top-down impact. This energy absorption provides a positive effect on the overall structural performance of the Clamshell by reducing its absorbed energy. The locking knobs on the outside of the top plate do not significantly absorb impact energy due to their geometry and location on the top plate. There is very low plastic strain in the VVER Clamshell structural walls which includes the main doors and base extrusions. See Figure 2-190. The general state of the plastic strain in the results demonstrate a very robust structural design.

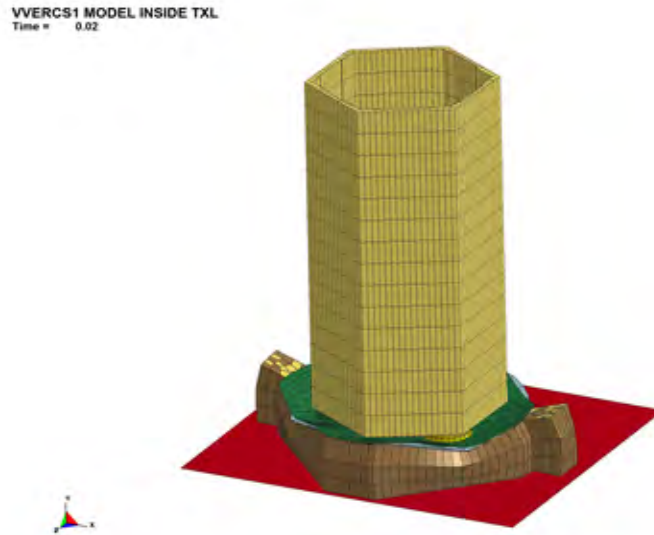


Figure 2-189 Deformed Shape of Model at 20ms

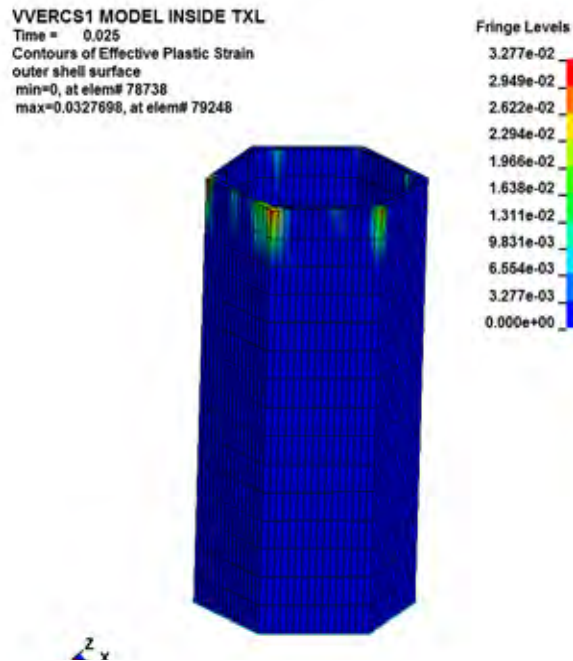


Figure 2-190 Max. Plastic Strain in the Clamshell Main Walls

Using the finite element results, the average deceleration of the Clamshell can be calculated. The deceleration is based on the total crushing Y-distance of the components below the Clamshell top plate. This includes the Pillow and the end limiter foam. At the top of the Pillow is a thick stainless steel "puncture plate." It is the 0.25 inch green plate shown in Figure 2-182. The displacement of this plate represents the total displacement of the Clamshell.

The total displacement of the crush plate is approximately 196.92 mm - 71.03 mm = 125.9 mm (4.96 inches).

The initial velocity of the package when dropped from 9.13 meters is:

$$V_f^2 = V_i^2 + 2 \times g \times d$$

Where: V_f is the velocity immediately at impact (mm/s)

V_i is the initial velocity when dropped (= 0)

g is the acceleration due to gravity, 9,810 mm/s²

d is the drop height, 9,130 mm (9.13 m)

Solving for V_f gives:

$$V_f = (2 \times 9810 \times 9130)^{0.5}$$

$$V_f = 13,380 \text{ mm/s (43.91 ft/s)}$$

During the impact, the Clamshell is decelerated to zero velocity after crushing 196.92 mm (4.96 inches). Using the same formula as above, the average Clamshell deceleration is:

$$V_f^2 = V_i^2 + 2 \times a_{ave} \times d$$

Where: V_f is 0

V_i is 13,380 mm/s (43.91 ft/s)

d is 125.9 mm (4.96 in)

a_{ave} is the average deceleration of the Clamshell structure

Then: $a_{ave} = - (13,380\text{mm/s})^2 / (2 \times 125.9 \text{ mm})$

$$a_{ave} = - 7.11\text{e}5 \text{ mm/s}^2$$

And dividing by the acceleration due to gravity (9810 mm/sec²) gives:

$$g_{ave} = 72.5 \text{ g's (decelerating)}$$

This relatively low deceleration ensures that the retaining top plate bolts are stressed to a lesser degree than the Traveller XL Clamshell in the same orientation.

Expected VVER Fuel Assembly Performance

Evaluation of VVER Fuel Assembly Performance Following NCT and HAC (Side Drop)

Traveller XL normal condition testing resulted in only localized Outerpack mechanical damage based upon visual inspection. This is due to the Outerpack design, which is the same structural design for the Traveller XL and Traveller VVER, and includes ductile stainless steel and foam that will plastically deform as they dissipate kinetic energy. After the normal and hypothetical accident condition tests, a visual inspection demonstrated that the Traveller XL Clamshell remained structurally intact. Since the Traveller VVER has shown by FEA for the 9-meter drop, the VVER Clamshell receives less applied force as compared to the Traveller XL, and that the Traveller XL Clamshell was essentially undamaged after the drop test series, therefore, the VVER Clamshell is expected to maintain its structural integrity. There are circumferential stiffeners on the Outerpack that plastically deform after a normal condition test when the package is dropped on its upper side. Therefore, it is expected that a normal condition side drop or a low-angle slap down could result in maximum VVER Clamshell and fuel assembly damage. Thus a side drop is used to perform the comparative energy absorption analysis.

The energy absorption capability comparison can be determined from the fuel assembly lateral stiffness values (impulse-dynamic effects are not considered for this comparison since those values are not available). Lateral stiffness is utilized for this comparison since the normal condition drop test considered is a side impact. Laboratory testing of VVER-1000 fuel and 17x17 XL fuel at 25.4 mm displacement at the center grid (of each fuel assembly) results in the following lateral stiffness values:

- VVER-1000: 64.5 N/mm
- 17x17 XL: 40.2 N/mm

The local energy absorption though the entire fuel assembly can be comparatively estimated by multiplying the stiffness by the number of fuel rods. The guide tubes will provide additional energy absorption, but are not considered for this comparative analysis. VVER-type fuel has 312 fuel rods and the 17x17-type fuel has 264 fuel rods. The energy absorption capability can be determined from the following spring work-energy principle. Where k is the stiffness and x is the displacement. For comparative purposes, the tested 25.4 mm deflection will be used for both fuel designs.

$$W = \frac{1}{2}(k)(x^2)$$

Table 2-59 provides the results of the work-energy analysis. It is evident that the VVER-1000 fuel assembly has more energy absorption capability compared to the 17x17 XL fuel assembly.

Table 2-59 Traveller VVER and Traveller XL Comparative Energy Absorption Capabilities		
Normal Condition (Side drop) Values	VVER-1000	17x17 XL
Local stiffness (at a fuel rod)	64.5 N/mm	40.2 N/mm
Total Lateral Stiffness (local stiffness * # fuel rods)	20.1 kN/mm	10.6 kN/mm
Energy Absorption Capability, W	6484 J	3419 J

Two 17x17 XL drop test series found that normal accident testing did not result in a fuel rod breach. Since the VVER fuel design can absorb more energy during an impact, it is expected to contain the fissile material.

An energy absorption comparison of the VVER fuel assembly and the 17x17 XL fuel assembly demonstrates that the VVER fuel assembly has more energy absorption capability than the tested 17x17 XL design. This is expected, as the VVER fuel assembly is a stiffer fuel assembly primarily by virtue of the double-bulge fuel rod design. Based upon the energy absorption comparative calculations and the 17x17 XL normal condition physical drop testing that did not result in loss of fissile material or Clamshell damage from the hypothetical accident drop, it can be concluded that the VVER fuel assembly will not lose fissile material.

Hypothetical Accident Condition (Vertical 9-meter Free Drop)

The Traveller XL FEA was benchmarked against physical drop tests and found to be in good agreement. The Traveller VVER Clamshell was modeled into the Traveller XL Outerpack and the free drop was re-run in order to evaluate the VVER Clamshell structural robustness. Drops oriented with the top nozzle down were conducted to evaluate the structural integrity of the VVER Clamshell top shear plates and bolts.

Table 2-60, below, provides a summary of calculated free-drop kinetic energy, impact force, deceleration event time, and average deceleration force value for the Traveller VVER and XL Clamshells from the FEA and/or hand calculations.

Table 2-60 Traveller VVER and Traveller XL Resultant FEA Comparisons		
FEA/Hand Calculated Results	VVER	XL
Kinetic Energy (imparted on Clamshell)	92 MJ	175 MJ
Impact Force (imparted on Clamshell)	597 kN	605 kN
Deceleration Event time (Clamshell)	20 ms	15 ms
Average Deceleration Force (imparted on Clamshell)	72.5 g	102 g

Traveller XL

The analytical 605 kN XL Clamshell impact force imparted by the fuel assembly was calculated using the baseline FEA (Section 2.12.4.2.5, Figure 2-56). The impact duration is also discussed in SAR Section 2.12.4.2.5 for the baseline FEA. The initial XL Clamshell impact onto the inner Outerpack occurs at 15 milliseconds into the impact event, and the Clamshell begins to rebound following the fuel assembly impact after 31 milliseconds. Thus, the XL Clamshell impact duration is 16 milliseconds.

The predicted analytical kinetic energy imparted by the falling XL fuel assembly onto the XL Clamshell is 175 MJ (Figure 2-168). Of note is that this FEA applies to the alternate XL Clamshell removable top plate design, and shows the initial Clamshell impact occurring at 1 millisecond and ending at 16 milliseconds for a total XL Clamshell impact duration of 15 milliseconds (Figure 2-167). This is in good agreement with the baseline FEA and gives confidence in the FEA model.

Traveller VVER

The FEA predicted analytical kinetic energy imparted by the falling VVER fuel assembly onto the VVER Clamshell is 92 MJ (Figure 2-188). The subsequent calculated average deceleration force is 72.5g. The calculated VVER Clamshell impact force imparted by the 1850 pound maximum fuel assembly is $F=mg$, or

$$F = (1850) \cdot (72.5) = 134,125 \text{ lbf (597 KN)}.$$

The impact duration occurs in 20 milliseconds as demonstrated in Figure 2-187. Since the XL Clamshell and fuel assembly are slightly heavier than the VVER Clamshell and fuel assembly, it is expected that the calculated kinetic energy and impact force of the XL will be more than VVER. The total time for the Clamshell and fuel assembly to decelerate to zero velocity was calculated using FEA, and the VVER Clamshell requires approximately 5 milliseconds more time to stop. This is attributed primarily to the relatively thinner VVER Clamshell top plate shear region (0.5 inches) compared to the XL Clamshell top plate shear region (1.38 inches). The thinner top plate shear region will deform more than a thicker plate resulting in a longer duration impact event. In addition, since the thinner plate is less rigid, the reacted impact forces will be less. The results in Table 2-60 support those impact energy principles since the XL package impact results in more kinetic energy (and impact force) and a shorter duration impact event as compared to the VVER package. The longer impact duration for Traveller VVER also results in less average deceleration force when compared to the Traveller XL.

A comparison of vertical 9-meter free drops onto the Traveller VVER and Traveller XL Clamshell top plates was conducted. The FEA and supporting hand calculations agree with the first principles of impact energy for the package. The evaluation concludes that the decelerations experienced by the Traveller VVER Clamshell are bounded by the Traveller XL design.

Slap-down Model Evaluation and Results

While the end drop represents the orientation which is the most structurally challenging to the fuel assemblies and Clamshell end features, a low-angle slap-down orientation is also very stressful for the Outerpack and Clamshell. Therefore, a second LS-Dyna model was created to analyze a low angle drop of 10 degrees. This model is shown in Figure 2-191. All material properties and initial conditions were applied to the slap-down model in a similar fashion to the top-down model. The initial velocity corresponded to the 9.13 m drop height. The impact angle was set to 10 degrees. The VVER Clamshell was also modeled using the wall thickness set to 0.436 inches which is a reasonable approximation of the composite wall thickness since the poison plate completely fills in the thinner sections of the extrusions, and the latch hinge and door hinges add even more material to the cross sectional strength. Most of the extraneous components such as the legs, lifting eyes, stiffeners, etc. associated with the Traveller were not modeled for the sake of simplicity, conservatism since they all add strength and reduce Clamshell forces by absorbing energy. Figure 2-192 shows the slap-down model with the upper Outerpack removed.

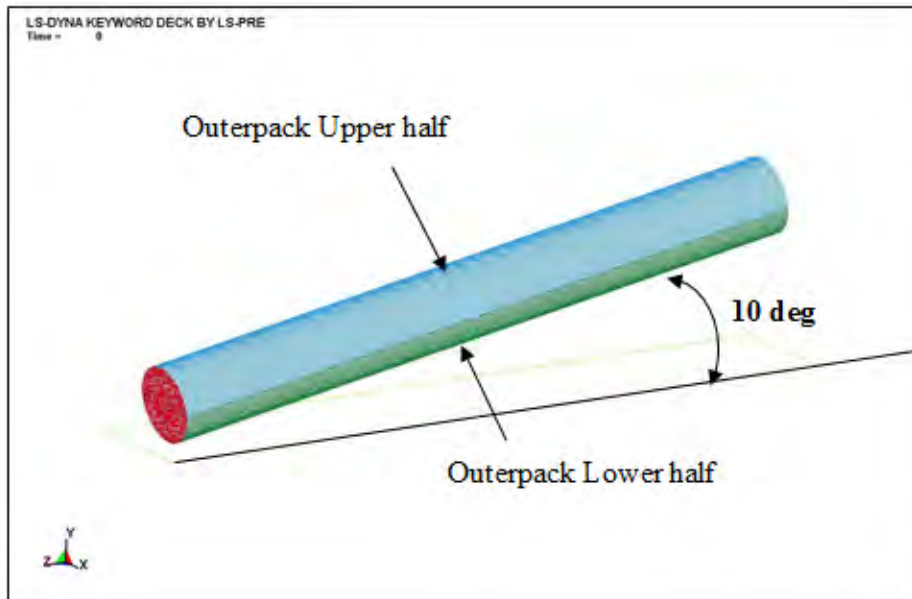


Figure 2-191 Slap-down Model

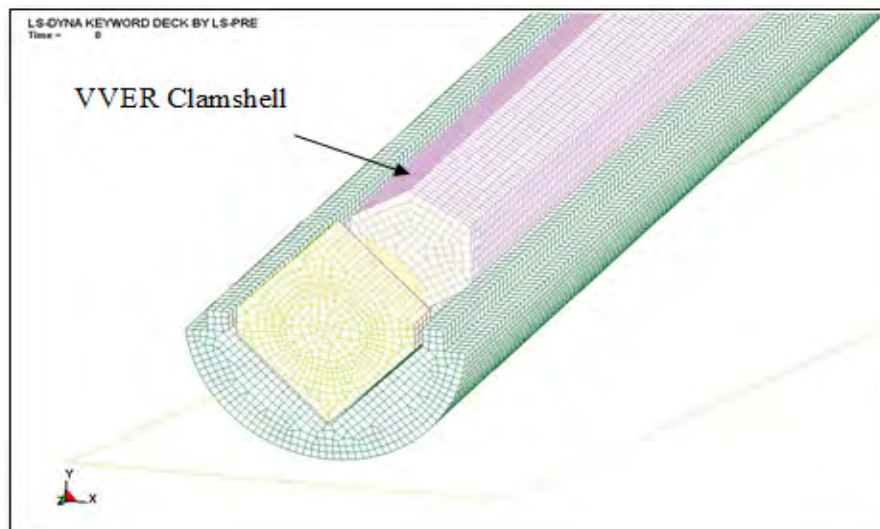


Figure 2-192 Model with Upper Outerpack Hidden to Show VVER Clamshell

The results of the low angle impact indicated robust structural performance. During the slap-down, the Outerpack and Clamshell experienced large longitudinal bending moments. The Outerpack survived this moment (peaked at 0.24 seconds) with minimal plastic deformation. As can be seen in Figure 2-193, the Outerpack survives this large bending moment with no significant structural damages other than a very slight buckle in the outer shell on the top surface. The simulated results are similar to actual slap-down tests and are consistent for the Traveller XL and Traveller VVER. The strength of an actual Outerpack is greater than the model by virtue of stiffeners, legs, hinges, etc. which were not included for simplicity and model size.

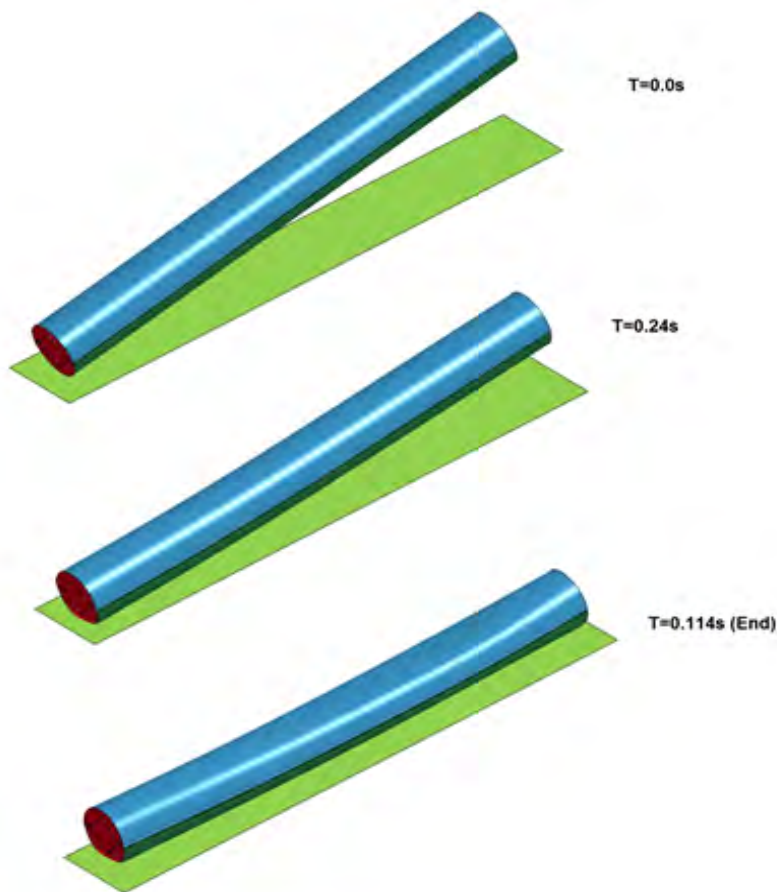


Figure 2-193 Max. Plastic Strain in the Clamshell Main Walls

Figure 2-194 shows approximately 0.12% plastic strain at peak bending, in the bottom edge, near the mid-span at the .0111 second time increment. No Clamshell damage at the first or second impact end was noted. The Clamshell extrusions including the base and wall demonstrate mechanical and geometric stability during a 30 foot slap-down impact. Based upon the robust Traveller XL Clamshell design, the VVER performed as expected. It is concluded that the VVER Clamshell has at least the structural integrity as the Traveller XL Clamshell for the slap-down event.

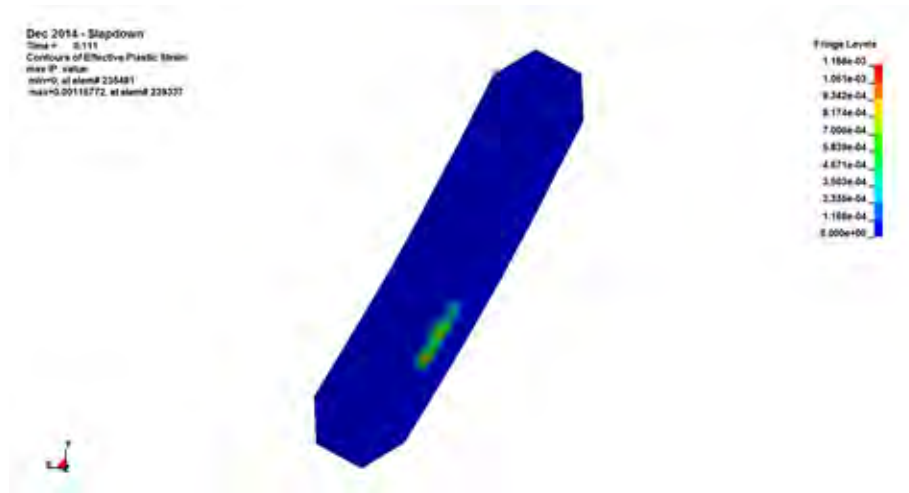


Figure 2-194 Slight Plastic Strain in Clamshell Extrusion

Figure 2-194 Slight Plastic Strain in Clamshell Extrusion

Shear Lip Strength Evaluation

During the top-down impact most of the force of the fuel assembly impact load path is directly through the top plate. Even so, the following calculation illustrates that the top plate shear lip can accommodate the entire shear load from the deceleration of the fuel assembly. The top plate shear lip is shown in Figure 2-195. The "shear lip" protrudes along 4 sides of the top plate and is engaged into the female groove on the shear lip component. When the fuel assembly collides with this top plate, the lip is loaded in shear. The calculated deceleration of the Clamshell was done above, therefore, the maximum load on the top plate cannot exceed the g's times the weight of the fuel assembly. This is an extremely conservative assumption since most of the energy of the fuel assembly collision is simply passed through the top plate and into the Pillow. The top plate is trapped between the two, and is loaded in compression. However, the calculation is still performed here to demonstrate the strength of the shear lip.

The total possible maximum load is therefore: $(72.5 \text{ g's}) \times (1850 \text{ lbs}) = 134,125 \text{ lbs}$

The allowable shear is assumed to be 60% of the yield strength of the material (6061-T6 aluminum, assume 35ksi yield per ASTM) times the shear area. Or, $(.6)(35\text{ksi})(\text{shear area})$

Where the shear area is = lip thickness x lip perimeter. The lip thickness is 0.36 inches and the perimeter is 21.60 inches.

The shear area is = $0.36 \times 21.60 = 7.78 \text{ sq. inches}$.

Then, the total allowable shear lip load (with no help from the Pillow) is:

$$= (0.6) \times (35,000\text{psi}) \times (7.78\text{sq. in.})$$

$$= 163,380 \text{ lbs.}$$

This calculation shows that the shear lip alone, with no load carried from the Pillow could decelerate the fuel assembly by itself and demonstrates the robust strength of the shear lip.

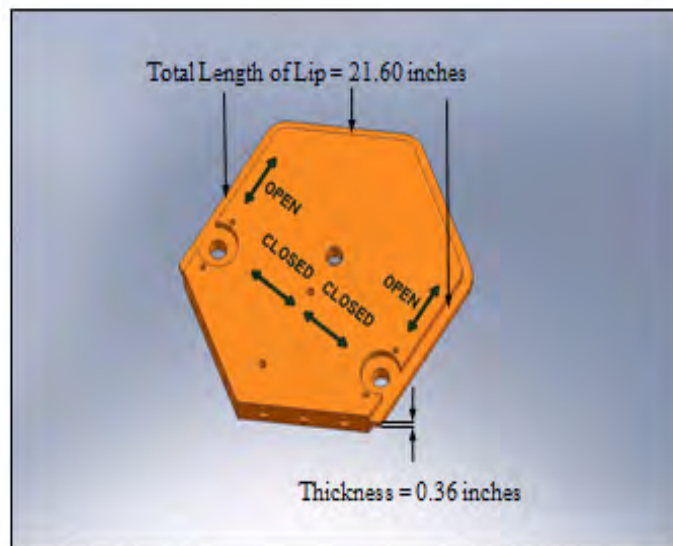


Figure 2-195 Traveller VVER Top Plate "Shear Lip"

2.12.9 Zirconium Alloy Performance During Testing

The choice of Standard Zirconium Alloy used during Traveller drop testing was based upon the energy absorbing capabilities the fuel cladding material used during construction of the fuel assemblies. The name Alloy is a generic naming convention because of the proprietary nature of these materials. Cladding may include a chromium coating or an Optimized ZIRLO Liner (OZL) to enhance in-reactor fuel performance. These cladding features are in addition to the base cladding material. All Alloys are compared to the Standard Zirconium Alloy when considering their structural performance, specifically the strain energy absorption capability up to failure during a 9-meter drop test, which demonstrates Standard Zirconium Alloy bounds all other Alloys. Table 2-61 compares all the Alloys' strain energy absorption capability up to failure to the HAC tested Standard Zirconium Alloy, and includes Alloy 1 (Optimized ZIRLO), Alloy 2, Alloy 3, Alloy 4, Alloy 5, chromium-coated Optimized ZIRLO, and OZL lined Optimized ZIRLO. As the base cladding defines the required cladding content specification, chemical or galvanic reactions with the existing packaging materials is evaluated and discussed in Section 2.2.2.

As Table 2-61 shows the tested Standard Zirconium Alloy is the least ductile of the six zirconium alloys considered including the chromium coated cladding and cladding with the inner liner. The failure of Standard Zirconium Alloy occurs at a much lower total strain energy than the other alloys making it the most susceptible to mechanical failure. Although the specification minimum tensile yield and ultimate stresses, as well as resilience strain energy, are greatest for the Standard Zirconium Alloy, its elongation at fracture is less than the other alloys. By virtue of having less ductility at fracture compared to the other alloys, Standard Zirconium Alloy possesses less total energy absorption capability compared to the more ductile Alloys 1-5 as well as chromium coated and OZL claddings.

Table 2-61 Fuel Rod Strain Energy Absorption Using Minimum Tensile Mechanical Properties			
Alloy	Minimum Strain Energy (psi – in/in)		
	Yield Strength	Resilience	Failure
Standard Zirconium Alloy	201	208	263
Alloy 1	177	162	683
Alloy 2	141	102	1266
Alloy 3	126	81	1159
Alloy 4	141	102	1282
Alloy 5	141	102	1224
Optimized ZIRLO with Chromium Coating	177	162	720
Optimized ZIRLO with Liner	161	133	29924

To bound individual Alloy material properties at elevated temperatures, the specification minimum yield and ultimate strengths were used during the prototype fuel bundle fabrication and during the HAC test sequence. Tables 2-62 and 2-63 provide the specification minimum yield and ultimate stresses at ambient, 20°C and 70°C temperatures for each of the zirconium alloys considered. For all alloys, the specification minimum mechanical properties bound or are representative of 20°C and 70°C temperature mechanical properties. When considering specification minimum material properties (and elevated temperatures), including elongation behavior, Standard Zirconium Alloy bounds other alloys with respect to total energy absorption capability. In addition, the base zirconium alloy used in all alloy cladding is a hexagonal closed pack (HCP) crystalline structure and those microstructures do not exhibit an apparent nil ductile-brittle transition at temperatures at or above -40°F (-40°C).

Alloy	Specification Minimum at Room Temperature (ksi)	Yield Stress at 68°F/20°C (ksi)	Yield Stress at 158°F/70°C (ksi)
Standard Zirconium Alloy	77	87	82
Alloy 1	68	73	69
Alloy 2	54	70	66
Alloy 3	48	56	53
Alloy 4	54	72	69
Alloy 5	54	70	66
Optimized ZIRLO with Chromium Coating	68	74	60
Optimized ZIRLO with Liner	62	73	54

Alloy	Specification Minimum Ultimate Stress at Room Temperature (ksi)	Ultimate Stress at 68°F/20°C (ksi)	Ultimate Stress at 158°F/70°C (ksi)
Standard Zirconium Alloy	103	116	108
Alloy 1	90	99	94
Alloy 2	80	83	79
Alloy 3	70	70	66
Alloy 4	80	84	80
Alloy 5	80	83	79
Optimized ZIRLO with Chromium Coating	90	102	78
Optimized ZIRLO with Liner (OZL)	80	91	68

2.12.9.1 Strain Energy Absorption Capability Calculation Method

The total strain energy absorption is the sum of the cladding’s moduli of resilience and toughness. These properties represent the elastic and elastic plus plastic areas under the stress-strain curve, as shown in Figure 2-196. The stress-strain curve is obtained from tensile test data to permit a direct comparison of all zirconium alloys. Axial tensile testing was performed on cladding samples, and each of the samples underwent room-temperature tensile testing to failure using industry standard controlled procedures.

After the stress-strain curve is plotted from tensile-test data, the area under the curve is determined by splitting the curve into two basic shapes; a triangle and a rectangle. The triangle is used up to 0.2% strain assuming the curve is still in the elastic region. The second half (plastic region) is estimated using a rectangle by arithmetically averaging the yield stress (S_y) from 0.2% strain with the ultimate stress (S_u) up to the elongation at fracture (failure).

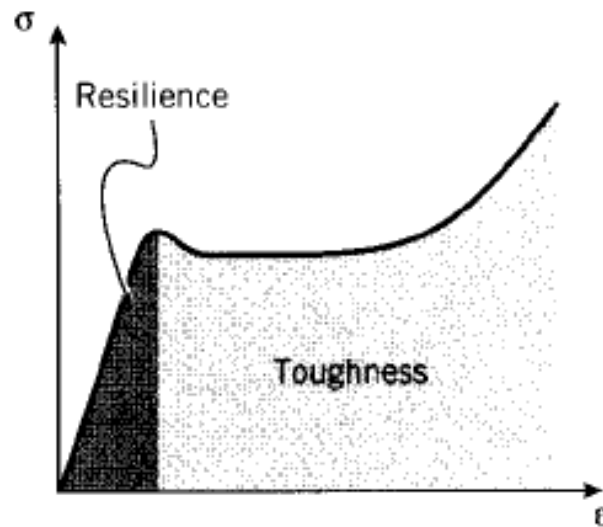


Figure 2-196 Resilience and Toughness (Strain Area)

The calculation for Standard Zirconium Alloy (i.e., ZIRLO) is shown below. Figure 2-197 provides the ZIRLO cladding stress-strain plot and shows the triangular and rectangular area representations.

Total Strain Energy, K, for Standard ZIRLO is:

$$K_{\text{ZIRLO}} = (0.5 \times (\epsilon_y \times S_{y-\text{min}})) + (S (\epsilon_{\text{failure}} - \epsilon_y))$$

]a,c

Therefore, strain energy calculations demonstrate that Standard Zirconium Alloy has the least total strain energy absorption value of all zirconium alloys and is therefore most susceptible to fracture as compared to other zirconium alloys. It was concluded the drop tested Standard Zirconium Alloy cladding bounds all other zirconium alloys to be transported in the Traveller package with respect to fracture susceptibility.

[]a,c

Figure 2-197 ZIRLO Cladding Stress-Strain Plot

To compare each Alloys' expected drop test structural performance, each claddings' mechanical tensile properties are compared considering uniaxial loading condition at the moment of impact. The total strain energy evaluation considers both elastic and plastic region which accurately represents cladding mechanical behavior resulting from a drop test as seen in Figure 2-153. It is noted from Figure 2-155 that 7.5% (20 of 264 rods) were cracked at the end plug location located at the four corners. This implies that the stresses at the corners was greater compared to the interior cells. Based upon the HAC 30 ft. (9 m) drop test discussed in Section 2.12.5.3 and Figure 2-154, the fuel rod failure did not occur at the base cladding. The failure occurred at the bottom end plug weld due to the bending moment applied at this region as the peripheral fuel rods slipped outwards due to the chamfered edge geometry of the bottom nozzle. Bending and buckling of the cladding occurred at the lower span due to the instantaneous axial load without any cladding fracture for the most brittle Standard Zirconium Alloy cladding. Therefore, bending and axial buckling of the cladding is not considered explicitly as a failure mechanism due to the weld failure mechanism during the 30 ft. (9 m) drop. This is further justified since the base alloys are in the partially or fully-recrystallized annealed condition. Therefore, the strength of the heat affected zone (HAZ) is slightly lower than the base material, and under large dynamic stress, the HAZ quickly hardens to the strength of the base material. Thus, the alloy total strain energy absorption is compared, as failure could occur anywhere in the cladding and is also highly dependent upon loading conditions and load path.

Chromium-coated cladding material and Optimized ZIRLO with OZL are expected have the same structural response to the 30 ft. (9 m) drop test since: 1) For Optimized ZIRLO with chromium coating, the coating stops prior to the ends of the tube, therefore, the HAZ region is unaffected and 2) the zirconium alloys have failed at the base cladding material instead of the HAZ region due to the ductility of the base cladding material.

2.12.9.2 Chromium Coated and OZL Cladding Evaluation

Axial tensile testing was conducted on both chromium-coated and OZL cladding to obtain yield and ultimate strength values, as well as elongation at failure. Each cladding's yield and ultimate stress values and their respective specification minimums are provided in Tables 2-62 and 2-63 to demonstrate that specification minimums bound or represent tensile properties up to 158°F (70°C). Stress-strain testing up to elongation at failure provides the elastic and plastic mechanical behavior and the data needed to perform the expected cladding behavior after the 30 ft. (9 m) HAC drop test. Axial tensile testing was performed on representative cladding samples as well as OZL cladding for the parametric energy evaluation. Each of the samples underwent room-temperature tensile testing to failure using industry standard methods per controlled procedures.

Testing Results and Total Strain Energy Evaluation

Data from the tensile tests was processed and plotted for both chromium-coated and OZL claddings to calculate the strain energy absorption capability in the same manner as previous alloys. The stress-strain plot for chromium-coated cladding is shown in Figure 2-198 and for OZL cladding in Figure 2-199. Below each figure is the total strain energy calculation result using the methodology shown in for Standard Zirconium Alloy in Section 2.12.9.1. Chromium-coated cladding total strain energy absorption capability was calculated to be 720 psi-in/in, and the calculated OZL cladding calculated total strain energy absorption capability is 29,924 psi-in/in. Both calculated values are greater than the tested Standard Zirconium Alloy (263 psi-in/in); therefore, both the chromium-coated and OZL lined Optimized ZIRLO claddings are less susceptible to mechanical failure after the 9-meter drop test. The same conclusion is reached from the comparison of all zirconium alloys as seen in Table 2-61. Based upon this evaluation, there will be no greater fuel assembly damage experienced by any evaluated alloys (i.e., lattice expansion) than what has already been considered in the criticality safety analysis.

[

]a,c

Figure 2-198 Chromium Coated Optimized ZIRLO Cladding Stress-Strain Curve

Total Strain Energy for Optimized ZIRLO cladding with chromium coating is:

$$K_{OPT_ZIRLO_CCmax} = (0.5 \times (\epsilon_y \times S_{y-min})) + (S (\epsilon_{failure} - \epsilon_y))$$

]a,c

[]a,c

Figure 2-199 OZL Lined Optimized ZIRLO Cladding Stress-Strain Curve

Total Strain Energy for Optimized ZIRLO cladding with liner (OZL) is:

$$K_{OPT_ZIRLO_LINERmax} = (0.5 \times (\epsilon_y \times S_{y-min})) + (S (\epsilon_{failure} - \epsilon_y))$$

]a,c

2.12.9.4 Advanced Fuel Cladding Feature Additional Details

All subsections and text of Section 2.12.9.4 is proprietary marked.

[

TABLE OF CONTENTS

3.0	THERMAL EVALUATION.....	3-1
3.1	Description of Thermal Design	3-1
3.1.1	Design Features	3-1
3.1.2	Contents Decay Heat	3-2
3.1.3	Summary Tables of Temperatures.....	3-2
3.1.4	Summary Tables of Maximum Pressures	3-3
3.2	Materials Properties and Component Specifications.....	3-3
3.2.1	Materials Properties	3-3
3.2.1.1	Cladding Materials	3-4A
3.2.2	Component Specifications	3-4C
3.3	General Considerations	3-5
3.3.1	Evaluation by Analysis	3-5
3.3.3.1	Traveller VVER	3-5A
3.3.2	Evaluation by Test	3-7
3.3.2.1	Seam Burn Test	3-7
3.3.2.2	Impact Limiter Burn Test	3-8
3.3.3	Margins of Safety	3-10
3.4	Thermal Evaluation Under Normal Conditions of Transport+	3-10
3.5	Thermal Evaluation Under Hypothetical Accident Conditions.....	3-10
3.5.1	Initial Conditions	3-13
3.5.2	Fire Test Conditions	3-13
3.5.3	Maximum Temperatures and Pressures.....	3-13
3.5.4	Accident Conditions for Fissile Material Packages for Air Transport	3-14A
3.6	Appendices	3-15
3.6.1	References	3-15A
3.6.2	Traveller Thermal Analysis	3-16
3.6.3	Traveller Seam Burn Tests	3-19
3.6.3.1	Test Results	3-21
3.6.3.2	Conclusions	3-25
3.6.4	Traveller Impact Limiter Burn Tests	3-26
3.6.4.1	First Impact Limiter Burn (December 15)	3-28
3.6.4.2	Second Impact Limiter Burn (December 16)	3-31
3.6.4.3	Test Conclusions	3-33
3.6.5	Traveller Certification Test Unit Burn Test	3-35
3.6.5.1	Test Procedures and Results.....	3-40

LIST OF TABLES

Table 3-1 Summary Table of Temperatures for Traveller Materials..... 3-2
Table 3-2 Room Temperature Properties of Key Traveller Materials..... 3-4
Table 3-3A Room Temperature Properties of Key Fuel Assembly Materials 3-4
Table 3-3B Room Temperature Properties of Key VVER Fuel Assembly Materials..... 3-4A
Table 3-3C VVER Fuel Assembly vs. 17X17 XL Fuel Assembly Thermal Analysis Parameters..... 3-5A
Table 3-4 Temperature Dependent Thermal Conductivity Used to Model Polyurethane Foam..... 3-17
Table 3-4A Summary of Recorded Temperatures During Burn Test..... 3-42A
Table 3-5 Optical Thermometer Data Sheet (West Side, Degrees C) 3-45
Table 3-6 Optical Thermometer Data Sheet (East Side, Degrees C)..... 3-46
Table 3-6A Moderator Block Weights..... 3-46A
Table 3-7 Wind Data Sheet..... 3-47

LIST OF FIGURES

Figure 3-1A	Burst Temperature Versus Internal Pressure for Chromium-Coated Optimized ZIRLO, STD ZIRLO and Optimized ZIRLO	3-4B
Figure 3-1	Calculated Radial Temperature Distribution for 30 Minute Fire (800°C)	3-6
Figure 3-2	Calculated Radial Temperature Distribution for 30 Minute Fire (1000°C)	3-6
Figure 3-3	Seam Burn Test	3-8
Figure 3-4	December 15, Impact Limiter Burn Test.....	3-9
Figure 3-5	Pool Fire Test Facility	3-11
Figure 3-6	Traveller CTU During Pool Fire Test	3-12
Figure 3-7	Thermocouple Locations Measuring Fire Temperature During CTU Burn Test.....	3-12
Figure 3-8	Temperature Strip Condition After CTU Burn Test	3-14
Figure 3-8A	Outerpack Flange Joint Showing Location of Packaging Weather Seal Gasket Options (1) Fiberglass Seal or (2) Silicone Rubber Seal	3-14A
Figure 3-9	Approach Used to Generate Analytical Model Geometry	3-16
Figure 3-10	Seam Burn Test Orientation	3-20
Figure 3-11	Package Exterior Wrapped with Ceramic Fiber Insulation	3-20
Figure 3-12	Measured Temperatures During Second Burn of the Control Section.....	3-21
Figure 3-13	Interior Temperature Measurements During Test of Continuous Hinge Section	3-23
Figure 3-14	Interior Temperature Measures After Test of Continuous Hinge Section	3-23
Figure 3-15	Interior Temperature Measurements During Test of Covered Moderator Section	3-24
Figure 3-16	Gaps in Outerpack Bottom Seam at Covered Moderator Test Section	3-25
Figure 3-17	Thermocouple Locations in Impact Limiter.....	3-26
Figure 3-18	Thermocouple Locations in Outerpack Interior	3-27
Figure 3-19	December 15, Impact Limiter Burn Test.....	3-28
Figure 3-20	Impact Limiter Pillow Temperatures	3-29
Figure 3-21	Internal Outerpack Skin Temperatures (December 15 Burn)	3-29
Figure 3-22	Flame Temperatures Measured by Optical Pyrometers	3-30
Figure 3-23	Outerpack Internals after December 15 Burn Test.....	3-30
Figure 3-24	Kaowool Layers on Outerpack Bottom Impact Limiter.....	3-31
Figure 3-25	December 16 Impact Limiter Burn	3-32
Figure 3-26	Internal Outerpack Skin Temperatures (December 16 Burn)	3-32
Figure 3-27	Impact Limiter Pillow Temperatures (December 16 Burn)	3-33
Figure 3-27A	Orientation of CTU for Thermal Test	3-35

LIST OF FIGURES (cont.)

Figure 3-27B Fire Fighters Standing by Fire Suppression System 3-35A

Figure 3-27C Approach to Suppress Pool Fire at End of Test 3-35B

Figure 3-28 Traveller CTU Burn Test 3-36

Figure 3-29 Thermocouple Locations on CTU Burn Test 3-36

Figure 3-30 Polyurethane Char in Outerpack Seam After Burn Test 3-37

Figure 3-31 Brown Polyurethane Residue Inside Outerpack After Burn Test 3-37

Figure 3-32 Test Stand for Fire Test 3-39

Figure 3-33 Test Setup with Steel Diffuser Plates 3-39

Figure 3-34 Test Article Under Tent to Maintain Temperature Overnight 3-40

Figure 3-35 Overnight Temperatures on East Side of Test Article 3-41

Figure 3-36 Overnight Temperatures on West Side of Test Article 3-41

Figure 3-37 Fire Temperatures Measured at the Corners of the Pool 3-42B

Figure 3-38 Data from Direction Flame Thermometers (DFTs) 3-43

Figure 3-39 Skin Temperature Data from East Side of CTU 3-43

Figure 3-40 Skin Temperature Data from West Side of CTU 3-44

Figure 3-41 Fire Temperature Data from East Side of CTU 3-44

Figure 3-42 Fire Temperature Data from West Side of CTU 3-45

Figure 3-43 Location of Possible Combustion of Moderator 3-48

Figure 3-44 Localized Melt Spot in Lid Moderator Block 3-48

Figure 3-45 Location and Indicated Temperatures of Temperature Strip Sets 3-49

Figure 3-46 Temperature Strip Set After Fire Test 3-50

3.0 THERMAL EVALUATION

The Traveller series packages are limited to use for transporting unirradiated, low enriched uranium, nuclear reactor core assemblies. There is no packaging design feature for heat removal because the contents does not contain heat generating radioactive material. The use of polyethylene as a moderator requires controlled heat-up during accident conditions, to prevent loss of hydrogen within the moderator.

3.1 DESCRIPTION OF THERMAL DESIGN

3.1.1 Design Features

The Traveller series packages, as described in section 2, utilize an aluminum Clamshell to contain a single unirradiated nuclear fuel assembly. The Clamshell is mounted within a cylindrical Outerpack fabricated from 304 stainless steel and flame retardant polyurethane foam. The stainless steel/foam sandwich provides thermal insulation during hypothetical fire conditions. Most of the heat capacity is within the Outerpack, provided by the polyethylene moderator, the aluminum Clamshell and the fuel assembly itself reducing the peak temperatures within the package.

The fuel rods, that contain the radioactive material, are designed to withstand temperatures of 1204°C (2200°F) without substantial damage. The primary temperature limitation is the polyethylene moderator located on the inside surface of the Outerpack. Polyethylene was selected because it retains its chemical composition and therefore its hydrogen content past melt temperature (between 120° and 137°C). Because of its very high viscosity, it will not flow significantly and will not change chemical composition unless significant amounts of high temperature oxygen are present (320-360°C).

The design and test strategy employed for the Traveller was to utilize design approaches that had previously passed the thermal test requirements. A review of previous designs and associated test results led to the selection of a stainless steel/polyurethane sandwich for the Outerpack. Based on this design approach, scoping tests and thermal analysis were performed to size the Outerpack structure. These analyses showed that sufficient polyurethane was incorporated to effectively insulate the interior of the Outerpack. As described in section 3.3.1 below, anticipated heat transfer due to conduction and radiation was so low that peak temperatures within the Outerpack would be below the melt temperature of the polyethylene and well below its ignition temperature. The primary concern was hot gas flow into the interior of the Outerpack. If both inner and outer skins of the Outerpack are ripped or if the seam between the Outerpack door and base are opened during the drop tests, hot gas from the fire could flow through the Outerpack significantly increasing its temperature. The Outerpack was made sufficiently robust that the defined drops did not create air infiltration paths within the Outerpack.

During the development process, three Traveller test articles were built. All were subjected to drop testing. Afterwards, these units were subjected to multiple burn tests. The information obtained during tests was incorporated into the final design of the Traveller Certification Test Unit (CTU). The CTU was subjected to drop testing as described above (Section 2.12.4). The CTU was then transported to Columbia, SC where it was burned in accordance with 10CFR71.73(c)(4) and TS-R-1, paragraph 728(a).

The package survived the test with maximum internal temperatures less than 180°C. The results of this test are described in section 3.5 and appendix 3.6.4.

3.1.2 Contents Decay Heat

Decay heat and radioactivity of the contents are not applicable for this package type.

3.1.3 Summary Tables of Temperatures

The maximum temperatures that affect structural integrity, containment, and criticality for both normal conditions of transport and hypothetical accident conditions are provided in Table 3-1. The table also includes the maximum measured temperature of the package components. All measured temperatures are within the limits specified. These results show that hypothetical accident thermal conditions will not materially affect the fuel assembly, the neutron poison plates, clamshell or the polyethylene moderator

During hypothetical accident conditions, the polyurethane insulation in the Outerpack protects the interior from excessive heat up. The Clamshell and its contents will not experience temperature increases significantly greater than 100°C. Therefore, room temperature material properties adequately describe the Clamshell and fuel assembly. The polyurethane foam will experience significant temperatures during the hypothetical accident. Because the lack of data at higher temperatures, the thermal analysis assumed foam properties above 340°C were equivalent to dry air. As shown by tests described in section 3.5 below, this approximation reasonably bounded actual properties.

Material	Temperature Limit and Rational (C)	Measured Temperature in CTU Fire Test (C)⁽¹⁾
Uranium oxide	2750 (melt) 1300 (compatibility with zirconium)	104
Zircalloy	1850 (melt)	104
Aluminum	660 (melt)	104
Stainless steel	1480-1530 (melt)	177 ⁽²⁾
UHMW Polyethylene	349 (boiling/ignition)	177 ⁽²⁾
Fiberglass seals (Thermojectet S)	1000°F (long term)	Temperature not measured/ Seals present after fire test
Silicone Rubber Gasket	500°F (long term)	Seals not present after fire test
Shock Mounts (fully cross-linked natural rubber)	greater than 300 (combustion)	177 ⁽²⁾
Refractory fiber felt insulation	2300°F (melt)	177 ⁽²⁾
Notes:		
(1) Temperature measurements made by non-reversible temperature strips. Exact time of peak temperature can be inferred from analysis. See section 3.3-1.		
(2) One location was unreadable on inside Outerpack shell. See section 3.6-4.		

3.1.4 Summary Tables of Maximum Pressures

The Traveller Outerpack surrounds the Clamshell and fuel assembly. It has silicone rubber or fiberglass seals to prevent rain, dirt, dust and spray from entering the package. The seals are not continuous, however, to avoid producing an air-tight seal. The Traveller Clamshell is not air tight and cannot maintain a different pressure than the air surrounding it. The double wall Traveller Outerpack also incorporates acetate seal plugs that melt in the event of a fire allowing decomposition products from the polyurethane insulate to vent to the outside air. Therefore, the Traveller interior pressure will always maintain itself in approximate equilibrium with external air pressure.

3.2 MATERIALS PROPERTIES AND COMPONENT SPECIFICATIONS

3.2.1 Materials Properties

The Traveller package series is fabricated primarily from four materials: 304 stainless steel, 6005 aluminum, Ultra-High Molecular Weight (UHMW) polyethylene, and flame retardant polyurethane foam. The Outerpack is fabricated from stainless steel and the polyurethane foam. The interior Clamshell holding the fuel assembly is fabricated from aluminum. The polyethylene is used as a neutron moderator and is located on the inside walls of the Outerpack, between the Outerpack and Clamshell. The important room temperature material properties are provided in Table 3-2, and applicable references are provided.

The melt temperature of the polyurethane foam is not provided because it is a thermoset material that decomposes before melting. The urethane foam selected for use will be a fire retardant foam that, when heated above 204.4°C, produces an intumescent char that seals voids and continues to provide insulation. This process is endothermic and produces gasses that must be vented. Vent plugs are placed along the length of the package to provide this venting. All Outerpack components containing polyurethane foam will have at least one vent plug.

The fuel assembly significantly affects the response of the overall package during a hypothetical fire. Because the fuel assembly may account for as much as 40% of the total package weight, the thermal capacity of the fuel assembly has a significant effect interior temperature. Key materials for the 17x17 XL fuel assembly to be shipped in the Traveller XL package is shown in Table 3-3A, and applicable references are provided. Key materials for the VVER fuel assembly to be shipped in the Traveller VVER package is shown in Table 3-3B.

Traveller VVER requires a thermal evaluation to ensure the package design and fissile contents are in a safe condition following normal and hypothetical accident conditions. Structural evaluations (Chapter 2) have demonstrated that the expected mechanical damage is bounded by the Traveller XL. Since Traveller VVER is a similar fresh fuel shipping package with respect to expected mechanical and thermal performance to a Traveller XL, the Traveller XL thermal methodology forms the basis for Traveller VVER evaluation. Section 3.3.1.1 provides the technical justification for use of Traveller XL thermal analysis.

Material	Density	Melt Temp	Conductivity	Specific Heat
304 Stainless Steel ⁽³⁾	8.3 g/cc .29 lb/in ³	1400-1455°C 2550-2650°F	14.2 W/m-K 8.2 BTU/hr-ft-F	0.5 J/g-°C 0.12 BTU/lb-°F
6005 Aluminum ⁽⁴⁾	2.8 g/cc .098 lb/in ³	582-652°C 1080-1210°F	167 W/m-K 96.1 BTU/hr-ft-F	0.88 J/g-°C 0.21 BTU/lb-°F
UHMW polyethylene ⁽⁵⁾	.932-.945 g/cc .0337 - .0341 lb/in ³	125-138°C 257-280°F	0.42 W/m-K .24 BTU/hr-ft-F	2.2 J/g-°C 0.526 BTU/lb-°F
Polyurethane Foam ⁽⁶⁾	0.166 g/cc .0058 lb/in ³	NA	0.041 W/m-K .023 BTU/hr-ft-F	1.15 J/g-°C 0.275 BTU/lb-°F
Fiberglass seals (Thermoject S)	NA ⁽²⁾	538°C ⁽¹⁾ 1000°F	NA ⁽²⁾	NA ⁽²⁾
Silicone rubber gasket	NA ⁽²⁾	-73 to 250°C ⁽¹⁾ -100 to 500°F	NA ⁽²⁾	NA ⁽²⁾
Refractory fiber felt insulation ⁽⁷⁾	0.097 g/cc .0035 lb/in ³	1260°C 2300°F	.06 W/m-K .034 BTU/hr-ft-F	1.0 J/g-°C 0.239 BTU/lb-°F

Notes:

(1) Temperature range that the gasket material and adhesive will withstand.

(2) Packaging weather gasket is to keep dust, dirt and spray from getting inside the Outerpack.

(3) Westinghouse Materials Property Manual, Chapter 3, "Type 304 and 304L Stainless Steel", Sections 3.5 and 3.6.

(4) Principles of Solar Engineering"; F. Kreith and J.F. Kreider; Hemisphere Publishing Co., page 701.

(5) Engineered Materials Handbook"; H.L. Stein, ASM International, page 169.

(6) General Plastics Last-A-Foam ®FR 3700 for Crash and Fire Protection of Nuclear Material Shipping Containers, General Plastics Manufacturing Company, Tacoma WA, USA.

(7) Westinghouse drawing 10014E35, Item 30, Note 4. McMaster-Carr Item 93285K24.

Material	Mass in FA ⁽⁵⁾	Melt Temp	Conductivity	Specific Heat
304 Stainless Steel	22 kg 49 lb	1400-1455°C 2550-2650°F	14.2 W/m-K 8.2 BTU/hr-ft-F	0.5 J/g-°C 0.12 BTU/lb-°F
Inconel ⁽¹⁾	2.7 kg 6 lb	1354-1413°C 2470-2580°F	14.9 W/m-K 8.6 BTU/hr-ft-F	0.44 J/g-°C 0.106 BTU/lb-°F
Zircalloy 4 ⁽²⁾	150 kg 330 lb	1850°C 3360°F	21.5 W/m-K 12.4 BTU/hr-ft-F	0.285 J/g-°C 0.0681 BTU/lb-°F
Uranium dioxide ⁽³⁾	650.5 kg 1434 lb	2750°C 4982°F	5.86 W/m-K 3.39 BTU/hr-ft-F	0.237 J/g-°C 0.0565 BTU/lb-°F
Uranium silicide ⁽⁴⁾	724.3 kg 1596 lb	1665°C 3029°F	8.46 W/m-K 4.89 BTU/hr-ft-F	0.192 J/g-°C 0.0458 BTU/lb-°F

Notes:

(1) Westinghouse Materials Property Manual, Chapter 5, "Alloy 718", Sections 5.5 and 5.6.

(2) Materials for Nuclear Engineers"; A.B. McIntosh and T.J. Heal; Interscience Publishers, pages 323, 351.

(3) Materials for Nuclear Engineers"; A.B. McIntosh and T.J. Heal; Interscience Publishers, pages 164-165.

(4) Westinghouse Materials Property Manual, Chapter 18, "Uranium Silicide (U₃Si₂)"

(5) Calculated based on drop tested 17x17 XL fuel assembly

Material	Mass in FA	Melt Temp	Conductivity	Specific Heat
304 Stainless Steel	47 kg 104 lb	1400-1455°C 2550-2650°F	14.2 W/m-K 8.2 BTU/hr-ft-F	0.5 J/g-°C 0.12 BTU/lb-°F
Inconel	5 kg 11 lb	1354-1413°C 2470-2580°F	14.9 W/m-K 8.6 BTU/hr-ft-F	0.44 J/g-°C 0.106 BTU/lb-°F
Zircalloy 4	152 kg 335 lb	1850°C 3360°F	21.5 W/m-K 12.4 BTU/hr-ft-F	0.285 J/g-°C 0.0681 BTU/lb-°F
Uranium dioxide	562 kg 1240 lb	2750°C 4982°F	5.86 W/m-K 3.39 BTU/hr-ft-F	0.237 J/g-°C 0.0565 BTU/lb-°F

3.2.1.1 Cladding Materials

Zircalloy cladding in-reactor performance can be enhanced by an external chromium coating or an internal zirconium-tin alloy lining, known as Optimized ZIRLO Liner (OZL). In both cases, the fuel rod base cladding is fabricated of zirconium (Zircalloy 4), with base cladding thermal properties described in Tables 3-1, 3-3A and 3-3B. As discussed in Section 2.12.9, there are variants of zirconium alloys which require performance evaluation for specific conditions. The HAC thermal tested fuel cladding is the Standard Zirconium Alloy.

Chromium-Coated Optimized ZILRO

[

]a,c

Optimized ZIRLO Liner

[

]a,c

Thermo-Mechanical Stability

[

]a,c

[]a,c
**Figure 3-1A Burst Temperature Versus Internal Pressure for Chromium-Coated Optimized ZIRLO,
STD ZIRLO and Optimized ZIRLO**

3.2.2 Component Specifications

Stainless steel and aluminum materials are procured to ASTM A240 304 SS and ASTM B209/B221 respectively. Welding is performed in accordance with ASME Section IX and inspected per AWS D1.6. The polyurethane foam is poured in accordance with approved procedures and specifications.

3.3 GENERAL CONSIDERATIONS

Thermal evaluations of the Traveller were performed by analysis and actual test. The Traveller package utilizes a double wall, insulated, Outerpack to protect an interior box (Clamshell) containing a fuel assembly and blocks of polyethylene moderator. Because of the large length to diameter ratio (8.8), heat transport in most of the package is primarily radial. The thermal analysis performed examined this heat transport path. The seam burn tests, examined radial heat flow with prototypical gas infiltration through the Outerpack seams. The impact limiter burn tests, examined and measured the heat transport through the ends of the package. The final QTU burn test combined all of the possible heat transport mechanism and demonstrated the suitability of the design.

3.3.1 Evaluation by Analysis

The thermal model of the Traveller package was created to examine the response to the hypothetical fire accident conditions described in 10 CFR 71 and IAEA Regulations for the Safe Transport of Radioactive Material, Section VII-728. This analysis was performed to bound the anticipated response and was done by analyzing the response of the package at 800°C external conditions with a fire emissivity of 0.9 and a package emissivity of 0.8 as defined by 10CFR71.73. The analysis was also performed assuming an average fire temperature of 1000°C anticipated during an actual burn test and an initial ambient temperature of 38°C. The analytical burn model did not include potential damage to the Outerpack because:

- Minimum damage was anticipated after drop test
- The anticipated minor damage would not have a significant impact of global performance
- The combined uncertainty of the package damage combined with uncertainty in modeling gas flow patterns around the package made a detailed thermal analysis undesirable.

The analysis results show that the outer skin of the package quickly rises to thermal equilibrium with the fire. The internal components heat up more slowly due to the insulation capability of the polyurethane foam between the inner and outer shell of the Outerpack. Fuel and Clamshell temperatures increase by approximately 50°C and are well within acceptable levels, see Figure 3-1 and Figure 3-2. This analysis is described in greater detail in appendix 3.6.1.

3.3.1.1 Traveller VVER

VVER fuel is comprised of the same materials of construction as Westinghouse type fuel design used in the thermal analysis. Table 3-3C provides a comparison of VVER fuel assembly thermal model input parameters compared to the 17X17 XL fuel design thermal model input parameters. The VVER fuel mass, clamshell length and heat sink mass are slightly less than the 17X17 XL corresponding parameters. Due to geometric differences in design, fuel assembly and clamshell masses per unit length are more than the 17x17 XL corresponding parameters. It is noted that the materials of construction are the same for the shipping packaging and fuel assemblies; thus those thermal properties are the same.

Table 3-3C VVER Fuel Assembly vs. 17X17 XL Fuel Assembly Thermal Analysis Parameters				
Parameter	VVER	17X17 XL	VVER Delta	Notes
FA Mass	767 kg 1690 lb	783 kg 1726 lb	2.1% less	See Table 3-3A for 17X17 XL materials of construction
Clamshell (CS) Mass	163 kg 360 lb	163 kg 360 lb	None	See Table 3-3A for 17X17 XL materials of construction
Heat Sink Mass (FA + CS)	930 kg 2050 lb	946 kg 2086 lb	1.7% less	
CS length	4.7 m 185 in	5.1 m 202 in	8.9% less	
FA Mass/Unit Length	163 kg/m 9.1 lb/in	153 kg/m 8.6 lb/in	6.1% more	
CS Mass/Unit Length	35 kg/m 2.0 lb/in	32 kg/m 1.8 lb/in	8.6% more	

The thermal model was re-run using the fuel assembly and Clamshell parameters. There was no significant change in the Traveller VVER model's predicted maximum temperature of 108°C (versus 106°C for Traveller XL) for either the 800°C or 1000°C flame temperatures. Thus, Figures 3-1 and 3-2 also represent the predicted VVER maximum temperatures.

Traveller XL thermal analysis consisted of a smeared model based upon simplified geometry. The analysis illustrated the fundamental thermal mechanisms involved and provides a general expected package response assuming no significant hot gas infusion or significant geometry changes (from the drop tests). The thermal analysis was utilized to ensure that peak polyethylene moderator temperatures were below the material's melt temperature. Despite fundamental limitations (i.e. response assuming no hot gas infusion or significant geometry changes), the analysis model demonstrated close agreement to the actual seam burn fire tests (a continuous Outerpack hinge). The internal predicted temperature rise predicted by analysis was 50°C, which is in excellent agreement with the measured temperature rise of 60°C for the continuous hinge burn testing. The analysis predicted a maximum temperature of 106°C on the moderator cover, as compared to an average measured temperature (of the CTU) of 143°C.

The Traveller XL thermal analysis inputs to the smeared model represent the Traveller VVER. The remaining thermal sections; 3.3.2 and 3.3.3 provide Traveller XL evaluation by testing. Sections 3.4 through and including 3.6 provide the Traveller detailed thermal analysis and testing which demonstrated the Traveller XL's thermal design acceptability.

It is concluded that the Traveller VVER, by virtue of its fundamental design similarities to the Traveller XL, and results of the thermal analysis, offers an acceptable thermal design. Hereafter, Traveller thermal evaluations and testing represent the bounding Traveller XL thermal evaluations and testing applicable to Traveller VVER.

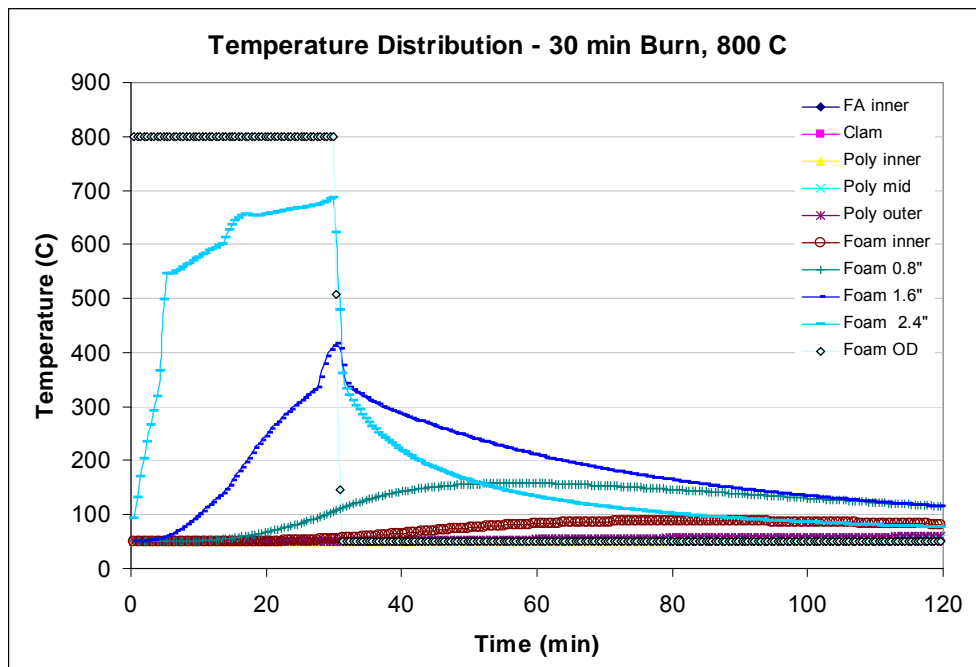


Figure 3-1 Calculated Radial Temperature Distribution for 30 Minute Fire (800°C)

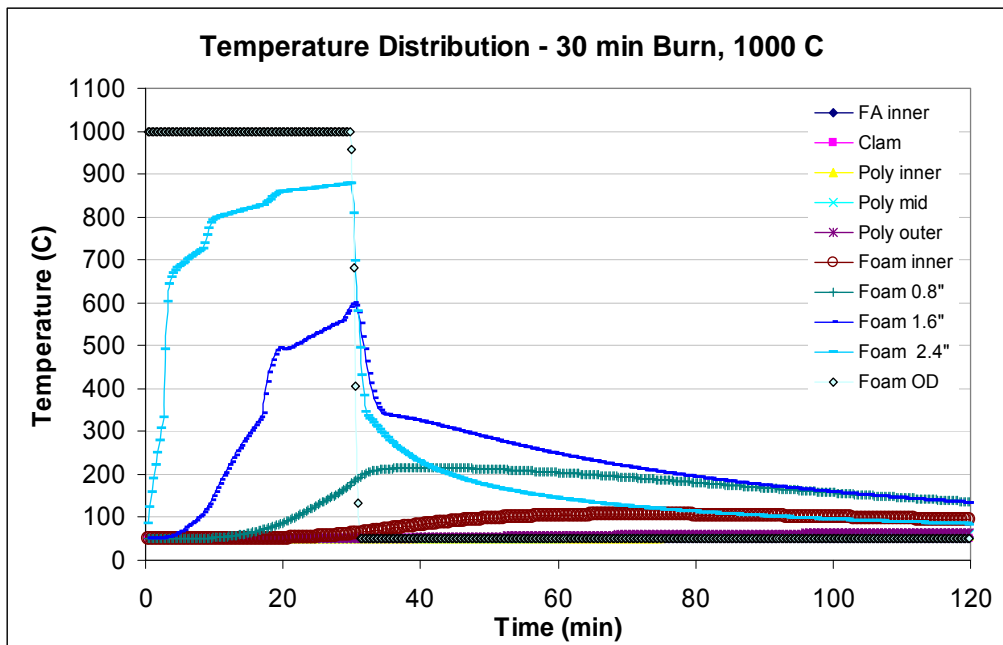


Figure 3-2 Calculated Radial Temperature Distribution for 30 Minute Fire (1000°C)

3.3.2 Evaluation by Test

Traveller performance under hypothetical accident conditions specified in 10CFR71.73 (c) and IAEA Regulations for the Safe Transport of Radioactive Material, Section VII-728 was initially calculated using the SCALE 4.4 thermal analysis code. The performance was subsequently demonstrated in a series of partial burn tests exposing selective portions of a full-scale package to pool fire conditions exceeding the hypothetical accident conditions. Finally, a full scale package was subjected to a full scale, fully engulfing, pool fire exceeding hypothetical accident conditions.

Two separate partial burn tests were performed to verify the final Traveller design. The first was the seam burn test. This test was designed to simulate the flow of hot gas through the Outerpack seams at the hinged joint between the Outerpack base and the Outerpack door and to measure the resulting heat transfer. The second, was the impact limiter burn test. This test subjected the end of a Traveller package to pool fire conditions to measure heat transfer at the package ends. These partial burn tests were then followed by a burn test of the qualification test article. This test, which followed the regulatory drop tests, completely immersed the full scale test unit in a pool fire for more than 30 minutes in flames significantly hotter than 800°C.

3.3.2.1 Seam Burn Test

The seam burn tests were designed to measure performance of different design approaches of protecting polyethylene moderator from excessive heat during the hypothetical fire conditions. Previous burn tests had revealed a tendency for package structures to deform in pool fires potentially allowing hot gasses to enter the package. The tests, performed in a previously burned package with large gaps left between the upper and lower Outerpack to allow hot gases to enter the package. One section, used as a control, had no protection for interior structures. The second section covered the Outerpack seam with stainless steel hinges to model a design with essentially continuous hinges. The third section used 26 gage stainless steel to cover the moderator blocks. The steel cover sheet was stitch welded in place, leaving gaps for combustion air to enter. The test approach is described in appendix 3.6.2

The first burn was of the control section. During the 30 minute burn, internal temperatures rose within the test section throughout the test due to the gap deliberately left in the seam between Outerpack base and lid. Peak internal temperatures over 500°C were observed, Figure 3-3.

The second test burn was of the section protected with essentially continuous hinge material. This section had a similar gap between the Outerpack base and lid, but gas flow through the package was minimized by the hinge sections. This burn lasted for 35 minutes with internal temperatures rising to 75°C (from an initial temperature of 35°C). After the burn was completed, interior temperatures continued to rise, peaking after 30 minutes at approximately 100°C.

The third test section was burned for 35 minutes as well. The internal temperatures measured show temperatures rose at a much higher rate than in the second test. This was expected because of the large gaps in the Outerpack seam (varying between 0.5 and 1.5 inches at the bottom seam). One thermocouple showed temperature at the bottom moderator blocks rose above 350°C within 25 minutes after the start of the burn.

After the pool fire was extinguished, some smoke was observed at the top Outerpack seam. This corresponded with a high temperature measurement on the moderator surface. Later examination showed that a small section of moderator burned for a limited period of time.

The seam burn tests showed that, where the Outerpack seam was covered by a hinge, that hot gas ingestion was virtually eliminated. Peak internal temperatures were approximately 100°C. With gaps in the Outerpack seams, peak internal temperatures exceeded the 350°C, the ignition temperature of polyethylene. Covering the moderator with stainless reduced the heat up rate, even with larger seam gaps, but moderator combustion took place near gaps in the stainless steel cover sheet. The tests showed that the best approach to prevent moderator combustion is to incorporate continuous hinge sections to prevent hot gas ingestion. The tests also showed that, to prevent combustion of moderator, assuming higher temperatures are experienced within the package, the stainless steel cover must be welded closed to prevent significant amounts of oxygen from reaching the polyethylene.



Figure 3-3 Seam Burn Test

3.3.2.2 Impact Limiter Burn Test

The seam burn tests described above examined the performance of the center portion of the package. The impact limiter burn test examined the thermal performance of the bottom end of the Traveller package. Both burns engulfed the bottom impact limiter and approximately 1.2 meters (four feet) of the package beyond the bottom impact limiter. Thermocouples were mounted at 16 locations inside and outside the package. The

test unit was mounted over the small weir built for the seam burn tests and burned for 40 minutes, Figure 3-4. Because the ambient temperature dropped below freezing during the night, initial temperatures inside the package started the test at approximately 0°C. Temperatures within the impact limiter pillow climbed to between 70 and 95°C depending on location during and after the burn test. Temperatures within the Outerpack interior cavity varied from 50 to 320°C. The only temperature measurements above 200°C were at locations near the outside skin of the Outerpack and well away from the moderator or impact limiter pillow.

The relatively high temperature observed at the Outerpack top seam led to questions of heat transfer. Was hot gas entering past the lip on the Outerpack door, or was the temperatures the result of heat conduction through the metal of the impact limiter bulkhead? The impact limiter burn test was therefore repeated but with Kaowool insulation stuffed into the Outerpack upper seam to prevent hot gasses from entering the package from that location. A 30 minute burn was performed in the late afternoon, so the initial temperatures inside the package were higher than the previous day. Temperatures within the Outerpack interior cavity varied from 80 to 340°C with the high temperatures being the closest to the Outerpack outer skin. Temperatures within the impact limiter pillow climbed to between 70 and 95°C depending on location during and after the burn test. The Outerpack top seam temperature rose to the same levels with insulation stuffed into the seam, demonstrating that the primary heat transport mechanism in this region is conduction. The slightly faster heat up rate can be attributed to several factors including the fact that the polyurethane insulating foam in the Outerpack had already been burned in earlier tests. These tests are described in greater detail in appendix 3.6.3 below.



Figure 3-4 December 15, Impact Limiter Burn Test

3.3.3 Margins of Safety

The Traveller protects its contents with a polyurethane insulated, double walled, stainless steel Outerpack. This Outerpack provides sufficient insulation to prevent significant heat conduction and maintain low interior temperatures during a hypothetical fire accident. The Outerpack also incorporates design features that prevent convective heat transfer. The tests described in 3.3.2 above, identified features (continuous hinge lengths and a large lip over the bottom seam) that prevent hot gases from entering the Outerpack seams. The results of these tests, as described in sections 3.5.2 and appendices 3.6.3 and 3.6.4 show that internal temperatures remain low when the Outerpack seams are adequately protected. These features were incorporated into the CTU test article and the production design. When the CTU was tested, significant margins of safety were observed as illustrated by Table 3-1 above. The most temperature sensitive component, the polyethylene moderator blocks, have an additional level of protection. The blocks are sealed by stainless steel cover sheets and are insulated at the ends. In the event that local conditions exceed the combustion temperature of the polyethylene, the moderator is protected by an insulating air gap (and refractory fiber felt insulation at the ends). Additionally, the moderator is isolated from oxygen preventing significant combustion.

3.4 THERMAL EVALUATION UNDER NORMAL CONDITIONS OF TRANSPORT+

The package will only be used to ship non-irradiated nuclear fuel. The contents contains no heat generating radioactive material. Therefore, the surface temperature of the package will not rise above ambient temperatures. As such, there is no need to evaluate by analysis or perform tests to demonstrate the maximum package surface temperature. All materials used within the Traveller package retain their desired properties over the entire range of possible ambient temperatures. The package is not hermetically sealed allowing interior pressure to adjust with changes in elevation and allowing expansion/contraction of internal air during temperature changes.

3.5 THERMAL EVALUATION UNDER HYPOTHETICAL ACCIDENT CONDITIONS

The primary verification of the Traveller's performance in a hypothetical accident was demonstrated in the burn test of a full-scale package loaded with a simulated fuel assembly. This unit was identified as the certification test unit (CTU). According to 10 CFR71.73 "Thermal. Exposure of the specimen fully engulfed, except for a simple support system, in a hydrocarbon fuel/air fire of sufficient extent, and in sufficiently quiescent ambient conditions, to provide an average emissivity coefficient of at least 0.9, with an average flame temperature of at least 800°C (1475°F) for a period of 30 minutes, or any other thermal test that provides the equivalent total heat input to the package and which provides a time averaged environmental temperature of 800°C. The fuel source must extend horizontally at least 1 m (40 in), but may not extend more than 3 m (10 ft), beyond any external surface of the specimen, and the specimen must be positioned 1 m (40 in) above the surface of the fuel source. For purposes of calculation, the surface absorptivity coefficient must be either that value which the package may be expected to possess if exposed to the fire specified or 0.8, whichever is greater; and the convective coefficient must be that value which may be demonstrated to exist if the package were exposed to the fire specified. Artificial cooling may not be applied after cessation of external heat input, and any combustion of materials of construction, must be allowed to proceed until it terminates naturally." (The IAEA Regulations for the Safe Transport of Radioactive Material, Section VII-728 have similar specifications.)

A Traveller XL package was fabricated by Columbiana High Tech to serve as the certification test article. This unit was subjected to a regulatory drop test performed February 5, 2004 in Columbiana, Ohio. This package was transported to the South Carolina Fire Academy in Columbia, South Carolina on February 6. The package was installed in the burn pool and subjected to a 32 minute burn test on February 10, 2004. Although the Outerpack had suffered minor damage that allowed some urethane decomposition products to escape into the package interior, the fuel assembly, Clamshell, and polyethylene moderator were essentially undamaged.

The testing was conducted on a calm day. To further minimize the impact of winds, the burn pool was surrounded with an insulated steel diffuser that extended to the top of the package and expanded the effective fire area. The maximum distance between the package and the diffuser was less than the 3 meters maximum proscribed distance, Figures 3-5 and 3-6.

Twenty-two, inconel sheathed type-K thermocouples were used to measure flame temperature immediately around the Traveller and the Outerpack outer skin as shown in Figure 3-7. Before and during the pool fire, temperature measurements were made at 16 locations using type K thermocouples located. During the test temperatures were measured at six locations on the package skin, at twelve locations inside the pool fire, at four locations using directional flame thermometers (DFTs) facing away from the package, and from outside the fire using two optical thermometers.



Figure 3-5 Pool Fire Test Facility



Figure 3-6 Traveller CTU During Pool Fire Test

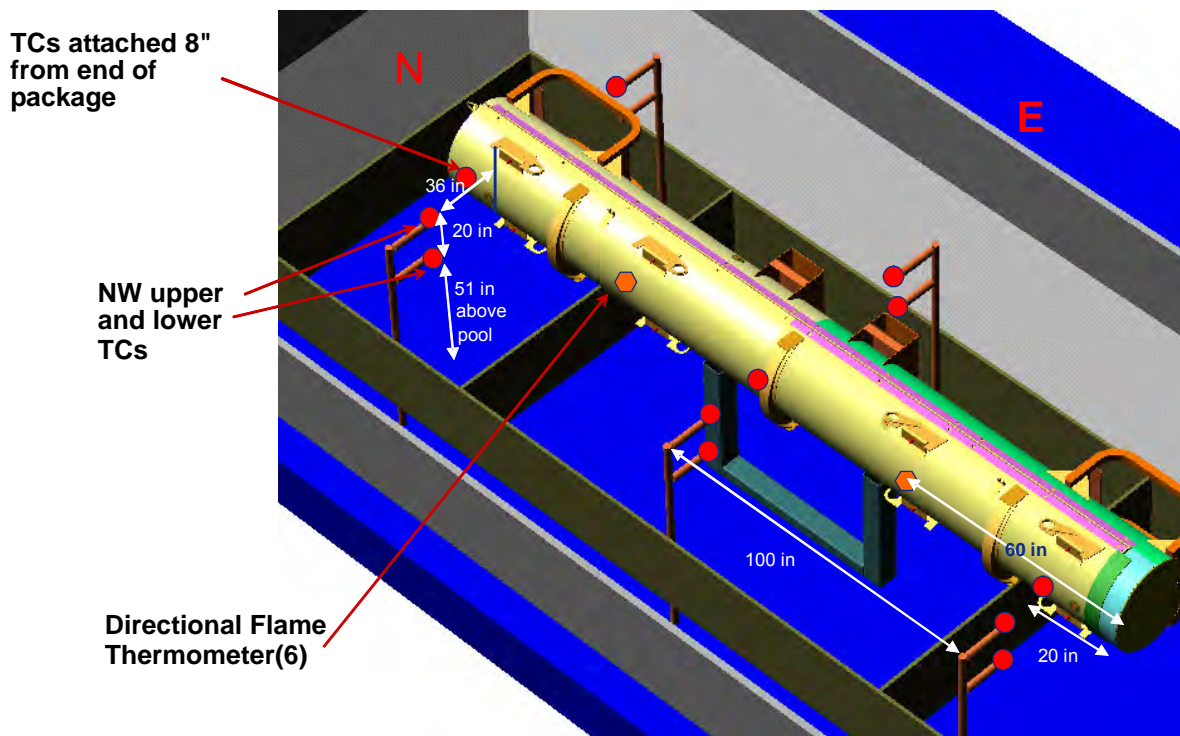


Figure 3-7 Thermocouple Locations Measuring Fire Temperature During CTU Burn Test

3.5.1 Initial Conditions

The package was covered with a canvas tent approximately 16 hours before the burn test. Two 44 kWth (150,000 BTU/hr) kerosene heaters were used, alternately, to maintain air temperature within the tent to above 37°C. The heaters were secured and the tent removed approximately 75 minutes before the beginning of the fire test. Air temperature around the package at this time averaged at 50°C (122°F). The air temperature and outside surface temperature dropped to approximately 5°C (41°F). Additional information can be found in appendix 3.6-4.

3.5.2 Fire Test Conditions

The CTU burn test was performed on a cool, calm, lightly overcast morning. The test article was located on a stand in a water pool. Fuel was pumped into manifolds under the surface of the pool to provide an even distribution of fuel for the pool fire. Approximately one minute after the fuel on the surface of the pool was ignited, the test article was completely engulfed. The fuel system continued to pump fuel into the fire until 32 minutes after the pool was lit. The pool fire was extinguished approximately one minute later. Fire temperatures were measured using four directional flame thermometers (DFTs) and 12 thermocouples suspended in the fire 0.9 m (3 feet) from the surface of the package. The 30 minute average temperatures measured by the DFTs were 833°C (1531°F). The 39 minute average temperature measured by the thermocouples suspended in the fire was 859°C (1578°F). Two, hand-held, optical thermometers that measured flame temperature from outside the pool supplemented these measurements. The average readings made with these thermometers was 958°C (1757°F).

3.5.3 Maximum Temperatures and Pressures

Temperatures were measured on the CTU Outerpack outer skin using six type K thermocouples, attached by screws. These thermocouples were located as shown in Figure 3-7 above. The 30 minute average temperature measured by these thermocouples was 904°C (1659°F). Temperatures inside the CTU Outerpack were measured using 13 sets of non-reversible temperature strips. One set on the inner stainless steel skin covering the Outerpack lid moderator was unreadable. All of the remaining temperature strips on the Outerpack lid recorded temperatures of 177°C (351°F) or below. Temperatures on the inside surface of the top and bottom impact limiters were 116 (241°F) and 149°C (300°F) respectively. Temperatures inside the Clamshell were below 104°C (219°F). An example of the temperature strip sets attached to the Outerpack lid moderator cover sheets is shown in Figure 3-8.



Figure 3-8 Temperature Strip Condition After CTU Burn Test

Although the thermal testing was done with the fiberglass seal, the detailed evaluation of the package after test revealed that the Outerpack hinge was the effective heat shield [1]. The temperature of the moderator blocks during this testing never reached even 100°C, well below the ignition temperature of the polyethylene moderator blocks or melting temperature of the aluminum clamshell material. The braided fiberglass gasket material alone was not an effective heat shield and did not provide any significant barrier to limiting the heat-up of the interior of the package during the thermal testing. The fiberglass seal was retained to provide packaging weather gasket to keep dust, dirt and spray from getting inside the Outerpack. The seal material may be either braided fiberglass or soft conformable silicone rubber as shown in Figure 3-8A.

The Traveller package design is non-pressurized and cannot retain internal pressure. Weather gasketing seals are discontinuous to prevent internal pressurization during the hypothetical fire and during normal variations in temperature and atmospheric pressure. The polyurethane foam space between the inner and outer shells of the Outerpack is protected from pressurization through the use of vent plugs. Every internal foam compartment within the Outerpack is protected by at least one acetate vent plug that will melt in the event of a fire and allow the internal spaces to vent. As a result, no significant increase in pressure was observed during the testing, nor is anticipated in any hypothetical accident condition.

The Traveller design surrounds the fuel assembly and polyethylene moderator with an insulated outer package. As a result, the outer surface of the package quickly reaches equilibrium with the fire while the interior remains cool. This is indicated by analysis and by the burn tests described above. The peak temperature measured on the Clamshell and the moderator covers were consistent between the seam burn test, the impact limiter burn test and the CTU burn test. All temperatures remained below 177°C and most locations remained below 100°C. No significant thermal damage was observed in the fuel assembly,

Clamshell or moderator blocks after the fire test. Moderator blocks were weighed before and after the fire test. No measurable reduction in mass was found.

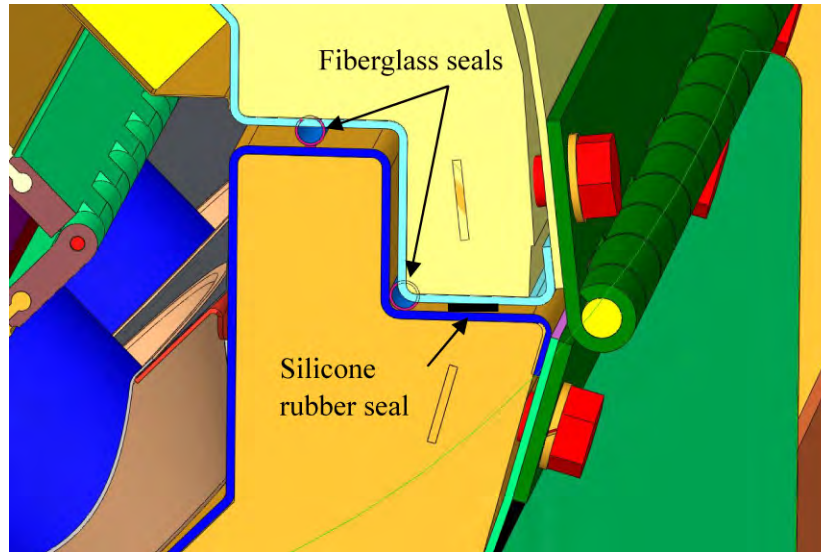


**Figure 3-8A Outerpack Flange Joint Showing Location of Packaging Weather Seal Gasket Options
(1) Fiberglass Seal or (2) Silicone Rubber Seal**

3.5.4 Accident Conditions for Fissile Material Packages for Air Transport

Application will be made for air transport at a later date.

This page intentionally left blank.

3.6 APPENDICES

The following appendices are included to provide amplifying information on material contained elsewhere in section 3.

- 3.6.1: References
- 3.6.2: Traveller Thermal Analysis
- 3.6.3: Traveller Seam Burn Tests
- 3.6.4: Traveller Impact Limiter Burn Tests
- 3.6.5: Traveller Certification Test Unit (CTU) Burn Test

3.6.1 References

1. CN-NFPE-09-86, (7/14/2009), "Justification for Removal of Traveller Heat Seal," Westinghouse Proprietary Class 2.

SSR-6, 2012 Ed. [2] has been incorporated by reference into 49 CFR 171.7 [3], replacing TS-R-1, 1996 Ed. (Revised). The intention of the regulation has not been changed by the new IAEA regulation reference, therefore, the package design maintains compliance to the intension of the updated regulatory reference. Note the section in-text reference has not been revised.

- [2] International Atomic Energy Agency, "Regulations for the Safe Transport of Radioactive Material," SSR-6, 2012.
- [3] U.S. Department of Transportation, Commission Code of Federal Regulations, Title 49 Subchapter C—Hazardous Materials Regulations, October 2016.
- [4] International Atomic Energy Agency, "Regulations for the Safe Transport of Radioactive Material," TS-R-1, 1996 Ed. (Revised).

This page intentionally left blank.

3.6.2 Traveller Thermal Analysis

A simplified computer model was developed using the HEATING7.2 code distributed by Oak Ridge National Laboratory as a part of SCALE 4.4. The model was built in cylindrical coordinates using the simplified geometry shown in Figure 3-9. This simplification was possible because:

- Primary temperature variations occur in the Outerpack foam that is cylindrical on the outside
- Simplifying interior foam surface by making it cylindrical is conservative
- The large length to diameter ratio (8.9:1) minimize end effects
- The ends have twice the thickness of polyurethane foam as the sides further reducing end effects

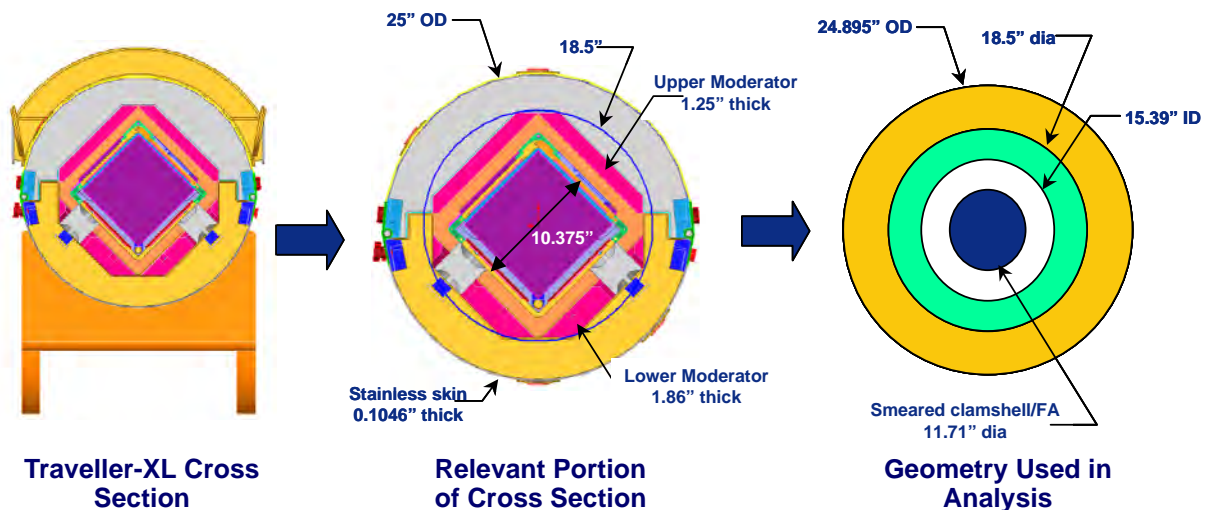


Figure 3-9 Approach Used to Generate Analytical Model Geometry

Three material regions were used in the analysis: Polyurethane foam with an average density of 10 lb/ft³, Polyethylene, and a smeared mixture representing the mid-section of the Clamshell and fuel assembly.

The Clamshell and fuel assembly region was modeled as a heat sink representing a 17x17 XL fuel assembly within the 9.50 inch (24.13 cm) inside dimension aluminum Clamshell. Because the end effects were to be ignored in this model, the fuel assembly nozzles and the Clamshell end plates were not included in this calculation. This resulted in the following material ratios:

- Aluminum Clamshell – 359.7 lb (163.2 kg) with a specific heat of 0.23 BTU/lb-°F (0.96 J/g-°C),
- Uranium Dioxide – 1341 lb (608.3 kg) with a specific heat of 0.0565 BTU/lb-°F (0.237 J/g-°C)
- Zircalloy 4 – 330 lb (149.7 kg) with a specific heat of 0.0681 BTU/lb-°F (0.285 J/g-°C)

The Traveller XL Clamshell is 202.0 inches (513.1 cm) long. The heat sink region weighs 2031 lb (921.1 kg), has an average specific heat of 0.891 BTU/lb-°F (0.373 J/g-°C) and a smeared density of 0.0934 lb/in³ (2.58 gm/cc).

A volumetric average conductivity was generated for the Clamshell and fuel assembly region by calculating a volume smeared conductivity by using the ratio of conductivity to volume for each material.

- Aluminum Clamshell – 3560 in³ (58,300 cc) with a conductivity of 104 BTU/hr-ft-F (182 W/m-K)
- Uranium Dioxide – 3380 in³ (54,500 cc) with a conductivity of 3.39 BTU/hr-ft-F (5.86 W/m-K)
- Zircalloy 4 – 1400 in³ (23,000 cc) with a conductivity of 12.4 BTU/hr-ft-(21.5 W/m-K)

Total volume used in the Clamshell/fuel assembly region is 21,700 in³ (356,000 cc). This results in a smeared conductivity of 18.3 BTU/hr-ft-F (32.1 W/m-K). This approximation is valid only because the heat input rate is very low allowing the region to be almost isothermal, even with low conductivities.

The Traveller XL Outerpack contains approximately 426 lb (193 kg) of UHMW polyethylene with specific heat of 0.526 BTU/lb-°F (2.2 J/g-°C) and a conductivity of 24 BTU/hr-ft-°F (0.42 W/m-°C). The total length of the moderator within the Outerpack is approximately 206 inches (523 cm). For the geometry defined for the model, this results in a smeared polyethylene density of 0.0249 lb/in³ (0.689 g/cc) which is 74% of predicted minimum density. The polyethylene acts as a heat sink and an insulation of primary heat sink.

The polyurethane foam room-temperature properties are given in Table 3-4. The properties change significantly, however, as the foam temperature increases resulting in pyrolyzation which occurs between 600 and 650°F (316 and 343°C). After charring, the material has the general appearance of very low density carbon foam. For the analytical model, the room temperature specific heat and conductivity were used up to 600F. Above 650°F, the temperature dependent conductivity of air was used instead. Between 600 and 650°F, foam specific heat is assumed to drop to zero.

Temperature (F)	Conductivity (BTU/hr-ft-F)	Conductivity (W/m-K)
100	.0230	.0398
600	.0230	.0398
650	.0249	.0431
700	.0268	.0464
800	.0286	.0495
1000	.0319	.0552
1500	.0400	.0692
2000	.0502	0.0869

The surface emissivity of the foam was set at 0.8. The first analysis performed modeled a 30 minute fire with flame temperature of 800°C. This analysis, Figure 3-1, showed significant temperature variation through the thickness of the polyurethane foam. Peak temperatures on the inside surface of the foam reached 100°C approximately 80 minutes after the beginning of the fire (50 minutes after the fire was put out).

Because the planned fire test facility burns at a higher temperature, the same analysis was performed assuming a 1000°C fire temperature. As shown in Figure 3-3, peak temperature within the polyethylene (at the interface between the polyurethane foam and the polyethylene) was calculated to reach 106°C. This is below the 125 – 138°C melt temperature of the polyethylene and well below the temperature that the melted polyethylene viscosity is low enough to flow easily.

The thermal analysis performed demonstrated several important features/characteristics of the design. Because of the urethane foam insulating the Outerpack, exterior skin temperatures quickly rise to near equilibrium with the fire outside the package. The clamshell and fuel assembly temperature, rise very slowly due to the insulation and the specific heat of the aluminum clamshell, polyethylene moderator, and the fuel assembly. The primary mechanisms that can result in significantly higher internal temperatures is hot gas infiltration during the fire and internal combustion during and after the fire test. We do not believe that these mechanisms can be accurately predicted by analysis. As a result, the Traveller team chose to demonstrate the package using pool fire tests, culminating with a full-scale fire test.

The seam burn tests with continuous hinge sections demonstrated approximately 60°C temperature rise during and after the test which was in close agreement with the 50°C temperature rise predicted by the analysis. The CTU burn test demonstrated internal temperatures between 116° and 177°C. This is 112° to 173°C higher than the air temperature that morning. These values are only 66° to 127°C higher than the equilibrium package temperatures maintained by heaters before the fire. As noted above, the external skin temperature at the middle of the package was significantly higher at the middle. Secondly, the amount of hot gas entering the package at different locations along the length clearly affects the local internal temperatures. Greater quantities of hot gas probably entered that package at that location.

Because of the fundamental limitations of the analysis (e.g., inability to predict precise geometry changes during the fire) the analysis model was never refined and exact agreement was never anticipated with test results. The analysis does illustrate the fundamental mechanisms involved and the general characteristics of the package response, assuming no significant gas infiltration or geometry changes.

3.6.3 Traveller Seam Burn Tests

This test examined two methods of protecting the polyethylene to prevent combustion and/or significant melting. One was the use of continuous hinges to seal the gap at the seam and the second was to cover the moderator with stainless steel sheet to prevent combustion. A third test section was also created to act as the test control. This section did not have any additional protection for the moderator.

The test was performed as series of three burns, heating the reference or control section, the section with additional hinge to model a package with continuous hinges, and the section with stainless covering over the moderator respectively. The first burn lasted 30 minutes. The two subsequent burns lasting for 35 minutes. A small pool fire (approximately 30 x 80 inches) was be created under the region of the package to be tested, Figure 3-10. Each region was approximately 57 cm (22.4 inches) across separated from the adjacent test region by 61 cm (24 inches) of refractory fiber felt insulation. This insulation was stuffed between the Clamshell and the moderator to prevent air flow from the section being tested to other test regions within the prototype package. The test regions were selected based having intact moderator left from previous tests. The test section with stainless steel cover over the moderator was selected based on the minimum distortion of the inner Outerpack shell and moderator blocks. The outside of the package was insulated on the bottom and sides using at least 2.5 cm (one inch) of refractory fiber felt insulation. This insulation will extend at least 1.2 m (48 inches) from each end of the test region, Figure 3-11.

Six thermocouples were attached in each test section. Two were screwed to the moderator bottom edge nearest the seam, one was screwed to the moderator/Outerpack where the two moderator blocks meet, one was screwed to the moderator block near the top seam, one was screwed to the Clamshell J-clip, and one was run through the bottom seam to hang approximately four inches below the package in the flames. Thermocouple connections and Teflon coated wires were routed out of the package at each end.

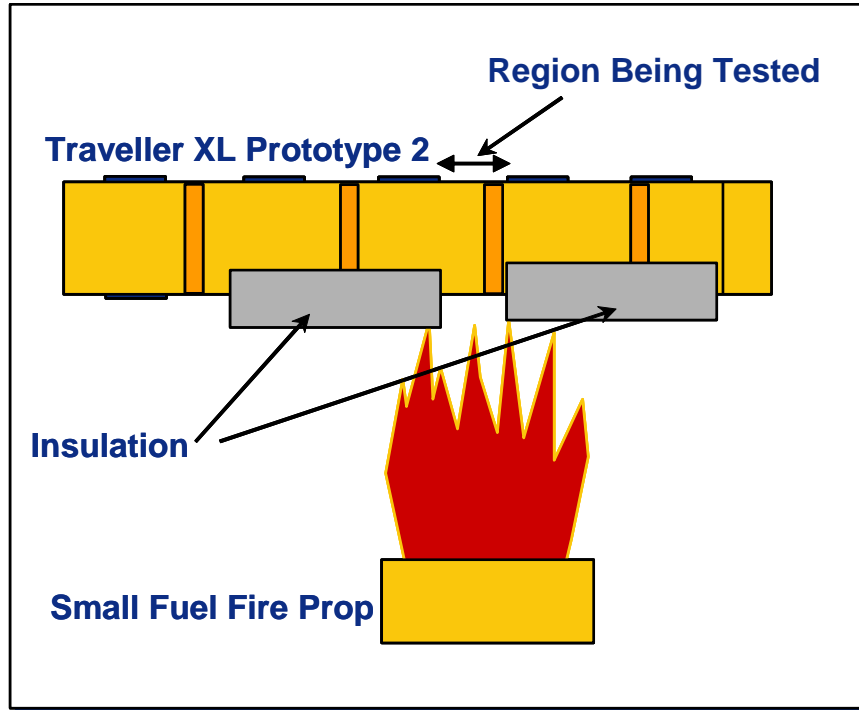


Figure 3-10 Seam Burn Test Orientation



Figure 3-11 Package Exterior Wrapped with Ceramic Fiber Insulation

3.6.3.1 Test Results

The first test burn was on the unprotected, control section of the package on October 3. Due to strong winds, flames did not stay on the test section. As a result, temperatures remained low and ultimately the thermocouple wires were burnt before the test was completed. Afterward, the weir was modified to extend the height up to the bottom of the package to confine the flames to the test region.

The burn of the control section was then repeated on October 6. The new weir confined the fire to the test section and temperatures rose within the test section throughout the test, Figure 3-12. After the pool fire was extinguished, burning polyurethane was observed along the top seam of the package and at the bottom seam of the test section. This was extinguished after approximately 10 minutes and the package was opened. Significant moderator was lost.

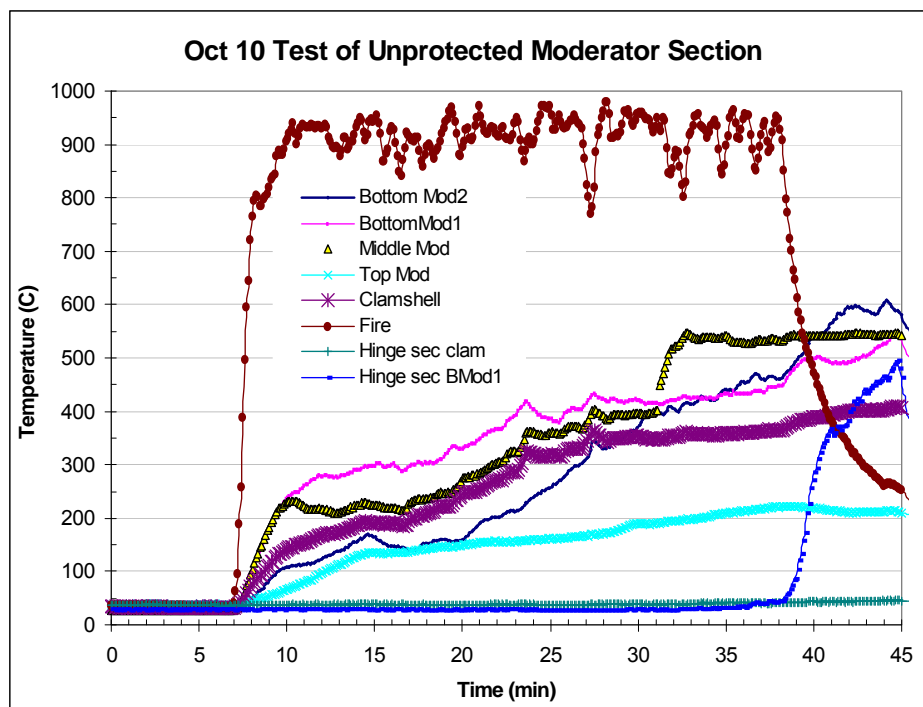


Figure 3-12 Measured Temperatures During Second Burn of the Control Section

The package was then closed, reinsulated, and the section modeling continuous hinges tested. This burn lasted for 35 minutes instead of the 30 minutes in the previous test. Thermocouple data, Figure 3-13, was incomplete because two of the channels (the external fire temperature and the middle moderator thermocouples) were bad. The latter produced very noisy data indicating that a connector was bad and the former did not change values throughout the test. Subsequent inspection revealed that the thermocouple itself was broken at the Outerpack seam. The data that was gathered from the internal thermocouples in the hinge test section and in the adjacent control section showed little change in internal temperatures. Temperatures rose very slowly during the burn test, with internal temperatures reaching a peak of 75°C at

the end of the test. After this data was collected and saved, additional temperature data was collected during the next 30 minutes after the burn, Figure 3-14. Temperatures slowly increased to approximately 100°C. This is consistent with thermal analysis that shows that heat transfer by conduction through the Outerpack polyurethane foam will continue to add heat to the interior for over an hour after the beginning of the burn, see section 3.1.

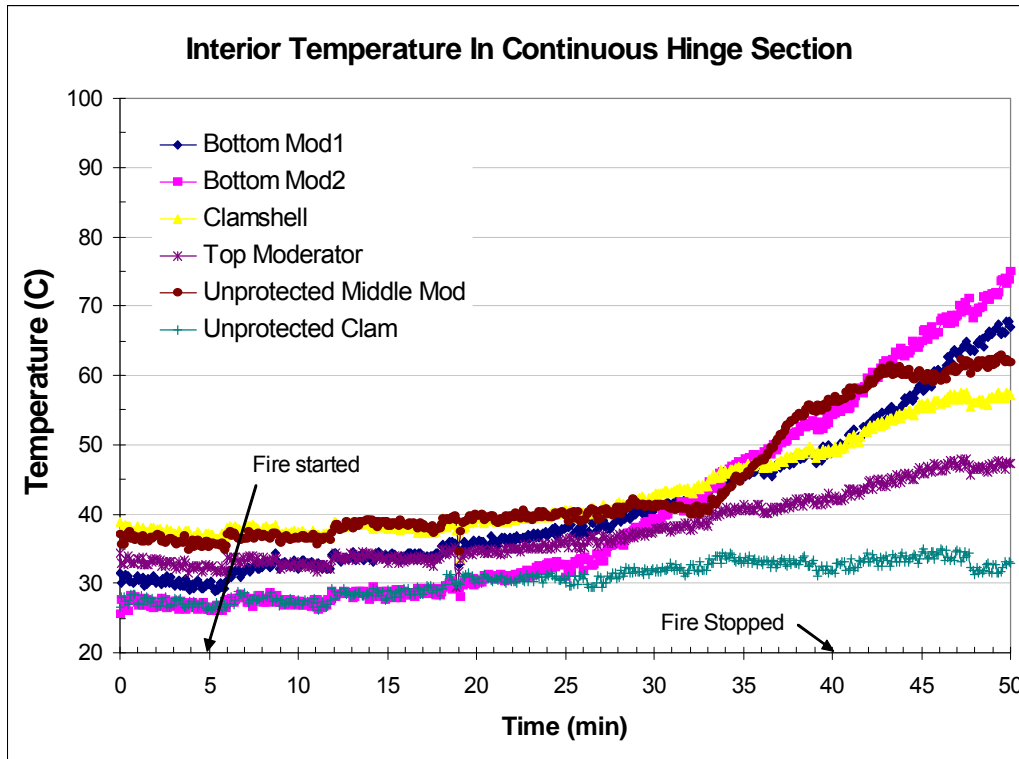


Figure 3-13 Interior Temperature Measurements During Test of Continuous Hinge Section



Figure 3-14 Interior Temperature Measures After Test of Continuous Hinge Section

The package was then moved on the test stand and positioned with the third test section, the covered moderator, over the burn weir. This section was burned for 35 minutes as well. The internal temperatures measured, Figure 3-15, show temperatures rose at a much higher rate than in the second test. This was expected because of the large gapes in the Outerpack seam (varying between 0.5 and 1.5 inches at the bottom seam), Figure 3-16. One thermocouple showed temperature at the bottom moderator blocks rose to above 350°C within 25 minutes after the start of the burn. After the pool fire was extinguished, some smoke was observed at the top Outerpack seam. This corresponded with an eventual rise in moderator temperature at one location after the external fire had been extinguished. After approximately 15 minutes, the package was cooled by water spray and removed from the burn pool. When opened, there was not initial sign of damage. After the stainless steel covering the moderator was removed, however, it was confirmed that small amounts of the moderator had burned.

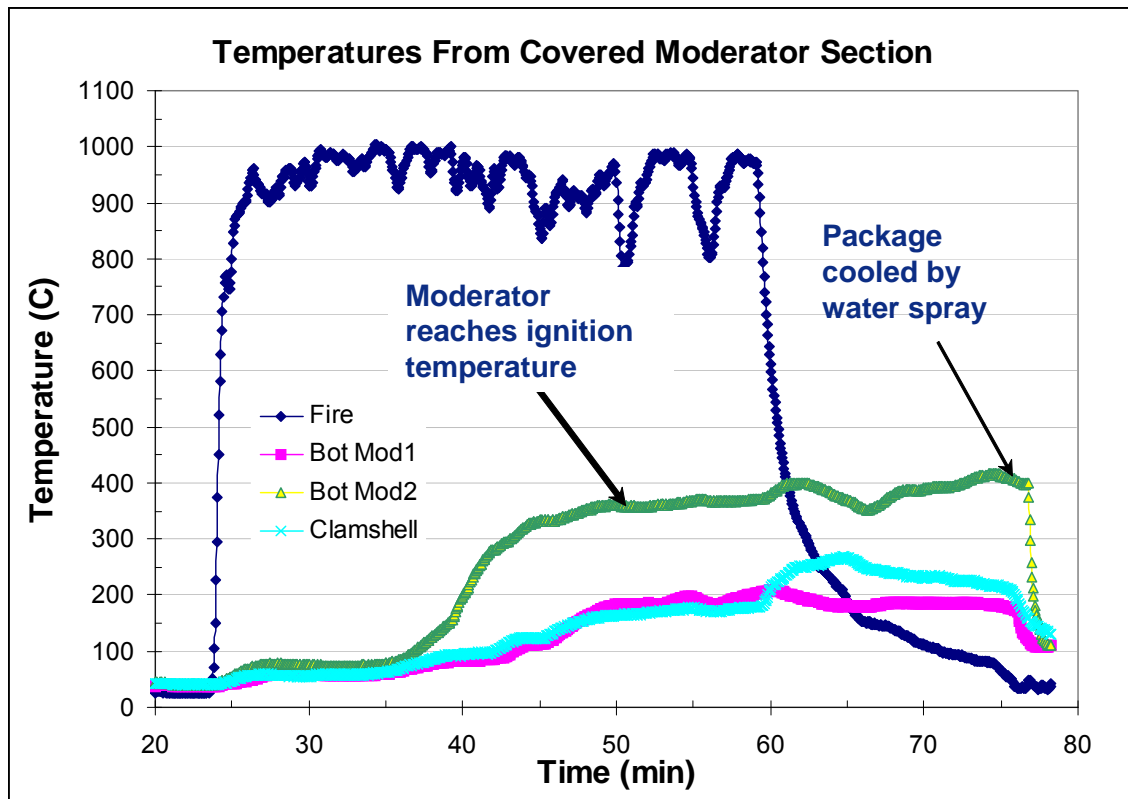


Figure 3-15 Interior Temperature Measurements During Test of Covered Moderator Section

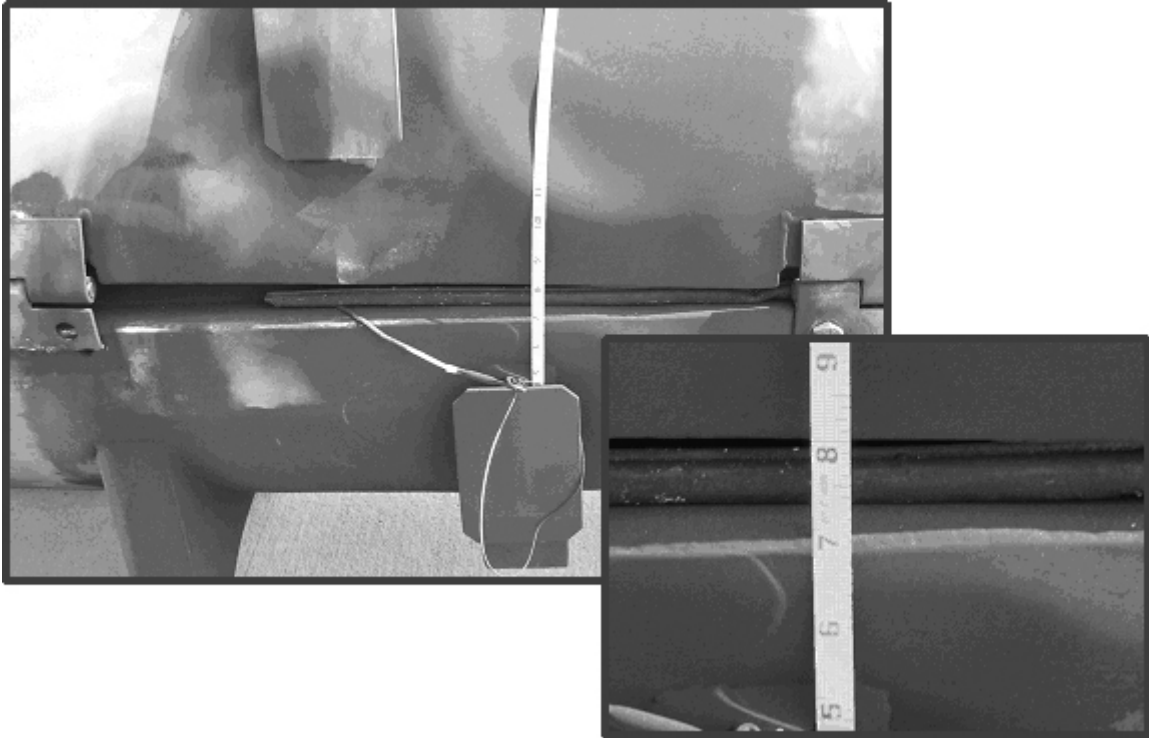


Figure 3-16 Gaps in Outerpack Bottom Seam at Covered Moderator Test Section

3.6.3.2 Conclusions

Tests showed that, where the Outerpack seam was covered by a hinge, that hot gas ingestion was virtually eliminated. Peak internal temperatures were approximately 100°C. With gaps in the Outerpack seams, peak internal temperatures exceeded the 350°C ignition temperature of polyethylene. Covering the moderator with stainless did appear to reduce heatup rate, even with larger seam gaps, but moderator combustion took place anyway. The tests showed that the best approach to prevent moderator combustion is to incorporate continuous hinge sections to prevent hot gas ingestion during the burn test.

3.6.4 Traveller Impact Limiter Burn Tests

A Traveller package was subjected to two burn tests after being tested in a full series of regulatory drops. This test series focused on the heat transfer characteristics of the bottom end of the package. This end is referred to as the bottom impact limiter. The top and bottom impact limiters are divided into two regions with high (20 lb/ft³) density foam in the outer regions and low density foam (6 lb/ft³) pillows inside. The foam pillow is separately encased in stainless steel with a 0.64 cm (0.25 inch) impact plate to minimize the chance of exposing the foam. Each pillow also has a 0.64 cm (0.25 inch) thick plate out the outer end as a heat sink to reduce peak temperatures in a fire. The foam pillow is also separated from the inside end of the outer impact limiter foam with approximately 0.32 cm (0.125 inches) of refractory fiber felt insulation.

During both tests, the package was instrumented with 16, inconel sheathed, type K thermocouples (Omega part numbers XCIB-K-4-2-10 and XCIB-K-2-3-10). Seven thermocouples were mounted on or around the impact limiter pillow, one midway through the outer impact limiter foam, and one on the outer impact limiter skin, Figure 3-17. The remaining seven thermocouples were mounted inside the Outerpack. The location of the thermocouples is shown in Figure 3-18.

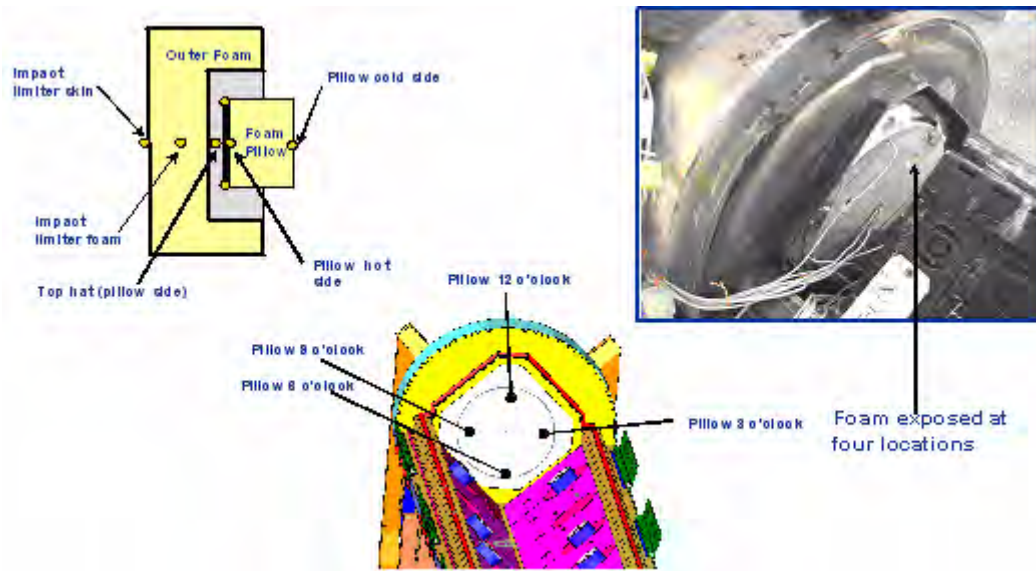


Figure 3-17 Thermocouple Locations in Impact Limiter

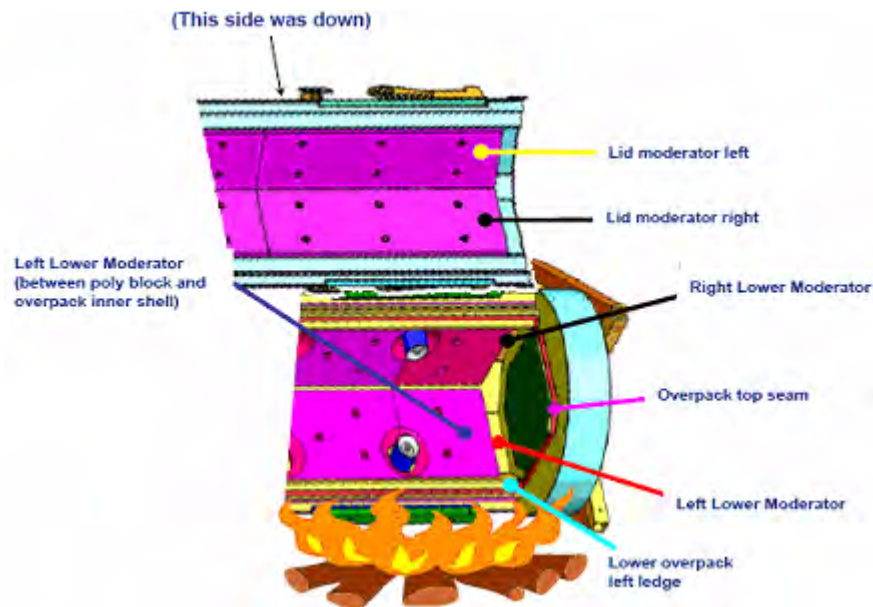


Figure 3-18 Thermocouple Locations in Outerpack Interior

The thermocouples were connected to thermocouple wire extensions using standard Type K plugs connecting the thermocouples to 20 gage type K extension wire. The 16 thermocouple cables were connected to two data acquisition systems. One system used an Omega OM-CP-OCTTEMP 8-channel data logger. This unit was set in operation before the test using a laptop computer and stored data from each channel at a rate of 12 samples per minute. After the test was completed, the data was download to the same laptop computer. The second system used an 8-channel Omega INET-100 external A/D box connected to an INET-230 PC-Card controller with a INET 311-2 power supply. This recorded data directly into the laptop computer allowing these channels to be monitored during the test.

Additional data was taken on external temperatures using two OMEGA OS523 handheld optical thermometers during the December 15 test. These units were used to measure flame temperatures and outside package skin temperature after the pool fire was extinguished.

A previously drop tested unit was modified to incorporate these changes in the bottom impact limiter and was subjected to two burns, one on December 15, and the second on December 16. Both burns engulfed the bottom impact limiter and approximately 3 feet of the package above the bottom impact limiter. Thermocouples were mounted at 16 locations inside and outside the package. Data from eight of the thermocouples were recorded by a laptop PC based Instrunet system that allowed data to be monitored in real time. The other eight channels were recorded using a battery powered Omega data logger.

3.6.4.1 First Impact Limiter Burn (December 15)

The test unit was mounted over the small weir built for the seam burn tests and burned for 40 minutes, Figure 3-19. Because the ambient temperature dropped below freezing during the night, initial temperatures inside the package started the test at approximately 0°C. Temperatures within the impact limiter pillow climbed to between 70 and 95°C depending on location during and after the burn test, Figure 3-20. Temperatures within the Outerpack interior cavity varied from 50 to 320°C, Figure 3-21.



Figure 3-19 December 15, Impact Limiter Burn Test

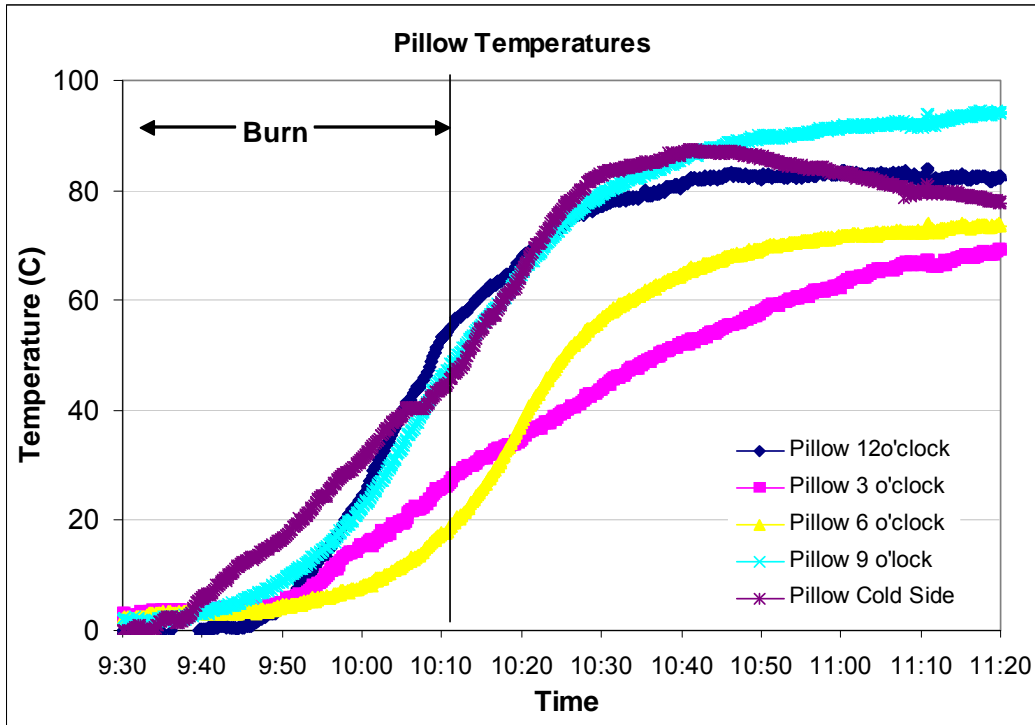


Figure 3-20 Impact Limiter Pillow Temperatures

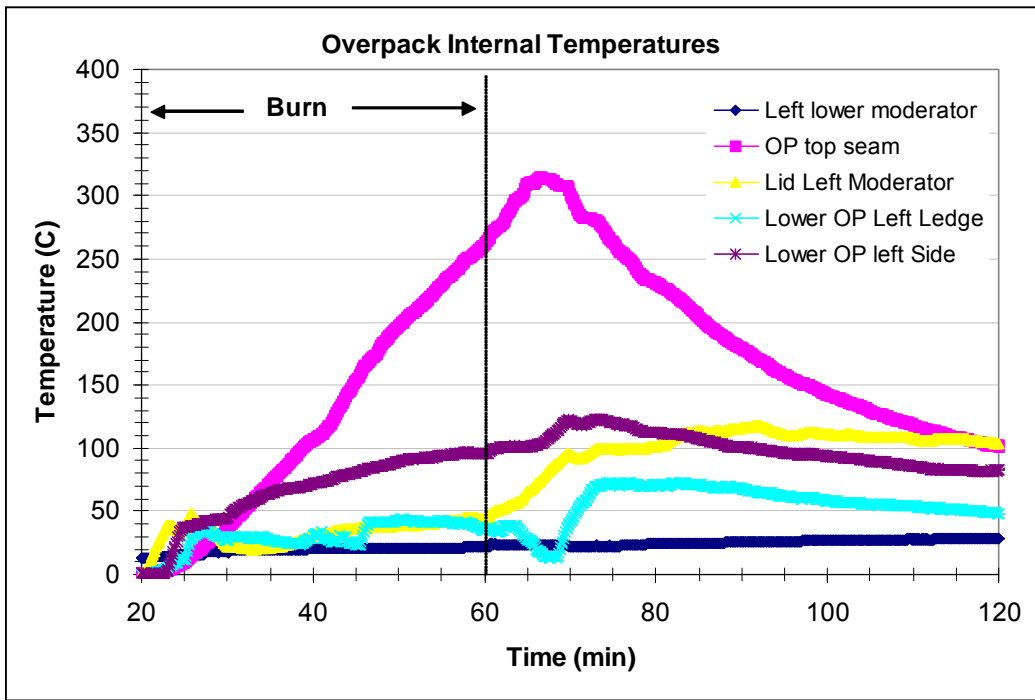


Figure 3-21 Internal Outerpack Skin Temperatures (December 15 Burn)

During this test, external temperatures were measured with two optical thermometers. Readings were taken every five minutes, Figure 3-22. After the test was completed, the Outerpack was opened. Other than a thin layer of soot lining the inside surfaces, there was no noticeable change in the Outerpack or Clamshell, Figure 3-23.

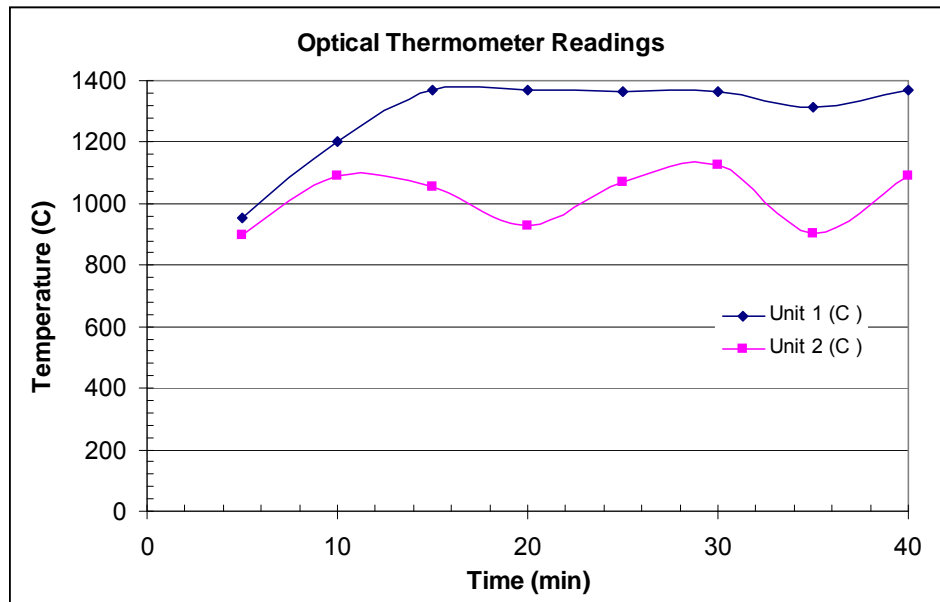


Figure 3-22 Flame Temperatures Measured by Optical Pyrometers



Figure 3-23 Outerpack Internals after December 15 Burn Test

3.6.4.2 Second Impact Limiter Burn (December 16)

The relatively high temperature observed at the Outerpack top seam led to questions of heat transfer. Was hot gas entering past the lip on the Outerpack door, or was the temperatures the result of heat conduction through the metal of the impact limiter bulkhead. The impact limiter burn test was therefore repeated but with Kaowool insulation stuffed into the Outerpack upper seam to prevent hot gasses from entering the package from that location, Figure 3-24. This burn lasted for 30 minutes, Figure 3-25. This test was performed in the late afternoon, so the initial temperatures inside the package were higher than the previous day. Temperatures within the Outerpack interior cavity varied from 80 to 340°C, Figure 3-26. Temperatures within the impact limiter pillow climbed to between 70 and 95°C depending on location during and after the burn test, Figure 3-27. The Outerpack top seam temperature rose to the same levels with insulation stuffed into the seam, demonstrating that the primary heat transport mechanism in this region is conduction.



Figure 3-24 Kaowool Layers on Outerpack Bottom Impact Limiter



Figure 3-25 December 16 Impact Limiter Burn

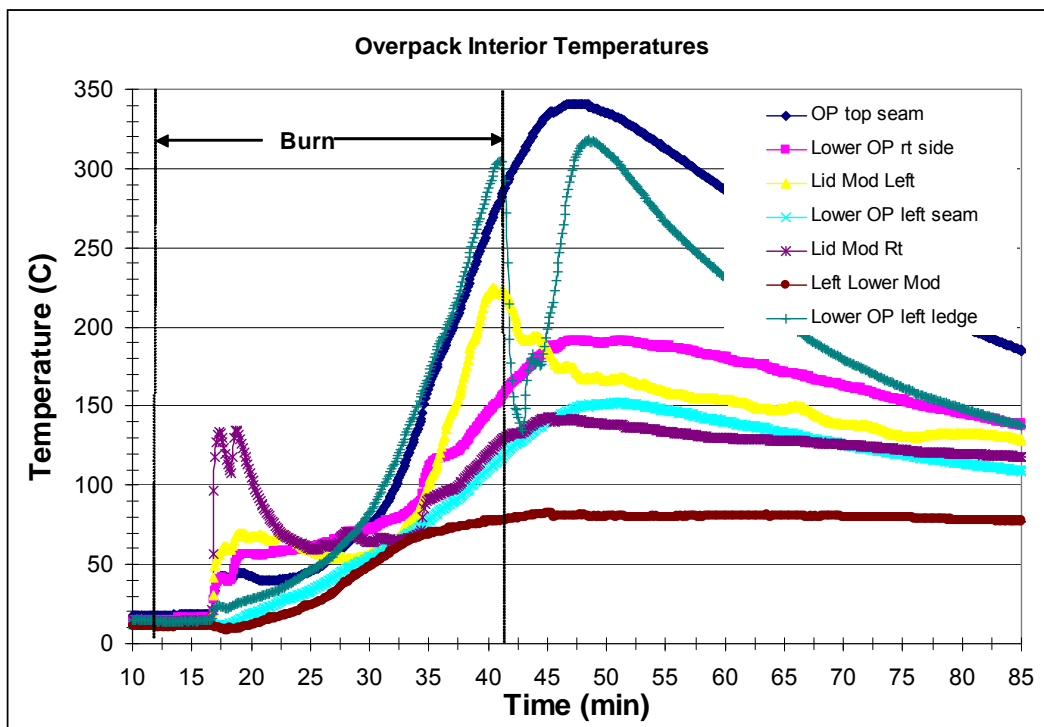


Figure 3-26 Internal Outerpack Skin Temperatures (December 16 Burn)

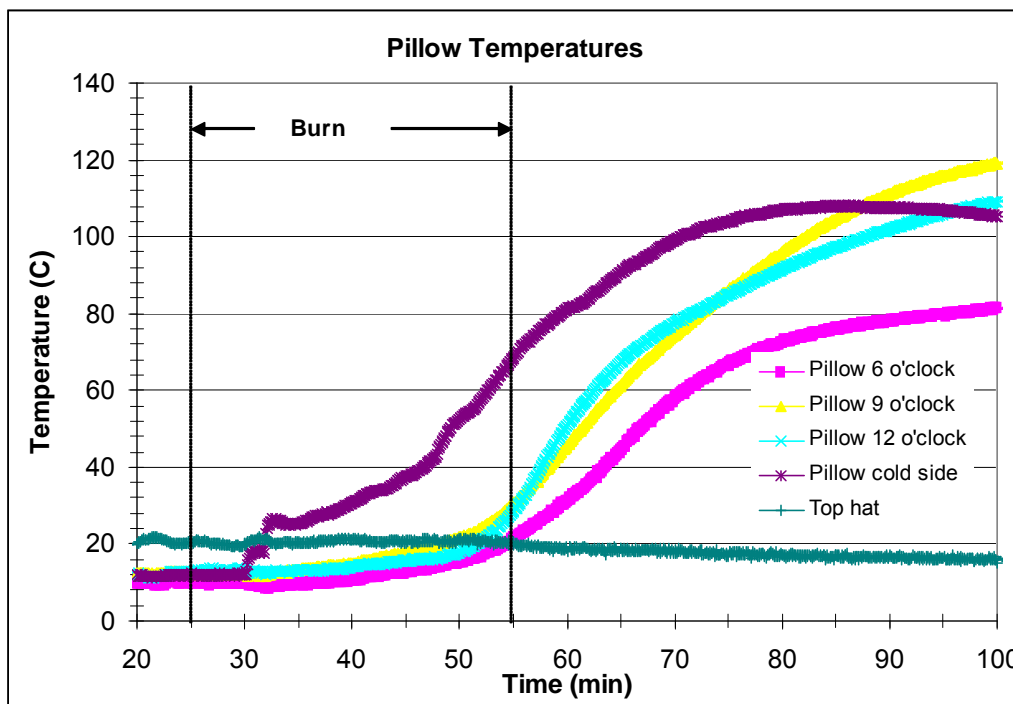


Figure 3-27 Impact Limiter Pillow Temperatures (December 16 Burn)

3.6.4.3 Test Conclusions

The purpose of the December 16 test was to repeat the previous day's test ensuring that hot gases did not flow around the Outerpack lid bottom lip. The heat up rate of the Outerpack top seam was slightly higher during the second burn than the first. Three factors may explain the higher temperatures during the second test.

- Foam in the impact limiter was charred during the first test resulting in higher heat transfer during the second test.
- The kaowool used to fill the bottom seam prevented the lid from closing as tightly as in the first test. This may have allow small amounts of combustion gas from the pool to enter the package
- During the first 5-6 minutes of the burn, fuel was sprayed directly on the outer skin of the package.

The test demonstrated that the revised impact limiter design will not overheat during a regulatory burn test. Even if the initial temperature is raised by 50°C, final temperature of the impact limiter pillow is anticipate to be less than 150°C. The test also demonstrated that very little gas is entering the Outerpack through the side or top seams. The interior skin is heating up however, due to conduction through metal parts of the Outerpack and through the polyurethane foam. The impact limiter tests results are conservative because the

foam in the cylindrical section of the package was not replaced and, therefore, did not provide the insulation that a unburnt package would have.

3.6.5 Traveller Certification Test Unit Burn Test

A Traveller XL package was fabricated by Columbiana High Tech to serve as the certification test article. This unit was subjected to a regulatory drop test performed February 5, 2004 in Columbiana, Ohio. This package was transported to the South Carolina Fire Academy in Columbia, South Carolina on February 6. The package was installed in the burn pool and burned February 10, 2004, Figure 3-28. Although the Outerpack had suffered minor damage that allowed some urethane decomposition products to escape into the package interior, the fuel assembly, Clamshell, and polyethylene moderator were essentially undamaged. (Please see section 2.12.4.2.3 in the Safety Analysis Report (pp 3-183 through 3-192) for description of the CTU drop tests and the resulting damage.)

The test was performed with the following objectives:

- Test Traveller package in manner that meets or exceeds regulatory requirements of TS-R-1 and 10CFR71.
- Demonstrate that the fuel assembly survives intact, without potential release of radioactivity.
- Demonstrate that the polyethylene moderator survives essentially intact retaining at least 90% of the hydrogen within the polyethylene.
- Demonstrate that the fuel assembly survives without cladding rupture caused by excessive temperatures inside the Clamshell

Figure 3-27A shows the orientation of the Certification Test Unit (CTU) for the thermal test. The bottom of the package was positioned approximately 1 meter from the top of the fire pool surface. The distance of the outer facility walls beyond the edge of the package were 67" at the ends and 71.5" at the sides.

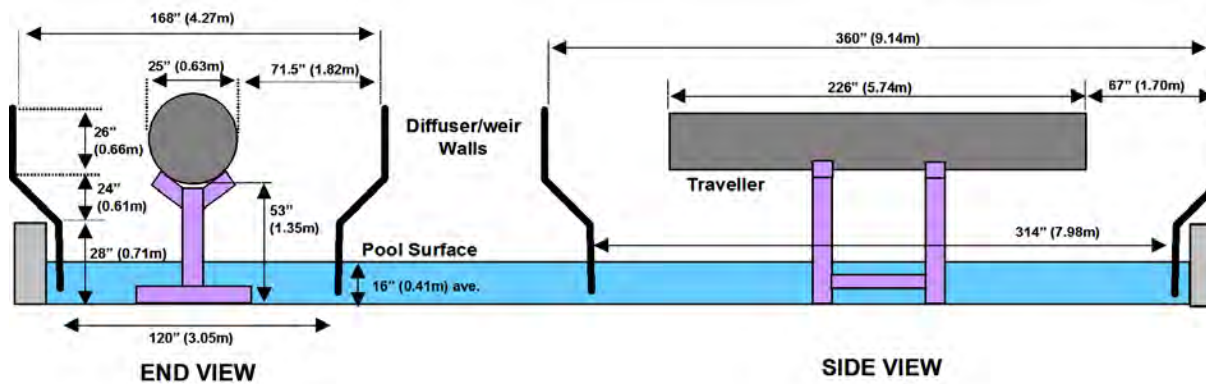


Figure 3-27A Orientation of CTU for Thermal Test

During this test, the package was engulfed for approximately 32 minutes. Prior to the burn test, the package was heated overnight to ensure that the interior of the package remained above 38°C (100°F). During the test temperatures were measured at six locations on the package skin, at twelve locations inside the pool fire, at four locations using directional flame thermometers (DFTs) facing away from the package, and from outside the fire using two optical thermometers, Figure 3-29. The 30 minute average temperatures were 904°C (1659°F) on the package skin, 859°C (1578°F) within the flame, 833°C (1531°F) as measured by the DFTs, and 958°C (1757°F) as measured by the optical thermometers.

The fire test facility was originally designed to terminate the fire test by shutting off fuel flow and allowing the fuel at the surface of the pool to burn off. Testing revealed that, in some circumstances, excess fuel could buildup on the pool surface causing the fire to continue burning for five minutes or longer. As a result, a simple fire suppression system was added to the facility. A water hose was connected to a nearby fire hydrant, Figure 3-27B. This hose utilized a suction line to siphon standard fire suppressant foam into the line, Figure 3-27C. The hose discharged into a single pipe that fed into the pool a few inches above the water level. When activated, the system would inject foam horizontally onto the surface of the pool, well below the test article. When used in combination with the fuel shutoff valves, the pool fire was extinguished within 60 seconds. This system did not cool the test article when in use and the package was allowed to naturally extinguish itself after the test. This was demonstrated by the CTU burn test, where the polyurethane at the Outerpack vent ports continued to burn many minutes after the fire suppressant was used on the pool surface.



Figure 3-27B Fire Fighters Standing by Fire Suppression System

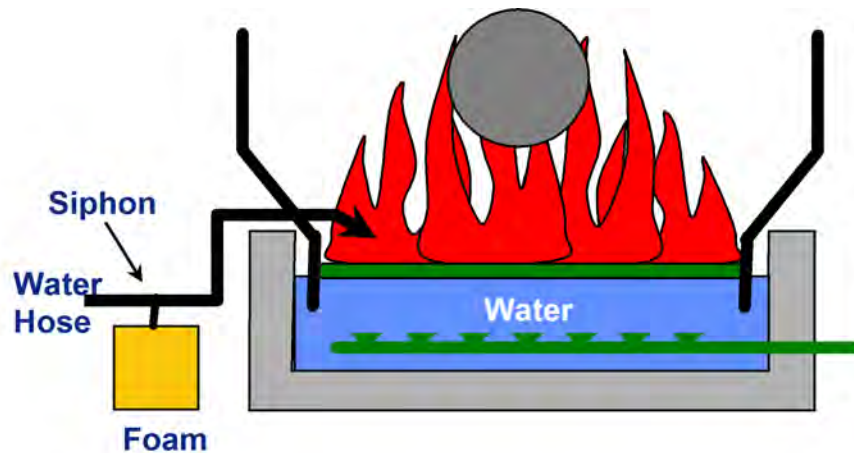


Figure 3-27C Approach to Suppress Pool Fire at End of Test

After the pool fire was extinguished, the package was removed from the pool and allowed to cool. Small amounts of smoke were observed to be coming from the package seams. The package was opened and the interior was examined. Significant amounts of polyurethane intumescence residue were observed along the Outerpack seam, Figure 3-30, and brown tar from the polyurethane was observed inside the package, Figure 3-31. Internal temperature strips recorded peak temperatures under 150°C throughout the package with one possible exception. Approximately 2 m (6 ft) from the bottom of the package, one set of temperature strips was unreadable due to heating and urethane deposits. An examination of the fuel assembly and the moderator blocks showed no significant heat damage.



Figure 3-28 Traveller CTU Burn Test

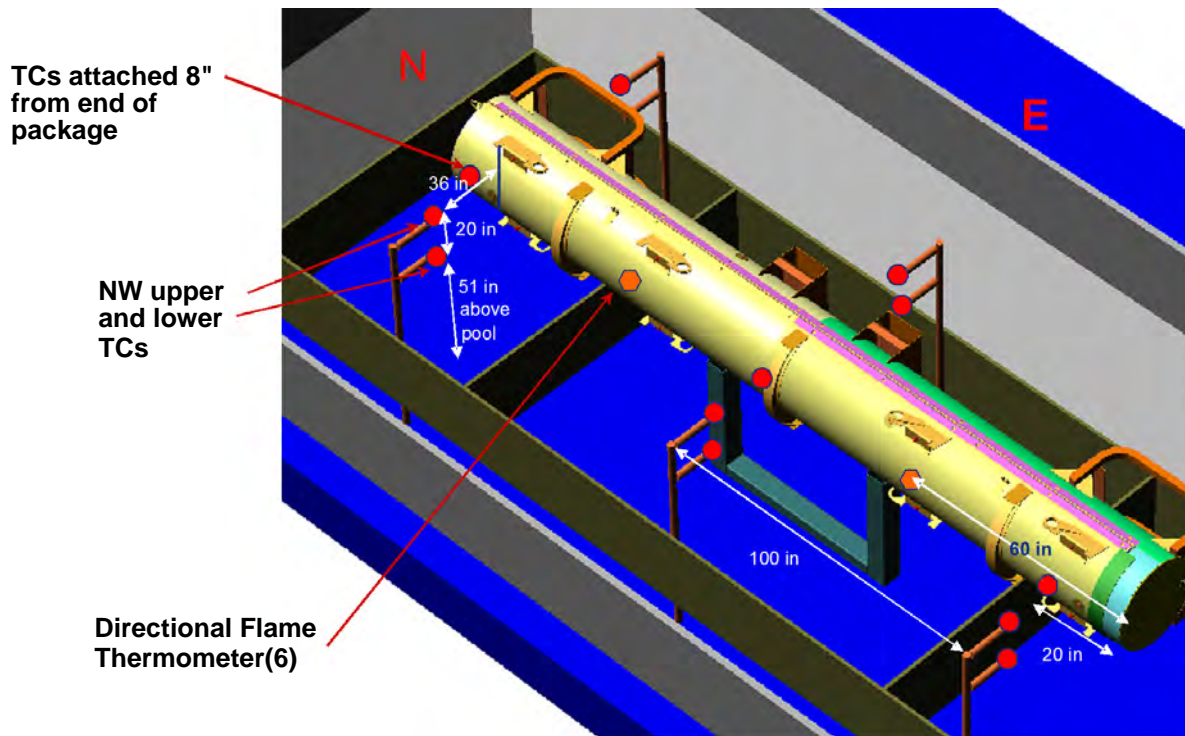


Figure 3-29 Thermocouple Locations on CTU Burn Test



Figure 3-30 Polyurethane Char in Outerpack Seam After Burn Test



Figure 3-31 Brown Polyurethane Residue Inside Outerpack After Burn Test

The following test equipment was used to conduct the burn test:

- Video cameras (4)
- Digital camera
- Omega type K thermocouples with Inconel overbraided 10' leads to measure skin temperature and flame temperature depending on location (XCIB-K-4-2-10 with screw attachment ends and XCIB-K-3-2-10 with air hoods)
- Omega OM-CP-OCTTEMP data loggers (2)
- Omega USB recorder Data Acquisition Modules with weather tight electronics box
- Laptop computer
- Hand held optical pyrometer with adjustable emissivity setting (s)
- Adhesive temperature measurement strips (TL-E-170, TL-E-250, TL-E-330)
- Edmund Scientific Propeller Wind Anometer

The package rested on a steel support structure placed in a burn pool, Figure 3-32. The burn pool was limited by a water cooled weir and the fuel was evenly distributed throughout the pool. The pool was also surrounded by a steel diffuser, Figure 3-33. The top of the diffuser was approximately 1.6 m (5.4 ft) above the top of the pool surface, the height of the top of the test article.

The primary sensors used in the tests were Omega XCIB-K-4-12 thermocouples connected via approximately 50 ft of 20 gage type K, Teflon coated, extension wire. The type K thermocouples have standard limit of 4°F (2.2°C) or 0.75% between 32° and 2282°F (0° and 1250°C). The 20 gage chromel/alumel wire has a resistance of 0.586 ohms per double foot of length. Two types of data recorders were used. Two Omega OM-CP-OCTTEMP 8 channel data recorders were used for 14 channels of data. These recorders have a -270° to 1370°C temperature measurement range for Type K thermocouples and 0.5°C accuracy for type K thermocouples. The recorders were purchased new from Omega and were used within the time limit of their original factory calibration. Eight channels of data were recorded using a Instronet, data acquisition system with an INET-100 external A/D box connected to a Toshiba Satellite notebook computer running Windows XP Professional using a INET-230 PC card controller. This system, with Type K thermocouples has an accuracy of $\pm 0.6^\circ\text{C}$ between -50° and 1360°C. The lowest average temperatures from the CTU burn test were the DFT readings which had an 834°C, 30 minute average temperature. Adding the worst case thermocouple and data recorder errors results in a 6.8°C average error. This is not sufficient to lower average temperature below 800°C.



Figure 3-32 Test Stand for Fire Test



Figure 3-33 Test Setup with Steel Diffuser Plates

3.6.5.1 Test Procedures and Results

The Certification Test Unit 1 (CTU) was burn tested on February 10, 2004. Because the overnight temperatures dropped to near freezing, the package was covered with a tarp, Figure 3-34 and heated by two 150,000 BTU/hr (44 kWt) kerosene heaters used alternatively. The heaters maintained the air temperature under the tent between 40 and 80°C (104 and 176°F) with readings at one location climbing to 115°C (239°F). The heater was turned off shortly after 7:15 AM and the tarp was removed between 7:20 and 8:00 AM. Temperatures around the package were measured and recorded on the two data loggers. This data is shown on, Figures 3-35 and 3-36. The ambient temperature shown is air temperature outside of the heated tent.

This test was performed between 8:32 and 9:06 AM Tuesday morning. Fuel was added to the pool starting at 8:26 AM and continued until 150 gal had been added. The pool was lit at 8:32 and full engulfment was achieved one minute later. After full engulfment was achieved, fuel flow was adjusted to between 61 and 83 l/min (16 and 22 gal/min) depending on the flame coverage within the pool. The fuel flow was secured at 9:04 and the fire suppression system was activated one minute later. The pool fire was extinguished within approximately one minute, although burning polyurethane from the package reignited residual fuel at one end of the pool shortly afterwards. This was extinguished using the fire suppression system.



Figure 3-34 Test Article Under Tent to Maintain Temperature Overnight

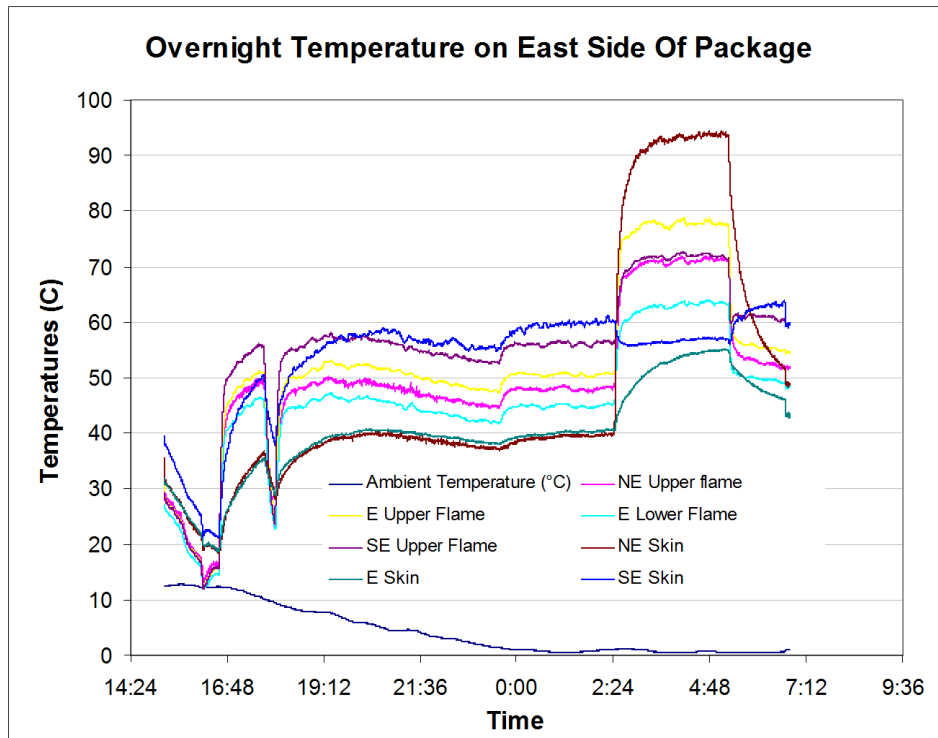


Figure 3-35 Overnight Temperatures on East Side of Test Article

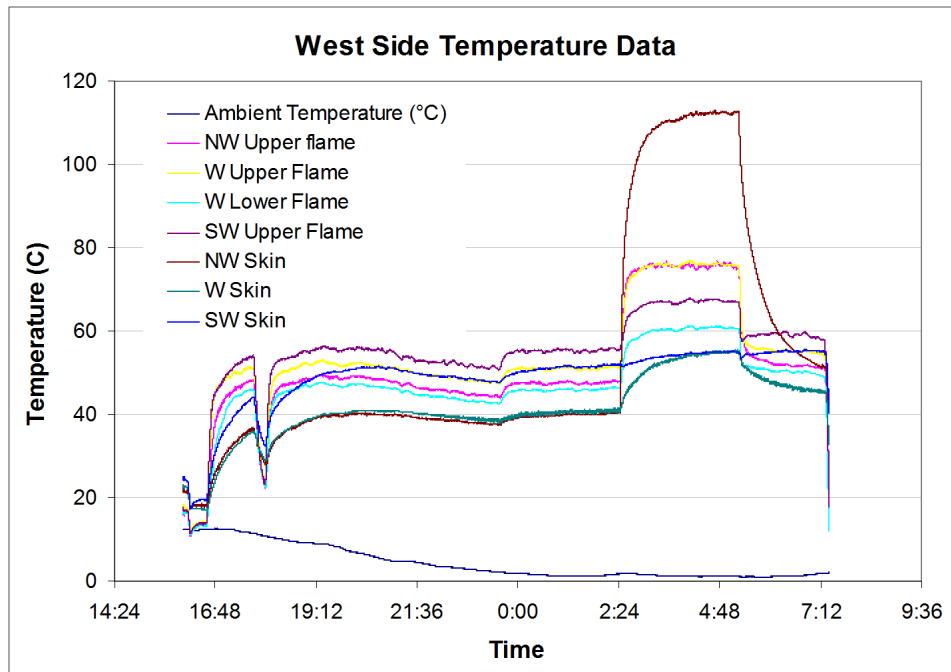


Figure 3-36 Overnight Temperatures on West Side of Test Article

During the fire test, data recorded by the instrument system was monitored in real time. This data included the following thermocouples:

- NE lower flame temperature (same height as center of test article)
- NE DFT
- SE DFT
- SE lower flame temperature
- NW lower flame temperature
- NW DFT
- SW DFT
- SW lower flame temperature

The data from the thermocouples within the fire is shown in, Figure 3-37. The data from the DFTs is shown in Figure 3-38.

Two data loggers were used to record a total of 14 channels of data. One data logger recorded temperatures on the east side of the CTU other, the west side of the CTU. Figures 3-39 and 3-40 show the skin temperature data collected on the east and west sides of the CTU. Figures 3-41 and 3-42 show data collected from the remaining thermocouples in the fire on the east and west sides respectively.

Twenty-two (22) thermocouples were used to measure external conditions on and around the Traveller package during the February 10, 2004 fire test. These sensors were located as shown in Figure 3-30 in the SAR. Due to the natural instability of open flames, combined with wind effects, these thermocouples were periodically uncovered. As shown in Figures 3-38 through 3-43, this resulted in large variations in measured temperature. These variations are largest at the corners of the pool fire where small disruptions in the flame would change air temperature at the thermocouple location. These disruptions were the smallest at the package skin because it was in the center of the pool fire.

Table 3-4A below, summarizes the thermocouple data for the test. Some of the thermocouples had average temperatures under 800°C but all experienced temperatures above 900°C during the test, demonstrating that the fire covered the complete pool area. Some of the minimum temperatures recorded are due to the time selected for the 30 minute average. A fire this size cannot start instantaneously, nor did it end instantaneously. As a result, the 30 minute period selected for averaging data includes data when some TC were beginning to heat up and when some were already cooling off after the fire. The data still shows that the average skin temperature, the average DFT temperature and the average temperature of TCs in the flame were all above 800°C for the 30 minute period selected.

Table 3-4A Summary of Recorded Temperatures During Burn Test			
TC Location	30 Minute Ave (°C)	Max Temp (°C)	Min Temp (°C)
NE Lower Flame	727	959	275
NE Upper Flame	925	1245	493
E Lower Flame	926	1155	489
E Upper Flame	904	1163	532
SE Lower Flame	714	962	291
SE Upper Flame	924	1245	484
NW Lower Flame	630	906	329
NW Upper Flame	748	1059	458
W Lower Flame	997	1162	640
W Upper Flame	1027	1173	661
SW Lower Flame	827	1032	230
SW Upper Flame	1000	1213	598
NE DFT	804	907	454
SE DFT	801	964	338
NW DFT	854	1016	541
SW DFT	876	1003	594
NE Skin	878	1058	610
E Skin	917	1073	699
SE Skin	903	1088	542
NW Skin	725	990	492
W Skin	974	1080	682
SW Skin	1028	1143	719

Because the thermocouples in the corners of the pool were not engulfed as long as the package itself, the 30 minute average temperature for the corners is lower than in the center of the pool. The total average for all of the thermocouples in the flame was 862°C versus 812°C for the corner thermocouples in the flame. The DFT average readings are also lower for similar reasons. The DFTs insulated the thermocouple and attached face plate from convective heat transfer. Radiative heat transfer was dominate by design. Because these devices faced away from the package, they recorded equilibrium temperature based on radiation from the fire and reradiation to cold surfaces outside the fire, without contribution from convection. The skin temperature is an equilibrium temperature that includes convective heat transfer from hot combustion gasses. As a result, its temperatures should be higher.

As described in the discussion of thermal analysis results (section 3.6.1) the long length to diameter ratio of the Traveller package minimizes the role of axial heat transfer inside the package. Non-uniform external temperatures produce non-uniform internal temperatures during fire tests. This fundamental mechanism allowed useful data to be obtained in the seam burn and impact limiter burn tests described in sections 3.6.2 and 3.6.3. This mechanism was demonstrated by the very low clamshell temperatures measured adjacent to the heated sections in those tests. During the CTU burn test, the average skin temperature at the North end, middle and South end of the package was 801°, 946°, and 915°C respectively. Peak interior temperatures recorded by the non-reversible temperatures strips were 116°C at the North end of the package, 177°C at the middle of the package, and 143°C at the South end of the package. At the center of the package, where the average exterior skin temperature was 946°C, the corresponding interior temperatures were acceptable for all materials in the package.

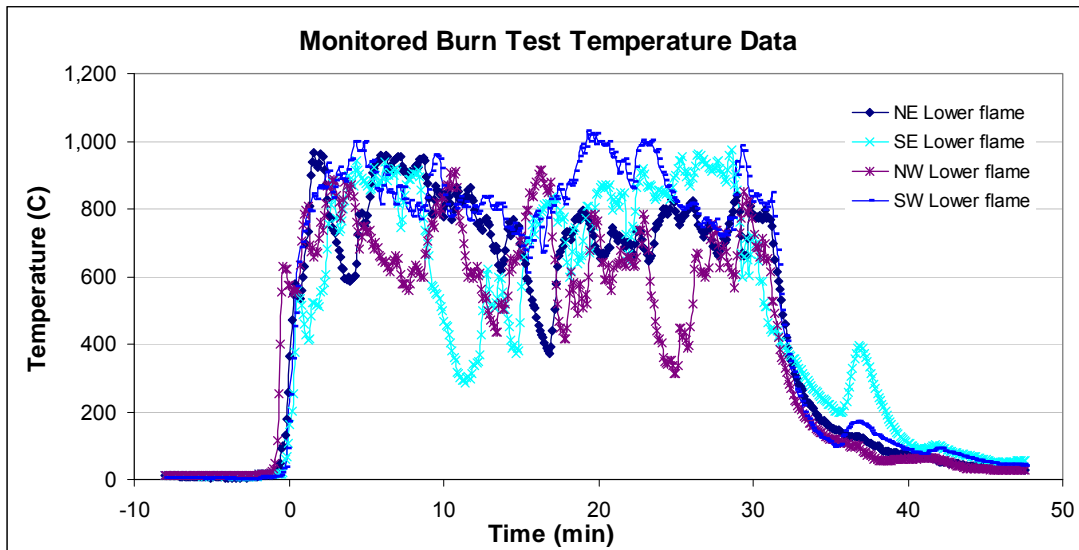


Figure 3-37 Fire Temperatures Measured at the Corners of the Pool

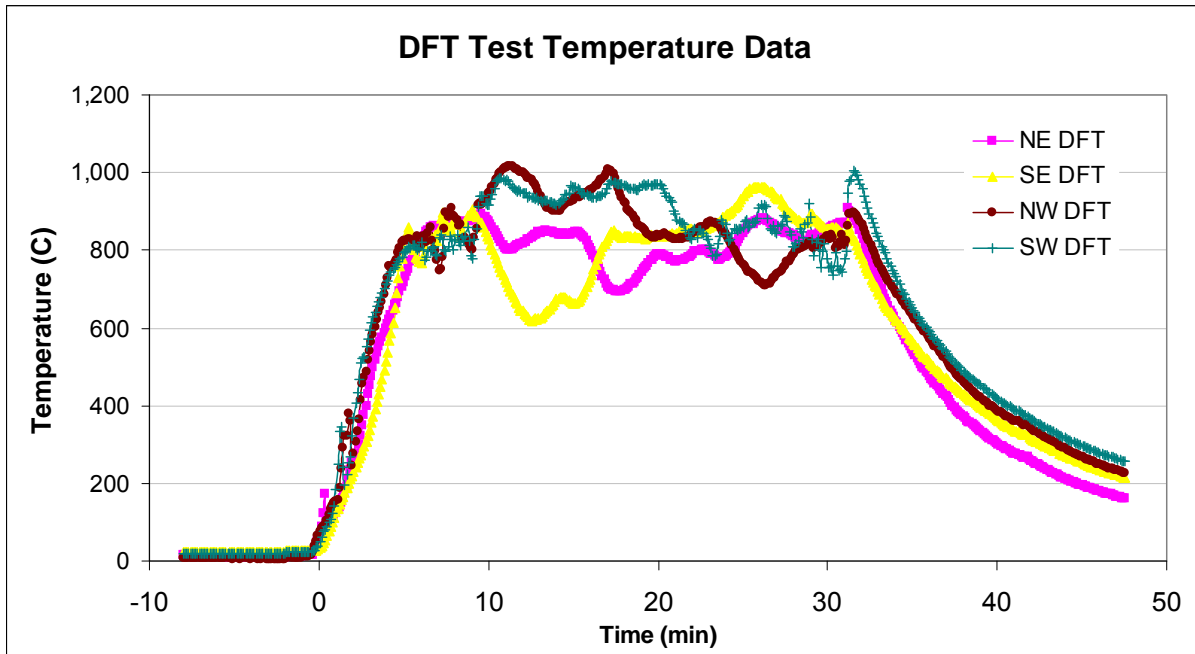


Figure 3-38 Data from Direction Flame Thermometers (DFTs)

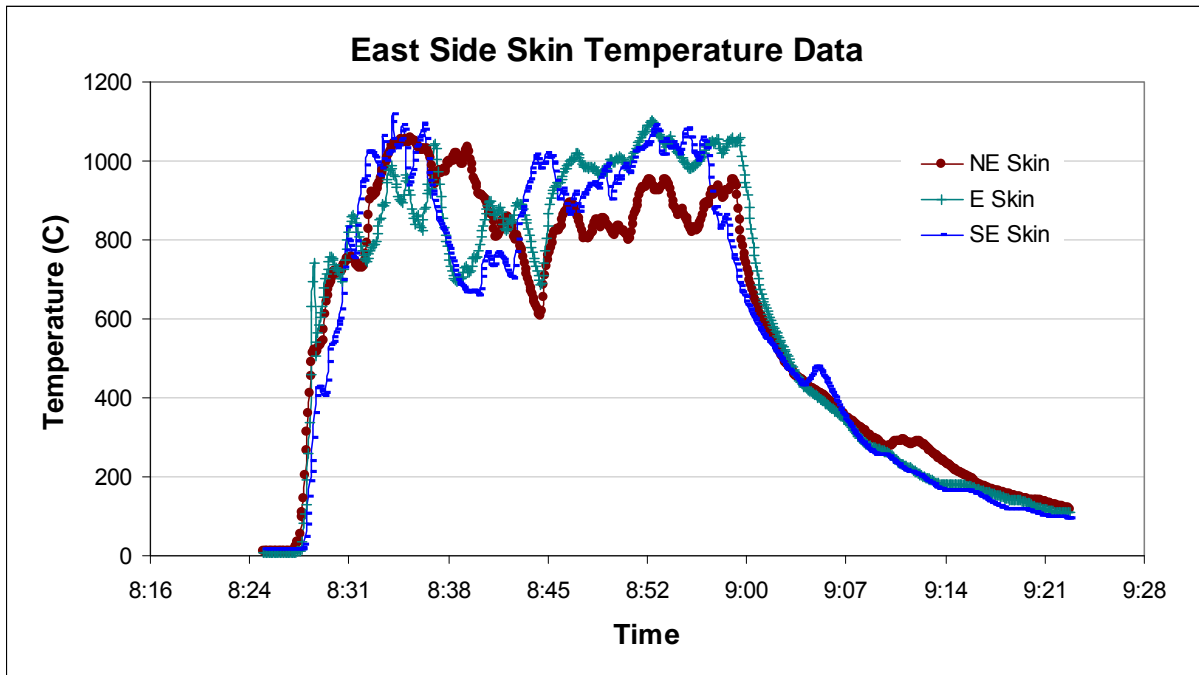


Figure 3-39 Skin Temperature Data from East Side of CTU

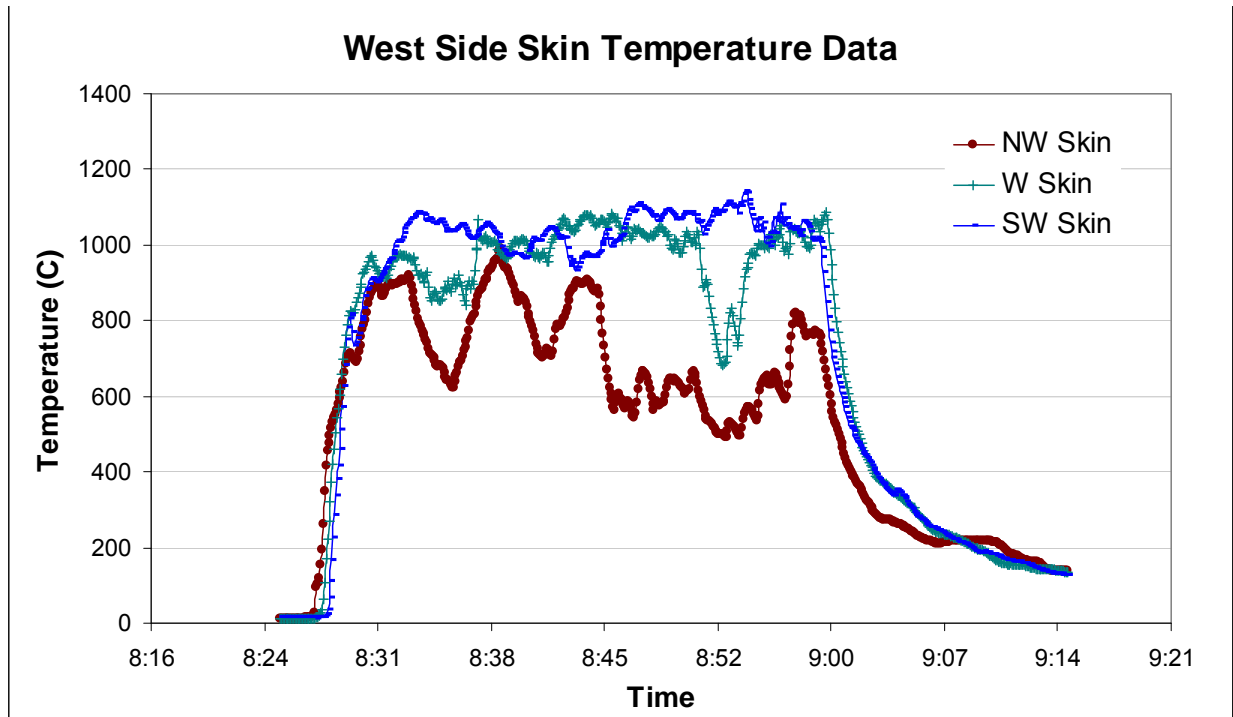


Figure 3-40 Skin Temperature Data from West Side of CTU

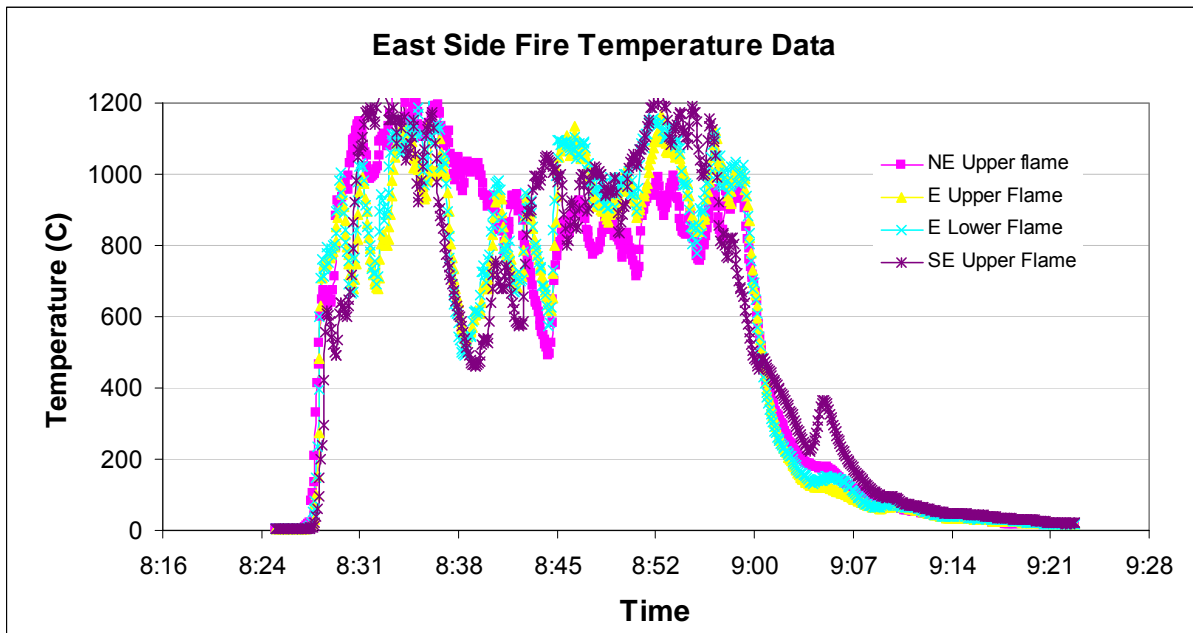


Figure 3-41 Fire Temperature Data from East Side of CTU

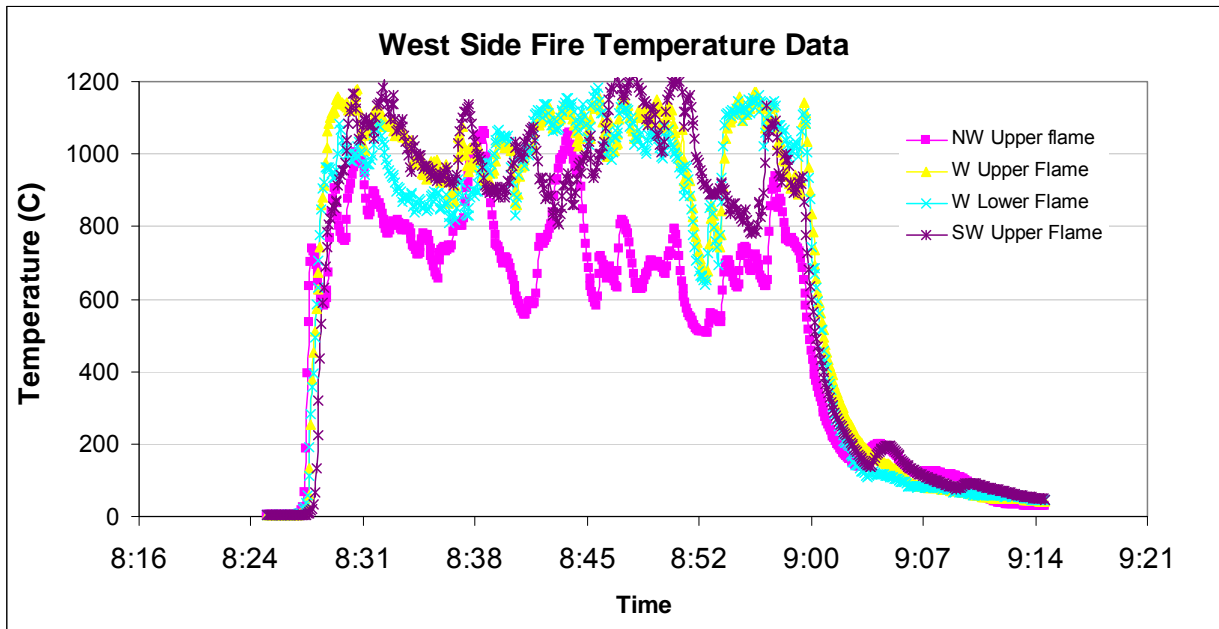


Figure 3-42 Fire Temperature Data from West Side of CTU

Temperature data was also collected using two portable, single wavelength optical thermometers. One was located on a raised platform on the west side of the package. The second was located on the east side of the package. Temperature data was recorded by hand. This data is shown in Tables 3-5 and 3-6.

Table 3-5 Optical Thermometer Data Sheet (West Side, Degrees C)			
Time After Pool Fire Ignition	Temperature (North End)	Temperature (Middle)	Temperature (South End)
0 minutes	922	944	874
5 minutes	1047	973	1025
10 minutes	1002	1092	993
15 minutes	937	847	987
20 minutes	1177	982	942
25 minutes	1062	1073	1058
30 minutes	898	1162	968
35 minutes	525	460	484
40 minutes	318	362	294

Time After Pool Fire Ignition	Temperature (North End)	Temperature (Middle)	Temperature (South End)
0 minutes	800	1000	936
5 minutes	978	1062	837
10 minutes	1037	948	932
15 minutes	842	996	835
20 minutes	590	1120	978
25 minutes	552	969	1048
30 minutes	1098	740	980
35 minutes	No Data	No Data	No Data
40 minutes	No Data	No Data	No Data

Wind speed measurements were made before, during and after the burn test. Average wind speed during the test was 0.9 miles per hour (0.4 m/s). Peak wind speed measured during the test was 2.2 miles per hour (1.0 m/s). The data was recorded by had at five minute intervals. This data is shown in Table 3-7.

An examination of the moderator blocks after the burn test revealed no significant damage. One small portion of moderator at the bottom end of the package showed signs of combustion, Figure 3-43. The very localized nature of the burn marks (on both the moderator and the refractory fiber felt insulation that covered the moderator) indicates that this was probably caused during the fabrication process. The stainless steel cover sheets are welded into place after the moderator blocks are bolted in and covered with insulation. It appears that the welding torch was applied to the moderator causing a small amount of damage. A brown spot was observed on the back side of one moderator block attached to the Outerpack lid. The polyethylene at this location appears to have been heated to melt temperature, Figure 3-44. A very small amount of flow occurred away from the hot spot. This melt spot was small, affecting only a few cubic centimeters of material. The twelve polyethylene moderator blocks were weighed before installation into the package, after the fire test, and subsequent disassembly. Table 3-6A compares the weight measurements before and after the fire test. Those measurements show that there was no significant weight loss within the accuracy of the measurements for all the blocks and therefore all blocks retained sufficient hydrogen content.

In addition to the polyethylene block post-test inspections, a visual examination of the shock mounts indicated that they were all intact.

Table 3-6A Moderator Block Weights		
Position	Weight Before Test (lb)	Weight After Test (lb)
Base top left	47.1	47.1
Base top right	47.2	47.2
Base lower left	44.6	44.8
Base lower right	46.3	46.2
Lid top left	40.4	40.7
Lid top right	40.4	40.1
Lid lower left	40.4	40.6
Lid lower right	40.4	40.3
Total	346.8	347.0

Ultra-high molecular weight (UHMW) polyethylene was selected as the neutron moderator for the Traveller package because of its high hydrogen content, its ductility at very low temperatures and its high viscosity at temperatures well above its melt point due to the long molecular chains (MW=3,000,000 to 6,000,000). The relative solution viscosity as measured by ASTM D4020 must be greater than 1.4¹ and is typically found to be 2.3 to 3.5 dl/gm² (at 135°C). As a result, UHMW polyethylene does not liquefy above its melt temperature and molded UHMW polyethylene parts are typically made at relatively high temperatures (190°–200°C) and very high pressures (70-100 bar)³. Its excellent stability allows it to be used in some applications at temperatures as high as 450°C⁴. Experience in the Traveller test program has shown that the material will soften but not run, even when heated to near vaporization temperature (349°C). However, the Traveller design encapsulates the moderator with stainless steel. This is primarily done to prevent oxygen from reaching the moderator, should it reach vaporization temperature, but it does serve a secondary function of ensuring that the moderator does not significantly distort or flow at high temperatures.

The highest measured temperature inside the package was 171°C which is lower than the typical process temperature used to create the UHMW sheets installed in the Traveller. Unchanged appearance and more importantly, unchanged weight indicate that the plastic did not lose a significant amount of its hydrogen during the test.

1. Stein, H.L., "Ultra High Molecular Weight Polyethylene (UHMWPE)," Engineered Materials Handbook, Vol. 2, Engineering Plastics, 1998.
2. This is a typical value observed in many manufacturers specifications: Crown Plastics (crownplastics.com/properties.htm).
3. Ticona Engineering Polymers information on compression molding, www.ticona.com/index/tech/processing/compression_molding/gurl.htm.
4. Stein, H.L., "Ultra High Molecular Weight Polyethylene (UHMWPE)," Engineered Materials Handbook, Vol. 2, Engineering Plastics, 1998

This page intentionally left blank.

|

Table 3-7 Wind Data Sheet			
Time	Wind Speed (mph)	Wind Direction	Temperature F
8:05	1.7	E	42
8:10	2.0	NE	-
8:15	1.7	E	-
8:20	2.0	E	42
8:25	0.8	E	-
8:30	0.8	E	42
8:35	0.8	E	-
8:40	0.6	E	42
8:45	1.3	E	-
8:50	2.2	N	42
8:55	0	-	-
9:00	1.5	N	-
9:05	0	-	43
9:10	1.3	W	-
9:20	1.7	SW	43
9:30	1.3	SW	44

Wind data was taken every five minutes starting approximately 15 minutes before the burn until 30 minutes after the burn was completed.

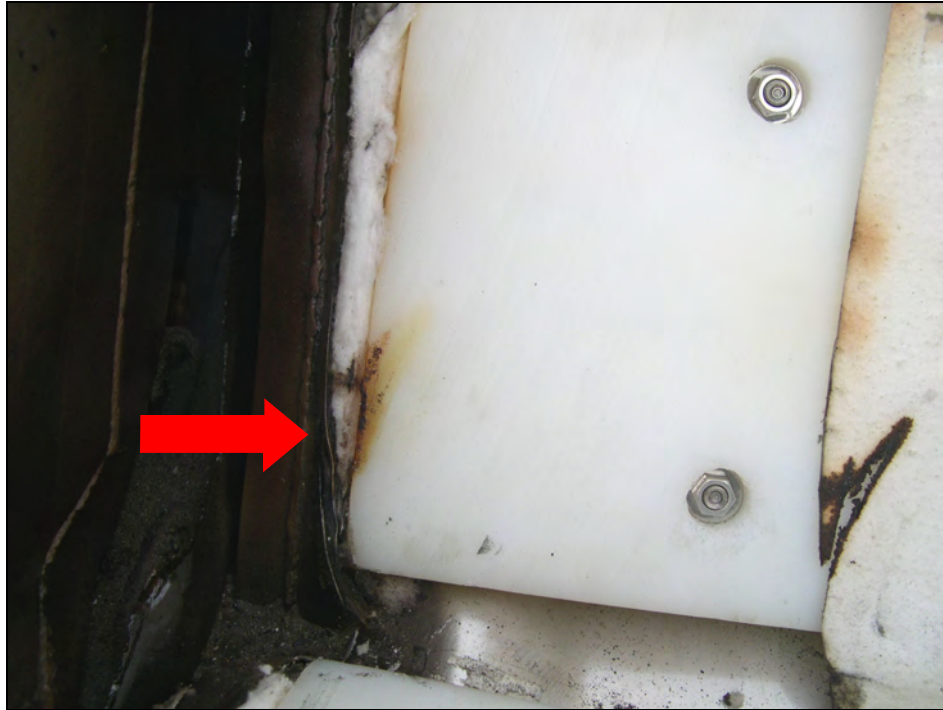


Figure 3-43 Location of Possible Combustion of Moderator



Figure 3-44 Localized Melt Spot in Lid Moderator Block

Twelve sets of non-reversible temperature strips were attached to the CTU. Two were placed on the inside faces of the impact limiters (one at each end), six were placed on the stainless steel covering the moderator in the Outerpack lid, and five were attached to the inside doors of the Clamshell. Except for one set that was unreadable after the test, the peak indicated temperature was 177°C. Locations of the temperature strip sets are shown in Figure 3-45. Readings on one of the Outerpack lid temperature strip sets is shown in Figure 3-46.

Earlier analysis and tests had shown that, if there was no substantial infiltration of hot gas into the package, interior temperatures would remain low during the fire test. This is shown in the results of both the seam burn tests and the impact limiter burn tests (sections 3.6.2 and 3.6.3). In these tests, interior temperatures rose between 50° and 110°C during and after the test. These values are conservative because the tests were performed on a previously burned package where the polyurethane had already turned to char. The primary design concern was hot gas infiltration during the CTU burn test. This would add substantially more heat and cause higher temperatures. This was observed in an earlier burn test (QTU-1). This package was oriented in the same fashion as the CTU, with one Outerpack seam facing the pool surface. Distortion of the Outerpack walls caused hot gasses to enter the package and flow around the clamshell. Because of the geometric arrangement of the Outerpack seam lip, this flow was directed preferentially over the top of the clamshell (as oriented when the package is resting on its feet). Polyurethane ignited at four locations in this region and burned. The moderator under the clamshell was undamaged. Based on this evidence, it seemed best to concentrate the temperature indicating strips on the moderator surface that was expected to be the hottest if significant hot gas infiltration occurred.

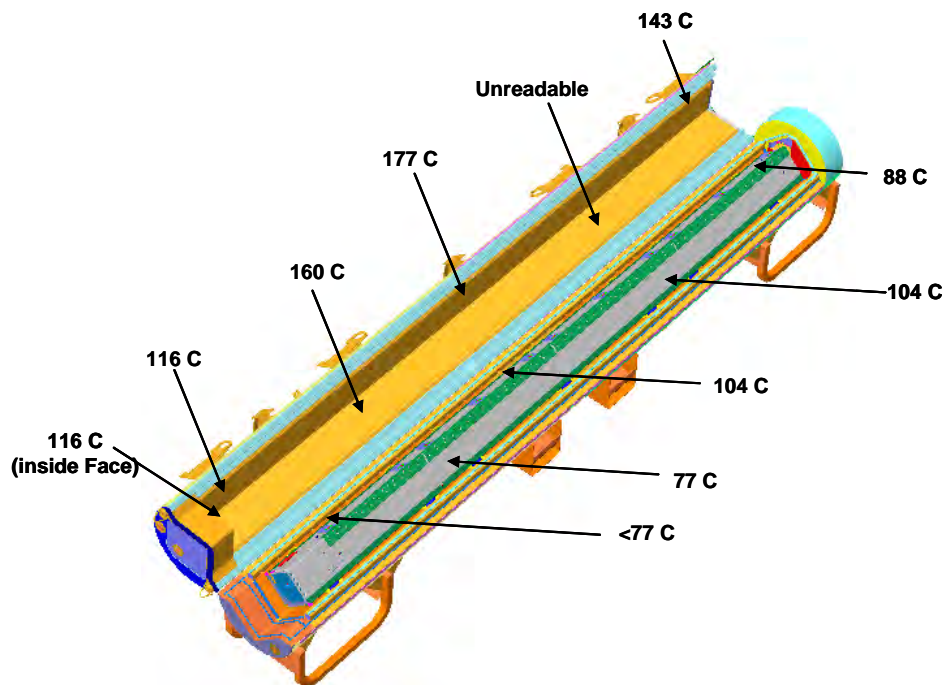


Figure 3-45 Location and Indicated Temperatures of Temperature Strip Sets



Figure 3-46 Temperature Strip Set After Fire Test

TABLE OF CONTENTS

4.0	CONTAINMENT	4-1
4.1	DESCRIPTION OF THE CONTAINMENT SYSTEM.....	4-1
4.2	CONTAINMENT UNDER NORMAL CONDITIONS OF TRANSPORT	4-1
4.3	APPENDICES.....	4-1
4.3.1	References.....	4-1

4.0 CONTAINMENT

4.1 DESCRIPTION OF THE CONTAINMENT SYSTEM

The Traveller package is limited to transporting Type A, low enriched commercial grade uranium, nuclear fuel assemblies and rods. The radioactive material, bound in sintered pellets having very limited solubility, has minimal propensity to suspend in air. These pellets are sealed in fuel tubes to form the fuel rod portion of each assembly. The welded seals of the fuel rods are verified for integrity. There is no pressure relief device that would allow release of radioactive contents.

Containment System is described in both SSR-6 (§213) [1] and 10CFR71.4 [2] as, “the assembly of components of the packaging intended to retain the radioactive material during transport.” The Containment System for the Traveller consists of the fuel rods.

4.2 CONTAINMENT UNDER NORMAL CONDITIONS OF TRANSPORT

For Type A fissile packages, no loss or dispersal of radioactive material is permitted under normal conditions of transport as specified in SSR-6 (§648) and 10CFR71.43(f). It has been demonstrated from repeated normal drop scenarios and subsequent evaluations that there is no loss of fissile material from the rods, and therefore no dispersal. Therefore, the containment system remains intact.

4.3 APPENDICES

4.3.1 References

- [1] International Atomic Energy Agency, "Regulations for the Safe Transport of Radioactive Material," SSR-6, 2012.
- [2] U.S. Nuclear Regulatory Commission Code of Federal Regulations, Title 10 Part 71, "Packaging and Transport of Radioactive Material", April 2016.

TABLE OF CONTENTS

5.0 SHIELDING EVALUATION	5-1
5.1 APPENDICES.....	5-1
5.1.1 References.....	5-1

5.0 SHIELDING EVALUATION

The enriched commercial grade uranium fuel assemblies do not emit any significant form of radiation to have an effect on package external dose rates. The negligible quantity of radiation emitted from contents and the shielding provided by the packaging materials of the Traveller effectively limit radiation levels on the external surface of the package. Under routine and normal conditions of transport, the radiation level does not exceed 2 mSv/hour (200 mrem/hour) at any point on the external surface of the package, meeting the requirements for a Type A fissile package specified in SSR-6 (§527) [1] and 10CFR71.47(a) [2].

5.1 APPENDICES

5.1.1 References

- [1] International Atomic Energy Agency, "Regulations for the Safe Transport of Radioactive Material," SSR-6, 2012.
- [2] U.S. Nuclear Regulatory Commission Code of Federal Regulations, Title 10 Part 71, "Packaging and Transport of Radioactive Material," 2016.

TABLE OF CONTENTS

6.0	CRITICALITY EVALUATION	6-1
6.1	DESCRIPTION OF CRITICALITY DESIGN	6-1
6.1.1	Design Features	6-1
6.1.1.1	Confinement System	6-1
6.1.1.2	Flux Traps.....	6-1
6.1.2	Summary Table of Criticality Evaluation	6-2
6.1.2.1	Contents Grouping	6-3
6.1.3	Criticality Safety Index.....	6-4
6.2	FISSILE MATERIAL CONTENTS	6-5
6.2.1	Group 1.....	6-6
6.2.2	Group 2.....	6-9
6.2.3	Group 3.....	6-10
6.2.4	Rod Pipe	6-11
6.3	GENERAL CONSIDERATIONS.....	6-12
6.3.1	Model Configuration	6-12
6.3.1.1	Rod Pipe	6-15
6.3.1.2	Conditions of Transport.....	6-16
6.3.2	Material Properties	6-17
6.3.2.1	Non-Fissile, Non-Radioactive Reactor Core Components	6-17
6.3.2.2	UO ₂	6-17
6.3.2.3	U ₃ Si ₂	6-17
6.3.2.4	Zircaloy Cladding.....	6-17
6.3.2.5	Guide Tubes/Instrument Tubes	6-18
6.3.2.6	Flooding and Reflecting Water.....	6-18
6.3.2.7	Fuel Assembly Structural Materials	6-18
6.3.2.8	Aluminum.....	6-18
6.3.2.9	304 Stainless Steel.....	6-18
6.3.2.10	Ultra-High Molecular Weight Polyethylene.....	6-18
6.3.2.11	BORAL Neutron Absorber Plates	6-19
6.3.2.12	Hydrogenous Packaging Materials.....	6-19
6.3.2.13	Hydrogenous Packing Materials.....	6-19
6.3.2.14	Extreme Cold Case (-40°C) Effects.....	6-20
6.3.2.15	Integral Absorbers	6-20
6.3.2.16	Summary of SCALE Material Compositions	6-21
6.3.3	Computer Codes and Cross-Section Libraries	6-22
6.3.3.1	Convergence Criteria.....	6-23
6.3.4	Demonstration of Maximum Reactivity	6-23
6.3.4.1	Categorized Fuel Assembly Determination.....	6-24
6.3.4.2	Baseline Case	6-24
6.3.4.3	Sensitivity Studies	6-30
6.4	SINGLE PACKAGE EVALUATION	6-43
6.4.1	Configuration.....	6-43
6.4.1.1	Baseline Configurations	6-43
6.4.1.2	Sensitivity Study Configurations.....	6-45
6.4.2	Results	6-46
6.4.2.1	Single Package – Maximum Reactivity Results Summary.....	6-46
6.4.2.2	Sensitivity Study Results.....	6-47
6.5	EVALUATION OF PACKAGE ARRAYS UNDER NORMAL CONDITIONS OF TRANSPORT... ..	6-70
6.5.1	Configuration.....	6-70
6.5.1.1	Baseline Configurations	6-70
6.5.1.2	Sensitivity Study Configurations.....	6-73
6.5.2	Results	6-74
6.5.2.1	NCT Package Array – Maximum Reactivity Results Summary.....	6-74

	6.5.2.2	Sensitivity Study Results.....	6-74
6.6		PACKAGE ARRAYS UNDER HYPOTHETICAL ACCIDENT CONDITIONS.....	6-86
	6.6.1	Configuration.....	6-86
	6.6.1.1	Baseline Configuration.....	6-86
	6.6.1.2	Sensitivity Study Configurations.....	6-89
	6.6.2	Results.....	6-91
	6.6.2.1	HAC Package Array – Maximum Reactivity Results Summary.....	6-91
	6.6.2.2	Sensitivity Study Results.....	6-91
6.7		FISSILE MATERIAL PACKAGES FOR AIR TRANSPORT.....	6-110
	6.7.1	Configuration.....	6-110
	6.7.2	Results.....	6-110
6.8		BENCHMARK EVALUATIONS.....	6-111
	6.8.1	Applicability of Benchmark Experiments.....	6-111
	6.8.2	Bias Determination.....	6-112
6.9		APPENDIX.....	6-114
	6.9.1	References.....	6-115
	6.9.2	Categorized Fuel Assembly Analysis.....	6-116
	6.9.2.1	CFA Results.....	6-116
	6.9.2.2	Organizing Fuel Assemblies into Bins.....	6-117
	6.9.2.3	Determination of Categorized Fuel Assemblies.....	6-118
	6.9.2.4	Determination of Most Reactive Secondary Parameters.....	6-120
	6.9.2.5	Bin Permutation Model.....	6-120
	6.9.2.6	CFA Most Reactive Secondary Parameters.....	6-121
	6.9.3	Baseline Detailed Results.....	6-134
	6.9.3.1	Single Package, Fuel Assembly.....	6-134
	6.9.3.2	Single Package, Rod Pipe.....	6-138
	6.9.3.3	Package Array, NCT, Fuel Assembly.....	6-142
	6.9.3.4	Package Array, NCT, Rod Pipe.....	6-144
	6.9.3.5	Package Array, HAC, Fuel Assembly.....	6-145
	6.9.3.6	Package Array, HAC, Rod Pipe.....	6-151
6.9.4		Combined Case Study Results.....	6-154

LIST OF TABLES

Table 6-1	Summary Table of Upper Subcritical Limits	6-3
Table 6-2	Summary Table of Criticality Evaluation.....	6-4
Table 6-3	Criticality Safety Index Summary	6-4
Table 6-4	Bin Listing for Each Fuel Assembly Group	6-5
Table 6-5	Group 1 Fuel Assembly Bins	6-7
Table 6-6	Group 1 Fuel Assembly Bins	6-7
Table 6-7	Group 1 Fuel Assembly Bins	6-7
Table 6-8	Group 2 Fuel Assembly Bins	6-9
Table 6-9	Group 3 Fuel Assembly Bin.....	6-10
Table 6-10	Major Dimensions of Each Traveller Variant Model	6-13
Table 6-11	Major Dimensions of Rod Pipe Model.....	6-15
Table 6-12	Summary of Compound Material Compositions.....	6-21
Table 6-13	Summary of Alloy/Mixture Material Compositions	6-21
Table 6-14	Summary of BORAL Plate Core Material Composition	6-22
Table 6-15	Bin Listing for Each Fuel Assembly Group	6-24
Table 6-16	Rod Pipe UO ₂ Baseline Evaluation - Fuel Rod and Pitch Values	6-28
Table 6-17	Rod Pipe U ₃ Si ₂ Baseline Evaluation - Fuel Rod and Pitch Values	6-29
Table 6-18	Baseline and Sensitivity Studies Configurations for Each Package Arrangement	6-31
Table 6-19	Cladding Diameter Tolerances Examined.....	6-39
Table 6-20	Fuel Pellet Diameter Tolerances Examined	6-39
Table 6-21	Fuel Rod Pitch Tolerances Examined	6-40
Table 6-22	Summary of Groups 1, 2, and 3 Single Package Configurations	6-43
Table 6-23	Summary of Rod Pipe Single Package Baseline Configurations	6-45
Table 6-24	Single Package Sensitivity Study Bounding Configurations - Groups 1, 2, and 3.....	6-45
Table 6-25	Rod Pipe Single Package Sensitivity Studies Bounding Configurations	6-46
Table 6-26	Single Package – Maximum Reactivity Results Summary	6-46
Table 6-27	Single Package Assessed Penalties, Δk_{eff} , Groups 1, 2, and 3	6-47
Table 6-28	Annular Blanket Sensitivity Results – Single Package, NCT, Groups 1, 2, and 3.....	6-48
Table 6-29	Fuel Assembly Position Sensitivity Results – Single Package, NCT, Groups 1, 2, and 3	6-49
Table 6-30	Polyethylene Packing Sensitivity Results – Single Package, NCT, Groups 1, 2, and 3.....	6-49
Table 6-31	SS Rod Replacement Sensitivity Results – Single Package, NCT, Groups 1, 2, and 3.....	6-50
Table 6-32	Tolerance Sensitivity Results – Single Package, NCT, Groups 1, 2, and 3.....	6-50
Table 6-33	Extended Active Fuel Length Results – Single Package, NCT, Group 3.....	6-51
Table 6-33A	ADOPT Fuel Results – Single Package, NCT, Groups 1 & 2.....	6-51
Table 6-34	Annular Blanket Sensitivity Results – Single Package, HAC, Groups 1, 2, and 3.....	6-52
Table 6-34A	Fuel Assembly Position Sensitivity Results – Single Package, HAC, Groups 1, 2, and 3.....	6-53
Table 6-35	Moderator Block Density Results – Single Package, HAC, Groups 1, 2, and 3	6-54
Table 6-36	Polyethylene Sensitivity Results – Single Package, HAC, Groups 1, 2, and 3	6-54
Table 6-37	Axial Rod Displacement Sensitivity Results – Single Package, HAC, Groups 1, 2, and 3.....	6-56
Table 6-38	SS Rod Replacement Sensitivity Results – Single Package, HAC, Groups 1, 2, and 3	6-57
Table 6-39	Tolerance Sensitivity Results – Single Package, HAC, Groups 1, 2, and 3.....	6-58
Table 6-40	Extended Active Fuel Length Results – Single Package, HAC, Group 3	6-59
Table 6-40A	ADOPT Fuel Results – Single Package, HAC, Groups 1 & 2	6-59
Table 6-41	Single Package Assessed Penalties, Δk_{eff} , Rod Pipe	6-59
Table 6-42	Annular Blanket Sensitivity Results – Single Package, NCT, Rod Pipe.....	6-60
Table 6-43	Rod Pipe Position Sensitivity Results – Single Package, NCT, Rod Pipe	6-61
Table 6-44	Polyethylene Packing Sensitivity Results – Single Package, NCT, Rod Pipe.....	6-62
Table 6-45	Tolerance Sensitivity Results – Single Package, NCT, Rod Pipe	6-63
Table 6-45A	ADOPT Fuel Results – Single Package, NCT, Rod Pipe.....	6-63
Table 6-46	Annular Blanket Sensitivity Results – Single Package, HAC, Rod Pipe	6-64
Table 6-47	Rod Pipe Position Sensitivity Results – Single Package, HAC, Rod Pipe.....	6-66
Table 6-48	Moderator Block Density Results – Single Package, HAC, Rod Pipe.....	6-66
Table 6-49	Polyethylene Sensitivity Results – Single Package, HAC, Rod Pipe.....	6-67
Table 6-50	Tolerance Sensitivity Results – Single Package, HAC, Rod Pipe.....	6-69

Table 6-50A	ADOPT Fuel Results – Single Package, HAC, Rod Pipe	6-69
Table 6-51	Summary of NCT Package Array Baseline Configuration.....	6-70
Table 6-52	Summary of Rod Pipe NCT Package Array Configurations	6-72
Table 6-53	NCT Package Array Sensitivity Study Bounding Configurations - Groups 1, 2, and 3.....	6-73
Table 6-54	NCT Package Array Sensitivity Study Bounding Configurations - Rod Pipe.....	6-74
Table 6-55	NCT Package Array – Maximum Reactivity Results Summary	6-74
Table 6-56	NCT Package Array Assessed Penalties, Δk_u	6-75
Table 6-57	Annular Blanket Sensitivity Results – Package Array, NCT, Groups 1, 2, and 3.....	6-75
Table 6-58	Fuel Assembly Position Sensitivity Results – Package Array, NCT, Groups 1, 2, and 3	6-77
Table 6-59	Package OD Tolerance Results – Package Array, NCT, Groups 1, 2, and 3	6-77
Table 6-60	Polyethylene Packing Sensitivity Results – Package Array, NCT, Groups 1, 2, and 3.....	6-78
Table 6-61	SS Rod Replacement Sensitivity Results – Package Array, NCT, Groups 1, 2, and 3.....	6-78
Table 6-62	Tolerance Sensitivity Results – Package Array, NCT, Groups 1, 2, and 3	6-79
Table 6-63	Steel Nozzle Reflector Sensitivity Results – Package Array, NCT, Groups 1, 2, and 3	6-80
Table 6-64	Extended Active Fuel Length Results – Package Array, NCT, Group 3.....	6-81
Table 6-64A	ADOPT Fuel Results – Package Array, NCT, Groups 1 & 2.....	6-81
Table 6-65	Rod Pipe NCT Package Array Assessed Penalties, Δk_u	6-81
Table 6-66	Annular Blanket Sensitivity Results – Package Array, NCT, Rod Pipe.....	6-82
Table 6-67	Rod Pipe Position Sensitivity Results – Package Array, NCT, Rod Pipe	6-83
Table 6-68	Package OD Tolerance Sensitivity Results – Package Array, NCT, Rod Pipe	6-83
Table 6-69	Polyethylene Packing Sensitivity Results – Package Array, NCT, Rod Pipe	6-84
Table 6-70	Tolerance Sensitivity Results – Package Array, NCT, Rod Pipe	6-85
Table 6-70A	ADOPT Fuel Results – Package Array, NCT, Rod Pipe.....	6-85
Table 6-71	Summary of Groups 1, 2, and 3 HAC Package Array Configurations	6-86
Table 6-72	Summary of Rod Pipe HAC Package Array Configurations.....	6-88
Table 6-73	HAC Package Array Sensitivity Study Bounding Configurations – Groups 1, 2, 3	6-90
Table 6-74	HAC Package Array Sensitivity Study Bounding Configurations – Rod Pipe	6-90
Table 6-75	HAC Package Array – Maximum Reactivity Results Summary.....	6-91
Table 6-76	HAC Package Array Assessed Penalties, Δk_u , Groups 1, 2, and 3.....	6-91
Table 6-77	Annular Blanket Sensitivity Results – HAC Package Array, Groups 1, 2, and 3	6-92
Table 6-78	Clamshell/Fuel Assembly Position Results – HAC Package Array, Groups 1, 2, and 3.....	6-94
Table 6-79	Moderator Block Density Results – HAC Package Array, Groups 1, 2, and 3	6-94
Table 6-80	Package Outer Diameter Tolerance Results – HAC Package Array, Groups 1, 2, and 3.....	6-95
Table 6-81	Polyethylene Sensitivity Results – HAC Package Array, Groups 1, 2, and 3	6-95
Table 6-82	Axial Rod Displacement Sensitivity Results – Single Package, HAC, Groups 1, 2, and 3.....	6-98
Table 6-83	SS Rod Replacement Sensitivity Results – Single Package, HAC, Groups 1, 2, and 3	6-100
Table 6-84	Tolerance Sensitivity Results – HAC Package Array, Groups 1, 2, and 3.....	6-100
Table 6-85	Steel Nozzle Reflector Sensitivity Results – HAC Package Array, Groups 1, 2, and 3.....	6-102
Table 6-86	Extended Active Fuel Length Results – HAC Package Array, Group 3	6-102
Table 6-86A	ADOPT Fuel Results – HAC Package Array, Groups 1 & 2.....	6-102
Table 6-87	HAC Package Array Assessed Penalties, Δk_u , Rod Pipe.....	6-103
Table 6-88	Annular Blanket Sensitivity Results – HAC Package Array, Rod Pipe	6-103
Table 6-89	Rod Pipe Position Sensitivity Results – HAC Package Array, Rod Pipe.....	6-105
Table 6-90	Moderator Block Density Results – HAC Package Array, Rod Pipe.....	6-105
Table 6-91	Package Outer Diameter Tolerance Sensitivity Results – HAC Package Array, Rod Pipe.....	6-105
Table 6-92	Polyethylene Sensitivity Results – HAC Package Array, Rod Pipe.....	6-106
Table 6-93	Tolerance Sensitivity Results – HAC Package Array, Rod Pipe.....	6-107
Table 6-94	Flooding Configuration Results – HAC Package Array, Rod Pipe.....	6-108
Table 6-94A	ADOPT Fuel Results – HAC Package Array, Rod Pipe	6-109
Table 6-95	Benchmark Experiment Summary	6-112
Table 6-96	Parameter Correlation Coefficient Results.....	6-112
Table 6-97	Categorized Fuel Assemblies for Input into Package Assessment.....	6-116
Table 6-98	Categorized Fuel Assemblies for Input into Package Assessment.....	6-117
Table 6-99	Categorized Fuel Assemblies for Input into Package Assessment.....	6-117
Table 6-100	Bin Organization Example	6-118
Table 6-101	Fuel Pellet Radius Range Determination	6-119

Table 6-102	Secondary Fuel Assembly Parameter Ranges	6-121
Table 6-103	Effect of Secondary Parameters on k-inf - 14 Bin 1.....	6-123
Table 6-104	Effect of Secondary Parameters on 14 Bin 2.....	6-124
Table 6-105	Effect of Secondary Parameters on 15 Bin 1.....	6-125
Table 6-106	Effect of Secondary Parameters on 15 Bin 2.....	6-126
Table 6-107	Effect of Secondary Parameters on 16 Bin 1.....	6-127
Table 6-108	Effect of Secondary Parameters on 16 Bin 2.....	6-128
Table 6-109	Effect of Secondary Parameters on 16 Bin 3.....	6-129
Table 6-110	Effect of Secondary Parameters on 17 Bin 1.....	6-130
Table 6-111	Effect of Secondary Parameters on 17 Bin 2.....	6-131
Table 6-112	Effect of Secondary Parameters on 18 Bin 1.....	6-132
Table 6-113	Effect of Secondary Parameters on VV Bin 1	6-133
Table 6-114	Single Package, CFA-Package Variant Comparison Results	6-134
Table 6-115	Axial Position Baseline Results – Single Package, NCT, Groups 1 & 2, and Group 3.....	6-135
Table 6-116	Axial Position Baseline Results – Single Package, HAC, Groups 1 & 2, and Group 3	6-136
Table 6-117	Single Package, NCT, Rod Pipe Package Variant Results.....	6-138
Table 6-118	Single Package, HAC, Rod Pipe Fuel OR-Pitch Combination – Maximum Results	6-139
Table 6-119	UO ₂ Single Package, HAC, Rod Pipe Fuel OR-Pitch Combination – Pitch Variation	6-140
Table 6-120	U ₃ Si ₂ Single Package, HAC, Rod Pipe Fuel OR-Pitch Combination – Pitch Variation.....	6-140
Table 6-121	UO ₂ Single Package, HAC, Rod Pipe Fuel OR-Pitch Combination – Refined Parameter Study.....	6-141
Table 6-122	Package Array, NCT, CFA Package Variant Results.....	6-142
Table 6-123	Axial Position Baseline Results –Package Array, NCT, Groups 1, 2, and 3.....	6-143
Table 6-124	Package Array, NCT, Rod Pipe-Package Variant Comparison Results	6-144
Table 6-125	Package Array, HAC, CFA Package Variant Results	6-145
Table 6-126	Axial Position Baseline Results –Package Array, HAC, Groups 1, 2, and 3	6-146
Table 6-127	Partial Flooding Baseline Results – Package Array, HAC, Groups 1, 2, and 3	6-147
Table 6-128	Preferential Flooding Baseline Results – Package Array, HAC, Groups 1, 2, and 3	6-148
Table 6-129	Package Array, HAC, Rod Pipe Fuel OR-Pitch Combination – Maximum Results	6-151
Table 6-130	UO ₂ Package Array, HAC, Rod Pipe Fuel OR-Pitch Combination – Pitch Variation	6-152
Table 6-131	U ₃ Si ₂ Package Array, HAC, Rod Pipe Fuel OR-Pitch Combination – Pitch Variation	6-152
Table 6-132	UO ₂ Package Array, HAC, Rod Pipe Fuel OR-Pitch Combination – Refined Parameter Study	6-153

LIST OF FIGURES

Figure 6-1	Cross Section of the Flux Trap System for STD/XL (Left) and VVER (Right).....	6-2
Figure 6-2	Group 1 Fuel Rod Patterns. Not to Scale.	6-8
Figure 6-3	Group 1 Fuel Rod Patterns. Not to Scale.	6-8
Figure 6-4	Group 1 Fuel Rod Patterns. Not to Scale.	6-8
Figure 6-5	Group 2 Fuel Rod Patterns. Not to Scale.	6-9
Figure 6-6	Group 3 Fuel Rod Pattern. Not to Scale.	6-10
Figure 6-7	Front Cross-Sections of the Traveller STD/XL (Left) and VVER (Right)	6-14
Figure 6-8	Top to bottom: Side Cross-Sections of the Traveller STD, XL, and VVER.....	6-14
Figure 6-9	Top to bottom: Top Moderator Block Cross-Sections of the Traveller STD, XL, and VVER	6-15
Figure 6-10	Side Cross Section of the Traveller Showing Fuel Assembly Axial Position Study.....	6-26
Figure 6-11	Cutaway of Traveller XL with 17 Bin 2 Showing the Lattice Pitch Expansion Section.....	6-26
Figure 6-12	The Six Groups 1, 2, and 3 Flooding Configurations.....	6-27
Figure 6-13	Rod Pipe, UO ₂ Fuel Array Modeling in Rod Pipe	6-29
Figure 6-14	Rod Pipe, U ₃ Si ₂ NCT Case (left) and Two HAC Cases (right).....	6-30
Figure 6-15	NCT Single Package Baseline Case vs. Fuel Assembly Shift.....	6-32
Figure 6-16	HAC Package Array Baseline Case vs. Clamshell and Fuel Assembly Shift	6-33
Figure 6-17	PWR Fuel Assembly Polyethylene Outer Wrap NCT Configuration	6-34
Figure 6-18	PWR Fuel Assembly Polyethylene Outer Wrap HAC Configurations	6-34
Figure 6-19	Uniform Polyethylene Melt HAC Configuration – PWR Fuel Assemblies	6-35
Figure 6-20	Uniform Polyethylene Wrap NCT/HAC Configuration – Rod Pipe	6-35
Figure 6-21	PWR Fuel Assembly Collected Polyethylene Melt Configuration	6-36
Figure 6-22	Rod Pipe Collected Polyethylene Melt Configuration	6-36
Figure 6-23	Corner Rod Displacement Configurations – 17 Bin 1 (top), VV Bin 1 (bottom).....	6-37
Figure 6-24	Random Rod Displacement Configurations – 17 Bin 1 (top), VV Bin 1 (bottom)	6-37
Figure 6-25	SS Replacement Rod Configurations – 17 Bin 1 (left) and VV Bin 1 (right)	6-38
Figure 6-26	Example of NCT Stainless Steel Nozzle Configuration, Shown in Green	6-40
Figure 6-27	Example of HAC Stainless Steel Nozzle Configuration, Shown in Green	6-41
Figure 6-28	Rod Pipe HAC Package Array Flooding Configurations	6-41
Figure 6-29	Cross-section NCT Single Package Baseline Case	6-44
Figure 6-30	Cross-section HAC Single Package Baseline Case.....	6-44
Figure 6-31	Annular Blanket Sensitivity – Single Package, NCT (Groups 1 & 2).....	6-48
Figure 6-32	Annular Blanket Sensitivity – Single Package, NCT (Group 3)	6-49
Figure 6-33	Annular Blanket Sensitivity Results – Single Package, HAC (Groups 1 & 2).....	6-53
Figure 6-34	Annular Blanket Sensitivity Results – Single Package, HAC (Group 3).....	6-53
Figure 6-35	Polyethylene Sensitivity Results – Single Package, HAC (Groups 1 & 2)	6-55
Figure 6-36	Polyethylene Sensitivity Results – Single Package, HAC (Group 3).....	6-55
Figure 6-37	Axial Rod Displacement Sensitivity Results – Single Package, HAC (Groups 1 & 2).....	6-56
Figure 6-38	Axial Rod Displacement Sensitivity Results – Single Package, HAC (Group 3)	6-57
Figure 6-39	Annular Blanket Sensitivity – Single Package, NCT (Rod Pipe UO ₂ Fuel Rods)	6-61
Figure 6-40	Annular Blanket Sensitivity – Single Package, NCT (Rod Pipe U ₃ Si ₂ Fuel Rods).....	6-61
Figure 6-41	Polyethylene Packing Sensitivity – Single Package, NCT (Rod Pipe UO ₂ Fuel Rods)	6-62
Figure 6-42	Polyethylene Packing Sensitivity – Single Package, NCT (Rod Pipe U ₃ Si ₂ Fuel Rods).....	6-63
Figure 6-43	Annular Blanket Sensitivity Results – Single Package, HAC (Rod Pipe UO ₂ Fuel Rods)	6-65
Figure 6-44	Annular Blanket Sensitivity Results – Single Package, HAC (Rod Pipe U ₃ Si ₂ Fuel Rods).....	6-65
Figure 6-45	Polyethylene Sensitivity Results – Single Package, HAC (Rod Pipe UO ₂ Fuel Rods)	6-68
Figure 6-46	Polyethylene Sensitivity Results – Single Package, HAC (Rod Pipe U ₃ Si ₂ Fuel Rods)	6-68
Figure 6-47	Group 1, NCT 250-package Array with Height of Two Packages.....	6-71
Figure 6-48	Group 2 NCT 60-package Array with Height of One Package.....	6-71
Figure 6-49	Group 3 NCT 250-package Array with Height of One Package	6-72
Figure 6-50	Rod Pipe NCT 379-package Array with Height of One Package	6-73
Figure 6-51	Annular Blanket Sensitivity – Package Array, NCT (Group 1)	6-76
Figure 6-52	Annular Blanket Sensitivity – Package Array, NCT (Group 2)	6-76
Figure 6-53	Annular Blanket Sensitivity – Package Array, NCT (Group 3)	6-77
Figure 6-54	Annular Blanket Sensitivity – Package Array, NCT (Rod Pipe UO ₂ Fuel Rods)	6-82

Figure 6-55	Annular Blanket Sensitivity – Package Array, NCT (Rod Pipe U ₃ Si ₂ Fuel Rods).....	6-83
Figure 6-56	Polyethylene Packing Sensitivity – Package Array, NCT (Rod Pipe UO ₂ Fuel Rods)	6-84
Figure 6-57	Polyethylene Packing Sensitivity – Package Array, NCT (Rod Pipe U ₃ Si ₂ Fuel Rods).....	6-85
Figure 6-58	Group 1, HAC 100-package Array.....	6-87
Figure 6-59	Group 2, HAC 24-package Array.....	6-87
Figure 6-60	Group 3, HAC 100-package Array.....	6-88
Figure 6-61	Rod Pipe, HAC 150-package Array	6-89
Figure 6-62	Annular Blanket Sensitivity – HAC Package Array (Group 1).....	6-93
Figure 6-63	Annular Blanket Sensitivity – HAC Package Array (Group 2).....	6-93
Figure 6-64	Annular Blanket Sensitivity – HAC Package Array (Group 3).....	6-94
Figure 6-65	Polyethylene Sensitivity Results – HAC Package Array (Group 1).....	6-97
Figure 6-66	Polyethylene Sensitivity Results – HAC Package Array (Group 2).....	6-97
Figure 6-67	Polyethylene Sensitivity Results – HAC Package Array (Group 3).....	6-97
Figure 6-68	Axial Rod Displacement Sensitivity Results – HAC Package Array (Group 1)	6-99
Figure 6-69	Axial Rod Displacement Sensitivity Results – HAC Package Array (Group 2)	6-99
Figure 6-70	Axial Rod Displacement Sensitivity Results – HAC Package Array (Group 3)	6-99
Figure 6-71	Annular Blanket Sensitivity – HAC Package Array (Rod Pipe UO ₂ Fuel Rods).....	6-104
Figure 6-72	Annular Blanket Sensitivity – HAC Package Array (Rod Pipe U ₃ Si ₂ Fuel Rods)	6-104
Figure 6-73	Polyethylene Sensitivity Results – HAC Package Array (Rod Pipe UO ₂ Fuel Rods).....	6-107
Figure 6-74	Polyethylene Sensitivity Results – HAC Package Array (Rod Pipe U ₃ Si ₂ Fuel Rods)	6-107
Figure 6-75	Flooding Configuration Sensitivity Results – HAC Package Array (Rod Pipe UO ₂ Fuel Rods).....	6-109
Figure 6-76	Flooding Configuration Sensitivity Results – HAC Package Array (Rod Pipe U ₃ Si ₂ Fuel Rods)	6-109
Figure 6-77	EALF USLSTATS Plot.....	6-113
Figure 6-78	Fuel Rod Patterns of 16 Bin 1 (left) and 16 Bin 2 (right) – Not to Scale	6-118
Figure 6-79	x-y (left) and x-z (right) Cross Sections of a Fuel Assembly Permutation. Not to Scale	6-120
Figure 6-80	Trend Plot of Effect of Secondary Parameters on k-inf – 14 Bin 1	6-123
Figure 6-81	Trend Plot of Effect of Secondary Parameters on k-inf – 14 Bin 2.....	6-124
Figure 6-82	Trend Plot of Effect of Secondary Parameters on k-inf – 15 Bin 1	6-125
Figure 6-83	Trend Plot of Effect of Secondary Parameters on k-inf – 15 Bin 2.....	6-126
Figure 6-84	Trend Plot of Effect of Secondary Parameters on k-inf – 16 Bin 1.....	6-127
Figure 6-85	Trend Plot of Effect of Secondary Parameters on k-inf – 16 Bin 2.....	6-128
Figure 6-86	Trend Plot of Effect of Secondary Parameters on k-inf – 16 Bin 3.....	6-129
Figure 6-87	Trend Plot of Effect of Secondary Parameters on k-inf – 17 Bin 1.....	6-130
Figure 6-88	Trend Plot of Effect of Secondary Parameters on k-inf – 17 Bin 2.....	6-131
Figure 6-89	Trend Plot of Effect of Secondary Parameters on k-inf – 18 Bin 1.....	6-132
Figure 6-90	Trend Plot of Effect of Secondary Parameters on k-inf – VV Bin 1	6-133
Figure 6-91	Axial Position Baseline Results – Single Package, NCT, Groups 1 & 2 (Left) and Group 3 (Right) ..	6-137
Figure 6-92	Axial Position Baseline Results – Single Package, HAC, Groups 1 & 2 (Left) and Group 3 (Right) .	6-137
Figure 6-93	Effect of Preferential Flooding Configuration on k _{eff} (Group 1).....	6-149
Figure 6-94	Effect of Preferential Flooding Configuration on k _{eff} (Group 2).....	6-150
Figure 6-95	Effect of Preferential Flooding Configuration on k _{eff} (Group 3).....	6-150

6.0 CRITICALITY EVALUATION

6.1 DESCRIPTION OF CRITICALITY DESIGN

A comprehensive description of the Traveller packaging is provided in Section 1. This section provides a description of the package (i.e. packaging and contents) that is sufficient for understanding the features of the Traveller that maintain criticality safety.

6.1.1 Design Features

The Traveller shipping package carries a single pressurized water reactor (PWR) fuel assembly or a single Rod Pipe that holds PWR and/or boiling water reactor (BWR) fuel rods. The Traveller is made up of two basic components: 1) an Outerpack and 2) a Clamshell that is a separate inner shell designed to support the contents. The Outerpack is a long cylindrical design consisting of a top and bottom half hinged together. Each half consists of a stainless steel (SS) outer shell, a layer of rigid polyurethane foam, and an inner SS shell. The inside of the Outerpack is lined with polyethylene moderator blocks. The neutron-moderating ultra-high molecular weight (UHMW) polyethylene moderator blocks are affixed to the upper and lower halves of the Outerpack. See Section 1.2 for additional features of the Traveller beyond criticality safety.

The Clamshell structural components consist of an aluminum base, two aluminum panel doors hinged to the base, a small top access door, and bottom and top end plates. BORAL® neutron absorber plates are located in each axial side of the Clamshell. For the Traveller STD and XL variants, the Clamshell is a rectangular aluminum box that completely encloses the contents and is mounted in the Outerpack with rubber shock mounts. For the Traveller VVER variant, the VVER Clamshell is a hexagonal aluminum box that completely encloses the contents and is mounted in the Outerpack with a bolted bracket on shock mounts. Both Clamshell configurations are designed such that they retain their original dimensions when subjected to the HAC tests. Figure 6-1 displays a cross-section view of the package criticality models.

The criticality model configurations are defined in Section 6.3. Details include conditions of transport and properties of materials of construction and moderating materials.

6.1.1.1 Confinement System

The *confinement system* for the Traveller consists of the fuel rods, the fuel assembly or Rod Pipe, the Clamshell assembly including the neutron absorber plates, and the Outerpack. These structural components are intended to maintain criticality safety of the package. The Clamshell assembly for all transport scenarios maintains confinement of the contents.

6.1.1.2 Flux Traps

The Traveller package features a unique flux trap system that does not require an accident condition (i.e. flooding) in order to function. The flux trap system reduces neutron communication between packages in an array. This system features BORAL neutron absorber plates located in each axial side of the Clamshell that act in conjunction with UHMW polyethylene moderator blocks, which are affixed to the walls of the Outerpack inner cavity. The BORAL plates have a minimum ^{10}B areal density of []^{a,c}. Neutrons leaving

one package must past through two regions of moderator blocks and then BORAL neutron absorber plates before reaching the contents of another package. In addition, the structural materials of the Traveller for which credit is taken in the criticality safety analysis provide additional neutron absorption. Any flooding enhances the performance of the flux trap in a package array. Figure 6-1 shows the flux trap in a single Traveller XL and Traveller VVER package. The Traveller STD has a smaller Clamshell configuration than the Traveller XL and the Traveller VVER has a hexagonal Clamshell.

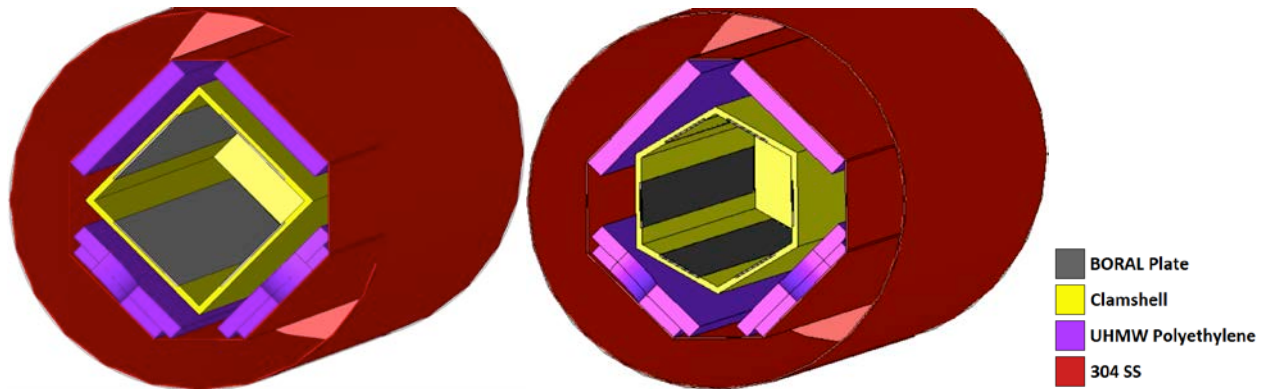


Figure 6-1 Cross Section of the Flux Trap System for STD/XL (Left) and VVER (Right)

6.1.2 Summary Table of Criticality Evaluation

The following analyses demonstrate that the Traveller complies fully with the requirements of 10 CFR 71 [1] and SSR-6 [2]. The nuclear criticality safety requirements for Type A, fissile material packages are satisfied for single package and array configurations under normal conditions of transport (NCT) and hypothetical accident conditions (HAC). A criticality safety evaluation was completed for the four package transport arrangements, including the Traveller STD, XL, and VVER packaging variants, and the contents consisting of three separate PWR fuel assembly Groups and loose rod contents in the Rod Pipe.

Allowance for sensitivity studies includes the following: material and fabrication tolerances and geometric or material representations of transport conditions, such as package testing conclusions. The parameter variation is quantified by direct perturbation methodology: evaluation by varying a parameter from the baseline case.

The sensitivity studies examine parameters independently of one another, i.e., each sensitivity study uses the baseline case as the starting or comparison point. A sensitivity study case is determined to have a more reactive result (i.e. penalizing) only if the case's increase in $k_{eff} + 2\sigma$ is greater than or equal to 2σ (i.e. statistically significant) from the baseline case ($k_{eff} + 2\sigma$) analyzed. The difference in $k_{eff} + 2\sigma$ from the baseline case value is tallied and summed for all parameters with a positive impact on neutron multiplication (Δk_u). No action is taken for sensitivity studies or parameter variations that result in a reduction in k_{eff} or statistically insignificant result (i.e. less than 2σ difference from the baseline case).

The maximum multiplication factor (*Maximum k_{eff}*) is used to summarize the limiting value for the contents and transport condition and used to demonstrate that criteria to establish subcriticality are satisfied. *Maximum k_{eff}* is the calculated multiplication factor k_{eff} (k_p) of the configuration plus the statistical uncertainty for k_p as 2 times the standard deviation (σ_p) for the calculation method plus the total summation of the parametric variations (Δk_u), as shown in the following equation:

$$\text{Maximum } k_{eff} = k_p + 2\sigma_p + \Delta k_u$$

Using the upper subcritical limit 1 (USL1) function presented in Section 6.8.2, the following USLs presented in Table 6-1 were calculated for each package arrangement using the energy of average lethargy causing fission (EALF) of each Group’s baseline case and an administrative margin (Δk_m) of 0.05. The *Maximum k_{eff}* for each package arrangement is listed in Table 6-2, Summary Table of the Criticality Evaluation.

Contents	Limiting EALF (eV)	Bias and Uncertainty ($\beta - \Delta\beta$)	USL ($1 - \Delta k_m + \beta - \Delta\beta$)
Groups 1 and 2 (Single)	0.294655	-0.00933	0.94067
Group 1 (Array)	0.195762	-0.00838	0.94162
Group 2 (Array)	0.270923	-0.00910	0.94090
Group 3 (Single and Array)	0.335131	-0.00971	0.94029
Rod Pipe UO ₂ Fuel Rods (Single and Array)	0.319064	-0.00956	0.94044
Rod Pipe U ₃ Si ₂ Fuel Rods (Single and Array)	0.310042	-0.00947	0.94053

6.1.2.1 Contents Grouping

PWR fuel assemblies are organized with similar fuel assemblies into defined bins. Three Groups define the allowable fuel assembly contents, with each Group containing like bins. The bounding parameters of the fuel assembly contents in a bin are represented by categorized fuel assemblies (CFA), for the criticality analyses. The Group 1 configuration is applicable to the Traveller STD and XL variants with square-pitch PWR fuel assemblies. The Group 2 configuration is applicable to only the Traveller XL variant with square-pitch PWR fuel assemblies. The Group 3 configuration is applicable to the Traveller VVER variant with hexagonal-pitch PWR fuel assemblies. The Rod Pipe configuration is applicable to the Traveller STD and/or XL variants, as defined by fuel rod content. This configuration allows for the shipment of loose PWR or BWR fuel rods in a Rod Pipe located inside the Clamshell. These restrictions are detailed in Section 6.2. For all contents listed in Table 6-2, *Maximum k_{eff}* is less than its respective USL.

Enrichment	Content	Limiting CFA / Fuel Parameters	Condition of Transport	Array Size	Maximum k_{eff}	Reference
5 wt.% ²³⁵ U	Groups 1 and 2 (Single)	18 Bin 1	NCT	--	0.92151	Table 6-26
		17 Bin 1	HAC		0.92087	
	Group 1 (Array)	17 Bin 2	NCT	5N = 250	0.30942	Table 6-55
		17 Bin 1	HAC	2N = 100	0.93783	Table 6-75
	Group 2 (Array)	16 Bin 1	NCT	5N = 60	0.31379	Table 6-55
		18 Bin 1	HAC	2N = 24	0.93945	Table 6-75
	Group 3 (Single)	VV Bin 1	NCT	--	0.88932	Table 6-26
			HAC		0.90028	
	Group 3 (Array)		NCT	5N = 250	0.39042	Table 6-55
			HAC	2N = 100	0.93064	Table 6-75
7 wt.% ²³⁵ U	Rod Pipe UO ₂ Fuel Rods (Single)	Fuel OR = 3.5 cm Fuel Half-Pitch = 3.5 cm	NCT	--	0.63579	Table 6-26
		Fuel OR = 0.55 cm Fuel Half-Pitch = 1.0 cm	HAC		0.79577	
	Rod Pipe UO ₂ Fuel Rods (Array)	Fuel OR = 3.5 cm Fuel Half-Pitch = 3.5 cm	NCT	5N = 379	0.59478	Table 6-55
		Fuel OR = 0.50 cm Fuel Half-Pitch = 1.0 cm	HAC	2N = 150	0.81588	Table 6-75
5 wt.% ²³⁵ U	Rod Pipe U ₃ Si ₂ Fuel Rods (Single)	Fuel OR = 0.4851 cm Fuel Half-Pitch = 0.4851 cm	NCT	--	0.72879	Table 6-26
		Fuel OR = 0.4851 cm Fuel Half-Pitch = 1.0101 cm	HAC		0.73961	
	Rod Pipe U ₃ Si ₂ Fuel Rods (Array)	Fuel OR = 0.4851 cm Fuel Half-Pitch = 0.4851 cm	NCT	5N = 379	0.69571	Table 6-55
		Fuel OR = 0.4851 cm Fuel Half-Pitch = 0.9851 cm	HAC	2N = 150	0.76836	Table 6-75

6.1.3 Criticality Safety Index

The CSI is equivalent to 50/N, rounded up to the nearest tenth. As described in Section 6.2, the contents are distinguished by which contents types are applicable to which variant(s) of the Traveller. The CSI for each package arrangement is listed in Table 6-3.

Content	5N	2N	N	CSI
Group 1	250	100	50	1.0
Group 2	60	24	12	4.2
Group 3	250	100	50	1.0
Rod Pipe	379	150	75	0.7

6.2 FISSILE MATERIAL CONTENTS

The contents consist of either a single PWR fuel assembly or loose fuel rods, as defined in Section 1.2.2, Contents. The UO_2 or U_3Si_2 fuel is modeled as a continuous rod, with no credit taken for dishing or chamfering on pellets, and with a maximum active fuel length defined by the respective bin. The organization of similar fuel assemblies into defined bins is described in Section 6.3.4. The UO_2 is modeled at theoretical density (10.96 g/cm^3) with the uranium modeled at the maximum permissible enrichment for the respective case (i.e. 5 wt.% or 7 wt.% ^{235}U) and the remaining uranium modeled as ^{238}U . For UO_2 contents, PWR fuel assemblies are limited to an enrichment of 5 wt.% ^{235}U and loose fuel rods are limited to an enrichment of 7 wt.% ^{235}U . Additionally, UO_2 contents in the form of loose fuel rods or fuel assemblies under PWR Group 1 or Group 2 may be ADOPT rods, doped with up to 700 ppm Cr_2O_3 and up to 200 ppm Al_2O_3 . The U_3Si_2 is modeled at theoretical density (12.2 g/cm^3) with the uranium modeled as 5 wt.% ^{235}U and the remaining uranium modeled as ^{238}U . For further material properties, see Section 6.3.2. Non-fissile, non-radioactive core components can be shipped with a PWR fuel assembly. There are also no restrictions on guide tubes and instrument tubes within a PWR fuel assembly.

Three Groups define the allowable fuel assembly contents, with each Group containing like bins. Table 6-4 shows the breakdown of the bins in each of the three Groups. The fourth content defines the loose fuel rods. English units are the design requirement for the content dimensions; hence, the conversion to SI units, which is required for modeling, is rounded.

Group 1		Group 2	Group 3
<ul style="list-style-type: none"> • 14 Bin 1 • 14 Bin 2 • 15 Bin 1 • 15 Bin 2 	<ul style="list-style-type: none"> • 16 Bin 2 • 16 Bin 3 • 17 Bin 1 • 17 Bin 2 	<ul style="list-style-type: none"> • 16 Bin 1 • 18 Bin 1 	<ul style="list-style-type: none"> • VV Bin 1

6.2.1 Group 1

The applicable parameters and fuel rod patterns for each bin in Group 1 are specified in Table 6-5 through Table 6-7 and Figure 6-2 through Figure 6-4. For any fuel assembly that meets the specification of a given bin, the most limiting configuration has been analyzed, as demonstrated in Section 6.3.4.

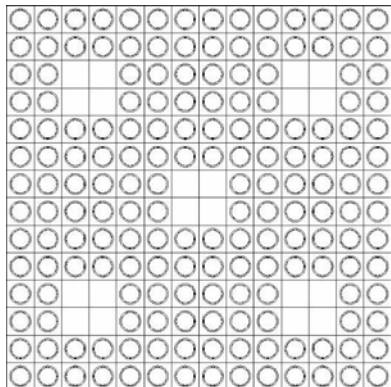
The following restrictions apply to all Group 1 bins:

- (1) All fuel must consist of only UO₂. Fuel rods in any location of the assembly may include ADOPT UO₂ pellets that are doped with up to 700 ppm Cr₂O₃ and up to 200 ppm Al₂O₃ (i.e. ADOPT rods).
- (2) For each parameter, the listed tolerance limit applies to all bins included in the table. For maximum parameters, only the positive tolerance is limited and for minimum parameters, only the negative tolerance is limited.
- (3) All rod cladding must be composed of a zirconium alloy. Cladding may include a chromium coating of 25 μm thick, nominally or include an Optimized ZIRLO Liner (OZL).
- (4) There is no restriction on the length of top and bottom annular blankets. The annular fuel pellet inner diameter in the blanket region must be ≥ 0.155 in. and ≤ 0.183 in. (≥ 0.3937 cm and ≤ 0.4648 cm).
- (5) Any quantity of stainless steel replacement rods is allowed in the fuel assembly.
- (6) Polyethylene packing materials are limited to 2.00 kg in the Clamshell and shall not have a hydrogen density greater than 0.1325 g/cm³.

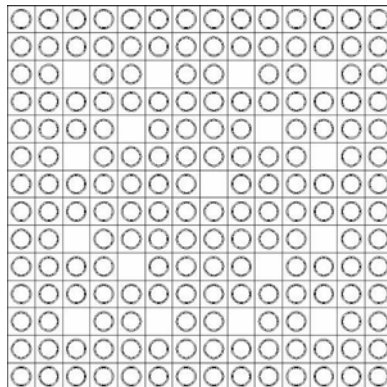
Description	Tolerance Limit	14 Bin 1	14 Bin 2	15 Bin 1
Array Size	-	14x14	14x14	15x15
Fuel Rods	-	176	179	204
Non-Fuel Holes	-	20	17	21
Nominal Pitch (in./cm)	+0.0050 (+0.0127)	0.580 (1.4732)	0.556 (1.4122)	0.563 (1.4300)
Minimum Fuel Pellet Outer Diameter (in./cm)	-0.0007 (-0.0018)	0.3805 (0.9665)	0.3439 (0.8735)	0.3582 (0.9097)
Minimum Cladding Inner Diameter (in./cm)	-0.0020 (-0.0051)	0.3855 (0.9792)	0.3489 (0.8862)	0.3636 (0.9237)
Minimum Cladding Thickness (in./cm)	-0.0020 (-0.0051)	0.0245 (0.0622)	0.0228 (0.0579)	0.0228 (0.0579)
Maximum Active Fuel Length (in./cm)	+0.50 (+1.27)	136.70 (347.22)	144.00 (365.76)	144.00 (365.76)

Description	Tolerance Limit	15 Bin 2
Array Size	-	15x15
Fuel Rods	-	205
Non-Fuel Holes	-	20
Nominal Pitch (in./cm)	+0.0118 (+0.03)	0.5630 (1.4300)
Minimum Fuel Pellet OD (in./cm)	-0.0007 (-0.0018)	0.3580 (0.9092)
Minimum Cladding ID (in./cm)	-0.002 (-0.0051)	0.3627 (0.9214)
Minimum Cladding Thickness (in./cm)	-0.002 (-0.0051)	0.0265 (0.0674)
Maximum Active Fuel Length (in./cm)	+0.50 (+1.27)	139.76 (355.00)

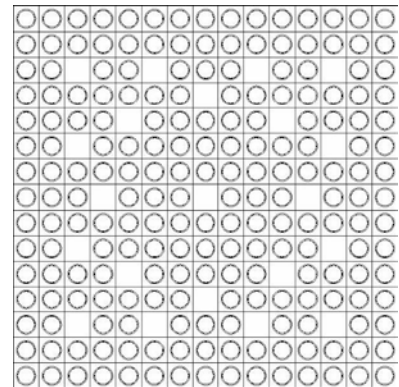
Description	Tolerance Limit	16 Bin 2	16 Bin 3	17 Bin 1	17 Bin 2
Array Size	-	16x16	16x16	17x17	17x17
Fuel Rods	-	236	235	264	264
Non-Fuel Holes	-	20	21	25	25
Nominal Pitch (in./cm)	+0.0050 (+0.0127)	0.506 (1.2852)	0.485 (1.2319)	0.496 (1.2598)	0.502 (1.2751)
Minimum Fuel Pellet OD (in./cm)	-0.0007 (-0.0018)	0.3220 (0.8179)	0.3083 (0.7831)	0.3083 (0.7831)	0.3238 (0.8225)
Minimum Cladding ID (in./cm)	-0.002 (-0.0051)	0.3265 (0.8293)	0.3125 (0.7938)	0.3125 (0.7938)	0.3276 (0.8321)
Minimum Cladding Thickness (in./cm)	-0.002 (-0.0051)	0.0210 (0.0533)	0.0210 (0.0533)	0.0210 (0.0533)	0.0220 (0.0559)
Maximum Active Fuel Length (in./cm)	+0.50 (+1.27)	150.00 (381.00)	144.00 (365.76)	168.00 (426.72)	144.00 (365.76)



14 Bin 1

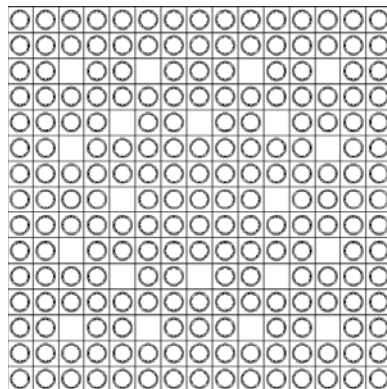


14 Bin 2



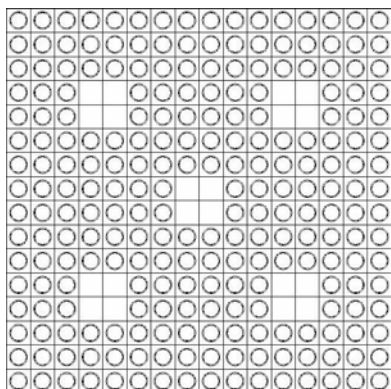
15 Bin 1

Figure 6-2 Group 1 Fuel Rod Patterns. Not to Scale.

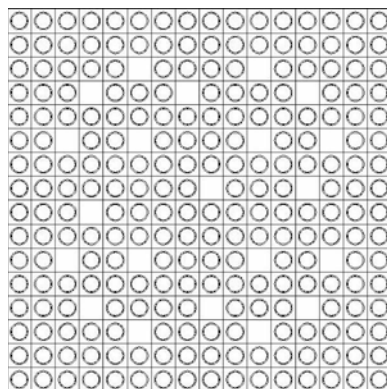


15 Bin 2

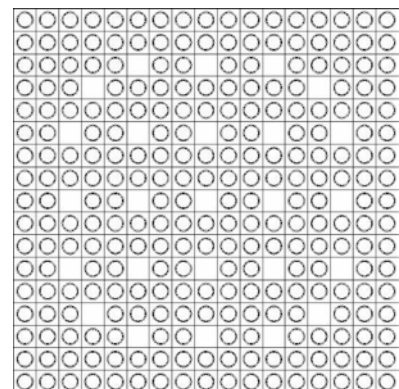
Figure 6-3 Group 1 Fuel Rod Patterns. Not to Scale.



16 Bin 2



16 Bin 3



17 Bin 1 / Bin 2

Figure 6-4 Group 1 Fuel Rod Patterns. Not to Scale.

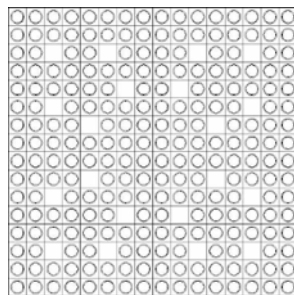
6.2.2 Group 2

The applicable parameters and fuel rod patterns for each bin in Group 2 are specified in Table 6-8 and Figure 6-5. For any fuel assembly that meets the specification of a given bin, the most limiting configuration has been analyzed, as demonstrated in Section 6.3.4.

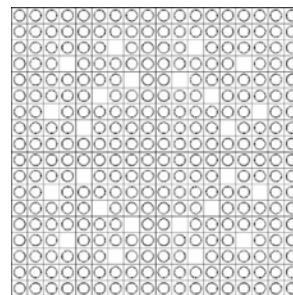
The following restrictions apply to all Group 2 bins:

- (1) All fuel must consist of only UO₂. Fuel rods in any location of the assembly may include ADOPT UO₂ pellets that are doped with up to 700 ppm Cr₂O₃ and up to 200 ppm Al₂O₃.
- (2) For each parameter, the listed tolerance limit applies to all bins included in the table. For maximum parameters, only the positive tolerance is limited and for minimum parameters, only the negative tolerance is limited.
- (3) All rod cladding must be composed of a zirconium alloy. Cladding may include a chromium coating of 25 µm thick, nominally or include an Optimized ZIRLO Liner.
- (4) The length of top and bottom annular blankets is limited to 20.0 in. (50.8 cm). The annular fuel pellet inner diameter in the blanket region must be ≥0.155 in. and ≤0.183 in. (≥0.3937 cm and ≤0.4648 cm).
- (5) Any quantity of stainless steel replacement rods is allowed in the fuel assembly.
- (6) Polyethylene packing materials are limited to 2.00 kg in the Clamshell and shall not have a hydrogen density greater than 0.1325 g/cm³.

Description	Tolerance Limit	16 Bin 1	18 Bin 1
Array Size	-	16x16	18x18
Fuel Rods	-	236	300
Non-Fuel Holes	-	20	24
Nominal Pitch (in./cm)	+0.0118 (+0.03)	0.563 (1.430)	0.500 (1.270)
Minimum Fuel Pellet OD (in./cm)	-0.0007 (-0.0018)	0.3581 (0.9097)	0.3165 (0.8039)
Minimum Cladding ID (in./cm)	-0.002 (-0.0051)	0.3665 (0.9310)	0.3236 (0.8220)
Minimum Cladding Thickness (in./cm)	-0.002 (-0.0051)	0.0283 (0.0720)	0.0252 (0.0640)
Maximum Active Fuel Length (in./cm)	+0.50 (+1.27)	153.54 (390.00)	153.54 (390.00)



16 Bin 1



18 Bin 1

Figure 6-5 Group 2 Fuel Rod Patterns. Not to Scale.

6.2.3 Group 3

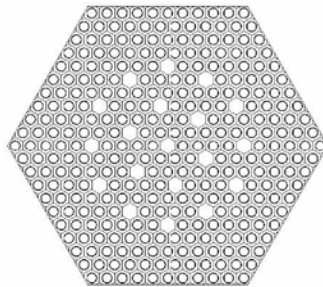
The applicable parameters and fuel rod pattern for the only bin of Group 3 is specified in Table 6-9 and Figure 6-6. For any fuel assembly that meets the specification of the given bin, the most limiting configuration has been analyzed, as demonstrated in Section 6.3.4.

The following restrictions apply to the Group 3 bin:

- (1) All fuel must consist of only UO₂.
- (2) For each parameter, the listed tolerance limit applies to all bins included in the table. For maximum parameters, only the positive tolerance is limited and for minimum parameters, only the negative tolerance is limited.
- (3) All rod cladding must be composed of a zirconium alloy. Cladding may include a chromium coating of 25 µm thick, nominally or include an Optimized ZIRLO Liner.
- (4) The length of top and bottom annular blankets is limited to 20.0 in. (50.8 cm). The annular fuel pellet inner diameter in the blanket region must be ≥0.155 in. and ≤0.183 in. (≥0.3937 cm and ≤0.4648 cm).
- (5) Any quantity of stainless steel replacement rods is allowed in the fuel assembly.
- (6) Polyethylene packing materials are limited to 2.00 kg in the Clamshell and shall not have a hydrogen density greater than 0.1325 g/cm³.

Table 6-9 Group 3 Fuel Assembly Bin		
Description	Tolerance Limit	VV Bin 1
Array Size	-	11x21 ^a
Fuel Rods	-	312
Non-Fuel Holes	-	19
Nominal Pitch (in./cm)	+0.001 (+0.003)	0.502 (1.2751)
Minimum Fuel Pellet OD (in./cm)	-0.0005 (-0.0013)	0.3083 (0.7831)
Minimum Cladding ID (in./cm)	-0.0015 (-0.0051)	0.3125 (0.7938)
Minimum Cladding Thickness (in./cm)	-0.0015 (-0.0051)	0.0210 (0.0533)
Maximum Active Fuel Length (in./cm)	+0.50 (+1.27)	143.70 (365.00)

Note: ^a (shortest row) x (longest row).



VV Bin 1

Figure 6-6 Group 3 Fuel Rod Pattern. Not to Scale.

6.2.4 Rod Pipe

The Rod Pipe contents category is only applicable to loose PWR or BWR fuel rod contents in the Rod Pipe. This category has the following restrictions for either UO_2 or U_3Si_2 fuel rods:

- (1) For UO_2 Fuel Rods,
 - a. Loose fuel rods may include ADOPT UO_2 pellets that are doped with up to 700 ppm Cr_2O_3 and up to 200 ppm Al_2O_3 .
 - b. Can only be shipped in the Traveller STD or XL Rod Pipe configuration.
 - c. Maximum uranium enrichment of 7.0 wt.% ^{235}U .
 - d. Fuel pellet diameter must be ≥ 0.308 in. (≥ 0.7823 cm).
 - e. Maximum stack length equivalent to the Rod Pipe inner length.
 - f. Maximum number of rods per Rod Pipe: up to Rod Pipe capacity.
 - g. All rod cladding must be composed of a zirconium alloy. Cladding may include a chromium coating of 25 μm thick, nominally or include an Optimized ZIRLO Liner.
 - h. Integral absorbers are allowed, including, but not limited to, gadolinia, erbia, boron, and hafnium.
 - i. No limit on annular fuel pellet blanket length. The annular fuel pellet inner diameter in the blanket region must be ≥ 0.155 in. and ≤ 0.183 in. (≥ 0.3937 cm and ≤ 0.4648 cm). For annular IDs > 0.183 in. (0.4648 cm), the annular ID must be equivalent to no more than 44% of the fuel pellet OD. Wrapping, sleeving, or packing materials inside the Rod Pipe shall not have a hydrogen density greater than 0.1325 g/cm³. There is no limit on the mass of packing materials in the Rod Pipe.
- (2) For U_3Si_2 Fuel Rods,
 - a. Can only be shipped in the Traveller STD Rod Pipe configuration.
 - b. Maximum uranium enrichment: 5.0 wt.% ^{235}U .
 - c. Maximum number of rods in the Rod Pipe: 60 rods.
 - d. Fuel pellet diameter must be ≥ 0.3078 in. and ≤ 0.3820 in. (≥ 0.7818 cm and ≤ 0.9703 cm).
 - e. Maximum stack length equivalent to the Rod Pipe inner length.
 - f. All rod cladding must be composed of a zirconium alloy. Cladding may include a chromium coating of 25 μm thick, nominally or include an Optimized ZIRLO Liner.
 - g. Integral absorbers are allowed, including, but not limited to, gadolinia, erbia, boron, and hafnium.
 - h. No limit on annular fuel pellet blanket length. The annular fuel pellet inner diameter in the blanket region must be ≥ 0.155 in. and ≤ 0.183 in. (≥ 0.3937 cm and ≤ 0.4648 cm).
 - i. Wrapping, sleeving, or packing materials inside the Rod Pipe shall not have a hydrogen density greater than 0.1325 g/cm³. There is no limit on the mass of packing materials in the Rod Pipe.

6.3 GENERAL CONSIDERATIONS

6.3.1 Model Configuration

The Traveller is a long, cylindrical packaging that can carry one PWR fuel assembly or loose PWR and/or BWR fuel rods in a Rod Pipe. The Outerpack of the Traveller is modeled as a single, cylindrical shell made of 12-gauge Type 304 Stainless Steel (SS304) sheet metal. No stacking or handling features are modeled, which reduces the effective spacing between packages in an array. The Outerpack inner shell is also modeled as 12-gauge SS304 sheet metal. These two Outerpack halves modeled are the only steel components for which credit is taken in the three Traveller variant models. Minor package components, including fastening fixtures, bolts, content skeletal materials, etc., are not modeled. Thus, no credit is taken for the absorption and reflection provided by these components in the criticality evaluation.

For all three Traveller variant models, the Outerpack inner cavity contains the UHMW moderator blocks and the Clamshell, which houses the fuel assembly or Rod Pipe. The Clamshell has grooves along the length of the inner walls that contain the BORAL neutron absorber plates. The positioning of the Clamshell in the inner cavity with respect to the moderator blocks is shown in Figure 6-7. As shown in Figure 6-8, the UHMW moderator blocks are modeled as the same length as the Clamshell even though they are physically longer than the Clamshell. This assumption is bounding by restricting the effective length of the flux trap. Moderator blocks have cutouts for the shock mounts, which provide shock absorption for the Clamshell in order to prevent damage to the contents during routine transport. The shock mount materials are not modeled in this analysis, however modeling the cutouts removes UHMW polyethylene and allows for increased neutron cross talk between packages in an array. The shock mount cutout configurations, as specified by the licensing drawing, are modeled as shown in Figure 6-9. In addition, the centering of the Clamshell in the Outerpack inner cavity provided by the shock mounts is credited. The major dimensions of each packaging variant's model are listed in Table 6-10. English units are the design requirement for the Traveller variant dimensions; hence the conversion to SI units, which is required for modeling, is rounded.

Component	Dimension	Traveller Variant		
		STD in. (cm)	XL in. (cm)	VVER in. (cm)
Outerpack	Overall Length	195.87 (497.5098)	224.87 (571.1698)	224.86 (571.1444)
	Diameter	25.0 (63.50)	25.0 (63.50)	25.0 (63.50)
	Outer Shell Thickness	0.1046 (0.2657)	0.1046 (0.2657)	0.1046 (0.2657)
	Inner Shell Thickness	0.1046 (0.2657)	0.1406 (0.2657)	0.1406 (0.2657)
	Top Pillow Length	8.21 (20.8534)	8.21 (20.8534)	8.32 (21.1328)
	Bottom Pillow Length	8.21 (20.8534)	8.21 (20.8534)	8.21 (20.8534)
	Cavity Height	18.28 (46.4312)	18.26 (46.3804)	18.26 (46.3804)
	Cavity Width	17.0 (43.18)	17.0 (43.18)	17.0 (43.18)
	Cavity Length	179.45 (455.803)	208.45 (529.463)	208.33 (529.1582)
Moderator Blocks	Upper Block Width	9.48 (24.0792)	9.48 (24.0792)	9.48 (24.0792)
	Upper Block Thickness	1.25 (3.175)	1.25 (3.175)	1.25 (3.175)
	Large Lower Block Width	9.34 (23.7236)	9.34 (23.7236)	9.34 (23.7236)
	Large Lower Block Thickness	1.00 (2.54)	1.00 (2.54)	1.00 (2.54)
	Small Lower Block Width	7.85 (19.939)	7.85 (19.939)	7.85 (19.939)
	Small Lower Block Thickness	0.75 (1.905)	0.75 (1.905)	0.75 (1.905)
Clamshell	Clamshell Length	173.0 (439.42)	202.0 (513.08)	184.0 (467.36)
	Inner width/height ¹	9.12 (23.1648)	9.62 (24.4348)	9.87 (25.0698)
	Wall Thickness	0.288 (0.7135)	0.288 (0.7315)	0.288 (0.7315)
	Top Plate Thickness	1.00 (2.54)	1.00 (2.54)	1.26 (3.2004)
	Bottom Plate Thickness	1.00 (2.54)	1.00 (2.54)	1.50 (3.81)
BORAL Plates	Active Poison Length	168.0 (426.72)	197.0 (500.38)	180.74 (459.0796)
	Width	6.00 (15.24)	6.00 (15.24)	3.00 (7.62)
	Thickness	[]a,c

Note: Dimensions defined by licensing drawings and verified to SolidWorks model; ¹ Dimension modeled includes +1 tolerance

The following model components are shown in Figure 6-7:

- (1) Outerpack shell (SS304)
- (2) Outerpack inner cavity shell (SS304)
- (3) UHMW moderator blocks (polyethylene)
- (4) Clamshell / VVER Clamshell (aluminum)
- (5) BORAL plates

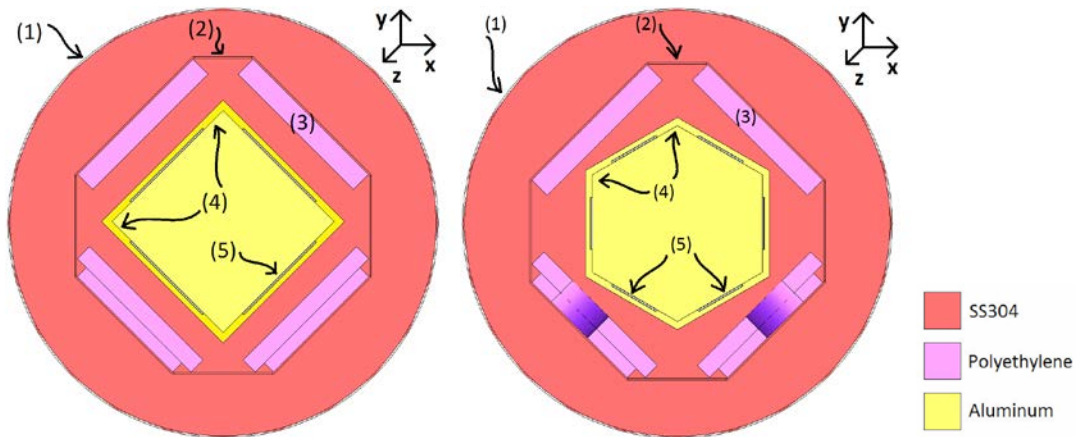


Figure 6-7 Front Cross-Sections of the Traveller STD/XL (Left) and VVER (Right)

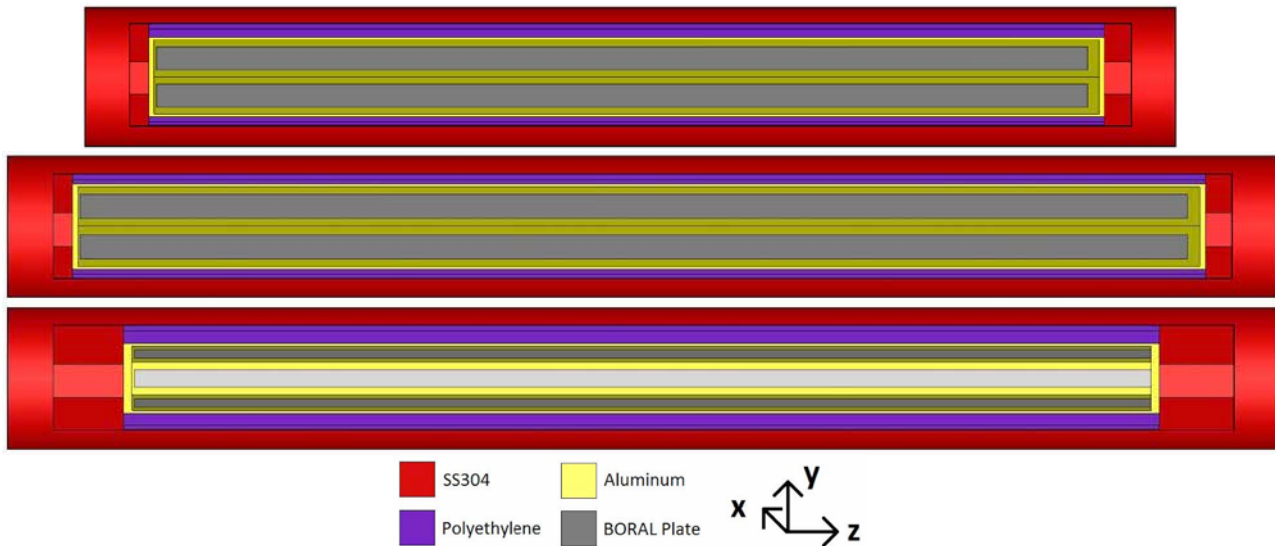


Figure 6-8 Top to bottom: Side Cross-Sections of the Traveller STD, XL, and VVER

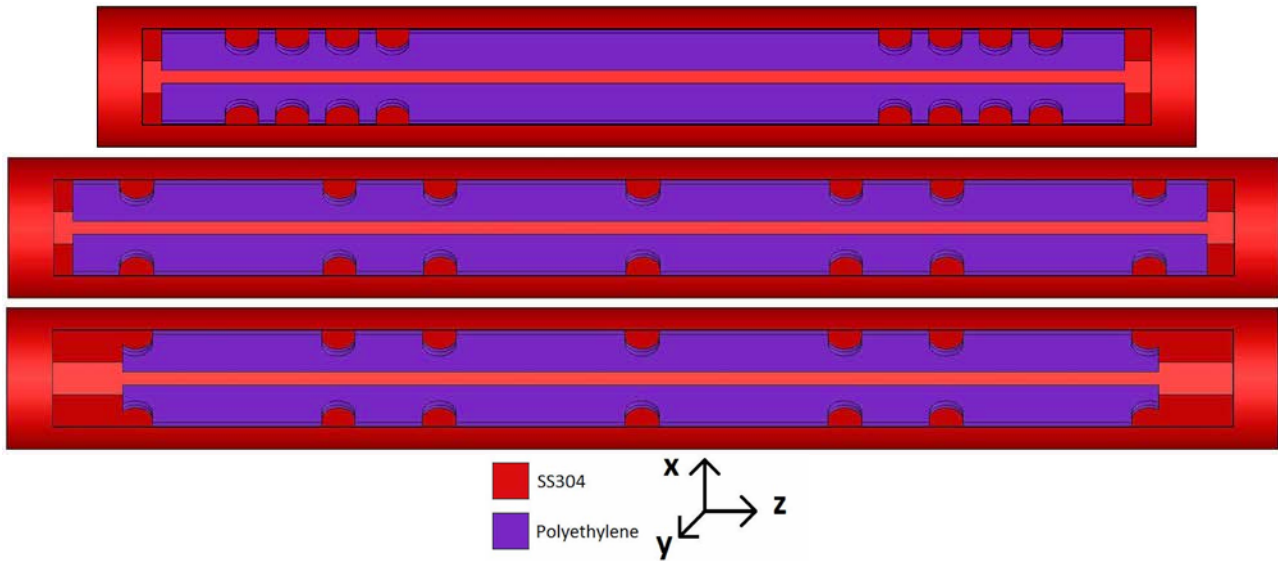


Figure 6-9 Top to bottom: Top Moderator Block Cross-Sections of the Traveller STD, XL, and VVER

6.3.1.1 Rod Pipe

The Rod Pipe is a 6-in. diameter, Schedule 40 SS304 pipe with end caps. The Rod Pipe licensing drawing specifies a maximum pipe length of 200 in. (pipe + end cap + end bolts), which is utilized for the Traveller XL model. The length is shortened to the Clamshell inner cavity length of 171 in. (pipe + end cap + end bolts) for the Traveller STD model. The pipe is modeled as a simple, hollow cylindrical shell. As a result, the pipe end bolts are not represented in the models, thus the pipe exterior length is 198 in. for the Traveller XL and 169 in. for the Traveller STD. The Rod Pipe end caps are flanged and square; however, the excess material outside the pipe OD is insignificant to the neutron activity and thus is neglected in the model. The major dimensions of each variant's Rod Pipe model are listed in Table 6-11.

Table 6-11 Major Dimensions of Rod Pipe Model				
Dimension	Traveller Variant			
	STD		XL	
	in.	cm	in.	cm
Pipe OD	6.63	16.8402	6.63	16.8402
Pipe ID	6.065	15.4051	6.065	15.4051
Pipe end plate	0.25	0.635	0.25	0.635
Pipe exterior length ¹	169	429.26	198	502.92
Pipe interior length ²	168.5	427.99	197.5	501.65
Pipe end bolts	1.0	2.54	1.0	2.54

Note: ¹ XL exterior length is pipe + end caps (no bolts), STD exterior length is Clamshell inner cavity length; ² Pipe interior length = exterior length – 2x end plates

6.3.1.2 Conditions of Transport

Before commencing the NCT and HAC sensitivity studies, a baseline case for NCT and a baseline case for HAC are established. These baseline cases are the most reactive NCT and HAC single package and package array configurations possible, based on the effects, as applicable, of axial positioning of the fuel assembly within the Clamshell, lattice pitch expansion length, and flooding configuration. Three studies are performed to determine which cases define the baseline cases. First, the Categorized Fuel Assembly (CFA) established for each bin (See Section 6.9.2) is modeled in all applicable Traveller variants under both conditions of transport to determine the most reactive CFA-package variant for the baseline cases. Using these baseline cases, sensitivity studies are then evaluated for both NCT and HAC to determine the most reactive configuration for each.

For NCT, no Outerpack deformation is modeled and the moderator blocks are modeled at full density. For the fuel assembly contents, no lattice expansion is modeled, and the CFA is modeled against the bottom inner surface of the Clamshell. Each fuel pin is modeled with its full nominal pitch, thus fuel rods closest to the Clamshell are spaced from the Clamshell by the nominal pitch distance. For the Rod Pipe contents, fuel rods are modeled close-packed with no lattice expansion. For a single package, the package is fully flooded including the fuel-clad gap. For a package array, no flooding is modeled, except for the Rod Pipe where the Rod Pipe is always flooded for package array evaluations. Under NCT, the model boundary has a 20 cm-thick water reflector.

During the HAC drop-test series, there was minimal concentrated deformation to the Outerpack. Therefore, no changes to Outerpack dimensions are modeled. However, the test fuel assembly did experience damage and lattice expansion because of the drop test. As discussed in Section 6.3.4.2.1.3, lattice pitch expansion was modeled as 20.0 in. long (50.8 cm) to bound the results of the drop test. There was minimal damage to the UHMW polyethylene moderator blocks of the packaging from the fire test. The effect of the loss of moderator block material was examined as a sensitivity study, as discussed in Section 6.3.4.3.3. The CFAs are modeled against the bottom inner surface of their respective Clamshell. The fuel-clad gap is modeled with full water flooding. Each fuel pin in the non-expanded lattice section of the CFA is modeled with its full nominal pitch, thus the fuel rods closest to the Clamshell are spaced from the Clamshell by the nominal pitch distance. For the Rod Pipe contents, fuel rods are modeled at the peak water-to-fuel ratio. In a single package, the entire package is flooded. For a package array, flooding to the most reactive credible extent in the Traveller is modeled, as discussed in Sections 6.3.4.2.1.4 and 6.3.4.3.13. Under HAC, the model boundary has a 20 cm-thick water reflector.

6.3.2 Material Properties

6.3.2.1 Non-Fissile, Non-Radioactive Reactor Core Components

Reactor core components that may be shipped with the radioactive/fissile contents of the Traveller are non-fissile, non-radioactive components that have specific functions within a reactor core but have no primary function in a transport scenario. The core component may function as a flux suppressant or as a neutron absorber during reactor operation and does not alter the design of the fuel assembly. As such, it is not evaluated in the package criticality safety analysis because its function as a neutron absorber decreases the reactivity of the system. In addition, for the transport evaluation, core components in a fuel assembly would displace water in a flooding condition of the criticality safety transport model and decrease moderation, and therefore decrease reactivity. Therefore, the non-fissile, non-radioactive reactor core components are not credited or modeled in the criticality safety analysis. These reactor core components are described further in Section 1.2.2.1.3.

6.3.2.2 UO₂

The UO₂ is modeled as the SCALE Standard Composition Library built-in compound “uo2.” The uranium consists of ²³⁵U at the maximum permissible enrichment for the respective case (i.e. 5 wt.% or 7 wt.% ²³⁵U) and the remainder of the uranium is modeled as ²³⁸U. The UO₂ is modeled at its theoretical density of 10.96 g/cm³. Other uranium isotopes are assumed to be ²³⁸U because these other isotopes (1) are not fissile, (2) only exist in small amounts, and (3) have thermal neutron absorption cross sections that are greater than ²³⁸U. This material is summarized in Table 6-12. ADOPT UO₂ fuel may include up to 700 ppm Cr₂O₃ and up to 200 ppm Al₂O₃. This material is added to the SCALE model with the elemental scale materials for chromium, aluminum and oxygen. The material composition for the ADOPT fuel is provided in Table 6-13.

6.3.2.3 U₃Si₂

The alternative loose rod fuel material U₃Si₂ is modeled as a compound composition of three atoms U and two atoms Si. The uranium consists of 5 wt.% ²³⁵U and 95 wt.% ²³⁸U, and the composition is modeled at its theoretical density of 12.2 g/cm³. Other uranium isotopes are assumed to be ²³⁸U because these other isotopes (1) are not fissile, (2) only exist in small amounts, and (3) have thermal neutron absorption cross sections that are greater than ²³⁸U. This material is summarized in Table 6-12.

6.3.2.4 Zircaloy Cladding

All cladding modeled is specified as the SCALE Standard Composition Library built-in alloy “zirc4,” which represents the alloy Zircaloy-4. This material is modeled at its theoretical density of 6.56 g/cm³ and it has the alloy composition listed in Table 6-13. As discussed in Section 2.12.9, the base zirconium alloy cladding may include features of chromium-coating or have an Optimized ZIRLO Liner (OZL). The addition of clad coatings and liners are neglected from the criticality analysis as they will have a negligible effect on the system reactivity through removal of moderation and presence of neutron absorbing materials. Additionally, the advanced cladding features are in addition to the base cladding and may not be credited in the minimum clad thickness requirement.

6.3.2.5 Guide Tubes/Instrument Tubes

Guide tubes/instrument tubes (GT/IT) are replaced with void under dry conditions and with light water under flooding conditions. Modeling the GT/IT as void under dry conditions allows for more neutron communication in an assembly and between packages in an array. Modeling the GT/IT as light water under flooding conditions promotes more neutron moderation and reflection in the fuel assembly envelope than the materials of construction of any GT/IT configuration. No credit is taken for the presence of GT/IT, thus there are no restrictions on guide tubes and instrument tubes.

6.3.2.6 Flooding and Reflecting Water

All water is modeled as the SCALE Standard Composition Library built-in compound “h₂o,” and is summarized in Table 6-12. This water consists of only ¹H and ¹⁶O with a S(α,β) thermal kernel. The water is modeled with SCALE’s nominal water density, 0.9982 g/cm³. In situations where a variation in water density is examined, the volume fraction of the material is altered.

6.3.2.7 Fuel Assembly Structural Materials

No credit is taken for fuel assembly structural materials (including rod end caps, top and bottom nozzles, and grid spacers) in this analysis. These materials are modeled as void in dry conditions and as full density light water in flooding conditions, as full density light water promotes more neutron moderation and reflection in the fuel assembly envelope than the structural materials of the fuel assembly and bounds any structural material configuration.

6.3.2.8 Aluminum

All structural aluminum of the packaging is modeled as elemental aluminum at its theoretical density of 2.702 g/cm³. This was determined to be bounding of the aluminum alloys of construction in the model (6061-T6 and 6005-T5/6005A-T5 aluminum alloys) as elemental aluminum has a lower density than these alloys and a reduced neutron cross-section compared to the alloy elements. This does not include the Type 1100 aluminum alloy cladding of the BORAL plates, which is discussed in Section 6.3.2.11.

6.3.2.9 304 Stainless Steel

The 304 stainless steel of the packaging is modeled as the 304 stainless steel composition presented in PNNL-15870 [3]. Its density is modeled as 8.0 g/cm³ and has the alloy composition listed in Table 6-13.

6.3.2.10 Ultra-High Molecular Weight Polyethylene

The moderator blocks of the Traveller are made of UHMW polyethylene, which is modeled as the SCALE Standard Composition Library built-in compound “polyethylene” with the chemical formula CH₂, which utilizes the hydrogen-in-polyethylene S(α,β) thermal kernel. Its density is modeled as 0.92 g/cm³ for both NCT and HAC. This material is summarized in Table 6-12.

6.3.2.11 BORAL Neutron Absorber Plates

BORAL is a clad composite of Type 1100 aluminum alloy and boron carbide (B_4C) that consists of three distinct layers: the two outer layers of cladding (solid, Type 1100 aluminum alloy) and the central layer (referred to as the “core”), consisting of a uniform aggregate of fine, B_4C particles held within a Type 1100 aluminum alloy matrix. See Table 6-13 for the composition of Type 1100 aluminum alloy.

6.3.2.11.1 BORAL Core Atom Number Density

The Traveller licensing drawings require a minimum ^{10}B areal density of []^{a,c} in the BORAL core. However, credit is only taken for 75% of the ^{10}B , as recommended in NUREG/CR-5661 [4]. This results in a modeled ^{10}B areal density of []^{a,c}. The number densities presented in Table 6-14 are calculated for a nominal BORAL core thickness of []^{a,c} and void fraction of []^{a,c}.

The number densities for each of the constituents of the BORAL core are calculated using the following process:

1. The ^{10}B number density is calculated based on the minimum areal density ([]^{a,c}), core thickness ([]^{a,c}), and atomic mass of ^{10}B
2. The ^{11}B number density is then calculated based on the natural abundances of ^{10}B and ^{11}B in Boron.
3. The Carbon in the B_4C portion of the BORAL Core is calculated using the total number density of Boron in the core, and the stoichiometric ratio of Boron to Carbon (4:1)
4. The number densities of the elements in the Type 1100 aluminum alloy portion of the core are determined by first calculating the volume fraction of the alloy in the core. This is calculated as the remainder of volume in the core, accounting for the B_4C and void (i.e. $V_{Al} = 1 - V_{B_4C} - []^{a,c}$). With this volume fraction and the nominal density of the alloy, the effective density of the alloy in the core is calculated. The number density of each element can then be calculated using this effective density and the weight fraction and atomic mass of the respective element in the alloy.

6.3.2.12 Hydrogenous Packaging Materials

The remaining materials specified in licensing drawings (rubber shock mounts, ceramic fiber blanket, polyurethane foam insulation, and acetate plugs) have all been determined to have lower hydrogen densities than water. Therefore, in flooding situations, these materials are replaced with water. In dry conditions, these materials are replaced with void. In the applicable transport condition models, both of these configurations have been determined to be bounding.

6.3.2.13 Hydrogenous Packing Materials

For routine conditions of transport, fuel assemblies and fuel rods are wrapped in sheets of polyethylene to protect the contents from foreign material such as dust and debris. Various types of hydrogenous materials may be used for packing. A bounding polyethylene density of 0.922 g/cm^3 is modeled, as it is a hydrogen-rich material. This material is used as the basis to define a hydrogen density limit for hydrogenous packing materials. Using polyethylene with a chemical formula of CH_2 , a density of 0.922 g/cm^3 , and the atomic weight of carbon (12.0107) and hydrogen (1.00794), a bounding hydrogen density of 0.1325 g/cm^3 is calculated. This material is summarized in Table 6-12.

6.3.2.14 Extreme Cold Case (-40°C) Effects

Any reactivity effect on a low-enriched uranium (LEU) fuel package due to an extreme cold case (-40°C) would be minimal. Reactivity effects would be due to the temperature effects on neutron cross-sections and changes in the density of the packaging and moderating materials.

A reduction in the temperature of LEU fuel would cause the ^{238}U thermal absorption resonances to become taller and thinner, narrowing the energy range of resonance peaks and decreasing the range of neutron energies absorbed in the resonance. As described in Section 6.3.3, the 293 K (20°C) cross sections were used. For a total temperature difference of 60°C (from 20°C to -40°C), this difference in resonance peaks is insignificant.

A change in the temperature of water from 20°C to -40°C would result in a phase change from liquid water to solid ice. As water freezes, it expands, reducing its density from $\sim 1 \text{ g/cm}^3$ to $\sim 0.92 \text{ g/cm}^3$. A reduction in water density results in a reduction in hydrogen density, effectively reducing neutron moderation in the system. Thus, any change in material densities due to a temperature change from 20°C to -40°C would not result in an increase in k_{eff} as there are no resulting changes to packaging components; there is only the potential for a reduction in moderation due to the expansion of water as a result of freezing.

6.3.2.15 Integral Absorbers

Integral absorbers are allowable contents within the fuel assembly or loose fuel rods, including, but not limited to, gadolinia, erbia, boron, chromium and hafnium. Integral absorber materials have specific functions within the fuel but have no primary function in a transport scenario. The integral absorber may function as a flux suppressant or as a neutron absorber during reactor operation and does not alter the design of the fuel assembly. As such, it is not evaluated in the package criticality safety analysis because its function as a neutron absorber decreases the reactivity of the system. Therefore, the integral absorbers are not credited or modeled in the criticality safety analysis.

6.3.2.16 Summary of SCALE Material Compositions

When elements are listed in Table 6-12, Table 6-13, or Table 6-14, the isotopic abundances of naturally occurring elements in the SCALE Standard Composition Library are used.

Material	Density (g/cm ³)	Constituent	Number of Atoms per Molecule
UO ₂ (5 wt.% ²³⁵ U, 95 wt.% ²³⁸ U / 7 wt.% ²³⁵ U, 93 wt.% ²³⁸ U)	10.96	U	1
		O	2
U ₃ Si ₂ (5 wt.% ²³⁵ U, 95 wt.% ²³⁸ U)	12.2	U	3
		Si	2
Light Water	0.9986	H	2
		O	1
UHMW Polyethylene (Moderator blocks)	0.92	C	1
		H	2
Polyethylene Packing Materials	0.922	C	1
		H	2

Material	Density (g/cm ³)	Constituent	Weight Fraction
Zircaloy-4	6.56	Zr	0.98230
		Sn	0.01450
		Fe	0.00210
		Cr	0.00100
		Hf	0.00010
304 Stainless Steel	8.00	C	0.00040
		Si	0.00500
		P	0.00023
		S	0.00015
		Cr	0.19000
		Mn	0.01000
		Fe	0.70173
		Ni	0.09250

Material	Density (g/cm ³)	Constituent	Weight Fraction
Type 1100 Aluminum Alloy	2.71	Al	0.99500
		Si	0.00162
		Mn	0.00017
		Fe	0.00162
		Cu	0.00125
		Zn	0.00034
ADOPT UO ₂ Fuel (700 ppm Cr ₂ O ₃ , 200 ppm Al ₂ O ₃)	10.96	UO ₂	0.999100
		Cr	0.000479
		Al	0.000106
		O	0.000315

Material	Density (g/cm ³)	Constituent	Atom Number Density (atoms/barn-cm)
BORAL Core (B ₄ C and Type 1100 Aluminum Alloy aggregate)	[] ^{a,c}	¹⁰ B	[] ^{a,c}
		¹¹ B	[] ^{a,c}
		C	[] ^{a,c}
		Al	[] ^{a,c}
		Si	[] ^{a,c}
		Mn	[] ^{a,c}
		Fe	[] ^{a,c}
		Cu	[] ^{a,c}
Zn	[] ^{a,c}		

6.3.3 Computer Codes and Cross-Section Libraries

The Criticality Safety Analysis Sequence with KENO-VI (CSAS6) of the SCALE 6.1.2 code package was used to calculate values of k_{eff} for this analysis [5]. KENO-VI is a Monte Carlo criticality program used to calculate the k_{eff} of three-dimensional (3-D) systems. The ENDF/B-VII.0 continuous energy neutron cross-section data were used for all cases in this analysis. Each case analyzed used the default room temperature (293 K) cross sections. SCALE is a categorized modeling and simulation suite for nuclear safety analysis and design developed and maintained by Oak Ridge National Laboratory under contract with the U.S. Nuclear Regulatory Commission, U.S. Department of Energy, and the National Nuclear Security Administration to perform reactor physics, criticality safety, radiation shielding, and spent fuel characterization for nuclear facilities and transportation/storage package designs.

6.3.3.1 Convergence Criteria

For each package arrangement examined, different neutron history configurations were utilized to obtain proper source convergence. For all analyses, a minimum of 450 total generations with a minimum of 10,000 neutrons per generation and a minimum of 150 skipped generations were analyzed for a minimum of 3,000,000 active neutron histories. The number of histories analyzed was increased as needed in order to achieve adequate source convergence. In addition, output files were examined to verify source convergence by examining the “average k-effective by generation” plot run, the “average k-effective by generation skipped” plot, and the “frequency for generations” plot.

6.3.4 Demonstration of Maximum Reactivity

The most reactive cases for each package variant, content Group, and condition of transport were determined through three sequential analyses:

- (1) Modeling CFAs that represent the most reactive configuration of a bin.
- (2) Determination of NCT and HAC baseline cases for each package arrangement.
- (3) Sensitivity studies analyzed for both baseline cases to demonstrate maximum reactivity for NCT and HAC safety case configurations and each package arrangement.

The first analysis determined the bounding CFA of each bin. A bin is a grouping of fuel assemblies that have in common three primary parameters: array size (e.g. 17x17), number and location of non-fueled holes, and as-designed nominal fuel rod pitch. Organizing fuel assemblies into bins reduces the quantity of fuel assemblies that need to be specified. The CFA of each bin is a bounding combination of three secondary fuel assembly design parameters: fuel pellet diameter, fuel-clad gap, and cladding thickness. The secondary parameter range of each bin is determined by the fuel assembly designs that constitute the bin. Every combination of these secondary parameters is evaluated to ensure that the fuel assembly permutations span the breadth of each secondary parameter range. By comparing all fuel assembly permutations, the effect of each secondary parameter on k_{eff} is determined. The in-depth CFA analysis is presented in Section 6.9.2, and the results of the CFA analysis are summarized in Section 6.3.4.1.

The second and third analyses modeled the CFAs with the Traveller packaging to demonstrate compliance with the regulatory requirements of 10 CFR 71 and SSR-6 for single packages and package arrays. The second analysis determines the baseline cases, which are bounding CFA-package variant combinations for each Group for both NCT and HAC. The baseline case evaluation models the CFAs for each Group in each applicable package variant to determine both the most reactive CFAs and package variant, as applicable. A similar method is applied to the Rod Pipe contents. The baseline case evaluation also determined which axial position of the content in the Clamshell is most reactive and the most reactive flooding configuration, as applicable to the transport condition. See Section 6.3.4.2 for the full baseline case explanation.

Upon determining the baseline cases, the third analysis evaluates sensitivity studies, independently of one another, to determine the reactivity effect of the baseline cases due to parametric variation studies. Parameters such as annular fuel pellet blankets, SS replacement rods, polyethylene packing material configurations, fuel tolerances, extended active fuel length, and various HAC testing resultant damage configurations were analyzed. If a sensitivity study resulted in a more reactive configuration than the baseline case, the increase in

$k_{eff} + 2\sigma (\Delta k_u)$ was summed for each sensitivity study and added to the k_{eff} of the baseline case ($k_p + 2\sigma_p$) in order to produce the final safety case value of k_{eff} (*Maximum k_{eff}*). See Section 6.3.4.3 for the full sensitivity study explanation. A combined case study is provided in Appendix 6.9.4 to compare the individual penalty method for each sensitivity study, as described in this section, to a single case combining all positive penalty configurations determined from each sensitivity study.

6.3.4.1 Categorized Fuel Assembly Determination

The CFA analysis, presented in Section 6.9.2, determined the bounding parameters for each bin. Each CFA represents the most reactive configuration of secondary parameters of a bin, all of which model the minimum fuel pellet diameter, cladding ID, and cladding thickness as the most reactive configuration. Since fuel assemblies are designed to be under-moderated for reactor operation, reducing the fuel pellet diameter, cladding ID, and cladding thickness to the evaluated minimum values increases neutron moderation in a transport evaluation by allowing for increased water presence within the fuel envelope. Presented in Table 6-15 are the bins applicable to each fuel assembly Group. A CFA is generated for each bin.

Table 6-15 Bin Listing for Each Fuel Assembly Group			
Group 1		Group 2	Group 3
• 14 Bin 1	• 16 Bin 2	• 16 Bin 1	• VV Bin 1
• 14 Bin 2	• 16 Bin 3	• 18 Bin 1	
• 15 Bin 1	• 17 Bin 1		
• 15 Bin 2	• 17 Bin 2		

6.3.4.2 Baseline Case

For each content and package variant combination, one baseline NCT case and one baseline HAC case were determined for single package and package array. Each baseline case is a bounding combination of the content and package variant for each condition of transport. The baseline configuration is based on the effects of modeling a CFA (or the Rod Pipe) in the packaging, axial positioning of the content within the Clamshell, and flooding configuration, as applicable to each condition of transport. The following outline shows the method used in selecting the NCT and HAC baseline cases for the CFA Package Array evaluation. The baseline case method for the Rod Pipe is described in Section 6.3.4.2.2.

Method Outline Application Example:

Group 1 Package Array NCT and HAC Baseline Case Determination

1. NCT Baseline Case
 - a. CFA-Package Variant Comparison
 - i. Compare Traveller variants by modeling equivalent CFAs in both the STD and XL
 - ii. Compare CFAs in most reactive Traveller variant (Traveller XL)
 - b. Baseline Case Determination
 - i. Compare axial positions of limiting CFA in most reactive Traveller variant
2. HAC Baseline Case
 - a. CFA-Package Variant Comparison
 - i. Compare Traveller variants by modeling equivalent CFAs in both the STD and XL
 - ii. Compare CFAs in most reactive Traveller variant (Traveller XL)
 - b. Baseline Case Determination
 - i. Compare axial positions of limiting CFA in most reactive Traveller variant
 - ii. Compare different flooding configurations for limiting flooding configuration

6.3.4.2.1 Fuel Assemblies

6.3.4.2.1.1 CFA-Package Variant Comparison

The first part of the baseline case determination is the CFA-package variant comparison. This examines the CFAs as presented in Section 6.9.2.1 in each applicable package variant for NCT and HAC with the following configuration:

- Active fuel lengths plus one fabrication tolerance.
- No lattice pitch expansion length considered for NCT and 20 in. (50.8 cm) of lattice pitch expansion length for HAC.
- Nominal fuel assembly lattice rests against the bottom of the Clamshell in the radial, x-y plane.
- All regions flooded for single package analyses. All floodable regions are modeled as void for NCT package array cases. For HAC package array cases, the fuel-clad gap, fuel assembly envelope, and Clamshell inner cavity modeled as fully flooded with all other floodable regions modeled as dry.
- Close, full water reflection (20+ cm thick) surrounding the single package and package arrays.

These comparisons result in one bounding CFA-package variant combination for each fuel assembly Group, for each NCT and HAC package arrangement. For Group 1, shorter fuel assemblies that are capable of being shipped in the STD were also modeled in the XL in order to perform a reactivity comparison between Traveller variants. It was determined in this analysis that the Traveller XL bounds all Traveller STD configurations in the Group 1 package arrangement. As stated in Section 6.2.2, the Traveller XL is the only applicable packaging variant in the Group 2 package arrangement, and, as stated in Section 6.2.3, the Traveller VVER is the only applicable packaging variant in the Group 3 package arrangement.

6.3.4.2.1.2 Axial Position of Fuel Assembly in Clamshell

As a part of the baseline evaluation, the axial position of the fuel assembly in the Clamshell is examined to determine the bounding position. Figure 6-10 shows three different cases from the axial position study. The axial position of the fuel assembly has an impact on k_{eff} for several reasons:

- (1) Small gaps exist between the BORAL plates and the axial ends of the Clamshell.
- (2) The shock mount cutouts (see Figure 6-9) in the moderator blocks can increase neutron communication between packages.
- (3) The centering of the fuel assembly affects axial reflection in the package due to the flooded Clamshell under HAC.

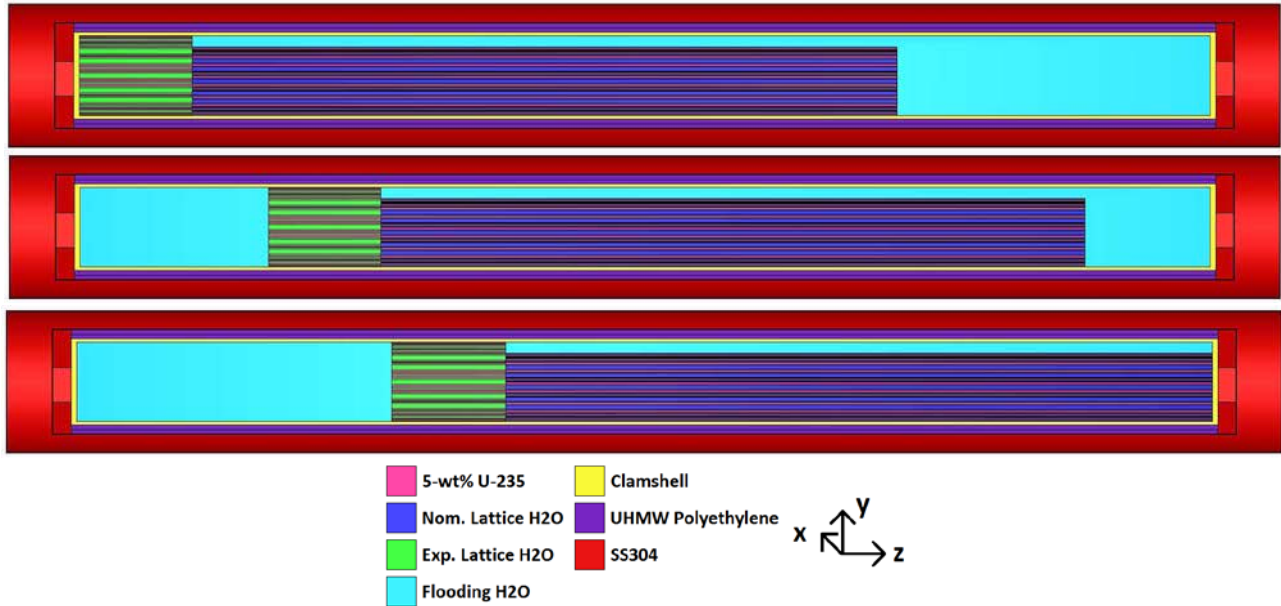


Figure 6-10 Side Cross Section of the Traveller Showing Fuel Assembly Axial Position Study

6.3.4.2.1.3 HAC Lattice Pitch Expansion Length

Under HAC, the lattice pitch expansion length is modeled as 20.0 in. long (50.8 cm) with the lattice pitch expanded fully and uniformly to the inner boundary of the Clamshell. Most testing resulted in the fuel assembly experiencing some kind of lattice modification. For the 20-in. span from the bottom nozzle to Grid 2, the fuel rod envelope expanded from 8-3/8 inches average nominal to 9-3/16 inches with a single rod bent outward approximately 1/2 in. Otherwise, the typical pitch pattern consisted of 2 rod rows touching and the remaining 14 rows at nominal pitch. See Section 2.12.5.3 for details. To bound drop test results, the lattice pitch expansion length is modeled at 20 in. (50.8 cm) with the lattice fully and uniformly expanded to the Clamshell boundary. This is a conservative modeling decision because only one fuel rod bowed during the drop test and no fuel rod expanded to the Clamshell boundary. Explicitly modeling the expanded lattice region results in a water-to-fuel ratio that is closer to the optimal value than the nominal fuel region. Lattice expansion is modeled for single package and package array configurations under HAC. A cross-section of the lattice pitch expansion as modeled in SCALE is shown in Figure 6-11.

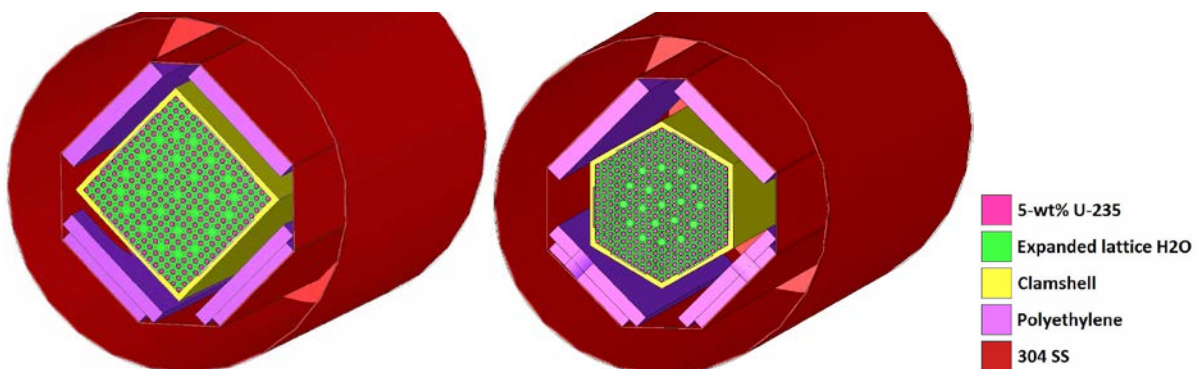


Figure 6-11 Cutaway of Traveller XL with 17 Bin 2 Showing the Lattice Pitch Expansion Section

6.3.4.2.1.4 HAC Package Array Flooding Configuration

Six different flooding configurations were examined for the Groups 1, 2, and 3, HAC package array cases in order to determine which flooding configuration is bounding. The first configuration, also known as the partial flooding scenario, is a more realistic scenario with a full-density water level that rises throughout the Outerpack inner cavity, Clamshell, and fuel assembly simultaneously. The five other configurations, known as the preferential flooding (also called differential or sequential flooding) scenarios, instead model the fuel assembly envelope and fuel-clad gap as always fully flooded and then vary the water density in one or more selected flooded regions of the Traveller packaging, while holding the remaining packaging regions as void. The five preferential flooding configurations are:

- (1) Outerpack inner cavity outside of the Clamshell,
- (2) The Clamshell cavity,
- (3) The Outerpack outer cavity,
- (4) The entire Traveller,
- (5) The region between packages (interspersed moderation).

These configurations are shown in Figure 6-12 for square Clamshell configurations. The most reactive flooding configuration for each fuel assembly package array arrangement consists of a fully flooded Clamshell cavity, including the fuel envelope and fuel-clad gap, with all other floodable regions of the package array as void (preferential flooding configuration 2). The optimum interspersed moderation configuration is void between packages in an array.

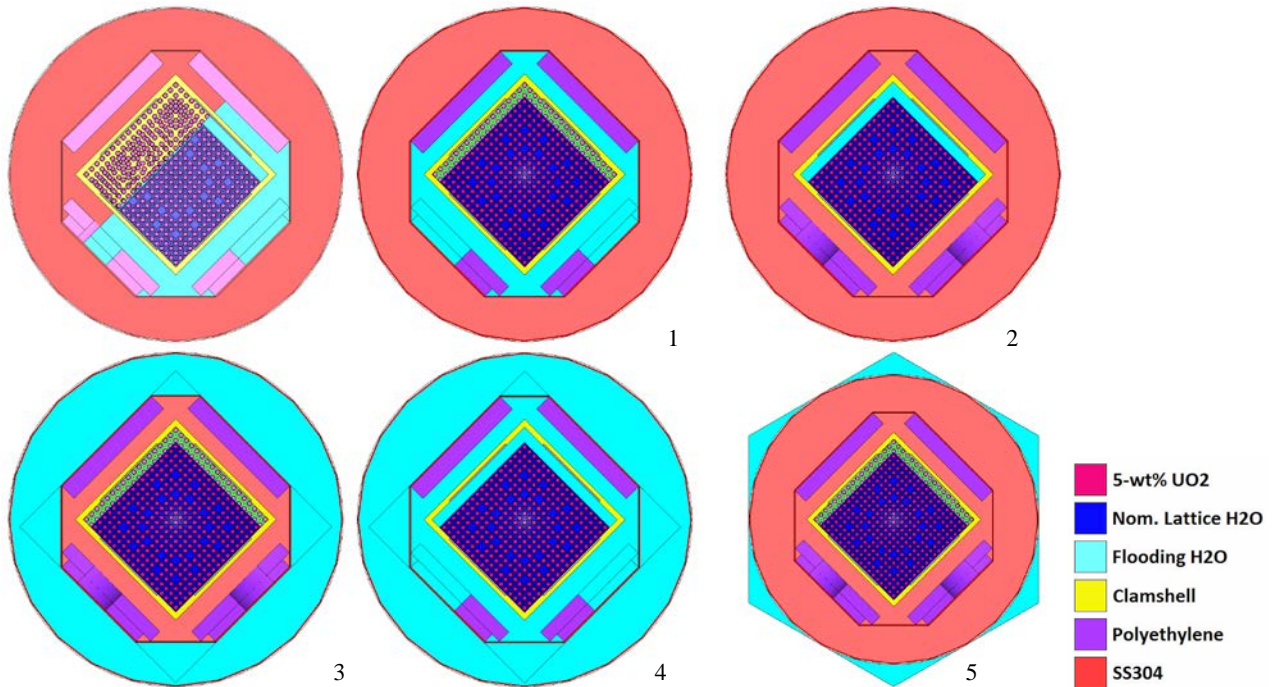


Figure 6-12 The Six Groups 1, 2, and 3 Flooding Configurations

6.3.4.2.2 Rod Pipe

For the UO₂ baseline evaluation, the range of fuel pellet outer radii (OR) evaluated is from 0.154 in. (0.3912 cm) to 2.756 in. (7.0002 cm), as shown in Table 6-16 for NCT, and from 0.154 in. (0.3912 cm) to 0.256 in. (0.650 cm) for HAC. The range of pellet OR only represents a variation in water-to-fuel ratio, to ensure peak reactivity is evaluated. The pitch is close-packed for all NCT examinations, thus the pitch is equivalent to the fuel pellet diameter. For HAC, the pitch is increased through a peak water-to-fuel ratio. Both square and hexagonal pitch types are modeled for each condition of transport. A baseline case is determined for the single package and package array and for NCT and HAC each. Comparison of results for the varying fuel pellet OR and half-pitch sets a bounding combination as the baseline for each transport condition for use in the sensitivity study analyses.

NCT ¹		HAC	
Fuel OR in. (cm)	Fuel OR continued in. (cm)	Fuel OR in. (cm)	Half-Pitch ² cm
0.154 (0.391)	0.394 (1.000)	0.154 (0.391)	Fuel OR
0.167 (0.425)	0.591 (1.500)	0.167 (0.425)	Fuel OR +0.10
0.177 (0.450)	0.787 (2.0)	0.177 (0.450)	Fuel OR +0.25
0.187 (0.475)	0.984 (2.5)	0.187 (0.475)	Fuel OR +0.50
0.197 (0.500)	1.181 (3.0)	0.197 (0.500)	Fuel OR +0.75
0.217 (0.550)	1.378 (3.5)	0.217 (0.550)	--
0.236 (0.600)	1.575 (4.0)	0.236 (0.600)	--
0.256 (0.650)	1.772 (4.5)	0.256 (0.650)	--
0.276 (0.700)	1.969 (5.0)	--	--
0.295 (0.750)	2.165 (5.5)	--	--
0.315 (0.800)	2.362 (6.0)	--	--
0.335 (0.850)	2.559 (6.5)	--	--
0.354 (0.900)	2.756 (7.0)	--	--
0.394 (1.000)	--	--	--

Note: ¹ Half-pitch = Fuel OR for NCT. ² All five half-pitch values are modeled for each fuel OR.

The number of pitch cells in the Rod Pipe defines the number of rods modeled, which is estimated by calculating the area of a single pitch cell and dividing the area of the Rod Pipe cavity by the single pitch cell area, as shown in Figure 6-13. With this method, the Rod Pipe inner radial boundary will cut through the pitch cells against the Rod Pipe inner boundary. The total number of rods includes these cut cells. The quantity of fuel rods that can be physically inserted into the Rod Pipe is less than the value evaluated due to the addition of packing materials that protect the fuel rods during transport.

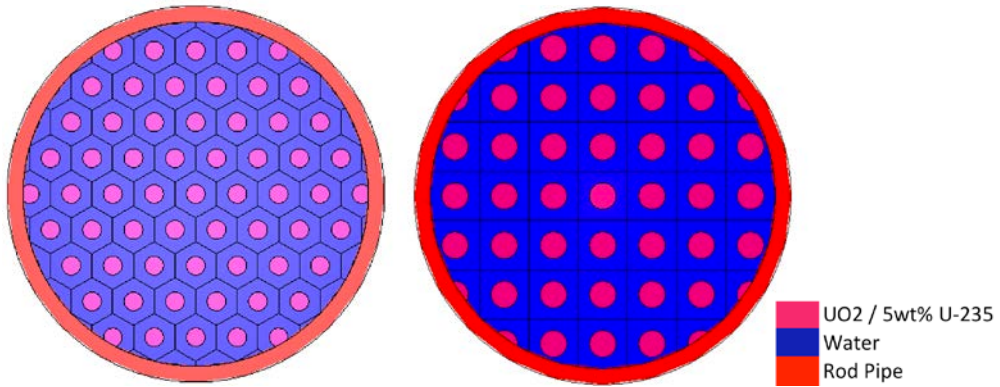


Figure 6-13 Rod Pipe, UO₂ Fuel Array Modeling in Rod Pipe

For the U₃Si₂ evaluation, the range of fuel pellet OR evaluated is from 0.154 in. (0.3909 cm) to 0.191 in. (0.4851 cm) for NCT and HAC, as shown in Table 6-17. The pitch is close-packed for all NCT examinations, thus the pitch is equivalent to the fuel pellet diameter, and the contents are centered in the Rod Pipe. For HAC, the pitch is increased to values that result in fewer than 60 fuel rods being modeled in the Rod Pipe in order to consider partial loadings and ensure the peak water-to-fuel ratio had been achieved. These configurations are shown in Figure 6-14.

NCT ^a	HAC	
Fuel OR in. (cm)	Fuel OR in. (cm)	Half-Pitch ^b cm
0.154 (0.391)	0.154 (0.391)	Fuel OR +0.15
0.163 (0.415)	0.163 (0.415)	Fuel OR +0.20
0.172 (0.438)	0.172 (0.438)	Fuel OR +0.25
0.182 (0.462)	0.182 (0.462)	Fuel OR +0.30
0.191 (0.485)	0.191 (0.485)	Fuel OR +0.35
--	--	Fuel OR +0.40
--	--	Fuel OR +0.425 ^c
--	--	Fuel OR +0.45
--	--	Fuel OR +0.475
--	--	Fuel OR +0.50
--	--	Fuel OR +0.525 ^d
--	--	Fuel OR +0.55
--	--	Fuel OR +0.60
--	--	Fuel OR +0.65
--	--	Fuel OR +0.70
--	--	Fuel OR +0.75
--	--	Fuel OR +0.80
--	--	Fuel OR +0.85

Note: ^a Half-pitch = Fuel OR for NCT. ^b All 17 half-pitch values are modeled for each fuel OR.

^c half-pitch only modeled for hexagonal pitch cases. ^d half-pitch only modeled for square pitch cases

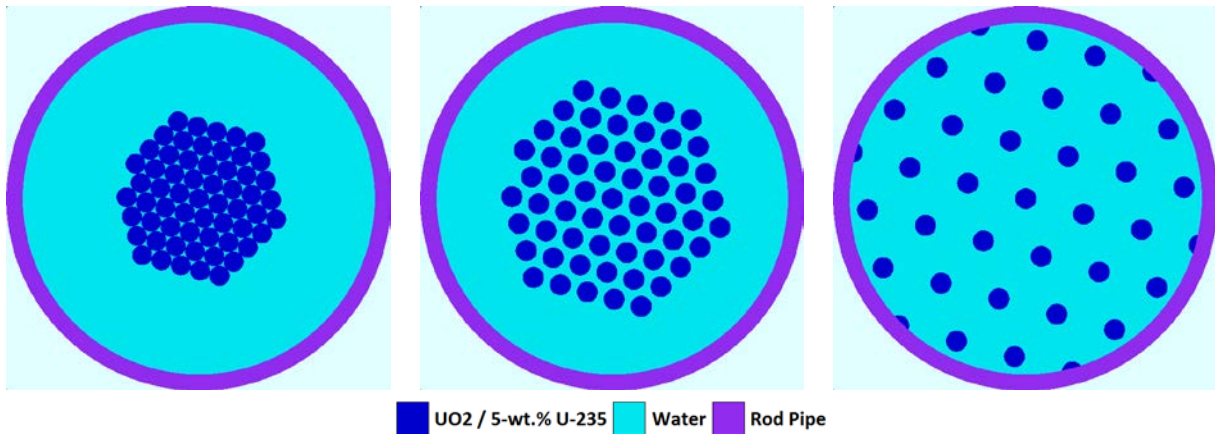


Figure 6-14 Rod Pipe, U₃Si₂ NCT Case (left) and Two HAC Cases (right)

For both loose rod contents, the lattice expansion study is not applicable, as the entire active fuel length is expanded through the optimum water-to-fuel ratio of the Rod Pipe. The axial position of the fuel inside the Rod Pipe is also not applicable because the fuel is modeled as the full inner length of the Rod Pipe.

6.3.4.3 Sensitivity Studies

The baseline cases, one each for NCT and HAC for each package arrangement, are subjected to several sensitivity studies, which are detailed in Table 6-18 and the following subsections. Note that Groups 1, 2, and 3 are grouped together in this table. Each Group is analyzed separately, but since they all contain PWR fuel assembly contents, the same sensitivity studies are evaluated. A sensitivity study case is determined to have a more reactive result (i.e. penalizing) only if the case's increase in $k_{\text{eff}} + 2\sigma$ is greater than or equal to 2σ (i.e. statistically significant) from the baseline case ($k_{\text{eff}} + 2\sigma$) analyzed. No action is taken for sensitivity studies or parameter variations that result in a reduction in k_{eff} or statistically insignificant result (i.e. less than 2σ difference from the base case). The summed increase in k_{eff} (Δk_u) is added to the baseline case ($k_p + 2\sigma_p$), producing a final value of k_{eff} (*Maximum* $k_{\text{eff}} = k_p + 2\sigma_p + \Delta k_u$), as detailed in Section 6.1.2. This process is repeated for all applicable package arrangements to demonstrate maximum reactivity for NCT and HAC of each package arrangement.

Case	Description	Groups 1, 2, and 3 (Single)		Groups 1, 2, and 3 (Arrays)		Rod Pipe (Single)		Rod Pipe (Arrays)	
		NCT	HAC	NCT	HAC	NCT	HAC	NCT	HAC
Lattice expansion	Expanded lattice pitch region.	--	X	--	X	--	--	--	--
Axial fuel position	Determination of the worst-case axial position of the fuel assembly in the Clamshell.	X	X	X	X	--	--	--	--
Flooding configuration	Assessment of several flooding configurations' effect on the behavior of k_{eff} .	--	--	--	X	--	--	--	X
Annular fuel pellet blanket study	Assessment of the behavior of k_{eff} with annular fuel pellet blankets in the fuel assembly.	X	X	X	X	X	X	X	X
Clamshell/fuel assembly/Rod Pipe shift study	Assessment of the behavior of k_{eff} by shifting the position of the Clamshell and/or fuel assembly in the inner cavity, or Rod Pipe in the Clamshell	X	X	X	X	X	X	X	X
Moderator block density study	Assessment of the behavior of k_{eff} with a 1% reduction in the density of the UHMW moderator blocks.	--	X	--	X	--	X	--	X
Package outer diameter tolerance study	Assessment of the behavior of k_{eff} upon examining the tolerance of the Outerpack outer diameter.	--	--	X	X	--	--	X	X
Polyethylene packing materials study	Assessment of the behavior of k_{eff} with polyethylene packing materials in the fuel assembly/Rod Pipe.	X	X	X	X	X	X	X	X
Axial rod displacement study	Assessment of the behavior of k_{eff} with rods shifted up axially in the fuel assembly as the result of an end drop.	--	X	--	X	--	--	--	--
Stainless Steel replacement rod study	Assessment of the behavior of k_{eff} with stainless steel rods replacing fuel rods in the fuel assembly.	X	X	X	X	--	--	--	--
Cladding diameter tolerance study	Assessment of the behavior of k_{eff} modeling fuel rod cladding diameter tolerances.	X	X	X	X	--	--	--	--
Fuel pellet diameter tolerance study	Assessment of the behavior of k_{eff} modeling fuel pellet diameter tolerances.	X	X	X	X	X	X	X	X
Fuel rod pitch tolerance study	Assessment of the behavior of k_{eff} modeling fuel rod pitch tolerances.	X	X	X	X	--	--	--	--
Steel nozzle reflector study	Assessment of the behavior of k_{eff} modeling two nozzle reflector configurations at both ends of a fuel assembly.	--	--	X	X	--	--	--	--
Extended active fuel length study	Assessment of the behavior of k_{eff} modeling longer active fuel lengths in Group 3 only.	X	X	X	X	--	--	--	--
ADOPT study	Assessment of the behavior of k_{eff} modeling ADOPT fuel instead of UO_2 . (Not applied to Group 3)	X	X	X	X	X	X	X	X

6.3.4.3.1 Annular Fuel Pellet Blanket Study

This study examined the addition of varying lengths of annular fuel pellet blanket lengths equally to the top and bottom of every rod in an assembly or Rod Pipe. The annulus ID was analyzed between 0.155 in. (0.3937 cm) and 0.183 in. (0.4648 cm). The fuel void resulting from the addition of an annulus to the fuel rod was modeled as flooded for all single package arrangements, void for NCT package array arrangements, and flooded for HAC package array arrangements.

For the Rod Pipe NCT assessments, proportionally larger-sized annular IDs were examined, as the limiting case for NCT involved large-diameter fuel rods with a pellet OR of 1.3780 in. (3.5 cm). As a result, modeling the nominal annular fuel pellet inner diameters typical of PWR fuel rods results in no meaningful effect to k_{eff} . Instead, for the loose rod contents, a proportional annular ID was modeled in order to better capture the effect of modeling annular fuel pellet blankets. The nominal annular fuel pellet IDs of PWR fuel assemblies are approximately 44% of their respective fuel pellet ODs. Therefore, for the 1.3780 in. (3.5 cm) fuel pellet ORs of the NCT single package and package array cases, a 0.6063 in. (1.54 cm) annular fuel pellet IR was modeled to capture this proportional effect.

6.3.4.3.2 Clamshell, Fuel Assembly, or Rod Pipe Shift Study

For the fuel assembly contents, two Clamshell and/or fuel assembly-shifting configurations were examined. In the baseline cases for all arrangements, the fuel assembly rests against the bottom of the Clamshell in the x-y plane, as shown in Figure 6-15.

For single package and package array NCT and HAC evaluations, the fuel assembly was modeled centered in the Clamshell, as the nozzles, grid structures, and packing would result in the fuel assembly being approximately centered in the Clamshell, as shown in Figure 6-15.

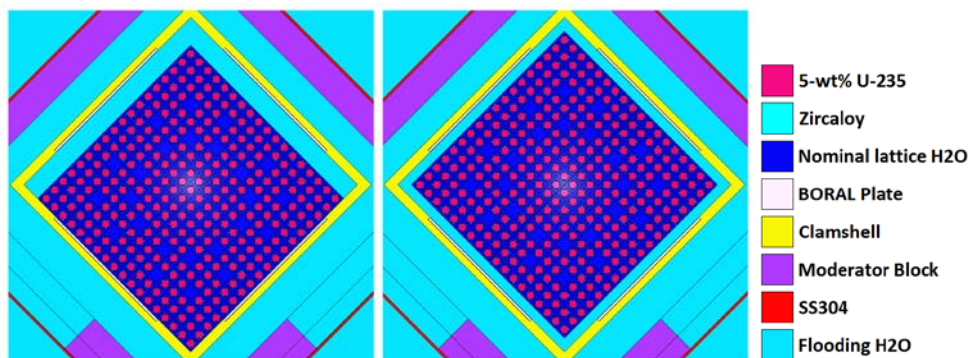


Figure 6-15 NCT Single Package Baseline Case vs. Fuel Assembly Shift

For the HAC package array evaluations, the Clamshell and fuel assembly were both shifted to the top of the inner cavity in order to simulate the package array flipping over in an accident condition. Refer to Figure 6-16. This scenario assumes the Clamshell separates from the shock mounts and rests nearly against the upper moderator blocks. However, this upward shift was not evaluated for HAC single packages because the HAC single package model is fully flooded. Therefore, minimal to no effect is expected from modeling the fuel assembly against the top of the cavity resting against the moderator blocks.

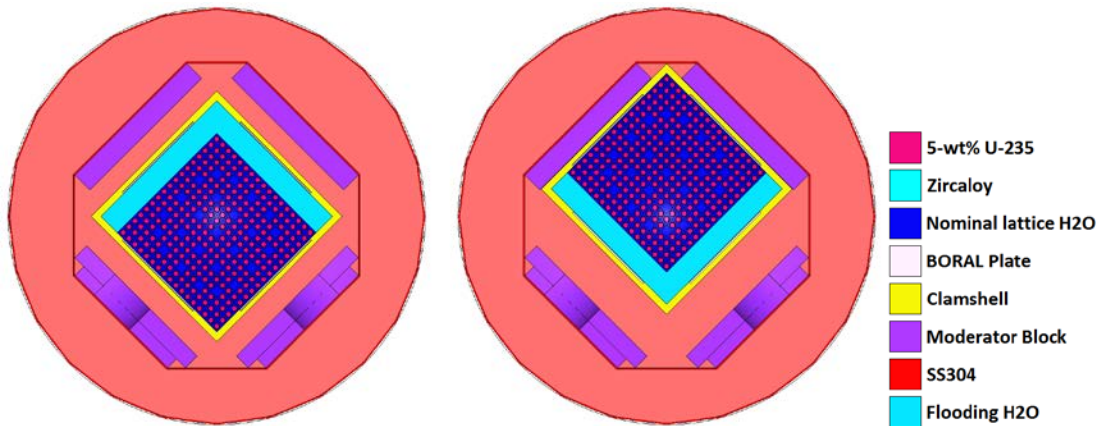


Figure 6-16 HAC Package Array Baseline Case vs. Clamshell and Fuel Assembly Shift

In the Rod Pipe single package and package array arrangements under NCT, the Rod Pipe was examined as both centered in the Clamshell and shifted down in the Clamshell. For HAC, the Rod Pipe was examined shifted up, centered, and shifted down in the Clamshell in order to determine the bounding positioning of the Rod Pipe.

6.3.4.3.3 Moderator Block Density Reduction Study

As described in detail in Section 6.1.1.2, the moderator blocks are designed to work in conjunction with the BORAL plates as part of the flux trap system, which reduces neutron communication between packages in an array. Therefore, a reduction in moderator block density results in more neutron communication between packages in an array. The density reduction of the polyethylene moderator blocks is examined for all HAC package arrangements in order to determine the effect on k_{eff} . The polyethylene density is examined at nominal density (0.92 g/cm^3) and a 1% density reduction (0.9108 g/cm^3).

An objective of the fire test presented in Section 3.6.5 was to show that greater than 90% of the hydrogen content of the moderator block was retained post-fire. The largest mass reduction experienced of any individual moderator block was -0.7%. As a result, a 1% reduction in all moderator block density was evaluated to bound the largest individual moderator block mass reduction.

6.3.4.3.4 Package Outer Diameter Sensitivity Study

The package outer diameter sensitivity study was only examined for the package arrays of each arrangement, as adjusting the spacing between packages in an array directly affects the effective fissile density. Licensing Drawings list the tolerance of the packaging's OD as $\pm 0.20 \text{ in.}$ ($\pm 0.508 \text{ cm}$). The package OD was examined at plus and minus one tolerance in order to determine the effect on k_{eff} .

6.3.4.3.5 Polyethylene Packing Materials Study

For routine conditions of transport, fuel assemblies and loose fuel rods in the Traveller are wrapped in sheets of polyethylene in order to protect the contents from foreign material, such as dust and debris. Various types of polyethylene are used with a density of 0.922 g/cm^3 modeled in this analysis. The mass of polyethylene present is varied to determine a packing material limit. The NCT cases are modeled as dry and the addition of

polyethylene may increase reactivity of the system during NCT. Therefore, the addition of polyethylene is evaluated to determine its effect on k_{eff} . Since polyethylene has a higher hydrogen density than light water, the addition of polyethylene wrap under HAC can result in an increased reactivity. Additionally, during a HAC fire event under extreme temperatures, the polyethylene wrap could potentially melt and redistribute in the contents, producing a more reactive system; therefore, three different configurations are examined for the polyethylene packing material HAC sensitivity study. However, it is important to note that none of the currently used polyethylene materials are likely to melt in an accident situation. During the package HAC testing, as described in Section 3.5, the highest temperature measured on the outside of the Clamshell during this process was below material melt temperatures.

6.3.4.3.5.1 Outer Wrap Configuration for Fuel Assembly Groups Only

The outer wrap configuration represents a routine condition for fuel assemblies. The polyethylene is modeled as wrapped around the fuel assembly under NCT and HAC. The polyethylene extends halfway from the fuel rod outer radius to the edge of the lattice cell. The NCT outer wrap configuration is modeled as shown in Figure 6-17. Under HAC, three different configurations of polyethylene wrap are examined to represent the movement of the wrap into the fuel assembly envelope due to melting and redistribution. The first configuration simulates the polyethylene as utilized in routine conditions of transport with it wrapped around the fuel assembly. As mass is added to the polyethylene, the additional polyethylene fills in towards the centerline of the fuel assembly such that the outer fuel rods become partially encapsulated in polyethylene, as shown in Figure 6-18.

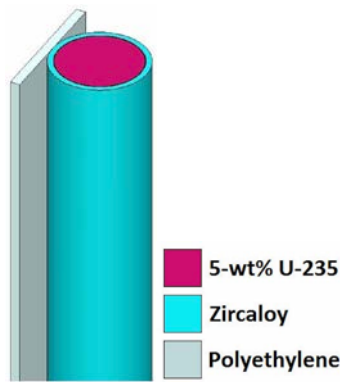


Figure 6-17 PWR Fuel Assembly Polyethylene Outer Wrap NCT Configuration

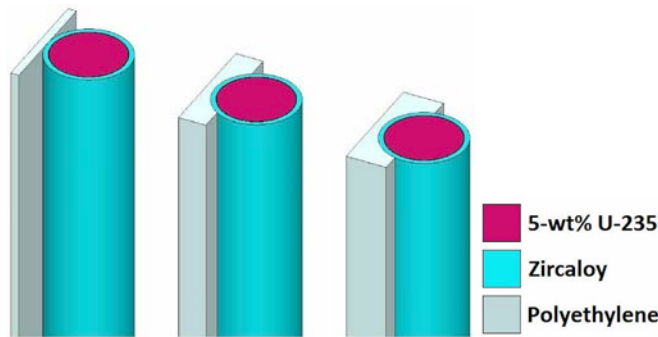


Figure 6-18 PWR Fuel Assembly Polyethylene Outer Wrap HAC Configurations

6.3.4.3.5.2 Uniform Melt Configuration for HAC Package Arrangements

The second configuration simulates the polyethylene melting from its outer wrap position and fully and uniformly encapsulating each fuel rod of the assembly in the radial direction, as shown in Figure 6-19. To model different masses of polyethylene, the thickness is adjusted.

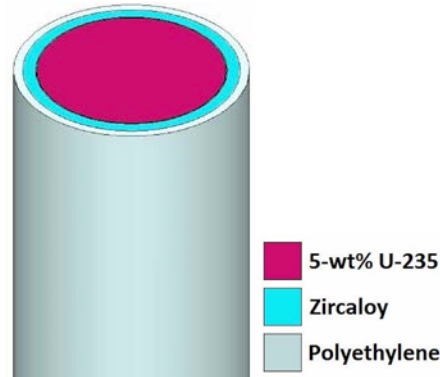


Figure 6-19 Uniform Polyethylene Melt HAC Configuration – PWR Fuel Assemblies

For both routine and normal conditions of transport of loose fuel rods, the rods are wrapped individually in sheets of polyethylene prior to being inserted into the Rod Pipe, which protects the fuel rods from rubbing against each other and foreign material. This configuration is examined for both NCT and HAC with the polyethylene fully and uniformly encapsulating each fuel rod in the radial direction, as shown in Figure 6-20. To model different masses of polyethylene, the thickness is adjusted.

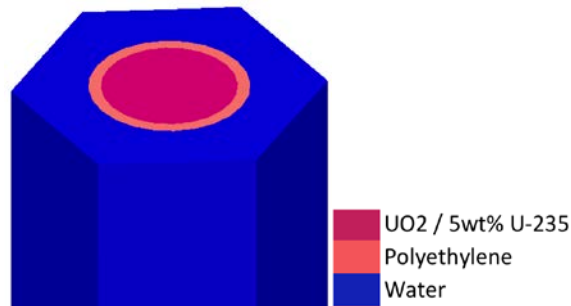


Figure 6-20 Uniform Polyethylene Wrap NCT/HAC Configuration – Rod Pipe

6.3.4.3.5.3 Collected Polyethylene Melt Configuration for HAC Package Arrangements

The third and final configuration simulates the polyethylene melting from its outer wrap position and collecting in the expanded lattice region, where the mass of polyethylene is modified by increasing the height of the modeled polyethylene. However, the lowest melting temperature of the polyethylene wrap material used is 111°C, and 190°C to induce a viscous melt. As presented in Section 3.5.3, the temperatures inside the Clamshell are estimated to be below 104°C (219°F). Therefore, melting of the polyethylene wrap to the extent modeled in this sensitivity study is not expected.

An example fuel assembly collected melt model is shown in Figure 6-21 and a Rod Pipe collected melt model is shown in Figure 6-22. Collected melt is typically the bounding configuration due to (1) the increased

moderation capability of polyethylene in comparison with water and (2) polyethylene collecting in the expanded lattice region, which is more reactive than the nominal lattice region.

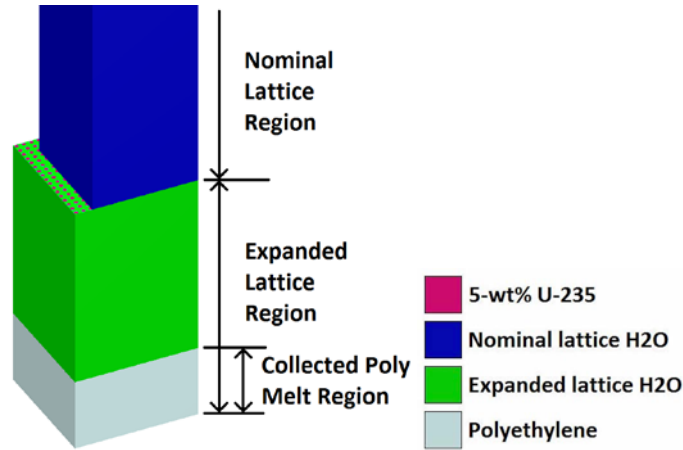


Figure 6-21 PWR Fuel Assembly Collected Polyethylene Melt Configuration

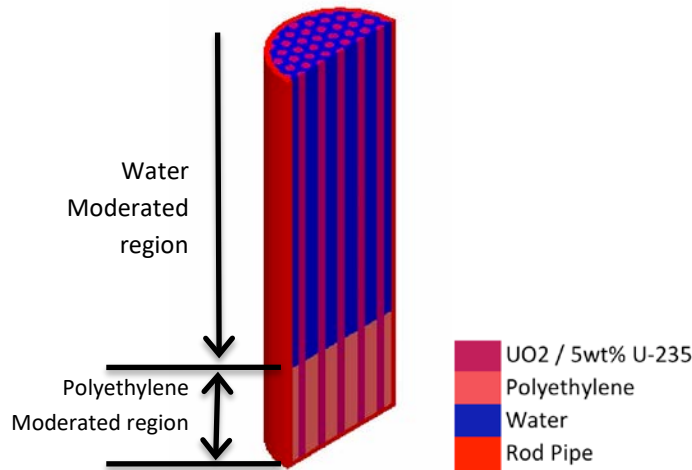


Figure 6-22 Rod Pipe Collected Polyethylene Melt Configuration

6.3.4.3.6 PWR Fuel Assembly Axial Rod Displacement Study

The axial displacement of individual fuel rods to the top of the Clamshell is a result of a package vertical drop during HAC. As detailed in Section 2.12.5.1, the guide pins buckled and four (4) fuel rods moved axially 1 inch but did not extend beyond the neutron poison plates. This displacement is modeled in two configurations: a corner displacement, where two adjacent edge rows are displaced in unison, or a random displacement, where random rods throughout the fuel assembly are all displaced to the axial top of the Clamshell. The random rods are selected in a symmetrical pattern, dispersed throughout the fuel assembly grid. 20, 40, and 64 (or 68, depending on the Group) displaced rods are evaluated. The largest number of displaced rods is equivalent to two adjacent rows of fuel rods on two adjacent sides of the lattice, as shown in Figure 6-23. The three random rod displacement cases model the same number of displaced rods as the three corner rod displacement configurations. This study is only applicable to Groups 1, 2, and 3. Examples of these two displaced fuel rod layouts are shown in Figure 6-23 and Figure 6-24.

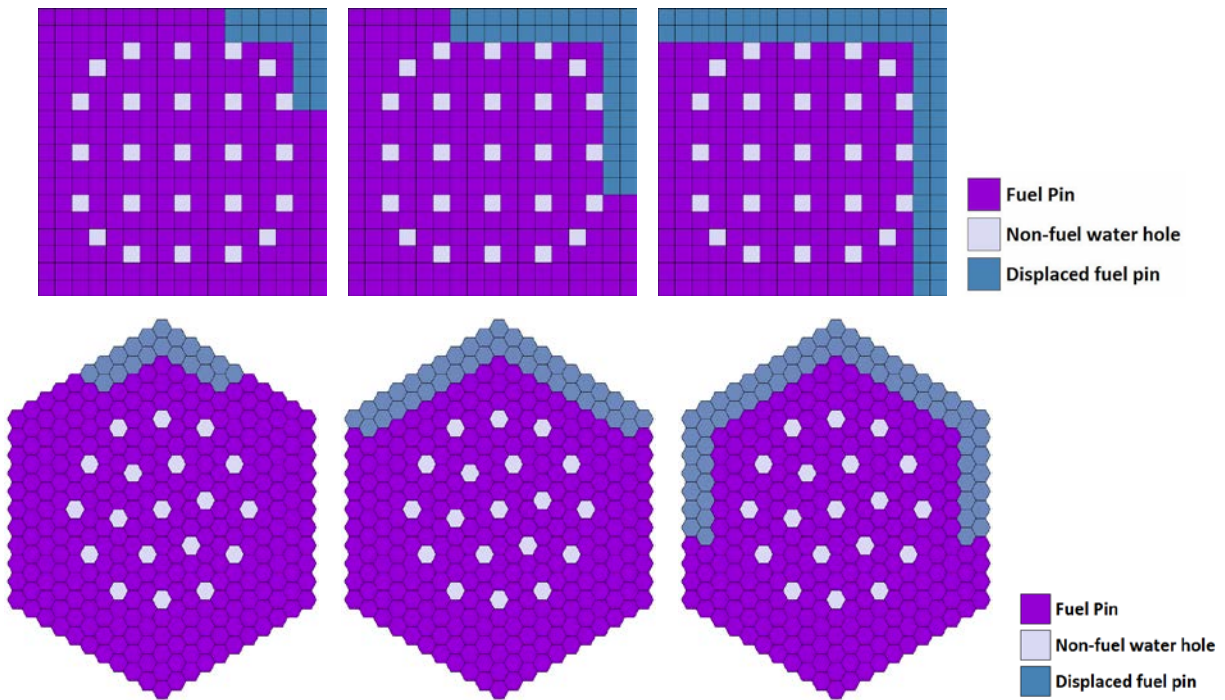


Figure 6-23 Corner Rod Displacement Configurations – 17 Bin 1 (top), VV Bin 1 (bottom)

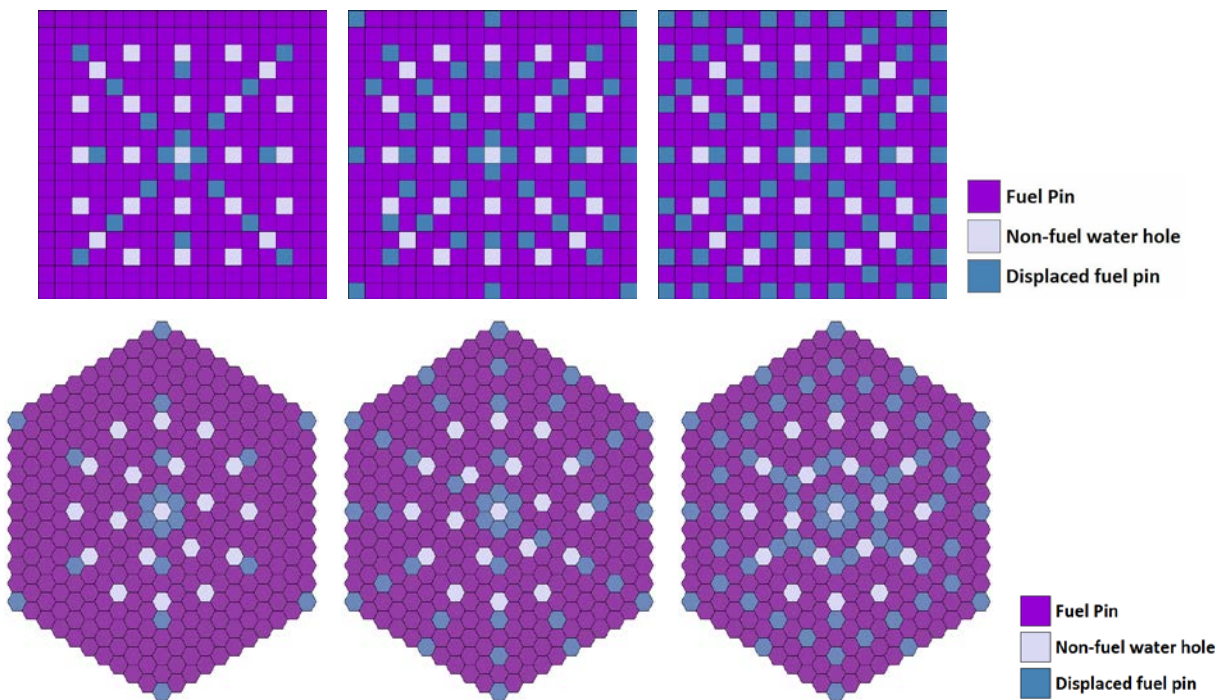


Figure 6-24 Random Rod Displacement Configurations – 17 Bin 1 (top), VV Bin 1 (bottom)

6.3.4.3.7 PWR Fuel Assembly Stainless Steel Replacement Rod Study

Replacement of fuel rods in the fuel assembly with SS rods may be necessary for core performance. This study is only applicable to Groups 1, 2, and 3, and examines the effect on k_{eff} . These rods are added in two configurations: the first configuration replaces two outer edge rows for Groups 1 and 2 and three outer edge rows for Group 3 with SS rods; the second configuration replaces fuel rods with SS rods in “random” locations throughout the fuel assembly. An example of both configurations is shown in Figure 6-25. The random rods are selected in a symmetrical pattern, but are dispersed throughout the fuel assembly grid. The SS rods are modeled with the same OD as their respective fuel rods. The random rod displacement configuration models the same number of displaced rods as the corner rod displacement configuration, while ensuring symmetry is maintained.

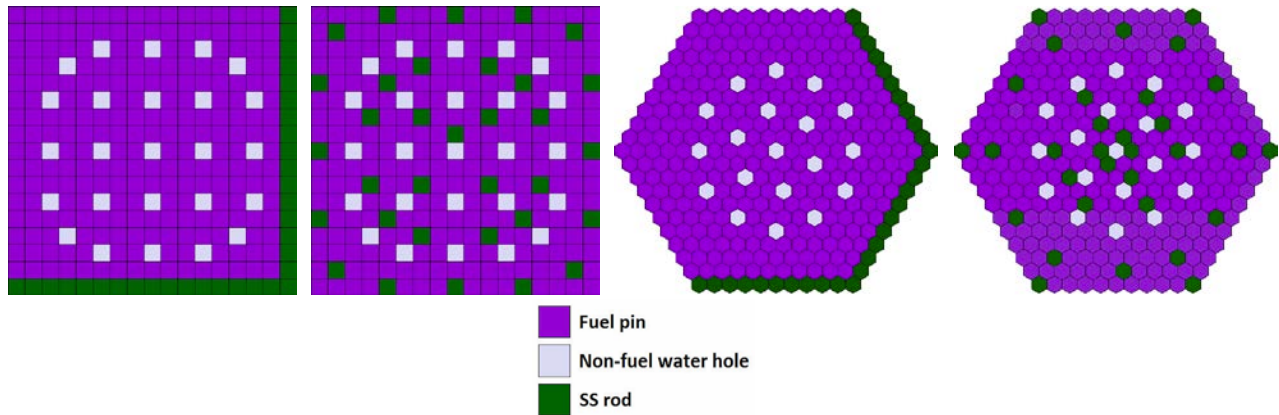


Figure 6-25 SS Replacement Rod Configurations – 17 Bin 1 (left) and VV Bin 1 (right)

Fuel rods in the fuel assembly may be replaced with lead-filled rods, as used in replica assemblies, per the SS replacement rod study. The lead-filled rods are replacing fuel rods, the replacement of which reduces the average fissile density of the fuel assembly, thereby decreasing k_{eff} . While lead has a higher density than steel, thus a potential increase in neutron reflection, this will not result in k_{eff} higher than the baseline case because fissile material is being removed thus decreasing k_{eff} . Finally, lead is not a significant neutron moderator or absorber. Given that lead is a high Z element, it is a strong neutron reflector than steel, but it will not increase the neutron moderation of the system, as any increases in neutron reflection will be negated by the removal of fissile material and the fact that no additional water, i.e. neutron moderation, is being added to the system. Therefore, the results of the SS rod study are applicable to fuel rod replacement by lead-filled rods.

6.3.4.3.8 Cladding Diameter Tolerance Study

The fuel rod cladding of each fuel assembly has a specified fabrication tolerance. Therefore, tolerance in cladding radial dimensions ID and OD and its effect on k_{eff} was examined. The tolerance ranges examined for each package arrangement are listed in Table 6-19 and are created based on the fuel assemblies of each bin. The tolerance is applied to the cladding ID and OD independently. Cladding tolerance was not examined for the Rod Pipe arrangement because no cladding was modeled in the Rod Pipe analysis.

Table 6-19 Cladding Diameter Tolerances Examined		
Contents	Cladding Diameter Tolerance	
	in.	cm
Group 1	±0.002	±0.0051
Group 2	±0.002	±0.0051
Group 3	±0.0015	±0.0038
Rod Pipe	--	--

6.3.4.3.9 Fuel Pellet Diameter Tolerance Study

The fuel pellet diameter of each fuel assembly has a specified fabrication tolerance. Therefore, the tolerance variation in the fuel pellet radial dimension and its effect on k_{eff} was examined. The tolerance ranges examined for each package arrangement are listed in Table 6-20 and are created based on the fuel assemblies of each bin. The largest tolerance of the Groups is applied to the Rod Pipe content.

Table 6-20 Fuel Pellet Diameter Tolerances Examined		
Contents	Fuel Pellet Diameter Tolerance	
	in.	cm
Group 1	±0.0005, ±0.0007	±0.0013, ±0.0018
Group 2	±0.0005, ±0.0007	±0.0013, ±0.0018
Group 3	±0.0005	±0.0013
Rod Pipe	±0.0010, ±0.0014	±0.0025, ±0.0036

6.3.4.3.10 Fuel Rod Pitch Tolerance Study

The fuel rod pitch of each fuel assembly has a specified fabrication tolerance. Therefore, its effect on k_{eff} was examined. The tolerance ranges examined are listed in Table 6-21 and are created based on the fuel assemblies of each bin. This study was not done for the Rod Pipe package arrangement, as the loose rods are not restricted to a design lattice configuration. The Group 1 single package fuel rod pitch tolerance range includes Group 1 and 2 tolerance values, because they were analyzed together in the single package evaluation. Therefore, Group 1 and 2 single package tolerance range is larger than the Group 1 package array fuel rod pitch tolerance. For HAC, only the pitch of the nominal lattice region is changed, because the maximum possible pitch is already modeled in the expanded lattice region.

Contents	Evaluation	Condition	Fuel Rod Pitch Tolerance	
			in.	cm
Groups 1 and 2	Single Package	NCT	-0.0685, -0.0343, +0.0059, +0.0118	-0.174, -0.087, +0.015, +0.03
		HAC	-0.0785, -0.0393, +0.0059, +0.0118	-0.1994, -0.0997, +0.015, +0.03
Group 1	Package Array	NCT and HAC	±0.001, ±0.005	±0.0025, ±0.0127
Group 2	Package Array	NCT	-0.0335, -0.0167, +0.0059, +0.0118	-0.085, -0.0425, +0.015, +0.03
		HAC	-0.0630, -0.0315, +0.0059, +0.0118	-0.16, -0.08, +0.015, +0.03
Group 3	Single Package, Package Array	NCT and HAC	±0.001	±0.0025
Rod Pipe	--	--	--	--

6.3.4.3.11 Steel Nozzle Reflector Study

This study is included to determine if modeling the top and bottom nozzles as their materials of construction, instead of replacing them with full-density light water, could result in an increase in reactivity for a package array under NCT or HAC. In the baseline cases, the top and bottom nozzles are modeled as void for NCT and the top and bottom nozzles are modeled as full-density light water for HAC. For this study, three configurations, one NCT and two HAC cases, are examined with a 30 kg SS304 top nozzle and a 15 kg of SS304 bottom nozzle. The nozzles are modeled as blocks, equivalent in the x- and y-dimensions to the fuel envelope of each assembly, with the height of the blocks being adjusted to accommodate the full mass of stainless steel.

For NCT, solid blocks that model 50% density SS304 are added to the top and bottom of the fuel assemblies. This configuration is shown in Figure 6-26 with the nozzle regions colored green. For the first HAC configuration, solid blocks are modeled as 50% density SS304 with the remaining volume of the blocks as full density water. The other HAC configuration models the top and bottom nozzles as 100% density SS304. An example of the HAC configuration is shown in Figure 6-27 with the nozzle regions colored green.

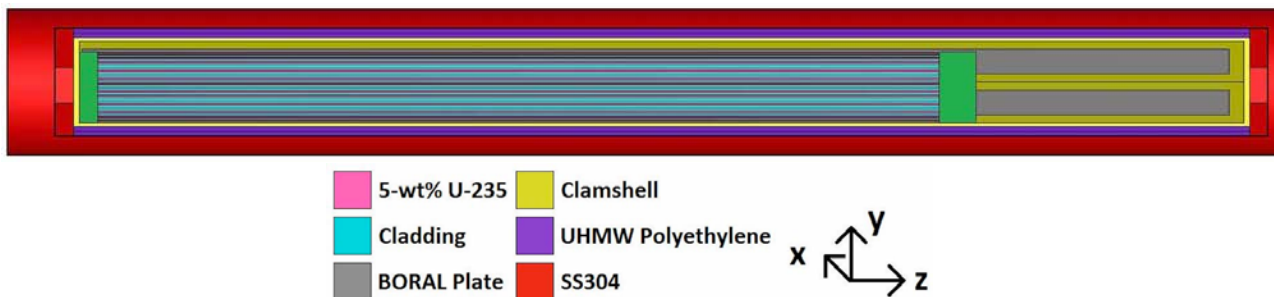


Figure 6-26 Example of NCT Stainless Steel Nozzle Configuration, Shown in Green

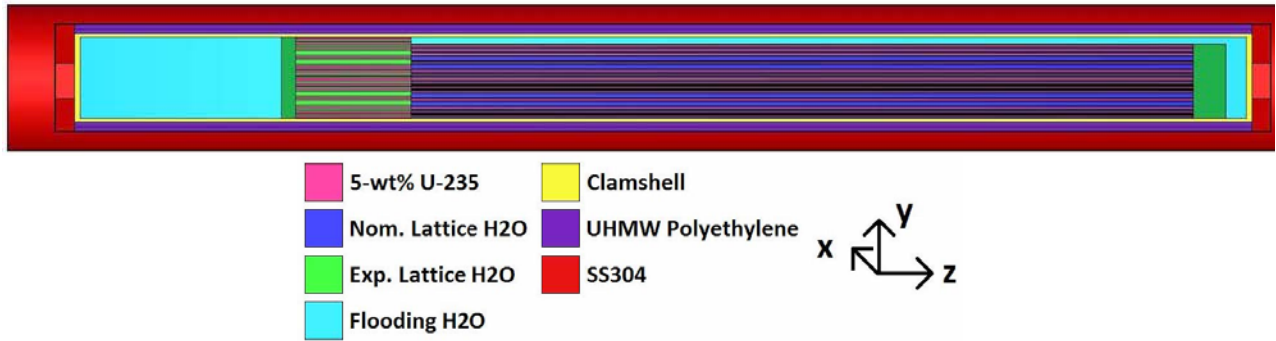


Figure 6-27 Example of HAC Stainless Steel Nozzle Configuration, Shown in Green

6.3.4.3.12 Extended Active Fuel Length Sensitivity Study

An extended active fuel length sensitivity study was only examined for Group 3 to assess the slightly longer active fuel lengths of future fuel designs. The extended range of examination includes the extended fuel length plus one tolerance, following the methodology in Section 6.9.2.1. The total extended range is less than one-inch and within two stacked tolerances. Therefore, the small extended length will have no significant impact on the results for the development of the baseline case, as defined in Section 6.9.3. Hence the extended active fuel length is evaluated as a sensitivity parameter.

6.3.4.3.13 HAC Rod Pipe Package Array Flooding Configuration Study

Preferential flooding is evaluated for package array HAC by holding one packaging cavity as flooded with full density water or void, while one or more of the other packaging cavities varies the water density. The first configuration floods the regions outside of the Clamshell, but not the Clamshell cavity. The second configuration floods only the Clamshell cavity. Figure 6-28 shows the regions that are moderated for each case.

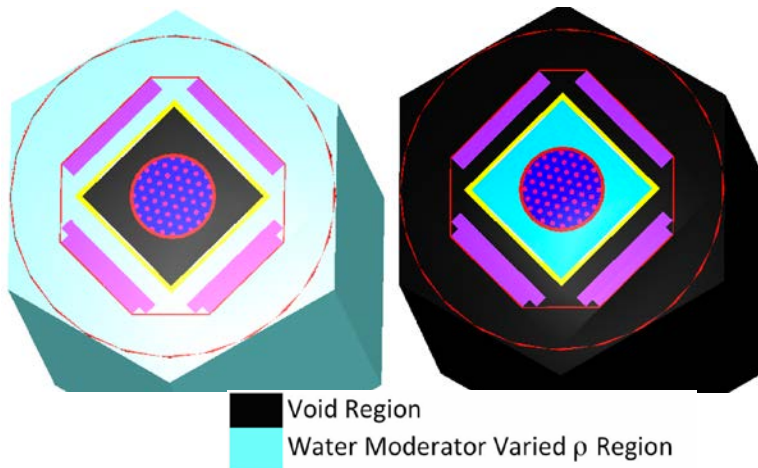


Figure 6-28 Rod Pipe HAC Package Array Flooding Configurations

6.3.4.3.14 ADOPT Fuel Study

This study evaluates the effect of UO_2 fuel with ADOPT fuel instead of standard UO_2 fuel. Because the additives in ADOPT rods are limited to very small quantities (700 ppm Cr_2O_3 and up to 200 ppm Al_2O_3), the reactivity effect is expected to be minimal. While fuel assemblies or the loose fuel rod contents may contain any number of ADOPT fuel rods in any location, this study models every rod in the fuel assembly or Rod Pipe with ADOPT fuel to analyze the maximum potential effect of the ADOPT fuel. This study is only applied to PWR Groups 1 and 2 and UO_2 loose fuel rods. ADOPT fuel is not allowable content in PWR Group 3 assemblies or U_3Si_2 loose fuel rods.

6.4 SINGLE PACKAGE EVALUATION

6.4.1 Configuration

For all single package arrangements and conditions of transport, all inner spaces of the package are modeled as flooded with full-density water, including the fuel-clad gap where applicable. Additional material modeling is specified in Section 6.3.2. Several materials, including fuel structural components and packaging components (e.g. Outerpack foam regions, ceramic fiber blankets, and shock mounts, etc.), are replaced with full-density water. The single package is reflected with 20 cm of full-density water.

6.4.1.1 Baseline Configurations

As described in Section 6.3.4.2, a baseline case is evaluated for all content Groups and Rod Pipe configurations under NCT and HAC. Baseline configurations represent a bounding model that is carried forward to the sensitivity studies to demonstrate maximum reactivity.

6.4.1.1.1 Fuel Assembly –Group 1, 2 and 3

For the baseline case determination, as defined in Section 6.3.4.2.1, first the bounding CFA-package variant combination is determined. For the single package assessment, the Traveller XL is consistently more reactive than the Traveller STD under NCT and HAC. As discussed in Section 6.3.4.2.1.2, the positioning of the fuel assembly is examined because of the physical properties of the packaging. Detailed results of the baseline case determination are shown in Section 6.9.3.1. The NCT baseline configuration is shown in Figure 6-29 and the HAC baseline configuration is shown in Figure 6-30. The baseline cases are summarized in Table 6-22.

Condition of Transport	Traveller Variant	Contents (Group)	Lattice Expansion Length (cm)	Axial Position (cm)	Flooding Configuration	$k_{eff} \pm \sigma$
NCT	XL	18 Bin 1 (1 & 2)	0.0	72.583	All Regions	0.88499 ± 0.00059
HAC	XL	17 Bin 1 (1 & 2)	50.8	87.122	All Regions	0.90209 ± 0.00049
NCT	VVER	VV Bin 1 (3)	0.0	51.854	All Regions	0.86201 ± 0.00025
HAC	VVER	VV Bin 1 (3)	50.8	51.854	All Regions	0.88241 ± 0.00025

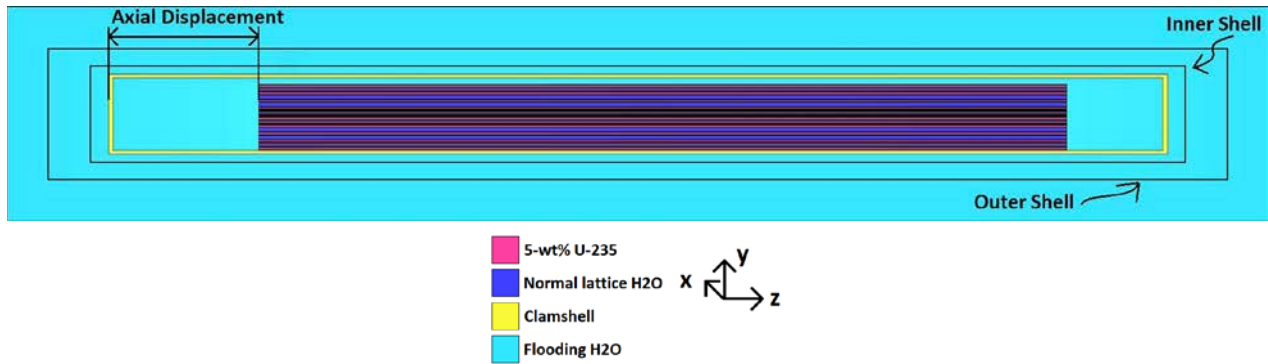


Figure 6-29 Cross-section NCT Single Package Baseline Case

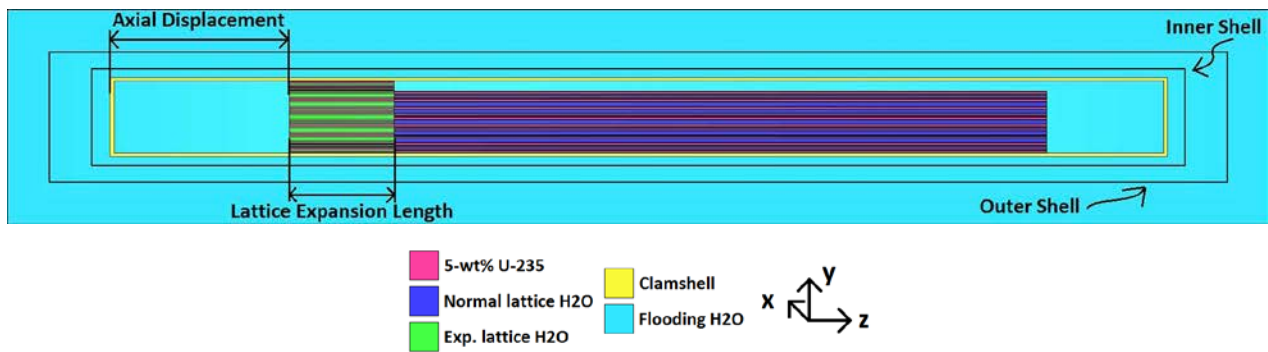


Figure 6-30 Cross-section HAC Single Package Baseline Case

6.4.1.1.2 Rod Pipe

For the baseline case determination, as defined in Section 6.3.4.2.2, loose rods are modeled in the Rod Pipe. The pitch is expanded starting with a close pack configuration for NCT expanding through a peak water-to-fuel ratio by increasing the pitch for HAC. The pitch type is modeled as both square and hexagonal as the small variation of geometry varies the water-to-fuel ratio slightly. The Traveller STD and Traveller XL packages are evaluated with the Rod Pipe as the only loose rod shipment configuration. The single package is fully flooded to increase moderation of the single package fissile content. Detailed results of the Rod Pipe contents analysis are shown in Section 6.9.3.2. Comparison of the Traveller STD to Traveller XL baseline results show that the Traveller XL is consistently more reactive than the Traveller STD. There are two Rod Pipe baseline cases for UO_2 fuel rods, which are bounding of all UO_2 Rod Pipe configurations under NCT and HAC for the Traveller STD and XL variants. There are two Rod Pipe baseline cases for U_3Si_2 fuel rods, which are bounding of all U_3Si_2 Rod Pipe configurations under NCT and HAC for the Traveller STD variant. The baseline cases are summarized in Table 6-23.

Contents	Condition of Transport	Traveller Variant	Fuel OR (cm)	Pitch-Type	Fuel Rod Half-Pitch (cm)	Flooding Configuration	$k_{eff} \pm \sigma$
UO ₂ Fuel Rods	NCT	XL	3.5	Square	3.5	All regions	0.56435 ± 0.00086
UO ₂ Fuel Rods	HAC	XL	0.55	Hexagonal	1.00	All regions	0.72106 ± 0.00047
U ₃ Si ₂ Fuel Rods	NCT	STD	0.4851	Square	0.4851	All regions	0.42948 ± 0.00037
U ₃ Si ₂ Fuel Rods	HAC	STD	0.4851	Hexagonal	1.0101	All regions	0.67492 ± 0.00049

6.4.1.2 Sensitivity Study Configurations

Several sensitivity studies are completed for the NCT and HAC single package evaluation. The following summary tables list the as-penalized configurations of each sensitivity study. An entry of “None” signifies that the study resulted in no penalty and an entry of “--” signifies that the study did not require analyzing based on transport condition. The baseline case ($k_p + 2\sigma_p$) with the sum of penalties from the sensitivity studies (Δk_{iu}) defines the most reactive configuration ($Maximum\ k_{eff} = k_p + 2\sigma_p + \Delta k_{iu}$) and demonstrates the maximum reactivity for single package transport condition.

6.4.1.2.1 Fuel Assembly – Group 1, 2 and 3

Listed in Table 6-24 are the bounding, as-penalized configurations of each sensitivity study for Groups 1, 2, and 3.

Sensitivity Study	Bounding Configuration Group 1 and 2		Bounding Configuration Group 3	
	NCT	HAC	NCT	HAC
Annular Fuel Pellet Blanket	Full-length	Full-length	Full-length	Full-length
Fuel Assembly Shift	Centered	Centered	None	Centered
Moderator Block Density	--	1% density reduction	--	1% density reduction
Polyethylene Packing Materials	5.54 kg of polyethylene	2.00 kg of polyethylene	4.96 kg of polyethylene	2.00 kg of polyethylene
Axial Rod Displacement	--	None	--	None
Stainless Steel Rods	None	None	None	None
Cladding (ID/OD) Dimensions Tolerance	Minimum cladding thickness	Minimum cladding thickness	Minimum cladding thickness	Minimum cladding thickness
Fuel Pellet Diameter Tolerance	None	None	None	Minimum Fuel Diameter
Extended Active Fuel Length	--	--	None	Longer length
Fuel Rod Pitch Tolerance	+ tolerance	+ tolerance	+ tolerance	None
ADOPT Fuel	None	ADOPT rods	--	--

Note: ‘--’ signifies the study was not applicable to the condition of transport analyzed. ‘None’ signifies that the sensitivity study did not result in a statistically significant increase in reactivity over the baseline case.

6.4.1.2.2 Rod Pipe

Listed in Table 6-25 are the bounding, as-penalized configurations of each sensitivity study for Rod Pipe content.

Sensitivity Study	Bounding Configuration UO ₂ Fuel Rods		Bounding Configuration U ₃ Si ₂ Fuel Rods	
	NCT	HAC	NCT	HAC
Annular Fuel Pellet Blanket	Full-length with proportional ID	Full-length	Full-length	None
Rod Pipe Position in Clamshell	None	None	None	None
Moderator Block Density	--	None	--	None
Polyethylene Packing Materials	0.5 cm-thick polyethylene wrap	Rod Pipe full of polyethylene	0.3654 cm-thick polyethylene wrap	Rod Pipe full of polyethylene
Fuel Pellet Diameter Tolerance	None	None	+0.0014 in. tolerance	None
ADOPT Fuel	None	None	--	--

Note: '--' signifies the study was not applicable to the condition of transport analyzed. 'None' signifies that the sensitivity study did not result in a statistically significant increase in reactivity over the baseline case.

6.4.2 Results

6.4.2.1 Single Package – Maximum Reactivity Results Summary

The maximum reactivity, *Maximum* k_{eff} , is defined by the bounding baseline $k_p + 2\sigma_p$ plus the sum of penalties assessed for each sensitivity study (Δk_u). See Table 6-26 for a summary of the *Maximum* k_{eff} results. Final values of maximum reactivity fall under the USL, as calculated per Section 6.8.

Condition of Transport	Traveller Variant	Bounding Content	$k_{eff} \pm \sigma$	$k_p + 2\sigma_p$	Δk_u	<i>Maximum</i> k_{eff}	USL
NCT	XL	18 Bin 1 (Group 1 & 2)	0.88499 ± 0.00059	0.88617	0.03534	0.92151	0.94067
HAC	XL	17 Bin 1 (Group 1 & 2)	0.90209 ± 0.00049	0.90307	0.01780	0.92087	0.94067
NCT	VVER	VV Bin 1 (Group 3)	0.86201 ± 0.00025	0.86251	0.02681	0.88932	0.94029
HAC	VVER	VV Bin 1 (Group 3)	0.88241 ± 0.00025	0.88291	0.01737	0.90028	0.94029
NCT	XL	Rod Pipe UO ₂ Fuel Rods	0.56435 ± 0.00086	0.56607	0.06972	0.63579	0.94044
HAC	XL	Rod Pipe UO ₂ Fuel Rods	0.72106 ± 0.00047	0.72200	0.07377	0.79577	0.94044
NCT	STD	Rod Pipe U ₃ Si ₂ Fuel Rods	0.42948 ± 0.00037	0.43022	0.29857	0.72879	0.94053
HAC	STD	Rod Pipe U ₃ Si ₂ Fuel Rods	0.67492 ± 0.00049	0.67590	0.06371	0.73961	0.94053

6.4.2.2 Sensitivity Study Results

As discussed in Section 6.3.4.3, the NCT and HAC baseline cases, for each package arrangement, are subjected to several sensitivity studies, which are detailed in Table 6-18. Each sensitivity study is compared to the baseline case. The most reactive configuration resulting in the largest positive difference in $k_{eff} + 2\sigma$ from the baseline case value is tallied and summed to define the total penalty assessed (Δk_u).

6.4.2.2.1 Fuel Assembly – Group 1, 2, and 3 Results Summary

Table 6-27 shows the summary of the penalty assessed for the sensitivity studies evaluated for the Groups 1, 2, and 3 contents. An entry of “0.0” signifies that the study resulted in no positive penalty on reactivity and an entry of “--” signifies that the study did not require analyzing based on transport condition.

Table 6-27 Single Package Assessed Penalties, Δk_u, Groups 1, 2, and 3				
Sensitivity Study	Penalty Assessed			
	Groups 1 and 2		Group 3	
	NCT	HAC	NCT	HAC
Annular Fuel Pellet Blanket	0.01273	0.0	0.02048	0.00749
Centered Fuel Assembly	0.00202	0.00266	0.0	0.00079
Moderator Block Density	--	0.00157	--	0.00064
Polyethylene Packing Materials	0.00168	0.00284	0.00077	0.00261
Axial Rod Displacement	--	0.0	--	0.0
Stainless Steel Rods	0.0	0.0	0.0	0.0
Cladding Dimensions Tolerance	0.00529	0.00495	0.00419	0.00395
Fuel Pellet Diameter Tolerance	0.0	0.0	0.0	0.00073
Fuel Rod Pitch Tolerance	0.01362	0.00457	0.00137	0.0
Extended Active Fuel Length	--	--	0.0	0.00116
ADOPT Fuel	0.0	0.00121	--	--
Total Penalty (Δk_u)	0.03534	0.01780	0.02681	0.01737

6.4.2.2.2 Fuel Assembly – Groups 1, 2, and 3 NCT Detailed Results

The annular blanket sensitivity study, as defined in Section 6.3.4.3.1, examined the addition of varying annular fuel pellet ID and lengths of annular fuel pellet blanket lengths equally to the top and bottom of an assembly. Table 6-28 defines the parameters evaluated and the results. Figure 6-31 and Figure 6-32 display the result trends for Groups 1, 2, and Group 3, respectively. The most reactive case is highlighted for each Group.

Contents (Group)	Traveller Variant	Annulus Diameter	Annulus Length (cm)	k_{eff}	σ	$k_{eff} + 2\sigma$	$\Delta(k_{eff} + 2\sigma)$		
18 Bin 1 (1 & 2)	XL	Baseline Case		0.88499	0.00059	0.88617	--		
		0.155 in. (0.3937 cm)	48.9	0.88628	0.00057	0.88742	0.00125		
			97.8	0.8897	0.00055	0.8908	0.00463		
			146.7	0.894	0.00048	0.89496	0.00879		
			195.6	0.89784	0.00053	0.8989	0.01273		
		0.183 in. (0.4648 cm)	48.9	0.88528	0.00053	0.88634	0.00017		
			97.8	0.88915	0.00058	0.89031	0.00414		
			146.7	0.89277	0.00048	0.89373	0.00756		
			195.6	0.89604	0.00053	0.89710	0.01093		
		VV Bin 1 (3)	VVER	Baseline Case		0.86201	0.00025	0.86251	--
				0.155 in. (0.3937 cm)	45.5	0.86348	0.00026	0.86400	0.00149
					91.1	0.87034	0.00024	0.87082	0.00831
136.6	0.8763				0.00026	0.87682	0.01431		
182.1	0.88049				0.00028	0.88105	0.01854		
0.183 in. (0.4648 cm)	45.5			0.86436	0.00024	0.86484	0.00233		
	91.1			0.87222	0.00025	0.87272	0.01021		
	136.6			0.87755	0.00027	0.87809	0.01558		
	182.1			0.88251	0.00024	0.88299	0.02048		

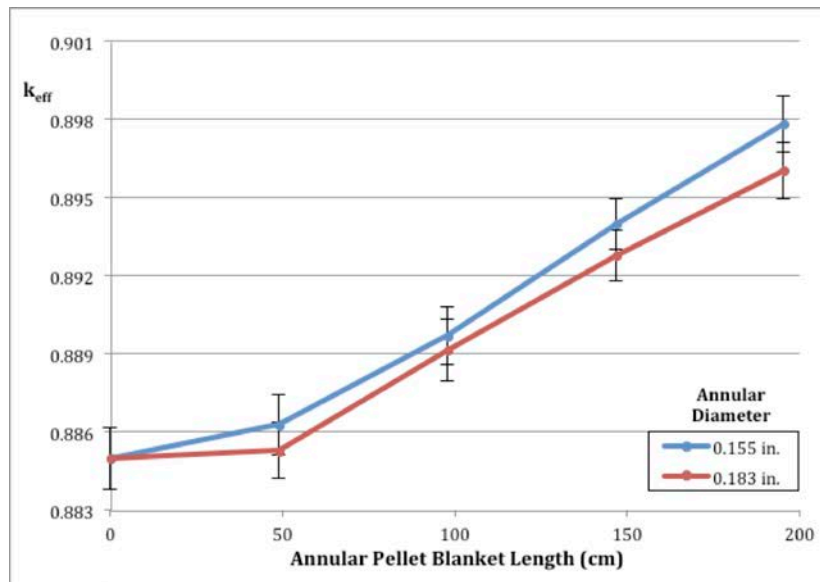


Figure 6-31 Annular Blanket Sensitivity – Single Package, NCT (Groups 1 & 2)

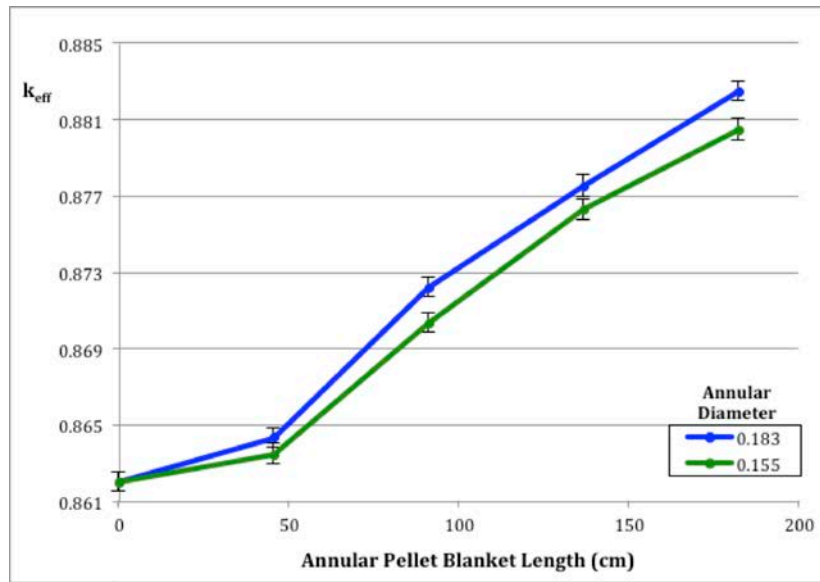


Figure 6-32 Annular Blanket Sensitivity – Single Package, NCT (Group 3)

The fuel assembly position sensitivity study, as defined in Section 6.3.4.3.2, examined the centering of the fuel assembly in the Clamshell. Table 6-29 defines the parameter evaluated and the results. The most reactive case is highlighted for each Group.

Contents (Group)	Traveller Variant	Fuel Assembly Position	k _{eff}	σ	k _{eff} + 2σ	Δ(k _{eff} + 2σ)
18 Bin 1 (1 & 2)	XL	Baseline Case	0.88499	0.00059	0.88617	--
		Centered	0.88715	0.00052	0.88819	0.00202
VV Bin 1 (3)	VVER	Baseline Case	0.86201	0.00025	0.86251	--
		Centered	0.86175	0.00028	0.86231	-0.0002

The polyethylene packing materials sensitivity study, as defined in Section 6.3.4.3.5, examined the presence of an outer wrap around the fuel assembly. Table 6-30 defines the parameter evaluated and the results. The most reactive case is highlighted for each Group.

Contents (Group)	Traveller Variant	Poly Model	Poly Mass (kg)	k _{eff}	σ	k _{eff} + 2σ	Δ(k _{eff} + 2σ)
18 Bin 1 (1 & 2)	XL	Baseline Case	0	0.88499	0.00059	0.88617	--
		Outer Wrap	5.54	0.88691	0.00047	0.88785	0.00168
VV Bin 1 (3)	VVER	Baseline Case	0	0.86201	0.00025	0.86251	--
		Outer Wrap	4.962	0.8628	0.00024	0.86328	0.00077

The SS replacement rod sensitivity study, as defined in Section 6.3.4.3.7, examined replacement of fuel rods with SS rod within the fuel assembly. Table 6-31 defines the parameters evaluated and the results. The most reactive case is highlighted for each Group.

Contents (Group)	Traveller Variant	SS Rod Configuration	k_{eff}	σ	$k_{eff} + 2\sigma$	$\Delta(k_{eff} + 2\sigma)$
18 Bin 1 (1 & 2)	XL	Baseline Case	0.88499	0.00059	0.88617	--
		Corner	0.85862	0.00051	0.85964	-0.02653
		Random	0.8353	0.00058	0.83646	-0.04971
VV Bin 1 (3)	VVER	Baseline Case	0.86201	0.00025	0.86251	--
		Corner	0.83091	0.00028	0.83147	-0.03104
		Random	0.81302	0.00024	0.8135	-0.04901

The tolerance sensitivity studies evaluate cladding dimensions, fuel pellet diameter, and fuel rod pitch, as defined in Sections 6.3.4.3.8, 6.3.4.3.9, and 6.3.4.3.10, respectively. Table 6-32 defines the parameter dimensions evaluated and the results. The most reactive case is highlighted for each Group and tolerance parameter.

Content (Group)	Traveller Variant	Tolerance Parameter		k_{eff}	σ	$k_{eff} + 2\sigma$	$\Delta(k_{eff} + 2\sigma)$
18 Bin 1 (1 & 2)	XL	Baseline Case		0.88499	0.00059	0.88617	--
VV Bin 1 (3)	VVER	Baseline Case		0.86201	0.00025	0.86251	--
Cladding Tolerance		ID Tolerance (in.)	OD Tolerance (in.)	k_{eff}	σ	$k_{eff} + 2\sigma$	$\Delta(k_{eff} + 2\sigma)$
18 Bin 1 (1 & 2)	XL	-0.002	-0.002	0.88547	0.00048	0.88643	0.00026
			nominal	0.88296	0.00049	0.88394	-0.00223
			+0.002	0.87955	0.00052	0.88059	-0.00558
		nominal	-0.002	0.88832	0.00061	0.88954	0.00337
			nominal	0.88499	0.00059	0.88617	--
			+0.002	0.88320	0.00052	0.88424	-0.00193
		+0.002	-0.002	0.89042	0.00052	0.89146	0.00529
			nominal	0.88805	0.00045	0.88895	0.00278
			+0.002	0.88548	0.00055	0.88658	0.00041
VV Bin 1 (3)	VVER	-0.0015	-0.0015	0.86201	0.00025	0.86251	0.00000
			nominal	0.85996	0.00025	0.86046	-0.00205
			+0.0015	0.85819	0.00024	0.85867	-0.00384
		nominal	-0.0015	0.86415	0.00027	0.86469	0.00218
			nominal	0.86201	0.00025	0.86251	--
			+0.0015	0.86018	0.00025	0.86068	-0.00183
		+0.0015	-0.0015	0.86618	0.00026	0.8667	0.00419
			nominal	0.86407	0.00024	0.86455	0.00204
			+0.0015	0.86185	0.00023	0.86231	-0.00020

Content (Group)	Traveller Variant	Tolerance Parameter	k_{eff}	σ	$k_{eff} + 2\sigma$	$\Delta(k_{eff} + 2\sigma)$
Pellet Diameter Tolerance		Pellet OD Tolerance (in.)	k_{eff}	σ	$k_{eff} + 2\sigma$	$\Delta(k_{eff} + 2\sigma)$
18 Bin 1 (1 & 2)	XL	-0.0007	0.88553	0.00035	0.88623	0.00006
		-0.0005	0.88562	0.00038	0.88638	0.00021
		+0.0005	0.8852	0.00038	0.88596	-0.00021
		+0.0007	0.88443	0.00036	0.88515	-0.00102
VV Bin 1 (3)	VVER	-0.0005	0.86243	0.00026	0.86295	0.00044
		+0.0005	0.86168	0.00025	0.86218	-0.00033
Pitch Tolerance		Pitch Tolerance (in.)	k_{eff}	σ	$k_{eff} + 2\sigma$	$\Delta(k_{eff} + 2\sigma)$
18 Bin 1 (1 & 2)	XL	-0.0685	0.76608	0.00056	0.7672	-0.11897
		-0.0343	0.83591	0.00048	0.83687	-0.04930
		+0.0059	0.89201	0.00055	0.89311	0.00694
		+0.0118	0.89863	0.00058	0.89979	0.01362
VV Bin 1 (3)	VVER	-0.001	0.86093	0.00026	0.86145	-0.00106
		+0.001	0.8633	0.00029	0.86388	0.00137

The fuel assembly position sensitivity study, as defined in Section 6.3.4.3.12, examined the extended active fuel length for Group 3. Table 6-33 defines the parameter evaluated and the results. The most reactive case is highlighted.

Contents (Group)	Traveller Variant	Active Fuel Length (cm)	k_{eff}	σ	$k_{eff} + 2\sigma$	$\Delta(k_{eff} + 2\sigma)$
VV Bin 1 (3)	VVER	Baseline Case 364.261	0.86201	0.00025	0.86251	--
		364.631	0.86191	0.00024	0.86239	-0.00012
		365.000	0.86193	0.00025	0.86243	-0.00008
		366.270	0.86244	0.00024	0.86292	0.00041

The ADOPT fuel sensitivity study, as defined in Section 6.3.4.3.14, examined the effect of replacing standard UO₂ fuel with ADOPT fuel. Table 6-33A lists the results of the study. The most reactive case is highlighted.

Contents (Group)	Traveller Variant	Fuel Material	k_{eff}	σ	$k_{eff} + 2\sigma$	$\Delta(k_{eff} + 2\sigma)$
18 Bin 1 (1 & 2)	XL	UO ₂	0.88499	0.00059	0.88617	--
		ADOPT	0.88470	0.00060	0.88590	-0.00027

6.4.2.2.3 Fuel Assembly – Groups 1, 2, and 3 HAC Detailed Results

The annular blanket sensitivity study, as defined in Section 6.3.4.3.1, examined the addition of varying annular fuel pellet ID and lengths of annular fuel pellet blanket lengths equally to the top and bottom of an assembly. Table 6-34 defines the parameters evaluated and the results. Figure 6-33 and Figure 6-34 display the result trends for Groups 1, 2, and Group 3, respectively. The most reactive case is highlighted for each Group.

Table 6-34 Annular Blanket Sensitivity Results – Single Package, HAC, Groups 1, 2, and 3									
Content (Group)	Traveller Variant	Annulus Diameter	Annulus Length (cm)	k_{eff}	σ	k_{eff} + 2σ	Δ(k_{eff} + 2σ)		
17 Bin 1 (1 & 2)	XL	Baseline Case		0.90209	0.00049	0.90307	--		
		0.155 in. (0.3937 cm)	13	0.90189	0.0006	0.90309	0.00002		
			26	0.89915	0.00048	0.90011	-0.00296		
			39	0.89378	0.00049	0.89476	-0.00831		
			50.8	0.88971	0.00058	0.89087	-0.01220		
			95.038	0.89038	0.0005	0.89138	-0.01169		
			139.277	0.89054	0.00048	0.8915	-0.01157		
			183.515	0.89123	0.00059	0.89241	-0.01066		
		0.183 in. (0.4648 cm)	13	0.90188	0.00054	0.90296	-0.00011		
			26	0.89602	0.00054	0.8971	-0.00597		
			39	0.88734	0.00058	0.8885	-0.01457		
			50.8	0.879	0.00052	0.88004	-0.02303		
			95.038	0.88073	0.00055	0.88183	-0.02124		
			139.277	0.88022	0.00061	0.88144	-0.02163		
			183.515	0.88055	0.00052	0.88159	-0.02148		
		VV Bin 1 (3)	VVER	Baseline Case		0.88241	0.00025	0.88291	--
				0.155 in. (0.3937 cm)	45.53	0.88308	0.00024	0.88356	0.00065
91.07	0.88499				0.00024	0.88547	0.00256		
136.6	0.88957				0.00026	0.89009	0.00718		
182.13	0.88982				0.00029	0.8904	0.00749		
0.183 in. (0.4648 cm)	45.53			0.88174	0.00025	0.88224	-0.00067		
	91.07			0.881	0.00028	0.88156	-0.00135		
	136.6			0.88717	0.00026	0.88769	0.00478		
	182.13			0.88709	0.00028	0.88765	0.00474		

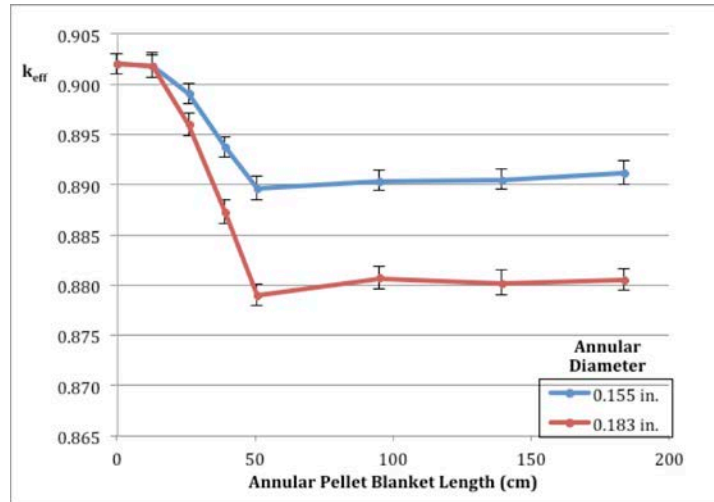


Figure 6-33 Annular Blanket Sensitivity Results – Single Package, HAC (Groups 1 & 2)

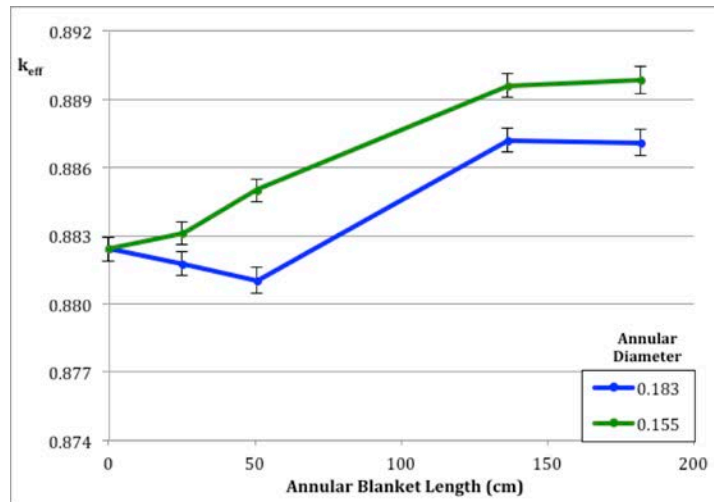


Figure 6-34 Annular Blanket Sensitivity Results – Single Package, HAC (Group 3)

The fuel assembly position sensitivity study, as defined in Section 6.3.4.3.2, examined the centering of the fuel assembly in the Clamshell. Table 6-34A defines the parameter evaluated and the results. The most reactive case is highlighted for each Group.

Contents (Group)	Traveller Variant	Fuel Assembly Position	k_{eff}	σ	$k_{eff} + 2\sigma$	$\Delta(k_{eff} + 2\sigma)$
18 Bin 1 (1 & 2)	XL	Baseline Case	0.90209	0.00049	0.90307	--
		Centered	0.90457	0.00058	0.90573	0.00266
VV Bin 1 (3)	VVER	Baseline Case	0.88241	0.00025	0.88291	--
		Centered	0.88320	0.00025	0.88370	0.00079

The moderator block density reduction sensitivity study, as defined in Section 6.3.4.3.3, examined the post-fire condition of the moderator block. Table 6-35 defines the parameter evaluated and the results. The most reactive case is highlighted for each Group.

Content (Group)	Traveller Variant	Moderator Block Density (g/cm ³)	k _{eff}	σ	k _{eff} + 2σ	Δ(k _{eff} + 2σ)
17 Bin 1 (1 & 2)	XL	Baseline Case	0.90209	0.00049	0.90307	--
		0.9108	0.90358	0.00053	0.90464	0.00157
VV Bin 1 (3)	VVER	Baseline Case	0.88241	0.00025	0.88291	--
		0.9108	0.88297	0.00029	0.88355	0.00064

The polyethylene packing materials sensitivity study, as defined in Section 6.3.4.3.5, examined a conservative representation of polyethylene packing materials through HAC. For the Traveller, 2.0 kg of polyethylene packing materials is the limit for the package, which is determined in Section 6.6 and applied here. Table 6-36 defines the parameters evaluated and the results. Figure 6-35 and Figure 6-36 display the result trends for Groups 1, 2, and Group 3, respectively. The most reactive 2.0 kg poly case is highlighted for each Group.

Content (Group)	Traveller Variant	Poly Model	Poly Mass (kg)	k _{eff}	σ	k _{eff} + 2σ	Δ(k _{eff} + 2σ)
17 Bin 1 (1 & 2)	XL	Baseline Case	0.0	0.90209	0.00049	0.90307	--
		Outer Wrap	2.27	0.90310	0.00048	0.90406	0.00099
			3.74	0.90267	0.00060	0.90387	0.00080
			4.83	0.90376	0.00064	0.90504	0.00197
			5.71	0.90499	0.00051	0.90601	0.00294
			6.46	0.90610	0.00077	0.90764	0.00457
			7.12	0.90562	0.00050	0.90662	0.00355
		Uniform Wrap	2.0	0.90402	0.00053	0.90508	0.00201
			4.0	0.90551	0.00058	0.90667	0.00360
			6.0	0.90546	0.00059	0.90664	0.00357
			8.0	0.90688	0.00064	0.90816	0.00509
			10.0	0.90865	0.00058	0.90981	0.00674
		Collected Melt	2.0	0.90473	0.00059	0.90591	0.00284
			4.0	0.90734	0.00055	0.90844	0.00537
			6.0	0.91456	0.00050	0.91556	0.01249
8.0	0.92283		0.00046	0.92375	0.02068		
VV Bin 1 (3)	VVER	Baseline Case	0.0	0.88241	0.00025	0.88291	--
		Outer Wrap	2.38	0.88304	0.00029	0.88362	0.00071
			3.94	0.88319	0.00027	0.88373	0.00082
			5.94	0.88367	0.00024	0.88415	0.00124
			7.94	0.88414	0.00025	0.88464	0.00173
			9.94	0.88456	0.00024	0.88504	0.00213
		Uniform Wrap	2.0	0.88424	0.00024	0.88472	0.00181
			4.0	0.88572	0.00024	0.88620	0.00329

Content (Group)	Traveller Variant	Poly Model	Poly Mass (kg)	k_{eff}	σ	$k_{eff} + 2\sigma$	$\Delta(k_{eff} + 2\sigma)$
			6.0	0.88773	0.00026	0.88825	0.00534
			8.0	0.88868	0.00028	0.88924	0.00633
			10.0	0.89044	0.00024	0.89092	0.00801
		Collected Melt	2.0	0.88504	0.00024	0.88552	0.00261
			4.0	0.89176	0.00026	0.89228	0.00937
			6.0	0.90390	0.00026	0.90442	0.02151
			8.0	0.91786	0.00027	0.91840	0.03549
			10.0	0.93016	0.00030	0.93076	0.04785

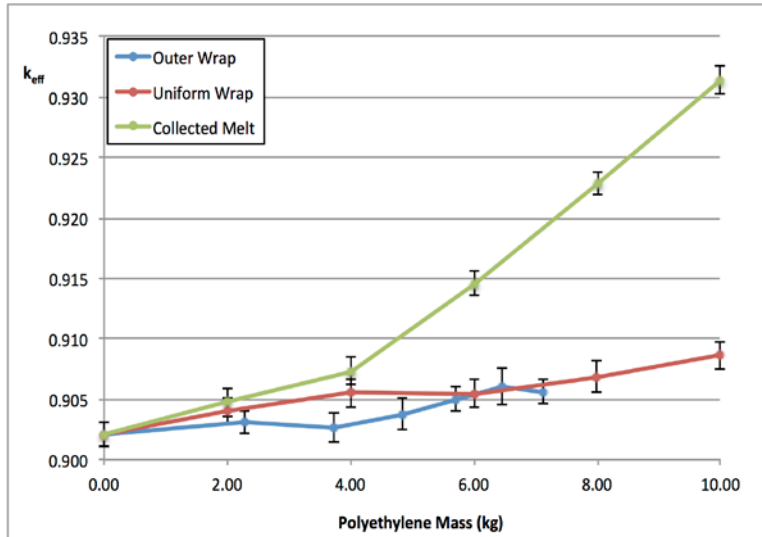


Figure 6-35 Polyethylene Sensitivity Results – Single Package, HAC (Groups 1 & 2)

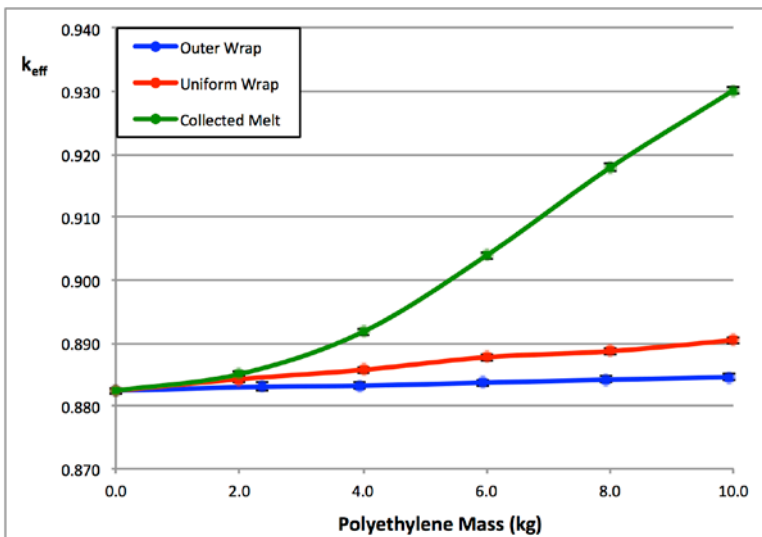


Figure 6-36 Polyethylene Sensitivity Results – Single Package, HAC (Group 3)

The axial rod displacement sensitivity study, as defined in Section 6.3.4.3.6, examined the movement of fuel rods out of the lattice because of drop testing. Table 6-37 defines the parameters evaluated and the results. Figure 6-37 and Figure 6-38 display the result trends for Groups 1, 2, and Group 3, respectively. The most reactive case is highlighted for each Group.

Content (Group)	Traveller Variant	Rod Configuration	Number of Rods	k_{eff}	σ	$k_{eff} + 2\sigma$	$\Delta(k_{eff} + 2\sigma)$		
17 Bin 1 (1 & 2)	XL	Baseline Case	0	0.90209	0.00049	0.90307	--		
		Corner	20	0.89365	0.0005	0.89465	-0.00842		
			40	0.88297	0.00068	0.88433	-0.01874		
			64	0.87615	0.00049	0.87713	-0.02594		
		Random	20	0.89533	0.00048	0.89629	-0.00678		
			40	0.89038	0.00059	0.89156	-0.01151		
			64	0.88085	0.00054	0.88193	-0.02114		
		VV Bin 1 (3)	VVER	Baseline Case	0	0.88241	0.00025	0.88291	--
				Corner	20	0.87756	0.00027	0.8781	-0.00481
40	0.87069				0.00028	0.87125	-0.01166		
64	0.8656				0.00026	0.86612	-0.01679		
Random	20			0.88132	0.00025	0.88182	-0.00109		
	40			0.88183	0.00025	0.88233	-0.00058		
	64			0.88089	0.00027	0.88143	-0.00148		

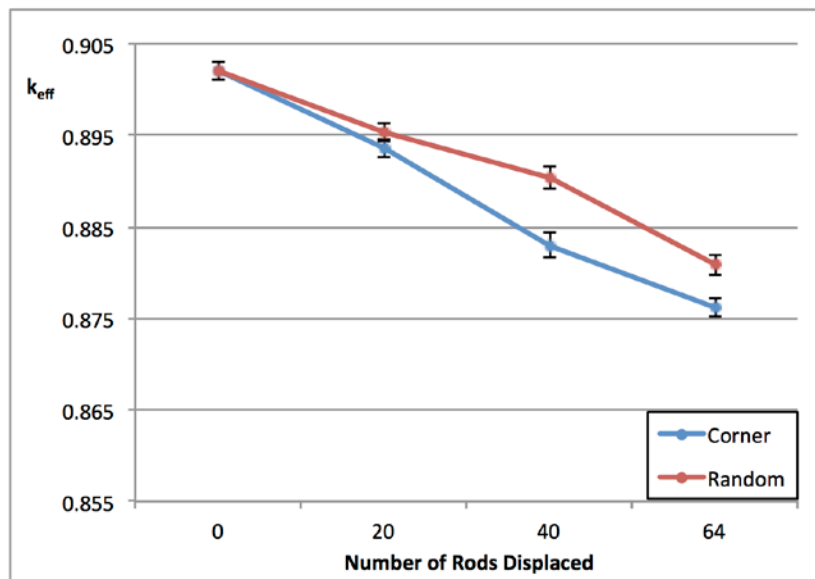


Figure 6-37 Axial Rod Displacement Sensitivity Results – Single Package, HAC (Groups 1 & 2)

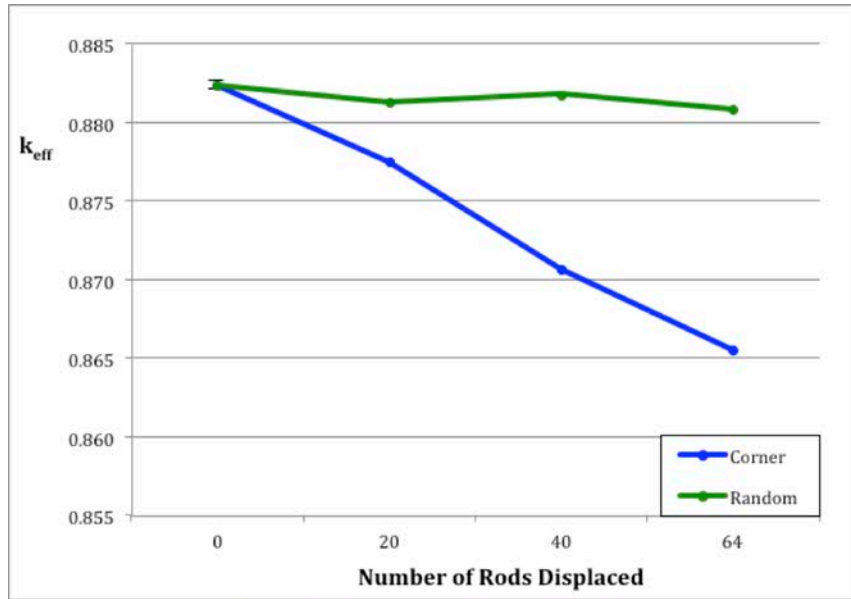


Figure 6-38 Axial Rod Displacement Sensitivity Results – Single Package, HAC (Group 3)

The SS replacement rod sensitivity study, as defined in Section 6.3.4.3.7, examined replacement of fuel rods with SS rod within the fuel assembly. Table 6-38 defines the parameters evaluated and the results. The most reactive case is highlighted for each Group.

Content (Group)	Traveller Variant	SS Rod Configuration	k_{eff}	σ	$k_{eff} + 2\sigma$	$\Delta(k_{eff} + 2\sigma)$
17 Bin 1 (1 & 2)	XL	Baseline Case	0.90209	0.00049	0.90307	--
		Corner	0.88409	0.0006	0.88529	-0.01778
		Random	0.84703	0.00056	0.84815	-0.05492
VV Bin 1 (3)	VVER	Baseline Case	0.88241	0.00025	0.88291	--
		Corner	0.86222	0.00026	0.86274	-0.02017
		Random	0.82794	0.00024	0.82842	-0.05449

The tolerance sensitivity studies evaluate cladding dimensions, fuel pellet diameter, and fuel rod pitch, as defined in Sections 6.3.4.3.8, 6.3.4.3.9, and 6.3.4.3.10, respectively. Table 6-39 defines the parameter dimensions evaluated and the results. The most reactive case is highlighted for each Group and tolerance parameter.

Content (Group)	Traveller Variant	Tolerance Parameter		k_{eff}	σ	k_{eff} + 2σ	Δ(k_{eff} + 2σ)
17 Bin 1 (1 & 2)	XL	Baseline Case		0.90209	0.00049	0.90307	--
VV Bin 1 (3)	VVER	Baseline Case		0.88241	0.00025	0.88291	--
Cladding Tolerance		ID Tolerance (in.)	OD Tolerance (in.)	k_{eff}	σ	k_{eff} + 2σ	Δ(k_{eff} + 2σ)
17 Bin 1 (1 & 2)	XL	-0.002	-0.002	0.90225	0.00052	0.90329	0.00022
			nominal	0.90131	0.00065	0.90261	-0.00046
			+0.002	0.90113	0.00061	0.90235	-0.00072
		nominal	-0.002	0.9049	0.0005	0.9059	0.00283
			nominal	0.90209	0.00049	0.90307	--
			+0.002	0.90076	0.00054	0.90184	-0.00123
		+0.002	-0.002	0.90662	0.0007	0.90802	0.00495
			nominal	0.90484	0.0005	0.90584	0.00277
			+0.002	0.90206	0.00072	0.9035	0.00043
VV Bin 1 (3)	VVER	-0.0015	-0.0015	0.88274	0.00025	0.88324	0.00033
			nominal	0.8806	0.00028	0.88116	-0.00175
			+0.0015	0.87927	0.00026	0.87979	-0.00312
		nominal	-0.0015	0.88483	0.00028	0.88539	0.00248
			nominal	0.88241	0.00025	0.88291	--
			+0.0015	0.88087	0.00025	0.88137	-0.00154
		+0.0015	-0.0015	0.88634	0.00026	0.88686	0.00395
			nominal	0.88448	0.00027	0.88502	0.00211
			+0.0015	0.88242	0.00029	0.883	0.00009
Pellet Diameter Tolerance		Pellet OD Tolerance (in.)		k_{eff}	σ	k_{eff} + 2σ	Δ(k_{eff} + 2σ)
17 Bin 1 (1 & 2)	XL	-0.0007		0.90314	0.00038	0.9039	0.00083
		-0.0005		0.90278	0.0004	0.90358	0.00051
		+0.0005		0.90209	0.00049	0.90307	0.00000
		+0.0007		0.90235	0.0004	0.90315	0.00008
VV Bin 1 (3)	VVER	-0.0005		0.88312	0.00026	0.88364	0.00073
		+0.0005		0.88288	0.00028	0.88344	0.00053
Pitch Tolerance		Pitch Tolerance (in.)		k_{eff}	σ	k_{eff} + 2σ	Δ(k_{eff} + 2σ)
17 Bin 1 (1 & 2)	XL	-0.0785		0.89208	0.00048	0.89304	-0.01003
		-0.0393		0.89594	0.00049	0.89692	-0.00615
		+0.0059		0.90504	0.00057	0.90618	0.00311
		+0.0118		0.9066	0.00052	0.90764	0.00457
VV Bin 1 (3)	VVER	-0.001		0.88288	0.00025	0.88338	0.00047
		+0.001		0.88281	0.00028	0.88337	0.00046

The fuel assembly position sensitivity study, as defined in Section 6.3.4.3.12, examined the extended active fuel length for Group 3. Table 6-40 defines the parameter evaluated and the results. The most reactive case is highlighted.

Contents (Group)	Traveller Variant	Active Fuel Length (cm)	k_{eff}	σ	$k_{eff} + 2\sigma$	$\Delta(k_{eff} + 2\sigma)$
VV Bin 1 (3)	VVER	Baseline Case 364.261	0.88241	0.00025	0.88291	--
		364.631	0.88266	0.00025	0.88316	0.00025
		365.000	0.88353	0.00027	0.88407	0.00116
		366.270	0.88277	0.00026	0.88329	0.00038

The ADOPT fuel sensitivity study, as defined in Section 6.3.4.3.14, examined the effect of replacing standard UO₂ fuel with ADOPT fuel. Table 6-40A lists the results of the study. The most reactive case is highlighted.

Contents (Group)	Traveller Variant	Fuel Material	k_{eff}	σ	$k_{eff} + 2\sigma$	$\Delta(k_{eff} + 2\sigma)$
17 Bin 1 (1 & 2)	XL	Baseline (UO ₂)	0.90209	0.00049	0.90307	--
		ADOPT	0.90310	0.00059	0.90428	0.00121

6.4.2.2.4 Rod Pipe

Table 6-41 shows the summary of the penalty assessed for the sensitivity studies evaluated for the Rod Pipe contents. An entry of “0.0” signifies that the study resulted in no positive penalty on reactivity and an entry of “--” signifies that the study did not require analyzing based on transport condition.

Sensitivity Study	Penalty Assessed			
	Rod Pipe UO ₂ Fuel Rods		Rod Pipe U ₃ Si ₂ Fuel Rods	
	NCT	HAC	NCT	HAC
Annular Blanket Length	0.04278	0.00427	0.02104	0.0
Rod Pipe Position in Clamshell	0.0	0.0	0.0	0.0
Moderator Block Density Reduction	--	0.0	--	0.0
Polyethylene Packing Materials	0.02694	0.06950	0.27573	0.06371
Fuel Pellet Tolerance	0.0	0.0	0.00180	0.0
ADOPT Fuel	0.0	0.0	--	--
Total Penalty (Δk_u)	0.06972	0.07377	0.29857	0.06371

6.4.2.2.4.1 Single Package, Rod Pipe, NCT Sensitivity Studies

The annular blanket sensitivity study, as defined in Section 6.3.4.3.1, examined the addition of varying annular fuel pellet ID and lengths of annular fuel pellet blanket lengths equally to the top and bottom of a fuel rod. Table 6-42 shows the parameters evaluated and the results, and Figure 6-39 and Figure 6-40 display the result trends. The most reactive case is highlighted for each content.

Contents	Traveller Variant	Annulus Diameter	Annulus Length (cm)	k_{eff}	σ	$k_{eff} + 2\sigma$	$\Delta(k_{eff} + 2\sigma)$		
Rod Pipe UO ₂ Fuel Rods	XL	Baseline Case		0.56435	0.00086	0.56607	--		
		0.155 in. (0.3937 cm)	13	0.56459	0.00037	0.56533	-0.00074		
			26	0.56514	0.00039	0.56592	-0.00015		
			39	0.5652	0.00047	0.56614	0.00007		
			78	0.56576	0.00040	0.56656	0.00049		
			250.825	0.56688	0.00051	0.56790	0.00183		
		0.183 in. (0.4648 cm)	13	0.56569	0.00041	0.56651	0.00044		
			26	0.56492	0.00044	0.56580	-0.00027		
			39	0.56532	0.00038	0.56608	0.00001		
			78	0.56567	0.00039	0.56645	0.00038		
			250.825	0.56645	0.00036	0.56717	0.00110		
		1.213 in. (3.0810 cm)	13	0.56525	0.00046	0.56617	0.00010		
			26	0.56758	0.00039	0.56836	0.00229		
			39	0.57760	0.00050	0.57860	0.01253		
			78	0.59614	0.00050	0.59714	0.03107		
			250.825	0.60801	0.00042	0.60885	0.04278		
		Rod Pipe U ₃ Si ₂ Fuel Rods	STD	Baseline Case		0.42948	0.00037	0.43022	--
				0.155 in. (0.3937 cm)	13	0.42961	0.00043	0.43047	0.00025
					26	0.43025	0.00040	0.43105	0.00083
					39	0.43036	0.00045	0.43126	0.00104
78	0.43733				0.00037	0.43807	0.00785		
213.995	0.44356				0.00041	0.44438	0.01416		
0.183 in. (0.4648 cm)	13			0.4298	0.00036	0.43052	0.00030		
	26			0.43079	0.00039	0.43157	0.00135		
	39			0.43225	0.00052	0.43329	0.00307		
	78			0.44193	0.00039	0.44271	0.01249		
	213.995			0.45020	0.00053	0.45126	0.02104		

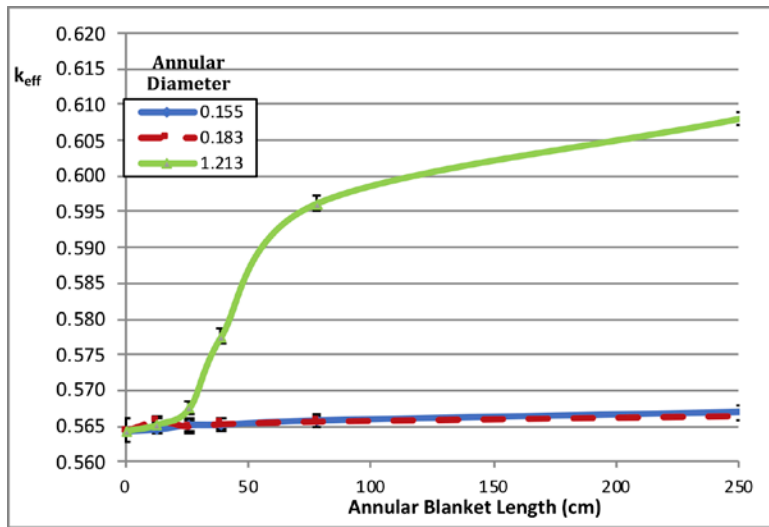


Figure 6-39 Annular Blanket Sensitivity – Single Package, NCT (Rod Pipe UO₂ Fuel Rods)

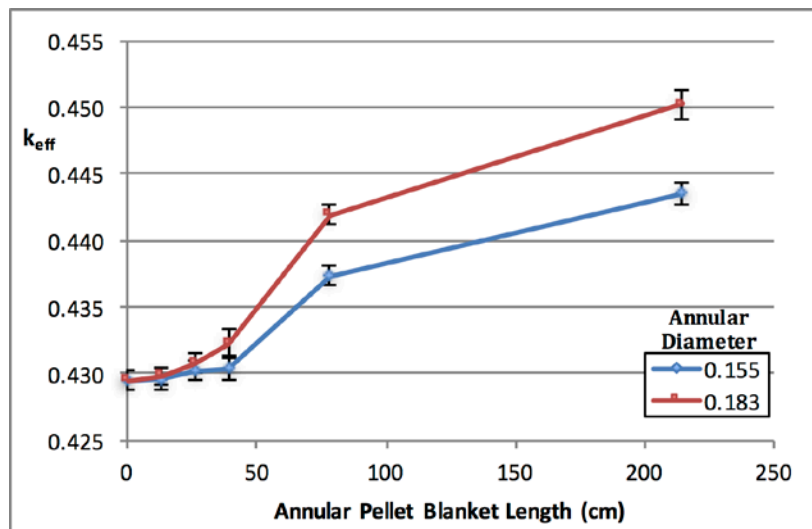


Figure 6-40 Annular Blanket Sensitivity – Single Package, NCT (Rod Pipe U₃Si₂ Fuel Rods)

The Rod Pipe position sensitivity study, as defined in Section 6.3.4.3.2, examined the shifting of the Rod Pipe in the Clamshell. Table 6-43 defines the parameter evaluated and the results. The most reactive case is highlighted for each content.

Table 6-43 Rod Pipe Position Sensitivity Results – Single Package, NCT, Rod Pipe						
Contents	Traveller Variant	Rod Pipe Position	k_{eff}	σ	$k_{eff} + 2\sigma$	$\Delta(k_{eff} + 2\sigma)$
Rod Pipe UO ₂ Fuel Rods	XL	Baseline Case	0.56435	0.00086	0.56607	--
		Down	0.53002	0.00069	0.53140	-0.03467
Rod Pipe U ₃ Si ₂ Fuel Rods	STD	Baseline Case	0.42948	0.00037	0.43022	--
		Down	0.42161	0.00037	0.42235	-0.00787

The polyethylene packing materials sensitivity study, as defined in Section 6.3.4.3.5, examined the presence of an outer wrap around each fuel rod. Table 6-44 defines the parameter evaluated and the results and Figure 6-41 and Figure 6-42 display the result trends. The most reactive case is highlighted for each content. The peak k_{eff} due to the polyethylene wrap addition encompasses the largest polyethylene addition modeled, with the highest value of $k_{eff} + 2\sigma$ far below the USL of 0.94044. Therefore, based on the single package NCT results, no limitation of polyethylene packing materials is imposed on the Traveller packaging with Rod Pipe.

Table 6-44 Polyethylene Packing Sensitivity Results – Single Package, NCT, Rod Pipe							
Contents	Traveller Variant	Poly Model	Poly Mass (kg)	k_{eff}	σ	$k_{eff} + 2\sigma$	$\Delta(k_{eff} + 2\sigma)$
Rod Pipe UO ₂ Fuel Rods	XL	Baseline Case	0.0	0.56435	0.00086	0.56607	--
		Outer Wrap	1.67	0.57444	0.00045	0.57534	0.00927
			2.19	0.57812	0.00039	0.5789	0.01283
			4.28	0.59052	0.0004	0.59132	0.02525
			18.32	0.59219	0.00041	0.59301	0.02694
			30.89	0.5825	0.00049	0.58348	0.01741
Rod Pipe U ₃ Si ₂ Fuel Rods	STD	Baseline Case	0.0	0.42948	0.00037	0.43022	--
		Outer Wrap	1.85	0.44955	0.00037	0.45029	0.02007
			3.79	0.47114	0.00042	0.47198	0.04176
			7.96	0.51601	0.00045	0.51691	0.08669
			17.41	0.60257	0.00048	0.60353	0.17331
			36.30	0.70497	0.00049	0.70595	0.27573

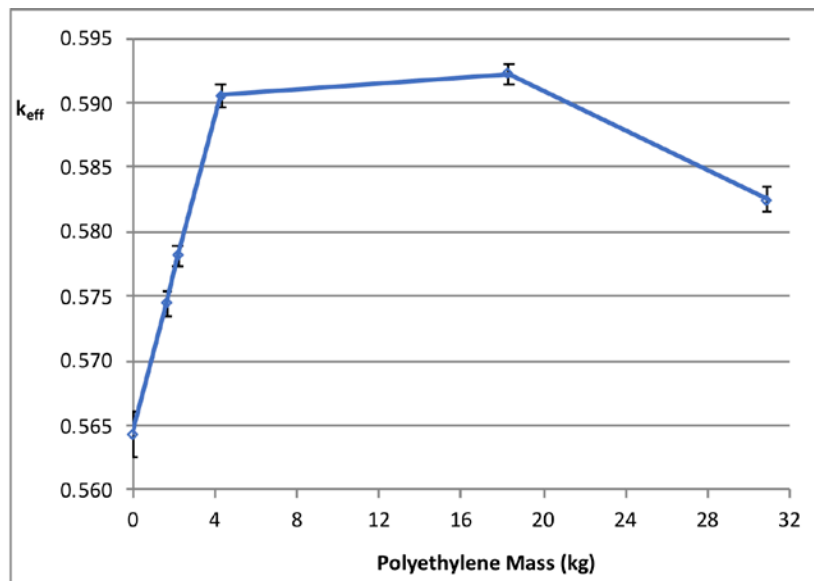


Figure 6-41 Polyethylene Packing Sensitivity – Single Package, NCT (Rod Pipe UO₂ Fuel Rods)

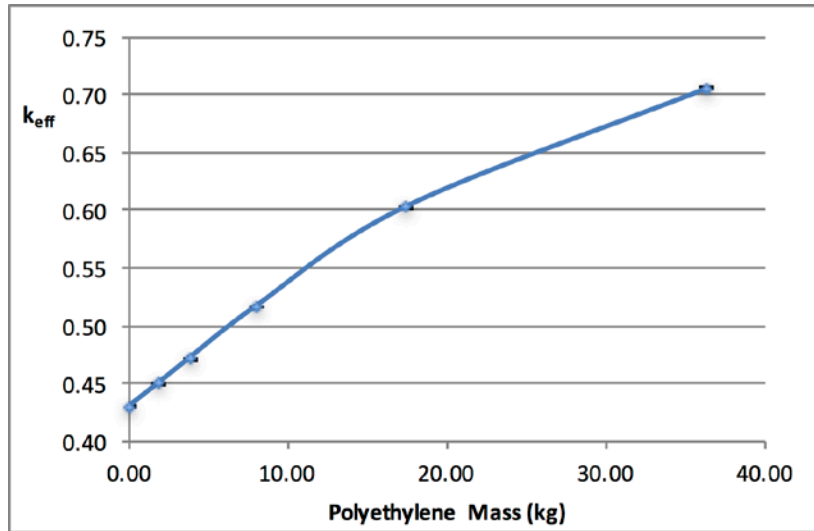


Figure 6-42 Polyethylene Packing Sensitivity – Single Package, NCT (Rod Pipe U₃Si₂ Fuel Rods)

The tolerance sensitivity study evaluates fuel pellet diameter only, as defined in Section 6.3.4.3.9. The Rod Pipe contents are not defined by cladding and pitch parameters, thus there is no tolerance evaluation as explained in Section 6.3.4.3.8 and 6.3.4.3.10, respectively. Table 6-45 defines the parameter dimensions evaluated and the results. The most reactive case is highlighted for each content and tolerance parameter.

Contents	Traveller Variant	Pellet OD Tolerance (in.)	k_{eff}	σ	$k_{eff} + 2\sigma$	$\Delta(k_{eff} + 2\sigma)$
Rod Pipe UO ₂ Fuel Rods	XL	-0.0014	0.56586	0.00038	0.56662	0.00055
		-0.0010	0.56534	0.00041	0.56616	0.00009
		Baseline Case	0.56435	0.00086	0.56607	--
		+0.0010	0.56500	0.00041	0.56582	-0.00025
		+0.0014	0.56506	0.00038	0.56582	-0.00025
Rod Pipe U ₃ Si ₂ Fuel Rods	STD	-0.0014	0.42895	0.00037	0.42969	-0.00053
		-0.0010	0.42891	0.00034	0.42959	-0.00063
		Baseline Case	0.42948	0.00037	0.43022	--
		+0.0010	0.42995	0.00037	0.43069	0.00047
		+0.0014	0.43130	0.00036	0.43202	0.00180

The ADOPT Fuel sensitivity study, as defined in Section 6.3.4.3.14, examined the effect of replacing standard UO₂ fuel with ADOPT fuel. Table 6-45A lists the results of the study. The most reactive case is highlighted.

Content	Traveller Variant	Fuel	k_{eff}	σ	$k_{eff} + 2\sigma$	$\Delta(k_{eff} + 2\sigma)$
Rod Pipe UO ₂ Fuel Rods	XL	Baseline (UO₂)	0.56435	0.00086	0.56607	--
		ADOPT	0.56616	0.00079	0.56774	0.00167

6.4.2.2.4.2 *Single Package, Rod Pipe, HAC Sensitivity Studies*

The annular blanket sensitivity study, as defined in Section 6.3.4.3.1, examined the addition of varying annular fuel pellet ID and lengths of annular fuel pellet blanket lengths equally to the top and bottom of a fuel rod. Table 6-46 defines the parameters evaluated and the results, and Figure 6-43 and Figure 6-44 display the result trends. The most reactive case is highlighted for each content.

Table 6-46 Annular Blanket Sensitivity Results – Single Package, HAC, Rod Pipe									
Contents	Traveller Variant	Annulus Diameter	Annulus Length (cm)	k_{eff}	σ	k_{eff} + 2σ	Δ(k_{eff} + 2σ)		
Rod Pipe UO ₂ Fuel Rods	XL	Baseline Case		0.72106	0.00047	0.72200	--		
		0.155 in. (0.3937 cm)	13.0	0.71982	0.00053	0.72088	-0.00112		
			26.0	0.71937	0.00051	0.72039	-0.00161		
			39.0	0.72075	0.00045	0.72165	-0.00035		
			78.0	0.72039	0.00055	0.72149	-0.00051		
			250.825	0.72362	0.00048	0.72458	0.00258		
		0.183 in. (0.4648 cm)	13.0	0.71964	0.00048	0.72060	-0.00140		
			26.0	0.72117	0.00054	0.72225	0.00025		
			39.0	0.72079	0.00051	0.72181	-0.00019		
			78.0	0.72103	0.00049	0.72201	0.00001		
			250.825	0.72515	0.00056	0.72627	0.00427		
		Rod Pipe U ₃ Si ₂ Fuel Rods	STD	Baseline Case		0.67492	0.00049	0.67590	--
				0.155 in. (0.3937 cm)	13.0	0.67441	0.00053	0.67547	-0.00043
					26.0	0.67528	0.00049	0.67626	0.00036
39.0	0.67498				0.0005	0.67598	0.00008		
78.0	0.67390				0.00051	0.67492	-0.00098		
213.995	0.66959				0.00043	0.67045	-0.00545		
0.183 in. (0.4648 cm)	13.0			0.67466	0.00049	0.67564	-0.00026		
	26.0			0.67508	0.00046	0.67600	0.00010		
	39.0			0.67542	0.00051	0.67644	0.00054		
	78.0			0.67460	0.00055	0.6757	-0.00020		
	213.995			0.66599	0.0005	0.66699	-0.00891		

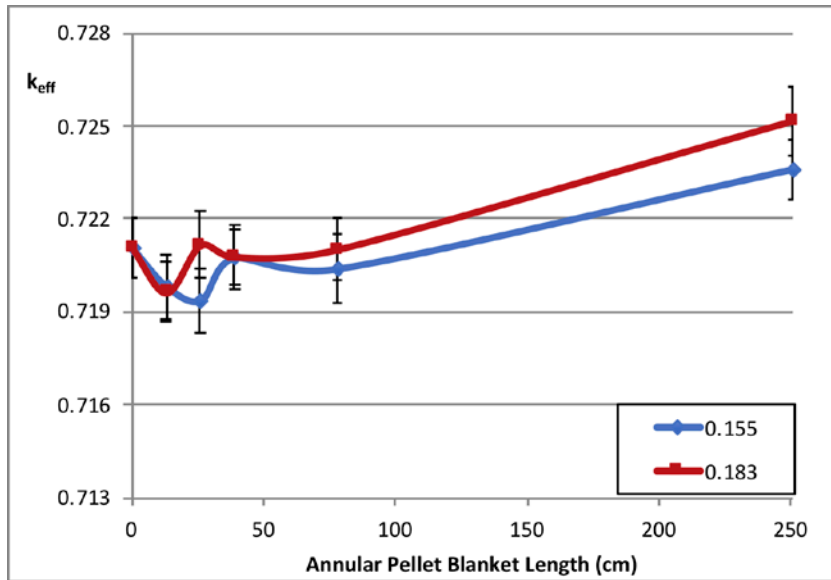


Figure 6-43 Annular Blanket Sensitivity Results – Single Package, HAC (Rod Pipe UO₂ Fuel Rods)

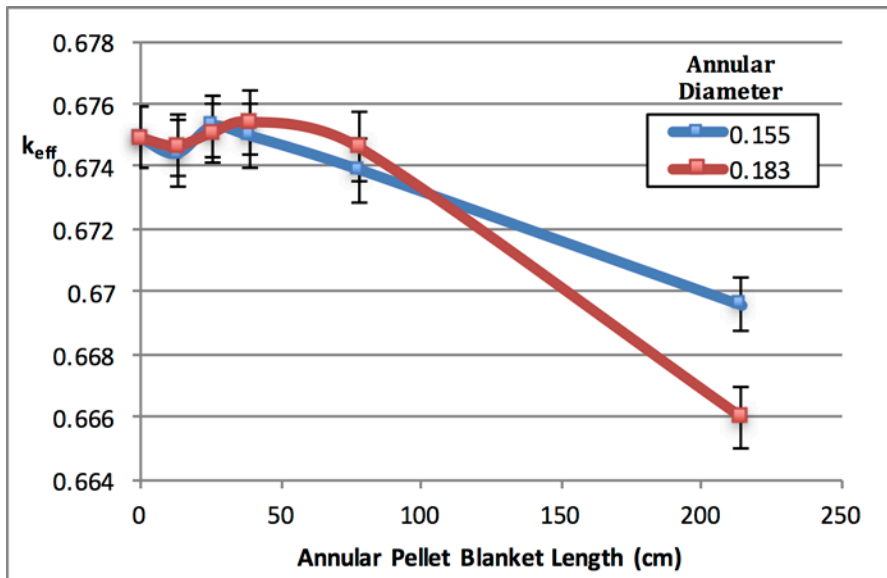


Figure 6-44 Annular Blanket Sensitivity Results – Single Package, HAC (Rod Pipe U₃Si₂ Fuel Rods)

The Rod Pipe position sensitivity study, as defined in Section 6.3.4.3.2, examined the shifting of the Rod Pipe in the Clamshell from the centerline, baseline position. Table 6-47 defines the parameter evaluated and the results. The most reactive case is highlighted for each content.

Contents	Traveller Variant	Fuel Assembly Position	k_{eff}	σ	$k_{eff} + 2\sigma$	$\Delta(k_{eff} + 2\sigma)$
Rod Pipe UO ₂ Fuel Rods	XL	Baseline Case	0.72106	0.00047	0.72200	--
		Up	0.69442	0.00053	0.69548	-0.02652
		Down	0.69464	0.00057	0.69578	-0.02622
Rod Pipe U ₃ Si ₂ Fuel Rods	STD	Baseline Case	0.67492	0.00049	0.67590	--
		Up	0.65502	0.00046	0.65594	-0.01996
		Down	0.65424	0.00045	0.65514	-0.02076

The moderator block density reduction sensitivity study, as defined in Section 6.3.4.3.3, examined the post-fire condition of the moderator block. Table 6-48 defines the parameter evaluated and the results. The most reactive case is highlighted for each content.

Content	Traveller Variant	Moderator Block Density (g/cm ³)	k_{eff}	σ	$k_{eff} + 2\sigma$	$\Delta(k_{eff} + 2\sigma)$
Rod Pipe UO ₂ Fuel Rods	XL	Baseline Case	0.72106	0.00047	0.72200	--
		0.9108	0.72012	0.00058	0.72128	-0.00072
Rod Pipe U ₃ Si ₂ Fuel Rods	STD	Baseline Case	0.67492	0.00049	0.67590	--
		0.9108	0.67526	0.00047	0.67620	0.00030

The polyethylene packing materials sensitivity study, as defined in Section 6.3.4.3.5, examined a conservative representation of polyethylene packing materials through HAC. Table 6-49 defines the parameters evaluated and the results, and Figure 6-45 and Figure 6-46 display the result trends. The most reactive case is highlighted for each content. As the full height melt is limiting, no limit on polyethylene packing materials is imposed on the Traveller packaging with the loose Rod Pipe as a result of the single package, HAC, polyethylene evaluation.

Table 6-49 Polyethylene Sensitivity Results – Single Package, HAC, Rod Pipe							
Content	Traveller Variant	Poly Model	Poly Mass (kg)	k_{eff}	σ	$k_{eff} + 2\sigma$	$\Delta(k_{eff} + 2\sigma)$
Rod Pipe UO ₂ Fuel Rods	XL	Baseline Case	0	0.72106	0.00047	0.72200	--
		Uniform Wrap	3.39	0.72304	0.00047	0.72398	0.00198
			4.50	0.72385	0.00046	0.72477	0.00277
			9.38	0.72977	0.00053	0.73083	0.00883
			20.33	0.74164	0.00056	0.74276	0.02076
			46.91	0.77311	0.00047	0.77405	0.05205
		Collected Melt	0.62	0.72065	0.00048	0.72161	-0.00039
			1.87	0.72025	0.0005	0.72125	-0.00075
			2.49	0.72307	0.00058	0.72423	0.00223
			3.12	0.73063	0.00052	0.73167	0.00967
			4.36	0.74779	0.0005	0.74879	0.02679
			6.24	0.76478	0.00059	0.76596	0.04396
			9.35	0.77659	0.00052	0.77763	0.05563
			12.47	0.78369	0.00058	0.78485	0.06285
		62.56	0.79048	0.00051	0.79150	0.06950	
Rod Pipe U ₃ Si ₂ Fuel Rods	STD	Baseline Case	0	0.67492	0.00049	0.67590	--
		Uniform Wrap	2.51	0.67631	0.00052	0.67735	0.00145
			3.33	0.67744	0.00048	0.67840	0.00250
			7.00	0.68013	0.00045	0.68103	0.00513
			15.30	0.68898	0.00044	0.68986	0.01396
			32.42	0.70946	0.00045	0.71036	0.03446
			51.32	0.73184	0.00049	0.73282	0.05692
		Collected Melt	0.68	0.67501	0.00045	0.67591	0.00001
			2.04	0.67508	0.00049	0.67606	0.00016
			2.72	0.67696	0.00047	0.67790	0.00200
			3.40	0.68373	0.00048	0.68469	0.00879
			4.76	0.69969	0.00049	0.70067	0.02477
			6.80	0.71436	0.00049	0.71534	0.03944
			10.19	0.72531	0.00051	0.72633	0.05043
			13.59	0.73053	0.00046	0.73145	0.05555
58.17	0.73847	0.00057	0.73961	0.06371			

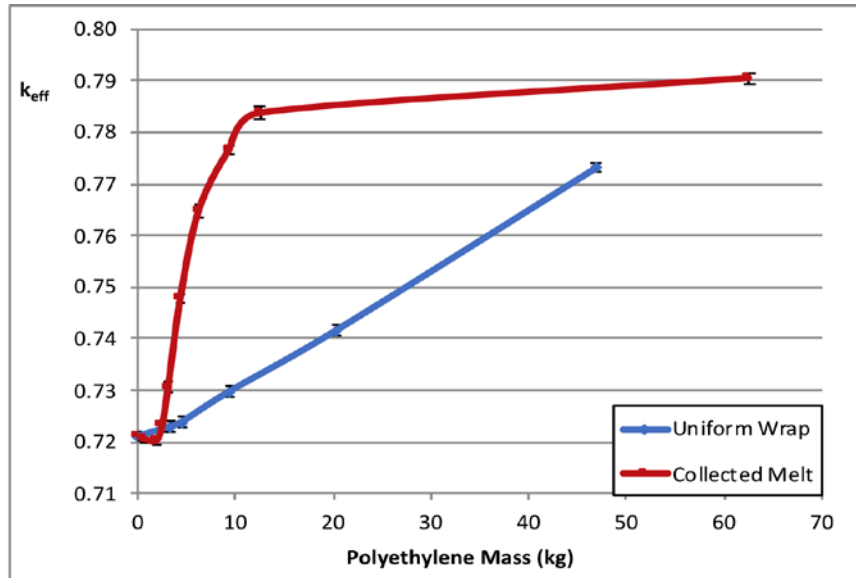


Figure 6-45 Polyethylene Sensitivity Results – Single Package, HAC (Rod Pipe UO₂ Fuel Rods)

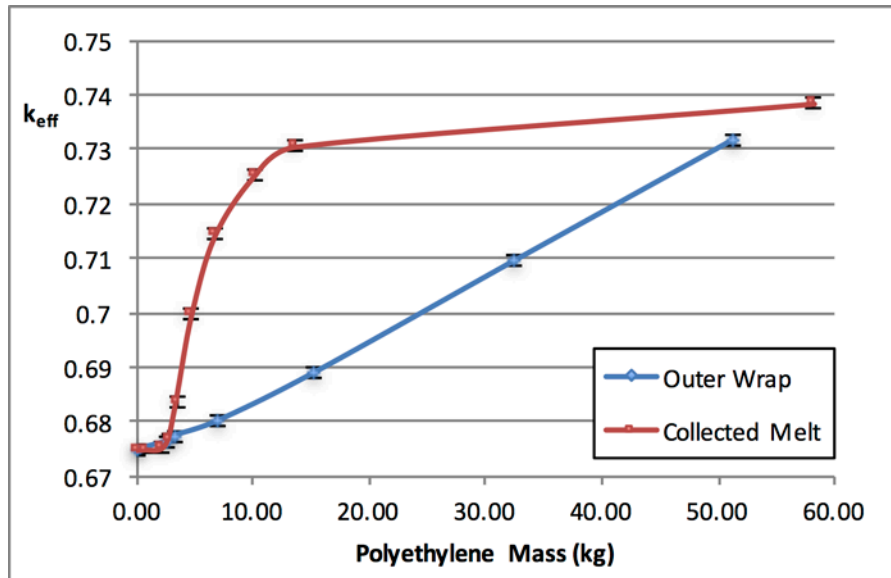


Figure 6-46 Polyethylene Sensitivity Results – Single Package, HAC (Rod Pipe U₃Si₂ Fuel Rods)

The tolerance sensitivity study evaluates fuel pellet diameter only, as defined in Section 6.3.4.3.9. The Rod Pipe contents are not defined by cladding and pitch parameters, thus there is no tolerance evaluation as explained in Section 6.3.4.3.8 and 6.3.4.3.10, respectively. Table 6-50 defines the parameter dimensions evaluated and the results. The most reactive case is highlighted.

Content	Traveller Variant	Pellet OD Tolerance (in.)	k_{eff}	σ	$k_{eff} + 2\sigma$	$\Delta(k_{eff} + 2\sigma)$
Rod Pipe UO ₂ Fuel Rods	XL	-0.0014	0.72049	0.00047	0.72143	-0.00057
		-0.0010	0.72083	0.00049	0.72181	-0.00019
		Baseline Case	0.72106	0.00047	0.72200	--
		+0.0010	0.72009	0.00044	0.72097	-0.00103
		+0.0014	0.72012	0.00050	0.72112	-0.00088
Rod Pipe U ₃ Si ₂ Fuel Rods	STD	-0.0014	0.67439	0.00059	0.67557	-0.00033
		-0.0010	0.67513	0.00049	0.67611	0.00021
		Baseline Case	0.67492	0.00049	0.67590	--
		+0.0010	0.67487	0.00050	0.67587	-0.00003
		+0.0014	0.67481	0.00051	0.67583	-0.00007

The ADOPT Fuel sensitivity study, as defined in Section 6.3.4.3.14, examined the effect of replacing standard UO₂ fuel with ADOPT fuel. Table 6-50A lists the results of the study. The most reactive case is highlighted.

Content	Traveller Variant	Fuel	k_{eff}	σ	$k_{eff} + 2\sigma$	$\Delta(k_{eff} + 2\sigma)$
Rod Pipe UO ₂ Fuel Rods	XL	Baseline (UO₂)	0.72106	0.00047	0.72200	--
		ADOPT	0.71964	0.00053	0.72070	-0.00130

6.5 EVALUATION OF PACKAGE ARRAYS UNDER NORMAL CONDITIONS OF TRANSPORT

6.5.1 Configuration

For the evaluation of package arrays under NCT, all inner spaces of the package are modeled as void, including the fuel-clad gap. Additional material modeling is specified in Section 6.3.2. Several materials, including fuel assembly structural components and packaging components (e.g. Outerpack foam regions, ceramic fiber blankets, and shock mounts, etc.), are replaced with void. The package array is reflected with 20 cm of full-density water.

6.5.1.1 Baseline Configurations

As described in Section 6.3.4.2, a baseline case is evaluated for all content Groups and Rod Pipe configurations under NCT. Baseline configurations represent a bounding model that is carried forward to the sensitivity studies to demonstrate maximum reactivity.

6.5.1.1.1 Fuel Assembly – Group 1, 2 and 3

For the baseline case determination, as defined in Section 6.3.4.2.1, first the bounding CFA-package variant combination is determined. For Groups 1 and 2, the Traveller XL is consistently more reactive than the Traveller STD for an array under NCT. As discussed in Section 6.3.4.2.1.2, the axial positioning of the fuel assembly is examined due to the physical geometry of the packaging. Detailed results of the baseline case determination are shown in Section 6.9.3.3.2. The NCT baseline configurations are summarized in Table 6-51. Each of the array configurations are shown in Figure 6-47, Figure 6-48, and Figure 6-49.

Traveller Variant	Contents (Group)	Array Size (5N)	Array Height	Axial Position (cm)	Flooding Configuration	$k_{eff} \pm \sigma$
XL	17 Bin 2 (1)	250	2	Top: 2.54 Bottom: 119.27	None	0.30888 ± 0.00027
XL	16 Bin 1 (2)	60	1	119.27	None	0.30950 ± 0.00026
VVER	VV Bin 1 (3)	250	1	3.81	None	0.38828 ± 0.00016

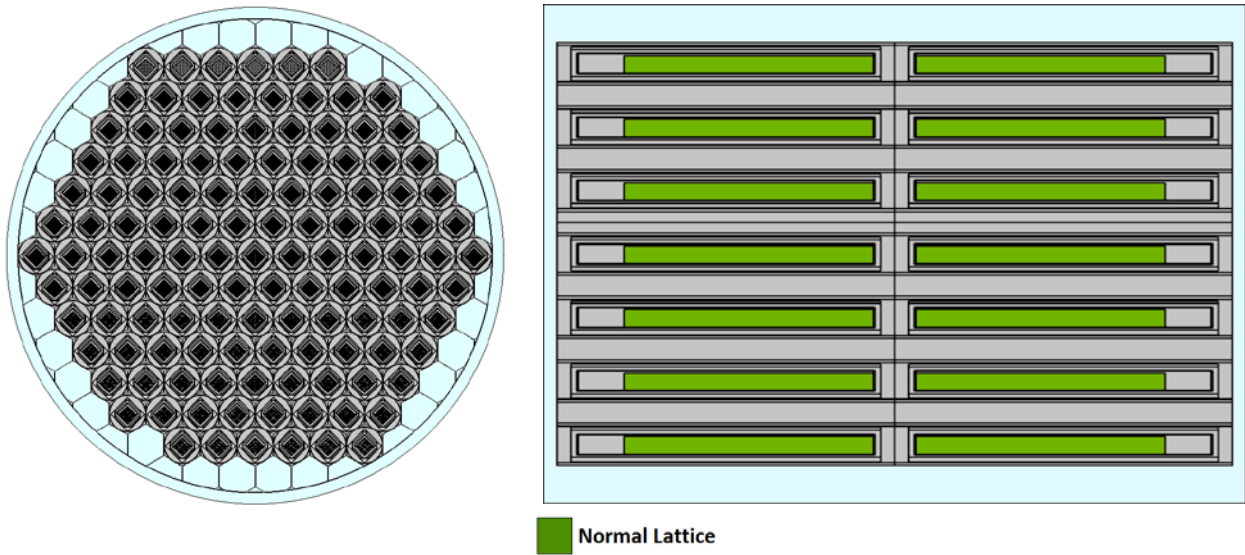


Figure 6-47 Group 1, NCT 250-package Array with Height of Two Packages

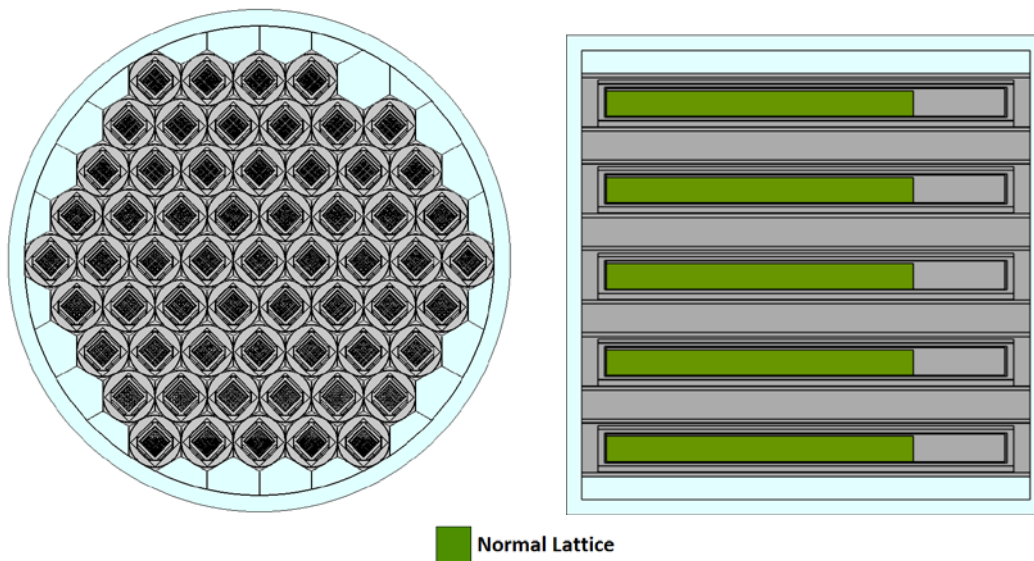


Figure 6-48 Group 2 NCT 60-package Array with Height of One Package

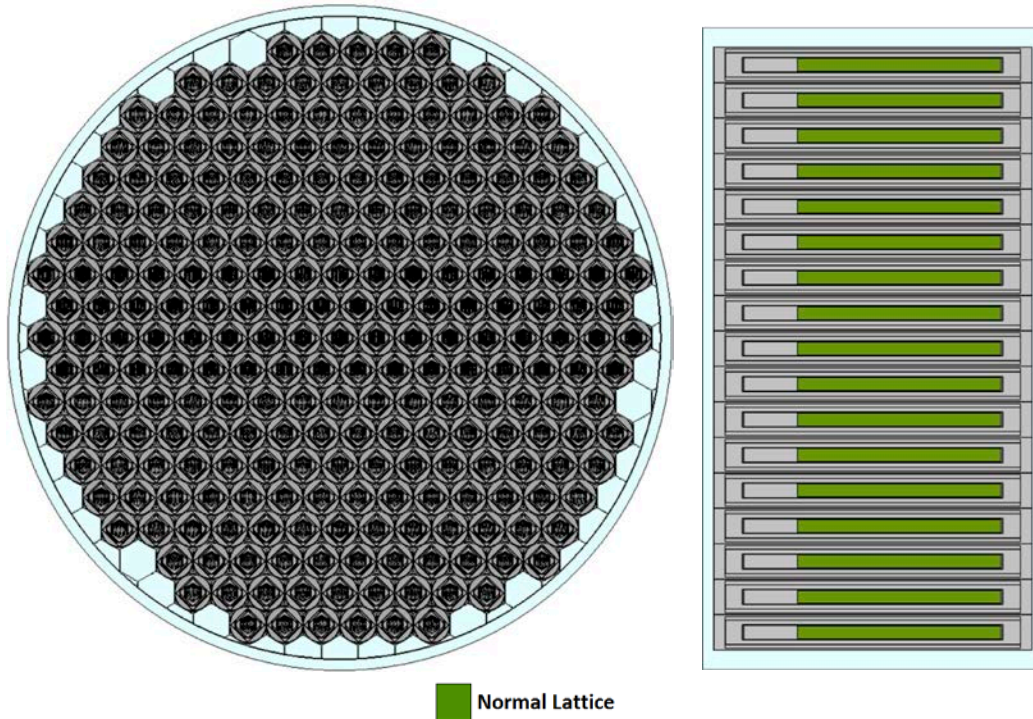


Figure 6-49 Group 3 NCT 250-package Array with Height of One Package

6.5.1.1.2 Rod Pipe

For the Rod Pipe, NCT package array baseline case determination, as defined in Section 6.3.4.2.2, loose rods are modeled in the Rod Pipe with a close-packed pitch equivalent to the fuel pellet OD. The pitch type is modeled as both square and hexagonal as the small variation of geometry varies the water-to-fuel ratio slightly. The Rod Pipe is flooded with full-density water with all remaining floodable regions void. Detailed results of the Rod Pipe NCT package array baseline case determination are shown in Section 6.9.3.4. For UO₂ fuel rods, comparison of the Traveller STD to Traveller XL baseline results show that, for the limiting fuel rod/pitch combination, the Traveller XL is consistently more reactive than the Traveller STD. The NCT package array baseline configurations for the Rod Pipe with UO₂ fuel rods and U₃Si₂ fuel rods is summarized in Table 6-52 and shown in Figure 6-50.

Table 6-52 Summary of Rod Pipe NCT Package Array Configurations								
Contents	Traveller Variant	Array Size (5N)	Array Height	Fuel OR (cm)	Pitch-Type	Fuel Half-Pitch (cm)	Flooding Configuration	k _{eff} ± σ
UO ₂ Fuel Rods	XL	379	1	3.5	Square	3.5	Inside Rod Pipe	0.46657 ± 0.00067
U ₃ Si ₂ Fuel Rods	STD	379	1	0.4851	Square	0.4851	Inside Rod Pipe	0.41633 ± 0.00035

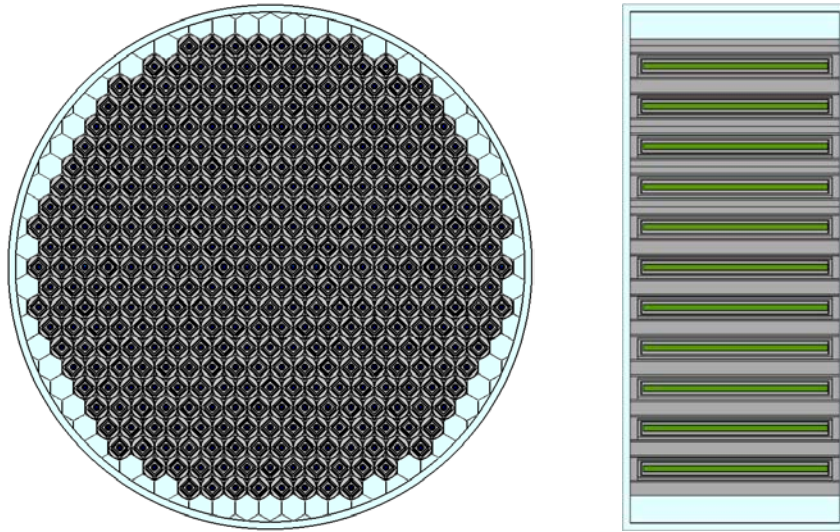


Figure 6-50 Rod Pipe NCT 379-package Array with Height of One Package

6.5.1.2 Sensitivity Study Configurations

Several sensitivity studies are completed for the NCT package array evaluation. The following summary tables list the bounding, as-penalized configurations of each sensitivity study. An entry of “None” signifies that the study resulted in no penalty and an entry of “--” signifies that the study did not require analyzing based on transport condition. The baseline case with the sum of penalties from sensitivity studies defines the most reactive configuration for demonstration of maximum reactivity.

6.5.1.2.1 Fuel Assembly – Group 1, 2 and 3

Listed in Table 6-53 are the bounding, as-penalized configurations of each sensitivity study for Groups 1, 2, and 3.

Sensitivity Study	Group 1	Group 2	Group 3
Annular Fuel Pellet Blanket	None	None	None
Clamshell/Fuel Assembly Shift	None	None	None
Package OD Tolerance	None	None	Minimum Package OD
Polyethylene Packing Materials	None	None	None
SS Rods	None	None	None
Cladding Tolerance	None	Minimum cladding thickness	Minimum Cladding Thickness
Fuel Pellet Diameter Tolerance	None	None	+ tolerance
Fuel Rod Pitch Tolerance	None	+ tolerance	None
Steel Reflector	None	None	None
Extended Active Fuel Length	--	--	None
ADOPT Fuel	None	None	--

Note: ‘--’ signifies the study was not applicable to the condition of transport analyzed. ‘None’ signifies that the sensitivity study did not result in a statistically significant increase in reactivity over the baseline case.

6.5.1.2.2 Rod Pipe

Listed in Table 6-54 are the bounding, as-penalized configurations of each sensitivity study for Rod Pipe content.

Sensitivity Study	Bounding Configuration UO ₂ Fuel Rods	Bounding Configuration U ₃ Si ₂ Fuel Rods
Annular Fuel Pellet Blanket	Full-length with proportional ID	Full-length
Rod Pipe Position in Clamshell	Down	None
Package OD Tolerance	None	None
Fuel Pellet Diameter Tolerance	+ tolerance	None
Polyethylene Packing Materials	1.0 cm-thick polyethylene wrap	0.3654 cm-thick polyethylene wrap
ADOPT Fuel	ADOPT rods	--

Note: '--' signifies the study was not applicable to the condition of transport analyzed. 'None' signifies that the sensitivity study did not result in a statistically significant increase in reactivity over the baseline case.

6.5.2 Results

6.5.2.1 NCT Package Array – Maximum Reactivity Results Summary

The maximum reactivity, *Maximum* k_{eff} , is defined by the bounding baseline $k_p + 2\sigma_p$ plus the sum of penalties assessed for each sensitivity study (Δk_u). See Table 6-55 for a summary of the *Maximum* k_{eff} results. All final values of maximum reactivity fall under the USL, as calculated per Section 6.8.

Traveller Variant	Bounding Content	$k_{eff} \pm \sigma$	$k_p + 2\sigma_p$	Δk_u	<i>Maximum</i> k_{eff}	USL
XL	Group 1 – 17 Bin 2	0.30888 ± 0.00027	0.30942	0.00000	0.30942	0.94162
XL	Group 2 – 16 Bin 1	0.30950 ± 0.00026	0.31002	0.00377	0.31379	0.94090
VVER	Group 3 – VV Bin 1	0.38828 ± 0.00016	0.38860	0.00182	0.39042	0.94029
XL	Rod Pipe UO ₂ Fuel Rods	0.46675 ± 0.00067	0.46809	0.12669	0.59478	0.94044
STD	Rod Pipe U ₃ Si ₂ Fuel Rods	0.41633 ± 0.00035	0.41703	0.27868	0.69571	0.94053

6.5.2.2 Sensitivity Study Results

As discussed in Section 6.3.4.2.1, the NCT package array baseline cases, for each package variant, are subjected to several sensitivity studies. Each sensitivity study is compared to the baseline case. The most reactive configuration resulting in the largest positive difference in $k_{eff} + 2\sigma$ from the baseline case value is tallied and summed to define the total penalty assessed (Δk_u).

6.5.2.2.1 Fuel Assembly – Groups 1, 2, and 3 Results Summary

Table 6-56 shows the summary of the penalty assessed for the sensitivity studies evaluated for all Group contents. An entry of “0.0” signifies that the study resulted in no positive penalty on reactivity.

Sensitivity Study	Group 1	Group 2	Group 3
Annular Fuel Pellet Blanket	0.0	0.0	0.0
Fuel Assembly Shift	0.0	0.0	0.0
Package OD Tolerance	0.0	0.0	0.00090
Polyethylene Packing Materials	0.0	0.0	0.0
SS Rods	0.0	0.0	0.0
Cladding Tolerance	0.0	0.00084	0.00042
Fuel Pellet Diameter Tolerance	0.0	0.0	0.00050
Fuel Rod Pitch Tolerance	0.0	0.00293	0.0
Steel Reflector	0.0	0.0	0.0
Extended Active Fuel Length	--	--	0.0
ADOPT Fuel	0.0	0.0	--
Total Penalty (Δk_u)	0.0	0.00377	0.00182

6.5.2.2.2 Fuel Assembly – Groups 1, 2, and 3 Detailed Results

The annular blanket sensitivity study, as defined in Section 6.3.4.3.1, examined the addition of annular fuel pellet blankets and varying the annular inner ID and blanket length. Annular fuel pellet blankets are added symmetrically to the top and bottom of an assembly. Table 6-57 defines the parameters evaluated and the results. Figure 6-51, Figure 6-52, and Figure 6-53 display the result trends for Groups 1, 2, and 3, respectively. The most reactive case is highlighted for each Group.

Contents (Group)	Traveller Variant	Annulus Diameter	Annulus Length (cm)	k_{eff}	σ	$k_{eff} + 2\sigma$	$\Delta(k_{eff} + 2\sigma)$
17 Bin 2 (1)	XL	Baseline Case		0.30888	0.00027	0.30942	--
		0.155 in. (0.3937 cm)	45.9	0.30217	0.00029	0.30275	-0.0067
			91.8	0.29643	0.00026	0.29695	-0.0125
			137.6	0.28650	0.00025	0.28700	-0.0224
			183.5	0.27587	0.00025	0.27637	-0.0331
		0.183 in. (0.4648 cm)	45.9	0.30054	0.00026	0.30106	-0.0084
			91.8	0.29203	0.00023	0.29249	-0.0169
			137.6	0.27831	0.00028	0.27887	-0.0306
			183.5	0.25951	0.00026	0.26003	-0.0494
		16 Bin 1 (2)	XL	Baseline Case		0.30950	0.00026
0.155 in. (0.3937 cm)	48.9			0.30691	0.00027	0.30745	-0.0026
	97.8			0.30246	0.00026	0.30298	-0.0070
	146.7			0.29423	0.00024	0.29471	-0.0153
	195.6			0.28265	0.00024	0.28313	-0.0269

Contents (Group)	Traveller Variant	Annulus Diameter	Annulus Length (cm)	k_{eff}	σ	$k_{eff} + 2\sigma$	$\Delta(k_{eff} + 2\sigma)$	
VV Bin 1 (3)	VVER	0.183 in. (0.4648 cm)	48.9	0.30619	0.00025	0.30669	-0.0033	
			97.8	0.29968	0.00023	0.30014	-0.0099	
			146.7	0.28801	0.00026	0.28853	-0.0215	
			195.6	0.27082	0.00025	0.27132	-0.0387	
		Baseline Case			0.38828	0.00016	0.3886	--
		0.155 in. (0.3937 cm)	45.53	0.38512	0.00015	0.38542	-0.0032	
			91.07	0.37857	0.00017	0.37891	-0.0097	
			136.60	0.36783	0.00018	0.36819	-0.0204	
			182.13	0.35187	0.00017	0.35221	-0.0364	
		0.183 in. (0.4648 cm)	45.53	0.38406	0.00016	0.38438	-0.0042	
			91.07	0.37514	0.00018	0.3755	-0.0131	
			136.60	0.35919	0.0002	0.35959	-0.0290	
182.13	0.33391		0.00015	0.33421	-0.0544			

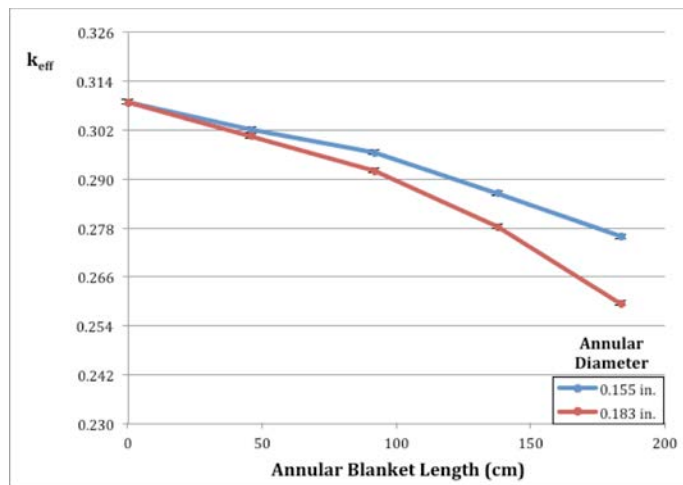


Figure 6-51 Annular Blanket Sensitivity – Package Array, NCT (Group 1)

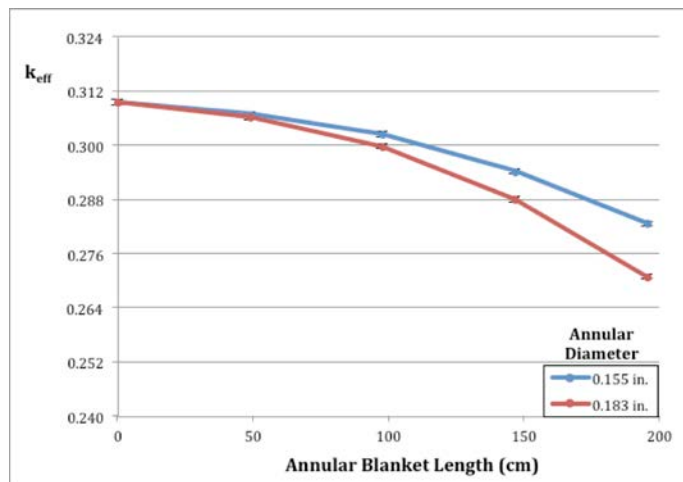


Figure 6-52 Annular Blanket Sensitivity – Package Array, NCT (Group 2)

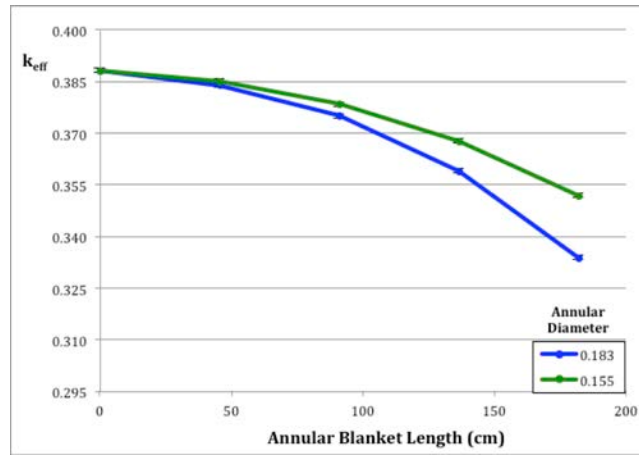


Figure 6-53 Annular Blanket Sensitivity – Package Array, NCT (Group 3)

The fuel assembly position sensitivity study, as defined in Section 6.3.4.3.2, examined the shifting of the fuel assembly in the Clamshell. Table 6-58 defines the parameter evaluated and the results. The most reactive case is highlighted for each Group.

Contents (Group)	Traveller Variant	Fuel Assembly Position	k _{eff}	σ	k _{eff} + 2σ	Δ(k _{eff} + 2σ)
17 Bin 2 (1)	XL	Baseline Case	0.30888	0.00027	0.30942	--
		Centered	0.30321	0.00023	0.30367	-0.00575
16 Bin 1 (2)	XL	Baseline Case	0.30950	0.00026	0.31002	--
		Centered	0.30755	0.00025	0.30805	-0.00197
VV Bin 1 (3)	VVER	Baseline Case	0.38828	0.00016	0.38860	--
		Centered	0.38604	0.00017	0.38638	-0.00222

The package outer diameter tolerance directly affects the spacing of the packages, thus the tolerance is evaluated, as defined in Section 6.3.4.3.4. Table 6-59 defines the parameter evaluated and the results. The most reactive case is highlighted for each Group.

Contents (Group)	Traveller Variant	Package Outer Diameter Tolerance (in.)	k _{eff}	σ	k _{eff} + 2σ	Δ(k _{eff} + 2σ)
17 Bin 2 (1)	XL	-0.2	0.30884	0.00031	0.30946	0.00004
		Nominal	0.30888	0.00027	0.30942	--
		+0.2	0.30811	0.00025	0.30861	-0.00081
16 Bin 1 (2)	XL	-0.2	0.31000	0.00024	0.31048	0.00046
		Nominal	0.30950	0.00026	0.31002	--
		+0.2	0.30930	0.00025	0.30980	-0.00022

Contents (Group)	Traveller Variant	Package Outer Diameter Tolerance (in.)	k_{eff}	σ	$k_{eff} + 2\sigma$	$\Delta(k_{eff} + 2\sigma)$
VV Bin 1 (3)	VVER	-0.2	0.38918	0.00016	0.3895	0.00090
		Nominal	0.38828	0.00016	0.38860	--
		+0.2	0.38728	0.00018	0.38764	-0.00096

The polyethylene packing materials sensitivity study, as defined in Section 6.3.4.3.5, examined the presence of an outer wrap around the fuel assembly for NCT configuration. Table 6-60 defines the parameter evaluated and the results. The most reactive case is highlighted for each Group.

Contents (Group)	Traveller Variant	Poly Model	Poly Mass (kg)	k_{eff}	σ	$k_{eff} + 2\sigma$	$\Delta(k_{eff} + 2\sigma)$
17 Bin 2 (1)	XL	Baseline Case	0.00	0.30888	0.00027	0.30942	--
		Outer Wrap	4.89	0.29270	0.00027	0.29324	-0.01618
16 Bin 1 (2)	XL	Baseline Case	0.00	0.30950	0.00026	0.31002	--
		Outer Wrap	5.90	0.29545	0.00024	0.29593	-0.01409
VV Bin 1 (3)	VVER	Baseline Case	0.0	0.38828	0.00016	0.3886	--
		Outer Wrap	4.962	0.35445	0.00016	0.35477	-0.03383

The SS replacement rod sensitivity study, as defined in Section 6.3.4.3.7, examined the replacement of fuel rods with SS rods in the fuel assembly. Table 6-61 defines the parameters evaluated and the results. The most reactive case is highlighted for each Group.

Bounding Content	Traveller Variant	SS Rod Configuration	k_{eff}	σ	$k_{eff} + 2\sigma$	$\Delta(k_{eff} + 2\sigma)$
17 Bin 2 (1)	XL	Baseline Case	0.30888	0.00027	0.30942	--
		Corner	0.26461	0.00028	0.26517	-0.04425
		Random	0.27926	0.00023	0.27972	-0.0297
16 Bin 1 (2)	XL	Baseline Case	0.30950	0.00026	0.31002	--
		Corner	0.26204	0.00024	0.26252	-0.0475
		Random	0.27269	0.00023	0.27315	-0.03687
VV Bin 1 (3)	VVER	Baseline Case	0.38828	0.00016	0.3886	--
		Corner	0.33747	0.00018	0.33783	-0.05077
		Random	0.35317	0.00015	0.35347	-0.03513

The tolerance sensitivity studies evaluate cladding dimensions, fuel pellet diameter, and fuel rod pitch, as defined in Section 6.3.4.3.8, 6.3.4.3.9, and 6.3.4.3.10, respectively. Table 6-62 defines the parameter dimensions evaluated and the results. The most reactive case is highlighted for each Group and tolerance parameter.

Content (Group)	Traveller Variant	Tolerance Parameter (in.)		k_{eff}	σ	k_{eff} + 2σ	Δ(k_{eff} + 2σ)
17 Bin 2 (1)	XL	Baseline Case		0.30888	0.00027	0.30942	--
16 Bin 1 (2)	XL	Baseline Case		0.30950	0.00026	0.31002	--
VV Bin 1 (3)	VVER	Baseline Case		0.38828	0.00016	0.3886	--
Cladding Tolerance		ID Tolerance (in.)	OD Tolerance (in.)	k_{eff}	σ	k_{eff} + 2σ	Δ(k_{eff} + 2σ)
17 Bin 2 (1)	XL	-0.002	-0.002	0.30850	0.00025	0.30900	-0.00042
			nominal	0.30849	0.00029	0.30907	-0.00035
			+0.002	0.30775	0.00026	0.30827	-0.00115
		nominal	-0.002	0.30909	0.00026	0.30961	0.00019
			nominal	0.30888	0.00027	0.30942	0.00000
			+0.002	0.30810	0.00028	0.30866	-0.00076
		+0.002	-0.002	0.30903	0.00024	0.30951	0.00009
			nominal	0.30878	0.00028	0.30934	-0.00008
			+0.002	0.30816	0.00025	0.30866	-0.00076
16 Bin 1 (2)	XL	-0.002	-0.002	0.30950	0.00024	0.30998	-0.00004
			nominal	0.30893	0.00029	0.30951	-0.00051
			+0.002	0.30919	0.00027	0.30973	-0.00029
		nominal	-0.002	0.31024	0.00025	0.31074	0.00072
			nominal	0.30950	0.00026	0.31002	0.00000
			+0.002	0.30953	0.00023	0.30999	-0.00003
		+0.002	-0.002	0.31036	0.00025	0.31086	0.00084
			nominal	0.31030	0.00027	0.31084	0.00082
			+0.002	0.30950	0.00025	0.31000	-0.00002
VV Bin 1 (3)	VVER	-0.0015	-0.0015	0.388	0.00018	0.38836	-0.00024
			nominal	0.38765	0.00017	0.38799	-0.00061
			+0.0015	0.38765	0.00017	0.38799	-0.00061
		nominal	-0.0015	0.38854	0.00016	0.38886	0.00026
			nominal	0.38828	0.00016	0.3886	0.00000
			+0.0015	0.38807	0.00016	0.38839	-0.00021
		+0.0015	-0.0015	0.3887	0.00016	0.38902	0.00042
			nominal	0.38834	0.00016	0.38866	0.00006
			+0.0015	0.38792	0.00015	0.38822	-0.00038
Pellet Diameter Tolerance		Pellet OD Tolerance (in.)		k_{eff}	σ	k_{eff} + 2σ	Δ(k_{eff} + 2σ)
17 Bin 2 (1)	XL	-0.0007		0.30801	0.00029	0.30859	-0.00083
		-0.0005		0.30773	0.00026	0.30825	-0.00117
		+0.0005		0.30903	0.00024	0.30951	0.00009
		+0.0007		0.30918	0.00031	0.30980	0.00038
16 Bin 1 (2)	XL	-0.0007		0.30922	0.00025	0.30972	-0.00030

		-0.0005	0.30951	0.00027	0.31005	0.00003
		+0.0005	0.30963	0.00027	0.31017	0.00015
		+0.0007	0.30992	0.00024	0.31040	0.00038
VV Bin 1 (3)	VVER	-0.0005	0.38765	0.00016	0.38797	-0.00063
		+0.0005	0.38876	0.00017	0.3891	0.00050
Pitch Tolerance		Pitch Tolerance (in.)	k_{eff}	σ	$k_{eff} + 2\sigma$	$\Delta(k_{eff} + 2\sigma)$
17 Bin 2 (1)	XL	-0.005	0.30744	0.00025	0.30794	-0.00148
		-0.001	0.30833	0.00024	0.30881	-0.00061
		+0.001	0.30868	0.00026	0.30920	-0.00022
		+0.005	0.30947	0.00024	0.30995	0.00053
16 Bin 1 (2)	XL	-0.0335	0.30154	0.00026	0.30206	-0.00796
		-0.0167	0.30487	0.00035	0.30557	-0.00445
		+0.0059	0.31090	0.00024	0.31138	0.00136
		+0.0118	0.31241	0.00027	0.31295	0.00293
VV Bin 1 (3)	VVER	-0.001	0.38807	0.00017	0.38841	-0.00019
		+0.001	0.38831	0.00019	0.38869	0.00009

The steel nozzle reflector sensitivity study, as defined in Section 6.3.4.3.11, examined the addition of two 50% density SS blocks at the top and bottom of the fuel assembly, simulating the top and bottom nozzles and their respective masses of steel. Table 6-63 defines the parameter evaluated and the results. The most reactive case is highlighted for each Group.

Contents (Group)	Traveller Variant	Stainless Steel Nozzle Configuration	k_{eff}	σ	$k_{eff} + 2\sigma$	$\Delta(k_{eff} + 2\sigma)$
17 Bin 2 (1)	XL	Baseline Case	0.30888	0.00027	0.30942	--
		50% density SS304	0.29967	0.00038	0.30043	-0.00899
16 Bin 1 (2)	XL	Baseline Case	0.30950	0.00026	0.31002	--
		50% density SS304	0.30718	0.00026	0.30770	-0.00232
VV Bin 1 (3)	VVER	Baseline Case	0.38828	0.00016	0.3886	--
		50% density SS304	0.38719	0.00017	0.38753	-0.00107

The fuel assembly position sensitivity study, as defined in Section 6.3.4.3.12, examined the extended active fuel length for Group 3. Table 6-64 defines the parameter evaluated and the results. The most reactive case is highlighted.

Table 6-64 Extended Active Fuel Length Results – Package Array, NCT, Group 3						
Contents (Group)	Traveller Variant	Active Fuel Length (cm)	k_{eff}	σ	$k_{eff} + 2\sigma$	$\Delta(k_{eff} + 2\sigma)$
VV Bin 1 (3)	VVER	Baseline Case 364.261	0.38828	0.00016	0.38860	--
		364.631	0.38836	0.0002	0.38876	0.00016
		365.000	0.38855	0.00018	0.38891	0.00031
		366.270	0.38843	0.00017	0.38877	0.00017

The ADOPT Fuel sensitivity study, as defined in Section 6.3.4.3.14, examined the effect of replacing standard UO₂ fuel with ADOPT fuel. Table 6-64A lists the results of the study. The most reactive case is highlighted.

Table 6-64A ADOPT Fuel Results – Package Array, NCT, Groups 1 & 2						
Contents (Group)	Traveller Variant	Fuel	k_{eff}	σ	$k_{eff} + 2\sigma$	$\Delta(k_{eff} + 2\sigma)$
17 Bin 2 (1)	XL	Baseline (UO₂)	0.30888	0.00027	0.30942	--
		ADOPT	0.30845	0.00027	0.30899	-0.00043
16 Bin 1 (2)	XL	Baseline (UO₂)	0.30950	0.00026	0.31002	--
		ADOPT	0.30939	0.00024	0.30987	-0.00015

6.5.2.2.3 Rod Pipe Results Summary

Table 6-65 shows the summary of the penalties assessed for the sensitivity studies analyzed for Rod Pipe NCT package array evaluation. An entry of “0.0” signifies that the study resulted in no positive penalty on reactivity.

Table 6-65 Rod Pipe NCT Package Array Assessed Penalties, Δk_u		
Sensitivity Study	Penalty Assessed	
	Rod Pipe UO ₂ Fuel Rods	Rod Pipe U ₃ Si ₂ Fuel Rods
Annular Fuel Pellet Blanket	0.05967	0.02234
Rod Pipe Position in Clamshell	0.00263	0.0
Package OD Tolerance	0.0	0.0
Polyethylene Packing Materials	0.06112	0.25634
Fuel Pellet Diameter Tolerance	0.00181	0.0
ADOPT Fuel	0.00146	--
Total Penalty (Δk_u)	0.12669	0.27868

6.5.2.2.4 Rod Pipe Detailed Results

The annular blanket sensitivity study, as defined in Section 6.3.4.3.1, examined the addition of varying annular fuel pellet ID and lengths of annular fuel pellet blanket lengths equally to the top and bottom of a fuel rod. Table 6-66 defines the parameters evaluated and the results, and Figure 6-54 and Figure 6-55 display the result trends. The most reactive case is highlighted for each content.

Contents	Traveller Variant	Annulus Diameter	Annulus Length (cm)	k_{eff}	σ	$k_{eff} + 2\sigma$	$\Delta(k_{eff} + 2\sigma)$		
Rod Pipe UO ₂ Fuel Rods	XL	Baseline Case		0.46675	0.00067	0.46809	--		
		0.155 in. (0.3937 cm)	13	0.46788	0.00037	0.46862	0.00053		
			26	0.46815	0.00036	0.46887	0.00078		
			39	0.46840	0.00036	0.46912	0.00103		
			78	0.46799	0.00036	0.46871	0.00062		
			250.825	0.46954	0.00037	0.47028	0.00219		
		0.183 in. (0.4648 cm)	13	0.46853	0.00043	0.46939	0.0013		
			26	0.46872	0.00041	0.46954	0.00145		
			39	0.46814	0.00039	0.46892	0.00083		
			78	0.4683	0.00035	0.46900	0.00091		
			250.825	0.46947	0.00039	0.47025	0.00216		
		1.213 in. (3.0810 cm)	13	0.46853	0.0004	0.46933	0.00124		
			26	0.47043	0.00045	0.47133	0.00324		
			39	0.47270	0.00041	0.47352	0.00543		
			78	0.48777	0.00039	0.48855	0.02046		
			250.825	0.52692	0.00042	0.52776	0.05967		
		Rod Pipe U ₃ Si ₂ Fuel Rods	STD	Baseline Case		0.41633	0.00035	0.41703	--
				0.155 in. (0.3937 cm)	13	0.41548	0.00040	0.41628	-0.00075
					26	0.41637	0.00037	0.41711	0.00008
					39	0.41653	0.00039	0.41731	0.00028
78	0.42092				0.00038	0.42168	0.00465		
213.995	0.43094				0.00039	0.43172	0.01469		
0.183 in. (0.4648 cm)	13			0.41625	0.00040	0.41705	0.00002		
	26			0.41679	0.00037	0.41753	0.00050		
	39			0.41799	0.00038	0.41875	0.00172		
	78			0.42454	0.00042	0.42538	0.00835		
	213.995			0.43849	0.00044	0.43937	0.02234		

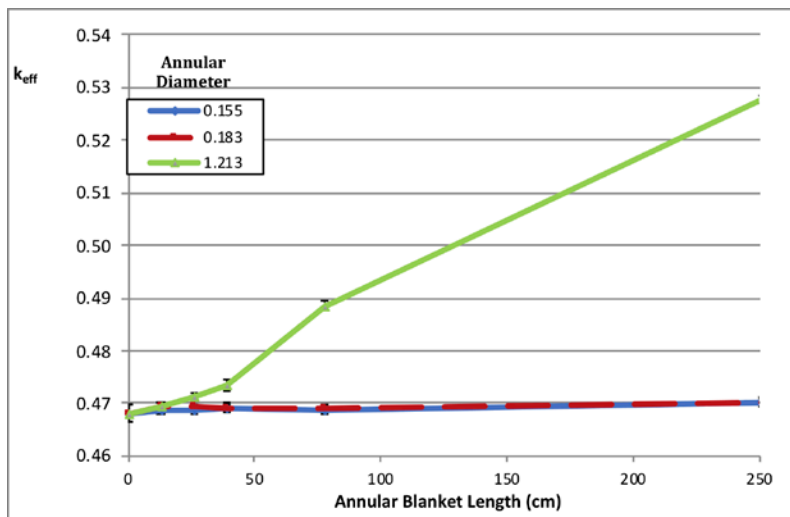


Figure 6-54 Annular Blanket Sensitivity – Package Array, NCT (Rod Pipe UO₂ Fuel Rods)

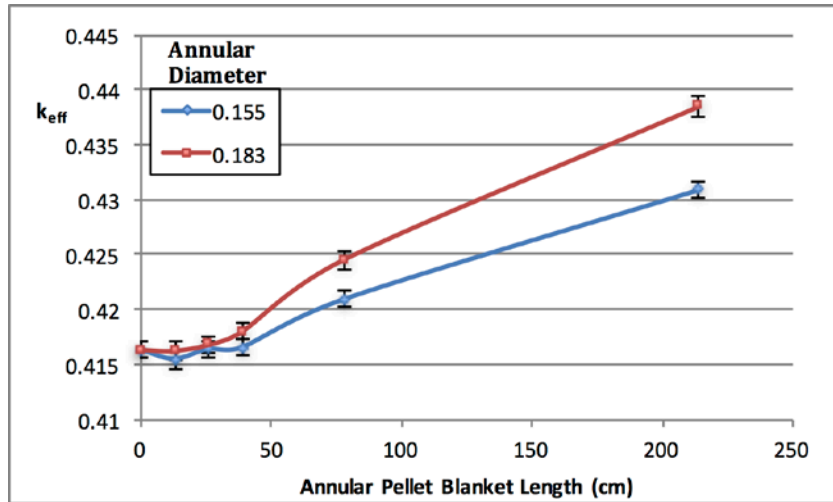


Figure 6-55 Annular Blanket Sensitivity – Package Array, NCT (Rod Pipe U₃Si₂ Fuel Rods)

The Rod Pipe position sensitivity study, as defined in Section 6.3.4.3.2, examined the shifting of the Rod Pipe in the Clamshell from the centered, baseline position. Table 6-67 defines the parameter evaluated and the results. The most reactive case is highlighted for each content.

Contents	Traveller Variant	Fuel Assembly Position	k_{eff}	σ	$k_{eff} + 2\sigma$	$\Delta(k_{eff} + 2\sigma)$
Rod Pipe UO ₂ Fuel Rods	XL	Baseline Case	0.46675	0.00067	0.46809	--
		Down	0.46982	0.00045	0.47072	0.00263
Rod Pipe U ₃ Si ₂ Fuel Rods	STD	Baseline Case	0.41633	0.00035	0.41703	--
		Down	0.41477	0.00039	0.41555	-0.00148

The package outer diameter tolerance directly affects the spacing of the packages in an array, thus the tolerance is evaluated, as defined in Section 6.3.4.3.4. Table 6-68 defines the parameter evaluated and the results. The most reactive case is highlighted for each content.

Contents	Traveller Variant	Package Outer Diameter (in.)	k_{eff}	σ	$k_{eff} + 2\sigma$	$\Delta(k_{eff} + 2\sigma)$
Rod Pipe UO ₂ Fuel Rods	XL	-0.2	0.46817	0.00041	0.46899	0.00090
		Nominal	0.46675	0.00067	0.46809	--
		+0.2	0.46721	0.00041	0.46803	-0.00006
Rod Pipe U ₃ Si ₂ Fuel Rods	STD	-0.2	0.41638	0.00038	0.41714	0.00011
		Nominal	0.41633	0.00035	0.41703	--
		+0.2	0.41571	0.00039	0.41649	-0.00054

The polyethylene packing materials sensitivity study for the Rod Pipe NCT package array evaluation, as defined in Section 6.3.4.3.5, examined the presence of a uniform wrap around each fuel rod. Table 6-69 defines the parameter evaluated and the results, and Figure 6-56 and Figure 6-57 display the trend. The most reactive case is highlighted for each content.

Table 6-69 Polyethylene Packing Sensitivity Results – Package Array, NCT, Rod Pipe							
Contents	Traveller Variant	Poly Model	Poly Mass (kg)	k_{eff}	σ	$k_{eff} + 2\sigma$	$\Delta(k_{eff} + 2\sigma)$
Rod Pipe UO ₂ Fuel Rods	XL	Baseline Case	0.0	0.46675	0.00067	0.46809	--
		Uniform Wrap	1.67	0.47942	0.00039	0.48020	0.01211
			2.19	0.48287	0.00036	0.48359	0.01550
			4.28	0.49650	0.00045	0.49740	0.02931
			18.32	0.52692	0.00039	0.52770	0.05961
			30.89	0.52825	0.00048	0.52921	0.06112
Rod Pipe U ₃ Si ₂ Fuel Rods	STD	Baseline Case	0.00	0.41633	0.00035	0.41703	--
		Uniform Wrap	1.85	0.4342	0.00042	0.43504	0.01801
			3.79	0.45568	0.00039	0.45646	0.03943
			7.96	0.49859	0.00039	0.49937	0.08234
			17.41	0.58134	0.00044	0.58222	0.16519
			36.30	0.67249	0.00044	0.67337	0.25634

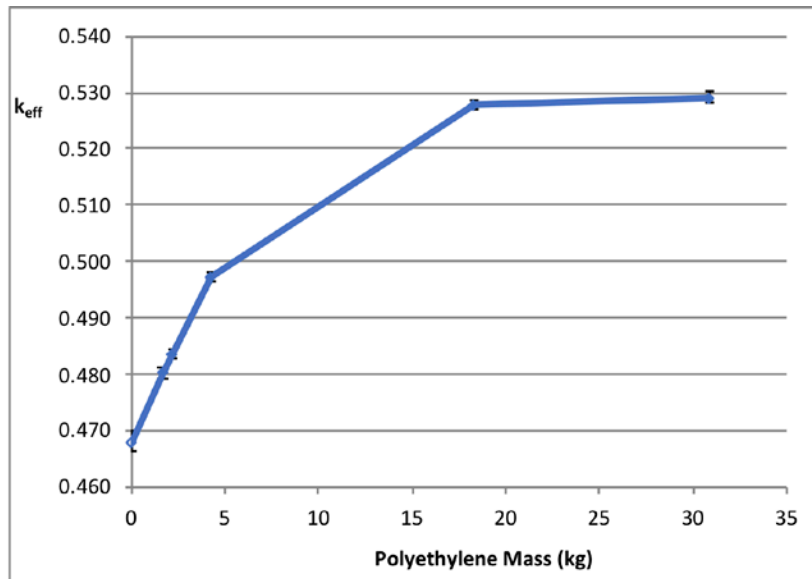


Figure 6-56 Polyethylene Packing Sensitivity – Package Array, NCT (Rod Pipe UO₂ Fuel Rods)

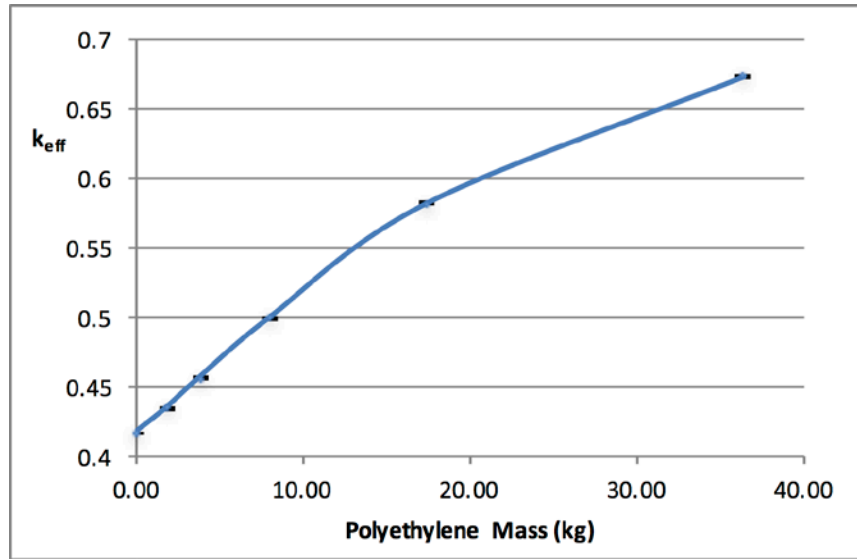


Figure 6-57 Polyethylene Packing Sensitivity – Package Array, NCT (Rod Pipe U₃Si₂ Fuel Rods)

The tolerance sensitivity study evaluates fuel pellet diameter only, as defined in Section 6.3.4.3.9. The Rod Pipe contents are not defined by cladding and pitch parameters, thus there is tolerance evaluation as explained in Section 6.3.4.3.8 and 6.3.4.3.10, respectively. Table 6-70 defines the parameter dimensions evaluated and the results. The most reactive case is highlighted for each content and tolerance parameter.

Table 6-70 Tolerance Sensitivity Results – Package Array, NCT, Rod Pipe						
Content	Traveller Variant	Pellet Diameter Tolerance (in.)	k_{eff}	σ	$k_{eff} + 2\sigma$	$\Delta(k_{eff} + 2\sigma)$
Rod Pipe UO ₂ Fuel Rods	XL	-0.0014	0.46806	0.00037	0.46880	0.00071
		-0.0010	0.46828	0.00040	0.46908	0.00099
		Nominal	0.46675	0.00067	0.46809	--
		+0.0010	0.46906	0.00042	0.46990	0.00181
		+0.0014	0.46768	0.00034	0.46836	0.00027
Rod Pipe U ₃ Si ₂ Fuel Rods	STD	-0.0014	0.41511	0.00037	0.41585	-0.00118
		-0.0010	0.41508	0.00036	0.41580	-0.00123
		Nominal	0.41633	0.00035	0.41703	--
		+0.0010	0.41664	0.00041	0.41746	0.00043
		+0.0014	0.41641	0.00037	0.41715	0.00012

The ADOPT Fuel sensitivity study, as defined in Section 6.3.4.3.14, examined the effect of replacing standard UO₂ fuel with ADOPT fuel. Table 6-70A lists the results of the study. The most reactive case is highlighted.

Table 6-70A ADOPT Fuel Results – Package Array, NCT, Rod Pipe						
Content	Traveller Variant	Fuel	k_{eff}	σ	$k_{eff} + 2\sigma$	$\Delta(k_{eff} + 2\sigma)$
Rod Pipe UO ₂ Fuel Rods	XL	Baseline (UO₂)	0.46675	0.00067	0.46809	--
		ADOPT	0.46823	0.00066	0.46955	0.00146

6.6 PACKAGE ARRAYS UNDER HYPOTHETICAL ACCIDENT CONDITIONS

6.6.1 Configuration

For all package array arrangements under hypothetical accident conditions, the Clamshell interior and fuel assembly envelope are modeled as flooded with full-density water, including the fuel-clad gap where applicable. Additional material modeling is specified in Section 6.3.2. Several materials, including fuel structural components and packaging components (e.g. Outerpack foam regions, ceramic fiber blankets, and shock mounts, etc.), are replaced with void, as this promotes the most neutron cross-talk between packages in an array. The package array is reflected with at least 20 cm of full-density water.

6.6.1.1 Baseline Configuration

As described in Section 6.3.4.2, a baseline case is evaluated for all content Groups and Rod Pipe configurations under HAC. Baseline configurations represent a bounding model that is carried forward to the sensitivity studies to demonstrate maximum reactivity.

6.6.1.1.1 Fuel Assembly – Groups 1, 2, and 3

Detailed results of the CFA-package variant comparison for the HAC package array assessment are shown in Section 6.9.3.5. The Traveller XL is consistently more reactive than the Traveller STD under HAC in a package array. In addition, an array with a height of one package is more reactive than a height of two packages. Therefore, the Traveller STD and packages arrays with a height of two packages are not further analyzed for the package array under HAC evaluation.

6.6.1.1.1.1 Baseline Case Determination

For the baseline case determination, as defined in Section 6.3.4.2.1, first the bounding CFAs-package variant combination is determined. For Groups 1 and 2, the Traveller XL is consistently more reactive than the Traveller STD for an array under HAC. As discussed in Section 6.3.4.2.1.2, the positioning of the fuel assembly is examined because of the physical properties of the packaging. Flooding configuration is examined in order to determine moderation by water to the most reactive, credible extent. Detailed results of the baseline case determination are shown in Section 6.9.3.5. The HAC baseline configurations are summarized in Table 6-71. Each of the array configurations are shown in Figure 6-58, Figure 6-59, and Figure 6-60.

Traveller Variant	Contents (Group)	Array Size (2N)	Array Height	Lattice Expansion Length (cm)	Axial Position (cm)	Flooding Configuration	$k_{eff} \pm \sigma$
XL	17 Bin 1 (1)	100	1	50.8	87.122	Fuel Assembly and Clamshell	0.92688 ± 0.00031
XL	18 Bin 1 (2)	24	1	50.8	72.583	Fuel Assembly and Clamshell	0.91690 ± 0.00025
VVER	VV Bin 1 (3)	100	1	50.8	3.81	Fuel Assembly and Clamshell	0.91373 ± 0.00024

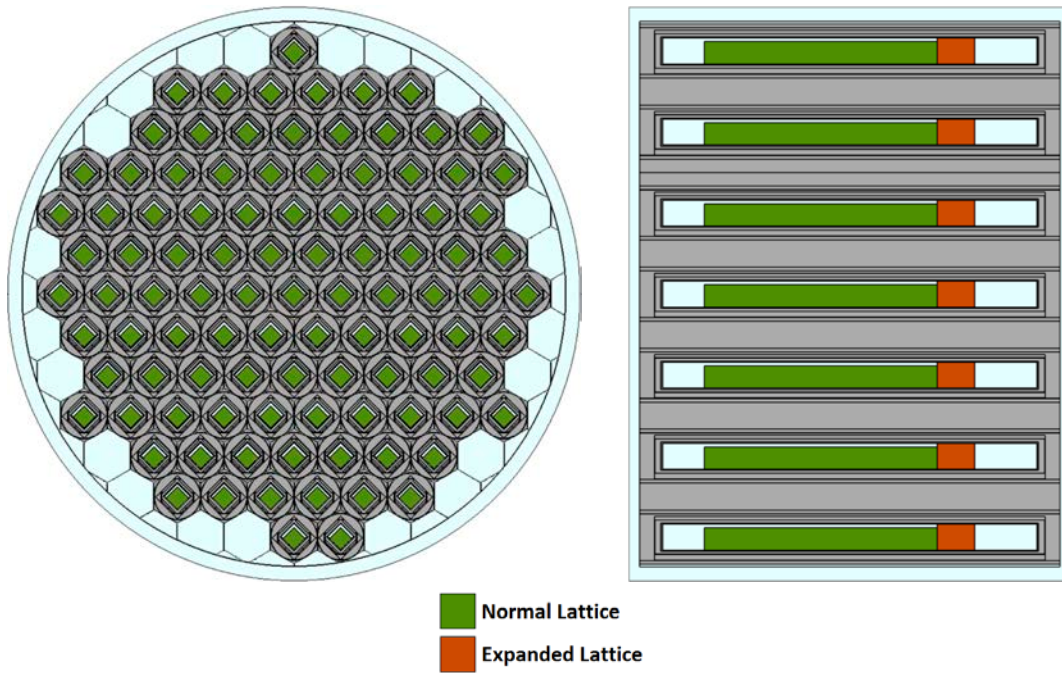


Figure 6-58 Group 1, HAC 100-package Array

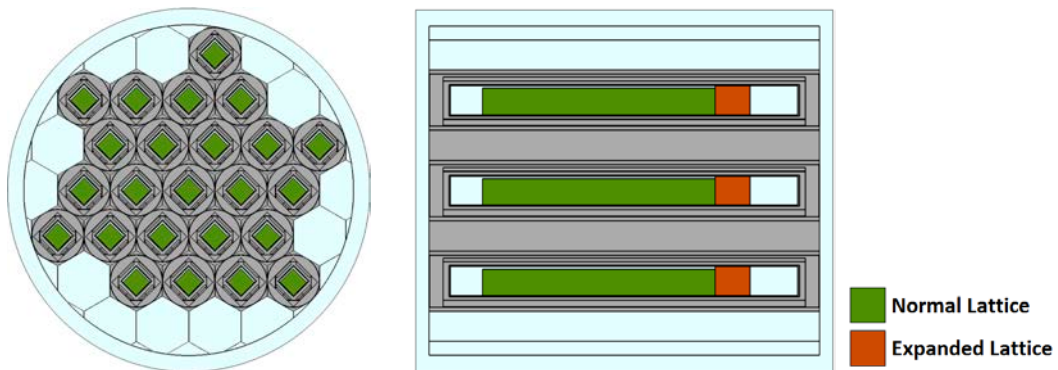


Figure 6-59 Group 2, HAC 24-package Array

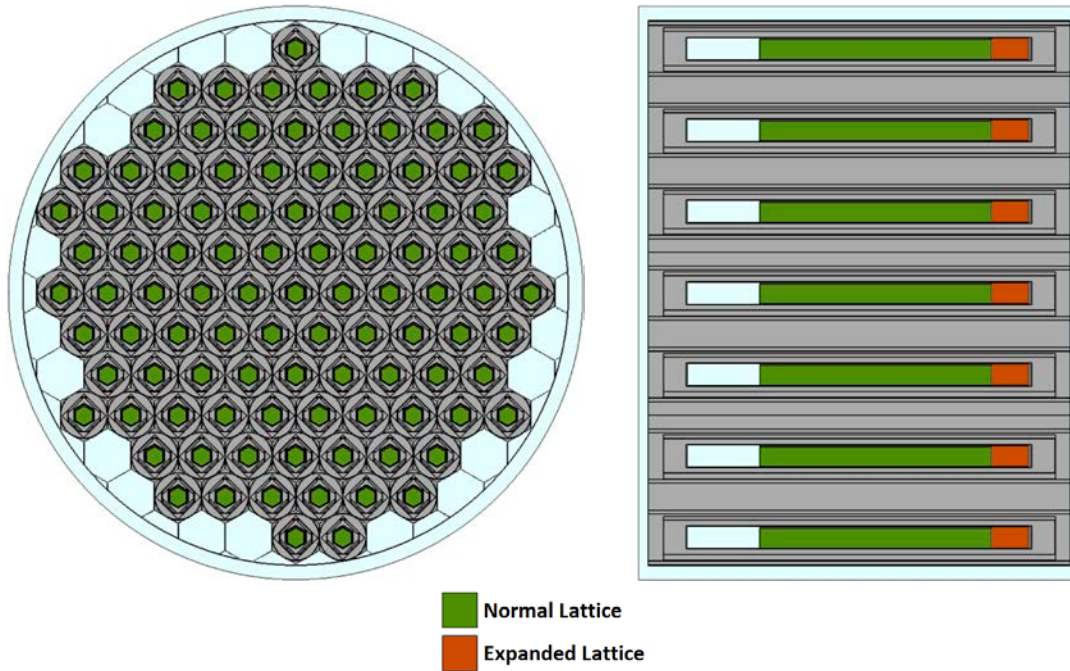


Figure 6-60 Group 3, HAC 100-package Array

6.6.1.1.2 Rod Pipe

For the Rod Pipe, HAC package array baseline case determination, as defined in Section 6.3.4.2.2, loose rods are modeled in the Rod Pipe and the pitch is expanded through a peak water-to-fuel ratio by changing the pitch for various fuel radii. The pitch type is modeled as both square and hexagonal, as this small variation in geometry varies the water-to-fuel ratio slightly. For the package array under HAC, the Clamshell and Rod Pipe interior regions are fully flooded with all other package interior and exterior regions modeled as void. Detailed results of the Rod Pipe HAC package array baseline case determination are shown in Section 6.9.3.6. For UO₂ fuel rods, comparison of the Traveller STD to Traveller XL baseline results show that, for the limiting fuel rod/pitch combination, the Traveller XL is consistently more reactive than the Traveller STD. The HAC package array baseline configurations for the Rod Pipe with UO₂ fuel rods and U₃Si₂ fuel rods are summarized in Table 6-72 and shown in Figure 6-61.

Table 6-72 Summary of Rod Pipe HAC Package Array Configurations								
Contents	Traveller Variant	Array Size (2N)	Array Height	Fuel OR (cm)	Pitch-Type	Fuel Rod Half-Pitch (cm)	Flooding Configuration	k _{eff} ± σ
UO ₂ Fuel Rods	XL	150	1	0.50	Hexagonal	1.0	Rod Pipe and Clamshell	0.66385 ± 0.00050
U ₃ Si ₂ Fuel Rods	STD	150	1	0.4851	Hexagonal	0.9851	Rod Pipe and Clamshell	0.62316 ± 0.00048

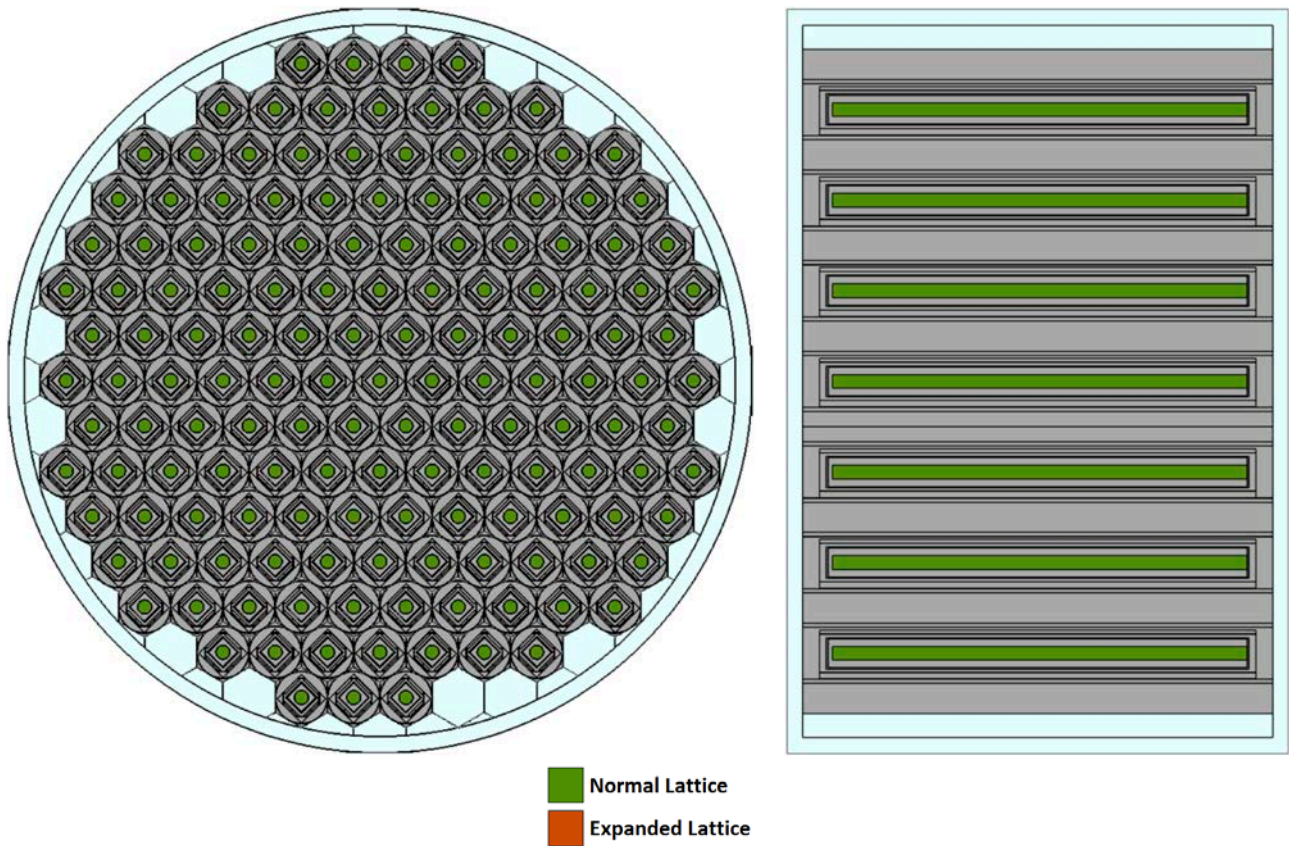


Figure 6-61 Rod Pipe, HAC 150-package Array

6.6.1.2 Sensitivity Study Configurations

Several sensitivity studies are analyzed for the HAC package array evaluation. The following summary tables list the bounding, as-penalized configurations of each sensitivity study. An entry of “None” signifies that the study resulted in no penalty and an entry of “--” signifies that the study did not require analyzing based on transport condition. The baseline case ($k_p + 2\sigma_p$) with the sum of penalties from the sensitivity studies (Δk_u) defines the most reactive configuration ($Maximum\ k_{eff} = k_p + 2\sigma_p + \Delta k_u$) and demonstrates the maximum reactivity for HAC package arrays.

6.6.1.2.1 Fuel Assembly – Groups 1, 2, and 3

Listed in Table 6-73 are the bounding, as-penalized configurations of each sensitivity study for the Groups 1, 2, and 3 HAC package array evaluations.

Sensitivity Study	Group 1	Group 2	Group 3
Annular Fuel Pellet Blanket	None	None	20.0 in. (50.8 cm) long
Clamshell/Fuel Assembly Shift	Clamshell/fuel assembly shifted up	Clamshell/fuel assembly shifted up	VVER Clamshell/fuel assembly shifted up
Moderator Density	None	None	1% density reduction
Package OD Tolerance	None	- Tolerance	- Tolerance
Polyethylene Packing Materials	2.00 kg of uniform melt	2.00 kg of collected melt	2.00 kg of uniform melt
Axial Rod Displacement	None	None	64 rods randomly shifted upward
Stainless Steel Rods	None	None	None
Cladding Tolerance	Minimum cladding thickness	Minimum cladding thickness	Minimum cladding thickness
Fuel Pellet Diameter Tolerance	None	- Tolerance	- Tolerance
Fuel Rod Pitch Tolerance	+ Tolerance	+ Tolerance	+ Tolerance
Steel Nozzle Reflector	None	None	None
Extended Active Fuel Length	--	--	Longer Length
ADOPT Fuel	None	None	--

Note: ‘None’ signifies that the sensitivity study did not result in a statistically significant increase in reactivity over the baseline case.
 ‘--’ signifies the study was not applicable to the condition of transport analyzed.

6.6.1.2.2 Rod Pipe

Listed in Table 6-74 are the bounding, as-penalized configurations of each sensitivity study for the Rod Pipe HAC package array evaluation.

Sensitivity Study	Bounding Configuration UO ₂ Fuel Rods	Bounding Configuration U ₃ Si ₂ Fuel Rods
Annular Fuel Pellet Blanket	Full-length	None
Rod Pipe Position in Clamshell	Centered	Centered
Moderator Density	None	1% density reduction
Package OD Tolerance	-Tolerance	- Tolerance
Fuel Pellet Diameter Tolerance	None	None
Polyethylene Packing Materials	Rod Pipe full of polyethylene	Rod Pipe full of polyethylene
Moderation Variation	Clamshell and Rod Pipe fully flooded	Clamshell and Rod Pipe fully flooded
ADOPT Fuel	None	--

Note: ‘None’ signifies that the sensitivity study did not result in a statistically significant increase in reactivity over the baseline case.
 ‘--’ signifies the study was not applicable to the condition of transport analyzed.

6.6.2 Results

6.6.2.1 HAC Package Array – Maximum Reactivity Results Summary

The maximum reactivity, *Maximum* k_{eff} , is defined by the bounding baseline ($k_p + 2\sigma_p$) plus the sum of penalties assessed for each sensitivity study (Δk_u). See Table 6-75 for a summary of the *Maximum* k_{eff} results. Final values of maximum reactivity fall under the USL, as calculated per Section 6.8.

Contents	Traveller Variant	Array Size (2N)	Array Height	Bin	$k_{eff} \pm \sigma$	$k_p + 2\sigma_p$	Δk_u	<i>Maximum</i> k_{eff}	USL
Group 1	XL	100	1	17 Bin 1	0.92688 ± 0.00031	0.92750	0.01033	0.93783	0.94162
Group 2	XL	24	1	18 Bin 1	0.91690 ± 0.00025	0.91740	0.02205	0.93945	0.94090
Group 3	VVER	100	1	VV Bin 1	0.91373 ± 0.00024	0.91421	0.01643	0.93064	0.94029
Rod Pipe UO ₂ Fuel Rods	XL	150	1	--	0.66385 ± 0.00050	0.66485	0.15103	0.81588	0.94044
Rod Pipe U ₃ Si ₂ Fuel Rods	STD	150	1	--	0.62316 ± 0.00048	0.62412	0.14424	0.76836	0.94053

6.6.2.2 Sensitivity Study Results

As discussed in Section 6.3.4.3, for each package arrangement, the HAC package array baseline cases are subjected to several sensitivity studies, which are detailed in Table 6-18. Each sensitivity study is compared to the baseline case. The most reactive configuration resulting in the largest positive difference in $k_{eff} + 2\sigma$ from the baseline case value is tallied and summed to define the total penalty assessed (Δk_u).

6.6.2.2.1 Fuel Assembly – Groups 1, 2, and 3 Results Summary

Table 6-76 shows the summary of the penalty assessed for the sensitivity studies evaluated for the Groups 1, 2, and 3 contents. An entry of “0.0” signifies that the study resulted in no positive penalty on reactivity.

Sensitivity Study	Group 1	Group 2	Group 3
Annular Fuel Pellet Blanket	0.0	0.0	0.00089
Clamshell/Fuel Assembly Shift	0.00353	0.00351	0.00094
Moderator Density	0.0	0.0	0.00082
Package OD Tolerance	0.0	0.00101	0.00051
Polyethylene Packing Materials	0.00079	0.00154	0.00154
Axial Rod Displacement	0.0	0.0	0.00529
Stainless Steel Rods	0.0	0.0	0.0

Sensitivity Study	Group 1	Group 2	Group 3
Cladding Tolerance	0.00310	0.00451	0.00421
Fuel Pellet Diameter Tolerance	0.0	0.00050	0.00052
Fuel Rod Pitch Tolerance	0.00291	0.01098	0.00117
Steel Nozzle Reflector	0.0	0.0	0.0
Extended Active Fuel Length	--	--	0.00054
ADOPT Fuel	0.0	0.0	--
Total Penalty (Δk_u)	0.01033	0.02205	0.01643

6.6.2.2.2 Fuel Assembly – Groups 1, 2, and 3 Detailed Results

The annular blanket sensitivity study, as defined in Section 6.3.4.3.1, examined the addition of varying annular fuel pellet ID and lengths of annular fuel pellet blanket lengths equally to the top and bottom of an assembly. Table 6-77 defines the parameters evaluated and the results. Figure 6-62, Figure 6-63, and Figure 6-64 display the result trends for Groups 1, 2, and 3, respectively. The most reactive case is highlighted for each Group.

Contents (Group)	Traveller Variant	Annulus Diameter	Annulus Length (cm)	k_{eff}	σ	$k_{eff} + 2\sigma$	$\Delta(k_{eff} + 2\sigma)$		
17 Bin 1 (1)	XL	Baseline Case		0.92688	0.00031	0.92750	--		
		0.155 in. (0.3937 cm)	13.0	0.92561	0.00030	0.92621	-0.00129		
			26.0	0.92288	0.00025	0.92338	-0.00412		
			39.0	0.91941	0.00027	0.91995	-0.00755		
			50.8	0.91674	0.00026	0.91726	-0.01024		
			95.0383	0.91693	0.00025	0.91743	-0.01007		
			139.2767	0.91789	0.00026	0.91841	-0.00909		
		183.5150	0.91828	0.00025	0.91878	-0.00872			
		0.183 in. (0.4648 cm)	13.0	0.92413	0.00025	0.92463	-0.00287		
			26.0	0.92016	0.00024	0.92064	-0.00686		
			39.0	0.91504	0.00024	0.91552	-0.01198		
			50.8	0.91111	0.00024	0.91159	-0.01591		
			95.0383	0.91117	0.00029	0.91175	-0.01575		
			139.2767	0.91067	0.00026	0.91119	-0.01631		
		183.5150	0.91016	0.00025	0.91066	-0.01684			
		18 Bin 1 (2)	XL	Baseline Case		0.91690	0.00025	0.91740	--
				0.155 in. (0.3937 cm)	13.0	0.91685	0.00024	0.91733	-0.00007
					26.0	0.91648	0.00026	0.91700	-0.00040
39.0	0.91544				0.00027	0.91598	-0.00142		
50.8	0.91547				0.00028	0.91603	-0.00137		
0.183 in. (0.4648 cm)	13.0			0.91650	0.00025	0.91700	-0.00040		
	26.0			0.91544	0.00024	0.91592	-0.00148		
	39.0			0.91436	0.00025	0.91486	-0.00254		
	50.8			0.91340	0.00024	0.91388	-0.00352		

Contents (Group)	Traveller Variant	Annulus Diameter	Annulus Length (cm)	k_{eff}	σ	$k_{eff} + 2\sigma$	$\Delta(k_{eff} + 2\sigma)$
VV Bin 1 (3)	VVER	Baseline Case		0.91373	0.00024	0.91421	--
		0.155 in. (0.3937 cm)	25.40	0.91366	0.00029	0.91424	0.00003
			50.80	0.91462	0.00024	0.91510	0.00089
			136.60	0.92357	0.00023	0.92403	0.00982
			182.13	0.92701	0.00027	0.92755	0.01334
		0.183 in. (0.4648 cm)	25.40	0.91294	0.00025	0.91344	-0.00077
			50.80	0.91296	0.0003	0.91356	-0.00065
			136.60	0.92215	0.00023	0.92261	0.00840
			182.13	0.92713	0.00027	0.92767	0.01346

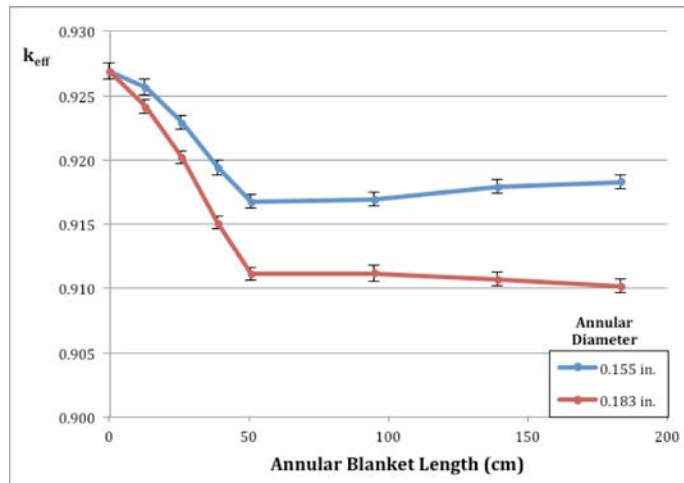


Figure 6-62 Annular Blanket Sensitivity – HAC Package Array (Group 1)

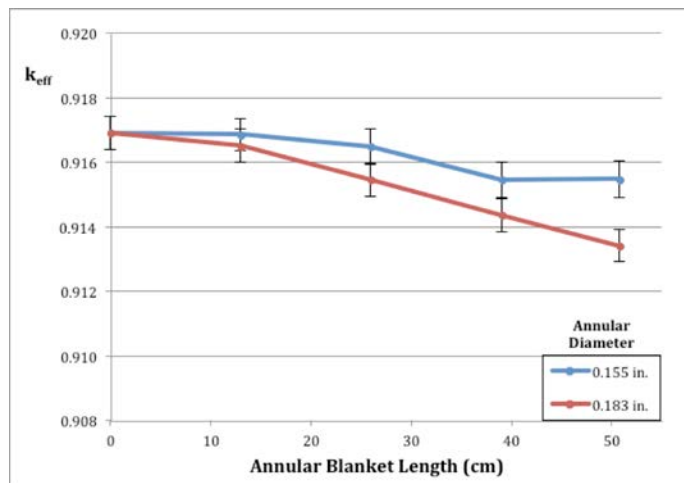


Figure 6-63 Annular Blanket Sensitivity – HAC Package Array (Group 2)

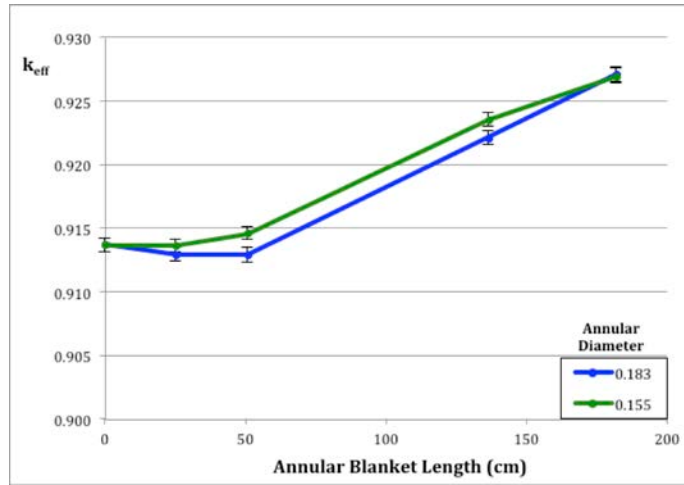


Figure 6-64 Annular Blanket Sensitivity – HAC Package Array (Group 3)

The Clamshell/fuel assembly position sensitivity study, as defined in Section 6.3.4.3.2, examined the shifting of the Clamshell to the top of the inner cavity and the fuel assembly to the top of the Clamshell in the x-y plane. Table 6-78 defines the parameter evaluated and the results. The most reactive case is highlighted for each Group.

Contents (Group)	Traveller Variant	Clamshell Position	Fuel Assembly Position	k _{eff}	σ	k _{eff} + 2σ	Δ(k _{eff} + 2σ)
17 Bin 1 (1)	XL	Baseline Case		0.92688	0.00031	0.92750	--
		Up	Up	0.93047	0.00028	0.93103	0.00353
18 Bin 1 (2)	XL	Baseline Case		0.91690	0.00025	0.91740	--
		Up	Up	0.92043	0.00024	0.92091	0.00351
VV Bin 1 (3)	VVER	Baseline Case		0.91373	0.00024	0.91421	--
		Up	Up	0.91463	0.00026	0.91515	0.00094

The moderator block density reduction sensitivity study, as defined in Section 6.3.4.3.3, examined the post-fire condition of the moderator block. Table 6-79 defines the parameter evaluated and the results. The most reactive case is highlighted for each Group.

Content (Group)	Traveller Variant	Moderator Block Density (g/cm ³)	k _{eff}	σ	k _{eff} + 2σ	Δ(k _{eff} + 2σ)
17 Bin 1 (1)	XL	Baseline Case	0.92688	0.00031	0.92750	--
		0.9108	0.92735	0.00028	0.92791	0.00041
18 Bin 1 (2)	XL	Baseline Case	0.91690	0.00025	0.91740	--
		0.9108	0.91721	0.00028	0.91777	0.00037
VV Bin 1 (3)	VVER	Baseline Case	0.91373	0.00024	0.91421	--
		0.9108	0.91453	0.00025	0.91503	0.00082

The package outer diameter tolerance sensitivity study, as defined in Section 6.3.4.3.4, examined the effect of the Traveller outer diameter tolerance on k_{eff} by altering the package spacing in an array. Table 6-80 defines the parameter evaluated and the results. The most reactive case is highlighted for each Group.

Content (Group)	Traveller Variant	Package Outer Diameter (in.)	k_{eff}	σ	$k_{eff} + 2\sigma$	$\Delta(k_{eff} + 2\sigma)$
17 Bin 1 (1)	XL	-0.2	0.92720	0.00026	0.92772	0.00022
		Nominal	0.92688	0.00031	0.92750	--
		+0.2	0.92617	0.00027	0.92671	-0.00079
18 Bin 1 (2)	XL	-0.2	0.91791	0.00025	0.91841	0.00101
		Nominal	0.91690	0.00025	0.91740	--
		+0.2	0.91729	0.00027	0.91783	0.00043
VV Bin 1 (3)	VVER	-0.2	0.91424	0.00024	0.91472	0.00051
		Nominal	0.91373	0.00024	0.91421	--
		+0.2	0.91274	0.00026	0.91326	-0.00095

The polyethylene packing materials sensitivity study, as defined in Section 6.3.4.3.5, examined a conservative representation of polyethylene packing materials through HAC. Table 6-81 defines the parameters evaluated and the results. Figure 6-65, Figure 6-66, and Figure 6-67 display the result trends for Groups 1, 2, and 3, respectively. A limit of 2.00 kg of polyethylene packing materials is imposed on these Groups. The bounding case corresponding to the polyethylene limit set is highlighted for each Group.

Content (Group)	Traveller Variant	Poly Model	Poly Mass (kg)	k_{eff}	σ	$k_{eff} + 2\sigma$	$\Delta(k_{eff} + 2\sigma)$
17 Bin 1 (1)	XL	Baseline Case	0.0	0.92688	0.00031	0.92750	--
		Outer Wrap	2.27	0.92619	0.00025	0.92669	-0.00081
			3.56	0.92758	0.00027	0.92812	0.00062
			4.69	0.92771	0.00024	0.92819	0.00069
			5.83	0.92797	0.00025	0.92847	0.00097
			7.03	0.92810	0.00026	0.92862	0.00112
			8.16	0.92879	0.00025	0.92929	0.00179
		Uniform Wrap	2.00	0.92775	0.00027	0.92829	0.00079
			4.00	0.92881	0.00024	0.92929	0.00179
			6.00	0.92974	0.00024	0.93022	0.00272
			8.00	0.93068	0.00024	0.93116	0.00366
		Collected Melt	10.00	0.93152	0.00026	0.93204	0.00454
			2.00	0.92744	0.00029	0.92802	0.00052
			4.00	0.92961	0.00028	0.93017	0.00267
				6.00	0.93429	0.00033	0.93495

Table 6-81 Polyethylene Sensitivity Results – HAC Package Array, Groups 1, 2, and 3							
Content (Group)	Traveller Variant	Poly Model	Poly Mass (kg)	k_{eff}	σ	$k_{eff} + 2\sigma$	$\Delta(k_{eff} + 2\sigma)$
			8.00	0.94120	0.00027	0.94174	0.01424
			10.00	0.94802	0.00027	0.94856	0.02106
18 Bin 1 (2)	XL	Baseline Case	0.00	0.91690	0.00025	0.91740	--
		Outer Wrap	2.34	0.91693	0.00025	0.91743	0.00003
			3.80	0.91718	0.00029	0.91776	0.00036
			5.06	0.91802	0.00025	0.91852	0.00112
			6.31	0.91851	0.00026	0.91903	0.00163
			7.59	0.91846	0.00025	0.91896	0.00156
			8.74	0.91924	0.00026	0.91976	0.00236
		Uniform Wrap	2.00	0.91822	0.00025	0.91872	0.00132
			4.00	0.91987	0.00023	0.92033	0.00293
			6.00	0.92080	0.00030	0.92140	0.00400
			8.00	0.92235	0.00029	0.92293	0.00553
		Collected Melt	10.00	0.92292	0.00025	0.92342	0.00602
			2.00	0.91846	0.00024	0.91894	0.00154
			4.00	0.92059	0.00026	0.92111	0.00371
			6.00	0.92481	0.00025	0.92531	0.00791
			8.00	0.93252	0.00026	0.93304	0.01564
		10.00	0.94194	0.00028	0.94250	0.02510	
		VV Bin 1 (3)	VVER	Baseline Case	0.0	0.91373	0.00024
Outer Wrap	2.38			0.91465	0.00027	0.91519	0.00098
	3.94			0.91378	0.00024	0.91426	0.00005
	5.94			0.91401	0.00028	0.91457	0.00036
	7.94			0.91431	0.00026	0.91483	0.00062
	9.94			0.91475	0.00024	0.91523	0.00102
Uniform Wrap	2.00			0.91527	0.00024	0.91575	0.00154
	4.00			0.9161	0.00024	0.91658	0.00237
	6.00			0.91833	0.00031	0.91895	0.00474
	8.00			0.91964	0.00026	0.92016	0.00595
	10.00			0.92168	0.00027	0.92222	0.00801
Collected Melt	2.00			0.91465	0.00026	0.91517	0.00096
	4.00			0.91675	0.00023	0.91721	0.00300
	6.00			0.92154	0.00025	0.92204	0.00783
	8.00			0.93031	0.00028	0.93087	0.01666
	10.00			0.94086	0.00024	0.94134	0.02713

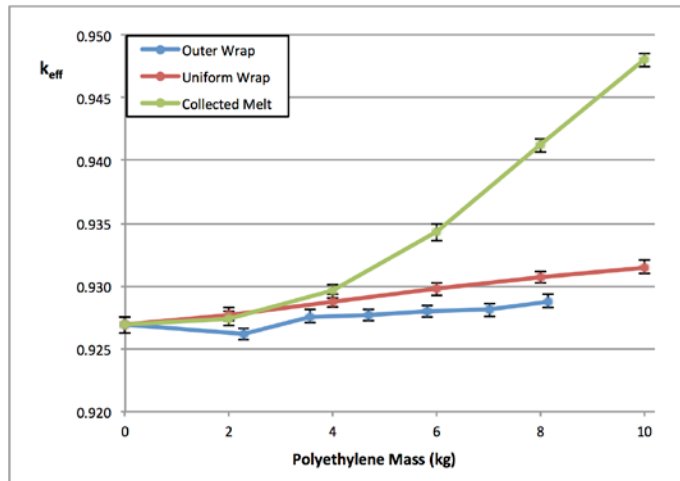


Figure 6-65 Polyethylene Sensitivity Results – HAC Package Array (Group 1)

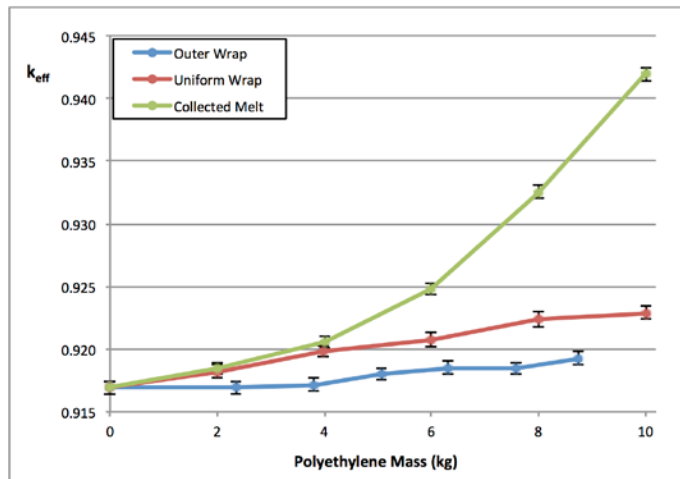


Figure 6-66 Polyethylene Sensitivity Results – HAC Package Array (Group 2)

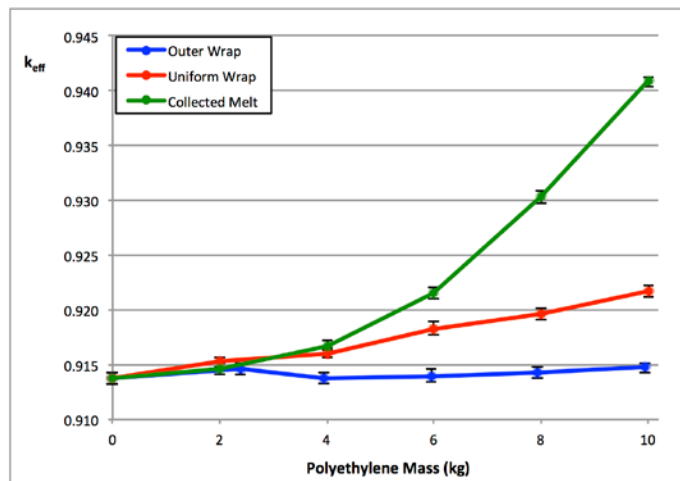


Figure 6-67 Polyethylene Sensitivity Results – HAC Package Array (Group 3)

The axial rod displacement sensitivity study, as defined in Section 6.3.4.3.6, examined the movement of fuel rods upward and out of the lattice during drop testing. Table 6-82 defines the parameters evaluated and the results. Figure 6-68, Figure 6-69, and Figure 6-70 display the result trends for Groups 1, 2, and 3, respectively. The most reactive case is highlighted for each Group.

Content (Group)	Traveller Variant	Rod Configuration	Number of Rods	k_{eff}	σ	$k_{eff} + 2\sigma$	$\Delta(k_{eff} + 2\sigma)$
17 Bin 1 (1)	XL	Baseline	0	0.92688	0.00031	0.92750	--
		Corner	20	0.91844	0.00026	0.91896	-0.00854
			40	0.91194	0.00024	0.91242	-0.01508
			64	0.90852	0.00027	0.90906	-0.01844
		Random	20	0.92141	0.00025	0.92191	-0.00559
			40	0.91722	0.00026	0.91774	-0.00976
			64	0.91294	0.00024	0.91342	-0.01408
18 Bin 1 (2)	XL	Baseline	0	0.91690	0.00025	0.91740	--
		Corner	20	0.91428	0.00024	0.91476	-0.00264
			40	0.91207	0.00029	0.91265	-0.00475
			68	0.90999	0.00025	0.91049	-0.00691
		Random	20	0.91631	0.00024	0.91679	-0.00061
			40	0.91661	0.00030	0.91721	-0.00019
			68	0.91413	0.00026	0.91465	-0.00275
VV Bin 1 (3)	VVER	Baseline	0	0.91373	0.00024	0.91421	--
		Corner	20	0.90879	0.00024	0.90927	-0.00494
			40	0.90508	0.00025	0.90558	-0.00863
			64	0.90311	0.00024	0.90359	-0.01062
		Random	20	0.91436	0.00024	0.91484	0.00063
			40	0.91607	0.00026	0.91659	0.00238
			64	0.91900	0.00025	0.91950	0.00529

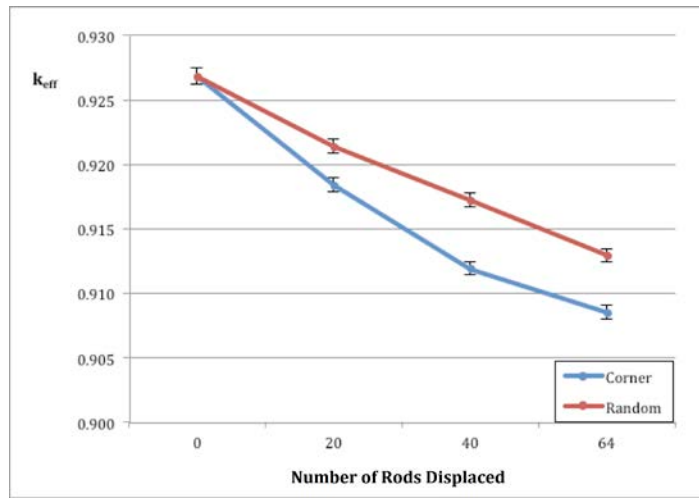


Figure 6-68 Axial Rod Displacement Sensitivity Results – HAC Package Array (Group 1)

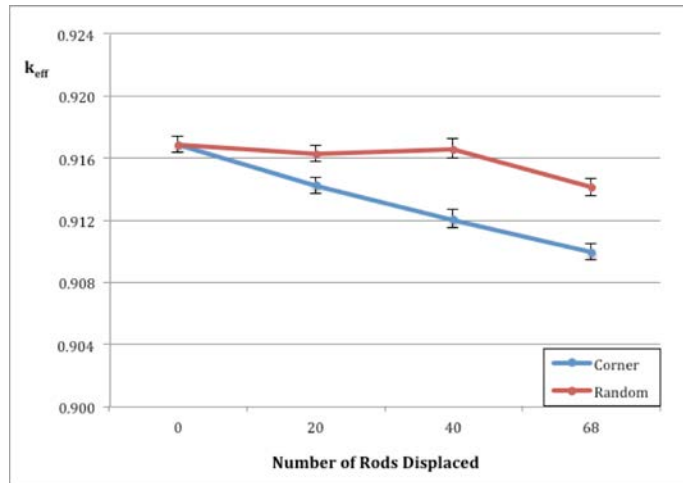


Figure 6-69 Axial Rod Displacement Sensitivity Results – HAC Package Array (Group 2)

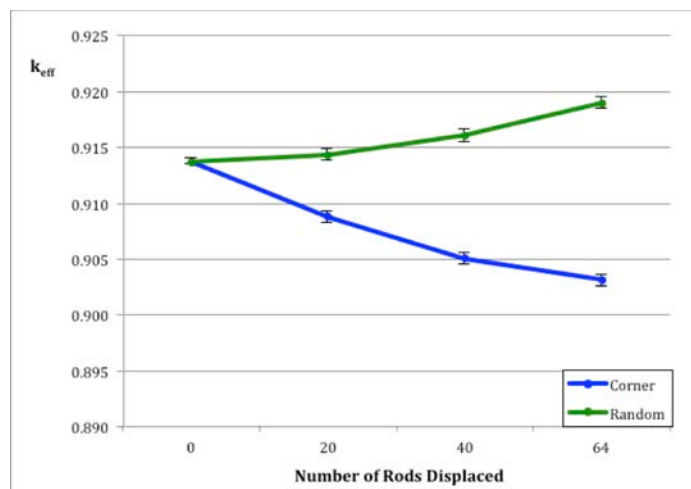


Figure 6-70 Axial Rod Displacement Sensitivity Results – HAC Package Array (Group 3)

The SS replacement rod sensitivity study, as defined in Section 6.3.4.3.7, examined the replacement of fuel rods with SS rods within the fuel assembly. Table 6-83 defines the parameters evaluated and the results. The most reactive case is highlighted for each Group.

Content (Group)	Traveller Variant	SS Rod Configuration	k_{eff}	σ	$k_{eff} + 2\sigma$	$\Delta(k_{eff} + 2\sigma)$
17 Bin 1 (1)	XL	Baseline Case	0.92688	0.00031	0.92750	--
		Corner	0.90189	0.00025	0.90239	-0.02511
		Random	0.86900	0.00022	0.86944	-0.05806
18 Bin 1 (2)	XL	Baseline Case	0.91690	0.00025	0.91740	--
		Corner	0.89297	0.00024	0.89345	-0.02395
		Random	0.86274	0.00024	0.86322	-0.05418
VV Bin 1 (3)	VVER	Baseline Case	0.91373	0.00024	0.91421	--
		Corner	0.88261	0.00023	0.88307	-0.03114
		Random	0.8605	0.00026	0.86102	-0.05319

The tolerance sensitivity studies evaluate cladding dimensions, fuel pellet diameter, and fuel rod pitch, as defined in Section 6.3.4.3.8, 6.3.4.3.9, and 6.3.4.3.10, respectively. Table 6-84 defines the parameter dimensions evaluated and the results. The most reactive case is highlighted for each Group and tolerance parameter.

Content (Group)	Traveller Variant	Tolerance Parameter		k_{eff}	σ	$k_{eff} + 2\sigma$	$\Delta(k_{eff} + 2\sigma)$
17 Bin 1 (1)	XL	Baseline Case		0.92688	0.00031	0.92750	--
18 Bin 1 (2)	XL	Baseline Case		0.91690	0.00025	0.91740	--
VV Bin 1 (3)	VVER	Baseline Case		0.91373	0.00024	0.91421	--
Cladding Tolerance		Cladding ID (in.)	Cladding OD (in.)	k_{eff}	σ	$k_{eff} + 2\sigma$	$\Delta(k_{eff} + 2\sigma)$
17 Bin 1 (1)	XL	-0.002	-0.002	0.92688	0.00024	0.92736	-0.00014
			Nominal	0.92498	0.00030	0.92558	-0.00192
			+0.002	0.92359	0.00025	0.92409	-0.00341
		Nominal	-0.002	0.92848	0.00024	0.92896	0.00146
			Nominal	0.92688	0.00031	0.92750	--
			+0.002	0.92504	0.00029	0.92562	-0.00188
		+0.002	-0.002	0.93006	0.00027	0.93060	0.00310
			Nominal	0.92785	0.00025	0.92835	0.00085
			+0.002	0.92614	0.00025	0.92664	-0.00086

18 Bin 1 (1)	XL	-0.002	-0.002	0.91785	0.00026	0.91837	0.00097
			Nominal	0.91516	0.00024	0.91564	-0.00176
			+0.002	0.91223	0.00028	0.91279	-0.00461
		Nominal	-0.002	0.91922	0.00026	0.91974	0.00234
			Nominal	0.91690	0.00025	0.91740	--
			+0.002	0.91504	0.00026	0.91556	-0.00184
		+0.002	-0.002	0.92143	0.00024	0.92191	0.00451
			Nominal	0.91889	0.00030	0.91949	0.00209
			+0.002	0.91647	0.00027	0.91701	-0.00039
VV Bin 1 (3)	VVER	-0.0015	-0.0015	0.91424	0.00024	0.91472	0.00051
			Nominal	0.91201	0.00027	0.91255	-0.00166
			+0.0015	0.90972	0.00024	0.9102	-0.00401
		Nominal	-0.0015	0.91589	0.00024	0.91637	0.00216
			Nominal	0.91373	0.00024	0.91421	--
			+0.0015	0.9116	0.00027	0.91214	-0.00207
		+0.0015	-0.0015	0.91786	0.00028	0.91842	0.00421
			Nominal	0.91515	0.00025	0.91565	0.00144
			+0.0015	0.9137	0.00024	0.91418	-0.00003
Pellet Diameter Tolerance		Pellet OD (in.)		k_{eff}	σ	k_{eff} + 2σ	Δ(k_{eff} + 2σ)
17 Bin 1 (1)	XL	-0.0007		0.92689	0.00026	0.92741	-0.00009
		-0.0005		0.92650	0.00023	0.92696	-0.00054
		+0.0005		0.92664	0.00025	0.92714	-0.00036
		+0.0007		0.92723	0.00024	0.92771	0.00021
18 Bin 1 (2)	XL	-0.0007		0.91738	0.00026	0.91790	0.00050
		-0.0005		0.91729	0.00026	0.91781	0.00041
		+0.0005		0.91713	0.00026	0.91765	0.00025
		+0.0007		0.91706	0.00025	0.91756	0.00016
VV Bin 1 (3)	VVER	-0.0005		0.91409	0.00032	0.91473	0.00052
		+0.0005		0.91339	0.00024	0.91387	-0.00034
Pitch Tolerance		Pitch Tolerance (in.)		k_{eff}	σ	k_{eff} + 2σ	Δ(k_{eff} + 2σ)
17 Bin 1 (1)	XL	-0.005		0.92460	0.00025	0.92510	-0.00240
		-0.001		0.92638	0.00023	0.92684	-0.00070
		+0.001		0.92727	0.00024	0.92775	0.00025
		+0.005		0.92993	0.00024	0.93041	0.00291
18 Bin 1 (2)	XL	-0.0630		0.88930	0.00027	0.88984	-0.02760
		-0.0315		0.89876	0.00027	0.89930	-0.0181
		+0.0059		0.92168	0.00025	0.92218	0.00478
		+0.0118		0.92788	0.00025	0.92838	0.01098
VV Bin 1 (3)	VVER	-0.001		0.91271	0.00028	0.91327	-0.00094
		+0.001		0.91482	0.00028	0.91538	0.00117

The steel nozzle reflector sensitivity study, as defined in Section 6.3.4.3.11, examined the presence of a SS304-water mixture and 100% density SS304 blocks at the ends of the fuel assembly, simulating the top and bottom nozzles in two different configurations. Table 6-85 defines the parameter evaluated and the results. The most reactive case is highlighted for each Group.

Table 6-85 Steel Nozzle Reflector Sensitivity Results – HAC Package Array, Groups 1, 2, and 3						
Contents (Group)	Traveller Variant	Stainless Steel Nozzle Configuration	k_{eff}	σ	$k_{eff} + 2\sigma$	$\Delta(k_{eff} + 2\sigma)$
17 Bin 1 (1)	XL	Baseline (Water)	0.92688	0.00031	0.92750	--
		50% SS304 / 50% water	0.92528	0.00024	0.92576	-0.00174
		100% density SS304	0.92601	0.00025	0.92651	-0.00099
18 Bin 1 (2)	XL	Baseline (Water)	0.91690	0.00025	0.91740	--
		50% SS304 / 50% water	0.91688	0.00029	0.91746	0.00006
		100% density SS304	0.91669	0.00029	0.91727	-0.00013
VV Bin 1 (3)	VVER	Baseline (Water)	0.91373	0.00024	0.91421	--
		50% SS304 / 50% water	0.91322	0.00025	0.91372	-0.00049
		100% density SS304	0.91325	0.00026	0.91377	-0.00044

The fuel assembly position sensitivity study, as defined in Section 6.3.4.3.12, examined the extended active fuel length for Group 3. Table 6-86 defines the parameter evaluated and the results. The most reactive case is highlighted.

Table 6-86 Extended Active Fuel Length Results – HAC Package Array, Group 3						
Contents (Group)	Traveller Variant	Active Fuel Length (cm)	k_{eff}	σ	$k_{eff} + 2\sigma$	$\Delta(k_{eff} + 2\sigma)$
VV Bin 1 (3)	VVER	Baseline Case 364.261	0.91373	0.00024	0.91421	--
		364.631	0.91359	0.00024	0.91407	-0.00014
		365.000	0.91384	0.00025	0.91434	0.00013
		366.270	0.91425	0.00025	0.91475	0.00054

The ADOPT Fuel sensitivity study, as defined in Section 6.3.4.3.14, examined the effect of replacing standard UO₂ fuel with ADOPT fuel. Table 6-86A lists the results of the study. The most reactive case is highlighted.

Table 6-86A ADOPT Fuel Results – HAC Package Array, Groups 1 & 2						
Contents (Group)	Traveller Variant	Fuel	k_{eff}	σ	$k_{eff} + 2\sigma$	$\Delta(k_{eff} + 2\sigma)$
17 Bin 1 (1)	XL	Baseline (UO₂)	0.92688	0.00031	0.92750	--
		ADOPT	0.92656	0.00025	0.92706	-0.00044
18 Bin 1 (2)	XL	Baseline (UO₂)	0.91690	0.00025	0.91740	--
		ADOPT	0.91672	0.00030	0.91732	-0.00008

6.6.2.2.3 Rod Pipe Results Summary

Table 6-87 shows the summary of the penalties assessed for the sensitivity studies evaluated for the Rod Pipe contents. An entry of “0.0” signifies that the study resulted in no positive penalty on reactivity.

Sensitivity Study	Penalty Assessed	
	UO ₂ Fuel Rods	U ₃ Si ₂ Fuel Rods
Annular Fuel Pellet Blanket	0.00187	0.0
Rod Pipe Position in Clamshell	0.0	0.0
Moderator Block Density Reduction	0.0	0.00102
Package OD Tolerance	0.00134	0.00101
Polyethylene Packing Materials	0.08270	0.08102
Fuel Pellet Diameter Tolerance	0.0	0.0
Moderator Variation	0.06512	0.06119
ADOPT Fuel	0.0	--
Total Penalty (Δk_u)	0.15103	0.14424

Note: '--' signifies the study was not applicable to the condition of transport analyzed.

6.6.2.2.4 Rod Pipe Detailed Results

The annular blanket sensitivity study, as defined in Section 6.3.4.3.1, examined the addition of varying annular fuel pellet ID and lengths of annular fuel pellet blanket lengths equally to the top and bottom of a fuel rod. Table 6-88 defines the parameters evaluated and the results, and Figure 6-71 and Figure 6-72 display the result trends. The most reactive case is highlighted for each content.

Contents	Traveller Variant	Annulus Diameter	Annulus Length (cm)	k_{eff}	σ	$k_{eff} + 2\sigma$	$\Delta(k_{eff} + 2\sigma)$		
Rod Pipe UO ₂ Fuel Rods	XL	Baseline Case		0.66385	0.00050	0.66485	--		
		0.155 in. (0.3937 cm)	13.0	0.66428	0.00062	0.66552	0.00067		
			26.0	0.6646	0.00052	0.66564	0.00079		
			39.0	0.66268	0.00052	0.66372	-0.00113		
			78.0	0.66562	0.00049	0.66660	0.00175		
			250.825	0.66574	0.00049	0.66672	0.00187		
		0.183 in. (0.4648 cm)	13.0	0.66298	0.00056	0.66410	-0.00075		
			26.0	0.66313	0.00058	0.66429	-0.00056		
			39.0	0.6636	0.00056	0.66472	-0.00013		
			78.0	0.6638	0.00049	0.66478	-0.00007		
			250.825	0.66364	0.00047	0.66458	-0.00027		
		Rod Pipe U ₃ Si ₂ Fuel Rods	STD	Baseline Case		0.62316	0.00048	0.62412	--
				0.155 in. (0.3937 cm)	13.0	0.62245	0.00046	0.62337	-0.00075
					26.0	0.62308	0.00048	0.62404	-0.00008
39.0	0.62329				0.00048	0.62425	0.00013		

Contents	Traveller Variant	Annulus Diameter	Annulus Length (cm)	k_{eff}	σ	$k_{eff} + 2\sigma$	$\Delta(k_{eff} + 2\sigma)$
		0.183 in. (0.4648 cm)	78.0	0.62270	0.00053	0.62376	-0.00036
			213.995	0.62294	0.00049	0.62392	-0.00020
			13.0	0.62274	0.00063	0.62400	-0.00012
			26.0	0.62266	0.00044	0.62354	-0.00058
			39.0	0.62326	0.00052	0.62430	0.00018
			78.0	0.62141	0.00056	0.62253	-0.00159
			213.995	0.62019	0.00058	0.62135	-0.00277

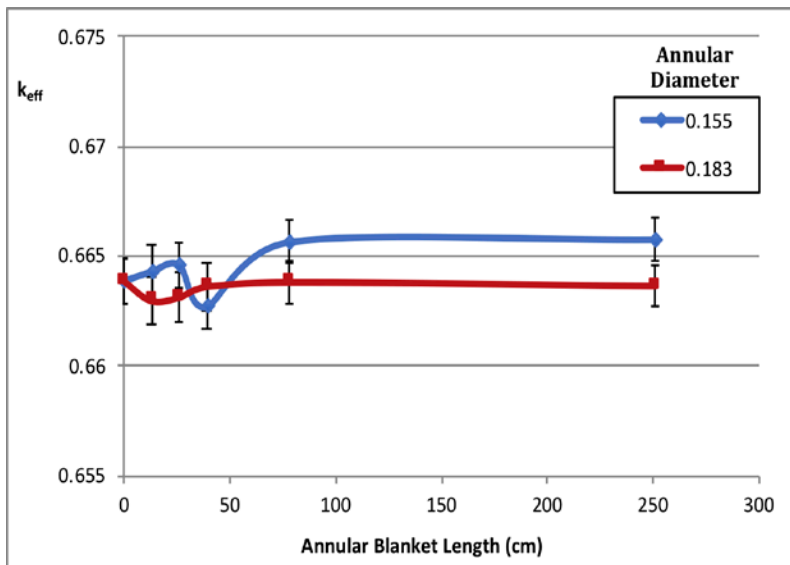


Figure 6-71 Annular Blanket Sensitivity – HAC Package Array (Rod Pipe UO₂ Fuel Rods)

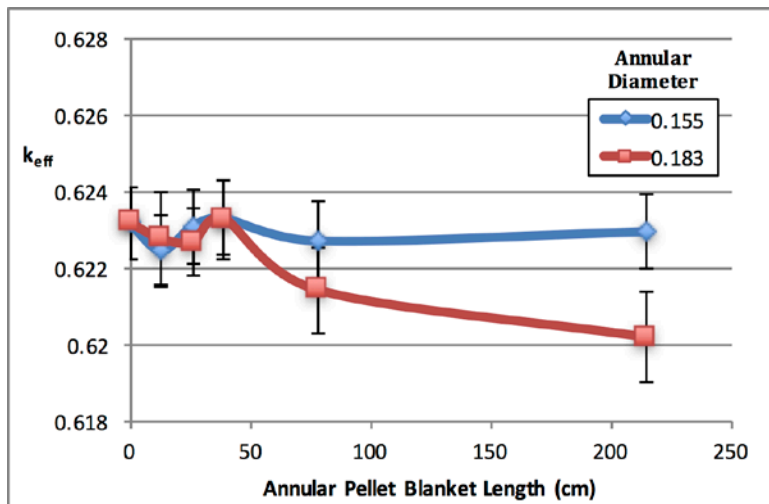


Figure 6-72 Annular Blanket Sensitivity – HAC Package Array (Rod Pipe U₃Si₂ Fuel Rods)

The Rod Pipe position sensitivity study, as defined in Section 6.3.4.3.2, examined the shifting of the Rod Pipe in the Clamshell. Table 6-89 defines the parameter evaluated and the results. The most reactive case is highlighted for each content.

Contents	Traveller Variant	Fuel Assembly Position	k_{eff}	σ	$k_{eff} + 2\sigma$	$\Delta(k_{eff} + 2\sigma)$
Rod Pipe UO ₂ Fuel Rods	XL	Up	0.66415	0.00061	0.66537	0.00052
		Baseline Case	0.66385	0.00050	0.66485	--
		Down	0.66449	0.00050	0.66549	0.00064
Rod Pipe U ₃ Si ₂ Fuel Rods	STD	Up	0.62307	0.00047	0.62401	-0.00011
		Baseline Case	0.62316	0.00048	0.62412	--
		Down	0.62337	0.00048	0.62433	0.00021

The moderator block density reduction sensitivity study, as defined in Section 6.3.4.3.3, examined the post-fire condition of the moderator block. Table 6-90 defines the parameter evaluated and the results. The most reactive case is highlighted for each content.

Content	Traveller Variant	Moderator Block Density (g/cm ³)	k_{eff}	σ	$k_{eff} + 2\sigma$	$\Delta(k_{eff} + 2\sigma)$
Rod Pipe UO ₂ Fuel Rods	XL	Baseline Case	0.66385	0.00050	0.66485	--
		0.9108	0.66471	0.00053	0.66577	0.00092
Rod Pipe U ₃ Si ₂ Fuel Rods	STD	Baseline Case	0.62316	0.00048	0.62412	--
		0.9108	0.62422	0.00046	0.62514	0.00102

The package outer diameter tolerance sensitivity study, as defined in Section 6.3.4.3.4, examined the effect of the Traveller outer diameter tolerance, which alters the package spacing in an array, on k_{eff} . Table 6-91 defines the parameter evaluated and the results. The most reactive case is highlighted for each content.

Content (Group)	Traveller Variant	Package Outer Diameter Tolerance (in.)	k_{eff}	σ	$k_{eff} + 2\sigma$	$\Delta(k_{eff} + 2\sigma)$
Rod Pipe UO ₂ Fuel Rods	XL	-0.2	0.66513	0.00053	0.66619	0.00134
		Baseline Case	0.66385	0.00050	0.66485	--
		+0.2	0.66305	0.00048	0.66401	-0.00084
Rod Pipe U ₃ Si ₂ Fuel Rods	STD	-0.2	0.62425	0.00044	0.62513	0.00101
		Baseline Case	0.62316	0.00048	0.62412	0
		+0.2	0.62269	0.00049	0.62367	-0.00045

The polyethylene packing materials sensitivity study, as defined in Section 6.3.4.3.5, examined a conservative representation of polyethylene packing materials through HAC. Table 6-92 defines the parameters evaluated and the results, and Figure 6-73 and Figure 6-74 display the result trends. The most reactive case is highlighted.

Content	Traveller Variant	Poly Model	Poly Mass (kg)	k_{eff}	σ	$k_{eff} + 2\sigma$	$\Delta(k_{eff} + 2\sigma)$
Rod Pipe UO ₂ Fuel Rods	XL	Baseline Case	0.0	0.66385	0.00050	0.66485	--
		Uniform Wrap	3.09	0.66719	0.00048	0.66815	0.00330
			4.10	0.66809	0.00052	0.66913	0.00428
			8.60	0.67304	0.00049	0.67402	0.00917
			58.64	0.73889	0.00055	0.73999	0.07514
		Collected Melt	0.60	0.65896	0.00048	0.65992	-0.00493
			1.79	0.66103	0.00052	0.66207	-0.00278
			2.39	0.66085	0.00057	0.66199	-0.00286
			2.99	0.66181	0.00048	0.66277	-0.00208
			4.19	0.67243	0.00052	0.67347	0.00862
			5.98	0.68886	0.00063	0.69012	0.02527
			8.97	0.70544	0.00055	0.70654	0.04169
			11.96	0.71558	0.00047	0.71652	0.05167
		60.00	0.74653	0.00051	0.74755	0.08270	
Rod Pipe U ₃ Si ₂ Fuel Rods	STD	Baseline Case	0.0	0.62316	0.00048	0.62412	--
		Uniform Wrap	2.64	0.62568	0.00046	0.62660	0.00248
			3.51	0.62667	0.00047	0.62761	0.00349
			7.36	0.63237	0.00053	0.63343	0.00931
			16.09	0.64447	0.00046	0.64539	0.02127
			31.76	0.66735	0.00051	0.66837	0.04425
			50.53	0.69422	0.00053	0.69528	0.07116
		Collected Melt	0.67	0.62368	0.00047	0.62462	0.00050
			2.01	0.62414	0.00044	0.62502	0.00090
			2.68	0.62464	0.00049	0.62562	0.00150
			3.35	0.62713	0.00052	0.62817	0.00405
			4.69	0.63900	0.00046	0.63992	0.01580
			6.70	0.65343	0.00057	0.65457	0.03045
			10.05	0.67179	0.00049	0.67277	0.04865
13.41	0.68087		0.00046	0.68179	0.05767		
57.38	0.70402	0.00056	0.70514	0.08102			

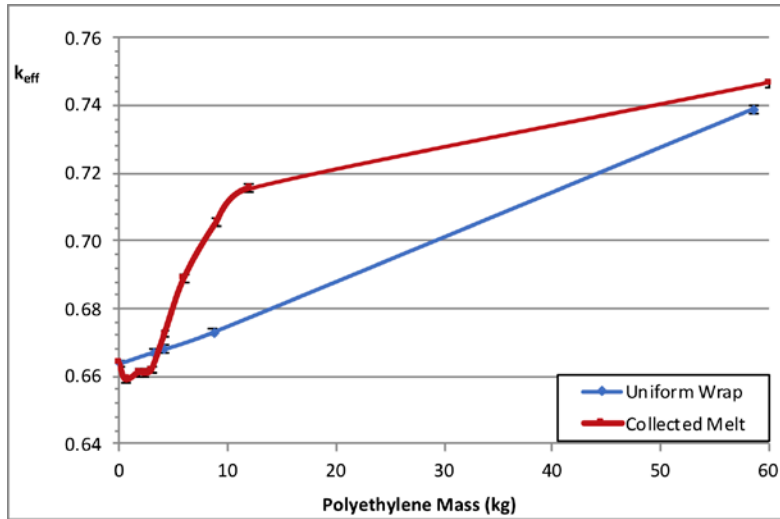


Figure 6-73 Polyethylene Sensitivity Results – HAC Package Array (Rod Pipe UO₂ Fuel Rods)

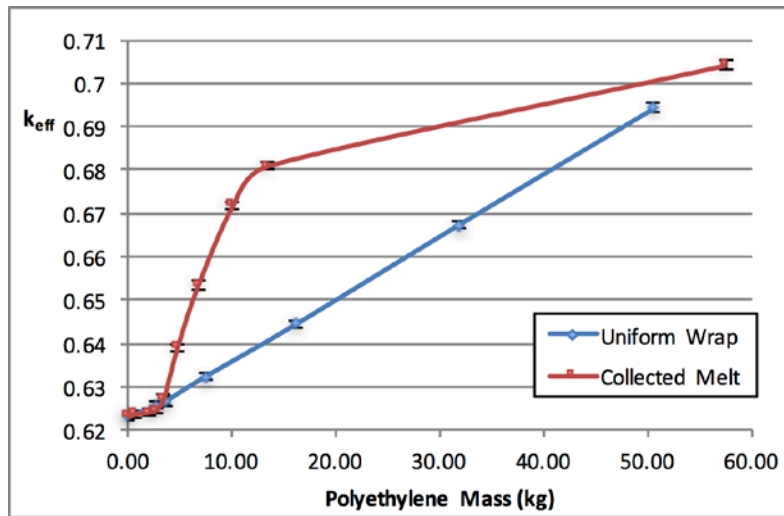


Figure 6-74 Polyethylene Sensitivity Results – HAC Package Array (Rod Pipe U₃Si₂ Fuel Rods)

The tolerance sensitivity study evaluates fuel pellet diameter only, as defined in Section 6.3.4.3.9. The Rod Pipe contents do not credit cladding or have a set pitch, therefore, these parameters are not evaluated. Table 6-93 defines the parameter dimensions evaluated and the results. The most reactive case is highlighted for each content and tolerance parameter.

Content	Traveller Variant	Pellet OD Tolerance (in.)	k_{eff}	σ	$k_{eff} + 2\sigma$	$\Delta(k_{eff} + 2\sigma)$
Rod Pipe UO ₂ Fuel Rods	XL	-0.0014	0.66325	0.00047	0.66419	-0.00066
		-0.0010	0.66353	0.00055	0.66463	-0.00022
		Baseline Case	0.66385	0.00050	0.66485	--
		+0.0010	0.66446	0.00054	0.66554	0.00069
		+0.0014	0.66473	0.00049	0.66571	0.00086

Content	Traveller Variant	Pellet OD Tolerance (in.)	k_{eff}	σ	$k_{eff} + 2\sigma$	$\Delta(k_{eff} + 2\sigma)$
Rod Pipe U ₃ Si ₂ Fuel Rods	STD	-0.0014	0.62335	0.00051	0.62437	0.00025
		-0.0010	0.62335	0.00050	0.62435	0.00023
		Baseline Case	0.62316	0.00048	0.62412	--
		+0.0010	0.62267	0.00047	0.62361	-0.00051
		+0.0014	0.62304	0.00059	0.62422	0.00010

The flooding configuration sensitivity study, as defined in Section 6.3.4.3.13, examined two different flooding scenarios in order to determine which was most reactive. Table 6-94 defines the parameters evaluated and the results, and Figure 6-75 and Figure 6-76 display the result trends. The most reactive case is highlighted.

Content	Traveller Variant	Flooding Configuration	Moderator Density (g/cm ³)	k_{eff}	σ	$k_{eff} + 2\sigma$	$\Delta(k_{eff} + 2\sigma)$
Rod Pipe UO ₂ Fuel Rods	XL	Baseline Case	0.0	0.66385	0.00050	0.66485	--
		Clamshell Void (Outerpack Cavity Flooded)	0.001	0.66351	0.00048	0.66447	-0.00038
			0.01	0.65884	0.00068	0.66020	-0.00465
			0.1	0.62875	0.00048	0.62971	-0.03514
			0.5	0.60516	0.00050	0.60616	-0.05869
			0.7	0.60526	0.00052	0.60630	-0.05855
			1.0	0.6075	0.00045	0.60840	-0.05645
		Outerpack Cavity Void (Clamshell Flooded)	0.001	0.66364	0.00055	0.66474	-0.00011
			0.01	0.6643	0.00047	0.66524	0.00039
			0.1	0.66599	0.00050	0.66699	0.00214
			0.5	0.69975	0.00045	0.70065	0.03580
			0.7	0.71337	0.00053	0.71443	0.04958
		1.0	0.72879	0.00059	0.72997	0.06512	
		Rod Pipe U ₃ Si ₂ Fuel Rods	STD	Baseline Case	0.0	0.62316	0.00048
Clamshell Void (Outerpack Cavity Flooded)	0.001			0.62245	0.0005	0.62345	-0.00067
	0.01			0.61712	0.00047	0.61806	-0.00606
	0.1			0.58969	0.00048	0.59065	-0.03347
	0.5			0.57012	0.00049	0.5711	-0.05302
	0.7			0.57096	0.00044	0.57184	-0.05228
	1.0			0.57298	0.00052	0.57402	-0.0501
Outerpack Cavity Void (Clamshell Flooded)	0.001			0.62255	0.00043	0.62341	-0.00071
	0.01			0.62233	0.00049	0.62331	-0.00081
	0.1			0.62469	0.00044	0.62557	0.00145
	0.5			0.65661	0.00045	0.65751	0.03339
	0.7			0.67019	0.00064	0.67147	0.04735
1.0	0.68433			0.00049	0.68531	0.06119	

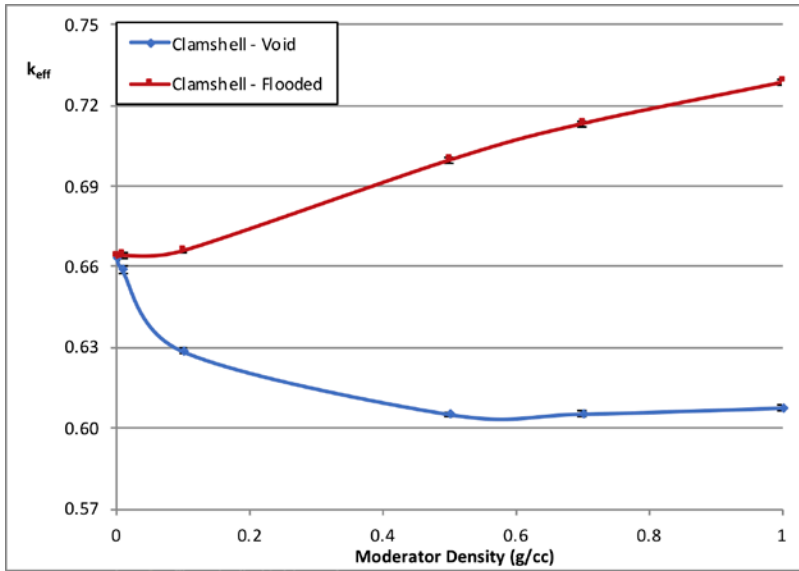


Figure 6-75 Flooding Configuration Sensitivity Results – HAC Package Array (Rod Pipe UO_2 Fuel Rods)

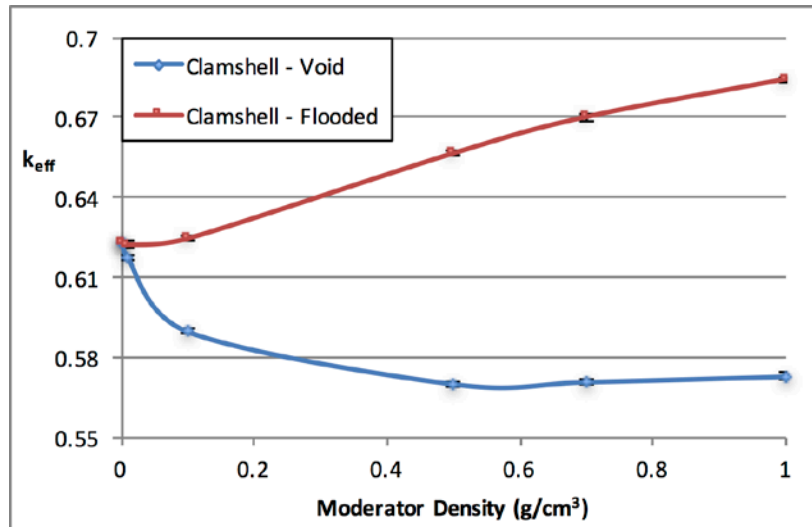


Figure 6-76 Flooding Configuration Sensitivity Results – HAC Package Array (Rod Pipe U_3Si_2 Fuel Rods)

The ADOPT Fuel sensitivity study, as defined in Section 6.3.4.3.14, examined the effect of replacing standard UO_2 fuel with ADOPT fuel. Table 6-94A lists the results of the study. The most reactive case is highlighted.

Content	Traveller Variant	Fuel	k_{eff}	σ	$k_{eff} + 2\sigma$	$\Delta(k_{eff} + 2\sigma)$
Rod Pipe UO_2 Fuel Rods	XL	Baseline (UO_2)	0.66385	0.0005	0.66485	--
		ADOPT	0.66347	0.00047	0.66441	-0.00044

6.7 FISSILE MATERIAL PACKAGES FOR AIR TRANSPORT

The Traveller is not presently authorized for air transport.

6.7.1 Configuration

Not applicable.

6.7.2 Results

Not applicable.

6.8 BENCHMARK EVALUATIONS

6.8.1 Applicability of Benchmark Experiments

Benchmark experiments are selected based on their applicability to the criticality analyses for which the USL function is being generated. Per NUREG/CR-6361, Section 5.1 [6]: “there are three fundamental parameters that should be considered in the selection of suitable experiments for use in the evaluation of transportation and storage package designs. They are the materials of construction (including fissionable material), the geometry of construction, and the inherent neutron energy spectrum affecting the fissionable material(s).” While there are no benchmarks that are entirely alike the application case, benchmark experiments are selected on the basis of being as similar as possible to the Traveller criticality analysis case.

The materials of construction for the Traveller criticality models are low-enriched UO_2 (5-7 wt.% ^{235}U) or U_3Si_2 (5 wt.% ^{235}U) fuel pellets bare or encapsulated by zirconium cladding, surrounded by the aluminum, BORAL, and stainless steel plates that make up the Traveller packaging. Moderation is provided by water that is modeled in the package to consider a flooding event. The geometry of construction for the Traveller criticality safety models are multiple square or hexagonal arrays of fuel rods, separated from each other by the materials of the Traveller packaging. The inherent neutron energy spectrum affecting the fissionable material in the Traveller criticality safety models is a thermalized spectrum, due to the low enrichment of the fuel, and flooding of the package.

In order to generate an applicable USL function for the Traveller criticality safety analysis, a group of benchmarks is selected from the ICSBEP Handbook [7]. All benchmark cases were selected from the series labeled ‘LEU-COMP-THERM-XXX’ shortened in this report to ‘LCT-XXX’ with ‘XXX’ as the identifier of the individual benchmark set. The title of each benchmark experiment is based on its defining characteristics:

- LEU – Low-Enriched Uranium
- COMP – Compound System (arrays of solid rods)
- THERM – Thermal Energy Spectrum

Thus, the ‘LCT-XXX’ series of experiments is the most similar to the application case of the Traveller packaging transporting a fuel assembly. Within the ‘LCT-XXX’ series, the experiments most like the application case are selected. The experiments have water-moderated UO_2 fuel rods, with materials of construction similar to the Traveller packaging (aluminum, stainless steel, Zirconium, and BORAL). The experiments are summarized in Table 6-95. The selected benchmarks included up to 10 wt% ^{235}U , ensuring the code known biases and uncertainties are sufficiently evaluated within the area of applicability (AOA).

Although the U_3Si_2 loose rod case has a different fuel composition than the UO_2 benchmark experiments, all other aspects of the benchmarks are similar. The U_3Si_2 loose rods are still a low enriched uranium compound system with a thermalized neutron energy spectrum. Thus, the USL function calculated is considered applicable to the U_3Si_2 loose rod analysis. It can also be noted that for both loose rod analyses (UO_2 and U_3Si_2 rods) there is a significant margin between the calculated values for the *Maximum k_{eff}* and USL, making any small change in the USL from rod composition insignificant.

Benchmark Group	No. Experiments	Enrichment (wt.% ²³⁵ U)	Clad Material	Array Shape	Pitch (cm)	Fuel OD ^a (cm)	Clad OD ^a (cm)
LCT-002	5	4.306	Aluminum	Square	2.54	1.265	1.415
LCT-006	18	2.600	Aluminum	Square	Varying	1.250	1.417
LCT-007	10	4.738	Aluminum	Square / Hex	Varying	0.789	0.940
LCT-009	9	4.306	Aluminum	Square	2.54	1.265	1.415
LCT-018	1	7.000	Stainless Steel	Square	1.32	0.743	0.843
LCT-020	7	5.000	Zirconium	Hexagonal	1.3	0.460	0.610
LCT-023	6	10.00	Stainless Steel	Hexagonal	1.4	0.416	0.510
LCT-025	4	7.410	Stainless Steel	Hexagonal	Varying	0.416	0.510
LCT-031	6	5.000	Zirconium	Hexagonal	0.8	0.460	0.610
LCT-034	6	4.738	Aluminum	Square	1.6	0.789	0.940
LCT-080	11	6.903	Aluminum	Square	0.8001	0.526	0.635

Note: ^a Values rounded to indicated precision.

6.8.2 Bias Determination

Using the trending parameter data and the k_{eff} results of the benchmark experiments, correlation coefficients are generated for each of the four trending parameters considered: energy of average lethargy causing fission (EALF), fuel enrichment, Water-to-Fuel (WtF) Volume Ratio, Hydrogen-to-Fissile Isotope (H/X) Ratio. The calculated correlation coefficients are provided in Table 6-96. A larger correlation coefficient for a parameter indicates a stronger correlation between the parameter and k_{eff} . From this table, it is evident that the trending parameters with the highest correlation coefficients are EALF and H/X ratio. The correlation coefficients of these parameters are effectively the same, considering the statistical error in the k_{eff} values used for the trends. Additionally, these two parameters are both used to characterize the same effect in degree of thermalization of the system. Thus, for consistency with the prior revisions of the Traveller criticality safety analysis, the EALF parameter is used to generate the USL with the USLSTATS code.

Parameter	R ²	Correlation Coefficient
EALF	0.23237	0.48205
Fuel Enrichment	0.01880	0.13711
WtF Volume Ratio	0.11719	0.34233
H/X Ratio	0.23724	0.48707

The USLSTATS input is produced using the typical values for the problem-specific second-line parameters (as described in Appendix C of NUREG/CR-6361) and the benchmark experiment data used to generate the correlation coefficients of Table 6-96. Using this input, the plot shown in Figure 6-77 is generated.

The USL is equivalent to:

$$USL = 1 - \Delta k_m + \beta - \Delta\beta$$

Where, Δk_m is the administrative margin equivalent to 0.05, β is the bias in the USL(1) calculation, and $\Delta\beta$ is the uncertainty in the USL(1) calculation.

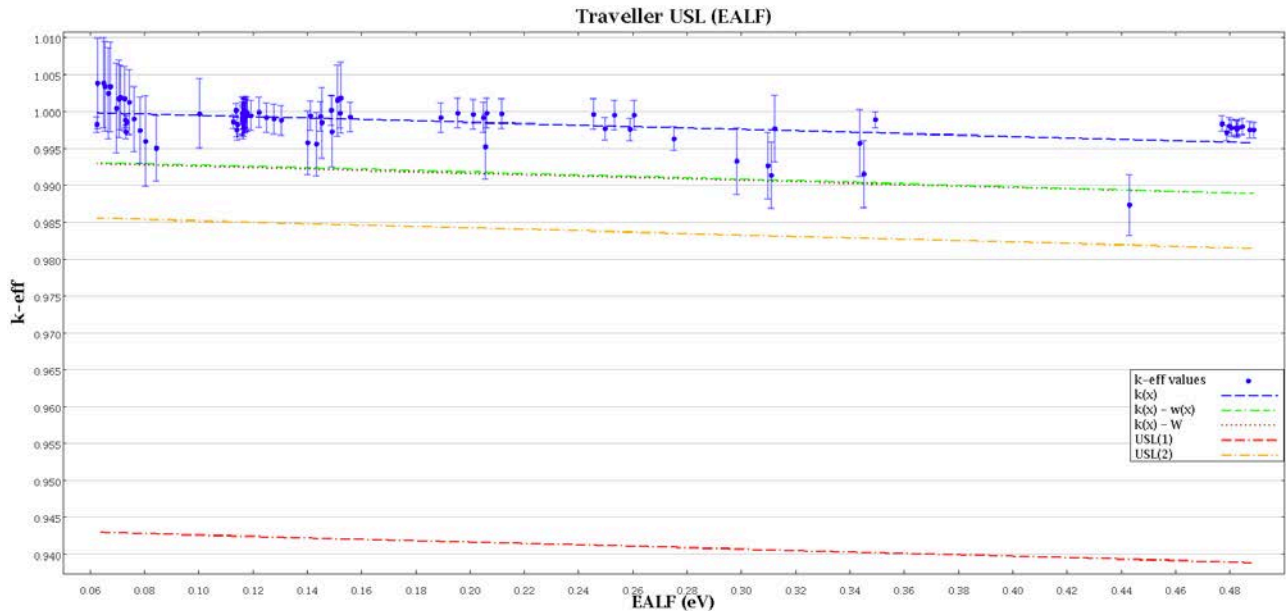


Figure 6-77 EALF USLSTATS Plot

The USLSTATS input also generates USL functions for both Method 1 and Method 2 as described in Appendix C of Reference 6. These USL functions are provided below, where the variable ‘X’ is the EALF of the system. USL(1) is the USL as calculated with Δk_m equivalent to 0.05. USL(2) is the USL as calculated with a purely statistical margin. If USL(1) is less than USL(2), the adequacy of the value of Δk_m selected is proven. The yellow (USL(2)) and red (USL(1)) curves in Figure 6-77 are generated with these functions. The USLSTATS output states that the data tests normal, verifying the validity of the USL functions generated. In addition, from Figure 6-77 it is clear that USL 1 is always less than USL 2, which verifies the administrative margin applied for Method 1 ($\Delta k_m = 0.05$) is sufficient. The Area of Applicability for these USL functions is between the minimum and maximum benchmark experiment EALF values: 0.063 to 0.489 eV.

The USL for the Traveller criticality safety analysis should be calculated by entering the EALF value of the limiting Traveller case in as the value ‘X’ in the USL1 function, and further reducing the value calculated to account for any additional sensitivity studies.

USL1 Function:

$$USL1 = 0.9435 + (-9.5714E-03) \cdot X$$

USL2 Function:

$$USL2 = 0.9861 + (-9.5714E-03) \cdot X$$

6.9 APPENDIX

The following appendices are included with Section 6:

- 6.9.1 References
- 6.9.2 Categorized Fuel Assembly Analysis
- 6.9.3 Baseline Detailed Results
- 6.9.4 Combined Case Study Results

6.9.1 References

- [1] U.S. Nuclear Regulatory Commission, "10 CFR Part 71 - Packaging and Transportation of Radioactive Material," 2016.
- [2] International Atomic Energy Agency, "Regulations for the Safe Transport of Radioactive Material," 2012 Edition.
- [3] R. J. McConn Jr., C. J. Gesh, R. T. Pagh, R. A. Rucker and R. G. Williams III, "Compendium of Material Composition Data for Radiation Transport Modeling," 2011.
- [4] H. R. Dyer and C. V. Parks, "Recommendations for Preparing the Criticality Safety Evaluation of Transportation Packages," 1997.
- [5] "Scale: A Comprehensive Modeling and Simulation Suite for Nuclear Safety Analysis and Design," 2011.
- [6] J. J. Lichtenwalter, S. M. Bowman, M. D. DeHart and C. M. Hopper, "Criticality Benchmark Guide for Light-Water-Reactor Fuel in Transportation and Storage Packages," 1997.
- [7] Organization for Economic Cooperation and Development - Nuclear Energy Agency (OECD-NEA), "International Handbook of Evaluated Criticality Safety Benchmark Experiments," 2014.

6.9.2 Categorized Fuel Assembly Analysis

Three fuel assembly parameters (primary parameters) are used in this analysis to define a bin: array size (e.g. a 17x17 array of lattice cells), fuel rod pattern (i.e. the number and location of fuel rods and non-fuel holes), and nominal fuel rod pitch. A unique combination of primary parameters that are characteristic of a set of fuel assembly designs is called a bin (e.g. 17 Bin 1). The nominal fuel assembly designs that constitute a bin form the basis for its range of secondary parameters (fuel pellet OD, cladding ID, and cladding thickness). The most reactive combination of secondary parameters of a bin is called the categorized fuel assembly (CFA) of that bin. These parameters are verified to be most reactive through a comparison of the variation of secondary parameters among the theoretical fuel assemblies of that bin.

6.9.2.1 CFA Results

For each bin in this analysis, the minimum values of all secondary parameters are determined to be the most reactive. This is primarily due to the fact that fuel assemblies are designed to be under-moderated, so reducing the fuel pellet radius, the fuel-clad gap, and the cladding thickness to their minimum values increases neutron moderation by allowing for the most water possible in the fuel envelope. The CFAs for each bin are summarized in Table 6-97, Table 6-98, and Table 6-99. The secondary parameter limits for each of the bins in these tables are based on the fuel designs that constitute the respective bin. The maximum fuel length for each bin is set as the maximum length of the fuel designs included in the respective bin, plus one tolerance (0.50 in.).

Description	14 Bin 1	14 Bin 2	15 Bin 1	15 Bin 2	16 Bin 1
Array Size	14x14	14x14	15x15	15x15	16x16
Fuel Rods	176	179	204	205	236
Non-Fuel Holes	20	17	21	20	20
Nominal Pitch (in./cm)	0.580 (1.47320)	0.556 (1.41224)	0.563 (1.43002)	0.563 (1.430 cm)	0.563 (1.430 cm)
Minimum Fuel Pellet OD (in./cm)	0.3805 (0.96647)	0.3439 (0.87351)	0.3582 (0.90973)	0.3580 (0.90922 cm)	0.3581 (0.9097 cm)
Minimum Cladding ID (in./cm)	0.3855 (0.97917)	0.3489 (0.88621)	0.3636 (0.92365)	0.3627 (0.92136 cm)	0.3665 (0.9310 cm)
Minimum Cladding Thickness (in./cm)	0.0245 (0.06223)	0.0228 (0.05791)	0.0228 (0.05791)	0.0265 (0.06742 cm)	0.0283 (0.0720 cm)
Cladding Material	Zirconium Alloy	Zirconium Alloy	Zirconium Alloy	Zirconium alloy	Zirconium Alloy
Maximum Active Fuel Length (in./cm)	137.20 (348.49)	144.50 (367.03)	144.50 (367.03)	140.26 (356.27)	154.04 (391.27)

Note: The secondary parameter limits for 16 Bin 1 are slightly different than the minimums listed in Section 6.9.2.6.5 due to unit conversions and rounding.

Description	16 Bin 2	16 Bin 3	17 Bin 1	17 Bin 2	18 Bin 1
Array Size	16x16	16x16	17x17	17x17	18x18
Fuel Rods	236	235	264	264	300
Non-Fuel Holes	20	21	25	25	24
Nominal Pitch (in.)	0.506 (1.28524)	0.485 (1.23190)	0.496 (1.25984)	0.502 (1.27508)	0.500 (1.270 cm)
Minimum Fuel Pellet OD (in.)	0.3220 (0.81788)	0.3083 (0.78308)	0.3083 (0.78308)	0.3238 (0.82245)	0.3165 (0.80392 cm)
Minimum Cladding ID (in.)	0.3265 (0.82931)	0.3125 (0.79375)	0.3125 (0.79375)	0.3276 (0.83210)	0.3236 (0.8220 cm)
Minimum Cladding Thickness (in.)	0.0210 (0.05334)	0.0210 (0.05334)	0.0210 (0.05334)	0.0220 (0.05588)	0.0252 (0.0640 cm)
Cladding Material	Zirconium Alloy	Zirconium Alloy	Zirconium Alloy	Zirconium Alloy	Zirconium Alloy
Maximum Active Fuel Length (in.)	150.50 (382.27)	144.50 (367.03)	168.50 (427.99)	144.50 (367.03)	154.04 (391.27)

Note: The secondary parameter limits for 18 Bin 1 are slightly different than the minimums listed in Section 6.9.2.6.10 due to unit conversions and rounding.

Description	VV Bin 1
Array Size	11x21 ^a
Fuel Rods	312
Non-Fuel Holes	19
Nominal Pitch (in.)	0.502
Minimum Fuel Pellet OD (in.)	0.3083
Minimum Cladding ID (in.)	0.3125
Minimum Cladding Thickness (in.)	0.0210
Cladding Material	Zirconium Alloy
Maximum Active Fuel Length (in.)	143.41 (364.27)

Note: ^a (shortest row) x (longest row).

6.9.2.2 Organizing Fuel Assemblies into Bins

Table 6-100 and Figure 6-78 present four fuel assembly designs and their relevant primary parameters to show how fuel assembly designs are organized into bins. The []^{a,c} fuel assembly is analyzed by itself in “16 Bin 1,” and the []^{a,c} fuel assemblies are analyzed together to create “16 Bin 2” because these three fuel assembly designs have identical array sizes, fuel rod patterns, and pitches. Although []^{a,c} shares the same number of fuel rods and non-fuel holes with the []^{a,c} assemblies, the fuel rod pattern and nominal fuel rod pitch differ. Figure 6-78 is included to demonstrate the variations in patterns and pitch between fuel assembly designs.

Table 6-100 Bin Organization Example				
Bin	16 Bin 1		16 Bin 2	
Fuel Assembly Type	[] ^{a,c}
<i>Primary Parameters of Fuel Assembly Designs</i>				
Array Size	16 x 16	16 x 16	16 x 16	16 x 16
No. of Fuel Rods per Assembly	236	236	236	236
No. of Non-Fuel Holes	20	20	20	20
Nominal Fuel Rod Pitch (in.)	[] ^{a,c}
<i>Secondary Parameters of Fuel Assembly Designs</i>				
Nominal Fuel Pellet Diameter (in.)	[] ^{a,c}
Nominal Clad Inner Diameter (in.)	[] ^{a,c}
Nominal Clad Outer Diameter (in.)	[] ^{a,c}

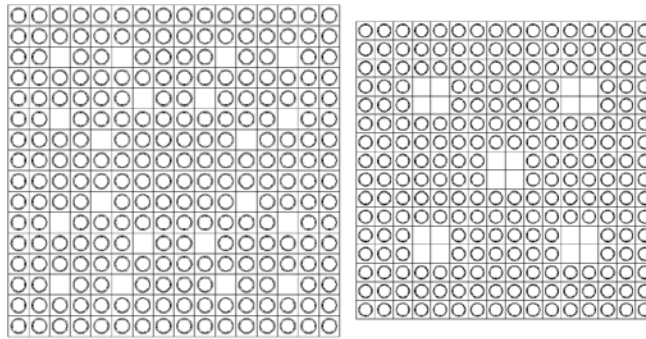


Figure 6-78 Fuel Rod Patterns of 16 Bin 1 (left) and 16 Bin 2 (right) – Not to Scale

6.9.2.3 Determination of Categorized Fuel Assemblies

Upon grouping the nominal fuel assembly designs into bins, the ranges of each secondary parameter (fuel pellet diameter, cladding ID, and cladding thickness) are examined by creating fuel assembly permutations that fully represent the secondary parameter ranges of each bin. Although cladding ID and cladding OD are the dimensions reported for fuel assembly designs, examining the secondary parameters in terms of fuel-clad gap (clad inner radius – fuel pellet radius) and cladding thickness (cladding outer radius – cladding inner radius) results in a more straightforward observation of trends in k_{∞} . The CFAs analyzed in Section 6.2 are based on secondary parameter limits set from the trends observed for each bin.

6.9.2.3.1 Determining Secondary Parameter Ranges

The fuel pellet radius range of a bin is determined using the nominal fuel pellet diameters of the fuel assemblies of that bin and their respective tolerances. If a bin has only one nominal fuel assembly design, the fuel pellet diameter range consists of the nominal fuel pellet diameter of that design plus or minus the fuel pellet diameter tolerance. If there is more than one fuel assembly design in a bin, the upper limit of the range is the largest

nominal fuel pellet diameter of the bin plus one tolerance and the lower limit is the smallest nominal fuel pellet diameter of the bin minus one tolerance. Up to two additional, equally spaced intervals between the upper and lower limits are then added depending on if more than one fuel assembly design applies to a bin. These two scenarios are shown in Table 6-101. This methodology also applies for the fuel-clad gap parameter range and the cladding thickness parameter range.

Table 6-101 Fuel Pellet Radius Range Determination			
Dimensions	16 Bin 2		17 Bin 2
	[]]a,c
Fuel Diameter (in.)	[]]a,c
Fuel Diameter Tolerance (in.)	[]]a,c
Minus Radius (in.)	[]]a,c
Nominal Radius (in.)	[]]a,c
Plus Radius (in.)	[]]a,c
Lower Limit (in.)	[]a,c
Interval 1 (in.)	[]a,c
Interval 2 (in.)	[]a,c		-
Upper Limit (in.)	[]a,c

6.9.2.3.2 Case Naming Convention

6.9.2.3.2.1 Bin Permutations

An example of a bin’s fuel assembly permutation case name is 14bin1_4_2_3_in. The nomenclature for each case name includes the bin (14bin1), three numbers separated by underscores (4_2_3) that signify which fuel radius (the fourth in the range), fuel-clad gap (the second in the range), and cladding thickness (the third in the range) are modeled, respectively.

6.9.2.3.2.2 Additional Cases

An example additional case name is 14bin1gp_1_in. The first part of this case name (14bin1) is the same as for the bin’s original permutations. These cases model additional fuel-clad gaps (gp) that are ± 1 and 2 tolerances from both the minimum and maximum fuel-clad gaps, with the following naming convention: -2 tolerances (1), -1 tolerance (2), +1 tolerance (3), and +2 tolerances (4). The addition of these cases results in a total fuel-clad gap range examined of approximately ± 3 to 4 tolerances. If the most reactive fuel assembly permutation is 14bin1_1_1_1_in, the additional fuel-clad gap cases also model fuel pellet radius 1 and cladding thickness 1. This same methodology is also applied to fuel pellet radius where applicable, replacing “gp” with “fr” in the case name. The cladding thickness ranges are always sufficiently large as to not require extra cases.

6.9.2.4 Determination of Most Reactive Secondary Parameters

The most reactive combination of secondary parameters of a bin defines the bin’s CFA. These parameters are deemed most reactive through comparative analyses of the fuel assembly permutations of a bin, which examine the individual effect of fuel pellet radius, fuel-clad gap, and cladding thickness on k_{∞} . In order to examine the effect of a secondary parameter on k_{∞} , the two other secondary parameters are held constant as the parameter of interest is varied. Each permutation models a unique combination of secondary parameters. The most reactive permutation of each bin is selected as the starting point of the comparative analyses of each bin because this permutation is hypothesized to model the most reactive secondary parameters.

Linear regression curves and R^2 values are added to the comparative study plots to better highlight the trends involved and prove the effect relating a secondary parameter to k_{∞} . The ranges examined are small; therefore, a linear regression was deemed acceptable. For example, fuel-clad gap does not have a strong effect on k_{∞} . Because of this, additional cases are added to all fuel-clad gap comparative studies. As shown in this appendix, the conclusion of all the studies is that these parameters examined are all negatively correlated to k_{∞} , proving that the minimum of all the parameters examined is the most reactive.

The figures in this appendix show the three secondary parameter variations of a bin in a single plot. This is accomplished by normalizing the secondary parameters, i.e., representing the secondary parameters as a difference from the minimum value of a secondary parameter range. For example, in Table 6-103, case 14bin1_1_1_1_in’s fuel pellet radius of 0.48324 cm is represented as 0 cm in Figure 6-80.

6.9.2.5 Bin Permutation Model

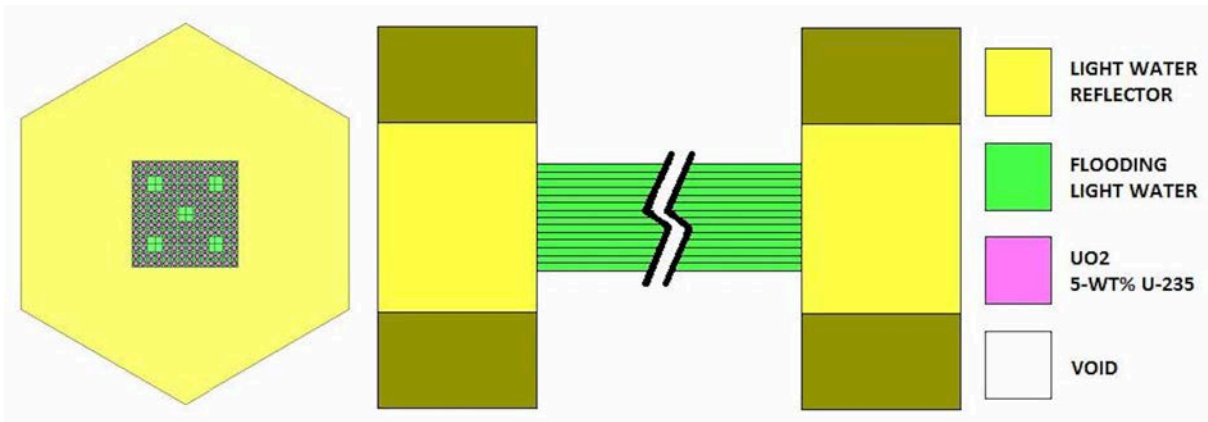


Figure 6-79 x-y (left) and x-z (right) Cross Sections of a Fuel Assembly Permutation. Not to Scale.

Fuel assemblies are modeled in hexagonally pitched arrays that are infinite in the x-y plane. The infinite planar array models white boundary conditions on the lateral faces of the hexagonal prism with 30.48 cm of full-density, light water reflection in the z direction (the long axis of the fuel assembly), and with void between the flooded fuel assembly envelope and the boundaries of the unit, as shown in Figure 6-79. No packaging materials are modeled in this analysis. However, the pitch of the fuel assemblies in the infinite array takes credit for the spacing afforded by the Traveller packaging outer diameter, but no credit is taken for any spacing provided by handling and stacking features. The fuel assemblies are centered in this spacing.

Several modeling conditions were chosen for this analysis that are bounding of actual conditions:

1. UO₂ is modeled at theoretical density (10.96 g/cm³) and at an enrichment of 5 wt.% ²³⁵U with the remaining uranium modeled solely as ²³⁸U, as this is the bounding configuration permitted in the Traveller.
2. All water is modeled as full density light water at room temperature.
3. All fuel cladding is modeled as the built-in Zircaloy-4 material of SCALE 6.1.2.
4. Active fuel length is modeled at 168.5 in. for all fuel assembly permutations, as this is the maximum active fuel length of all fuel assembly designs considered, with the largest tolerance of the active fuel length applied, 0.5 in. No credit is taken for fuel pellet dishing or chamfering in this analysis as no individual fuel pellets are modeled. Instead, the fuel is modeled as one continuous cylinder of UO₂.
5. The entire fuel assembly envelope is modeled as flooded with light water, including all fuel-clad gaps.

6.9.2.6 CFA Most Reactive Secondary Parameters

For all bins analyzed, the minimum fuel pellet diameter, fuel-clad gap, and cladding thickness are bounding for each bin. The range of examination of secondary fuel assembly parameters for each bin is listed in Table 6-102.

Table 6-102 Secondary Fuel Assembly Parameter Ranges				
Bin		Parameter		
		Fuel Pellet OD	Cladding ID	Cladding OD
14 Bin 1	Maximum in. (cm)	[] ^{a,c}
	Minimum in. (cm)	[] ^{a,c}
14 Bin 2	Maximum in. (cm)	[] ^{a,c}
	Minimum in. (cm)	[] ^{a,c}
15 Bin 1	Maximum in. (cm)	[] ^{a,c}
	Minimum in. (cm)	[] ^{a,c}
15 Bin 2	Maximum in. (cm)	[] ^{a,c}
	Minimum in. (cm)	[] ^{a,c}
16 Bin 1	Maximum in. (cm)	[] ^{a,c}
	Minimum in. (cm)	[] ^{a,c}
16 Bin 2	Maximum in. (cm)	[] ^{a,c}
	Minimum in. (cm)	[] ^{a,c}
16 Bin 3	Maximum in. (cm)	[] ^{a,c}

Table 6-102 Secondary Fuel Assembly Parameter Ranges				
Bin		Parameter		
		Fuel Pellet OD	Cladding ID	Cladding OD
	Minimum in. (cm)	[] ^{a,c}
17 Bin 1	Maximum in. (cm)	[] ^{a,c}
	Minimum in. (cm)	[] ^{a,c}
17 Bin 2	Maximum in. (cm)	[] ^{a,c}
	Minimum in. (cm)	[] ^{a,c}
18 Bin 1	Maximum in. (cm)	[] ^{a,c}
	Minimum in. (cm)	[] ^{a,c}
VV Bin 1	Maximum in. (cm)	[] ^{a,c}
	Minimum in. (cm)	[] ^{a,c}

6.9.2.6.1 14 Bin 1

The following comparative analyses, shown in Table 6-103 and Figure 6-80, demonstrate the effect of fuel pellet radius, fuel-clad gap, and cladding thickness on k_{∞} for 14 Bin 1 and verify that the minimum dimension is the most reactive for all three secondary parameters. The minimum value of each secondary parameter range is shaded in gray in Table 6-103.

Case	Fuel Pellet Radius (cm)	Delta from Minimum (cm)	k_{∞}	σ
14bin1fr_1_in	[] ^{a,c}	-0.00127	1.40062	0.00026
14bin1fr_2_in	[] ^{a,c}	-0.00064	1.40053	0.00027
14bin1_1_1_1_in	[] ^{a,c}	0.0	1.40061	0.00026
14bin1_2_1_1_in	[] ^{a,c}	0.00063	1.40061	0.00033
14bin1_3_1_1_in	[] ^{a,c}	0.00127	1.39959	0.00028
14bin1fr_3_in	[] ^{a,c}	0.00190	1.39897	0.00027
14bin1fr_4_in	[] ^{a,c}	0.00254	1.39959	0.00031
Case	Fuel-Clad Gap Thickness (cm)	Delta from Minimum (cm)	k_{∞}	σ
14bin1gp_1_in	[] ^{a,c}	-0.00508	1.40084	0.00031
14bin1gp_2_in	[] ^{a,c}	-0.00254	1.40068	0.00027
14bin1_1_1_1_in	[] ^{a,c}	0.0	1.40061	0.00026
14bin1_1_2_1_in	[] ^{a,c}	0.00254	1.40019	0.00029
14bin1_1_3_1_in	[] ^{a,c}	0.00508	1.39982	0.00027
14bin1gp_3_in	[] ^{a,c}	0.00762	1.39980	0.00026
14bin1gp_4_in	[] ^{a,c}	0.01016	1.39987	0.00029
Case	Clad Thickness (cm)	Delta from Minimum (cm)	k_{∞}	σ
14bin1_1_1_1_in	[] ^{a,c}	0.0	1.40061	0.00026
14bin1_1_1_2_in	[] ^{a,c}	0.00423	1.39826	0.00029
14bin1_1_1_3_in	[] ^{a,c}	0.00847	1.39655	0.00028

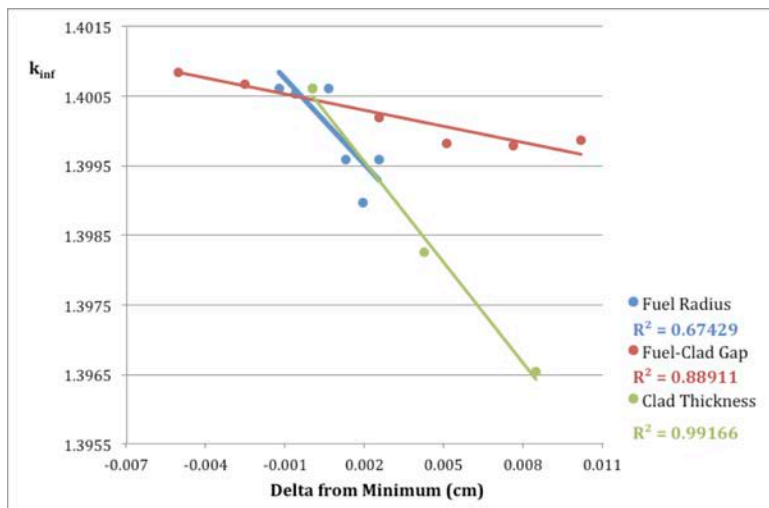


Figure 6-80 Trend Plot of Effect of Secondary Parameters on k_{∞} – 14 Bin 1

6.9.2.6.2 14 Bin 2

The following comparative analyses, shown in Table 6-104 and Figure 6-81, demonstrate the effect of fuel pellet radius, fuel-clad gap, and cladding thickness on k_{∞} for 14 Bin 2 and verify that the minimum dimension is the most reactive for all three secondary parameters. The minimum value of each secondary parameter range is shaded in gray in Table 6-104.

Table 6-104 Effect of Secondary Parameters on 14 Bin 2				
Case	Fuel Pellet Radius (cm)	Delta from Minimum (cm)	k_{∞}	σ
14bin2_1_1_1_in	[] ^{a,c}	0.0	1.41129	0.00027
14bin2_2_1_1_in	[] ^{a,c}	0.00953	1.40719	0.00030
14bin2_3_1_1_in	[] ^{a,c}	0.01905	1.40301	0.00030
14bin2_4_1_1_in	[] ^{a,c}	0.02858	1.39757	0.00028
Case	Fuel-Clad Gap Thickness (cm)	Delta from Minimum (cm)	k_{∞}	σ
14bin2gp_1_in	[] ^{a,c}	-0.00508	1.41176	0.00030
14bin2gp_2_in	[] ^{a,c}	-0.00254	1.41163	0.00031
14bin2_1_1_1_in	[] ^{a,c}	0.0	1.41129	0.00027
14bin2_1_2_1_in	[] ^{a,c}	0.00191	1.41139	0.00032
14bin2_1_3_1_in	[] ^{a,c}	0.00381	1.41089	0.00026
14bin2_1_4_1_in	[] ^{a,c}	0.00572	1.41136	0.00028
14bin2gp_3_in	[] ^{a,c}	0.00826	1.41073	0.00031
14bin2gp_4_in	[] ^{a,c}	0.01080	1.41091	0.00027
Case	Clad Thickness (cm)	Delta from Minimum (cm)	k_{∞}	σ
14bin2_1_1_1_in	[] ^{a,c}	0.0	1.41129	0.00027
14bin2_1_1_2_in	[] ^{a,c}	0.00381	1.40960	0.00029
14bin2_1_1_3_in	[] ^{a,c}	0.00762	1.40802	0.00034

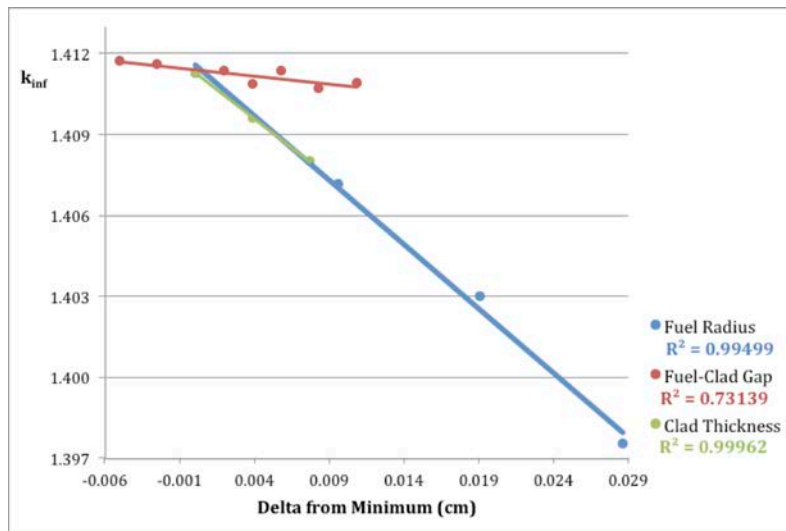


Figure 6-81 Trend Plot of Effect of Secondary Parameters on k_{inf} – 14 Bin 2

6.9.2.6.3 15 Bin 1

The following comparative analyses, shown in Table 6-105 and Figure 6-82, demonstrate the effect of fuel pellet radius, fuel-clad gap, and cladding thickness on k_{∞} for 15 Bin 1 and verify that the minimum dimension is the most reactive for all three secondary parameters. The minimum value of each secondary parameter range is shaded in gray in Table 6-105.

Case	Fuel Pellet Radius (cm)	Delta from Minimum (cm)	k_{∞}	σ
15bin1_1_1_1_in	[] ^{a,c}	0	1.42514	0.00029
15bin1_2_1_1_in	[] ^{a,c}	0.00348	1.42381	0.00026
15bin1_3_1_1_in	[] ^{a,c}	0.00697	1.42180	0.00026
15bin1_4_1_1_in	[] ^{a,c}	0.01046	1.42039	0.00031
Case	Fuel-Clad Gap Thickness (cm)	Delta from Minimum (cm)	k_{∞}	σ
15bin1gp_1_in	[] ^{a,c}	-0.00508	1.42573	0.00028
15bin1gp_2_in	[] ^{a,c}	-0.00254	1.42528	0.00025
15bin1_1_1_1_in	[] ^{a,c}	0	1.42514	0.00029
15bin1_1_2_1_in	[] ^{a,c}	0.00170	1.42504	0.00026
15bin1_1_3_1_in ¹	[] ^{a,c}	0.00340	1.42493	0.00027
15bin1_1_4_1_in	[] ^{a,c}	0.00511	1.42465	0.00031
15bin1gp_3_in	[] ^{a,c}	0.00765	1.42437	0.00035
15bin1gp_4_in	[] ^{a,c}	0.01019	1.42406	0.00026
Case	Clad Thickness (cm)	Delta from Minimum (cm)	k_{∞}	σ
15bin1_1_1_1_in	[] ^{a,c}	0	1.42514	0.00029
15bin1_1_1_2_in	[] ^{a,c}	0.00613	1.42294	0.00024
15bin1_1_1_3_in	[] ^{a,c}	0.01227	1.41969	0.00032
15bin1_1_1_4_in	[] ^{a,c}	0.01840	1.41615	0.00026

Note: ¹ More histories were modeled to improve source convergence.

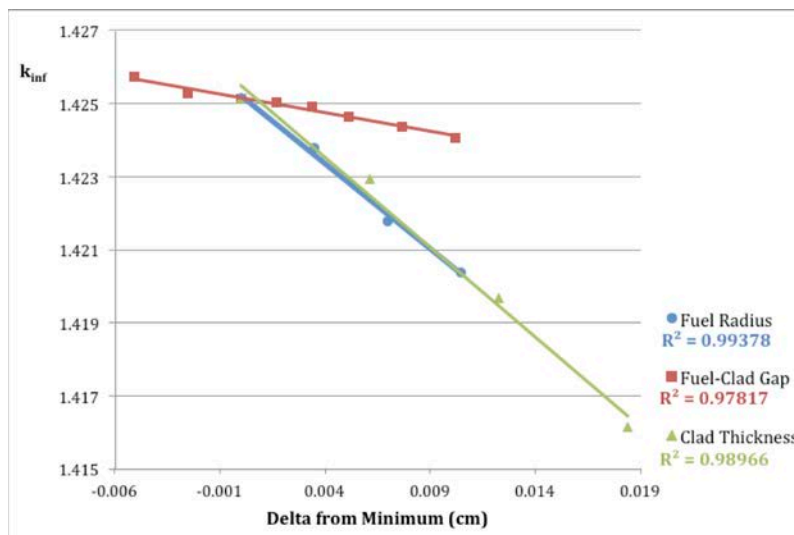


Figure 6-82 Trend Plot of Effect of Secondary Parameters on k-inf – 15 Bin 1

6.9.2.6.4 15 Bin 2

The following comparative analyses, shown in Table 6-106 and Figure 6-83, demonstrate the effect of fuel pellet radius, fuel-clad gap, and cladding thickness on k_{∞} for 15 Bin 2 and verify that the minimum dimension is the most reactive for all three secondary parameters. The minimum value of each secondary parameter range is shaded in gray in Table 6-106.

Case	Fuel Pellet Radius (cm)	Delta from Minimum (cm)	k_{∞}	σ
15bin2fr_1_in	[] ^{a,c}	-0.00178	1.42131	0.00026
15bin2fr_2_in	[] ^{a,c}	-0.00089	1.42082	0.00028
15bin2_1_1_1_in	[] ^{a,c}	0.0	1.42018	0.00029
15bin2_2_1_1_in	[] ^{a,c}	0.00089	1.4199	0.00032
15bin2_3_1_1_in	[] ^{a,c}	0.00178	1.41932	0.00029
15bin2fr_3_in	[] ^{a,c}	0.00267	1.41933	0.00025
15bin2fr_4_in	[] ^{a,c}	0.00356	1.41857	0.00026
Case	Fuel-Clad Gap Thickness (cm)	Delta from Minimum (cm)	k_{∞}	σ
15bin2gp_1_in	[] ^{a,c}	-0.00607	1.42142	0.00027
15bin2gp_2_in	[] ^{a,c}	-0.00343	1.4205	0.00036
15bin2_1_1_1_in	[] ^{a,c}	0.0	1.42018	0.00029
15bin2_1_2_1_in	[] ^{a,c}	0.00343	1.42024	0.00026
15bin2_1_3_1_in	[] ^{a,c}	0.00686	1.41958	0.00025
15bin2gp_3_in	[] ^{a,c}	0.01029	1.41944	0.00026
15bin2gp_4_in ¹	[] ^{a,c}	0.01372	1.41899	0.00026
Case	Clad Thickness (cm)	Delta from Minimum (cm)	k_{∞}	σ
15bin2_1_1_1_in	[] ^{a,c}	0.0	1.42018	0.00029
15bin2_1_1_2_in	[] ^{a,c}	0.00508	1.41822	0.00027
15bin2_1_1_3_in	[] ^{a,c}	0.01016	1.41463	0.00029

Note: ¹ More histories were modeled to improve source convergence.

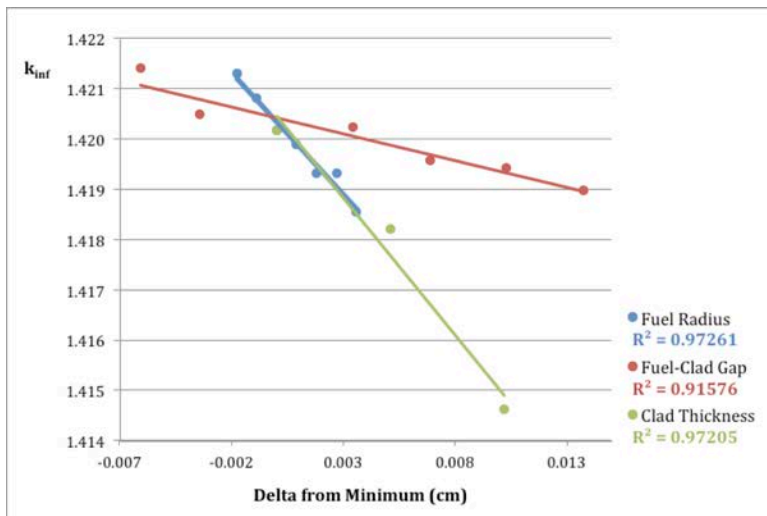


Figure 6-83 Trend Plot of Effect of Secondary Parameters on k_{inf} – 15 Bin 2

6.9.2.6.5 16 Bin 1

The following comparative analyses, shown in Table 6-107 and Figure 6-84, demonstrate the effect of fuel pellet radius, fuel-clad gap, and cladding thickness on k_{∞} for 16 Bin 1 and verify that the minimum dimension is the most reactive for all three secondary parameters. The minimum value of each secondary parameter range is shaded in gray in Table 6-107.

Case	Fuel Pellet Radius (cm)	Delta from Minimum (cm)	k_{∞}	σ
16bin1fr_1_in	[] ^{a,c}	-0.00127	1.43165	0.00029
16bin1fr_2_in	[] ^{a,c}	-0.00064	1.43083	0.00027
16bin1_1_1_1_in	[] ^{a,c}	0.0	1.43101	0.00026
16bin1_2_1_1_in	[] ^{a,c}	0.00063	1.43050	0.00032
16bin1_3_1_1_in	[] ^{a,c}	0.00127	1.43020	0.00027
16bin1fr_3_in	[] ^{a,c}	0.00190	1.42978	0.00026
16bin1fr_4_in	[] ^{a,c}	0.00254	1.42961	0.00033

Case	Fuel-Clad Gap Thickness (cm)	Delta from Minimum (cm)	k_{∞}	σ
16bin1gp_1_in	[] ^{a,c}	-0.00508	1.43156	0.00026
16bin1gp_2_in	[] ^{a,c}	-0.00254	1.43089	0.00025
16bin1_1_1_1_in	[] ^{a,c}	0.0	1.43101	0.00026
16bin1_1_2_1_in	[] ^{a,c}	0.00254	1.43074	0.00031
16bin1_1_3_1_in	[] ^{a,c}	0.00508	1.43009	0.00025
16bin1gp_3_in	[] ^{a,c}	0.00762	1.42970	0.00027
16bin1gp_4_in	[] ^{a,c}	0.01016	1.42918	0.00027

Case	Clad Thickness (cm)	Delta from Minimum (cm)	k_{∞}	σ
16bin1_1_1_1_in	[] ^{a,c}	0.0	1.43101	0.00026
16bin1_1_1_2_in	[] ^{a,c}	0.00381	1.42896	0.00032
16bin1_1_1_3_in	[] ^{a,c}	0.00762	1.42678	0.00025

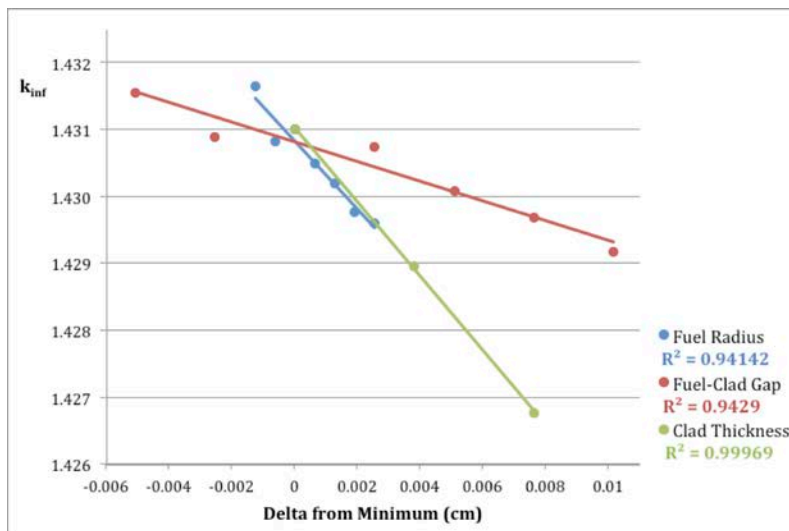


Figure 6-84 Trend Plot of Effect of Secondary Parameters on k_{∞} – 16 Bin 1

6.9.2.6.6 16 Bin 2

The following comparative analyses, shown in Table 6-108 and Figure 6-85, demonstrate the effect of fuel pellet radius, fuel-clad gap, and cladding thickness on k_{∞} for 16 Bin 2 and verify that the minimum dimension is the most reactive for all three secondary parameters. The minimum value of each secondary parameter range is shaded in gray in Table 6-108.

Case	Fuel Pellet Radius (cm)	Delta from Minimum (cm)	k_{∞}	σ
16bin2_1_1_1_in	[] ^{a,c}	0.0	1.40585	0.00032
16bin2_2_1_1_in	[] ^{a,c}	0.00169	1.40476	0.00028
16bin2_3_1_1_in	[] ^{a,c}	0.00339	1.40361	0.00031
16bin2_4_1_1_in	[] ^{a,c}	0.00508	1.40339	0.00031
Case	Fuel-Clad Gap Thickness (cm)	Delta from Minimum (cm)	k_{∞}	σ
16bin2gp_1_in	[] ^{a,c}	-0.00508	1.40650	0.00028
16bin2gp_2_in	[] ^{a,c}	-0.00254	1.40585	0.00026
16bin2_1_1_1_in	[] ^{a,c}	0.0	1.40585	0.00032
16bin2_1_2_1_in	[] ^{a,c}	0.00190	1.40513	0.00028
16bin2_1_3_1_in	[] ^{a,c}	0.00381	1.40540	0.00036
16bin2_1_4_1_in	[] ^{a,c}	0.00571	1.40501	0.00034
16bin2gp_3_in	[] ^{a,c}	0.00825	1.40510	0.00030
16bin2gp_4_in	[] ^{a,c}	0.01079	1.40506	0.00031
Case	Clad Thickness (cm)	Delta from Minimum (cm)	k_{∞}	σ
16bin2_1_1_1_in	[] ^{a,c}	0.0	1.40585	0.00032
16bin2_1_1_2_in	[] ^{a,c}	0.00487	1.40297	0.00026
16bin2_1_1_3_in	[] ^{a,c}	0.00974	1.40048	0.00026
16bin2_1_1_4_in	[] ^{a,c}	0.01461	1.39717	0.00030

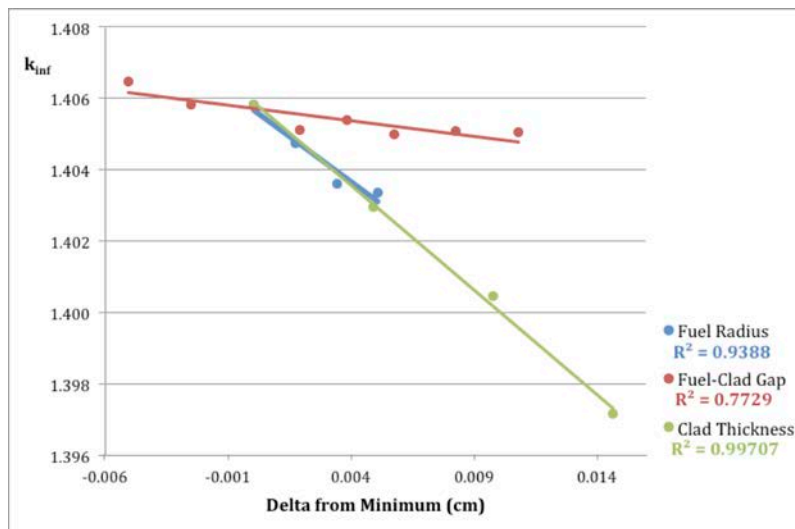


Figure 6-85 Trend Plot of Effect of Secondary Parameters on k_{inf} – 16 Bin 2

6.9.2.6.7 16 Bin 3

The following comparative analyses, shown in Table 6-109 and Figure 6-86, demonstrate the effect of fuel pellet radius, fuel-clad gap, and cladding thickness on k_{∞} for 16 Bin 3 and verify that the minimum dimension is the most reactive for all three secondary parameters. The minimum value of each secondary parameter range is shaded in gray in Table 6-109.

Case	Fuel Pellet Radius (cm)	Delta from Minimum (cm)	k_{∞}	σ
16bin3_1_1_1_in	[] ^{a,c}	0.0	1.40154	0.00028
16bin3_2_1_1_in	[] ^{a,c}	0.00622	1.39711	0.00027
16bin3_3_1_1_in	[] ^{a,c}	0.01245	1.39245	0.00029
16bin3_4_1_1_in	[] ^{a,c}	0.01867	1.38813	0.00027
Case	Fuel-Clad Gap Thickness (cm)	Delta from Minimum (cm)	k_{∞}	σ
16bin3gp_1_in	[] ^{a,c}	-0.00508	1.40173	0.00029
16bin3gp_2_in	[] ^{a,c}	-0.00254	1.40181	0.00028
16bin3_1_1_1_in	[] ^{a,c}	0.0	1.40154	0.00028
16bin3_1_2_1_in	[] ^{a,c}	0.00182	1.40128	0.00026
16bin3_1_3_1_in	[] ^{a,c}	0.00364	1.40070	0.00025
16bin3_1_4_1_in	[] ^{a,c}	0.00547	1.40020	0.00030
16bin3gp_3_in	[] ^{a,c}	0.00801	1.40038	0.00030
16bin3gp_4_in	[] ^{a,c}	0.01055	1.40003	0.00027
Case	Clad Thickness (cm)	Delta from Minimum (cm)	k_{∞}	σ
16bin3_1_1_1_in	[] ^{a,c}	0.0	1.40154	0.00028
16bin3_1_1_2_in	[] ^{a,c}	0.00381	1.39948	0.00028
16bin3_1_1_3_in	[] ^{a,c}	0.00762	1.39686	0.00028

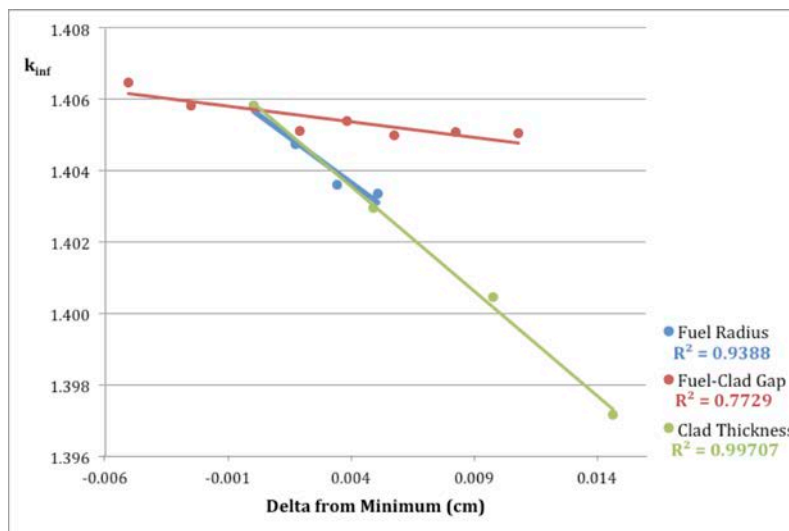


Figure 6-86 Trend Plot of Effect of Secondary Parameters on k_{inf} – 16 Bin 3

6.9.2.6.8 17 Bin 1

The following comparative analyses, shown in Table 6-110 and Figure 6-87, demonstrate the effect of fuel pellet radius, fuel-clad gap, and cladding thickness on k_{∞} for 17 Bin 1 and verify that the minimum dimension is the most reactive for all three secondary parameters. The minimum value of each secondary parameter range is shaded in gray in Table 6-110.

Case	Fuel Pellet Radius (cm)	Delta from Minimum (cm)	k_{∞}	σ
17bin1_1_1_1_in	[] ^{a,c}	0.0	1.42552	0.00027
17bin1_2_1_1_in	[] ^{a,c}	0.00622	1.42288	0.00027
17bin1_3_1_1_in	[] ^{a,c}	0.01245	1.41930	0.00025
17bin1_4_1_1_in	[] ^{a,c}	0.01867	1.41459	0.00030
Case	Fuel-Clad Gap Thickness (cm)	Delta from Minimum (cm)	k_{∞}	σ
17bin1gp_1_in	[] ^{a,c}	-0.00508	1.42622	0.00024
17bin1gp_2_in	[] ^{a,c}	-0.00254	1.42604	0.00029
17bin1_1_1_1_in	[] ^{a,c}	0.0	1.42552	0.00027
17bin1_1_2_1_in	[] ^{a,c}	0.00182	1.42531	0.00026
17bin1_1_3_1_in	[] ^{a,c}	0.00364	1.42570	0.00031
17bin1_1_4_1_in ¹	[] ^{a,c}	0.00547	1.42501	0.00029
17bin1gp_3_in	[] ^{a,c}	0.00801	1.42535	0.00027
17bin1gp_4_in	[] ^{a,c}	0.01055	1.42506	0.00026
Case	Clad Thickness (cm)	Delta from Minimum (cm)	k_{∞}	σ
17bin1_1_1_1_in	[] ^{a,c}	0.0	1.42552	0.00027
17bin1_1_1_2_in	[] ^{a,c}	0.00381	1.42391	0.00026
17bin1_1_1_3_in	[] ^{a,c}	0.00762	1.42198	0.00035

Note: ¹ More histories were modeled to improve source convergence.

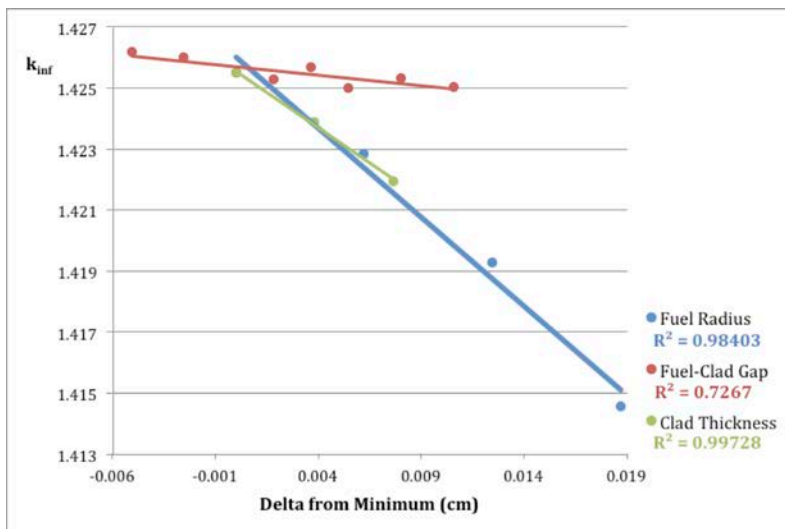


Figure 6-87 Trend Plot of Effect of Secondary Parameters on k_{∞} – 17 Bin 1

6.9.2.6.9 17 Bin 2

The following comparative analyses, shown in Table 6-111 and Figure 6-88, demonstrate the effect of fuel pellet radius, fuel-clad gap, and cladding thickness on k_{∞} for 17 Bin 2 and verify that the minimum dimension is the most reactive for all three secondary parameters. The minimum value of each secondary parameter range is shaded in gray in Table 6-111.

Case	Fuel Pellet Radius (cm)	Delta from Minimum (cm)	k_{∞}	σ
17bin2fr_1_in	[] ^{a,c}	-0.00178	1.42032	0.00031
17bin2fr_2_in	[] ^{a,c}	-0.00089	1.41992	0.00026
17bin2_1_1_1_in	[] ^{a,c}	0.0	1.41936	0.00029
17bin2_2_1_1_in	[] ^{a,c}	0.00089	1.41834	0.00028
17bin2_3_1_1_in	[] ^{a,c}	0.00177	1.41802	0.00024
17bin2fr_3_in	[] ^{a,c}	0.00266	1.41771	0.00029
17bin2fr_4_in	[] ^{a,c}	0.00355	1.41661	0.00027

Case	Fuel-Clad Gap Thickness (cm)	Delta from Minimum (cm)	k_{∞}	σ
17bin2gp_1_in	[] ^{a,c}	-0.00483	1.41964	0.00026
17bin2gp_2_in	[] ^{a,c}	-0.00343	1.41969	0.00028
17bin2_1_1_1_in	[] ^{a,c}	0.0	1.41936	0.00029
17bin2_1_2_1_in	[] ^{a,c}	0.00343	1.41891	0.00028
17bin2_1_3_1_in	[] ^{a,c}	0.00685	1.41849	0.00028
17bin2gp_3_in	[] ^{a,c}	0.01028	1.41784	0.00026
17bin2gp_4_in	[] ^{a,c}	0.01371	1.41771	0.00028

Case	Clad Thickness (cm)	Delta from Minimum (cm)	k_{∞}	σ
17bin2_1_1_1_in	[] ^{a,c}	0.0	1.41936	0.00029
17bin2_1_1_2_in	[] ^{a,c}	0.00508	1.41665	0.00031
17bin2_1_1_3_in	[] ^{a,c}	0.01016	1.41308	0.00025

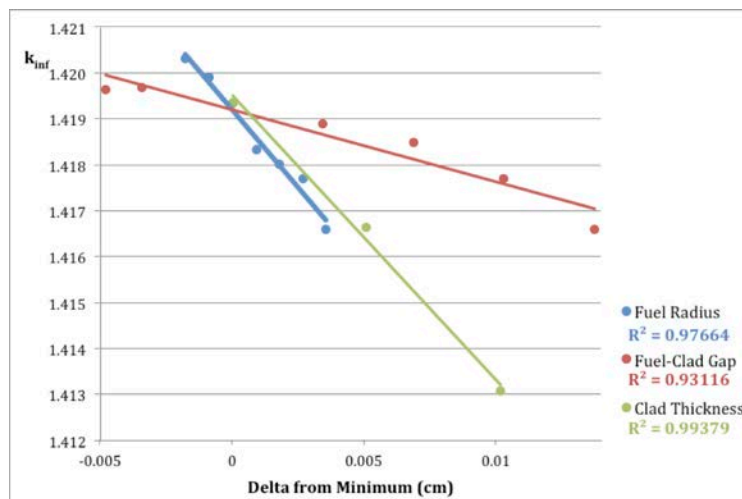


Figure 6-88 Trend Plot of Effect of Secondary Parameters on k_{inf} – 17 Bin 2

6.9.2.6.10 18 Bin 1

The following comparative analyses, shown in Table 6-112 and Figure 6-89, demonstrate the effect of fuel pellet radius, fuel-clad gap, and cladding thickness on k_{∞} for 18 Bin 1 and verify that the minimum dimension is the most reactive for all three secondary parameters. The minimum value of each secondary parameter range is shaded in gray in Table 6-112.

Case	Fuel Pellet Radius (cm)	Delta from Minimum (cm)	k_{∞}	σ
18bin1fr_1_in	[a,c]	-0.00127	1.43029	0.00026
18bin1fr_2_in	[a,c]	-0.00064	1.42971	0.00031
18bin1_1_1_1_in	[a,c]	0.0	1.42963	0.00036
18bin1_2_1_1_in	[a,c]	0.00063	1.42865	0.00027
18bin1_3_1_1_in	[a,c]	0.00127	1.42825	0.00025
18bin1fr_3_in	[a,c]	0.00190	1.42784	0.00028
18bin1fr_4_in	[a,c]	0.00254	1.42743	0.00025

Case	Fuel-Clad Gap Thickness (cm)	Delta from Minimum (cm)	k_{∞}	σ
18bin1gp_1_in	[a,c]	-0.00508	1.42943	0.00030
18bin1gp_2_in	[a,c]	-0.00254	1.42970	0.00028
18bin1_1_1_1_in	[a,c]	0.0	1.42963	0.00036
18bin1_1_2_1_in	[a,c]	0.00254	1.42885	0.00029
18bin1_1_3_1_in	[a,c]	0.00508	1.42858	0.00027
18bin1gp_3_in	[a,c]	0.00762	1.42807	0.00032
18bin1gp_4_in	[a,c]	0.01016	1.42803	0.00026

Case	Clad Thickness (cm)	Delta from Minimum (cm)	k_{∞}	σ
18bin1_1_1_1_in	[a,c]	0.0	1.42963	0.00036
18bin1_1_1_2_in	[a,c]	0.00381	1.42606	0.00025
18bin1_1_1_3_in	[a,c]	0.00762	1.42493	0.00029

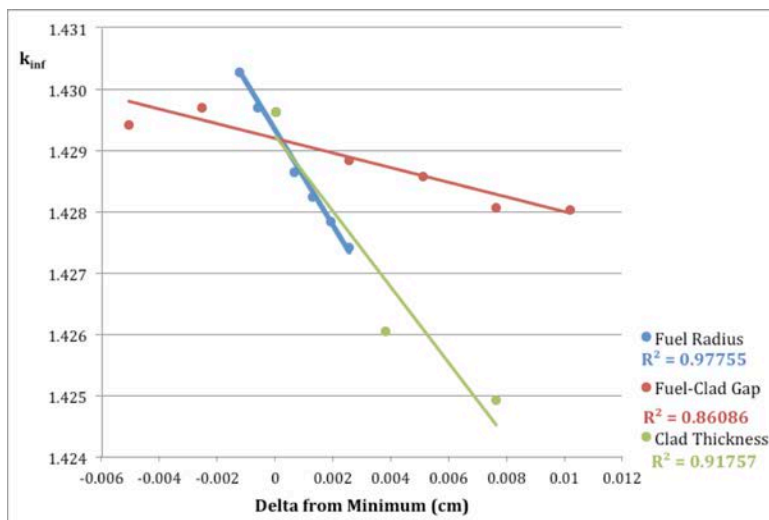


Figure 6-89 Trend Plot of Effect of Secondary Parameters on k_{inf} – 18 Bin 1

6.9.2.6.11 VV Bin 1

The following comparative analyses, shown in Table 6-113 and Figure 6-90, demonstrate the effect of fuel pellet radius, fuel-clad gap, and cladding thickness on k_{∞} for VV Bin 1 and verify that the minimum dimension is the most reactive for all three secondary parameters. The minimum value of each secondary parameter range is shaded in gray in Table 6-113.

Case	Fuel Pellet Radius (cm)	Delta from Minimum (cm)	k_{∞}	σ	
VVERbin1fr_1_in]a,c	-0.001269	1.40345	0.00023
VVERbin1fr_2_in]a,c	-0.000634	1.40294	0.00020
VVERbin1_1_1_1_in	[]a,c	0.0	1.40216	0.00019
VVERbin1_2_1_1_in	[]a,c	0.00064	1.40165	0.00021
VVERbin1_3_1_1_in	[]a,c	0.00127	1.40079	0.00021
VVERbin1fr_3_in]a,c	0.001906	1.40070	0.00019
VVERbin1fr_4_in]a,c	0.002541	1.40009	0.00024

Case	Fuel-Clad Gap Thickness (cm)	Delta from Minimum (cm)	k_{∞}	σ	
VVERbin1gp_1_in	[]a,c	-0.00508	1.40340	0.00021
VVERbin1gp_2_in	[]a,c	-0.00254	1.40225	0.00019
VVERbin1_1_1_1_in	[]a,c	0.0	1.40216	0.00019
VVERbin1_1_2_1_in	[]a,c	0.00254	1.40169	0.00021
VVERbin1_1_3_1_in	[]a,c	0.00508	1.40135	0.00020
VVERbin1gp_3_in	[]a,c	0.00762	1.40132	0.00020
VVERbin1gp_4_in	[]a,c	0.01016	1.40062	0.00021

Case	Clad Thickness (cm)	Delta from Minimum (cm)	k_{∞}	σ	
VVERbin1_1_1_1_in	[a,c	0.0	1.40216	0.00019
VVERbin1_1_1_2_in	[a,c	0.00381	1.39894	0.00019
VVERbin1_1_1_3_in	[a,c	0.00762	1.39633	0.00022

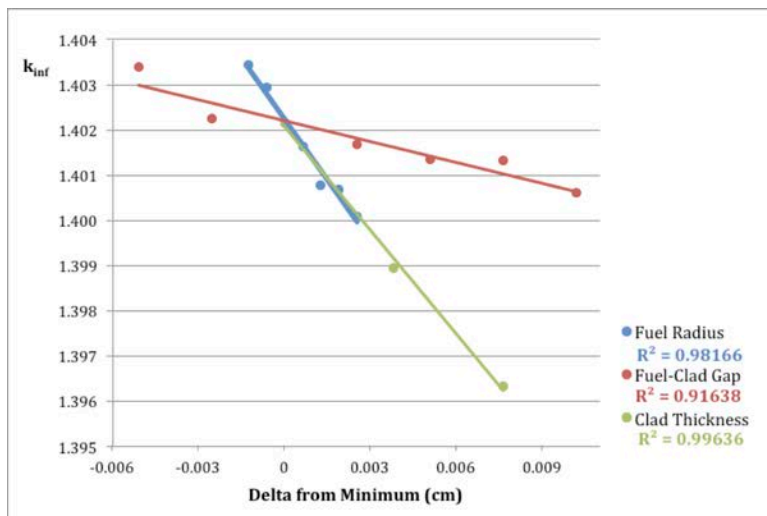


Figure 6-90 Trend Plot of Effect of Secondary Parameters on k_{inf} – VV Bin 1

6.9.3 Baseline Detailed Results

6.9.3.1 Single Package, Fuel Assembly

6.9.3.1.1 CFA Package Variant Comparison Results

For the bins 16 Bin 2 and 17 Bin 1, the maximum active fuel length can only fit in the Traveller XL. For this reason in the CFA-package variant comparison, these bins are broken up into 2 CFAs. The longer CFA (with suffix ‘a’) is the maximum fuel length for the bin, which only fits in the Traveller XL. The shorter CFA (no suffix) is the fuel length of an existing fuel design in the bin that fits in both the STD and XL. For the Groups 1 & 2 Single Package evaluation under NCT, 16 Bin 1 and 18 Bin 1 in the Traveller XL are selected as the most reactive CFA-package variants for evaluation in the baseline case determination. For Group 1 and 2 single package HAC, 17 Bin 1, 17 Bin 1a, and 17 Bin 2 in the Traveller XL are selected as the most reactive CFA-package variants for evaluation in the baseline case determination. The results are tabulated in Table 6-114. For Group 3 there is only one CFA-package variant combination possible.

Traveller Variant	CFA	Active Fuel Length (in.)	NCT			HAC		
			k_{eff}	σ	$k_{eff} + 2\sigma$	k_{eff}	σ	$k_{eff} + 2\sigma$
STD	14 Bin 1	137.20	0.82687	0.00057	0.82801	0.85417	0.00063	0.85543
	14 Bin 2	144.50	0.82905	0.00055	0.83015	0.85961	0.00059	0.86079
	15 Bin 1	144.50	0.85594	0.00050	0.85694	0.87093	0.00074	0.87241
	15 Bin 2	140.26	0.84727	0.00085	0.84897	0.86367	0.00053	0.86473
	16 Bin 2	137.20	0.83498	0.00048	0.83594	0.86204	0.00057	0.86318
	16 Bin 3	144.50	0.82091	0.00055	0.82201	0.86419	0.00062	0.86543
	17 Bin 1	144.50	0.85691	0.00048	0.85787	0.87226	0.00053	0.87332
	17 Bin 2	144.50	0.85304	0.00048	0.85400	0.86943	0.00053	0.87049
XL	14 Bin 1	137.20	0.84081	0.00051	0.84183	0.88205	0.00050	0.88305
	14 Bin 2	144.50	0.83904	0.00062	0.84028	0.88247	0.00054	0.88355
	15 Bin 1	144.50	0.87324	0.00049	0.87422	0.90031	0.00048	0.90127
	15 Bin 2	140.26	0.86513	0.00087	0.86687	0.89637	0.00050	0.89737
	16 Bin 1	154.04	0.88423	0.00055	0.88533	0.89874	0.00050	0.89974
	16 Bin 2	137.20	0.84900	0.00053	0.85006	0.88942	0.00049	0.89040
	16 Bin 2a *	150.50	0.84815	0.00047	0.84909	0.88881	0.00054	0.88989
	16 Bin 3	144.50	0.83133	0.00047	0.83227	0.89059	0.00050	0.89159
	17 Bin 1	144.50	0.87474	0.00049	0.87572	0.90301	0.00052	0.90405
	17 Bin 1a *	168.50	0.87576	0.00060	0.87696	0.90347	0.00051	0.90449
	17 Bin 2	144.50	0.87033	0.00055	0.87143	0.90188	0.00049	0.90286
	18 Bin 1	154.04	0.88464	0.00053	0.88570	0.90069	0.00054	0.90177

Note: * These cases model an active fuel length that cannot be shipped in the STD and are therefore only modeled in the XL.

6.9.3.1.2 Baseline Determination Results

For Groups 1 & 2 under NCT, the baseline case is chosen as 18 Bin 1 in the Traveller XL with an axial displacement of the fuel of 72.583 cm. Although there is no clear most reactive case, this case was chosen because, as shown in Figure 6-91 and listed in Table 6-115, there is no statistically significant trend in the effect of the axial position of the fuel on k_{eff} . Therefore, the more reactive of the two contents (18 Bin 1) approximately centered in the Clamshell (72.583 cm) was selected as the baseline configuration to promote axial reflection for the fuel assembly in the Clamshell. It was determined for these cases that the difference in k_{eff} was based on the statistical nature of the Monte Carlo code rather than a true physical effect of repositioning the fuel assembly.

For Group 3 under NCT, the baseline case is chosen as VV Bin 1 in the Traveller VVER with an axial displacement of the fuel of 51.854 cm. As shown in Figure 6-91 and Table 6-115, the change in k_{eff} is insignificant until the fuel displaces to the top of the Clamshell, where k_{eff} drops off. Therefore, the fuel assembly centered axially in the Clamshell was chosen as the baseline configuration to promote axial reflection for the fuel assembly in the Clamshell. It was determined for these cases that the difference in k_{eff} was based on the statistical nature of the Monte Carlo code rather than a true physical effect of repositioning the fuel assembly

Group	Content	Traveller Variant	Axial Position (cm)	k_{eff}	σ	$k_{eff} + 2\sigma$
1 & 2	16 Bin 1	XL	2.540	0.88423	0.00055	0.88533
			25.888	0.88384	0.00050	0.88484
			49.235	0.88456	0.00055	0.88566
			72.583	0.88481	0.00055	0.88591
			95.931	0.88427	0.00048	0.88523
			119.278	0.88509	0.00048	0.88605
	18 Bin 1	XL	2.540	0.88464	0.00053	0.88570
			25.888	0.88555	0.00052	0.88659
			49.235	0.88520	0.00053	0.88626
			72.583	0.88499	0.00059	0.88617
			95.931	0.88594	0.00053	0.88700
			119.278	0.88601	0.00048	0.88697
3	VV Bin 1	VVER	3.810	0.86195	0.00025	0.86245
			27.832	0.86204	0.00025	0.86254
			51.854	0.86201	0.00025	0.86251
			75.876	0.8619	0.00026	0.86242
			99.899	0.86157	0.00024	0.86205

For Groups 1 & 2 under HAC, the baseline case is chosen as 17 Bin 1 in the Traveller XL with an axial displacement of the fuel of 87.122 cm. Although there is no clear most reactive case, this case was chosen

because, as shown in Figure 6-92, there is no statistically significant trend in the effect of the axial position of the fuel on k_{eff} for all three CFAs, despite 17 Bin 1a modeling a longer fuel assembly than 17 Bin 1. Therefore, 17 Bin 1 with an axial displacement of the fuel of 87.122 cm was selected as the baseline configuration to promote axial reflection for the fuel assembly in the Clamshell. It was determined for these cases that the difference in k_{eff} was based on the statistical nature of the Monte Carlo code rather than a true physical effect of repositioning the fuel assembly.

For Group 3 under HAC, the baseline case is chosen as VV Bin 1 in the Traveller VVER with an axial displacement of the fuel of 51.854 cm. As shown in Figure 6-92, k_{eff} remains constant and statistically indistinguishable as the axial displacement of the fuel is increased. Therefore, the fuel assembly centered axially in the Clamshell was chosen as the baseline configuration to promote axial reflection for the fuel assembly in the Clamshell. It was determined for these cases that the difference in k_{eff} was based on the statistical nature of the Monte Carlo code rather than a true physical effect of repositioning the fuel assembly.

Group	Content	Traveller Variant	Axial Position (cm)	k_{eff}	σ	$k_{eff} + 2\sigma$
1 & 2	17 Bin 1	XL	2.540	0.90301	0.00052	0.90405
			30.734	0.90320	0.00055	0.90430
			58.928	0.90219	0.00052	0.90323
			87.122	0.90209	0.00049	0.90307
			115.316	0.90340	0.00056	0.90452
			143.510	0.90368	0.00056	0.90480
	17 Bin 1a	XL	2.540	0.90347	0.00051	0.90449
			18.542	0.90372	0.00048	0.90468
			34.544	0.90347	0.00054	0.90455
			50.546	0.90364	0.00051	0.90466
			66.548	0.90222	0.00049	0.90320
			82.550	0.90304	0.00064	0.90432
	17 Bin 2	XL	2.540	0.90188	0.00049	0.90286
			30.734	0.90268	0.00055	0.90378
			58.928	0.90374	0.00046	0.90466
			87.122	0.90228	0.00059	0.90346
			115.316	0.90249	0.00056	0.90361
			143.510	0.90300	0.00055	0.90410
3	VV Bin 1	VVER	3.810	0.88279	0.00026	0.88331
			27.832	0.88293	0.00027	0.88347
			51.854	0.88241	0.00025	0.88291
			75.876	0.88286	0.00028	0.88342
			99.899	0.88254	0.00027	0.88308

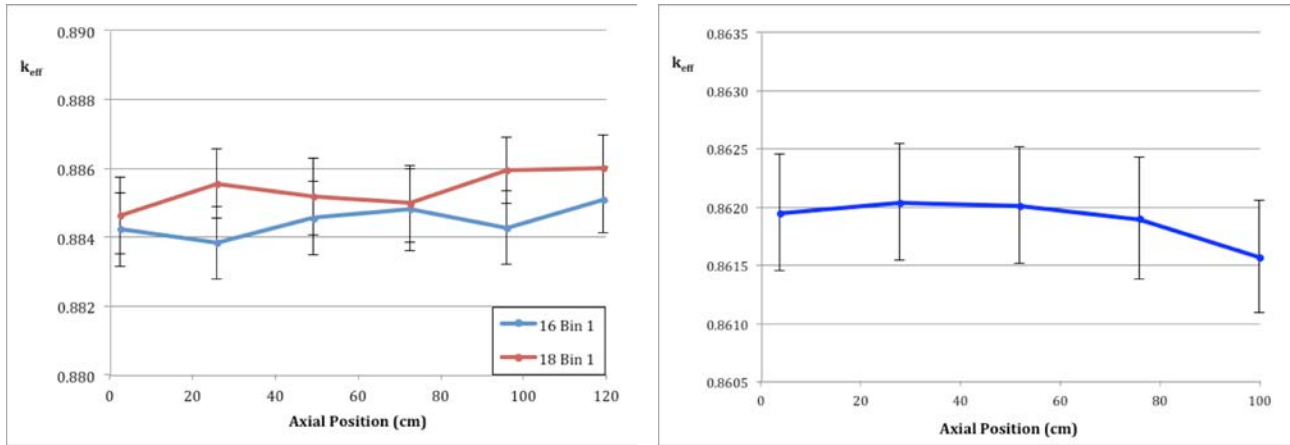


Figure 6-91 Axial Position Baseline Results – Single Package, NCT, Groups 1 & 2 (Left) and Group 3 (Right)

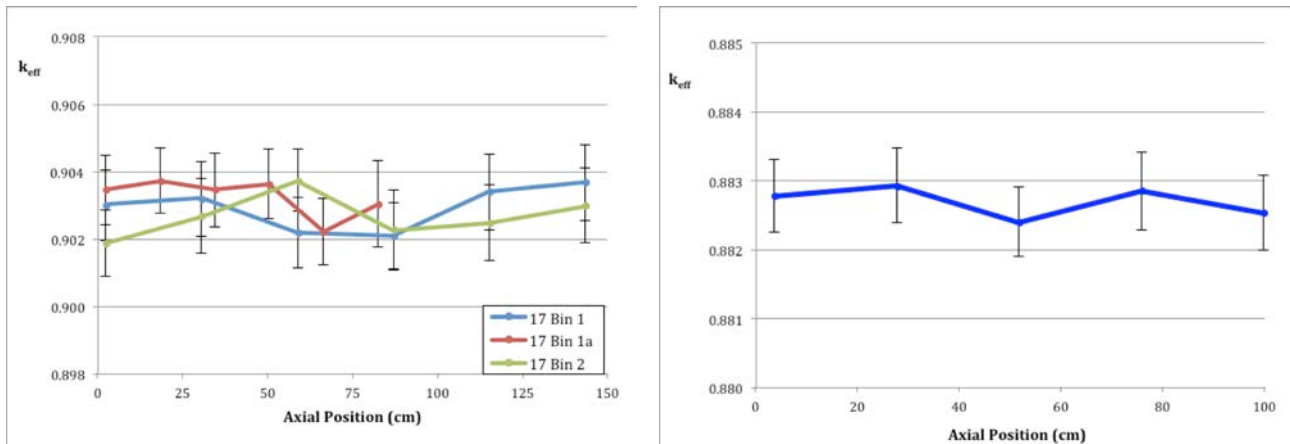


Figure 6-92 Axial Position Baseline Results – Single Package, HAC, Groups 1 & 2 (Left) and Group 3 (Right)

6.9.3.2 Single Package, Rod Pipe

6.9.3.2.1 Baseline Determination Results

The bounding fuel OR data for each baseline configuration is shown in Table 6-117 for Single Package NCT. Only the square pitch-type was examined beyond a fuel OR of 0.65 cm, as square pitch was more reactive than hexagonal pitch. For UO₂ fuel rods, the resultant bounding fuel OR is much larger than a standard LWR fuel pellet, with a fuel OR of 3.5 cm and an equivalent half-pitch of 3.5 cm. For U₃Si₂ fuel rods, the bounding fuel OR is the upper limit of examination, 0.4851 cm, with an equivalent square half-pitch of 0.4851 cm.

Content	Traveller Variant	Fuel OR (cm)	Half-Pitch (cm)	Hexagonal Pitch-Type			Square Pitch-Type		
				k _{eff}	σ	k _{eff} + 2σ	k _{eff}	σ	k _{eff} + 2σ
UO ₂ Fuel Rods	STD	0.39	0.39	0.46567	0.00063	0.46693	0.51224	0.00079	0.51382
		0.425	0.425	0.46632	0.00061	0.46754	0.51370	0.00067	0.51504
		0.45	0.45	0.46553	0.00060	0.46673	0.51232	0.00062	0.51356
		0.475	0.475	0.46678	0.00055	0.46788	0.51263	0.00066	0.51395
		0.5	0.5	0.46598	0.00070	0.46738	0.51231	0.00061	0.51353
		0.55	0.55	0.46567	0.00059	0.46685	0.51453	0.00070	0.51593
		0.6	0.6	0.46620	0.00059	0.46738	0.51496	0.00069	0.51634
	0.65	0.65	0.46713	0.00065	0.46843	0.51540	0.00064	0.51668	
	XL	0.39	0.39	0.47715	0.00058	0.47831	0.52178	0.00063	0.52304
		0.425	0.425	0.47613	0.00063	0.47739	0.52237	0.00068	0.52373
		0.45	0.45	0.47609	0.00059	0.47727	0.52128	0.00070	0.52268
		0.475	0.475	0.47754	0.00060	0.47874	0.52267	0.00066	0.52399
		0.5	0.5	0.47638	0.00059	0.47756	0.52236	0.00063	0.52362
		0.55	0.55	0.47840	0.00064	0.47968	0.52426	0.00063	0.52552
		0.6	0.6	0.47755	0.00063	0.47881	0.52416	0.00065	0.52546
		0.65	0.65	0.47703	0.00063	0.47829	0.52432	0.00064	0.52560
		0.7	0.7	--	--	--	0.52673	0.0007	0.52813
		0.75	0.75	--	--	--	0.52715	0.00068	0.52851
		0.8	0.8	--	--	--	0.52535	0.00071	0.52677
		0.85	0.85	--	--	--	0.52505	0.00069	0.52643
		0.9	0.9	--	--	--	0.52908	0.00069	0.53046
		1.0	1.0	--	--	--	0.52906	0.00072	0.53050
		1.2	1.2	--	--	--	0.53460	0.00067	0.53594
		1.5	1.5	--	--	--	0.52953	0.00068	0.53089
		2.0	2.0	--	--	--	0.54344	0.00071	0.54486
		2.5	2.5	--	--	--	0.52381	0.00062	0.52505
		3.0	3.0	--	--	--	0.54699	0.00067	0.54833
		3.5	3.5	--	--	--	0.56435	0.00086	0.56607
		4.0	4.0	--	--	--	0.55588	0.00074	0.55736
		4.5	4.5	--	--	--	0.52236	0.00068	0.52372
5.0		5.0	--	--	--	0.50621	0.00064	0.50749	
5.5	5.5	--	--	--	0.48890	0.00066	0.49022		
6.0	6.0	--	--	--	0.47085	0.00056	0.47197		
6.5	6.5	--	--	--	0.45437	0.00068	0.45573		
7.0	7.0	--	--	--	0.44140	0.00058	0.44256		

Content	Traveller Variant	Fuel OR (cm)	Half-Pitch (cm)	Hexagonal Pitch-Type			Square Pitch-Type		
				k_{eff}	σ	$k_{eff} + 2\sigma$	k_{eff}	σ	$k_{eff} + 2\sigma$
U ₃ Si ₂ Fuel Rods	STD	0.3909	0.3909	0.37181	0.00042	0.37265	0.39207	0.00042	0.39291
		0.4145	0.4145	0.38052	0.00036	0.38124	0.40264	0.00036	0.40336
		0.438	0.438	0.39037	0.0004	0.39117	0.41198	0.00041	0.41280
		0.4616	0.4616	0.39893	0.00035	0.39963	0.42104	0.00037	0.42178
		0.4851	0.4851	0.40592	0.00035	0.40662	0.42948	0.00037	0.43022

For the Rod Pipe Single Package under HAC, a full study was done that examined several pitch values for each fuel OR listed in order to determine the peak reactivity. For each fuel OR value, five half-pitch values were examined such that a curve was developed for each fuel OR. Table 6-118 lists the peak value of each of these curves, with the overall maximum shaded in gray. Table 6-119 and Table 6-120 show the fuel pitch variation curve for the most reactive fuel OR of each package variant and pitch type. The full range of fuel OR and half-pitch values examined are listed in Table 6-16. Table 6-121 takes the overall most reactive UO₂ fuel rod case (the Traveller XL with fuel OR = 0.55 cm and half-pitch = 1.05 cm with a hexagonal pitch-type) and examines finer pitch values for fuel OR of 0.50, 0.55, and 0.60 cm in order to better determine the optimum fuel OR-fuel pitch combination. The Rod Pipe, UO₂ Fuel Rod, Single Package, HAC baseline case models the Traveller XL with a fuel OR of 0.55 cm and a hexagonal half-pitch of 1.00 cm. The Rod Pipe, U₃Si₂ Fuel Rod, Single Package, HAC baseline case models the Traveller STD with a fuel OR of 0.4851 cm and a square half-pitch of 1.0101 cm.

Contents	Traveller Variant	Fuel OR (cm)	Hexagonal Pitch-Type				Square Pitch-Type			
			Half-Pitch (cm)	k_{eff}	σ	$k_{eff} + 2\sigma$	Half-Pitch (cm)	k_{eff}	σ	$k_{eff} + 2\sigma$
UO ₂ Fuel Rods	STD	0.390	0.640	0.70158	0.00084	0.70326	0.640	0.71305	0.00091	0.71487
		0.425	0.925	0.69713	0.00095	0.69903	0.675	0.70660	0.00100	0.70860
		0.450	0.950	0.70226	0.00086	0.70398	0.700	0.70507	0.00087	0.70681
		0.475	0.975	0.70917	0.00085	0.71087	0.725	0.70577	0.00085	0.70747
		0.500	1.000	0.71458	0.00088	0.71634	0.750	0.70148	0.00097	0.70342
		0.550	1.050	0.71759	0.00088	0.71935	1.050	0.69789	0.00074	0.69937
		0.600	1.100	0.70806	0.00088	0.70982	1.100	0.70211	0.00084	0.70379
	0.650	1.150	0.69349	0.00084	0.69517	1.150	0.70220	0.00082	0.70384	
	XL	0.390	0.640	0.70650	0.00100	0.70850	0.640	0.71643	0.00090	0.71823
		0.425	0.925	0.70070	0.00080	0.70230	0.675	0.71244	0.00086	0.71416
		0.450	0.950	0.70703	0.00080	0.70863	0.700	0.71048	0.00079	0.71206
		0.475	0.975	0.71213	0.00092	0.71397	0.725	0.71372	0.00086	0.71544
		0.500	1.000	0.71842	0.00084	0.72010	0.750	0.70775	0.00091	0.70957
		0.550	1.050	0.72148	0.00091	0.72330	1.050	0.70213	0.00081	0.70375
0.600		1.100	0.71222	0.00084	0.71390	1.100	0.70750	0.00079	0.70908	
0.650	1.150	0.69830	0.00084	0.69998	1.150	0.70862	0.00093	0.71048		
U ₃ Si ₂ Fuel Rods	STD	0.3909	0.9409	0.64433	0.00047	0.64527	0.8909	0.64625	0.00043	0.64711
		0.4145	0.9645	0.65555	0.00050	0.65655	0.8895	0.65556	0.00051	0.65658
		0.4380	0.9880	0.66260	0.00044	0.66348	0.8880	0.66275	0.00048	0.66371
		0.4616	1.0116	0.66958	0.00045	0.67048	0.8866	0.66790	0.00051	0.66892
		0.4851	1.0101	0.67492	0.00049	0.67590	0.9101	0.67170	0.00044	0.67258

Traveller Variant	Hexagonal Pitch-Type Fuel OR = 0.55 cm				Square Pitch-Type Fuel OR = 0.39 cm			
	Half-Pitch (cm)	k _{eff}	σ	k _{eff} + 2σ	Half-Pitch (cm)	k _{eff}	σ	k _{eff} + 2σ
STD	0.550	0.46567	0.00059	0.46685	0.39	0.51224	0.00079	0.51382
	0.650	0.57384	0.00070	0.57524	0.49	0.64028	0.00080	0.64188
	0.800	0.67225	0.00078	0.67381	0.64	0.71305	0.00091	0.71487
	1.050	0.71759	0.00088	0.71935	0.89	0.69093	0.00080	0.69253
	1.300	0.67762	0.00091	0.67944	1.14	0.60186	0.00077	0.60340
XL	0.550	0.47840	0.00064	0.47968	0.39	0.52178	0.00063	0.52304
	0.650	0.58179	0.00070	0.58319	0.49	0.64570	0.00085	0.64740
	0.800	0.67945	0.00084	0.68113	0.64	0.71643	0.00090	0.71823
	1.050	0.72148	0.00091	0.72330	0.89	0.69441	0.00083	0.69607
	1.300	0.68201	0.00082	0.68365	1.14	0.60238	0.00074	0.60386

Traveller Variant	Hexagonal Pitch-Type Fuel OR = 0.4851 cm				Square Pitch-Type Fuel OR = 0.4851 cm			
	Half-Pitch (cm)	k _{eff}	σ	k _{eff} + 2σ	Half-Pitch (cm)	k _{eff}	σ	k _{eff} + 2σ
STD	0.6351	0.50275	0.00039	0.50353	0.6351	0.53921	0.00044	0.54009
	0.6851	0.53725	0.00043	0.53811	0.6851	0.57200	0.00043	0.57286
	0.7351	0.57009	0.00044	0.57097	0.7351	0.60327	0.00047	0.60421
	0.7851	0.59831	0.00047	0.59925	0.7851	0.63083	0.00048	0.63179
	0.8351	0.62586	0.00048	0.62682	0.8351	0.65343	0.00051	0.65445
	0.8851	0.64822	0.00051	0.64924	0.8851	0.66937	0.00049	0.67035
	0.9351	0.66411	0.00051	0.66513	0.9101	0.67170	0.00044	0.67258
	0.9601	0.66978	0.00046	0.67070	0.9351	0.66719	0.00049	0.66817
	0.9851	0.67377	0.0005	0.67477	0.9601	0.65913	0.00046	0.66005
	1.0101	0.67492	0.00049	0.67590	0.9851	0.65365	0.00047	0.65459
	1.0351	0.67343	0.00047	0.67437	1.0351	0.64914	0.00046	0.65006
	1.0851	0.65959	0.00048	0.66055	1.0851	0.63989	0.00046	0.64081
	1.1351	0.63237	0.00051	0.63339	1.1351	0.62649	0.00040	0.62729
	1.1851	0.62553	0.00044	0.62641	1.1851	0.61949	0.00048	0.62045
	1.2351	0.62486	0.00046	0.62578	1.2351	0.59977	0.00046	0.60069
	1.2851	0.61578	0.00068	0.61714	1.2851	0.57214	0.00047	0.57308
	1.3351	0.60152	0.00043	0.60238	1.3351	0.55316	0.00038	0.55392

Table 6-121 UO₂ Single Package, HAC, Rod Pipe Fuel OR-Pitch Combination – Refined Parameter Study				
Fuel OR (cm)	Half-Pitch (cm)	k_{eff}	σ	k_{eff} + 2σ
0.50	0.50	0.47715	0.00038	0.47791
	0.60	0.59249	0.00041	0.59331
	0.75	0.68716	0.00048	0.68812
	0.90	0.71225	0.00053	0.71331
	0.95	0.71069	0.00053	0.71175
	1.00	0.71899	0.00056	0.72011
	1.05	0.71636	0.00054	0.71744
	1.10	0.69702	0.00051	0.69804
	1.15	0.67265	0.00044	0.67353
	1.20	0.67062	0.00049	0.67160
	1.25	0.66829	0.00049	0.66927
0.55	0.55	0.47725	0.00033	0.47791
	0.65	0.58184	0.00038	0.58260
	0.80	0.67930	0.00044	0.68018
	0.95	0.70537	0.00045	0.70627
	1.00	0.72106	0.00047	0.72200
	1.05	0.72104	0.00046	0.72196
	1.10	0.70821	0.00056	0.70933
	1.15	0.68711	0.00047	0.68805
	1.20	0.68673	0.00051	0.68775
	1.25	0.68652	0.00050	0.68752
	1.30	0.68179	0.00047	0.68273
0.60	0.60	0.47726	0.00039	0.47804
	0.70	0.57688	0.00040	0.57768
	0.85	0.67549	0.00055	0.67659
	1.00	0.71384	0.00047	0.71478
	1.05	0.71834	0.00051	0.71936
	1.10	0.71201	0.00052	0.71305
	1.15	0.69473	0.00051	0.69575
	1.20	0.69488	0.00050	0.69588
	1.25	0.69882	0.00048	0.69978
	1.30	0.69745	0.00046	0.69837
	1.35	0.69157	0.00051	0.69259

6.9.3.3 Package Array, NCT, Fuel Assembly

6.9.3.3.1 CFA-Package Variant Comparison Results

Table 6-122 details the results of the Package Array, NCT evaluation for Groups 1, 2, and 3. For Group 1, the most reactive CFA-Package Variant combination is the Traveller XL with 17 Bin 2 and an array stack height of 2 packages. For Group 2, the most reactive CFA-Package Variant combination is the Traveller XL with 16 Bin 1 and an array stack height of 1 package. For Group 3, there is only one possible CFA-Package Variant combination and the array stack height of 1 package is the most reactive.

Table 6-122 Package Array, NCT, CFA Package Variant Results									
Traveller Variant	Group	CFA	Active Fuel Length (in.)	Array Stack Height = 2			Array Stack Height = 1		
				k_{eff}	σ	$k_{eff} + 2\sigma$	k_{eff}	σ	$k_{eff} + 2\sigma$
STD	1	14 Bin 1	137.20	0.28743	0.00024	0.28791	0.27923	0.00024	0.27971
		14 Bin 2	144.50	0.26258	0.00032	0.26322	0.25522	0.00027	0.25576
		15 Bin 1	144.50	0.29497	0.00029	0.29555	0.28814	0.00026	0.28866
		15 Bin 2	140.26	0.29413	0.00026	0.29465	0.28671	0.00025	0.28721
		16 Bin 2	137.20	0.28149	0.00023	0.28195	0.27367	0.00024	0.27415
		16 Bin 3	144.50	0.26860	0.00028	0.26916	0.26127	0.00023	0.26173
		17 Bin 1	144.50	0.28916	0.00025	0.28966	0.28211	0.00026	0.28263
		17 Bin 2	144.50	0.30307	0.00028	0.30363	0.29554	0.00025	0.29604
XL	1	14 Bin 1	137.20	0.29419	0.00037	0.29493	0.28865	0.00026	0.28917
		14 Bin 2	144.50	0.27142	0.00026	0.27194	0.26686	0.00026	0.26738
		15 Bin 1	144.50	0.30100	0.00025	0.30150	0.29587	0.00025	0.29637
		15 Bin 2	140.26	0.29981	0.00032	0.30045	0.29434	0.00022	0.29478
		16 Bin 2	137.20	0.28892	0.00024	0.28940	0.28302	0.00024	0.28350
		16 Bin 2a *	150.50	0.28997	0.00026	0.29049	0.28544	0.00025	0.28594
		16 Bin 3	144.50	0.27758	0.00029	0.27816	0.27242	0.00023	0.27288
		17 Bin 1	144.50	0.29550	0.00030	0.29610	0.29036	0.00024	0.29084
		17 Bin 1a *	168.50	0.29696	0.00026	0.29748	0.29368	0.00030	0.29428
		17 Bin 2	144.50	0.30888	0.00027	0.30942	0.30338	0.00024	0.30386
	2	16 Bin 1	154.04	0.29991	0.00026	0.30043	0.30847	0.00031	0.30909
18 Bin 1	154.04	0.29864	0.00026	0.29916	0.30660	0.00026	0.30712		
VVER	3	VV Bin 1	143.41	0.38772	0.00017	0.38806	0.38828	0.00016	0.3886

Note: * these cases model an active fuel length that cannot be shipped in the STD and are therefore only modeled in the XL.

6.9.3.3.2 Baseline Determination Results

For Group 1, the baseline case has a most reactive axial fuel position of 2.54 cm, modeling the CFA of 17 Bin 2 at the bottom of the Clamshell. The axial positions listed in Table 6-123 represent the axial positions of the fuel assemblies in the top package. An axial position of 2.54 cm represents the fuel assemblies of the top and bottom package as close to one another as possible, which is the most reactive configuration, whereas an axial position of 143.51 cm represents the fuel assemblies as far from each other as possible. For Group 2, the baseline case has a most reactive axial fuel position of 119.278 cm, modeling the CFA of 16 Bin 1 at the top of the Clamshell. For Group 3, the baseline case has a most reactive axial fuel position of 3.81 cm, modeling the CFA of VV Bin 1 at the bottom of the Clamshell.

Table 6-123 Axial Position Baseline Results –Package Array, NCT, Groups 1, 2, and 3					
Content (Group)	Traveller Variant	Axial Position (cm)	k_{eff}	σ	k_{eff} + 2σ
17 Bin 2 (1)	XL	2.540	0.30888	0.00027	0.30942
		30.734	0.29814	0.00025	0.29864
		58.928	0.29714	0.00029	0.29772
		87.122	0.29670	0.00035	0.29740
		115.316	0.29660	0.00027	0.29714
		143.510	0.30040	0.00024	0.30088
16 Bin 1 (2)	XL	2.540	0.30847	0.00031	0.30909
		25.888	0.30664	0.00028	0.30720
		49.235	0.30649	0.00023	0.30695
		72.583	0.30664	0.00025	0.30714
		95.931	0.30652	0.00025	0.30702
		119.278	0.30950	0.00026	0.31002
VV Bin 1 (3)	VVER	3.810	0.38828	0.00016	0.38860
		27.832	0.38682	0.00017	0.38716
		51.854	0.38682	0.00017	0.38716
		75.876	0.38702	0.00017	0.38736
		99.899	0.3879	0.00017	0.38824

6.9.3.4 Package Array, NCT, Rod Pipe

6.9.3.4.1 Baseline Determination Results

The bounding fuel OR data for each baseline configuration is shown in Table 6-124 for Package Array, NCT. For UO₂ fuel rods, only the square pitch-type was examined beyond a fuel OR of 0.65 cm, as it was evident that the square pitch-type was more reactive than the hexagonal pitch-type. The resultant bounding fuel OR is much larger than a standard LWR fuel pellet, with peak reactivity at a fuel OR of 3.5 cm with an equivalent half-pitch of 3.5 cm. For U₃Si₂ fuel rods, the bounding fuel OR is 0.4851 cm with an equivalent square half-pitch of 0.4851 cm.

Contents	Traveller Variant	Fuel OR (cm)	Half-Pitch (cm)	Hexagonal Pitch-Type			Square Pitch-Type		
				k _{eff}	σ	k _{eff} + 2σ	k _{eff}	σ	k _{eff} + 2σ
UO ₂ Fuel Rods	STD	0.390	0.390	0.36250	0.00074	0.36398	0.41675	0.00052	0.41779
		0.450	0.450	0.36264	0.00052	0.36368	0.41782	0.00070	0.41922
		0.475	0.475	0.36306	0.00056	0.36418	0.41960	0.00066	0.42092
		0.500	0.500	0.36204	0.00057	0.36318	0.41929	0.00059	0.42047
		0.550	0.550	0.36251	0.00048	0.36347	0.42081	0.00053	0.42187
		0.600	0.600	0.36337	0.00049	0.36435	0.41983	0.00065	0.42113
		0.650	0.650	0.36451	0.00049	0.36549	0.42114	0.00061	0.42236
		0.700	0.700	0.36401	0.00048	0.36497	0.42225	0.00058	0.42341
		0.750	0.750	0.36380	0.00054	0.36488	0.42248	0.00059	0.42366
	XL	0.390	0.390	0.36722	0.00049	0.36820	0.42171	0.00059	0.42289
		0.450	0.450	0.36710	0.00046	0.36802	0.42188	0.00060	0.42308
		0.475	0.475	0.36664	0.00048	0.36760	0.42174	0.00061	0.42296
		0.500	0.500	0.36601	0.00051	0.36703	0.42209	0.00056	0.42321
		0.550	0.550	0.36709	0.00050	0.36809	0.42317	0.00055	0.42427
		0.600	0.600	0.36795	0.00052	0.36899	0.42435	0.00062	0.42559
		0.650	0.650	0.36697	0.00049	0.36795	0.42515	0.00060	0.42635
		0.700	0.700	0.36813	0.00051	0.36915	0.42507	0.00058	0.42623
		0.750	0.750	0.36709	0.00049	0.36807	0.42608	0.00060	0.42728
		0.800	0.800	--	--	--	0.42641	0.00056	0.42753
		0.950	0.950	--	--	--	0.42861	0.0006	0.42981
		1.000	1.000	--	--	--	0.42964	0.00057	0.43078
		1.500	1.500	--	--	--	0.43248	0.00061	0.4337
		2.000	2.000	--	--	--	0.44342	0.00055	0.44452
		2.500	2.500	--	--	--	0.43539	0.00069	0.43677
3.000	3.000	--	--	--	0.45212	0.00064	0.4534		
3.500	3.500	--	--	--	0.46675	0.00067	0.46809		
4.000	4.000	--	--	--	0.45741	0.00075	0.45891		

Contents	Traveller Variant	Fuel OR (cm)	Half-Pitch (cm)	Hexagonal Pitch-Type			Square Pitch-Type		
				k_{eff}	σ	$k_{eff} + 2\sigma$	k_{eff}	σ	$k_{eff} + 2\sigma$
U ₃ Si ₂	STD	0.3909	0.3909	0.36594	0.00036	0.36666	0.38418	0.00046	0.3851
		0.4145	0.4145	0.37462	0.00035	0.37532	0.39369	0.00042	0.39453
		0.438	0.438	0.38208	0.00038	0.38284	0.40172	0.00035	0.40242
		0.4616	0.4616	0.38886	0.00037	0.38960	0.40923	0.00041	0.41005
		0.4851	0.4851	0.39364	0.00044	0.39452	0.41633	0.00035	0.41703

6.9.3.5 Package Array, HAC, Fuel Assembly

6.9.3.5.1 CFA-Package Variant Comparison Results

Table 6-125 details the results of the Package Array, HAC evaluation for Groups 1, 2, and 3. For Group 1, the most reactive CFA-Package Variant combinations model the Traveller XL with 17 Bin 1, 17 Bin 1a, and 17 Bin 2, and an array stack height of 1 package. For Group 2, the most reactive CFA-Package Variant combination is the Traveller XL with 18 Bin 1 and an array stack height of 1 package. For Group 3, there is only one possible CFA-Package Variant combination and the array stack height of 1 package is the most reactive.

Group	Traveller Variant	Content	Active Fuel Length (in.)	Array Stack Height = 2			Array Stack Height = 1		
				k_{eff}	σ	$k_{eff} + 2\sigma$	k_{eff}	σ	$k_{eff} + 2\sigma$
1	STD	14 Bin 1	137.20	0.87847	0.00024	0.87895	0.88074	0.00024	0.88122
		14 Bin 2	144.50	0.88017	0.00027	0.88071	0.88301	0.00024	0.88349
		15 Bin 1	144.50	0.90231	0.00025	0.90281	0.90515	0.00026	0.90567
		15 Bin 2	140.26	0.89559	0.00024	0.89607	0.89775	0.00029	0.89833
		16 Bin 2	137.20	0.88621	0.00035	0.88691	0.88900	0.00024	0.88948
		16 Bin 3	144.50	0.88231	0.00025	0.88281	0.88517	0.00032	0.88581
		17 Bin 1	144.50	0.90404	0.00026	0.90456	0.90726	0.00026	0.90778
		17 Bin 2	144.50	0.90015	0.00026	0.90067	0.90314	0.00027	0.90368
	XL	14 Bin 1	137.20	0.89879	0.00027	0.89933	0.90104	0.00024	0.90152
		14 Bin 2	144.50	0.89606	0.00026	0.89658	0.89901	0.00024	0.89949
		15 Bin 1	144.50	0.92220	0.00027	0.92274	0.92413	0.00026	0.92465
		15 Bin 2	140.26	0.91581	0.00026	0.91633	0.91885	0.00026	0.91937
		16 Bin 2	137.20	0.90670	0.00024	0.90718	0.90894	0.00026	0.90946
		16 Bin 2a *	150.50	0.90602	0.00031	0.90664	0.90850	0.00027	0.90904
		16 Bin 3	144.50	0.90457	0.00029	0.90515	0.90676	0.00025	0.90726
17 Bin 1	144.50	0.92391	0.00026	0.92443	0.92612	0.00026	0.92664		
17 Bin 1a *	168.50	0.92377	0.00027	0.92431	0.92646	0.00027	0.92700		

Group	Traveller Variant	Content	Active Fuel Length (in.)	Array Stack Height = 2			Array Stack Height = 1		
				k_{eff}	σ	$k_{eff} + 2\sigma$	k_{eff}	σ	$k_{eff} + 2\sigma$
		17 Bin 2	144.50	0.92331	0.00027	0.92385	0.92573	0.00026	0.92625
2	XL	16 Bin 1	154.04	0.90565	0.00024	0.90613	0.91484	0.00024	0.91532
		18 Bin 1	154.04	0.90697	0.00026	0.90749	0.91633	0.00026	0.91685
3	VVER	VV Bin 1	143.41	0.89492	0.00025	0.89542	0.90035	0.00023	0.90081

Note: * these cases model an active fuel length that cannot be shipped in the STD and are therefore only modeled in the XL.

6.9.3.5.2 Baseline Determination Results

Table 6-126 details the results of the Package Array, HAC evaluation for Groups 1, 2, and 3. For Group 1, the baseline case models the 17 Bin 1 CFA with a most reactive axial fuel position of 87.122 cm, approximately centered in the Clamshell. For Group 2, the baseline case has a most reactive axial fuel position of 72.583 cm, modeling the CFA of 16 Bin 1 approximately centered. For Group 3, the baseline case has a most reactive axial fuel position of 3.81 cm, modeling the CFA of VV Bin 1 at the bottom of the Clamshell.

Group	Traveller Variant	Content	Axial Position (cm)	k_{eff}	σ	$k_{eff} + 2\sigma$
1	XL	17 Bin 1	2.540	0.92612	0.00026	0.92664
			30.734	0.92410	0.00026	0.92462
			58.928	0.92563	0.00027	0.92617
			87.122	0.92688	0.00031	0.92750
			115.316	0.92566	0.00028	0.92622
			143.510	0.92574	0.00028	0.92630
		17 Bin 1a	2.540	0.92646	0.00027	0.92700
			18.542	0.92524	0.00023	0.92570
			34.544	0.92375	0.00023	0.92421
			50.546	0.92486	0.00027	0.92540
			66.548	0.92605	0.00024	0.92653
			82.550	0.92665	0.00024	0.92713
		17 Bin 2	2.540	0.92573	0.00026	0.92625
			30.734	0.92375	0.00027	0.92429
			58.928	0.92492	0.00025	0.92542
			87.122	0.92590	0.00027	0.92644
			115.316	0.92567	0.00027	0.92621
			143.510	0.92507	0.00029	0.92565

Group	Traveller Variant	Content	Axial Position (cm)	k_{eff}	σ	$k_{eff} + 2\sigma$
2	XL	18 Bin 1	2.540	0.91633	0.00026	0.91685
			25.888	0.91629	0.00032	0.91693
			49.235	0.91633	0.00024	0.91681
			72.583	0.91690	0.00025	0.91740
			95.931	0.91628	0.00024	0.91676
			119.278	0.91603	0.00029	0.91661
3	VVER	VV Bin 1	3.810	0.90035	0.00023	0.90081
			51.854	0.89846	0.00032	0.89910
			75.876	0.89892	0.00026	0.89944
			99.899	0.89891	0.00027	0.89945
			24.022	0.89811	0.00027	0.89865

Table 6-127 displays the results of the partial flooding baseline study. For Groups 1, 2, and 3, the highest water level is the most reactive, but the preferential flooding study presented in Table 6-128 is ultimately more reactive. For Groups 1, 2, and 3, a fully flooded Clamshell with all other package regions, and the package exterior, modeled as dry results in the most reactive flooding configuration, as shown in Figure 6-93, Figure 6-94, and Figure 6-95, respectively. For all three Groups, this is the baseline flooding configuration.

Content (Group)	Traveller Variant	Water Level *	k_{eff}	σ	$k_{eff} + 2\sigma$
17 Bin 1 (1)	XL	1	0.28275	0.00014	0.28303
		2	0.27528	0.00016	0.27560
		3	0.51721	0.00022	0.51765
		4	0.79216	0.00030	0.79276
		5	0.90268	0.00032	0.90332
		6	0.91304	0.00030	0.91364
18 Bin 1 (2)	XL	1	0.28637	0.00014	0.28665
		2	0.28263	0.00014	0.28291
		3	0.52063	0.00022	0.52107
		4	0.76388	0.00031	0.76450
		5	0.89435	0.00029	0.89493
		6	0.90525	0.00025	0.90575

Content (Group)	Traveller Variant	Water Level *	k_{eff}	σ	$k_{eff} + 2\sigma$
VV Bin 1 (3)	VVER	1	0.37926	0.00019	0.37964
		2	0.35042	0.0002	0.35082
		3	0.46402	0.00019	0.4644
		4	0.68574	0.00023	0.6862
		5	0.82992	0.00024	0.8304
		6	0.88931	0.00024	0.88979
		7	0.89122	0.00026	0.89174

Note: * Water Levels 1 – 6 (or 7) represent water rising diagonally through the clamshell as shown in Figure 6-12, where Water Level 1 is empty and Water Level 6 (or 7) is full.

Preferential Flooding Configuration	Water Density (g/cm ³)	Group 1	Group 2	Group 3
		Traveller XL		Traveller VVER
		$k_{eff} + 2\sigma$		
Outerpack Inner Cavity	0.0000	0.90967	0.89848	--
	0.0010	0.90920	0.89921	0.9004
	0.0100	0.90896	0.89840	0.89946
	0.1000	0.90673	0.89726	0.89454
	0.5000	0.90133	0.89418	0.88673
	0.7000	0.89971	0.89328	0.88551
	0.9982	0.89790	0.89239	0.88492
Clamshell	0.0000	0.90967	0.89848	--
	0.0010	0.90859	0.89838	0.90037
	0.0100	0.90940	0.89878	0.90004
	0.1000	0.91182	0.90137	0.90133
	0.5000	0.91975	0.90916	0.90661
	0.7000	0.92310	0.91150	0.90923
	0.9982	0.92750	0.91740	0.91421
Outerpack Outer Cavity	0.0000	0.90967	0.89848	--
	0.0010	0.90922	0.89843	0.8999
	0.0100	0.90798	0.89727	0.89795
	0.1000	0.89574	0.88772	0.87858
	0.5000	0.87478	0.86863	0.84963
	0.7000	0.87227	0.86691	0.84634
	0.9982	0.87039	0.86501	0.84434

Preferential Flooding Configuration	Water Density (g/cm ³)	Group 1	Group 2	Group 3
		Traveller XL		Traveller VVER
		$k_{eff} + 2\sigma$		
Entire Package	0.0000	0.90967	0.89848	--
	0.0010	0.90907	0.89907	0.90004
	0.0100	0.90790	0.89728	0.89672
	0.1000	0.89745	0.88912	0.87786
	0.5000	0.89509	0.88805	0.87292
	0.7000	0.89862	0.89160	0.87753
	0.9982	0.90418	0.89688	0.88385
Interspersed Moderation	0.0000	0.90967	0.89848	--
	0.0010	0.90888	0.89899	0.90067
	0.0100	0.90899	0.89797	0.90002
	0.1000	0.90670	0.89712	0.89522
	0.5000	0.89696	0.88904	0.88044
	0.7000	0.89420	0.88684	0.87649
	0.9982	0.89039	0.88318	0.87091

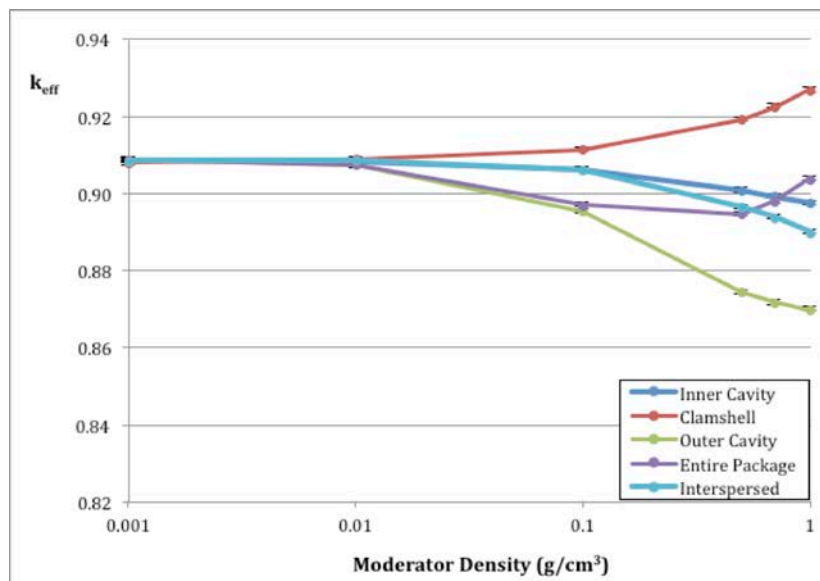


Figure 6-93 Effect of Preferential Flooding Configuration on k_{eff} (Group 1)

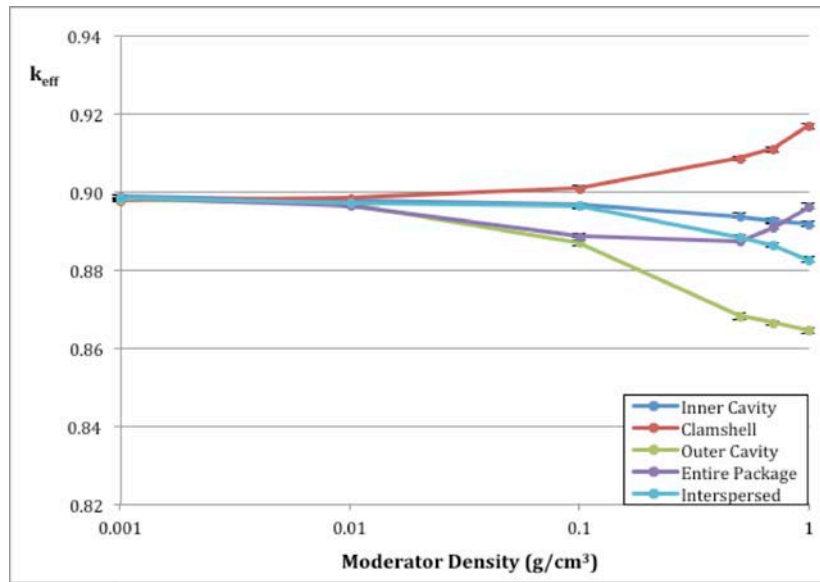


Figure 6-94 Effect of Preferential Flooding Configuration on k_{eff} (Group 2)

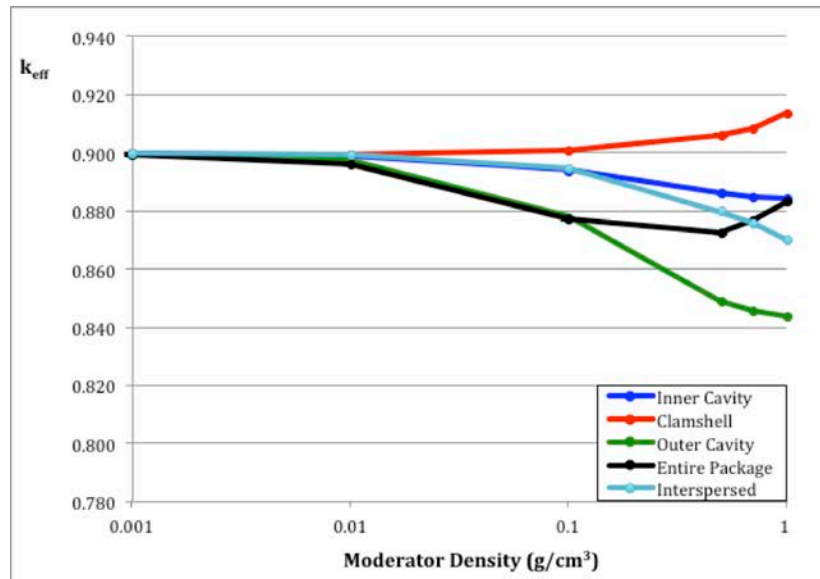


Figure 6-95 Effect of Preferential Flooding Configuration on k_{eff} (Group 3)

6.9.3.6 Package Array, HAC, Rod Pipe

6.9.3.6.1 Baseline Determination Results

For the Rod Pipe Package Array under HAC, a full study was done that examined several pitch values for each fuel OR listed in order to determine the peak reactivity. Table 6-129 lists the peak value of each of these curves, with the overall maximum shaded in gray. Table 6-129, Table 6-130, and Table 6-131 show the fuel pitch variation curve for the most reactive fuel OR of each package variant and pitch type. The full range of fuel OR and half-pitch values examined are listed in Table 6-16. Table 6-132 takes the overall most reactive UO₂ fuel rod case (the Traveller XL with fuel OR = 0.5 cm and half-pitch = 1.0 cm with a hexagonal pitch-type) and examines finer pitch values for fuel OR of 0.45, 0.5, and 0.55 cm in order to better determine the optimum fuel OR-fuel pitch combination. The Rod Pipe UO₂ Fuel Rods Package Array, HAC baseline case models the Traveller XL with a fuel OR of 0.5 cm and a hexagonal half-pitch of 1.00 cm. The Rod Pipe U₃Si₂ Fuel Rods Package Array, HAC baseline case models the Traveller STD with a fuel OR of 0.4851 cm and a square half-pitch of 0.9851 cm.

Contents	Traveller Variant	Fuel OR (cm)	Hexagonal Pitch-Type				Square Pitch-Type			
			Half-Pitch (cm)	k _{eff}	σ	k _{eff} + 2σ	Half-Pitch (cm)	k _{eff}	σ	k _{eff} + 2σ
UO ₂ Fuel Rods	STD	0.390	0.890	0.65080	0.00100	0.65280	0.640	0.65546	0.00082	0.65710
		0.450	0.950	0.65670	0.00100	0.65870	0.700	0.64712	0.00079	0.64870
		0.475	0.975	0.65896	0.00084	0.66064	0.975	0.64482	0.00096	0.64674
		0.500	1.000	0.66131	0.00088	0.66307	1.000	0.64560	0.00100	0.64760
		0.550	1.050	0.65958	0.00080	0.66118	1.050	0.65110	0.00092	0.65294
		0.600	1.100	0.65142	0.00092	0.65326	1.100	0.65190	0.00100	0.65390
		0.650	1.150	0.64336	0.00096	0.64528	1.150	0.64818	0.00087	0.64992
		0.700	1.200	0.64161	0.00078	0.64317	1.200	0.64719	0.00086	0.64891
		0.750	1.250	0.64006	0.00085	0.64176	1.250	0.64409	0.00078	0.64565
	XL	0.390	0.890	0.65219	0.00091	0.65401	0.640	0.65671	0.00086	0.65843
		0.450	0.950	0.65800	0.00100	0.66000	0.700	0.64847	0.00089	0.65025
		0.475	0.975	0.66092	0.00084	0.66260	0.975	0.64641	0.00082	0.64805
		0.500	1.000	0.66404	0.00090	0.66584	1.000	0.65015	0.00089	0.65193
		0.550	1.050	0.66278	0.00088	0.66454	1.050	0.65587	0.00084	0.65755
		0.600	1.100	0.65487	0.00083	0.65653	1.100	0.65278	0.00081	0.65440
		0.650	1.150	0.64503	0.00081	0.64665	1.150	0.65232	0.00080	0.65392
		0.700	1.200	0.64394	0.00084	0.64562	1.200	0.65153	0.00081	0.65315
		0.750	1.250	0.64204	0.00078	0.64360	1.250	0.64680	0.00093	0.64866
U ₃ Si ₂ Fuel Rods	STD	0.3909	0.9159	0.60523	0.00055	0.60633	0.8659	0.60508	0.00047	0.60602
		0.4145	0.9395	0.61310	0.00045	0.61400	0.8645	0.61139	0.00048	0.61235
		0.4380	0.9380	0.61677	0.00068	0.61813	0.8630	0.61641	0.00050	0.61741
		0.4616	0.9866	0.62163	0.00044	0.62251	0.8866	0.61943	0.00056	0.62055
		0.4851	0.9851	0.62316	0.00048	0.62412	0.9101	0.61984	0.00049	0.62082

Traveller Variant	Hexagonal Pitch-Type Fuel OR = 0.50 cm				Square Pitch-Type Fuel OR = 0.39 cm			
	Half-Pitch (cm)	k _{eff}	σ	k _{eff} + 2σ	Half-Pitch (cm)	k _{eff}	σ	k _{eff} + 2σ
STD	0.5	0.36030	0.00051	0.36132	0.39	0.41473	0.00057	0.41587
	0.6	0.49679	0.00077	0.49833	0.49	0.56512	0.00085	0.56682
	0.75	0.61458	0.00079	0.61616	0.64	0.65546	0.00082	0.65710
	1.0	0.66131	0.00088	0.66307	0.89	0.64367	0.00090	0.64547
	1.25	0.62189	0.00084	0.62357	1.14	0.56496	0.00081	0.56658
XL	0.5	0.36481	0.00051	0.36583	0.39	0.41863	0.00055	0.41973
	0.6	0.50205	0.00070	0.50345	0.49	0.56960	0.00087	0.57134
	0.75	0.61877	0.00078	0.62033	0.64	0.65671	0.00086	0.65843
	1.0	0.66404	0.00090	0.66584	0.89	0.64537	0.00092	0.64721
	1.25	0.62488	0.00091	0.62670	1.14	0.56566	0.00091	0.56748

Traveller Variant	Hexagonal Pitch-Type Fuel OR = 0.4851 cm				Square Pitch-Type Fuel OR = 0.4851 cm			
	Half-Pitch (cm)	k _{eff}	σ	k _{eff} + 2σ	Half-Pitch (cm)	k _{eff}	σ	k _{eff} + 2σ
STD	0.6351	0.48303	0.00040	0.48383	0.6351	0.51485	0.00040	0.51565
	0.6851	0.51369	0.00056	0.51481	0.6851	0.54510	0.00049	0.54608
	0.7351	0.54171	0.00052	0.54275	0.7351	0.57244	0.00044	0.57332
	0.7851	0.56883	0.00047	0.56977	0.7851	0.59382	0.00042	0.59466
	0.8351	0.59099	0.00050	0.59199	0.8351	0.60970	0.00046	0.61062
	0.8851	0.60725	0.00053	0.60831	0.8851	0.61963	0.00057	0.62077
	0.9351	0.61865	0.00048	0.61961	0.9101	0.61984	0.00049	0.62082
	0.9601	0.62188	0.00048	0.62284	0.9351	0.61657	0.00046	0.61749
	0.9851	0.62316	0.00048	0.62412	0.9601	0.61307	0.00051	0.61409
	1.0101	0.62295	0.00053	0.62401	0.9851	0.60988	0.00046	0.61080
	1.0351	0.62181	0.00048	0.62277	1.0351	0.60517	0.00046	0.60609
	1.0851	0.61007	0.00046	0.61099	1.0851	0.59670	0.00049	0.59768
	1.1351	0.59411	0.00052	0.59515	1.1351	0.58495	0.00048	0.58591
	1.1851	0.58921	0.00051	0.59023	1.1851	0.57452	0.00049	0.57550
	1.2351	0.5839	0.00046	0.58482	1.2351	0.55718	0.00042	0.55802
	1.2851	0.57329	0.00050	0.57429	1.2851	0.53699	0.00043	0.53785
	1.3351	0.55946	0.00044	0.56034	1.3351	0.52171	0.00043	0.52257

Fuel OR (cm)	Half-Pitch (cm)	k_{eff}	σ	k_{eff} + 2σ
0.475	0.475	0.36435	0.00029	0.36493
	0.575	0.50652	0.00038	0.50728
	0.725	0.62531	0.00045	0.62621
	0.875	0.66157	0.00043	0.66243
	0.925	0.65967	0.00066	0.66099
	0.975	0.66217	0.00044	0.66305
	1.025	0.65971	0.00050	0.66071
	1.075	0.65040	0.00061	0.65162
	1.125	0.63150	0.00054	0.63258
	1.175	0.62186	0.00046	0.62278
	1.225	0.61769	0.00063	0.61895
0.5	0.5	0.36489	0.00030	0.36549
	0.6	0.50025	0.00041	0.50107
	0.75	0.61898	0.00045	0.61988
	0.9	0.65602	0.00052	0.65706
	0.95	0.65915	0.00049	0.66013
	1	0.66385	0.00050	0.66485
	1.05	0.66147	0.00057	0.66261
	1.1	0.64822	0.00048	0.64918
	1.15	0.63379	0.00050	0.63479
	1.2	0.62922	0.00047	0.63016
	1.25	0.62453	0.00056	0.62565
0.550	0.55	0.36474	0.00033	0.36540
	0.65	0.49089	0.00039	0.49167
	0.8	0.60868	0.00049	0.60966
	0.95	0.65168	0.00051	0.65270
	1	0.66151	0.00054	0.66259
	1.05	0.66253	0.00047	0.66347
	1.1	0.65524	0.00048	0.65620
	1.15	0.64444	0.00052	0.64548
	1.2	0.64255	0.00050	0.64355
	1.25	0.64131	0.00051	0.64233
	1.3	0.63354	0.00057	0.63468

6.9.4 Combined Case Study Results

This appendix evaluates combined cases that model all the penalizing configurations to demonstrate that the independent penalty method described in Section 6.3.4 is bounding. This is primarily because penalties from each study are indiscriminately summed for a total penalty, while for multiple studies the penalty is due to the same effect (e.g. increased moderation). Thus, the increase in k_{eff} from independently adding penalties from separate studies is greater than the cumulative effect from modeling all positive penalty configurations in a single model. This study is only evaluated for the HAC package array cases, as these are the bounding cases that are closest to the USL.

A summary of the bounding configurations for each of the PWR Groups and the Loose Rod pipe are provided in Table 6-133 and Table 6-134, respectively, based on the results summarized in Table 6-73 and Table 6-74. A comparison between the HAC Package Array Maximum k_{eff} value listed in Table 6-75 using the method outlined in Section 6.3.4 and k_{eff} from the combined cases is presented in Table 6-135. These results support the use of the individual penalty method for a bounding result in the criticality analysis.

Study	Bounding Configuration		
	PWR Group 1	PWR Group 2	PWR Group 3
Annular Blanket	None	None	0.155 in. ID x 20 in. Long
Clamshell/fuel assembly shift	Shifted up	Shifted up	Shifted up
Moderator Block Density	None	None	Reduced Density
Package OD Tolerance	None	Min. Package OD	Min. Package OD
Poly Melt	2 kg of uniform melt	2 kg of collected melt	2 kg uniform melt
Axial rod displacement	None	None	64 rods shifted up
Stainless Steel Rods	None	None	None
Fuel Clad Tolerance	Min. Clad Thickness	Min. Clad Thickness	Min. Clad Thickness
Fuel Pellet Tolerance	None	Min. Pellet OD	Min. Pellet OD
Fuel Rod Pitch Tolerance	Max. Pitch	Max. Pitch	Max. Pitch
Nozzle Reflection	None	None	None
Extended Active Fuel Length	--	--	Extended Length
ADOPT Fuel Rods	None	None	--

Study	Bounding Configuration	
	Loose Rods (UO ₂)	Loose Rods (U ₃ Si ₂)
Annular Fuel Pellet Blanket	Full-length	None
Rod Pipe Position in Clamshell	Centered	Centered
Moderator Density	None	Reduced Density
Package OD Tolerance	Min. Package OD	Min. Package OD
Fuel Pellet Diameter Tolerance	None	None
Polyethylene Packing Materials	Full Rod Pipe	Full Rod Pipe
Moderation Variation	Clamshell Fully Flooded	Clamshell Fully Flooded
ADOPT Fuel Rods	None	--

Case		k_{eff}	σ	Total Penalty	k_{eff}+2σ
PWR Group 1	Independent Penalty	0.92688	0.00031	0.01033	0.93783
	Combined	0.93671	0.00024	-	0.93719
PWR Group 2	Independent Penalty	0.91690	0.00025	0.02205	0.93945
	Combined	0.93641	0.00025	-	0.93691
PWR Group 3	Independent Penalty	0.91373	0.00024	0.01643	0.93064
	Combined	0.92402	0.00023	-	0.92448
Loose Rods (UO ₂)	Independent Penalty	0.66385	0.00050	0.15103	0.81588
	Combined	0.79627	0.00046	-	0.79719
Loose Rods (U ₃ Si ₂)	Independent Penalty	0.62316	0.00048	0.14424	0.76836
	Combined	0.74746	0.00056	-	0.74858

TABLE OF CONTENTS

7.0 PACKAGE OPERATIONS..... 7-1

7.1 PACKAGE LOADING..... 7-1

7.1.1 Preparation for Loading..... 7-1

7.1.1.1 Receive Shipping Package 7-1

7.1.1.2 Clean Shipping Package 7-1

7.1.1.3 Refurbish Shipping Package..... 7-2

7.1.1.4 Configure Package for Fuel Assembly Loading 7-2

7.1.1.5 Inspection 7-2

7.1.2 Loading Contents and Closing Package 7-2

7.1.3 Preparation for Transport..... 7-3

7.1.3.1 Conveyance Loading of Shipping Packages 7-3

7.1.3.2 Regulatory 7-4

7.1.3.3 Inspection 7-4

7.2 PACKAGE UNLOADING 7-4

7.2.1 Receipt of Package from Carrier 7-4

7.2.2 Removal of Contents 7-4

7.3 PREPARATION OF EMPTY PACKAGE FOR TRANSPORT 7-5

7.4 APPENDICES 7-6

7.4.1 References..... 7-6

7.0 PACKAGE OPERATIONS

The following information contains the significant events relating to the routine use of fuel assembly shipping packages. Complete detailed instructions are outlined within the individual plant operating procedures and quality control instructions pertinent to each specific operation. It should be considered that in this section the term “Traveller package” refers to all variants (STD, XL, and VVER) and the term “Clamshell” refers to both the rectangular Clamshell and the hexagonal VVER Clamshell.

7.1 PACKAGE LOADING

Operations at the loading site include the span of activities from receiving and inspecting the package to loading and preparing the loaded package for transport. Each loading site must provide fully trained personnel and operating procedures to cover all of the activities.

7.1.1 Preparation for Loading

For contents to be acceptable for shipment in the Traveller package the requirements of (a) or (b) shall be met, as described in Section 1.2.2.2:

- a. The uranium content meets the “unirradiated uranium” definition of SSR-6 para. 527 [1] and 10 CFR 71.4 [2].

Unirradiated uranium means uranium containing not more than 2×10^3 Bq of plutonium per gram of ^{235}U , not more than 9×10^6 Bq of fission products per gram of ^{235}U , and not more than 5×10^{-3} g of ^{236}U per gram of ^{235}U .

- b. If the ^{236}U requirement of the “unirradiated uranium” definition is not met, the content may still be shipped if the following criteria are met:
 - 1) The contents meet the requirements of the UF_6 Enriched Commercial Grade specification of ASTM C 996 [3], specifically the ^{236}U limit ($250 \mu\text{g } ^{236}\text{U/gU}$), as outlined in Table 1-2.
 - 2) There is less than a Type A quantity of material in the content.
 - For an A_2 calculation, the *U(enriched to 20% or less) - Unlimited* value may not be used.
 - The A_2 calculation must be completed using the A_2 values in 10 CFR 71 Appendix A₂ Table A-1 for the individual isotopes in the fuel content, using the “slow lung absorption” values for uranium isotopes (i.e., for a UO_2 or U_3Si_2 compound).

Note: plutonium and fission products are not allowed in the Traveller Type A packages.

7.1.1.1 Receive Shipping Package

- Unload the shipping package from the truck.
- Report any obvious damage to the package engineer.
- Prepare a package identification route card.

7.1.1.2 Clean Shipping Package

- Use soap or a suitable detergent and/or water to clean the package, as required.
- Move the package to the refurbishing or lay down areas.

7.1.1.3 Refurbish Shipping Package

- Check package upper and lower Outerpack exterior for damage.
- Open Outerpack and check for internal damage or excessive wear.
- Repair/rework as required.
- Check Clamshell for loose parts, and if found, secure per specifications and drawings.
- Check the Clamshell for any mechanical damage or excessive wear.
- Vacuum package to collect foreign debris.

7.1.1.4 Configure Package for Fuel Assembly Loading

- Configure (install) top axial restraint(s) and axial spacer (as needed) for specific fuel assembly type.
- Install accelerometers as required per site procedure.
- Check installed accelerometers for QC seal, calibration, and tripped condition. If found in tripped condition, replace with un-tripped and calibrated accelerometer.

7.1.1.5 Inspection

- Verify that the package interior/exterior Outerpack and Clamshell are clean, and in good condition.
- Verify that the top axial restraint(s), axial spacer (as needed), and grid pads are present and in good working condition.
- Verify that the BORAL neutron absorber plates are present and in good visual condition.
- Verify that outstanding applicable package non-conformances have been closed prior to release for loading.

7.1.2 Loading Contents and Closing Package

- Secure Outerpack in Upender by engaging lock pins or latch.
- Remove all but at least one of the upper Outerpack bolts on one side of the package. (All other hinge bolts remain in place).
- Raise shipping package to vertical position. Lockout support arms when using mechanical Upenders.
- Remove the remaining hinge bolt(s) from the one side.
- Loosen Outerpack swing bolts and rotate away from package.
- Open upper Outerpack door and fully rotate away from package.
- Remove the hinge pin and open Clamshell top door.
- Loosen and remove Clamshell top axial restraint assembly.
- Open lower Clamshell doors by turning latches to open position.
- Install Clamshell door stop.
- Check upper and lower accelerometers are not tripped. If found in tripped condition, replace with un-tripped and calibrated accelerometer.
- Verify that the fuel assembly has been released by Quality Assurance. Install fuel assembly by resting it on Clamshell bottom plate.
- Verify that the fuel assembly is properly oriented in the package.

- Check that grid pads are positioned at fuel assembly structural grids and nozzles.
- Remove door stop.
- Close lower Clamshell doors and secure latches by turning to lock position.
- Remove fuel tool.
- Install Clamshell top axial restraint assembly and secure axial restraint.
- Close Clamshell top door and install hinge pin.
- Close the upper Outerpack.
- Rotate Outerpack swing bolts into bracket and secure.
- Install at least one Outerpack bolt.
- Disengage upper support arm lock pins on mechanical Upender. Lower package to horizontal position. Disengage latch on powered Upender.
- Verify general cleanliness and absence of debris on the Outerpack after closing the upper Outerpack door.
- Torque the swing bolts to 20 ± 1 ft-lb (27.1 ± 1.4 N-m) and torque the Outerpack bolts to 60 ± 5 ft-lb (81.3 ± 6.8 N-m).
- Verify one approved tamper proof security seal is installed on each opposite side of the package.
- Verify that the required decals, license plates, labels, stencil markings, etc. are present and legible.

7.1.3 Preparation for Transport

7.1.3.1 Conveyance Loading of Shipping Packages

- Place shipping package(s) on conveyance equipped to permit chaining and strapping package(s) securely.
 - When lifting by the four (4) upper Outerpack lift eyes:
 - A maximum of two (2) stacked Traveller STDs may be lifted at a time.
 - A maximum of one (1) Traveller XL may be lifted at a time.
 - A maximum of one (1) Traveller VVER may be lifted at a time.
- Center and place package lengthwise on conveyance.
- Install spacer bars, if required, and install quick release lockout pin.
- Secure packages to conveyance with stops or locating pins.
- Chain or strap the package(s) to conveyance using “come along” tighteners with chains of 3/8 in (0.95 cm) minimum diameter and/or nylon straps with a minimum 5000 lb (22.24 kN) Working Load Limit (WLL).
- Place webbing swings over spacer bars, if required, and secure to conveyance.

7.1.3.2 Regulatory

- Conduct direct alpha surveys on both the package(s) and the accessible areas of the flatbed.
- Conduct radiation survey of the package(s) and transport vehicle consistent with 10 CFR 71.47 and SSR-6 para. 527. Note: A neutron and gamma radiation survey shall be performed.
- Perform the removable alpha and beta-gamma external smear surveys on both the package(s) and the accessible areas of the flatbed. If any of the following measurements are met or exceeded, notify Regulatory Engineering or appropriate site personnel for instructions on decontamination:
 - 0.4 Bq/cm^2 ($1 \times 10^{-5} \text{ } \mu\text{Ci/cm}^2$ or $2400 \text{ dpm/100 cm}^2$) for beta and gamma emitters and low toxicity alpha emitters
 - 0.04 Bq/cm^2 ($1 \times 10^{-6} \text{ } \mu\text{Ci/cm}^2$ or 240 dpm/100 cm^2) for all other alpha emitters

7.1.3.3 Inspection

- Verify that package(s) are properly stacked and secured.
- Verify that required Health Physics, Radioactive and any other placards or labels have been properly placed.
- Verify that two tamper proof security seals have been properly placed on each package.

7.2 PACKAGE UNLOADING

Operations at the unloading site include receipt and inspection of the loaded package and removal of contents. Each unloading facility must provide fully trained personnel and will be supplied with detailed operating procedures to cover all activities as required by 10 CFR 71.89.

7.2.1 Receipt of Package from Carrier

- Conduct radiation and contamination surveys of the package(s) and transport vehicle as outlined in site-specific procedures.
- Perform an external inspection of the unopened package and record any significant observations.
- Verify that two tamper proof security seals have been properly placed on each package. If either seal is missing or damaged, record the damage and follow site procedures for possible security issues.
- When lifting by the four (4) upper Outerpack lift eyes, a maximum of two (2) stacked Traveller STDs may be lifted and a maximum of one (1) Traveller XL or one (1) Traveller VVER may be lifted at a time.

7.2.2 Removal of Contents

- Secure Outerpack in Upender by engaging the lock pins or a latch on a powered Upender.
- Remove all but at least one of the upper Outerpack bolts on one side of the package. (All other hinge bolts remain in place).
- Raise shipping package to vertical position. Lockout support arms when using mechanical Upenders.
- Remove the remaining hinge bolt(s) from the one side.
- Loosen Outerpack swing bolts and rotate away from package.
- Open upper Outerpack door and fully rotate away from package.
- Check upper and lower accelerometers for tripped condition. If in tripped condition, disposition fuel

assembly per applicable Field Specification.

- Remove the Clamshell top hinge pin and open Clamshell top door.
- Loosen and remove Clamshell top axial restraint assembly.
- Install and latch the plant fuel tool to the fuel assembly/component.
- Tension the crane cable between 100 to 1000 lb (0.44 kN to 4.45 kN) as needed to take load off the Clamshell bottom plate.
- Turn lower Clamshell door latches to open position and open main doors.
- Install Clamshell door stop.
- Lift fuel assembly at least 1.5 in (3.81 cm) above Clamshell bottom plate.
- Carefully remove fuel assembly from Clamshell.
- Move fuel assembly to dry storage or other desired location.
- Prepare to close Clamshell by removing Clamshell door stop.
- Close main Clamshell doors and secure latches.
- Install Clamshell top axial restraint assembly.
- Close Clamshell top door and install hinge pin.
- Rotate Outerpack swing bolts into bracket and install at least one Outerpack bolt.
- Verify the swing bolts and Outerpack bolts are at least hand tight using standard hand tools.
- Disengage upper support arm lock pins on mechanical Upender. Lower package to horizontal position. Disengage latch if using a powered Upender.

7.3 PREPARATION OF EMPTY PACKAGE FOR TRANSPORT

The requirements for preparing an empty Traveller package for transport are intended to meet the relevant requirements for shipping an empty radioactive material package in 49 CFR 173 [4] and SSR-6 paras. 422 and 427 [1]:

- Verify the package is empty of contents.
- Verify radiation levels do not exceed limits prescribed in 49 CFR 173.421(b).
- Verify non-fixed radioactive surface contamination does not exceed limits prescribed in 49 CFR 173.421(c).
- Verify the package does not contain fissile material unless an exception of 49 CFR 173.453 is met.
- Verify the packaging is in unimpaired condition and is securely closed.
- Verify the internal contamination does not exceed 100 times the limits as prescribed by 49 CFR 173.428(d).
- Remove any previously applied labels affixed for fuel shipments.
- Affix an “Empty” label.

7.4 APPENDICES

7.4.1 References

- [1] International Atomic Energy Agency, "Regulations for the Safe Transport of Radioactive Material," SSR-6, 2012.
- [2] U.S. Nuclear Regulatory Commission Code of Federal Regulations, Title 10 Part 71, "Packaging and Transport of Radioactive Material," 2016.
- [3] American Society for Testing and Materials, "Standard Specification for Uranium Hexafluoride Enriched to Less Than 5% ²³⁵U," ASTM C 996-15, 2015.
- [4] U.S. Department of Transportation Code of Federal Regulations, Title 49 Subchapter C, "Hazardous Materials Regulations," 2016.

TABLE OF CONTENTS

8.0	ACCEPTANCE TESTS AND MAINTENANCE PROGRAM.....	8-1
8.1	ACCEPTANCE TESTS.....	8-1
8.1.1	Visual Inspections and Measurements.....	8-1
8.1.2	Weld Examinations	8-1
8.1.3	Structural and Pressure Tests.....	8-1
8.1.4	Leakage Tests.....	8-1
8.1.5	Component and Material Tests.....	8-2
8.1.5.1	Polyurethane Foam.....	8-2
8.1.5.2	Neutron Absorber Plates	8-5
8.1.5.3	Polyethylene Moderator Blocks	8-8
8.1.6	Shielding Tests	8-8
8.1.7	Thermal Tests	8-8
8.2	MAINTENANCE PROGRAM.....	8-8
8.2.1	Structural and Pressure Tests.....	8-8
8.2.2	Leakage Tests	8-8
8.2.3	Component and Material Tests.....	8-9
8.2.3.1	Fasteners.....	8-9
8.2.3.2	Weather Gasket	8-9
8.2.3.3	Shock Mounts.....	8-9
8.2.4	Thermal	8-9
8.2.5	Neutron Absorber Plates.....	8-9
8.2.6	Periodic Weld Examinations	8-9
8.2.7	Periodic Acetate Plug Examinations	8-10
8.3	APPENDICES.....	8-11
8.3.1	References	8-11

LIST OF TABLES

Table 8-1 Packaging Rigid Polyurethane Foam Density Requirements.....8-2
Table 8-2 Packaging Rigid Polyurethane Foam Property Compressive Strength Range8-3
Table 8-3 Packaging Rigid Polyurethane Foam Thermal Conductivity Properties.....8-4
Table 8-4 Packaging Material Test Methods8-7

8.0 ACCEPTANCE TESTS AND MAINTENANCE PROGRAM

8.1 ACCEPTANCE TESTS

Per the requirements of 10 CFR 71.85 [1] and SSR-6 para. 501 [2], this section discusses the inspections and acceptance tests to be performed prior to first use of the Traveller package. The Traveller package is procured under an NRC-approved Quality Assurance (QA) program meeting the requirements of 10 CFR 71 Subpart H.

8.1.1 Visual Inspections and Measurements

The Traveller STD, Traveller XL, and Traveller VVER packages have manufacturing drawings that are controlled within a quality assurance program. The drawings have quality control characteristics that must be inspected during the manufacturing process. Source inspection and final release of the package will be performed by Westinghouse to verify the quality characteristics were inspected and that the package is acceptable. Any characteristic that is out of specification must be reported. It will then be dispositioned according to Westinghouse procedure.

8.1.2 Weld Examinations

All Traveller packaging welds shall be examined to verify conformance with all applicable codes, standards and notes on each applicable drawing or specification. All Traveller packaging materials of construction and welds shall be examined in accordance with the requirements delineated in Table 2-2 of Section 2. Non-destructive examination procedures and acceptance standards are based on the ASME Code, Section III, Subsection NF-5000 (Reference [3] or a later edition as approved by Engineering at time of the manufacturing). For the Support Shelf Welds and the Fork Lift Leg Sub-Assembly, a non-destructive examination technique, such as liquid penetrant testing, is required to verify the integrity of these welds.

Weld examination verifies that locations, types and sizes of welds match drawing specifications. Further, it must be verified that there are no cracks, incomplete fusion or lack of penetration. Parts that do not meet their respective specification are repaired or replaced in accordance with Westinghouse procedure and re-inspected.

8.1.3 Structural and Pressure Tests

The Traveller packaging includes hoist rings, which require acceptance inspection. Prior to first-time use, the hoist rings need to be tested at 125% of their maximum rated loading for a minimum of ten minutes.

The Traveller packaging is not pressurized, therefore no pressure testing of the packaging is required.

8.1.4 Leakage Tests

The Traveller packaging does not have any requirements for leak testing.

8.1.5 Component and Material Tests

8.1.5.1 Polyurethane Foam

The Traveller packaging utilizes a closed-cell, polyurethane foam and must be certified to meet the requirements and acceptance criteria for installation, inspection, and testing as defined in this section.

The finished foam product shall be greater than 85% closed cell polyurethane plastic foam of the self-extinguishing variety of the density specified. The closed cell configuration will ensure that the foam will not be susceptible to significant water absorption.

If the polyurethane foam does not meet the required mechanical, thermal, and water absorption properties, the material shall be rejected.

8.1.5.1.1 Density

Rigid polyurethane foam shall have a density per Table 8-1.

Part	lb/ft³ (pcf)
Endcap Impact Limiters	20.0 ± 2.0
Outerpack Package Body	10.0 ± 1.0
Inner Pillow Impact Limiters	6.0 ± 1.0

Density shall be determined in accordance with ASTM D-1622 with the following exceptions:

- a) A minimum of one specimen per pour shall be taken, distributed regularly throughout the batch.
- b) Conditioning shall be 70°F to 80°F and 40% – 60% relative humidity for 12 hours minimum.
- c) Test conditions shall be 70°F to 80°F and 30% – 70% relative humidity.
- d) Length, width, and thickness measurements shall be made with a 6-inch digital or dial caliper.
- e) Measurements shall be made and reported to the nearest 0.001 inches.
- f) Density shall be reported in pounds per cubic foot (pcf) and no correction is made for the (negligible) buoyant effect of air.
- g) The standard deviation of the three density determinations need not be calculated or reported.

8.1.5.1.2 Mechanical Properties

Exhibited foam compressive strength for 10% strain parallel to foam rise shall be determined in accordance with ASTM D-1621, with the exceptions noted below, and shall fall within the range of values presented in Table 8-2.

Part	Density (pcf)	Compressive Strength	
		Min	Max
Endcap Impact Limiters	20.0 ± 2.0	888 psi	1332 psi
Outerpack Package Body	10.0 ± 1.0	262 psi	393 psi
Inner Pillow Impact Limiters	6.0 ± 1.0	132 psi	198 psi

- a) Specimen shall be right rectangular prisms 1.0 ± 0.1 in thick x 2.0 ± 0.1 in x 2.0 ± 0.1 in with the 1.0 ± 0.1 in dimension parallel to the direction of foam rise.
- b) A specimen from each batch shall be tested.
- c) Conditioning shall be 70°F to 80°F and 40% – 60% relative humidity for 12 hours minimum.
- d) Test conditions shall be 70°F to 80°F and 30% – 70% relative humidity.
- e) Length, width, and thickness measurements shall be made with a 6-inch digital or dial caliper.
- f) Measurements shall be made and reported to the nearest 0.001 inches.
- g) Strain rate shall be 0.1 ± 0.05 in/in – min.
- h) Only actual values (not averages or standard deviations) need be reported.

8.1.5.1.3 Flame Retardant Characteristics

Flame retardant characteristics shall be qualified by demonstrating compliance with the following requirements. The requirements shall be demonstrated by flame testing described in FAA Powerplant Engineering Report No. 3A. Additional certification testing to validate the flame-retardant characteristics shall also be performed in accordance with ASTM F-501-93. The test described in b) below is not applicable to the 6 pcf foam.

- a) Foam shall not be capable of sustaining a flame for a period greater than five (5) minutes, following the removal of the heat source and after being exposed to temperatures up to 1,500°F. A heat source with a flame temperature of at least 1,500°F is applied until the foam is ignited. The heat source is removed after ignition of the foam and the time until self-extinguishment of the flame (absence of flame) will be monitored and compared against the 5-minute acceptance criteria.
- b) Prepare a representative sample of the foam material and test in accordance with the following:
 - 1) Cut two pieces of sheet metal (16 gauge maximum/25 gauge minimum) to a size sufficient to cover a 10 inch diameter test sample.
 - 2) Attach a thermocouple at the approximate center of one side of each piece of sheet metal.
 - 3) Prepare a representative sample of the foam material inside a 10-inch inner diameter by 6-inch long steel cylinder. Foam to fill the entire length of the cylinder and the full 10-inch diameter.
 - 4) Sandwich the sample between the two pieces of sheet metal, with the thermocouples in

contact with the foam.

- 5) Expose one end of the foam sample (sheet metal) to a heat source. Apply enough heat to cause the indicated thermocouple temperature to increase from ambient temperature to 1,475°F minimum on the exposed side.
- 6) Hold the sample at a minimum of 1,475°F for a minimum period of thirty (30) minutes.

Acceptance criteria shall be as follows:

During the period that heat is applied, the thermocouple on the non-exposed end of the sample shall not exceed 180°F. The thermocouple on the back side (away from the flame) shall be isolated from the sheet metal to prevent heat from radiating from the metal instead of traversing the foam core. The thermocouple can be isolated using a piece of Nomex cloth or approved equivalent.

8.1.5.1.4 Thermal Properties

The foam shall exhibit the following nominal thermal characteristics for the 6 pcf, 10 pcf, and 20 pcf nominal density pours, minimum of three specimens per qualification:

- a) Thermal Conductivity (Table 8-3)

Table 8-3 Packaging Rigid Polyurethane Foam Thermal Conductivity Properties			
Part	Thermal Conductivity (Test Method – ASTM C-177 at 75°F mean temperature)	Density (pcf)	k-factor (BTU/Hr-ft ² -F/inch)
Inner Pillow Impact Limiters	LAST-A-FOAM® FR-3706	6.0 ± 1.0	0.240
Outerpak Package Body	LAST-A-FOAM® FR-3710	10.0 ± 1.0	0.279
Endcap Impact Limiters	LAST-A-FOAM® FR-3720	20.0 ± 2.0	0.376

- b) Specific Heat
 0.353 BTU/lb-°F (Test Method – ASTM E-1269)

8.1.5.1.5 Water Absorption Properties

The average water absorption by the foam observed through testing using ASTM D-2842, with the following testing exceptions, shall not be more than 5% by volume. The construction of the Traveller will further ensure that, in actual operation, significantly lower water absorption rate would be observed.

- a) Length, width and thickness measurements shall be made with a digital or dial caliper.
- b) Measurements shall be made and reported to the nearest 0.001 inches.
- c) A single specimen of the qualifying material shall be molded to the density range as stated in the density chart above.
- d) The specimen shall consist of a single 3.0 inches x 6.0 inches x 6.0 inches (tolerance on dimensions is 0.5 inches) block of foam.
- e) No correction shall be made for cut or open cells in the specimen’s volume calculations.

8.1.5.1.6 Chemical Composition

The chemical composition of the foam shall be as follows:

C:	50% – 70%
O:	14% – 34%
N:	4% – 12%
H:	4% – 10%
P:	0% – 2%
Si:	< 1%
Cl:	< 1800 PPM
Leachable Chlorides:	< 1 PPM
Other:	< 1%

The foam is a rigid polyether polyurethane formed as reaction product of the primary chemicals: polyphenylene, polymethylene, polyisocyanate (polymeric isocyanate) and polyoxypropylene glycols (polyether polyols). These materials react to produce a rigid, polyether, polyurethane foam. The foam will not contain halogen containing flame retardant or trichloromonofluoromethane (Freon 11).

Leachable chloride testing is required when using stainless steel as the container structure because free chloride ions in contact with the container sides have been faulted as a contributor to stress corrosion cracking. Leachable chlorides will not be greater than 1 ppm when tested in accordance with either (1) GP-TM9510: Method for Sample Preparation and Determination of Leachable Chlorides in Rigid Polyurethane Foam or (2) EPA 300.0: Determination of Inorganic Anions by Ion Chromatography.

8.1.5.2 Neutron Absorber Plates

Neutron absorber plates are installed along the four faces of the Clamshell or six faces of the VVER Clamshell to meet the requirements specified in Section 6 of this document. The neutron absorber material, BORAL, is a hot-rolled composite aluminum sheet consisting of a core of uniformly distributed boron carbide and aluminum particles, which is enclosed within layers of pure aluminum forming a solid barrier against the environment. The plates are used to ensure subcriticality during transportation as a neutron absorber and are not relied upon for the conductivity or mechanical properties. The service conditions are not so severe as to promote significant alterations of these plates. Therefore, durability of these neutron absorbing materials is regarded to meet or exceed the service requirements of this application.

To ensure the BORAL meets the drawing requirements, the plates will be inspected on a periodic basis not to exceed five years per Section 8.2.5. This will ensure that the BORAL maintains its durability throughout its service lifetime. The visual inspection will verify that the plates are present and in good condition. This includes inspection of the BORAL core for chipping or flaking resulting from brittleness. There are no significant routine loads applied to the BORAL plates, therefore no durability problems should arise during normal conditions of transport.

No processing changes are anticipated for the production of BORAL since the established process will be used to produce the packages.

8.1.5.2.1 Boron-10 Areal Density

The BORAL neutron absorber plate minimum ^{10}B areal density for the final thickness of []^{a,c} is []^{a,c}. Acceptance testing to ensure that the manufacturing process is operating in a satisfactory manner may be conducted using neutronics transmission or chemical analysis to ensure an effective minimum ^{10}B areal density of []^{a,c}.

Neutron Transmittance is a neutron counting testing technique performed to determine the concentration of an isotope in a material. Testing involves placement of test coupons in a calibrated neutron source beam and measuring the number of neutrons allowed to pass through the test material. Based on the neutron count, the areal density of the coupon can be calculated and compared to certified standards. Chemical analysis is assay testing performed on a sample taken from test coupons to determine the boron content.

8.1.5.2.2 Neutron Absorption Testing Requirements

Neutron Transmittance testing shall be performed at thermal neutron energies per approved test method to verify the minimum required ^{10}B concentration. Test coupons are considered acceptable when the transmittance data indicates a ^{10}B areal density equal to or greater than []^{a,c}. Statistical data on transmissivity may be coupled with luminescence test data to demonstrate uniformity of the boron material.

Neutron Radiograph testing shall be performed for each selected sample with a luminance test or approved equivalent to verify the uniformity of the ^{10}B distribution in the sheet at thermal neutron energies. Neutron Radiograph (luminance) testing is a non-destructive imaging technique for the internal evaluation of materials. It involves attenuation of a neutron beam by an object to be radiographed, and registration of the attenuation process (as an image) on film or video. Inspection results shall be recorded using the appropriate data recording method by the testing facility.

8.1.5.2.3 Chemical Testing Requirements

Chemical testing may be employed as an acceptable substitute to the neutronics testing to verify the minimum areal density of ^{10}B is present in the neutron absorber plate. Prior to ^{10}B verification by chemical testing, the process shall be demonstrated to be equivalent to the neutronics testing described with respect to ^{10}B uniformity and isotopic composition. Test coupons are considered acceptable when the calculated ^{10}B areal density is equal to or greater than is []^{a,c}.

8.1.5.2.4 Sampling Rates and Test Methods

The inspection levels shall be as stipulated in the supplier submitted process specification(s). Test methods, when not referenced herein, shall be reviewed by Westinghouse Engineering. Sample coupons shall be randomly selected and be representative of the configuration, material, and lot being evaluated. The test methods are outlined in Table 8-4.

Table 8-4 Packaging Material Test Methods		
Requirement	Number of Tests Per Lot	Test Method
Aluminum Alloy Compositions	1 per Heat	ASTM B209/B221 and Approved Procedure
Neutron Radiograph	100% ⁽¹⁾	WEC Approved Procedure
Neutron Transmittance for ¹⁰ B Areal Density	100% ⁽¹⁾	WEC Approved Procedure
Chemical Testing	100% ⁽²⁾	WEC Approved Procedure
Notes:		
(1) For every lot, initial sampling of coupons for neutron transmission measurements and radiograph/ radioscopy shall be 100%, which shall be considered normal sampling. Rejection of a given coupon shall result in rejection of any contiguous plate(s). Reduced sampling (50%) may be introduced based upon acceptance of all coupons in the first 25% of the lot. The approved process specification shall reflect the use of reduced sampling, as applicable. A rejection during reduced inspection will require a return to 100% inspection of the lot.		
(2) For every lot, initial sampling of coupons for chemical testing shall be 100%, which shall be considered normal sampling. Rejection of a given coupon shall result in rejection of any contiguous plate(s). Reduced sampling of the lot to 95/95 confidence sampling is acceptable based upon acceptance of all coupons in the first 25% of the lot. The approved process specification shall reflect the use of reduced sampling, as applicable. A rejection during reduced inspection will require a return to 100% inspection of the lot.		

8.1.5.2.5 Mechanical Tests

The neutron absorber plates perform a neutronic function of the Traveller package. Thus, no mechanical testing is required.

8.1.5.2.6 Visual Inspection

For all plates, the finished plate shall be free of visual surface cracks, blisters, pores, or foreign inclusions.

Evidence of foreign material shall be cause for rejection (embedded pieces of B₄C matrix are not considered foreign material). Creases or other surface discontinuities are acceptable on the cladding of the BORAL provided the core is not exposed. If necessary, the plate shall be examined by visual inspection per approved procedure(s) to determine if a surface indication is a crease or a crack. Surface roughness shall not exceed 125 RMS roughness maximum.

8.1.5.2.7 Test Terminology

Acceptance test criteria are as follows:

- a) Lot Definition – A lot shall consist of all plate of the same nominal size, condition and finish that is produced from the same heat, processed in the same manner, and presented for inspection at the same time.
- b) Heat Definition – A heat shall consist of the total molten metal output from a single heating in a batch melting process or the total metal output from essentially a single heating in a continuous

melting operation and targeted at a fixed metal chemistry at the furnace spout.

- c) Coupon (BORAL) – A selected sample of the thinnest section of a lot of the neutron absorber used for acceptance testing of the candidate material.

8.1.5.3 Polyethylene Moderator Blocks

This section establishes the requirements and acceptance criteria for inspection and testing of Ultra High Molecular Weight (UHMW) Polyethylene moderator blocks utilized within the Traveller packaging.

The supplier shall certify that the polyethylene is Ultra High Molecular Weight (UHMW) and complies with ASTM D4020, including a specific gravity greater than 0.93.

8.1.6 Shielding Tests

The Traveller package does not contain any purpose-built shielding components. Therefore, shielding tests are not required.

8.1.7 Thermal Tests

The material properties utilized in Chapter 3, Thermal Evaluation, are consistently conservative for the Normal Conditions of Transport (NCT) thermal analysis performed. The Hypothetical Accident Condition (HAC) fire certification testing of the Traveller package (see Section 3.6.5) verified material performance in the HAC thermal environment. As such, with the exception of the tests required for specific packaging components as discussed in Section 8.1.5, Component and Material Tests, specific acceptance tests for material thermal properties are not required or performed.

8.2 MAINTENANCE PROGRAM

This section describes the maintenance program used to ensure continued performance of the Traveller package.

Visual inspection for damage of all exposed surfaces will be performed before each use. Individual components will also be inspected as described in the sections below. If any defects are found during inspection, the package will be segregated and dispositioned by standard site procedure before its next use.

8.2.1 Structural and Pressure Tests

The Traveller packaging does not contain any structural or lifting/tie-down devices that require testing.

The Traveller packaging is not pressurized. Therefore, no pressure testing of the packaging is required.

8.2.2 Leakage Tests

The Traveller packaging does not have any requirements for leak testing.

8.2.3 Component and Material Tests

8.2.3.1 Fasteners

Threaded components shall be inspected prior to each use for deformed or stripped threads. Damaged components shall be repaired or replaced prior to further use.

8.2.3.2 Weather Gasket

Prior to each use, visual inspection of the silicone rubber or fiberglass weather gasket shall be performed for tears, damage, or deterioration. Unacceptable seals shall be replaced.

8.2.3.3 Shock Mounts

Prior to first use and at an interval not to exceed five years or 50 cycles, whichever is more limiting, each Lord Sandwich Shock Mount (Part Number J-5425-275 [STD and XL], J-3424-21 [VVER], or engineering approved equivalent) shall be visually inspected. The inspection shall verify the condition of the shock mount for tears, missing material or deterioration from aging. A load shall be placed on the Clamshell to tension the shock mounts to visual inspect. A light source with a videoscope is used to inspect the full circumference of each shock mount. Damaged or suspect shock mounts shall be replaced with Lord Sandwich Shock Mount Part Number J-5425-275 [STD and XL], J-3424-21 [VVER], or engineering approved equivalent.

8.2.4 Thermal

Because the Outerpack of the Traveller package is constructed of rigid polyurethane foam encapsulated in stainless steel, no degradation of heat transfer capability will occur during normal conditions of transport. Therefore, routine thermal tests are not necessary to ensure continued thermal performance of the Traveller packaging.

8.2.5 Neutron Absorber Plates

On a periodic basis (not to exceed five years or 50 cycles, whichever is more limiting), packages will be inspected to verify the neutron absorber plate configuration complies with the drawing requirements. Quality Control Instructions and Mechanical Operating Procedures will define the specific inspection requirements. In accordance with established site procedures, a visual inspection will be conducted of the visible side of the neutron absorber plates. Personnel will visually verify that the plates are present and in good condition. Any neutron absorber plate with deep scratches or gouges, which expose the inner boron carbide center, shall be replaced. Neutron absorber plates covered with cork rubber shall be visually inspected at each screw location and the cork rubber inspected for signs of tampering. Documentation relating to these inspections, repairs, and part replacements will be produced and maintained.

8.2.6 Periodic Weld Examinations

During routine, scheduled maintenance not to exceed two (2) years, external Outerpack and internal Clamshell structural welds are inspected visually per ASME Section III, Sub-section NF-5221 Class 2 (c), or an approved Engineering equivalent standard including European EN standard. The lifting eye and forklift

leg sub-assembly leg welds, in lieu of visual inspections, may be inspected by non-destructive test methods, such as liquid dye penetrant or magnetic particle, per ASME Section III, Sub-Section NF-5221 Class 2 (a), or an approved Engineering equivalent standard including European EN standard.

8.2.7 Periodic Acetate Plug Examinations

During routine, scheduled maintenance not to exceed two (2) years, the Outerpack acetate plugs are inspected visually for obvious physical damage. The visual and functional inspection requires that acetate plugs be replaced if any of the following conditions are found:

- Thru-the-wall cracks are present or cracking along full length/width of plug.
- During tightening (hand tool, 9/16 inch or 15mm ratchet wrench), cracking is observed.
- During tightening (hand tool, 9/16 inch or 15mm ratchet wrench), the acetate plug will not thread into the threaded vent port.

8.3 APPENDICES

8.3.1 References

- [1] U.S. Nuclear Regulatory Commission Code of Federal Regulations, Title 10 Part 71, "Packaging and Transport of Radioactive Material," 2016.
- [2] International Atomic Energy Agency (IAEA), "Regulations for the Safe Transport of Radioactive Material," 2012.
- [3] American Society of Mechanical Engineers, "ASME Boiler and Pressure Vessel Code, Rules for Construction of Nuclear Power Plant Components, Section III," 2001 with 2003 Addenda.
- [4] International Atomic Energy Agency, "Regulations for the Safe Transport of Radioactive Material," SSR-6, 2012.
- [5] American Society for Testing and Materials, "Standard Specification for Uranium Hexafluoride Enriched to Less Than 5% ²³⁵U," ASTM C 996-15, 2015.